

Resource-Economical C–H Activation for Late-Stage Functionalization

Dissertation

for the award of the degree

“Doctor rerum naturalium” (Dr.rer.nat.)

of the Georg-August-Universität Göttingen



within the doctoral program of chemistry
of the Georg-August-Universität School of Science (GAUSS)

Submitted by
Nikolaos Kaplaneris
From Athens, Greece

Göttingen, 2021

Thesis Committee

Prof. Dr. Lutz Ackermann, Georg-August-Universität Göttingen Institut für Organische und Biomolekulare Chemie

Prof. Dr. Konrad Koszinowski, Georg-August-Universität Göttingen Institut für Organische und Biomolekulare Chemie

Members of the Examination Board

Reviewer: Prof. Dr. Lutz Ackermann, Georg-August-Universität Göttingen Institut für Organische und Biomolekulare Chemie

Second Reviewer: Prof. Dr. Konrad Koszinowski, Georg-August-Universität Göttingen Institut für Organische und Biomolekulare Chemie

Further members of the Examination Board

Prof. Dr. Dr. h.c.mult. Lutz F. Tietze, Georg-August-Universität Göttingen Institut für Organische und Biomolekulare Chemie

Prof. Dr. Ricardo Mata, Georg-August-Universität Göttingen Institut für Physikalische Chemie

Dr. Daniel Janßen-Müller, Georg-August-Universität Göttingen Institut für Organische und Biomolekulare Chemie

Dr. Michael John, Georg-August-Universität Göttingen Institut für Organische und Biomolekulare Chemie

Date of the oral examination: 30.06.2021

List of Abbreviations

Å	Ångström
Ac	acetyl
Alk	alkyl
AMLA	ambiphilic metal-ligand activation
aq.	aqueous
Ar	aryl
atm	atmospheric pressure
BIES	base-assisted internal electrophilic substitution
Bn	benzyl
Boc	<i>tert</i> -butyloxycarbonyl
Bu	butyl
Bz	benzoyl
calc.	calculated
<i>cat.</i>	catalytic
Cbz	benzyloxycarbonyl
CMD	concerted-metalation-deprotonation
conv.	conversion
Cp*	pentamethylcyclopentadienyl
Cy	cyclohexyl
δ	chemical shift

d	doublet
DCE	1,2-dichloroethane
dd	doublet of doublet
DFT	density functional theory
DG	directing group
DME	dimethoxyethane
DMF	<i>N,N</i> -dimethylformamide
dt	doublet of triplet
EI	electron ionization
equiv	equivalent
ES	electrophilic substitution
ESI	electrospray ionization
Et	ethyl
FG	functional group
g	gram
GC	gas chromatography
h	hour
Hal	halogen
Het	heteroatom
Hept	heptyl
Hex	hexyl

HFIP	hexafluoro-2-propanol
HPLC	high performance liquid chromatography
HR-MS	high resolution mass spectrometry
Hz	Hertz
<i>i</i>	<i>iso</i>
IR	infrared spectroscopy
IES	internal electrophilic substitution
<i>J</i>	coupling constant
KIE	kinetic isotope effect
L	ligand
<i>m</i>	<i>meta</i>
m	multiplet
M	molar
[M] ⁺	molecular ion peak
Me	methyl
Mes	mesityl
mg	milligram
MHz	megahertz
min	minute
mL	milliliter
mmol	millimol

M. p.	melting point
MS	mass spectrometry
<i>m/z</i>	mass-to-charge ratio
NCTS	<i>N</i> -cyano-4-methyl- <i>N</i> -phenyl benzenesulfonamide
NMP	<i>N</i> -methylpyrrolidinone
NMR	nuclear magnetic resonance
<i>o</i>	<i>ortho</i>
OA	oxidative addition
OPV	oil pump vacuum
<i>p</i>	<i>para</i>
Ph	phenyl
PhMe	toluene
PMP	<i>para</i> -methoxyphenyl
Piv	pivaloyl
ppm	parts per million
Pr	propyl
py	pyridyl
pym	pyrimidyl
pyr	pyrazol
q	quartet
RT	ambient temperature

s	singlet
sat.	saturated
SPPS	solid phase peptide synthesis
SPS	solvent purification system
<i>t</i>	<i>tert</i>
t	triplet
T	temperature
THF	tetrahydrofuran
TIPS	triisopropylsilyl
TLC	thin layer chromatography
TM	transition metal
TMP	3,4,5-trimethoxyphenyl
TMS	trimethylsilyl
Ts	<i>para</i> -toluenesulfonyl
TS	transition state
<i>t_r</i>	retention time
<i>wt%</i>	weight percentage
UV	ultraviolet
X	(pseudo)halide

Table of Contents

1. Introduction.....	1
1.1. Transition Metal-Catalyzed C–H Functionalizations.....	1
1.2. Ruthenium-Catalyzed C–H Activation	8
1.3. Manganese-Catalyzed C–H Activation.....	18
1.3.1. Manganese-Catalyzed C–H Activation: Early Report.....	18
1.3.2. Manganese-Catalyzed C–H Hydroarylation.....	20
1.3.3. Manganese-Catalyzed Substitutive C–H Activation	26
1.3.4. Domino Processes Initiated by Manganese-Catalyzed C–H Activation.....	28
1.4. Late-Stage Functionalization of Peptides <i>via</i> C–H Activation.....	31
1.4.1. Functionalization of Amino Acid Derivatives <i>via</i> C–H Activation	31
1.4.2. Functionalization of Peptides <i>via</i> C–H Activation.....	36
1.4.3. Peptide Macrocyclization <i>via</i> C–H Activation.....	47
2. Objectives	55
3. Results and Discussion.....	60
3.1. Sequential <i>meta-/ortho</i> -C–H Functionalization of Aryl Oxazolines <i>via</i> Ruthenium Catalysis	60
3.1.1. Optimization Studies for Ruthenium-Catalyzed <i>meta</i> -C–H Alkylation <i>via</i> Oxazoline Assistance..	61
3.1.2. Scope of the Ruthenium-Catalyzed <i>meta</i> -C–H Functionalization <i>via</i> Oxazoline Assistance	62
3.1.3. Diversification of the Functionalized Oxazolines.....	69
3.1.4. Mechanistic Studies.....	70
3.1.4. Proposed Catalytic Cycle for the Ruthenium-Catalyzed C–H <i>meta</i> -Alkylation <i>via</i> Oxazoline Assistance	72
3.2. Palladium-Catalyzed C(<i>sp</i> ²)-H and C(<i>sp</i> ³)-H Late-Stage Glycosylation	74
3.2.1. Scope of the Palladium-Catalyzed C(<i>sp</i> ²)-H Glycosylation.....	75
3.2.2. Scope of the Palladium-Catalyzed C(<i>sp</i> ³)-H Glycosylation.....	76
3.3. Ruthenium(II)-Catalyzed Peptide C–H Functionalization <i>via</i> Hydroarylation	79
3.3.1. Acid-Enabled C–H Cleavage and Protodemetalation	80
3.3.2. Scope of the Ruthenium(II)-Catalyzed Peptide Alkylation	81
3.3.3. Late-Stage Removal of the Pyridyl Group.....	87
3.3.4. Peptide Alkenylation <i>via</i> Ruthenium(II)-Catalyzed Hydroarylation.....	88
3.4. 3d-Transition Metal-Catalyzed Allylation of Drug Scaffolds and Peptides.....	90
3.4.1. Optimization Studies for C–H Allylation of Peptides Under Manganese(I) Catalysis	91
3.4.2. Scope of the Manganese(I)-Catalyzed C–H Allylation of Tryptophan-Containing Peptides and Biomolecules	92
3.4.3. Synthetic Applications of the Manganese(I)-Catalyzed C–H Allylation Manifold	99
3.4.4. Manganese(I)-Catalyzed Macrocyclization <i>via</i> an Allylation Manifold.....	101

3.4.5. Late-Stage Removal of the Pyridyl Group.....	102
3.4.6. Manganese(I)-Catalyzed C–H Alkylation of Heteroarenes with Protected MBH-Adducts.....	103
3.4.7. Late-Stage Cobalt(III)-Catalyzed C–H Alkylation of Tryptophan-Containing Peptides	106
3.5. Manganese(I)-Catalyzed Peptide C–H Ligation and Macrocyclization	108
3.5.1. Optimization Studies for Peptide Stitching <i>via</i> C–H Hydroarylation of Propiolates with Tryptophan-Containing Peptides.....	109
3.5.2. Manganese(I)-Catalyzed C–H Stitching	111
3.5.3. Synthetic Applications of the Manganese(I)-Catalyzed Hydroarylation Manifold	117
3.5.4. Manganese(I)-Catalyzed Macrocyclization <i>via</i> a Hydroarylation Manifold.....	119
3.5.5. Traceless Removal of the Pyridyl Group from the Cyclic Peptide 285d	123
3.6. Manganese(I)-Catalyzed C–H BODIPY-Labeling of Tryptophan-Containing Peptides	125
3.6.1. Optimization Studies for Manganese(I)-Catalyzed Labeling of Tryptophan with BODIPY-Alkynes	126
3.6.2. Scope of the Manganese(I)-Catalyzed Labeling of Tryptophan-Containing Peptides	127
3.6.3. Traceless Azine Removal: Access to <i>NH</i> -Free Fluorescent Tryptophan Derivative	137
4. Summary and Outlook.....	139
5. Experimental Part.....	145
5.1. General Remarks	145
5.2. General Procedures	148
5.2.1. General Procedure A: Ruthenium(II)-Catalyzed <i>meta</i> -Alkylation of Oxazolines	148
5.2.2. General Procedure B: Ruthenium(II)-Catalyzed <i>meta</i> -Alkylation/ <i>ortho</i> -Arylation of Oxazolines.....	148
5.2.3. General Procedure C: Palladium-Catalyzed C(<i>sp</i> ²)-H Glycosylation with TAM ^{Bu}	148
5.2.4. General Procedure D: Palladium-Catalyzed Peptide C(<i>sp</i> ³)-H Glycosylation with TAM	149
5.2.5. General Procedure E: Ruthenium(II)-Catalyzed C–H Alkylation of Tryptophan	149
5.2.6. General Procedure F: Ruthenium(II)-Catalyzed C–H Alkylation of Peptides	149
5.2.7. General Procedure G: Ruthenium(II)-Catalyzed C–H Ligation of Peptides.....	149
5.2.8. General Procedure H: Traceless Removal of 2-Pyridyl Group from Alkylated Peptides	150
5.2.9. General Procedure I: Manganese(I)-Catalyzed Late-Stage C–H Alkylation on Peptides with MBH Adducts.....	150
5.2.10. General Procedure J: Manganese(I)-Catalyzed Late-Stage C–H Alkylation on (Hetero)Arenes with MBH Adducts.....	150
5.2.11. General Procedure K: Traceless Removal of 2-Pyridyl Group from Alkylated Peptides.....	151
5.2.12. General Procedure L: Cobalt(III)-Catalyzed Late-Stage C–H Alkylation on Peptides.....	151
5.2.13. General Procedure M: Manganese(I)-Catalyzed Late-Stage C–H Hydroarylation on Peptides.....	151
5.2.14. General Procedure N: Manganese(I)-Catalyzed C–H Macrocyclization of Peptides	151
5.2.15. General Procedure O: Manganese(I)-Catalyzed Late-Stage C–H Alkylation on Peptides	152
5.3. Sequential <i>meta</i> -/ <i>ortho</i> -C–H Functionalization of Oxazolines <i>via</i> Ruthenium Catalysis	153

5.3.1. Characterization Data	153
5.3.2. Mechanistic Studies	172
5.4. Palladium-Catalyzed C(sp ²)-H and C(sp ³)-H Late-Stage Glycosylation	179
5.4.1. Characterization Data	179
5.5. Ruthenium(II)-Catalyzed Peptide C-H Functionalization <i>via</i> Hydroarylation Manifold	193
5.5.1. Characterization Data	193
5.5.1. Mechanistic Studies	222
5.6. 3d-Transition Metal-Catalyzed Allylation of Drug Scaffolds and Peptides	224
5.6.1. Characterization Data	224
5.7. Manganese(I)-Catalyzed Peptide C-H Ligation and Macrocyclization	279
5.7.1. Characterization Data	279
5.7. Manganese(I)-Catalyzed C-H BODIPY-Labeling of Tryptophan-Containing Peptides	321
5.7.1. Characterization Data	321
6. References	358
7. Acknowledgements	374
8. NMR Spectra	376

1. Introduction

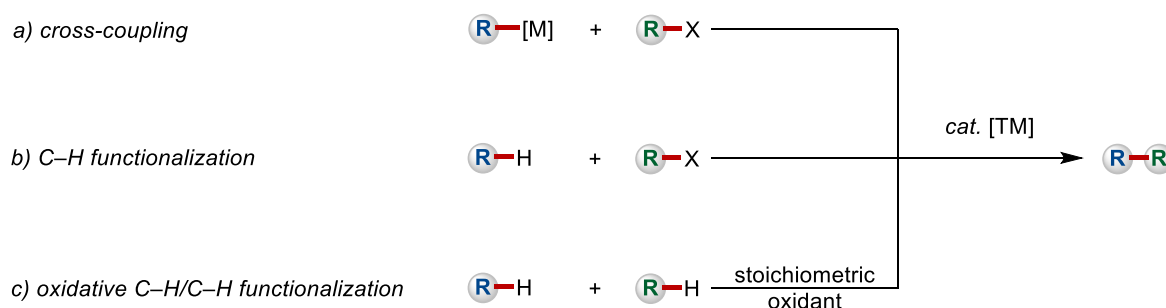
Based on the environmental issues that have risen during the last decades, new and efficient processes are in high demand for replacing old and waste-generating technologies in order to provide a sustainable future for the next generation. This paradigm shift reflects that we are now aware of our present practices having enormous impact on future generations, this is now also observed in molecular synthesis. Thus, due to the increased need for sustainable molecular syntheses, new strategies and technologies are highly desired. Catalysis represents one significant approach for the minimization of the environmental footprint as was recognized by Anastas and Werner in their 12 Principles of Green Chemistry.^[1] Apart from that, catalysis can provide new disconnections to the practitioner in a step-, atom- and resource economical manner.^[2]

1.1. Transition Metal-Catalyzed C–H Functionalizations

The design of mild, robust and predictable reactions for forging C–C and C–Het bonds is of utmost importance in organic synthesis, as these methods would facilitate the synthesis of a plethora of life-saving drugs, among others, in an expedient and efficient manner. In this context, transition metal-catalyzed reactions represent one of the most well-established and reliable approaches for the synthesis of these scaffolds. Transition metals offer an enormous amount of modes of action, thus providing a new avenue for new types of disconnections, which have been inaccessible by "traditional" chemistry. Among the plethora of reaction manifolds, metathesis^[3] and cross-coupling^[4] have truly revolutionized the way we approach organic synthesis. The understanding of the distinct mechanistic steps of these reaction manifolds led to significant advancements, thus cross-coupling has been sharpened into a modular and predictable tool, with applications in academia and industries. Among the transition metals, palladium^[5] is the most used for cross-couplings, due to general and mild reaction conditions that are typically employed. Thus, many palladium-catalyzed cross-couplings reaction have been developed, namely Kumada-Corriu,^[6] Negishi,^[7] Magita-Kosogi-Stille,^[8] Suzuki-Miyaura,^[9] Hiyama^[10] cross-coupling enabled the expedient synthesis of biaryls *via* the coupling of an aryl halides or pseudo-halides with various organometallic nucleophiles (Scheme 1.1.1a). In addition, the Mizoroki-Heck reaction^[11] enabled the alkenylation of an aryl halides or pseudo-halides, the Sonogashira-Hagihara^[12] reaction allowed for the alkynylation of aryl halides or

1. Introduction

pseudo-halides and the Tsuji-Trost^[13] reaction enabled the substitutive allylation of allyl electrophiles with various organic and organometallic nucleophiles. The translational nature of these new reaction manifolds was recognized with the Nobel Prize in Chemistry in 2010 to A. Suzuki, E.-i. Negishi and R. F. Heck.^[14] While these methods entirely changed the way synthetic chemists think and practice organic chemistry,^[15] they still require pre-functionalized materials, thus jeopardizing the atom- and step-economy of this approach. Furthermore, some organometallic nucleophiles utilized are either air- or moisture- sensitive, such as organomagnesium reagents used in the Kumada-Corriu cross-coupling or organozinc reagents used in the Negishi cross-coupling. Lastly, organostannane reagents used in Stille coupling are typically toxic. Thus, the chemical waste associated with the preparation of the starting materials and the stoichiometric byproducts of these reaction significantly intensifies their environmental footprint. To bypass these shortcomings, the synthetic community in search of a more straightforward approach for molecular synthesis, demonstrated that C–H functionalization provides a sustainable alternative to the "traditional" cross-coupling technologies.^[16] In this approach, the organometallic nucleophile is replaced by an inert C–H bond, therefore eliminating the need for multi-step sequences for accessing the sensitive and potentially toxic organic nucleophile (Scheme 1.1b). Interestingly, the stitching of two carbon atoms bearing a hydrogen atom *via* an oxidative C–H/C–H functionalization represents *a priori* an ideal transformation, albeit a stoichiometric oxidant is normally required (Scheme 1.1c).



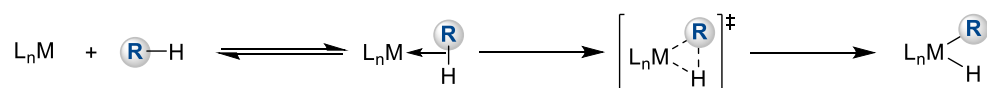
Scheme 1.1.1. Conceptual advantages of C–H functionalization over classical cross-couplings.

Due to the inherent benefits of the C–H functionalization approach in terms of atom- and step-economy, great efforts had been devoted to the understanding of the C–H bond cleavage step. Excluding the radical-type outer-sphere mechanisms, the

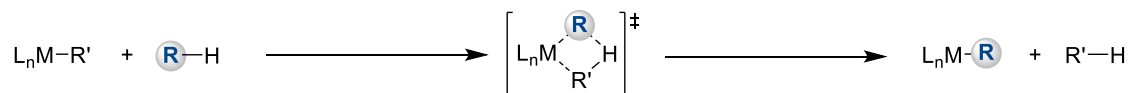
organometallic C–H bond cleavage mainly proceeds *via* five different pathways, depending by on nature of the metal, ligands and the oxidation state (Scheme 1.1.2).^[17] These modes of C–H activation are oxidative addition, σ -bond metathesis, 1,2-addition, electrophilic substitution and base-assisted metalation. C–H bond cleavage by oxidative addition is typically observed in electron-rich metal centers, thus cyclometalation with d^8 -electron configuration at iridium(I), rhodium(I) and ruthenium(0) typically occurs *via* this pathway. The key interaction of the σ^* orbital of the C–H bond with the metal center induces a formal two-electron transfer from the metal to the ligand. Cyclometalation *via* σ -bond metathesis is considered the main mechanistic pathway for high-valent early transition metals. In addition, this mode of action has been proposed to be operative with metal hydrides and metal alkyl complexes. The 1,2-addition is observed for metals with a M=X bond, mostly group IV and V metal imido-complexes. This mode of action usually takes place with early transition metals. C–H bond cleavage *via* electrophilic substitution is generally observed with electron-poor late transition metals. A classic example is palladium(II)-mediated C(sp^2)–H activation. Mechanistic investigations demonstrated that electron-rich arenes react preferentially to electron-poor ones, analogous to "classical" electrophilic substitution. The base-assisted metalation is observed for complexes bearing a chelating base, e.g. carboxylate or carbonate and resembles the electrophilic substitution, but with the assistance from the coordinated base. Under this mechanistic manifold the C–H bond cleavage occurs simultaneously to the formation of the R–[M] bond.

1. Introduction

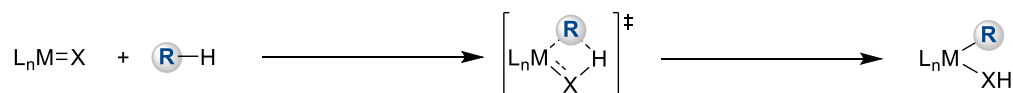
a) oxidative addition



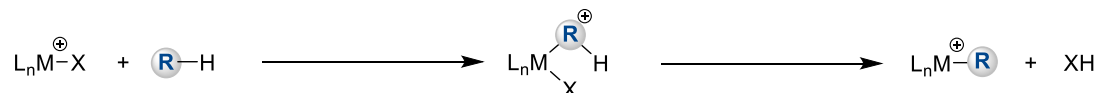
b) σ -bond metathesis



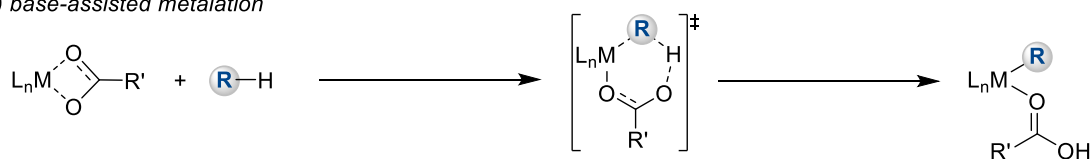
c) 1,2-addition



d) electrophilic substitution

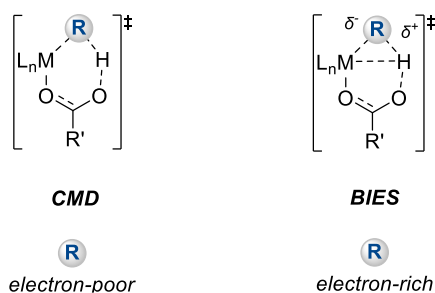


e) base-assisted metalation



Scheme 1.1.2. Different modes of organometallic C–H bond cleavage.

Among these different modes of transition-metal catalyzed C–H bond cleavage base-assisted metalation is by far the most practical in terms of mildness and robustness and consequently the most studied. Thus, based on the transition state structure and the resulting accumulation of partial charges, the base-assisted metalation pathway can be further categorized (Scheme 1.1.3).^[18] For a deprotonative transition state as first put forward by Sakaki,^[19] the term concerted metalation-deprotonation (CMD) was introduced by Fagnou.^[20] The same mode of action, although featuring an agostic interaction between the C–H bond and the metal center, was also studied by Macgregor and Davies and named ambiphilic metal ligand activation (AMLA).^[21] Due to the deprotonative nature of this pathway, a preferential activation of electron-deficient substrates is observed through kinetic C–H acidity control. In contrast, the base-assisted internal electrophilic substitution (BIES) was introduced by Ackermann for the preferred activation of electron-rich substrates and proceeds in a deprotonative/electrophilic substitution-type pathway.^[22]



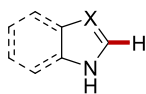
Scheme 1.1.3. Comparison of transition state structures in base-assisted metalation.

C–H functionalization has been established as a transformative tool with applications ranging from natural product synthesis^[23] and material sciences^[24] to predominantly medicinal chemistry.^[25] Otherwise unreactive C–H bonds are utilized as latent functional groups enabled by a variety of diverse reaction manifolds. Although this implies a straightforward approach towards molecular complexity, site-selectivity issues arise, since organic molecules typically display multiple C–H bonds with comparable dissociation energies. Thus, different approaches have been developed for achieving synthetically useful selectivities (Scheme 1.1.4a). Selectivity can be achieved by the inherent properties of the molecule. For instance, based on electronic or steric factors. This approach is limited albeit powerful for specific type of substrates. Another approach, perhaps the most well-established and predictable, relies on Lewis-basic functionalities that chemoselectively bring the catalyst into close proximity to a specific C–H bond to enable the crucial chelation-assisted C–H cleavage.^[16c] During the last two decades, directed C–H functionalization has flourished with many major contributions with regards to the type of substrates, reactions and transition metals used. Chelation-assisted C–H activation has matured into an indispensable tool for molecular synthesis, as it allows a reliable and predictable manifold for the functionalization of inert C–H bonds under exceedingly mild conditions (Scheme 1.1.4b). Great efforts from the synthetic community have established the use of precious 4d and 5d metals, as well as more recently Earth-abundant 3d transition metals for the functionalization of C(*sp*²)–H and C(*sp*³)–H bonds.^[26]

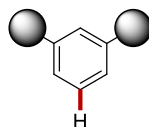
1. Introduction

a) Strategies for selectivity control

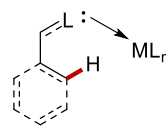
electronic bias



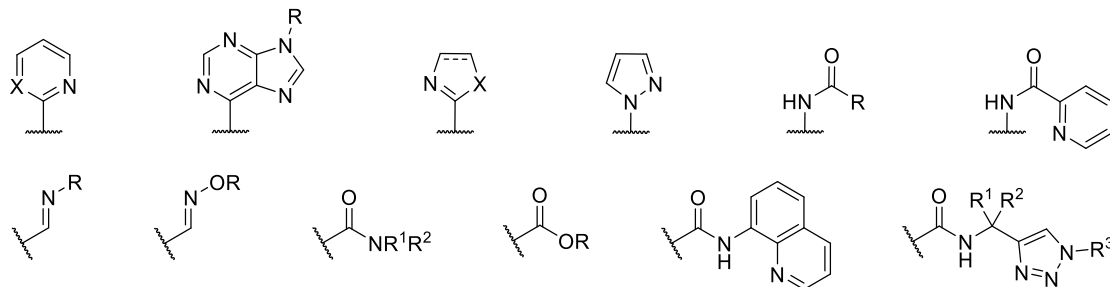
steric control



directed



b) Typical directing groups

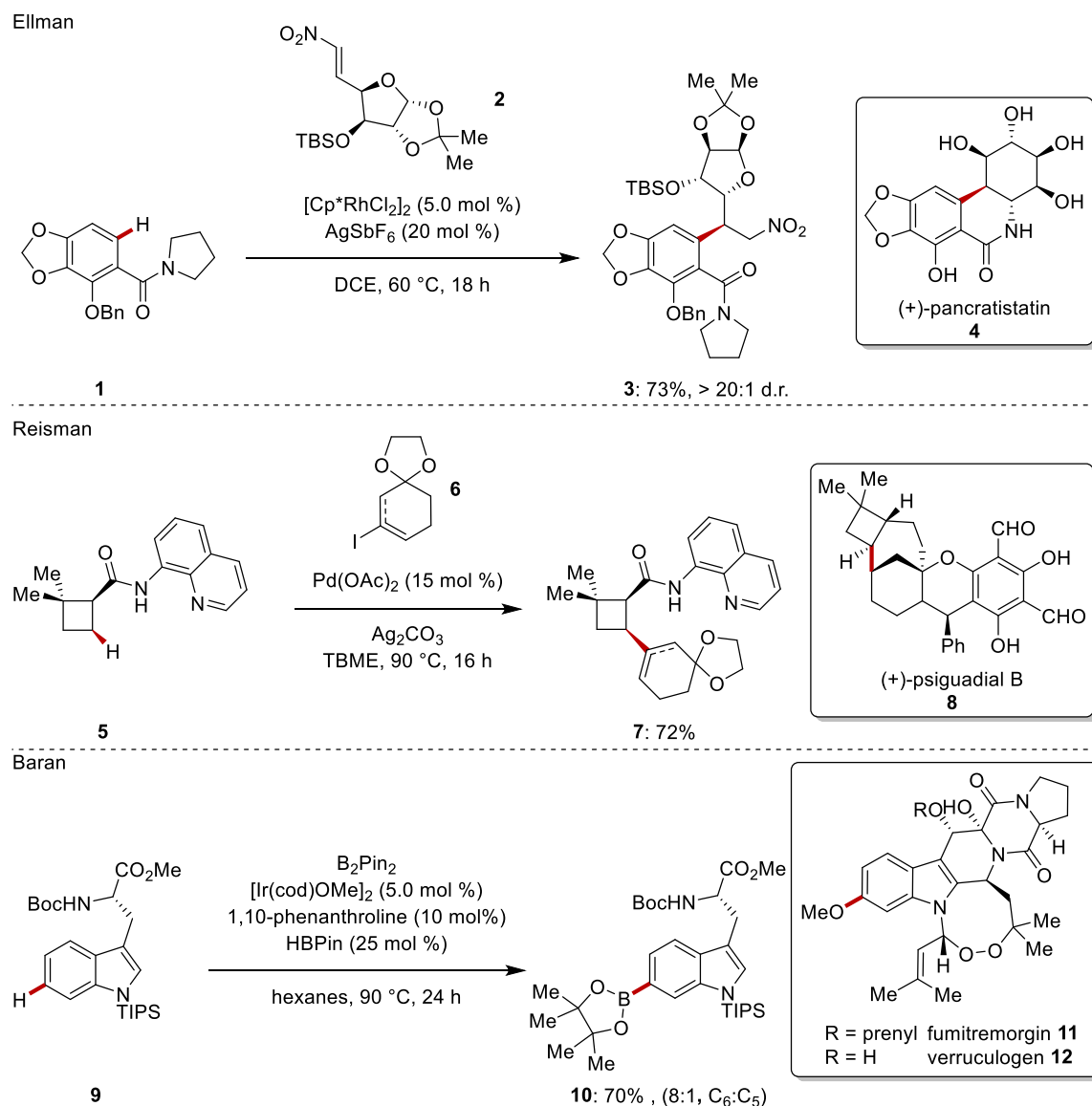


Scheme 1.1.4. Strategies for selectivity control and typical directing groups.

A remarkable testament to the transformative application of C–H functionalization is its use in natural product synthesis, allowing disconnections previously unimaginable. Furthermore, the continuous efforts from the synthetic community to shape C–H functionalization into a mild and robust method is reflected by its applications to complex settings in many total synthesis campaigns. In Scheme 1.1.5, three examples are presented where various modes of action are utilized to construct key structural motifs. Ellman used rhodium(III)-catalyzed C–H hydroarylation of sugar-derived nitroalkene **2** directed by a tertiary amide *en route* to (+)-pancratistatin (**4**).^[27] This Michael-type addition occurred with excellent levels of diastereoselectivity. Furthermore, the nitro group that was essential for achieving a regioselective addition, subsequently was reduced to afford the *trans*-fused 3,4-dihydroisoquinolin-1(2*H*)-one moiety. Among the transition metals, palladium is the most prominent in terms of directed C(*sp*³)–H functionalization assisted by a plethora of different directing groups and under various reaction manifolds. Reisman utilized the well-established 8-aminoquinoline (AQ) as the bidentate directing group to functionalize the cyclobutane ring by forging a key C–C bond in their total synthesis of (+)-psiguadial B (**8**).^[28] The C–H alkenylation with the vinyl-iodide **6** occurred with excellent *cis* stereoselectivity, without racemization. Although the use of exogenous directing groups provides a robust and predictable site-selective C–H activation regime, their utilization is in contrast to atom- and step-economic nature of C–H functionalization as the installation and subsequent removal of the directing group requires additional steps. Thus, the use

1. Introduction

of sterically control iridium(I)-catalyzed C–H borylation of fully protected tryptophan derivative **9** by Baran demonstrates the remarkable efficiency of such approach.^[29] As it is already established, the choice of the *N,N*-ligand is crucial for achieving good turnover numbers and to improve the site-selectivity.^[16k] As it is expected, 4d and 5d transition metals have dominated this area since methods catalyzed by them have been developed much earlier than those with 3d transition metals.^[26]



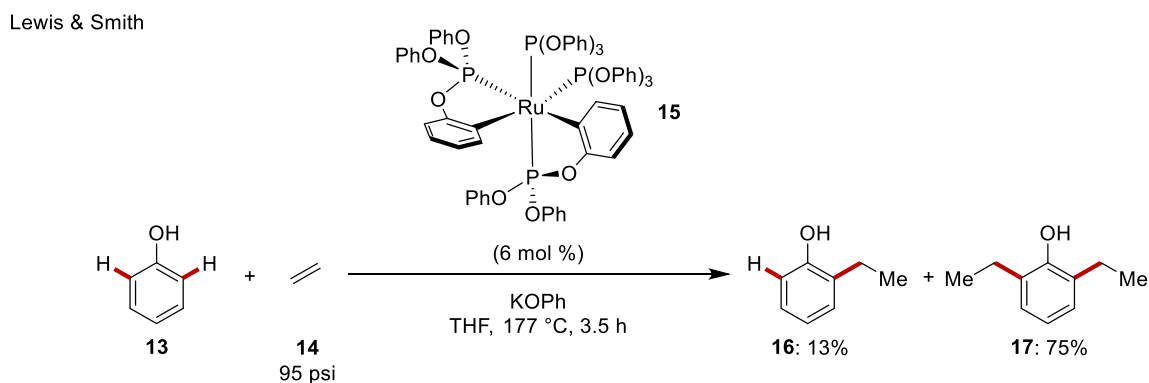
Scheme 1.1.5. Recent applications of C–H functionalization to total syntheses.

1. Introduction

1.2. Ruthenium-Catalyzed C–H Activation

During the last two decades enormous progress has been made in C–H functionalization *via* organometallic C–H bond cleavage, thus providing a new synthetic toolbox for molecular synthesis. In terms of the transition metals used in these methods, 4d and 5d transition metals have been the metals of choice. Despite having established a plethora of reaction manifolds under mild reaction conditions, sustainability and resource-economy issues arise, since most of these metals are expensive and potentially toxic. However, although ruthenium is a 4d transition metal, it is cost-effective and offers a wide range of distinct catalytic applications.^[30]

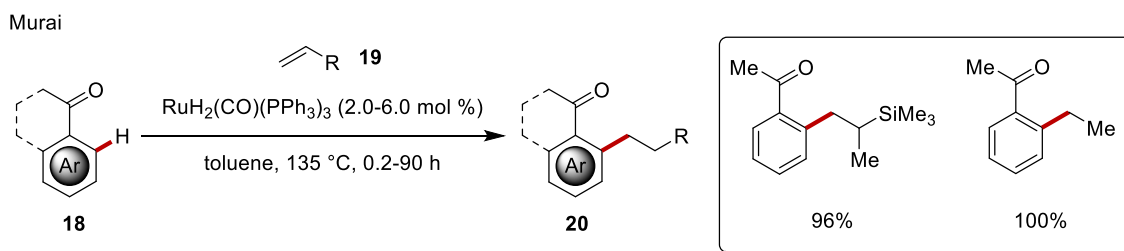
One of the earliest examples of ruthenium-catalyzed C–H activation was reported by Lewis and Smith in 1986,^[31] inspired by earlier stoichiometric studies by Chatt.^[32] In an elegant approach, using the first transient directing group approach,^[33] the ruthenium-catalyzed hydroarylation of ethylene gas with phenol **13** was realized, affording a mixture of mono- and disubstituted products (Scheme 1.2.1). Despite the harsh reaction conditions, this report clearly provided the impetus for further applications of ruthenium-catalyzed C–H activation.



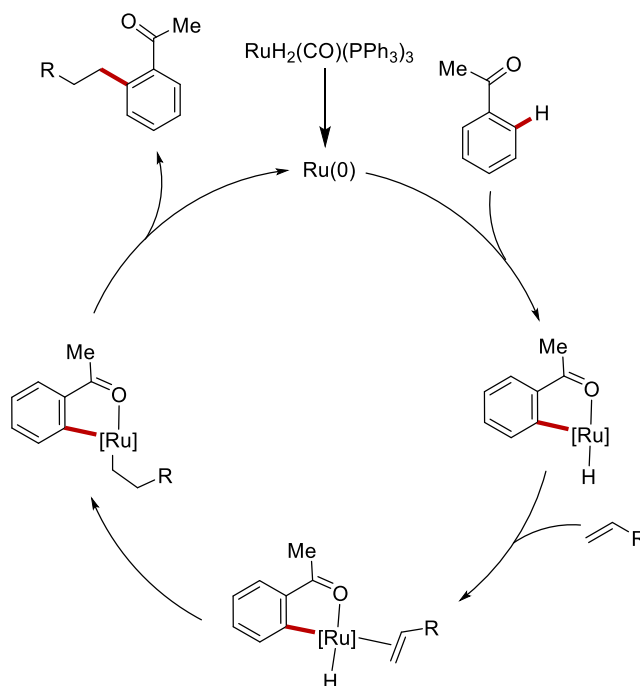
Scheme 1.2.1. First ruthenium catalyzed C–H alkylation *via* phosphite assistance.

Almost a decade later, Murai published his seminal work on ruthenium(0)-catalyzed C–H hydroarylation of unisomerizable olefins **19** *via* ketone assistance (Scheme 1.2.2).^[34] The ruthenium precatalyst $\text{RuH}_2(\text{CO})(\text{PPh}_3)_3$ upon heating generated a ruthenium(0) species that enabled the crucial C–H cleavage *via* an oxidative addition resulting in a ruthenium hydride species that inserted into the olefin, that underwent reductive elimination giving rise to linear anti-Markovnikov addition products. The reaction manifold proved applicable to many aromatic ketones **18** and various olefins

19 resulting in chemo- and site-selective functionalization under relatively mild and synthetically-useful reaction conditions.



Proposed catalytic cycle

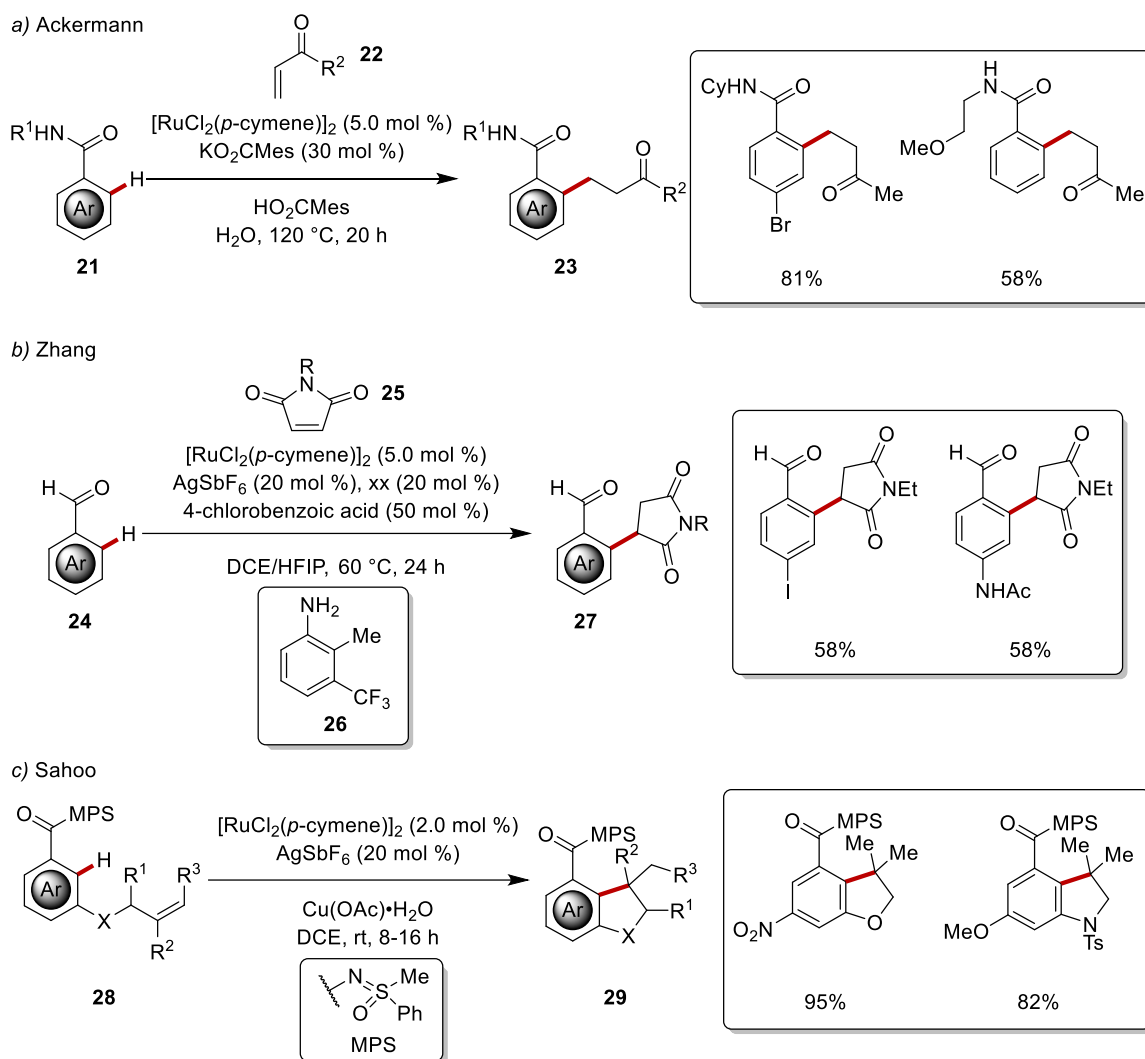


Scheme 1.2.2. Ruthenium-catalyzed C–H hydroarylation *via* ketone assistance.

After this early contributions, many ruthenium-catalyzed C–H activation reactions have been well established, including arylations,^[35] alkylations,^[36] amination/amidations,^[37] oxygenations,^[38] among others. Importantly, the user-friendly, air- and moisture-stable $[\text{RuCl}_2(p\text{-cymene})]_2$ and related complexes have provided a robust and reliable solution even on large scale. Among these reaction manifolds, hydroarylation^[39] is perhaps the most appealing since theoretically nearly perfect atom-economy is observed. In addition, olefins are widely available and inexpensive. Thus, the hydroarylation manifold has been expanded greatly with activated olefins being the most widely used coupling partners. It should be stated that under oxidative conditions, alkenylation regime can be operative by employing chemical oxidants,^[40] molecular oxygen,^[41] or even electrons as a resource-economical oxidant.^[42]

1. Introduction

Ackermann demonstrated that various activated olefins, such as α,β -unsaturated esters, amides and ketones, are suitable substrates under ruthenium(II)-catalysis via weak-amide assistance (Scheme 1.2.3a).^[43] Remarkably, water outperformed common organic solvents, showcasing the robustness of the ruthenium(II)-catalysis. Furthermore, the single component ruthenium carboxylate complex Ru(O₂CMes)₂(*p*-cymene) proved to be similarly efficient catalyst. This method tolerated a wide range of substituents both at the arene scaffold as well as at the olefin coupling partner. Lastly, this strategy enabled the functionalization of anilides and under oxidative conditions allowed expedient access to isoquinolines. Recently, Zhang employed the transient directing group strategy for the hydroarylation of maleimides with aromatic benzaldehydes under ruthenium(II)-catalysis (Scheme 1.2.3b).^[44] In this method, the condensation of the benzaldehyde **24** and the aniline **26**, resulted the formation of the corresponding aldimine, this transient species enabled the site-selective C–H cleavage and subsequent functionalization. The intramolecular hydroarylation of suitably tethered olefins is also feasible under ruthenium(II)-catalysis as Sahoo reported the methyl phenyl sulfoxime (MPS) directed cyclization (Scheme 1.2.3c).^[45] Under mild reaction conditions various substrates **28** were efficiently converted to 2,3-dihydrobenzofuran and indoline derivatives **29**. Furthermore, the directing group could be easily employed for a sequential C–H functionalization at the remaining *ortho*-position.

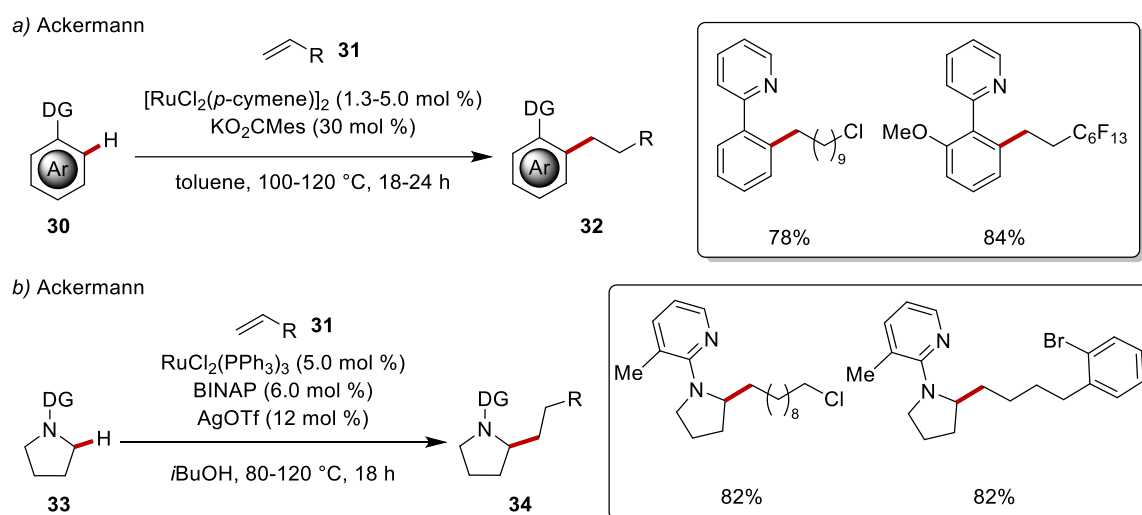


Scheme 1.2.3. Ruthenium(II)-catalyzed C–H hydroarylation with activated olefins.

These contributions, among others, demonstrated the remarkable efficacy of ruthenium(II)-catalysis for the C–H hydroarylation of activated olefins either *via* electronic or *via* topological activation. The general and practical utilization of unbiased olefins under ruthenium(II)-catalysis was elegantly developed by Ackermann in 2013 (Scheme 1.2.4a).^[46] Thus, various (hetero)-arenes **30**, such as pyrazoles, pyridines and indoles among others, were efficiently alkylated with a plethora of olefins **31**, featuring many sensitive functional groups *via* the key assistance by the bulky potassium carboxylate KO_2CMes . Remarkably, also fluorinated olefins proved to be suitable substrates under otherwise similar reaction conditions. Control experiments ruled out the formation of ruthenium(0) species as the key intermediate. Despite that the cleavage of $\text{C}(sp^2)\text{--H}$ bonds under ruthenium-catalysis is well established and has been used for various reaction manifolds, the cleavage of $\text{C}(sp^3)\text{--H}$ bonds, even

1. Introduction

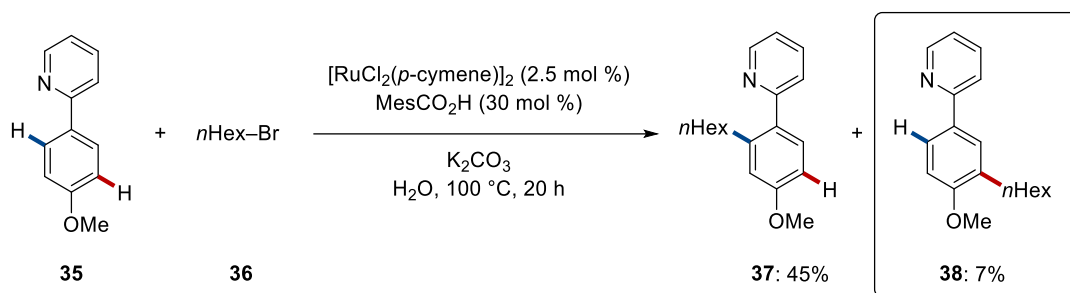
though having lower BDE, is significantly more challenging and only palladium provides a robust and general platform for various $C(sp^3)$ -H functionalizations. Thus, Ackermann devised a protocol for the C-H functionalization of pyrrolidine rings *via* pyridine assistance under ruthenium catalysis (Scheme 1.2.4b).^[47] The key for the selective functionalization was the use of bisphosphine ligand BINAP in combination with $RuCl_2(PPh_3)_2$ that allowed the cleavage of the C-H bond proximal to the nitrogen and subsequent hydroarylation of the olefin **31**. The authors demonstrated that this method was applicable to a wide variety of substrates that featured sensitive functional groups. Remarkably, aryl bromides were chemoselectively used, overriding the tendency towards arylation manifolds.



Scheme 1.2.4. Ruthenium(II)-catalyzed C-H hydroarylation with unactivated olefins **31**.

The proximity-induced C-H functionalization by transition metals is a powerful tool for molecular synthesis, albeit limited in terms of the C-H bonds that can be efficiently functionalized, since cyclometalation is required. Therefore, strategies for remote functionalization of C-H bonds are in high demand since the powerful C-H functionalization manifold would be applied to a plethora of C-H bonds.^[48] The most prominent strategies require either the use of mediators, for example norbornene derivatives in a Catellani-type manifold,^[49] or the installation of elaborate templates^[50] that direct the transition metal to the proximity of *meta* or even *para* C-H bond of the arene. These methods rely on the metalation of the remote C-H bond and subsequent functionalization. A mechanistically different approach was unraveled in a catalytic fashion by Ackermann in 2011, when the *ortho*-alkylation of ketimines was

investigated.^[36b] After careful examination of the reaction with electron-rich phenyl pyridine **35** significant amounts of *meta*-alkylated product **38** were isolated in combination with the expected *ortho*-alkylated product **37** (Scheme 1.2.5). This unexpected result led to extensive mechanistic investigations in order to shed light into this mysterious reaction manifold and provided the stimulus for the development of a robust platform for ruthenium-catalyzed *meta*-C–H functionalizations *via* unique σ -activation. These studies led to the development of mild reaction conditions for the decarboxylative *ortho*-alkylation.^[36c, 51]

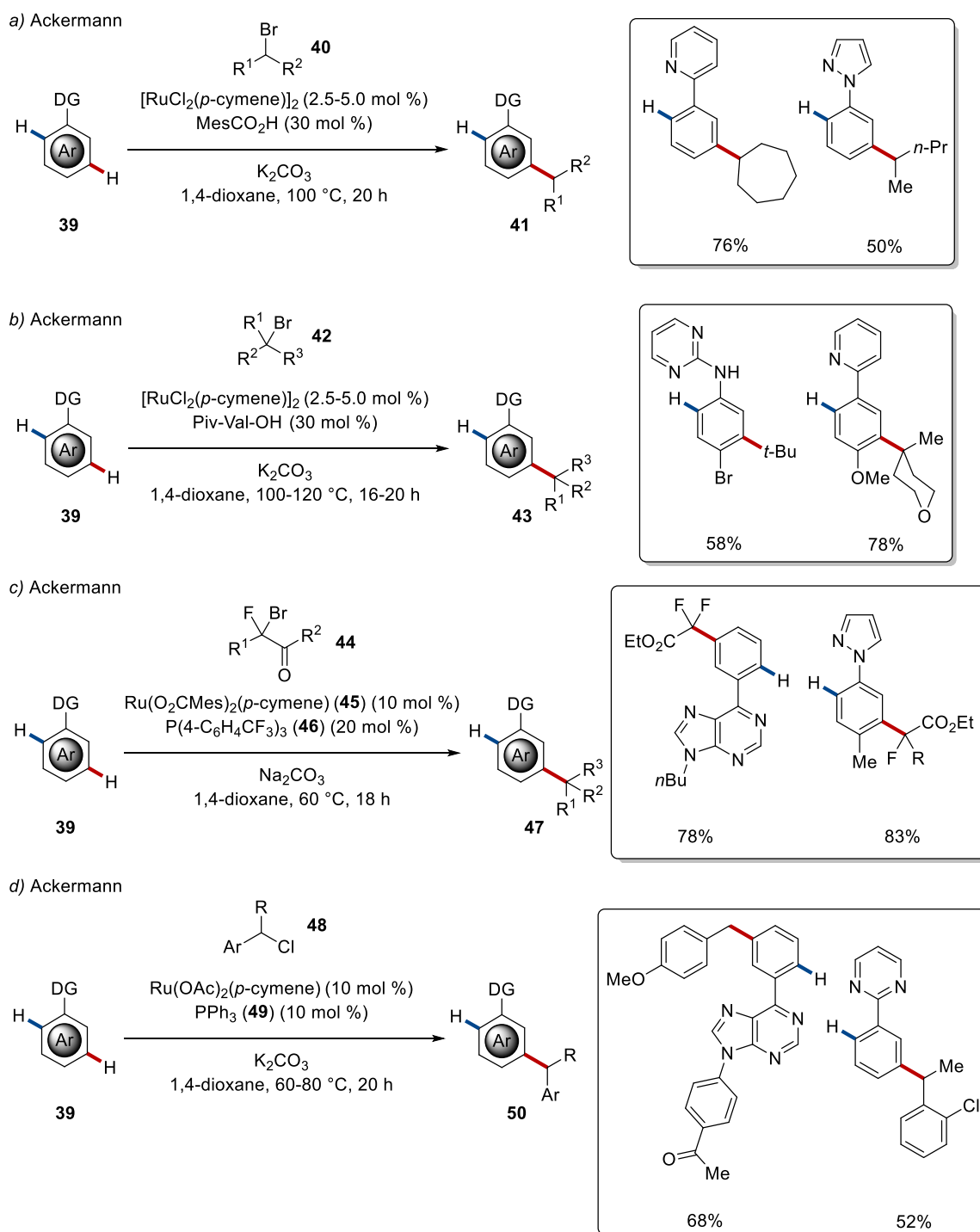


Scheme 1.2.5. First ruthenium(II)-catalyzed *meta* C–H alkylation with primary alkyl-bromide **36**.

After this early report, the Ackermann group demonstrated that this strategy is applicable for the *meta*-C–H alkylations using secondary alkyl bromides **40** *via* carboxylate-assisted *ortho*-ruthenation, leading to the formation of *meta*-alkylated arenes **41** with excellent levels of position-selectivity (Scheme 1.2.6a).^[52] A plethora of heteroarenes served as efficient directing groups, including pyridines, pyrimidines, and azoles. Detailed mechanistic studies suggested a reversible C–H ruthenation and subsequent site-selective alkylation, which was proposed to be guided by the effect of the Ru–C(*sp*²) σ -bond, including *para*-to-the-ruthenium radical addition. Moreover, addition of the typical radical scavenger, TEMPO fully inhibited the reaction, providing strong evidence that radical species are involved in the reaction. In 2015, Ackermann reported on the ruthenium-catalyzed tertiary *meta*-C–H alkylation of arenes and aniline derivatives (Scheme 1.2.6b).^[53] Similarly, carboxylate-assisted cycloruthenation was key to the success, as Piv-Val-OH was employed as the ligand for ruthenium-catalyzed C–H bond cleavage. A plethora of arenes and aniline derivatives were efficiently functionalized with various tertiary alkyl bromides, featuring sensitive functional groups, in chemo- and site-selective fashion. Remarkably, this method allowed the

1. Introduction

regioselective *meta*-alkylation of aniline derivative completely overriding the innate reactivity that usually would lead to *ortho*- and *para*-substituted derivatives via an electrophilic aromatic substitution type manifold. Almost at the same time, Frost reported a related tertiary *meta*-C–H alkylation, albeit this protocol was restricted to the functionalization of 2-aryl-pyridines.^[54] Since organofluorine compounds play a key role in agrochemicals, pharmaceuticals, and material sciences, the site-selective incorporation of fluorine-containing groups into arenes is in high demand.^[55] Thus, by the synergy of phosphine **46** and carboxylate ligand in ruthenium(II) catalysis, Ackermann realized the *meta*-C–H mono- and difluoromethylations using alkyl bromides **44** (Scheme 1.2.6c).^[56] Subsequently, Wang reported on a dual ruthenium and palladium catalysis approach for a related transformation.^[57] Recently, Ackermann reported on the *meta*-selective benzylation of a plethora of arenes **39** with primary and secondary benzyl chlorides **48** (Scheme 1.2.6d).^[58] Similarly, the synergy of triphenylphosphine **49** and acetate ligand in ruthenium(II) catalysis led to the switch in selectivity, as the same group had already demonstrated the *ortho*-benzylation under ruthenium(II) catalysis.^[36d] It is noteworthy that this synergistic ruthenium manifold was fully compatible with a plethora of biomolecules, such as peptides, nucleotides, lipids and sugars. Detailed mechanistic studies shed light on the reaction mechanism, suggesting a radical pathway to be operative. Reports that combine a reagent-controlled generation of benzyl radical with ruthenium(II) catalysis have also been disclosed, but the harsh reaction conditions severely jeopardize their synthetic utility.^[59]

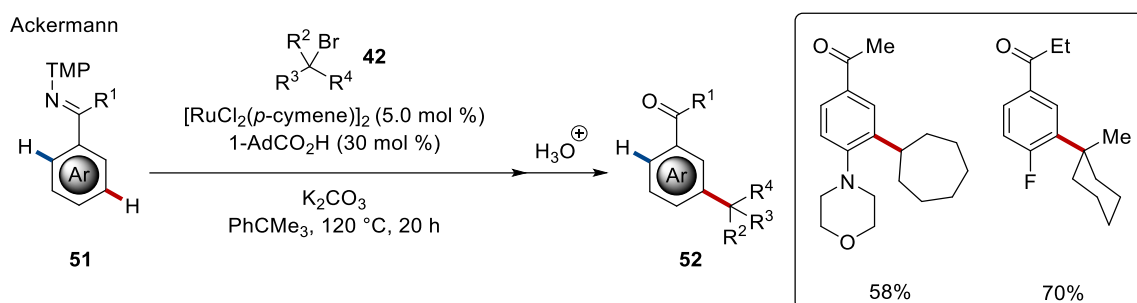


Scheme 1.2.6. Ruthenium(II)-catalyzed *meta* C–H alkylation.

One limitation of the aforementioned strategies is that they required a non-removable strongly coordinating directing group, except from the pyrimidine-aniline functionalization. To bypass this impediment, Ackermann elegantly developed the *meta*-C–H alkylation of ketimines **51** that upon acidic hydrolysis furnished the *meta*-decorated ketones **52** (Scheme 1.2.7).^[60] The method showed excellent levels of functional group tolerance, as a number of acetophenones was obtained featuring

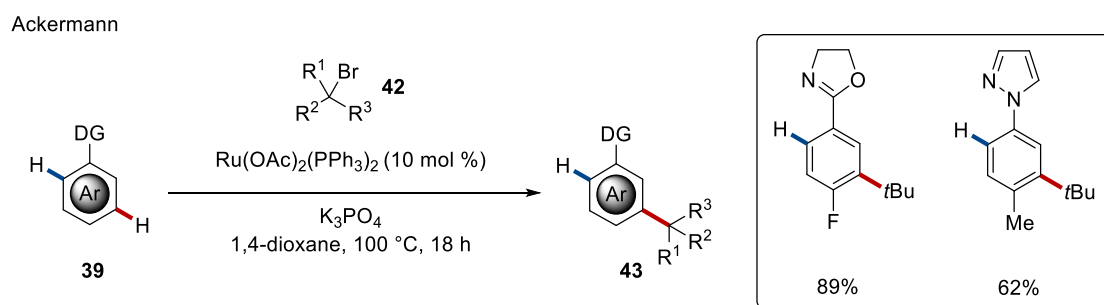
1. Introduction

electrophilic functional groups and saturated heterocycles, among others. In addition, since acetophenones are highly versatile building blocks the functionalized ketones **52** were efficiently transformed into a myriad of structural motifs, such as phenols, anilines, benzoic acids, and indoles.



Scheme 1.2.7. Ruthenium(II)-catalyzed *meta* C–H alkylation via ketimine-assistance.

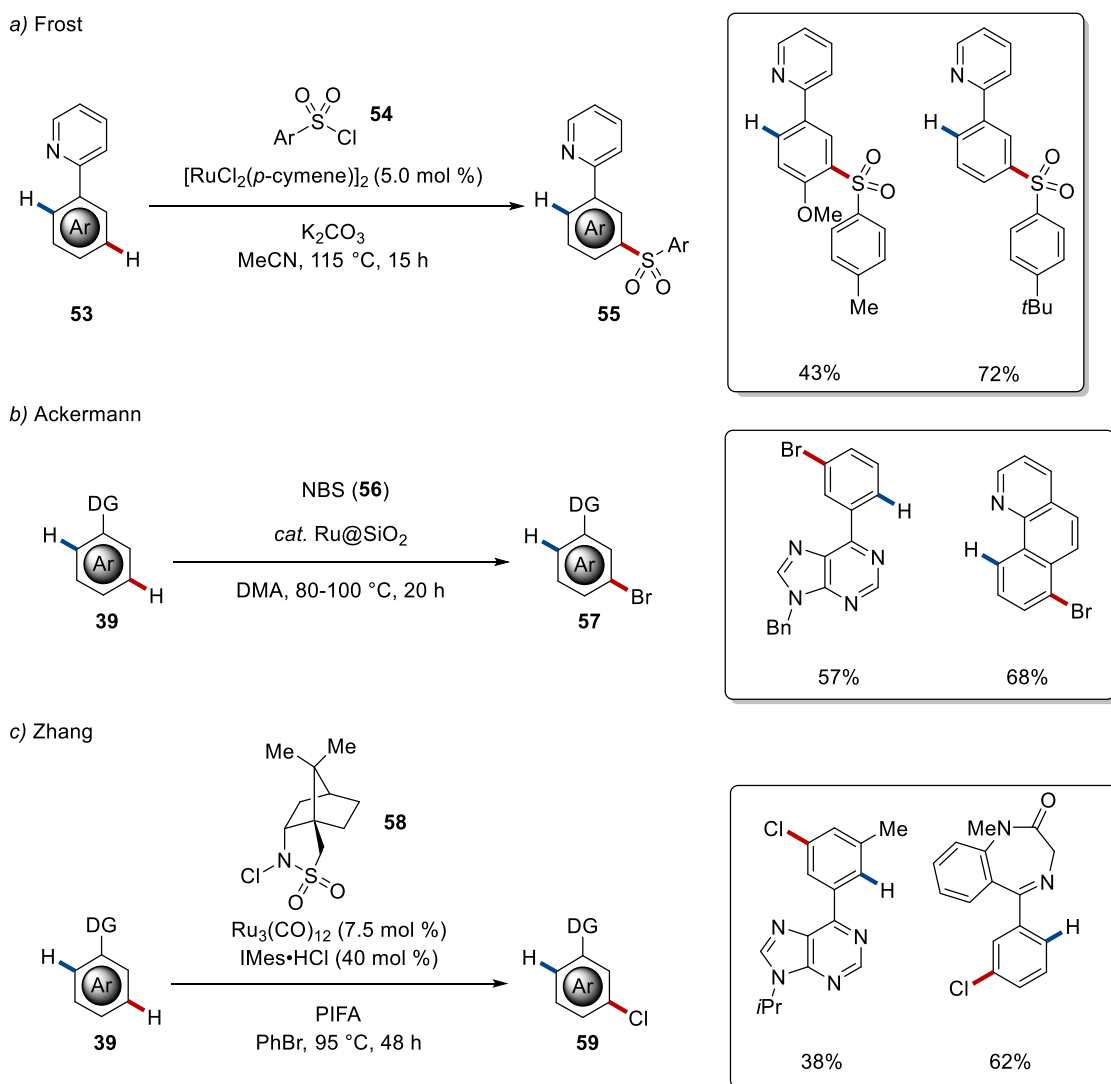
These manifolds for the *meta*-alkylation of arenes typically are catalyzed by air- and moisture-stable $[\text{RuX}_2(p\text{-cymene})]_n$ complexes with or without the synergistic effect of carboxylate or phosphine ligands. A major breakthrough, in terms of both mechanistic and synthetic application, was achieved by Ackermann by using the well-defined arene-ligand-free $\text{Ru}(\text{OAc})_2(\text{PPh}_3)_2$ as the catalyst for the regioselective *meta*-alkylation of various (hetero)arenes (Scheme 1.2.8).^[61]



Scheme 1.2.8. Arene-ligand-free ruthenium(II)-catalyzed *meta* C–H alkylation.

The ruthenium-catalyzed *meta*-functionalization is not restricted to the formation of C–C bonds but has also found application to the construction of C–Het bonds. In this context, Frost reported on a *meta*-selective C–H sulfonylation of 2-aryl-pyridines **53** using $[\text{RuCl}_2(p\text{-cymene})]_2$ and arylsulfonyl chlorides **54** (Scheme 1.2.9a).^[62] Their initial rationale for the *meta*-selectivity was attributed to the formation of a ruthenacycle which directs an electrophilic-type sulfonylation *para*-to-the-ruthenium.^[63] Based on subsequent mechanistic studies a radical-type addition was suggested for the C–S bond forming step, by ruthenium-promoted sulfonyl radical generation. Subsequently,

Ackermann developed the first heterogeneous *meta*-C–H bromination utilizing Ru@SiO₂ and NBS as the brominating agent (Scheme 1.2.9b).^[64] Interestingly this heterogeneous catalytic system outperformed our commonly used ruthenium complexes and led to the site-selective bromination of various (hetero)arenes and purine bases. Furthermore, the sustainable nature of this heterogeneous manifold was reflected by the ease of recycling the catalyst and subsequent reuse of up to seven times without loss of efficacy. Very recently, Ackermann disclosed an unprecedented hybrid ruthenium catalyst for the remote C–H alkylation of a plethora of arenes.^[65] In 2018, Zhang reported on the *meta*-C–H chlorination of various arenes, including purines and benzodiazepines, under a combination of ruthenium(0) catalyst with a *N*-heterocyclic carbene ligand, PIFA as terminal oxidant and *N*-chloro-2,10-camphorsultam as chlorinating agent, albeit with limited efficiency (Scheme 1.2.9c).^[66]

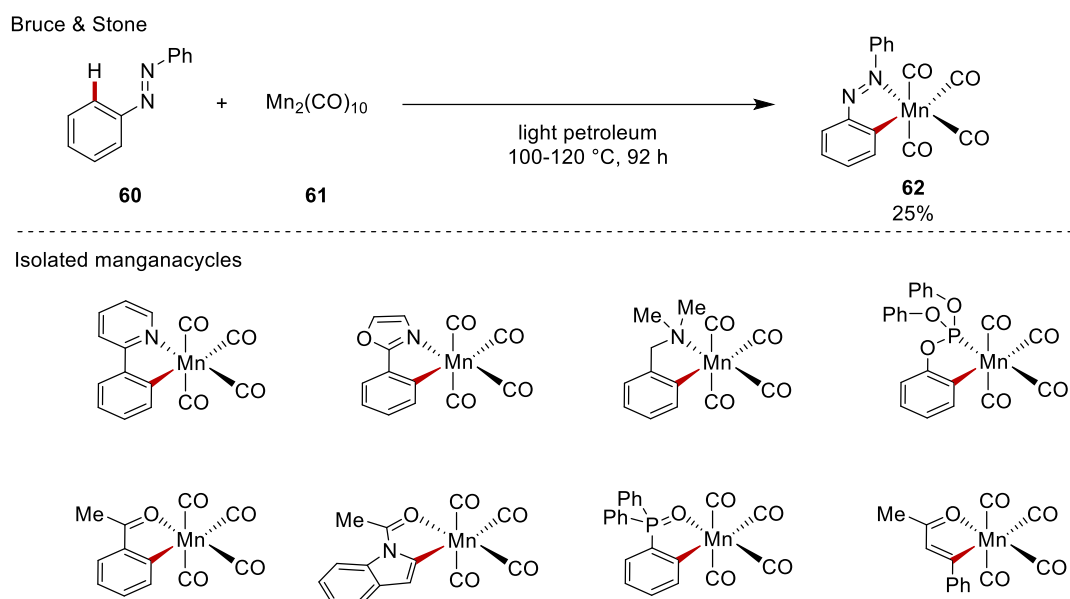


Scheme 1.2.9. Ruthenium-catalyzed *meta* C–het bond forming manifolds.

1. Introduction

1.3. Manganese-Catalyzed C–H Activation

Despite major advances in C–H activation, the continuous demand for sustainable and eco-friendly approaches, forced the synthetic community away from the use of 4d and 5d transition metals. Thus, Earth-abundant 3d transition metals offer an excellent alternative,^[26] and more specifically, manganese as the third most abundant transition metal is particularly cost-effective.^[67] Stoichiometric studies on manganese C–H activation has already reported in 1970 by Stone and Bruce, for the cyclometalation of azobenzene (**60**) with $\text{Mn}_2(\text{CO})_{10}$ as the manganese source (Scheme 1.3.1).^[68] Thereafter, several examples of reactions involving manganacycles have been reported by Nicholson/Main,^[69] Woodgate,^[70] and Liebeskind,^[71] among others, showcasing the potential of these intermediates and motivating the synthetic community to develop catalytic manifolds.



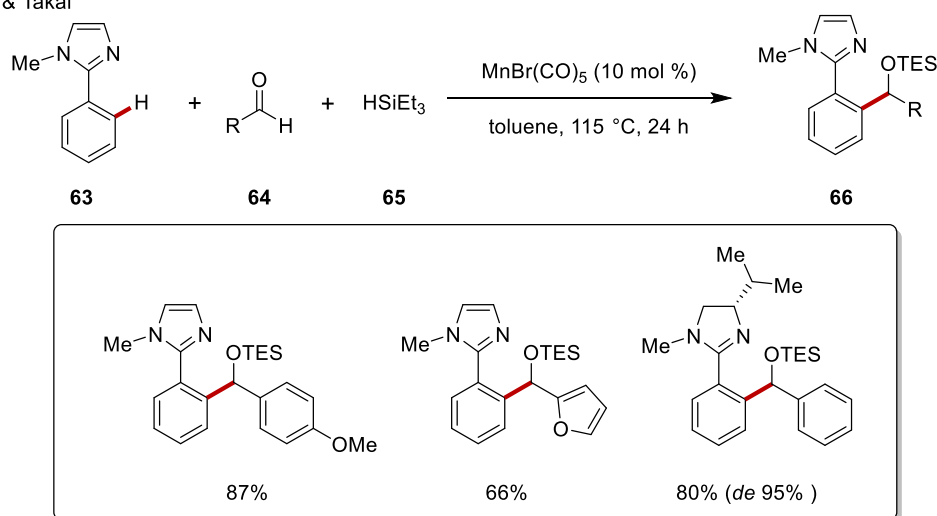
Scheme 1.3.1. Pioneering example of stoichiometric C–H activation by manganese and selected isolated manganacycles.

1.3.1. Manganese-Catalyzed C–H Activation: Early Report

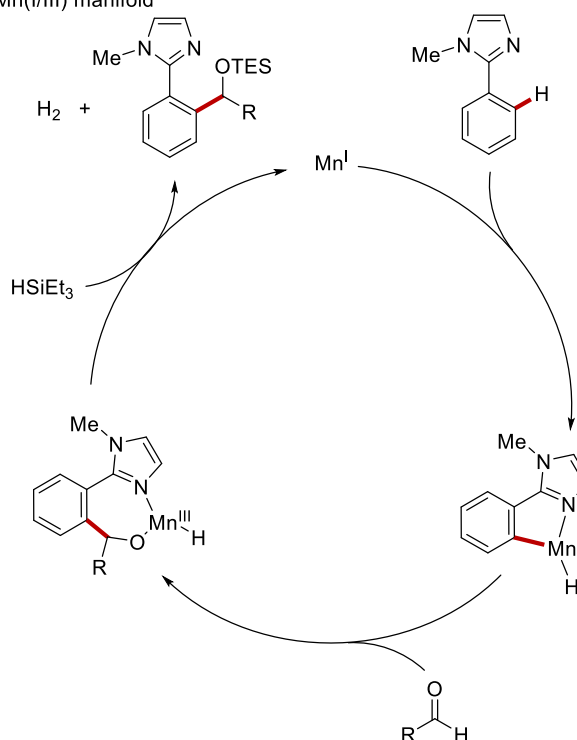
In 2007, Kuninobu and Takai demonstrated that $\text{MnBr}(\text{CO})_5$ could facilitate the addition of aromatic C–H bonds onto electrophilic aldehydes, in the presence of silanes (Scheme 1.3.2).^[72] The reaction had broad scope in terms of the directing groups and the aldehydes used. Imidazoles and oxazolines were shown to be effective directing groups. Remarkably when chiral oxazolines were used highly diastereoselective

addition to the aldehydes occurred. In addition, presumably due to the capping of the resulting alcohol as the silyl-ether, electron-poor and electron-rich aldehydes were used, despite the tendency of the later for reversible additions.^[73] In terms of the mechanism of this pioneering transformation, some mechanistic evidence led to the hypothesis that the C–H bond cleavage occurred *via* oxidative addition leading to a Mn(III)-hydride species, and then the C–Mn bond underwent selective insertion into the aldehyde followed by silyl protection *via* formation of H₂.

Kuninobu & Takai



Proposed Catalytic Cycle: Mn(I/III) manifold

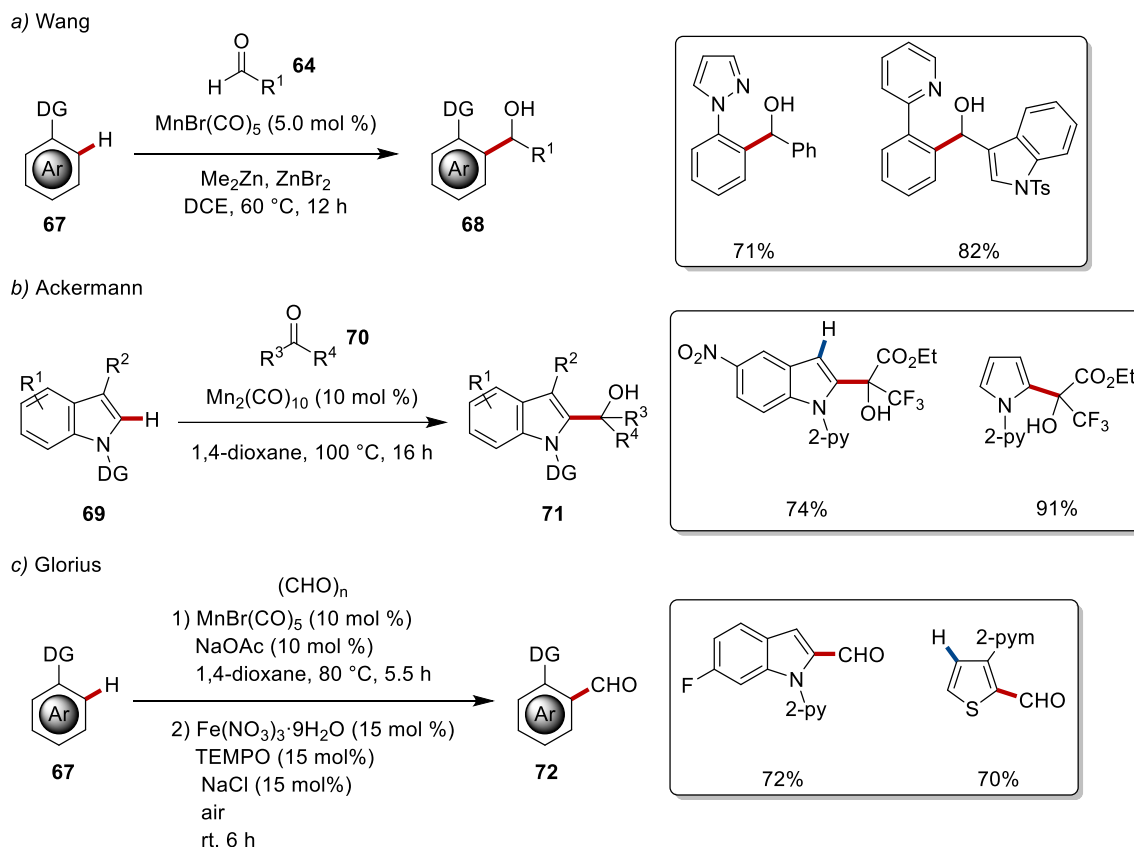


Scheme 1.3.2. Manganese(I,III)-catalyzed addition of aromatic C(*sp*²)-H onto aldehydes **64**.

1. Introduction

1.3.2. Manganese-Catalyzed C–H Hydroarylation

After the early contribution of Kuninobu and Takai and together with the clear movement towards sustainable synthesis by utilizing Earth-abundant metals as catalysts, Wang reported on the addition of aromatic and alkenyl C(*sp*²)–H bonds to aldehydes and nitriles, providing a straightforward route to secondary alcohols and ketones respectively (Scheme 1.3.3a).^[74] In contrast to the previous report by Kuninobu and Takai, extensive optimization revealed that a combination of Me₂Zn and ZnBr₂ was essential for an efficient reaction. The organozinc reagent presumably activates the manganese precatalyst by forming *in situ* the more reactive MnMe(CO)₅, which was shown to be catalytically active, thus realizing silane-free conditions. The Lewis acid coordinates to the electrophile making it prone to nucleophilic addition. Concurrently, Ackermann demonstrated that ketones, despite being inherently less reactive, can be effective coupling partners under manganese catalysis.^[75] After extensive screening of various metal salts, MnBr(CO)₅ and Mn₂(CO)₁₀ were the only catalysts that enabled the selective C2 addition of activated ketones to the indole derivatives, under user-friendly reaction conditions (Scheme 1.3.3b). This method clearly overrides the innate reactivity of indole for C3 electrophilic substitution manifold. Recently, Glorius realized the formylation of arenes by one-pot manganese(I) and iron(III) relay catalysis (Scheme 1.3.3c).^[76] The mild nature and robustness of manganese catalysis was reflected by the preparative ease of the methodology since the hydroxymethylated product was directly used for the iron catalyzed oxidation without any purification yielding the desired products in good yields.



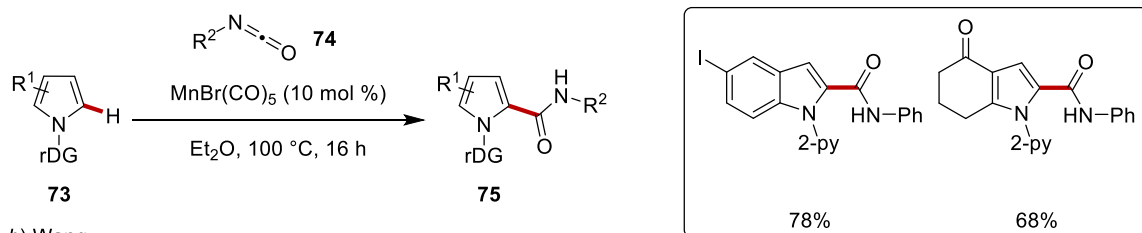
Scheme 1.3.3. Manganese-catalyzed C–H addition to carbonyl compounds.

Since nitrogen containing compounds play an important role in pharmaceutical and medicinal industries isocyanates and imines were also explored as coupling partners under manganese(I) catalysis. Thus, Ackermann developed the aminocarbonylation of indoles and pyrroles under additive free reaction conditions, taking advantage of reactive and versatile isocyanates (Scheme 1.3.4a).^[77] The robustness of this method was clearly reflected by the site-selective functionalization of various indoles and pyrroles featuring sensitive electrophilic functional groups, such as bromides, iodides and ketones. Detailed mechanistic studies supported a facile and reversible C–H activation step. Imines, were envisioned as a suitable substrate for the addition on the highly nucleophilic C–Mn bonds. Thus, Wang reported on the chemoselective addition of C(*sp*²)-H of ketones **76** to electron-deficient imines taking advantage of their previous established system featuring Me₂Zn and ZnBr₂ (Scheme 1.3.4b).^[78] Fine-tuning of the reaction temperature enabled the divergent access to either the benzylic amines **78** or the *exo*-olefinic-containing isoindolines *via* subsequent condensation under slightly more forcing reactions conditions. Expanding on their previous report, Ackermann demonstrated that imines **79** can be suitable coupling partners for

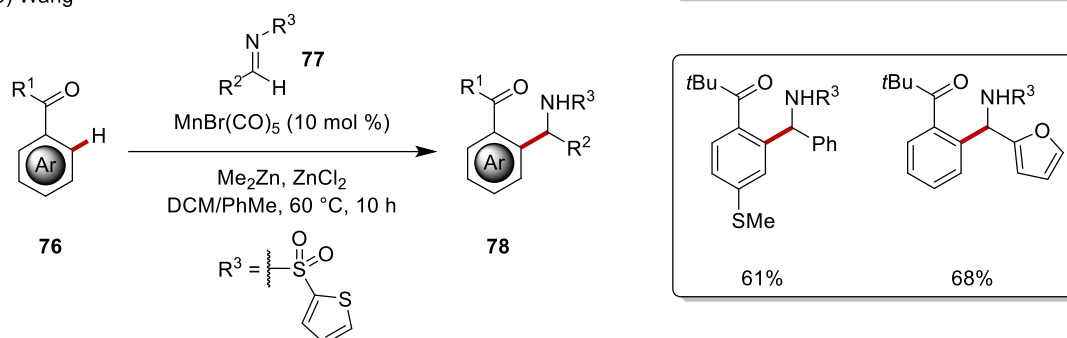
1. Introduction

manganese-catalyzed C–H activation, under organozinc reagent-free reaction conditions.^[75] Thus, the use of *n*Bu₂O as solvent under additive-free reaction conditions enabled excellent functional group tolerance for the C2 functionalization of indoles, completely bypassing any Friedel-Crafts regime. Moreover, they showcased that the directing group can be efficiently removed in good yield producing synthetically useful indole derivatives (Scheme 1.3.4c).

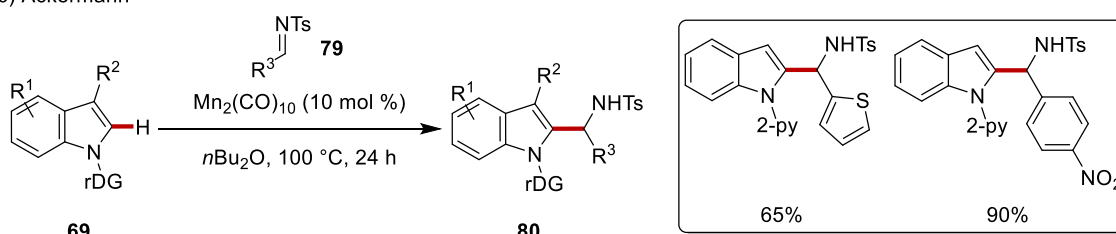
a) Ackermann



b) Wang



c) Ackermann

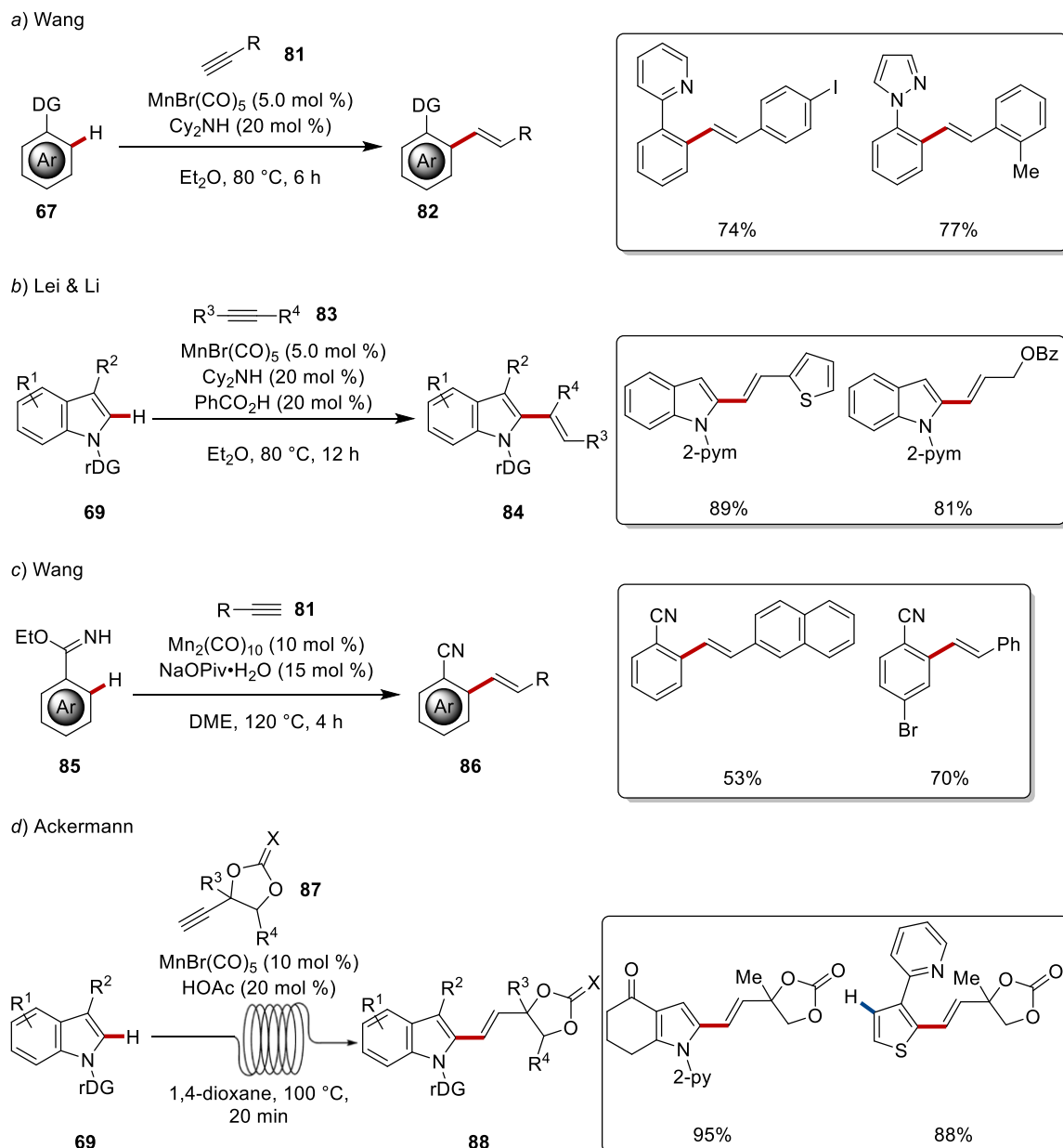


Scheme 1.3.4. Manganese-catalyzed C–H addition to isocyanates **74** and imines **77** or **79**.

The reactivity of manganese(I) complexes in C–H activation is not restricted to addition reactions to electrophilic C–Het multiple bonds, but hydroarylation regime of alkynes and alkenes is also feasible. Thus, Wang and coworkers reported on the manganese-catalyzed C–H alkenylation by means of hydroarylation of terminal alkynes (Scheme 1.3.5a).^[79] Remarkably the catalytic system consisting of MnBr(CO)₅ and Cy₂NH performed well, without signs of side-reactions of the terminal alkynes, providing an efficient route for the construction of highly functionalized alkenes. Computational studies suggested a base-promoted C–H activation step and a C(*sp*)–H mediated

protodemetalation pathway. Subsequently, Lei and Li realizing the limitation of Wang's report, devised a catalytic manifold containing catalytic amounts of $\text{MnBr}(\text{CO})_5$, DIPEA and PhCO_2H that was able to utilize internal alkynes as well (Scheme 1.3.5b).^[80] Later, Wang demonstrated that aromatic *N-H* imidates can be engaged in the hydroarylation regime to access synthetically useful nitriles, showcasing that imidates can direct *ortho*-manganation and act as masked nitriles (Scheme 1.3.5c).^[81] Notably, internal alkynes **83** reacted in a highly regioselective fashion, providing trisubstituted alkenes albeit in low yields. Regioselective hydroarylation of alkynes **87** bearing heteroatoms at the α -position remains a synthetic challenge due to facile β -heteroatom elimination and the high synthetic value of the obtained allylic systems bearing heteroatoms. Thus, Ackermann realized a highly selective hydroarylation regime of indole derivatives with propargylic carbonates under manganese(I) catalysis, featuring a crucial Brønsted acid-catalyzed protodemetalation, to ensure that the normally facile β -heteroatom elimination is completely suppressed (Scheme 1.3.5d).^[82] Notable features of the protocol included short reaction times that were achieved by performing the reaction in flow and wide diversification of the obtained allylic carbonates. Later, Glorius demonstrated that propargylic carbonates under manganese(I) catalysis provided the corresponding allenes through a migratory insertion/ β -oxygen elimination manifold.^[83] In contrast to Ackermann's system for the hydroarylation of propargylic carbonates, NaOAc was necessary in order to achieve good catalytic turnover.

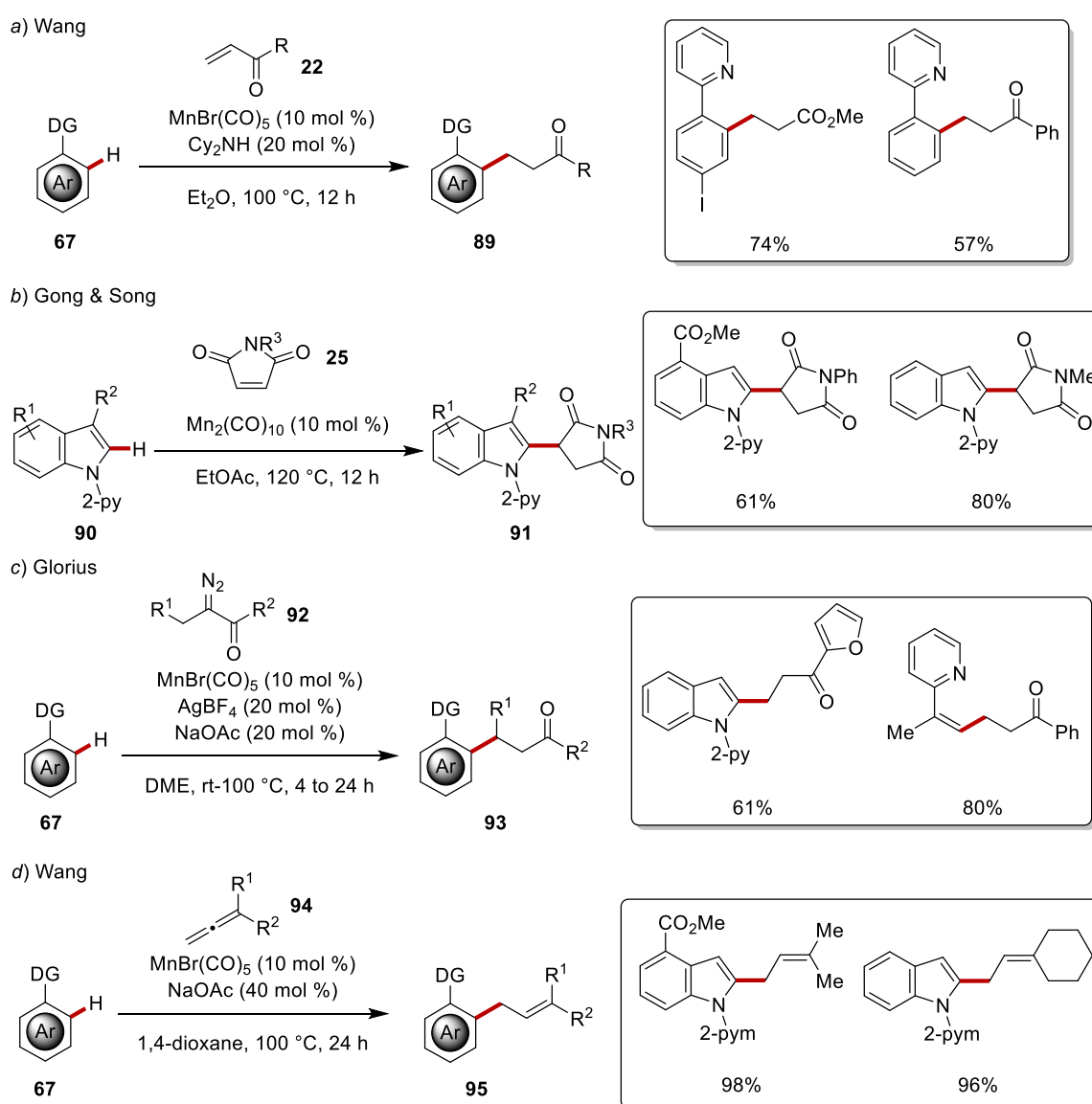
1. Introduction



Scheme 1.3.5. Manganese(I)-catalyzed C–H hydroarylation of alkenes.

Alkenes bearing electron-withdrawing groups have been widely used in C–H activation reactions under precious metal catalysis, and since they are modular motifs and readily available their implementation in the manganese-catalyzed C–H activation is highly desirable. Inspired by their earlier report on the hydroarylation of alkynes by manganese catalysis Wang utilized α,β -unsaturated carbonyls to gain access to formally alkylated arenes (Scheme 1.3.6a).^[84] Their catalytic system of choice consisting of MnBr(CO)_5 and Cy_2NH proved efficient for promoting this conjugate addition with high levels of mono-selectivity. In addition, Gong and Song extended the methodology to maleimides **25**, devising a direct route towards

decorated five-membered nitrogen heterocycles (Scheme 1.3.6b).^[85] Taking advantage of the outstanding robustness of manganese(I) catalysis, Glorius developed a protocol for the *in situ* generation of α,β -unsaturated ketones **22** from the corresponding α -diazo ketones catalyzed by a silver salt, that were swiftly employed in a hydroarylation regime (Scheme 1.3.6c).^[86] Allenes **94** offer diverse reactivity manifolds due to their structure, mainly based on the nature of their substitution pattern. Wang employed 1,1-dialkyl allenenes for the allylations of arenes obtained from the migratory insertion on the resulting manganacycle to the less substituted double bond (Scheme 1.3.6d).^[87] Notably, when 1,1-dimethylallene **94a** was employed prenylated arenes **95** were obtained, highlighting the synthetic utility of their method, as prenyl groups are found in a plethora of natural products.



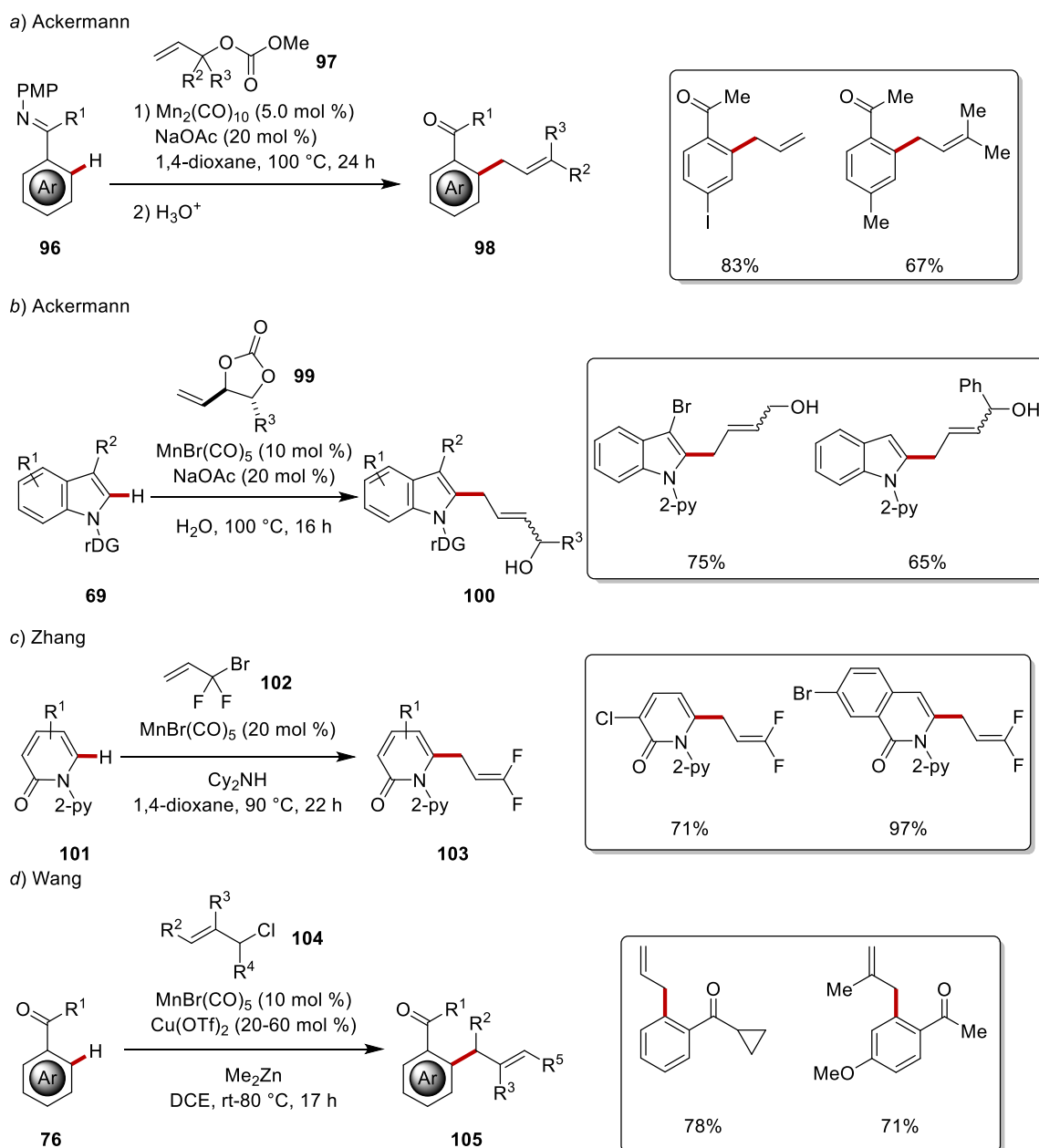
Scheme 1.3.6. Manganese(I)-catalysed C–H hydroarylation of alkenes and allenenes.

1. Introduction

1.3.3. Manganese-Catalyzed Substitutive C–H Activation

1.3.3.1. Manganese-Catalyzed C–H Allylation

The allyl group is frequently used in organic synthesis, since it is easily converted to a myriad of other functional groups by well-established methods. Thus, the development of novel and sustainable allylation reactions is of utmost importance. To this end, Ackermann developed the first manganese-catalyzed reaction employing synthetically useful ketimines and substituted allyl-methyl-carbonates (Scheme 1.3.7a).^[88] The catalytic system consisting of $\text{MnBr}(\text{CO})_5$ and NaOAc proved extremely tolerant towards a variety of electrophilic functional groups, as well as nucleophilic/coordinating functional groups. Along the same lines, Ackermann and coworkers utilized the highly versatile allyl substituted cyclic carbonate to gain access to allylic alcohols, remarkably, water outperformed common organic solvents once again highlighting the sustainable nature of manganese(I)-catalysis (Scheme 1.3.7b).^[89] Thereafter, Zhang demonstrated that 3-bromo-3,3-difluoropropene was reactive under manganese catalysis for the 3,3-difluoroallylation of pyridones among other arenes (Scheme 1.3.7c).^[90] Recently, Wang employed their established catalytic system consisting of $\text{MnBr}(\text{CO})_5$ and a combination of Me_2Zn and $\text{Cu}(\text{OTf})_2$ for the efficient *ortho*-allylation of aromatic ketones (Scheme 1.3.7d).^[91] Detailed mechanistic studies demonstrated the importance of both additives for the crucial cyclometalation step. In 2018, Glorius reported on the manganese catalyzed propargylation of arenes by means of regioselective allene insertion followed by β -bromine elimination, notably, K_3PO_4 , and H_2O were crucial for good regioselectivity.^[92]



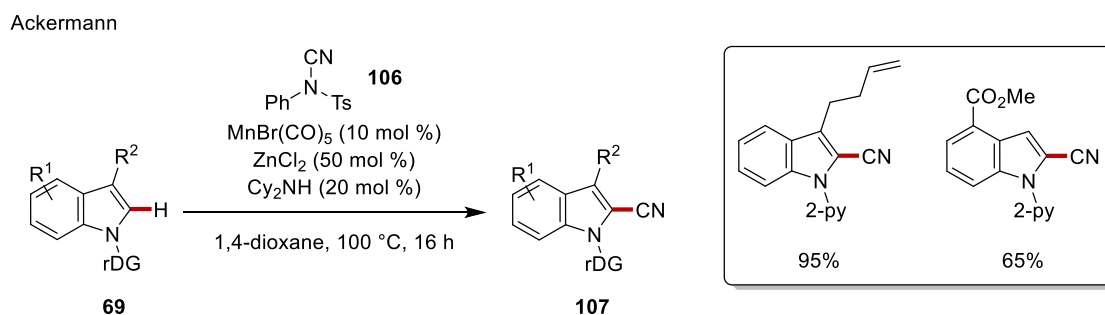
Scheme 1.3.7. Manganese(I)-catalyzed substitutive C–H allylations.

1.3.3.2. Manganese-Catalyzed C–H Cyanation

In 2016, Ackermann reported on the first manganese-catalyzed C–H cyanation of arenes with NCTS, among others, as user-friendly cyanating reagent (Scheme 1.3.8).^[93] After extensive optimization, the authors demonstrated that a combination of $\text{MnBr}(\text{CO})_5$, with co-catalytic amounts of Cy_2NH and ZnCl_2 were optimal for the efficient cyanation of indole moieties. Mechanistic and computational studies shed light on the mechanism of the reaction highlighting a heterobimetallic regime. The coordination of ZnCl_2 to the cyano-toluenesulfonamide facilitates the cyano group

1. Introduction

transfer *via* an addition/elimination reaction manifold.

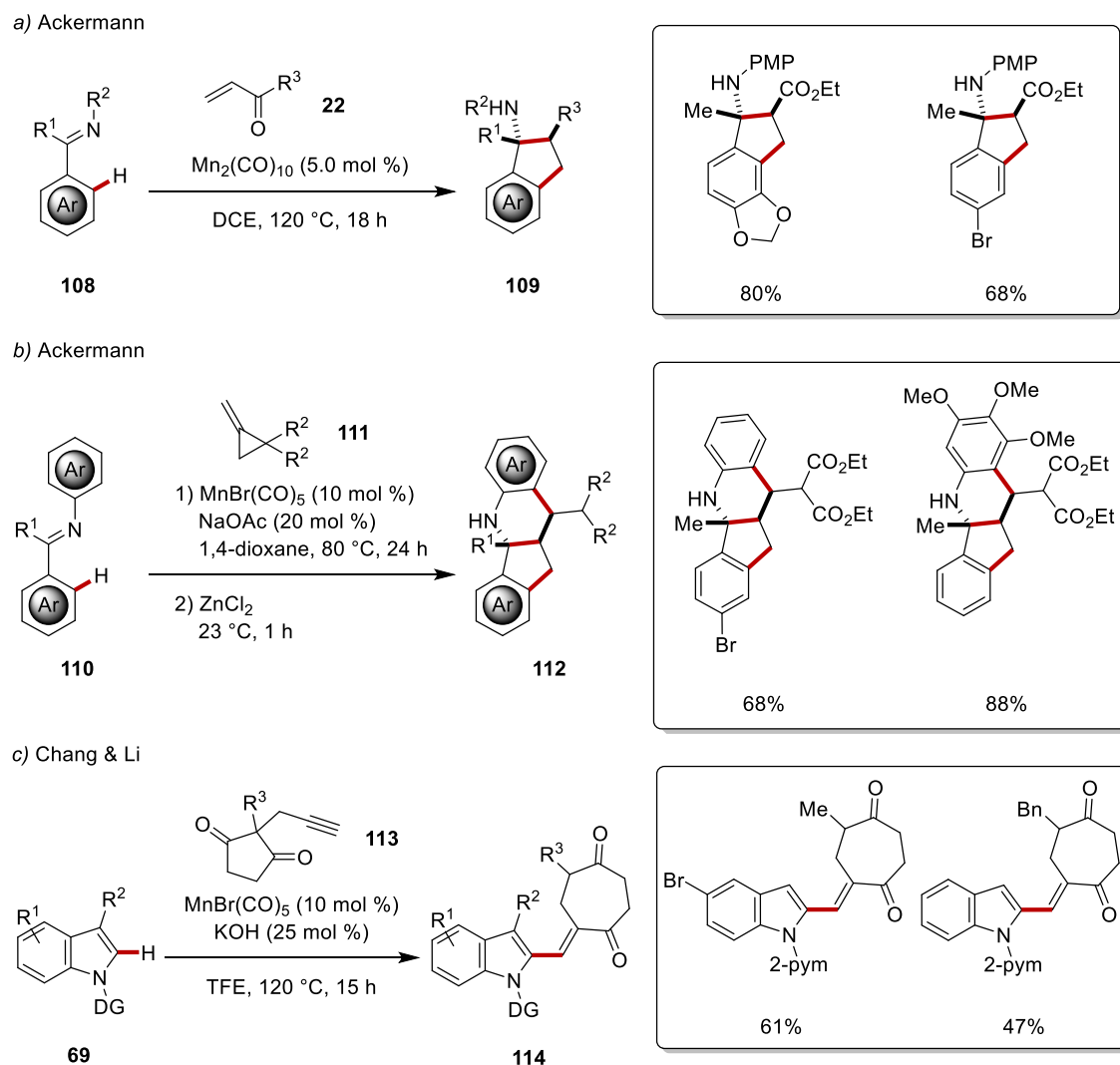


Scheme 1.3.8. Manganese(I)-catalyzed C–H cyanation.

1.3.4. Domino Processes Initiated by Manganese-Catalyzed C–H Activation

Domino reactions are increasingly useful for the construction of complex molecular architectures in a sustainable and step-economic fashion. Despite their undeniable merits, the design of efficient domino reactions is not straightforward due to the possible side-reactions that can jeopardize their efficacy. Thus, their use commonly requires careful design and precise optimization of the reaction conditions to ensure productive transformations.^[94] Robust and mild catalytic processes are ideal for this highly important endeavor, thus manganese-catalyzed C–H activation has been used as a viable platform for the construction of multiple bonds in a single reaction vessel. Thus, Ackermann realized the synthesis of *cis*- β -amino acid esters **109**, by intercepting the intermediate formed after the insertion of a manganacycle to an acrylate (Scheme 1.3.9a).^[95] The proposed intermediate possess a highly nucleophilic character, that enabled the diastereoselective intramolecular addition to the tethered imine. Subsequently, Ding, Peng and co-workers, reported a related method using allenes to form similar scaffolds possessing an exocyclic olefin.^[96] In 2017, Ackermann used methylenecyclopropanes **111** that upon C–C cleavage by the cyclometallated complex furnished a manganese dienolate that was able to insert into the imine forging a five membered ring. Concurrently, zinc-mediated Michael addition of the electron-rich aniline to the newly formed α,β -unsaturated ester led to the formation of the fused tetrahydroquinoline scaffolds (Scheme 1.3.9b).^[97] In the same year, Wang devised a different approach for the synthesis of fused tetrahydroquinolines, using aromatic ketimines and 1,1-disubstituted allenes. Upon formation of the corresponding allylated ketimines, AgOTf catalyzed Povarov reaction led to the fused tetrahydroquinolines.^[98] Notably, a different diastereoisomer

was formed, highlighting a complementary working mode. Recently, Chang and Li reported a manganese-catalyzed cascade for the synthesis of medium sized rings (Scheme 1.3.9c).^[99] Their approach relied on the insertion of an alkyne into manganese cycle, addition of the Mn–C bond to a tethered ketone, forming a bicycle[3.2.0]heptane system that under the basic reaction conditions ring expanded *via* a retro-aldol reaction.

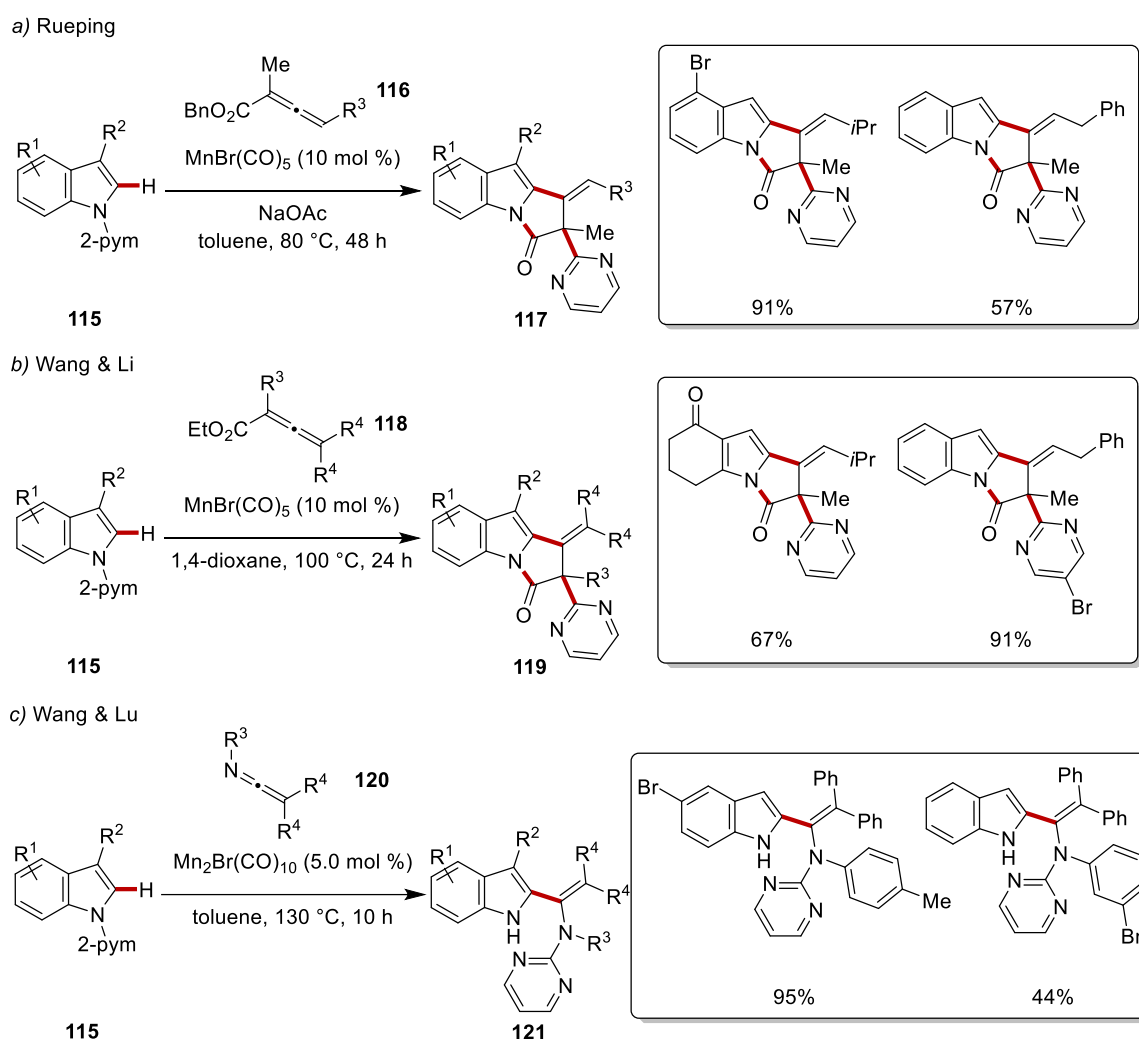


Scheme 1.3.9. Manganese(I)-catalyzed domino reactions *via* insertion of newly formed C–Mn bonds to imines and ketones.

In 2017, the groups of Rueping^[100] and Wang/Li^[101] independently reported on the manganese-catalyzed hydroarylation of electron-deficient allenes **116** or **118** followed by a Smiles rearrangement, resulting in the migration of the heteroaryl directing group (Scheme 1.3.10a and 1.3.10b). Interestingly, Rueping demonstrated that the judicious choice of the reaction temperature resulted in different products, as

1. Introduction

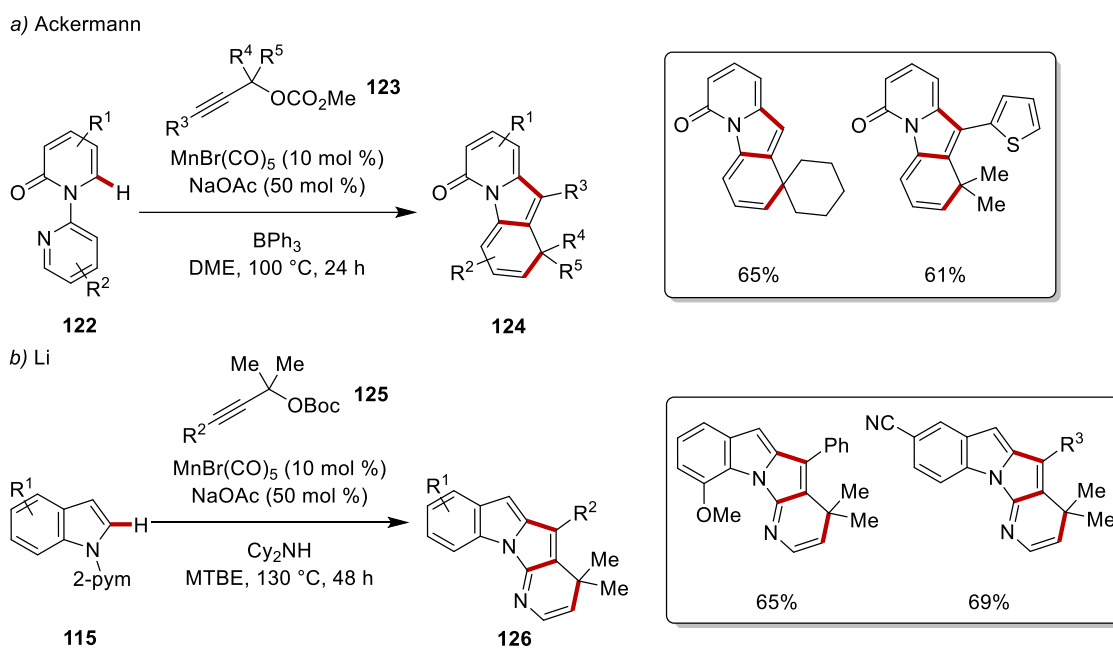
at lower temperature, the hydroarylation product is observed *via* a protodemetalation pathway, whereas at higher temperature the intermediate of the allene insertion is able to engage in a Smiles rearrangement. Later, Lu and Wang achieved a related transformation using ketenimines **120**, thus after insertion to C=N bond, migration of the pyrimidine directing group was also observed (Scheme 1.3.10c).^[102] Very recently, Ruan utilized ketenimines under rhenium and manganese catalysis with 6-indole-purines as substrates, interestingly, the reaction proceeded without migration of the directing group.^[103]



Scheme 1.3.10. Domino manganese(I)-catalyzed C–H activation/Smiles rearrangement.

In 2019, Ackermann envisioned a sequence that after C–H allenylation the tethered allene would engage in a series of Diels-Alder reactions with the pyridine directing group, furnishing a highly decorated polycyclic system. After careful optimization, the

combination of $\text{MnBr}(\text{CO})_5$, NaOAc and BPh_3 was capable of promoting this domino sequence (Scheme 1.3.11a).^[104] Computational studies revealed the crucial role of the Lewis-acid, as a promoter for the inverse-electron demand Diels-Alder, followed by extrusion of HCN to furnish the desired product **124**. At the same time, Li developed a related transformation, using Cy_2NH instead of the BPh_3 and prolonged reaction times, thus they were able to access fused indole scaffolds when pyrimidine was used as the directing group on the indole moiety (Scheme 1.3.11b).^[105]



Scheme 1.3.11. Manganese(I)-catalyzed C–H activation/Diels Alder domino reaction.

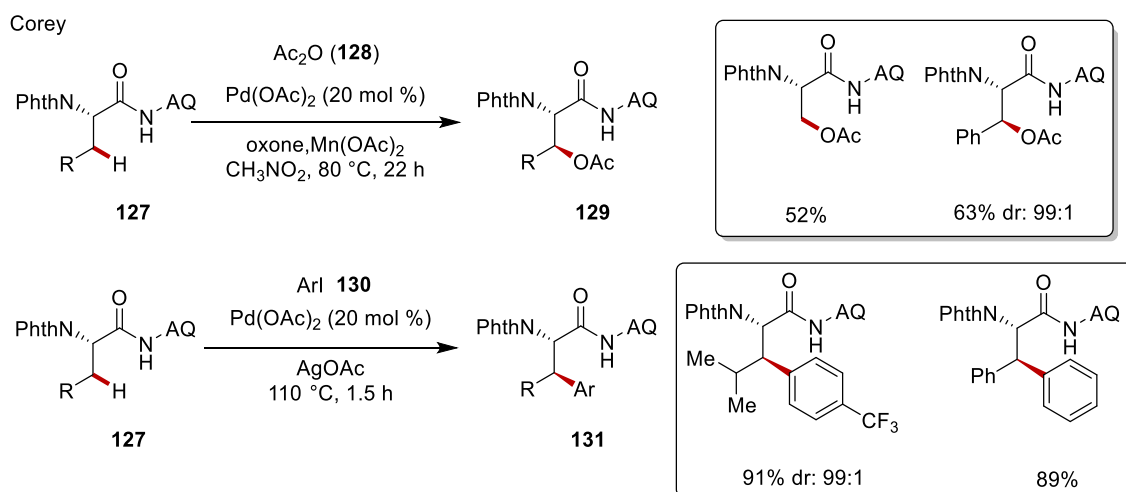
1.4. Late-Stage Functionalization of Peptides *via* C–H Activation

1.4.1. Functionalization of Amino Acid Derivatives *via* C–H Activation

The ability to functionalize amino acids to gain access to new scaffolds is of paramount importance for various fields of chemistry. This approach offers an atom-economical route towards a diverse set of building blocks, taking advantage the existence of the stereocenter, thus avoiding the need for developing asymmetric syntheses of these derivatives. Despite this conceptual asset, the sensitive nature of some amino acids requires very mild reaction conditions in order to avoid loss of the stereointegrity of the amino acid derivative. In this regard, in 2006 Corey demonstrated that the 8-aminoquinoline directing group could be used for the functionalization of a plethora of amino acids (Scheme 1.4.1).^[106] Under palladium catalysis, the $\beta\text{-C}(sp^3)\text{-H}$ acetoxylation and arylations were achieved with excellent levels of stereocontrol.

1. Introduction

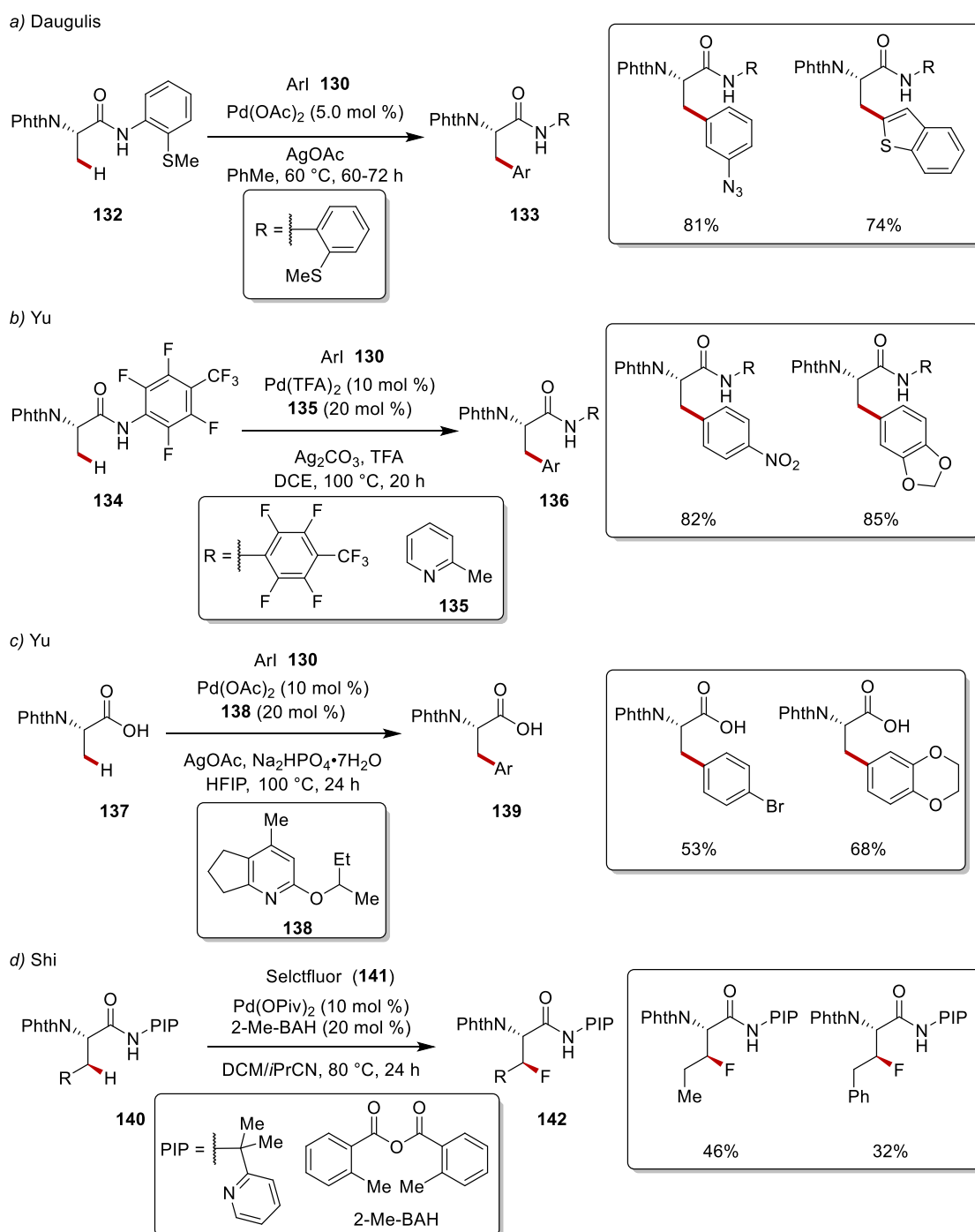
Interestingly, when valine or isoleucine were used in these methods, γ -primary $C(sp^3)$ -H over β -tertiary $C(sp^3)$ -H activation was observed, presumably due to steric reasons. Despite the limited scope of these transformations, the synthetic community recognized the potential of this strategy for gaining access to a myriad of amino acid derivatives.



Scheme 1.4.1. Palladium-catalyzed acetoxylation and arylation of amino acids.

After this early report, many groups expanded on this approach, by utilizing different directing groups, which are more user-friendly in terms of their removal, and by developing new transformation to unlock new parts of the chemical space. Thus, in 2012, Daugulis achieved the arylation of amino acid derivatives featuring various directing groups at the C-terminus (Scheme 1.4.2a).^[107] Remarkably, they recognized that 2-methylthio-aniline was an efficient directing group for palladium catalysis and was easily removed under acidic conditions. With the optimized reactions conditions in hand, various (hetero)arylalanine derivatives **133** were obtained in good yields. The early examples of the amino acid $C(sp^3)$ -H functionalization typically used bidentate directing groups to ensure good reactivities and turnover numbers. Thus, in 2014, Yu introduced an electron-deficient amide as a monodentate directing group for $C(sp^3)$ -H activation (Scheme 1.4.2b).^[108] In this work, a pyridine ligand was crucial for an efficient reaction. Thus, alanine derivatives were efficiently arylated under palladium catalysis. Importantly, the reaction occurred in a stereoselective fashion and allowed sequential arylation. Based on this report, Yu expanded on the monodentate $C(sp^3)$ -H arylation by using the native carboxylic acid as the directing group (Scheme 1.4.2c).^[109] Despite this advancement, this method was not as efficient as the amide directed C-H

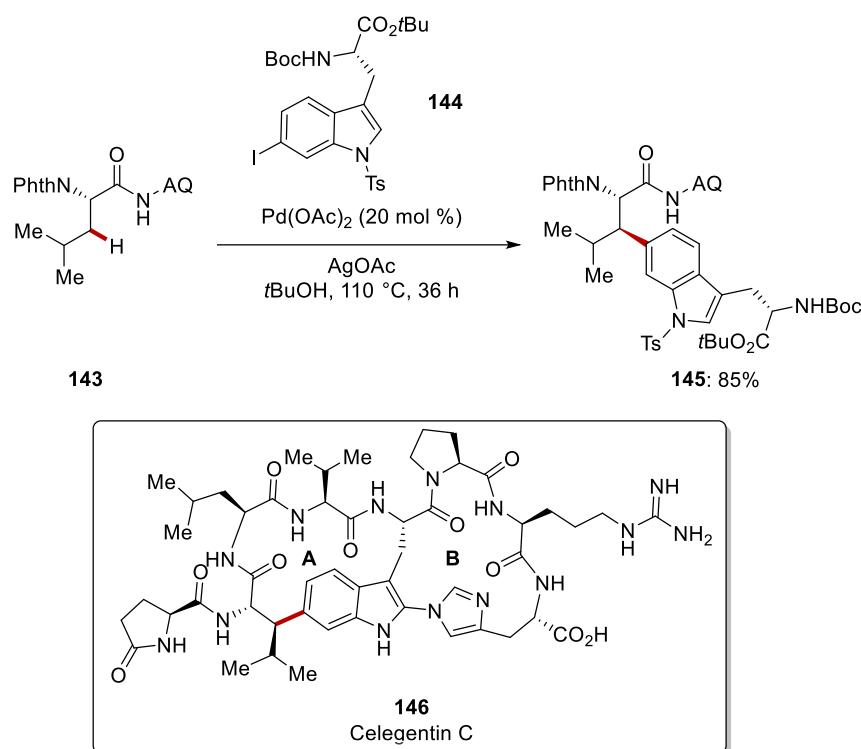
arylation. The directed C(sp^3)–H functionalization of amino acid derivatives is not restricted to the formation of C–C bonds, as in 2015 Shi developed the oxidative C–H fluorination using Selectfluor as the oxidant and fluoride source (Scheme 1.4.2d).^[110] This method tolerated sensitive functional groups and gave rise to a plethora of fluorinated amino acid derivatives **142** in a stereo- and position-selective fashion albeit with moderate efficacy.



Scheme 1.4.2. Palladium-catalyzed C(sp^3)–H functionalization of amino acids.

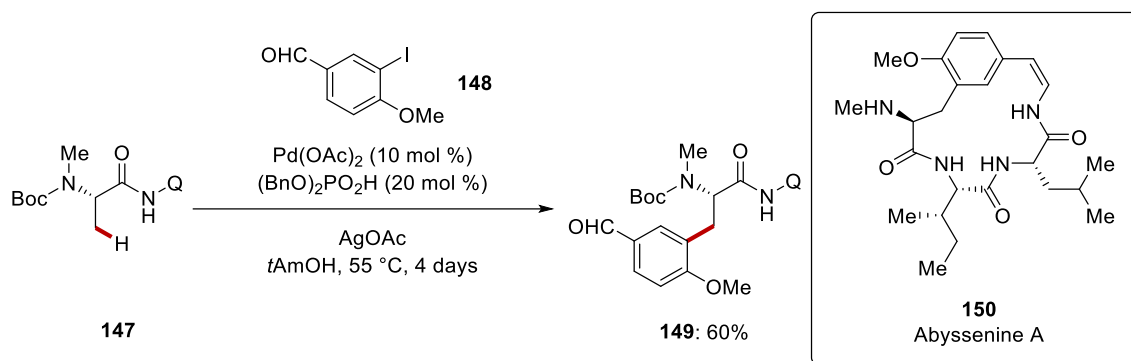
1. Introduction

Apart from the synthesis of amino acid derivatives as building blocks for various purposes, the transformative nature of $C(sp^3)$ -H activation of amino acid derivatives was demonstrated by Chen in the total synthesis of Celegentin C (Scheme 1.4.3).^[111] More specifically, leucine derivative **143** was arylated in stereo-, site- and chemoselective fashion using iodinated tryptophan derivative **144** under palladium catalysis. Gratifyingly, the stereochemical outcome of the reaction matched the one found in the natural product thus providing an easy route to this exotic linkage of leucine and tryptophan.



Scheme 1.4.3. Palladium-catalyzed $C(sp^3)$ -H arylation *en route* to Celegentin C **146**.

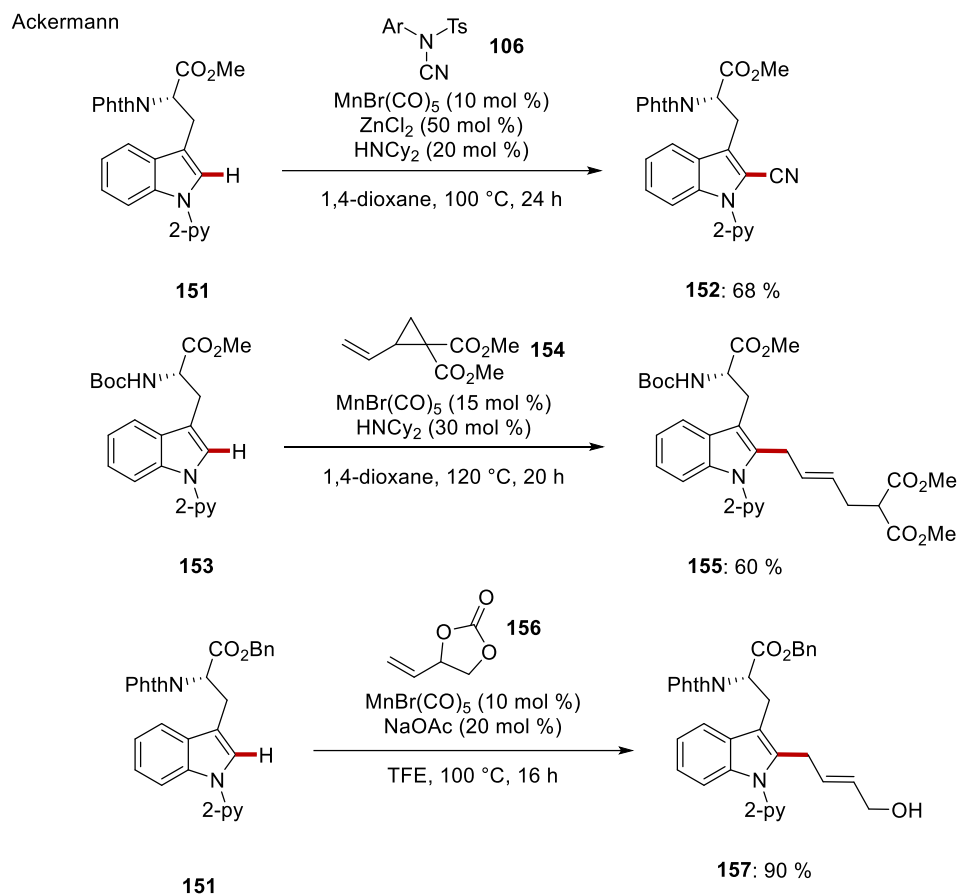
Another application that demonstrated the translation potential of palladium-catalyzed $C(sp^3)$ -H arylation was reported by Kazmaier when under 8-aminoquinoline assistance, a key precursor **149** of the natural product Abyssenine A **150** was expediently obtained (Scheme 1.4.4).^[112] Remarkably, the phthalyl protection on the nitrogen was not essential, and Boc-protected *N*-methylated alanine was a viable substrate simplifying the overall synthetic plan. In addition, *N*-methylated amino acids are important structural motifs in various biologically active cyclic peptides and other natural products.^[113]



Scheme 1.4.4. Palladium-catalyzed $\text{C}(\text{sp}^3)\text{-H}$ arylation *en route* to Abyssenine A.

The C–H functionalization of amino acids is not restricted to $\text{C}(\text{sp}^3)\text{-H}$, but $\text{C}(\text{sp}^2)\text{-H}$ can also be functionalized under different metal catalysis. Among the amino acids that have been functionalized, tryptophan is the best studied. For the site-selective functionalization of tryptophan different strategies have been used, such as introduction of directing groups or the use of the innate reactivity of the indole core. The nucleophilic character of the indole moiety has been exploited under electrophilic palladium(II) catalysis for the diversification of tryptophan and tryptophan containing-peptides (*vide infra*). On the other hand, Ackermann enabled the functionalization of the C2 position of the tryptophan derivatives *via* the incorporation of a nitrogen based directing group on the indole moiety. Thus under manganese(I) catalysis the substitutive cyanation,^[93] allylation *via* C–H/C–C activation^[114] and allylation *via* C–H/C–O activation^[89] were achieved (Scheme 1.4.5). Despite these elegant findings, these methods were only applied in amino acid derivatives.

1. Introduction



Scheme 1.4.5. Manganese-catalyzed C(sp^2)-H functionalization of tryptophan derivatives **151** and **153**.

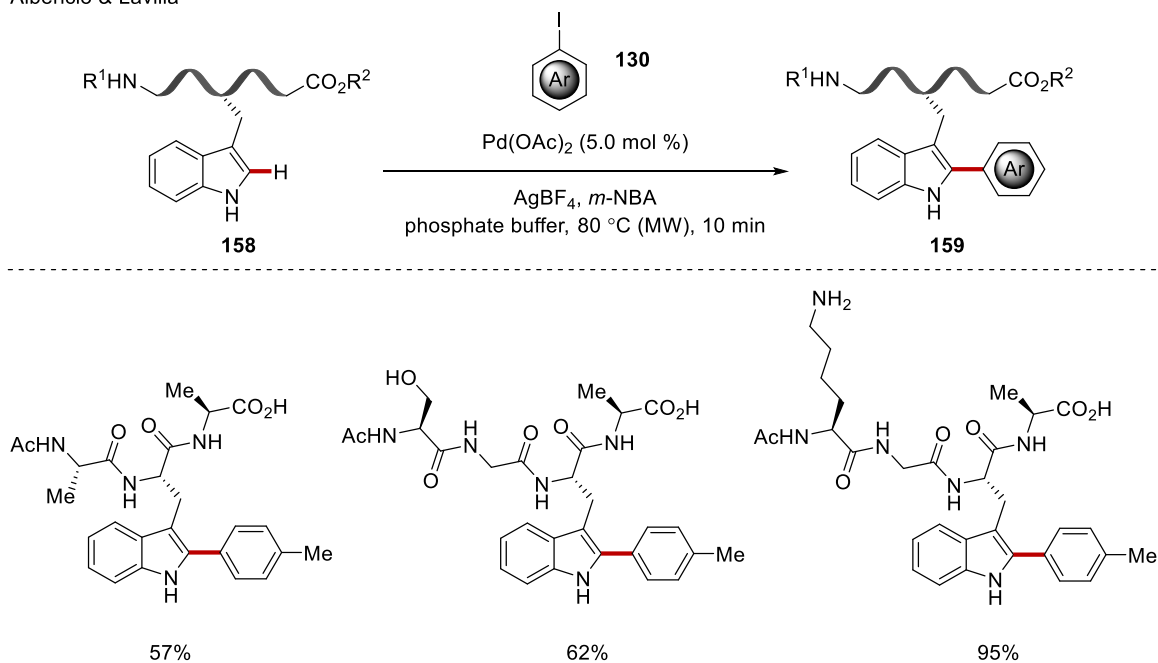
1.4.2. Functionalization of Peptides via C-H Activation

These undisputed advances have provided new avenues for the functionalization of a plethora of amino acids, thus enabling the facile synthesis of functionalized peptides and proteins *via* iterative peptide synthesis protocols. Whereas this approach has significantly boosted molecular synthesis, the direct functionalization of peptides represents a more efficient and elegant strategy, albeit more challenging. Specifically, the sensitive nature of many peptides requires mild catalytic manifolds that can selectively engage in productive pathways with the desired amino acid in the presence of myriad of other functional groups.

In 2010, Albericio and Lavilla developed the C2 arylation of tryptophans and tryptophan-containing peptides **158** under electrophilic palladium catalysis (Scheme 1.4.6).^[115] Remarkably, the reaction tolerated unprotected amino acids and the key to this efficient method was the use of acidic phosphate buffer that was sufficient to

solubilize the peptides at 80 °C under microwave irradiation. In addition, they demonstrated that this method allowed the arylation of tryptophan derivatives in DMF as solvent at 150 °C. This method was expanded to the functionalization of biologically relevant tryptophan-containing diketopiperazines.^[116]

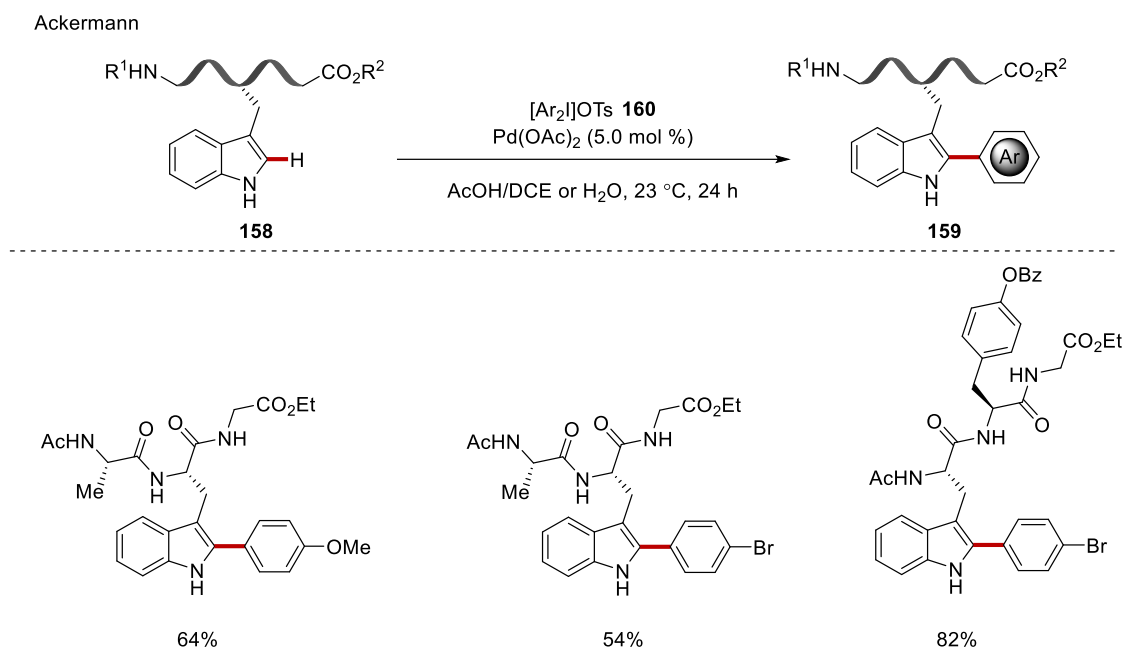
Albericio & Lavilla



Scheme 1.4.6. Palladium-catalyzed C–H arylation of tryptophan-containing peptides.

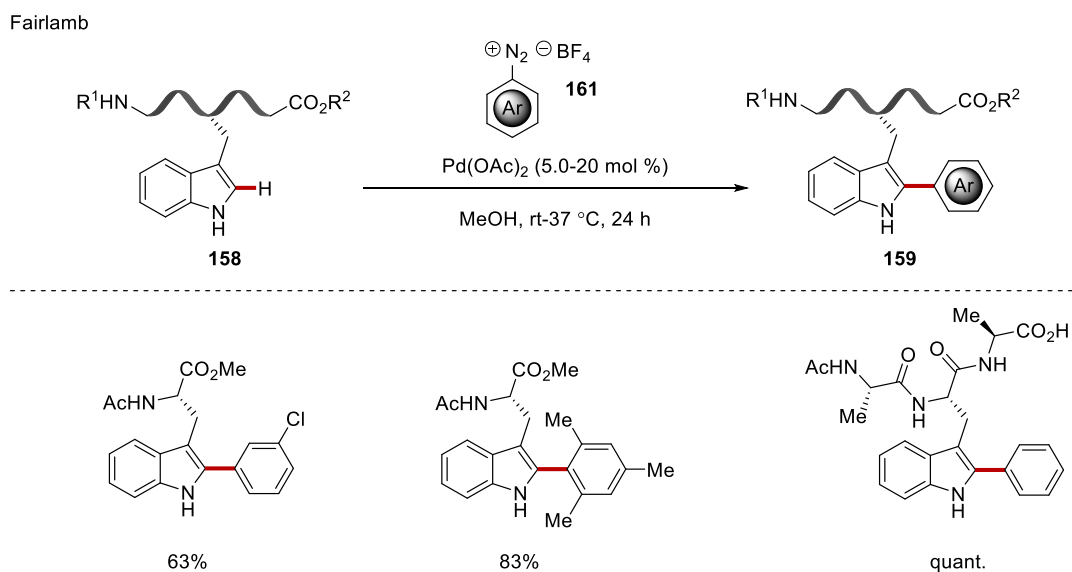
The sensitive nature of peptides requires mild reaction conditions, thus Ackermann unravelled a room temperature C2-arylation of tryptophan-containing peptides **158** with iodonium salts **160** (Scheme 1.4.7).^[117] The high reactivity of these arylating agents required careful optimization that showed acetic acid or water as the most suitable solvents. Under the optimized reaction conditions, a plethora of peptides, containing various functional groups, were functionalized in a site- and chemo-selective fashion, under exceedingly mild reaction conditions that did not jeopardize the stereo-integrity of the peptidic backbone.

1. Introduction



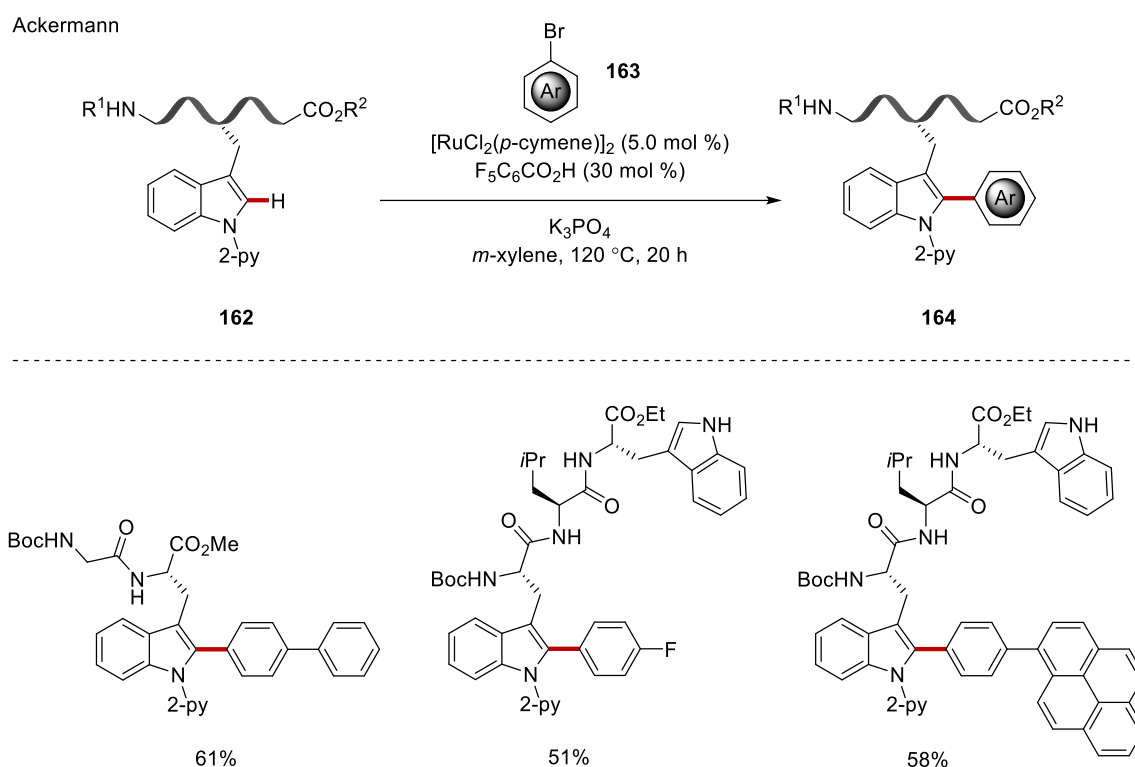
Scheme 1.4.7. Room temperature palladium-catalyzed C–H arylation of tryptophan-containing peptides **158**.

Subsequently, Fairlamb demonstrated that reactive aryl diazonium salts **161** can also be utilized for the C2 selective arylation of tryptophan moieties by palladium catalysis (Scheme 1.4.8).^[118] The reaction tolerated several functional groups on the aryl scaffold and was extended to tryptophan containing peptides **158**, albeit with limited scope. This protocol was an extension of their previously reported oxidative C2-arylation of tryptophan moieties with aryl boronic acids.^[119]



Scheme 1.4.8. Palladium-catalyzed C–H arylation of tryptophan moieties with aryl diazonium salts **161**.

These early and elegant reports were based on the well-established palladium-catalyzed C–H activation manifolds. However, the use of other transition metals in the functionalization of peptides would be highly desirable, to devise new reaction pathways. Thus, in 2017 Ackermann developed the first ruthenium-catalyzed arylation of tryptophan-containing peptides **162** under the crucial carboxylate assistance,^[120] building on their earlier studies (Scheme 1.4.9).^[121] After considerable optimization, pentafluorobenzoic acid was identified as the optimal carboxylic acid that facilitated the carboxylate-assisted C–H cleavage. Remarkably, this manifold allowed the efficient synthesis of larger peptides *via* C–H ligation and the late-stage fluorescent labeling of peptides. Moreover, a slight modification in the reaction conditions allowed the C–H arylation to be conducted in aqueous medium.

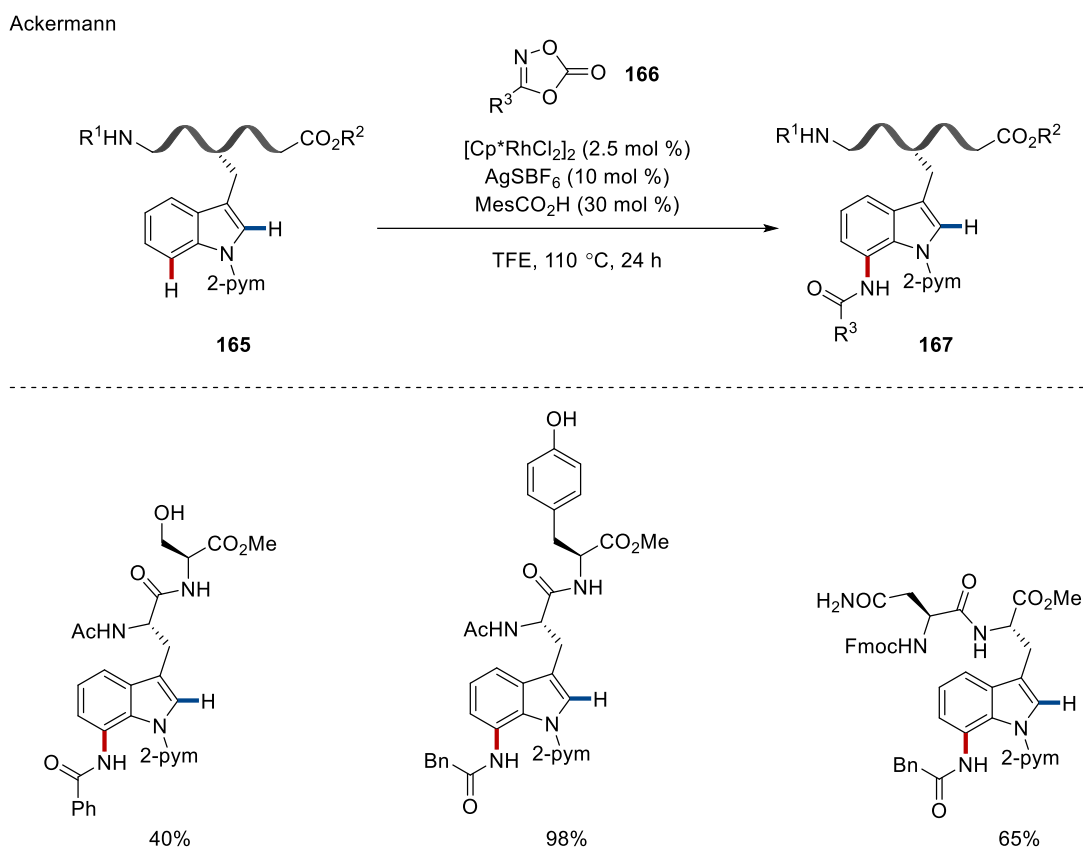


Scheme 1.4.9. Ruthenium-catalyzed C–H arylation of tryptophan-containing peptides moieties with aryl bromides **163**.

Very recently, Ackermann unravelled an elegant strategy for the C7-selective amidation of tryptophan-containing peptides **165** under rhodium(III)-catalysis, using the highly modular and easily accessible dioxazolones **166** (Scheme 1.4.10).^[122] This strategy relied on the reversible C–H activation step and subsequent rate-limiting C–N bond formation, as was supported by mechanistic and computational studies. Under

1. Introduction

the optimized reaction conditions a plethora of peptides, possessing a myriad of different functional groups, were amidated in a chemo- and site-selective fashion. Furthermore, the modular nature of dioxazolones **166** allowed the expedient stitch of peptides with peptides, natural products and drug molecules, leading to various peptide-conjugates.

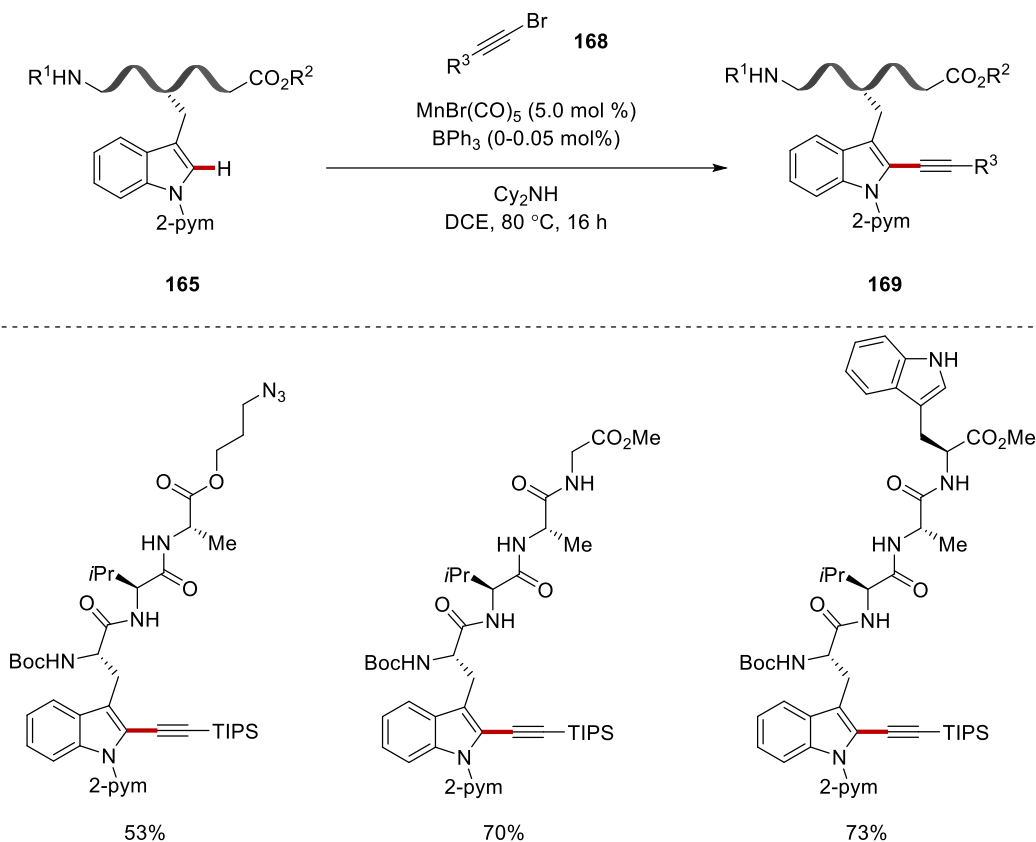


Scheme 1.4.10. Rhodium-catalyzed C7–H amidation of tryptophan-containing peptides.

In the quest for more sustainable strategies for late-stage functionalization *via* C–H activation the development of novel methodologies utilizing Earth-abundant, non-toxic 3d transition metals is in high demand and is a very active research field. In 2017, Ackermann disclosed the first manganese(I)-catalyzed C–H alkynylations of tryptophan-containing peptides using modular bromo-alkynes **168** (Scheme 1.4.11).^[123] This regime tolerated a wide range of functional groups, such as azides and *NH*-free tryptophans. Remarkably, after considerable optimization the reaction was expediently expanded to alkyl- and aryl-bromoalkynes by using BPh_3 , that presumably accelerates the key β -bromide elimination. This approach enormously

enhanced the potential for bioorthogonal post-synthetic modifications as a plethora of alkyne handles can be chemo- and site-selectively incorporated into a peptide.

Ackermann

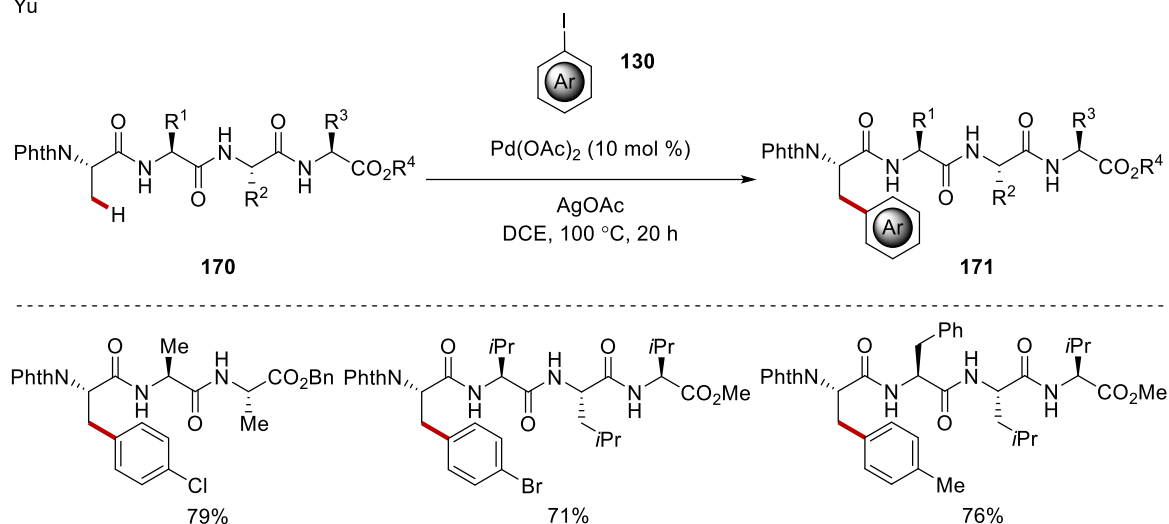


Scheme 1.4.11. Manganese-catalyzed C–H alkylation of tryptophan-containing peptides.

Despite those undisputed advances, $\text{C}(\text{sp}^3)\text{-H}$ activation is often more challenging for organometallic C–H activation. This issue is significantly more prominent in peptides, since they possess multiple $\text{C}(\text{sp}^3)\text{-H}$ in close proximity to multiple Lewis-basic functional groups that can pose selectivity hurdles. Thus, since the early stages of practical C–H activation, the utilization of a designed directing group was necessary with rare exceptions. In this context, Yu demonstrated that the peptidic backbone can act as directing groups under palladium catalysis, if the C–H to be functionalized is positioned at the *N*-terminus (Scheme 1.4.12).^[124] Thus, various tri- and tetrapeptides, possessing an alanine residue at the *N*-terminus were chemo- and site-selectively arylated, presumably *via* the intermediacy of a palladacycle under the peptidic backbone bidentate assistance.

1. Introduction

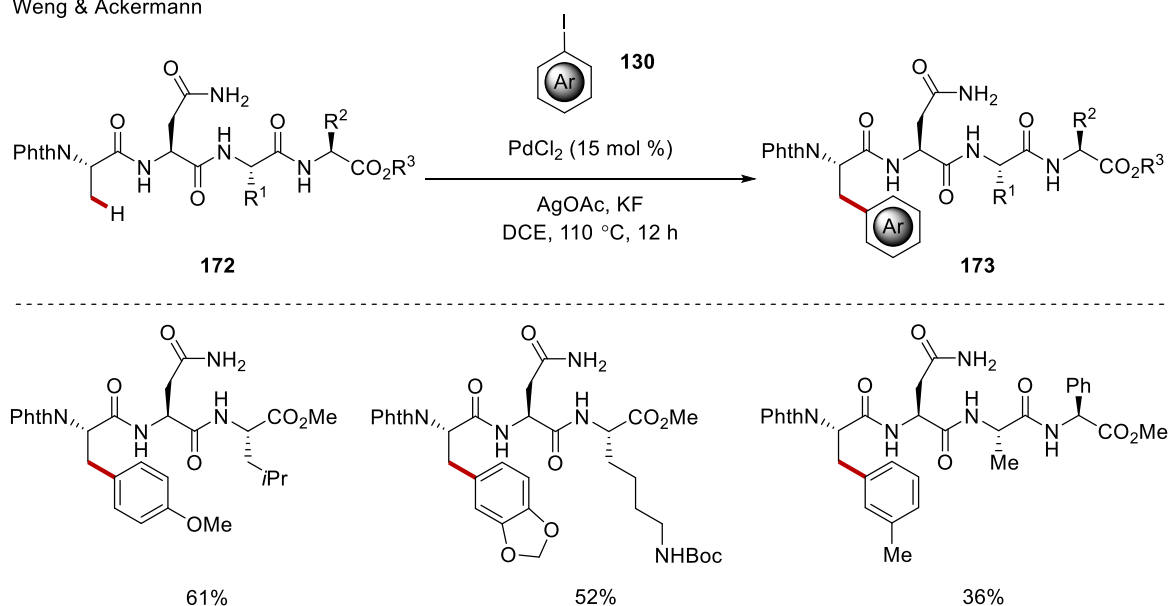
Yu



Scheme 1.4.12. Palladium-catalyzed C(sp³)-H arylation of peptides **170** via bidentate backbone assistance.

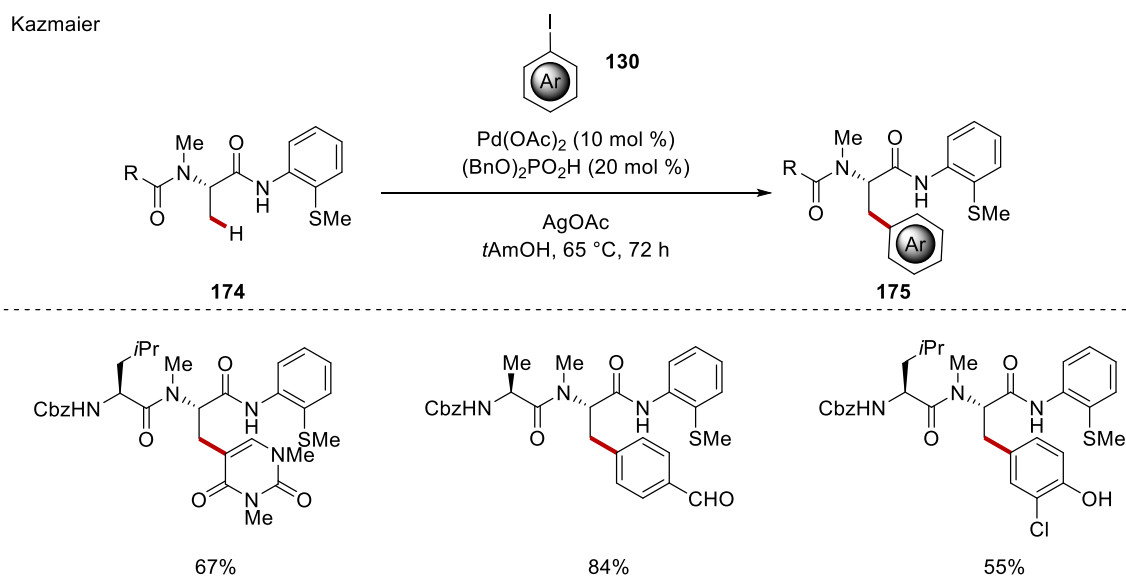
Recently, Weng and Ackermann demonstrated that the side chain of asparagine, containing the Lewis-basic primary amide moiety, could direct a site-selective C(sp³)-H arylation of alanine moieties, *via* an unprecedented 5,6-fused palladacycle (Scheme 1.4.13).^[125] This method allowed the expedient synthesis of various tri-, tetra-, penta- and even hexapeptides **172** functionalized with a plethora of aryl moieties. The translational potential of the method was demonstrated by the expedient access to AGRP loop analogues that were subsequently incorporated into cyclic octapeptides.

Weng & Ackermann



Scheme 1.4.13. Palladium-catalyzed C(sp³)-H arylation of peptides *via* asparagine assistance.

Very recently, Kazmaier unravelled a mono selective arylation of *N*-methylated-alanine moieties, positioned at the *C*-terminus, via the key bidentate assistance of 8-aminoquinoline or 2-methylthio-aniline (Scheme 1.4.14).^[126] Remarkably, *N*-phthaloyl protection was not crucial at the alanine residue, thus enabling the straightforward functionalization of various peptides with a plethora of densely functionalized aryl iodides **130**, featuring heterocycles and halogenated phenols leading to halogenated tyrosine derivative found in many bioactive peptides.^[127]

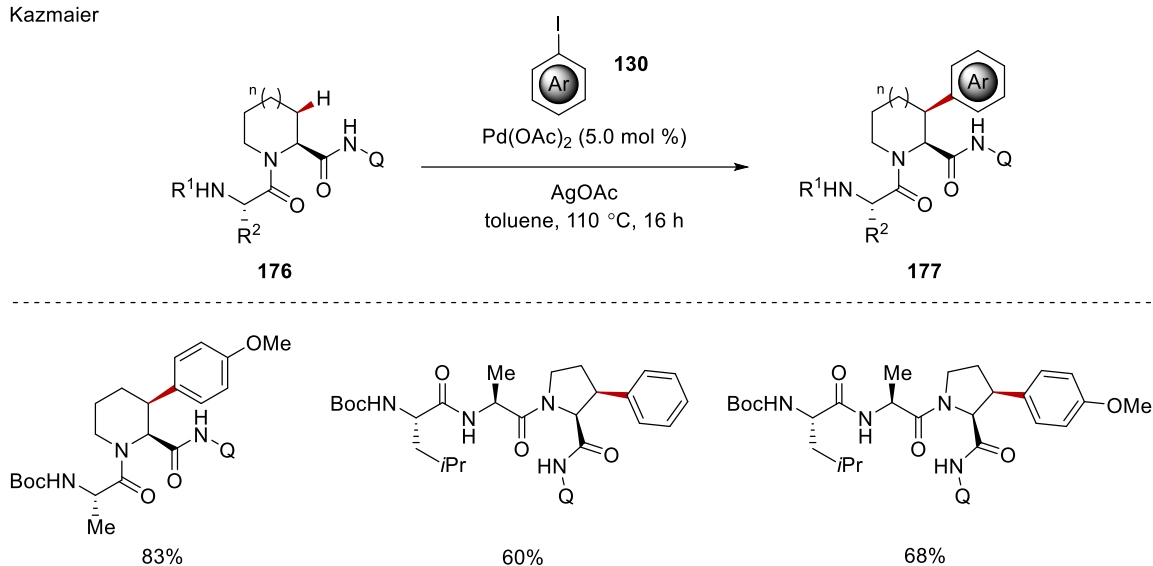


Scheme 1.4.14. Palladium-catalyzed C–H arylation of *N*-methylated alanine-containing peptides **174**.

Secondary C(*sp*³)–H functionalizations are significantly more challenging endeavor due to steric hindrance and stereoselectivity issues, in combination with chemo- and site-selectivity issues. Thus, the functionalization of amino acid residues possessing a substituent at the β -position is highly desirable. In this context, Bull disclosed the β -*syn*-arylation of Cbz-protected proline moieties by 8-aminoquinoline assistance.^[128] Shortly after, Kazmaier developed mild reaction conditions for the stereoselective β -*syn*-arylation of proline-containing peptides (Scheme 1.4.15).^[129] Furthermore, this methodology exhibited excellent stereo- and site-selectivity in the functionalization of L-pipecolic acid-containing peptides.

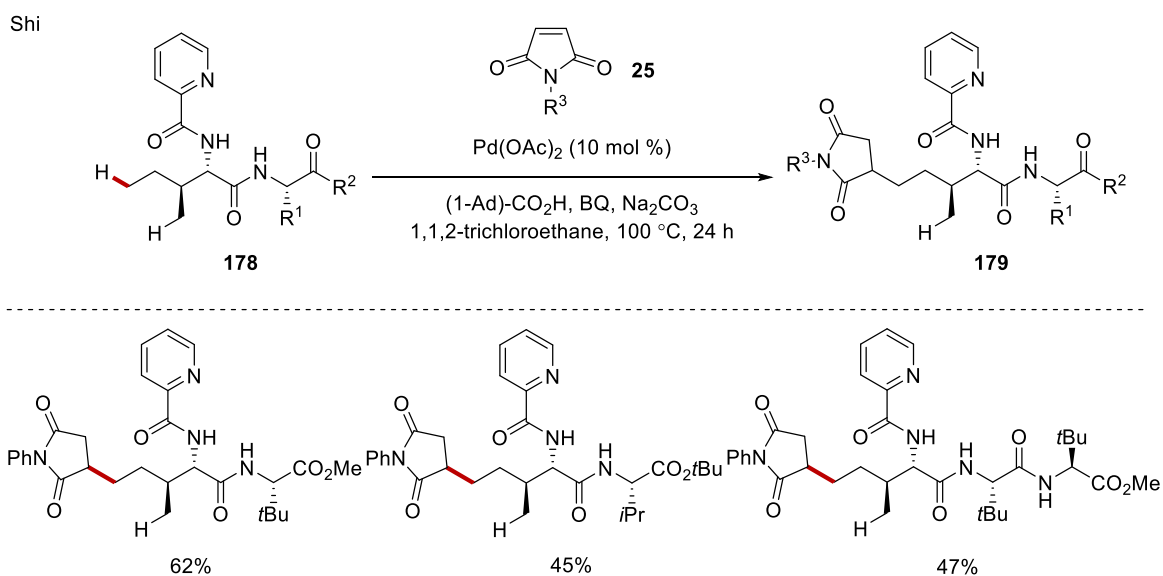
1. Introduction

Kazmaier



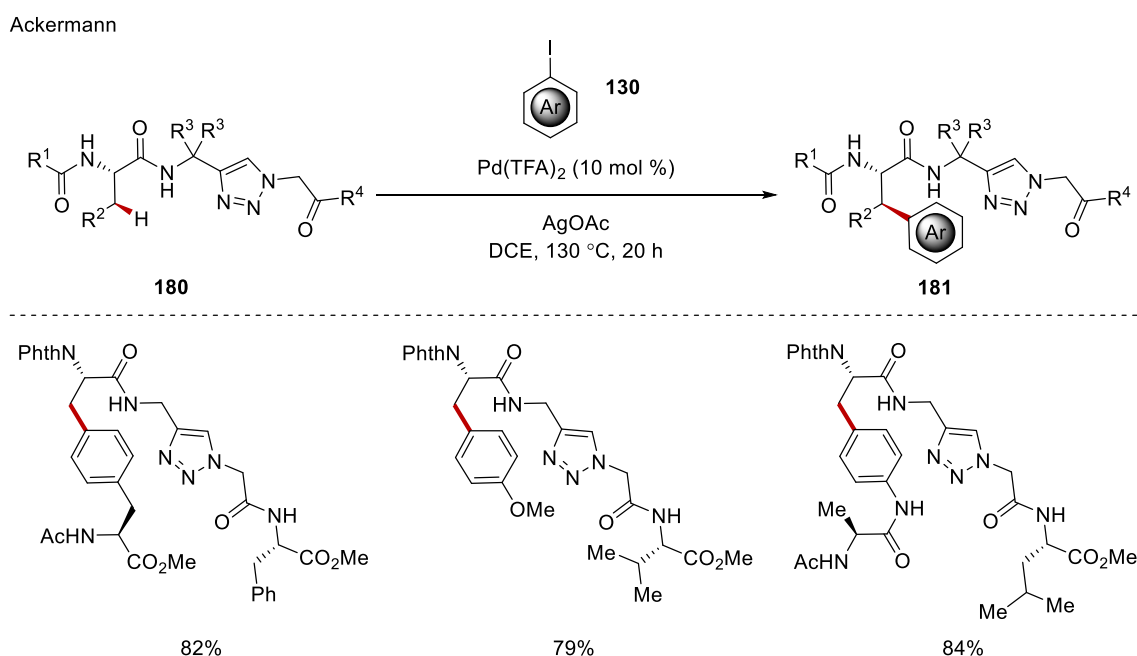
Scheme 1.4.15. Palladium-catalyzed C–H arylation of proline-containing peptides.

The functionalization of terminal amino acids of the peptide chain is not only restricted to the C-terminus, indeed the incorporation of a suitable directing group at the N-terminus is also feasible. Thus, Shi after installing the 2-picolinic acid at the N-terminus, that acted as a bidentate directing group, achieved the palladium-catalyzed site-selective δ C–H alkylation with maleimides **25** of isoleucine-containing peptides **178** (Scheme 1.4.16).^[130] The observed selectivity was attributed to the easier primary δ over the secondary γ C(sp^3)–H activation, thus limiting the protocol for functionalizing peptides featuring amino acids equipped with γ -methyl groups at the N-terminus.



Scheme 1.4.16. Palladium-catalyzed δ C(sp^3)–H alkylation with maleimides **25**.

Despite these undisputed advances on C(sp^3)-H functionalization of peptides, these methodologies enabled the modification of amino acids only at the *N*- or *C*-terminus, thus significantly hampering their translational potential. In contrast, in 2018, Ackermann disclosed the site-selective palladium-catalyzed primary and secondary C(sp^3)-H arylation of structurally complex peptides under triazole assistance (Scheme 1.4.17).^[131] The selection of triazole-based amide as the bidentate directing group as an peptide isostere was based on its presence in various bioactive peptidomimetics as they share common electrical and topological properties.^[132] Furthermore, the highly modular synthesis of 1,2,3-triazoles allows the expedient access to various peptides.^[133] Thus, the incorporation of the triazole based directing group led to the efficient functionalization of various amino acids such as alanine and phenylalanine, among others, in a stereo-, chemo- and site- selective fashion. This strategy tolerated plethora of sensitive functional groups on the aryl scaffold. Having established a robust protocol for the functionalization of amino acids derivatives, they installed a peptidic backbone on the triazole core, *via* a 1,4 substitution pattern, thus obtaining triazole-peptidomimetics destined for palladium-catalyzed C-H arylation. After considerable optimization, larger peptides were selectively arylated in the presence of many C-H bonds, leading to functionalized and ligated peptides.

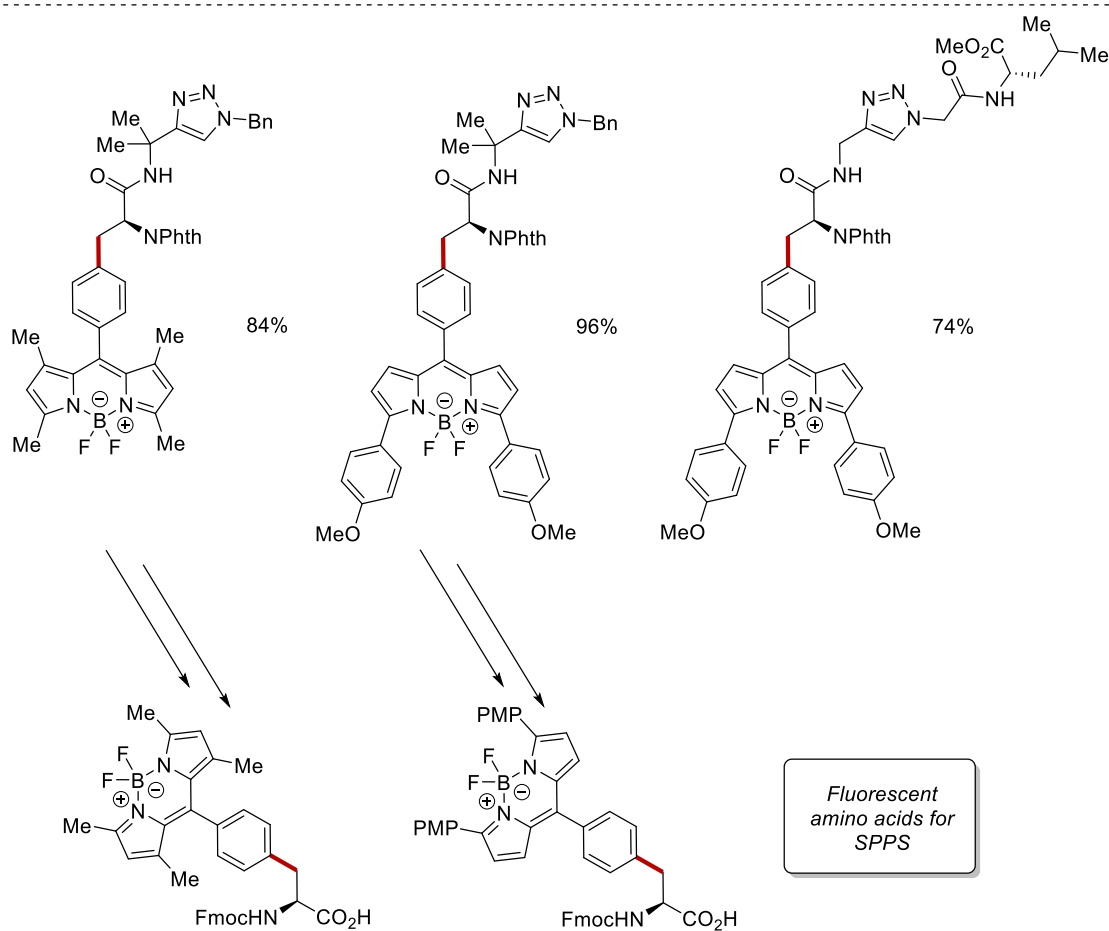
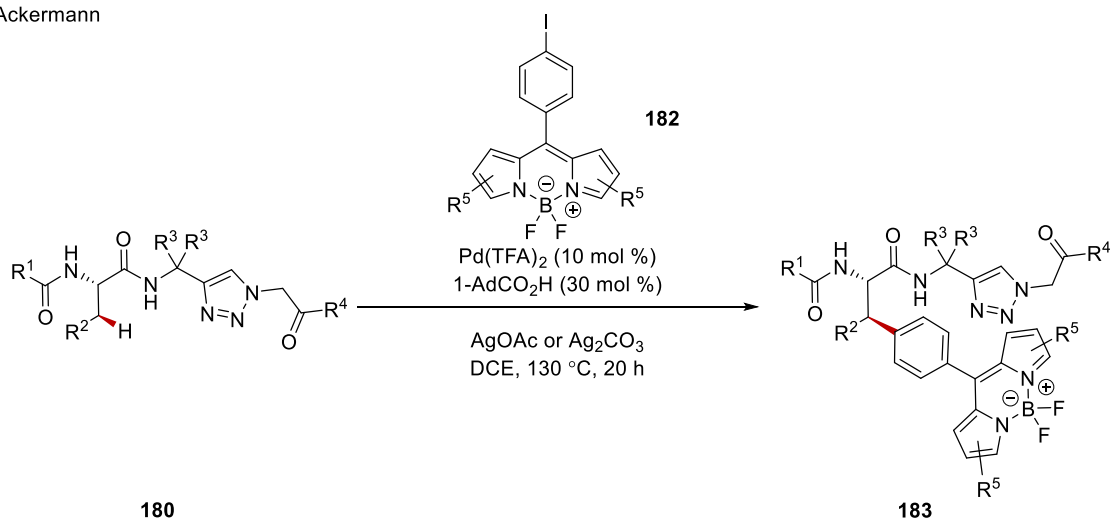


Scheme 1.4.17. Palladium-catalyzed C-H arylation of triazole-peptidomimetics.

1. Introduction

Having established a reliable platform for the internal C(sp³)-H arylation of triazole containing peptidomimetics, the authors expanded this manifold for the late-stage labeling of peptides using iodo-BODIPY dyes **182** as the arylating agent (Scheme 1.4.18).^[134] Hence by means of palladium catalysis with co-catalytic amounts of 1-adamantanecarboxylic acid various amino acid derivatives were efficiently labeled with various BODIPY dyes, possessing distinct fluorescent properties, under triazole assistance. This approach, after standard protecting group manipulations, led to the synthesis of fluorescent Fmoc-protected amino acids, destined for the synthesis of larger peptides *via* SPPS. Furthermore, the primary and secondary C(sp³)-H labeling was efficiently applied to the internal functionalization of larger peptidomimetics.

Ackermann



Scheme 1.4.18. Palladium-catalyzed C–H labeling.

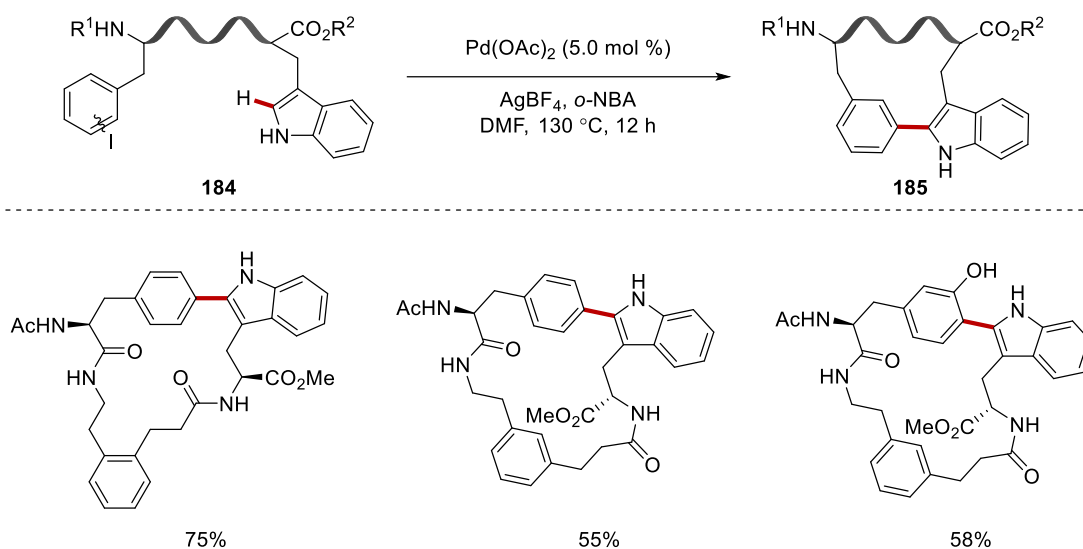
1.4.3. Peptide Macrocyclization via C–H Activation

One of the earliest examples of C–H macrocyclization for the synthesis of cyclic peptides was reported in 2012 by James, where tryptophan residues were intramolecularly arylated under palladium catalysis using a suitably positioned tethered aryl iodide moiety.^[135] In this protocol, for the C(*sp*²)-H macrocyclization *o*-nitro-

1. Introduction

benzoic acid was used, in *N,N*-dimethylformamide as solvent at 130 °C (Scheme 1.4.19). Thus, the relatively harsh reaction conditions limited the scope of this transformation to a few specifically engineered linear precursors, that possessed an *ortho* or *meta* substitution pattern at the aryl iodide scaffold. This enabled the necessary conformational rigidity for a successful intramolecular reaction, without extensive side-reactions. Despite these limitations, this provided the impetus for further applications as milder and more selective reaction manifolds were rapidly developed.

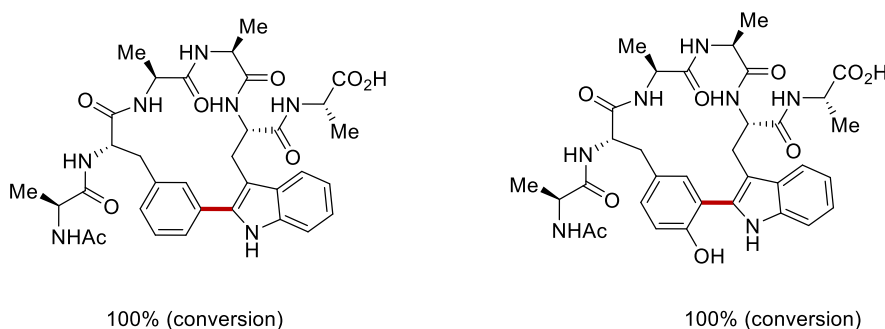
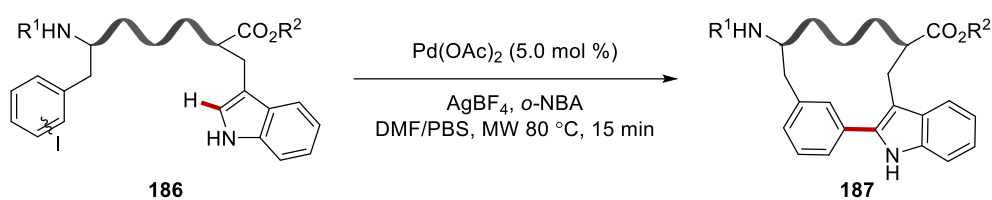
James



Scheme 1.4.19. Palladium-catalyzed C–H macrocyclization via C2 tryptophan arylation.

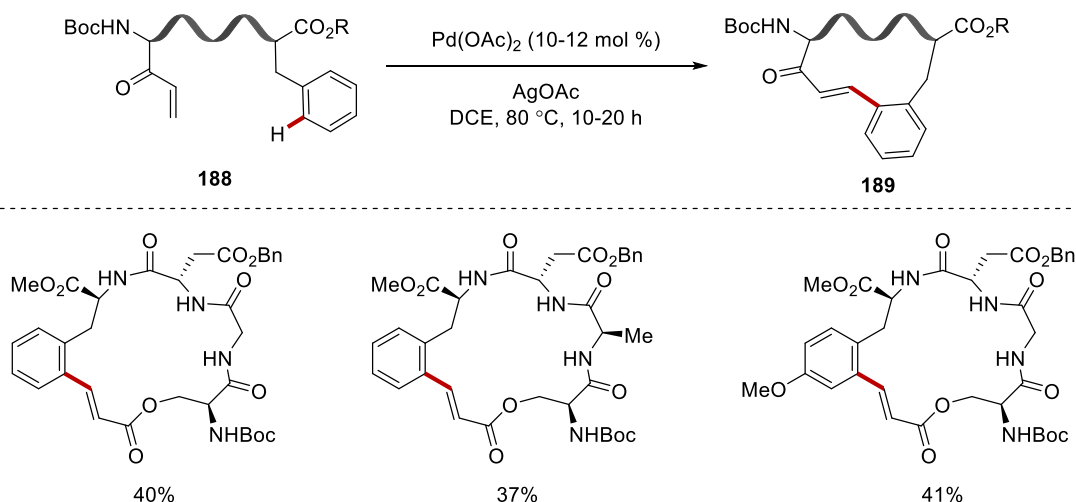
Palladium-catalyzed $\text{C}(\text{sp}^2)\text{--H}$ arylations of tryptophan moieties was later exploited by Albericio and Lavilla for the synthesis of stapled peptides using linear precursors equipped with an iodinated phenylalanine or tyrosine moiety (Scheme 1.4.20).^[136] After an extensive optimization, a mixture of *N,N*-dimethylformamide and acidic phosphate buffer solution at 80 °C under microwave irradiation was crucial for solubilizing the linear peptide **186** and ensuring sufficient macrocyclization. Thus, a number of cyclic peptides were synthesized possessing many sensitive functional groups, providing access to biaryl-containing peptides, a structural motif found in myriad of biologically active natural products.^[137] Furthermore, this strategy was efficient for the bis-cyclization of the linear precursor containing two tryptophan residues, on the *N*- and *C*-terminus, and a bis-iodinated tyrosine residue, leading to a fused bis-macrocyclic peptide.

Albericio/ Lavilla

**Scheme 1.4.20.** Palladium-catalyzed synthesis of stapled peptides.

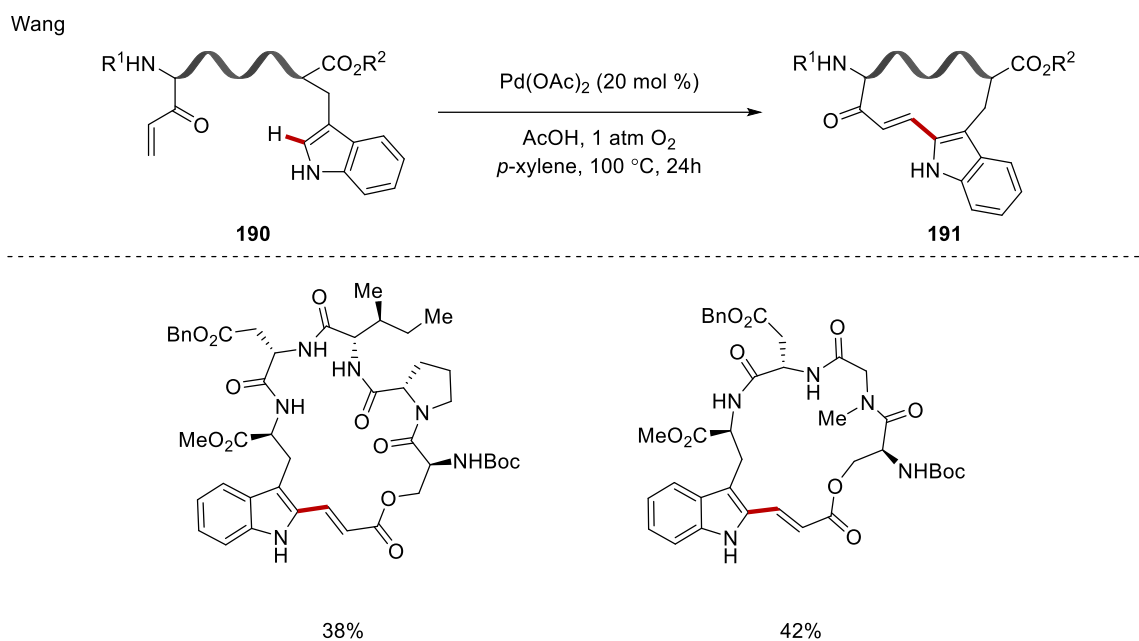
Recently, Wang applied the backbone-directed $\text{C}(\text{sp}^2)\text{-H}$ *ortho*-alkenylation of phenylalanine derivatives in a macrocyclization setting, for the synthesis of *E*-olefin-containing cyclic peptides under palladium catalysis (Scheme 1.4.21).^[138] Remarkably, the reaction occurred selectively at the δ position of the phenylalanine residue positioned at the C-terminus, both for the intra- and intermolecular manifold, giving rise to ligated and cyclic peptides in a site- and chemoselective fashion. Furthermore, the reaction manifold was applicable to the oxidative alkenylation with unactivated olefins

Wang

**Scheme 1.4.21.** Palladium-catalyzed backbone directed $\text{C}(\text{sp}^2)\text{-H}$ activation towards cyclic peptides.

1. Introduction

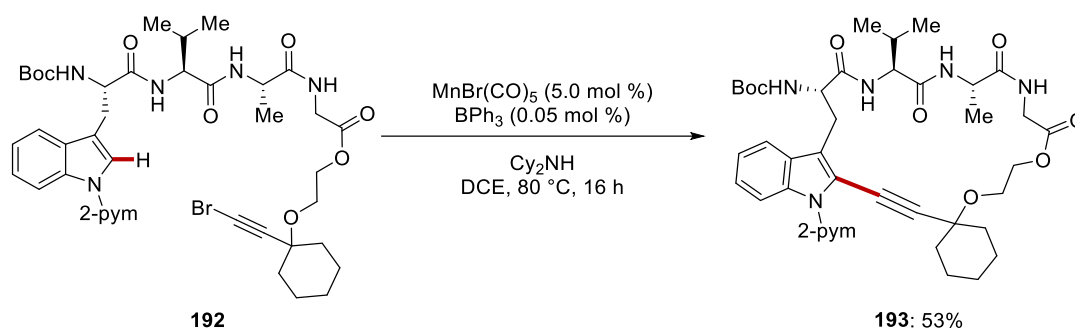
This oxidative alkenylation manifold was recently expanded to tryptophan-containing peptides. Thus, *NH*-free tryptophan moieties were alkenylated with a tethered alkene selectively at the C2-position (Scheme 1.4.22).^[139] As before, the method was efficiently applied for the synthesis of ligated and cyclic peptides with excellent levels of site- and chemoselectivity. This methodology tolerated some amino acids and forged from 18 to 26-membered rings albeit with moderate efficiency, presumably due to the sensitive nature of the linear precursors **190**.



Scheme 1.4.22. Palladium-catalyzed C(*sp*²)-H alkenylation towards cyclic peptides.

In 2017, Ackermann unravelled a 3d-metal, namely manganese,-catalyzed alkynylation regime for the late-stage diversification of peptides (Scheme 1.4.23).^[123] The chemoselective nature and robustness of this manifold enabled facile access to cyclic peptides *via* a regioselective insertion/BPh₃ enabled β -bromide elimination pathway.

Ackermann

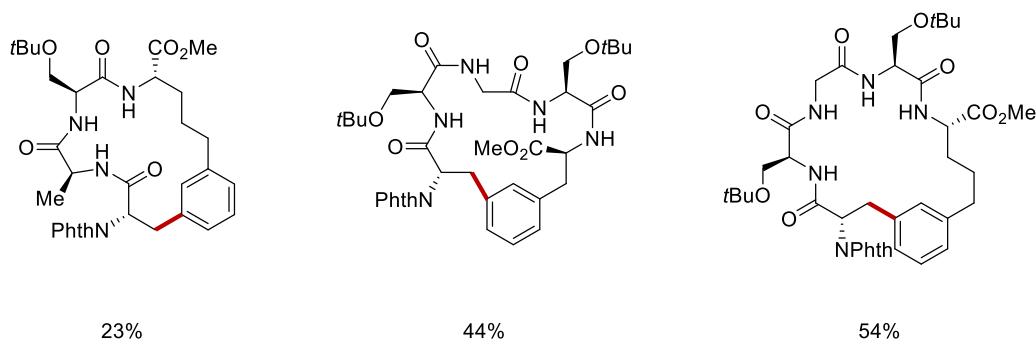
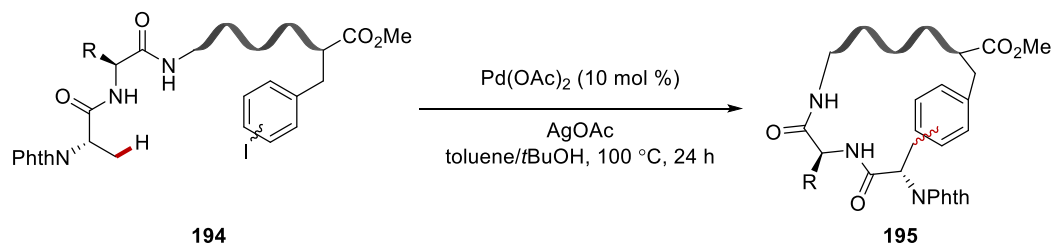


Scheme 1.4.23. Manganese-catalyzed C–H alkylation towards cyclic peptide **192**.

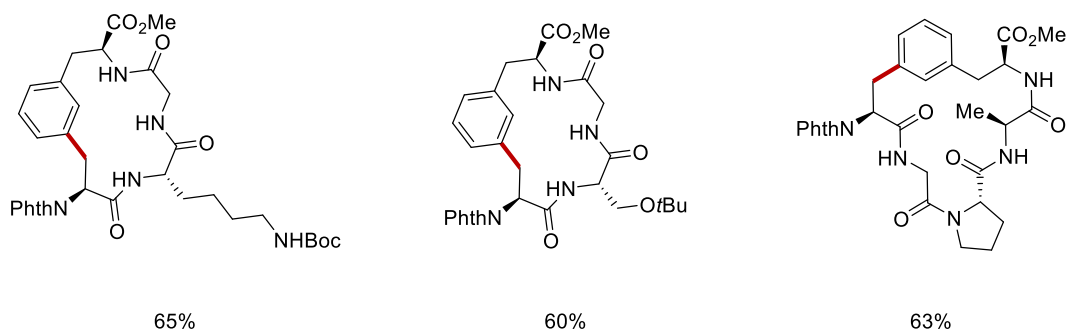
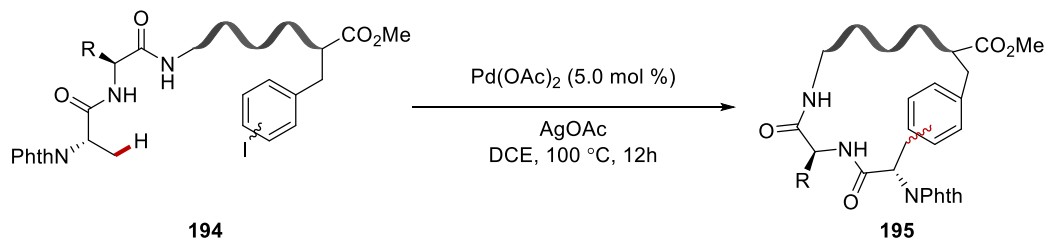
The C–H macrocyclization manifold *en route* to cyclic peptides is not restricted to C(sp^2)–H activation but is also applied to the more challenging C(sp^3)–H activation. Thus, in 2017, Noisier, Albericio^[140] and Wang^[141] independently reported the backbone-directed macrocyclization of peptides featuring alanine and iodinated phenylalanine residues linked together *via* a peptidic chain (Scheme 1.4.24). Both protocols demonstrated high levels of site- and chemoselectivities. Remarkably, in this manifold detrimental dimerizations were not observed, in sharp contrast to the previous tryptophan-based macrocyclization methodologies. This can be attributed to the favorable conformational change during the backbone-directed C–H activation that forces the chain to adopt a suitable conformation for the crucial oxidative addition step. Furthermore, Wang demonstrated that their method could be utilized for the formal synthesis of Celogentin C **146** *via* a diastereoselective C–H macrocyclization leading, after two additional steps, to an advanced intermediate of the Chen synthesis.

1. Introduction

a) Noisier/Albericio



b) Wang

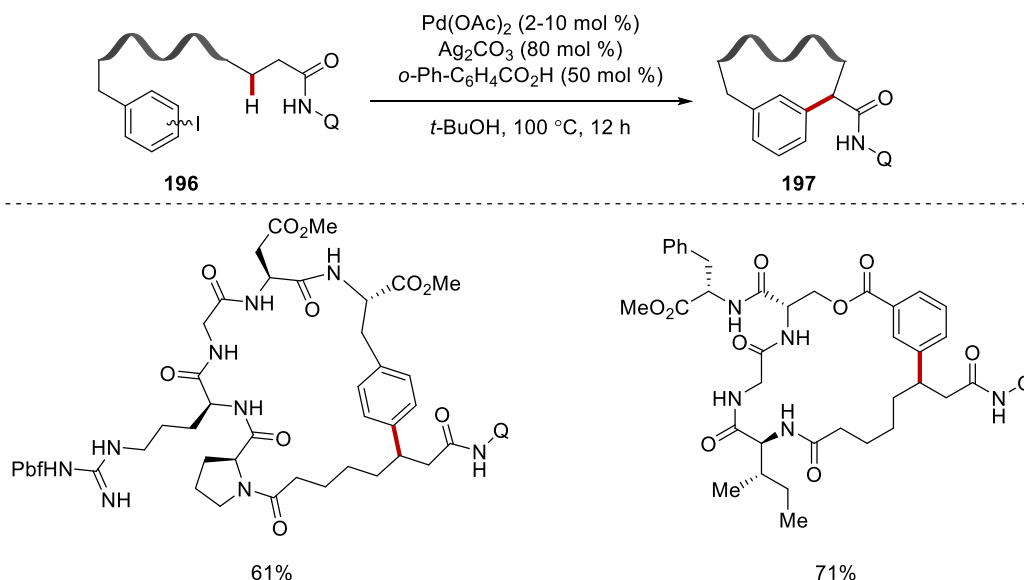


Scheme 1.4.24. Palladium-catalyzed intramolecular $\text{C}(sp^3)\text{-H}$ activation towards cyclic peptides **195**.

In 2018 He, Qi, Liu and Chen developed a *C*-terminus \rightarrow *N*-terminus macrocyclization by employing the 8-aminoquinoline directing group under palladium catalysis. Under the optimized reaction conditions, featuring Pd(OAc)_2 at as low as 2 mol %, *ortho*-phenylbenzoic acid as ligand in *t*BuOH various linear precursors **196**, featuring protected and some unprotected amino acids, were efficiently cyclized under high dilution conditions (Scheme 1.4.25).^[142] Remarkably, this manifold enabled the synthesis of highly-strained 13-membered *ortho*- or *meta*-cyclophanes, featuring bent

arenes. In addition, larger cyclic peptides were smoothly obtained in good yields, albeit without stereocontrol at the newly formed stereocenter. The use of an electron-rich 8-aminoquinoline surrogate, developed by Daugulis,^[143] allowed the oxidative cleavage of the directing group.

He, Qi, Shen, Liu & Chen

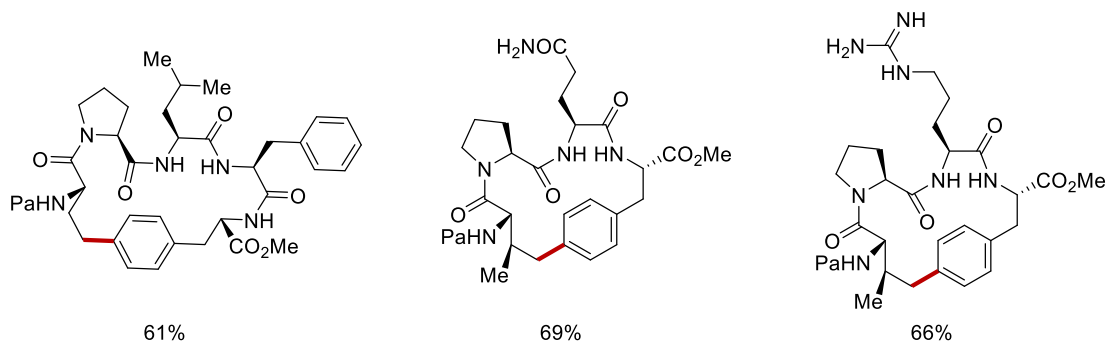
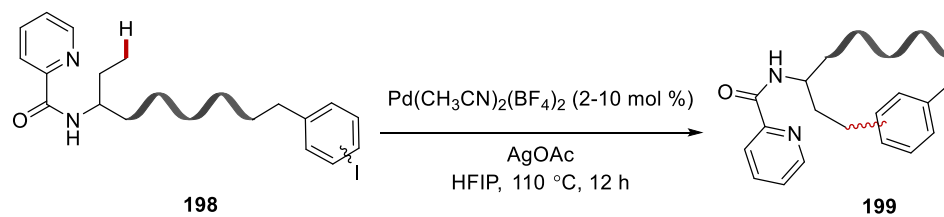


Scheme 1.4.25. Palladium-catalyzed macrocyclization under C-terminus bidentate assistance.

Recently, Chen utilized picolinic acid as the directing group for the *N*-terminus→*C*-terminus $\text{C}(\text{sp}^3)\text{-H}$ macrocyclization. Thus, various linear peptides **198** with amino acids with $\gamma\text{-C-H}$ positioned at the *N*-terminus equipped with a suitably tethered aryl iodide moiety at the *C*-terminus were efficiently cyclized in a stereo- and site-selective fashion (Scheme 1.4.26).^[144] Remarkably, this robust protocol tolerated a plethora of coordinating groups found in the side chains of amino acids, such as amides, amines and guanidine groups, without loss of catalytic efficiency. Furthermore, the linear precursors were easily obtained under standard SPPS techniques, thus facilitating the rapid and facile synthesis of a library of cyclic peptides. Lastly, the directing group was cleanly removed by treatment with zinc in acidic aqueous solution yielding the free-amine cyclic peptide that could be further elongated.

1. Introduction

Chen



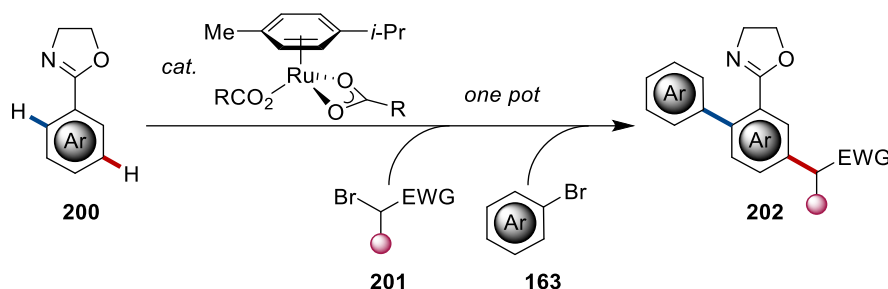
Scheme 1.4.26. Palladium-catalyzed macrocyclization by *N*-terminus bidentate assistance.

2. Objectives

The development of novel and robust C–H functionalization strategies for the expedient diversification of molecules of interest is gaining recent momentum, with translational impact on natural product synthesis,^[23, 145] material chemistry^[24] and medicinal chemistry.^[25a, 25b, 25e] The modular nature of the late-stage C–H functionalization strategy allows an atom- and step-economical exploration of the chemical space. In this regard, 4d and 5d transition metals have dominated the field, relying heavily on significant advancements in palladium-catalyzed cross-coupling technologies. The implementation of Earth-abundant transition metals in C–H activation has recently gained considerable momentum, due to the generally lower cost and toxicity of 3d transition metals compared to their 4d and 5d counterparts.^[26, 146] Thus, the aim of this thesis is directed towards the development of efficient strategies for the late-stage functionalization of (bio)molecules *en route* to complex molecular architectures. Furthermore, in order to address the increasing need for more environmentally-benign C–H transformations, the focus is shifted to inexpensive 3d transition metals, mainly manganese.

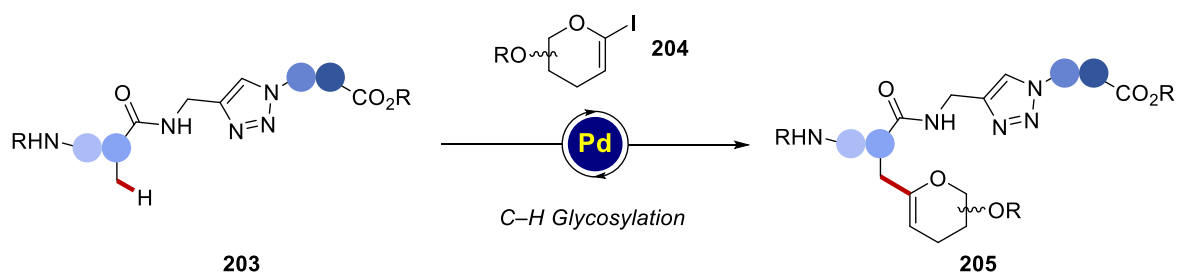
Among the most common ways to ensure sustainability in molecular synthesis, the one-pot strategy is arguably the most straightforward. In this context, elegant domino strategies are most effective, as several new bonds are forged in a single synthetic operation.^[94f] Hence, one-pot reactions are still highly desirable, for the same reasons, but require a sequential addition of reagents. However, these strategies require robust catalysts and precise optimization of the reaction conditions to ensure productive transformations. Thus, within this thesis, a new protocol for the remote functionalization was intended to be merged with the well-established ruthenium-catalyzed *ortho*-C–H arylation in an one-pot fashion. Detailed mechanistic studies were performed to delineate the unique reactivity of the ruthenium-catalyzed remote C–H alkylation manifold (Scheme 2.1).

2. Objectives



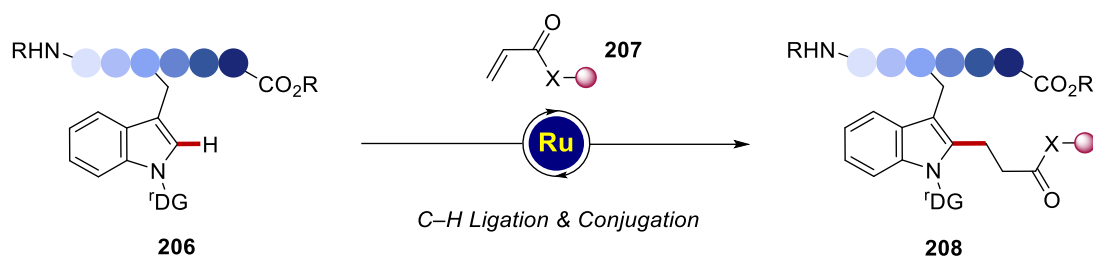
Scheme 2.1. Ruthenium-catalyzed *meta-ortho*-difunctionalization.

Despite undisputed advances, C(*sp*³)-H activation is often more challenging for organometallic C-H activation.^[16e] Palladium-catalyzed C-H activation has been recognized as a reliable tool for this valuable transformation. Recently, the mild and robust nature of this regime led to the efficient functionalization of peptides. Inspired by these advances, we decided to probe the utilization of a suitable sugar-fragment for the late-stage glycosylation of peptides (Scheme 2.2). To enhance the impact of this methodology on medical chemistry, modular triazole-based peptidomimetics were explored as the substrates.



Scheme 2.2. Palladium-catalyzed C-H glycosylation.

Despite significant advances in the functionalization of amino acids and peptides *via* C-H activation, these methods have heavily relied on arylation strategies, with very few exceptions.^[25b, 25g, 147] In the context of sustainable molecular syntheses, hydroarylation manifolds exhibit perfect atom-economy. Furthermore, ruthenium-catalysis has been established as one of the most powerful regimes in the realm of C-H activation, albeit with limited applications in the late-stage functionalization of peptides.^[120] Thus, we became interested in exploiting the potent ruthenium catalysis in an hydroarylation regime for the late-stage diversification and ligation of peptides. Thus, tryptophan was selected as the amino acid to be functionalized due to the ease of incorporating a suitable guiding group onto the indole moiety (Scheme 2.3).

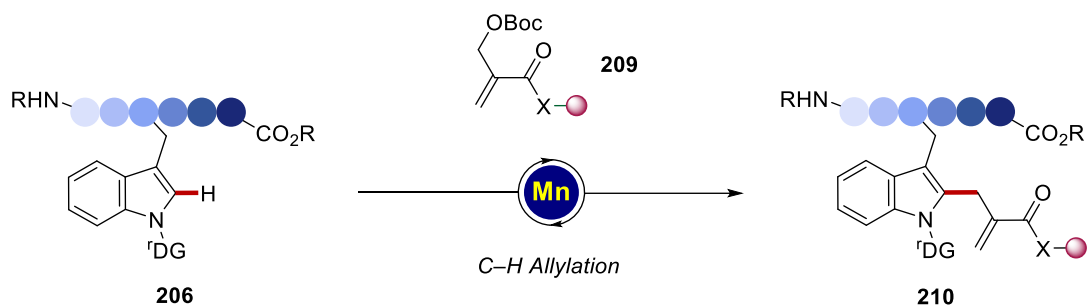


Scheme 2.3. Peptide functionalization under ruthenium-catalysis.

Chelation-assisted C–H activation has matured into an indispensable tool for molecular synthesis, as it allows a reliable and predictable strategy for the functionalization of inert C–H bonds under exceedingly mild conditions. Early efforts have established the use of precious metals for C(sp^2)–H and C(sp^3)–H functionalizations. Thus, various directing groups ranging from nitrogen containing heterocycles to amides and carboxylic acids, among others, have been elegantly utilized.^[16c] Recently, the quest towards sustainability has encouraged the synthetic community to explore Earth-abundant 3d transition metals, as they are typically inexpensive and less toxic.^[26] However, the functionalization of peptides with 3d transition metals is still in its infancy.^[123]

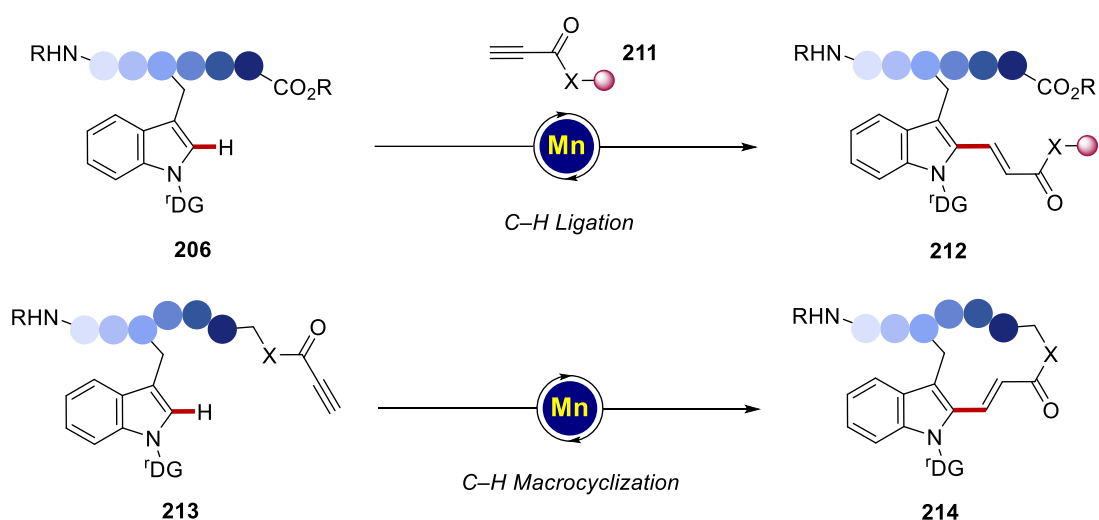
The incorporation of reactive functional groups in peptides in a site-selective fashion is of paramount importance in modern chemical biology. Traditionally, very reactive residues, such as cysteine or lysine, have been exploited for the functionalization of peptides and proteins *via* condensation, (cyclo)additions and more recently cross-coupling manifolds. Thus, the functionalization of inert C–H bonds will greatly enhance our ability to diversify biomolecules. In this context, C–H activation has lately made significant strides by utilizing precious transition metals. Therefore, we decided to explore whether the versatile manganese-catalyzed C–H allylation^[88-89, 92] could be employed for the site-selective functionalization of peptides. The choice of the protected Morita-Baylis-Hillman adducts as allylating agents was based on the final incorporation of the reactive α,β -unsaturated carbonyl moiety in the peptide (Scheme 2.4).

2. Objectives



Scheme 2.4. Manganese-catalyzed C–H allylation of peptides.

The late-stage modification of peptides is not restricted to the incorporation of small substituents. Indeed, the stitching of two distinct biomolecules together results in multifunctional hybrids with many potential applications. More importantly, the coupling of two large peptide fragments is an elegant alternative to traditional iterative peptide couplings, that is routinely utilized. Thus, taking into consideration the remarkable robustness and mildness of manganese(I)-catalysis, our aim was to develop a manganese-catalyzed C–H peptide ligation. Furthermore, the intramolecular variant of this manifold could give rise to a challenging macrocyclization (Scheme 2.5). For this transformation careful optimization of the reaction conditions was required to ensure productive reactions. In order to unlock the full potential of this strategy modular propiolates were selected as the coupling partner.

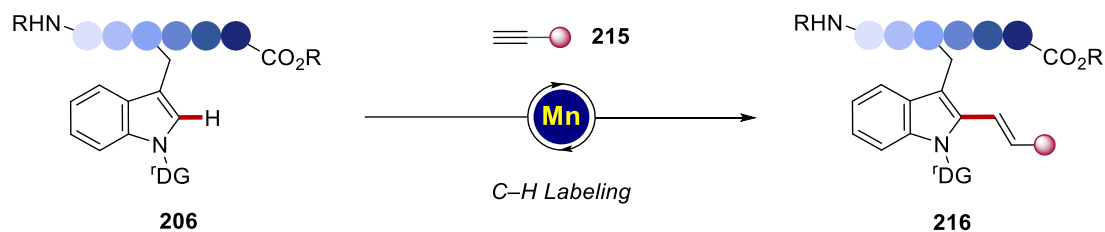


Scheme 2.5. Manganese-catalyzed C–H ligation and macrocyclization.

The labeling of peptides is of paramount importance in many fields of chemical biology, particularly as a tool for the elucidation of biological functions. Traditionally, the labeling of peptides and proteins relies either on lengthy *de novo* strategies, utilizing fluorescent

2. Objectives

building blocks, or on the late-stage labeling of polar residues, such as cysteine or lysine. Inspired by the success of the manganese(I)-catalyzed C–H activation manifold, we decided to probe the modular hydroarylation approach for the labeling of tryptophan-containing peptides (Scheme 2.6). To this end, BODIPY fluorophores were chosen, as their modular nature can swiftly provide versatile probes.



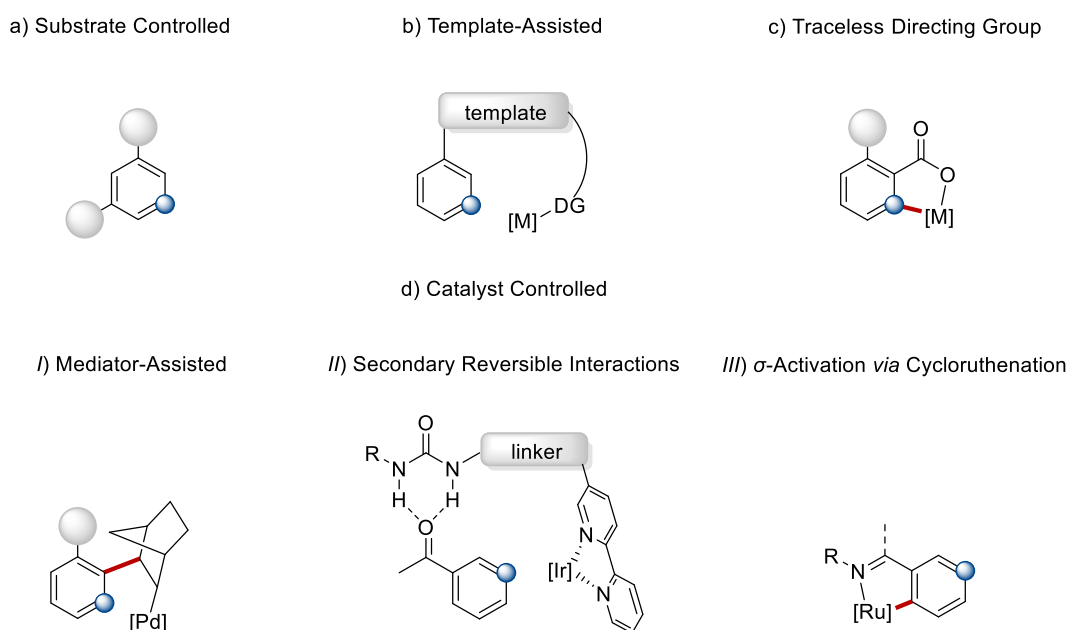
Scheme 2.6. Manganese-catalyzed C–H labeling.

3. Results and Discussion

3. Results and Discussion

3.1. Sequential *meta/ortho*-C–H Functionalization of Aryl Oxazolines via Ruthenium Catalysis

During the beginning of the utilization of C–H activation in molecular synthesis, the *ortho*-functionalization was the most widely used, as many reaction types that had been developed relied on the proximity induced C–H cleavage. Whereas, these advancements had profound impact on the synthetic organic chemistry, they are inherently restricted to *ortho*-functionalization. To unlock the full potential of C–H activation, new strategies for the functionalization of remote C–H bonds had to be developed. In this regard, if the selective *meta* or *para* C–H cleavage can be achieved, the downstream functionalization of the organometallic intermediate would result in a plethora of new remote transformation, under similar reaction conditions utilized for *ortho*-functionalization. Recently, strategies for achieving remote metalation have been developed, based on substrate control,^[16k] templates,^[48, 50] traceless directing group (formal *meta*-functionalization),^[148] and elaborate mediators,^[49] ligands^[149] and catalysts^[36b, 52-53] (Scheme 3.1.1). In contrast these strategies, σ -activation *via* cycloruthenation is unique, since it relies on the *ortho*-cycloruthenation that directs the addition of a nucleophilic or electrophilic alkyl radical *para*-to-the-ruthenium.



Scheme 3.1.1. Strategies for remote C–H functionalization.

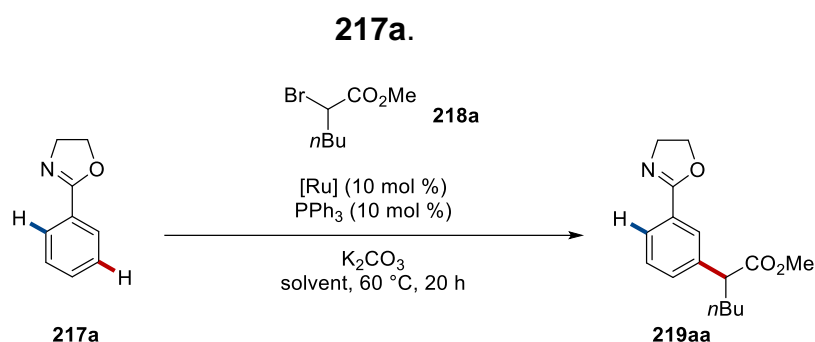
Despite, the powerful nature of σ -activation *via* cycloruthenation, to date only strongly coordinating directing groups, such as pyridines and pyrazoles, have been utilized. These auxiliary groups are usually difficult to remove, or to transform to other synthetically useful functional groups, with scarce exceptions.^[60] These, limitations severely limit the broad utilization of such methodologies. Thereby, we became interested in the development of an atom- and step-economical method for the *meta*-alkylation of versatile aryl oxazolines, which are surrogates of carboxylic acids. We chose as coupling partners the reactive and modular α -bromo carbonyl compounds. Furthermore, we reasoned that the powerful ruthenium-catalyzed *ortho*-C–H activation manifold could be combined with the *meta*-functionalization manifold in a sequential difunctionalization regime.

3.1.1. Optimization Studies for Ruthenium-Catalyzed *meta*-C–H Alkylation *via* Oxazoline Assistance

After initial optimization for the remote ruthenium-catalyzed alkylation *via* strongly coordinating pyrimidine assistance by Dr. K. Korvorapun, we probed whether the powerful ruthenium-catalyzed *meta*-alkylation regime could be applicable for the functionalization of synthetically useful oxazolines. Hence, we chose the functionalization of 2-phenyl-4,5-dihydrooxazole **217a** with methyl 2-bromohexanoate **218a** under ruthenium catalysis as our model system (Table 3.1.1). Thus, we commenced our studies for the desired functionalization by probing different ruthenium-based catalytic systems employing PPh₃ as the ligand and K₂CO₃ as the base (entries 1-5). Carboxylate assistance was found to be essential for the envisioned remote alkylation process, whereas, 1,4-dioxane was shown to be the optimal solvent (entry 7). The reaction showed similar efficiency even at 40 °C (entry 9), further reflecting the high catalytic efficacy of the ruthenium(II)-biscarboxylate catalysis manifold. Control experiment demonstrated the crucial role of the phosphine additive (entry 10), suggesting a synergistic regime to be operative.

3. Results and Discussion

Table 3.1.1. Optimization of the ruthenium-catalyzed *meta*-alkylation of oxazoline



Entry	[Ru]	Solvent	Yield (%)
1	-	1,4-dioxane	-
2	Ru ₃ (CO) ₁₂	1,4-dioxane	-
3	[RuCl ₂ (<i>p</i> -cymene)] ₂	1,4-dioxane	(<5)
4	[RuCl ₂ (<i>p</i> -cymene)] ₂	1,4-dioxane	(<5) ^{a, b}
5	[Ru(O ₂ CMes) ₂ (<i>p</i> -cymene)]	toluene	(17)
6	[Ru(O ₂ CMes) ₂ (<i>p</i> -cymene)]	DCE	(10)
7	[Ru(O₂CMes)₂(<i>p</i>-cymene)]	1,4-dioxane	76
8	[Ru(O ₂ CAd) ₂ (<i>p</i> -cymene)]	1,4-dioxane	73
9	[Ru(O ₂ CMes) ₂ (<i>p</i> -cymene)]	1,4-dioxane	65 ^c
10	[Ru(O ₂ CMes) ₂ (<i>p</i> -cymene)]	1,4-dioxane	(<5) ^a

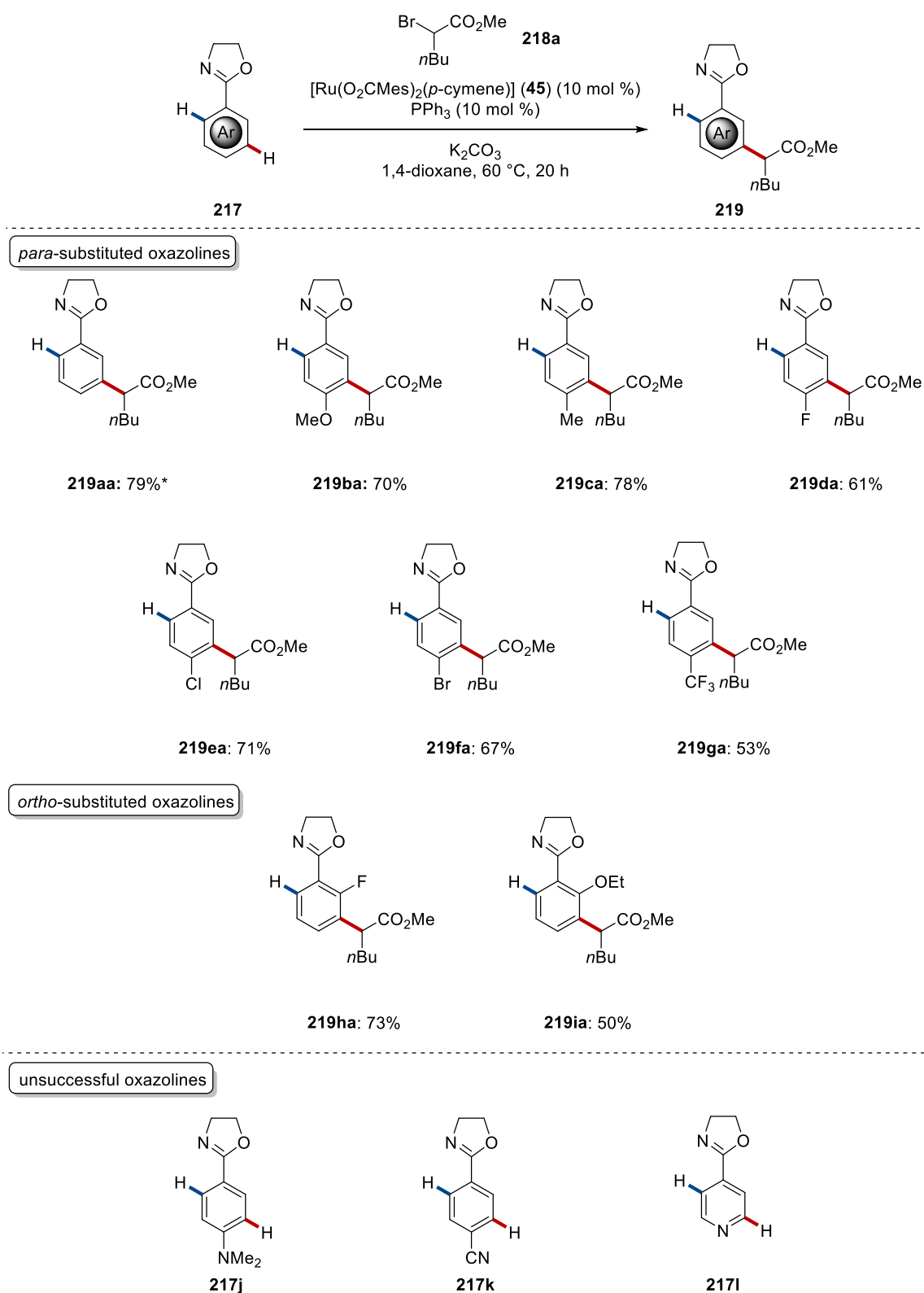
Reaction conditions: **217a** (0.50 mmol), **218a** (1.5 mmol), [Ru] (10 mol %), PPh₃ (10 mol %), K₂CO₃ (1.0 mmol), solvent (2.0 mL), 60 °C, 20 h. Yields of isolated product. Conversion are given in parentheses based on ¹H-NMR analysis with CH₂Br₂ as internal standard. ^a Without PPh₃. ^b With AgSbF₆ (20 mol %). ^c The reaction was performed at 40 °C.

3.1.2. Scope of the Ruthenium-Catalyzed *meta*-C–H Functionalization via Oxazoline Assistance

With the optimized reaction conditions in hand for the ruthenium(II)-catalyzed *meta*-alkylation of 2-aryl-oxazolines **217** with 2-bromo carbonyl compounds **218** we explored

its versatility by probing different aryl-oxazolines **217** as substrates (Scheme 3.1.2). The robustness of our alkylation manifold was reflected by the gram scale synthesis of alkylated oxazoline **219**, with similar efficiency, even when utilizing a reduced catalyst loading. To our delight, electron-rich and electron-deficient arenes **217** were smoothly alkylated in a chemo- and site-selective fashion. Thus, many functional groups at the *para*-position of the aryl moiety, such as fluoro, chloro, bromo and trifluoromethyl were well tolerated, exclusively leading to *meta*-functionalizations. In addition, *ortho*-substituted aryl oxazolines **217h** and **217i** were regioselectively alkylated leading to the more sterically-hindered 1,2,3-substituted oxazolines **219ha** and **217ia**. Unfortunately, *meta*-substituted oxazolines led to unsatisfactory results under otherwise similar reaction conditions. Furthermore, dimethylamino, cyano and pyridine groups were not tolerated on the aryl moiety.

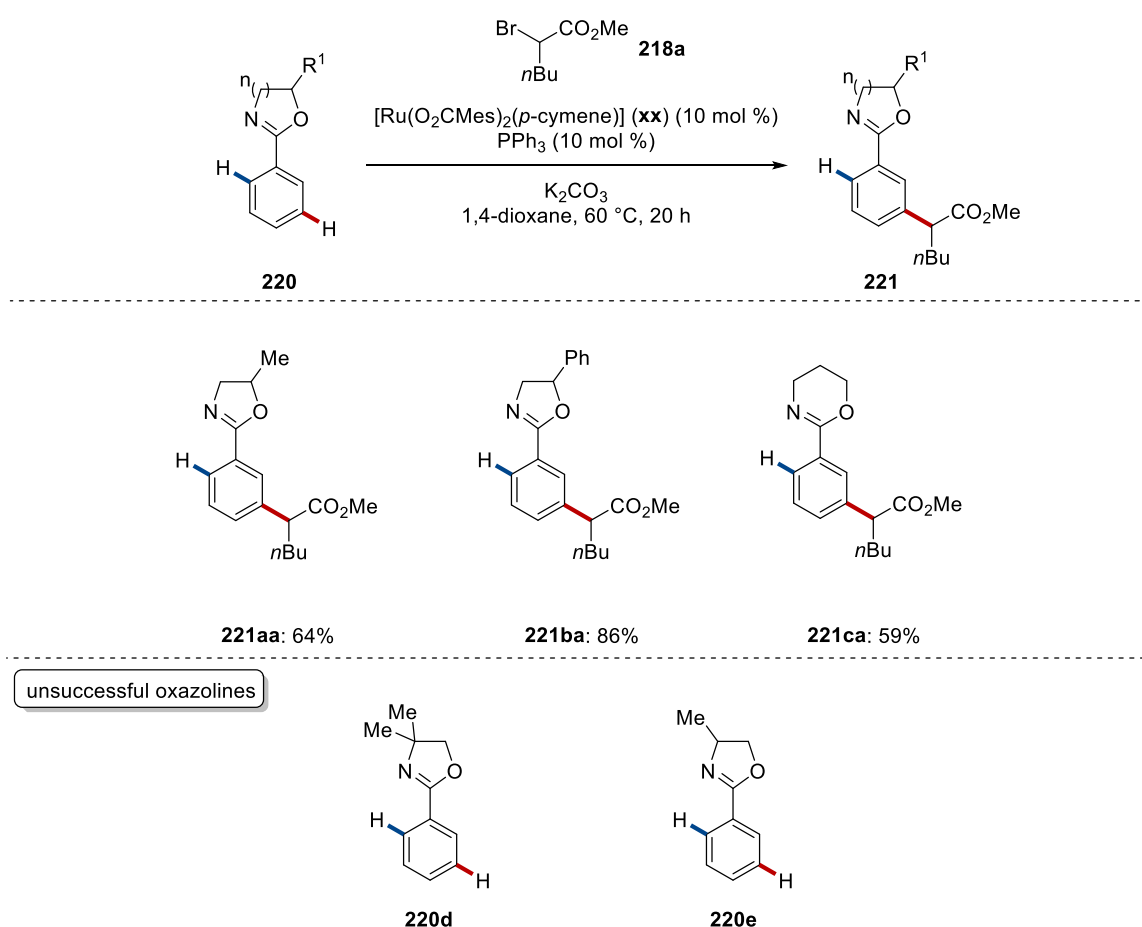
3. Results and Discussion



Scheme 3.1.2. Ruthenium(II)-biscarboxylate catalysis for the *meta*-alkylation via oxazoline assistance. ^a Gram-scale, [Ru(O₂CMe)₂(*p*-cymene)] (**45**) (5.0 mol %), PPh₃ (5.0 mol %).

3. Results and Discussion

Next, the substitution pattern on the unsaturated heterocyclic ring was investigated. Thus, alkylated and arylated oxazolines as well as their six-membered counterpart, oxazines, were subjected to our remote-alkylation manifold (Scheme 3.1.3). To our delight, alkyl and aryl substituents α to the oxygen were well tolerated, and *meta*-alkylated oxazolines **220a** and **220b** were obtained in a site-selective fashion. Unfortunately, substituents α to the nitrogen were not tolerated, presumably due to the increased steric hindrance during the key cycloruthenation step. Lastly, oxazine **220c** was efficiently alkylated in a chemo- and site-selective manner, albeit with slightly diminished efficiency.

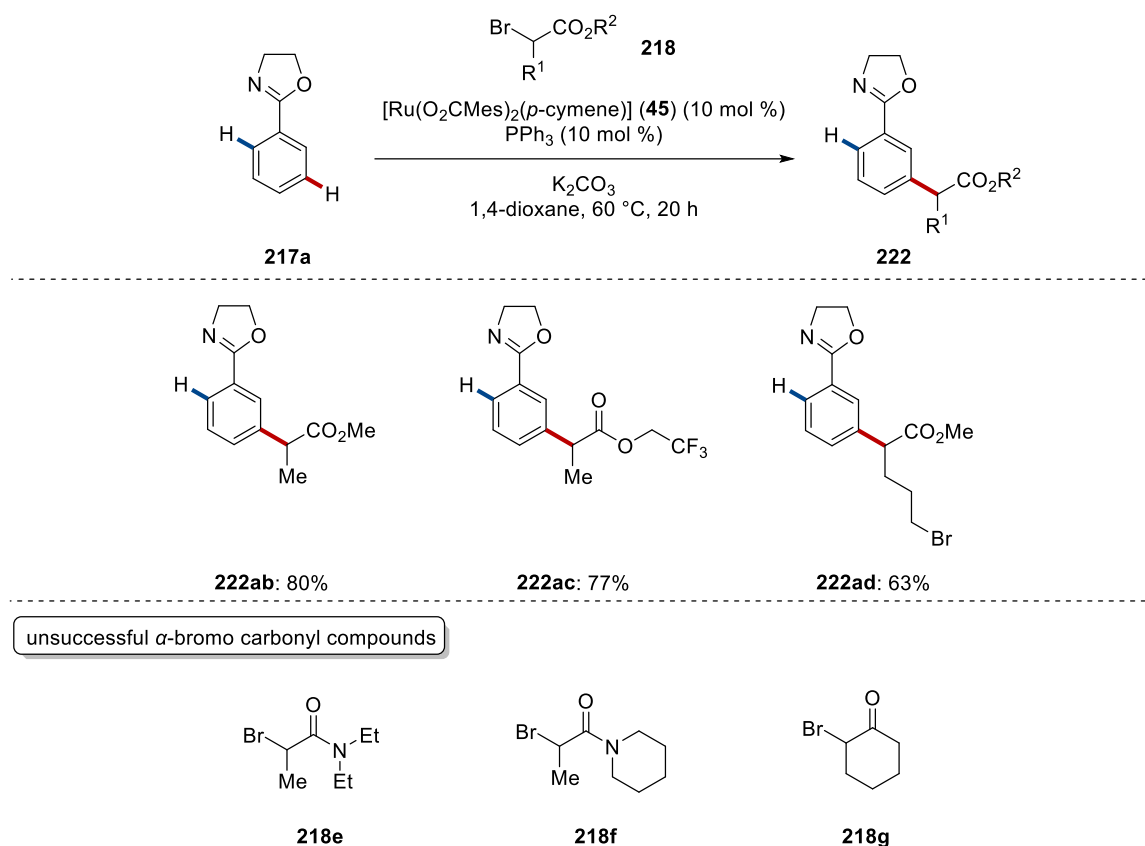


Scheme 3.1.3. Ruthenium(II)-biscarboxylate catalysis for the *meta*-alkylation via *N*-coordination with various heterocycles.

Next, the substrate scope of the α -bromo carbonyl compound partner was investigated (Scheme 3.1.4). Thus, various α -bromo esters were efficiently employed in our remote-alkylation manifold, remarkably the *meta*-functionalized oxazoline **222** featuring the primary alkyl bromide moiety was obtained with excellent levels of chemoselectivity,

3. Results and Discussion

completely bypassing *ortho*-alkylative regimes.^[36a-c] Unfortunately, α -bromo ketones and amides gave unsatisfactory results under otherwise similar reaction conditions.

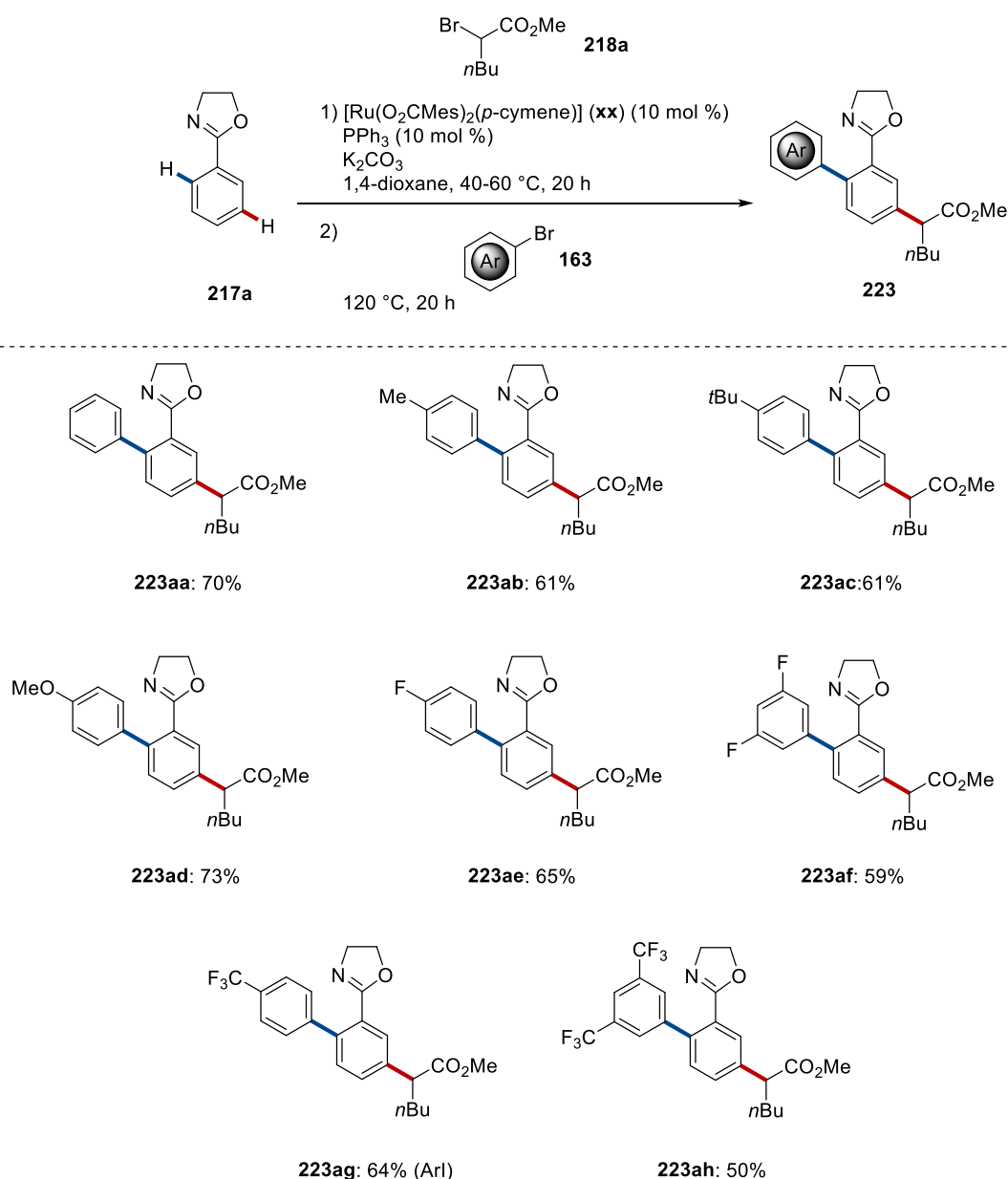


Scheme 3.1.4. Ruthenium(II)-biscarboxylate catalysis for the *meta*-alkylation with various α -bromo esters **218**.

Having established a mild and robust methodology for the *meta*-alkylation of a variety of substituted oxazolines with modular α -bromo esters and taking into consideration the powerful ruthenium-catalyzed *ortho*-C–H activation manifolds, we probed whether a sequential *meta*-/*ortho*-C–H difunctionalization type of regime could be unraveled.^[150] We reasoned whether upon completion of the *meta*-C–H alkylation the addition of an appropriate coupling partner would lead to the site-selective 1,4-difunctionalization of arene moiety by sterically-controlled C–H cycloruthenation. Among the plethora of ruthenium(II)-catalyzed reactions, the *ortho*-arylation was selected as the most suitable, due to its remarkable robustness.^[151] To our delight, after completion of the reaction of 2-phenyl-4,5-dihydrooxazole (**217a**) with methyl 2-bromohexanoate (**218a**), and hence resulting in the formation of *meta*-alkylated oxazoline **219aa**, the simple addition of bromo arene **163a** led to the site-selective

formation of difunctionalized oxazoline **223aa**. Key features of this sequential method that led to the observed selectivity are a) the initial *meta*-functionalization is remarkably mono-selective and b) the introduced *meta* substituent is large enough to block its *ortho* positions. Thus, our strategy allowed for the chemo- and site-selective difunctionalization under ruthenium(II)-biscarboxylate catalysis, under two mechanistically distinct pathways. Encouraged by this finding, the scope with regards to the aryl electrophile **163** was explored (Scheme 3.1.5). Electron-rich arenes **163** bearing methyl, *tert*-butyl and methoxy substituents were efficiently employed leading to the desired products **223ab**, **223ac** and **223ad** with excellent levels of site-selectivity. Furthermore, fluorinated aryl bromides **163e** and **163f**, featuring distinct substitution patterns, were also smoothly employed. Moreover, difunctionalized oxazolines **223ag** and **223ah** bearing trifluoromethyl groups were obtained in an efficient and site-selective manner.

3. Results and Discussion

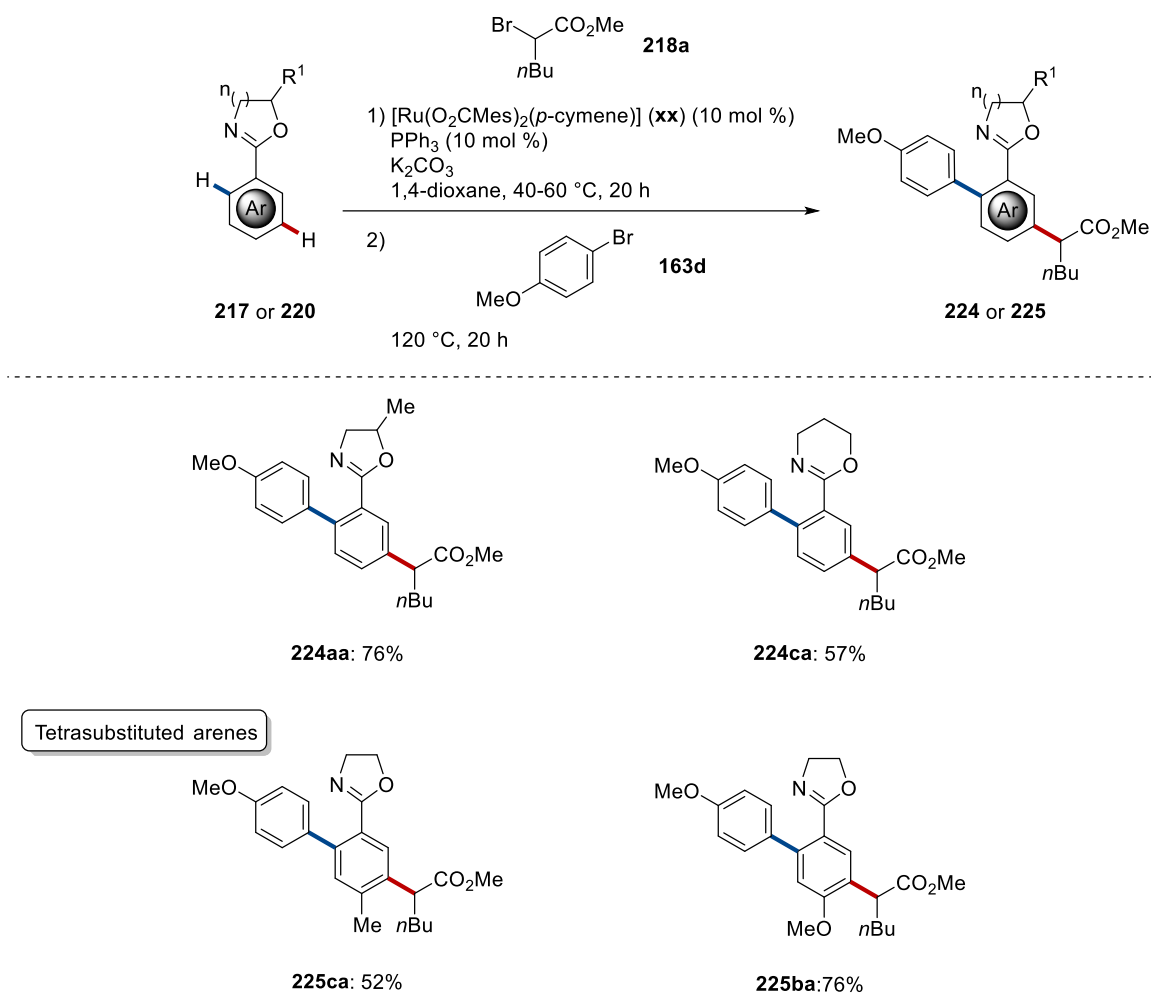


Scheme 3.1.5. Ruthenium(II)-biscarboxylate catalysis for the one-pot *meta-/ortho*-difunctionalization *via* oxazoline assistance. ^a Aryl iodide **163g** was used.

Having established a robust and site-selective manifold for the 1,4-difunctionalization of aryl oxazolines **223** with various aryl electrophiles, we moved on to explore the generality of our process with regards to the oxazoline moiety (Scheme 3.1.6). Thus, substituted oxazoline **221a** and oxazine **22ac** were subjected to our sequential *meta-/ortho*-functionalization approach. Under the optimized reaction conditions both scaffolds were selectively difunctionalized leading to the desired oxazoline **224aa** and oxazine **224ca**, respectively. Thereby, our approach led to the synthesis of 1,2,4-trisubstituted arenes *via* ruthenium-catalyzed difunctionalization, hence we became

3. Results and Discussion

intrigued to probe whether tetrasubstituted arenes could be obtained. Remarkably, when *para*-substituted oxazolines **217** were utilized in our difunctionalization manifold, 1,2,4,5-tetrasubstituted arenes **225ca** and **225ba** were obtained in a site-selective manner.

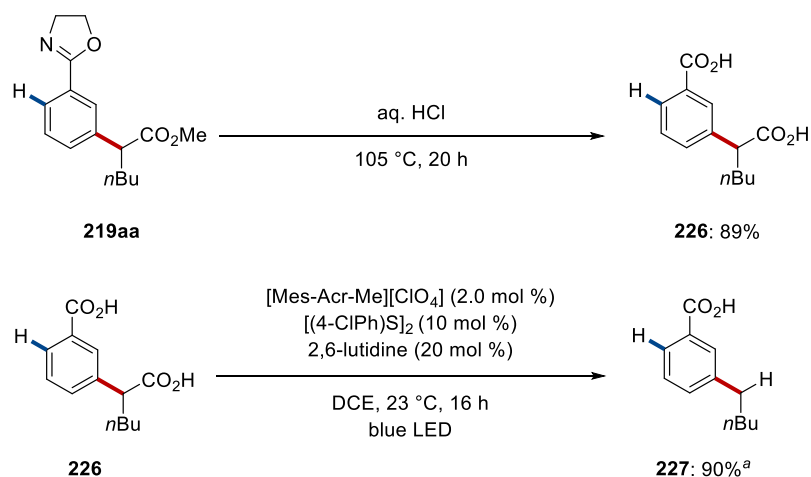


Scheme 3.1.6. One-pot ruthenium(II)-biscarboxylate catalysis for the *meta*-/*ortho*-difunctionalization of various oxazolines.

3.1.3. Diversification of the Functionalized Oxazolines

Our strategy provided an expedient access to various mono- and difunctionalized oxazolines **219** and **223**. Since oxazolines are versatile building blocks in organic synthesis, we probed whether we could modify this scaffold to other valuable functional group (Scheme 3.1.7). Thus, oxazoline **219aa** was subjected to acidic hydrolysis conditions resulting in the formation of the di-acid **226** in excellent yield. The di-acid **226** was then reductively decarboxylated under photoredox conditions, thereby obtaining the *meta*-alkylated benzoic acid **227**.

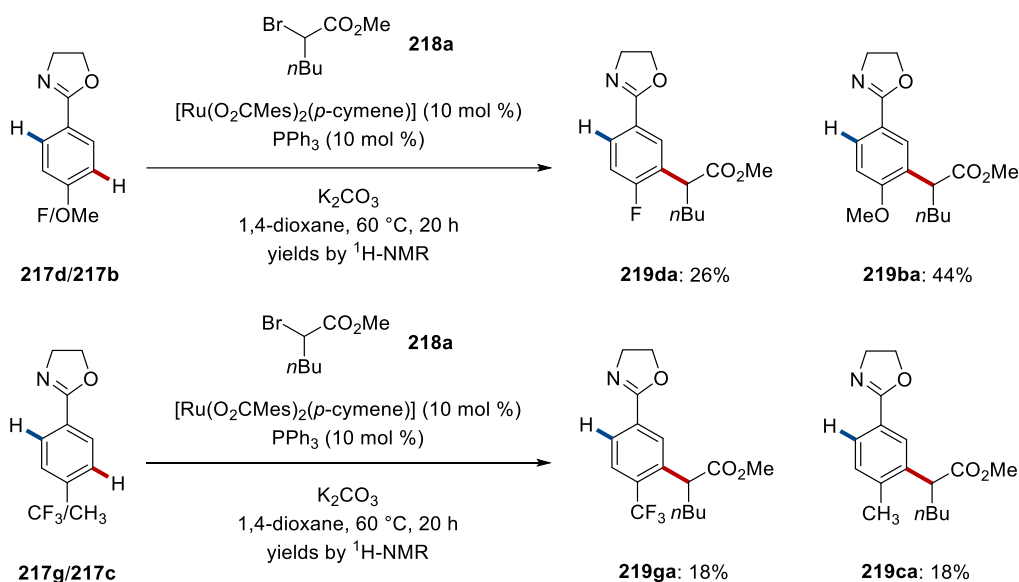
3. Results and Discussion



Scheme 3.1.7. Diversification of the *meta*-alkylated oxazoline. ^a Performed by Dr. K. Korvorapun.

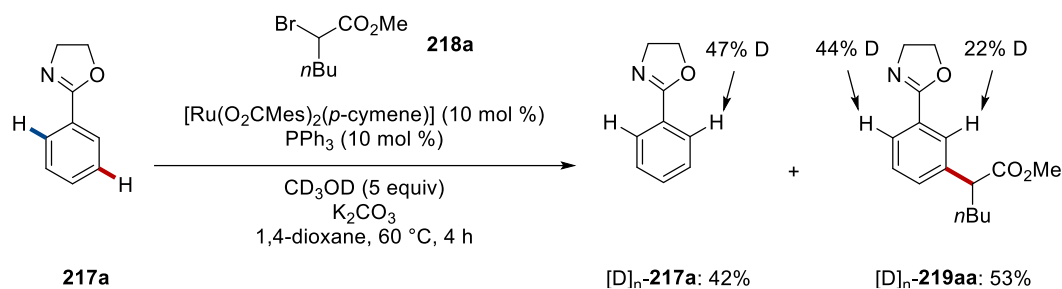
3.1.4. Mechanistic Studies

To shed light into the ruthenium(II)-catalyzed *meta*-alkylation, mechanistic studies were conducted next. Competition experiments between electron-rich and electron-deficient aryl oxazolines **217** were performed under our optimized reaction conditions (Scheme 3.1.8). The results, showed a slight preference for electron-rich oxazolines, thus ruling out a CMD pathway. Instead a BIES type C–H activation manifold is likely operative.



Scheme 3.1.8. Intermolecular competition experiments for the ruthenium-catalyzed *meta*-alkylation *via* oxazoline assistance.

Next, the key cycloruthenation step was examined. Initially, an H/D exchange experiment with deuterated methanol was performed. The recovered starting material **217a** and the product **219aa** showed significant levels of H/D scrambling, suggesting a reversible cycloruthenation (Scheme 3.1.9). Furthermore, the larger D-incorporation in the least hindered *ortho*-position of the product **219aa** showcased the observed positional selectivity of our *meta*-/*ortho*-difunctionalization regime.



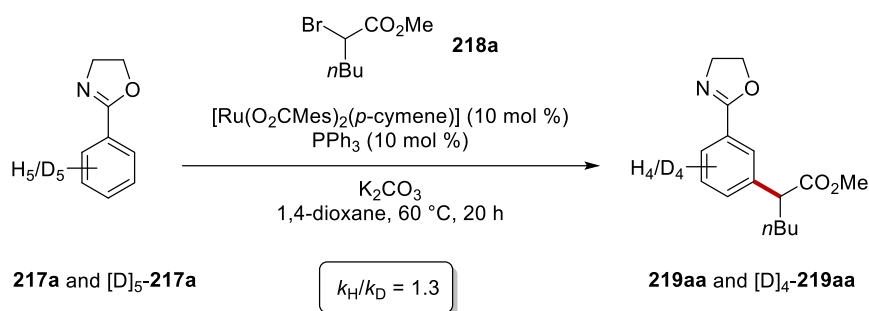
Scheme 3.1.9. H/D exchange experiment with CD_3OD .

After confirming a reversible C–H cycloruthenation, experiments to determine the deuterium kinetic isotope effect were conducted (Scheme 3.1.10). To this end, an intermolecular competition experiment between **217a** and $[\text{D}]_5\text{-217a}$ was performed resulting in a minor KIE of $k_{\text{H}}/k_{\text{D}} = 1.3$. Furthermore, the KIE was also determined *via* the comparison of the relative reaction rates of **217a** and $[\text{D}]_5\text{-217a}$, by independent experiments, under the optimized reaction conditions. Similarly, **217a** showed only a slightly higher reaction rate than $[\text{D}]_5\text{-217a}$, therefore strongly suggesting that the C–H activation step is not kinetically relevant. Hence, the crucial C–H-cycloruthenation is fast.

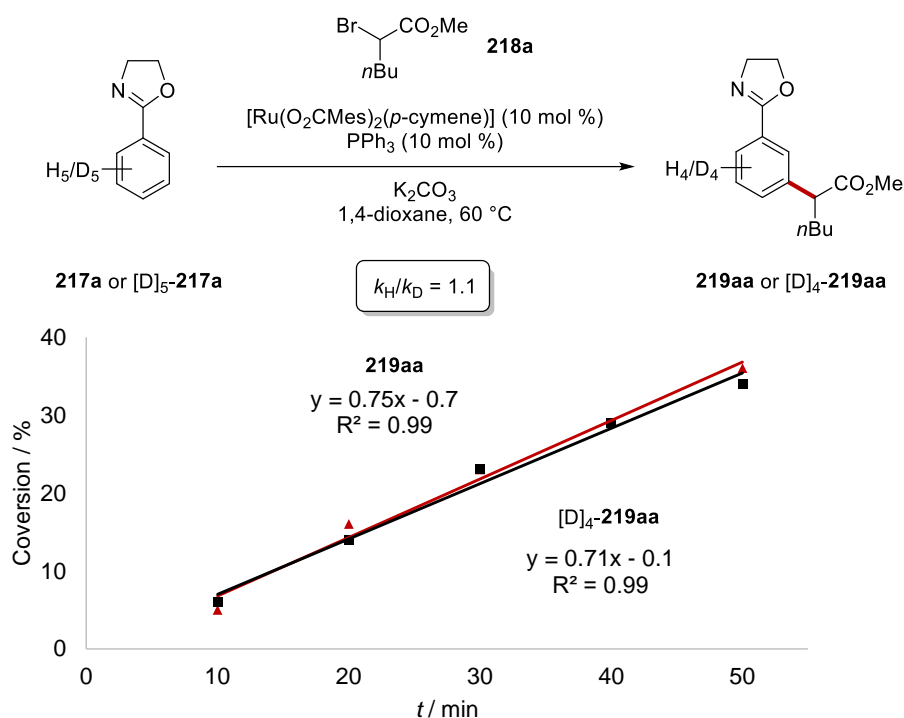
Additional mechanistic studies, performed by Dr. K. Korvorapun, revealed the involvement of radical species in the mechanism. This was strongly suggested by inhibition of the reaction by radical scavengers, the trapping of the stabilized alkyl radical as the TEMPO-adduct, the loss of the stereogenic information from an enantioenriched alkyl bromide during the conversion to the product and finally by the detection of an alkyl radical species by spin-trap label EPR studies. Furthermore, to rationalize the positional selectivity of the *meta*-alkylation manifold, computation studies, analyzing Fukui Indices, were performed by Dr. T. Rogge, which showcased that the dissociation of the *p*-cymene ligand from the ruthenium catalyst was crucial for achieving the observed selectivity. Recent studies by Ackermann also support an arene ligand-free manifold for a plethora of *meta*-alkylations *via* N-assistance.^[61]

3. Results and Discussion

a) Intermolecular KIE by competition



b) Intermolecular KIE by independent experiments

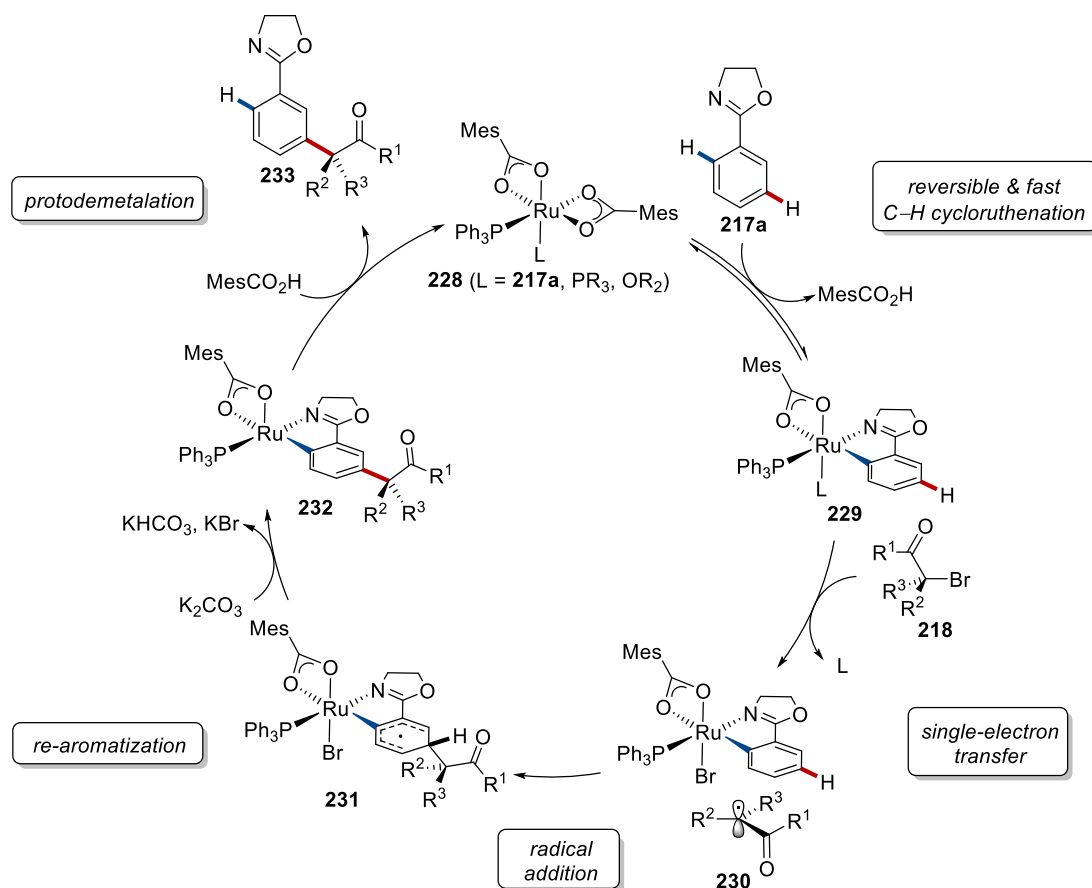


Scheme 3.1.10. KIE experiments for the ruthenium-catalyzed *meta*-alkylation via oxazoline assistance.

3.1.4. Proposed Catalytic Cycle for the Ruthenium-Catalyzed C–H *meta*-Alkylation via Oxazoline Assistance

Based on our mechanistic and computational findings we propose a plausible catalytic cycle to commence by reversible and facile carboxylate-assisted C–H cycloruthenation (Scheme 3.1.11). Thereafter, SET occurs from the ruthenium(II) complex **229** to the alkyl halide **218**, generating after halide transfer the cyclometalated ruthenium(III) intermediate **229**. Radical addition on the aromatic moiety then proceeds at the position *para*-to-the-ruthenium, leading to species **231**, subsequent re-aromatization

furnishes ruthenacycle **232**. Finally, protodemetalation delivers the desired *meta*-substituted product **233**, and at the same time regenerates the catalytically active ruthenium(II) complex **228**.

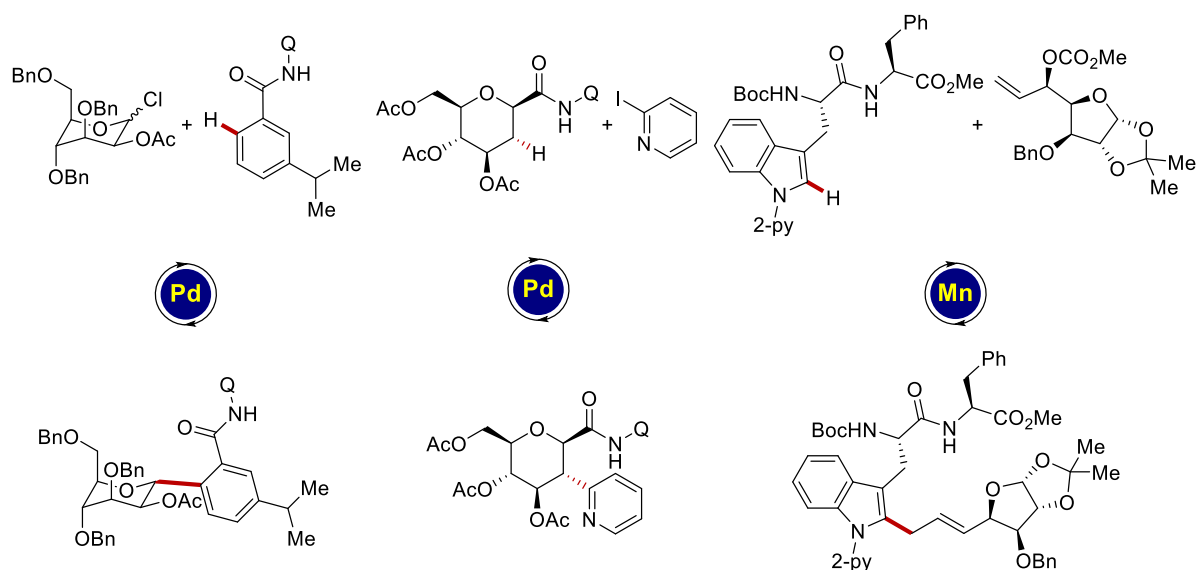


Scheme 3.1.11. Plausible catalytic cycle for the ruthenium-catalyzed *meta*-alkylation.

3. Results and Discussion

3.2. Palladium-Catalyzed C(sp²)-H and C(sp³)-H Late-Stage Glycosylation

Sugars are a class of biomolecules which have notably found applications to *inter alia* drug development.^[152] Thus, the efficient and precise manipulation of naturally occurring sugar motifs is of utmost importance in terms of synthetic applications as well as pharmaceutical applications. In this context, glycopeptides hold a special place as many glycopeptides, such as vancomycin, telavancin and ramoplanin, among others, exhibit high antibiotic potency.^[153] The assembly of these daunting targets typically require many synthetic steps, therefore their expedient implementation in clinical settings is severely hindered. Furthermore, the elucidation of key structure-activity relationships that is necessary for developing highly potent antibiotics is resource- and time-intensive. Recently, palladium-catalyzed C-H activation has made some initial forays with a few C(sp²)-H glycosylation strategies by utilizing aryl iodides,^[154] 1-iodoglucals,^[155] or glycosyl halides,^[156] in arylation, vinylation or alkylation manifolds, respectively (Scheme 3.2.1). Very recently, manganese catalysis gave expedient access to allylated glycopeptides featuring a C(sp²)-C(sp³) bond between a tryptophan residue and a sugar scaffold.^[157]



Scheme 3.2.1. Selected emerging strategies for C-H glycosylations.

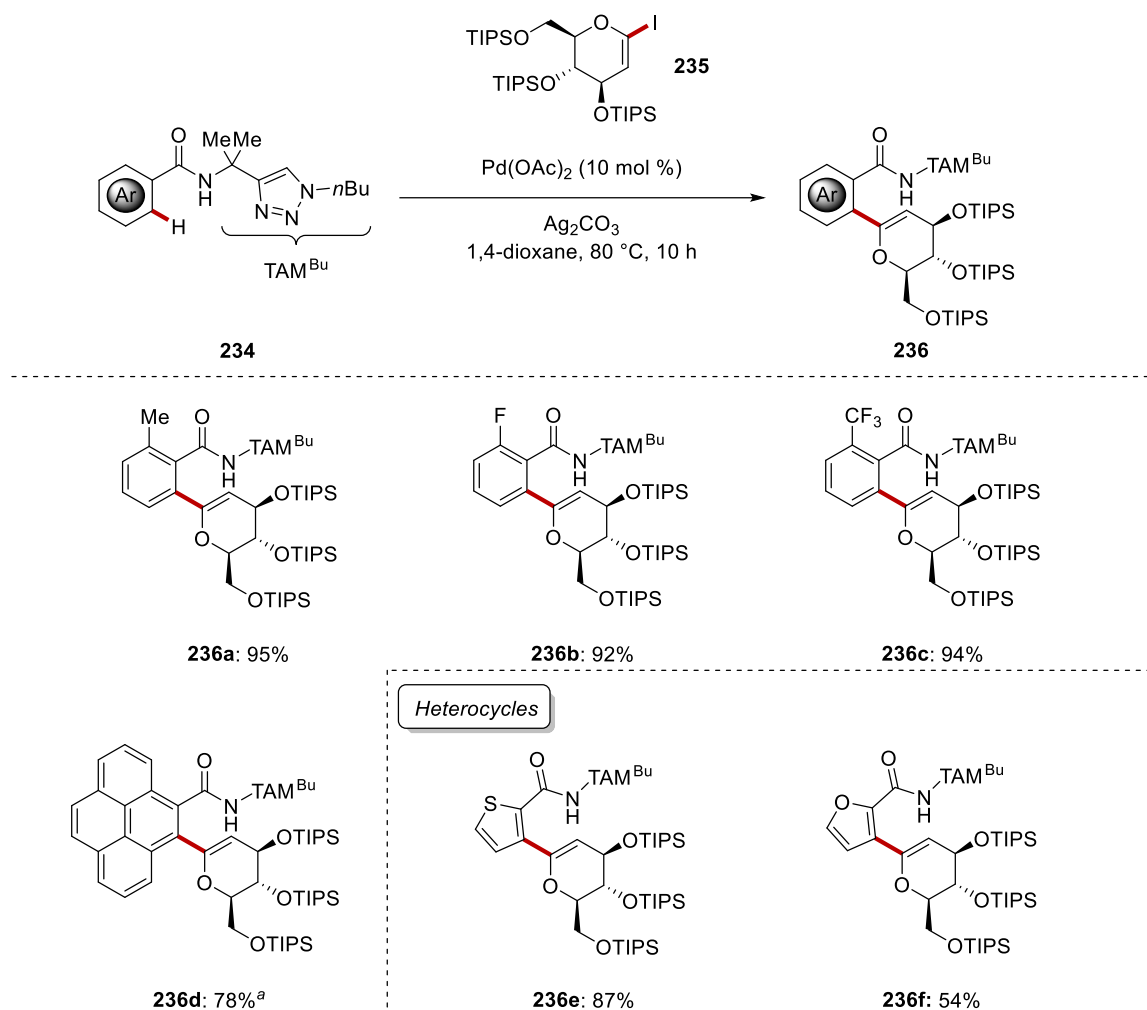
Therefore, we became interested in the development of an atom- and step-economical method for the late-stage C-H glycosylation of arenes and peptides. Despite the significant recent progress in the late-stage functionalization of amino acids and peptides,^[25b, 25g, 147] the efficient functionalization of sugar scaffolds is still in its infancy

as many potential pitfalls could appear. This is the case due to the sensitivity of the densely functionalized polyoxygenated rings and to the stereochemical issues associated with the chiral environment. Hence, we decided to probe whether palladium catalysis, *via* bidentate assistance, could be used for establishing a reliable platform for the late-stage glycosylation by utilizing 1-iodo-glucals. Furthermore, the reliable palladium catalysis would potentially allow not only the C(*sp*²)-H but also the significantly more challenging C(*sp*³)-H glycosylation. To this end, the modular family of triazole-based directing group was selected, since this would allow the implementation of this approach to the internal peptide glycosylation.

3.2.1. Scope of the Palladium-Catalyzed C(*sp*²)-H Glycosylation

Initial optimization studies, performed by J. Wu, showcased the importance of the bidentate directing group on the benzoic acid moiety. Among the commonly utilized bidentate directing groups examined, the triazole-based directing group, TAM, demonstrated the highest efficacy for the desired C(*sp*²)-H glycosylation by utilizing iodo-glucal **235**. Thus, under the optimized reaction conditions, consisting of catalytic amounts of palladium acetate along with stoichiometric amounts of silver carbonate in 1,4-dioxane at 80 °C, various (hetero)arenes were chemo- and site-selectively glycosylated (Scheme 3.2.2). More precisely, substituted arenes with electron-donating and electron-withdrawing groups were efficiently converted to the desired C-aryl glycosides **236**, featuring methyl, fluoro, and trifluoromethyl groups. Moreover, 1-substituted pyrene-derived benzamide **234d** was selectively glycosylated at the C2 and not at the *peri* C10 position, due to the preferential formation of the 5,5 fused bicyclic palladacycle over the 5,6 fused bicyclic palladacycle. The *para*-substituted benzamides **234** gave inseparable mixtures of *mono*- and *di*-functionalized products, thus limiting their applicability in this methodology. Furthermore, heteroarenes equipped with the TAM^{Bu} directing group were similarly glycosylated, under the optimized reaction conditions. Thus, electron-rich five-membered heterocycles, such thiophene and furan, were efficiently converted to the corresponding C-aryl glycosides **236e** and **236f**.

3. Results and Discussion



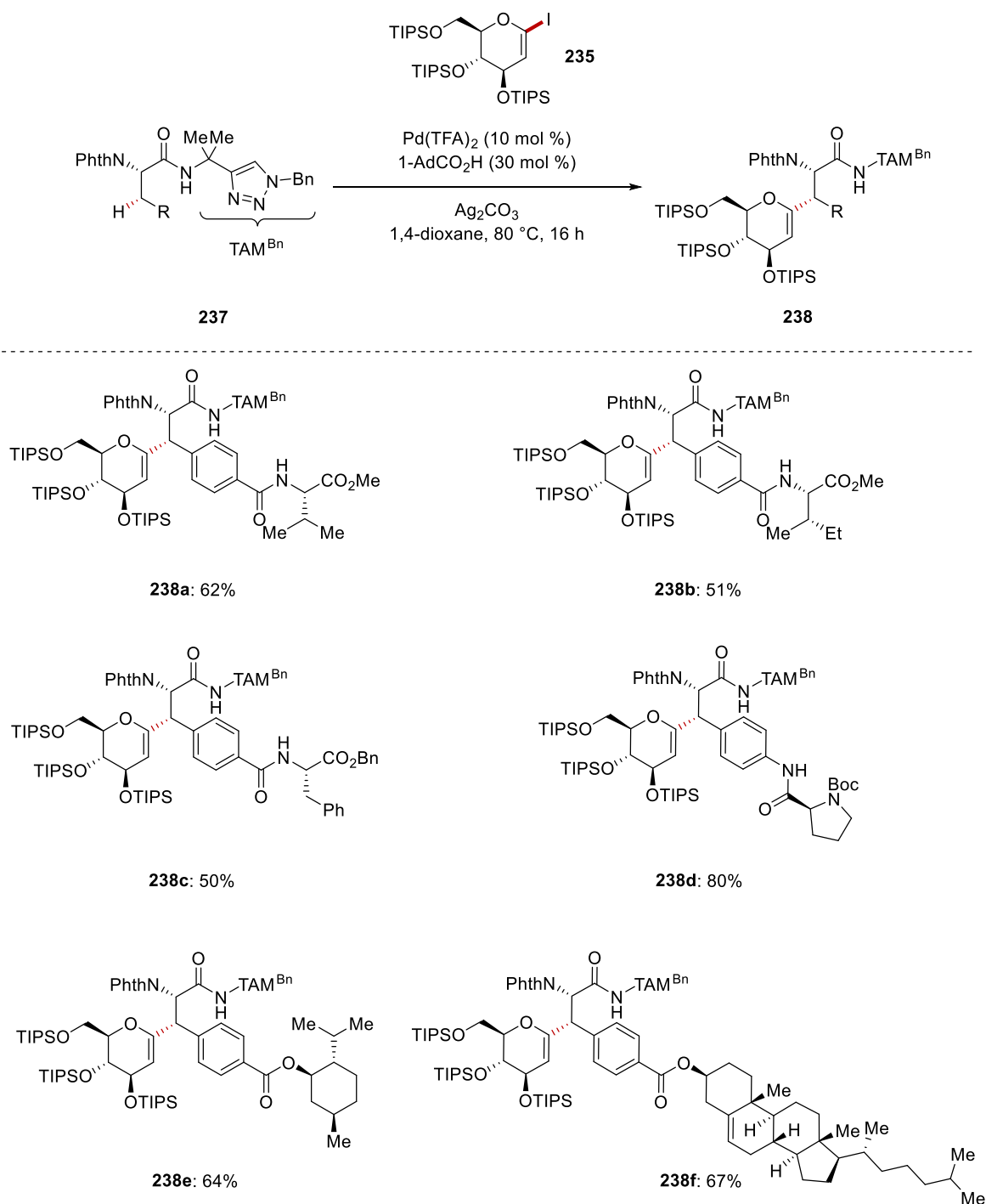
Scheme 3.2.2. Late-stage C(*sp*²)-H glycosylation *en route* to C-aryl glycosides. ^a Performed by J. Wu.

3.2.2. Scope of the Palladium-Catalyzed C(*sp*³)-H Glycosylation

Having established a robust and site-selective C(*sp*²)-H glycosylation approach, we probed whether the powerful palladium catalysis could be utilized for the late-stage C(*sp*³)-H glycosylation of amino-acids and peptides. This approach would lead to the synthesis of C-alkyl glycosides. In this context, under slightly modified reaction conditions, consisting of catalytic amounts of palladium trifluoroacetate and 1-adamantanecarboxylic acid along with stoichiometric amounts of silver carbonate in 1,4-dioxane at 80 °C, a plethora of amino acid derivatives **237** were chemo- and site-selectively glycosylated. Remarkably, the challenging secondary C(*sp*³)-H activation proceeded with excellent levels of stereocontrol, due to the formation of the least sterically congested palladacycle.^[131] Thus, decorated phenylalanine moieties **238**, featuring amino acids and natural products on the side chain, were efficiently

3. Results and Discussion

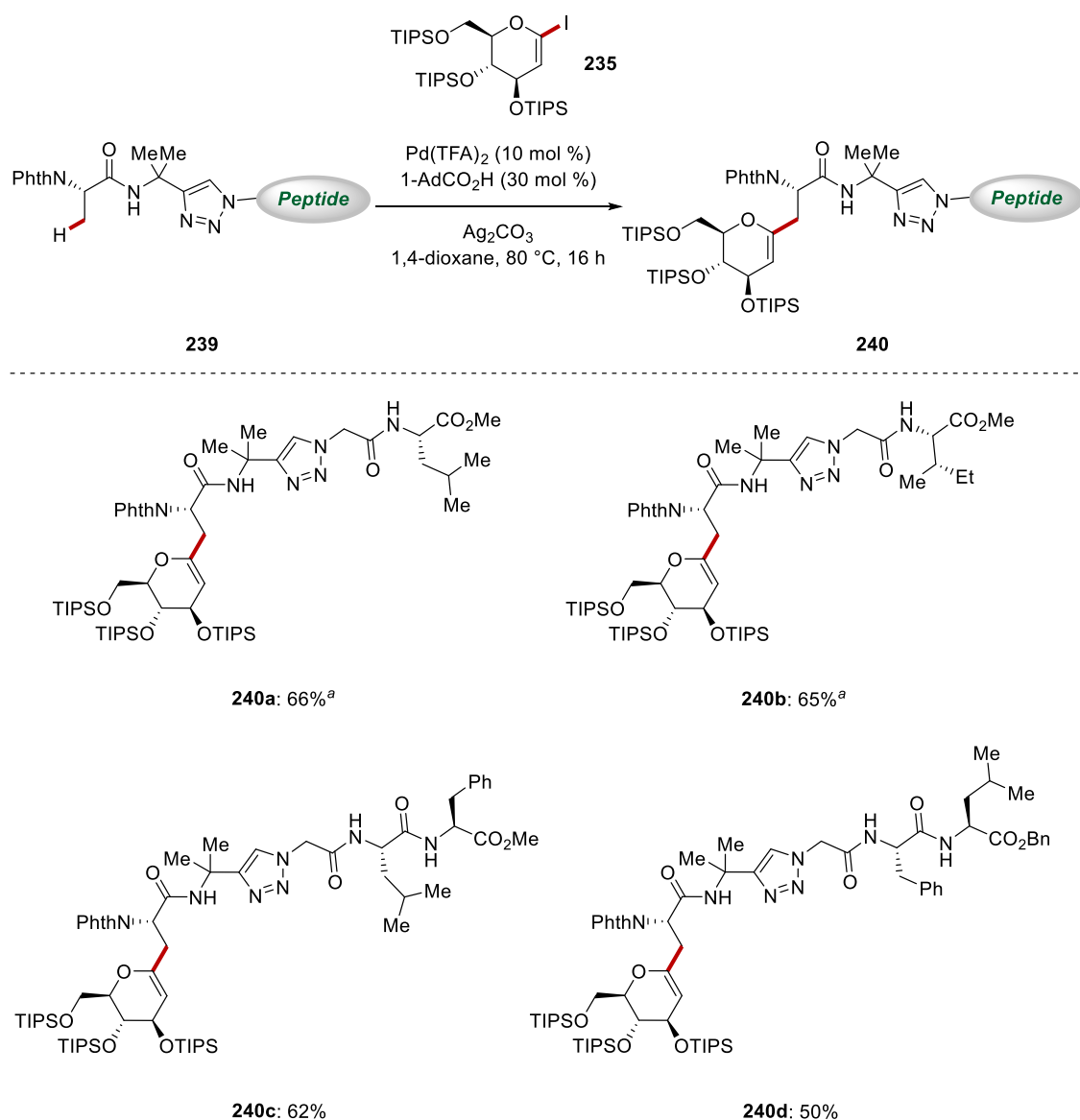
glycosylated with the iodo-glucal **235**. Gratifyingly, various amino acids, such as valine, isoleucine, phenylalanine and proline, as well as menthol and cholesterol were successfully utilized affording the glycopeptides **238a-238d** and glycolamino acid hybrids **238e** and **238f** (Scheme 3.2.3).



Scheme 3.2.3 Palladium-catalyzed C(sp³)-H glycosylation of amino acid derivatives **237**.

3. Results and Discussion

In order to illustrate the robustness of our C(sp^3)-H activation strategy, we probed whether the unprecedented late-stage glycosylation of internal peptides was feasible within our catalytic manifold (Scheme 3.2.4). The triazole-based directing group, an amide surrogate sharing common electronic and topological properties with peptide bonds, is suitable for the incorporation in larger peptides. To our delight, the corresponding peptidomimetics proved viable substrates for the late-stage glycosylation. Thus, various tetra- and pentapeptides **239** were chemo- and site-selectively glycosylated under our palladium-catalyzed manifold in a late-stage fashion. This approach paves the way for more time- and resource-economical syntheses of glycopeptides without relying on lengthy and costly *de novo* syntheses.

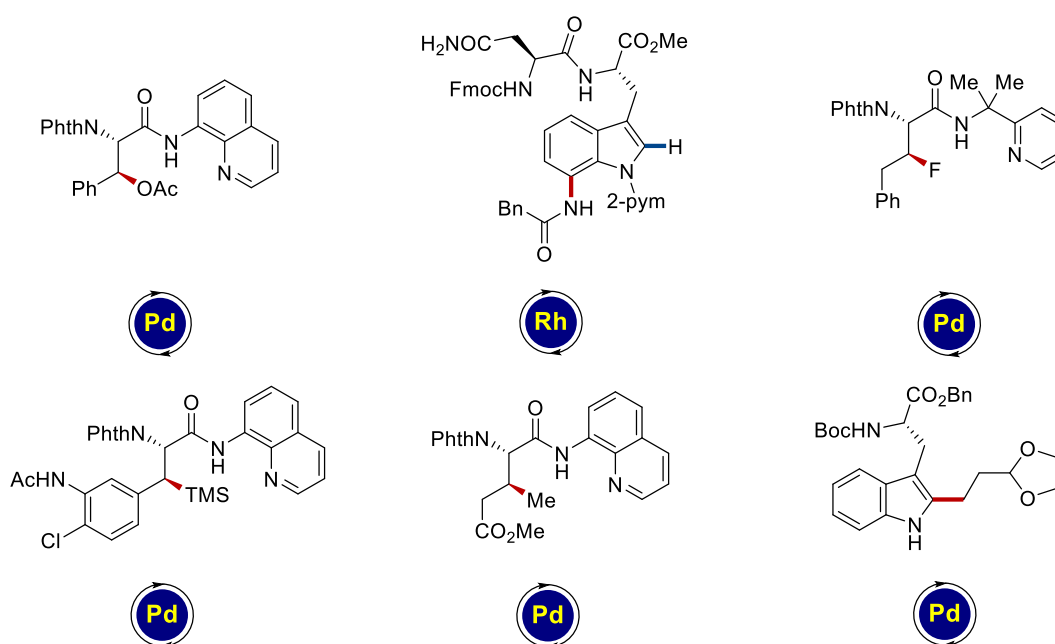


Scheme 3.2.4 Late-stage C(sp^3)-H glycosylation *via* internal triazole assistance.^a

Performed by J. Wu.

3.3. Ruthenium(II)-Catalyzed Peptide C–H Functionalization *via* Hydroarylation

Thus far, the functionalization of amino acids and peptides *via* C–H activation has relied heavily on arylative manifolds, with scarce exceptions. Hence, methodologies that enable the formation of C–Het or C–C(sp^3) bonds are in high demand as this will unlock a vast section of chemical space, beyond the aromatic flattened structures. Recently, oxygenations,^[106] amidations,^[122] fluorinations,^[110] and silylations^[158] have been disclosed using palladium or rhodium catalysis. In this context, the C–H alkylation of amino acids and peptides have been reported utilizing primary alkyl halides under palladium catalysis (Scheme 3.3.1).^[49c, 159]



Scheme 3.3.1. Representative examples of amino acid or peptide functionalization *via* the formation of C–Het or C–C(sp^3) bonds.

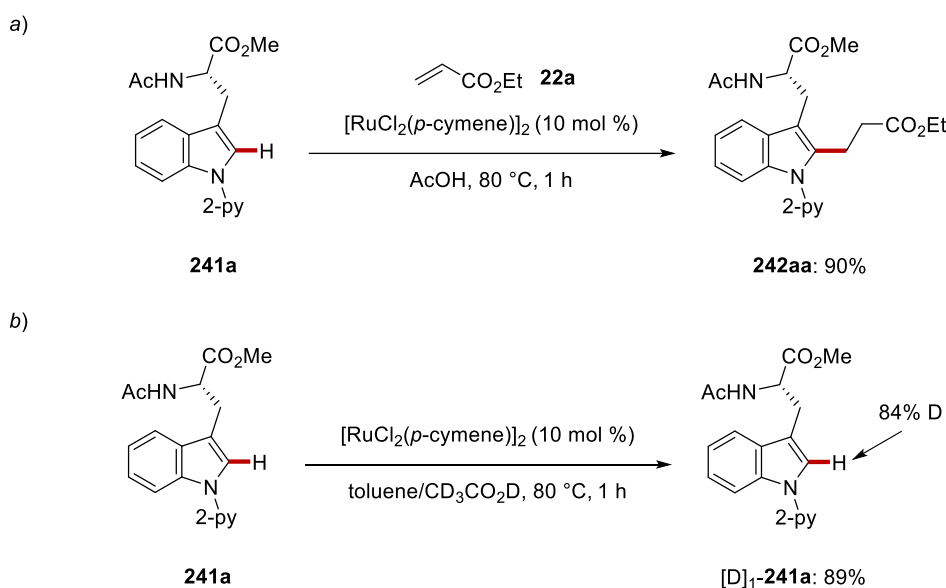
Therefore, we became interested in developing an atom- and step-economical method for chemo- and site-selective alkylation of tryptophan-containing peptides *via* a C–H activation manifold. Thus, ruthenium-catalysis was chosen due to its relative low-cost, among other 4d transition metals, and its remarkable functional group tolerance.^[120] We recognized that the choice of alkylating agent is crucial for achieving high levels of chemoselectivity. In this context, electrophilic alkyl halides could prove detrimental for the functionalization of complex peptides due to possible alkylation of polar residues *via* nucleophilic substitution pathways. Thus, acrylates were selected as modular

3. Results and Discussion

alkylating agents *via* a hydroarylation mechanism. This strategy would allow, among others, the expedient ligation of peptides and stitching of various biomolecules leading to multifunctional conjugates.^[160]

3.3.1. Acid-Enabled C–H Cleavage and Protodemetalation

Initial optimization studies by Dr. A. Schischko for the alkylation of tryptophan derivative **241a** with ethyl acrylate **22a** showcased that catalytic amounts of $[\text{RuCl}_2(p\text{-cymene})]_2$ in acetic acid under air were suitable for ensuring chemo- and site-selective functionalization (Scheme 3.3.2a). Importantly, Dr. A. Schischko demonstrated the importance of acetic acid as solvent, since its use was crucial for achieving high turnover numbers. An H/D exchange experiment with deuterated acetic acid was conducted, and the recovered starting material **241a** showed significant levels of D incorporation, suggesting a reversible and fast cycloruthenation (Scheme 3.3.2b). To unravel the mode of action of acetic acid, computational studies were performed by Dr. T. Rogge that provided strong support for a facile C–H cycloruthenation and rate-limiting protodemetalation by the acetic acid solvent.

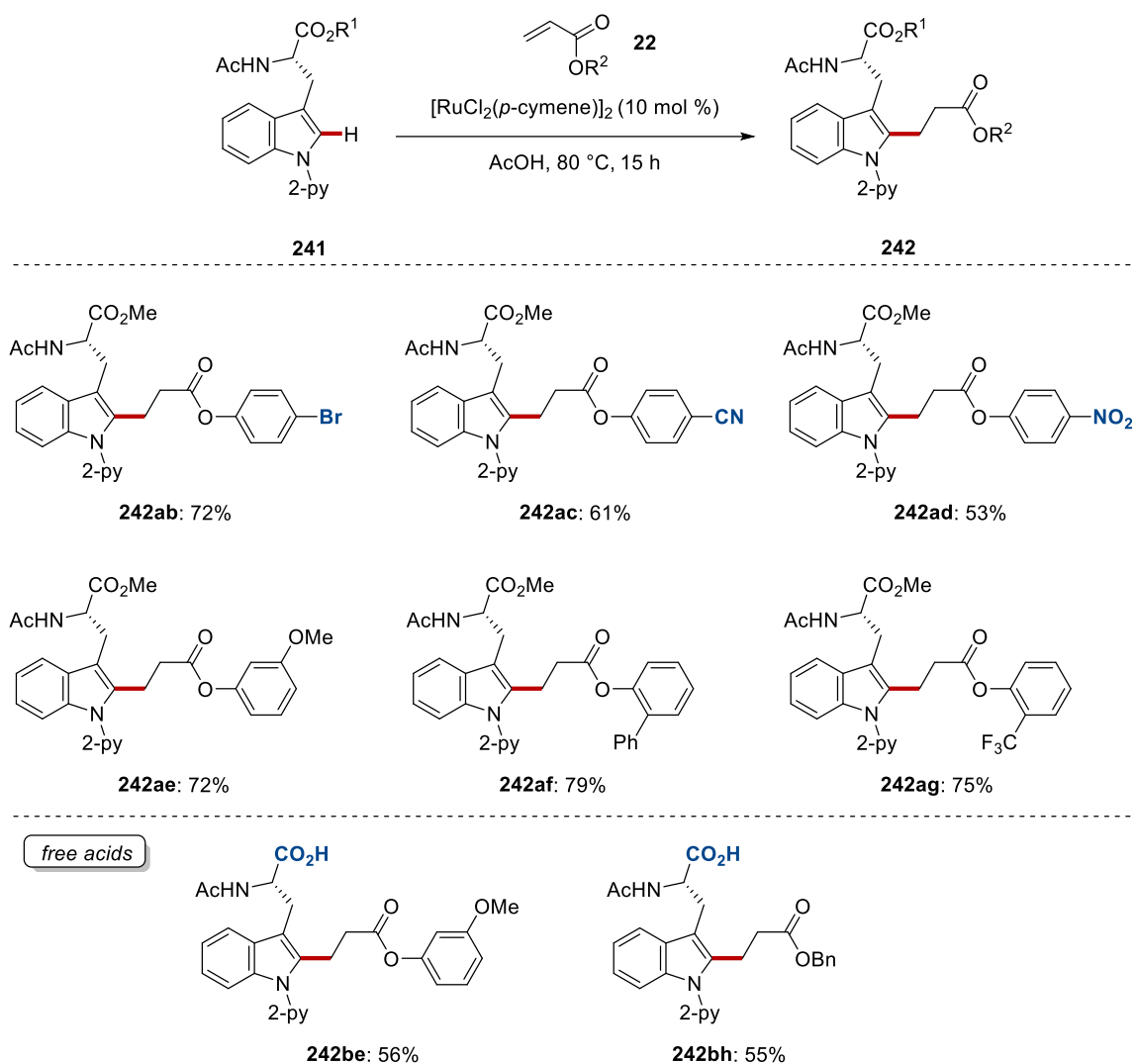


Scheme 3.3.2. a) Ruthenium(II)-catalyzed C–H alkylation of tryptophan derivative **241a**. b) Acid-enabled facile H/D exchange.

3.3.2. Scope of the Ruthenium(II)-Catalyzed Peptide Alkylation

With the optimized reaction conditions in hand we explored the generality of our hydroarylation manifold, utilizing a plethora of tryptophan-containing peptides^[121] and α,β -unsaturated carbonyl compounds. Initially, the functional group tolerance with regards to the coupling partner was examined (Scheme 3.3.3). Thus, tryptophan derivative **241** was coupled with various substituted phenol acrylates with excellent levels of chemo- and site-selectivity. Remarkably, electrophilic functional groups on the arene moiety, such as bromide, cyano and nitro, were well tolerated, as it is reflected from the examples **242ab-242ad**. Furthermore, substrates bearing substituents at the *meta*- and even *ortho*-position on the phenol ring were efficiently converted to the desired alkylated tryptophan derivatives **242ae-242ag**. The acidic conditions, under which our hydroarylation manifold is performed motivated us to investigate whether carboxylic acid-free tryptophan derivative **241b** could be a viable substrate. Gratifyingly, alkylated tryptophan derivatives **242be** and **242bh**, featuring aryl and benzyl acrylates, were obtained in a chemo- and site-selective fashion, albeit with slightly diminished efficiency. Moreover, Dr. A. Schischko demonstrated that α,β -unsaturated ketones, thioesters and maleimides are viable coupling partners under otherwise similar reaction conditions.

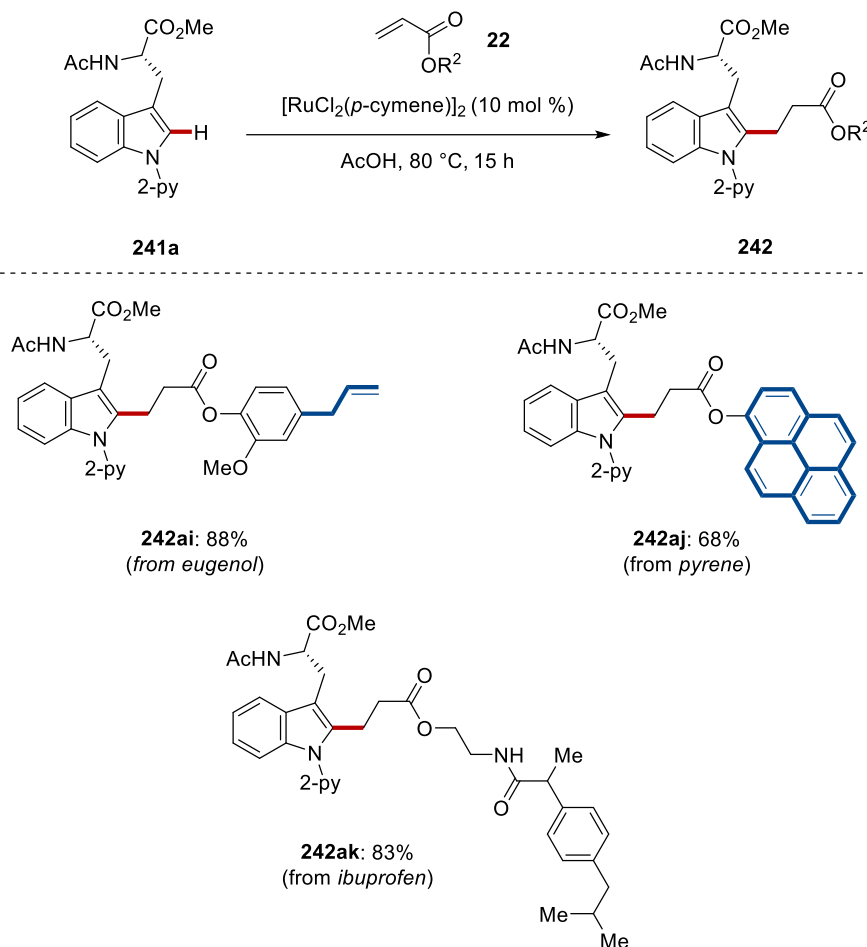
3. Results and Discussion



Scheme 3.3.3. Ruthenium(II)-catalyzed C–H alkylation of tryptophan derivative **241** via hydroarylation.

Having established a robust and reliable method for the stitching of various α,β -unsaturated carbonyl compounds to the C2 position of tryptophan derivative **241a**, we probed whether more complex acrylates could be used. Thus, acrylates containing natural products, drug scaffolds and fluorescent tags were employed (Scheme 3.3.4). To our delight, *eugenol* containing acrylate gave rise to the conjugate **242ai** in excellent yield. For the functionalization with the *eugenol* acrylate **22i** a mixture of toluene and acetic acid was used as solvent, in order to diminish the acid-catalyzed isomerization of the allyl moiety to the more substituted styryl-type. Furthermore, *ibuprofen* containing acrylate **22k** was smoothly employed generating the amino acid-drug conjugate **242ak** in excellent yield. Finally, the fluorescent labeling of tryptophan derivative **241a** was efficiently accomplished with pyrene containing acrylate **22j**.

3. Results and Discussion

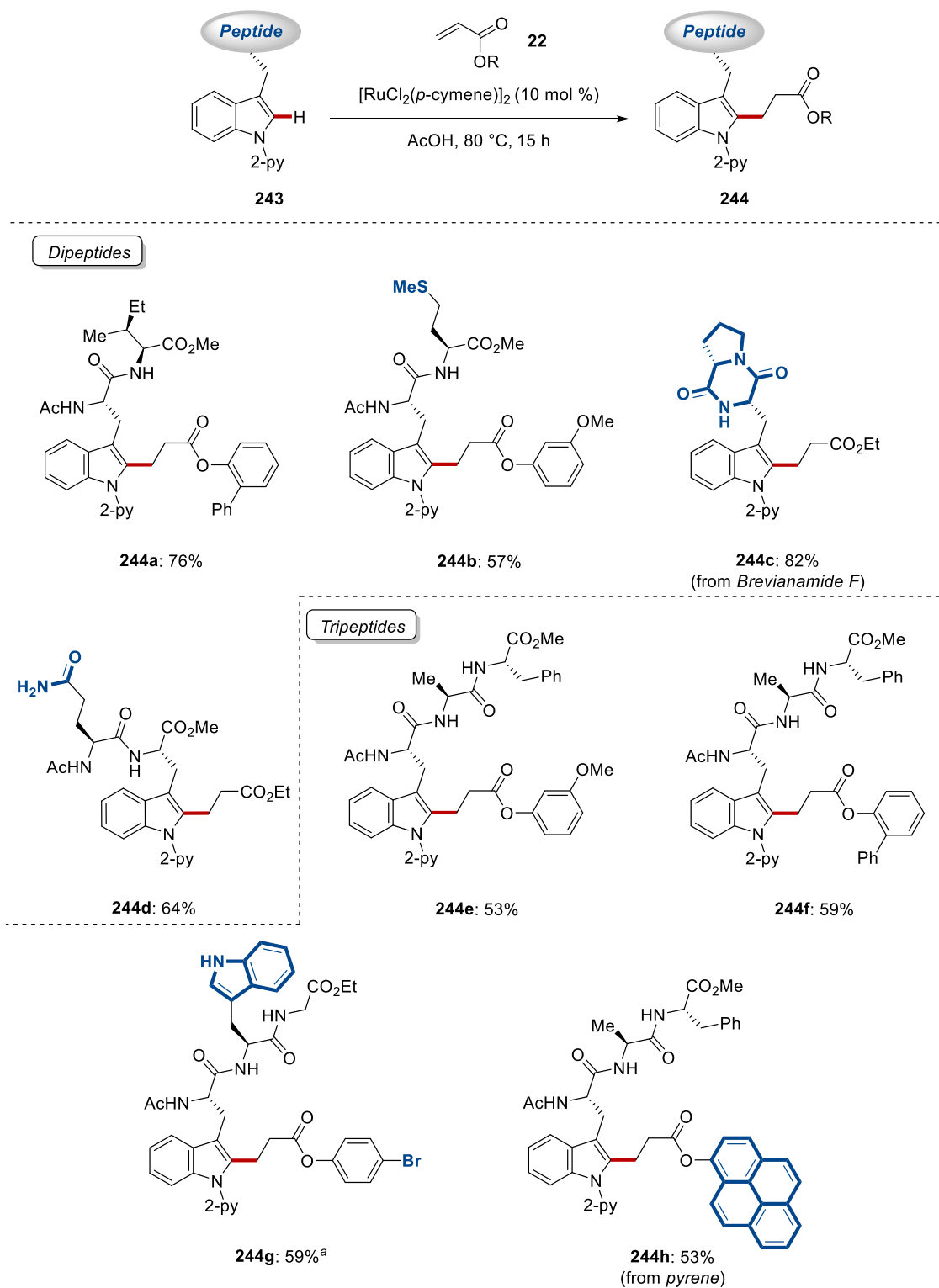


Scheme 3.3.4. Ruthenium(II)-catalyzed C–H conjugation. ^a Toluene/AcOH 1/1 was used as solvent.

After demonstrating a broad substrate scope with regards to the α,β -unsaturated carbonyl compounds, the generality of our hydroarylation reaction was assessed in the setting of C–H functionalization of structurally complex peptides. Thus, various di- and tripeptides were employed in our C–H alkylation regime, featuring a diverse set of functional groups. More precisely, dipeptides containing isoleucine, methionine, proline and glutamine were chemo- and site-selectively alkylated with aryl and alkyl substituted acrylates (Scheme 3.3.5). Remarkably, the oxidation prone thioether moiety found in the methionine-containing dipeptide **243b** was smoothly employed in our method. Along these lines, the 2,5-diketopiperazine moiety found in numerous naturally occurring cyclic dipeptides, such as in *Brevianamide F* derivative **243c**, was well tolerated. Motivated by the robustness of our ruthenium(II)-catalyzed C–H alkylation manifold for the site-selective functionalization of dipeptides we probed whether tripeptides would be viable substrates. Thereby, alkylated tripeptides **244** featuring *NH*-free indole moiety, aryl bromide and fluorescent pyrene tag were

3. Results and Discussion

efficiently obtained under the optimized reaction conditions, without signs of epimerization.

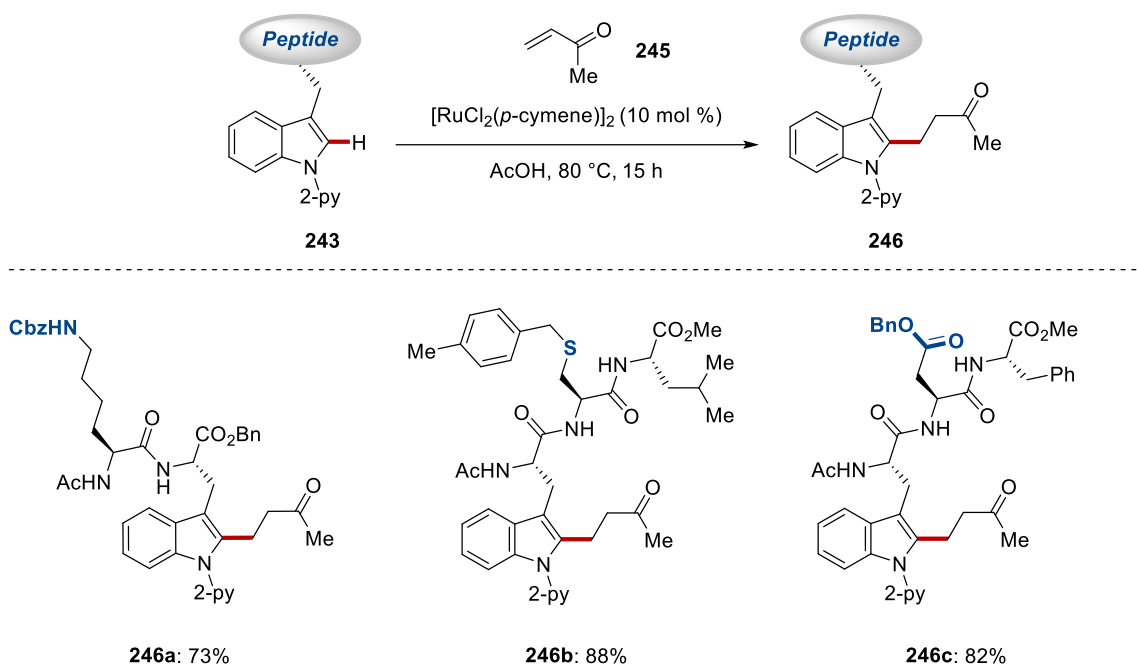


Scheme 3.3.5. Ruthenium(II)-catalyzed C–H alkylation of di- and tripeptides. ^a

Performed by Dr. A. Schischko.

3. Results and Discussion

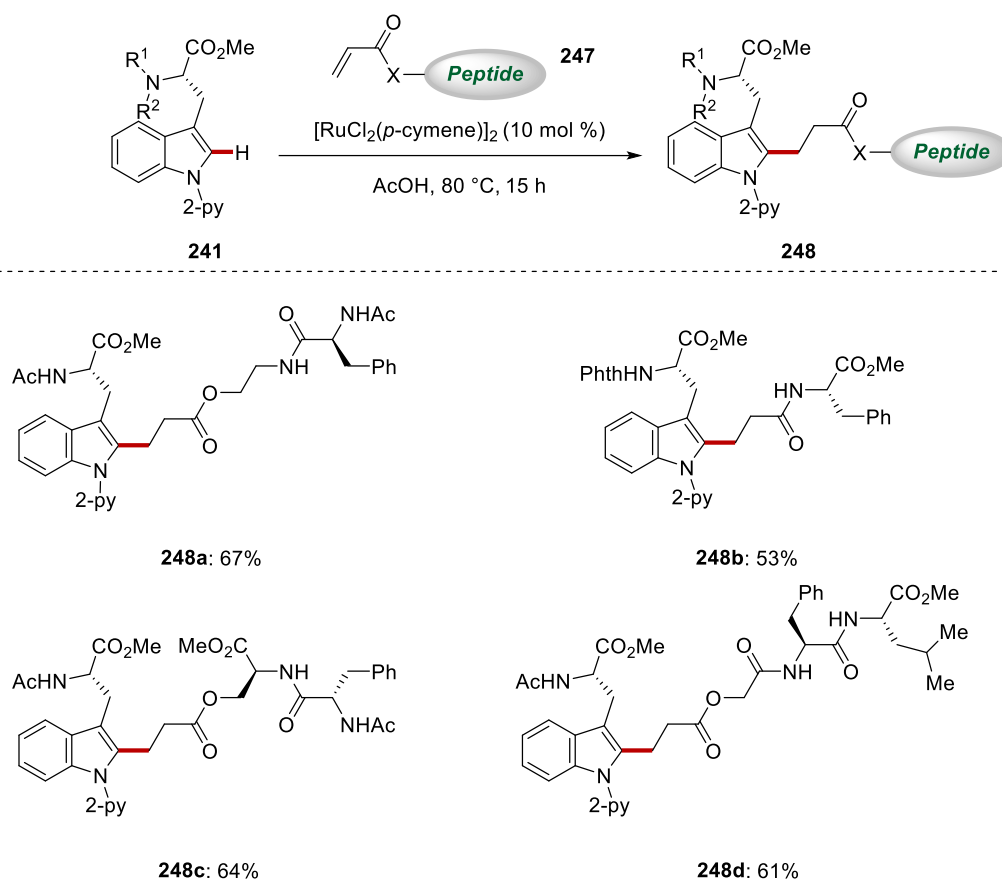
Having demonstrated that the modular α,β -unsaturated esters are suitable substrates for the site-selective functionalization of di- and tripeptides, we investigated the efficiency of our method with the more reactive α,β -unsaturated ketones (Scheme 3.3.6). Thus, di- and tripeptides were subjected to our ruthenium(II)-catalyzed C–H alkylation manifold. To our delight, peptides featuring protected lysine, cysteine and aspartic acid were efficiently converted to the desired alkylated peptides **246a–246c** with excellent yields in a chemo- and site-selective fashion, without signs of epimerization.



Scheme 3.3.6. Ruthenium(II)-catalyzed C–H alkylation of di- and tripeptides with methyl vinyl ketone (**245**).

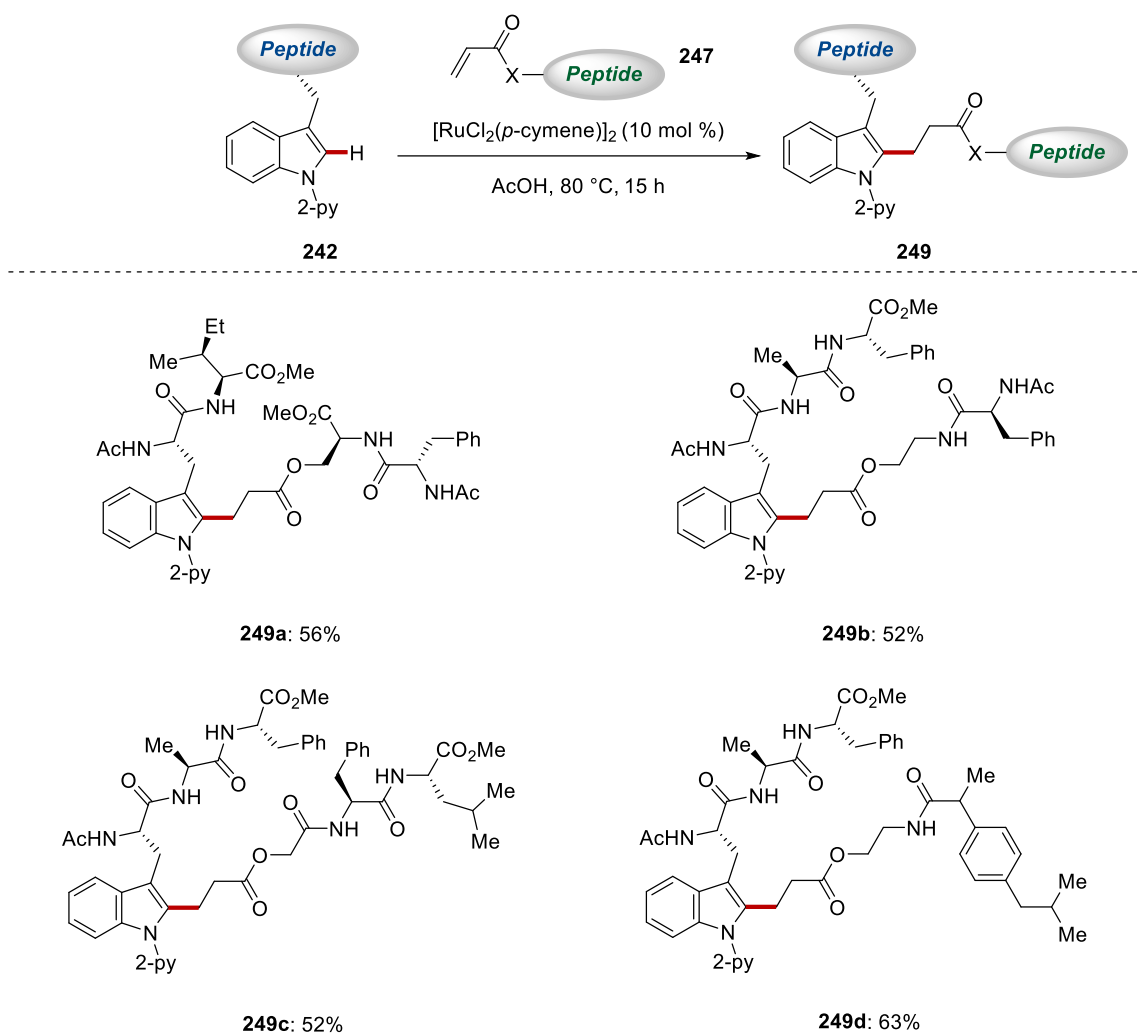
Intrigued by the robustness of our ruthenium(II)-catalyzed C–H alkylation and taking into consideration the modular nature of α,β -unsaturated carbonyl compounds we probed if our regime would be suitable for the C–H ligation of peptides. To put this hypothesis into practice we examined the stitching of various peptide-containing acrylates to the tryptophan derivative **241a** (Scheme 3.3.7). To our delight, a diverse set of acrylates linked to *N*- or *C*- terminus or even to the hydroxy group of serine proved viable substrates, giving rise to peptides **248a–248d** with distinct ligation patterns. In the case of phenylalanine derived acrylate **247b** *N*-phthaloyl protection was crucial to suppress competing *aza*-Michael pathways. Hence, under the optimized reaction conditions unnatural di-, tri- and tetrapeptides were obtained in good yields.

3. Results and Discussion



Scheme 3.3.7. Ruthenium(II)-catalyzed C–H ligation of tryptophan derivatives.

Motivated by these results, we pursued on expanding this strategy to the ligation of more complex peptides. Thus, di- and tripeptides were used as substrates in our C–H ligation approach with various peptide- or drug-derived acrylates (Scheme 3.3.8). To our delight, our regime gave expedient access to various tetra- and hexapeptides **242** via an C2-selective alkylation manifold. Lastly, the conjugation of tripeptide **243e** with *ibuprofen*-derived acrylate **22k** was efficiently accomplished giving rise to hybrid molecule **249d**.

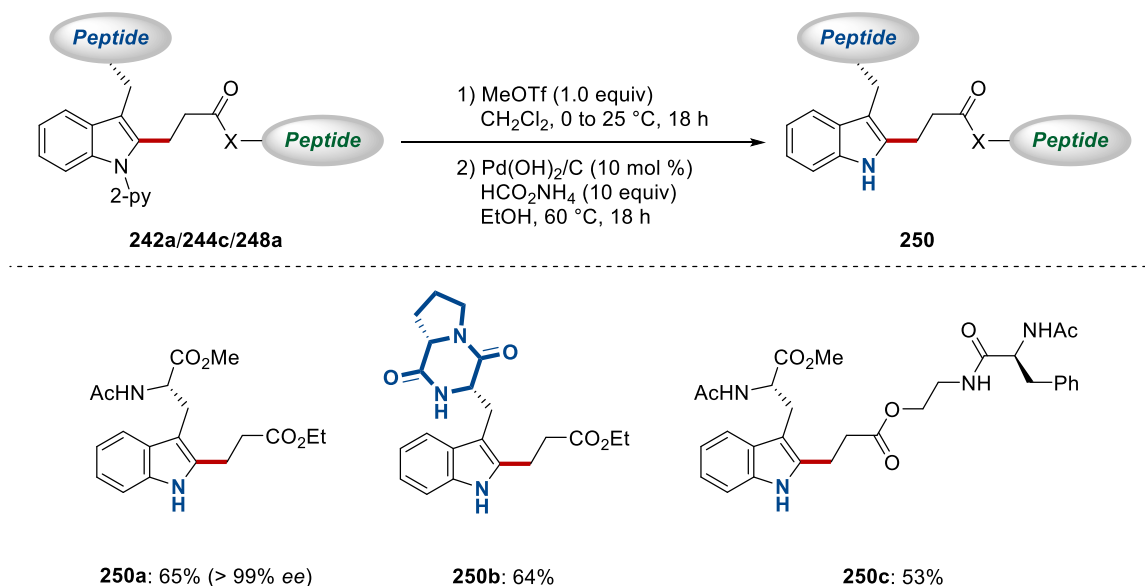


Scheme 3.3.8. Ruthenium(II)-catalyzed C–H ligation of peptides.

3.3.3. Late-Stage Removal of the Pyridyl Group

With a robust and reliable alkylation manifold in hand for the late-stage diversification and ligation of structurally complex tryptophan-containing peptides we focused on the removal of the essential 2-pyridyl directing group, under mild reaction conditions without jeopardizing the peptidic backbone. Hence, selective *N*-methylation with methyl triflate followed by hydrogenation of the resulting pyridinium salt led to the cleavage of the directing group providing the *NH*-free indole-containing peptides **250a–250c** (Scheme 3.3.9). Remarkably, the C–H alkylation and directing group cleavage proceeded without erosion of the enantiopurity of the alkylated amino acid **250a**. Accordingly, alkylated and ligated peptides were smoothly employed in this sequence yielding the desired derivatives in moderate yields.

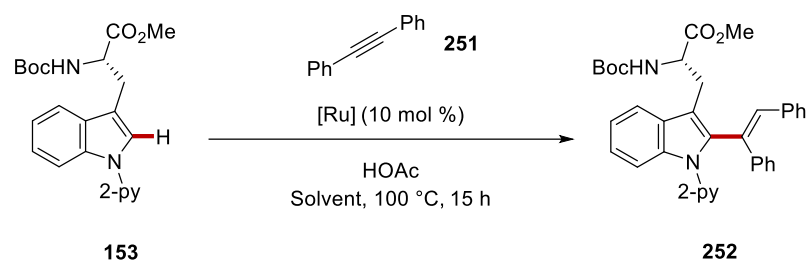
3. Results and Discussion



Scheme 3.3.9. Traceless removal of the 2-azinyll group.

3.3.4. Peptide Alkenylation via Ruthenium(II)-Catalyzed Hydroarylation

The ruthenium(II)-catalyzed hydroarylation is not restricted to alkenes but it is also applicable to alkynes.^[80, 161] Notably, electronically unbiased alkynes are typical coupling partners in ruthenium-catalyzed C–H activation,^[41c, 42a, 42b, 42e, 162] in sharp contrast to alkenes that generally require an additional activating group. Thus, we challenged whether the acid-enabled hydroarylation manifold we had developed for activated alkenes could be expanded to alkynes. We commenced our optimization studies by probing various reaction conditions for the envisioned C–H alkenylation of tryptophan derivative **153** with diphenylacetylene **251** utilizing catalytic amounts of [RuCl₂(*p*-cymene)]₂ and stoichiometric amounts HOAc at 100 °C, in various solvents (Table 3.3.1). Among a representative set of solvents toluene proved to be optimal (entry 2), giving rise to the desired functionalized amino acid **252** in 85% yield. Then, ruthenium(II)-biscarboxylate complexes were assessed (entries 4-7), with [Ru(OAc)₂(*p*-cymene)] providing the best result. Remarkably, our hydroarylation manifold did not require the use of silver(I) salts for the generation of the a cationic ruthenium complex. In all cases the product was formed with complete *E*-selectivity.

Table 3.3.1. Optimization studies for ruthenium(II)-catalyzed alkenylation *via* a hydroarylation manifold.

Entry	[Ru]	Solvent	Yield (%)
1	[RuCl ₂ (<i>p</i> -cymene)] ₂	1,4-dioxane	43
2	[RuCl ₂ (<i>p</i> -cymene)] ₂	toluene	85
3	[RuCl ₂ (<i>p</i> -cymene)] ₂	DMF	-
4	[Ru(OCMe) ₂ (<i>p</i> -cymene)]	toluene	79
5	[Ru(OAc)₂(<i>p</i>-cymene)]	toluene	87
6	[Ru(MeCN) ₆][SbF ₆] ₂	toluene	-
7	[Ru(<i>t</i> BuCN) ₆][PF ₆] ₂	toluene	-

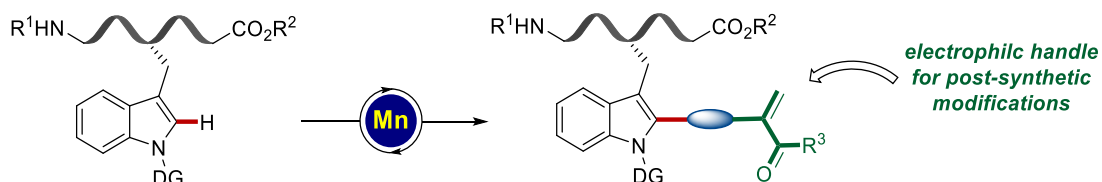
Reaction conditions: **153** (0.15 mmol), **251** (0.22 mmol), [Ru] (10 mol %), HOAc (1.0 equiv), solvent (0.6 mL), 100 °C, 15 h. Yields of isolated product.

3. Results and Discussion

3.4. 3d-Transition Metal-Catalyzed Allylation of Drug Scaffolds and Peptides

Recently, the growing importance of peptides and proteins in therapeutic and biomedical applications has provided enormous motivation to the synthetic community for developing mild and robust methodologies for the chemo- and site-selective modification of peptides.^[163] Traditionally, the existing methods for late-stage, post-assembly, modification of peptides are limited mainly to reactions based on polar nucleophilic side chains, found mainly in cysteine and lysine.^[164] Recently, the powerful cross-coupling regime has enabled the modification of peptides equipped with the appropriate handles, that are generally unnatural.^[165] Thus, these strategies are generally not suitable for the modification of hydrophobic amino acids. In this regard, C–H functionalization has proven invaluable, as omnipresent C–H bonds are substituted with a plethora of functional groups. During the last decade, C–H activation has become an increasingly viable tool for molecular syntheses.^[25a, 25e] Enormous efforts have been devoted to establishing C–H functionalizations of amino acids and peptides using toxic 4d transition metals, mainly palladium and ruthenium,^[25b, 147, 166] whilst Earth-abundant 3d transition metal catalysis continues to be scarce.^[123] Manganese complexes typically demonstrate low toxicity, thus its utilization in late-stage C–H functionalization of peptides is highly desirable. Furthermore, the site-selective incorporation of functional groups that enable plethora of post-synthetic manipulations are highly desirable, rapidly expanding the chemical space. In this regard, α,β -unsaturated carbonyl compounds are one of the most widely used synthetic handles for the modification of peptides and proteins due to their highly electrophilic character.^[167]

Therefore, we became interested in the development of an atom- and step economical method for the incorporation of α,β -unsaturated carbonyl moiety into the peptidic chain via a C–H activation manifold (Scheme 3.4.1). Thus, manganese catalysis was chosen due to its lower toxicity and cost-effectiveness as well as high natural abundance of manganese.^[26] Recognizing the remarkable efficiency of manganese(I)-catalyzed C–H allylation,^[88-89, 91] we probed whether the Morita-Baylis-Hillman (MBH) adducts,^[168] possessing a bis-electrophilic character, could be suitable substrates for the chemo- and site-selective functionalization of tryptophan-containing peptides.



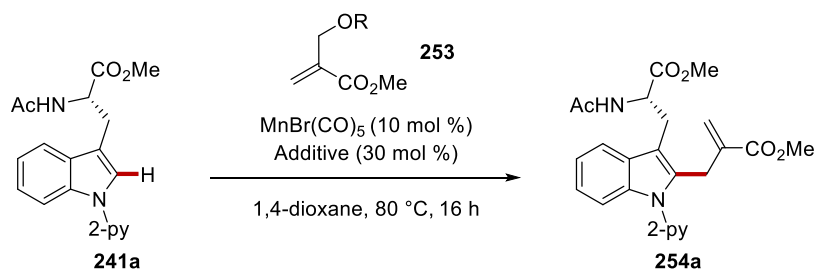
Scheme 3.4.1. Manganese(I)-catalyzed incorporation of α,β -unsaturated carbonyl moiety to peptides.

3.4.1. Optimization Studies for C–H Allylation of Peptides Under Manganese(I) Catalysis

We commenced our optimization studies by probing various reaction conditions for the envisioned C–H allylation of tryptophan derivative **241a** with Boc-protected MBH-adduct **253a** with catalytic amounts of $\text{MnBr}(\text{CO})_5$ and NaOAc at 80 °C, in various solvents (Table 3.4.1). Among the tested solvents, 1,4-dioxane provided the highest isolated yield (entry 3), albeit reactions in toluene and DCE gave nearly quantitative yields as well (entries 1 and 2). The nature of the leaving group was then examined. This demonstrated the essential role of the carbonate moiety, as both free MBH adduct and acetyl-protected-MBH adduct failed to provide the desired product **254a** (entries 4 and 5). This can be attributed either to the need for pre-coordination of the leaving group prior to the migratory insertion or to the ease of β -oxygen elimination of the different leaving groups. Control experiments revealed the importance of NaOAc, that presumably leads to the formation of $\text{Mn}(\text{OAc})(\text{CO})_5$, thus facilitating the initial C–H activation step *via* carboxylate assistance,^[17a] and the essential nature of the $\text{MnBr}(\text{CO})_5$ (entries 6 and 7). Notably, the reaction proceeded without erosion of the enantiointegrity of the tryptophan scaffold, demonstrating the exceedingly mild nature of this manganese(I)-catalyzed allylation manifold.

3. Results and Discussion

Table 3.4.1. Optimization studies for the manganese(I)-catalyzed allylation of tryptophan derivative **241a** with MBH adduct **253**.



Entry	Solvent	Additive	R	Yield (%)
1	toluene	NaOAc	Boc	93
2	DCE	NaOAc	Boc	93
3	1,4-dioxane	NaOAc	Boc	98
4	1,4-dioxane	NaOAc	H	---
5	1,4-dioxane	NaOAc	Ac	---
6	1,4-dioxane	---	Boc	73
7	1,4-dioxane	NaOAc	Boc	--- ^a

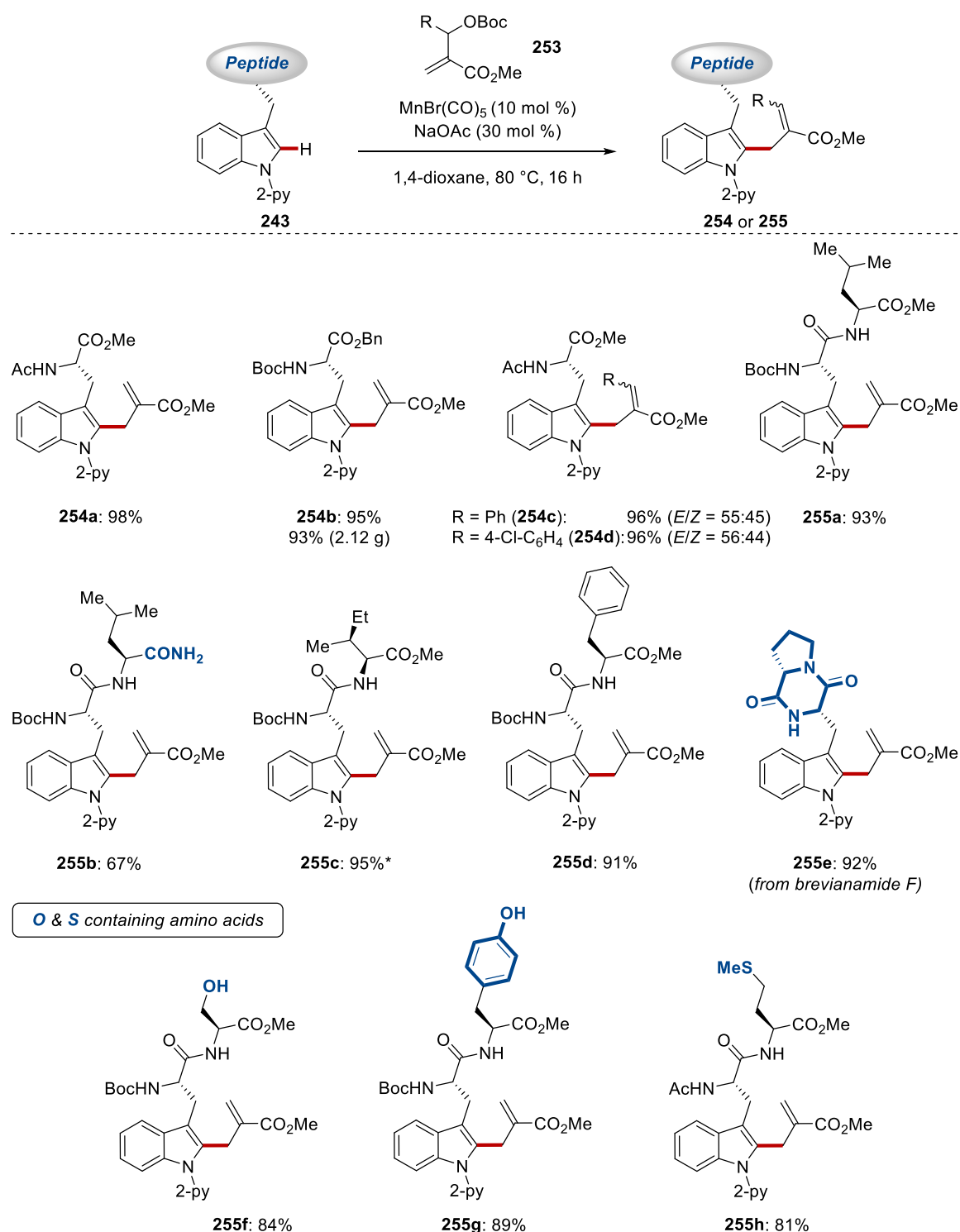
Reaction conditions: **241a** (0.20 mmol), **253** (0.40 mmol), $\text{MnBr}(\text{CO})_5$ (10 mol %), additive (30 mol %), solvent (0.6 mL), 16 h. Yields of isolated product. ^a Without $\text{MnBr}(\text{CO})_5$.

3.4.2. Scope of the Manganese(I)-Catalyzed C–H Allylation of Tryptophan-Containing Peptides and Biomolecules

With the optimized reaction conditions in hand, we first tested different tryptophan derivatives with orthogonal protecting groups in order to provide access to functionalized amino acids suitable for peptide synthesis, featuring the reactive α,β -unsaturated ester moiety (Scheme 3.4.2). Thus, **254a** and **254b** were isolated in excellent yields. Remarkably, the Boc-Trp^{py}-OBn was allylated in excellent yield even

on gram-scale, demonstrating the user-friendly nature of this manganese(I)-catalyzed C–H allylation. In addition, different MBH-adducts were efficiently converted under this allylation manifold, thus **254c** and **254b** were isolated in excellent yields, albeit with moderate *E/Z* ratio. After establishing a robust strategy for the functionalization of amino acids, we investigated whether tryptophan-containing dipeptides **243** were suitable substrates (Scheme 3.4.2). Gratifyingly, a plethora of dipeptides **243** were efficiently functionalized under the optimized reaction conditions with the excellent levels of chemo- and site-selectivity. Precisely, dipeptides with aliphatic and aromatic amino acids, like leucine, isoleucine, and phenylalanine were well tolerated, leading to the functionalized dipeptides **255a**, **255b** and **255c** in a chemo- and site-selective fashion. Moreover, the terminal primary amide featured in the dipeptide **243k** did not affect the efficacy of our C–H allylation manifold. The *brevianamide F* derivative **243c**, bearing the 2,5-diketopiperazine moiety found in a myriad of natural products,^[169] was efficiently functionalized under the optimized reaction conditions. Furthermore, hydroxyl-containing amino acids, such as serine and tyrosine, were well tolerated, as reflected by the chemo- and site-selective allylation of dipeptides **243n** and **243o**, completely bypassing the innate reactivity for *oxa*-Michael addition that would lead, after E1cB of the -OBoc group, to the *O*-allylation. Remarkably, the methionine-containing dipeptide **243b**, featuring the oxidation prone sulfide, was efficiently allylated without the formation of undesired oxidation by-products.

3. Results and Discussion

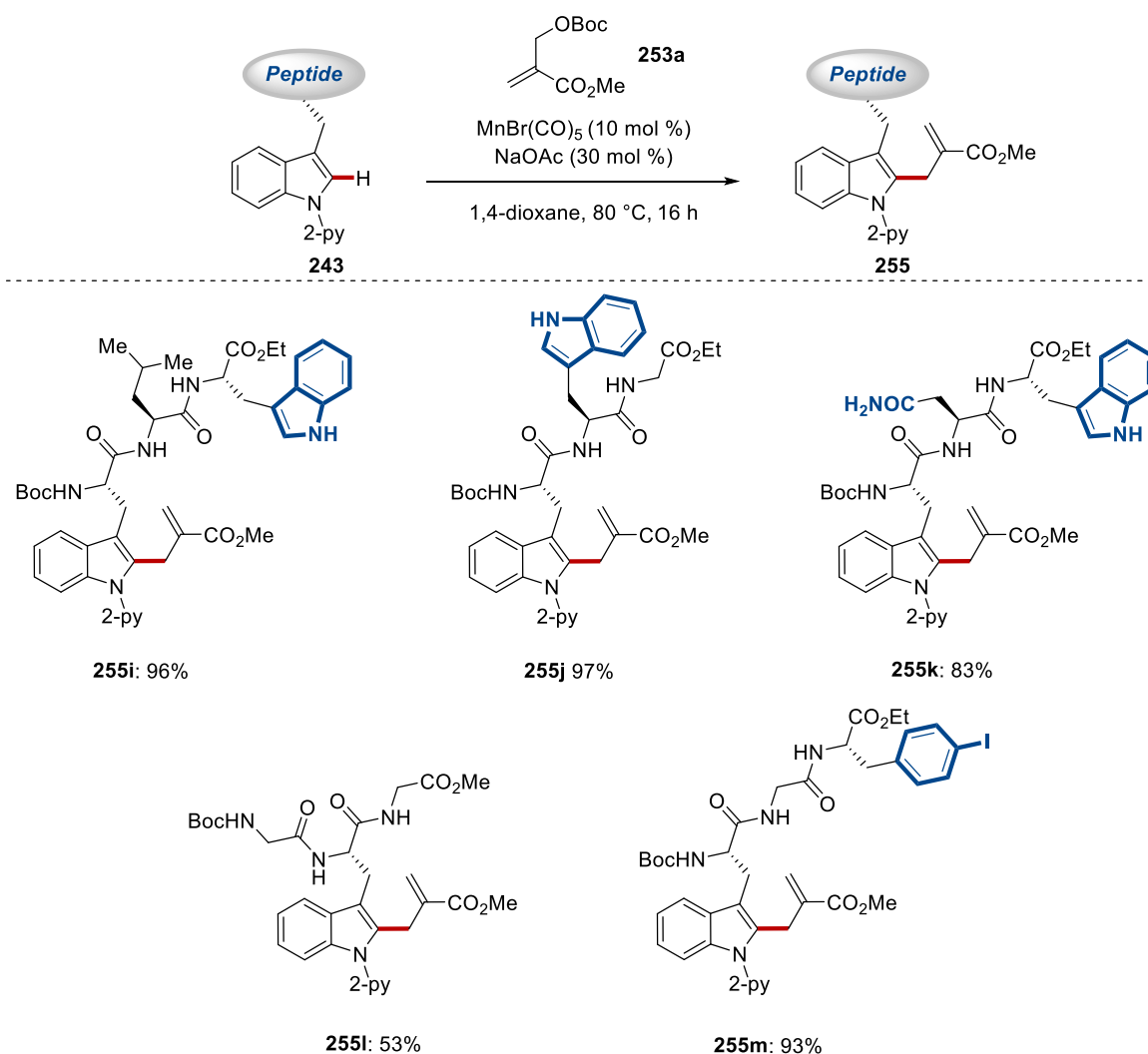


Scheme 3.4.2. Manganese(I)-catalyzed C–H allylation of dipeptides. * Performed by R. Yin.

Having established a robust method for the late-stage diversification of various dipeptides we shifted our attention to the functionalization of more complex peptides in order to demonstrate the full potential of our C–H allylation regime. Thus, tripeptides containing free *NH*-tryptophan and 4-iodo-phenylalanine were efficiently functionalized

3. Results and Discussion

in a chemo- and site-selective fashion, giving rise to allylated tripeptides with good to excellent yields (Scheme 3.4.3). Hence, the highly predictable positional selectivity of the manganese(I)-catalyzed C–H allylation was reflected by the selective functionalization of peptides **243p**, **243q** and **243r**, featuring two different tryptophan residues, one equipped with the directing group and the other without protecting or directing group without signs of *aza*-Michael byproducts. Remarkably, tripeptide **243s** featuring the tryptophan moiety in the middle of the peptidic sequence was efficiently functionalized despite the increased steric hindrance, albeit with diminished efficiency. In addition, the aryl iodide found in the product **255m** should prove invaluable for further post-synthetic modifications.

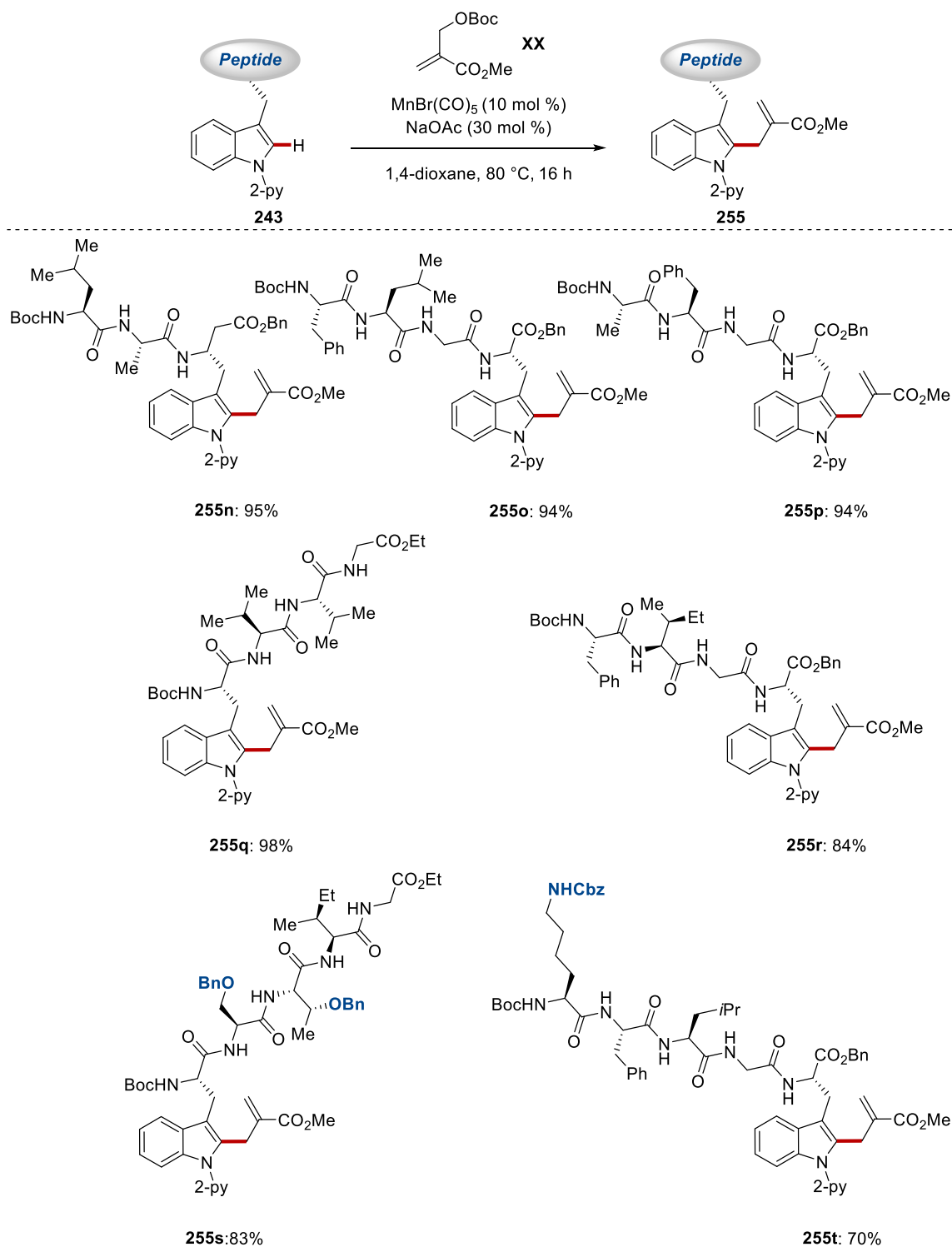


Scheme 3.4.3. Manganese(I)-catalyzed C–H allylation of tripeptides.

To further test the versatility of our manganese(I)-catalyzed C–H allylation we next examined whether even larger peptides could be efficiently allylated in a site-selective

3. Results and Discussion

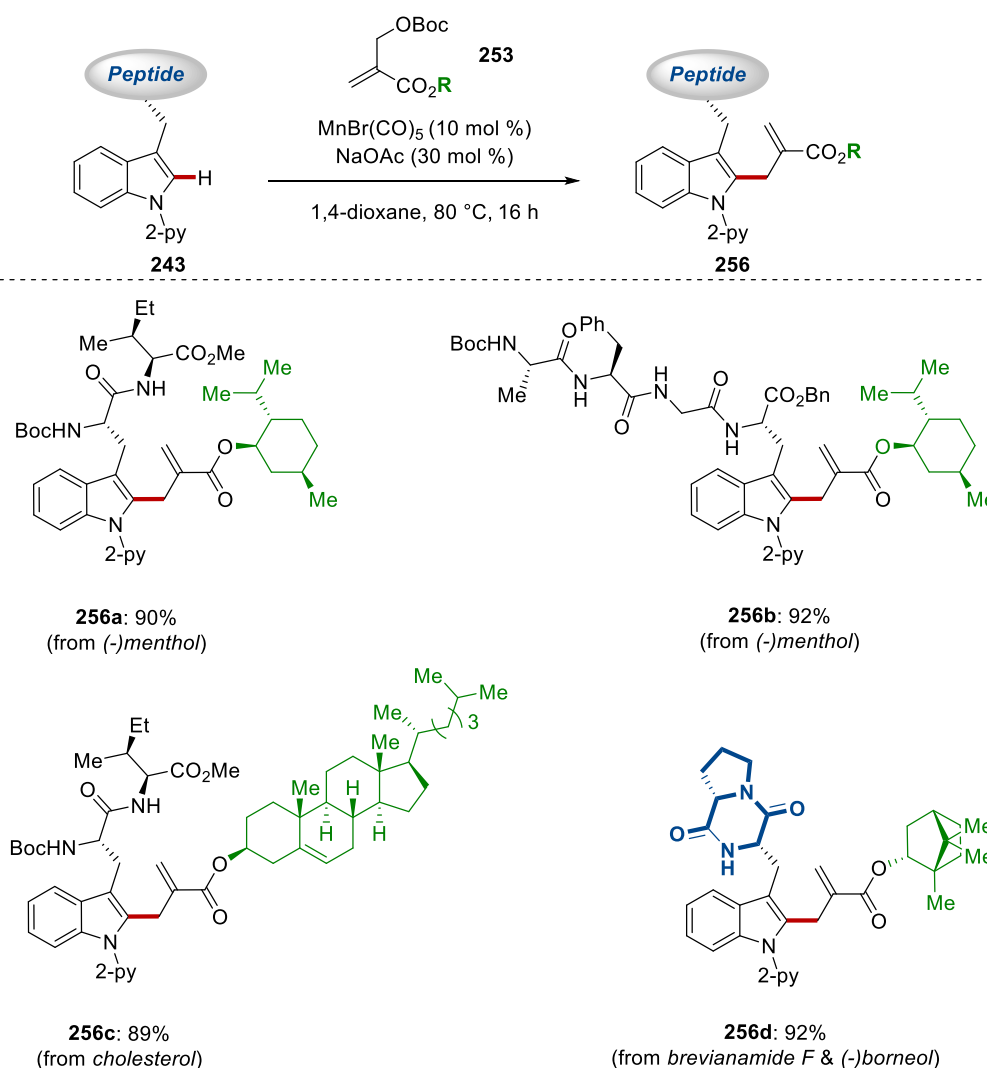
fashion. To our delight, tetra- and pentapeptides were identified as suitable substrates providing the desired functionalized peptides in excellent yields (Scheme 3.4.4). Notably, protected hydroxyl-containing amino acids such as serine and threonine, and orthogonally protected lysine were well tolerated, leading to site- and chemo-selectively functionalized peptides **255s** and **255t**.



Scheme 3.4.4. Manganese(I)-catalyzed C–H allylation of tetra- and pentapeptides.

3. Results and Discussion

The modularity of the MBH-adducts enabled the synthesis of hybrid molecules *via* the manganese(I)-catalyzed C–H allylation, utilizing natural product-derived MBH-adducts **253d**, **253e** and **253f** (Scheme 3.4.5). Thus, the assembly of peptide/terpene and peptide/steroid conjugates was efficiently achieved under the optimized reaction conditions, utilizing *menthol*, *borneol* and *cholesterol* tethered MBH-adducts. More precisely, the di- and tetrapeptides were functionalized in a chemo- and site-selective fashion, giving rise to conjugates featuring an otherwise reactive α,β -unsaturated ester moiety.

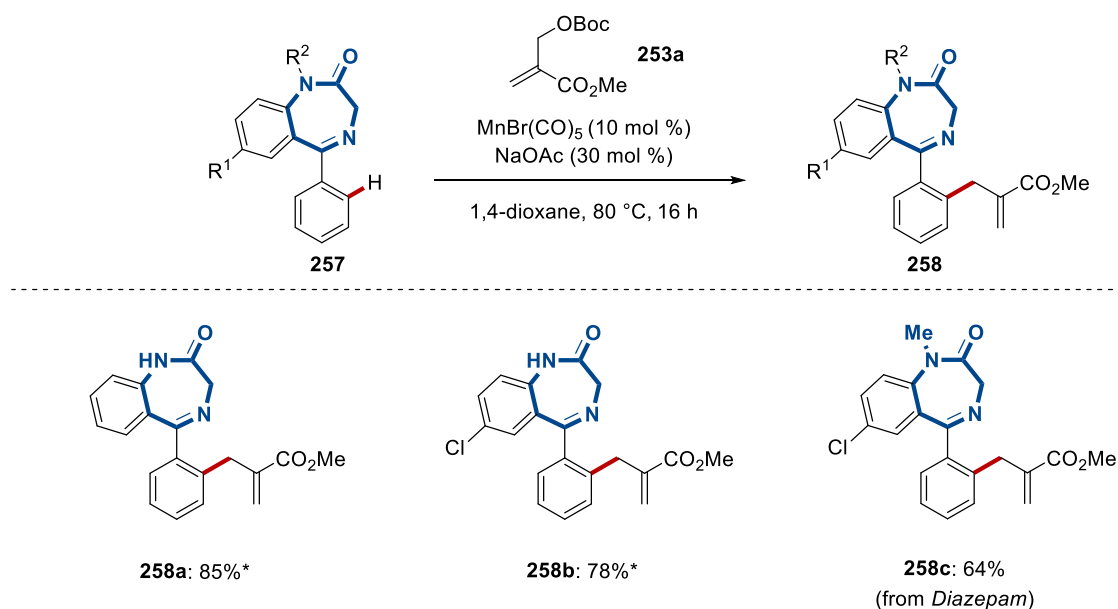


Scheme 3.4.5. Manganese(I)-catalyzed synthesis of peptide conjugates **256** *via* C–H allylation.

Having established a mild and robust method for the late-stage functionalization of structurally complex peptides with versatile protected MBH-adducts, we probed whether our approach could be employed for the diversification of drug-like scaffolds

3. Results and Discussion

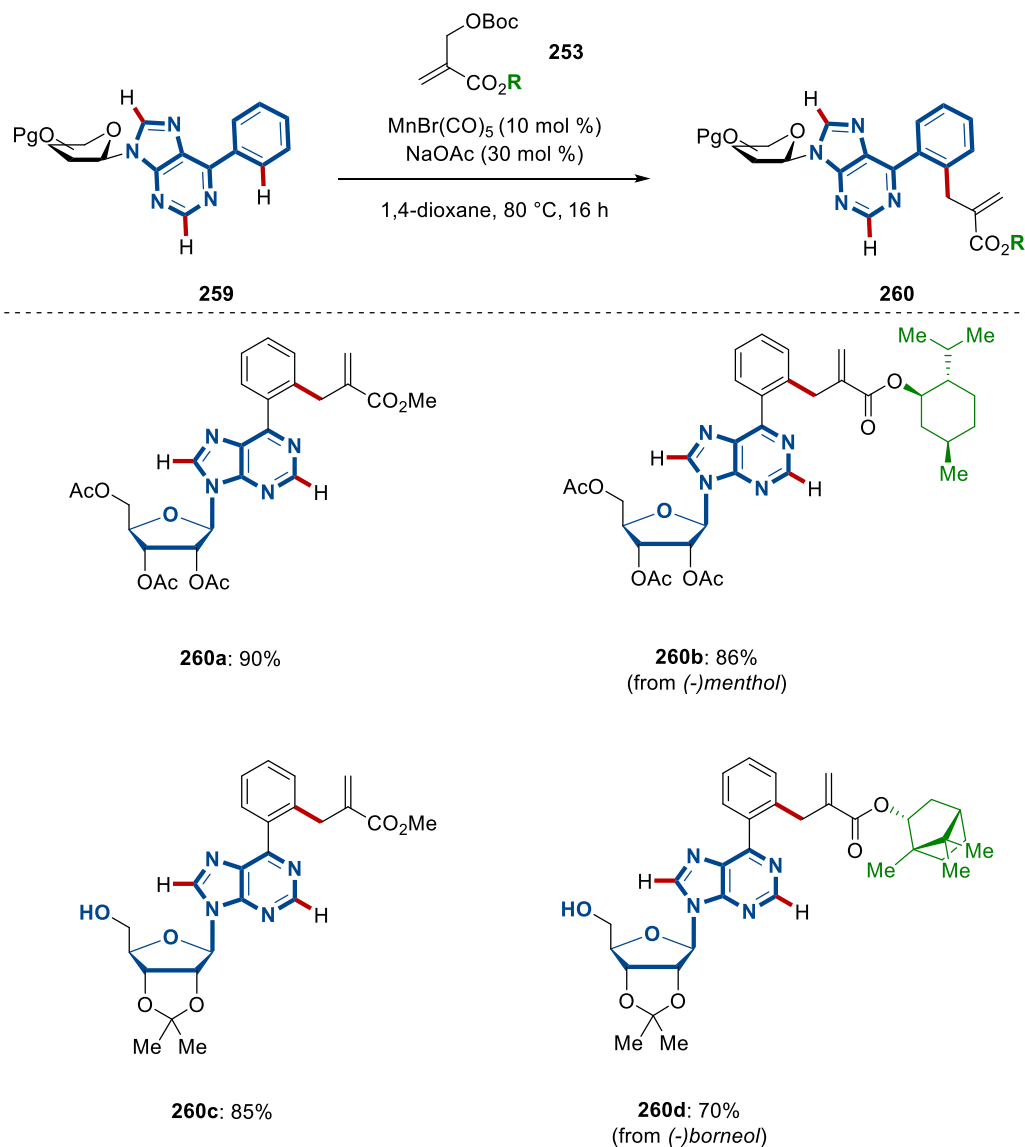
(Scheme 3.4.6). The implementation of the C–H activation strategy in the late-stage functionalization of drugs can be straightforward, as many drugs typically possess nitrogen containing heterocycles that are powerful coordinating groups for various transition metals, yet the presence of these Lewis-basic functionalities can also pose selectivity and inhibition issues.^[25e] Thus, we were delighted to achieve the selective functionalization of benzodiazepines. In this case, the imine-type nitrogen provided the crucial chelation-assistance to the manganese catalyst in order to enable the proximity induced C–H cleavage and subsequent allylation. Notably, *Diazepam* **257c** was functionalized under the optimized reaction conditions in a chemo- and site-selective fashion. Thus, the functionalization of drug-like and drugs scaffolds was accomplished by means of non-toxic and Earth-abundant manganese(I)-catalyzed C–H activation.



Scheme 3.4.6. Manganese(I)-catalyzed C–H allylation of benzodiazepines. *
Performed by R. Yin.

The generality of this method is also mirrored by the chemo- and site-selective functionalization of unnatural nucleoside **259**, featuring the purine derivative 6-phenyl-purine as nucleobase (Scheme 3.4.7). Here, the purine core acts as the essential chelating element to direct the C–H activation. The robustness of our method allowed the complete tolerance of the densely functionalized furanose core, free alcohols, acid-sensitive acetals, together with the nitrogen-rich purine scaffold that could engage in undesired coordination with the manganese(I)-catalyst, normally leading to diminished reaction efficiency. Despite these potential pitfalls, the manganese(I)-catalysis gave

expedient access to functionalized nucleotides and nucleotide/natural product conjugates, featuring the α,β -unsaturated ester moiety.



Scheme 3.4.7. Manganese(I)-catalyzed C–H allylation of nucleotides **259**.

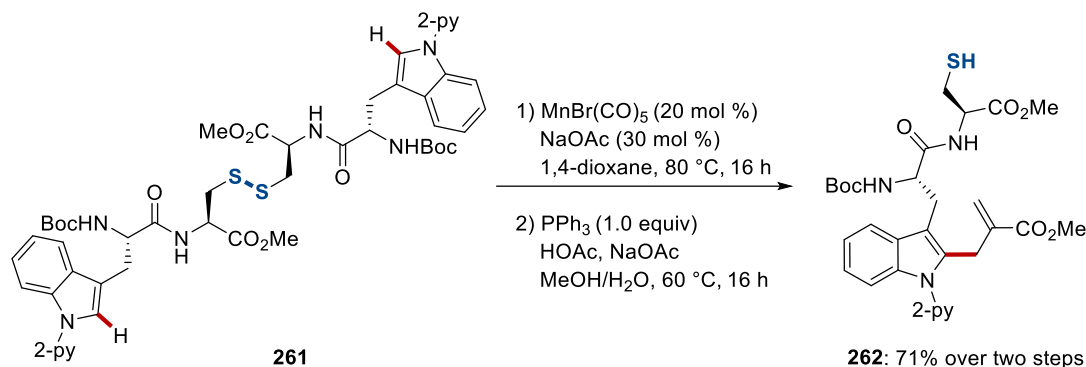
3.4.3. Synthetic Applications of the Manganese(I)-Catalyzed C–H Allylation Manifold

Recognizing the incompatibility of the protected MBH-adduct with the free-thiol moiety found in cysteine, we envisioned that a peptide dimer featuring a disulfide bond could act as an atom-economical protecting group surrogate. Thus, symmetric cysteine-containing tetrapeptide **261** was employed in a two-fold C–H functionalization strategy to obtain the difunctionalized tetrapeptide with excellent chemo- and site-selectivity (Scheme 3.4.8a). Subsequent triphenylphosphine-mediated disulfide reduction yielded

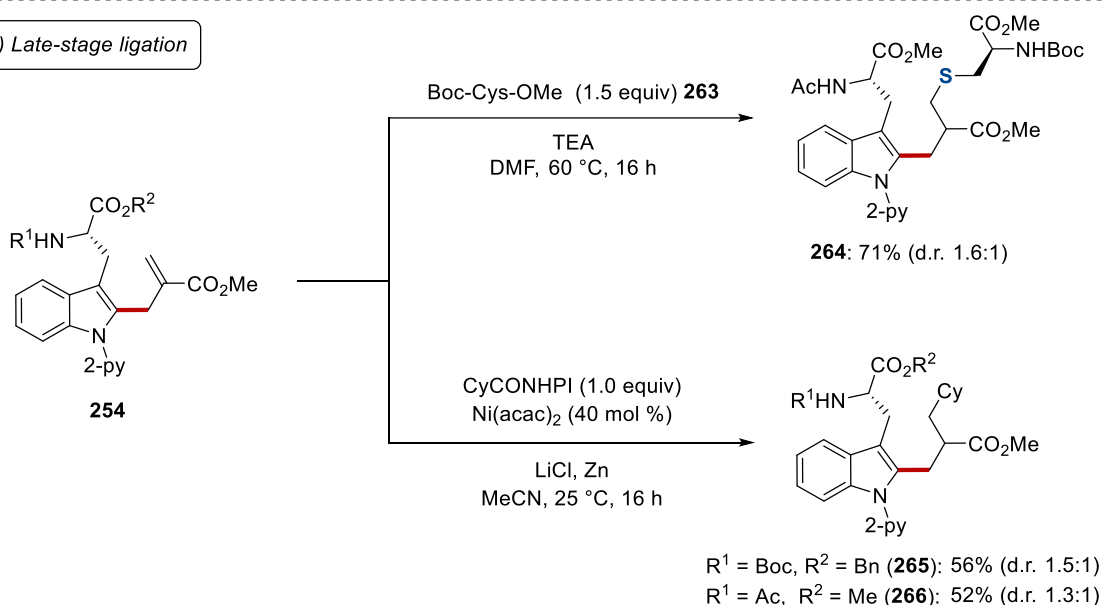
3. Results and Discussion

the desired functionalized dipeptide **262** in 71% yield over two steps. Remarkably, dipeptide **262** consists of highly nucleophilic thiol moiety and highly electrophilic α,β -unsaturated ester moiety, demonstrating the mild nature and chemoselectivity of our strategy. Having established a robust method for the incorporation of the reactive α,β -unsaturated ester moiety in structurally complex peptides, we probed whether Michael-type addition of various polar or radical nucleophiles could be applicable in a late-stage fashion, thus fully exploiting the bis-electrophilic nature of the protected MBH-adducts. To put this hypothesis into practice, the allylated amino acid **254** was efficiently converted *via* a *sulfa*-Michael addition of Boc-Cys-OMe **263** to the α,β -unsaturated ester with moderate stereocontrol, generating a diastereoisomeric mixture of the unnatural dipeptide **264** (Scheme 3.4.8b). Furthermore, radical addition to α,β -unsaturated ester *via* a nickel-catalyzed Giese coupling using *N*-hydroxy-phthalimide derived redox active ester as radical precursor yielded the functionalized amino acid derivatives **265** and **266**, albeit with moderate stereocontrol.^[170] Regarding the nickel-catalyzed Giese coupling, slight modification from the reported conditions was crucial in order to avoid the addition of the cyclohexyl radical to the pyridine ring *via* a Minisci type manifold, thus the redox active ester was used as the limiting reagent.

a) Two-fold C–H activation towards free-SH cysteine



b) Late-stage ligation



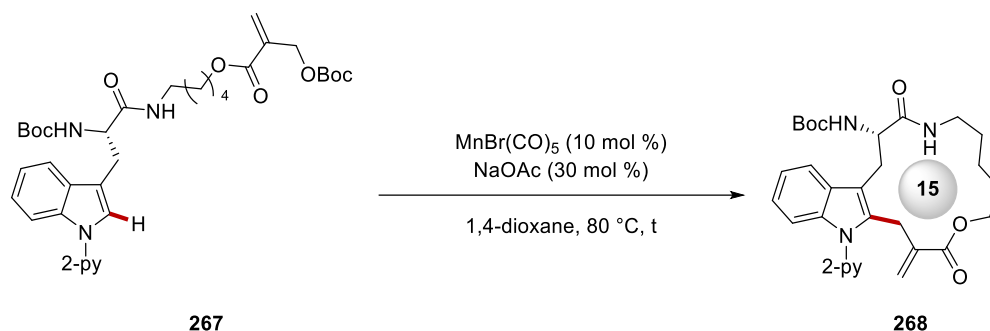
Scheme 3.4.8. a) Access to functionalized cysteine-containing dipeptide. b) Late-stage ligation *via* polar and radical type Michael addition.

3.4.4. Manganese(I)-Catalyzed Macrocyclization via an Allylation Manifold

Motivated by the unique robustness of our method, we probed the utility of the intramolecular C–H activation towards tryptophan-based macrocycles. To this end, we incorporated the conformationally unbiased linker 1,5-aminopentanol, which is devoid of a β -turn motif, into the tryptophan scaffold (Table 3.4.2). To our delight, after a short optimization the desired 15-membered macrocycle **268** was obtained in 57% yield, featuring the highly reactive exocyclic olefin. Further testament to the user-friendly and robust nature of our C–H allylation manifold is the straightforward scale-up of the macrocyclization in 1.0 mmol scale, obtaining the desired macrocycle **268** in even slightly better yield.

3. Results and Discussion

Table 3.4.2. Optimization studies for the manganese(I)-catalyzed C–H macrocyclization.

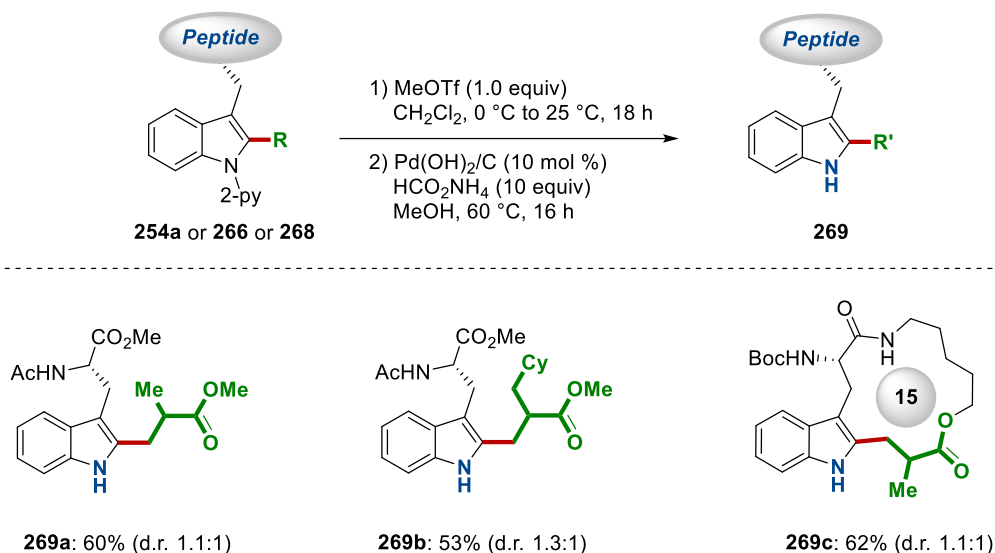


Entry	Concentration (mM)	t (h)	Yield (%)
1	20	20	53
2	20	40	62
3	40	20	57 (62)^a

Reaction conditions: **267** (0.20 mmol), $\text{MnBr}(\text{CO})_5$ (10 mol %), NaOAc (30 mol %), 1,4-dioxane, reaction time (t). Yields of isolated product. ^a On 1.0 mmol scale, by G. Sirvinskaite.

3.4.5. Late-Stage Removal of the Pyridyl Group

After the development of an efficient and reliable method for the late-stage diversification of structurally complex peptides featuring the 2-pyridyl moiety as the directing group, we were pleased to be able to remove the directing group *via* a methylation/hydrogenation manifold (Scheme 3.4.9). Thus, selective *N*-methylation with methyl triflate followed by hydrogenation of the resulting pyridinium salt led to the labile amination that after hydrolysis yielded the peptide **269** with the free indole scaffold, with concurrent hydrogenation of the olefin. Hence, functionalized amino acids were easily employed in this sequence yielding the desired derivative in moderate yields. Lastly, the 15-membered macrocycle **268** reacted efficiently under the reaction conditions giving rise to the azine group-free macrocycle as a diastereoisomeric mixture.



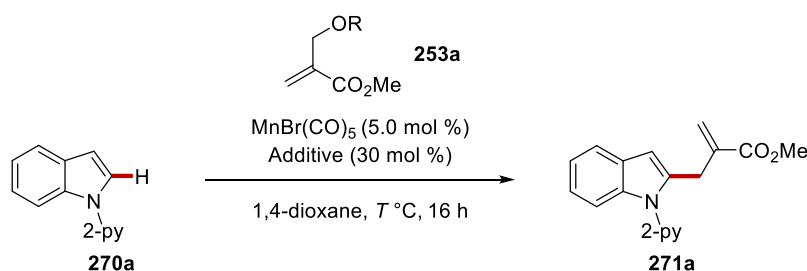
Scheme 3.4.9. Traceless removal of the directing group.

3.4.6. Manganese(I)-Catalyzed C–H Allylation of Heteroarenes with Protected MBH-Adducts

The efficiency of our manganese(I)-catalyzed C–H allylation of peptides with protected MBH-adducts **253a** prompted us to explore the feasibility of the functionalization of simpler heteroarenes, at exceedingly mild reaction conditions (Table 3.4.3). Thus, we began our optimization studies for the allylation of 1-(pyridin-2-yl)-1*H*-indole **270a** employing similar reaction conditions to those already developed for the functionalization of tryptophan-containing peptides, albeit with reduced catalyst loading. The allylated heteroarene **271a** was isolated in excellent yield (entry 1). Hence, the solvent effect was evaluated at lower reaction temperatures (entries 2-5), with 1,4-dioxane outperforming the solvents that were tested at 60 °C (entry 2). Gratifyingly, the desired allylation proceeded efficiently at 40 °C (entry 6). Further lowering of the reaction temperature at 25 °C led to slightly diminished efficiency, albeit the desired heteroarene **271a** could be obtained in good yield (entry 7).

3. Results and Discussion

Table 3.4.3. Optimization studies for the manganese(I)-catalyzed allylation of indole **270a**.



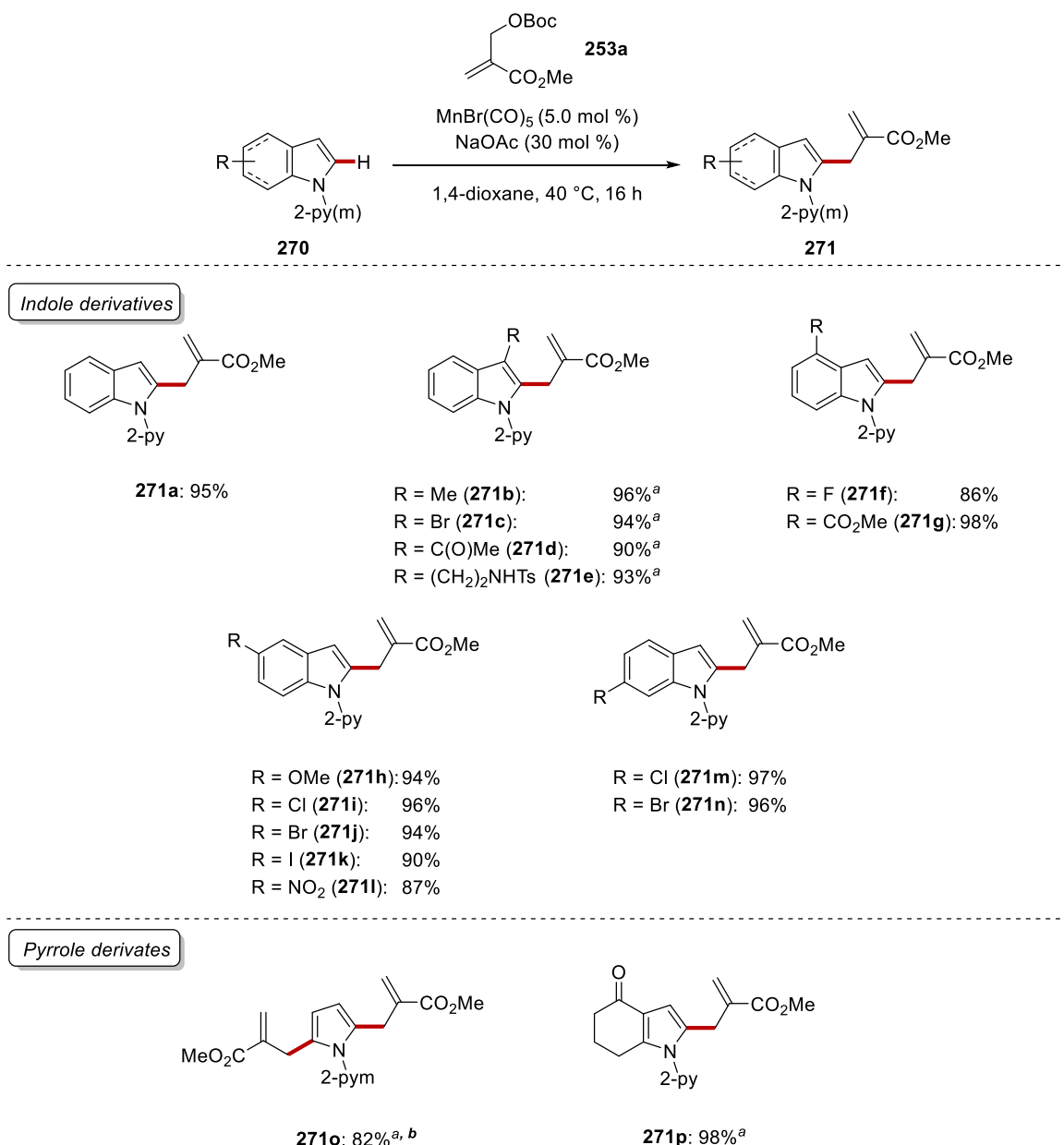
Entry	Solvent	Temperature (°C)	Yield (%)
1	1,4-dioxane	80	98
2	1,4-dioxane	60	98
3	DCE	60	97
4	TFE	60	98
5	H ₂ O	60	90
6	1,4-dioxane	40	95
7	1,4-dioxane	25	68

Reaction conditions: **270a** (0.25 mmol), **253a** (0.38 mmol), MnBr(CO)₅ (5.0 mol %), NaOAc (30 mol %), solvent (1.0 mL), 16 h. Yields of isolated product.

With the optimized reaction conditions in hand, we on explored the substrate scope of our allylation regime with diversely-decorated indole and pyrrole derivatives equipped with the 2-pyridyl or 2-pyrimidyl directing group (Scheme 3.4.10). 3-Substituted indole derivates **270** featuring bromo, keto or protected amine groups, among others, were efficiently allylated, albeit they required a higher reaction temperature, presumably due the increased steric hindrance. Next, the effect of the substitution pattern on the 4, 5 and 6 position on the indole scaffold was investigated. To our delight, a plethora of functional groups, including fluorides, bromides, iodide, esters and nitro, were efficiently tolerated, leading to the desired allylated heteroarenes **271** in a chemo- and

3. Results and Discussion

site-selective fashion. Furthermore, pyrrole derivatives were also viable substrates under standard reactions, whereas requiring higher reaction temperature to ensure good conversions. Remarkably, the two-fold C–H allylation of the unsubstituted pyrrole derivative **270o** proceeded with good efficiency, giving rise to the bis-allylated heteroarene.



Scheme 3.4.10. Manganese(I)-catalyzed C–H allylation of indoles and pyrroles **270**.

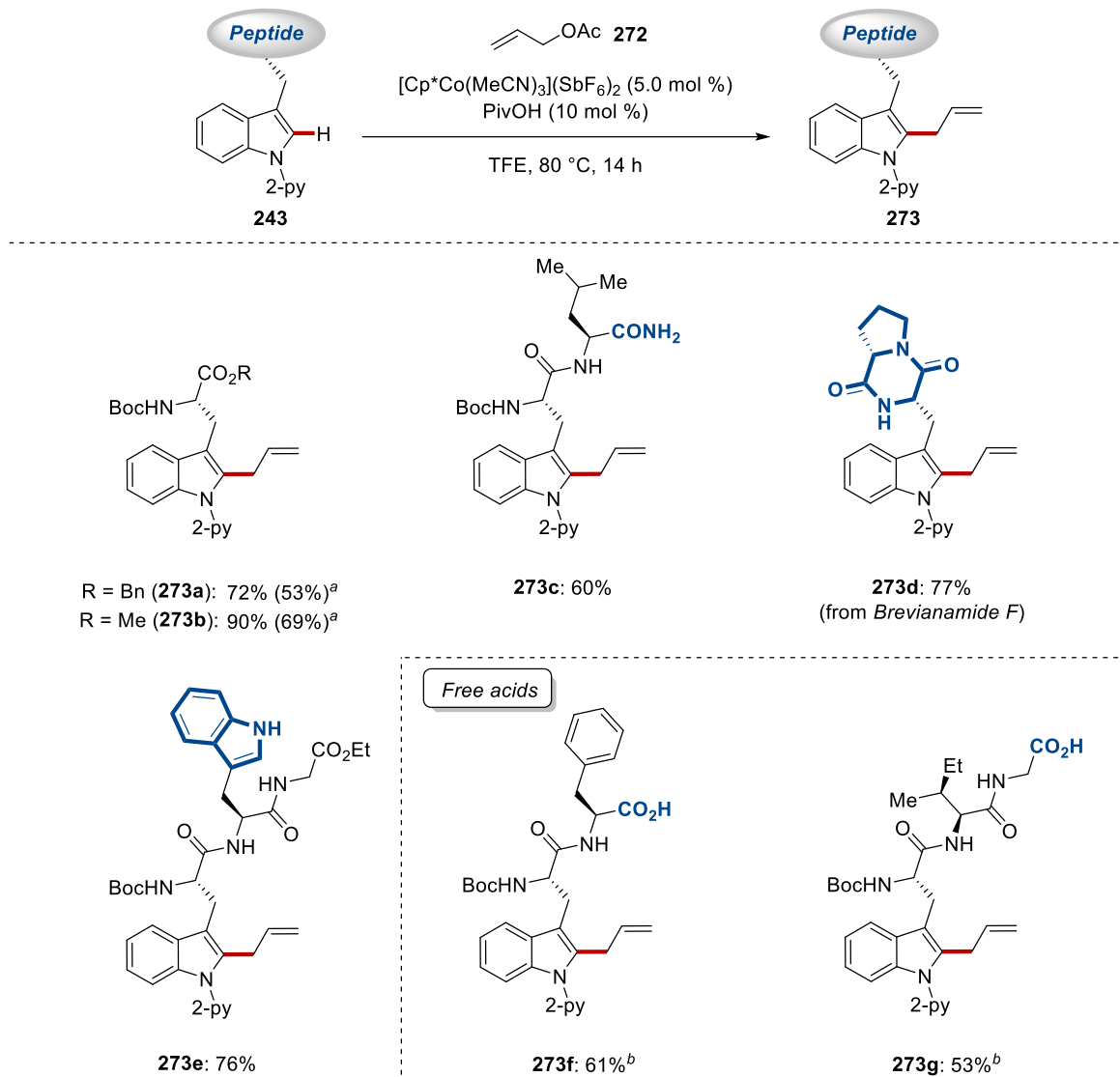
^a Reaction at 80 °C. ^b 3.0 equiv of **253a** were used.

3. Results and Discussion

3.4.7. Late-Stage Cobalt(III)-Catalyzed C–H Allylation of Tryptophan-Containing Peptides

Cobalt(III)-catalysis has emerged as a powerful strategy for the functionalization of inert C–H bonds.^[171] Particularly, substitutive C–H allylations on simple (hetero)arenes have been well-established,^[172] as the allyl moiety is easily transformed to a variety of valuable functional groups. Motivated by these reports, Dr. M. Lorion developed the allylation of tryptophan residues **243** with allyl acetate **272**, utilizing cationic $[\text{Cp}^*\text{Co}(\text{MeCN})_3](\text{SbF}_6)_2$ as the catalyst along with co-catalytic amounts of pivalic acid. Thus, the scope of this method was investigated with various amino acid derivatives and small peptides **243** (Scheme 3.4.11). The C–H allylations showed good functional group tolerance and robustness, as the addition of superstoichiometric amounts of H_2O did not diminish the desired reactivity. Furthermore, peptides bearing primary amides, *NH*-free indoles, and free carboxylic acids were efficiently allylated in a chemo- and site-selective fashion.

3. Results and Discussion

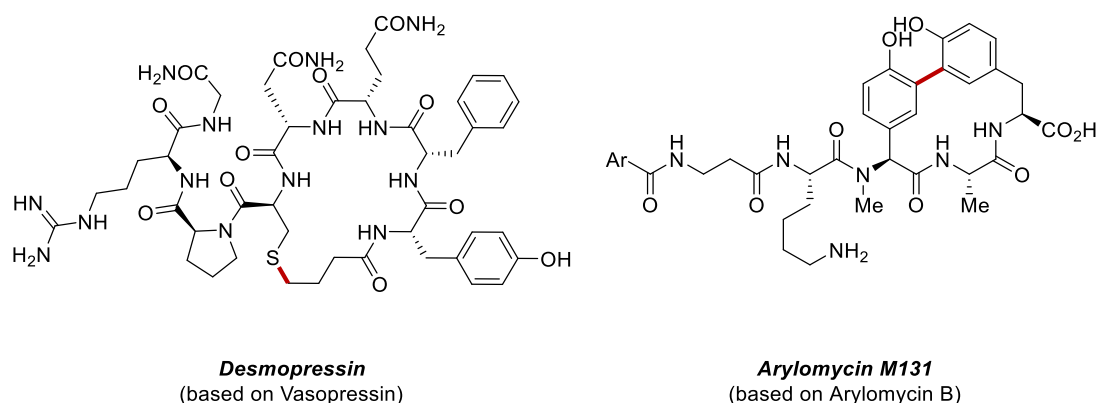


Scheme 3.4.11. Cobalt(III)-catalyzed C–H allylation . ^a In the presence of H₂O(10 equiv). ^b With 10 mol % of [Cp*Co(MeCN)₃](SbF₆)₂.

3. Results and Discussion

3.5. Manganese(I)-Catalyzed Peptide C–H Ligation and Macrocyclization

Peptides are responsible for a plethora of biological events, thus, they have been utilized as therapeutics for the treatment of many types of diseases.^[173] Furthermore, peptides and proteins are essential for proteomics, diagnosis and drug delivery. While natural peptides, such as insulin, are of great importance in present drug market and drug discovery programs, new strategies for enhancing their activities, making them more suitable drug candidates, have appeared.^[174] In this context, unnatural amino acids, unconventional linkages or cyclization of linear precursors offer new avenues for expanding the viable chemical space (Scheme 3.5.1). Traditionally, peptide syntheses rely on iterative coupling/deprotection regime, that has been automated, enabling facile access to large peptides.^[175]



Scheme 3.5.1. Bioactive cyclic peptides featuring exotic linkages.

This strategy can be used to produce native peptides as well as unnatural peptides by using amino acids with modified side chains. Despite the enormous applications of SPSS, unnatural linkages within the peptidic backbone are not easily accessible. In this context, new methods for the chemo- and site-selective stitching of a peptidic fragment with another peptidic or sugar fragment are of utmost importance as multifunctional conjugates are produced.^[176] In addition, more recently, medicinal and biological chemists have shifted their attention to cyclic peptides, due to their recognized pharmacological advantages of these macrocyclic molecules over their acyclic counterparts.^[177] This can be partially attributed to improved membrane permeability and metabolic resistance. Macrocycles are conformationally constrained molecules. However, due to their large ring sizes they have appreciable degrees of flexibility and hence exist in distinct conformations. Due to this subtle conformational

interplay, they can adopt various conformations with minimum entropic cost, thus, enabling efficient binding to biological targets.

As a consequence, we became interested in the development of an atom- and step-economical method for the C–H ligation and macrocyclization of tryptophan-containing peptides. Despite the significant progress in the late-stage functionalization of amino acids and peptides, this is mainly achieved by noble metal-catalyzed C–H activation manifolds.^[25g] While these regimes enabled the assembly of challenging cyclic peptides, toxic and costly palladium catalysts were required, which, among others could prove detrimental due to their costs and trace metal impurities of the toxic and precious metal. In contrast, 3d-transition metal-catalyzed C–H activation has only recently gained considerable attention.^[26] Hence, we decided to probe whether non-toxic manganese(I) complexes can enable the peptide stitching and macrocyclization. In order to develop a user-friendly and robust methodology, the functionalization of tryptophan moieties with modular propiolates was envisioned.

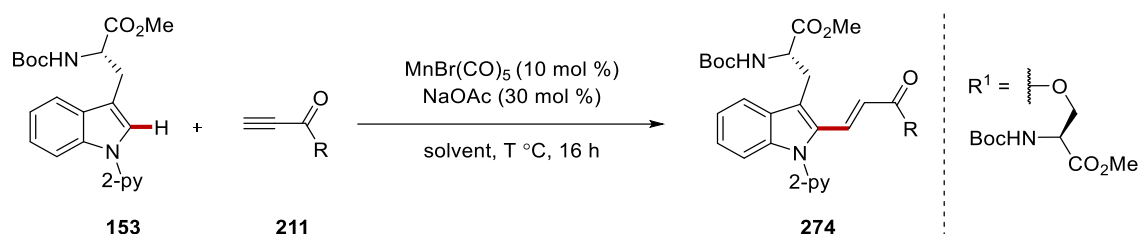
3.5.1. Optimization Studies for Peptide Stitching *via* C–H Hydroarylation of Propiolates with Tryptophan-Containing Peptides

At the outset of our optimization studies we chose tryptophan derivative **153** featuring the 2-pyridyl as directing group, ethyl propiolate **211a** as the coupling partner and catalytic amounts of MnBr(CO)₅ in combination with NaOAc at 100 °C as our initial conditions (Table 3.5.1). After testing various polar, non-polar, protic and aprotic solvents, 1,4-dioxane and DME showed the best results, as the desired product was isolated in excellent yields with complete *E*-selectivity (entries 3 and 4). Interestingly, manganese(I)-catalysis showed reasonable reactivity even in the presence water (entry 6), albeit with a diminished isolated yield. In consideration of the near quantitative yield obtained at 100 °C, further efforts to reduce the reaction temperature, in order to provide a milder reaction protocol, demonstrated that the reaction was efficient even at 60 °C, similarly providing the product in near quantitative yield (entry 8). Control experiments showed the importance of NaOAc, that presumably enabled the formation of Mn(OAc)(CO)₅ thus facilitating the C–H activation step *via* carboxylate assistance,^[17a] and the essential nature of the MnBr(CO)₅ (entries 10 and 11). Under the optimized reaction conditions, serine-derived propiolate **211b** was tested giving rise to the unnatural dipeptide **274b** in 86% yield (entry 12). To increase the efficiency of the unnatural dipeptide formation higher reaction temperatures were tested (entries

3. Results and Discussion

13 and,14). Gratifyingly, the desired product was obtained in 95% ($E/Z \geq 95:5$) at 100 °C. Notably, the reaction proceeded without erosion of the enantiointegrity of the tryptophan scaffold, demonstrating the mild nature of this manganese(I) hydroarylation manifold.

Table 3.5.1. Optimization studies for the manganese(I)-catalyzed C–H alkenylation.



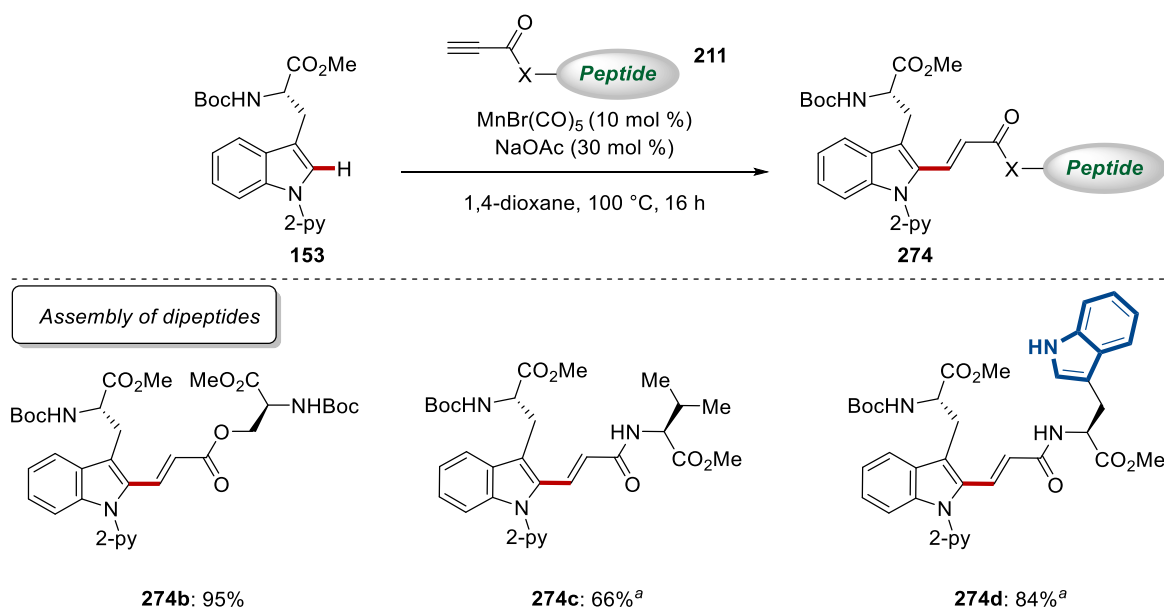
Entry	R	Solvent	Temperature (°C)	Yield (%)
1	OEt	toluene	100	37
2	OEt	DCE	100	83
3	OEt	DME	100	97
4	OEt	1,4-dioxane	100	98
5	OEt	DMF	100	---
6	OEt	H ₂ O	100	43
7	OEt	1,4-dioxane	80	97
8	OEt	1,4-dioxane	60	97
9	OEt	1,4-dioxane	40	58
10	OEt	1,4-dioxane	60	85 ^a
11	OEt	1,4-dioxane	60	--- ^b

12	R ¹	1,4-dioxane	60	86
13	R ¹	1,4-dioxane	80	90
14	R¹	1,4-dioxane	100	95

Reaction conditions: **153** (0.15 mmol), **211** (0.23 mmol), MnBr(CO)₅ (10 mol %), NaOAc (30 mol %), solvent (0.6 mL), 16 h. Yields of isolated product. ^a Without NaOAc. ^b Without MnBr(CO)₅.

3.5.2. Manganese(I)-Catalyzed C–H Stitching

With the optimized reactions in hand, we probed whether different propiolates **211** featuring amino acids could be suitable substrates (Scheme 3.5.2). Thus, valine- and tryptophan-derived propiolates, featuring an amide linkage, provided the desired dipeptides in good to excellent yields. Gratifyingly, peptide **274d** was formed in site-selective fashion, despite the presence of a second tryptophan moiety.



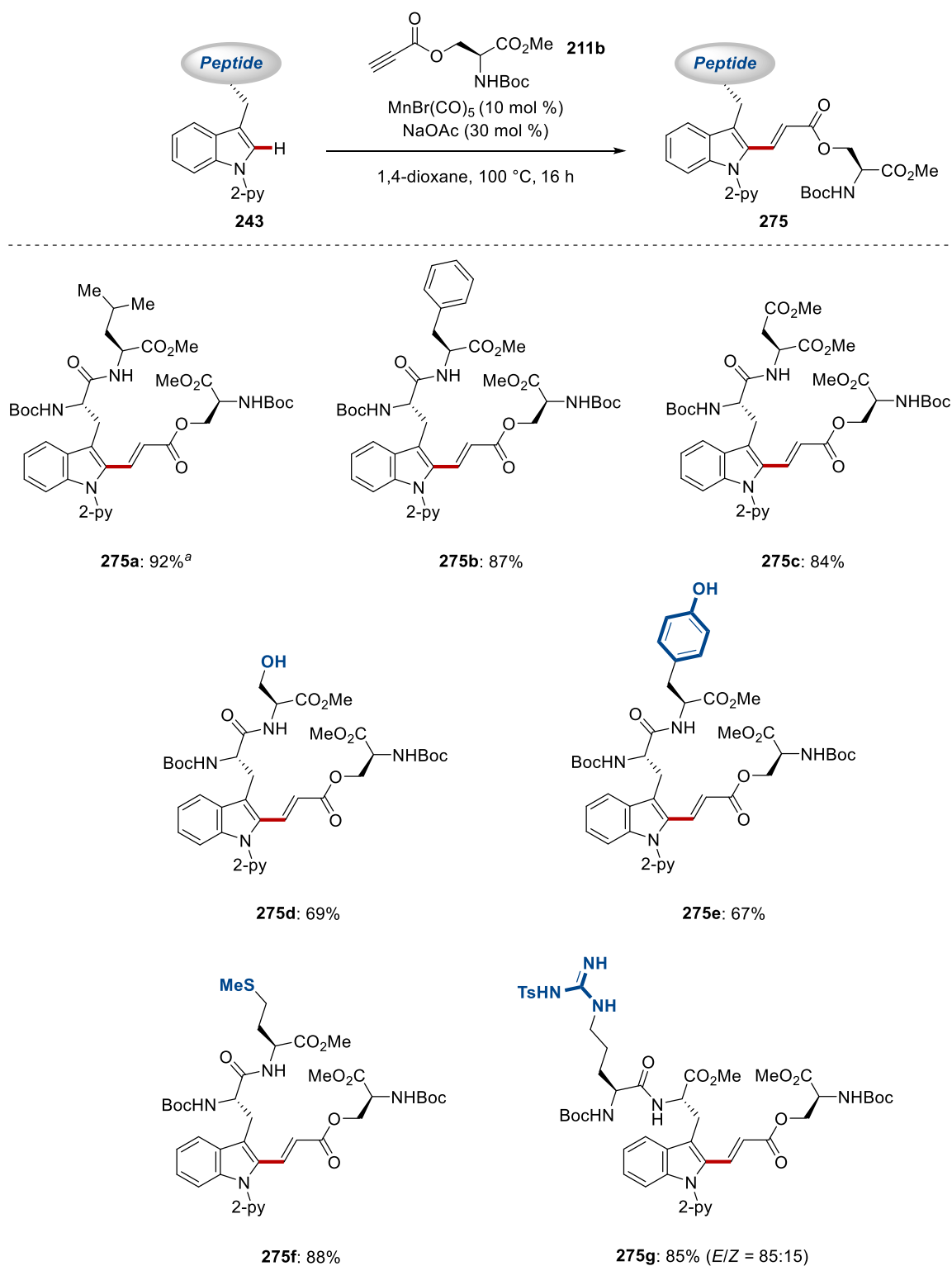
Scheme 3.5.2. Manganese(I)-catalyzed synthesis of unnatural dipeptides. ^a

Performed by G. Sirvinskaite.

Encouraged by the efficient synthesis of unnatural dipeptides we examined whether under the optimized reaction conditions tripeptides could be obtained in chemo- and site-selective fashion (Scheme 3.5.3). To our delight, our methodology was able to

3. Results and Discussion

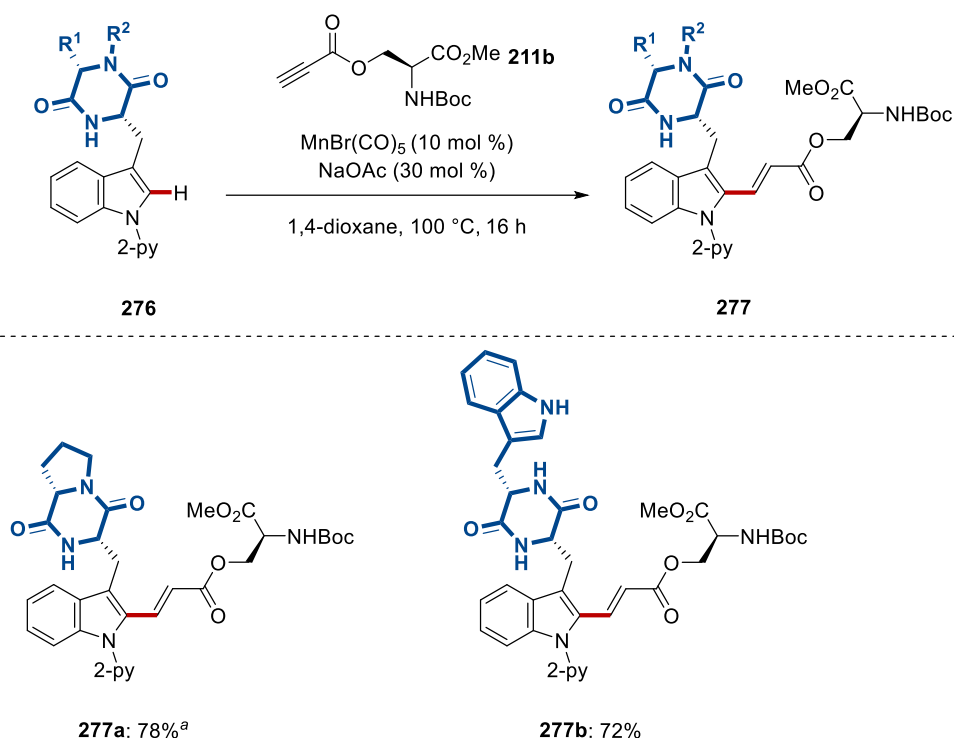
stitch various dipeptides with the serine-derived propiolate **211b**, showcasing the mild and chemo-selective nature of manganese(I)-catalyzed hydroarylation manifold. Thus, dipeptides containing aliphatic and aromatic side chains were efficiently utilized. In addition, dipeptide containing protected aspartic acid was utilized giving rise to the desired tripeptide **275c** in 84%. Moreover, dipeptides containing free serine and tyrosine, possessing unprotected hydroxyl and phenol groups were efficiently converted with excellent levels of chemo-selectivity, as the potentially competing oxa-Michael addition was not observed. In addition, dipeptide featuring methionine was employed, giving rise to the sulfide containing tripeptide **275f** in 88% yield. Lastly, dipeptide **243ad** bearing the nitrogen-rich guanidine group was efficiently converted to the desired tripeptide, albeit with a moderate stereoselectivity.



Scheme 3.5.3. Manganese(I)-catalyzed synthesis of unnatural tripeptides.

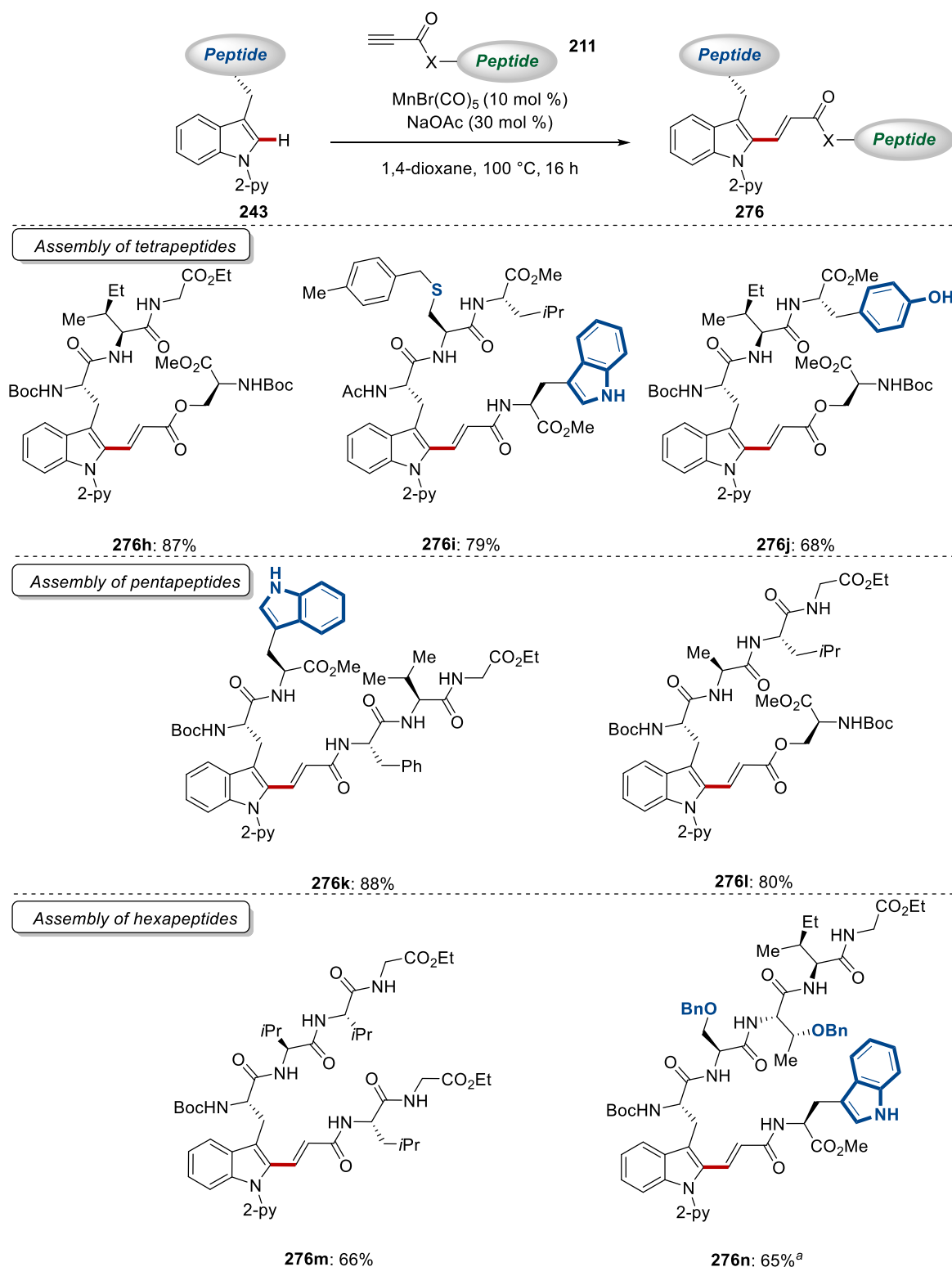
The site-selective functionalization of dipeptides *en route* to tripeptides was not limited to linear peptides. Thus, cyclic dipeptides featuring the 2,5-diketopiperazine scaffold, were utilized in this methodology providing expedient access to derivatives of *Brevianamide F* **277a** and *Fellutanine A* **277b** in excellent yields (Scheme 3.5.4).

3. Results and Discussion



Scheme 3.5.4. Manganese(I)-catalyzed C–H functionalization of 2,5-diketopiperazines. ^a Performed by G. Sirvinskaite.

Motivated by our chemo- and site-selective method to stitch peptides *via* C–H hydroarylation we strode to expand our approach to more complex peptides **243** and propiolates **211**. In sharp contrast to the traditional peptide syntheses that rely on iterative couplings, this strategy would provide a more step-economical and convergent methodology for the synthesis of large peptides (Scheme 3.5.5). Thus, tetrapeptides were readily synthesized bearing protecting cysteine and unprotected tyrosine among other amino acids. Furthermore, tripeptide-derived propiolate **211f** was efficiently used as coupling partner with the dipeptide **243ac** providing the pentapeptide **276k** in excellent yield. Moreover, our strategy gave rise to hexapeptides, *via* either a 4+2 or a 5+1 approach, in site-selective fashion and good yields, utilizing peptides bearing protected serine and threonine as well as *NH*-free tryptophan.

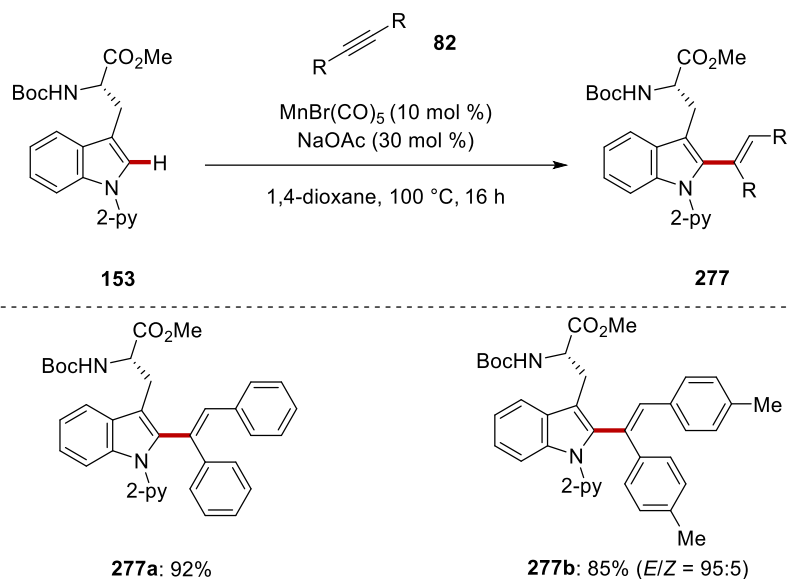


Scheme 3.5.5. Manganese(I)-catalyzed assembly of large peptides via C–H hydroarylation. ^a Performed by G. Sirvinskaite.

Our hydroarylation manifold was not restricted to activated and terminal alkynes. Indeed, symmetrical diaryl alkynes **82** were also efficiently converted to the desired trisubstituted-olefin containing tryptophan derivatives **277a** and **277b** under otherwise

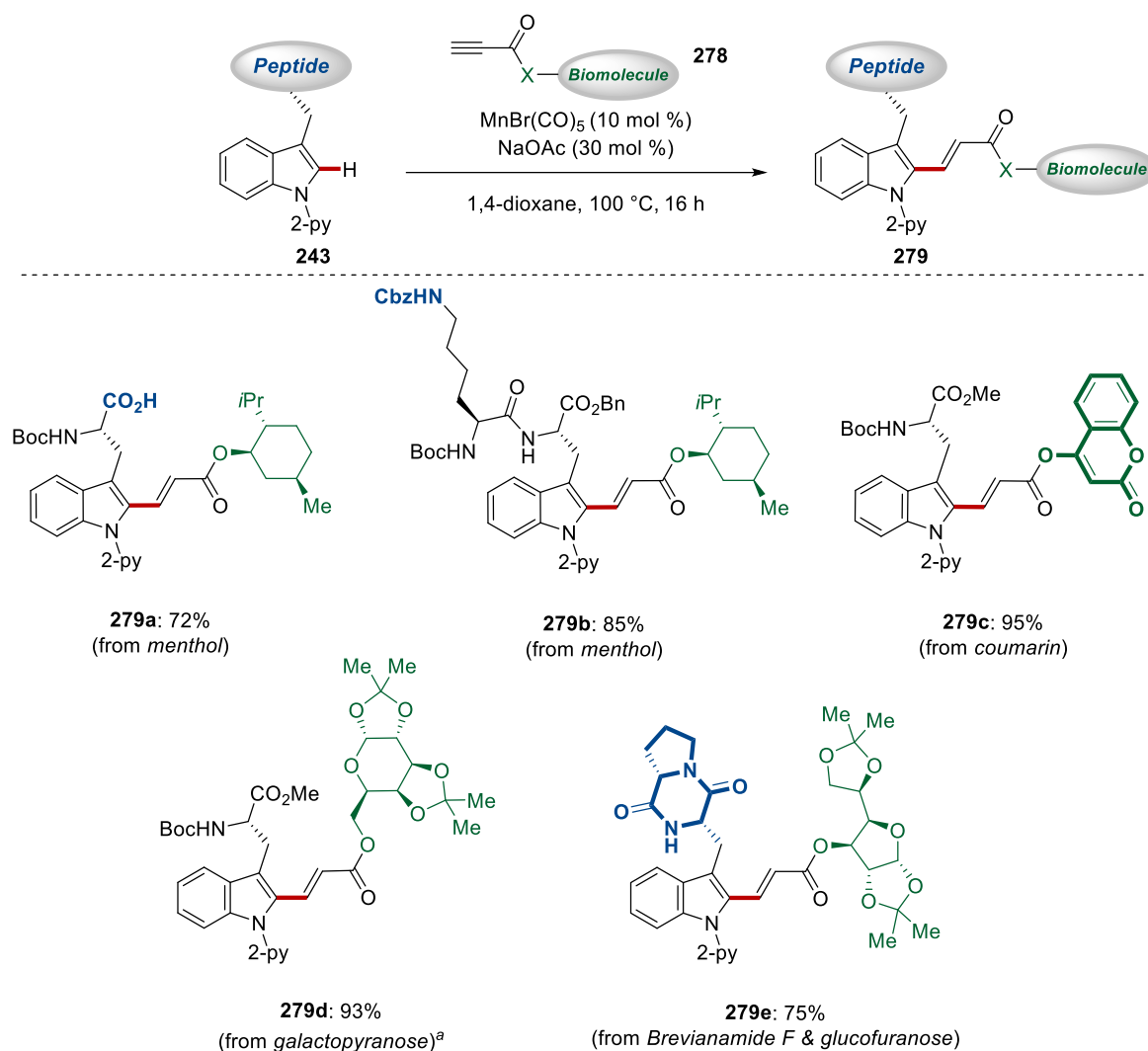
3. Results and Discussion

similar reaction conditions (Scheme 3.5.6). Aryl-substituted propiolates gave inseparable mixtures of regioisomers, limiting their synthetic application.



Scheme 3.5.6. Manganese(I)-catalyzed synthesis of tryptophan derivatives **153**, bearing trisubstituted olefins.

The ability to stitch fragments that perform two distinct functions, based on their molecular architecture, is of utmost importance since new multi-functional molecules arise.^[160b-d] Thus, we became intrigued to investigate whether our strategy could be employed for this purpose (Scheme 3.5.7). Gratifyingly, Boc-Trp^{py}-OH was efficiently sewed with the menthol-derived propiolate **211f**, giving rise to the alkenylated product **279a** destined for iterative peptide synthesis. Furthermore, dipeptide **243ac**, featuring orthogonally bis-protected lysine, was efficiently used, allowing the selective expansion of the peptide chain *via* selective *N*-deprotection. The coumarin-based fluorescent tag was easily incorporated into the tryptophan moiety ensuring access to an amino acid with altered fluorescent properties. Lastly, sugar fragments, featuring protected galactopyranose and glucofuranose, were efficiently utilized under this methodology providing the glucopeptides **279d** and **279e** in excellent yields.



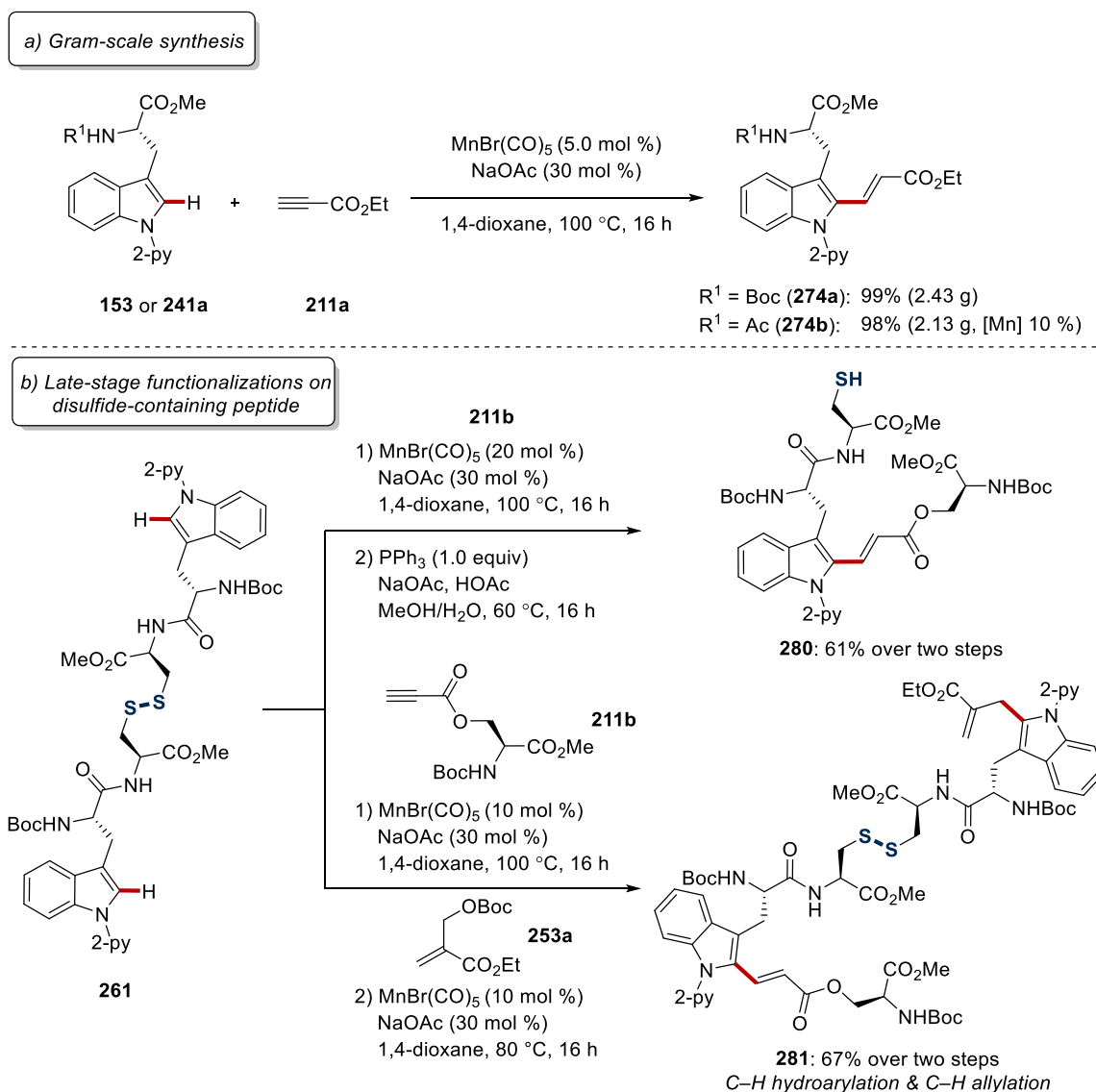
Scheme 3.5.7. Manganese(I)-catalyzed synthesis of hybrid molecules **279** via C–H hydroarylation. ^a Performed by G. Sirvinskaite.

3.5.3. Synthetic Applications of the Manganese(I)-Catalyzed Hydroarylation Manifold

The user-friendly nature of our hydroarylation manifold was reflected by the efficient gram-scale (5.0 mmol) synthesis of the functionalized amino acid **274a** and **274b** in near quantitative yields (Scheme 3.5.8a). The robustness of this process is showcased by the high catalytic efficiency even in reduced catalyst loading under otherwise similar reaction conditions. Furthermore, in order to obtain alkenylated peptides with free cysteine, a two-fold C–H activation strategy of cysteine-containing peptide **261** was employed, where the disulfide bond acts as an atom-economical protecting-group surrogate (Scheme 3.5.8b). Thus, the two-fold C–H functionalization followed by triphenylphosphine-mediated disulphide reduction yielded the desired thiol-containing

3. Results and Discussion

peptide in 61% over two steps. The cystine-containing peptide **261** possessing two azinyl-tryptophan residues, allows the sequential functionalization, after judicious tuning of the stoichiometry of the initial C–H functionalization, under two distinct reaction manifolds (Scheme 3.5.8b). Therefore, the manganese(I)-catalyzed hydroarylation manifold, utilizing the serine-derived propiolate as the limiting reagent to ensure synthetically useful mono-selectivity, was combined with manganese(I)-catalyzed allylation with protected PPH₃ MBH-adducts, thus affording the difunctionalized tetrapeptide in 67% yield over two steps. The orchestration of the sequential difunctionalization of the symmetric tetrapeptide **281** occurred in a chemo- and site-selective fashion.



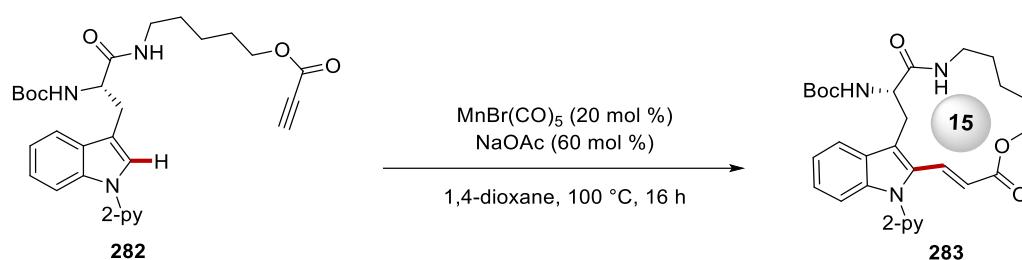
Scheme 3.5.8. a) Gram-scale manganese(I)-catalyzed hydroarylation. b) Late-stage functionalizations of cystine-containing peptide **261**.

3.5.4. Manganese(I)-Catalyzed Macrocyclization via a Hydroarylation Manifold

Having established a reliable method for the ligation of peptides with peptides, sugars and natural products, *via* a C–H hydroarylation manifold, we probed whether this strategy could be expanded to the synthesis of cyclic peptides *via* a C–H macrocyclization. The synthesis of macrocycles is a challenging transformation,^[178] since fine-tuning of the reaction conditions has to be performed for different classes of molecules as even small conformational changes of the starting material can lead to side-reactions.^[179] This holds especially true for peptides, since their conformation is sequence dependent. Thus, the macrocyclization disconnection for the cyclization of a pentapeptide is not obvious and various disconnections have to be examined in order to develop efficient macrocyclization. In addition, traditional macrolactamization methods, like carbodiimides, active esters, phosphonium salts and aminium/uronium salts, can potentially lead to epimerization of the residue that is activated due to the slow rate of the amide formation.^[180] Thus, alternative methods have been developed featuring cross-coupling, olefin-metathesis and recently C–H activation strategies.^[181] In the field of C–H macrocyclization palladium has dominated, with many examples in C(*sp*²)–H and C(*sp*³)–H bond activations, leading to the elegant formal synthesis of *Celogentin C* by Wang.^[141] To examine whether our C–H hydroarylation manifold is suitable for this demanding transformation, linear precursor **282** was reacted under high dilution conditions, utilizing higher catalyst loading to ensure synthetically useful reaction rates (Table 3.5.2). Gratifyingly, the desired 15-membered cyclic amide was isolated in 64% at 5 mM concentration. Remarkably the formation of dimer was not observed under the reaction conditions tested, based on careful LC-MS analysis, thus facilitating the isolation of the macrocycle.

3. Results and Discussion

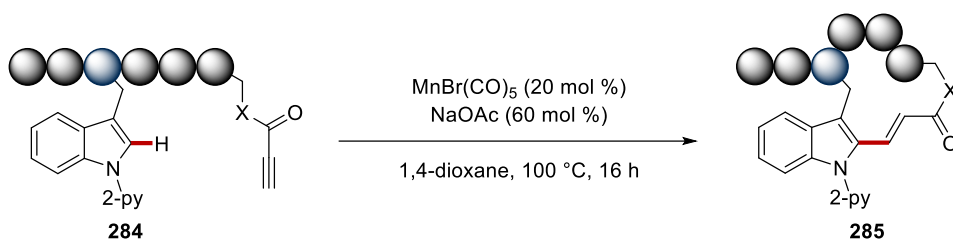
Table 3.5.2. Optimization studies for the manganese(I)-catalyzed C–H macrocyclization.



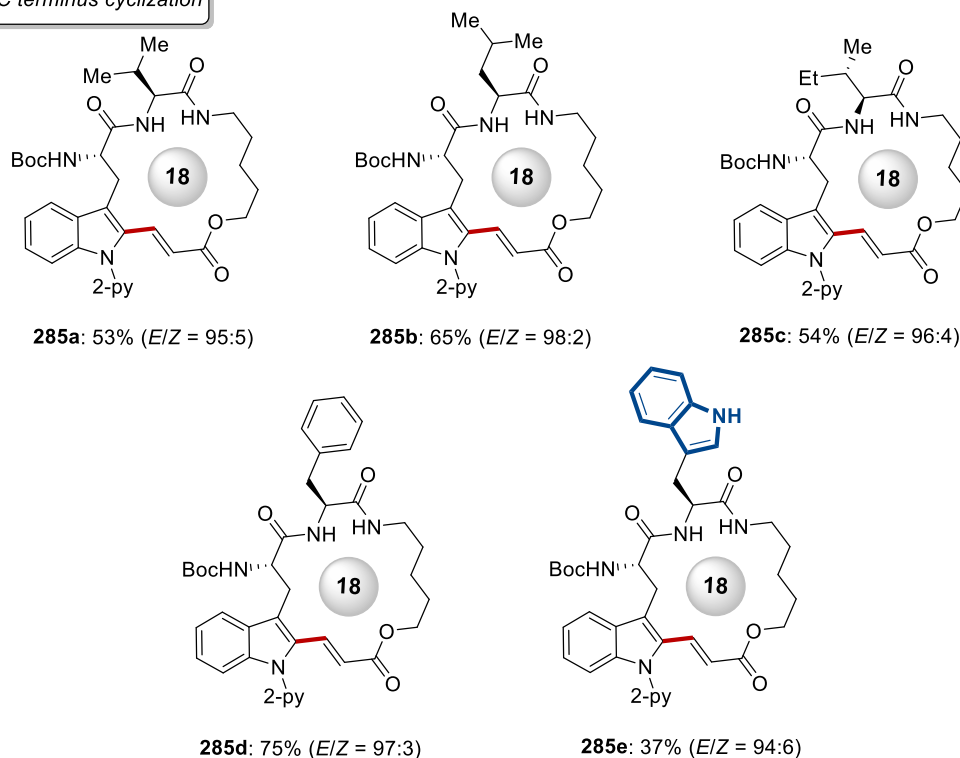
Entry	Concentration (mM)	Yield (%)
1	20	27
2	10	38
3	5	64

Reaction conditions: **282** (0.15 mmol), $\text{MnBr}(\text{CO})_5$ (20 mol %), NaOAc (60 mol %), 1,4-dioxane, 16 h. Yields of isolated product.

With the optimized reaction conditions in hand, we tested various dipeptides **284** bearing the tethered propiolate moiety. The reaction proceeded efficiently for aliphatic and aromatic amino acids embedded in the peptidic sequence, providing the desired 18-membered macrocycles in good to excellent yields and *E*-selectivity (Scheme 3.5.9). The excellent positional selectivity was reflected by the synthesis of cyclic dipeptide **285e** featuring two different tryptophan moieties, one bearing the 2-pyridyl directing group while the other having its indole scaffold unprotected.



Trp → C terminus cyclization

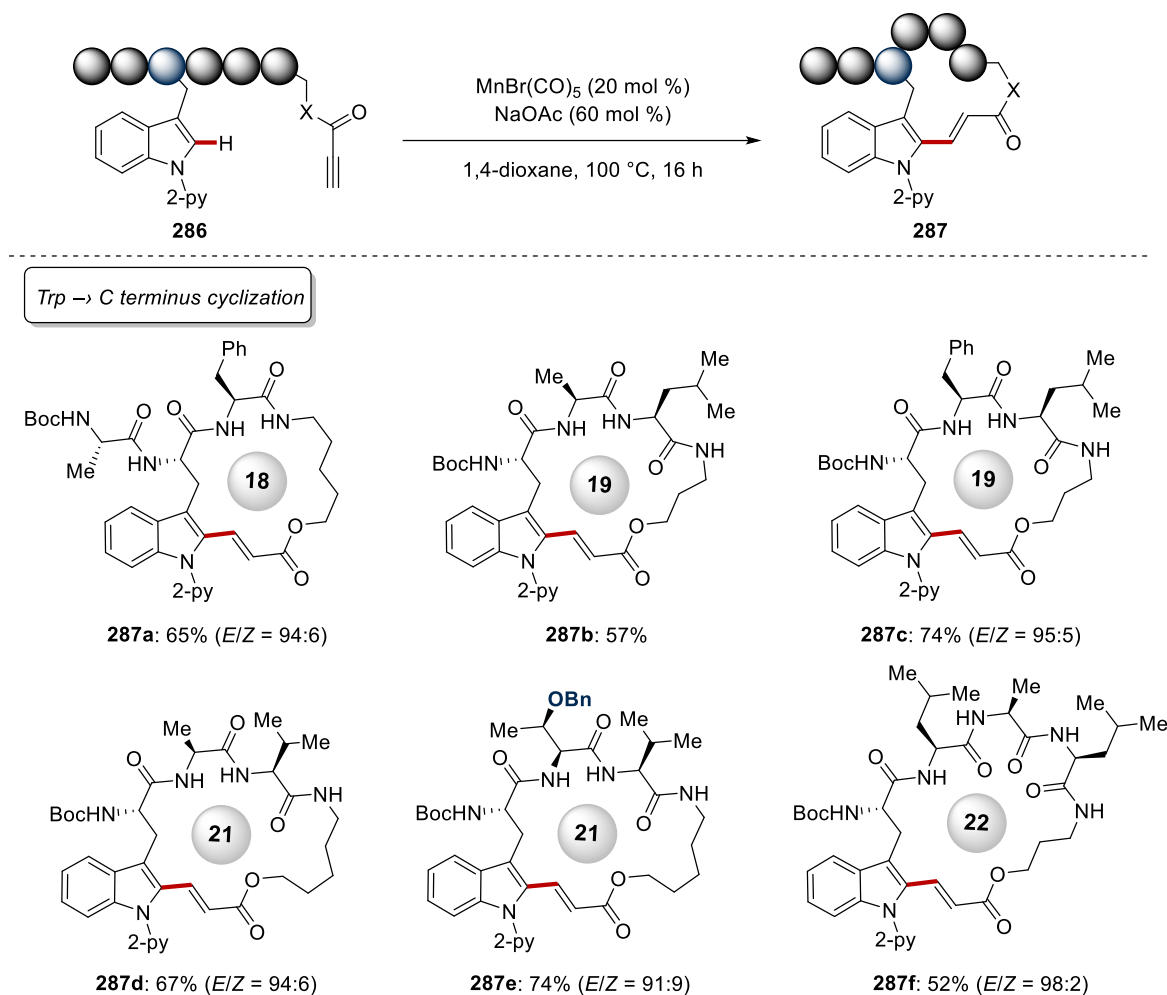


Scheme 3.5.9. Manganese(I)-catalyzed synthesis of cyclic dipeptides **285** via C–H hydroarylation.

Motivated by the remarkable efficiency of the synthesis of cyclic dipeptides **285** by our hydroarylation manifold we probed whether longer linear precursors can be effectively cyclized under this method. Thus, tri- and tetrapeptides were used as substrates for this manganese(I)-catalyzed macrocyclization (Scheme 3.5.10). Pleasingly, in all the cases good to excellent yields were observed along with excellent stereo- and chemo-selectivities. The cyclization of peptides at a residue that is not at a terminal position is challenging, due to steric hindrance and conformational restraints. In addition, traditional directing groups incorporated at the C or N terminus, as is the case for the majority of palladium-catalyzed C–H macrocyclizations, would fall short in this type of transformation. Gratifyingly, peptide **287a**, featuring the tryptophan residue in the middle of the peptidic sequence, was obtained in 65%. Remarkably, the high efficiency in the assembly of **287a**, compared to its simpler counterpart **285d**, where tryptophan

3. Results and Discussion

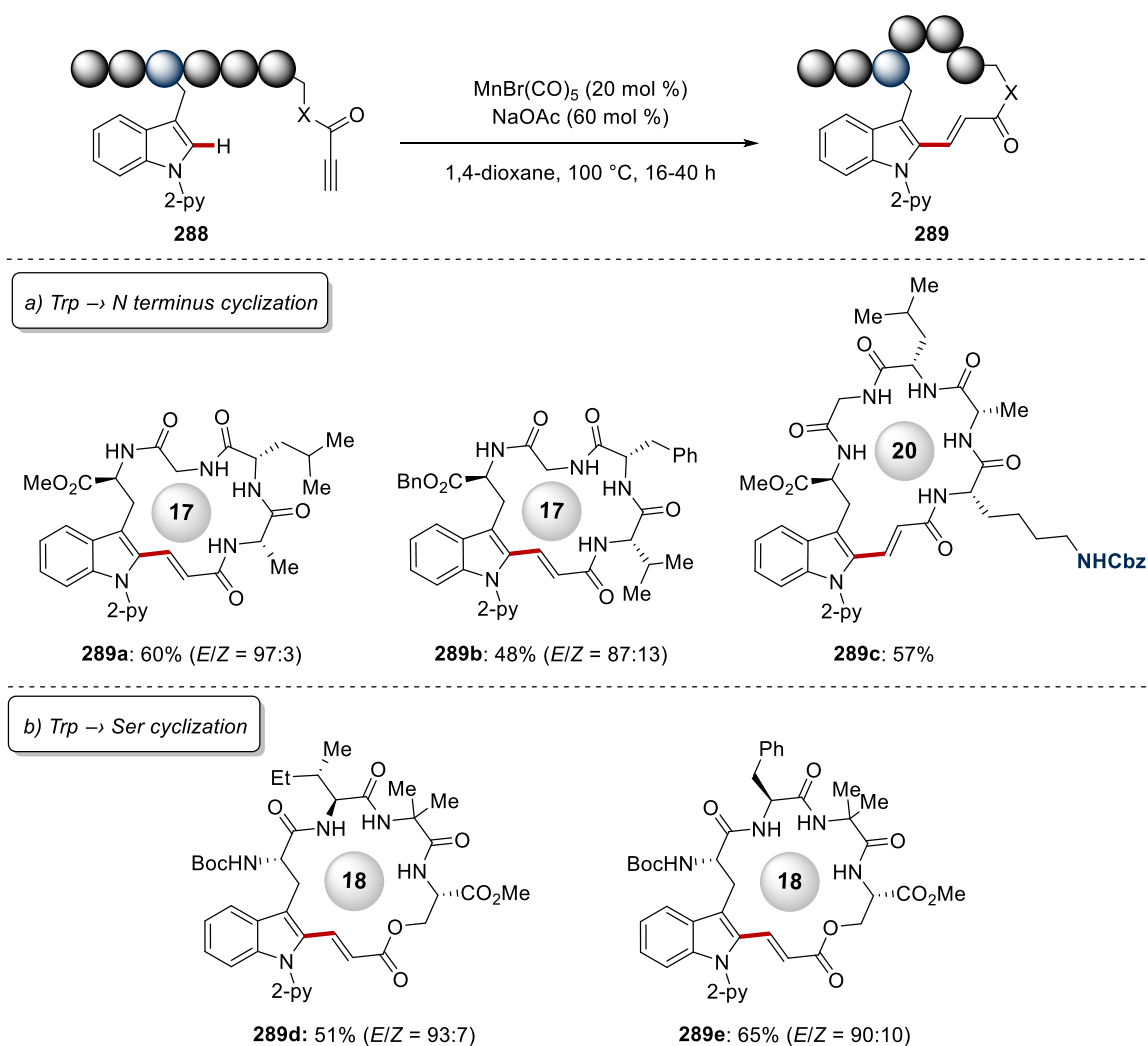
is at the terminal position, demonstrated the generality of our manganese(I)-catalyzed hydroarylation manifold that is not hampered by the steric hindrance or the conformational flexibility of the linear peptides.



Scheme 3.5.10. Manganese(I)-catalyzed synthesis of cyclic tri- and tetrapeptides *via* C–H hydroarylation.

Thus far, our method gave expedient access to cyclic peptides *via* a Trp→C terminus macrocyclization strategy utilizing α,ω -aminoalcohols as linkers. In order to complement our approach we recognized that the propiolate could be introduced in the peptidic chain at the *N* terminus or at the side chain of amino acids that bear the proper handle e.g. serine, threonine and lysine (Scheme 3.5.11a). Thus, the propiolate moiety was installed in the *N*-terminus of tetra- and pentapeptides and under prolonged reaction times and under higher dilution conditions, the desired peptides **289a**, **289b** and **289c** were obtained in good to excellent yields leading to 17- and 20-membered macrocycles. The higher dilution conditions were required as the lower reactivity of the

propiolamide moiety resulted in lower macrocyclization rate and as a consequence led to degradation pathways. The prolonged reaction time balanced the lower reaction rate at the higher dilution conditions. Serine was selected as the alcohol containing amino acid suitable for the installation of the propiolate moiety (Scheme 3.5.11b). Gratifyingly, under the optimized reaction conditions cyclic tetrapeptides **289d** and **289e** were efficiently obtained in good yields and excellent chemo- and stereoselectivities.



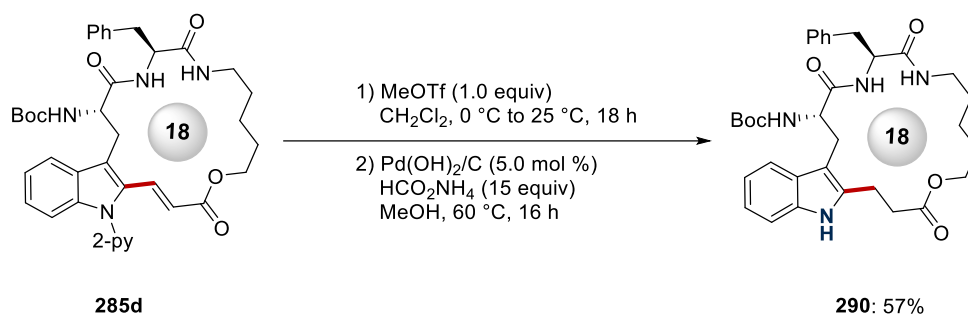
Scheme 3.5.11. a) Trp → *N* terminus manganese(I)-catalyzed cyclization. b) Trp → Ser manganese(I)-catalyzed cyclization.

3.5.5. Traceless Removal of the Pyridyl Group from the Cyclic Peptide **285d**

After the development of an efficient and reliable method for the synthesis of cyclic peptides featuring the 2-pyridyl moiety, we were delighted to be able to remove the directing group *via* a methylation/hydrogenation manifold (Scheme 3.5.12). Thus, selective *N*-methylation with methyl triflate and subsequent hydrogenation of the

3. Results and Discussion

resulting pyridinium salt gave the labile aminal, that after hydrolysis yielded the cyclic peptide **290** with the *NH*-free indole scaffold.



Scheme 3.5.12. Traceless removal of the directing group.

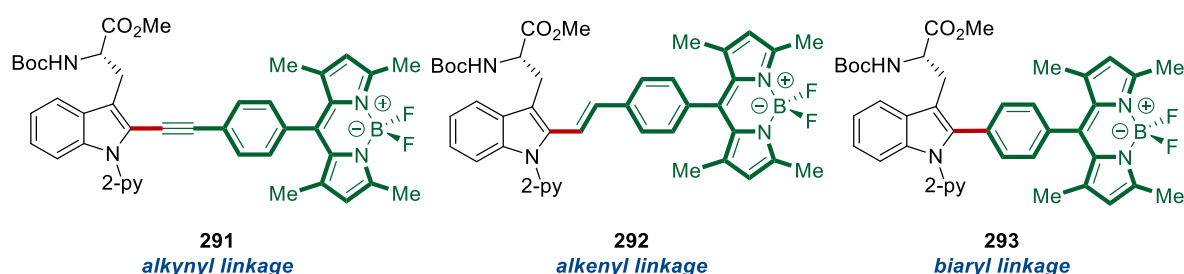
3.6. Manganese(I)-Catalyzed C–H BODIPY-Labeling of Tryptophan-Containing Peptides

Small molecules had long been regarded as the ultimate drug scaffolds. However, in recent years, the pharmaceutical industries have experienced a paradigm shift, as the use of peptides, proteins and monoclonal antibodies is now experiencing a renaissance.^[173] Hence, apart from purely academic endeavor, the elucidation of the working mode of bioactive peptides is of utmost importance, with immediate translational potential. The fluorescent labeling of peptides has been recognized as an efficient tool for shedding light into various biological pathways.^[182] Among many dyes that have been attached to biomolecules, BODIPYs hold a special place due to their highly tunable nature and physiochemical properties.^[183] More precisely, the BODIPY core, that is responsible for their fluorescent properties can be easily modified giving rise to fluorescent molecules with a large emission maxima (λ_{exc}) window.^[184] Furthermore, they are biocompatible and generally have a high cell permeability. These properties enable their utilization in many biological studies.^[185] Recently, a palladium-catalyzed C(*sp*²)–H and C(*sp*³)–H BODIPY-labeling was reported showcasing the translational potential of C–H activation regime.^[134, 186] Thus, the development of new methods for the incorporation of these scaffolds in peptides are highly desirable, especially when a modular strategy can be achieved.

Hence, we became interested in developing an atom- and step-economical method for the C–H labeling of tryptophan-containing peptides. During the last decade, noble metal-catalyzed C–H functionalizations of amino acids and peptides have provided an efficient strategy for late-stage diversification under mild and robust conditions.^[25b, 25g, 147] In this context, and despite the recent momentum towards Earth-abundant 3d transition metal-catalyzed C–H activation, this sustainable approach for the diversification of amino acids and peptides continues to be limited. Inspired by this advances, Dr. J. Son probed a strategy for a divergent assembly of fluorescent peptides with tunable optical properties by identifying internal bromoalkynes and terminal alkynes as appropriate substrates, *via* an alkynylation^[123] or alkenylation^[79-80] manifold, respectively. Thus, by employing these strategies, we could gain access to fluorescent imaging probes, where the phenyl-BODIPY fluorescent core would be stitched to the indole-moiety of the tryptophan amino acid *via* a linear alkynyl or a bent alkenyl spacer, while at the same time extending the conjugate π -system to fine-tune

3. Results and Discussion

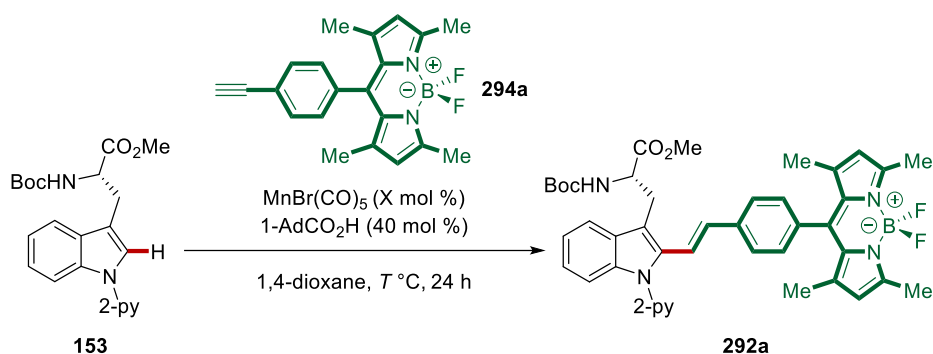
the fluorogenic behavior. In addition, this linkage would not only alter the fluorescent properties of the peptide but also due to different rotation barriers, could render novel fluorescent molecular rotors. Furthermore, the well-established ruthenium(II)-catalyzed arylation of tryptophan moieties^[120] enabled the stitching of the phenyl-BODIPY fluorescent core to indole moiety of the tryptophan *via* a biaryl linkage, thus obtaining three different fluorescent probes (Scheme 3.6.1). Initial studies in collaboration with Professor M. Vendrell, demonstrated that among these three novel fluorescent probes **291**, **292** and **293**, molecule **292** featuring the alkenyl linkage between the indole moiety and phenyl-BODIPY core leads to high viscosity-dependent fluorescence. More accurately compound **292** displayed viscosity sensitivity coefficient of around 0.7, being among the most sensitive fluorescent rotors reported to date.^[187]



Scheme 3.6.1. Tryptophan-BODIPY conjugates with different linkages.

3.6.1. Optimization Studies for Manganese(I)-Catalyzed Labeling of Tryptophan with BODIPY-Alkynes

After initial optimization by Dr. J. Son for the manganese(I)-catalyzed labeling of tryptophan-containing peptides, the labeling of tryptophan derivative **153** with terminal BODIPY-alkyne **294a** was further studied to establish a milder reaction manifold (Table 3.6.1). Thus, under the optimized reaction conditions consisting of catalytic amounts of $\text{MnBr}(\text{CO})_5$, co-catalytic amounts of 1-adamantanecarboxylic acid, in 1,4-dioxane at 100 °C for 24 h the desired fluorescent tryptophan derivative **292a** was obtained in 88% yield (entry 1). Gratifyingly, reducing the reaction temperature, even to physiological temperature of 37 °C, led to only slight decrease in the reaction efficacy (entries 2-4). Lastly, decreasing the catalyst loading led to a small decrease in the isolated yield.

Table 3.6.1. Optimization of the manganese(I)-catalyzed labeling of tryptophan **153**.

Entry	X	Temperature (°C)	Yield (%)
1	20	100	88 ^a
2	20	80	83
3	20	60	80
3	20	60	80
4	20	37	52
5	10	100	60

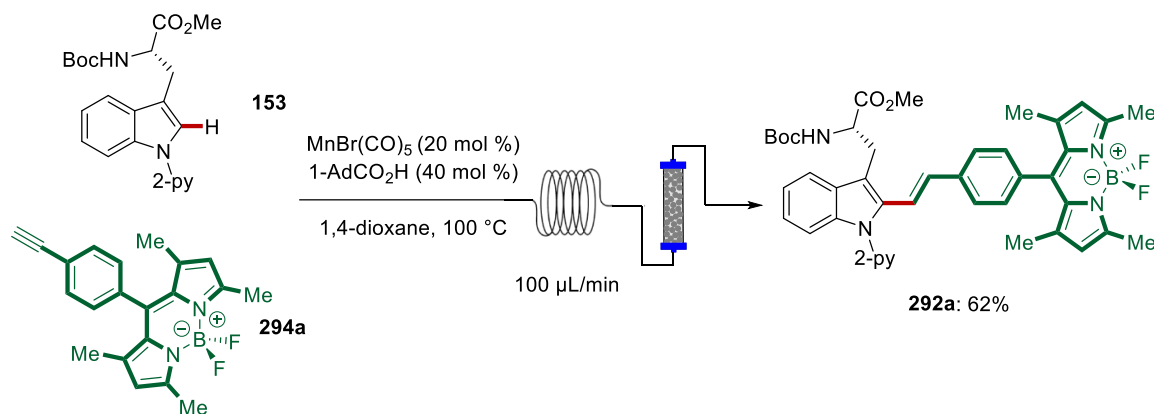
Reaction conditions: **153** (0.10 mmol), **294a** (0.10 mmol), MnBr(CO)₅, 1-AdCO₂H (40 mol %), 1,4-dioxane (1.0 mL), 24 h. Yields of isolated product. ^a Performed by Dr. J. Son.

3.6.2. Scope of the Manganese(I)-Catalyzed Labeling of Tryptophan-Containing Peptides

With the optimized reaction conditions in hand and taking into consideration the remarkable robustness of the manganese(I)-catalyzed C–H activation, we probed whether our regime could be conducted in a flow setup, thus, due to enhanced heat and mass transfer the reaction time could be significantly reduced.^[188] Furthermore, flow setups allow facile incorporation of metal-scavenging techniques to remove trace-metal impurities that might be detrimental for further biological applications. Therefore, using a standardized flow reactor the reaction time could be significantly reduced to

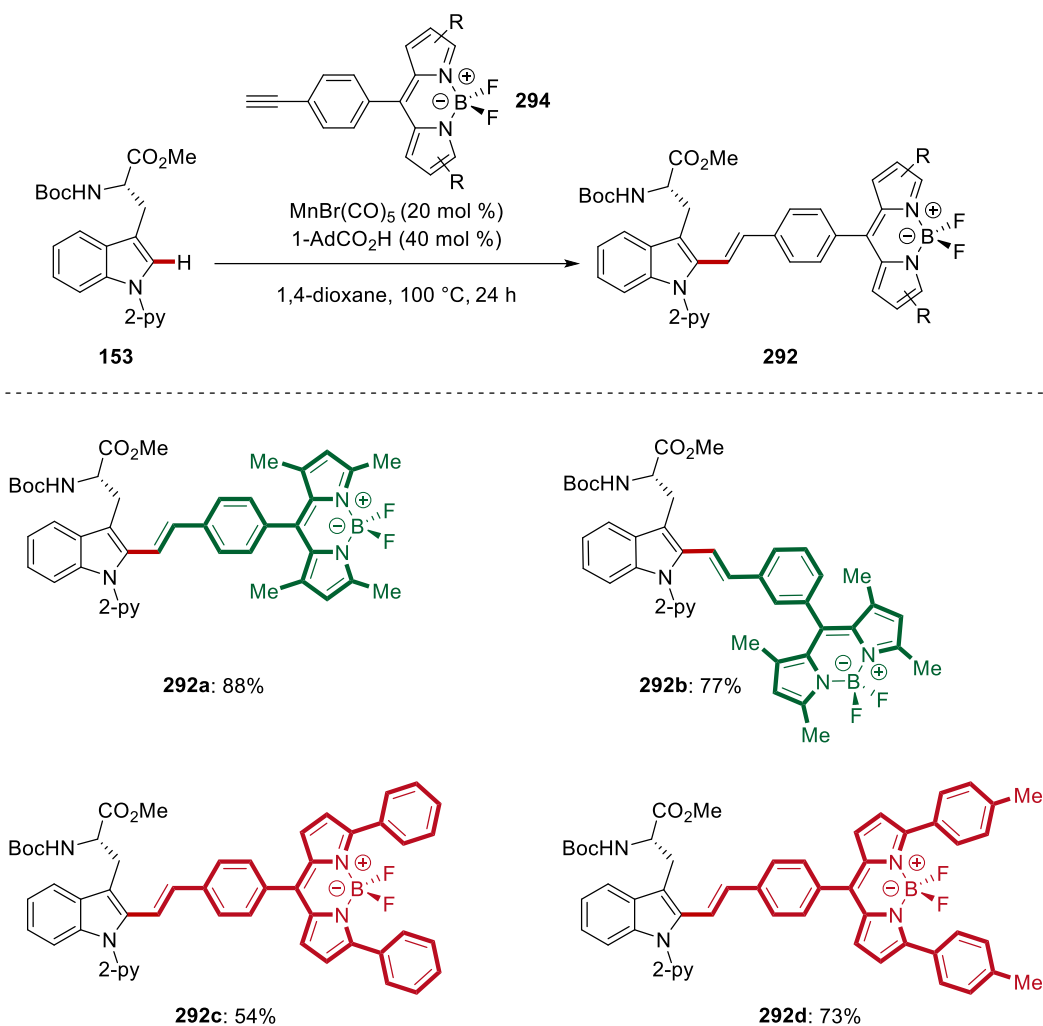
3. Results and Discussion

only 100 min. In addition, a cartridge filled with the metal scavenger, QuadraPure™ IDA could be connected after the reactor (Scheme 3.6.2). Thereby, the residual manganese level was reduced to 6.1 ppm, as determined by inductively coupled plasma mass spectrometry (ICP-MS) analysis. The analysis was conducted in collaboration with I. Maksso in the Ackermann group.



Scheme 3.6.2. Manganese(I)-catalyzed tryptophan C–H labeling in flow.

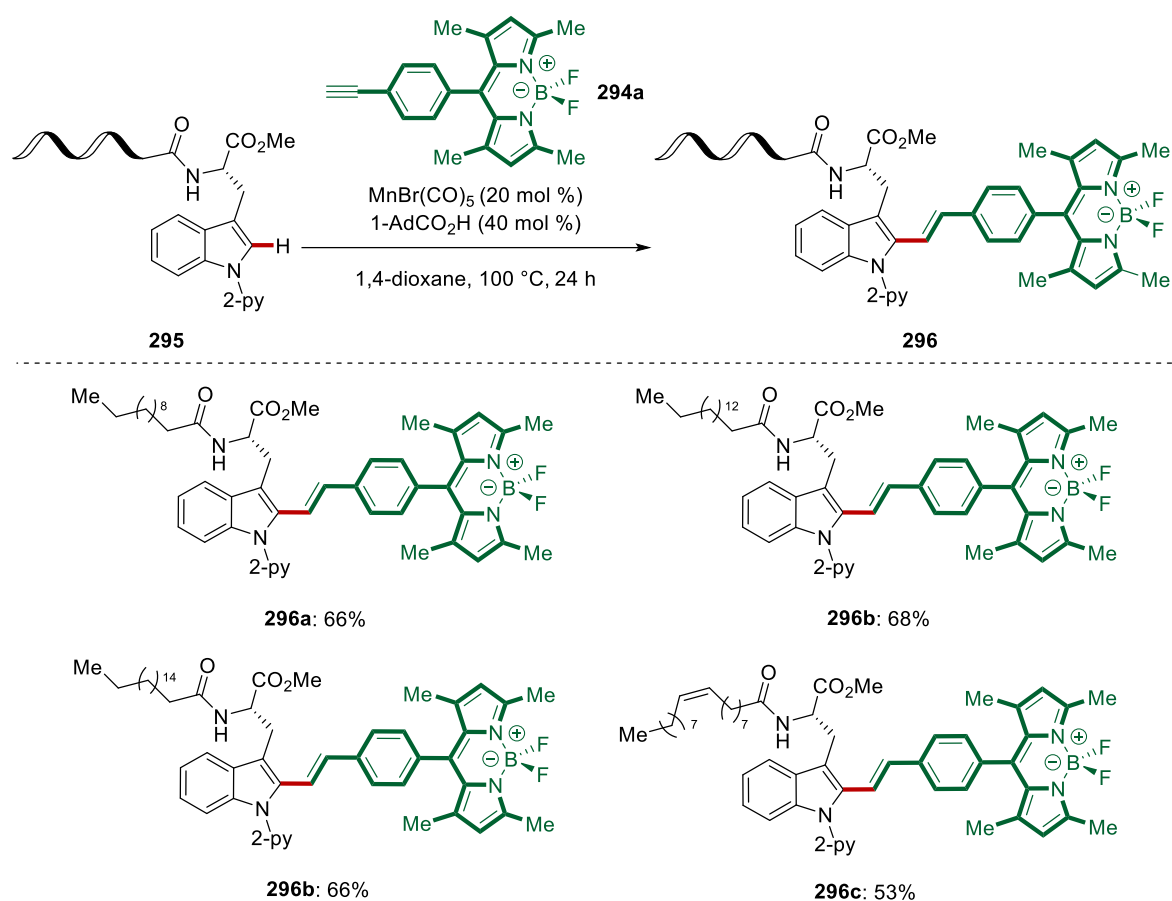
The modular nature of BODIPY dyes allows expedient access to distinct fluorescent dyes, since small changes in the substituents and/or substitution pattern on the pyrrole core result in significant changes at the fluorescent properties. Thus, BODIPY-alkynes featuring the 2,4-dimethyl-pyrrole core tethered with *para*- or *meta*-substituted aromatic linkage were efficiently incorporated into tryptophan-derived substrate **153** leading to the fluorescent amino acid derivatives **292a** and **292b** with strong green fluorescence (Scheme 3.6.3). Furthermore, BODIPY-alkynes **294** derived from C2-arylated pyrroles bathochromically shift the emission wavelength of obtained fluorescent amino acid derivatives **292c** and **292d**, thus leading to strong yellow fluorescence (Scheme 3.6.3).



Scheme 3.6.3. Access to BODIPY-tryptophan derivatives with various fluorescent properties.

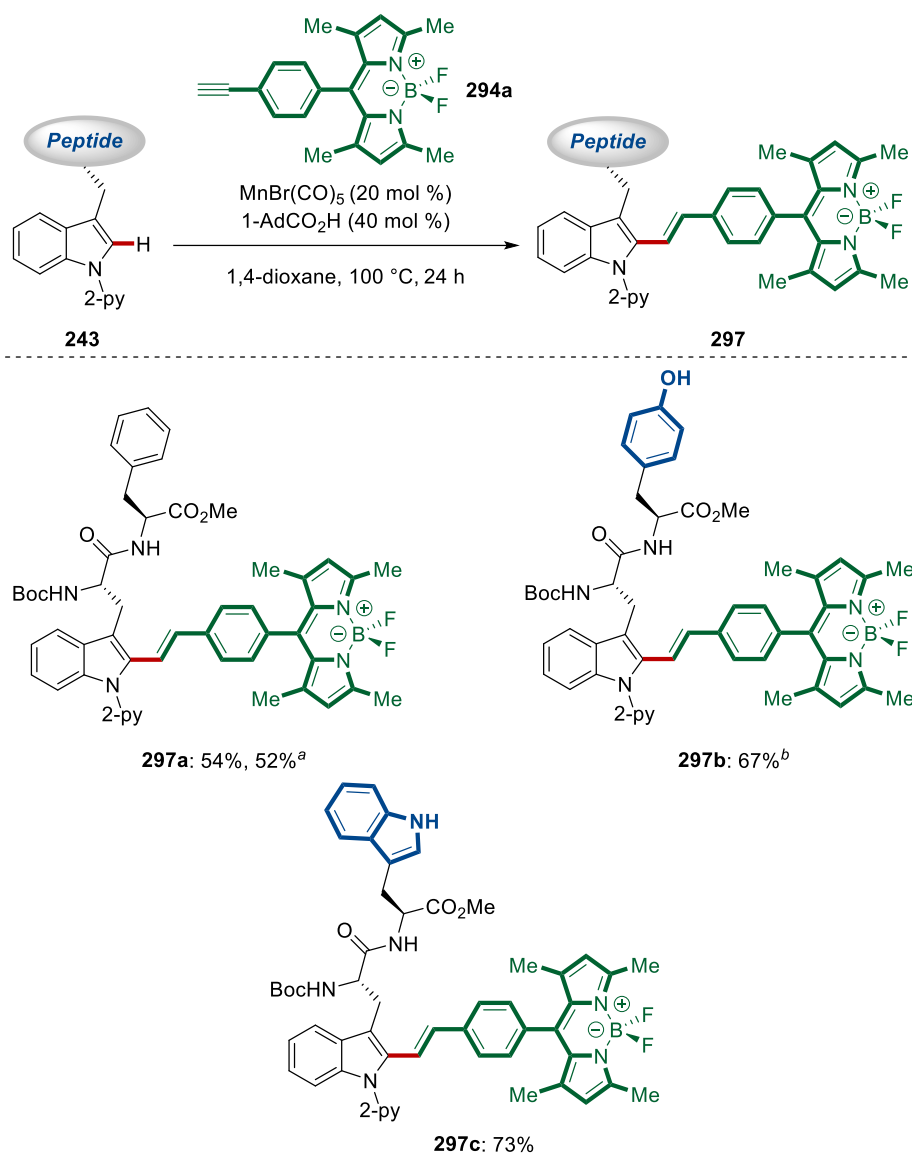
Since our strategy enabled the modular and efficient synthesis of various fluorescent amino acid derivatives, we probed whether a designed modification to the tryptophan-BODIPY conjugates would lead to fluorogenic probes with translational impact. The fluorogenic properties of the alkenylated tryptophan derivative **294** led us to probe whether it can act as membrane viscosity probe. Thus, tryptophan derivatives containing lipophilic tails at the *N*-terminus were also subjected to the labeling process to afford modulated lipophilic rotors that could potentially be anchored on membranes. Thus, upon utilizing lauric, palmitic, stearic and *cis*-oleic acids attached to tryptophan, under our optimized reaction conditions we thus gained access to *E*-bent fluorogenic tryptophan derivatives **296a-296d** (Scheme 3.6.4).

3. Results and Discussion



Scheme 3.6.4. Manganese(I)-catalyzed labeling of lipopeptides.

After establishing that our manganese(I)-catalyzed labeling regime tolerated a wide range of different BODIPY-alkynes **294** for the functionalization of tryptophan derivative **153** we probed the diversification of the more challenging dipeptides (Scheme 3.6.5). Thus, dipeptides containing phenylalanine, free tyrosine and free tryptophan were subjected to our hydroarylation manifold. Gratifyingly, the corresponding dipeptides were efficiently labeled in chemo- and site-selective fashion with the BODIPY-alkyne **294a**. Furthermore, the labeling of dipeptide **243m** was also conducted at 60 °C and the functionalized dipeptide **297a** was obtained with equally high efficiency, being a strong testament to the mildness and robustness of our manganese(I)-catalyzed hydroarylation regime.

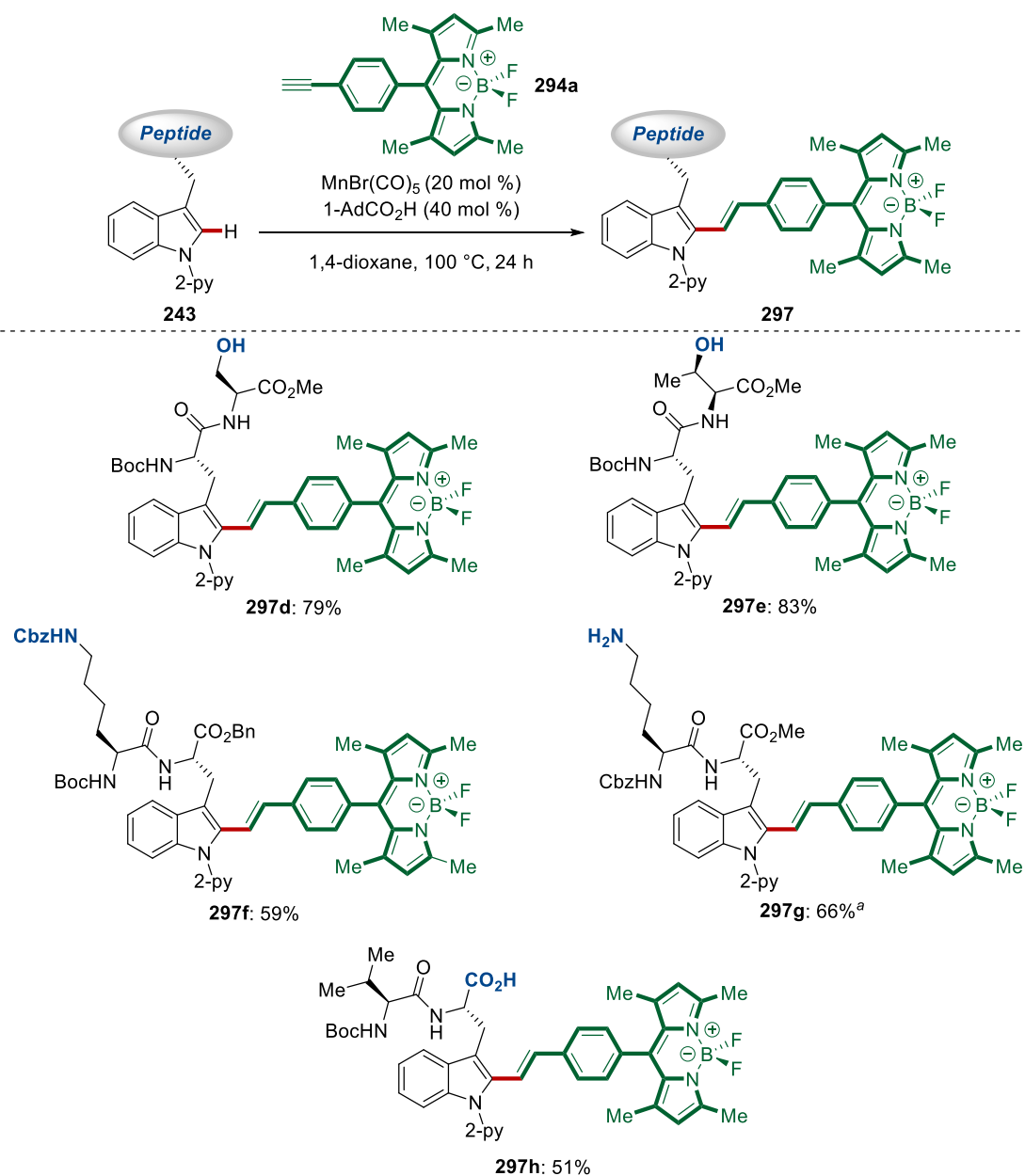


Scheme 3.6.5. Manganese(I)-catalyzed labeling of tryptophan dipeptides **243** containing aromatic amino acids. ^a 60 °C. ^b Performed by Dr. J. Son.

An efficient method for late-stage functionalizations not only requires to be mild, but also needs to be extremely selective, guaranteeing that the desired transformation is not hindered by other structural motifs. Thus, polar functional groups, found in the side chains of some amino acids, can potentially hinder the functionalization of peptides featuring these amino acids in their unprotected form. In this context, it should be mentioned that the vast majority of large peptides are synthesized with their side-chains protected. Hence, various dipeptides featuring free-alcohols, amines or carboxylic acids were subjected to our hydroarylation manifold (Scheme 3.6.6). Remarkably, serine- and threonine-containing dipeptides were efficiently labeled in a chemoselective fashion, without any sign of diminished efficacy caused by the

3. Results and Discussion

unprotected alcohol, leading to fluorescent dipeptides **297d** and **297e**. With regards to the more nucleophilic and coordinating amine group in lysine, orthogonally bis-protected fluorescent dipeptide **297f** was obtained by our manganese(I)-catalysis. This approach can enable the selective elongation of the peptidic chain, after judicious deprotection conditions. Moreover, free-lysine was tolerated when using stoichiometric amounts of $\text{MnBr}(\text{CO})_5$. Thus, the unprotected-lysine-containing fluorescent dipeptide **297g** was obtained in 66% yield, completely bypassing hydroamination regimes. Lastly, under the optimized reaction conditions fluorescent dipeptide **297h** featuring unprotected C-terminus carboxylic acid was obtained in good yield.

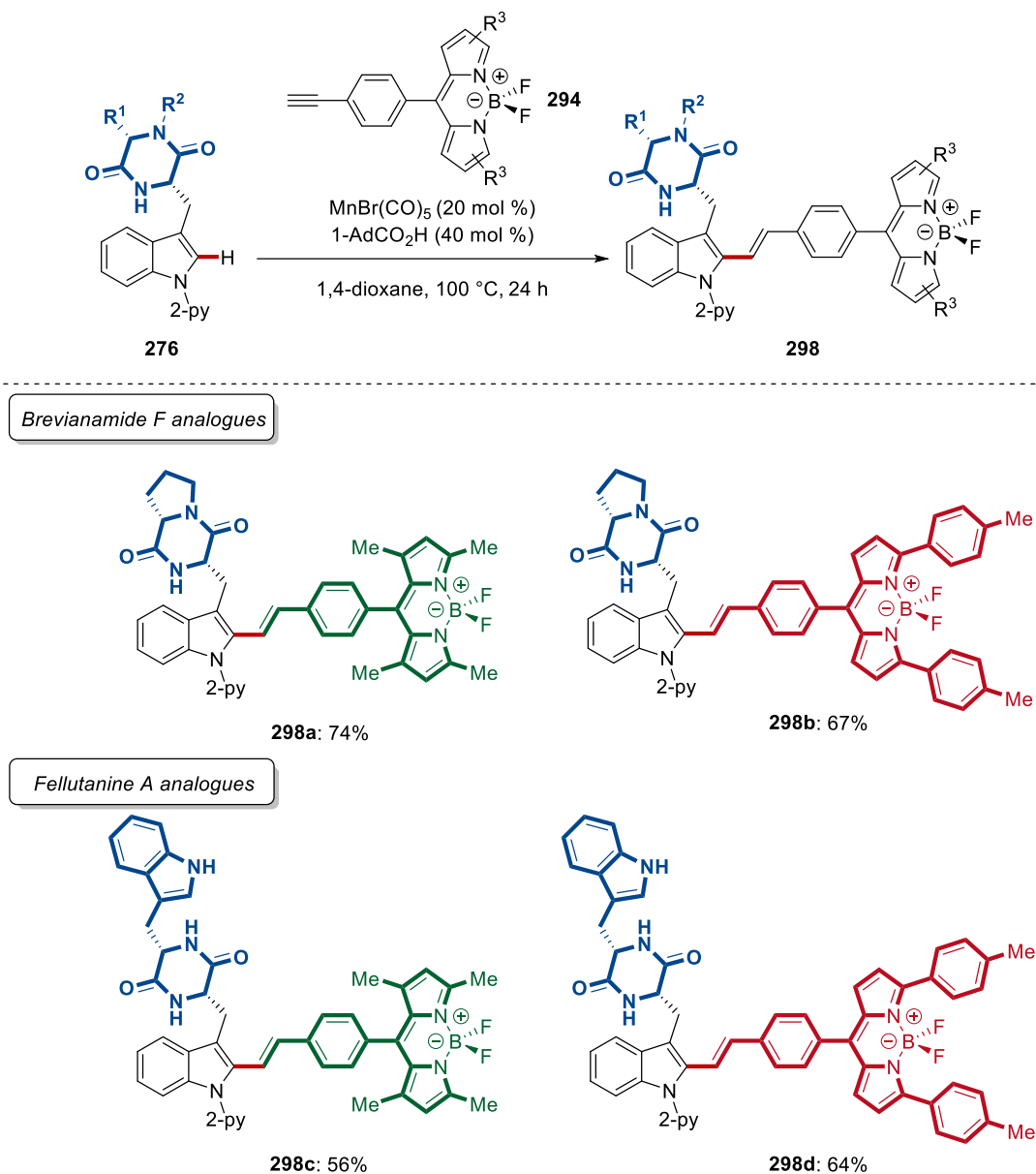


Scheme 3.6.6. Manganese(I)-catalyzed C–H labeling of dipeptides featuring polar functional groups. ^a The reaction was performed with $\text{MnBr}(\text{CO})_5$ (1.0 equiv) and 1-AdCO₂H (1.4 equiv).

The 2,5-diketopiperazine scaffold is found in many bioactive natural products. Thus the labeling of such moieties would potentially find application in deciphering their molecular mode of action. Encouraged by the robustness of our manganese(I)-hydroarylation regime we choose *Brevianamide F* cyclo-[L-Trp^{py}-L-Pro] and *Fellutanine A* cyclo-[L-Trp^{py}-L-Trp] derivatives for applying our method. Remarkably, both natural products **276a** and **276b** were efficiently labeled with either

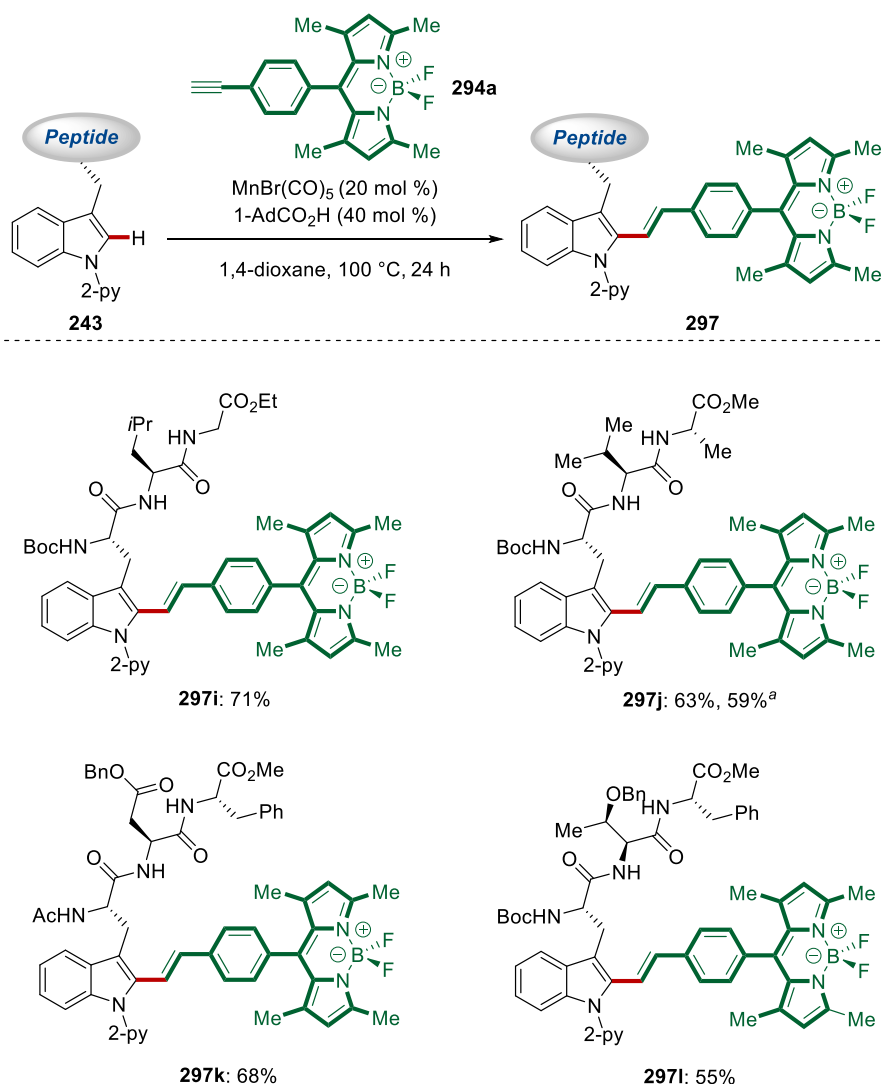
3. Results and Discussion

dimethylpyrrole- or arylated-pyrrole-based BODIPYs, thus having either strong green or yellow fluorescence (Scheme 3.6.7).



Scheme 3.6.7. Manganese(I)-catalyzed labeling of 2,5-diketopiperazines **276**.

Inspired by the robustness of our hydroarylation regime we probed the functionalization of tripeptides **243** (Scheme 3.6.8). Hence, various labeled tripeptides featuring protected aspartic acid and threonine, among others, were efficiently obtained with high chemo- and site-selectivity. In addition, the labeling of tripeptide **297ac** was efficiently conducted at 60 °C with similar efficiency.

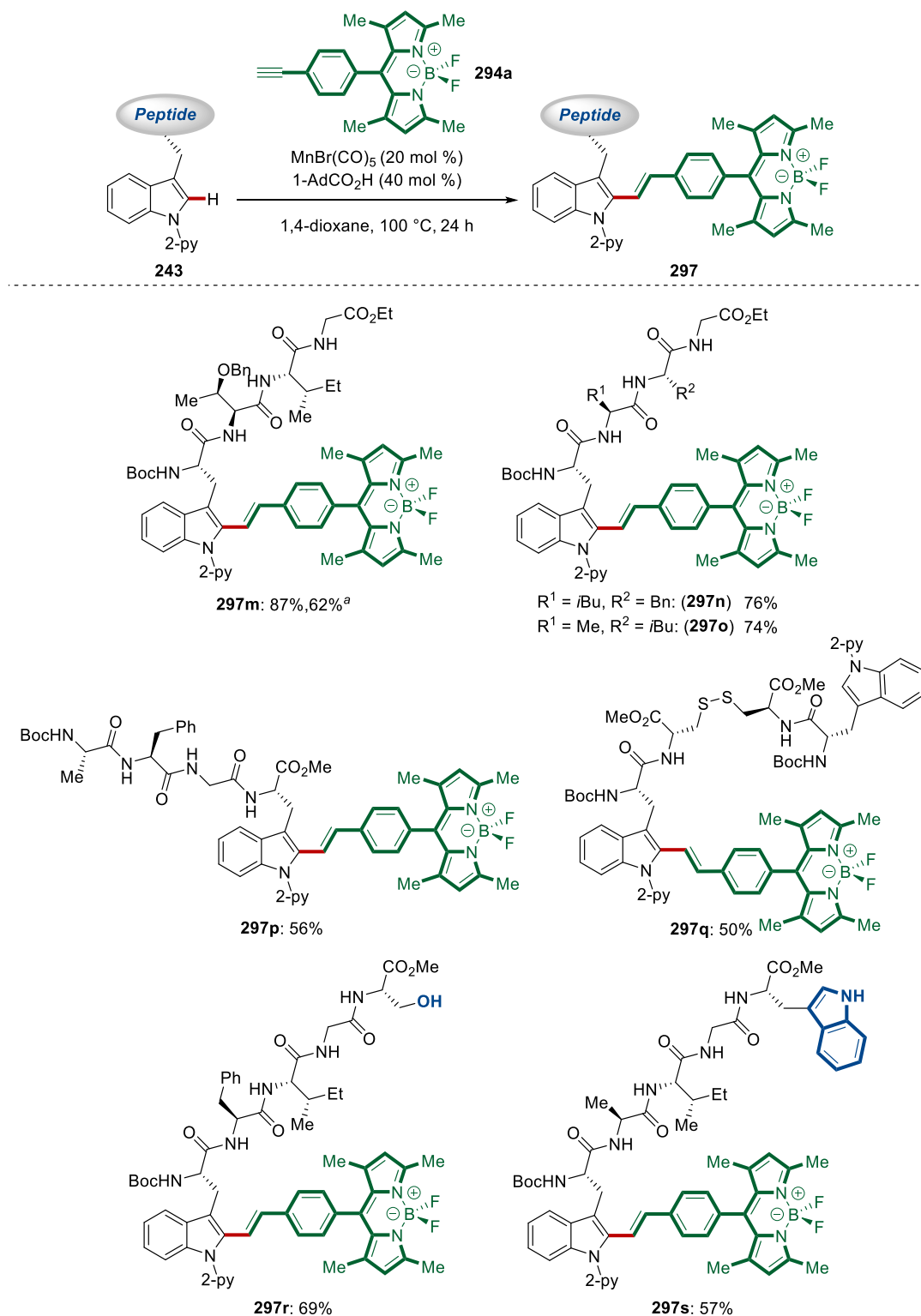


Scheme 3.6.8. Manganese(I)-catalyzed BODIPY-labeling of tripeptides. ^a 60 °C.

Encouraged by the efficiency of our manganese(I)-catalyzed labeling of di- and tripeptides we examined the viability of larger peptides as suitable substrates. To our delight, labeled tetra- and pentapeptides **243** were obtained under mild and epimerization-free reaction conditions in a chemo- and site-selective manner (Scheme 3.6.9). Remarkably, even in this complex setting, the manganese(I)-catalyzed hydroarylation regime tolerated unprotected serine and tryptophan, found in labeled pentapeptides **243ad** and **243ae**, respectively. In addition, the sensitive disulfide bridge, found in a plethora of naturally occurring peptides was fully tolerated, as it is evident from the expedient access to fluorescent tetrapeptide **297q**. Furthermore, the labeled tetrapeptide **297m** was also obtained, when the reaction was carried out at 60 °C, albeit with slightly diminished efficiency. Thus, the efficient, chemo- and site-selective labeling of large peptides, even at as low as 60 °C, demonstrated the mild

3. Results and Discussion

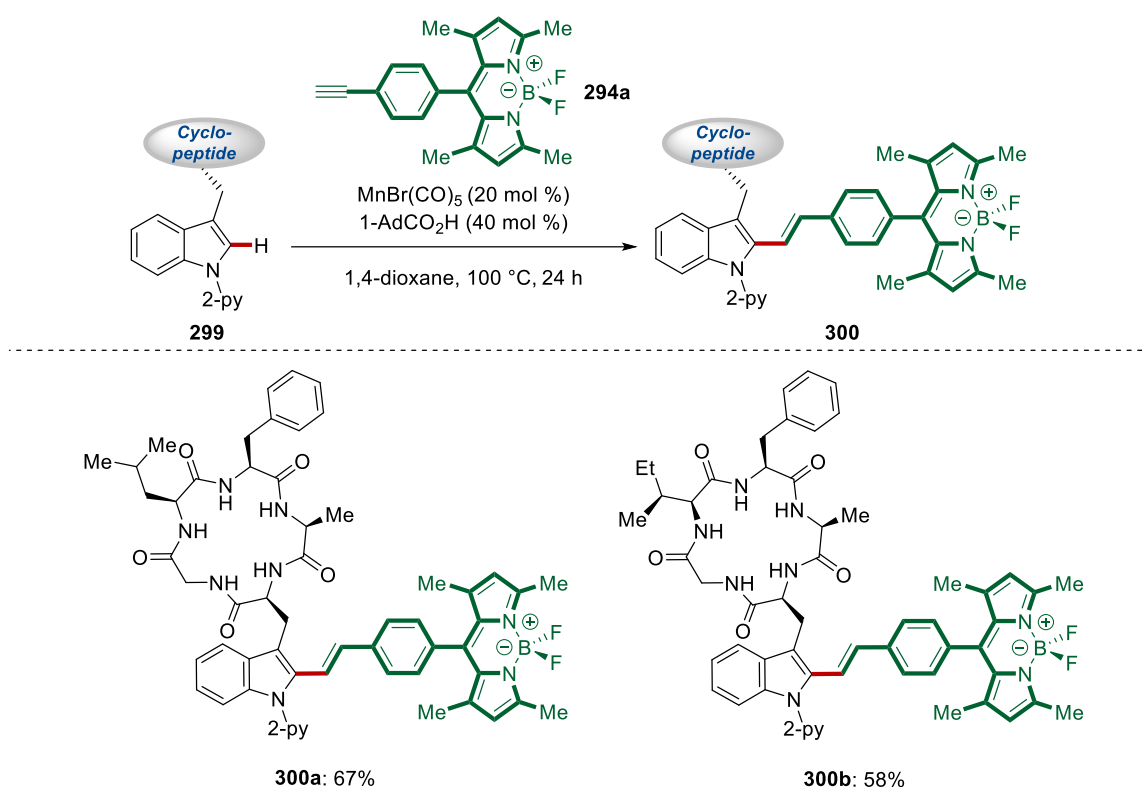
and robust nature of our manganese(I)-catalyzed C–H hydroarylation manifold, utilizing modular terminal BODIPY-alkynes.



Scheme 3.6.9. Manganese(I)-catalyzed labeling of tetra- and pentapeptides **243**.^a

60 °C.

Cyclic peptides hold a very prominent place among naturally occurring peptides, since they are generally more stable in terms of proteolytic degradation. Thus, they have favorable properties for medicinal purposes. The late-stage functionalization of cyclic peptides is hence of utmost importance, since a plethora of analogues would be readily available, without the need for step- and resource-intensive *de novo* peptide synthesis and finally a challenging macrocyclization. To our delight, our manganese(I)-catalyzed hydroarylation manifold provided expedient access to fluorescent cyclic peptides **300a** and **300b** (Scheme 3.6.10).

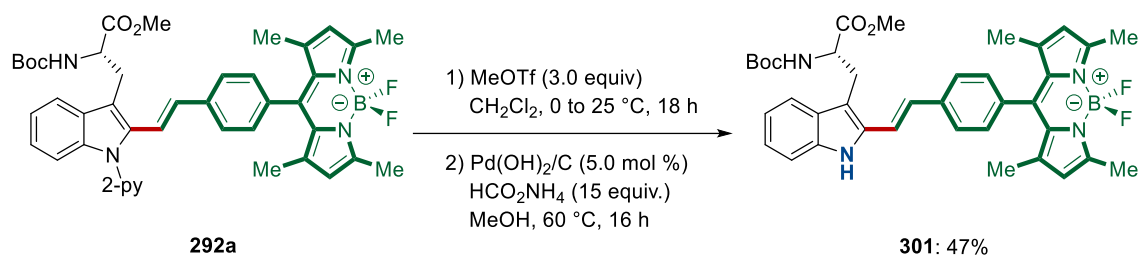


Scheme 3.6.10. Late-stage BODIPY-labeling of tryptophan-containing cyclic peptides.

3.6.3. Traceless Azine Removal: Access to *NH*-Free Fluorescent Tryptophan Derivative

Having established a robust protocol for the chemo- and site-selective labeling of tryptophan-containing peptides we probed whether the 2-pyridyl group could be removed, preferably without affecting the olefin. Gratifyingly, selective methylation of the pyridine moiety and subsequent hydrogenation with Pearlman's catalyst cleanly cleaved the directing group and left the disubstituted olefin untouched (Scheme 3.6.11).

3. Results and Discussion



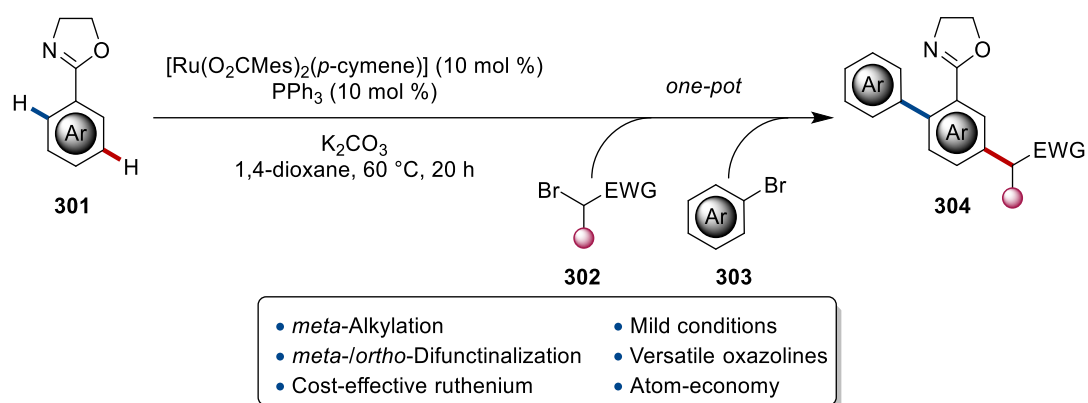
Scheme 3.6.11. Traceless removal of the 2-pyridyl group.

4. Summary and Outlook

Organic synthesis has traditionally relied on step-, time- and resource-intensive strategies, namely the functional group interconversion and, more recently, on cross-coupling reactions. These approaches have enabled the synthetic community to synthesize every imaginable molecule, given the necessary time and resources. Thus, the next major challenge in the field of organic synthesis is the efficiency, scalability, and sustainability.^[2b, 189] In this context, transition metal-catalyzed C–H activation has emerged as a powerful tool, as the time- and resource-consuming prefunctionalizations of starting materials are minimized, since inert and omnipresent C–H bonds are utilized as latent functional groups. In this thesis, the primary focus was the development of novel strategies for increasing the molecular complexity of simple precursors *via* an one-pot difunctionalization approach and the late-stage diversification of peptides. Moreover, in order to address the need for more environmentally-benign C–H transformations we focused on the use of inexpensive Earth-abundant 3d transition metals, namely manganese and cobalt.

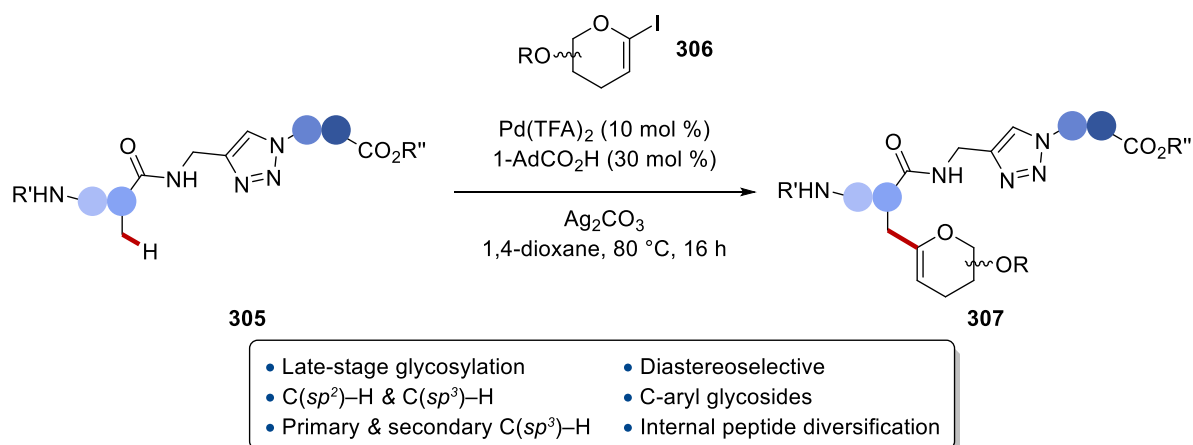
Within the first project, a highly efficient *meta/ortho*-difunctionalization of aryl-oxazolines under ruthenium catalysis was developed (Scheme 4.1).^[190] Mild and robust reaction conditions ensured ample substrate scope featuring a plethora of valuable functional groups. The synergy of the ruthenium(II)-biscarboxylate catalyst and of the phosphine ligand allowed the site-selective *meta*-alkylation of various aryl-oxazolines with α -bromo carbonyl compounds. The robust ruthenium catalyst allowed the sequential *meta*-alkylation/*ortho*-arylation of arenes by the simple addition of the arylating agent upon completion of the initial alkylation. Detailed mechanistic studies by experimentation and computation shed light on an unprecedented ruthenium(II/III) manifold.

4. Summary and Outlook



Scheme 4.1. Ruthenium-catalyzed double *meta/ortho*-C–H difunctionalization.

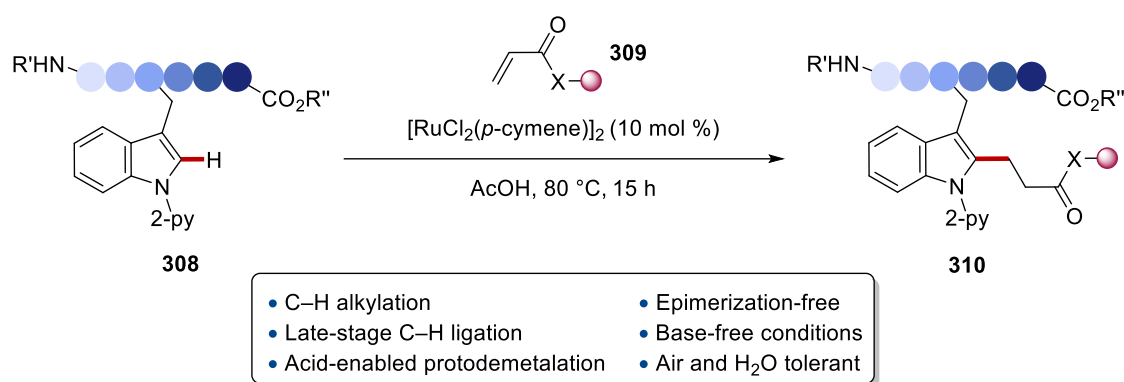
In the second project, we developed a versatile C(*sp*³)-H/C(*sp*²)-H glycosylation strategy of peptidomimetics, featuring the 1,4-disubstituted triazole moiety, an amide surrogate, as the essential bidentate directing group. (Scheme 4.2).^[191] Consequently, the synthesis of structurally complex C-aryl glycosides, C-alkyl glycoamino acids, and glycopeptides was achieved by palladium-catalyzed C–H activation in a regio-, chemo- and diastereoselective fashion. The synthetic utility of our approach was reflected by the expedient assembly of BODIPY fluorescent labeled glycoamino acids and the epimerization-free late-stage diversification of structurally complex molecules. Considering the importance of C-aryl glycosides and glycopeptides in drug discovery, these studies are expected to inspire further developments in the field of transition metal-catalyzed C–H functionalization of saccharide scaffolds.



Scheme 4.2. Palladium-catalyzed C(*sp*³)-H/C(*sp*²)-H glycosylation.

In the third project, we realized a ruthenium(II)-catalyzed peptide C–H alkylation manifold for the epimerization-free diversification of complex peptides in a

bioorthogonal manner (Scheme 4.3).^[192] Gratifyingly, the air- and water-tolerant $[\text{RuCl}_2(p\text{-cymene})]_2$ catalyst set the stage for the chemo- and site-selective diversification of amino acids and peptides. The robustness of the ruthenium(II) catalysis was reflected by the C–H modification and ligation of structurally complex peptides with modular acrylates. This method provided facile access to hybrid architectures bearing natural products, drug scaffolds and even fluorescent tags. These findings should prove invaluable for applications to medicinal chemistry, illustrating the robust nature of the ruthenium(II)-catalyzed C–H activation. Furthermore, our approach demonstrated the outstanding synthetic utility of ruthenium(II)-catalyzed C–H activation towards complex peptides bypassing the need for lengthy and resource-demanding *de novo* strategies.

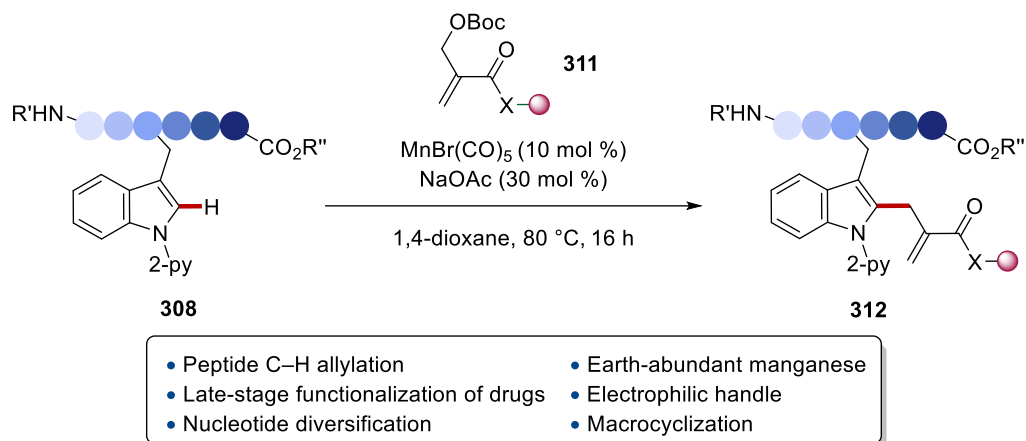


Scheme 4.3. Diversification of peptides by ruthenium(II)-catalyzed C–H alkylation.

Thus far, the late-stage diversification of peptides *via* C–H activation has relied heavily on precious transition metals, mostly palladium. In this regard the use of expensive and potentially toxic 4d and 5d transition metal hinders the inherent sustainable nature of the C–H functionalization strategy. Hence, in the fourth project, we developed an unprecedented manganese(I)-catalyzed C–H allylation strategy towards decorated peptides, nucleotides, and drug molecules (Scheme 4.4).^[193] The chemo- and site-selective diversification of biomolecules was accomplished under exceedingly mild and epimerization-free reaction conditions. Consequently, a plethora of sensitive functional groups was fully tolerated, reflecting the robustness and mildness of the C–H activation regime. Our findings further highlight the user-friendly nature of manganese(I)-catalyzed C–H activation for the late-stage peptide and drug diversification, as well as the bioorthogonal assembly of hybrid peptides and macrocycles. The C–H allylation of peptides with 3d transition metals was not restricted to manganese. Indeed cobalt(III)

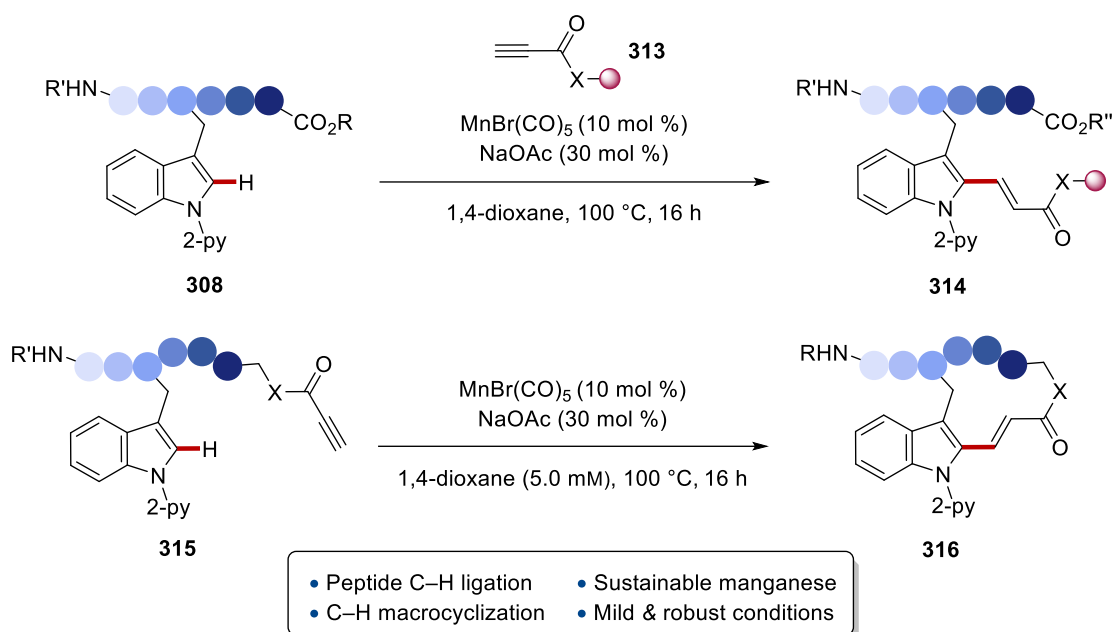
4. Summary and Outlook

catalysis enabled the position-selective allylation of tryptophan containing peptides.^[194] The robust C–H allylation was elegantly combined with the ruthenium-catalyzed olefin metathesis leading to stapled peptides.



Scheme 4.4. Manganese-catalyzed C–H allylation of peptides with MBH adducts.

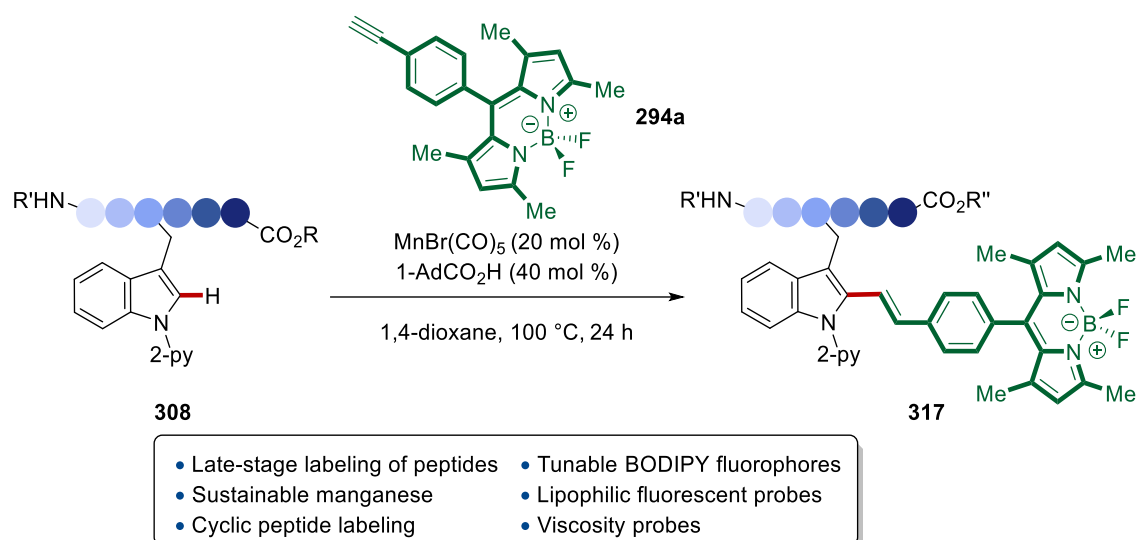
In the fifth project, we developed an unprecedented manganese(I)-catalyzed C–H hydroarylation on complex peptides, that enabled the highly valuable C–H ligation (Scheme 4.5).^[195] The chemo- and site-selective peptide stitching was characterized by an excellent functional group tolerance featuring a plethora of delicate functional groups, under mild and epimerization-free reaction conditions. We then focused on assembling hybrid molecules by stitching tryptophan-containing peptides with natural products, sugars, and fluorescent tags. The generality of our intermolecular regime prompted us to explore the more challenging intramolecular macrocyclization version. Gratifyingly, our robust method paved the way for a highly efficient access to cyclic peptides *via* a C–H macrocyclization regime. Furthermore, the modular nature of our approach with propiolates, allowed for the synthesis of stapled peptides *via* Trp→C terminus, Trp→N terminus, or Trp→Ser cyclization. Our general route towards tryptophan-containing peptides will enable the expedient discovery of constrained bioactive macrocyclic scaffolds.



Scheme 4.5. Manganese-catalyzed C–H ligation and macrocyclization.

Finally, a strategy for the late-stage manganese(I)-catalyzed C–H labeling of structurally complex peptides with BODIPY probes was established (Scheme 4.6).^[196] The tunable nature of the BODIPY fluorophores allowed facile access to fluorescent peptides with distinct photophysical properties, enabling their potential use in various biological applications. Moreover, the manganese(I)-catalyzed carboxylate-assisted hydroarylation manifold gave access to a myriad of fluorescent complex peptides, cyclic peptides, and cyclic peptides, decorated with sensitive functional groups under mild, epimerization-free reaction conditions. The hindered rotation of the alkenyl linkage would favour the charge transfer between the indole and phenyl-BODIPY groups, showing excellent fluorogenic character. Remarkably, the alkenylated tryptophan-BODIPY conjugate exhibited high viscosity-dependent fluorescence. Thus, in collaboration with the Vendrell group in Edinburgh, we incorporated this scaffold into a lipophilic tail that enabled the anchoring of the viscosity-sensitive dye in cell membranes. Furthermore, we identified a fluidity-sensitive probe, which emits bright fluorescence in response to cholesterol found in cell membranes, and we utilized it to establish a fluorescence-based screening platform for the identification of small molecule modulators of CD8⁺ T cells. Overall, our manganese(I)-catalyzed C–H hydroarylation strategy will establish novel avenues in the development of functional fluorophores to image cell function and in the late-stage labeling peptides.

4. Summary and Outlook



Scheme 4.6. Manganese-catalyzed C–H labeling with BODIPY fluorophores **294**.

5. Experimental Part

5.1. General Remarks

All reactions involving air- and/or moisture-sensitive compounds were conducted under a dry nitrogen atmosphere using pre-dried glassware and standard Schlenk techniques. If not otherwise noted, yields refer to isolated compounds, which were estimated to be >95% pure based on $^1\text{H-NMR}$.

Vacuum

The following average pressure was measured on the used rotary vane pump RD4 from Vacuubrand®: 0.8·10⁻¹ mbar (uncorrected value).

Melting Points

Melting points were measured on a Stuart® Melting Point Apparatus SMP3 from Barloworld Scientific. Values are uncorrected.

Chromatography

Analytical thin layer chromatography (TLC) was performed on silica gel 60 F254 aluminium sheets from Merck. Plates were either visualized under irradiation at 254 nm or 365 nm or developed by treatment with a potassium permanganate solution followed by careful warming. Chromatographic purifications were accomplished by column chromatography on Merck Geduran® silica gel, grade 60 (40–63 μm , 70–230 mesh ASTM).

Gel permeation chromatography (GPC)

GPC purifications were performed on a JAI system (JAI-LC-9260 II NEXT) equipped with two sequential columns (JAIGEL-2HR, gradient rate: 5.000; JAIGEL-2.5HR, gradient rate: 20.000; internal diameter = 20 mm; length = 600 mm; Flush rate = 10.0 mL/min and CHCl_3 (HPLC-quality with 0.6% EtOH as stabilizer) was used as the eluent.

Infrared Spectroscopy

IR spectra were recorded using a Bruker® Alpha-P ATR spectrometer. Liquid samples were measured as film and solid samples neat. Spectra were recorded in the range from 4000 to 400 cm^{-1} . Analysis of the spectral data was carried out using Opus 6. Absorption is given in wave numbers (cm^{-1}).

5. Experimental Part

Nuclear Magnetic Resonance Spectroscopy

NMR spectra were recorded on Mercury Plus 300, VNMRs 300, Inova 500 and 600 from Varian®, or Avance 300, Avance III 300 and 400, Avance III HD 400 and 500 from Bruker®. Chemical shifts are reported in δ -values in ppm relative to the residual proton peak or carbon peak of the deuterated solvent.

The coupling constants J are reported in hertz (Hz). Analysis of the recorded spectra was carried out using MestReNova 10.0 software.

	¹ H-NMR	¹³ C-NMR
CDCl ₃	7.26	77.16
CD ₂ Cl ₂	5.32	54.00
(CD ₃) ₂ SO	2.50	39.51

Gas Chromatography

Monitoring of reaction process *via* gas chromatography or coupled gas chromatography-mass spectrometry was performed using a 7890 GC-system with/without mass detector 5975C (Triple-Axis-Detector) or a 7890B GC-system coupled with a 5977A mass detector, both from Agilent Technologies®.

Mass Spectrometry

Electron ionization (EI) and EI high resolution mass spectra (HR-MS) were measured on a time-of-flight mass spectrometer AccuTOF from JEOL. Electrospray ionization (ESI) mass spectra were recorded on an Io-Trap mass spectrometer LCQ from Finnigan, a quadrupole time-of-flight maXis from Bruker Daltonic or on a time-of-flight mass spectrometer microTOF from Bruker Daltonic. ESI-HR-MS spectra were recorded on a Bruker Apex IV or Bruker Daltonic 7T, Fourier transform ion cyclotron resonance (FTICR) mass spectrometer. The ratios of mass to charge (m/z) are indicated, intensities relative to the base peak ($I = 100$) are written in parentheses.

Chiral HPLC

Chiral HPLC chromatograms were recorded on an Agilent 1290 Infinity using CHIRALPAK® IA-3, IB-3, IC-3, ID-3, IE-3 and IF-3 columns (3.0 μ m particle size; ϕ : 4.6 mm and 250 mm length) at ambient temperature.

Solvents

All solvents for reactions involving air- and/or moisture-sensitive reagents were dried, distilled and stored under an N₂ atmosphere according to the following standard procedures.

1,2-Dichloroethane (DCE) and toluene (PhMe) were dried over CaH₂ for 8 h, degassed and distilled under reduced pressure. 1,4-Dioxane and di-*n*-butylether (*n*Bu₂O) were dried over Na for 8 h, degassed and distilled under reduced pressure.

CH₂Cl₂, DMF, THF, Et₂O were obtained from a MBRAUN MB SPS-800 solvent purification system.

Chemicals

Chemicals obtained from commercial sources with a purity >95% were used as received without further purification.

The following compounds were known from the literature and synthesized according to previously known methods: oxazolines **217**,^[197] indoles **270**,^[121] triazole-containing peptides **237** and **239**,^[131, 134] pyridylated peptides **243**,^[120] acrylates **22**,^[84] protected MBH adducts **253**.^[198]

The following compounds were kindly synthesized and provided by the persons listed below:

Karsten Rauch: [RuCl₂(*p*-cymene)]₂, [Ru(OCMe)₂(*p*-cymene)], [Ru(OAc)₂(*p*-cymene)], dry and/or degassed solvents.

Dr. Korkit Korvorapun: nucleotides **260**.

Dr. Cuiju Zhu: triazole-containing benzamides **234**.

Jun Wu: 1-iodo glucal **235**.

Adelina Kopp: BODIPY alkynes **294**.

Rongxin Yin: MBH-adducts **253f** and **253i**.

Giedre Sirvinskaite: propiolates **211**, peptides **284**.

Felix Kaltenhäuser: peptides **286**.

5. Experimental Part

5.2. General Procedures

5.2.1. General Procedure A: Ruthenium(II)-Catalyzed *meta*-Alkylation of Oxazolines

Oxazoline **217** or **220** (0.50 mmol), [Ru(O₂CMes)₂(*p*-cymene)] (28.1 mg, 10 mol %), PPh₃ (13.1 mg, 10 mol %) and K₂CO₃ (138 mg, 1.00 mmol) were placed in a Schlenk tube. The tube was evacuated and purged with N₂ three times. 1,4-Dioxane (2.0 mL) and alkyl bromide **218** (1.50 mmol) were then added and the mixture was stirred at 60 °C. After 20 h, the resulting mixture was filtered through silica gel pad and washed with EtOAc. The filtrate was concentrated *in vacuo*. Purification by column chromatography on silica gel (*n*-hexane/EtOAc) afforded the desired product.

5.2.2. General Procedure B: Ruthenium(II)-Catalyzed *meta*-Alkylation/*ortho*-Arylation of Oxazolines

Oxazoline **217** or **220** (0.50 mmol), [Ru(O₂CMes)₂(*p*-cymene)] (28.1 mg, 10 mol %), PPh₃ (13.1 mg, 10 mol %) and K₂CO₃ (276 mg, 2.00 mmol) were placed in a Schlenk tube. The tube was evacuated and purged with N₂ three times. 1,4-Dioxane (2.0 mL) and alkyl bromide **218** (1.50 mmol) were then added and the mixture was stirred at 40 °C. After 20 h, bromoarene **163** (1.50 mmol) was added to the reaction mixture at ambient temperature and the mixture was stirred at 120 °C for an additional 20 h. The resulting mixture was filtered through silica gel pad and washed with EtOAc. The filtrate was concentrated *in vacuo*. Purification by column chromatography on silica gel (*n*-hexane/EtOAc) afforded desired product.

5.2.3. General Procedure C: Palladium-Catalyzed C(sp²)-H Glycosylation with TAM^{Bu}

Amide **234** (0.1 mmol), Pd(OAc)₂ (2.2 mg, 10 mol %), Ag₂CO₃ (55 mg, 0.2 mmol), were added to Schlenk tube. The tube was evacuated and purged with N₂ three times. Then, 1-iodo glycal **235** (0.15 mmol) in 1,4-dioxane (0.50 mL) was added. The tube was sealed and heated at 80 °C for 10 h. After cooling to ambient temperature, the resulting reaction mixture was diluted with CH₂Cl₂ and concentrated *in vacuo*. Purification by column chromatography on silica gel (*n*-hexane/EtOAc) afforded the desired product.

5.2.4. General Procedure D: Palladium-Catalyzed Peptide C(sp³)-H Glycosylation with TAM

Amide **237** or **239** (0.1 mmol), Pd(TFA)₂ (3.3 mg, 10 mol %), Ag₂CO₃ (55 mg, 0.2 mmol), 1-AdCO₂H (5.4 mg, 30 mol %) were placed in an oven-dried Schlenk tube. The mixture was evacuated and purged with N₂ three times. Then, 1-iodo glycal **235** (0.15 mmol) in 1,4-dioxane (0.50 mL) was added. The tube was sealed and heated at 80 °C for 10 -16 h. After cooling to ambient temperature, the resulting reaction mixture was diluted with CH₂Cl₂ and concentrated *in vacuo*. Purification by column chromatography on silica gel (*n*-hexane/EtOAc) afforded the desired product.

5.2.5. General Procedure E: Ruthenium(II)-Catalyzed C-H Alkylation of Tryptophan

A test tube with a stir bar was charged with pyridylated tryptophane **241** (0.15 mmol, 1.0 equiv) and [RuCl₂(*p*-cymene)]₂ (9.2 mg, 10mol %). AcOH (0.15 mL) and acrylate **22** (1.1 – 3.0 equiv.) were added. The tube was fitted with a septum and the mixture was heated to 80 °C for 15 h. After cooling to ambient temperature, the resulting reaction mixture was diluted with PhMe and concentrated *in vacuo*. Purification by column chromatography on silica gel afforded the desired product.

5.2.6. General Procedure F: Ruthenium(II)-Catalyzed C-H Alkylation of Peptides

A test tube with a stir bar was charged with pyridylated peptide **243** (0.15 mmol, 1.0 equiv) and [RuCl₂(*p*-cymene)]₂ (9.2 mg, 10mol %). AcOH (0.15 mL) and acrylate **22** or vinyl ketone **245** (1.1 – 3.0 equiv.) were added. The tube was fitted with a septum and the mixture was heated to 80 °C for 15 h. After cooling to ambient temperature, the resulting reaction mixture was diluted with PhMe and concentrated *in vacuo*. Purification by column chromatography on silica gel afforded the desired product.

5.2.7. General Procedure G: Ruthenium(II)-Catalyzed C-H Ligation of Peptides

A test tube with a stir bar was charged with pyridylated peptide **241** or **243** (0.15 mmol, 1.0 equiv), acryloyl peptide **247** (0.17 mmol, 1.1 equiv.) and [RuCl₂(*p*-cymene)]₂ (9.2 mg, 10mol %). AcOH (0.15 mL) were added. The tube was fitted with a septum and the mixture was heated to 80 °C for 15 h. After cooling to ambient temperature,

5. Experimental Part

the resulting reaction mixture was diluted with PhMe and concentrated *in vacuo*. Purification by column chromatography on silica gel afforded the desired product.

5.2.8. General Procedure H: Traceless Removal of 2-Pyridyl Group from Alkylated Peptides

To a stirred solution of peptide **242a** or **244c** or **248a** (1.0 equiv) in CH₂Cl₂ (0.25 M) was added MeOTf (1.0 equiv) at 0 °C. After 30 min, the mixture was allowed to warm up to 25 °C and stirred for 18 h. The crude mixture was concentrated under reduced pressure to afford a bright yellow solid. In a sealed-tube, the crude product, Pd(OH)₂/C (10 mol %, 20 wt%) and ammonium formate (10.0 equiv) were dissolved in ethanol (0.5 M) and stirred at 60 °C for 16 hours. The mixture was filtered through a short plug of celite, concentrated under reduced pressure and purified by column chromatography on silica gel afforded the desired product.

5.2.9. General Procedure I: Manganese(I)-Catalyzed Late-Stage C–H Allylation on Peptides with MBH Adducts

A suspension of pyridylated peptide **243** (1.0 equiv), MBH adduct **253** (2.0 equiv), MnBr(CO)₅ (10 mol %) and NaOAc (30 mol %) in 1,4-dioxane (0.33 M) was stirred at 80 °C for 16 h under N₂. After cooling to ambient temperature, CH₂Cl₂ (10 mL) was added and the mixture concentrated *in vacuo*. Purification by column chromatography on silica gel afforded the desired product.

5.2.10. General Procedure J: Manganese(I)-Catalyzed Late-Stage C–H Allylation on (Hetero)Arenes with MBH Adducts

A suspension of (hetero)arenes **257** or **259** (0.20 mmol, 1.0 equiv), MBH adduct **2** (0.40 mmol, 2.0 equiv), MnBr(CO)₅ (5.5 mg, 10 mol %) and NaOAc (4.9 mg, 30 mol %) in 1,4-dioxane (1.0 mL) was stirred at 80 °C for 16 h under N₂. After cooling to ambient temperature, CH₂Cl₂ (10 mL) was added and the mixture concentrated *in vacuo*. Purification by column chromatography on silica gel afforded the desired products.

5.2.11. General Procedure K: Traceless Removal of 2-Pyridyl Group from Allylated Peptides

To a stirred solution of **254a** or **269b** or **268** (1.0 equiv) in CH₂Cl₂ (0.25 M) was added methyl trifluoromethanesulfonate (1.0 equiv) at 0 °C. After 30 min, the mixture was allowed to warm up to 25 °C and stirred for 18 h. The crude mixture was concentrated under reduced pressure to afford a bright yellow solid. In a sealed-tube, the crude product, Pd(OH)₂/C (10 mol %, 20 wt%), and ammonium formate (10.0 equiv) were dissolved in methanol (0.5 M), and stirred at 60 °C for 16 hours. The mixture was filtered through a short plug of celite, concentrated under reduced pressure and purified by column chromatography on silica gel afforded the desired product.

5.2.12. General Procedure L: Cobalt(III)-Catalyzed Late-Stage C–H Allylation on Peptides

A mixture of peptide **243** (1.00 equiv), allyl acetate **272** (30 µL, 2.00 equiv), [Cp*Co(MeCN)₃](SbF₆)₂ (5.9 mg, 5.0 mol %) and PivOH (1.5 mg, 10 mol %) in TFE (1.0 mL) was stirred at 80 °C for 14 h under N₂. After cooling to ambient temperature, EtOAc (15 mL) was added and the mixture concentrated *in vacuo*. Purification by column chromatography on silica gel afforded the desired product.

5.2.13. General Procedure M: Manganese(I)-Catalyzed Late-Stage C–H Hydroarylation on Peptides

A suspension of peptide **243** (0.15 mmol, 1.0 equiv), propiolate **211** (0.23 mmol, 1.5 equiv), MnBr(CO)₅ (10 mol %) and NaOAc (30 mol %) in 1,4-dioxane (0.25 M) was stirred at 100 °C for 16 h under N₂. After cooling to ambient temperature, CH₂Cl₂ (10 mL) was added and the mixture concentrated *in vacuo*. Purification by column chromatography on silica gel afforded the desired product.

5.2.14. General Procedure N: Manganese(I)-Catalyzed C–H Macrocyclization of Peptides

A suspension of peptide **284** or **286** or **288** (0.15 mmol, 1.0 equiv), MnBr(CO)₅ (20 mol %) and NaOAc (60 mol %) in 1,4-dioxane (30 mL) was stirred at 100 °C for 16 h under N₂. After cooling to ambient temperature, CH₂Cl₂ (10 mL) was added and the

5. Experimental Part

mixture concentrated *in vacuo*. Purification by column chromatography on silica gel afforded the desired product **10**.

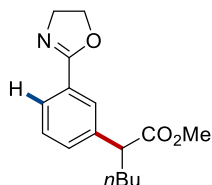
5.2.15. General Procedure O: Manganese(I)-Catalyzed Late-Stage C–H Alkylation on Peptides

A suspension of peptide **243** or **299** (0.10 mmol, 1.0 equiv), BODIPY-alkyne **294** (0.11-0.20 mmol, 1.1 -2.0 equiv), $\text{MnBr}(\text{CO})_5$ (5.5 mg, 20 mol %) and 1-AdCO₂H (7.2 mg, 40 mol %) in 1,4-dioxane (1.0 mL) was stirred at 100 °C for 24 h. After cooling to ambient temperature, CH₂Cl₂ (10 mL) was added and the mixture was concentrated *in vacuo*. Purification by column chromatography on silica gel afforded the desired product.

5.3. Sequential *meta-ortho*-C–H Functionalization of Oxazolines *via* Ruthenium Catalysis

5.3.1. Characterization Data

Methyl 2-[3-(4,5-dihydrooxazol-2-yl)phenyl]hexanoate (**219aa**)

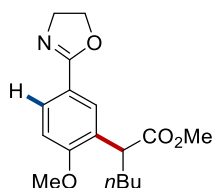


The general procedure **A** was followed using 2-phenyl-4,5-dihydrooxazole **217a** (73.5 mg, 0.50 mmol), methyl 2-bromohexanoate **218a** (314 mg, 1.50 mmol), [Ru(O₂CMes)₂(*p*-cymene)] (28.1 mg, 10 mol %), PPh₃ (13.1 mg, 10 mol %) and K₂CO₃ (138 mg, 1.00 mmol) in 1,4-dioxane (2.0 mL). Purification by column chromatography on silica gel (*n*-hexane/EtOAc: 5/1 → 3/1) yielded **219aa** (104.7 mg, 76%) as a brown oil. Gram scale reaction: 2-phenyl-4,5-dihydrooxazole **217a** (1.18 g, 8.00 mmol), [Ru(O₂CMes)₂(*p*-cymene)] (224 mg, 0.40 mmol, 5.0 mol %), PPh₃ (105 mg, 0.40 mmol, 5.0 mol %) and K₂CO₃ (2.20 mg, 16.0 mmol) were placed in a pre-dried 100 mL schlenk flask. The mixture was evacuated and purged with N₂ for three times. Methyl 2-bromohexanoate **218a** (4.99 g, 24.0 mmol) and 1,4-dioxane (32.0 mL) were then added and the mixture was stirred at 60 °C. After 20 h, the resulting mixture was filtered over silica gel pad and washed with EtOAc. The filtrate was concentrated *in vacuo*. Purification by column chromatography on silica gel (*n*-hexane/EtOAc: 5/1 → 3/1) yielded **219aa** (1.74 g, 79%).

¹H-NMR (300 MHz, CDCl₃): δ 7.85 (td, *J* = 1.6, 0.9 Hz, 1H), 7.79 (dt, *J* = 7.6, 1.6 Hz, 1H), 7.42–7.37 (m, 1H), 7.32 (td, *J* = 7.6, 0.7 Hz, 1H), 4.39 (t, *J* = 9.4 Hz, 2H), 4.02 (t, *J* = 9.4 Hz, 2H), 3.61 (s, 3H), 3.54 (t, *J* = 7.7 Hz, 1H), 2.06 (dddd, *J* = 13.3, 9.5, 7.9, 5.7 Hz, 1H), 1.75 (dddd, *J* = 13.5, 9.3, 7.6, 5.9 Hz, 1H), 1.37–1.09 (m, 4H), 0.82 (t, *J* = 7.1 Hz, 3H). **¹³C-NMR** (126 MHz, CDCl₃): δ 174.0 (C_q), 164.3 (C_q), 139.4 (C_q), 130.6 (CH), 128.5 (CH), 127.9 (CH), 127.8 (C_q), 126.7 (CH), 67.6 (CH₂), 54.9 (CH₂), 51.9 (CH₃), 51.4 (CH), 33.2 (CH₂), 29.7 (CH₂), 22.4 (CH₂), 13.9 (CH₃). **IR** (ATR): 2952, 2872, 1733, 1649, 1357, 1160, 950, 709 cm⁻¹. **MS** (ESI): *m/z* (relative intensity): 298 (14) [M+Na]⁺, 276 (100) [M+H]⁺. **HR-MS** (ESI): *m/z* calcd for C₁₆H₂₂NO₃⁺ [M+H]⁺: 276.1594, found: 276.1597.

5. Experimental Part

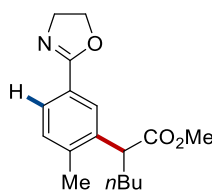
Methyl 2-[5-(4,5-dihydrooxazol-2-yl)-2-methoxyphenyl]hexanoate (219ba)



The general procedure **A** was followed using 2-(4-methoxyphenyl)-4,5-dihydrooxazole **217b** (88.6 mg, 0.50 mmol), methyl 2-bromohexanoate **218a** (314 mg, 1.50 mmol), [Ru(O₂CMes)₂(*p*-cymene)] (28.1 mg, 10 mol %), PPh₃ (13.1 mg, 10 mol %) and K₂CO₃ (138 mg, 1.00 mmol) in 1,4-dioxane (2.0 mL). Purification by column chromatography on silica gel (*n*-hexane/EtOAc: 5/1 → 3/1) yielded **219ba** (107.4 mg, 70%) as a pale yellow solid.

M.p.: 79 – 80 °C. **¹H-NMR** (600 MHz, CDCl₃): δ 7.81 (d, *J* = 2.2 Hz, 1H), 7.79 (dd, *J* = 8.6, 2.2 Hz, 1H), 6.83 (d, *J* = 8.6 Hz, 1H), 4.34 (t, *J* = 9.5 Hz, 2H), 3.97 (t, *J* = 9.5 Hz, 2H), 3.92 (t, *J* = 7.6 Hz, 1H), 3.81 (s, 3H), 3.59 (s, 3H), 2.11–1.95 (m, 1H), 1.71 (dddd, *J* = 13.2, 9.8, 7.6, 5.4 Hz, 1H), 1.35–1.08 (m, 4H), 0.81 (t, *J* = 7.2 Hz, 3H). **¹³C-NMR** (126 MHz, CDCl₃): δ 174.3 (C_q), 164.2 (C_q), 159.1 (C_q), 128.5 (CH), 128.4 (CH), 128.0 (C_q), 120.2 (C_q), 110.1 (CH), 67.4 (CH₂), 55.6 (CH₃), 54.8 (CH₂), 51.8 (CH₃), 44.1 (CH), 31.8 (CH₂), 29.7 (CH₂), 22.5 (CH₂), 13.9 (CH₃). **IR** (ATR): 2953, 2872, 1733, 1648, 1607, 1459, 1433, 1249, 1107, 952 cm⁻¹. **MS** (ESI): *m/z* (relative intensity): 306 (100) [M+H]⁺. **HR-MS** (ESI): *m/z* calcd for C₁₇H₂₄NO₄⁺ [M+H]⁺: 306.1700, found: 306.1701.

Methyl 2-[5-(4,5-dihydrooxazol-2-yl)-2-methylphenyl]hexanoate (219ca)

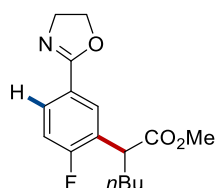


The general procedure **A** was followed using 2-(*p*-tolyl)-4,5-dihydrooxazole **217c** (80.6 mg, 0.50 mmol), methyl 2-bromohexanoate **218a** (314 mg, 1.50 mmol), [Ru(O₂CMes)₂(*p*-cymene)] (28.1 mg, 10 mol %), PPh₃ (13.1 mg, 10 mol %) and K₂CO₃ (138 mg, 1.00 mmol) in 1,4-dioxane (2.0 mL). Purification by column chromatography on silica gel (*n*-hexane/EtOAc: 5/1 → 4/1) yielded **219ca** (112.7 mg, 78%) as a white solid.

M.p.: 73 – 74 °C. **¹H-NMR** (600 MHz, CDCl₃): δ 7.86 (d, *J* = 1.8 Hz, 1H), 7.69 (dd, *J* = 8.0, 1.8 Hz, 1H), 7.17 (d, *J* = 8.0 Hz, 1H), 4.42–4.33 (m, 2H), 4.01 (t, *J* = 9.5 Hz, 2H), 3.79 (dd, *J* = 8.0, 7.1 Hz, 1H), 3.61 (s, 3H), 2.37 (s, 3H), 2.12 (dddd, *J* = 13.4, 10.2,

8.0, 5.1 Hz, 1H), 1.74 (dddd, $J = 13.4, 9.9, 7.1, 5.5$ Hz, 1H), 1.36–1.11 (m, 4H), 0.84 (t, $J = 7.2$ Hz, 3H). $^{13}\text{C-NMR}$ (126 MHz, CDCl_3): δ 174.1 (C_q), 164.4 (C_q), 139.7 (C_q), 137.9 (C_q), 130.4 (CH), 126.7 (CH), 126.6 (CH), 125.9 (C_q), 67.5 (CH_2), 54.9 (CH_2), 51.9 (CH_3), 47.0 (CH), 32.6 (CH_2), 29.9 (CH_2), 22.6 (CH_2), 20.0 (CH_3), 14.0 (CH_3). **IR** (ATR): 2952, 2929, 2871, 1733, 1649, 1215, 1160, 723 cm^{-1} . **MS** (ESI) m/z (relative intensity): 290 (100) $[\text{M}+\text{H}]^+$. **HR-MS** (ESI): m/z calcd for $\text{C}_{17}\text{H}_{24}\text{NO}_3^+$ $[\text{M}+\text{H}]^+$: 290.1751, found: 290.1752.

Methyl 2-[5-(4,5-dihydrooxazol-2-yl)-2-fluorophenyl]hexanoate (**219da**)

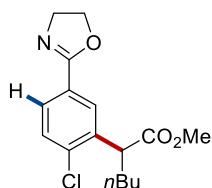


The general procedure **A** was followed using 2-(4-fluorophenyl)-4,5-dihydrooxazole **217d** (82.6 mg, 0.50 mmol), methyl 2-bromohexanoate **218a** (314 mg, 1.50 mmol), $[\text{Ru}(\text{O}_2\text{CMes})_2(p\text{-cymene})]$ (28.1 mg, 10 mol %), PPh_3 (13.1 mg, 10 mol %) and K_2CO_3 (138 mg, 1.00 mmol) in 1,4-dioxane (2.0 mL). Purification by column chromatography on silica gel ($n\text{-hexane}/\text{EtOAc}$: 5/1 \rightarrow 4/1) yielded **219da** (89.5 mg, 61%) as a colorless oil.

$^1\text{H-NMR}$ (300 MHz, CDCl_3): δ 7.94 (dd, $J = 7.1, 2.2$ Hz, 1H), 7.83 (ddd, $J = 8.6, 5.1, 2.2$ Hz, 1H), 7.07 (dd, $J = 9.6, 8.6$ Hz, 1H), 4.42 (t, $J = 9.4$ Hz, 2H), 4.04 (t, $J = 9.4$ Hz, 2H), 3.90 (t, $J = 7.5$ Hz, 1H), 3.66 (s, 3H), 2.11 (dddd, $J = 12.8, 9.8, 7.5, 5.5$ Hz, 1H), 1.87–1.67 (m, 1H), 1.41–1.10 (m, 4H), 0.85 (t, $J = 7.0$ Hz, 3H). $^{13}\text{C-NMR}$ (126 MHz, CDCl_3): δ 173.5 (C_q), 163.7 (C_q), 162.3 (d, $^1J_{\text{C-F}} = 252$ Hz, C_q), 129.5 (d, $^3J_{\text{C-F}} = 5$ Hz, CH), 128.9 (d, $^3J_{\text{C-F}} = 9$ Hz, CH), 126.7 (d, $^2J_{\text{C-F}} = 16$ Hz, C_q), 124.2 (d, $^4J_{\text{C-F}} = 3$ Hz, C_q), 115.6 (d, $^2J_{\text{C-F}} = 24$ Hz, CH), 67.7 (CH_2), 54.9 (CH_2), 52.1 (CH_3), 43.6 (d, $^3J_{\text{C-F}} = 2$ Hz, CH), 32.0 (CH_2), 29.6 (CH_2), 22.4 (CH_2), 13.7 (CH_3). $^{19}\text{F-NMR}$ (471 MHz, CDCl_3): δ -113.35 (ddd, $J = 9.6, 7.1, 5.1$ Hz). **IR** (ATR): 2954, 2873, 1736, 1651, 1997, 1359, 1228, 1169, 1104, 979 cm^{-1} . **MS** (EI): m/z (relative intensity): 293 (25) $[\text{M}]^+$, 234 (100) $[\text{M}-\text{CO}_2\text{Me}]^+$, 178 (90). **HR-MS** (EI): m/z calcd for $\text{C}_{16}\text{H}_{20}\text{FNO}_3^+$ $[\text{M}]^+$: 293.1422, found: 293.1422.

5. Experimental Part

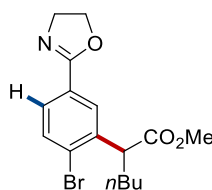
Methyl 2-[2-chloro-5-(4,5-dihydrooxazol-2-yl)phenyl]hexanoate (219ea)



The general procedure **A** was followed using 2-(4-chlorophenyl)-4,5-dihydrooxazole **217e** (90.8 mg, 0.50 mmol), methyl 2-bromohexanoate **218a** (314 mg, 1.50 mmol), [Ru(O₂CMes)₂(*p*-cymene)] (28.1 mg, 10 mol %), PPh₃ (13.1 mg, 10 mol %) and K₂CO₃ (138 mg, 1.00 mmol) in 1,4-dioxane (2.0 mL). Purification by column chromatography on silica gel (*n*-hexane/EtOAc: 5/1 → 3/1) yielded **219ea** (110.3 mg, 71%) as a white solid.

M.p.: 62 – 64 °C. **¹H-NMR** (300 MHz, CDCl₃): δ 7.91 (d, *J* = 2.1 Hz, 1H), 7.72 (dd, *J* = 8.4, 2.1 Hz, 1H), 7.37 (d, *J* = 8.4 Hz, 1H), 4.38 (t, *J* = 9.2 Hz, 2H), 4.10 (t, *J* = 7.6 Hz, 1H), 4.01 (t, *J* = 9.2 Hz, 2H), 3.63 (s, 3H), 2.19–2.01 (m, 1H), 1.76 (dddd, *J* = 13.4, 9.7, 7.5, 5.6 Hz, 1H), 1.41–1.10 (m, 4H), 0.83 (t, *J* = 7.0 Hz, 3H). **¹³C-NMR** (126 MHz, CDCl₃): δ 173.3 (C_q), 163.5 (C_q), 137.2 (C_q), 137.0 (C_q), 129.5 (CH), 128.5 (CH), 127.7 (CH), 126.7 (C_q), 67.7 (CH₂), 55.0 (CH₂), 52.1 (CH₃), 47.2 (CH), 32.4 (CH₂), 29.6 (CH₂), 22.4 (CH₂), 13.9 (CH₃). **IR** (ATR): 2954, 2872, 1735, 1651, 1358, 1251, 1166, 731 cm⁻¹. **MS** (ESI): *m/z* (relative intensity) 332 (15) [M+Na]⁺, 310 (100) [M+H]⁺. **HR-MS** (ESI): *m/z* calcd for C₁₆H₂₁³⁵CINO₃⁺ [M+H]⁺: 310.1204, found: 310.1207.

Methyl 2-[2-bromo-5-(4,5-dihydrooxazol-2-yl)phenyl]hexanoate (219fa)

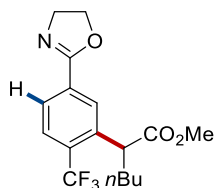


The general procedure **A** was followed using 2-(4-bromophenyl)-4,5-dihydrooxazole **217f** (113.0 mg, 0.50 mmol), methyl 2-bromohexanoate **218a** (314 mg, 1.50 mmol), [Ru(O₂CMes)₂(*p*-cymene)] (28.1 mg, 10 mol %), PPh₃ (13.1 mg, 10 mol %) and K₂CO₃ (138 mg, 1.00 mmol) in 1,4-dioxane (2.0 mL). Purification by column chromatography on silica gel (*n*-hexane/EtOAc: 5/1 → 3/1) yielded **219fa** (119.2 mg, 67%) as a white solid.

M.p.: 66 – 68 °C. **¹H-NMR** (400 MHz, CDCl₃): δ 7.88 (d, *J* = 2.1 Hz, 1H), 7.62 (dd, *J* = 8.3, 2.1 Hz, 1H), 7.55 (d, *J* = 8.3 Hz, 1H), 4.35 (t, *J* = 9.6 Hz, 2H), 4.10 (t, *J* = 7.6 Hz, 1H), 3.97 (t, *J* = 9.6 Hz, 2H), 3.61 (s, 3H), 2.05 (dddd, *J* = 13.4, 10.1, 7.6, 5.0 Hz, 1H),

1.74 (dddd, $J = 13.2, 9.9, 7.5, 5.5$ Hz, 1H), 1.35–1.09 (m, 4H), 0.81 (t, $J = 7.1$ Hz, 3H). $^{13}\text{C-NMR}$ (126 MHz, CDCl_3): δ 173.2 (C_q), 163.5 (C_q), 138.9 (C_q), 132.8 (CH), 128.2 (CH), 128.0 (C_q), 127.8 (CH), 127.3 (C_q), 67.6 (CH_2), 54.9 (CH_2), 52.0 (CH_3), 49.8 (CH), 32.7 (CH_2), 29.5 (CH_2), 22.4 (CH_2), 13.8 (CH_3). **IR** (ATR): 2953, 2872, 1743, 1650, 1193, 1166, 1078, 909, 731 cm^{-1} . **MS** (ESI): m/z (relative intensity) 354 (100) $[\text{M}+\text{H}]^+$. **HR-MS** (ESI): m/z calcd for $\text{C}_{16}\text{H}_{21}^{79}\text{BrNO}_3^+$ $[\text{M}+\text{H}]^+$: 354.0699, found: 354.0703.

Methyl 2-[5-(4,5-dihydrooxazol-2-yl)-2-(trifluoromethyl)phenyl]hexanoate (219ga)

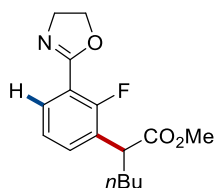


The general procedure **A** was followed using 2-[4-(trifluoromethyl)phenyl]-4,5-dihydrooxazole **217g** (108.1 mg, 0.50 mmol), methyl 2-bromohexanoate **218a** (314 mg, 1.50 mmol), $[\text{Ru}(\text{O}_2\text{CMes})_2(p\text{-cymene})]$ (28.1 mg, 10 mol %), PPh_3 (13.1 mg, 10 mol %) and K_2CO_3 (138 mg, 1.00 mmol) in 1,4-dioxane (2.0 mL). Purification by column chromatography on silica gel ($n\text{-hexane}/\text{EtOAc}$: 5/1 \rightarrow 4/1) yielded **219ga** (90.9 mg, 53%) as a colorless oil.

$^1\text{H-NMR}$ (300 MHz, CDCl_3): δ 8.16 (dd, $J = 1.7, 0.8$ Hz, 1H), 7.90 (ddd, $J = 8.2, 1.7, 0.9$ Hz, 1H), 7.66 (d, $J = 8.3$ Hz, 1H), 4.48–4.37 (m, 2H), 4.13–3.96 (m, 3H), 3.64 (s, 3H), 2.22–2.05 (m, 1H), 1.84–1.67 (m, 1H), 1.41–1.09 (m, 4H), 0.84 (t, $J = 7.0$ Hz, 3H). $^{13}\text{C-NMR}$ (126 MHz, CDCl_3): δ 173.3 (C_q), 163.2 (C_q), 138.5 (m, C_q), 131.3 (C_q), 130.7 (q, $^2J_{\text{C-F}} = 30$ Hz, C_q), 128.6 (CH), 126.6 (CH), 125.9 (q, $^3J_{\text{C-F}} = 6$ Hz, CH), 123.8 (q, $^1J_{\text{C-F}} = 274$ Hz, C_q), 67.8 (CH_2), 55.1 (CH_2), 52.2 (CH_3), 46.4 (CH), 34.2 (CH_2), 29.8 (CH_2), 22.4 (CH_2), 13.8 (CH_3). $^{19}\text{F-NMR}$ (282 MHz, CDCl_3): δ -58.7 (s). **IR** (ATR): 2955, 1737, 1652, 1310, 1160, 1123, 1038, 980 cm^{-1} . **MS** (EI): m/z (relative intensity): 343 (15) $[\text{M}]^+$, 287 (100) $[\text{M}-\text{Bu}]^+$, 284 (90) $[\text{M}-\text{CO}_2\text{Me}]^+$, 229 (67). **HR-MS** (EI): m/z calcd for $\text{C}_{17}\text{H}_{20}\text{F}_3\text{NO}_3^+$ $[\text{M}]^+$: 343.1390, found: 343.1393.

5. Experimental Part

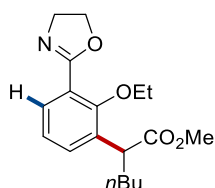
Methyl 2-[3-(4,5-dihydrooxazol-2-yl)-2-fluorophenyl]hexanoate (**219ha**)



The general procedure **A** was followed using 2-(2-fluorophenyl)-4,5-dihydrooxazole **217h** (82.6 mg, 0.50 mmol), methyl 2-bromohexanoate **218a** (314 mg, 1.50 mmol), [Ru(O₂CMe)₂(*p*-cymene)] (28.1 mg, 10 mol %), PPh₃ (13.1 mg, 10 mol %) and K₂CO₃ (138 mg, 1.00 mmol) in 1,4-dioxane (2.0 mL). Purification by column chromatography on silica gel (*n*-hexane/EtOAc: 5/1 → 4/1) yielded **219ha** (107.3 mg, 73%) as a colorless oil.

¹H-NMR (300 MHz, CDCl₃): δ 7.76 (ddd, *J* = 7.8, 6.8, 1.8 Hz, 1H), 7.46 (ddd, *J* = 8.1, 6.6, 1.8 Hz, 1H), 7.16 (td, *J* = 7.8, 0.8 Hz, 1H), 4.41 (td, *J* = 9.4, 1.0 Hz, 2H), 4.17–4.05 (m, 2H), 3.98 (t, *J* = 7.6 Hz, 1H), 3.66 (s, 3H), 2.17–1.99 (m, 1H), 1.86–1.67 (m, 1H), 1.39–1.11 (m, 4H), 0.85 (t, *J* = 7.1 Hz, 3H). **¹³C-NMR** (125 MHz, CDCl₃): δ 173.5 (C_q), 161.2 (d, ³*J*_{C-F} = 6 Hz, C_q), 158.7 (d, ¹*J*_{C-F} = 258 Hz, C_q), 131.8 (d, ³*J*_{C-F} = 5 Hz, CH), 129.6 (d, ⁴*J*_{C-F} = 2 Hz, CH), 127.6 (d, ²*J*_{C-F} = 15 Hz, C_q), 123.8 (d, ³*J*_{C-F} = 4 Hz, CH), 116.1 (d, ²*J*_{C-F} = 12 Hz, C_q), 67.1 (CH₂), 55.3 (CH₂), 52.1 (CH₃), 43.3 (d, ³*J*_{C-F} = 4 Hz, CH), 32.3 (CH₂), 29.6 (CH₂), 22.4 (CH₂), 13.9 (CH₃). **¹⁹F-NMR** (282 MHz, CDCl₃): δ –115.3 (t, *J* = 6.7 Hz). **IR** (ATR): 2956, 1738, 1651, 1455, 1217, 1163, 743 cm⁻¹. **MS** (EI): *m/z* (relative intensity) 293 (20) [M]⁺, 234 (100) [M–CO₂Me]⁺. **HR-MS** (EI): *m/z* calcd for C₁₆H₂₀FNO₃⁺ [M]⁺: 293.1422, found: 293.1427.

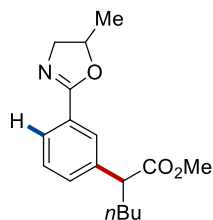
Methyl 2-[3-(4,5-dihydrooxazol-2-yl)-2-ethoxyphenyl]hexanoate (**219ia**)



The general procedure **A** was followed using 2-(2-ethoxyphenyl)-4,5-dihydrooxazole **217i** (95.6 mg, 0.50 mmol), methyl 2-bromohexanoate **218a** (314 mg, 1.50 mmol), [Ru(O₂CMe)₂(*p*-cymene)] (28.1 mg, 10 mol %), PPh₃ (13.1 mg, 10 mol %) and K₂CO₃ (138 mg, 1.00 mmol) in 1,4-dioxane (2.0 mL). Purification by column chromatography on silica gel (*n*-hexane/EtOAc: 5/1 → 1/1) yielded **219ia** (79.8 mg, 50%) as a colorless oil.

¹H-NMR (300 MHz, CDCl₃): δ 7.64 (dd, *J* = 7.7, 1.8 Hz, 1H), 7.44 (dd, *J* = 7.8, 1.8 Hz, 1H), 7.08 (dd, *J* = 7.8, 7.7 Hz, 1H), 4.46–4.32 (m, 2H), 4.16–3.85 (m, 5H), 3.62 (s, 3H), 2.02 (dddd, *J* = 13.0, 10.2, 8.0, 5.0 Hz, 1H), 1.74–1.58 (m, 1H), 1.39 (t, *J* = 7.0 Hz, 3H), 1.35–1.06 (m, 4H), 0.83 (t, *J* = 7.1 Hz, 3H). **¹³C-NMR** (125 MHz, CDCl₃): δ 174.5 (C_q), 163.3 (C_q), 155.9 (C_q), 134.0 (C_q), 130.8 (CH), 129.9 (CH), 123.7 (CH), 121.8 (C_q), 70.8 (CH₂), 67.3 (CH₂), 55.2 (CH₂), 51.9 (CH₃), 43.5 (CH), 33.4 (CH₂), 29.9 (CH₂), 22.5 (CH₂), 15.6 (CH₃), 13.9 (CH₃). **IR** (ATR): 2916, 2848, 1737, 1465, 1238, 1054, 719 cm⁻¹. **MS** (ESI): *m/z* (relative intensity): 342 (20) [M+Na]⁺, 320 (100) [M+H]⁺. **HR-MS** (ESI): *m/z* calcd for C₁₈H₂₆NO₄⁺ [M+H]⁺: 320.1856, found: 320.1858.

Methyl 2-[3-(5-methyl-4,5-dihydrooxazol-2-yl)phenyl]hexanoate (**221aa**)

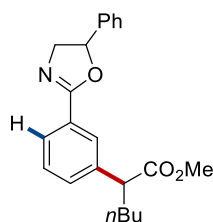


The general procedure **A** was followed using 5-methyl-2-phenyl-4,5-dihydrooxazole **220a** (80.5 mg, 0.50 mmol), methyl 2-bromohexanoate **218a** (314 mg, 1.50 mmol), [Ru(O₂CMe)₂(*p*-cymene)] (28.1 mg, 10 mol %), PPh₃ (13.1 mg, 10 mol %) and K₂CO₃ (138 mg, 1.00 mmol) in 1,4-dioxane (2.0 mL). Purification by column chromatography on silica gel (*n*-hexane/EtOAc: 5/1 → 1/1) yielded **221aa** (92.5 mg, 64%) as a colorless oil.

¹H-NMR (600 MHz, CDCl₃, mixture of diastereoisomers, dr 1.0:1.0): δ 7.88–7.84 (m, 2H), 7.83–7.78 (m, 2H), 7.44–7.39 (m, 2H), 7.36–7.31 (m, 2H), 4.90–4.76 (m, 2H), 4.18–4.08 (m, 2H), 3.63 (s, 3H), 3.63 (s, 3H), 3.61–3.54 (m, 4H), 2.12–2.03 (m, 2H), 1.82–1.72 (m, 2H), 1.42–1.39 (m, 6H), 1.35–1.11 (m, 8H), 0.87–0.77 (m, 6H). **¹³C-NMR** (126 MHz, CDCl₃, mixture of diastereoisomers, dr 1.0:1.0): δ 174.1 (C_q), 163.5 (C_q), 139.4 (C_q), 130.5 (CH), 130.5 (CH), 128.4 (CH), 128.3 (C_q), 127.7 (CH), 127.7 (CH), 126.8 (CH), 76.3 (CH), 61.6 (CH₂), 51.9 (CH₃), 51.5 (CH), 51.5 (CH), 33.2 (CH₂), 33.1 (CH₂), 29.7 (CH₂), 22.4 (CH₂), 21.1 (CH₃), 13.9 (CH₃). **IR** (ATR): 2952, 2928, 2869, 1735, 1646, 1434, 1260, 1068, 994, 712 cm⁻¹. **MS** (ESI): *m/z* (relative intensity) 312 (25) [M+Na]⁺, 290 (100) [M+H]⁺. **HR-MS** (ESI): *m/z* calcd for C₁₇H₂₄NO₃⁺ [M+H]⁺: 290.1751, found: 290.1746.

5. Experimental Part

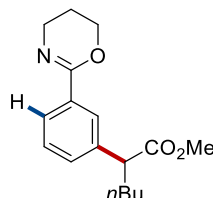
Methyl 2-[3-(5-phenyl-4,5-dihydrooxazol-2-yl)phenyl]hexanoate (**221ba**)



The general procedure **A** was followed using 2,5-diphenyl-4,5-dihydrooxazole **220b** (116.5 mg, 0.50 mmol), methyl 2-bromohexanoate **218a** (314 mg, 1.50 mmol), [Ru(O₂CMe)₂(*p*-cymene)] (28.1 mg, 10 mol %), PPh₃ (13.1 mg, 10 mol %) and K₂CO₃ (138 mg, 1.00 mmol) in 1,4-dioxane (2.0 mL). Purification by column chromatography on silica gel (*n*-hexane/EtOAc: 9/1 → 5/1) yielded **221ba** (151.4 mg, 86%) as a colorless oil.

¹H-NMR (400 MHz, CDCl₃, mixture of diastereoisomers, dr 1.0:1.0): δ 8.00–7.93 (m, 2H), 7.95–7.87 (m, 2H), 7.51–7.43 (m, 2H), 7.41–7.29 (m, 12H), 5.69–5.60 (m, 2H), 4.53–4.39 (m, 2H), 4.09–3.92 (m, 2H), 3.65 (s, 3H), 3.64 (s, 3H), 3.65–3.55 (m, 2H), 2.16–2.04 (m, 2H), 1.87–1.73 (m, 2H), 1.36–1.17 (m, 8H), 0.92–0.81 (m, 6H). **¹³C-NMR** (100 MHz, CDCl₃, mixture of diastereoisomers, dr 1.0:1.0): δ 174.2 (C_q), 174.1 (C_q), 163.8 (C_q), 140.9 (C_q), 139.6 (C_q), 130.8 (CH), 130.8 (CH), 128.7 (CH), 128.6 (CH), 128.2 (CH), 128.0 (CH), 128.0 (CH), 127.9 (C_q), 127.1 (CH), 127.1 (CH), 125.7 (CH), 125.7 (CH), 81.0 (CH), 63.1 (CH₂), 51.9 (CH₃), 51.4 (CH), 33.2 (CH₂), 33.0 (CH₂), 29.7 (CH₂), 29.6 (CH₂), 22.3 (CH₂), 22.3 (CH₂), 13.8 (CH₃). **IR** (ATR): 2953, 2871, 1731, 1649, 1584, 1493, 1161, 697 cm⁻¹. **MS** (ESI): *m/z* (relative intensity) 352 (100) [M+H]⁺. **HR-MS** (ESI): *m/z* calcd for C₂₂H₂₆NO₃⁺ [M+H]⁺: 352.1907, found: 352.1908.

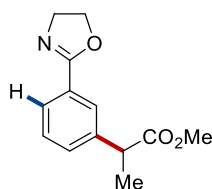
Methyl 2-[3-(5,6-dihydro-4*H*-1,3-oxazin-2-yl)phenyl]hexanoate (**221ca**)



The general procedure **A** was followed using 2-phenyl-5,6-dihydro-4*H*-1,3-oxazine **220c** (80.6 mg, 0.50 mmol), methyl 2-bromohexanoate **218a** (314 mg, 1.50 mmol), [Ru(O₂CMe)₂(*p*-cymene)] (28.1 mg, 10 mol %), PPh₃ (13.1 mg, 10 mol %) and K₂CO₃ (138 mg, 1.00 mmol) in 1,4-dioxane (2.0 mL). Purification by column chromatography on silica gel (*n*-hexane/EtOAc: 5/1) yielded **221ca** (85.4 mg, 59%) as a colorless oil.

¹H-NMR (600 MHz, CDCl₃): δ 7.81 (t, *J* = 1.6 Hz, 1H), 7.77 (dt, *J* = 7.6, 1.6 Hz, 1H), 7.36 (dt, *J* = 7.8, 1.6 Hz, 1H), 7.30 (t, *J* = 7.6 Hz, 1H), 4.34 (t, *J* = 5.5 Hz, 2H), 3.62 (s, 3H), 3.61–3.53 (m, 3H), 2.14–1.95 (m, 1H), 2.00–1.91 (m, 2H), 1.76 (dddd, *J* = 13.2, 9.5, 7.4, 5.7 Hz, 1H), 1.35–1.11 (m, 4H), 0.84 (t, *J* = 7.2 Hz, 3H). **¹³C-NMR** (101 MHz, CDCl₃): δ 174.4 (C_q), 155.4 (C_q), 139.1 (C_q), 134.3 (C_q), 129.6 (CH), 128.2 (CH), 126.6 (CH), 125.7 (CH), 65.1 (CH₂), 51.8 (CH₃), 51.5 (CH), 42.6 (CH₂), 33.2 (CH₂), 29.7 (CH₂), 22.4 (CH₂), 21.9 (CH₂), 13.8 (CH₃). **IR** (ATR): 2952, 2858, 1734, 1653, 1347, 1272, 1160, 1130, 716 cm⁻¹. **MS** (ESI): *m/z* (relative intensity) 290 (100) [M+H]⁺. **HR-MS** (ESI): *m/z* calcd for C₁₇H₂₄NO₃ [M+H]⁺: 290.1751, found: 290.1753.

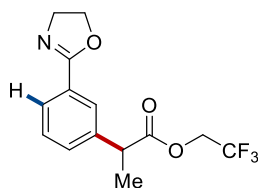
Methyl 2-[3-(4,5-dihydrooxazol-2-yl)phenyl]propanoate (222ab)



The general procedure **A** was followed using 2-phenyl-4,5-dihydrooxazole **217a** (73.5 mg, 0.50 mmol) and methyl 2-bromopropanoate **218b** (247 mg, 1.50 mmol). Purification by column chromatography on silica gel (*n*-hexane/EtOAc: 5/1 → 2/1) yielded **222ab** (93.3 mg, 80%) as a colorless oil.

¹H-NMR (300 MHz, CDCl₃): δ 7.85 (t, *J* = 1.7 Hz, 1H), 7.80 (dt, *J* = 7.5, 1.7 Hz, 1H), 7.39 (dt, *J* = 7.5, 1.7 Hz, 1H), 7.34 (d, *J* = 7.5 Hz, 1H), 4.39 (t, *J* = 9.5 Hz, 2H), 4.02 (t, *J* = 9.5 Hz, 2H), 3.73 (q, *J* = 7.2 Hz, 1H), 3.62 (s, 3H), 1.48 (d, *J* = 7.2 Hz, 3H). **¹³C-NMR** (126 MHz, CDCl₃): δ 174.4 (C_q), 164.3 (C_q), 140.6 (C_q), 130.2 (CH), 128.5 (CH), 127.9 (C_q), 127.3 (CH), 126.8 (CH), 67.6 (CH₂), 54.9 (CH₂), 52.0 (CH₃), 45.2 (CH), 18.5 (CH₃). **IR** (ATR): 2951, 2872, 1733, 1648, 1607, 1251, 1077, 947 cm⁻¹. **MS** (EI): *m/z* (relative intensity) 233 (40) [M]⁺, 174 (100) [M-CO₂Me]⁺. **HR-MS** (EI): *m/z* calcd for C₁₃H₁₅NO₃⁺ [M]⁺: 233.1046, found: 233.1040.

2,2,2-Trifluoroethyl 2-[3-(4,5-dihydrooxazol-2-yl)phenyl]propanoate (222ac)

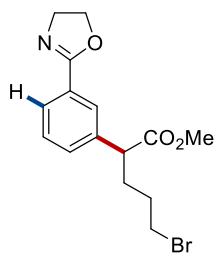


The general procedure **A** was followed using 2-phenyl-4,5-dihydrooxazole **217a** (73.5 mg, 0.50 mmol), 2,2,2-trifluoroethyl 2-bromopropanoate **218c** (353 mg, 1.50 mmol),

5. Experimental Part

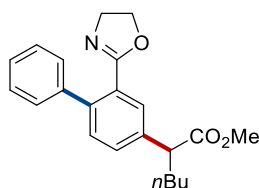
[Ru(O₂CMe_s)₂(*p*-cymene)] (28.1 mg, 10 mol %), PPh₃ (13.1 mg, 10 mol %) and K₂CO₃ (138 mg, 1.00 mmol) in 1,4-dioxane (2.0 mL). Purification by column chromatography on silica gel (*n*-hexane/EtOAc: 5/1) yielded **222ac** (116.2 mg, 77%) as a colorless oil. **¹H-NMR** (500 MHz, CDCl₃): δ 7.89 (t, *J* = 1.2 Hz, 1H), 7.85 (dt, *J* = 6.9, 1.2 Hz, 1H), 7.44–7.33 (m, 2H), 4.60–4.29 (m, 4H), 4.05 (t, *J* = 9.5 Hz, 2H), 3.86 (q, *J* = 7.2 Hz, 1H), 1.56 (d, *J* = 7.2 Hz, 3H). **¹³C-NMR** (126 MHz, CDCl₃): δ 172.4 (C_q), 164.1 (C_q), 139.4 (C_q), 130.2 (CH), 128.7 (CH), 128.2 (C_q), 127.2 (CH), 127.2 (CH), 122.7 (q, ¹*J*_{C-F} = 277 Hz, C_q), 67.6 (CH₂), 60.5 (q, ²*J*_{C-F} = 37 Hz, CH₂), 54.9 (CH₂), 44.9 (CH), 18.3 (CH₃). **¹⁹F-NMR** (282 MHz, CDCl₃): δ -73.9 (t, *J* = 8.4 Hz). **IR** (ATR): 2884, 1755, 1650, 1279, 1163, 976, 949 cm⁻¹. **MS** (ESI): *m/z* (relative intensity) 302 [M+H]⁺. **HR-MS** (ESI): *m/z* calcd for C₁₄H₁₅F₃NO₃⁺ [M+H]⁺: 302.0999, found: 302.1009.

Methyl 5-bromo-2-[3-(4,5-dihydrooxazol-2-yl)phenyl]pentanoate (**222ad**)



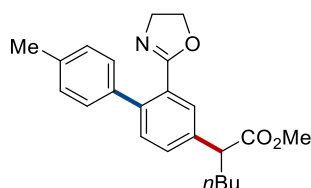
The general procedure **A** was followed using 2-phenyl-4,5-dihydrooxazole **217a** (73.5 mg, 0.50 mmol), methyl 2,5-dibromopentanoate **218d** (411 mg, 1.50 mmol), [Ru(O₂CMe_s)₂(*p*-cymene)] (28.1 mg, 10 mol %), PPh₃ (13.1 mg, 10 mol %) and K₂CO₃ (138 mg, 1.00 mmol) in 1,4-dioxane (2.0 mL). Purification by column chromatography on silica gel (*n*-hexane/EtOAc: 8/1 → 5/1) yielded **222ad** (107.2 mg, 63%) as a colorless oil.

¹H-NMR (300 MHz, CDCl₃): δ 7.91–7.83 (m, 1H), 7.84 (dt, *J* = 7.6, 1.7 Hz, 1H), 7.42 (dt, *J* = 7.6, 1.7 Hz, 1H), 7.37 (dd, *J* = 7.6, 7.6 Hz, 1H), 4.43 (td, *J* = 9.5, 0.8 Hz, 2H), 4.06 (td, *J* = 9.6, 0.8 Hz, 2H), 3.65 (s, 3H), 3.60 (t, *J* = 7.6 Hz, 1H), 3.44–3.28 (m, 2H), 2.23 (dddd, *J* = 12.5, 9.7, 7.5, 5.0 Hz, 1H), 2.04–1.91 (m, 1H), 1.88–1.69 (m, 2H). **¹³C-NMR** (126 MHz, CDCl₃): δ 173.4 (C_q), 164.2 (C_q), 138.7 (C_q), 130.5 (CH), 128.7 (CH), 128.2 (C_q), 127.7 (CH), 127.2 (CH), 67.6 (CH₂), 55.0 (CH₂), 52.2 (CH₃), 50.6 (CH), 32.9 (CH₂), 31.9 (CH₂), 30.6 (CH₂). **IR** (ATR): 2949, 1730, 1649, 1433, 1358, 1165, 1068, 710 cm⁻¹. **MS** (ESI): *m/z* (relative intensity) 340 (100) [M+H]⁺. **HR-MS** (ESI): *m/z* calcd for C₁₅H₁₉⁷⁹BrNO₃ [M+H]⁺: 340.0543, found: 340.0546.

Methyl 2-[2-(4,5-dihydrooxazol-2-yl)-[1,1'-biphenyl]-4-yl]hexanoate (223aa)

The general procedure **B** was followed using 2-phenyl-4,5-dihydrooxazole **217a** (73.5 mg, 0.50 mmol), methyl 2-bromohexanoate **218a** (314 mg, 1.50 mmol), bromobenzene **163a** (236 mg, 1.50 mmol), [Ru(O₂CMe)₂(*p*-cymene)] (28.1 mg, 50.0 μmol, 10.0 mol %), PPh₃ (13.1 mg, 50.0 μmol, 10.0 mol %) and K₂CO₃ (276 mg, 2.00 mmol) in 1,4-dioxane (2.0 mL). Purification by column chromatography on silica gel (*n*-hexane/EtOAc 5/1: → 1/1) yielded **223aa** (123.4 mg, 70%) as a colorless oil.

¹H-NMR (400 MHz, CDCl₃): δ 7.68 (dd, *J* = 2.0, 0.5 Hz, 1H), 7.43 (ddd, *J* = 7.9, 2.0, 0.5 Hz, 1H), 7.38–7.27 (m, 6H), 4.15–4.05 (m, 2H), 3.94–3.85 (m, 2H), 3.65 (s, 3H), 3.58 (t, *J* = 8.0 Hz, 1H), 2.09 (dddd, *J* = 13.4, 9.5, 8.1, 5.7 Hz, 1H), 1.80 (dddd, *J* = 13.4, 9.2, 8.0, 6.0 Hz, 1H), 1.37–1.16 (m, 4H), 0.86 (t, *J* = 7.1 Hz, 3H). **¹³C-NMR** (100 MHz, CDCl₃): δ 174.2 (C_q), 165.9 (C_q), 140.8 (C_q), 140.7 (C_q), 138.3 (C_q), 130.6 (CH), 129.9 (CH), 129.8 (CH), 128.2 (CH), 127.9 (CH), 127.6 (C_q), 127.1 (CH), 67.7 (CH₂), 54.9 (CH₂), 51.9 (CH₃), 51.1 (CH), 33.1 (CH₂), 29.7 (CH₂), 22.4 (CH₂), 13.8 (CH₃). **IR** (ATR): 2953, 2927, 2870, 1734, 1648, 1434, 1348, 1224, 749 cm⁻¹. **MS** (ESI): *m/z* (relative intensity) 352 (100) [M+H]⁺. **HR-MS** (ESI): *m/z* calcd for C₂₂H₂₆NO₃⁺ [M+H]⁺: 352.1907, found: 352.1907.

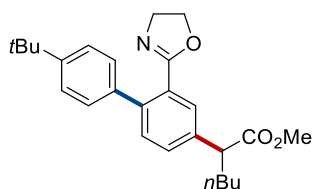
Methyl 2-[2-(4,5-dihydrooxazol-2-yl)-4'-methyl-[1,1'-biphenyl]-4-yl]hexanoate (223ab)

The general procedure **B** was followed using 2-phenyl-4,5-dihydrooxazole **217a** (73.5 mg, 0.50 mmol), methyl 2-bromohexanoate **218a** (314 mg, 1.50 mmol), 4-bromotoluene **163b** (256 mg, 1.50 mmol), [Ru(O₂CMe)₂(*p*-cymene)] (28.1 mg, 10 mol %), PPh₃ (13.1 mg, 10 mol %) and K₂CO₃ (276 mg, 2.00 mmol) in 1,4-dioxane (2.0 mL). Purification by column chromatography on silica gel (*n*-hexane/EtOAc 5/1: → 1/1) yielded **223ab** (111.0 mg, 61%) as a colorless oil.

5. Experimental Part

¹H-NMR (400 MHz, CDCl₃): δ 7.66 (d, *J* = 2.0 Hz, 1H), 7.44–7.40 (m, 1H), 7.31 (d, *J* = 8.0 Hz, 1H), 7.24 (d, *J* = 8.1 Hz, 2H), 7.16 (d, *J* = 8.1 Hz, 2H), 4.15–4.08 (m, 2H), 3.90 (t, *J* = 9.5 Hz, 2H), 3.65 (s, 3H), 3.57 (t, *J* = 7.7 Hz, 1H), 2.36 (s, 3H), 2.09 (dddd, *J* = 13.3, 9.4, 7.7, 5.7 Hz, 1H), 1.79 (dddd, *J* = 13.3, 9.2, 7.7, 6.0 Hz, 1H), 1.40–1.16 (m, 4H), 0.86 (t, *J* = 7.1 Hz, 3H). **¹³C-NMR** (101 MHz, CDCl₃): δ 174.2 (C_q), 166.0 (C_q), 140.6 (C_q), 138.0 (C_q), 137.9 (C_q), 136.8 (C_q), 130.6 (CH), 129.9 (CH), 129.8 (CH), 128.7 (CH), 128.1 (CH), 127.6 (C_q), 67.8 (CH₂), 54.9 (CH₂), 51.9 (CH₃), 51.1 (CH), 33.1 (CH₂), 29.7 (CH₂), 22.4 (CH₂), 21.1 (CH₃), 13.8 (CH₃). **IR** (ATR): 2952, 2871, 1733, 1650, 1484, 1434, 1348, 1162, 817 cm⁻¹. **MS** (ESI): *m/z* (relative intensity) 366 (100) [M+H]⁺. **HR-MS** (ESI): *m/z* calcd for C₂₃H₂₈NO₃⁺ [M+H]⁺: 366.2064, found: 366.2064.

Methyl 2-[4'-(*tert*-butyl)-2-(4,5-dihydrooxazol-2-yl)-[1,1'-biphenyl]-4-yl]hexanoate (223ac)

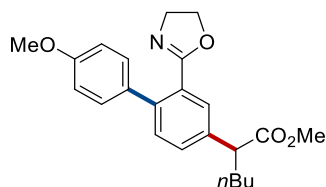


The general procedure **B** was followed using 2-phenyl-4,5-dihydrooxazole **217a** (73.5 mg, 0.50 mmol), methyl 2-bromohexanoate **218a** (314 mg, 1.50 mmol), 1-bromo-4-*tert*-butylbenzene **163c** (319 mg, 1.50 mmol), [Ru(O₂CMes)₂(*p*-cymene)] (28.1 mg, 10 mol %), PPh₃ (13.1 mg, 10 mol %) and K₂CO₃ (276 mg, 2.00 mmol) in 1,4-dioxane (2.0 mL). Purification by column chromatography on silica gel (*n*-hexane/EtOAc 5/1 → 1/1) yielded **223ac** (124.2 mg, 61%) as a colorless oil.

¹H-NMR (400 MHz, CDCl₃): 7.67 (d, *J* = 1.9 Hz, 1H), 7.44 (dd, *J* = 8.0, 1.9 Hz, 1H), 7.39 (d, *J* = 8.7 Hz, 2H), 7.34 (d, *J* = 8.0 Hz, 1H), 7.30 (d, *J* = 8.7 Hz, 2H), 4.15–4.09 (m, 2H), 3.96–3.89 (m, 2H), 3.67 (s, 3H), 3.59 (t, *J* = 7.7 Hz, 1H), 2.11 (dddd, *J* = 13.4, 9.3, 8.1, 5.7 Hz, 1H), 1.81 (dddd, *J* = 13.4, 9.2, 7.3, 6.0 Hz, 1H), 1.35 (s, 9H), 1.34–1.18 (m, 4H), 0.88 (t, *J* = 7.1 Hz, 3H). **¹³C-NMR** (101 MHz, CDCl₃): 174.2 (C_q), 166.1 (C_q), 150.0 (C_q), 140.6 (C_q), 138.0 (C_q), 137.8 (C_q), 130.6 (CH), 129.8 (CH), 129.7 (CH), 127.8 (CH), 127.6 (C_q), 124.9 (CH), 67.8 (CH₂), 54.9 (CH₂), 51.9 (CH₃), 51.1 (CH), 34.5 (C_q), 33.2 (CH₂), 31.3 (CH₃), 29.7 (CH₂), 22.4 (CH₂), 13.8 (CH₃). **IR** (ATR): 2954, 2862, 1736, 1650, 1485, 1191, 1112, 827 cm⁻¹. **MS** (ESI): *m/z* (relative intensity)

837 (15) [2M+Na]⁺, 815 (15) [2M+H]⁺, 408 (100) [M+H]⁺. **HR-MS** (ESI): *m/z* calcd for C₂₆H₃₄NO₃⁺ [M+H]⁺ 408.2533, found 408.2535.

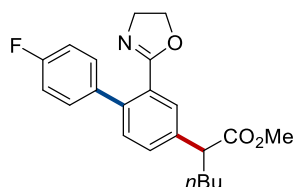
Methyl 2-[2-(4,5-dihydrooxazol-2-yl)-4'-methoxy-[1,1'-biphenyl]-4-yl]hexanoate (223ad)



The general procedure **B** was followed using 2-phenyl-4,5-dihydrooxazole **217a** (73.5 mg, 0.50 mmol), methyl 2-bromohexanoate **218a** (314 mg, 1.50 mmol), 4-bromoanisole **163d** (280 mg, 1.50 mmol), [Ru(O₂CMes)₂(*p*-cymene)] (28.1 mg, 10 mol %), PPh₃ (13.1 mg, 10 mol %) and K₂CO₃ (276 mg, 2.00 mmol) in 1,4-dioxane (2.0 mL). Purification by column chromatography on silica gel (*n*-hexane/EtOAc: 5/1 → 1/1) yielded **223ad** (139.4 mg, 73%) as a colorless oil.

¹H-NMR (300 MHz, CDCl₃): δ 7.64 (d, *J* = 1.9 Hz, 1H), 7.41 (dd, *J* = 8.0, 1.9 Hz, 1H), 7.35–7.19 (m, 3H), 6.89 (d, *J* = 8.8 Hz, 2H), 4.20–4.06 (m, 2H), 3.90 (td, *J* = 9.6, 1.3 Hz, 2H), 3.81 (s, 3H), 3.64 (s, 3H), 3.57 (t, *J* = 7.7 Hz, 1H), 2.16–2.00 (m, 1H), 1.89–1.71 (m, 1H), 1.38–1.15 (m, 4H), 0.86 (t, *J* = 7.0 Hz, 3H). **¹³C-NMR** (126 MHz, CDCl₃): δ 174.1 (C_q), 165.9 (C_q), 158.8 (C_q), 140.2 (C_q), 137.8 (C_q), 133.2 (C_q), 130.4 (CH), 129.8 (CH), 129.8 (CH), 129.3 (CH), 127.5 (C_q), 113.4 (CH), 67.8 (CH₂), 55.2 (CH₃), 55.0 (CH₂), 52.0 (CH₃), 51.1 (CH), 33.2 (CH₂), 29.8 (CH₂), 22.5 (CH₂), 13.9 (CH₃). **IR** (ATR): 2952, 2871, 1732, 1649, 1608, 1246, 1177, 1162, 828 cm⁻¹. **MS** (ESI): *m/z* (relative intensity) 382 (100) [M+H]⁺. **HR-MS** (ESI): *m/z* calcd for C₂₃H₂₈NO₄⁺ [M+H]⁺: 382.2013, found: 382.2015.

Methyl 2-[2-(4,5-dihydrooxazol-2-yl)-4'-fluoro-[1,1'-biphenyl]-4-yl]hexanoate (223ae)



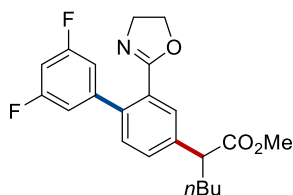
The general procedure **B** was followed using 2-phenyl-4,5-dihydrooxazole **217a** (73.5 mg, 0.50 mmol), methyl 2-bromohexanoate **218a** (314 mg, 1.50 mmol), 1-bromo-4-fluorobenzene **163e** (263 mg, 1.50 mmol), [Ru(O₂CMes)₂(*p*-cymene)] (28.1 mg, 10 mol

5. Experimental Part

%), PPh₃ (13.1 mg, 10 mol %) and K₂CO₃ (276 mg, 2.00 mmol) in 1,4-dioxane (2.0 mL). Purification by column chromatography on silica gel (*n*-hexane/EtOAc: 5:1 → 3:1) yielded **223ae** (120.2 mg, 65%) as a colorless oil.

¹H-NMR (300 MHz, CDCl₃): δ 7.68 (d, *J* = 2.0 Hz, 1H), 7.43 (dd, *J* = 8.0, 2.0 Hz, 1H), 7.34–7.22 (m, 3H), 7.08–6.99 (m, 2H), 4.17–4.07 (m, 2H), 3.94–3.83 (m, 2H), 3.65 (s, 3H), 3.58 (t, *J* = 7.7 Hz, 1H), 2.16–2.01 (m, 1H), 1.90–1.71 (m, 1H), 1.39–1.14 (m, 4H), 0.86 (t, *J* = 7.0 Hz, 3H). **¹³C-NMR** (126 MHz, CDCl₃): δ 174.0 (C_q), 165.5 (C_q), 162.1 (d, ¹*J*_{C-F} = 246 Hz, C_q), 139.6 (C_q), 138.4 (C_q), 136.8 (d, ⁴*J*_{C-F} = 3 Hz, C_q), 130.5 (CH), 129.8 (d, ³*J*_{C-F} = 8 Hz, CH), 129.8 (CH), 129.8 (CH), 127.6 (C_q), 114.8 (d, ²*J*_{C-F} = 22 Hz, CH), 67.7 (CH₂), 55.0 (CH₂), 52.0 (CH₃), 51.1 (CH), 33.2 (CH₂), 29.8 (CH₂), 22.5 (CH₂), 13.9 (CH₃). **¹⁹F-NMR** (282 MHz, CDCl₃): δ – 115.6 (tt, *J* = 8.8, 5.4 Hz). **IR** (ATR): 2954, 2873, 1734, 1650, 1485, 1350, 1221, 1192, 830 cm⁻¹. **MS** (ESI): *m/z* (relative intensity): 392 (5) [M+Na]⁺, 370 (100) [M+H]⁺. **HR-MS** (ESI): *m/z* calcd for C₂₂H₂₅FNO₃⁺ [M+H]⁺: 370.1813, found: 370.1814.

Methyl 2-[2-(4,5-dihydrooxazol-2-yl)-3',5'-difluoro-[1,1'-biphenyl]-4-yl]hexanoate (**223af**)

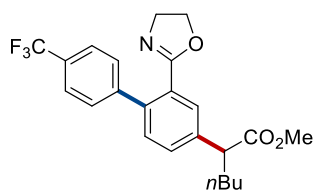


The general procedure **B** was followed using 2-phenyl-4,5-dihydrooxazole **217a** (73.5 mg, 0.50 mmol), methyl 2-bromohexanoate **218a** (314 mg, 1.50 mmol), 1-bromo-3,5-difluorobenzene **163f** (289 mg, 1.50 mmol), [Ru(O₂CMes)₂(*p*-cymene)] (28.1 mg, 10 mol %), PPh₃ (13.1 mg, 10 mol %) and K₂CO₃ (276 mg, 2.00 mmol) in 1,4-dioxane (2.0 mL). Purification by column chromatography on silica gel (*n*-hexane/EtOAc: 5/1 → 3/1) yielded **223af** (114.3 mg, 59%) as a colorless oil.

M.p.: 99 – 100 °C. **¹H-NMR** (400 MHz, CDCl₃): δ 7.71 (d, *J* = 1.9 Hz, 1H), 7.45 (dd, *J* = 8.0, 2.0 Hz, 1H), 7.27 (d, *J* = 8.0 Hz, 1H), 6.98–6.81 (m, 2H), 6.76 (tt, *J* = 9.0, 2.3 Hz, 1H), 4.21–4.11 (m, 2H), 3.92 (td, *J* = 9.5, 0.9 Hz, 2H), 3.65 (s, 3H), 3.58 (t, *J* = 7.7 Hz, 1H), 2.09 (dddd, *J* = 13.1, 9.4, 7.8, 5.5 Hz, 1H), 1.79 (dddd, *J* = 13.4, 9.1, 7.4, 5.9 Hz, 1H), 1.40–1.12 (m, 4H), 0.86 (t, *J* = 7.1 Hz, 3H). **¹³C-NMR** (101 MHz, CDCl₃): δ 174.0 (C_q), 165.0 (C_q), 162.6 (dd, ^{1,3}*J*_{C-F} = 248, 13 Hz, C_q), 144.2 (t, ^{3,3}*J*_{C-F} *J* = 10 Hz, C_q), 139.4 (C_q), 138.4 (t, ^{4,4}*J*_{C-F} *J* = 2 Hz, C_q), 130.3 (CH), 130.1 (CH), 130.0 (CH), 127.6

(C_q), 111.4 (dd, $^2J_{C-F} = 18.7, 6.9$ Hz, CH), 102.6 (t, $^2J_{C-F} = 25$ Hz, CH), 67.9 (CH₂), 55.1 (CH₂), 52.1 (CH₃), 51.1 (CH), 33.2 (CH₂), 29.7 (CH₂), 22.4 (CH₂), 13.8 (CH₃). **¹⁹F-NMR** (376 MHz, CDCl₃): δ (-110.5) – (-110.6) (m). **IR** (ATR): 2955, 2930, 1736, 1623, 1594, 1162, 1045, 987 cm⁻¹. **MS** (ESI): *m/z* (relative intensity) 410 (15) [M+Na]⁺, 388 (100) [M+H]⁺. **HR-MS** (ESI): *m/z* calcd for C₂₂H₂₄F₂NO₃⁺ [M+H]⁺: 388.1719, found: 388.1719.

Methyl 2-[2-(4,5-dihydrooxazol-2-yl)-4'-(trifluoromethyl)-[1,1'-biphenyl]-4-yl]hexanoate (223ag)

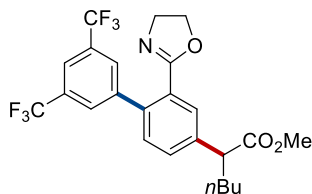


The general procedure **B** was followed using 2-phenyl-4,5-dihydrooxazole **217a** (73.5 mg, 0.50 mmol), methyl 2-bromohexanoate **218a** (314 mg, 1.50 mmol), 4-iodobenzotrifluoride **163g** (408 mg, 1.50 mmol), [Ru(O₂CMes)₂(*p*-cymene)] (28.1 mg, 10 mol %), PPh₃ (13.1 mg, 10 mol %) and K₂CO₃ (276 mg, 2.00 mmol) in 1,4-dioxane (2.0 mL). Purification by column chromatography on silica gel (*n*-hexane/EtOAc: 5/1 → 3/1) yielded **223ag** (134.2 mg, 64%) as a colorless oil.

¹H-NMR (400 MHz, CDCl₃): δ 7.75 (d, $J = 1.9$ Hz, 1H), 7.62 (dt, $J = 8.0, 0.7$ Hz, 2H), 7.52 – 7.42 (m, 3H), 7.30 (d, $J = 8.0$ Hz, 1H), 4.12 (t, $J = 9.7$ Hz, 2H), 3.90 (t, $J = 9.7$ Hz, 2H), 3.67 (s, 3H), 3.61 (t, $J = 7.7$ Hz, 1H), 2.12 (dtd, $J = 10.0, 8.1, 5.2$ Hz, 1H), 1.88–1.76 (m, 1H), 1.43–1.20 (m, 4H), 0.87 (t, $J = 7.1$ Hz, 3H). **¹³C-NMR** (101 MHz, CDCl₃): δ 174.1 (C_q), 165.2 (C_q), 144.6 (C_q), 139.3 (C_q), 139.1 (C_q), 130.5 (CH), 130.1 (CH), 129.9 (CH), 129.2 (q, $^2J_{C-F} J = 33$ Hz, C_q), 128.6 (CH), 127.5 (C_q), 124.8 (q, $^3J_{C-F} = 4$ Hz, CH), 124.2 (q, $^1J_{C-F} = 272$ Hz, C_q), 67.8 (CH₂), 55.0 (CH₂), 52.0 (CH₃), 51.1 (CH), 33.2 (CH₂), 29.7 (CH₂), 22.4 (CH₂), 13.8 (CH₃). **¹⁹F-NMR** (376 MHz, CDCl₃): δ – 62.4 (s). **IR** (ATR): 2953, 2872, 1734, 1647, 1323, 1160, 1122, 1084, 1021, 831 cm⁻¹. **MS** (ESI): *m/z* (relative intensity) 442 (12) [M+Na]⁺, 420 [M+H]⁺. **HR-MS** (ESI): *m/z* calcd for C₂₃H₂₅F₃NO₃⁺ [M+H]⁺: 420.1781, found: 420.1781.

5. Experimental Part

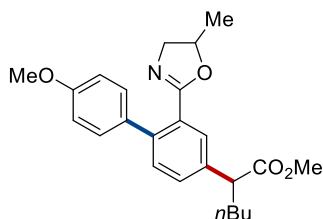
Methyl 2-[2-(4,5-dihydrooxazol-2-yl)-3',5'-bis(trifluoromethyl)-[1,1'-biphenyl]-4-yl]hexanoate (**223ah**)



The general procedure **B** was followed using 2-phenyl-4,5-dihydrooxazole **217a** (73.5 mg, 0.50 mmol), methyl 2-bromohexanoate **218a** (314 mg, 1.50 mmol), 1,3-bis(trifluoromethyl)-5-bromobenzene **163h** (439 mg, 1.50 mmol), [Ru(O₂CMe)₂(*p*-cymene)] (28.1 mg, 10 mol %), PPh₃ (13.1 mg, 10 mol %) and K₂CO₃ (276 mg, 2.00 mmol) in 1,4-dioxane (2.0 mL). Purification by column chromatography on silica gel (*n*-hexane/EtOAc: 5/1 → 4/1) yielded **223ah** (122.2 mg, 50%) as a white solid.

M.p.: 96 – 98 °C. **¹H-NMR** (300 MHz, CDCl₃): δ 7.84 (s, 1H), 7.83–7.80 (m, 3H), 7.52 (dd, *J* = 8.0, 2.0 Hz, 1H), 7.36 (d, *J* = 8.0 Hz, 1H), 4.22–4.10 (m, 2H), 3.99–3.85 (m, 2H), 3.68 (s, 3H), 3.63 (t, *J* = 7.7 Hz, 1H), 2.13 (dddd, *J* = 13.3, 9.3, 7.7, 5.8 Hz, 1H), 1.83 (dddd, *J* = 13.5, 9.1, 7.7, 6.0 Hz, 1H), 1.41–1.16 (m, 4H), 0.89 (t, *J* = 7.0 Hz, 3H). **¹³C-NMR** (100 MHz, CDCl₃): δ 173.8 (C_q), 164.4 (C_q), 142.8 (C_q), 140.0 (C_q), 137.5 (C_q), 131.1 (q, ²*J*_{C-F} = 33 Hz, C_q), 130.5 (CH), 130.4 (CH), 130.2 (C_q), 123.3 (q, ¹*J*_{C-F} = 272 Hz, C_q), 128.7 (CH), 127.6 (CH), 120.8 (sept, ³*J*_{C-F} = 3.9 Hz, CH), 67.8 (CH₂), 55.1 (CH₂), 52.1 (CH₃), 51.2 (CH), 33.2 (CH₂), 29.8 (CH₂), 22.5 (CH₂), 13.9 (CH₃). **¹⁹F-NMR** (282 MHz, CDCl₃): δ – 62.8 (s). **IR** (ATR): 2957, 2932, 1737, 1380, 1277, 1169, 1131, 898, 681 cm⁻¹. **MS** (ESI): *m/z* (relative intensity) 510 (38) [M+Na]⁺, 488 (100) [M+H]⁺. **HR-MS** (ESI): *m/z* calcd for C₂₄H₂₄F₆NO₃⁺ [M+H]⁺: 488.1655, found: 488.1649.

Methyl 2-[4'-methoxy-2-(5-methyl-4,5-dihydrooxazol-2-yl)-[1,1'-biphenyl]-4-yl]hexanoate (**224aa**)

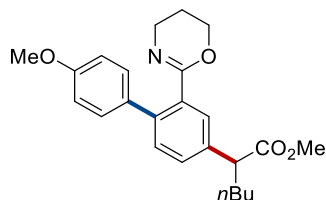


The general procedure **B** was followed using 5-methyl-2-phenyl-4,5-dihydrooxazole **220a** (80.6 mg, 0.50 mmol), methyl 2-bromohexanoate **218a** (314 mg, 1.50 mmol), 4-bromoanisole **163d** (280 mg, 1.50 mmol), [Ru(O₂CMe)₂(*p*-cymene)] (28.1 mg, 10 mol %), PPh₃ (13.1 mg, 10 mol %) and K₂CO₃ (276 mg, 2.00 mmol) in 1,4-dioxane (2.0

mL). Purification by column chromatography on silica gel (*n*-hexane/EtOAc: 5/1 → 3/1) yielded **224aa** (150.3 mg, 76%) as a colorless oil.

¹H-NMR (600 MHz, CDCl₃, mixture of diastereoisomers, dr 1.0:1.0): δ 7.66–7.63 (m, 2H), 7.45–7.39 (m, 2H), 7.32–7.27 (m, 6H), 6.92–6.88 (m, 4H), 4.62–4.53 (m, 2H), 4.05–3.97 (m, 2H), 3.86–3.81 (m, 6H), 3.68–3.64 (m, 6H), 3.61–3.56 (m, 2H), 3.51–3.43 (m, 2H), 2.20–2.00 (m, 2H), 1.85–1.75 (m, 2H), 1.44–1.20 (m, 8H), 1.17 (d, *J* = 6.0 Hz, 3H), 1.16 (d, *J* = 5.9 Hz, 3H), 0.91–0.84 (m, 6H). **¹³C-NMR** (126 MHz, CDCl₃, mixture of diastereoisomers, dr 1.0:1.0): δ 174.1 (C_q), 174.1 (C_q), 165.1 (C_q), 158.8 (C_q), 140.2 (C_q), 137.8 (C_q), 133.2 (C_q), 130.5 (CH), 130.5 (CH), 129.7 (CH), 129.7 (CH), 129.6 (CH), 129.5 (CH), 129.5 (CH), 128.0 (C_q), 127.9 (C_q), 113.3 (CH), 76.3 (CH), 61.7 (CH₂), 55.3 (CH₃), 52.0 (CH₃), 51.1 (CH), 33.2 (CH₂), 33.2 (CH₂), 29.8 (CH₂), 22.5 (CH₂), 20.8 (CH₃), 13.9 (CH₃). **IR** (ATR): 2928, 1733, 1650, 1608, 1519, 1245, 1176, 1162, 1037, 827 cm⁻¹. **MS** (ESI): *m/z* (relative intensity) 813 (21) [2M+Na]⁺, 791 (18) [2M+H]⁺, 418 (17) [M+Na]⁺, 396 (100) [M+H]⁺. **HR-MS** (ESI): *m/z* calcd for C₂₄H₃₀NO₄⁺ [M+H]⁺: 396.2169, found: 396.2162.

Methyl 2-[2-(5,6-dihydro-4*H*-1,3-oxazin-2-yl)-4'-methoxy-[1,1'-biphenyl]-4-yl]hexanoate (224ca)



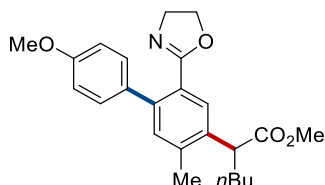
The general procedure **B** was followed using 2-phenyl-5,6-dihydro-4*H*-1,3-oxazine **220c** (80.6 mg, 0.50 mmol), methyl 2-bromohexanoate **218a** (314 mg, 1.50 mmol), 4-bromoanisole **163d** (280 mg, 1.50 mmol), [Ru(O₂CMes)₂(*p*-cymene)] (28.1 mg, 10 mol %), PPh₃ (13.1 mg, 10 mol %) and K₂CO₃ (276 mg, 2.00 mmol) in 1,4-dioxane (2.0 mL). Purification by column chromatography on silica gel (*n*-hexane/EtOAc: 5/1 → 2/1) yielded **224ca** (104.4 mg, 57%) as a colorless oil.

¹H-NMR (400 MHz, CDCl₃): δ 7.46 (d, *J* = 2.0 Hz, 1H), 7.39–7.30 (m, 2H), 7.25 (d, *J* = 8.6 Hz, 2H), 6.90 (d, *J* = 8.6 Hz, 2H), 3.94–3.85 (m, 2H), 3.81 (s, 3H), 3.62 (s, 3H), 3.54 (t, *J* = 7.7 Hz, 1H), 3.47 (t, *J* = 5.9 Hz, 2H), 2.07 (dddd, *J* = 13.3, 9.3, 8.2, 5.6 Hz, 1H), 1.88–1.72 (m, 3H), 1.37–1.16 (m, 4H), 0.85 (t, *J* = 7.1 Hz, 3H). **¹³C-NMR** (101 MHz, CDCl₃): δ 174.4 (C_q), 158.6 (C_q), 158.4 (C_q), 139.1 (C_q), 137.8 (C_q), 134.6 (C_q), 133.8 (C_q), 130.1 (CH), 129.2 (CH), 129.0 (CH), 128.7 (CH), 113.4 (CH), 65.0 (CH₂),

5. Experimental Part

55.2 (CH₃), 51.9 (CH₃), 51.1 (CH), 42.7 (CH₂), 33.2 (CH₂), 29.8 (CH₂), 22.4 (CH₂), 21.5 (CH₂), 13.8 (CH₃). **IR** (ATR): 2952, 2857, 1732, 1656, 1464, 1246, 1176, 827, 731 cm⁻¹. **MS** (ESI): *m/z* (relative intensity) 813 (12) [2M+Na]⁺, 791 (30) [2M+H]⁺, 396 (100) [M+H]⁺. **HR-MS** (ESI): *m/z* calcd for C₂₄H₃₀NO₄⁺ [M+H]⁺: 396.2169, found: 396.2165.

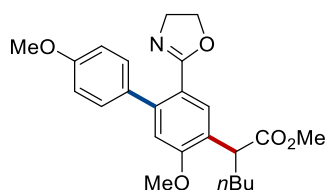
Methyl 2-[2-(4,5-dihydrooxazol-2-yl)-4',5-dimethoxy-[1,1'-biphenyl]-4-yl]hexanoate (**225ca**)



The general procedure **B** was followed using 2-(4-methoxyphenyl)-4,5-dihydrooxazole **217c** (88.5 mg, 0.50 mmol), methyl 2-bromohexanoate **218a** (314 mg, 1.50 mmol), 4-bromoanisole **163d** (280 mg, 1.50 mmol), [Ru(O₂CMe)₂(*p*-cymene)] (28.1 mg, 10 mol %), PPh₃ (13.1 mg, 10 mol %) and K₂CO₃ (276 mg, 2.00 mmol) in 1,4-dioxane (2.0 mL). The first step was performed at 60 °C Purification by column chromatography on silica gel (*n*-hexane/EtOAc: 5/1 → 2/1) yielded **225ca** (156.2 mg, 76%) as a colorless oil.

¹H-NMR (300 MHz, CDCl₃): δ 7.66 (s, 1H), 7.29 (dm, *J* = 8.9 Hz, 2H), 6.90 (dm, *J* = 8.9 Hz, 2H), 6.79 (s, 1H), 4.16–4.04 (m, 2H), 3.98 (t, *J* = 7.5 Hz, 1H), 3.92–3.84 (m, 5H), 3.82 (s, 3H), 3.64 (s, 3H), 2.08 (dddd, *J* = 13.4, 9.1, 7.5, 3.0 Hz, 1H), 1.76 (dddd, *J* = 13.4, 9.3, 7.5, 5.7 Hz, 1H), 1.40–1.19 (m, 4H), 0.87 (t, *J* = 7.0 Hz, 3H). **¹³C-NMR** (126 MHz, CDCl₃): δ 174.3 (C_q), 165.6 (C_q), 158.8 (C_q), 158.0 (C_q), 141.7 (C_q), 133.7 (C_q), 130.4 (CH), 129.2 (CH), 126.6 (C_q), 119.6 (C_q), 113.3 (CH), 112.3 (CH), 67.4 (CH₂), 55.7 (CH₃), 55.1 (CH₃), 54.9 (CH₂), 51.8 (CH₃), 43.7 (CH), 32.0 (CH₂), 29.7 (CH₂), 22.5 (CH₂), 13.9 (CH₃). **IR** (ATR): 2956, 2853, 1733, 1608, 1494, 1245, 1225, 1173, 908, 728 cm⁻¹. **MS** (ESI): *m/z* (relative intensity) 412 (100) [M+H]⁺. **HR-MS** (ESI): *m/z* calcd for C₂₄H₃₀NO₅⁺ [M+H]⁺ 412.2118, found 412.2119.

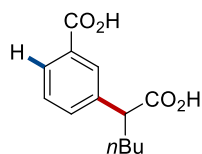
Methyl 2-[2-(4,5-dihydrooxazol-2-yl)-4'-methoxy-5-methyl-[1,1'-biphenyl]-4-yl]hexanoate (225ba)



The general procedure **B** was followed using 2-(*p*-tolyl)-4,5-dihydrooxazole **217b** (80.6 mg, 0.50 mmol), methyl 2-bromohexanoate **218a** (314 mg, 1.50 mmol), 4-bromoanisole **163a** (280 mg, 1.50 mmol), [Ru(O₂CMes)₂(*p*-cymene)] (28.1 mg, 10 mol %), PPh₃ (13.1 mg, 10 mol %) and K₂CO₃ (276 mg, 2.00 mmol) in 1,4-dioxane (2.0 mL). The first step was performed at 60 °C. Purification by column chromatography on silica gel (*n*-hexane/EtOAc: 5/1 → 2/1) yielded **225ba** (103.2 mg, 52%) as a colorless oil.

¹H-NMR (600 MHz, CDCl₃): δ 7.68 (s, 1H), 7.29 (d, *J* = 8.8 Hz, 2H), 7.16 (s, 1H), 6.90 (d, *J* = 8.8 Hz, 2H), 4.18–4.09 (m, 2H), 3.91 (ddd, *J* = 10.3, 9.1, 1.9 Hz, 2H), 3.86–3.79 (m, 4H), 3.66 (s, 3H), 2.41 (s, 3H), 2.23–2.09 (m, 1H), 1.77 (dddd, *J* = 13.4, 9.6, 6.9, 5.5 Hz, 1H), 1.41–1.21 (m, 4H), 0.89 (t, *J* = 7.1 Hz, 3H). **¹³C-NMR** (126 MHz, CDCl₃): δ 174.2 (C_q), 165.9 (C_q), 158.7 (C_q), 139.8 (C_q), 138.6 (C_q), 136.4 (C_q), 133.4 (C_q), 132.3 (CH), 129.3 (CH), 128.7 (CH), 125.4 (C_q), 113.4 (CH), 67.6 (CH₂), 55.2 (CH₃), 55.0 (CH₂), 52.0 (CH₃), 46.7 (CH), 32.8 (CH₂), 30.0 (CH₂), 22.6 (CH₂), 19.9 (CH₃), 14.0 (CH₃). **IR** (ATR): 2953, 2872, 1733, 1609, 1457, 1244, 1174, 1032, 832 cm⁻¹. **MS** (ESI): *m/z* (relative intensity) 396 [M+H]⁺. **HR-MS** (ESI): *m/z* calcd for C₂₄H₃₀NO₄⁺ [M+H]⁺: 396.2169, found: 396.2171.

3-(1-Carboxypentyl)benzoic acid (226)



Methyl 2-[3-(4,5-dihydrooxazol-2-yl)phenyl]hexanoate **219aa** (412.5 mg, 1.50 mmol) was placed in a round bottom flask and aqueous HCl (6M, 10 mL) was added. The resulting solution was stirred at 105 °C for 20 h. At ambient temperature, the solution was extracted with Et₂O (3 × 20 mL). The combined organic layers were washed with brine (20 ml), dried over Na₂SO₄ and the filtrate was concentrated *in vacuo* to afford **226** (315.0 mg, 89%) as a white solid.

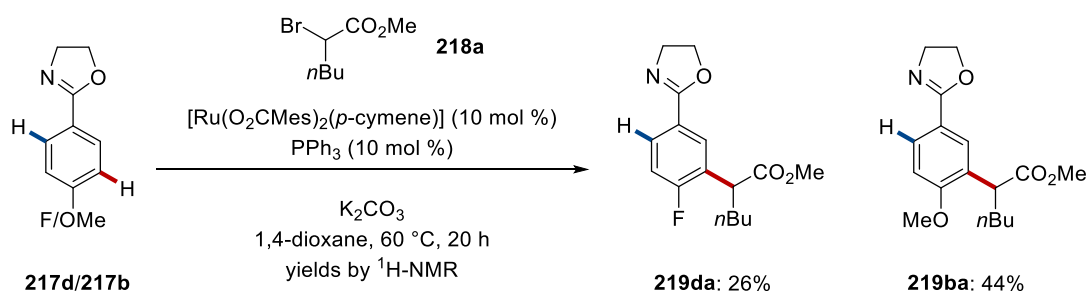
5. Experimental Part

M.p.: 117 – 121 °C. **¹H-NMR** (400 MHz, DMSO-*d*₆): δ 12.61 (br s, 2H), 7.87 (t, *J* = 1.6 Hz, 1H), 7.83 (dt, *J* = 7.6, 1.6 Hz, 1H), 7.54 (dt, *J* = 7.6, 1.6 Hz, 1H), 7.45 (t, *J* = 7.6 Hz, 1H), 3.59 (t, *J* = 7.6 Hz, 1H), 1.96 (dddd, *J* = 13.0, 9.9, 7.6, 5.1 Hz, 1H), 1.65 (dddd, *J* = 13.0, 9.5, 7.6, 5.5 Hz, 1H), 1.35–1.05 (m, 4H), 0.82 (t, *J* = 7.2 Hz, 3H).

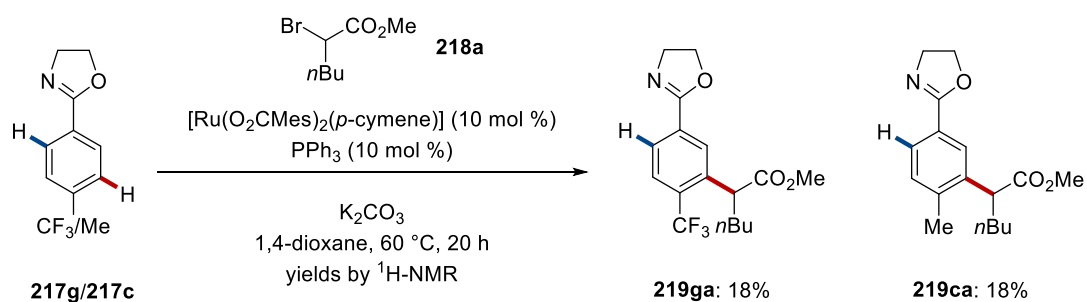
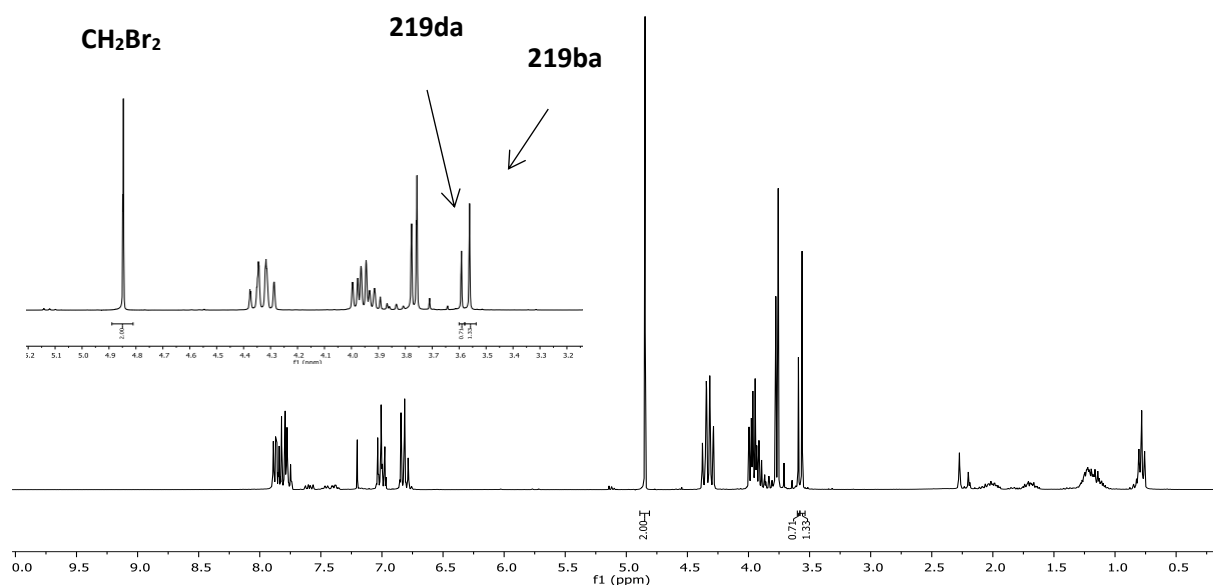
¹³C-NMR (101 MHz, DMSO-*d*₆): δ 174.6 (C_q), 167.3 (C_q), 140.3 (C_q), 132.4 (CH), 131.0 (C_q), 128.8 (CH), 128.6 (CH), 127.9 (CH), 50.6 (CH), 32.7 (CH₂), 29.2 (CH₂), 21.9 (CH₂), 13.8 (CH₃). **IR** (ATR): 2957, 1691, 1606, 1587, 1282, 1195, 1109, 929, 733 cm⁻¹. **MS** (ESI): *m/z* (relative intensity) 471 (35) [2M-H]⁻, 235 (25) [M-H]⁻, 191 (100) [M-CO₂H]⁻. **HR-MS** (ESI): *m/z* calcd for C₁₃H₁₅O₄⁻ [M-H]⁻: 235.0976, found: 235.0977.

5.3.2. Mechanistic Studies

5.3.2.1. Intermolecular Competition Experiments

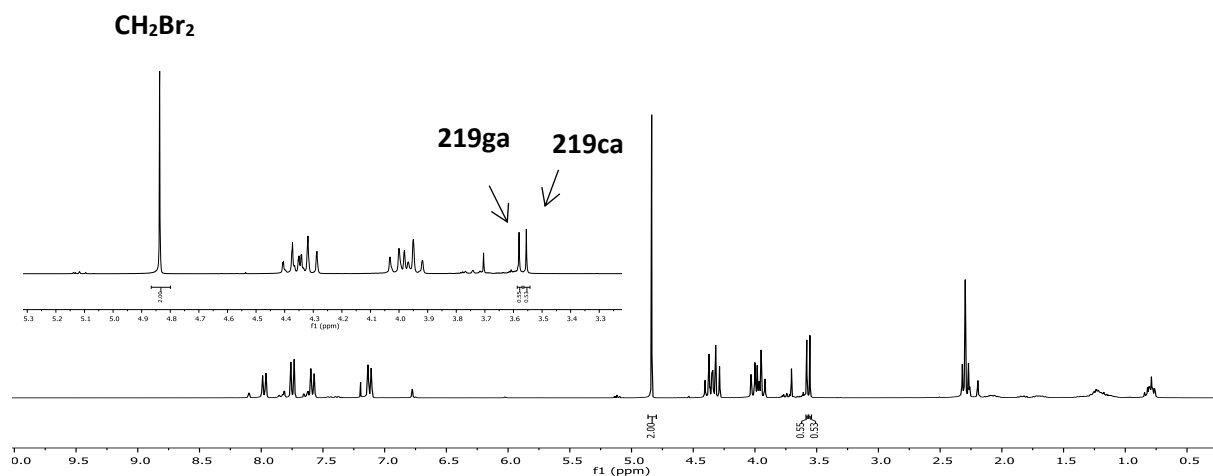


Oxazoline **217d** (82.6 mg, 0.50 mmol), oxazoline **217b** (88.6 mg, 0.50 mmol), [Ru(O₂CMes)₂(*p*-cymene)] (28.1 mg, 10 mol %), PPh₃ (13.1 mg, 10 mol %) and K₂CO₃ (138 mg, 1.00 mmol) were placed in a Schlenk tube. The tube was evacuated and purged with N₂ for three times. 1,4-Dioxane (2.0 mL) and alkyl bromide **218a** (104 mg, 0.50 mmol) were then added and the mixture was stirred at 60 °C. After 20 h, the resulting mixture was filtered through silica gel pad and washed with EtOAc. The filtrate was concentrated *in vacuo*. Yields of products were determined by ¹H-NMR spectroscopy using CH₂Br₂ (86.9 mg, 0.50 mmol) as internal standard.

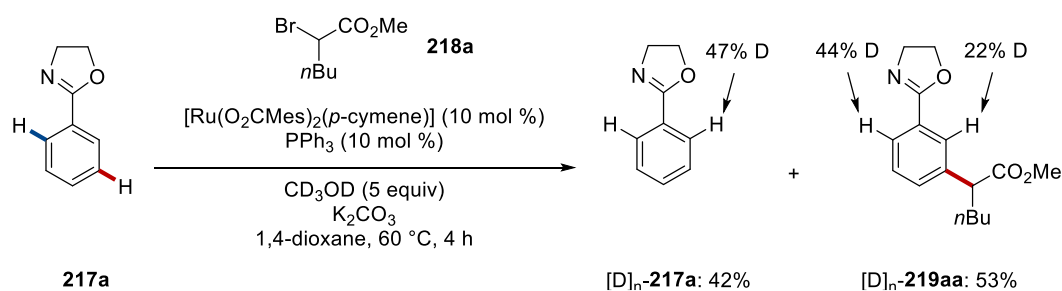


Oxazoline **217g** (107.6 mg, 0.50 mmol), oxazoline **217c** (80.6 mg, 0.50 mmol), $[\text{Ru}(\text{O}_2\text{CMes})_2(p\text{-cymene})]$ (28.1 mg, 10 mol %), PPh_3 (13.1 mg, 10 mol %) and K_2CO_3 (138 mg, 1.00 mmol) were placed in a Schlenk tube. The tube was evacuated and purged with N_2 for three times. 1,4-Dioxane (2.0 mL) and alkyl bromide **218a** (104 mg, 0.50 mmol) were then added and the mixture was stirred at 60 °C. After 20 h, the resulting mixture was filtered through silica gel pad and washed with EtOAc. The filtrate was concentrated *in vacuo*. Yields of products were determined by $^1\text{H-NMR}$ spectroscopy using CH_2Br_2 (86.9 mg, 0.50 mmol) as internal standard.

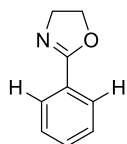
5. Experimental Part



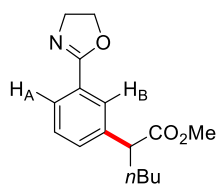
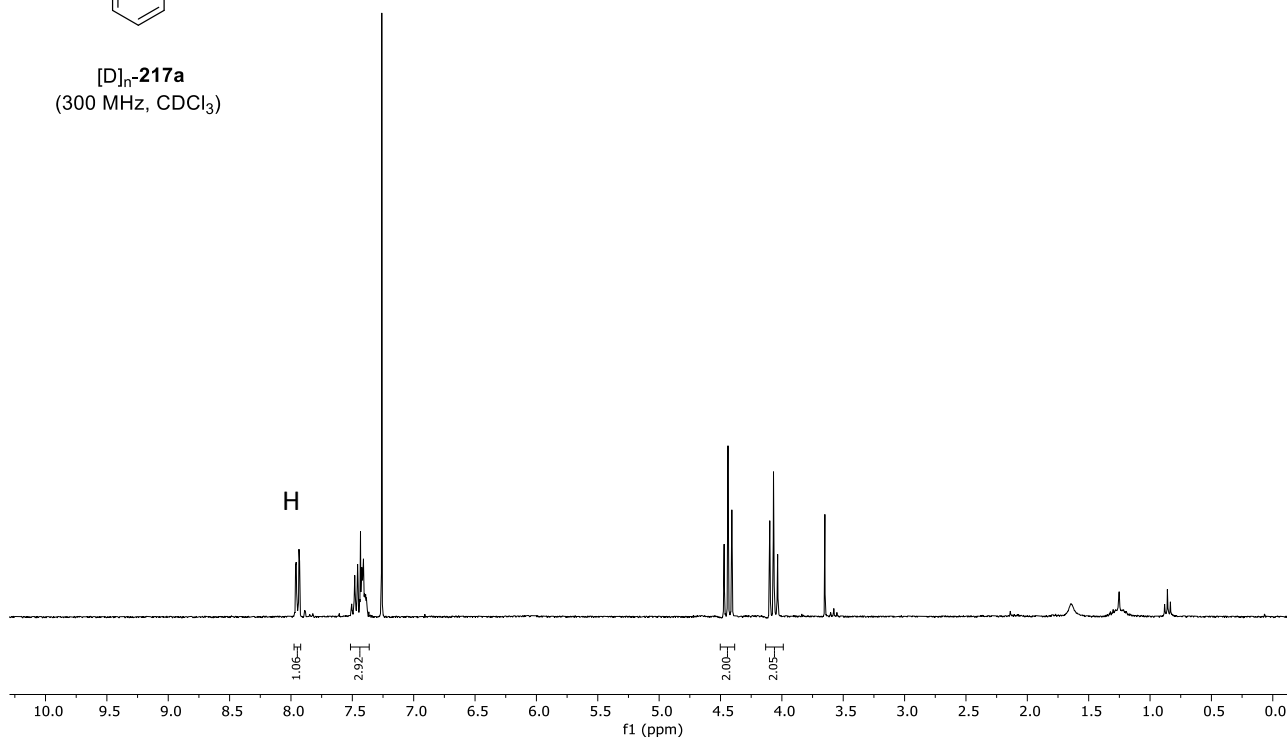
5.3.2.2. H/D Exchange Study



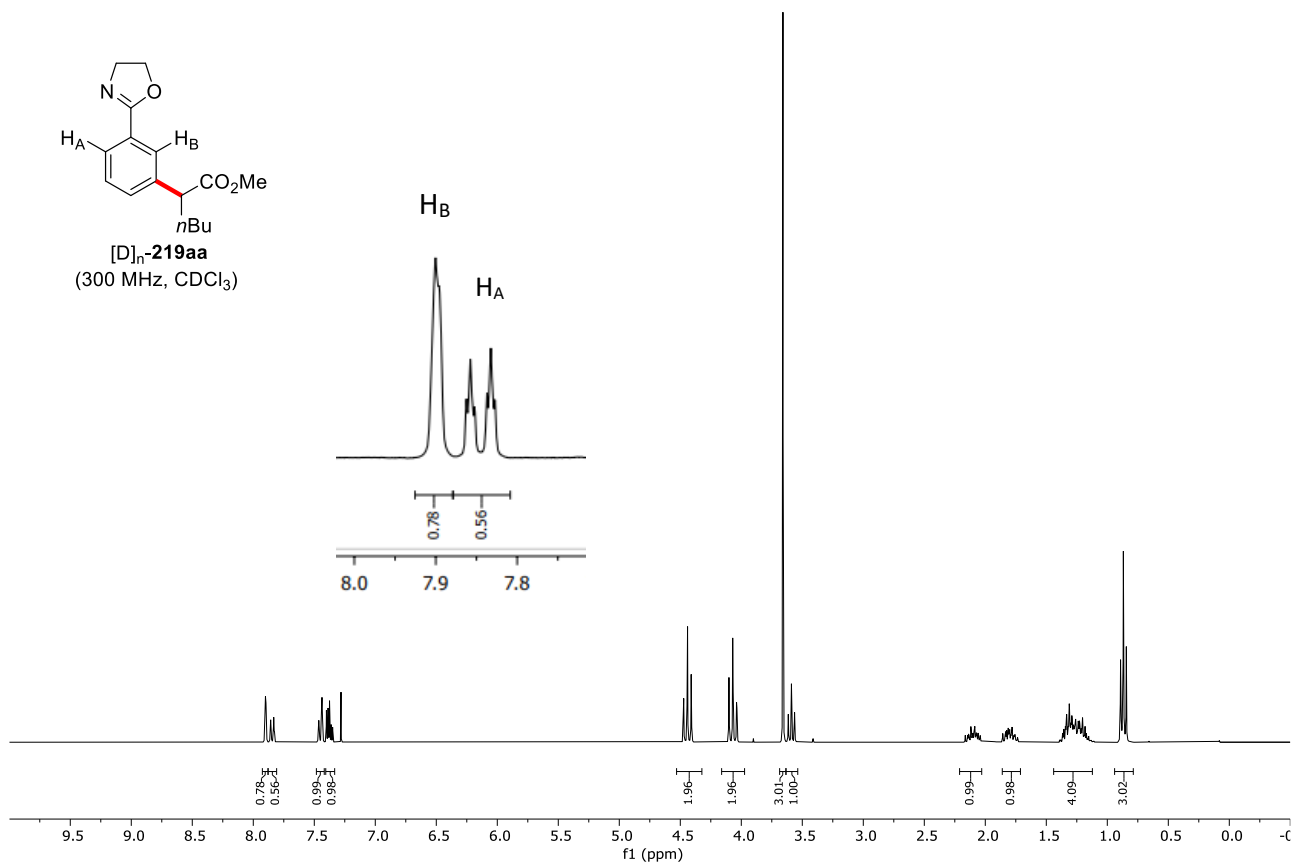
Oxazoline **217a** (73.5 mg, 0.50 mmol), $[\text{Ru}(\text{O}_2\text{CMes})_2(p\text{-cymene})]$ (28.1 mg, 50.0 μmol , 10.0 mol %), PPh_3 (13.1 mg, 10 mol %) and K_2CO_3 (138 mg, 1.00 mmol) were placed in a pre-dried 25 mL schlenk tube. The tube was evacuated and purged with N_2 for three times. 1,4-Dioxane (2.0 mL), alkyl bromide **218a** (314 mg, 1.50 mmol) and CD_3OD (90.1 mg, 2.50 mmol) were then added and the mixture was stirred at 60 $^\circ\text{C}$. After 4 h, Purification by column chromatography on silica gel (*n*-hexane/EtOAc 10:1) yielded $[\text{D}]_n\text{-217a}$ (31.5 mg, 42%) and $[\text{D}]_n\text{-219aa}$ (73.5 mg, 53%). The H/D exchange result was determined by $^1\text{H-NMR}$ spectroscopy.



[D]_n-217a
(300 MHz, CDCl₃)

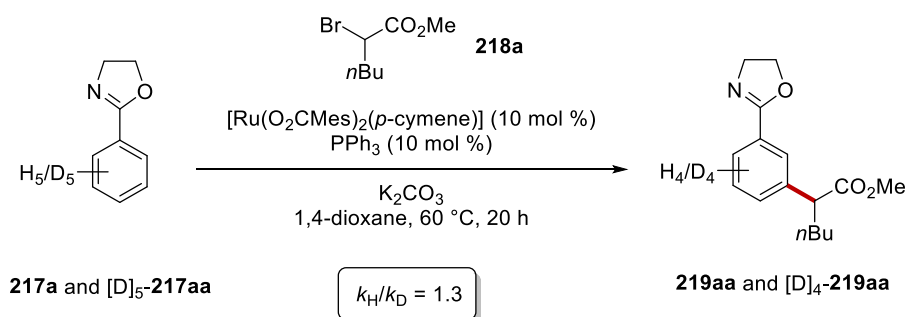


[D]_n-219aa
(300 MHz, CDCl₃)

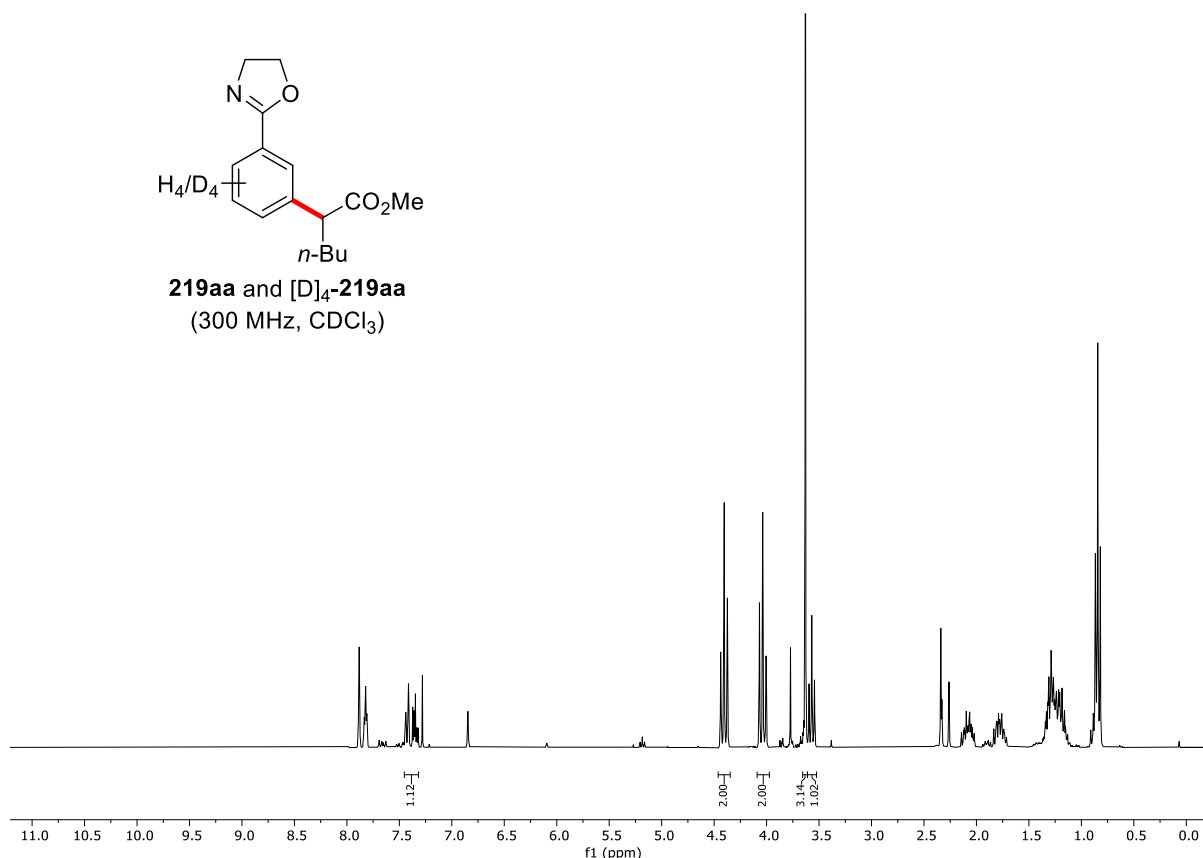


5. Experimental Part

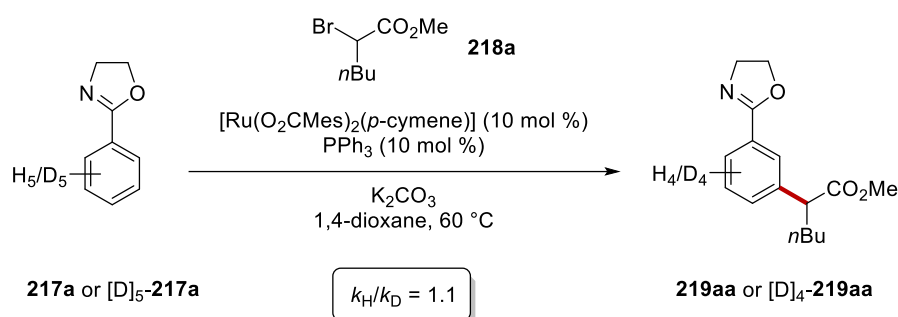
5.3.2.3. Intermolecular KIE by One-Pot Procedure



Oxazoline **217a** (73.6 mg, 0.50 mmol), $[D]_5\text{-219aa}$ (76.1 mg, 0.50 mmol), $[\text{Ru}(\text{O}_2\text{CMes})_2(p\text{-cymene})]$ (28.1 mg, 10 mol %), PPh_3 (13.1 mg, 10 mol %) and K_2CO_3 (138 mg, 2.00 mmol) were placed in a Schlenk tube. The tube was evacuated and purged with N_2 for three times. 1,4-Dioxane (2.0 mL) and alkyl bromide **218a** (314 mg, 1.50 mmol) were then added and the mixture was stirred at 60 °C. After 20 h, the resulting mixture was filtered through silica gel pad and washed with EtOAc. The filtrate was concentrated *in vacuo*. Purification by column chromatography on silica gel (*n*-hexane/EtOAc 5:1 to 3:1) yielded **219aa** and $[D]_4\text{-219aa}$. (191.4 mg, 69%). The kinetic isotope effect of this reaction was determined to be $k_{\text{H}}/k_{\text{D}} = 1.27$ as estimated by ^1H -NMR spectroscopy.



5.3.2.4. Intermolecular KIE by Independent Experiments



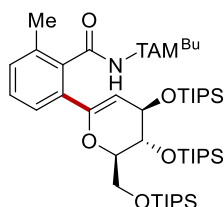
Two parallel reactions of **218a** with **217a** or **[D]₅-217a** were performed to determine the corresponding KIE value. The general procedure **A** was followed using **217a** (147.1 mg, 1.00 mmol) or **[D]₅-217a** (152.2 mg, 1.00 mmol), **218a** (630 mg, 3.00 mmol), **[Ru(O₂CMes)₂(*p*-cymene)]** (56.2 mg, 10 mol %), **PPh₃** (26.2 mg, 10 mol %), **K₂CO₃** (276 mg, 2.0 mmol), 1,3,5-trimethoxybenzene (168.2 mg, 1.00 mmol) as internal standard and 1,4-dioxane (4.0 mL). The mixture was stirred at 60 °C, and a periodic aliquot (0.10 mL) was removed by syringe and analyzed by ¹H-NMR to determine the following conversions:

5. Experimental Part

t (min) yield (%)	10	20	30	40	50
219aa	5	16	23	29	36
[D]₄-219aa	6	14	23	29	34

5.4. Palladium-Catalyzed C(sp²)-H and C(sp³)-H Late-Stage Glycosylation

5.4.1. Characterization Data

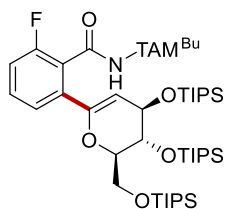
2-({2*R*,3*R*,4*R*}-3,4-Bis{[(triisopropylsilyl)oxy]-2-[(triisopropylsilyl)oxy]methyl}-3,4-dihydro-2*H*-pyran-6-yl)-*N*-[2-(1-butyl-1*H*-1,2,3-triazol-4-yl)propan-2-yl]-6-methylbenzamide (236a)

The general procedure **C** was followed using *N*-[2-(1-butyl-1*H*-1,2,3-triazol-4-yl)propan-2-yl]-2-methylbenzamide **234a** (30 mg, 0.10 mmol), [(2*R*,3*R*,4*R*)-6-iodo-2-[(triisopropylsilyl)oxy]methyl]-3,4-dihydro-2*H*-pyran-3,4-diyl]bis(oxy)]bis(triisopropylsilane) **235** (111 mg, 0.15 mmol), Pd(OAc)₂ (2.2 mg, 10 mol %), Ag₂CO₃ (55 mg, 0.20 mmol), in 1,4-dioxane (0.50 mL). Purification by column chromatography on silica gel (*n*-hexane/EtOAc 9:1 → 8:2) yielded **236a** (87 mg, 95%) as a colorless oil.

¹H NMR (300 MHz, CDCl₃): δ 7.57 (s, 1H), 7.54 (d, *J* = 7.7 Hz, 1H), 7.21 (dd, *J* = 7.7, 7.7 Hz, 1H), 7.10 (d, *J* = 7.7 Hz, 1H), 6.22 (s, 1H), 5.44 (d, *J* = 4.4 Hz, 1H), 4.42 (dd, *J* = 8.2, 4.4 Hz, 1H), 4.32 (t, *J* = 7.3 Hz, 2H), 4.23 – 4.06 (m, 3H), 3.84 (dd, *J* = 11.2, 4.3 Hz, 1H), 2.20 (s, 3H), 1.94 – 1.81 (m, 5H), 1.73 (s, 3H), 1.43 – 1.30 (m, 2H), 1.11 – 1.01 (m, 63H), 0.95 (t, *J* = 7.4 Hz, 3H). **¹³C NMR** (101 MHz, CDCl₃): δ 169.2 (C_q), 153.0 (C_q), 148.1 (C_q), 135.7 (C_q), 135.0 (C_q), 133.4 (C_q), 130.1 (CH), 128.1 (CH), 126.3 (CH), 120.5 (CH), 101.7 (CH), 81.0 (CH), 71.1 (CH), 67.1 (CH), 60.9 (CH₂), 51.6 (C_q), 50.0 (CH₂), 32.3 (CH₂), 28.4 (CH₃), 26.9 (CH₃), 19.7 (CH₂), 18.9 (CH₃), 18.2 (CH₃), 18.2 (CH₃), 18.1 (CH₃), 18.1 (CH₃), 18.0 (CH₃), 13.5 (CH₃), 12.5 (CH), 12.3 (CH), 12.0 (CH). (One CH₃ resonance of the TIPS group is missing due to overlap, the overlap was verified by analysis of the HSQC spectrum). **IR** (ATR): 2942, 2865, 1660, 1462, 1383, 1050, 1012, 881, 680 cm⁻¹. **MS** (ESI): *m/z* (relative intensity) 936 (100) [M+Na]⁺, 913 (62) [M+H]⁺. **HR-MS** (ESI): *m/z* calcd for C₅₀H₉₃N₄O₅Si₃⁺ [M+H]⁺: 913.6448 found: 913.6441.

5. Experimental Part

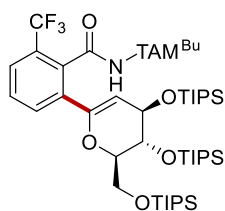
2-({2*R*,3*R*,4*R*}-3,4-Bis{[(triisopropylsilyl)oxy]-2-[(triisopropylsilyl)oxy]methyl}-3,4-dihydro-2*H*-pyran-6-yl)-*N*-[2-(1-butyl-1*H*-1,2,3-triazol-4-yl)propan-2-yl]-6-fluorobenzamide (**236b**)



The general procedure **C** was followed using *N*-[2-(1-butyl-1*H*-1,2,3-triazol-4-yl)propan-2-yl]-2-fluorobenzamide **234b** (30 mg, 0.10 mmol), [({2*R*,3*R*,4*R*}-6-iodo-2-[(triisopropylsilyl)oxy]methyl}-3,4-dihydro-2*H*-pyran-3,4-diyl)bis(oxy)]bis(triisopropylsilane) **235** (111 mg, 0.15 mmol), Pd(OAc)₂ (2.2 mg, 10 mol %), Ag₂CO₃ (55 mg, 0.20 mmol), in 1,4-dioxane (0.50 mL). Purification by column chromatography on silica gel (*n*-hexane/EtOAc 9:1) yielded **236b** (85 mg, 92%) as a colorless oil.

¹H NMR (400 MHz, CDCl₃): δ 7.58 (s, 1H), 7.53 (d, *J* = 7.9 Hz, 1H), 7.32 (ddd, *J* = 7.9, 7.4, 5.8 Hz, 1H), 7.05 (dd, *J* = 9.1, 7.4 Hz, 1H), 6.26 (s, 1H), 5.52 (d, *J* = 4.6 Hz, 1H), 4.45 (dd, *J* = 7.9, 4.6 Hz, 1H), 4.34 (t, *J* = 7.4 Hz, 2H), 4.22 – 4.10 (m, 3H), 3.87 (dd, *J* = 11.3, 4.4 Hz, 1H), 1.96 – 1.85 (m, 5H), 1.74 (s, 3H), 1.40 (tq, *J* = 7.9, 7.4 Hz, 2H), 1.14 – 1.02 (m, 63H), 0.98 (t, *J* = 7.4 Hz, 3H). **¹³C NMR** (101 MHz, CDCl₃): δ 164.3 (C_q), 159.3 (d, ¹*J*_{C-F} = 245.5 Hz, C_q), 153.0 (C_q), 147.2 (d, ⁴*J*_{C-F} = 3.0 Hz, C_q), 135.8 (d, ³*J*_{C-F} = 3.8 Hz, C_q), 129.8 (d, ³*J*_{C-F} = 8.8 Hz, CH) 124.4 (d, ²*J*_{C-F} = 19.9 Hz, C_q), 124.4 (d, ⁴*J*_{C-F} = 3.0 Hz, CH), 120.3 (d, ⁷*J*_{C-F} = 2.9 Hz, CH), 115.4 (d, ²*J*_{C-F} = 22.1 Hz, CH), 102.3 (CH), 81.2 (CH), 70.6 (CH), 66.8 (CH), 60.9 (CH₂), 52.7 (C_q), 50.0 (CH₂), 32.2, (CH₂) 29.1 (CH₃), 27.3 (CH₃), 19.7 (CH₂), 18.2 (CH₃), 18.2 (CH₃), 18.1 (CH₃), 18.1 (CH₃), 18.0 (CH₃), 18.0 (CH₃), 13.5 (CH₃), 12.5 (CH), 12.4 (CH), 12.0 (CH). **¹⁹F NMR** (282 MHz, CDCl₃): δ – 117.5 (s). **IR** (ATR): 2942, 2865, 1673, 1508, 1461, 1082, 1052, 881, 758, 679 cm⁻¹. **MS** (ESI): *m/z* (relative intensity) 940 (100) [M+Na]⁺, 917 (55) [M+H]⁺. **HR-MS** (ESI): *m/z* calcd for C₄₉H₉₀N₄O₅Si₃F⁺ [M+H]⁺: 917.6198 found: 917.6188.

2-[(2*R*,3*R*,4*R*)-3,4-Bis((triisopropylsilyl)oxy)-2-[(triisopropylsilyl)oxy]methyl]-3,4-dihydro-2*H*-pyran-6-yl]-*N*-[2-(1-butyl-1*H*-1,2,3-triazol-4-yl)propan-2-yl]-6-(trifluoromethyl)benzamide (236c**)**

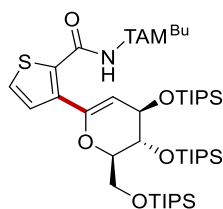


The general procedure **C** was followed using *N*-[2-(1-butyl-1*H*-1,2,3-triazol-4-yl)propan-2-yl]-2-(trifluoromethyl)benzamide **234c** (35 mg, 0.10 mmol), [(2*R*,3*R*,4*R*)-6-iodo-2-[(triisopropylsilyl)oxy]methyl]-3,4-dihydro-2*H*-pyran-3,4-diyl)bis(oxy)]bis(triisopropylsilane) **235** (111 mg, 0.15 mmol), Pd(OAc)₂ (2.2 mg, 10 mol %), Ag₂CO₃ (55 mg, 0.20 mmol), in 1,4-dioxane (0.50 mL). Purification by column chromatography on silica gel (*n*-hexane/EtOAc 9:1) yielded **236c** (91 mg, 94%) as a colorless oil.

¹H NMR (400 MHz, CDCl₃): δ 7.99 (d, *J* = 7.9 Hz, 1H), 7.63 (d, *J* = 7.9 Hz, 1H), 7.59 (s, 1H), 7.46 (dd, *J* = 7.9, 7.9 Hz, 1H), 6.45 (s, 1H), 5.55 (d, *J* = 4.6 Hz, 1H), 4.47 – 4.41 (m, 1H), 4.40 – 4.22 (m, 3H), 4.17 (d, *J* = 4.7 Hz, 1H), 4.08 (s, 1H), 3.81 (d, *J* = 11.3 Hz, 1H), 1.94 – 1.85 (m, 5H), 1.79 (s, 3H), 1.39 (tq, *J* = 7.5, 7.5 Hz, 2H), 1.14 – 1.07 (m, 63H), 0.98 (t, *J* = 7.5 Hz, 3H). **¹³C NMR** (101 MHz, CDCl₃): δ 165.6 (C_q), 152.7 (C_q), 146.5 (C_q), 135.8 (C_q), 133.9 (q, ³*J*_{C-F} = 1.6 Hz, C_q), 133.5 (CH), 128.5 (CH), 127.4 (q, ²*J*_{C-F} = 31.3 Hz, C_q), 126.0 (q, ³*J*_{C-F} = 4.9 Hz, CH), 123.7 (q, ¹*J*_{C-F} = 274.4 Hz, C_q), 120.2 (CH), 103.4 (CH), 81.2 (CH), 71.1 (CH), 66.9 (CH), 60.6 (CH₂), 52.7 (C_q), 50.0 (CH₂), 32.2 (CH₂), 28.2 (CH₃), 27.2 (CH₃), 19.7 (CH₂), 18.2 (CH₃), 18.1 (CH₃), 18.1 (CH₃), 18.1 (CH₃), 18.0 (CH₃), 18.0 (CH₃), 13.4 (CH₃), 12.4 (CH), 12.3 (CH), 11.9 (CH). **¹⁹F NMR** (376 MHz, CDCl₃): δ – 58.5 (s). **IR** (ATR): 2942, 2865, 1664, 1320, 1133, 1075, 1058, 881, 734, 673 cm⁻¹. **MS** (ESI): *m/z* (relative intensity) 990 (100) [M+Na]⁺, 967 (34) [M+H]⁺. **HR-MS** (ESI): *m/z* calcd for C₅₀H₉₀N₄O₅Si₃F₃⁺ [M+H]⁺: 967.6166 found: 967.6150.

5. Experimental Part

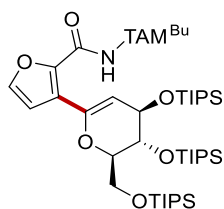
3-({2*R*,3*R*,4*R*}-3,4-Bis{[(triisopropylsilyl)oxy]-2-[(triisopropylsilyl)oxy]methyl}-3,4-dihydro-2*H*-pyran-6-yl)-*N*-[2-(1-butyl-1*H*-1,2,3-triazol-4-yl)propan-2-yl]thiophene-2-carboxamide (**236e**)



The general procedure **C** was followed using *N*-[2-(1-butyl-1*H*-1,2,3-triazol-4-yl)propan-2-yl]thiophene-2-carboxamide **234e** (29 mg, 0.10 mmol), [(*2R*,*3R*,*4R*)-6-iodo-2-[(triisopropylsilyl)oxy]methyl]-3,4-dihydro-2*H*-pyran-3,4-diyl)bis(oxy)]bis(triisopropylsilane) **235** (111 mg, 0.15 mmol), Pd(OAc)₂ (2.2 mg, 10 mol %), Ag₂CO₃ (55 mg, 0.20 mmol), in 1,4-dioxane (0.50 mL). Purification by column chromatography on silica gel (*n*-hexane/EtOAc 8:1 → 8:2) yielded **236e** (79 mg, 87%) as a colorless oil.

¹H NMR (400 MHz, CDCl₃): δ 8.33 (s, 1H), 7.54 (s, 1H), 7.34 (d, *J* = 5.1 Hz, 1H), 7.11 (d, *J* = 5.1 Hz, 1H), 5.38 (d, *J* = 5.0 Hz, 1H), 4.58 – 4.49 (m, 1H), 4.28 (t, *J* = 7.4 Hz, 2H), 4.24 – 4.12 (m, 3H), 3.91 (dd, *J* = 11.4, 3.8 Hz, 1H), 1.94 – 1.76 (m, 8H), 1.37 (q, *J* = 7.6 Hz, 2H), 1.15 – 0.96 (m, 63H), 0.95 (t, *J* = 7.6 Hz, 3H). **¹³C NMR** (101 MHz, CDCl₃): δ = 161.0 (C_q), 152.5 (C_q), 146.6 (C_q), 138.7 (C_q), 134.6 (C_q), 130.3 (CH), 128.2 (CH), 121.0 (CH), 102.7 (CH), 82.2 (CH), 69.5 (CH), 65.8 (CH), 61.7 (CH₂), 51.8 (C_q), 49.9 (CH₂), 32.2 (CH₂), 28.8 (CH₃), 28.6 (CH₃), 19.8 (CH₂), 18.1 (CH₃), 18.1 (CH₃), 17.9 (CH₃), 17.9 (CH₃), 13.5 (CH₃), 12.5 (CH), 12.4 (CH), 11.9 (CH). (2 CH₃ resonances of the TIPS groups are missing due to overlap, the overlap was verified by analysis of the HSQC spectrum). **IR** (ATR): 2942, 2865, 1649, 1462, 1300, 1060, 1012, 881, 680 cm⁻¹. **MS** (ESI): *m/z* (relative intensity) 928 (100) [M+Na]⁺, 905 (23) [M+H]⁺. **HR-MS** (ESI): *m/z* calcd for C₄₇H₈₉N₄O₅Si₃S⁺ [M+H]⁺: 905.5856 found: 905.5857.

3-({2*R*,3*R*,4*R*}-3,4-Bis{[(triisopropylsilyl)oxy]methyl}-3,4-dihydro-2*H*-pyran-6-yl)-*N*-[2-(1-butyl-1*H*-1,2,3-triazol-4-yl)propan-2-yl]furan-2-carboxamide (236f)

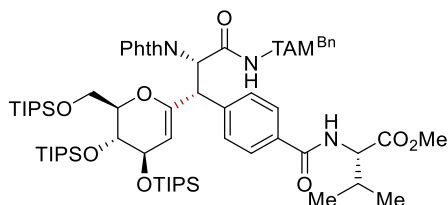


The general procedure **C** was followed using *N*-[2-(1-butyl-1*H*-1,2,3-triazol-4-yl)propan-2-yl]furan-2-carboxamide **234f** (28 mg, 0.10 mmol), [({2*R*,3*R*,4*R*}-6-iodo-2-[(triisopropylsilyl)oxy]methyl}-3,4-dihydro-2*H*-pyran-3,4-diyl)bis(oxy)]bis(triisopropylsilane) **235** (111 mg, 0.15 mmol), Pd(OAc)₂ (2.2 mg, 10 mol %), Ag₂CO₃ (55 mg, 0.20 mmol), in 1,4-dioxane (0.50 mL). Purification by column chromatography on silica gel (*n*-hexane/EtOAc 9:1 → 8:2) yielded **26f** (48 mg, 54%) as a colorless oil.

¹H NMR (400 MHz, CDCl₃): δ 8.44 (s, 1H), 7.56 (s, 1H), 7.40 (d, *J* = 1.8 Hz, 1H), 6.52 (d, *J* = 1.8 Hz, 1H), 5.57 (dd, *J* = 5.4, 1.5 Hz, 1H), 4.57 – 4.43 (m, 1H), 4.26 (t, *J* = 7.4 Hz, 2H), 4.20 – 4.07 (m, 3H), 3.85 (dd, *J* = 11.5, 3.5 Hz, 1H), 1.92 – 1.77 (m, 8H), 1.35 (tq, *J* = 7.4, 7.4 Hz, 2H), 1.10 – 0.96 (m, 63H), 0.93 (t, *J* = 7.4 Hz, 3H). **¹³C NMR** (101 MHz, CDCl₃): δ 157.8 (C_q), 152.7 (C_q), 143.6 (C_q), 143.4 (C_q), 143.0 (CH), 122.8 (C_q), 121.2 (CH), 111.8 (CH), 102.2 (CH), 82.3 (CH), 69.3 (CH), 65.6 (CH), 61.8 (CH₂), 51.6 (C_q), 49.9 (CH₂), 32.3 (CH₂), 28.6 (CH₃), 28.5 (CH₃), 19.8 (CH₂), 18.2 (CH₃), 18.1 (CH₃), 18.1 (CH₃), 18.0 (CH₃), 17.9 (CH₃), 17.9 (CH₃), 13.5 (CH₃), 12.5 (CH), 12.4 (CH), 11.9 (CH). **IR** (ATR): 2942, 2865, 1670, 1462, 1095, 1058, 881, 755, 679 cm⁻¹. **MS** (ESI): *m/z* (relative intensity) 912 (100) [M+Na]⁺, 889 (22) [M+H]⁺. **HR-MS** (ESI): *m/z* calcd for C₄₇H₈₉N₄O₆Si₃⁺ [M+H]⁺: 889.6084 found: 889.6089.

5. Experimental Part

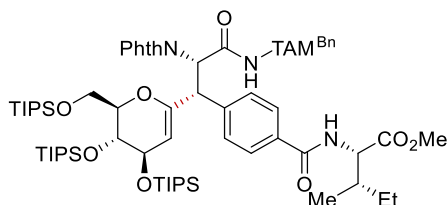
Methyl 4-[(1*S*,2*S*)-3-({2-[1-benzyl-1*H*-1,2,3-triazol-4-yl]propan-2-yl}amino)-1-({2*R*,3*R*,4*R*}-3,4-bis[{triisopropylsilyl]oxy}-2-[(triisopropylsilyl)oxy]methyl)-3,4-dihydro-2*H*-pyran-6-yl)-2-(1,3-dioxoisindolin-2-yl)-3-oxopropyl]benzoyl]-*L*-valinate (238a**)**



The general procedure **D** was followed using methyl [4-({*S*}-3-[[2-(1-benzyl-1*H*-1,2,3-triazol-4-yl)propan-2-yl]amino]-2-{1,3-dioxoisindolin-2-yl}-3-oxopropyl)benzoyl]-*L*-valinate **237a** (65 mg, 0.10 mmol), [({2*R*,3*R*,4*R*}-6-iodo-2-[(triisopropylsilyl)oxy]methyl)-3,4-dihydro-2*H*-pyran-3,4-diy]bis(oxy)]bis(triisopropylsilane) **235** (111 mg, 0.15 mmol), Pd(TFA)₂ (3.3 mg, 10 mol %), 1-AdCO₂H (5.4 mg, 30 mol %), Ag₂CO₃ (55 mg, 0.20 mmol), in 1,4-dioxane (0.50 mL). Purification by column chromatography on silica gel (*n*-hexane/EtOAc 2:1) yielded **238a** (78 mg, 62%) as a colorless oil.

¹H NMR (400 MHz, CDCl₃): δ 7.71 – 7.57 (m, 4H), 7.52 (d, *J* = 8.0 Hz, 2H), 7.42 (s, 1H), 7.36 (d, *J* = 8.0 Hz, 2H), 7.34 – 7.27 (m, 3H), 7.24 – 7.17 (m, 2H), 6.96 (s, 1H), 6.41 (d, *J* = 8.6 Hz, 1H), 5.56 (d, *J* = 11.8 Hz, 1H), 5.42 (s, 2H), 5.10 (d, *J* = 5.3 Hz, 1H), 4.79 – 4.60 (m, 2H), 4.45 – 4.26 (m, 1H), 4.15 – 3.93 (m, 4H), 3.74 (s, 3H), 2.28 – 2.17 (m, 1H), 1.78 (s, 3H), 1.73 (s, 3H), 1.14 – 1.05 (m, 42H), 0.93 (t, *J* = 7.2 Hz, 6H), 0.88 – 0.83 (m, 21H). **¹³C NMR** (101 MHz, CDCl₃): δ 172.5 (C_q), 167.8 (C_q), 166.8 (C_q), 166.4 (C_q), 153.0 (C_q), 150.6 (C_q), 142.8 (C_q), 134.9 (C_q), 133.9 (CH), 132.5 (C_q), 131.3 (C_q), 128.9 (CH), 128.4 (CH), 128.4 (CH), 127.9 (CH), 126.8 (CH), 123.4 (CH), 120.9 (CH), 99.2 (CH), 81.1 (CH), 69.3 (CH), 66.6 (CH), 61.2 (CH₂), 57.2 (CH), 54.8 (CH), 53.9 (CH₂), 52.2 (C_q), 52.2 (CH₃), 50.0 (CH), 31.6 (CH), 28.4 (CH₃), 28.2 (CH₃), 18.9 (CH₃), 18.2 (CH₃), 18.2 (CH₃), 18.1 (CH₃), 18.0 (CH₃), 18.0 (CH₃), 17.9 (CH₃), 17.8 (CH₃), 12.4 (CH), 12.3 (CH), 12.2 (CH). **IR** (ATR): 2943, 2865, 2197, 1717, 1464, 1383, 1102, 1060, 681 cm⁻¹. **MS** (ESI): *m/z* (relative intensity) 1286 (81) [M+Na]⁺, 1263(92) [M+H]⁺. **HR-MS** (ESI): *m/z* calcd for C₆₉H₁₀₇N₆O₁₀Si₃⁺ [M+H]⁺: 1263.7351 found: 1263.7335.

Methyl [4-[(1*R*,2*R*)-3-({2-[1-benzyl-1*H*-1,2,3-triazol-4-yl]propan-2-yl)amino)-1-({2*R*,3*R*,4*R*}-3,4-bis[triisopropylsilyloxy]-2-[(triisopropylsilyloxy)methyl]-3,4-dihydro-2*H*-pyran-6-yl)-2-(1,3-dioxo-2,3-dihydro-1*H*-inden-2-yl)-3-oxopropyl]benzoyl]-L-isoleucinate (238b)

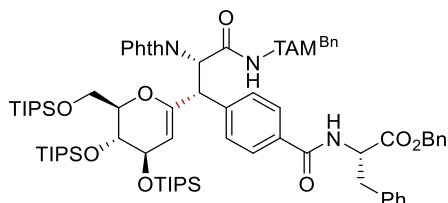


The general procedure **D** was followed using methyl [4-({*S*}-3-[[2-(1-benzyl-1*H*-1,2,3-triazol-4-yl)propan-2-yl]amino]-2-{{1,3-dioxoisindolin-2-yl}-3-oxopropyl)benzoyl]-L-isoleucinate **237b** (67 mg, 0.10 mmol), [({2*R*,3*R*,4*R*}-6-iodo-2-[[triisopropylsilyloxy]methyl]-3,4-dihydro-2*H*-pyran-3,4-diyloxy]bis(triisopropylsilane) **235** (111 mg, 0.15 mmol), Pd(TFA)₂ (3.3 mg, 10 mol %), 1-AdCO₂H (5.4 mg, 30 mol %), Ag₂CO₃ (55 mg, 0.20 mmol), in 1,4-dioxane (0.50 mL). Purification by column chromatography on silica gel (*n*-hexane/EtOAc 2:1) yielded **238b** (65 mg, 51%) as a colorless oil.

¹H NMR (400 MHz, CDCl₃): δ 7.72 – 7.56 (m, 4H), 7.52 (d, *J* = 8.0 Hz, 2H), 7.42 (s, 1H), 7.36 (d, *J* = 8.0 Hz, 2H), 7.33 – 7.27 (m, 3H), 7.25 – 7.17 (m, 2H), 6.96 (s, 1H), 6.44 (d, *J* = 8.4 Hz, 1H), 5.56 (d, *J* = 11.9 Hz, 1H), 5.42 (s, 2H), 5.10 (d, *J* = 5.4 Hz, 1H), 4.79 – 4.64 (m, 2H), 4.43 – 4.28 (m, 1H), 4.14 – 3.92 (m, 4H), 3.74 (s, 3H), 1.99 – 1.90 (m, 1H), 1.78 (s, 3H), 1.73 (s, 3H), 1.52 – 1.42 (m, 1H), 1.24 – 1.16 (m, 1H), 1.15 – 1.03 (m, 42H), 0.97 – 0.88 (m, 6H), 0.88 – 0.80 (m, 21H). **¹³C NMR** (101 MHz, CDCl₃): δ 172.4 (C_q), 167.7 (C_q), 166.6 (C_q), 166.4 (C_q), 153.0 (C_q), 150.6 (C_q), 142.7 (C_q), 134.9 (C_q), 133.9 (CH), 132.4 (C_q), 131.2 (C_q), 128.9 (CH), 128.4 (CH), 128.3 (CH), 127.9 (CH), 126.8 (CH), 123.4 (CH), 120.8 (CH), 99.1 (CH), 81.0 (CH), 69.3 (CH), 66.6 (CH), 61.2 (CH₂), 56.5 (CH), 54.8 (CH), 53.9 (CH₂), 52.2 (C_q), 52.1 (CH₃), 50.0 (CH), 38.2 (CH), 28.4 (CH₃), 28.2 (CH₃), 25.2 (CH₂), 18.2 (CH₃), 18.2 (CH₃), 18.1 (CH₃), 18.0 (CH₃), 17.9 (CH₃), 17.9 (CH₃), 15.4 (CH₃), 12.3 (CH), 12.2 (CH), 12.1 (CH), 11.5 (CH₃). **IR** (ATR): 2942, 2865, 1717, 1665, 1462, 1382, 1095, 1052, 882, 682 cm⁻¹. **MS** (ESI): *m/z* (relative intensity) 1300 (84) [M+Na]⁺, 1277 (100) [M+H]⁺. **HR-MS** (ESI): *m/z* calcd for C₇₀H₁₀₉N₆O₁₀Si₃⁺ [M+H]⁺: 1277.7507 found: 1277.7483.

5. Experimental Part

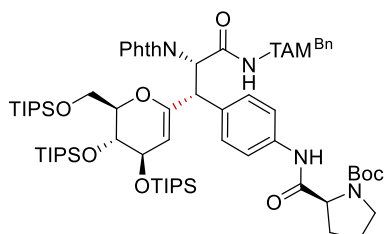
Benzyl 4-[(1*S*,2*S*)-3-({2-[1-benzyl-1*H*-1,2,3-triazol-4-yl]propan-2-yl}amino)-1-({2*R*,3*R*,4*R*}-3,4-bis[{triisopropylsilyl]oxy}-2-[(triisopropylsilyl)oxy]methyl)-3,4-dihydro-2*H*-pyran-6-yl)-2-(1,3-dioxoisindolin-2-yl)-3-oxopropyl]benzoyl]-*L*-phenylalaninate (**238c**)



The general procedure **D** was followed using benzyl [4-({*S*}-3-[[2-(1-benzyl-1*H*-1,2,3-triazol-4-yl)propan-2-yl]amino]-2-{1,3-dioxoisindolin-2-yl}-3-oxopropyl)benzoyl]-*L*-phenylalaninate **237c** (77 mg, 0.10 mmol), [({2*R*,3*R*,4*R*}-6-iodo-2-[(triisopropylsilyl)oxy]methyl)-3,4-dihydro-2*H*-pyran-3,4-diy]bis(oxy)]bis(triisopropylsilane) **235** (111 mg, 0.15 mmol), Pd(TFA)₂ (3.3 mg, 10 mol %), 1-AdCO₂H (5.4 mg, 30 mol %), Ag₂CO₃ (55 mg, 0.20 mmol), in 1,4-dioxane (0.50 mL). Purification by column chromatography on silica gel (*n*-hexane/EtOAc 2/1 → 1/1) yielded **238c** (69 mg, 50%) as a colorless oil.

¹H NMR (400 MHz, CDCl₃): δ 7.72 – 7.54 (m, 4H), 7.47 – 7.40 (m, 3H), 7.39 – 7.27 (m, 10H), 7.25 – 7.14 (m, 5H), 7.01 – 6.92 (m, 3H), 6.42 – 6.31 (m, 1H), 5.54 (d, *J* = 12.1 Hz, 1H), 5.42 (s, 2H), 5.27 – 4.97 (m, 4H), 4.72 (dd, *J* = 12.1, 1.9 Hz, 1H), 4.41 – 4.30 (m, 1H), 4.17 – 3.91 (m, 4H), 3.34 – 3.03 (m, 2H), 1.78 (s, 3H), 1.74 (s, 3H), 1.14 – 1.06 (m, 42H), 0.87 – 0.83 (m, 21H). **¹³C NMR** (101 MHz, CDCl₃): δ 171.3 (C_q), 167.7 (C_q), 166.4 (C_q), 166.3 (C_q), 153.0 (C_q), 150.5 (C_q), 142.7 (C_q), 135.6 (C_q), 135.0 (C_q), 134.9 (C_q), 133.9 (CH), 132.2 (C_q), 131.2 (C_q), 129.2 (CH), 128.9 (CH), 128.6 (CH), 128.6 (CH), 128.5 (CH), 128.5 (CH), 128.4 (CH), 128.3 (CH), 127.9 (CH), 127.0 (CH), 126.7 (CH), 123.3 (CH), 120.8 (CH), 99.2 (CH), 81.0 (CH), 69.3 (CH), 67.3 (CH₂), 66.6 (CH), 61.1 (CH₂), 54.9 (CH), 53.9 (CH₂), 53.3 (CH), 52.2 (C_q), 50.0 (CH), 37.8 (CH₂), 28.3 (CH₃), 28.2 (CH₃), 18.2 (CH₃), 18.2 (CH₃), 18.1 (CH₃), 18.0 (CH₃), 17.9 (CH₃), 17.9 (CH₃), 12.3 (CH), 12.2 (CH), 12.1 (CH). **IR** (ATR): 2942, 2865, 1715, 1664, 1461, 1050, 881, 718, 681 cm⁻¹. **MS** (ESI): *m/z* (relative intensity) 1411 (100) [M+Na]⁺, 1387 (33) [M+H]⁺. **HR-MS** (ESI): *m/z* calcd for C₇₉H₁₁₁N₆O₁₀Si₃⁺ [M+H]⁺: 1387.7664 found: 1387.7636.

tert-Butyl (S)-2-([4-((1*s*,2*s*)-3-([2-(1-benzyl-1*H*-1,2,3-triazol-4-yl)propan-2-yl]amino)-1-({2*R*,3*R*,4*R*}-3,4-bis{[(triisopropylsilyl)oxy]-2-[(triisopropylsilyl)oxy]methyl}-3,4-dihydro-2*H*-pyran-6-yl)-2-(1,3-dioxoisindolin-2-yl)-3-oxopropyl]phenyl)carbamoyl]pyrrolidine-1-carboxylate (238d)



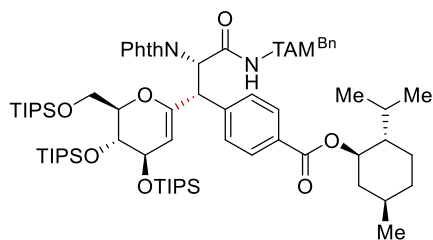
The general procedure **D** was followed using *tert*-butyl (S)-2-[[4-((S)-3-[[2-(1-benzyl-1*H*-1,2,3-triazol-4-yl)propan-2-yl]amino)-2-{{1,3-dioxoisindolin-2-yl}-3-oxopropyl]phenyl]carbamoyl]pyrrolidine-1-carboxylate **237d** (71 mg, 0.10 mmol), [({2*R*,3*R*,4*R*}-6-iodo-2-[[triisopropylsilyl]oxy]methyl)-3,4-dihydro-2*H*-pyran-3,4-diyl]bis(oxy)]bis(triisopropylsilane) **235** (111 mg, 0.15 mmol), Pd(TFA)₂ (3.3 mg, 10 mol %), 1-AdCO₂H (5.4 mg, 30 mol %), Ag₂CO₃ (55 mg, 0.20 mmol), in 1,4-dioxane (0.50 mL). Purification by column chromatography on silica gel (hexane/EtOAc 2:1 → 1:1) yielded **238d** (106 mg, 80%) as a colorless oil.

¹H NMR (600 MHz, DMSO-*d*₆, 100 °C): δ 9.27 (s, 1H), 7.74 – 7.71 (m, 3H), 7.70 – 7.66 (m, 2H), 7.37 (s, 1H), 7.35 – 7.27 (m, 3H), 7.25 (d, *J* = 8.6 Hz, 2H), 7.24 – 7.21 (m, 2H), 7.06 – 7.03 (m, 2H), 5.48 (s, 2H), 5.28 (d, *J* = 11.4 Hz, 1H), 5.01 (dd, *J* = 5.2, 1.5 Hz, 1H), 4.52 (d, *J* = 11.4 Hz, 1H), 4.24 (ddt, *J* = 7.6, 6.0, 1.8 Hz, 1H), 4.18 (dd, *J* = 1.8, 1.8 Hz, 1H), 4.13 (dd, *J* = 8.4, 4.1 Hz, 1H), 4.11 – 4.05 (m, 1H), 4.04 (dt, *J* = 4.4, 1.8 Hz, 1H), 3.74 (dd, *J* = 10.7, 5.6 Hz, 1H), 3.38 (ddd, *J* = 10.2, 7.5, 5.6 Hz, 1H), 3.32 (dt, *J* = 10.2, 6.7 Hz, 1H), 2.14 – 2.05 (m, 1H), 1.89 – 1.71 (m, 3H), 1.66 (s, 3H), 1.61 (s, 3H), 1.24 (s, 9H), 1.10 – 1.07 (m, 21H), 1.05 – 1.01 (m, 21H), 0.98 – 0.94 (m, 21H). **¹³C NMR** (151 MHz, DMSO-*d*₆, 100 °C): δ 170.2 (C_q), 166.5 (C_q), 164.9 (C_q), 152.9 (C_q), 152.6 (C_q), 151.6 (C_q), 137.3 (C_q), 135.3 (C_q), 133.8 (CH), 132.8 (C_q), 130.4 (C_q), 128.0 (CH), 127.6 (CH), 127.3 (CH), 127.2 (CH), 122.3 (CH), 120.3 (CH), 117.9 (CH), 96.9 (CH), 80.2 (CH), 78.0 (C_q), 69.3 (CH), 66.2 (CH), 60.9 (CH₂), 59.8 (CH), 54.5 (CH), 52.4 (CH₂), 51.1 (C_q), 47.8 (CH), 46.0 (CH₂), 29.9 (CH₂), 27.6 (CH₃), 27.5 (CH₃), 27.3 (CH₃), 22.8 (CH₂), 17.4 (CH₃), 17.4 (CH₃), 17.2 (CH₃), 17.2 (CH₃), 17.2 (CH₃), 17.2 (CH₃), 11.5 (CH), 11.5 (CH), 11.1 (CH). **IR** (ATR): 2943, 2865, 1708, 1526, 1383, 1098, 1052, 1026, 882, 715, 679 cm⁻¹. **MS** (ESI): *m/z* (relative intensity) 1341 (100)

5. Experimental Part

[M+Na]⁺, 1318 (7) [M+H]⁺. **HR-MS** (ESI): *m/z* calcd for C₇₂H₁₁₂N₇O₁₀Si₃⁺ [M+H]⁺: 1318.7773 found: 1318.7750.

(1*R*,2*S*,5*R*)-2-isopropyl-5-methylcyclohexyl 4-[(1*S*,2*S*)-3-({2-[1-benzyl-1*H*-1,2,3-triazol-4-yl]propan-2-yl)amino)-1-({2*R*,3*R*,4*R*}-3,4-bis{[(triisopropylsilyl)oxy]-2-[(triisopropylsilyl)oxy]methyl}-3,4-dihydro-2*H*-pyran-6-yl)-2-(1,3-dioxisoindolin-2-yl)-3-oxopropyl]benzoate (238e)

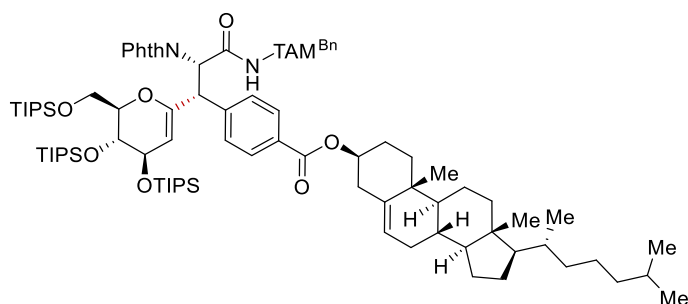


The general procedure **D** was followed using (1*R*,2*S*,5*R*)-2-isopropyl-5-methylcyclohexyl 4-({*S*}-3-{{2-(1-benzyl-1*H*-1,2,3-triazol-4-yl)propan-2-yl]amino}-2-{1,3-dioxisoindolin-2-yl}-3-oxopropyl)benzoate **237e** (68 mg, 0.10 mmol), [({2*R*,3*R*,4*R*}-6-iodo-2-[(triisopropylsilyl)oxy]methyl}-3,4-dihydro-2*H*-pyran-3,4-diyl)bis(oxy)]bis(triisopropylsilane) **235** (111 mg, 0.15 mmol), Pd(TFA)₂ (3.3 mg, 10 mol %), 1-AdCO₂H (5.4 mg, 30 mol %), Ag₂CO₃ (55 mg, 0.20 mmol), in 1,4-dioxane (0.50 mL). Purification by column chromatography on silica gel (*n*-hexane/EtOAc 4:1) yielded **238e** (82 mg, 64%) as a colorless oil.

¹H NMR (400 MHz, CDCl₃): δ 7.75 (d, *J* = 8.2 Hz, 2H), 7.69 – 7.64 (m, 2H), 7.64 – 7.58 (m, 2H), 7.42 (s, 1H), 7.37 – 7.29 (m, 5H), 7.24 – 7.19 (m, 2H), 6.97 (s, 1H), 5.56 (d, *J* = 11.9 Hz, 1H), 5.42 (s, 2H), 5.10 (dd, *J* = 5.5, 1.4 Hz, 1H), 4.81 (ddd, *J* = 10.8, 10.8, 4.3 Hz, 1H), 4.72 (d, *J* = 11.9 Hz, 1H), 4.36 (ddd, *J* = 7.8, 4.9, 3.1 Hz, 1H), 4.13 – 4.05 (m, 2H), 4.02 (dd, *J* = 11.2, 6.1 Hz, 1H), 3.97 (dd, *J* = 4.9, 2.5 Hz, 1H), 2.03 (dd, *J* = 12.0, 4.2 Hz, 1H), 1.90 (dtd, *J* = 13.9, 7.2, 2.8 Hz, 1H), 1.78 (s, 3H), 1.75 – 1.65 (m, 5H), 1.57 – 1.42 (m, 2H), 1.13 – 1.06 (m, 42H), 1.03 – 0.98 (m, 1H), 0.93 – 0.82 (m, 29H), 0.72 (d, *J* = 6.9 Hz, 3H). **¹³C NMR** (101 MHz, CDCl₃): δ 167.7 (C_q), 166.4 (C_q), 165.9 (C_q), 153.0 (C_q), 150.6 (C_q), 143.7 (C_q), 134.9 (C_q), 133.8 (CH), 131.3 (C_q), 129.3 (C_q), 129.3 (CH), 128.9 (CH), 128.3 (CH), 128.1 (CH), 127.9 (CH), 123.3 (CH), 120.8 (CH), 99.1 (CH), 81.0 (CH), 74.5 (CH), 69.3 (CH), 66.6 (CH), 61.2 (CH₂), 54.8 (CH), 53.9 (CH₂), 52.2 (C_q), 50.1 (CH), 47.1 (CH), 40.9 (CH₂), 34.2 (CH₂), 31.3 (CH), 28.4 (CH₃), 28.2 (CH₃), 26.2 (CH), 23.4 (CH₂), 22.0 (CH₃), 20.8 (CH₃), 18.2 (CH₃), 18.2 (CH₃), 18.1 (CH₃), 18.0 (CH₃), 17.9 (CH₃), 17.9 (CH₃), 16.3 (CH₃), 12.3 (CH), 12.2

(CH), 12.1 (CH). **IR** (ATR): 2942, 2865, 1714, 1462, 1382, 1274, 1107, 1049, 882, 717, 657 cm^{-1} . **MS** (ESI): m/z (relative intensity) 1311 (100) $[\text{M}+\text{Na}]^+$, 1288 (7) $[\text{M}+\text{H}]^+$. **HR-MS** (ESI): m/z calcd for $\text{C}_{73}\text{H}_{114}\text{N}_5\text{O}_9\text{Si}_3^+$ $[\text{M}+\text{H}]^+$: 1288.7919 found: 1288.7885.

(3*S*,8*S*,9*S*,10*R*,13*R*,14*S*,17*R*)-10,13-Dimethyl-17-[(*R*)-6-methylheptan-2-yl]-2,3,4,7,8,9,10,11,12,13,14,15,16,17-tetradecahydro-1*H*-cyclopenta[*a*]phenanthren-3-yl 4-((1*S*,2*S*)-3-((2-(1-benzyl-1*H*-1,2,3-triazol-4-yl)propan-2-yl)amino)-1-({2*R*,3*R*,4*R*}-3,4-bis{[(triisopropylsilyl)oxy]-2-[(triisopropylsilyl)oxy]methyl}-3,4-dihydro-2*H*-pyran-6-yl)-2-(1,3-dioxoisindolin-2-yl)-3-oxopropyl)benzoate (238f)



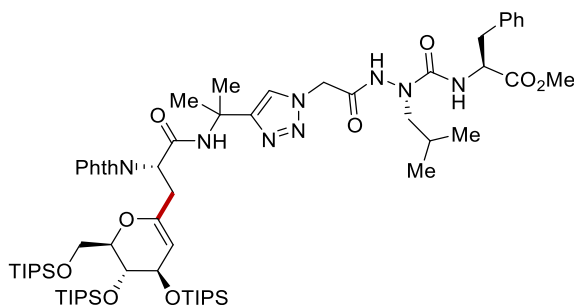
The general procedure **D** was followed using (3*S*,8*S*,9*S*,10*R*,13*R*,14*S*,17*R*)-10,13-dimethyl-17-[(*R*)-6-methylheptan-2-yl]-2,3,4,7,8,9,10,11,12,13,14,15,16,17-tetradecahydro-1*H*-cyclopenta[*a*]phenanthren-3-yl 4-({*S*}-3-[[2-(1-benzyl-1*H*-1,2,3-triazol-4-yl)propan-2-yl]amino]-2-{1,3-dioxoisindolin-2-yl}-3-oxopropyl)benzoate **237f** (91 mg, 0.10 mmol), [({2*R*,3*R*,4*R*}-6-iodo-2-[(triisopropylsilyl)oxy]methyl}-3,4-dihydro-2*H*-pyran-3,4-diyl)bis(oxy)]bis(triisopropylsilane) **235** (111 mg, 0.15 mmol), $\text{Pd}(\text{TFA})_2$ (3.3 mg, 10 mol %), 1-AdCO₂H (5.4 mg, 30 mol %), Ag₂CO₃ (55 mg, 0.20 mmol), in 1,4-dioxane (0.50 mL). Purification by column chromatography on silica gel (*n*-hexane/EtOAc 7:3) yielded **238f** (101 mg, 67%,) as a colorless oil.

¹H NMR (400 MHz, CDCl₃): δ 7.74 (d, J = 8.4 Hz, 2H), 7.69 – 7.63 (m, 2H), 7.60 (dd, J = 5.5, 3.0 Hz, 2H), 7.43 (s, 1H), 7.36 – 7.29 (m, 5H), 7.25 – 7.19 (m, 2H), 6.98 (s, 1H), 5.55 (d, J = 11.9 Hz, 1H), 5.43 (s, 2H), 5.40 – 5.36 (m, 1H), 5.10 (dd, J = 5.6, 1.5 Hz, 1H), 4.81 – 4.67 (m, 2H), 4.35 (dddd, J = 7.1, 6.7, 3.2, 3.2 Hz, 1H), 4.14 – 4.06 (m, 1H), 4.06 – 3.93 (m, 1H), 2.38 (d, J = 8.2 Hz, 2H), 2.03 (dt, J = 12.7, 3.2 Hz, 2H), 1.98 – 1.82 (m, 5H), 1.78 (s, 3H), 1.74 (s, 3H), 1.66 – 1.43 (m, 8H), 1.43 – 1.32 (m, 4H), 1.25 – 1.14 (m, 5H), 1.11 – 1.07 (m, 43H), 1.05 (s, 3H), 0.93 (d, J = 6.5 Hz, 3H), 0.91 – 0.85 (m, 28H), 0.70 (s, 3H). **¹³C NMR** (101 MHz, CDCl₃): δ 167.7 (C_q), 166.4 (C_q), 165.8 (C_q), 153.0 (C_q), 150.7 (C_q), 143.8 (C_q), 139.6 (C_q), 135.0 (C_q), 133.9 (CH), 131.3

5. Experimental Part

(C_q), 129.4 (CH), 129.4 (C_q), 128.9 (CH), 128.4 (CH), 128.1 (CH), 127.9 (CH), 123.3 (CH), 122.7 (CH), 120.9 (CH), 99.1 (CH), 81.1 (CH), 74.2 (CH), 69.4 (CH), 66.6 (CH), 61.2 (CH₂), 56.7 (CH), 56.1 (CH), 54.8 (CH), 53.9 (CH₂), 52.2 (C_q), 50.1 (CH), 50.0 (CH), 42.3 (C_q), 39.7 (CH₂), 39.5 (CH₂), 38.2 (CH₂), 37.0 (CH₂), 36.6 (C_q), 36.2 (CH₂), 35.8 (CH), 31.9 (CH), 31.9 (CH₂), 28.4 (CH₃), 28.2 (CH₂), 28.2 (CH₃), 28.0 (CH₂), 27.8 (CH), 24.3 (CH₂), 23.8 (CH₂), 22.8 (CH₃), 22.6 (CH₃), 21.0 (CH₂), 19.3 (CH₃), 18.7 (CH₃), 18.2 (CH₃), 18.2 (CH₃), 18.1 (CH₃), 18.0 (CH₃), 18.0 (CH₃), 17.9 (CH₃), 12.4 (CH), 12.3 (CH), 12.1 (CH), 11.9 (CH₃). **IR** (ATR): 2941, 2865, 1716, 1464, 1272, 1050, 882, 717, 681 cm⁻¹. **MS** (ESI): *m/z* (relative intensity) 1542 (100) [M+Na]⁺, 1519 (30) [M+H]⁺. **HR-MS** (ESI): *m/z* calcd for C₉₀H₁₄₀N₅O₉Si₃ [M+H]⁺: 1519.9985 found: 1519.9961.

Methyl [2-(4-{2-[(*S*)-3-({2*R*,3*R*,4*R*}-3,4-bis{[(triisopropylsilyl)oxy]-2-[(triisopropylsilyl)oxy]methyl}-3,4-dihydro-2*H*-pyran-6-yl)-2-(1,3-dioxoisindolin-2-yl)propanamido]propan-2-yl}-1*H*-1,2,3-triazol-1-yl)acetyl]-L-leucyl-L-phenylalaninate (240c)

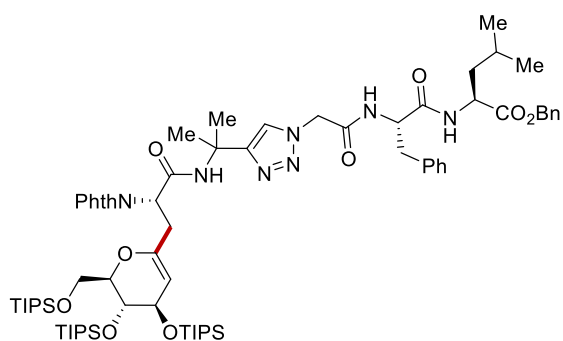


The general procedure **D** was followed using methyl {2-[2-(4-{2-[(*S*)-2-(1,3-dioxoisindolin-2-yl)propanamido]propan-2-yl}-1*H*-1,2,3-triazol-1-yl)acetyl]-1-isobutylhydrazine-1-carbonyl]-L-phenylalaninate **239c** (66 mg, 0.10 mmol), [({2*R*,3*R*,4*R*}-6-iodo-2-[(triisopropylsilyl)oxy]methyl)-3,4-dihydro-2*H*-pyran-3,4-diyl]bis(oxy)]bis(triisopropylsilane) **235** (111 mg, 0.15 mmol), Pd(TFA)₂ (3.3 mg, 10 mol %), 1-AdCO₂H (5.4 mg, 30 mol %), Ag₂CO₃ (55 mg, 0.20 mmol), in 1,4-dioxane (0.50 mL). Purification by column chromatography on silica gel (*n*-hexane/EtOAc 1:1 → 1:2) yielded **239c** (79 mg, 62%) as a colorless oil.

¹H NMR (600 MHz, CDCl₃): δ 7.78 (dd, *J* = 5.4, 3.0 Hz, 2H), 7.68 – 7.64 (m, 2H), 7.58 (s, 1H), 7.28 – 7.22 (m, 2H), 7.22 – 7.16 (m, 1H), 7.11 – 7.05 (m, 2H), 6.98 (s, 1H), 6.48 (d, *J* = 7.9 Hz, 1H), 6.43 (d, *J* = 7.8 Hz, 1H), 4.98 (dd, *J* = 8.2, 5.8 Hz, 1H), 4.89 (s, 2H), 4.78 (ddd, *J* = 8.0, 6.7, 5.7 Hz, 1H), 4.73 (dd, *J* = 5.3, 1.4 Hz, 1H), 4.32 (td, *J*

= 8.5, 6.0 Hz, 1H), 4.22 (ddt, $J = 7.2, 5.6, 1.9$ Hz, 1H), 4.02 – 3.97 (m, 1H), 3.91 – 3.81 (m, 3H), 3.68 (s, 3H), 3.11 (dd, $J = 13.9, 5.7$ Hz, 1H), 3.07 – 2.98 (m, 2H), 2.93 (dd, $J = 14.8, 5.8$ Hz, 1H), 1.71 (s, 3H), 1.70 (s, 3H), 1.54 (ddd, $J = 13.5, 7.4, 5.8$ Hz, 1H), 1.48 – 1.37 (m, 2H), 1.03 – 1.00 (m, 21H), 0.98 – 0.97 (m, 21H), 0.95 – 0.91 (m, 21H), 0.80 (d, $J = 6.4$ Hz, 3H), 0.77 (d, $J = 6.4$ Hz, 3H). ^{13}C NMR (151 MHz, CDCl_3): δ 171.7 (C_q), 170.8 (C_q), 167.9 (C_q), 167.7 (C_q), 165.4 (C_q), 153.2 (C_q), 149.1 (C_q), 135.7 (C_q), 133.9 (CH), 131.9 (C_q), 129.2 (CH), 128.5 (CH), 127.1 (CH), 123.4 (CH), 122.7 (CH), 99.2 (CH), 81.4 (CH), 69.1 (CH), 66.0 (CH), 61.8 (CH_2), 53.1 (CH), 53.0 (CH), 52.6 (CH_2), 52.3 (CH), 52.2 (CH_3), 51.7 (C_q), 40.2 (CH_2), 37.7 (CH_2), 34.8 (CH_2), 28.3 (CH_3), 27.8 (CH_3), 24.6 (CH), 22.6 (CH_3), 21.9 (CH_3), 18.1 (CH_3), 18.1 (CH_3), 18.0 (CH_3), 18.0 (CH_3), 12.3 (CH), 11.9 (CH) (1 CH_3 and 1 CH resonances of the TIPS groups are missing due to overlap, the overlap was verified by analysis of the HSQC spectrum). IR (ATR): 3263, 2942, 2865, 1718, 1660, 1556, 1381, 1051, 881, 679 cm^{-1} . MS (ESI): m/z (relative intensity) 1295 (100) $[\text{M}+\text{Na}]^+$, 1272 (2) $[\text{M}+\text{H}]^+$. HR-MS (ESI): m/z calcd for $\text{C}_{67}\text{H}_{110}\text{N}_7\text{O}_{11}\text{Si}_3^+$ $[\text{M}+\text{H}]^+$: 1272.7566 found: 1272.7537.

Benzyl [2-(4-{2-[(S)-3-({2R,3R,4R}-3,4-bis[triisopropylsilyl]oxy)-2-[(triisopropylsilyl)oxy]methyl}-3,4-dihydro-2H-pyran-6-yl)-2-(1,3-dioxoisindolin-2-yl)propanamido]propan-2-yl}-1H-1,2,3-triazol-1-yl)acetyl]-L-phenylalanyl-L-leucinate (240d)



The general procedure **D** was followed using benzyl [2-(4-{2-[(S)-2-(1,3-dioxoisindolin-2-yl)propanamido]propan-2-yl}-1H-1,2,3-triazol-1-yl)acetyl]-L-phenylalanyl-L-leucinate **239d** (74 mg, 0.10 mmol), [({2R,3R,4R}-6-iodo-2-[(triisopropylsilyl)oxy]methyl)-3,4-dihydro-2H-pyran-3,4-diyl]bis(oxy)]bis(triisopropylsilane) **235** (111 mg, 0.15 mmol), $\text{Pd}(\text{TFA})_2$ (3.3 mg, 10 mol %), 1-AdCO₂H (5.4 mg, 30 mol %), Ag_2CO_3 (55 mg, 0.20 mmol), in 1,4-dioxane (0.50 mL). Purification by column chromatography on silica gel (*n*-hexane/EtOAc 3:2 → 2:3) yielded **240d** (68 mg, 50%) as a colorless oil.

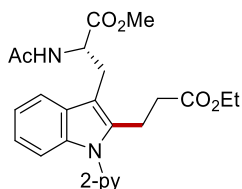
5. Experimental Part

¹H NMR (400 MHz, CDCl₃): δ 7.78 (d, *J* = 5.5 Hz, 2H), 7.66 (dd, *J* = 5.5 Hz, 2H), 7.54 (s, 1H), 7.40 – 7.28 (m, 5H), 7.24 – 7.14 (m, 3H), 7.06 (d, *J* = 7.1 Hz, 2H), 7.01 (s, 1H), 6.60 (d, *J* = 7.6 Hz, 1H), 6.22 (d, *J* = 8.1 Hz, 1H), 5.12 (s, 2H), 5.01 (dd, *J* = 8.2, 5.8 Hz, 1H), 4.92 (d, *J* = 16.8 Hz, 1H), 4.87 (d, *J* = 16.8 Hz, 1H), 4.75 (d, *J* = 5.1 Hz, 1H), 4.65 – 4.42 (m, 2H), 4.25 (t, *J* = 6.2 Hz, 1H), 4.02 (s, 1H), 3.95 – 3.81 (m, 3H), 3.08 (dd, *J* = 14.8, 8.3 Hz, 1H), 3.02 – 2.88 (m, 3H), 1.76 – 1.68 (s, 6H), 1.61 – 1.51 (m, 1H), 1.51 – 1.40 (m, 2H), 1.06 – 1.02 (m, 21H), 1.00 (s, 21H), 0.96 – 0.91 (m, 21H), 0.88 – 0.78 (m, 6H). **¹³C NMR** (101 MHz, CDCl₃): δ 172.1 (C_q), 169.7 (C_q), 167.8 (C_q), 167.7 (C_q), 165.2 (C_q), 153.2 (C_q), 149.1 (C_q), 136.0 (C_q), 135.3 (C_q), 133.9 (CH), 131.9 (C_q), 129.2 (CH), 128.6 (CH), 128.6 (CH), 128.4 (CH), 128.2 (CH), 127.0 (CH), 123.4 (CH), 122.5 (CH), 99.2 (CH), 81.4 (CH), 69.1 (CH), 67.0 (CH₂), 66.0 (CH), 61.8 (CH₂), 54.9 (CH), 53.0 (CH), 52.6 (CH₂), 51.7 (C_q), 51.0 (CH), 41.2 (CH₂), 37.6 (CH₂), 34.9 (CH₂), 28.4 (CH₃), 27.7 (CH₃), 24.7 (CH), 22.6 (CH₃), 21.8 (CH₃), 18.1 (CH₃), 18.1 (CH₃), 18.0 (CH₃), 18.0 (CH₃), 12.3 (CH), 11.9 (CH). (2 CH₃ and 1 CH resonances of the TIPS groups are missing due to overlap, the overlap was verified by analysis of the HSQC spectrum). **IR** (ATR): 3307, 2942, 2866, 1716, 1651, 1463, 1383, 881, 730, 680 cm⁻¹. **MS** (ESI): *m/z* (relative intensity) 1371 (100) [M+Na]⁺, 1348 (2) [M+H]⁺. **HR-MS** (ESI): *m/z* calcd for C₇₃H₁₁₄N₇O₁₁Si₃⁺ [M+H]⁺: 1348.7879 found: 1348.7852.

5.5. Ruthenium(II)-Catalyzed Peptide C–H Functionalization *via* Hydroarylation Manifold

5.5.1. Characterization Data

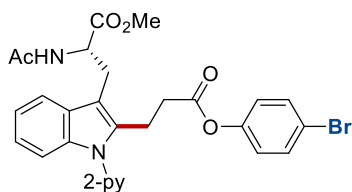
Methyl acetyl-1-(2-pyridyl)-2-(ethyl propionate-3-yl)-L-tryptophanate (**242aa**)



The general procedure **E** was followed using methyl acetyl-1-(2-pyridyl)-L-tryptophanate **241a** (50.6 mg, 0.15 mmol), ethyl acrylate **22a** (45 mg, 0.45 mmol), $[\text{RuCl}_2(p\text{-cymene})]_2$ (9.2 mg, 10 mol %) in acetic acid (0.15 mL). Purification by column chromatography on silica gel (EtOAc) yielded **242aa** (59 mg, 90%) as a colorless oil.

¹H NMR (300 MHz, CDCl_3): δ 8.63 (dd, $J = 4.9, 1.8$ Hz, 1H), 7.91 (ddd, $J = 7.7, 7.7, 1.9$ Hz, 1H), 7.59–7.51 (m, 1H), 7.46 (d, $J = 7.8$ Hz, 1H), 7.34 (dd, $J = 7.2, 5.1$ Hz, 1H), 7.30–7.24 (m, 1H), 7.18–7.09 (m, 2H), 6.36 (d, $J = 7.6$ Hz, 1H), 4.96 (ddd, $J = 7.7, 6.0, 6.0$ Hz, 1H), 4.02 (q, $J = 7.2$ Hz, 2H), 3.70 (s, 3H), 3.38 (dd, $J = 14.7, 6.0$ Hz, 1H), 3.31 (dd, $J = 14.7, 6.0$ Hz, 1H), 3.27–3.13 (m, 2H), 2.29 (ddd, $J = 9.0, 7.1, 2.5$ Hz, 2H), 1.95 (s, 3H), 1.16 (t, $J = 7.2$ Hz, 3H). **¹³C NMR** (126 MHz, CDCl_3): δ 172.4 (C_q), 172.2 (C_q), 169.7 (C_q), 150.9 (C_q), 149.4 (CH), 138.7 (CH), 136.8 (C_q), 136.6 (C_q), 128.5 (C_q), 122.4 (CH), 122.2 (CH), 120.9 (CH), 120.7 (CH), 118.5 (CH), 109.8 (CH), 109.4 (C_q), 60.5 (CH_2), 52.8 (CH), 52.3 (CH_3), 33.7 (CH_2), 27.1 (CH_2), 23.1 (CH_3), 20.3 (CH_2), 14.1 (CH_3). **IR** (ATR): 2954, 2927, 1731, 1655, 1470, 1459, 1436, 1369, 1176, 742 cm^{-1} . **MS** (ESI): m/z (relative intensity) 897 (24) $[\text{2M}+\text{Na}]^+$, 460 (79) $[\text{M}+\text{Na}]^+$, 438 (100) $[\text{M}+\text{H}]^+$. **HR-MS** (ESI): m/z calcd for $\text{C}_{24}\text{H}_{28}\text{N}_3\text{O}_5^+$ $[\text{M}+\text{H}]^+$: 438.2023, found: 438.2026.

Methyl acetyl-1-(2-pyridyl)-2-(4-bromophenyl propionate-3-yl)-L-tryptophanate (**242ab**)



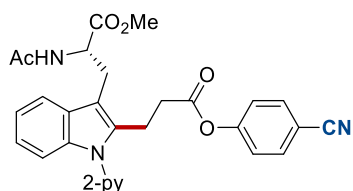
The general procedure **E** was followed using methyl acetyl-1-(2-pyridyl)-L-tryptophanate **242ab** (50.6 mg, 0.15 mmol), 4-bromophenyl acrylate **22b** (41 mg,

5. Experimental Part

0.23 mmol) and $[\text{RuCl}_2(p\text{-cymene})]_2$ (9.2 mg, 10 mol %) in acetic acid (0.15 mL). Purification by column chromatography on silica gel (hexanes/EtOAc: 1/1 \rightarrow 1/3) yielded **242ab** (61 mg, 72%) as a white solid.

M.p.: 126 – 129 °C. **$^1\text{H NMR}$** (300 MHz, CDCl_3): δ 8.65 (ddd, $J = 4.9, 2.0, 0.8$ Hz, 1H), 7.93 (ddd, $J = 8.0, 7.5, 2.0$ Hz, 1H), 7.60–7.53 (m, 1H), 7.50 (ddd, $J = 8.0, 1.0, 1.0$ Hz, 1H), 7.43 (d, $J = 8.9$ Hz, 2H), 7.38–7.28 (m, 2H), 7.22–7.13 (m, 2H), 6.83 (d, $J = 8.9$ Hz, 2H), 6.25 (d, $J = 7.8$ Hz, 1H), 4.97 (ddd, $J = 7.8, 6.0, 6.0$ Hz, 1H), 3.69 (s, 3H), 3.55–3.18 (m, 4H), 2.65–2.57 (m, 2H), 1.92 (s, 3H). **$^{13}\text{C NMR}$** (126 MHz, CDCl_3): δ 172.4 (C_q), 170.5 (C_q), 169.6 (C_q), 151.1 (C_q), 149.6 (CH), 149.4 (C_q), 138.5 (CH), 136.6 (C_q), 136.3 (C_q), 132.3 (CH), 128.5 (C_q), 123.1 (CH), 122.6 (CH), 122.3 (CH), 120.8 (CH), 120.8 (CH), 118.8 (C_q), 118.5 (CH), 110.0 (CH), 109.6 (C_q), 52.9 (CH), 52.4 (CH_3), 33.9 (CH_2), 27.2 (CH_2), 23.1 (CH_3), 20.3 (CH_2). **IR** (ATR): 2928, 1745, 1654, 1585, 1471, 1437, 1199, 1134, 744 cm^{-1} . **MS** (ESI): m/z (relative intensity) 586 (100) $[\text{M}+\text{Na}]^+$, 564 (50) $[\text{M}+\text{H}]^+$. **HR-MS** (ESI): m/z calcd for $\text{C}_{28}\text{H}_{27}^{79}\text{BrN}_3\text{O}_5^+$ $[\text{M}+\text{H}]^+$: 564.1129, found: 564.1130.

Methyl acetyl-1-(2-pyridyl)-2-(4-cyanophenyl propionate-3-yl)-L-tryptophanate (**242ac**)

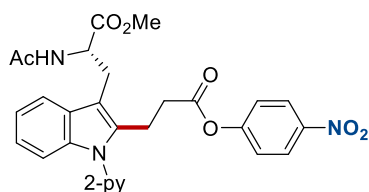


The general procedure **E** was followed using methyl acetyl-1-(2-pyridyl)-L-tryptophanate **241a** (50.6 mg, 0.15 mmol), 4-cyanophenyl acrylate **22c** (40 mg, 0.23 mmol) and $[\text{RuCl}_2(p\text{-cymene})]_2$ (9.2 mg, 10 mol %) in acetic acid (0.15 mL). Purification by column chromatography on silica gel (hexanes/EtOAc: 1/1 \rightarrow 1/3) yielded **242ac** (47 mg, 61%) as a colorless oil.

$^1\text{H NMR}$ (300 MHz, CDCl_3): δ 8.66 (ddd, $J = 4.9, 2.0, 0.8$ Hz, 1H), 7.94 (ddd, $J = 8.0, 7.5, 2.0$ Hz, 1H), 7.63 (d, $J = 8.8$ Hz, 2H), 7.58–7.48 (m, 2H), 7.42–7.28 (m, 2H), 7.23–7.13 (m, 2H), 7.10 (d, $J = 8.8$ Hz, 2H), 6.20 (d, $J = 7.9$ Hz, 1H), 4.96 (ddd, $J = 7.9, 6.0, 6.0$ Hz, 1H), 3.68 (s, 3H), 3.40–3.25 (m, 4H), 2.69 (dd, $J = 8.0, 7.0$ Hz, 2H), 1.94 (s, 3H). **$^{13}\text{C NMR}$** (126 MHz, CDCl_3): δ 172.4 (C_q), 170.0 (C_q), 169.6 (C_q), 153.6 (C_q), 151.0 (C_q), 149.6 (CH), 138.6 (CH), 136.6 (C_q), 136.1 (C_q), 133.5 (CH), 128.6 (C_q), 122.7 (CH), 122.5 (CH), 122.3 (CH), 120.9 (CH), 120.8 (CH), 118.5 (CH), 118.1 (C_q),

110.0 (CH), 109.7 (C_q), 109.7 (C_q), 52.9 (CH), 52.4 (CH₃), 34.0 (CH₂), 27.3 (CH₂), 23.2 (CH₃), 20.3 (CH₂). **IR** (ATR): 2930, 2228, 1743, 1653, 1586, 1472, 1438, 1209, 1121, 744 cm⁻¹. **MS** (ESI): *m/z* (relative intensity) 533 (100) [M+Na]⁺, 511 (69) [M+H]⁺. **HR-MS** (ESI): *m/z* calcd for C₂₉H₂₇N₄O₅⁺ [M+H]⁺: 511.1976, found: 511.1982.

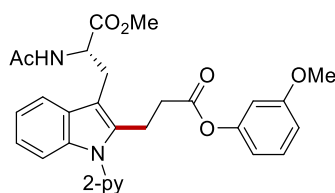
Methyl acetyl-1-(2-pyridyl)-2-(4-nitrophenyl propionate-3-yl)-L-tryptophanate (242ad)



The general procedure **E** was followed using methyl acetyl-1-(2-pyridyl)-L-tryptophanate **241a** (50.6 mg, 0.15 mmol), 4-nitrophenyl acrylate **22d** (44 mg, 0.23 mmol) and [RuCl₂(*p*-cymene)]₂ (9.2 mg, 10 mol %) in acetic acid (0.15 mL). Purification by column chromatography on silica gel (hexanes/EtOAc: 1/1 → 1/3) yielded **242ad** (42 mg, 53%) as a white solid.

M.p.: 102 – 104 °C. **¹H NMR** (300 MHz, CDCl₃): δ 8.66 (ddd, *J* = 4.9, 2.0, 0.8 Hz, 1H), 8.21 (d, *J* = 9.3 Hz, 2H), 7.94 (ddd, *J* = 8.0, 7.5, 2.0 Hz, 1H), 7.57–7.48 (m, 2H), 7.39–7.30 (m, 2H), 7.23–7.12 (m, 4H), 6.20 (d, *J* = 7.9 Hz, 1H), 4.96 (ddd, *J* = 7.9, 6.0, 6.0 Hz, 1H), 3.68 (s, 3H), 3.44–3.24 (m, 4H), 2.72 (dd, *J* = 8.2, 7.0 Hz, 2H), 1.95 (s, 3H). **¹³C NMR** (126 MHz, CDCl₃): δ 172.4 (C_q), 170.0 (C_q), 169.6 (C_q), 155.1 (C_q), 151.1 (C_q), 149.7 (CH), 145.2 (C_q), 138.5 (CH), 136.6 (C_q), 136.1 (C_q), 128.6 (C_q), 125.0 (CH), 122.7 (CH), 122.3 (CH), 122.2 (CH), 120.9 (CH), 120.8 (CH), 118.5 (CH), 110.1 (CH), 109.7 (C_q), 53.0 (CH), 52.4 (CH₃), 34.1 (CH₂), 27.3 (CH₂), 23.2 (CH₃), 20.3 (CH₂). **IR** (ATR): 2923, 1743, 1653, 1589, 1522, 1458, 1437, 1370, 1347, 1156, 745 cm⁻¹. **MS** (ESI): *m/z* (relative intensity) 553 (100) [M+Na]⁺, 531 (68) [M+H]⁺. **HR-MS** (ESI): *m/z* calcd for C₂₈H₂₇N₄O₇⁺ [M+H]⁺: 531.1874, found: 531.1881.

Methyl acetyl-1-(2-pyridyl)-2-(3-methoxyphenyl propionate-3-yl)-L-tryptophanate (242ae)

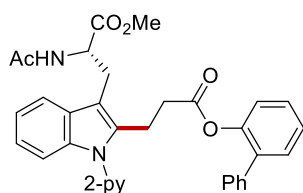


5. Experimental Part

The general procedure **E** was followed using methyl acetyl-1-(2-pyridyl)-L-tryptophanate **241a** (50.6 mg, 0.15 mmol), 3-methoxyphenyl acrylate **22e** (41 mg, 0.23 mmol) and $[\text{RuCl}_2(p\text{-cymene})]_2$ (9.2 mg, 10 mol %) in acetic acid (0.15 mL). Purification by column chromatography on silica gel (hexanes/EtOAc: 1/1 \rightarrow 1/3) yielded **242ae** (56 mg, 72%) as a colorless oil.

$^1\text{H NMR}$ (300 MHz, CDCl_3): δ 8.67 (ddd, $J = 4.9, 2.0, 0.9$ Hz, 1H), 7.93 (ddd, $J = 8.0, 7.5, 2.0$ Hz, 1H), 7.61–7.54 (m, 1H), 7.51 (ddd, $J = 8.0, 0.9, 0.9$ Hz, 1H), 7.40–7.29 (m, 2H), 7.24–7.13 (m, 3H), 6.73 (ddd, $J = 8.2, 2.4, 0.9$ Hz, 1H), 6.53 (ddd, $J = 8.2, 2.4, 0.9$ Hz, 1H), 6.42 (dd, $J = 2.4, 2.4$ Hz, 1H), 6.24 (d, $J = 7.7$ Hz, 1H), 4.98 (ddd, $J = 7.7, 6.0, 6.0$ Hz, 1H), 3.71 (s, 3H), 3.70 (s, 3H), 3.48–3.21 (m, 4H), 2.70–2.45 (m, 2H), 1.89 (s, 3H). **$^{13}\text{C NMR}$** (126 MHz, CDCl_3): δ 172.5 (C_q), 170.8 (C_q), 169.7 (C_q), 160.3 (C_q), 151.3 (C_q), 151.1 (C_q), 149.7 (CH), 138.5 (CH), 136.7 (C_q), 136.3 (C_q), 129.6 (CH), 128.6 (C_q), 122.6 (CH), 122.3 (CH), 120.8 (CH), 120.8 (CH), 118.6 (CH), 113.5 (CH), 111.8 (CH), 110.0 (CH), 109.6 (C_q), 107.2 (CH), 55.4 (CH_3), 52.8 (CH), 52.4 (CH_3), 33.8 (CH_2), 27.2 (CH_2), 23.1 (CH_3), 20.4 (CH_2). **IR** (ATR): 2950, 1745, 1655, 1588, 1489, 1471, 1458, 1437, 1139, 744 cm^{-1} . **MS** (ESI): m/z (relative intensity) 538 (65) $[\text{M}+\text{Na}]^+$, 516 (100) $[\text{M}+\text{H}]^+$. **HR-MS** (ESI): m/z calcd for $\text{C}_{29}\text{H}_{30}\text{N}_3\text{O}_6^+$ $[\text{M}+\text{H}]^+$: 516.2129, found: 516.2134.

Methyl acetyl-1-(2-pyridyl)-2-(2-phenylphenyl propionate-3-yl)-L-tryptophanate (**242af**)

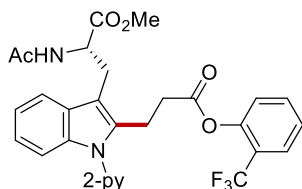


The general procedure **E** was followed using methyl acetyl-1-(2-pyridyl)-L-tryptophanate **241a** (50.6 mg, 0.15 mmol), 2-phenylphenyl acrylate **22f** (52 mg, 0.23 mmol) and $[\text{RuCl}_2(p\text{-cymene})]_2$ (9.2 mg, 10 mol %) in acetic acid (0.15 mL). Purification by column chromatography on silica gel (hexanes/EtOAc: 1/1 \rightarrow 1/2) yielded **242af** (66 mg, 79%) as a colorless oil.

$^1\text{H NMR}$ (300 MHz, CDCl_3): δ 8.57–8.52 (m, 1H), 7.87 (ddd, $J = 7.8, 7.8, 1.9$ Hz, 1H), 7.61–7.48 (m, 1H), 7.41–7.20 (m, 11H), 7.18–7.11 (m, 2H), 7.01–6.95 (m, 1H), 6.15 (d, $J = 7.8$ Hz, 1H), 4.93 (ddd, $J = 7.8, 5.9, 5.9$ Hz, 1H), 3.65 (s, 3H), 3.33 (dd, $J = 14.8, 6.1$ Hz, 1H), 3.23 (dd, $J = 14.8, 5.9$ Hz, 1H), 3.15–3.02 (m, 2H), 2.39 (t, $J = 7.7$ Hz,

2H), 1.85 (s, 3H). ^{13}C NMR (126 MHz, CDCl_3): δ 172.4 (C_q), 170.8 (C_q), 169.7 (C_q), 151.0 (C_q), 149.6 (CH), 147.5 (C_q), 138.4 (CH), 137.4 (C_q), 136.6 (C_q), 136.4 (C_q), 134.7 (C_q), 130.7 (CH), 128.7 (CH), 128.6, (C_q) 128.4 (CH), 128.1 (CH), 127.3 (CH), 126.3 (CH), 122.6 (CH), 122.5 (CH), 122.2 (CH), 120.8 (CH), 120.7 (CH), 118.5 (CH), 110.0 (CH), 109.4 (C_q), 52.8 (CH), 52.4 (CH_3), 33.7 (CH_2), 27.1 (CH_2), 23.1 (CH_3), 20.2 (CH_2). IR (ATR): 3056, 2925, 1749, 1654, 1584, 1541, 1136, 701 cm^{-1} . MS (ESI): m/z (relative intensity) 584 (49) $[\text{M}+\text{Na}]^+$, 562 (100) $[\text{M}+\text{H}]^+$. HR-MS (ESI): m/z calcd for $\text{C}_{34}\text{H}_{32}\text{N}_3\text{O}_5^+$ $[\text{M}+\text{H}]^+$: 562.2336, found: 562.2334.

Methyl acetyl-1-(2-pyridyl)-2-(2-trifluoromethylphenyl propionate-3-yl)-L-tryptophanate (**242ag**)

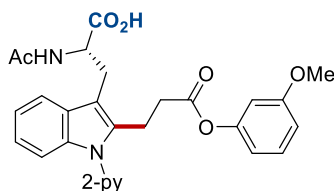


The general procedure **E** was followed using methyl acetyl-1-(2-pyridyl)-L-tryptophanate **241a** (50.6 mg, 0.15 mmol), 2-(trifluoromethyl)phenyl acrylate **22g** (50 mg, 0.23 mmol) and $[\text{RuCl}_2(p\text{-cymene})]_2$ (9.2 mg, 10 mol %) in acetic acid (0.15 mL). Purification by column chromatography on silica gel (hexanes/EtOAc: 1/1 \rightarrow 1/2) yielded **242ag** (62 mg, 75%) as a colorless oil.

^1H NMR (300 MHz, CDCl_3): δ 8.66 (ddd, $J = 4.9, 2.0, 0.8$ Hz, 1H), 7.93 (ddd, $J = 8.0, 7.5, 2.0$ Hz, 1H), 7.68–7.46 (m, 4H), 7.39–7.27 (m, 3H), 7.20–7.14 (m, 2H), 7.11 (d, $J = 8.2$ Hz, 1H), 6.24 (d, $J = 7.9$ Hz, 1H), 5.00 (ddd, $J = 7.9, 5.9, 5.9$ Hz, 1H), 3.70 (s, 3H), 3.49–3.21 (m, 4H), 2.70 (dd, $J = 8.5, 7.3$ Hz, 2H), 1.91 (s, 3H). ^{13}C NMR (126 MHz, CDCl_3): δ 172.4 (C_q), 170.2 (C_q), 169.6 (C_q), 151.0 (C_q), 149.7 (CH), 147.8 (q, $^3J_{\text{C-F}} = 2.2$ Hz, C_q), 138.5 (CH), 136.6 (C_q), 136.2 (C_q), 132.9 (CH), 128.6 (C_q), 126.7 (q, $^3J_{\text{C-F}} = 4.8$ Hz, CH), 125.7 (CH), 124.3 (CH), 122.8 (q, $^1J_{\text{C-F}} = 272.3$ Hz, C_q), 122.5 (CH), 122.4 (q, $^2J_{\text{C-F}} = 33.9$ Hz, C_q), 122.3 (CH), 120.8 (CH), 120.7 (CH), 118.5 (CH), 110.0 (CH), 109.5 (C_q), 52.8 (CH_3), 52.4 (CH), 33.7 (CH_2), 27.2 (CH_2), 23.1 (CH_3), 20.3 (CH_2). ^{19}F NMR (282 MHz, CDCl_3): δ -61.8 (s). IR (ATR): 3055, 2952, 1745, 1655, 1588, 1472, 1438 1371, 1131, 744 cm^{-1} . MS (ESI): m/z (relative intensity) 576 (78) $[\text{M}+\text{Na}]^+$, 554 (100) $[\text{M}+\text{H}]^+$. HR-MS (ESI): m/z calcd for $\text{C}_{29}\text{H}_{27}\text{F}_3\text{N}_3\text{O}_5^+$ $[\text{M}+\text{H}]^+$: 554.1897, found: 554.1903.

5. Experimental Part

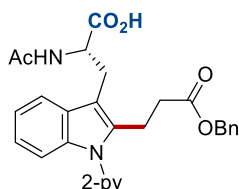
(S)-2-acetamido-3-{2-[3-(3-methoxyphenoxy)-3-oxopropyl]-1-[pyridin-2-yl]-1H-indol-3-yl}propanoic acid (**242be**)



The general procedure **E** was followed using *N*^a-acetyl-1-(pyridin-2-yl)-L-tryptophan **242be** (48.5 mg, 0.15 mmol), 3-methoxyphenyl acrylate **22e** (41 mg, 0.23 mmol), and [RuCl₂(*p*-cymene)]₂ (9.2 mg, 10 mol %) in acetic acid (0.15 mL). Purification by column chromatography on silica gel (CH₂Cl₂/MeOH: 30/1 → 20/1) yielded **242be** (42 mg, 84 μmol, 56%) as a white solid.

M.p.: 116 – 118 °C. **¹H NMR** (400 MHz, CDCl₃): δ 8.73 (d, *J* = 4.9 Hz, 1H), 7.99 (dd, *J* = 7.7, 7.7 Hz, 1H), 7.59 (d, *J* = 7.4 Hz, 1H), 7.51 (d, *J* = 7.7 Hz, 1H), 7.45 (dd, *J* = 7.4, 4.9 Hz, 1H), 7.22–7.11 (m, 2H), 7.11–6.98 (m, 2H), 6.93–6.83 (m, 1H), 6.70 (dd, *J* = 8.1, 2.2 Hz, 1H), 6.43 (dd, *J* = 8.1, 2.2 Hz, 1H), 6.31 (d, *J* = 2.2 Hz, 1H), 5.08–4.99 (m, 1H), 3.64 (s, 3H), 3.39–3.16 (m, 3H), 3.16 – 2.96 (m, 1H), 2.45–2.28 (m, 2H), 1.81 (s, 3H). **¹³C NMR** (101 MHz, CDCl₃): δ 174.0 (C_q), 171.3 (C_q), 170.7 (C_q), 160.4 (C_q), 151.2 (C_q), 150.6 (C_q), 149.2 (CH), 139.7 (CH), 136.9 (C_q), 136.4 (C_q), 129.7 (CH), 128.6 (C_q), 123.1 (CH), 122.6 (CH), 122.1 (CH), 120.8 (CH), 119.0 (CH), 113.4 (CH), 112.0 (CH), 110.1 (C_q), 109.6 (CH), 107.1 (CH), 55.3 (CH₃), 52.2 (CH), 33.5 (CH₂), 26.5 (CH₂), 22.7 (CH₃), 20.2 (CH₂). **IR** (ATR): 3341, 3053, 2932, 1731, 1586, 1471, 1437, 1163, 742 cm⁻¹. **MS** (ESI): *m/z* (relative intensity) 1003 (26) [2M+H]⁺, 524 (34) [M+Na]⁺, 502 (100) [M+H]⁺. **HR-MS** (ESI): *m/z* calcd for C₂₈H₂₈N₃O₆⁺ [M+H]⁺: 502.1973; found: 502.1974.

(S)-2-Acetamido-3-{2-[3-(benzyloxy)-3-oxopropyl]-1-[pyridin-2-yl]-1H-indol-3-yl}propanoic acid (**242bh**)

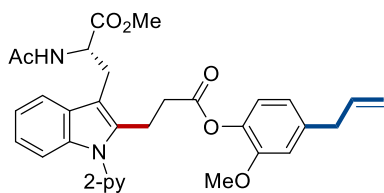


The general procedure **E** was followed using *N*^a-acetyl-1-(pyridin-2-yl)-L-tryptophan **241b** (48.5 mg, 0.15 mmol), benzyl acrylate **22h** (37 mg, 0.23 mmol) and [RuCl₂(*p*-cymene)]₂ (9.2 mg, 10 mol %) in AcOH (0.15 mL). Purification by column

chromatography on silica gel (CH₂Cl₂/MeOH: 30/1 → 20/1) yielded **242bh** (40 mg, 83 μmol, 55%) as a white solid.

M.p.: 110 – 112 °C. **¹H NMR** (400 MHz, CDCl₃): δ 8.67 (dd, *J* = 5.0, 1.7 Hz, 1H), 8.03–7.90 (m, 1H), 7.56 (dd, *J* = 6.9, 1.8 Hz, 1H), 7.46–7.33 (m, 2H), 7.31–7.21 (m, 3H), 7.20–7.11 (m, 2H), 7.13–6.95 (m, 4H), 5.11–4.84 (m, 3H), 3.27–2.85 (m, 4H), 2.34–2.21 (m, 2H), 1.85 (s, 3H). **¹³C NMR** (101 MHz, CDCl₃): δ 174.2 (C_q), 173.2 (C_q), 170.8 (C_q), 150.9 (C_q), 149.4 (CH), 139.7 (CH), 137.0 (C_q), 136.9 (C_q), 135.5 (C_q), 128.7 (CH), 128.6 (C_q), 128.5 (CH), 128.3 (CH), 123.1 (CH), 122.6 (CH), 122.2 (CH), 120.8 (CH), 119.0 (CH), 109.9 (C_q), 109.8 (CH), 66.8 (CH₂), 52.1 (CH), 33.8 (CH₂), 26.5 (CH₂), 23.0 (CH₃), 20.4 (CH₂). **IR** (ATR): 3366, 3056, 2929, 1752, 1608, 1589, 1471, 1438, 1138, 742 cm⁻¹. **MS** (ESI) *m/z* (relative intensity) 993 (16) [2M+Na]⁺, 971 (20) [2M+H]⁺, 508 (33) [M+Na]⁺, 486 (100) [M+H]⁺. **HR-MS** (ESI): *m/z* calcd for C₂₈H₂₈N₃O₅⁺ [M+H]⁺: 486.2023, found: 486.2024.

Methyl acetyl-1-(2-pyridyl)-2-(4-allyl-2-methoxyphenyl propionate-3-yl)-L-tryptophanate (**242ai**)



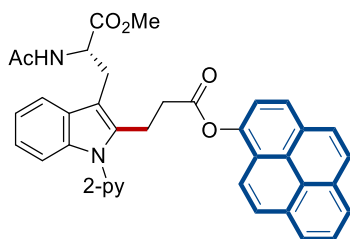
The general procedure **E** was followed using methyl acetyl-1-(2-pyridyl)-L-tryptophanate **241a** (50.6 mg, 0.15 mmol), 4-allyl-2-methoxyphenyl acrylate **22i** (50 mg, 0.23 mmol) and [RuCl₂(*p*-cymene)]₂ (9.2 mg, 10 mol %) in toluene/AcOH (1:1, 0.15 mL). Purification by column chromatography on silica gel (hexanes/EtOAc: 1/1 → 1/2) yielded **242ai** (73 mg, 88%) as a pale yellow solid.

M.p.: 77 – 79 °C. **¹H NMR** (600 MHz, CDCl₃): δ 8.66 (ddd, *J* = 5.0, 1.9, 0.9 Hz, 1H), 7.93 (ddd, *J* = 7.8, 7.8, 2.0 Hz, 1H), 7.62–7.56 (m, 1H), 7.52 (dd, *J* = 8.0, 0.9 Hz, 1H), 7.35 (dd, *J* = 7.5, 4.9 Hz, 1H), 7.33–7.29 (m, 1H), 7.20–7.14 (m, 2H), 6.78 (dd, *J* = 8.0, 0.7 Hz, 1H), 6.73–6.63 (m, 2H), 6.32 (d, *J* = 7.6 Hz, 1H), 5.92 (ddtd, *J* = 16.9, 10.2, 6.7, 0.7 Hz, 1H), 5.08 (ddd, *J* = 9.2, 1.2, 0.8 Hz, 1H), 5.06 (q, *J* = 1.2 Hz, 1H), 4.99 (ddd, *J* = 7.6, 6.1, 6.1 Hz, 1H) 3.72 (s, 3H), 3.63 (s, 3H), 3.46–3.26 (m, 6H), 2.60 (ddd, *J* = 16.7, 8.6, 6.0 Hz, 1H), 2.54 (ddd, *J* = 16.3, 8.7, 7.3 Hz, 1H), 1.85 (s, 3H). **¹³C NMR** (126 MHz, CDCl₃): δ 172.5 (C_q), 170.7 (C_q), 169.9 (C_q), 151.1 (C_q), 150.5 (C_q), 149.7 (CH), 138.9 (C_q), 138.5 (CH), 137.6 (C_q), 136.8 (CH), 136.7 (C_q), 136.5 (C_q), 128.5

5. Experimental Part

(C_q), 122.5 (CH), 122.2 (CH), 122.2 (CH), 120.9 (CH), 120.7 (CH), 120.5 (CH), 118.6 (CH), 116.0 (CH₂), 112.6 (CH), 109.9 (CH), 109.6 (C_q), 55.6 (CH₃), 52.8 (CH), 52.4 (CH₃), 40.0 (CH₂), 33.3 (CH₂), 27.1 (CH₂), 23.0 (CH₃), 20.4 (CH₂). **IR** (ATR): 2951, 1745, 1656, 1507, 1437, 1137, 1123, 742 cm⁻¹. **MS** (ESI): *m/z* (relative intensity) 578 (62) [M+Na]⁺, 556 (100) [M+H]⁺. **HR-MS** (ESI): *m/z* calcd for C₃₂H₃₄N₃O₆⁺ [M+H]⁺: 556.2442, found: 556.2438.

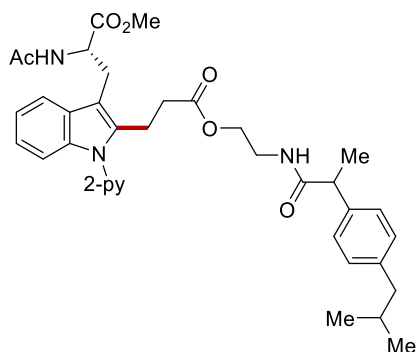
Methyl acetyl-1-(2-pyridyl)-2-(1-pyrenyl propionate-3-yl)-L-tryptophanate (**242aj**)



The general procedure **E** was followed using methyl acetyl-1-(2-pyridyl)-L-tryptophanate **241a** (50.6 mg, 0.15 mmol), pyren-1-yl acrylate **22j** (62 mg, 0.23 mmol) and [RuCl₂(*p*-cymene)]₂ (9.2 mg, 10 mol %) in AcOH (0.15 mL). Purification by column chromatography on silica gel (hexanes/EtOAc: 1/1 → 1/2) yielded **242aj** (62 mg, 68%) as a white solid.

M.p.: 205 – 207 °C. **¹H NMR** (300 MHz, CDCl₃): δ 8.76 (dd, *J* = 4.9, 1.2 Hz, 1H), 8.26–8.08 (m, 3H), 8.07–7.88 (m, 4H), 7.78 (d, *J* = 9.2 Hz, 1H), 7.70–7.57 (m, 4H), 7.48–7.35 (m, 2H), 7.33–7.24 (m, 2H), 6.29 (d, *J* = 7.7 Hz, 1H), 5.04 (ddd, *J* = 7.7, 6.1, 6.1 Hz, 1H), 3.72 (s, 3H), 3.64–3.33 (m, 4H), 2.98–2.84 (m, 2H), 1.81 (s, 3H). **¹³C NMR** (126 MHz, CDCl₃): δ 172.6 (C_q), 171.6 (C_q), 170.0 (C_q), 151.2 (C_q), 149.7 (CH), 144.0 (C_q), 138.9 (CH), 136.9 (C_q), 136.3 (C_q), 131.0 (C_q), 130.8 (C_q), 129.3 (C_q), 128.8 (C_q), 128.1 (CH), 127.1 (CH), 127.0 (CH), 126.3 (CH), 125.5 (CH), 125.4 (C_q), 125.3 (CH), 124.9 (CH), 124.4 (C_q), 122.9 (C_q), 122.8 (CH), 122.5 (CH), 121.1 (CH), 121.0 (CH), 119.9 (CH), 119.5 (CH), 118.8 (CH), 110.2 (C_q), 110.1 (CH), 52.8 (CH), 52.4 (CH₃), 33.8 (CH₂), 27.1 (CH₂), 22.9 (CH₃), 20.6 (CH₂). **IR** (ATR): 3276, 3074, 2962, 2930, 1742, 1647, 1542, 1472, 1459, 1148, 743 cm⁻¹. **MS** (ESI): *m/z* (relative intensity) 1241 (100) [2M+Na]⁺, 632 (59) [M+Na]⁺, 610 (33) [M+H]⁺. **HR-MS** (ESI): *m/z* calcd for C₃₈H₃₂N₃O₅⁺ [M+H]⁺: 610.2336, found: 610.2336.

Methyl acetyl-1-(2-pyridyl)-2-{2-[2-(4-isobutylphenyl)propanamido]ethyl propionate-3-yl}-L-tryptophanate (242ak)

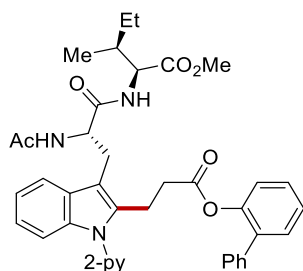


The general procedure **E** was followed using methyl acetyl-1-(2-pyridyl)-L-tryptophanate **241a** (50.6 mg, 0.15 mmol), 2-[2-(4-isobutylphenyl)propanamido]ethyl acrylate **22k** (69 mg, 0.23 mmol) and $[\text{RuCl}_2(p\text{-cymene})]_2$ (9.2 mg, 10 mol %) in AcOH (0.15 mL). Purification by column chromatography on silica gel (hexanes/EtOAc: 1/1 \rightarrow 1/2) yielded **242ak** (80 mg, 83%) as a white solid.

M.p.: 123 – 126 °C. **$^1\text{H NMR}$** (600 MHz, CDCl_3 , mixture of diastereoisomers 1.0/1.0): δ 8.60 (dd, $J = 4.7, 2.9$ Hz, 1H), 7.94–7.85 (m, 1H), 7.49 (ddd, $J = 5.8, 1.8, 1.8$ Hz, 1H), 7.41 (d, $J = 7.7$ Hz, 1H), 7.33 (dd, $J = 7.3, 4.8$ Hz, 1H), 7.17–7.09 (m, 4H), 7.04 (d, $J = 7.6$ Hz, 2H), 6.41–6.35 (m, 2H), 4.91–4.81 (m, 1H), 4.15–3.90 (m, 2H), 3.64 (s, 1.5H), 3.63 (s, 1.5H), 3.57–3.44 (m, 1H), 3.44–3.23 (m, 2H), 3.22–3.10 (m, 2H), 2.38 (d, $J = 7.2$ Hz, 3H), 2.32–2.23 (m, 2H), 1.94 (s, 1.5H), 1.91 (s, 1.5H), 1.83–1.74 (m, 1H), 1.43 (d, $J = 7.1$ Hz, 1.5H), 1.42 (d, $J = 6.9$ Hz, 1.5H), 0.84 (d, $J = 6.6$ Hz, 6H). **$^{13}\text{C NMR}$** (126 MHz, CDCl_3): δ 174.5 (C_q), 172.4 (C_q), 172.4 (C_q), 171.9 (C_q), 169.8 (C_q), 151.0 (C_q), 149.6 (CH), 140.3 (C_q), 138.6 (C_q), 138.5 (C_q), 138.5 (CH), 136.6 (C_q), 136.6 (C_q), 136.5 (C_q), 129.3 (CH), 128.4 (C_q), 128.4 (C_q), 127.1 (CH), 122.4 (CH), 122.3 (CH), 120.8 (CH), 120.7 (CH), 118.2 (CH), 118.2 (CH), 110.0 (CH), 109.3 (C_q), 63.5 (CH_2), 53.1 (CH), 53.1 (CH), 52.4 (CH_3), 46.3 (CH), 46.3 (CH), 45.0 (CH_2), 38.6 (CH_2), 34.0 (CH_2), 33.9 (CH_2), 30.1 (CH), 27.2 (CH_2), 27.2 (CH_2), 23.2 (CH_3), 23.2 (CH_3), 22.4, 20.5 (CH_2), 18.7 (CH_3), 18.6 (CH_3). **IR** (ATR): 3276, 3074, 2962, 1742, 1647, 1542, 1472, 1459, 1148, 743 cm^{-1} . **MS** (ESI): m/z (relative intensity) 1304 (22) $[2\text{M}+\text{Na}]^+$ 663 (63) $[\text{M}+\text{Na}]^+$, 641 (100) $[\text{M}+\text{H}]^+$. **HR-MS** (ESI): m/z calcd for $\text{C}_{37}\text{H}_{45}\text{N}_4\text{O}_6^+$ $[\text{M}+\text{H}]^+$: 641.3334, found: 641.1331.

5. Experimental Part

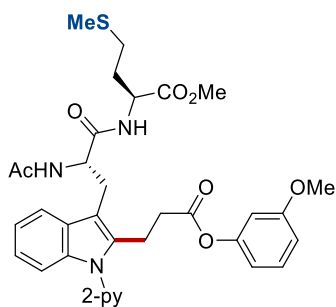
Methyl *N*-acetyl-1-(2-pyridyl)-2-(2-phenylphenyl propionate-3-yl)-L-tryptophyl-L-isoleucinate (**244a**)



The general procedure **F** was followed using methyl *N*-acetyl-1-(2-pyridyl)-L-tryptophyl-L-isoleucinate **243a** (67.5 mg, 0.15 mmol), 2-phenylphenyl acrylate **22f** (52 mg, 0.23 mmol) and [RuCl₂(*p*-cymene)]₂ (9.2 mg, 10 mol %) in AcOH (0.15 mL). Purification by column chromatography on silica gel (CH₂Cl₂/MeOH: 40/1 → 30/1 → 20/1) yielded **244a** (77 mg, 76%) as a white solid.

M.p.: 102 – 105 °C. **¹H NMR** (600 MHz, CDCl₃): δ 8.54 (ddd, *J* = 5.0, 2.0, 0.8 Hz, 1H), 7.87 (dd, *J* = 7.7, 7.7, 2.0 Hz, 1H), 7.70–7.66 (m, 1H), 7.46 (d, *J* = 8.0 Hz, 1H), 7.34 (dd, *J* = 7.3, 1.9 Hz, 1H), 7.32–7.28 (m, 6H), 7.29–7.26 (m, 2H), 7.26–7.24 (m, 1H), 7.18–7.11 (m, 2H), 7.04 (dd, *J* = 7.9, 1.5 Hz, 1H), 6.50 (d, *J* = 7.5 Hz, 1H), 6.29 (d, *J* = 8.1 Hz, 1H), 4.82 (ddd, *J* = 8.7, 7.5, 6.3 Hz, 1H), 4.34 (dd, *J* = 8.1, 4.9 Hz, 1H), 3.47 (s, 3H), 3.31 (dd, *J* = 14.5, 6.2 Hz, 1H), 3.16 (dd, *J* = 8.0, 6.7 Hz, 2H), 3.10 (dd, *J* = 14.5, 8.8 Hz, 1H), 2.57 (ddd, *J* = 17.1, 6.9, 6.9 Hz, 1H), 2.40 (ddd, *J* = 17.1, 7.8, 7.8 Hz, 1H), 1.93 (s, 3H), 1.71–1.66 (m, 1H), 1.27–1.19 (m, 1H), 1.02–0.93 (m, 1H), 0.80 (t, *J* = 7.4 Hz, 3H), 0.70 (d, *J* = 6.9 Hz, 3H). **¹³C NMR** (126 MHz, CDCl₃): δ 171.2 (C_q), 170.9 (C_q), 170.9 (C_q), 169.7 (C_q), 151.2 (C_q), 149.5 (CH), 147.5 (C_q), 138.3 (CH), 137.4 (C_q), 136.7 (C_q), 136.4 (C_q), 134.6 (C_q), 130.6 (CH), 128.7 (CH), 128.3 (CH), 128.3 (C_q), 128.1 (CH), 127.3 (CH), 126.2 (CH), 122.8 (CH), 122.3 (CH), 122.1 (CH), 120.9 (CH), 120.8 (CH), 118.7 (CH), 110.1 (C_q), 109.9 (CH), 56.6 (CH), 53.6 (CH), 51.8 (CH₃), 38.1 (CH), 33.5 (CH₂), 28.1 (CH₂), 25.1 (CH₂), 23.2 (CH₃), 20.1 (CH₂), 15.2 (CH₃), 11.6 (CH₃). **IR** (ATR): 2961, 2923, 1747, 1646, 1472, 1436, 743 cm⁻¹. **MS** (ESI): *m/z* (relative intensity) 697 (100) [M+Na]⁺, 675 (36) [M+H]⁺. **HR-MS** (ESI): *m/z* calcd for C₄₀H₄₃N₄O₆⁺ [M+H]⁺: 675.3177, found: 675.3165.

Methyl ((S)-2-acetamido-3-{2-[3-(3-methoxyphenoxy)-3-oxopropyl]-1-[pyridin-2-yl]-1H-indol-3-yl}propanoyl)-L-methioninate (244b)

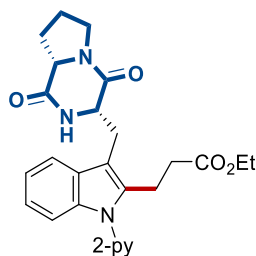


The general procedure **F** was followed using methyl *N*^α-acetyl-1-(pyridin-2-yl)-L-tryptophyl-L-methioninate **243b** (70.2 mg, 0.15 Mmol), 3-methoxyphenyl acrylate **22e** (40 mg, 0.23 mmol) and [RuCl₂(*p*-cymene)]₂ (9.2 mg, 10 mol %) in AcOH (0.45 mL). Purification by column chromatography on silica gel (EtOAc) yielded **244b** (55.2 mg, 57%) as a white solid.

M.p.: 88 – 89 °C. **¹H NMR** (600 MHz, CDCl₃): δ 8.66 (ddd, *J* = 4.9, 2.0, 0.9 Hz, 1H), 7.93 (ddd, *J* = 7.8, 7.8, 2.0 Hz, 1H), 7.68–7.62 (m, 1H), 7.58 (ddd, *J* = 7.8, 0.9, 0.9 Hz, 1H), 7.36 (ddd, *J* = 7.5, 4.9, 0.9 Hz, 1H), 7.32–7.27 (m, 1H), 7.18 (dd, *J* = 8.2, 8.2 Hz, 1H), 7.16–7.12 (m, 2H), 6.72 (ddd, *J* = 8.2, 2.2, 0.8 Hz, 1H), 6.55 (ddd, *J* = 8.2, 2.2, 0.8 Hz, 1H), 6.52 (d, *J* = 7.4 Hz, 1H), 6.47 (dd, *J* = 2.2 Hz, 1H), 6.42 (d, *J* = 7.1 Hz, 1H), 4.84 (ddd, *J* = 9.1, 7.4, 6.0 Hz, 1H), 4.44 (ddd, *J* = 7.1, 7.1, 5.1 Hz, 1H), 3.70 (s, 3H), 3.51 (s, 3H), 3.43–3.34 (m, 3H), 3.15 (dd, *J* = 14.4, 9.1 Hz, 1H), 2.75 (ddd, *J* = 16.7, 6.7, 6.7 Hz, 1H), 2.56 (ddd, *J* = 16.7, 7.8, 7.8 Hz, 1H), 2.29 (ddd, *J* = 13.3, 9.1, 6.1 Hz, 1H), 2.23 (ddd, *J* = 13.3, 9.1, 6.1 Hz, 1H), 1.96 (s, 3H), 1.94 (s, 3H), 1.83–1.66 (m, 2H). **¹³C NMR** (126 MHz, CDCl₃): δ 171.2 (C_q), 171.0 (C_q), 170.9 (C_q), 169.8 (C_q), 160.3 (C_q), 151.3 (C_q), 151.3 (C_q), 149.6 (CH), 138.5 (CH), 136.8 (C_q), 136.3 (C_q), 129.5 (CH), 128.3 (C_q), 122.4 (CH), 122.2 (CH), 121.0 (CH), 120.8 (CH), 118.6 (CH), 113.6 (CH), 111.7 (CH), 110.2 (C_q), 109.9 (CH), 107.4 (CH), 55.4 (CH₃), 53.7 (CH), 52.3 (CH₃), 51.6 (CH), 33.5 (CH₂), 31.9 (CH₂), 29.6 (CH₂), 28.1 (CH₂), 23.2 (CH₃), 20.4 (CH₂), 15.4 (CH₃). **IR** (ATR): 3277, 2921, 1744, 1645, 1459, 1436, 1137, 741 cm⁻¹. **MS** (ESI): *m/z* (relative intensity) 1316 (58) [2M+Na]⁺, 669 (100) [M+Na]⁺, 647 (82) [M+H]⁺. **HR-MS** (ESI): *m/z* calcd for C₃₄H₃₉N₄O₇S⁺ [M+H]⁺: 647.2534, found: 647.2527.

5. Experimental Part

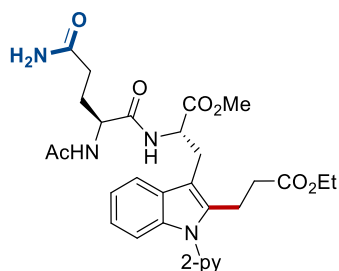
Ethyl 3-(3-{[(3*S*,8*aS*)-1,4-dioxooctahydropyrrolo[1,2-*a*]pyrazin-3-yl]methyl}-1-[pyridin-2-yl]-1*H*-indol-2-yl)propanoate (**244c**)



The general procedure **F** was followed using 3-[[1-(pyridin-2-yl)-1*H*-indol-3-yl]methyl]hexahydropyrrolo[1,2-*a*]pyrazine-1,4-dione **243c** (54 mg, 150 μ mol), ethyl acrylate **22a** (45 mg, 0.45 mmol) and $[\text{RuCl}_2(p\text{-cymene})]_2$ (9.2 mg, 10 mol %) in AcOH (0.45 mL). Purification by column chromatography on silica gel (EtOAc) yielded **244c** (57 mg, 82%) as a pale yellow solid.

M.p.: 97 – 98 °C. **$^1\text{H NMR}$** (600 MHz, CDCl_3): δ 8.62 (ddd, $J = 4.8, 2.0, 1.0$ Hz, 1H), 7.91 (ddd, $J = 7.5, 7.5, 1.8$ Hz, 1H), 7.55 – 7.50 (m, 1H), 7.47 (dd, $J = 7.9, 1.0$ Hz, 1H), 7.37 – 7.31 (m, 1H), 7.29 (ddd, $J = 7.5, 1.0, 1.0$ Hz, 1H), 7.22 – 7.08 (m, 2H), 5.86 (s, 1H), 4.47 (dd, $J = 11.5, 3.8$ Hz, 1H), 4.10 – 3.97 (m, 3H), 3.74 (dd, $J = 15.2, 3.8$ Hz, 1H), 3.67 (ddd, $J = 11.7, 7.9, 7.9$ Hz, 1H), 3.57 (ddd, $J = 11.7, 8.8, 3.1$ Hz, 1H), 3.26 – 3.15 (m, 2H), 3.06 (ddd, $J = 15.2, 11.7, 1.0$ Hz, 1H), 2.43 (ddd, $J = 15.9, 8.8, 7.1$ Hz, 1H), 2.39 – 2.28 (m, 2H), 2.09 – 1.97 (m, 2H), 1.93 – 1.83 (m, 1H), 1.15 (t, $J = 7.2$ Hz, 3H). **$^{13}\text{C NMR}$** (126 MHz, CDCl_3): δ 172.1 (C_q), 169.3 (C_q), 165.5 (C_q), 150.8 (C_q), 149.7 (CH), 138.4 (CH), 137.3 (C_q), 136.8 (C_q), 127.6 (C_q), 122.8 (CH), 122.4 (CH), 121.0 (CH), 120.9 (CH), 118.1 (CH), 110.3 (CH), 108.5 (C_q), 60.6 (CH_2), 59.3 (CH), 54.5 (CH), 45.5 (CH_2), 34.0 (CH_2), 28.4 (CH_2), 25.7 (CH_2), 22.7 (CH_2), 20.6 (CH_2), 14.2 (CH_3). **IR** (ATR): 2979, 2930, 1718, 1585, 1469, 1436, 1164, 782, 732 cm^{-1} . **MS** (ESI): m/z (relative intensity) 943 (50) $[2\text{M}+\text{Na}]^+$, 483 (100) $[\text{M}+\text{Na}]^+$, 461 (93) $[\text{M}+\text{H}]^+$. **HR-MS** (ESI): m/z calcd for $\text{C}_{26}\text{H}_{29}\text{N}_4\text{O}_4^+$ $[\text{M}+\text{H}]^+$: 461.2183, found: 461.2186.

Methyl (S)-2-[(S)-2-acetamido-5-amino-5-oxopentanamido]-3-(2-(3-ethoxy-3-oxopropyl)-1-(pyridin-2-yl)-1H-indol-3-yl)propanoate (244d)

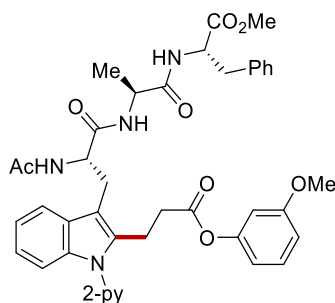


The general procedure **F** was followed using methyl *N*^a-(acetyl-L-glutaminy)-1-(pyridin-2-yl)-L-tryptophanate **243d** (70 mg, 0.15 mmol), ethyl acrylate **22a** (45 mg, 0.45 mmol) and [RuCl₂(*p*-cymene)]₂ (9.2 mg, 10 mol %) in AcOH (0.15 mL). Purification by column chromatography on silica gel (CH₂Cl₂/MeOH: 20/1) yielded **244d** (54 mg, 64%) as a white solid.

M.p.: 206 – 209 °C. **¹H NMR** (300 MHz, CDCl₃): δ 8.65 (d, *J* = 4.7 Hz, 1H), 7.95 (dd, *J* = 7.9, 7.4 Hz, 1H), 7.61–7.58 (m, 2H), 7.52 (d, *J* = 7.9 Hz, 1H), 7.39–7.35 (dd, *J* = 7.4, 4.7 Hz, 1H), 7.30–7.25 (m, 1H), 7.18–7.15 (m, 2H), 6.64 (d, *J* = 6.7 Hz, 1H), 6.32 (s, 1H), 5.61 (s, 1H), 4.95 (ddd, *J* = 6.4, 6.4, 6.4 Hz, 1H), 4.48 (ddd, *J* = 6.7, 6.7, 6.7 Hz, 1H), 4.07 (q, *J* = 7.0, 2H), 3.76 (s, 3H), 3.42 (dd, *J* = 6.4 Hz, 5.5 Hz, 1H), 3.33–3.18 (m, 3H), 2.40–2.22 (m, 4H), 2.11–2.04 (m, 1H), 2.01–1.96 (m, 1H), 1.94 (s, 3H), 1.18 (t, *J* = 7.0 Hz, 3H). **¹³C NMR** (101 MHz, CDCl₃): δ 175.2 (C_q), 172.9 (C_q), 172.6 (C_q), 171.3 (C_q), 170.1 (C_q), 151.2 (C_q), 149.8 (CH), 138.7 (CH), 136.91 (C_q), 136.90 (C_q), 128.2 (C_q), 122.5 (CH), 122.4 (CH), 121.1 (CH), 120.8 (CH), 118.5 (CH), 110.0 (CH), 109.3 (C_q), 60.8 (CH₂), 52.9 (CH), 52.5 (CH₃), 52.2 (CH), 33.4 (CH₂), 31.6 (CH₂), 29.0 (CH₂), 26.8 (CH₂), 23.1 (CH₃), 20.1 (CH₂), 14.1 (CH₃). **IR** (ATR): 3394, 3280, 3226, 3064, 2952, 1734, 1687, 1633, 1585, 1539. **MS** (ESI): *m/z* (relative intensity) 588 (100) [M+Na]⁺, 566 (20) [M+H]⁺. **HR-MS** (ESI) *m/z* calcd for C₂₉H₃₅N₅O₇Na⁺ [M+Na]⁺: 588.2434, found: 588.2431.

5. Experimental Part

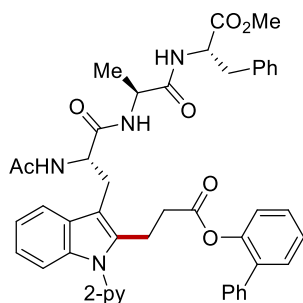
Methyl *N*-acetyl-1-(2-pyridyl)-2-(3-methoxyphenyl propionate-3-yl)-L-tryptophyl-L-alaninyl-L-phenylalaninate (**244e**)



The general procedure **F** was followed using methyl *N*-acetyl-1-(2-pyridyl)-L-tryptophyl-L-alaninyl-L-phenylalaninate **243e** (84.6 mg, 0.15 mmol), 3-methoxyphenyl acrylate **22e** (41 mg, 0.23 mmol) and [RuCl₂(*p*-cymene)]₂ (9.2 mg, 10 mol %) in AcOH (0.15 mL). Purification by column chromatography on silica gel (CH₂Cl₂/MeOH: 40/1 → 30/1 → 20/1) yielded **244e** (58 mg, 53%) as a white solid.

M.p.: 202 – 204 °C. **¹H NMR** (300 MHz, CDCl₃): δ 8.63 (ddd, *J* = 4.9, 2.0, 0.8 Hz, 1H), 7.90 (ddd, *J* = 8.0, 7.4, 2.0 Hz, 1H), 7.72–7.63 (m, 1H), 7.55 (d, *J* = 8.0 Hz, 1H), 7.37–7.08 (m, 8H), 7.07–7.00 (m, 2H), 6.70 (ddd, *J* = 8.2, 2.2, 0.9 Hz, 1H), 6.64–6.53 (m, 3H), 6.51 (ddd, *J* = 8.2, 2.2, 0.9 Hz, 1H), 6.41 (dd, *J* = 2.2, 2.2 Hz, 1H), 4.80 (ddd, *J* = 7.1, 7.1, 7.1 Hz, 1H), 4.65 (ddd, *J* = 7.8, 6.2, 6.2 Hz, 1H), 4.33 (dq, *J* = 7.0, 7.0 Hz, 1H), 3.65 (s, 3H), 3.64 (s, 3H), 3.42–3.12 (m, 4H), 2.98 (d, *J* = 6.2 Hz, 2H), 2.69 (ddd, *J* = 16.6, 7.2, 6.1 Hz, 1H), 2.56 (ddd, *J* = 16.6, 7.7, 7.7 Hz, 1H), 1.83 (s, 3H), 1.17 (d, *J* = 7.1 Hz, 3H). **¹³C NMR** (126 MHz, CDCl₃): δ 171.5 (C_q), 171.4 (C_q), 171.0 (C_q), 170.2 (C_q), 160.3 (C_q), 151.3 (C_q), 151.2 (C_q), 149.6 (CH), 138.5 (CH), 136.8 (C_q), 136.3 (C_q), 135.8 (C_q), 129.6 (CH), 129.1 (CH), 128.5 (CH), 128.3 (C_q), 127.0 (CH), 122.6 (CH), 122.3 (CH), 121.1 (CH), 120.8 (CH), 118.8 (CH), 113.6 (CH), 111.9 (CH), 110.2 (C_q), 110.0 (CH), 107.3 (CH), 55.4 (CH₃), 53.7 (CH), 53.4 (CH), 52.3 (CH₃), 49.0 (CH), 37.8 (CH₂), 33.7 (CH₂), 27.6 (CH₂), 23.0 (CH₃), 20.4 (CH₂), 18.2 (CH₃). **IR** (ATR): 2919, 1748, 1628, 1541, 1521, 1472, 1141, 744 cm⁻¹. **MS** (ESI): *m/z* (relative intensity) 756 (100) [M+Na]⁺, 734 (76) [M+H]⁺. **HR-MS** (ESI): *m/z* calcd for C₄₁H₄₄N₅O₈⁺ [M+H]⁺: 734.3184, found: 734.3178.

Methyl *N*-acetyl-1-(2-pyridyl)-2-(2-phenylphenyl propionate-3-yl)-L-tryptophyl-L-alaninyl-L-phenylalaninate (244f)

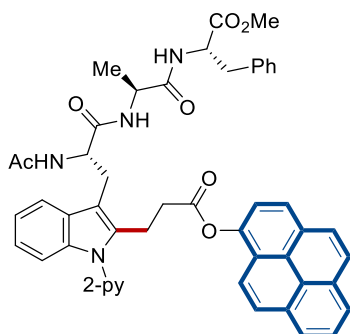


The general procedure **F** was followed using methyl *N*-acetyl-1-(2-pyridyl)-L-tryptophyl-L-alaninyl-L-phenylalaninate **243e** (84.6 mg, 0.15 mmol), 2-phenylphenyl acrylate **22f** (52 mg, 0.23 mmol) and [RuCl₂(*p*-cymene)]₂ (9.2 mg, 10 mol %) in AcOH (0.15 mL). Purification by column chromatography on silica gel (CH₂Cl₂/MeOH: 40/1 → 30/1 → 20/1) yielded **244f** (69 mg, 59%) as a white solid.

M.p.: 206 – 209 °C. **¹H NMR** (300 MHz, CDCl₃): δ 8.52 (ddd, *J* = 4.9, 2.0, 0.8 Hz, 1H), 7.85 (ddd, *J* = 8.0, 7.5, 2.0 Hz, 1H), 7.71–7.60 (m, 1H), 7.43 (ddd, *J* = 8.0, 1.0, 1.0 Hz, 1H), 7.35–7.22 (m, 10H), 7.22–7.17 (m, 3H), 7.16–7.08 (m, 2H), 7.07–6.90 (m, 3H), 6.71–6.59 (m, 3H), 4.78 (ddd, *J* = 7.0, 7.0, 7.0 Hz, 1H), 4.64 (ddd, *J* = 7.7, 6.3, 6.3 Hz, 1H), 4.35 (dq, *J* = 7.0, 7.0 Hz, 1H), 3.62 (s, 3H), 3.41–3.01 (m, 4H), 3.02–2.95 (m, 2H), 2.54–2.33 (m, 2H), 1.82 (s, 3H), 1.17 (d, *J* = 7.0 Hz, 3H). **¹³C NMR** (126 MHz, CDCl₃): δ 171.5 (C_q), 171.3 (C_q), 171.1 (C_q), 171.0 (C_q), 170.2 (C_q), 151.1 (C_q), 149.5 (CH), 147.4 (C_q), 138.4 (CH), 137.3 (C_q), 136.8 (C_q), 136.3 (C_q), 135.8 (C_q), 134.6 (C_q), 130.7 (CH), 129.1 (CH), 128.6 (CH), 128.4 (CH), 128.4 (CH), 128.2 (C_q), 128.1 (CH), 127.3 (CH), 127.0 (CH), 126.3 (CH), 122.7 (CH), 122.5 (CH), 122.1 (CH), 121.0 (CH), 120.8 (CH), 118.8 (CH), 110.0 (C_q), 109.9 (CH), 53.6 (CH), 53.4 (CH), 52.2 (CH₃), 49.0 (CH), 37.8 (CH₂), 33.6 (CH₂), 27.6 (CH₂), 23.0 (CH₃), 20.1 (CH₂), 18.3 (CH₃). **IR** (ATR): 2923, 2853, 1748, 1683, 1637, 1507, 1473, 1188, 742 cm⁻¹. **MS** (ESI): *m/z* (relative intensity) 1582 (19) [2M+Na]⁺, 802 (100) [M+Na]⁺, 780 (66) [M+H]⁺. **HR-MS** (ESI): *m/z* calcd for C₄₆H₄₆N₅O₇⁺ [M+H]⁺: 780.3392, found: 780.3380.

5. Experimental Part

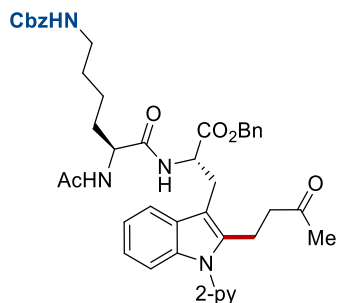
Methyl *N*-acetyl-1-(2-pyridyl)-2-(1-pyrenyl propionate-3-yl)-*L*-tryptophyl-*L*-alaninyl-*L*-phenylalaninate (**244h**)



The general procedure **F** was followed using methyl *N*-acetyl-1-(2-pyridyl)-*L*-tryptophyl-*L*-alaninyl-*L*-phenylalaninate **243e** (84.6 mg, 0.15 mmol), pyren-1-yl acrylate **22j** (62 mg, 0.23 mmol) and [RuCl₂(*p*-cymene)]₂ (9.2 mg, 10 mol %) in AcOH (0.15 mL). Purification by column chromatography on silica gel (hexanes/EtOAc: 1/1 → 1/2) yielded **244h** (66 mg, 53%) as a white solid.

M.p.: 237 °C (decomposition). **¹H NMR** (300 MHz, CDCl₃): δ 8.73 (dd, *J* = 5.2, 1.8 Hz, 1H), 8.23–7.92 (m, 7H), 7.84–7.71 (m, 2H), 7.71–7.58 (m, 3H), 7.45–7.35 (m, 2H), 7.27–7.15 (m, 5H), 7.06–6.91 (m, 2H), 6.69–6.53 (m, 3H), 4.87 (ddd, *J* = 7.0, 7.0, 7.0 Hz, 1H), 4.66 (ddd, *J* = 6.7, 6.7, 6.7 Hz, 1H), 4.35 (dq, *J* = 7.0, 7.0 Hz, 1H), 3.64 (s, 3H), 3.58–3.45 (m, 2H), 3.43–3.18 (m, 2H), 3.09–2.83 (m, 4H), 1.66 (s, 3H), 1.14 (d, *J* = 6.9 Hz, 3H). **¹³C NMR** (75 MHz, CDCl₃): δ 172.2 (C_q), 171.7 (C_q), 171.3 (C_q), 171.2 (C_q), 170.5 (C_q), 151.5 (C_q), 149.8 (CH), 144.1 (C_q), 138.7 (CH), 137.1 (C_q), 136.4 (C_q), 135.8 (C_q), 131.1 (C_q), 130.9 (C_q), 129.4 (C_q), 129.1 (CH), 128.5 (C_q), 128.5 (CH), 128.2 (CH), 127.2 (CH), 127.1 (CH), 127.0 (CH), 126.4 (CH), 125.5 (CH), 125.5 (C_q), 125.3 (CH), 124.9 (CH), 124.4 (C_q), 123.0 (C_q), 122.8 (CH), 122.5 (CH), 121.3 (CH), 121.1 (CH), 120.0 (CH), 119.6 (CH), 119.1 (CH), 110.7 (C_q), 110.2 (CH), 53.7 (CH), 53.3 (CH), 52.2 (CH₃), 49.0 (CH), 37.7 (CH₂), 33.7 (CH₂), 27.6 (CH₂), 22.8 (CH₃), 20.5 (CH₂), 18.1 (CH₃). **IR** (ATR): 3050, 2949, 2929, 1760, 1748, 1625, 1472, 1210, 848, 741 cm⁻¹. **MS** (ESI): *m/z* (relative intensity) 1677 (54) [2M+Na]⁺, 850 (100) [M+Na]⁺, 828 (86) [M+H]⁺. **HR-MS** (ESI): *m/z* calcd for C₅₀H₄₆N₅O₇⁺ [M+H]⁺: 828.3392, found: 828.3393.

Benzyl (S)-2-({S}-2-acetamido-6-[(benzyloxy)carbonyl]amino)hexanamido)-3-[2-(3-oxobutyl)-1-(pyridin-2-yl)-1H-indol-3-yl]propanoate (246a)

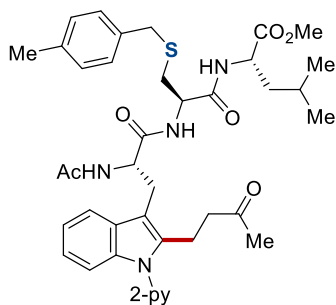


The general procedure **F** was followed using benzyl *N*^a-{*N*²-acetyl-*N*⁶-[(benzyloxy)carbonyl]-L-lysyl}1-(pyridin-2-yl)-L-tryptophanate **243g** (99 mg, 0.15 mmol), but-3-en-2-one **245** (32 mg, 0.45 mmol) and [RuCl₂(*p*-cymene)]₂ (9.2 mg, 10 mol %) in AcOH (0.45 mL). Purification by column chromatography on silica gel (CH₂Cl₂/MeOH: 40/1) yielded **246a** (82 mg, 73%) as a white solid.

M.p.: 178 – 180 °C. **¹H NMR** (600 MHz, CDCl₃): δ 8.60 (dd, *J* = 5.0, 1.9 Hz, 1H), 7.89 (ddd, *J* = 7.7, 7.7, 1.9 Hz, 1H), 7.57–7.50 (m, 1H), 7.38 (d, *J* = 7.9 Hz, 1H), 7.35–7.16 (m, 12H), 7.15–7.07 (m, 2H), 7.02–6.96 (m, 1H), 6.21 (d, *J* = 7.1 Hz, 1H), 5.16–5.00 (m, 5H), 4.95 (ddd, *J* = 7.0, 7.0, 7.0 Hz, 1H), 4.39 (ddd, *J* = 7.1, 7.1, 7.1 Hz, 1H), 3.34 (dd, *J* = 14.8, 6.1 Hz, 1H), 3.27 (dd, *J* = 14.8, 7.6 Hz, 1H), 3.15–3.06 (m, 4H), 2.57–2.34 (m, 2H), 1.96 (s, 3H), 1.87 (s, 3H), 1.79–1.69 (m, 1H), 1.60–1.51 (m, 1H), 1.48–1.35 (m, 2H), 1.32–1.24 (m, 2H). **¹³C NMR** (126 MHz, CDCl₃): δ 208.0 (C_q), 171.7 (C_q), 171.5 (C_q), 169.7 (C_q), 156.4 (C_q), 151.1 (C_q), 149.6 (CH), 138.5 (CH), 137.2 (C_q), 136.8 (C_q), 136.6 (C_q), 135.1 (C_q), 128.4 (CH), 128.4 (CH), 128.2 (CH), 128.2 (CH), 128.2 (C_q), 127.9 (CH), 127.9 (CH), 122.4 (CH), 122.3 (CH), 121.0 (CH), 120.8 (CH), 118.4 (CH), 109.9 (CH), 109.0 (C_q), 67.4 (CH₂), 66.5 (CH₂), 52.9 (CH), 52.5 (CH), 42.7 (CH₂), 40.4 (CH₂), 32.2 (CH₂), 30.0 (CH₃), 29.3 (CH₂), 27.1 (CH₂), 23.2 (CH₃), 22.0 (CH₂), 19.0 (CH₂). **IR** (ATR): 3297, 2934, 1712, 1649, 1530, 1471, 1438, 1264, 1246, 735 cm⁻¹. **MS** (ESI): *m/z* (relative intensity): 784 (65) [M+K]⁺, 769 (96) [M+Na]⁺, 746 (100) [M+H]⁺. **HR-MS** (ESI): *m/z* calcd for C₄₃H₄₈N₅O₇⁺ [M+H]⁺: 746.3548, found: 746.3540.

5. Experimental Part

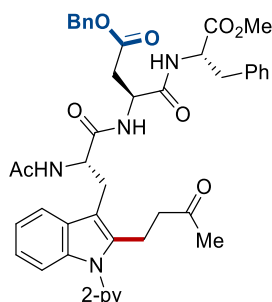
Methyl *N*-{[*S*]-2-acetamido-3-[2-(3-oxobutyl)-1-(pyridin-2-yl)-1*H*-indol-3-yl]propanoyl}-*S*-(4-methylbenzyl)-*L*-cysteinyl-*L*-leucinate (**246b**)



The general procedure **F** was followed using methyl methyl *N*-[*N*^a-acetyl-1-(pyridin-2-yl)-*L*-tryptophyl]-*S*-(4-methylbenzyl)-*L*-cysteinyl-*L*-leucinate **243h** (97 mg, 150 μ mol), but-3-en-2-one **245** (32 mg, 0.45 mmol) and [RuCl₂(*p*-cymene)]₂ (9.2 mg, 10 mol %) in AcOH (0.30 mL). Purification by column chromatography on silica gel (CH₂Cl₂/MeOH: 40/1 \rightarrow 30/1) yielded **246b** (96 mg, 88%) as a white solid.

M.p.: 143 – 145 °C. **¹H NMR** (600 MHz, CDCl₃): δ 8.64–8.51 (m, 1H), 7.89 (ddd, *J* = 7.7, 7.7, 1.9 Hz, 1H), 7.69–7.60 (m, 1H), 7.49 (d, *J* = 7.9 Hz, 1H), 7.33 (ddd, *J* = 7.5, 4.8, 1.0 Hz, 1H), 7.23–7.19 (m, 1H), 7.17 (d, *J* = 7.8 Hz, 2H), 7.12–7.06 (m, 2H), 7.06 (d, *J* = 7.8 Hz, 2H), 6.94–6.89 (m, 2H), 6.79 (d, *J* = 6.5 Hz, 1H), 4.79 (ddd, *J* = 6.5, 6.5, 6.5 Hz, 1H), 4.49–4.35 (m, 2H), 3.68–3.65 (m, 5H), 3.30 (dd, *J* = 14.7, 7.0 Hz, 1H), 3.23 (dd, *J* = 14.7, 6.9 Hz, 1H), 3.10 (dd, *J* = 7.1, 7.1 Hz, 2H), 2.89 (dd, *J* = 14.1, 4.9 Hz, 1H), 2.63–2.43 (m, 3H), 2.28 (s, 3H), 1.98 (s, 3H), 1.94 (s, 3H), 1.71–1.47 (m, 3H), 0.90 (d, *J* = 5.9 Hz, 3H), 0.85 (d, *J* = 5.9 Hz, 3H). **¹³C NMR** (126 MHz, CDCl₃): δ 207.9 (C_q), 172.5 (C_q), 171.2 (C_q), 170.5 (C_q), 169.5 (C_q), 151.3 (C_q), 149.5 (CH), 138.4 (CH), 137.1 (C_q), 136.8 (C_q), 136.6 (C_q), 134.9 (C_q), 129.1 (CH), 128.8 (CH), 128.2 (C_q), 122.3 (CH), 122.2 (CH), 121.3 (CH), 120.7 (CH), 118.5 (CH), 109.9 (CH), 109.4 (C_q), 54.1 (CH), 52.3 (CH), 52.2 (CH), 51.3 (CH₃), 42.7 (CH₂), 40.8 (CH₂), 36.4 (CH₂), 33.7 (CH₂), 30.0 (CH₃), 27.5 (CH₂), 24.8 (CH), 23.1 (CH₃), 22.8 (CH₃), 21.9 (CH₃), 21.1 (CH₃), 19.1 (CH₂). **IR** (ATR): 3283, 2955, 1743, 1713, 1640, 1542, 1460, 1437, 1204, 738 cm⁻¹. **MS** (ESI): *m/z* (relative intensity): 1477 (12) [2M+Na]⁺, 750 (89) [M+Na]⁺, 728 (100) [M+H]⁺. **HR-MS** (ESI): *m/z* calcd for C₄₀H₅₀N₅O₆S⁺ [M+H]⁺: 728.3476, found: 728.3473.

Benzyl (S)-3-{[S]-2-acetamido-3-[2-(3-oxobutyl)-1-(pyridin-2-yl)-1H-indol-3-yl]propanamido}-4-[(S)-1-methoxy-1-oxo-3-phenylpropan-2-yl]amino}-4-oxobutanoate (246c)

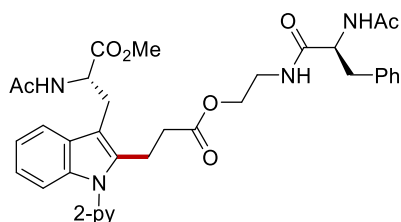


The general procedure **F** was followed using benzyl (S)-3-{[S]-2-acetamido-3-[1-(pyridin-2-yl)-1H-indol-3-yl]propanamido}-4-[(S)-1-methoxy-1-oxo-3-phenylpropan-2-yl]amino}-4-oxobutanoate **243i** (99 mg, 0.15 mmol), but-3-en-2-one **245** (32 mg, 0.45 mmol) and [RuCl₂(*p*-cymene)]₂ (9.2 mg, 10 mol %) in AcOH (0.60 mL). Purification by column chromatography on silica gel (CH₂Cl₂/MeOH: 40/1) yielded **246c** (93 mg, 82%) as a white solid.

M.p.: 96 – 98 °C. **¹H NMR** (600 MHz, CDCl₃): δ 8.60 (d, *J* = 3.2 Hz, 1H), 7.88 (ddd, *J* = 7.7, 7.7, 1.8 Hz, 1H), 7.61 (dd, *J* = 7.2, 1.6 Hz, 1H), 7.47 (d, *J* = 7.9 Hz, 1H), 7.35–7.25 (m, 8H), 7.23–7.18 (m, 2H), 7.13–7.05 (m, 5H), 7.03 (d, *J* = 7.5 Hz, 1H), 6.63 (d, *J* = 6.5 Hz, 1H), 5.03 (d, *J* = 12.3 Hz, 1H), 4.99 (d, *J* = 12.3 Hz, 1H), 4.76–4.66 (m, 2H), 4.61 (ddd, *J* = 7.5, 7.5, 5.9 Hz, 1H), 3.61 (s, 3H), 3.27 (dd, *J* = 14.7, 7.1 Hz, 1H), 3.18 (dd, *J* = 14.7, 6.9 Hz, 1H), 3.11 (t, *J* = 7.2 Hz, 2H), 3.04 (dd, *J* = 14.0, 5.9 Hz, 1H), 2.98 (dd, *J* = 14.0, 7.5 Hz, 1H), 2.90 (dd, *J* = 17.3, 4.1 Hz, 1H), 2.61–2.42 (m, 3H), 1.98 (s, 3H), 1.89 (s, 3H). **¹³C NMR** (126 MHz, CDCl₃): δ 207.7 (C_q), 171.4 (C_q), 171.2 (C_q), 171.2 (C_q), 170.5 (C_q), 169.4 (C_q), 151.2 (C_q), 149.5 (CH), 138.4 (CH), 137.1 (C_q), 136.8 (C_q), 136.0 (C_q), 135.2 (C_q), 129.1 (CH), 128.4 (CH), 128.4 (CH), 128.2 (C_q), 128.2 (CH), 128.0 (CH), 126.9 (CH), 122.4 (CH), 122.3 (CH), 121.2 (CH), 120.8 (CH), 118.5 (CH), 109.9 (CH), 109.4 (C_q), 66.7 (CH₂), 54.1 (CH), 53.8 (CH), 52.2 (CH₃), 49.1 (CH), 42.7 (CH₂), 37.5 (CH₂), 35.8 (CH₂), 30.0 (CH₃), 27.2 (CH₂), 23.0 (CH₃), 19.0 (CH₂). **IR** (ATR): 3296, 3061, 2950, 1738, 1715, 1643, 1526, 1471, 1169, 742 cm⁻¹. **MS** (ESI): *m/z* (relative intensity) 1542 (29) [2M+Na]⁺, 782 (100) [M+Na]⁺, 760 (82) [M+H]⁺. **HR-MS** (ESI): *m/z* calcd for C₄₃H₄₆N₅O₈⁺ [M+H]⁺: 760.3341, found: 760.3338.

5. Experimental Part

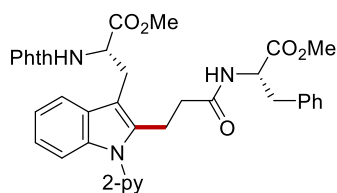
Methyl *N*-acetyl-1-(2-pyridyl)-2-[[*N*-acetylphenylalaninyl]-2-aminoethane-1-yl] propionate-3-yl]-*L*-tryptophanate (**248a**)



The general procedure **G** was followed using methyl acetyl-1-(2-pyridyl)-*L*-tryptophanate **241a** (50.6 mg, 0.15 mmol), *N*-acetyl-*L*-phenylalaninyl-2-aminoethane-1-yl acrylate **247a** (46 mg, 0.17 mmol) and [RuCl₂(*p*-cymene)]₂ (9.2 mg, 10 mol %) in AcOH (0.15 mL). Purification by column chromatography on silica gel (CH₂Cl₂/MeOH: 40/1 → 30/1) yielded **248a** (64 mg, 67%) as a white solid.

M.p.: 145 – 146 °C. **¹H NMR** (400 MHz, CDCl₃): δ 8.64 (ddd, *J* = 4.9, 2.0, 0.8 Hz, 1H), 7.94–7.84 (m, 1H), 7.53–7.45 (m, 1H), 7.43 (dd, *J* = 8.0, 0.9 Hz, 1H), 7.33 (ddd, *J* = 7.5, 4.9, 1.0 Hz, 1H), 7.30–7.26 (m, 1H), 7.24–7.18 (m, 2H), 7.18–7.09 (m, 6H), 6.70 (d, *J* = 8.0 Hz, 1H), 6.57 (d, *J* = 8.1 Hz, 1H), 4.84 (ddd, *J* = 7.8, 6.4, 6.4 Hz, 1H), 4.69 (ddd, *J* = 8.0, 6.9, 6.9 Hz, 1H), 4.11–3.82 (m, 2H), 3.62 (s, 3H), 3.40 (dddd, *J* = 14.4, 6.2, 6.2, 3.2 Hz, 1H), 3.34–3.26 (m, 2H), 3.25–3.10 (m, 3H), 3.09–2.93 (m, 2H), 2.43–2.21 (m, 2H), 1.97 (s, 3H), 1.94 (s, 3H). **¹³C NMR** (126 MHz, CDCl₃): δ 172.7 (C_q), 171.9 (C_q), 171.2 (C_q), 170.1 (C_q), 169.7 (C_q), 151.0 (C_q), 149.7 (CH), 138.5 (CH), 136.6 (C_q), 136.6 (C_q), 136.5 (C_q), 129.1 (CH), 128.3 (C_q), 128.3 (CH), 126.7 (CH), 122.4 (CH), 122.3 (CH), 120.7 (CH), 118.2 (CH), 110.0 (CH), 109.4 (C_q), 63.4 (CH₂), 54.4 (CH), 53.3 (CH), 52.5 (CH₃), 38.8 (CH₂), 38.5 (CH₂), 34.3 (CH₂), 27.5 (CH₂), 23.1 (CH₃), 23.1 (CH₃), 20.7 (CH₂). **IR** (ATR): 3062, 2951, 1735, 1650, 1541, 1471, 1458, 1225, 1174, 745 cm⁻¹. **MS** (ESI): *m/z* (relative intensity) 664 (74) [M+Na]⁺, 642 (100) [M+H]⁺, 341 (31). **HR-MS** (ESI): *m/z* calcd for C₃₅H₄₀N₅O₇⁺ [M+H]⁺: 642.2922, found: 642.2917.

Methyl (S)-2-(1,3-dioxisoindolin-2-yl)-3-[2-(3-((S)-1-methoxy-1-oxo-3-phenylpropan-2-yl)amino)-3-oxopropyl)-1-(pyridin-2-yl)-1H-indol-3-yl]propanoate (248b)

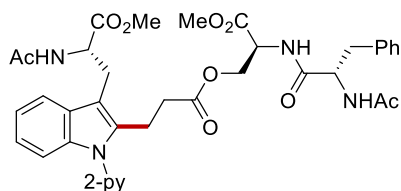


The general procedure **G** was followed using methyl (S)-2-(1,3-dioxisoindolin-2-yl)-3-[1-(pyridin-2-yl)-1H-indol-3-yl]propanoate **241c** (64 mg, 0.15 mmol), methyl acryloyl-L-phenylalaninate **247b** (70 mg, 0.30 mmol) and $[\text{RuCl}_2(p\text{-cymene})]_2$ (9.2 mg, 10 mol %) in AcOH (0.45 mL). Purification by column chromatography on silica gel (EtOAc) yielded **248b** (52.3 mg, 53%) as a white solid.

M.p.: 178 – 180 °C. **$^1\text{H NMR}$** (400 MHz, CDCl_3): δ 8.55 (dd, $J = 5.0, 1.8$ Hz, 1H), 7.86 (ddd, $J = 7.7, 7.7, 2.0$ Hz, 1H), 7.76–7.68 (m, 2H), 7.69–7.62 (m, 2H), 7.61–7.55 (m, 1H), 7.35–7.30 (m, 2H), 7.26–7.18 (m, 4H), 7.10–7.02 (m, 4H), 6.29 (d, $J = 7.8$ Hz, 1H), 5.32 (dd, $J = 9.7, 5.9$ Hz, 1H), 4.84 (ddd, $J = 7.8, 6.0, 6.0$ Hz, 1H), 3.82 (s, 3H), 3.79–3.68 (m, 2H), 3.65 (s, 3H), 3.24–3.16 (m, 2H), 3.12 (dd, $J = 13.9, 5.9$ Hz, 1H), 3.05 (dd, $J = 13.9, 6.1$ Hz, 1H), 2.37–2.27 (m, 1H), 2.27–2.16 (m, 1H). **$^{13}\text{C NMR}$** (101 MHz, CDCl_3): δ 172.0 (C_q), 171.3 (C_q), 169.5 (C_q), 167.6 (C_q), 151.2 (C_q), 149.6 (CH), 138.5 (CH), 137.0 (C_q), 136.7 (C_q), 136.0 (C_q), 134.0 (CH), 131.7 (C_q), 129.2 (CH), 128.4 (CH), 128.2 (C_q), 126.9 (CH), 123.4 (CH), 122.3 (CH), 122.2 (CH), 121.0 (CH), 120.6 (CH), 118.3 (CH), 110.0 (CH), 109.7 (C_q), 53.0 (CH), 52.9 (CH_3), 52.4 (CH_3), 52.1 (CH), 37.9 (CH_2), 36.3 (CH_2), 24.5 (CH_2), 21.4 (CH_2). **IR** (ATR): 3057, 2952, 1742, 1713, 1672, 1436, 1388, 1368, 1204, 731 cm^{-1} . **MS** (ESI): m/z (relative intensity) 681 (100) $[\text{M}+\text{Na}]^+$, 659 (59) $[\text{M}+\text{H}]^+$. **HR-MS** (ESI): m/z calcd for $\text{C}_{38}\text{H}_{35}\text{N}_4\text{O}_7^+$ $[\text{M}+\text{H}]^+$: 659.2500, found: 659.2508.

5. Experimental Part

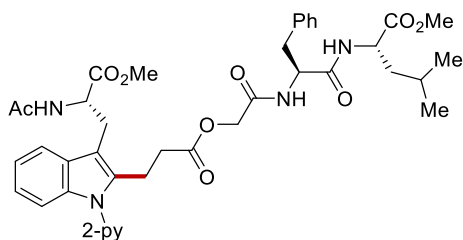
Methyl (*N*-acetyl-1-(2-pyridyl)-2-[[methyl (acetyl-L-phenylalanyl)-L-alanine-3-yl] propionate-3-yl]-L-tryptophanate) (**248c**)



The general procedure **G** was followed using methyl acetyl-1-(2-pyridyl)-L-tryptophanate **241a** (50.6 mg, 0.15 mmol), [methyl (*N*-acetyl-L-phenylalaninyl)-L-alaninate-3-yl] acrylate **247c** (60 mg, 0.17 mmol) and [RuCl₂(*p*-cymene)]₂ (9.2 mg, 10 mol %) in AcOH (0.15 mL). Purification by column chromatography on silica gel (CH₂Cl₂/MeOH: 40/1 → 30/1 → 20/1) yielded **248c** (67 mg, 64%) as a white solid.

M.p.: 116 – 118 °C. **¹H NMR** (600 MHz, CDCl₃): δ 8.67–8.56 (m, 1H), 7.89 (ddd, *J* = 7.7, 7.7, 1.9 Hz, 1H), 7.53–7.47 (m, 1H), 7.43 (ddd, *J* = 8.0, 0.9, 0.9 Hz, 1H), 7.39 (d, *J* = 7.5 Hz, 1H), 7.33 (ddd, *J* = 7.4, 4.9, 0.9 Hz, 1H), 7.28–7.25 (m, 1H), 7.26–7.21 (m, 2H), 7.20–7.10 (m, 5H), 6.59 (d, *J* = 7.9 Hz, 1H), 6.49 (d, *J* = 8.0 Hz, 1H), 4.89 (ddd, *J* = 7.9, 6.5, 6.5 Hz, 1H), 4.80 (ddd, *J* = 8.0, 6.7, 6.7 Hz, 1H), 4.75 (ddd, *J* = 7.5, 3.6, 3.6 Hz, 1H), 4.35 (dd, *J* = 8.2, 3.7 Hz, 1H) 4.33 (dd, *J* = 8.2, 3.7 Hz, 1H), 3.69 (s, 3H), 3.62 (s, 3H), 3.36–3.25 (m, 2H), 3.19–3.11 (m, 3H), 2.99 (dd, *J* = 14.0, 7.1 Hz, 1H), 2.50–2.28 (m, 2H), 1.97 (s, 3H), 1.92 (s, 3H). **¹³C NMR** (126 MHz, CDCl₃): δ 172.8 (C_q), 171.6 (C_q), 171.0 (C_q), 170.1 (C_q), 170.0 (C_q), 169.2 (C_q), 150.9 (C_q), 149.6 (CH), 138.5 (CH), 136.7 (C_q), 136.5 (C_q), 136.4 (C_q), 129.2 (CH), 128.4 (C_q), 128.4 (CH), 126.7 (CH), 122.5 (CH), 122.3 (CH), 120.8 (CH), 120.8 (CH), 118.3 (CH), 110.0 (CH), 109.3 (C_q), 63.7 (CH₂), 54.0 (CH), 53.0 (CH), 52.8 (CH₃), 52.5 (CH₃), 51.8 (CH), 38.1 (CH₂), 34.3 (CH₂), 27.4 (CH₂), 23.2 (CH₃), 23.1 (CH₃), 20.6 (CH₂). **IR** (ATR): 3054, 2953, 1742, 1653, 1541, 1458, 1222, 744 cm⁻¹. **MS** (ESI): *m/z* (relative intensity) 722 (100) [M+Na]⁺, 700 (49) [M+H]⁺, 426 (30). **HR-MS** (ESI): *m/z* calcd for C₃₇H₄₂N₅O₉⁺ [M+H]⁺: 700.2977, found: 700.2971.

Methyl ([methyl *N*-acetyl-1-(2-pyridyl)-*L*-tryptophanate-2-yl]-3-propanoate-3-yl)methylcarbonyl [*L*-phenylalanyl-*L*-leucinate]) (248d)

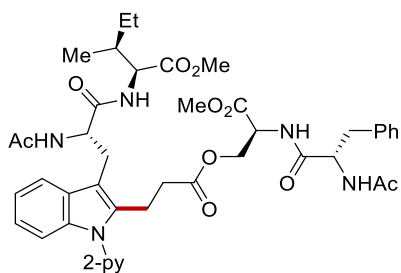


The general procedure **G** was followed using methyl acetyl-1-(2-pyridyl)-*L*-tryptophanate **241a** (50.6 mg, 0.15 mmol), methyl [2-(acryloyloxy)acetyl]-*L*-phenylalanyl-*L*-leucinate **247d** (67 mg, 0.17 mmol) and [RuCl₂(*p*-cymene)]₂ (9.2 mg, 10 mol %) in AcOH (0.15 mL). Purification by column chromatography on silica gel (CH₂Cl₂/MeOH: 40/1 → 20/1) yielded **248d** (68 mg, 61%) as a white solid.

M.p.: 179 – 180 °C. **¹H NMR** (600 MHz, CDCl₃): δ 8.65–8.62 (m, 1H), 7.91 (ddd, *J* = 7.7, 7.7, 1.7 Hz, 1H), 7.54–7.49 (m, 1H), 7.46 (d, *J* = 7.9 Hz, 1H), 7.34 (dd, *J* = 7.4, 4.9 Hz, 1H), 7.28–7.25 (m, 1H), 7.25–7.20 (m, 2H), 7.19–7.11 (m, 5H), 7.08 (d, *J* = 7.6 Hz, 1H), 6.41 (d, *J* = 7.8 Hz, 1H), 6.31 (d, *J* = 7.8 Hz, 1H), 4.91 (ddd, *J* = 7.6, 7.6, 7.6 Hz, 1H), 4.63 (ddd, *J* = 7.8, 7.8, 7.8 Hz, 1H), 4.51–4.37 (m, 3H), 3.67 (s, 3H), 3.63 (s, 3H), 3.33 (dd, *J* = 14.7, 6.9 Hz, 1H), 3.28 (dd, *J* = 14.7, 5.6 Hz, 1H), 3.25–3.13 (m, 2H), 3.09–2.97 (m, 2H), 2.54–2.40 (m, 2H), 1.94 (s, 3H), 1.60–1.39 (m, 3H), 0.85 (d, *J* = 6.3 Hz, 6H). **¹³C NMR** (126 MHz, CDCl₃): δ 172.5 (C_q), 172.4 (C_q), 170.9 (C_q), 170.0 (C_q), 169.9 (C_q), 166.8 (C_q), 150.9 (C_q), 149.7 (CH), 138.6 (CH), 136.6 (C_q), 136.3 (C_q), 136.3 (C_q), 129.2 (CH), 128.5 (C_q), 128.5 (CH), 126.9 (CH), 122.5 (CH), 122.4 (CH), 120.8 (CH), 120.8 (CH), 118.4 (CH), 110.1 (CH), 109.6 (C_q), 62.8 (CH₂), 54.2 (CH), 53.0 (CH), 52.4 (CH₃), 52.2 (CH₃), 51.0 (CH), 41.3 (CH₂), 37.7 (CH₂), 33.8 (CH₂), 27.5 (CH₂), 24.8 (CH), 23.2 (CH₃), 22.7 (CH₃), 22.0 (CH₃), 20.4 (CH₂). **IR** (ATR): 2956, 1743, 1654, 1541, 1472, 1478, 1159, 745 cm⁻¹. **MS** (ESI): *m/z* (relative intensity) 764 (100) [M+Na]⁺, 742 (78) [M+H]⁺. **HR-MS** (ESI): *m/z* calcd for C₄₀H₄₈N₅O₉⁺ [M+H]⁺: 742.3447, found: 742.3437.

5. Experimental Part

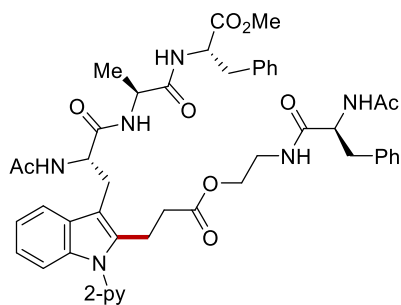
Methyl (*N*-acetyl-1-(2-pyridyl)-2-[[methyl (acetyl-L-phenylalanyl)-L-alanine-3-yl] propionate-3-yl]-L-tryptophyl-L-isoleucinate) (**249a**)



The general procedure **G** was followed using methyl *N*-acetyl-1-(2-pyridyl)-L-tryptophyl-L-isoleucinate **243a** (67.5 mg, 0.15 mmol), [methyl (*N*-acetyl-L-phenylalaninyl)-L-alanine-3-yl] acrylate **247c** (60 mg, 0.17 mmol) and [RuCl₂(*p*-cymene)]₂ (9.2 mg, 10 mol %) in AcOH (0.30 mL). Purification by column chromatography on silica gel (CH₂Cl₂/MeOH: 40/1 → 30/1 → 20/1) yielded **249a** (68 mg, 56%) as a white solid.

M.p.: 135 – 137 °C. **¹H NMR** (600 MHz, CDCl₃): δ 8.63 (ddd, *J* = 4.9, 2.0, 0.8 Hz, 1H), 7.89 (ddd, *J* = 7.7, 7.7, 1.9 Hz, 1H), 7.82 (d, *J* = 8.0 Hz, 1H), 7.58–7.55 (m, 1H), 7.49 (dd, *J* = 8.0, 1.0 Hz, 1H), 7.32 (ddd, *J* = 7.7, 4.8, 1.0 Hz, 1H), 7.30–7.27 (m, 1H), 7.25–7.17 (m, 3H), 7.17–7.10 (m, 4H), 6.88 (d, *J* = 8.0 Hz, 1H), 6.61–6.54 (m, 2H), 4.90 (ddd, *J* = 6.9, 6.9, 6.9 Hz, 1H), 4.88–4.79 (m, 2H), 4.42 (dd, *J* = 11.3, 4.4 Hz, 1H), 4.38 (dd, *J* = 8.4, 5.0 Hz, 1H), 4.34 (dd, *J* = 11.3, 3.2 Hz, 1H), 3.74 (s, 3H), 3.44 (s, 3H), 3.30–3.09 (m, 5H), 3.00 (dd, *J* = 14.0, 6.8 Hz, 1H), 2.48 (ddd, *J* = 15.6, 9.2, 6.0 Hz, 1H), 2.37 (ddd, *J* = 15.6, 9.1, 6.5 Hz, 1H), 1.97 (s, 3H), 1.94 (s, 3H), 1.77–1.69 (m, 1H), 1.37–1.24 (m, 1H), 1.05 (ddq, *J* = 14.4, 9.3, 7.4 Hz, 1H), 0.82 (t, *J* = 7.4 Hz, 3H), 0.77 (d, *J* = 6.8 Hz, 3H). **¹³C NMR** (126 MHz, CDCl₃): δ 171.9 (C_q), 171.2 (C_q), 171.1 (C_q), 171.0 (C_q), 169.9 (C_q), 169.8 (C_q), 169.6 (C_q), 151.1 (C_q), 149.6 (CH), 138.4 (CH), 136.6 (C_q), 136.6 (C_q), 136.4 (C_q), 129.2 (CH), 128.5 (C_q), 128.3 (CH), 126.7 (CH), 122.3 (CH), 122.1 (CH), 120.9 (CH), 120.8 (CH), 118.2 (CH), 110.0 (CH), 109.7 (C_q), 63.7 (CH₂), 56.6 (CH), 53.9 (CH), 53.8 (CH), 52.8 (CH₃), 51.9 (CH), 51.8 (CH₃), 38.3 (CH), 38.2 (CH₂), 34.3 (CH₂), 28.0 (CH₂), 25.2 (CH₂), 23.3 (CH₃), 23.1 (CH₃), 20.6 (CH₂), 15.2 (CH₃), 11.6 (CH₃). **IR** (ATR): 3050, 2949, 2929, 1744, 1656, 1584, 1458, 1335, 1120, 736 cm⁻¹. **MS** (ESI): *m/z* (relative intensity) 835 (100) [M+Na]⁺, 813 (29) [M+H]⁺, 426 (30). **HR-MS** (ESI): *m/z* calcd for C₄₃H₅₃N₆O₁₀⁺ [M+H]⁺: 813.3818, found 813.3816.

Methyl *N*-acetyl-1-(2-pyridyl)-2-[[*N*-acetylphenylalaninyl]-2-aminoethane-1-yl] propionate-3-yl]-L-tryptophyl-L-alaninyl-L-phenylalaninate (249b**)**

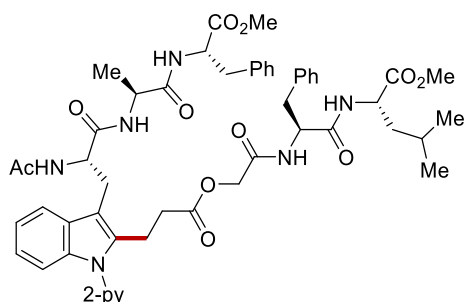


The general procedure **G** was followed using methyl *N*-acetyl-1-(2-pyridyl)-L-tryptophyl-L-alaninyl-L-phenylalaninate **243e** (84.6 mg, 0.15 mmol), *N*-acetyl-L-phenylalaninyl-2-aminoethane-1-yl acrylate **247a** (46 mg, 0.17 mmol) and [RuCl₂(*p*-cymene)]₂ (9.2 mg, 10 mol %) in AcOH (0.15 mL). Purification by column chromatography on silica gel (CH₂Cl₂/MeOH: 40/1 → 20/1) yielded **249b** (67 mg, 52%) as a white solid.

M.p.: 192 °C (decomposition). **¹H NMR** (600 MHz, CDCl₃): δ 8.59 (dd, *J* = 4.8, 1.6 Hz, 1H), 7.85 (ddd, *J* = 7.7, 7.7, 2.0 Hz, 1H), 7.70–7.60 (m, 1H), 7.49 (dd, *J* = 8.0, 1.0 Hz, 1H), 7.39 (dd, *J* = 6.0, 6.0 Hz, 1H), 7.30 (ddd, *J* = 7.5, 4.8, 1.0 Hz, 1H), 7.26–7.23 (m, 2H), 7.22–7.19 (m, 4H), 7.18–7.16 (m, 1H), 7.15–7.10 (m, 5H), 7.04–7.01 (m, 2H), 6.92 (d, *J* = 7.3 Hz, 1H), 6.83–6.77 (m, 2H), 4.80–4.68 (m, 2H), 4.57 (ddd, *J* = 7.7, 6.4, 6.4 Hz, 1H), 4.50 (dq, *J* = 7.0, 7.0 Hz, 1H), 4.05 (ddd, *J* = 11.4, 6.8, 2.9 Hz, 1H), 3.95 (ddd, *J* = 11.4, 6.6, 2.9 Hz, 1H), 3.61 (s, 3H), 3.48–3.39 (m, 1H), 3.37–3.31 (m, 1H), 3.27 (dd, *J* = 14.5, 6.3 Hz, 1H), 3.16–3.00 (m, 4H), 2.99–2.92 (m, 3H), 2.45–2.24 (m, 2H), 1.96 (s, 3H), 1.88 (s, 3H), 1.23 (d, *J* = 7.0 Hz, 3H). **¹³C NMR** (126 MHz, CDCl₃): δ 172.0 (C_q), 171.6 (C_q), 171.5 (C_q), 171.3 (C_q), 171.0 (C_q), 170.1 (C_q), 170.1 (C_q), 151.1 (C_q), 149.6 (CH), 138.4 (CH), 136.8 (C_q), 136.6 (C_q), 136.6 (C_q), 136.5 (C_q), 135.8 (C_q), 129.2 (CH), 129.0 (CH), 128.4 (CH), 128.3 (CH), 127.0 (CH), 126.7 (CH), 122.5 (CH), 122.2 (CH), 121.1 (CH), 120.9 (CH), 118.4 (CH), 110.1 (CH), 109.6 (C_q), 63.5 (CH₂), 54.5 (CH), 54.4 (CH), 53.6 (CH), 52.2 (CH₃), 48.8 (CH), 38.7 (CH₂), 38.5 (CH₂), 37.8 (CH₂), 34.7 (CH₂), 28.0 (CH₂), 23.3 (CH₃), 23.1 (CH₃), 20.7 (CH₂), 19.1 (CH₃). **IR** (ATR): 2957, 2921, 2851, 1734, 1647, 1541, 1457, 1438, 744 cm⁻¹. **MS** (ESI): *m/z* (relative intensity) 882 (100) [M+Na]⁺, 860 (46) [M+H]⁺. **HR-MS** (ESI): *m/z* calcd for C₄₇H₅₄N₇O₉⁺ [M+H]⁺: 860.3978, found: 860.3968.

5. Experimental Part

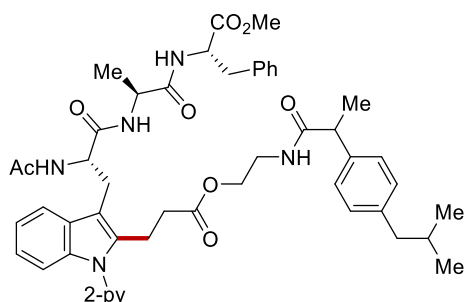
Methyl {[methyl ({[*N*-acetyl-1-(2-pyridyl)-*L*-tryptophyl-2-yl]-3-propanoate-3-yl)methyl-carbonyl [*L*-phenylalanyl-*L*-leucinate]]-*L*-alaninyl-*L*-phenylalaninate} (249c)



The general procedure **G** was followed using methyl *N*-acetyl-1-(2-pyridyl)-*L*-tryptophyl-*L*-alaninyl-*L*-phenylalaninate **243e** (84.6 mg, 0.15 mmol), methyl (2-(acryloyloxy)acetyl)-*L*-phenylalanyl-*L*-leucinate **247d** (67 mg, 0.17 mmol) and [RuCl₂(*p*-cymene)]₂ (9.2 mg, 10 mol %) in AcOH (0.30 mL). Purification by column chromatography on silica gel (CH₂Cl₂/MeOH: 40/1 → 30/1 → 20/1) yielded **249c** (75 mg, 52%) as a white solid.

M.p.: 152 – 154 °C. **¹H NMR** (600 MHz, CDCl₃): δ 8.60 (dd, *J* = 5.0, 1.9 Hz, 1H), 7.88 (ddd, *J* = 7.7, 7.7, 2.0 Hz, 1H), 7.64–7.61 (m, 1H), 7.54–7.49 (m, 1H), 7.35–7.29 (m, 2H), 7.27–7.23 (m, 3H), 7.23–7.16 (m, 7H), 7.12–7.08 (m, 2H), 7.04–6.97 (m, 2H), 6.73 (d, *J* = 7.3 Hz, 1H), 6.66–6.61 (m, 2H), 4.79 (ddd, *J* = 8.0, 8.0, 5.3 Hz, 1H), 4.63 (ddd, *J* = 7.4, 7.4, 7.4 Hz, 1H), 4.60 (ddd, *J* = 7.7, 7.7 Hz, 1H), 4.52–4.43 (m, 2H), 4.41–4.32 (m, 2H), 3.66 (s, 3H), 3.61 (s, 3H), 3.34–3.10 (m, 4H), 3.06 (d, *J* = 7.2 Hz, 2H), 2.94 (d, *J* = 6.2 Hz, 2H), 2.43 (t, *J* = 7.8 Hz, 2H), 1.93 (s, 3H), 1.59–1.48 (m, 2H), 1.45 (ddd, *J* = 12.5, 8.8, 5.1 Hz, 1H), 1.21 (d, *J* = 7.0 Hz, 3H), 0.85 (d, *J* = 6.4 Hz, 6H). **¹³C NMR** (126 MHz, CDCl₃): δ 172.5 (C_q), 171.5 (C_q), 171.2 (C_q), 171.1 (C_q), 170.8 (C_q), 170.3 (C_q), 169.9 (C_q), 167.0 (C_q), 151.1 (C_q), 149.6 (CH), 138.4 (CH), 136.7 (C_q), 136.5 (C_q), 136.3 (C_q), 135.7 (C_q), 129.2 (CH), 129.0 (CH), 128.5 (CH), 128.5 (CH), 128.4 (C_q), 127.1 (CH), 126.9 (CH), 122.5 (CH), 122.2 (CH), 121.1 (CH), 120.8 (CH), 118.6 (CH), 110.1 (CH), 109.8 (C_q), 63.0 (CH₂), 54.5 (CH), 53.8 (CH), 53.4 (CH), 52.3 (CH₃), 52.2 (CH₃), 51.1 (CH), 48.8 (CH), 41.2 (CH₂), 37.8 (CH₂), 37.8 (CH₂), 33.9 (CH₂), 27.8 (CH₂), 24.8 (CH₃), 23.3 (CH₃), 22.7 (CH₃), 22.0 (CH), 20.4 (CH₂), 18.8 (CH₃). **IR** (ATR): 2921, 1745, 1652, 1541, 1473, 1457, 1158, 745 cm⁻¹. **MS** (ESI): *m/z* (relative intensity) 982 (100) [M+Na]⁺, 961 (14) [M+H]⁺. **HR-MS** (ESI): *m/z* calcd for C₅₂H₆₂N₇O₁₁⁺ [M+H]⁺: 961.4502, found: 961.4502.

Methyl *N*-acetyl-1-(2-pyridyl)-2-{2-[2-(4-isobutylphenyl)propanamido]ethyl propionate-3-yl}-L-tryptophyl-L-alaninyl-L-phenylalaninate (249d)



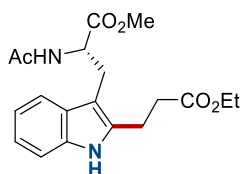
The general procedure **G** was followed using methyl *N*-acetyl-1-(2-pyridyl)-L-tryptophyl-L-alaninyl-L-phenylalaninate **243c** (84.6 mg, 0.15 mmol), 2-[2-(4-isobutylphenyl)propanamido]ethyl acrylate **22k** (69 mg, 0.23 mmol) and RuCl₂(*p*-cymene)]₂ (9.2 mg, 10 mol %) in AcOH (0.15 mL). Purification by column chromatography on silica gel (CH₂Cl₂/MeOH: 40/1 → 20/1) yielded **249d** (82 mg, 95 μmol, 63%) as a white solid.

M.p.: 135 – 139 °C. **¹H NMR** (600 MHz, CDCl₃, mixture of diastereoisomers): δ 8.60 (ddd, *J* = 4.6, 2.1, 2.1 Hz, 1H), 7.95–7.82 (m, 1H), 7.67–7.60 (m, 1H), 7.50 (dd, *J* = 8.0, 3.4 Hz, 1H), 7.33 (ddd, *J* = 5.1, 5.1, 2.4 Hz, 1H), 7.26 (s, 3H), 7.25–7.18 (m, 1H), 7.19–7.14 (m, 2H), 7.12–7.07 (m, 4H), 7.05 (d, *J* = 6.6 Hz, 2H), 6.88–6.67 (m, 3H), 6.53–6.47 (m, 1H), 4.76 (ddd, *J* = 7.2, 7.2, 7.2 Hz, 1H), 4.67 (dq, *J* = 6.7, 6.7 Hz, 1H), 4.42–4.32 (m, 1H), 4.12–3.92 (m, 2H), 3.65 (s, 3H), 3.54–3.35 (m, 2H), 3.31–3.08 (m, 5H), 3.02 (dd, *J* = 6.3, 4.7 Hz, 2H), 2.42–2.27 (m, 4H), 1.94–1.91 (m, 3H), 1.83–1.74 (m, 1H), 1.44 (d, *J* = 7.1 Hz, 1.5H), 1.41 (d, *J* = 7.1 Hz, 1.5H), 1.25 (t, *J* = 6.9 Hz, 3H), 0.86 (d, *J* = 6.6 Hz, 6H). **¹³C NMR** (126 MHz, CDCl₃, mixture of diastereoisomers): δ 174.6 (C_q), 172.5 (C_q), 172.4 (C_q), 171.6 (C_q), 171.0 (C_q), 171.0 (C_q), 170.9 (C_q), 170.0 (C_q), 151.1 (C_q), 151.1 (C_q), 149.5 (CH), 140.3 (C_q), 140.2 (C_q), 138.6 (C_q), 138.6 (C_q), 138.5 (C_q), 136.7 (C_q), 136.7 (C_q), 136.5 (C_q), 136.4 (C_q), 135.7 (C_q), 129.3 (CH), 129.2 (CH), 129.1 (CH), 128.5 (CH), 128.3 (C_q), 128.3 (C_q), 127.1 (CH), 127.1 (CH), 122.4 (CH), 122.3 (CH), 122.3 (CH), 121.2 (CH), 121.1 (CH), 120.7 (CH), 118.5 (CH), 118.4 (CH), 110.0 (CH), 109.9 (C_q), 63.4 (CH₂), 54.1 (CH), 53.5 (CH), 52.2 (CH₃), 49.0 (CH), 46.3 (CH), 46.3 (CH), 45.0 (CH₂), 38.5 (CH₂), 37.9 (CH₂), 33.9 (CH₂), 33.8 (CH₂), 30.2 (CH₃), 28.0 (CH₂), 27.9 (CH₂), 23.2 (CH), 22.4 (CH₃), 20.5 (CH₂), 20.5 (CH₂), 18.7 (CH₃), 18.7 (CH₃), 18.6 (CH₃). **IR** (ATR): 2950, 2923, 1734, 1683, 1647, 1637, 1541,

5. Experimental Part

1523, 1508 cm^{-1} . **MS** (ESI): m/z (relative intensity) 882 (100) $[\text{M}+\text{Na}]^+$, 859 (35) $[\text{M}+\text{H}]^+$. **HR-MS** (ESI): m/z calcd for $\text{C}_{49}\text{H}_{59}\text{N}_6\text{O}_8^+$ $[\text{M}+\text{H}]^+$: 859.4389, found: 859.4385.

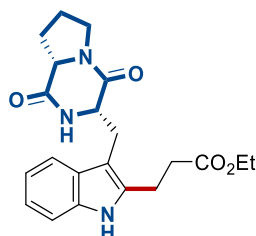
(S)-methyl 2-acetamido-3-[2-(3-ethoxy-3-oxopropyl)-1H-indol-3-yl]propanoate (250a)



The general procedure **H** was followed using methyl (S)-2-acetamido-3-[2-(3-ethoxy-3-oxopropyl)-1-(pyridin-2-yl)-1H-indol-3-yl]propanoate **242a** (87.4 mg, 0.20 mmol). Purification by column chromatography on silica gel (EtOAc) yielded **250a** (46.8 mg, 65%) as a colorless oil.

^1H NMR (400 MHz, CDCl_3): δ 8.82 (s, 1H), 7.42 (dd, $J = 7.5, 1.1$ Hz, 1H), 7.28–7.22 (m, 1H), 7.10 (ddd, $J = 8.1, 7.1, 1.3$ Hz, 1H), 7.04 (ddd, $J = 8.1, 7.1, 1.0$ Hz, 1H), 6.18 (d, $J = 7.8$ Hz, 1H), 4.86 (ddd, $J = 7.8, 5.7, 5.7$ Hz, 1H), 4.15 (q, $J = 7.1$ Hz, 2H), 3.64 (s, 3H), 3.30–3.24 (m, 1H), 3.24–3.18 (m, 1H), 3.00–2.91 (m, 2H), 2.68–2.60 (m, 2H), 1.91 (s, 3H), 1.23 (t, $J = 7.1$ Hz, 3H). **^{13}C NMR** (101 MHz, CDCl_3): δ 174.1 (C_q), 172.6 (C_q), 169.8 (C_q), 135.8 (C_q), 135.3 (C_q), 128.4 (C_q), 121.5 (CH), 119.4 (CH), 118.0 (CH), 110.7 (CH), 105.6 (C_q), 61.0 (CH_2), 53.1 (CH), 52.3 (CH_3), 34.0 (CH_2), 26.7 (CH_2), 23.1 (CH_3), 20.3 (CH_2), 14.1 (CH_3). **IR** (ATR): 3333, 2969, 1734, 1655, 1528, 1438, 1374, 1202, 745 cm^{-1} . **MS** (ESI): m/z (relative intensity) 743 (17) $[2\text{M}+\text{Na}]^+$, 383 (100) $[\text{M}+\text{Na}]^+$, 361 (28) $[\text{M}+\text{H}]^+$. **HR-MS** (ESI): m/z calcd for $\text{C}_{19}\text{H}_{25}\text{N}_2\text{O}_5^+$ $[\text{M}+\text{H}]^+$: 361.1758, found: 361.1755.

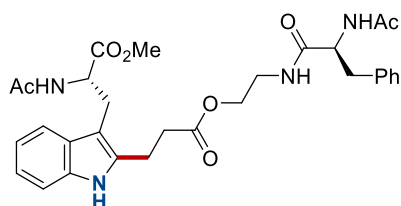
Ethyl 3-{3-[(1,4-dioxooctahydropyrrolo[1,2-a]pyrazin-3-yl)methyl]-1H-indol-2-yl}propanoate (250b)



The general procedure **H** was followed using ethyl 3-{3-[(1,4-dioxooctahydropyrrolo[1,2-a]pyrazin-3-yl)methyl]-1-[pyridin-2-yl]-1H-indol-2-yl}propanoate (250b).

yl]propanoate **244c** (92.1 mg, 0.20 mmol). Purification by column chromatography on silica gel (EtOAc) yielded **250b** (48.9 mg, 64%) as a pale yellow solid.

M.p.: 92 – 94 °C. **¹H NMR** (400 MHz, CDCl₃): δ 8.86 (s, 1H), 7.48–7.41 (m, 1H), 7.29 (dd, *J* = 8.1, 0.9 Hz, 1H), 7.14 (ddd, *J* = 8.0, 7.1, 0.9 Hz, 1H), 7.06 (ddd, *J* = 8.0, 7.1, 0.9 Hz, 1H), 5.73 (s, 1H), 4.36 (ddd, *J* = 11.3, 4.3, 1.5 Hz, 1H), 4.14 (q, *J* = 7.1 Hz, 2H), 4.03 (ddd, *J* = 8.0, 7.2, 1.6 Hz, 1H), 3.74 – 3.48 (m, 3H), 3.09–2.88 (m, 3H), 2.77–2.55 (m, 2H), 2.38–2.23 (m, 1H), 2.07–1.94 (m, 2H), 1.93–1.79 (m, 1H), 1.22 (t, *J* = 7.1 Hz, 3H). **¹³C NMR** (101 MHz, CDCl₃): δ 173.8 (C_q), 169.4 (C_q), 165.7 (C_q), 136.2 (C_q), 135.6 (C_q), 127.4 (C_q), 122.1 (CH), 119.8 (CH), 117.8 (CH), 111.0 (CH), 105.2 (C_q), 61.1 (CH₂), 59.2 (CH), 54.6 (CH), 45.4 (CH₂), 34.0 (CH₂), 28.3 (CH₂), 25.6 (CH₂), 22.6 (CH₂), 20.5 (CH₂), 14.1 (CH₃). **IR** (ATR): 3282, 2979, 2925, 1726, 1655, 1460, 1419, 1188, 733 cm⁻¹. **MS** (ESI): *m/z* (relative intensity) 789 (46) [2M+Na]⁺, 406 (100) [M+Na]⁺, 384 (23) [M+H]⁺. **HR-MS** (ESI): *m/z* calcd for C₂₁H₂₆N₃O₄⁺ [M+H]⁺: 384.1918, found: 384.1916.

(S)-methyl**2-acetamido-3-[2-(3-{2-[(S)-2-acetamido-3-****phenylpropanamido]ethoxy}-3-oxopropyl)-1*H*-indol-3-yl]propanoate (**250c**)**

The general procedure **H** was followed using (S)-methyl 2-acetamido-3-[2-(3-{2-[(S)-2-acetamido-3-phenylpropanamido]ethoxy}-3-oxopropyl)-1-(pyridin-2-yl)-1*H*-indol-3-yl]propanoate **248a** (128.3 mg, 0.20 mmol). Purification by column chromatography on silica gel (CH₂Cl₂/MeOH: 40/1 → 20/1) yielded **250c** (59.8 mg, 53%) as a pale yellow solid.

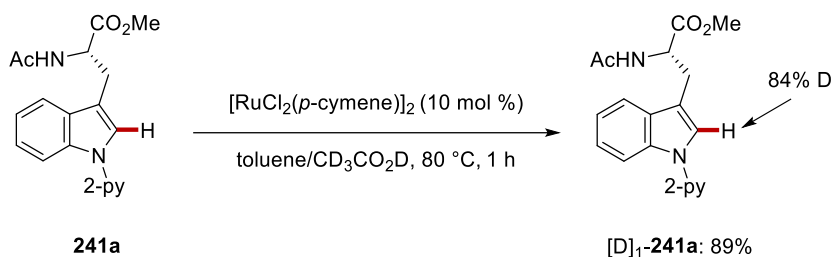
M. p.: 107 – 109 °C. **¹H NMR** (400 MHz, CDCl₃): δ 9.19 (s, 1H), 7.45 (d, *J* = 7.6 Hz, 1H), 7.29–7.03 (m, 8H), 6.95–6.86 (m, 1H), 6.66 (d, *J* = 7.2 Hz, 1H), 6.51 (d, *J* = 7.7 Hz, 1H), 4.86 (ddd, *J* = 6.7, 6.7, 6.7 Hz, 1H), 4.74–4.64 (m, 1H), 4.21–3.94 (m, 2H), 3.67 (s, 3H), 3.45–3.35 (s, 2H), 3.33–3.17 (m, 2H), 3.10–2.95 (m, 4H), 2.74–2.60 (m, 2H), 1.95–1.90 (m, 6H). **¹³C NMR** (126 MHz, CDCl₃): δ 173.3 (C_q), 172.8 (C_q), 171.6 (C_q), 170.5 (C_q), 170.1 (C_q), 136.5 (C_q), 135.5 (C_q), 135.4 (C_q), 129.1 (CH), 128.5 (CH), 128.4 (C_q), 126.9 (CH), 121.5 (CH), 119.4 (CH), 117.9 (CH), 110.7 (CH), 105.7 (C_q), 63.3 (CH₂), 54.5 (CH), 53.2 (CH), 52.4 (CH₃), 38.4 (CH₂), 38.3 (CH₂), 33.8 (CH₂), 26.9

5. Experimental Part

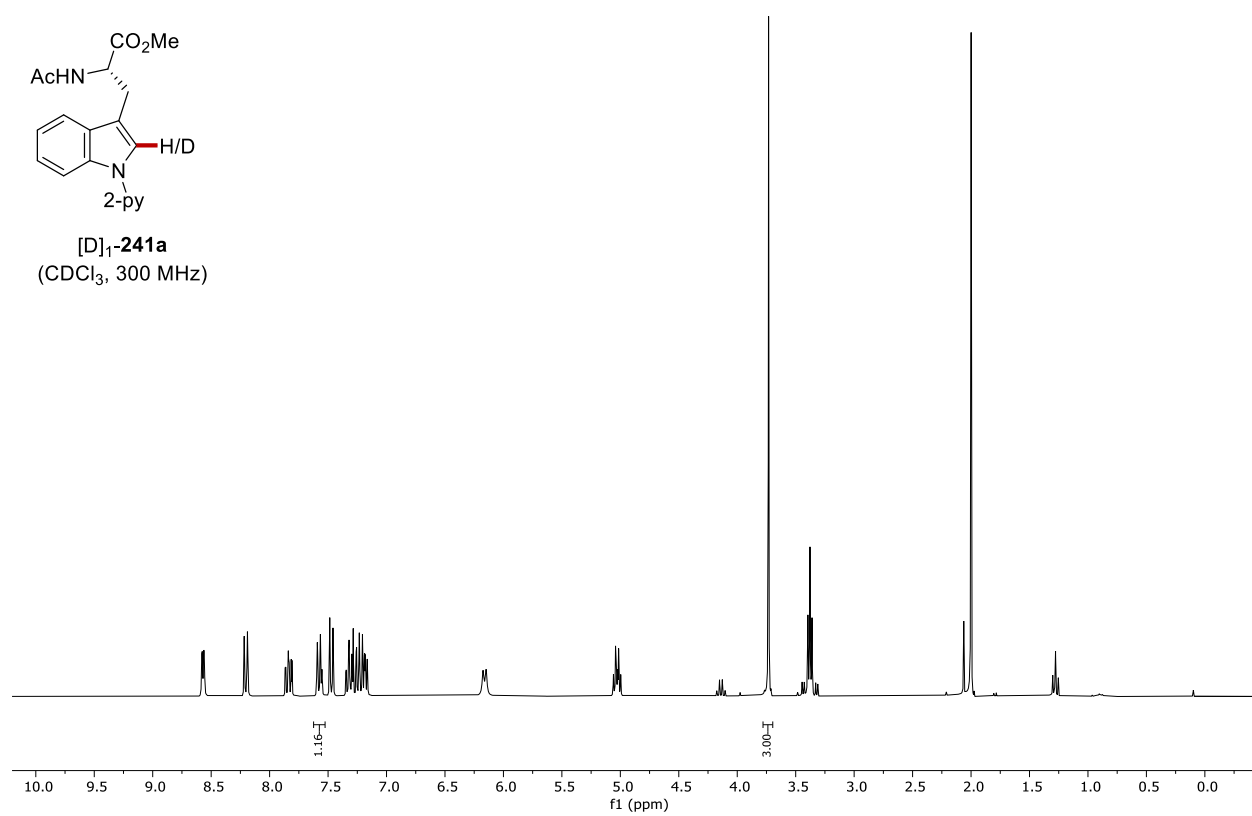
(CH₂), 23.0 (CH₃), 22.9 (CH₃), 20.8 (CH₂). **IR** (ATR): 3296, 3062, 2952, 1731, 1648, 1531, 1178, 731, 699 cm⁻¹. **MS** (ESI): *m/z* (relative intensity) 587 (100) [M+Na]⁺, 565 (26) [M+H]⁺. **HR-MS** (ESI): *m/z* calcd for C₃₀H₃₇N₄O₇⁺ [M+H]⁺: 565.2657, found: 565.2651.

5.5.1. Mechanistic Studies

5.5.1.2. H/D Exchange Study



A 10 mL conical-bottom test tube with a stir bar was charged with pyridylated tryptophan **241a** (0.15 mmol) and $[\text{RuCl}_2(p\text{-cymene})]_2$ (9.2 mg, 10 mol %). Toluene/ D_4 -acetic acid (1:1, 150 μL) were added. The tube was fitted with a septum and the mixture was heated to 80 °C for 1 h. After cooling to ambient temperature, the reaction mixture was diluted with toluene (5.0 mL). Purification by column chromatography (hexanes/EtOAc 1:1→1:2) yielded $[\text{D}]_1\text{-241a}$ (45 mg, 89%) as a white solid. The H/D exchange result was determined by ¹H-NMR spectroscopy.

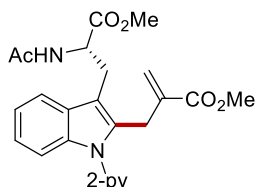


5. Experimental Part

5.6. 3d-Transition Metal-Catalyzed Allylation of Drug Scaffolds and Peptides

5.6.1. Characterization Data

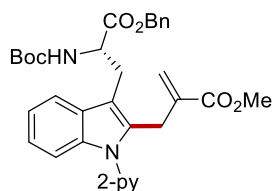
Methyl (S)-2-[[3-(2-acetamido-3-methoxy-3-oxopropyl)-1-(pyridin-2-yl)-1H-indol-2-yl]methyl]acrylate (**254a**)



The general procedure **I** was followed using (S)-methyl 2-acetamido-3-[1-(pyridin-2-yl)-1H-indol-3-yl]propanoate **241a** (67.5 mg, 0.20 mmol), methyl 2-[[*tert*-butoxycarbonyl]oxy]methyl]acrylate **253a** (86.5 mg, 0.40 mmol), MnBr(CO)₅ (5.5 mg, 10 mol %) and NaOAc (4.9 mg, 30 mol %) in 1,4-dioxane (0.6 mL). Purification by column chromatography on silica gel (*n*-hexane/EtOAc: 2/1 → 1/1) yielded **254a** (85.3 mg, 98%) as a white foam.

M. p. 52 – 56 °C. **¹H NMR** (300 MHz, CDCl₃): δ 8.56 (ddd, *J* = 4.9, 2.0, 0.8 Hz, 1H), 7.82 (ddd, *J* = 7.9, 7.4, 2.0 Hz, 1H), 7.64 – 7.47 (m, 1H), 7.34 (ddd, *J* = 8.0, 0.8, 0.8 Hz, 1H), 7.32 – 7.21 (m, 2H), 7.19 – 7.07 (m, 2H), 6.32 (d, *J* = 7.5 Hz, 1H), 5.92 (td, *J* = 1.8, 1.1 Hz, 1H), 5.01 (td, *J* = 2.2, 1.1 Hz, 1H), 4.92 (dt, *J* = 7.5, 6.0 Hz, 1H), 3.94 (dd, *J* = 2.2, 1.8 Hz, 2H), 3.67 (s, 3H), 3.65 (s, 3H), 3.38 – 3.24 (m, 2H), 1.92 (s, 3H). **¹³C NMR** (126 MHz, CDCl₃): δ 172.4 (C_q), 169.6 (C_q), 166.5 (C_q), 151.1 (C_q), 149.4 (CH), 138.2 (CH), 137.3 (C_q), 136.8 (C_q), 134.2 (C_q), 128.4 (C_q), 126.1 (CH₂), 122.5 (CH), 122.1 (CH), 120.9 (CH), 120.7 (CH), 118.5 (CH), 110.4 (C_q), 110.1 (CH), 52.8 (CH), 52.4 (CH₃), 51.9 (CH₃), 27.2 (CH₂), 27.1 (CH₂), 23.1 (CH₃). **IR** (ATR): 3054, 2951, 1718, 1656, 1585, 1470, 1436, 1370, 1256, 1138, 737 cm⁻¹. **MS** (ESI): *m/z* (relative intensity): 458 (62) [M+Na]⁺, 436 (100) [M+H]⁺. **HR-MS** (ESI): *m/z* calcd for C₂₄H₂₆N₃O₅⁺ [M+H]⁺: 436.1867, found: 436.1871.

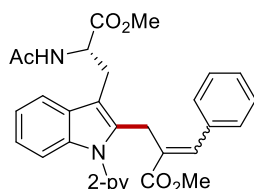
Methyl (S)-2-[(3-{3-[benzyloxy]-2-[(*tert*-butoxycarbonyl)amino]-3-oxopropyl]-1-(pyridin-2-yl)-1*H*-indol-2-yl)methyl]acrylate (254b)



The general procedure I was followed using (*S*)-benzyl 2-[(*tert*-butoxycarbonyl)amino]-3-[1-(pyridin-2-yl)-1*H*-indol-3-yl]propanoate **153** (94.3 mg, 0.20 mmol), methyl 2-[[(*tert*-butoxycarbonyl)oxy]methyl]acrylate **253a** (86.5 mg, 0.40 mmol), MnBr(CO)₅ (5.5 mg, 10 mol %) and NaOAc (4.9 mg, 30 mol %) in 1,4-dioxane (0.6 mL). Purification by column chromatography on silica gel (*n*-hexane/EtOAc: 4/1 → 2/1) yielded **254b** (108.2 mg, 95%) as a white solid.

M. p. 62 – 64 °C. **¹H NMR** (300 MHz, CDCl₃): δ 8.56 (ddd, *J* = 4.8, 2.0, 0.9 Hz, 1H), 7.80 (ddd, *J* = 8.1, 7.4, 2.0 Hz, 1H), 7.62 – 7.53 (m, 1H), 7.35 – 7.20 (m, 6H), 7.21 – 7.09 (m, 4H), 5.93 (td, *J* = 2.1, 1.0 Hz, 1H), 5.19 (d, *J* = 7.0 Hz, 1H), 5.07 (d, *J* = 12.2 Hz, 1H), 5.01 – 4.92 (m, 2H), 4.67 (dt, *J* = 7.0 Hz, 1H), 3.94 (dd, *J* = 1.6, 1.0 Hz, 2H), 3.64 (s, 3H), 3.30 (d, *J* = 7.0 Hz, 2H), 1.39 (s, 9H). **¹³C NMR** (125 MHz, CDCl₃): δ 172.1 (C_q), 166.5 (C_q), 154.9 (C_q), 151.1 (C_q), 149.3 (CH), 138.1 (CH), 137.3 (C_q), 136.7 (C_q), 135.1 (C_q), 134.2 (C_q), 128.4 (C_q), 128.3 (CH), 128.2 (CH), 128.1 (CH), 126.0 (CH₂), 122.4 (CH), 122.0 (CH), 120.8 (CH), 120.6 (CH), 118.6 (CH), 110.6 (C_q), 110.1 (CH), 79.7 (C_q), 67.2 (CH₂), 54.2 (CH), 51.8 (CH₃), 28.3 (CH₃), 27.7 (CH₂), 27.0 (CH₂). **IR** (ATR): 2976, 2951, 1708, 1585, 1498, 1470, 1437, 1254, 733 cm⁻¹. **MS** (ESI): *m/z* (relative intensity): 592 (100) [M+Na]⁺, 570 (75) [M+H]⁺, 514 (38). **HR-MS** (ESI): *m/z* calcd for C₃₃H₃₆N₃O₆⁺ [M+H]⁺: 570.2599, found: 570.2598.

(S)-Methyl 2-[[3-(2-acetamido-3-methoxy-3-oxopropyl)-1-(pyridin-2-yl)-1*H*-indol-2-yl]methyl]-3-phenylacrylate (254c)



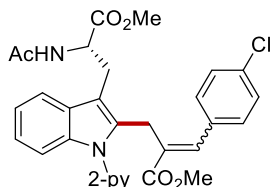
The general procedure I was followed using (*S*)-methyl 2-acetamido-3-[1-(pyridin-2-yl)-1*H*-indol-3-yl]propanoate **241a** (67.5 mg, 0.20 mmol), methyl 2-[[(*tert*-butoxycarbonyl)oxy][phenyl]methyl]acrylate **253d** (116.9 mg, 0.40 mmol), MnBr(CO)₅

5. Experimental Part

(5.5 mg, 10 mol %) and NaOAc (4.9 mg, 30 mol %) in 1,4-dioxane (0.6 mL). Purification by column chromatography on silica gel (*n*-hexane/EtOAc: 2/1 → 1/1) yielded **254c** (98.2 mg, 96%, *E/Z* = 1.2) as a white solid.

M. p.: 153 – 156 °C. **¹H NMR** (400 MHz, CDCl₃): δ 8.64 (ddd, *J* = 4.9, 2.0, 0.8 Hz, 0.55H), 8.06 (ddd, *J* = 4.9, 2.0, 0.8 Hz, 0.45H), 7.82 (ddd, *J* = 8.0, 7.5, 2.0 Hz, 0.55H), 7.73 (ddd, *J* = 7.9, 7.5, 2.0 Hz, 0.45H), 7.62 – 7.49 (m, 1H), 7.39 (dt, *J* = 8.0, 1.0 Hz, 0.58H), 7.35 – 7.22 (m, 4H), 7.21 – 7.04 (m, 5H), 6.92 – 6.84 (m, 1.5H), 6.35 (d, *J* = 7.5 Hz, 0.55H), 6.15 (s, 0.55H), 5.02 – 4.88 (m, 1H), 4.39 (dd, *J* = 16.1, 1.2 Hz, 0.45H), 4.22 (dd, *J* = 16.2, 1.7 Hz, 0.45H), 4.09 (dd, *J* = 1.7, 0.9 Hz, 1.1H), 3.72 (s, 1.35H), 3.68 (s, 1.65H), 3.57 (s, 1.35H), 3.43 (s, 1.65H), 3.40 – 3.24 (m, 2H), 1.93 (s, 1.35H), 1.92 (s, 1.65H). **¹³C NMR** (101 MHz, CDCl₃): *Major diastereomer.* δ 172.5 (C_q), 169.9 (C_q), 168.8 (C_q), 151.1 (C_q), 149.5 (CH), 138.3 (CH), 136.9 (C_q), 135.6 (C_q), 135.3 (CH), 133.8 (C_q), 130.8 (C_q), 129.5 (CH), 128.4 (C_q), 127.8 (CH), 122.7 (CH), 122.2 (CH), 121.3 (CH), 121.0 (CH), 120.7 (CH), 118.7 (CH), 110.7 (C_q), 110.0 (CH), 52.8 (CH), 52.4 (CH₃), 51.5 (CH₃), 30.1 (CH₂), 26.9 (CH₂), 23.0 (CH₃). *Minor diastereomer.* δ 172.9 (C_q), 170.4 (C_q), 167.9 (C_q), 150.9 (C_q), 149.5 (CH), 139.8 (CH), 137.9 (CH), 137.0 (C_q), 135.3 (C_q), 134.4 (C_q), 129.3 (C_q), 128.7 (CH), 128.2 (C_q), 127.8 (CH), 127.8 (CH), 122.3 (CH), 122.0 (CH), 121.0 (CH), 120.5 (CH), 118.5 (CH), 109.6 (C_q), 109.6 (CH), 52.8 (CH), 52.3 (CH₃), 52.0 (CH₃), 26.8 (CH₂), 24.1 (CH₂), 22.7 (CH₃). **IR** (ATR): 3363, 3057, 2951, 1741, 1714, 1658, 1587, 1471, 1437, 1225, 743 cm⁻¹. **MS** (ESI): *m/z* (relative intensity) 534 (100) [M+Na]⁺, 512 (83) [M+H]⁺. **HR-MS** (ESI): *m/z* calcd for C₃₀H₂₉N₃O₅⁺ [M+H]⁺: 512.2180, found: 512.2176.

(*S*)-Methyl 2-[[3-(2-acetamido-3-methoxy-3-oxopropyl)-1-(pyridin-2-yl)-1*H*-indol-2-yl]methyl]-3-(4-chlorophenyl)acrylate (**254e**)



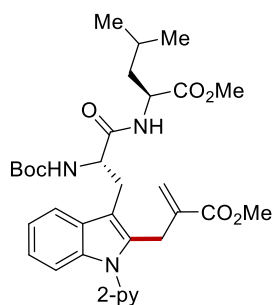
The general procedure **I** was followed using (*S*)-methyl 2-acetamido-3-[1-(pyridin-2-yl)-1*H*-indol-3-yl]propanoate **241a** (67.5 mg, 0.20 mmol), methyl 2-[[*tert*-butoxycarbonyl]oxy][4-chlorophenyl]methyl]acrylate **253e** (130.7 mg, 0.40 mmol), MnBr(CO)₅ (5.5 mg, 10 mol %) and NaOAc (4.9 mg, 30 mol %) in 1,4-dioxane (0.6 mL). Purification by column chromatography on silica gel (*n*-hexane/EtOAc: 2/1 → 1/1)

yielded **254e** (104.8mg, 96%, *E/Z* = 1.2) as a white solid.

M. p. 157 – 159 °C. **¹H NMR** (300 MHz, CDCl₃): δ 8.62 (dd, *J* = 5.1, 2.0 Hz, 0.56H), 8.14 – 8.05 (m, 0.44H), 7.88 – 7.64 (m, 1H), 7.63 – 7.45 (m, 1H), 7.37 (dt, *J* = 8.0, 1.0 Hz, 0.56H), 7.33 – 7.19 (m, 3H), 7.19 – 7.04 (m, 5H), 6.86 (d, *J* = 6.5 Hz, 0.44H), 6.84 – 6.76 (m, 1H), 6.32 (d, *J* = 7.5 Hz, 0.56H), 6.09 (s, 0.56H), 5.02 – 4.86 (m, 1H), 4.35 (dd, *J* = 16.2, 1.3 Hz, 0.44H), 4.19 (dd, *J* = 16.1, 1.7 Hz, 0.44H), 4.09 (s, 1.16H), 3.71 (s, 1.32H), 3.67 (s, 1.68H), 3.57 (s, 1.32H), 3.45 (s, 1.68H), 3.41 – 3.22 (m, 2H), 1.93 (s, 1.32H), 1.92 (s, 1.68H).

¹³C NMR (126 MHz, CDCl₃): *Major diastereomer.* δ 172.7 (C_q), 169.7 (C_q), 168.3 (C_q), 151.0 (C_q), 149.4 (CH), 138.3 (CH), 136.7 (C_q), 134.8 (C_q), 134.1 (CH), 134.0 (C_q), 133.5 (C_q), 131.3 (C_q), 129.1 (CH), 128.3 (CH), 128.0 (C_q), 122.6 (CH), 122.2 (CH), 121.1 (CH), 120.6 (CH), 118.6 (CH), 110.7 (C_q), 110.0 (CH), 52.9 (CH), 52.4 (CH₃), 51.6 (CH₃), 30.1 (CH₂), 27.0 (CH₂), 22.7 (CH₃). *Minor diastereomer.* δ 172.3 (C_q), 170.1 (C_q), 167.5 (C_q), 150.8 (C_q), 149.4 (CH), 138.2 (CH), 137.8 (CH), 136.8 (C_q), 134.5 (C_q), 133.5 (C_q), 132.7 (C_q), 130.6 (CH), 129.9 (C_q), 128.3 (CH), 128.1 (C_q), 122.2 (CH), 121.9 (CH), 120.9 (CH), 120.5 (CH), 118.4 (CH), 109.8 (C_q), 109.5 (CH), 52.8 (CH), 52.3 (CH₃), 52.0 (CH₃), 26.9 (CH₂), 24.2 (CH₂), 23.1 (CH₃). **IR** (ATR): 3352, 3056, 2951, 1715, 1660, 1471, 1437, 1224, 740 cm⁻¹. **MS** (ESI): *m/z* (relative intensity) 568 (86) [M+Na]⁺, 546 (100) [M+H]⁺. **HR-MS** (ESI): *m/z* calcd for C₃₀H₂₉N₃O₅³⁵Cl⁺ [M+H]⁺: 546.1790, found: 546.1779.

(S)-Methyl 2-({S}-2-[(*tert*-butoxycarbonyl)amino]-3-{2-[2-(methoxycarbonyl)allyl]-1-[pyridin-2-yl]-1*H*-indol-3-yl]propanamido)-4-methylpentanoate (255a)



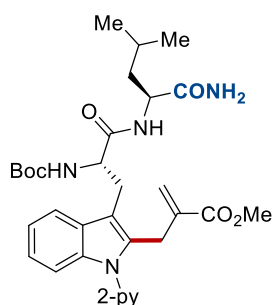
The general procedure **I** was followed using (S)-methyl 2-[[S]-2-[(*tert*-butoxycarbonyl)amino]-3-[1-(pyridin-2-yl)-1*H*-indol-3-yl]propanamido]-4-methylpentanoate **243j** (101.7 mg, 0.20 mmol), methyl 2-[[(*tert*-butoxycarbonyl)oxy]methyl]acrylate **253a** (86.5 mg, 0.40 mmol), MnBr(CO)₅ (5.5 mg,

5. Experimental Part

10 mol %) and NaOAc (4.9 mg, 30 mol %) in 1,4-dioxane (0.6 mL). Purification by column chromatography on silica gel (*n*-hexane/EtOAc: 4/1) yielded **255a** (112.8 mg, 93%) as a white solid.

M. p. 74 – 77 °C. **¹H NMR** (600 MHz, CDCl₃): δ 8.56 (ddd, *J* = 4.9, 2.0, 0.8 Hz, 1H), 7.82 (ddd, *J* = 7.7, 7.7, 2.0 Hz, 1H), 7.62 (d, *J* = 6.9 Hz, 1H), 7.38 (dt, *J* = 8.0, 1.0 Hz, 1H), 7.27 (ddd, *J* = 7.4, 4.9, 1.0 Hz, 1H), 7.25 – 7.22 (m, 1H), 7.14 – 7.08 (m, 2H), 6.38 (d, *J* = 7.9 Hz, 1H), 5.89 (td, *J* = 1.9, 1.2 Hz, 1H), 5.32 (brs, 1H), 5.05 (s, 1H), 4.57 – 4.49 (m, 1H), 4.43 (ddd, *J* = 8.4, 8.4, 5.3 Hz, 1H), 3.98 (s, 2H), 3.64 (s, 3H), 3.52 (s, 3H), 3.34 – 3.25 (m, 1H), 3.19 – 3.10 (m, 1H), 1.55 – 1.44 (m, 2H), 1.42 – 1.36 (s, 10H), 0.85 (d, *J* = 6.0 Hz, 3H), 0.82 (d, *J* = 6.0 Hz, 3H). **¹³C NMR** (126 MHz, CDCl₃): δ 172.3 (C_q), 171.1 (C_q), 166.7 (C_q), 155.2 (C_q), 151.3 (C_q), 149.3 (CH), 138.1 (CH), 137.3 (C_q), 136.9 (C_q), 134.2 (C_q), 128.3 (C_q), 126.2 (CH₂), 122.3 (CH), 122.1 (CH), 121.2 (CH), 120.7 (CH), 118.7 (CH), 110.8 (C_q), 109.9 (CH), 79.8 (C_q), 54.6 (CH), 52.1 (CH₃), 52.0 (CH₃), 50.7 (CH), 42.1 (CH₂), 28.3 (CH₃), 27.9 (CH₂), 27.5 (CH₂), 24.7 (CH), 22.7 (CH₃), 22.2 (CH₃). **IR** (ATR): 3352, 2954, 1714, 1672, 1471, 1437, 1367, 1202, 784 cm⁻¹. **MS** (ESI): *m/z* (relative intensity) 1235 (23) [2M+Na]⁺, 629 (73) [M+Na]⁺, 607 (100) [M+H]⁺, 507 (27). **HR-MS** (ESI): *m/z* calcd for C₃₃H₄₃N₄O₇⁺ [M+H]⁺: 607.3126, found: 607.3124.

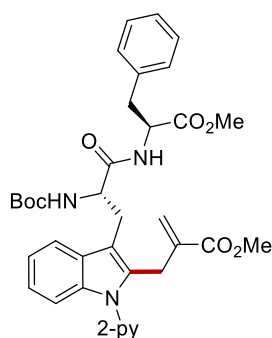
Methyl 2-[[3-({S}-3-[(S)-1-amino-4-methyl-1-oxopentan-2-yl]amino)-2-[[*tert*-butoxycarbonyl]amino]-3-oxopropyl)-1-(pyridin-2-yl)-1*H*-indol-2-yl]methyl]acrylate (**255b**)



The general procedure I was followed using *tert*-butyl ({S}-1-[(S)-1-amino-4-methyl-1-oxopentan-2-yl]amino)-1-oxo-3-{1-[pyridin-2-yl]-1*H*-indol-3-yl}propan-2-yl)carbamate **243k** (98.7 mg, 0.20 mmol), methyl 2-[[(*tert*-butoxycarbonyl)oxy]methyl]acrylate **253a** (86.5 mg, 0.40 mmol), MnBr(CO)₅ (5.5 mg, 10 mol %) and NaOAc (4.9 mg, 30mol %) in 1,4-dioxane (0.6 mL). Purification by column chromatography on silica gel (*n*-hexane/EtOAc: 1/2 → 1/5) yielded **255b** (79.2 mg, 67%) as a white solid.

M. p. 104 – 107 °C. **¹H NMR** (600 MHz, CDCl₃): δ 8.57 (dd, *J* = 4.8, 1.8 Hz, 1H), 7.83 (ddd, *J* = 7.7, 7.7, 1.9 Hz, 1H), 7.70 – 7.62 (m, 1H), 7.33 (d, *J* = 7.9 Hz, 1H), 7.30 (ddd, *J* = 7.5, 4.9, 1.0 Hz, 1H), 7.19 (dd, *J* = 7.7, 1.5 Hz, 1H), 7.17 – 7.08 (m, 2H), 6.42 (d, *J* = 8.3 Hz, 1H), 5.87 (d, *J* = 1.3 Hz, 1H), 5.66 (brs, 1H), 5.43 (brs, 2H), 4.99 (d, *J* = 1.3 Hz, 1H), 4.54 (ddd, *J* = 7.6, 7.6, 7.6 Hz, 1H), 4.34 (ddd, *J* = 10.0, 8.3, 4.8 Hz, 1H), 3.97 (dt, *J* = 17.3, 1.7 Hz, 1H), 3.89 (d, *J* = 17.3 Hz, 1H), 3.62 (s, 3H), 3.30 – 3.15 (m, 2H), 1.63 (ddd, *J* = 13.8, 9.1, 4.7 Hz, 1H), 1.57 – 1.50 (m, 1H), 1.39 (s, 9H), 1.31 (ddd, *J* = 13.8, 10.0, 5.1 Hz, 1H), 0.83 (d, *J* = 6.6 Hz, 3H), 0.81 (d, *J* = 6.6 Hz, 3H). **¹³C NMR** (126 MHz, CDCl₃): δ 173.8 (C_q), 171.8 (C_q), 166.6 (C_q), 155.5 (C_q), 150.9 (C_q), 149.4 (CH), 138.4 (CH), 137.0 (C_q), 136.9 (C_q), 134.3 (C_q), 127.8 (C_q), 126.4 (CH₂), 122.7 (CH), 122.5 (CH), 121.5 (CH), 120.9 (CH), 118.7 (CH), 110.2 (C_q), 110.0 (CH), 80.2 (C_q), 55.1 (CH), 52.0 (CH₃), 51.4 (CH), 40.2 (CH₂), 28.3 (CH₃), 27.7 (CH₂), 27.5 (CH₂), 24.7 (CH), 23.0 (CH₃), 21.6 (CH₃). **IR** (ATR): 3318, 2954, 1664, 1586, 1508, 1437, 1253, 738 cm⁻¹. **MS** (ESI): *m/z* (relative intensity) 614 (100) [M+Na]⁺, 592 (96) [M+H]⁺. **HR-MS** (ESI): *m/z* calcd for C₃₂H₄₂N₅O₆⁺ [M+H]⁺: 592.3130, found: 592.3129.

Methyl 2-[[3-((S)-2-[(tert-butoxycarbonyl)amino]-3-[(S)-1-methoxy-1-oxo-3-phenylpropan-2-yl]amino)-3-oxopropyl)-1-(pyridin-2-yl)-1H-indol-2-yl]methyl]acrylate (255d)



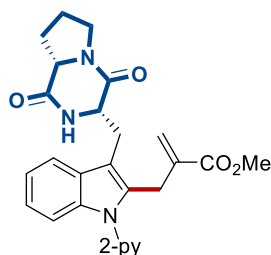
The general procedure **I** was followed using (S)-methyl 2-[[S]-2-[(tert-butoxycarbonyl)amino]-3-[1-(pyridin-2-yl)-1H-indol-3-yl]propanamido]-3-phenylpropanoate **243m** (108.5 mg, 0.20 mmol), methyl 2-[[tert-butoxycarbonyl]oxy]methyl]acrylate **253a** (86.5 mg, 0.40 mmol), MnBr(CO)₅ (5.5 mg, 10 mol %) and NaOAc (4.9 mg, 30 mol %) in 1,4-dioxane (0.6 mL). Purification by column chromatography on silica gel (*n*-hexane/EtOAc: 4/1 → 2/1) yielded **255d** (116.6 mg, 91%) as a white solid.

M. p.: 80 – 82 °C. **¹H NMR** (600 MHz, CDCl₃): δ 8.55 (dd, *J* = 5.1, 1.9 Hz, 1H), 7.79 (ddd, *J* = 7.8, 7.8, 1.9 Hz, 1H), 7.59 (d, *J* = 7.5 Hz, 1H), 7.35 (d, *J* = 7.8 Hz, 1H), 7.26

5. Experimental Part

(ddd, $J = 7.5, 4.9, 1.0$ Hz, 1H), 7.19 (dd, $J = 7.1, 1.6$ Hz, 1H), 7.16 – 7.05 (m, 5H), 6.91 – 6.85 (m, 2H), 6.37 (d, $J = 7.3$ Hz, 1H), 5.80 (s, 1H), 5.38 (d, $J = 5.9$ Hz, 1H), 5.00 (s, 1H), 4.66 – 4.45 (m, 2H), 4.01 (d, $J = 17.0$ Hz, 1H), 3.97 (d, $J = 17.0$ Hz, 1H), 3.47 – 3.45 (m, 6H), 3.37 – 3.25 (m, 1H), 3.13 – 3.06 (m, 1H), 2.96 (dd, $J = 13.7, 5.7$ Hz, 1H), 2.90 (dd, $J = 13.7, 5.4$ Hz, 1H), 1.41 (s, 9H). **^{13}C NMR** (126 MHz, CDCl_3): δ 171.0 (C_q), 170.6 (C_q), 166.6 (C_q), 155.0 (C_q), 151.2 (C_q), 149.3 (CH), 138.1 (CH), 137.3 (C_q), 136.9 (C_q), 135.7 (C_q), 134.2 (C_q), 129.2 (CH), 128.3 (C_q), 128.2 (CH), 126.7 (CH), 126.1 (CH_2), 122.3 (CH), 122.1 (CH), 121.2 (CH), 120.6 (CH), 118.7 (CH), 110.7 (C_q), 109.7 (CH), 79.7 (C_q), 54.4 (CH), 53.4 (CH), 51.9 (CH_3), 51.9 (CH_3), 38.2 (CH_2), 28.4 (CH_3), 27.8 (CH_2). (One aliphatic CH_2 is missing due to overlap, the overlap was verified by HSQC analysis, showing that the peak at 28.4 ppm corresponds to two carbons). **IR** (ATR): 3346, 2976, 2952, 1712, 1670, 1586, 1471, 1437, 1253, 734 cm^{-1} . **MS** (ESI): m/z (relative intensity): 1303 (30) $[\text{2M}+\text{Na}]^+$, 663 (63) $[\text{M}+\text{Na}]^+$, 641 (100) $[\text{M}+\text{H}]^+$. **HR-MS** (ESI): m/z calcd for $\text{C}_{36}\text{H}_{41}\text{N}_4\text{O}_7^+$ $[\text{M}+\text{H}]^+$: 641.2970, found: 641.2962.

Methyl 2-[(3-[(3*S*,8*aS*)-1,4-dioxooctahydropyrrolo[1,2-*a*]pyrazin-3-yl)methyl]-1-(pyridin-2-yl)-1*H*-indol-2-yl)methyl]acrylate (**255e**)

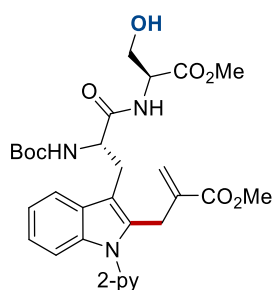


The general procedure **I** was followed using (3*S*,8*aS*)-3-[[1-(pyridin-2-yl)-1*H*-indol-3-yl]methyl]hexahydropyrrolo[1,2-*a*]pyrazine-1,4-dione **243c** (72.1 mg, 0.20 mmol), methyl 2-[[(*tert*-butoxycarbonyl)oxy]methyl]acrylate **253a** (86.5 mg, 0.40 mmol), $\text{MnBr}(\text{CO})_5$ (5.5 mg, 10 mol %) and NaOAc (4.9 mg, 30 mol %) in 1,4-dioxane (0.6 mL). Purification by column chromatography on silica gel (*n*-hexane/EtOAc: 2/1 \rightarrow 1/2) yielded **255e** (84.3 mg, 92%) as a colorless oil.

^1H NMR (600 MHz, CDCl_3): δ 8.59 (dd, $J = 4.9, 1.8$ Hz, 1H), 7.86 (ddd, $J = 7.7, 7.7, 2.0$ Hz, 1H), 7.61 – 7.55 (m, 1H), 7.38 (dd, $J = 8.0, 1.0$ Hz, 1H), 7.34 – 7.29 (m, 2H), 7.21 – 7.15 (m, 2H), 6.00 (s, 1H), 5.97 (d, $J = 1.4$ Hz, 1H), 5.05 (d, $J = 1.4$ Hz, 1H), 4.51 – 4.37 (m, 1H), 4.10 – 4.01 (m, 2H), 3.94 (d, $J = 17.7$ Hz, 1H), 3.75 (dd, $J = 15.3, 3.8$ Hz, 1H), 3.67 (s, 3H), 3.67 – 3.63 (m, 1H), 3.57 (ddd, $J = 12.0, 8.9, 3.2$ Hz, 1H), 3.05 (dd, $J = 15.3, 11.2$ Hz, 1H), 2.32 (ddt, $J = 11.2, 7.1, 3.7$ Hz, 1H), 2.16 – 1.97 (m,

2H), 1.95 – 1.85 (m, 1H). ^{13}C NMR (126 MHz, CDCl_3): δ 169.3 (C_q), 166.5 (C_q), 165.5 (C_q), 150.8 (C_q), 149.4 (CH), 138.3 (CH), 137.1 (C_q), 137.0 (C_q), 134.6 (C_q), 127.6 (C_q), 126.2 (CH_2), 122.9 (CH), 122.3 (CH), 121.0 (CH), 121.0 (CH), 118.1 (CH), 110.4 (CH), 109.7 (C_q), 59.2 (CH), 54.7 (CH), 52.0 (CH_3), 45.4 (CH_2), 28.3 (CH_2), 27.4 (CH_2), 25.7 (CH_2), 22.7 (CH_2). IR (ATR): 3053, 2951, 2879, 1716, 1661, 1470, 1458, 1436, 1142, 786 cm^{-1} . MS (ESI): m/z (relative intensity): 939 (19) $[2\text{M}+\text{Na}]^+$, 481 (63) $[\text{M}+\text{Na}]^+$, 459 (100) $[\text{M}+\text{H}]^+$. HR-MS (ESI): m/z calcd for $\text{C}_{26}\text{H}_{27}\text{N}_4\text{O}_4^+$ $[\text{M}+\text{H}]^+$: 459.2027, found: 459.2024.

Methyl 2-[[3-((S)-2-[(tert-butoxycarbonyl]amino)-3-[(S)-3-hydroxy-1-methoxy-1-oxopropan-2-yl]amino]-3-oxopropyl)-1-(pyridin-2-yl)-1H-indol-2-yl]methyl]acrylate (255f)



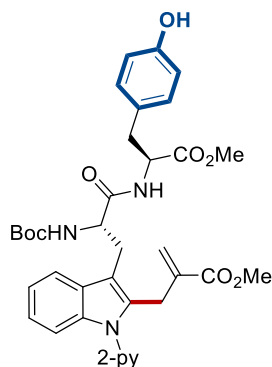
The general procedure I was followed using (S)-methyl 2-[[S]-2-[(tert-butoxycarbonyl]amino]-3-[1-(pyridin-2-yl)-1H-indol-3-yl]propanamido]-3-hydroxypropanoate **243n** (96.5 mg, 0.20 mmol), methyl 2-[[tert-butoxycarbonyl]oxy]methyl]acrylate **253a** (86.5 mg, 0.40 mmol), $\text{MnBr}(\text{CO})_5$ (5.5 mg, 10 mol %) and NaOAc (4.9 mg, 30 mol %) in 1,4-dioxane (0.6 mL). Purification by column chromatography on silica gel (*n*-hexane/EtOAc: 2/1 \rightarrow 1/2) yielded **255f** (97.5 mg, 84%) as a white solid.

M. p. 97 – 99 °C. ^1H NMR (300 MHz, CDCl_3): δ 8.59 (dd, $J = 5.0, 1.8$ Hz, 1H), 7.90 (td, $J = 7.7, 1.9$ Hz, 1H), 7.72 – 7.60 (m, 1H), 7.45 (d, $J = 7.9$ Hz, 1H), 7.35 (ddd, $J = 7.6, 4.9, 1.0$ Hz, 1H), 7.27 – 7.11 (m, 3H), 6.85 (d, $J = 6.7$ Hz, 1H), 5.92 (s, 1H), 5.43 (d, $J = 7.4$ Hz, 1H), 5.03 (s, 1H), 4.61 (ddd, $J = 7.4, 7.4, 7.4$ Hz, 1H), 4.42 (ddd, $J = 6.7, 3.2, 3.2$ Hz, 1H), 4.10 – 3.74 (m, 4H), 3.69 – 3.62 (s, 6H), 3.53 – 3.39 (m, 1H), 3.22 (dd, $J = 14.5, 7.4$ Hz, 1H), 2.22 (brs, 1H), 1.45 (s, 9H). ^{13}C NMR (76 MHz, CDCl_3): δ 171.9 (C_q), 170.2 (C_q), 166.8 (C_q), 155.4 (C_q), 151.1 (C_q), 149.5 (CH), 138.7 (CH), 137.3 (C_q), 137.1 (C_q), 134.5 (C_q), 128.4 (C_q), 126.3 (CH_2), 122.7 (CH), 122.6 (CH), 121.7 (CH), 121.0 (CH), 118.6 (CH), 110.9 (C_q), 109.9 (CH), 80.2 (C_q), 62.5 (CH_2), 55.1 (CH), 55.1

5. Experimental Part

(CH), 52.5 (CH₃), 52.0 (CH₃), 28.4 (CH₃), 28.3 (CH₂), 27.6 (CH₂). **IR** (ATR): 3337, 2951, 1744, 1715, 1671, 1472, 1368, 1162, 740 cm⁻¹. **MS** (ESI): *m/z* (relative intensity) 1183 (24) [2M+Na]⁺, 603 (100) [M+Na]⁺, 581 (66) [M+H]⁺, 481 (38). **HR-MS** (ESI): *m/z* calcd for C₃₀H₃₇N₄O₈⁺ [M+H]⁺: 581.2606, found: 581.2607.

Methyl 2-[[3-((S)-2-[(*tert*-butoxycarbonyl)amino]-3-[[(*S*)-3-(4-hydroxyphenyl)-1-methoxy-1-oxopropan-2-yl]amino]-3-oxopropyl)-1-(pyridin-2-yl)-1*H*-indol-2-yl]methyl]acrylate (255g)

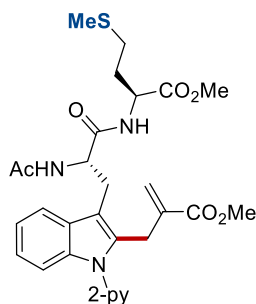


The general procedure **I** was followed using (*S*)-methyl 2-[[*S*]-2-[(*tert*-butoxycarbonyl)amino]-3-[1-(pyridin-2-yl)-1*H*-indol-3-yl]propanamido]-3-(4-hydroxyphenyl)propanoate **243o** (111.7 mg, 0.20 mmol), methyl 2-[[(*tert*-butoxycarbonyl)oxy]methyl]acrylate **253a** (86.5 mg, 0.40 mmol), MnBr(CO)₅ (5.5 mg, 10 mol %) and NaOAc (4.9 mg, 30 mol %) in 1,4-dioxane (0.6 mL). Purification by column chromatography on silica gel (*n*-hexane/EtOAc: 2/1 → 1/2) yielded **255g** (116.9 mg, 89%) as a white solid.

M. p. 97 – 100 °C. **¹H NMR** (600 MHz, CDCl₃): δ 8.55 (dd, *J* = 4.9, 1.8 Hz, 1H), 7.81 (ddd, *J* = 7.8, 7.8, 1.9 Hz, 1H), 7.64 – 7.53 (m, 1H), 7.35 (d, *J* = 7.8 Hz, 1H), 7.28 (dd, *J* = 7.5, 4.9 Hz, 1H), 7.19 – 7.16 (m, 1H), 7.10 – 7.06 (m, 2H), 7.03 – 6.93 (m, 1H), 6.63 – 6.56 (m, 2H), 6.54 – 6.41 (m, 3H), 5.82 (s, 1H), 5.33 (brs, 1H), 4.98 (s, 1H), 4.63 – 4.57 (m, 1H), 4.54 – 4.43 (m, 1H), 3.93 (s, 2H), 3.49 (s, 3H), 3.47 (s, 3H), 3.40 – 3.28 (m, 1H), 3.12 – 3.07 (m, 1H), 2.92 – 2.84 (m, 1H), 2.79 (dd, *J* = 14.0, 5.8 Hz, 1H), 1.39 (s, 9H). **¹³C NMR** (126 MHz, CDCl₃): δ 171.2 (C_q), 170.8 (C_q), 166.7 (C_q), 155.2 (C_q), 155.1 (C_q), 151.1 (C_q), 149.1 (CH), 138.4 (CH), 137.1 (C_q), 136.9 (C_q), 134.3 (C_q), 130.1 (CH), 128.3 (C_q), 126.8 (CH₂), 126.2 (C_q), 122.4 (CH), 121.6 (CH), 120.7 (CH), 118.9 (CH), 115.3 (CH), 110.6 (C_q), 109.6 (CH), 79.9 (C_q), 54.3 (CH), 53.4 (CH), 52.0 (CH₃), 52.0 (CH₃), 37.2 (CH₂), 28.3 (CH₃), 27.9 (CH₂), 27.7 (CH₂). (One aromatic CH is missing due to overlap, the overlap was verified by HSQC analysis, showing that the

peak at 122.4 ppm corresponds to two carbons). **IR** (ATR): 3342, 2974, 2954, 2926, 1715, 1669, 1515, 1473, 1439, 1367, 1225, 1170, 745 cm^{-1} . **MS** (ESI): m/z (relative intensity) 679 (100) $[\text{M}+\text{Na}]^+$, 657 (84) $[\text{M}+\text{H}]^+$, 320 (37). **HR-MS** (ESI): m/z calcd for $\text{C}_{36}\text{H}_{41}\text{N}_4\text{O}_8^+$ $[\text{M}+\text{H}]^+$: 657.2919, found: 657.2921.

(S)-Methyl 2-((S)-2-acetamido-3-{2-[2-(methoxycarbonyl)allyl]-1-[pyridin-2-yl]-1H-indol-3-yl}propanamido)-4-(methylthio)butanoate (255h)



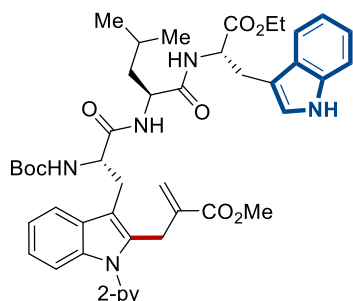
The general procedure **I** was followed using (S)-methyl 2-[(S)-2-acetamido-3-[1-(pyridin-2-yl)-1H-indol-3-yl]propanamido]-4-(methylthio)butanoate **243b** (93.7 mg, 0.20 mmol), methyl 2-[[*tert*-butoxycarbonyl]oxy]methyl]acrylate **253a** (86.5 mg, 0.40 mmol), $\text{MnBr}(\text{CO})_5$ (5.5 mg, 10 mol %) and NaOAc (4.9 mg, 30 mol %) in 1,4-dioxane (0.6 mL). Purification by column chromatography on silica gel (*n*-hexane/EtOAc: 1/1 \rightarrow 1/2) yielded **255h** (91.8 mg, 81%) as a white solid.

M. p. 106 – 108 °C. **$^1\text{H NMR}$** (600 MHz, CDCl_3): δ 8.56 (ddd, $J = 4.9, 1.9, 0.8$ Hz, 1H), 7.82 (ddd, $J = 7.6, 7.6, 2.0$ Hz, 1H), 7.60 – 7.55 (m, 1H), 7.40 (ddd, $J = 7.9, 1.0, 1.0$ Hz, 1H), 7.27 (ddd, $J = 7.6, 4.9, 1.0$ Hz, 1H), 7.21 – 7.18 (m, 1H), 7.11 – 7.04 (m, 2H), 6.65 – 6.58 (m, 2H), 5.83 (t, $J = 1.3$ Hz, 1H), 5.06 (t, $J = 1.3$ Hz, 1H), 4.88 (ddd, $J = 9.3, 7.3, 6.0$ Hz, 1H), 4.37 (ddd, $J = 6.9, 6.9, 5.2$ Hz, 1H), 4.06 (dt, $J = 16.9, 1.3$ Hz, 1H), 3.99 (dt, $J = 16.9, 1.3$ Hz, 1H), 3.61 (s, 3H), 3.48 (s, 3H), 3.37 (dd, $J = 14.4, 6.1$ Hz, 1H), 3.08 (dd, $J = 14.2, 9.2$ Hz, 1H), 2.34 (ddd, $J = 13.4, 9.2, 6.2$ Hz, 1H), 2.27 (ddd, $J = 13.4, 9.2, 6.0$ Hz, 1H), 2.02 – 1.99 (m, 1H), 1.98 (s, 3H), 1.97 (s, 3H), 1.81 (dddd, $J = 14.2, 9.1, 6.9, 6.0$ Hz, 1H). **$^{13}\text{C NMR}$** (126 MHz, CDCl_3): δ 171.1 (C_q), 170.9 (C_q), 169.7 (C_q), 166.7 (C_q), 151.2 (C_q), 149.3 (CH), 138.1 (CH), 137.1 (C_q), 136.9 (C_q), 134.4 (C_q), 128.3 (C_q), 126.4 (CH_2), 122.2 (CH), 122.2 (CH), 121.3 (CH), 120.6 (CH), 118.4 (CH), 110.5 (C_q), 109.7 (CH), 53.5 (CH), 52.3 (CH_3), 52.0 (CH_3), 51.6 (CH), 32.0 (CH_2), 29.6 (CH_2), 28.0 (CH_2), 27.9 (CH_2), 23.3 (CH_3), 15.4 (CH_3). **IR** (ATR): 3282, 3056, 2952, 2918, 1741, 1718, 1585, 1542, 1205, 732 cm^{-1} . **MS** (ESI): m/z (relative intensity) 1155 (56) $[\text{2M}+\text{Na}]^+$, 589 (63) $[\text{M}+\text{Na}]^+$, 567 (100) $[\text{M}+\text{H}]^+$. **HR-MS** (ESI): m/z

5. Experimental Part

calcd for C₂₉H₃₅N₄O₆S⁺ [M+H]⁺: 567.2272, found: 567.2268.

Ethyl (6*S*,9*S*,12*S*)-12-[(1*H*-indol-3-yl)methyl]-9-isobutyl-6-({2-[2-(methoxycarbonyl)allyl]-1-[pyridin-2-yl]-1*H*-indol-3-yl)methyl}-2,2-dimethyl-4,7,10-trioxo-3-oxa-5,8,11-triazatridecan-13-oate (255i)

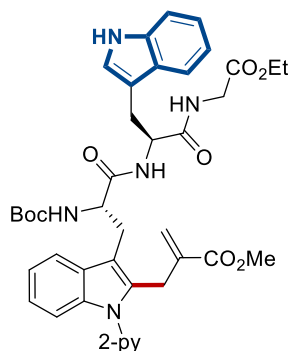


The general procedure I was followed using (6*S*,9*S*,12*S*)-ethyl 12-[(1*H*-indol-3-yl)methyl]-9-isobutyl-2,2-dimethyl-4,7,10-trioxo-6-[[1-(pyridin-2-yl)-1*H*-indol-3-yl)methyl]-3-oxa-5,8,11-triazatridecan-13-oate **243p** (141.8 mg, 0.20 mmol), methyl 2-[[*tert*-butoxycarbonyl]oxy]methyl]acrylate **253a** (86.5 mg, 0.40 mmol), MnBr(CO)₅ (5.5 mg, 10.0 mol %) and NaOAc (4.9 mg, 30.0 mol %) in 1,4-dioxane (0.6 mL). Purification by column chromatography on silica gel (*n*-hexane/EtOAc: 2/1 → 1/2) yielded **255i** (154.8 mg, 96%) as a white solid.

M. p.: 102 – 107 °C. **¹H NMR** (600 MHz, CDCl₃): δ 8.76 (brs, 1H), 8.58 (ddd, *J* = 4.8, 2.0, 0.8 Hz, 1H), 7.81 (ddd, *J* = 7.7, 7.7, 2.0 Hz, 1H), 7.67 – 7.62 (m, 1H), 7.50 (dd, *J* = 7.7, 1.0 Hz, 1H), 7.36 (d, *J* = 8.0 Hz, 1H), 7.29 – 7.25 (m, 3H), 7.15 – 7.10 (m, 3H), 7.06 (ddd, *J* = 8.0, 6.9, 1.0 Hz, 1H), 6.91 – 6.87 (m, 1H), 6.63 (d, *J* = 7.7 Hz, 1H), 6.48 (d, *J* = 8.2 Hz, 1H), 5.93 (td, *J* = 2.0, 1.2 Hz, 1H), 5.24 (d, *J* = 7.6 Hz, 1H), 5.02 (td, *J* = 2.3, 1.2 Hz, 1H), 4.75 (ddd, *J* = 7.7, 5.8, 5.8 Hz, 1H), 4.57 – 4.45 (m, 1H), 4.37 (ddd, *J* = 7.8, 7.8, 7.8 Hz, 1H), 4.14 – 4.03 (m, 2H), 4.00 (d, *J* = 17.5 Hz, 1H), 3.95 (d, *J* = 17.4 Hz, 1H), 3.64 (s, 3H), 3.36 – 3.14 (m, 4H), 1.63 – 1.54 (m, 1H), 1.51 – 1.44 (m, 1H), 1.37 (s, 9H), 1.33 – 1.25 (m, 1H), 1.18 (t, *J* = 7.1 Hz, 3H), 0.79 (t, *J* = 6.8 Hz, 6H). **¹³C NMR** (126 MHz, CDCl₃): δ 171.5 (C_q), 171.4 (C_q), 170.7 (C_q), 166.8 (C_q), 155.5 (C_q), 151.1 (C_q), 149.3 (CH), 138.2 (CH), 137.2 (C_q), 136.9 (C_q), 136.0 (C_q), 134.3 (C_q), 128.2 (C_q), 127.3 (C_q), 126.2 (CH₂), 123.3 (CH), 122.5 (CH), 122.2 (CH), 121.7 (CH), 121.2 (CH), 120.8 (CH), 119.2 (CH), 118.9 (CH), 118.3 (CH), 111.2 (CH), 110.7 (C_q), 110.0 (CH), 109.3 (C_q), 80.3 (C_q), 61.4 (CH₂), 54.8 (CH), 52.7 (CH), 52.0 (CH₃), 51.6 (CH), 40.7 (CH₂), 28.3 (CH₃), 27.5 (CH₂), 27.3 (CH₂), 27.1 (CH₂), 24.5 (CH), 22.7 (CH₃), 22.3 (CH₃), 14.1 (CH₃). **IR** (ATR): 3309, 2956, 2929, 1716, 1650, 1520, 1459,

1438, 1367, 1165, 741 cm^{-1} . **MS** (ESI): m/z (relative intensity) 829 (100) $[\text{M}+\text{Na}]^+$, 807 (91) $[\text{M}+\text{H}]^+$, 432 (32). **HR-MS** (ESI): m/z calcd for $\text{C}_{45}\text{H}_{55}\text{N}_6\text{O}_8^+$ $[\text{M}+\text{H}]^+$: 807.4076, found: 807.4067.

Ethyl (6S,9S)-9-[(1H-indol-3-yl)methyl]-6-({2-[2-(methoxycarbonyl)allyl]-1-[pyridin-2-yl]-1H-indol-3-yl)methyl}-2,2-dimethyl-4,7,10-trioxo-3-oxa-5,8,11-triazatridecan-13-oate (255j)



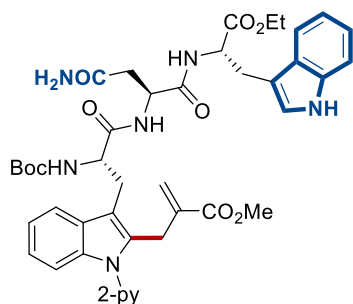
The general procedure **I** was followed using (6S,9S)-ethyl 9-[(1H-indol-3-yl)methyl]-2,2-dimethyl-4,7,10-trioxo-6-[[1-(pyridin-2-yl)-1H-indol-3-yl)methyl]-3-oxa-5,8,11-triazatridecan-13-oate **243q** (130.5 mg, 0.20 mmol), methyl 2-[[*tert*-butoxycarbonyl]oxy]methyl]acrylate **253a** (86.5 mg, 0.40 mmol), $[\text{MnBr}(\text{CO})_5]$ (5.5 mg, 10.0 mol %) and NaOAc (4.9 mg, 30.0 mol %) in 1,4-dioxane (0.6 mL). Purification by column chromatography on silica gel (*n*-hexane/EtOAc: 1/1 \rightarrow 1/2) yielded **255j** (145.5 mg, 97%) as a white solid.

M. p.: 109 – 111 $^{\circ}\text{C}$. **$^1\text{H NMR}$** (600 MHz, CDCl_3): δ 8.77 (brs, 1H), 8.60 (dd, $J = 5.0, 1.9$ Hz, 1H), 7.83 (ddd, $J = 7.7, 7.7, 2.0$ Hz, 1H), 7.65 – 7.59 (m, 1H), 7.35 (ddd, $J = 8.1, 1.0, 1.0$ Hz, 1H), 7.33 – 7.25 (m, 2H), 7.22 (d, $J = 8.1$ Hz, 1H), 7.18 – 7.10 (m, 3H), 7.05 (dd, $J = 7.7, 7.7$ Hz, 1H), 6.88 (t, $J = 7.6$ Hz, 1H), 6.74 (brs, 2H), 6.52 (d, $J = 7.9$ Hz, 1H), 5.84 (d, $J = 1.5$ Hz, 1H), 5.03 (d, $J = 6.2$ Hz, 1H), 4.92 (d, $J = 1.5$ Hz, 1H), 4.70 (ddd, $J = 6.5, 6.5, 6.5$ Hz, 1H), 4.38 (ddd, $J = 6.2, 6.2, 6.2$ Hz, 1H), 4.09 (q, $J = 7.1$ Hz, 2H), 3.97 (d, $J = 17.5$ Hz, 1H), 3.91 (d, $J = 17.5$, 1H), 3.85 (dd, $J = 17.5, 5.3$ Hz, 1H), 3.72 (dd, $J = 17.5, 5.6$ Hz, 1H), 3.60 (s, 3H), 3.35 – 3.24 (m, 2H), 3.15 (dd, $J = 14.8, 6.5$ Hz, 1H), 3.01 (dd, $J = 14.8, 6.1$ Hz, 1H), 1.24 – 1.15 (m, 12H). **$^{13}\text{C NMR}$** (126 MHz, CDCl_3): δ 171.7 (C_q), 171.2 (C_q), 169.0 (C_q), 166.4 (C_q), 155.6 (C_q), 150.9 (C_q), 149.3 (CH), 138.4 (CH), 137.0 (C_q), 136.9 (C_q), 135.8 (C_q), 134.3 (C_q), 128.1 (C_q), 127.4 (C_q), 126.3 (CH_2), 123.5 (CH), 122.7 (CH), 122.4 (CH), 121.7 (CH), 121.2 (CH), 120.9 (CH), 119.4 (CH), 118.9 (CH), 118.0 (CH), 111.1 (CH), 110.2 (C_q), 110.0 (CH),

5. Experimental Part

109.2 (C_q), 80.1 (C_q), 61.0 (CH₂), 55.3 (CH), 53.7 (CH), 51.9 (CH₃), 41.3 (CH₂), 28.0 (CH₃), 27.2 (CH₂), 26.7 (CH₂), 26.5 (CH₂), 14.1 (CH₃). **IR** (ATR): 3310, 2979, 2929, 1716, 1686, 1507, 1472, 1368, 1368, 1198, 1163, 741 cm⁻¹. **MS** (ESI): *m/z* (relative intensity) 1523 (48) [2M+Na]⁺, 773 (63) [M+Na]⁺, 751 (100) [M+H]⁺. **HR-MS** (ESI): *m/z* calcd for C₄₁H₄₇N₆O₈⁺ [M+H]⁺: 751.3450, found: 751.3445.

(6S,9S,12S)-Ethyl 12-[(1*H*-indol-3-yl)methyl]-9-(2-amino-2-oxoethyl)-6-({2-[2-(methoxycarbonyl)allyl]-1-[pyridin-2-yl]-1*H*-indol-3-yl)methyl}-2,2-dimethyl-4,7,10-trioxo-3-oxa-5,8,11-triazatridecan-13-oate (255k)

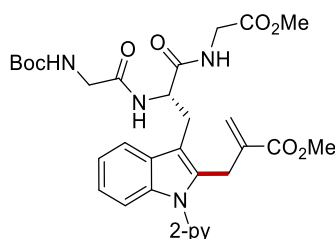


The general procedure **I** was followed using (6*S*,9*S*,12*S*)-ethyl 12-[(1*H*-indol-3-yl)methyl]-9-(2-amino-2-oxoethyl)-2,2-dimethyl-4,7,10-trioxo-6-[[1-(pyridin-2-yl)-1*H*-indol-3-yl]methyl]-3-oxa-5,8,11-triazatridecan-13-oate **243r** (141.9 mg, 0.20 mmol), methyl 2-[[*tert*-butoxycarbonyl]oxy]methyl]acrylate **253a** (86.5 mg, 0.40 mmol), MnBr(CO)₅ (5.5 mg, 10 mol %) and NaOAc (4.9 mg, 30 mol %) in 1,4-dioxane (0.6 mL). Purification by column chromatography on silica gel (CH₂Cl₂/MeOH: 60/1 → 40/1) yielded **255k** (134.4 mg, 83%) as a pale yellow solid.

M. p.: 126 – 128 °C. **¹H NMR** (600 MHz, DMSO-*d*₆): δ 10.85 (s, 1H), 8.56 (dd, *J* = 5.0, 1.9 Hz, 1H), 8.21 (d, *J* = 7.2 Hz, 1H), 8.14 (d, *J* = 7.9 Hz, 1H), 7.98 (ddd, *J* = 7.7, 7.7, 2.0 Hz, 1H), 7.74 – 7.70 (m, 1H), 7.49 – 7.45 (m, 2H), 7.41 (dd, *J* = 7.5, 4.9 Hz, 1H), 7.39 – 7.37 (m, 1H), 7.33 (d, *J* = 8.1 Hz, 1H), 7.27 – 7.21 (m, 1H), 7.18 – 7.15 (m, 1H), 7.10 (dt, *J* = 6.3, 3.8 Hz, 2H), 7.08 – 7.03 (m, 1H), 7.00 – 6.94 (m, 2H), 6.87 (d, *J* = 8.8 Hz, 1H), 5.84 (s, 1H), 4.97 (s, 1H), 4.64 (q, *J* = 6.9 Hz, 1H), 4.46 (q, *J* = 7.0 Hz, 1H), 4.25 (td, *J* = 9.2, 4.3 Hz, 1H), 4.08 – 3.83 (m, 4H), 3.58 (s, 3H), 3.18 (dd, *J* = 14.6, 4.3 Hz, 1H), 3.13 (dd, *J* = 14.6, 6.8 Hz, 1H), 3.08 (dd, *J* = 14.6, 7.1 Hz, 1H), 2.95 (dd, *J* = 14.6, 9.7 Hz, 1H), 1.24 (s, 9H), 1.03 (t, *J* = 7.1 Hz, 3H). (Two aliphatic protons are missing due to overlap, the overlap was verified by HMBC analysis, showing that the peaks are overlapping with the residual solvent peak). **¹³C NMR** (126 MHz, DMSO-*d*₆): δ 171.4 (C_q), 171.2 (C_q), 171.1 (C_q), 170.6 (C_q), 165.9 (C_q), 154.8 (C_q), 150.4 (C_q),

149.0 (CH), 138.8 (CH), 136.9 (C_q), 136.0 (C_q), 135.9 (C_q), 133.7 (C_q), 128.0 (C_q), 126.9 (CH₂), 125.4 (C_q), 123.6 (CH), 122.3 (CH), 121.9 (CH), 121.8 (CH), 120.7 (CH), 119.9 (CH), 118.7 (CH), 118.2 (CH), 117.7 (CH), 111.7 (C_q), 111.2 (CH), 109.8 (C_q), 108.9 (CH), 78.1 (C_q), 60.3 (CH₂), 55.3 (CH), 53.3 (CH), 51.7 (CH₃), 49.2 (CH), 37.3 (CH₂), 28.0 (CH₃), 27.0 (CH₂), 26.9 (CH₂), 26.4 (CH₂), 13.8 (CH₃). **IR** (ATR): 3292, 2975, 1715, 1676, 1498, 1465, 1431, 1243, 733 cm⁻¹. **MS** (ESI): *m/z* (relative intensity) 830 (100) [M+Na]⁺, 808 (73) [M+H]⁺. **HR-MS** (ESI): *m/z* calcd for C₄₃H₅₀N₇O₉⁺ [M+H]⁺: 808.3665, found: 808.3661.

(S)-Methyl 9-({2-[2-(methoxycarbonyl)allyl]-1-[pyridin-2-yl]-1H-indol-3-yl}methyl)-2,2-dimethyl-4,7,10-trioxo-3-oxa-5,8,11-triazatridecan-13-oate (255I)



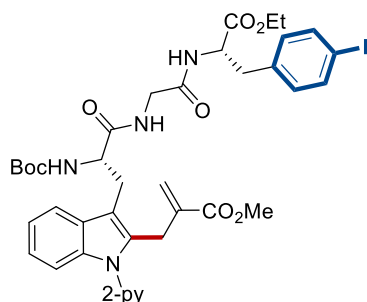
The general procedure I was followed using (S)-methyl 2,2-dimethyl-4,7,10-trioxo-9-{{1-(pyridin-2-yl)-1H-indol-3-yl}methyl}-3-oxa-5,8,11-triazatridecan-13-oate **243s** (101.9 mg, 0.20 mmol), methyl 2-{{(*tert*-butoxycarbonyl)oxy}methyl}acrylate **253a** (86.5 mg, 0.40 mmol), MnBr(CO)₅ (5.5 mg, 10 mol %) and NaOAc (4.9 mg, 30 mol %) in 1,4-dioxane (0.6 mL). Purification by column chromatography on silica gel (*n*-hexane/EtOAc: 1/1 → 1/3) yielded **255I** (64.4 mg, 53%) as a white solid.

M. p.: 100 – 102 °C. **¹H NMR** (600 MHz, CDCl₃): δ 8.56 (dd, *J* = 5.0, 1.8 Hz, 1H), 7.83 (ddd, *J* = 7.7, 7.7, 2.0 Hz, 1H), 7.66 – 7.59 (m, 1H), 7.38 (d, *J* = 7.9 Hz, 1H), 7.30 – 7.26 (m, 1H), 7.24 – 7.21 (m, 1H), 7.15 – 7.07 (m, 2H), 6.98 (d, *J* = 7.4 Hz, 1H), 6.62 (brs, 1H), 5.87 (d, *J* = 1.4 Hz, 1H), 5.26 (brs, 1H), 5.02 (d, *J* = 1.4 Hz, 1H), 4.87 (ddd, *J* = 8.3, 7.3, 6.3 Hz, 1H), 4.04 – 3.94 (m, 2H), 3.92 (dd, *J* = 18.1, 5.5 Hz, 1H), 3.77 – 3.72 (m, 2H), 3.68 (dd, *J* = 18.1, 4.9 Hz, 1H), 3.63 (s, 3H), 3.60 (s, 3H), 3.36 (dd, *J* = 14.6, 6.3 Hz, 1H), 3.19 (dd, *J* = 14.6, 8.3 Hz, 1H), 1.39 (s, 9H). **¹³C NMR** (126 MHz, CDCl₃): δ 171.1 (C_q), 169.3 (C_q), 169.1 (C_q), 166.7 (C_q), 155.9 (C_q), 151.1 (C_q), 149.3 (CH), 138.2 (CH), 137.1 (C_q), 136.9 (C_q), 134.5 (C_q), 128.2 (C_q), 126.4 (CH₂), 122.5 (CH), 122.2 (CH), 121.2 (CH), 120.8 (CH), 118.5 (CH), 110.7 (C_q), 110.0 (CH), 80.1 (C_q), 53.4 (CH), 52.2 (CH₃), 52.0 (CH₃), 44.2 (CH₂), 41.3 (CH₂), 28.3 (CH₃), 27.7 (CH₂), 27.6 (CH₂). **IR** (ATR): 3305, 2953, 2927, 1716, 1655, 1471, 1459, 1209, 1169, 739 cm⁻¹.

5. Experimental Part

1. **MS** (ESI): m/z (relative intensity): 1237 (45) $[2M+Na]^+$, 630 (100) $[M+Na]^+$, 608 (50) $[M+H]^+$, 508 (23). **HR-MS** (ESI): m/z calcd for $C_{31}H_{38}N_5O_8^+$ $[M+H]^+$: 608.2715, found: 608.2712.

(6S,12S)-Ethyl 6-[[2-(2-aminoallyl)-1-(pyridin-2-yl)-1H-indol-3-yl]methyl]-12-(4-iodobenzyl)-2,2-dimethyl-4,7,10-trioxo-3-oxa-5,8,11-triazatridecan-13-oate (255m)

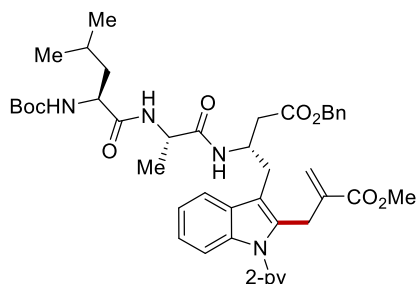


The general procedure **I** was followed using (6S,12S)-ethyl 12-(4-iodobenzyl)-2,2-dimethyl-4,7,10-trioxo-6-[[1-(pyridin-2-yl)-1H-indol-3-yl]methyl]-3-oxa-5,8,11-triazatridecan-13-oate **243t** (147.9 mg, 0.20 mmol), methyl 2-[[*tert*-butoxycarbonyl]oxy]methyl]acrylate **253a** (86.5 mg, 0.40 mmol), $MnBr(CO)_5$ (5.5 mg, 10 mol %) and NaOAc (4.9 mg, 30 mol %) in 1,4-dioxane (0.6 mL). Purification by column chromatography on silica gel (*n*-hexane/EtOAc: 1/3 \rightarrow 0/1) yielded **255m** (155.8 mg, 93%) as a white solid.

M. p.: 109 – 111 °C. **1H NMR** (500 MHz, $CDCl_3$): δ 8.55 (dd, $J = 4.8, 1.8$ Hz, 1H), 7.81 (ddd, $J = 7.7, 7.7, 1.8$ Hz, 1H), 7.66 – 7.50 (m, 3H), 7.35 (d, $J = 7.9$ Hz, 1H), 7.30 – 7.21 (m, 3H), 7.17 – 7.06 (m, 2H), 6.94 – 6.79 (m, 2H), 6.65 (t, $J = 5.4$ Hz, 1H), 5.91 (s, 1H), 5.39 (d, $J = 6.9$ Hz, 1H), 5.03 (s, 1H), 4.68 (ddd, $J = 6.8, 6.8, 6.8$ Hz, 1H), 4.45 (ddd, $J = 7.1, 7.1, 7.1$ Hz, 1H), 4.08 (q, $J = 7.1$ Hz, 2H), 4.00 – 3.87 (m, 3H), 3.62 (s, 3H), 3.53 (dd, $J = 16.9, 4.7$ Hz, 1H), 3.34 – 3.10 (m, 2H), 3.00 (dd, $J = 13.8, 6.1$ Hz, 1H), 2.94 (dd, $J = 13.8, 6.4$ Hz, 1H), 1.37 (s, 9H), 1.16 (t, $J = 7.1$ Hz, 3H). **^{13}C NMR** (126 MHz, $CDCl_3$): δ 172.2 (C_q), 170.9 (C_q), 168.2 (C_q), 166.7 (C_q), 155.4 (C_q), 151.1 (C_q), 149.4 (CH), 138.3 (CH), 137.5 (CH), 137.2 (C_q), 136.8 (C_q), 135.7 (C_q), 134.3 (C_q), 131.3 (CH), 128.2 (C_q), 126.4 (CH_2), 122.6 (CH), 122.3 (CH), 121.1 (CH), 120.8 (CH), 118.6 (CH), 110.7 (C_q), 110.0 (CH), 92.5 (C_q), 80.0 (C_q), 61.5 (CH_2), 55.0 (CH), 53.1 (CH), 52.0 (CH_3), 43.1 (CH_2), 37.3 (CH_2), 28.2 (CH_3), 27.5 (CH_2), 27.3 (CH_2), 14.0 (CH_3). **IR** (ATR): 3306, 2978, 1714, 1654, 1509, 1471, 1437, 1367, 1163, 735 cm^{-1} . **MS** (ESI): m/z (relative intensity): 1697 (38) $[2M+Na]^+$, 860 (65) $[M+Na]^+$, 838 (100)

[M+H]⁺. **HR-MS** (ESI): *m/z* calcd for C₃₉H₄₅IN₅O₈⁺ [M+H]⁺: 838.2307, found: 838.2304.

Benzyl (6S,9S,12S)-6-isobutyl-12-({2-[2-(methoxycarbonyl)allyl]-1-[pyridin-2-yl]-1H-indol-3-yl)methyl}-2,2,9-trimethyl-4,7,10-trioxo-3-oxa-5,8,11-triazatetradecan-14-oate (255n)



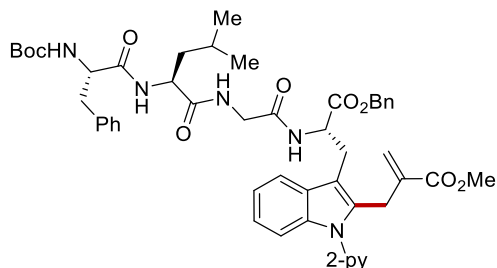
The general procedure **I** was followed using (6S,9S,12S)-benzyl 6-isobutyl-2,2,9-trimethyl-4,7,10-trioxo-12-[[1-(pyridin-2-yl)-1H-indol-3-yl]methyl]-3-oxa-5,8,11-triazatetradecan-14-oate **243u** (133.9 mg, 0.20 mmol), methyl 2-[[*tert*-butoxycarbonyl]oxy]methyl]acrylate **253a** (86.5 mg, 0.40 mmol), MnBr(CO)₅ (5.5 mg, 10 mol %) and NaOAc (4.9 mg, 30 mol %) in 1,4-dioxane (0.6 mL). Purification by column chromatography on silica gel (*n*-hexane/EtOAc: 2/1 → 1/1) yielded **255u** (145.8 mg, 95%) as a white solid.

M. p.: 123 – 125 °C. **¹H NMR** (600 MHz, CDCl₃): δ 8.59 (ddd, *J* = 4.9, 2.0, 0.8 Hz, 1H), 7.83 (ddd, *J* = 7.7, 7.7, 2.0 Hz, 1H), 7.71 – 7.64 (m, 1H), 7.38 – 7.33 (m, 5H), 7.33 – 7.26 (m, 3H), 7.17 – 7.10 (m, 2H), 7.01 (d, *J* = 8.0 Hz, 1H), 6.66 (d, *J* = 7.3 Hz, 1H), 5.91 (d, *J* = 1.4 Hz, 1H), 5.13 (d, *J* = 13.4 Hz, 1H), 5.11 (d, *J* = 13.4 Hz, 1H), 5.07 (d, *J* = 7.9 Hz, 1H), 4.99 (d, *J* = 1.4 Hz, 1H), 4.72 – 4.59 (m, 1H), 4.37 (dt, *J* = 7.0, 7.0 Hz, 1H), 4.13 – 4.05 (m, 1H), 3.99 (d, *J* = 17.5 Hz, 1H), 3.95 (d, *J* = 17.5 Hz, 1H), 3.67 (s, 3H), 3.13 (dd, *J* = 14.5, 6.6 Hz, 1H), 3.04 (dd, *J* = 14.5, 8.2 Hz, 1H), 2.68 (dd, *J* = 16.3, 5.4 Hz, 1H), 2.63 (dd, *J* = 16.3, 5.7 Hz, 1H), 1.68 – 1.63 (m, 1H), 1.58 (ddd, *J* = 13.8, 8.7, 5.1 Hz, 1H), 1.52 – 1.44 (m, 1H), 1.44 (s, 9H), 1.26 (d, *J* = 7.0 Hz, 3H), 0.90 (t, *J* = 6.9 Hz, 6H). **¹³C NMR** (126 MHz, CDCl₃): δ 172.1 (C_q), 171.3 (C_q), 171.3 (C_q), 166.7 (C_q), 155.6 (C_q), 151.1 (C_q), 149.3 (CH), 138.2 (CH), 137.2 (C_q), 136.8 (C_q), 135.5 (C_q), 133.9 (C_q), 128.4 (CH), 128.3 (C_q), 128.3 (CH), 128.2 (CH), 126.2 (CH₂), 122.4 (CH), 122.1 (CH), 121.1 (CH), 120.7 (CH), 118.9 (CH), 111.8 (C_q), 110.0 (CH), 80.0 (C_q), 66.5 (CH₂), 53.2 (CH), 52.0 (CH₃), 48.8 (CH), 47.0 (CH), 41.3 (CH₂), 37.3 (CH₂), 29.0 (CH₂), 28.4 (CH₃), 27.3 (CH₂), 24.8 (CH), 23.1 (CH₃), 21.9 (CH₃), 18.4 (CH₃). **IR** (ATR): 3292, 2955, 2930, 1717, 1646, 1519, 1471, 1437, 1366, 1253, 1161, 738 cm⁻¹. **MS** (ESI): *m/z* (relative intensity) 1558 (28) [2M+Na]⁺, 790 (58) [M+Na]⁺, 768 (100) [M+H]⁺.

5. Experimental Part

HR-MS (ESI): m/z calcd for $C_{43}H_{54}N_5O_8^+$ $[M+H]^+$: 768.3967, found: 768.3966.

Benzyl (6S,9S,15S)-6-benzyl-9-isobutyl-15-({2-[2-(methoxycarbonyl)allyl]-1-[pyridin-2-yl]-1H-indol-3-yl)methyl} 2,2-dimethyl-4,7,10,13-tetraoxo-3-oxa-5,8,11,14-tetraazahexadecan-16-oate (255o)

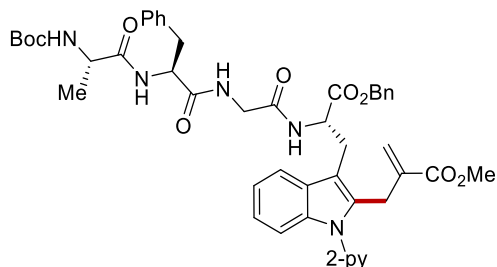


The general procedure **I** was followed using (6S,9S,15S)-benzyl 6-benzyl-9-isobutyl-2,2-dimethyl-4,7,10,13-tetraoxo-15-[[1-(pyridin-2-yl)-1H-indol-3-yl]methyl]-3-oxa-5,8,11,14-tetraazahexadecan-16-oate **243v** (78.9 mg, 0.10 mmol), methyl 2-[[*tert*-butoxycarbonyl]oxy]methyl]acrylate **253a** (43.2 mg, 0.20 mmol), $MnBr(CO)_5$ (2.7 mg, 10 mol %) and NaOAc (2.5 mg, 30 mol %) in 1,4-dioxane (0.3 mL). Purification by column chromatography on silica gel (*n*-hexane/EtOAc: 1/1 \rightarrow 1/4) yielded **255o** (83.3 mg, 94%) as a white solid.

M. p.: 93 – 96 °C. **1H NMR** (600 MHz, $CDCl_3$): δ 8.53 – 8.47 (m, 1H), 7.82 (ddd, J = 7.7, 7.7, 2.0 Hz, 1H), 7.57 – 7.48 (m, 1H), 7.31 – 7.25 (m, 6H), 7.21 – 7.15 (m, 5H), 7.15 – 7.11 (m, 2H), 7.11 – 7.09 (m, 2H), 7.00 – 6.95 (m, 1H), 6.75 (d, J = 4.6 Hz, 1H), 6.38 (d, J = 7.7 Hz, 1H), 5.89 (td, J = 1.8, 1.1 Hz, 1H), 5.33 (s, 1H), 5.11 (d, J = 12.3 Hz, 1H), 4.99 – 4.93 (m, 3H), 4.34 (ddd, J = 9.6, 7.7, 5.0 Hz, 1H), 4.07 (d, J = 7.6 Hz, 1H), 4.02 (dd, J = 17.0, 6.2 Hz, 1H), 3.91 (d, J = 17.4 Hz, 1H), 3.85 (d, J = 17.4 Hz, 1H), 3.77 – 3.69 (m, 1H), 3.62 (s, 3H), 3.33 (d, J = 6.6 Hz, 1H), 3.32 (d, J = 6.3 Hz, 1H), 3.05 (dd, J = 13.8, 6.6 Hz, 1H), 2.99 (dd, J = 13.8, 6.6 Hz, 1H), 1.59 (ddd, J = 13.8, 8.9, 5.0 Hz, 1H), 1.53 – 1.46 (m, 1H), 1.42 – 1.35 (m, 1H), 1.36 (s, 9H), 0.86 – 0.79 (m, 6H). **^{13}C NMR** (126 MHz, $CDCl_3$): δ 171.7 (C_q), 171.6 (C_q), 171.6 (C_q), 168.5 (C_q), 166.6 (C_q), 155.4 (C_q), 150.8 (C_q), 149.1 (CH), 138.5 (CH), 136.9 (C_q), 136.7 (C_q), 136.7 (C_q), 134.9 (C_q), 134.3 (C_q), 129.2 (CH), 128.4 (CH), 128.4 (CH), 128.3 (C_q), 128.2 (CH), 128.2 (CH), 126.8 (CH), 126.4 (CH_2), 122.5 (CH), 122.3 (CH), 121.2 (CH), 121.0 (CH), 118.6 (CH), 110.3 (C_q), 110.1 (CH), 80.2 (C_q), 67.4 (CH_2), 56.0 (CH), 52.8 (CH), 52.1 (CH_3), 51.7 (CH), 42.9 (CH_2), 40.2 (CH_2), 37.3 (CH_2), 28.3 (CH_3), 27.3 (CH_2), 27.2 (CH_2), 24.5 (CH), 23.1 (CH_3), 21.7 (CH_3). **IR** (ATR): 3285, 2954, 2927, 1717, 1639, 1521, 1471, 1438, 1252, 784 cm^{-1} . **MS** (ESI): m/z (relative intensity) 1797

(20) $[M+Na]^+$, 909 (100) $[M+Na]^+$, 887 (95) $[M+H]^+$. **HR-MS** (ESI): m/z calcd for $C_{50}H_{59}N_6O_9^+$ $[M+H]^+$: 887.4338, found: 887.4334.

(6S,9S,15S)-Benzyl 9-benzyl-15-({2-[2-(methoxycarbonyl)allyl]-1-[pyridin-2-yl]-1H-indol-3-yl)methyl}-2,2,6-trimethyl-4,7,10,13-tetraoxo-3-oxa-5,8,11,14-tetraazahexadecan-16-oate (255p)



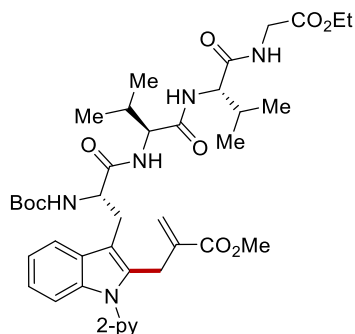
The general procedure **I** was followed using (6S,9S,15S)-benzyl 9-benzyl-2,2,6-trimethyl-4,7,10,13-tetraoxo-15-[[1-(pyridin-2-yl)-1H-indol-3-yl]methyl]-3-oxa-5,8,11,14-tetraazahexadecan-16-oate **243w** (74.7 mg, 0.10 mmol), methyl 2-[[*tert*-butoxycarbonyl]oxy]methyl]acrylate **253a** (43.2 mg, 0.20 mmol), $MnBr(CO)_5$ (2.7 mg, 10 mol %) and NaOAc (2.5 mg, 30 mol %) in 1,4-dioxane (0.3 mL). Purification by column chromatography on silica gel (*n*-hexane/EtOAc: 1/1 \rightarrow 1/4) yielded **255p** (79.4 mg, 94%) as a white solid.

M. p.: 104 – 106 °C. **1H NMR** (600 MHz, $CDCl_3$): δ 8.53 – 8.48 (m, 1H), 7.81 (td, J = 7.7, 2.0 Hz, 1H), 7.60 – 7.51 (m, 1H), 7.29 – 7.23 (m, 6H), 7.21 – 7.19 (m, 2H), 7.17 – 7.15 (m, 1H), 7.13 – 7.07 (m, 7H), 6.95 – 6.88 (m, 2H), 5.86 (d, J = 1.3 Hz, 1H), 5.07 – 5.01 (m, 2H), 4.97 – 4.91 (m, 2H), 4.87 (ddd, J = 7.0, 7.0, 7.0 Hz, 1H), 4.57 (ddd, J = 7.0, 7.0, 7.0 Hz, 1H), 4.05 – 3.99 (m, 1H), 3.97 – 3.84 (m, 3H), 3.80 (dd, J = 16.8, 5.4 Hz, 1H), 3.61 (s, 3H), 3.32 (dd, J = 14.7, 6.9 Hz, 1H), 3.27 (dd, J = 14.7, 6.7 Hz, 1H), 3.07 (dd, J = 13.9, 6.5 Hz, 1H), 3.02 (dd, J = 13.9, 7.2 Hz, 1H), 1.35 (s, 9H), 1.15 (d, J = 7.0 Hz, 3H). **^{13}C NMR** (126 MHz, $CDCl_3$): δ 172.7 (C_q), 171.5 (C_q), 170.9 (C_q), 168.3 (C_q), 166.6 (C_q), 155.5 (C_q), 150.9 (C_q), 149.2 (CH), 138.4 (CH), 137.0 (C_q), 136.8 (C_q), 136.4 (C_q), 135.0 (C_q), 134.3 (C_q), 129.1 (CH), 128.5 (CH), 128.3 (CH), 128.2 (C_q), 128.2 (CH), 128.1 (CH), 126.9 (CH), 126.4 (CH_2), 122.6 (CH), 122.2 (CH), 121.2 (CH), 120.8 (CH), 118.5 (CH), 110.5 (C_q), 110.1 (CH), 80.2 (C_q), 67.3 (CH_2), 54.5 (CH), 53.0 (CH), 52.0 (CH_3), 50.5 (CH), 43.0 (CH_2), 37.6 (CH_2), 28.3 (CH_3), 27.3 (CH_2), 18.2 (CH_3). (One aliphatic CH_2 is missing due to overlap, the overlap was verified by HSQC analysis, showing that the peak at 27.3 ppm corresponds to two carbons). **IR** (ATR): 3288, 2928, 1714, 1640, 1519, 1471, 1252, 734 cm^{-1} . **MS** (ESI):

5. Experimental Part

m/z (relative intensity) 1712 (15) $[2M+Na]^+$, 867 (100) $[M+Na]^+$, 845 (95) $[M+H]^+$. **HR-MS** (ESI): m/z calcd for $C_{47}H_{53}N_6O_9^+$ $[M+H]^+$: 845.3869, found: 845.3865.

(6S,9S,12S)-Ethyl 9,12-diisopropyl-6-{{2-[2-(methoxycarbonyl)allyl]-1-[pyridin-2-yl]-1H-indol-3-yl]methyl}-2,2-dimethyl-4,7,10,13-tetraoxo-3-oxa-5,8,11,14-tetraazahexadecan-16-oate (255q)

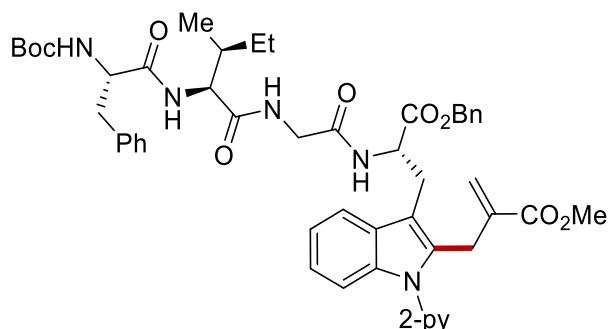


The general procedure **I** was followed using (6S,9S,12S)-ethyl 9,12-diisopropyl-2,2-dimethyl-4,7,10,13-tetraoxo-6-[[1-(pyridin-2-yl)-1H-indol-3-yl]methyl]-3-oxa-5,8,11,14-tetraazahexadecan-16-oate **243x** (66.4 mg, 0.10 mmol), methyl 2-[[*tert*-butoxycarbonyl]oxy]methyl]acrylate **253a** (43.2 mg, 0.20 mmol), $MnBr(CO)_5$ (2.7 mg, 10 mol %) and NaOAc (2.5 mg, 30 mol %) in 1,4-dioxane (0.3 mL). Purification by column chromatography on silica gel (*n*-hexane/EtOAc: 1/1 \rightarrow 1/4) yielded **255q** (74.9 mg, 98%) as a white solid.

M. p.: 217 – 220 °C. **1H NMR** (600 MHz, $CDCl_3$): δ 8.56 (dd, $J = 5.1, 1.5$ Hz, 1H), 7.82 (ddd, $J = 7.7, 7.7, 2.0$ Hz, 1H), 7.61 (ddd, $J = 7.3, 3.6, 3.6$ Hz, 1H), 7.41 – 7.31 (m, 2H), 7.27 (ddd, $J = 7.4, 4.9, 1.0$ Hz, 1H), 7.27 – 7.21 (m, 1H), 7.14 – 7.07 (m, 2H), 7.05 – 6.93 (m, 2H), 5.91 (d, $J = 1.5$ Hz, 1H), 5.50 (brs, 1H), 4.99 (d, $J = 1.5$ Hz, 1H), 4.55 (ddd, $J = 6.2, 6.2, 6.2$ Hz, 1H), 4.48 – 4.39 (m, 1H), 4.25 (dd, $J = 5.9, 5.9$ Hz, 1H), 4.15 (q, $J = 7.1$ Hz, 2H), 4.04 – 3.92 (m, 4H), 3.63 (s, 3H), 3.31 (dd, $J = 15.0, 5.1$ Hz, 1H), 3.27 – 3.20 (m, 1H), 2.32 – 2.24 (m, 1H), 2.22 – 2.14 (m, 1H), 1.33 (s, 9H), 1.22 (t, $J = 7.1$ Hz, 3H), 0.93 (t, $J = 6.2$ Hz, 6H), 0.84 (d, $J = 6.8$ Hz, 3H), 0.81 (d, $J = 6.8$ Hz, 3H). **^{13}C NMR** (126 MHz, $CDCl_3$): δ 172.9 (C_q), 171.3 (C_q), 170.9 (C_q), 169.5 (C_q), 166.6 (C_q), 155.8 (C_q), 151.0 (C_q), 149.3 (CH), 138.3 (CH), 137.2 (C_q), 136.9 (C_q), 134.3 (C_q), 128.1 (C_q), 126.3 (CH_2), 122.6 (CH), 122.2 (CH), 121.1 (CH), 120.8 (CH), 118.8 (CH), 110.4 (C_q), 110.0 (CH), 80.4 (C_q), 61.2 (CH_2), 59.5 (CH), 58.7 (CH), 55.6 (CH), 52.0 (CH_3), 41.3 (CH_2), 30.0 (CH), 30.0 (CH), 28.2 (CH_3), 27.2 (CH_2), 27.0 (CH_2), 19.3 (CH_3), 19.2 (CH_3), 17.7 (CH_3), 14.2 (CH_3). (One aliphatic CH_3 is missing due to overlap, the overlap was verified by HSQC analysis, showing that the peak at 17.7 ppm

corresponds to two carbons). **IR** (ATR): 3281, 2963, 2931, 1719, 1634, 1471, 1437, 1253, 1195, 737 cm^{-1} . **MS** (ESI): m/z (relative intensity): 785 (79) $[\text{M}+\text{Na}]^+$, 763 (100) $[\text{M}+\text{H}]^+$, 401 (21). **HR-MS** (ESI): m/z calcd for $\text{C}_{40}\text{H}_{54}\text{N}_6\text{O}_9^+$ $[\text{M}+\text{H}]^+$: 763.4025, found: 763.4012.

(6S,9S,15S)-Benzyl 6-benzyl-9-[(S)-sec-butyl]-15-({2-[2-(methoxycarbonyl)allyl]-1-[pyridin-2-yl]-1H-indol-3-yl)methyl}-2,2-dimethyl-4,7,10,13-tetraoxo-3-oxa-5,8,11,14-tetraazahexadecan-16-oate (255r)



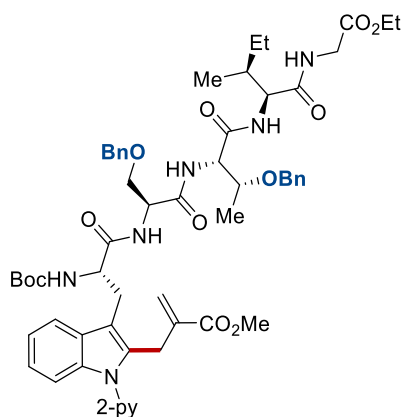
The general procedure **I** was followed using (6S,9S,15S)-benzyl 6-benzyl-9-[(S)-sec-butyl]-2,2-dimethyl-4,7,10,13-tetraoxo-15-[[1-(pyridin-2-yl)-1H-indol-3-yl]methyl]-3-oxa-5,8,11,14-tetraazahexadecan-16-oate **243y** (78.9 mg, 0.10 mmol), methyl 2-[[*tert*-butoxycarbonyl]oxy]methyl]acrylate **253a** (43.2 mg, 0.20 mmol), $\text{MnBr}(\text{CO})_5$ (2.7 mg, 10 mol %) and NaOAc (2.5 mg, 30 mol %) in 1,4-dioxane (0.3 mL). Purification by column chromatography on silica gel (*n*-hexane/EtOAc: 1/1 \rightarrow 1/4) yielded **255r** (74.5 mg, 84%) as a white solid.

M. p.: 108 – 111 °C. **$^1\text{H NMR}$** (600 MHz, CDCl_3): δ 8.55 (d, $J = 3.6$ Hz, 1H), 7.81 (ddd, $J = 7.7, 7.7, 1.9$ Hz, 1H), 7.60 – 7.50 (m, 1H), 7.29 – 7.23 (m, 6H), 7.22 – 7.20 (m, 2H), 7.18 – 7.08 (m, 7H), 7.03 (d, $J = 7.4$ Hz, 1H), 6.66 (brs, 1H), 6.48 (d, $J = 7.0$ Hz, 1H), 5.86 (td, $J = 1.8, 1.1$ Hz, 1H), 5.14 (d, $J = 7.8$ Hz, 1H), 5.09 (d, $J = 12.2$ Hz, 1H), 5.00 – 4.90 (m, 3H), 4.28 – 4.15 (m, 2H), 4.00 – 3.85 (m, 4H), 3.62 (s, 3H), 3.35 (dd, $J = 14.7, 6.8$ Hz, 1H), 3.31 (dd, $J = 14.7, 6.5$ Hz, 1H), 3.04 (dd, $J = 13.9, 6.6$ Hz, 1H), 3.00 (dd, $J = 13.9, 7.3$ Hz, 1H), 1.84 – 1.79 (m, 1H), 1.37 (s, 9H), 1.36 – 1.32 (m, 1H), 0.97 (ddd, $J = 13.5, 9.6, 7.2$ Hz, 1H), 0.82 – 0.71 (m, 6H). **$^{13}\text{C NMR}$** (126 MHz, CDCl_3): δ 171.5 (C_q), 171.3 (C_q), 170.7 (C_q), 168.2 (C_q), 166.7 (C_q), 155.5 (C_q), 151.0 (C_q), 149.4 (CH), 138.3 (CH), 137.0 (C_q), 136.8 (C_q), 136.5 (C_q), 135.0 (C_q), 134.4 (C_q), 129.2 (CH), 128.6 (CH), 128.4 (CH), 128.2 (CH), 128.2 (CH), 126.8 (CH), 126.5 (CH_2), 122.5 (CH), 122.2 (CH), 121.1 (CH), 120.8 (CH), 118.6 (CH), 110.3 (C_q), 110.1 (CH), 80.3 (C_q), 67.4 (CH_2), 58.0 (CH), 56.0 (CH), 52.9 (CH), 52.1 (CH_3), 42.8 (CH_2), 37.7 (CH_2),

5. Experimental Part

36.6 (CH), 28.3 (CH₃), 27.4 (CH₂), 27.3, (CH₂) 24.7 (CH₂), 15.5 (CH₃), 11.4 (CH₃). (One aromatic C_q is missing due to overlap, the overlap was verified by HSQC and HMBC analysis, showing that the peak at 128.2 ppm corresponds to two carbons). **IR** (ATR): 3288, 2960, 2925, 1716, 1635, 1520, 1470, 1366, 1252, 735, 697 cm⁻¹. **MS** (ESI): *m/z* (relative intensity) 909 (73) [M+Na]⁺, 887 (100) [M+H]⁺. **HR-MS** (ESI): *m/z* calcd for C₅₀H₅₉N₆O₉⁺ [M+H]⁺: 887.4338, found: 887.4344.

Ethyl (6*S*,9*S*,12*S*,15*S*)-12-[(*R*)-1-(benzyloxy)ethyl]-9-[(benzyloxy)methyl]-15-[(*S*)-*sec*-butyl]-6-[(2-[2-(methoxycarbonyl)allyl]-1-[pyridin-2-yl]-1*H*-indol-3-yl)methyl]-2,2-dimethyl-4,7,10,13,16-pentaoxo-3-oxa-5,8,11,14,17-pentaazanonadecan-19-oate (**255s**)

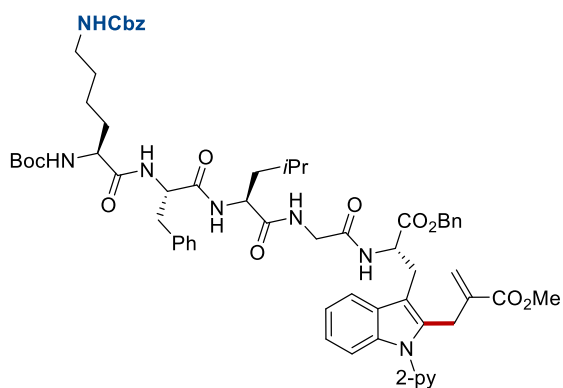


The general procedure **I** was followed using (6*S*,9*S*,12*S*,15*S*)-ethyl 12-[(*R*)-1-(benzyloxy)ethyl]-9-[(benzyloxy)methyl]-15-[(*S*)-*sec*-butyl]-2,2-dimethyl-4,7,10,13,16-pentaoxo-6-[[1-(pyridin-2-yl)-1*H*-indol-3-yl]methyl]-3-oxa-5,8,11,14,17-pentaazanonadecan-19-oate **243z** (94.8 mg, 0.10 mmol), methyl 2-[[(*tert*-butoxycarbonyl)oxy]methyl]acrylate **253a** (43.2 mg, 0.20 mmol), MnBr(CO)₅ (2.7 mg, 10 mol %) and NaOAc (2.5 mg, 30 mol %) in 1,4-dioxane (0.3 mL). Purification by column chromatography on silica gel (*n*-hexane/EtOAc: 1/2 → 0/1) yielded **255s** (86.8 mg, 83%) as a white solid.

M. p.: 140 – 144 °C. **¹H NMR** (600 MHz, CDCl₃): δ 8.57 (dd, *J* = 5.1, 1.9 Hz, 1H), 7.82 (ddd, *J* = 7.7, 7.7, 2.0 Hz, 1H), 7.60 (d, *J* = 7.2 Hz, 1H), 7.36 (dd, *J* = 7.7, 1.0 Hz, 1H), 7.30 – 7.18 (m, 13H), 7.15 – 7.09 (m, 2H), 7.01 – 6.93 (m, 3H), 5.91 (d, *J* = 1.4 Hz, 1H), 5.34 (d, *J* = 5.6 Hz, 1H), 5.01 (d, *J* = 1.4 Hz, 1H), 4.55 (d, *J* = 11.7 Hz, 1H), 4.47 – 4.35 (m, 7H), 4.21 (d, *J* = 7.0 Hz, 1H), 4.14 (q, *J* = 7.1 Hz, 2H), 4.05 – 3.98 (m, 1H), 3.96 (dd, *J* = 6.8, 1.6 Hz, 2H), 3.87 (dd, *J* = 17.9, 5.3 Hz, 1H), 3.80 (dd, *J* = 10.3, 3.6 Hz, 1H), 3.64 (s, 3H), 3.49 (dd, *J* = 9.7, 6.2 Hz, 1H), 3.23 (d, *J* = 6.7 Hz, 2H), 1.51 –

1.41 (m, 1H), 1.32 – 1.27 (m, 10H), 1.22 (t, $J = 7.1$ Hz, 3H), 1.14 (d, $J = 6.4$ Hz, 3H), 1.11 – 1.04 (m, 1H), 0.87 (d, $J = 6.8$ Hz, 3H), 0.78 (t, $J = 7.4$ Hz, 3H). ^{13}C NMR (126 MHz, CDCl_3): δ 172.6 (C_q), 171.1 (C_q), 170.2 (C_q), 169.8 (C_q), 169.5 (C_q), 166.6 (C_q), 155.5 (C_q), 151.1 (C_q), 149.4 (CH), 138.3 (CH), 137.8 (C_q), 137.2 (C_q), 137.0 (C_q), 136.9 (C_q), 134.3 (C_q), 128.3 (CH), 128.2 (CH), 128.1 (C_q), 127.8 (CH), 127.6 (CH), 127.6 (CH), 127.5 (CH), 126.2 (CH_2), 122.6 (CH), 122.3 (CH), 121.2 (CH), 120.7 (CH), 118.7 (CH), 110.4 (C_q), 110.0 (CH), 80.3 (C_q), 73.7 (CH), 73.4 (CH_2), 71.3 (CH_2), 68.8 (CH_2), 61.2 (CH_2), 58.6 (CH), 58.3 (CH), 55.4 (CH), 54.0 (CH), 52.0 (CH_3), 41.3 (CH_2), 36.5 (CH), 28.1 (CH_3), 27.3 (CH_2), 24.6 (CH_2), 16.2 (CH_3), 15.6 (CH_3), 14.2 (CH_3), 11.6 (CH_3). (One aliphatic CH_2 is missing due to overlap, the overlap was verified by HSQC analysis, showing that the peak at 27.3 ppm corresponds to two carbons). IR (ATR): 3280, 2972, 2932, 1719, 1633, 1523, 1471, 1199, 783 cm^{-1} . MS (ESI): m/z (relative intensity): 1068 (100) $[\text{M}+\text{Na}]^+$, 1046 (74) $[\text{M}+\text{H}]^+$. HR-MS (ESI): m/z calcd for $\text{C}_{57}\text{H}_{72}\text{N}_7\text{O}_{12}^+$ $[\text{M}+\text{H}]^+$: 1046.5233, found: 1046.5229.

Benzyl (9S,12S,15S,21S)-12-benzyl-9-[(*tert*-butoxycarbonyl)amino]-15-isobutyl-21-([2-[2-(methoxycarbonyl)allyl]-1-[pyridin-2-yl]-1*H*-indol-3-yl)methyl]-3,10,13,16,19-pentaoxo-1-phenyl-2-oxa-4,11,14,17,20-pentaazadocosan-22-oate (255t)



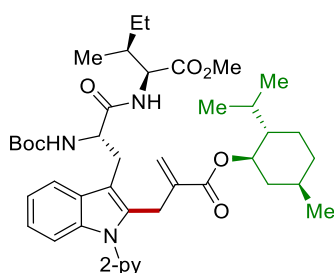
The general procedure I was followed using (9S,12S,15S,21S)-benzyl 12-benzyl-9-[(*tert*-butoxycarbonyl)amino]-15-isobutyl-3,10,13,16,19-pentaoxo-1-phenyl-21-[[1-(pyridin-2-yl)-1*H*-indol-3-yl)methyl]-2-oxa-4,11,14,17,20-pentaazadocosan-22-oate **243aa** (105.1 mg, 0.10 mmol), methyl 2-[[*tert*-butoxycarbonyl]oxy]methyl]acrylate **253a** (43.2 mg, 0.20 mmol), $\text{MnBr}(\text{CO})_5$ (2.7 mg, 10 mol %) and NaOAc (2.5 mg, 30 mol %) in 1,4-dioxane (0.3 mL). Purification by column chromatography on silica gel (*n*-hexane/EtOAc: 1/1 \rightarrow 1/4) yielded **255t** (80.4 mg, 70%) as a white solid.

M. p.: 100 – 102 °C. ^1H NMR (600 MHz, CDCl_3): δ 8.55 – 8.50 (m, 1H), 7.77 (ddd, $J =$

5. Experimental Part

7.7, 7.7, 2.0 Hz, 1H), 7.56 (dd, $J = 6.1, 3.1$ Hz, 1H), 7.36 – 7.29 (m, 4H), 7.30 – 7.21 (m, 6H), 7.21 – 7.15 (m, 6H), 7.14 – 7.06 (m, 5H), 6.95 – 6.89 (m, 2H), 6.78 (d, $J = 6.6$ Hz, 1H), 5.85 (s, 1H), 5.57 (brs, 1H), 5.18 – 5.02 (m, 3H), 4.98 – 4.87 (m, 2H), 4.84 – 4.75 (m, 2H), 4.60 – 4.54 (m, 1H), 4.52 – 4.44 (m, 1H), 4.06 – 3.98 (m, 2H), 3.93 (d, $J = 17.7$ Hz, 1H), 3.88 – 3.78 (m, 2H), 3.60 (s, 3H), 3.29 – 3.23 (m, 1H), 3.19 – 3.08 (m, 3H), 3.04 (dd, $J = 14.0, 5.9$ Hz, 1H), 1.79 – 1.64 (m, 2H), 1.62 – 1.54 (m, 1H), 1.54 – 1.33 (m, 7H), 1.29 (s, 9H), 0.88 (d, $J = 6.4$ Hz, 3H), 0.83 (d, $J = 6.5$ Hz, 3H). ^{13}C NMR (126 MHz, CDCl_3): δ 173.3 (C_q), 172.3 (C_q), 171.8 (C_q), 170.9 (C_q), 168.9 (C_q), 166.7 (C_q), 156.8 (C_q), 156.6 (C_q), 151.0 (C_q), 149.3 (CH), 138.2 (CH), 137.1 (C_q), 136.7 (C_q), 136.4 (C_q), 135.8 (C_q), 135.0 (C_q), 134.1 (C_q), 129.0 (CH), 128.7 (CH), 128.4 (CH), 128.3 (C_q), 128.2 (CH), 128.0 (CH), 128.0 (CH), 127.9 (CH), 127.2 (CH), 126.2 (CH_2), 122.4 (CH), 122.4 (CH), 122.1 (CH), 121.0 (CH), 120.7 (CH), 118.6 (CH), 110.6 (C_q), 110.1 (CH), 80.7 (C_q), 67.2 (CH_2), 66.7 (CH_2), 55.7 (CH), 54.9 (CH), 53.1 (CH), 52.1 (CH), 51.9 (CH_3), 43.1 (CH_2), 40.0 (CH_2), 39.8 (CH_2), 36.9 (CH_2), 30.8 (CH_2), 29.5 (CH_2), 28.3 (CH_3), 27.5 (CH_2), 27.1 (CH_2), 24.5 (CH), 23.2 (CH_3), 22.0 (CH_2), 21.2 (CH_3). IR (ATR): 3281, 2952, 1702, 1633, 1520, 1438, 1248, 1168, 734 cm^{-1} . MS (ESI): m/z (relative intensity): 1172 (41) $[\text{M}+\text{Na}]^+$, 1150 (50) $[\text{M}+\text{H}]^+$, 586 (100) 525 (100). HR-MS (ESI): m/z calcd for $\text{C}_{64}\text{H}_{76}\text{N}_8\text{O}_{12}^+$ $[\text{M}+\text{H}]^+$: 1149.5655, found: 1149.5647.

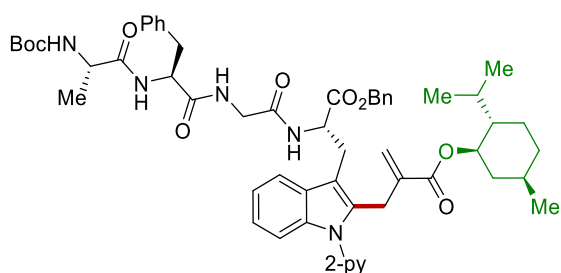
(2S,3S)-Methyl 2-({S}-2-[(*tert*-butoxycarbonyl)amino]-3-{2-[2-({(1R,2S,5R)-2-isopropyl-5-methylcyclohexyl}oxy)carbonyl]allyl}-1-[pyridin-2-yl]-1*H*-indol-3-yl]propanamido)-3-methylpentanoate (256a)



The general procedure I was followed using 2-[[S]-2-[(*tert*-butoxycarbonyl)amino]-3-[1-(pyridin-2-yl)-1*H*-indol-3-yl]propanamido]-3-methylpentanoate **243f** (101.7 mg, 0.20 mmol), (1*R*,2*S*,5*R*)-2-isopropyl-5-methylcyclohexyl 2-[[(*tert*-butoxycarbonyl)oxy]methyl]acrylate **253f** (136.2 mg, 0.40 mmol), $\text{MnBr}(\text{CO})_5$ (5.5 mg, 10 mol %) and NaOAc (4.9 mg, 30 mol %) in 1,4-dioxane (0.6 mL). Purification by column chromatography on silica gel (*n*-hexane/EtOAc: 1/1) yielded **256a** (130.9 mg, 90%) as a white solid.

M.p.: 87 – 89°C. **¹H NMR** (600 MHz, CDCl₃): δ 8.53 (dd, *J* = 5.0, 1.8 Hz, 1H), 7.78 (ddd, *J* = 7.7, 7.7, 2.0 Hz, 1H), 7.56 (d, *J* = 6.7 Hz, 1H), 7.38 (d, *J* = 7.9 Hz, 1H), 7.26 – 7.22 (m, 1H), 7.21 – 7.18 (m, 1H), 7.10 – 7.04 (m, 2H), 6.52 (d, *J* = 7.8 Hz, 1H), 5.84 (d, *J* = 1.4 Hz, 1H), 5.38 (d, *J* = 8.2 Hz, 1H), 5.05 (td, *J* = 2.5, 1.4 Hz, 1H), 4.60 (ddd, *J* = 10.9, 10.9, 4.4 Hz, 1H), 4.50 (ddd, *J* = 7.8, 7.8, 7.8 Hz, 1H), 4.32 (d, *J* = 6.3 Hz, 1H), 3.98 (s, 2H), 3.44 (s, 3H), 3.31 (s, 1H), 3.12 (dd, *J* = 14.4, 8.8 Hz, 1H), 1.94 – 1.87 (m, 1H), 1.73 – 1.57 (m, 4H), 1.40 (s, 9H), 1.36 – 1.25 (m, 4H), 1.08 – 0.92 (m, 2H), 0.85 – 0.80 (m, 7H), 0.79 (d, *J* = 7.0 Hz, 3H), 0.72 (d, *J* = 6.8 Hz, 3H), 0.65 (d, *J* = 6.9 Hz, 3H). **¹³C NMR** (126 MHz, CDCl₃): δ 171.0 (C_q), 170.9 (C_q), 165.5 (C_q), 155.1 (C_q), 151.3 (C_q), 149.2 (CH), 138.0 (CH), 137.7 (C_q), 136.8 (C_q), 134.5 (C_q), 128.4 (C_q), 125.9 (CH₂), 122.1 (CH), 122.0 (CH), 121.3 (CH), 120.5 (CH), 118.5 (CH), 110.6 (C_q), 109.7 (CH), 79.7 (C_q), 74.5 (CH), 56.4 (CH), 54.8 (CH), 51.7 (CH₃), 47.1 (CH), 40.7 (CH₂), 38.3 (CH), 34.2 (CH₂), 31.4 (CH), 28.4 (CH₃), 28.0 (CH₂), 27.9 (CH₂), 26.3 (CH), 25.2 (CH₂), 23.6 (CH₂), 22.0 (CH₃), 20.8 (CH₃), 16.5 (CH₃), 15.1 (CH₃), 11.6 (CH₃). **IR** (ATR): 2957, 2871, 1706, 1472, 1366, 1252, 737 cm⁻¹. **MS** (ESI): *m/z* (relative intensity): 1484 (9) [2M+Na]⁺, 753 (100) [M+Na]⁺, 731 (61) [M+H]⁺. **HR-MS** (ESI): *m/z* calcd for C₄₂H₅₉N₄O₇⁺ [M+H]⁺: 731.4378, found: 731.4374.

(6S,9S,15S)-Benzyl 9-benzyl-15-({2-[2-((1R,2S,5R)-2-isopropyl-5-methylcyclohexyl)oxy}carbonyl)allyl[-1-(pyridin-2-yl)-1H-indol-3-yl]methyl)-2,2,6-trimethyl-4,7,10,13-tetraoxo-3-oxa-5,8,11,14-tetraazahexadecan-16-oate (256b)

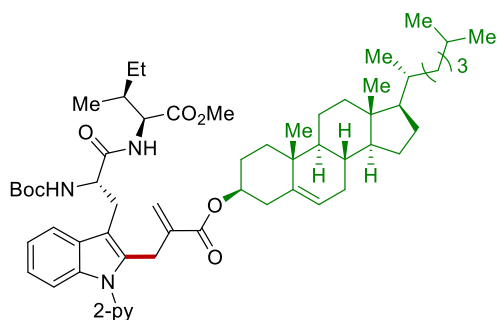


The general procedure I was followed using (6S,9S,15S)-benzyl 9-benzyl-2,2,6-trimethyl-4,7,10,13-tetraoxo-15-[[1-(pyridin-2-yl)-1H-indol-3-yl]methyl]-3-oxa-5,8,11,14-tetraazahexadecan-16-oate **243v** (74.7 mg, 0.10 mmol), (1R,2S,5R)-2-isopropyl-5-methylcyclohexyl 2-[[*tert*-butoxycarbonyl]oxy]methyl]acrylate **253g** (68.1 mg, 0.20 mmol), MnBr(CO)₅ (2.7 mg, 10 mol %) and NaOAc (2.5 mg, 30 mol %) in 1,4-dioxane (0.3 mL). Purification by column chromatography on silica gel (*n*-hexane/EtOAc: 2/1 → 1/2) yielded **256b** (89.2 mg, 83%) as a white solid.

5. Experimental Part

M. p.: 112 – 114 °C. **¹H NMR** (600 MHz, CDCl₃): δ 8.48 (dd, *J* = 5.0, 1.8 Hz, 1H), 7.78 (ddd, *J* = 7.7, 7.7, 2.0 Hz, 1H), 7.53 (dd, *J* = 6.0, 3.1 Hz, 1H), 7.29 – 7.23 (m, 6H), 7.22 – 7.20 (m, 2H), 7.19 – 7.15 (m, 1H), 7.15 – 7.09 (m, 6H), 7.06 (d, *J* = 7.0 Hz, 1H), 7.00 (d, *J* = 7.7 Hz, 1H), 6.90 (brs, 1H), 5.84 (d, *J* = 1.3 Hz, 1H), 5.08 – 5.04 (m, 2H), 4.97 – 4.91 (m, 2H), 4.88 (q, *J* = 6.9 Hz, 1H), 4.65 – 4.53 (m, 2H), 4.03 (d, *J* = 9.4 Hz, 1H), 3.97 – 3.84 (m, 3H), 3.79 (dd, *J* = 16.8, 5.3 Hz, 1H), 3.34 (dd, *J* = 14.8, 7.0 Hz, 1H), 3.30 (dd, *J* = 15.1, 6.9 Hz, 1H), 3.07 (dd, *J* = 14.0, 6.6 Hz, 1H), 3.02 (dd, *J* = 13.8, 7.2 Hz, 1H), 1.91 – 1.75 (m, 1H), 1.69 – 1.50 (m, 3H), 1.47 – 1.38 (m, 1H), 1.36 (s, 9H), 1.31 – 1.21 (m, 1H), 1.13 (d, *J* = 7.0 Hz, 3H), 1.06 – 0.94 (m, 1H), 0.91 – 0.78 (m, 5H), 0.75 (d, *J* = 7.0 Hz, 3H), 0.62 (d, *J* = 7.0 Hz, 3H). **¹³C NMR** (126 MHz, CDCl₃): δ 172.7 (C_q), 171.5 (C_q), 170.8 (C_q), 168.2 (C_q), 165.6 (C_q), 155.4 (C_q), 151.1 (C_q), 149.2 (CH), 138.2 (CH), 137.5 (C_q), 136.7 (C_q), 136.4 (C_q), 135.0 (C_q), 134.7 (C_q), 129.1 (CH), 128.5 (CH), 128.4 (C_q), 128.3 (CH), 128.2 (CH), 128.1 (CH), 126.8 (CH₂), 125.8 (CH), 122.5 (CH), 122.1 (CH), 121.1 (CH), 120.7 (CH), 118.5 (CH), 110.3 (C_q), 110.1 (CH), 80.2 (C_q), 74.6 (CH), 67.4 (CH₂), 54.4 (CH), 53.0 (CH), 50.5 (CH), 47.0 (CH), 43.0 (CH₂), 40.8 (CH₂), 37.6 (CH₂), 34.2 (CH₂), 31.3 (CH), 28.3 (CH₃), 27.3 (CH₂), 27.2 (CH₂), 26.3 (CH), 23.5 (CH₂), 22.0 (CH₃), 20.7 (CH₃), 18.2 (CH₃), 16.5 (CH₃). **IR** (ATR): 3290, 2955, 2926, 2869, 1707, 1638, 1520, 1471, 1438, 1250, 737 cm⁻¹. **MS** (ESI): *m/z* (relative intensity): 991 (100) [M+Na]⁺, 970 (83) [M+H]⁺, 504 (46). **HR-MS** (ESI): *m/z* calcd for C₅₆H₆₉N₆O₉⁺ [M+H]⁺: 969.5121, found: 969.5111.

Methyl **[(S)-2-((tert-butoxycarbonyl)amino)-3-(2-{2-[[{3S,8S,9S,10R,13R,14S,17R]-10,13-dimethyl-17-[(R)-6-methylheptan-2-yl]-2,3,4,7,8,9,10,11,12,13,14,15,16,17-tetradecahydro-1H-cyclopenta[a]phenanthren-3-yl]oxy)carbonyl]allyl}-1-(pyridin-2-yl)-1H-indol-3-yl)propanoyl]-L-isoleucinate (256c)**



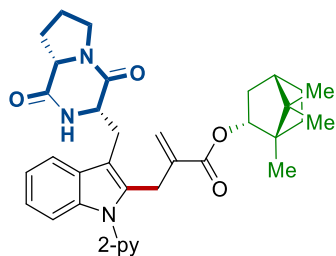
The general procedure I was followed using (2S,3S)-methyl 2-[[S]-2-[(tert-butoxycarbonyl)amino]-3-[1-(pyridin-2-yl)-1H-indol-3-yl]propanamido]-3-

methylpentanoate **243i** (50.9 mg, 0.10 mmol), (3*S*,8*S*,9*S*,10*R*,13*R*,14*S*,17*R*)-10,13-dimethyl-17-[(*R*)-6-methylheptan-2-yl]-2,3,4,7,8,9,10,11,12,13,14,15,16,17-tetradecahydro-1*H*-cyclopenta[*a*]phenanthren-3-yl 2-[[(*tert*-butoxycarbonyl)oxy]methyl]acrylate **253h** (114.2 mg, 0.20 mmol), MnBr(CO)₅ (2.7 mg, 10 mol %) and NaOAc (2.5 mg, 30 mol %) in 1,4-dioxane (0.3 mL). Purification by column chromatography on silica gel (*n*-hexane/EtOAc: 2/1 → 1/2) yielded **256c** (85.6 mg, 89%) as a colorless oil.

¹H NMR (600 MHz, CDCl₃): δ 8.58 (ddd, *J* = 4.9, 2.0, 0.8 Hz, 1H), 7.82 (td, *J* = 7.7, 1.9 Hz, 1H), 7.57 (d, *J* = 7.0 Hz, 1H), 7.45 – 7.41 (m, 1H), 7.28 (ddd, *J* = 7.4, 4.8, 1.0 Hz, 1H), 7.22 – 7.18 (m, 1H), 7.12 – 7.06 (m, 2H), 6.59 (d, *J* = 6.7 Hz, 1H), 5.83 (d, *J* = 1.3 Hz, 1H), 5.52 – 5.34 (m, 1H), 5.28 (d, *J* = 5.6 Hz, 1H), 5.06 (s, 1H), 4.62 – 4.55 (m, 2H), 4.32 (dd, *J* = 8.2, 4.9 Hz, 1H), 4.05 (d, *J* = 17.0 Hz, 1H), 3.98 (d, *J* = 17.0 Hz, 1H), 3.46 (s, 3H), 3.37 – 3.29 (m, 1H), 3.18 – 3.08 (m, 1H), 2.31 – 2.19 (m, 2H), 2.00 (dt, *J* = 12.7, 3.5 Hz, 1H), 1.97 – 1.90 (m, 1H), 1.86 – 1.76 (m, 3H), 1.70 (tddd, *J* = 8.3, 6.1, 4.2, 1.7 Hz, 1H), 1.60 – 1.20 (m, 21H), 1.18 – 0.94 (m, 13H), 0.92 – 0.89 (m, 4H), 0.86 (d, *J* = 2.7 Hz, 3H), 0.85 (d, *J* = 2.7 Hz, 3H), 0.83 (t, *J* = 7.4 Hz, 3H), 0.74 (d, *J* = 6.9 Hz, 3H), 0.67 (s, 3H). **¹³C NMR** (126 MHz, CDCl₃): δ 171.1 (C_q), 170.9 (C_q), 165.5 (C_q), 155.1 (C_q), 151.4 (C_q), 149.2 (CH), 139.5 (C_q), 138.0 (CH), 137.8 (C_q), 136.9 (C_q), 134.4 (C_q), 128.4 (C_q), 125.9 (CH₂), 122.5 (CH), 122.1 (CH), 122.1 (CH), 121.4 (CH), 120.5 (CH), 118.5 (CH), 110.5 (CH), 109.6 (C_q), 79.6 (C_q), 74.2 (CH), 56.7 (CH), 56.4 (CH), 56.1 (CH), 54.5 (CH), 51.7 (CH₃), 50.1 (CH), 42.3 (C_q), 39.7 (CH₂), 39.5 (CH₂), 38.4 (CH), 37.9 (CH₂), 37.0 (CH₂), 36.6 (CH₂), 36.2 (C_q), 35.8 (CH), 31.9 (CH₂), 31.9 (CH), 28.4 (CH₃), 28.3 (CH₂), 28.1 (CH), 28.0 (CH₂), 28.0 (CH₂), 27.7 (CH₂), 25.1 (CH₂), 24.3 (CH₂), 23.9 (CH₂), 22.9 (CH₃), 22.6 (CH₃), 21.1 (CH₂), 19.4 (CH₃), 18.8 (CH₃), 15.2 (CH₃), 11.9 (CH₃), 11.7 (CH₃). **IR** (ATR): 3346, 2948, 2868, 1740, 1710, 1675, 1472, 1437, 1366, 1159, 736 cm⁻¹. **MS** (ESI): *m/z* (relative intensity): 984 (100) [M+Na]⁺, 962 (39) [M+H]⁺. **HR-MS** (ESI): *m/z* calcd for C₅₉H₈₅N₄O₇⁺ [M+H]⁺: 961.6413, found: 961.6391.

5. Experimental Part

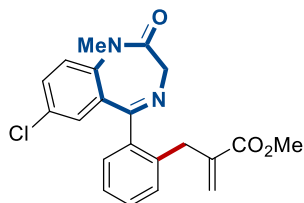
(1*S*,2*R*,4*S*)-1,7,7-trimethylbicyclo[2.2.1]heptan-2-yl 2-[(3-[(3*S*,8*aS*)-1,4-dioxooctahydropyrrolo[1,2-*a*]pyrazin-3-yl)methyl]-1-(pyridin-2-yl)-1*H*-indol-2-yl)methyl]acrylate (**256d**)



The general procedure I was followed using 3(3*S*,8*aS*)-3-[[1-(pyridin-2-yl)-1*H*-indol-3-yl]methyl]hexahydropyrrolo[1,2-*a*]pyrazine-1,4-dione **243c** (36.1 mg, 0.10 mmol), (1*S*,2*R*,4*S*)-1,7,7-trimethylbicyclo[2.2.1]heptan-2-yl 2-[[*tert*-butoxycarbonyloxy]methyl]acrylate **253i** (67.7 mg, 0.20 mmol), MnBr(CO)₅ (2.7 mg, 10 mol %) and NaOAc (2.5 mg, 30 mol %) in 1,4-dioxane (0.3 mL). Purification by column chromatography on silica gel (*n*-hexane/EtOAc: 1/2) yielded **256d** (56.3 mg, 97%) as a white solid.

M. p.: 95 – 96 °C. **¹H NMR** (600 MHz, CDCl₃): δ 8.57 (ddd, *J* = 4.9, 2.0, 0.9 Hz, 1H), 7.86 – 7.80 (m, 1H), 7.60 – 7.53 (m, 1H), 7.36 (ddd, *J* = 8.0, 1.0, 1.0 Hz, 1H), 7.33 – 7.26 (m, 2H), 7.21 – 7.14 (m, 2H), 5.97 (s, 1H), 5.97 (s, 1H), 5.04 (s, 1H), 4.84 (ddd, *J* = 10.0, 3.5, 2.1 Hz, 1H), 4.47 – 4.39 (m, 1H), 4.08 – 4.00 (m, 2H), 3.92 (dt, *J* = 17.8, 1.7 Hz, 1H), 3.74 (dd, *J* = 15.3, 3.8 Hz, 1H), 3.65 (dt, *J* = 12.1, 8.2 Hz, 1H), 3.57 (ddd, *J* = 12.0, 8.9, 3.2 Hz, 1H), 3.03 (dd, *J* = 15.3, 11.4 Hz, 1H), 2.35 – 2.27 (m, 2H) 2.11 – 1.96 (m, 2H), 1.94 – 1.78 (m, 2H), 1.71 (tt, *J* = 12.1, 4.0 Hz, 1H), 1.64 (t, *J* = 4.5 Hz, 1H), 1.26 (dddd, *J* = 17.8, 11.6, 6.0, 3.6 Hz, 1H), 1.18 (ddd, *J* = 12.0, 9.4, 4.4 Hz, 1H), 0.92 – 0.88 (m, 1H), 0.87 (s, 3H), 0.84 (s, 3H), 0.76 (s, 3H). **¹³C NMR** (126 MHz, CDCl₃): δ 169.3 (C_q), 166.2 (C_q), 165.5 (C_q), 150.8 (C_q), 149.5 (CH), 138.2 (CH), 137.8 (C_q), 137.0 (C_q), 134.9 (C_q), 127.7 (C_q), 125.5 (CH₂), 122.9 (CH), 122.3 (CH), 121.1 (CH), 120.9 (CH), 118.1 (CH), 110.5 (CH), 109.7 (C_q), 80.5 (CH), 59.3 (CH), 54.8 (CH), 48.9 (C_q), 47.8 (C_q), 45.5 (CH₂), 44.9 (CH), 36.7 (CH₂), 28.4 (CH₂), 28.0 (CH₂), 27.3 (CH₂), 27.3 (CH₂), 25.7 (CH₂), 22.7 (CH₂), 19.7 (CH₃), 18.9 (CH₃), 13.6 (CH₃). **IR** (ATR): 3054, 2953, 2878, 1663, 1586, 1470, 1458, 1262, 1138, 784 cm⁻¹. **MS** (ESI): *m/z* (relative intensity) 603 (100) [M+Na]⁺, 581 (82) [M+H]⁺, 117 (35). **HR-MS** (ESI): *m/z* calcd for C₃₅H₄₁N₄O₄⁺ [M+H]⁺: 581.3122, found: 581.3124.

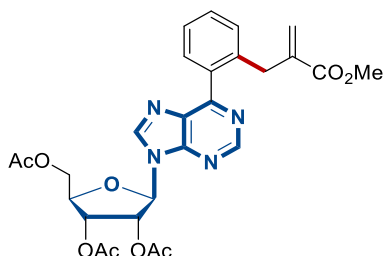
Methyl 2-[2-(7-chloro-1-methyl-2-oxo-2,3-dihydro-1H-benzo[e][1,4]diazepin-5-yl)benzyl]acrylate (258c)



The general procedure **J** was followed using 7-chloro-1-methyl-5-phenyl-1H-benzo[e][1,4]diazepin-2(3H)-one **257c** (56.9 mg, 0.20 mmol), methyl 2-[[*tert*-butoxycarbonyl]oxy]methyl]acrylate **253a** (86.5 mg, 0.40 mmol), MnBr(CO)₅ (5.5 mg, 10 mol %) and NaOAc (4.9 mg, 30 mol %) in 1,4-dioxane (1.0 mL). Purification by column chromatography on silica gel (*n*-hexane/EtOAc: 4/1 → 2/1) yielded **258c** (49.8 mg, 65%) as a colorless oil.

¹H NMR (300 MHz, CDCl₃): δ 7.44 – 7.29 (m, 4H), 7.23 – 7.14 (m, 2H), 6.99 (dd, *J* = 2.5, 0.3 Hz, 1H), 6.10 (td, *J* = 1.8, 1.2 Hz, 1H), 5.15 (td, *J* = 2.3, 1.2 Hz, 1H), 4.81 (d, *J* = 10.9 Hz, 1H), 3.75 (d, *J* = 10.9 Hz, 1H), 3.64 (s, 3H), 3.46 (d, *J* = 17.1 Hz, 1H), 3.35 (s, 3H), 3.26 (d, *J* = 17.1 Hz, 1H). **¹³C NMR** (126 MHz, CDCl₃): δ 170.2 (C_q), 169.4 (C_q), 166.9 (C_q), 141.5 (C_q), 138.9 (C_q), 138.3 (C_q), 136.5 (C_q), 131.3 (CH), 131.2 (C_q), 130.9 (CH), 130.3 (CH), 129.8 (CH), 129.3 (C_q), 129.3 (CH), 126.8 (CH), 126.5 (CH₂), 122.3 (CH), 56.8 (CH₂), 51.9 (CH₃), 35.1 (CH₂), 34.7 (CH₃). **IR** (ATR): 2950, 2917, 2849, 1716, 1673, 1613, 1480, 1341, 1196, 946, 732 cm⁻¹. **MS** (ESI): *m/z* (relative intensity) 405 (74) [M+Na]⁺, 383 (100) [M+H]⁺. **HR-MS** (ESI): *m/z* calcd for C₂₁H₂₀³⁵ClN₂O₃⁺ [M+H]⁺: 383.1157, found: 383.1156.

(2R,3R,4R,5R)-2-(acetoxymethyl)-5-(6-{2-[2-(methoxycarbonyl)allyl]phenyl}-9H-purin-9-yl)tetrahydrofuran-3,4-diyl diacetate (260a)



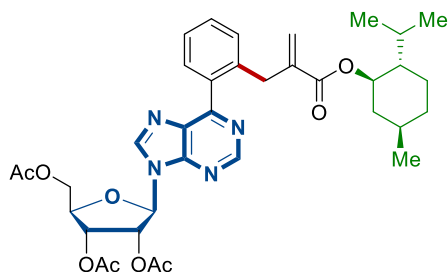
The general procedure **J** was followed using (2R,3R,4R,5R)-2-(acetoxymethyl)-5-(6-phenyl-9H-purin-9-yl)tetrahydrofuran-3,4-diyl diacetate **259a** (90.9 mg, 0.20 mmol), methyl 2-[[*tert*-butoxycarbonyl]oxy]methyl]acrylate **253a** (86.5 mg, 0.40 mmol), MnBr(CO)₅ (5.5 mg, 10 mol %) and NaOAc (4.9 mg, 30 mol %) in 1,4-dioxane (1.0 mL).

5. Experimental Part

Purification by column chromatography on silica gel (*n*-hexane/EtOAc: 5/1 → 2/1) yielded **260a** (99.4 mg, 90%) as a colorless oil.

¹H NMR (600 MHz, CDCl₃): δ 9.00 (s, 1H), 8.22 (s, 1H), 7.74 (dd, *J* = 7.6, 1.5 Hz, 1H), 7.47 – 7.37 (m, 2H), 7.37 – 7.34 (m, 1H), 6.28 (d, *J* = 5.1 Hz, 1H), 6.05 (ddd, *J* = 1.8, 1.8, 1.3 Hz, 1H), 6.01 (t, *J* = 5.3 Hz, 1H), 5.71 (dd, *J* = 5.6, 4.7 Hz, 1H), 5.20 (ddd, *J* = 2.3, 2.3, 1.3 Hz, 1H), 4.50 – 4.45 (m, 2H), 4.40 (dd, *J* = 13.0, 5.2 Hz, 1H), 3.96 (d, *J* = 16.6 Hz, 1H), 3.93 (d, *J* = 16.6 Hz, 1H), 3.60 (s, 3H), 2.15 (s, 3H), 2.11 (s, 3H), 2.10 (s, 3H). **¹³C NMR** (126 MHz, CDCl₃): δ 170.1 (C_q), 169.4 (C_q), 169.2 (C_q), 167.1 (C_q), 158.9 (C_q), 152.2 (CH), 151.3 (C_q), 142.8 (CH), 139.6 (C_q), 137.7 (C_q), 134.6 (C_q), 132.6 (C_q), 131.2 (CH), 130.9 (CH), 129.9 (CH), 126.5 (CH), 126.2 (CH₂), 86.5 (CH), 80.3 (CH), 73.1 (CH), 70.6 (CH), 63.0 (CH₂), 51.8 (CH₃), 35.1 (CH₂), 20.8 (CH₃), 20.6 (CH₃), 20.5 (CH₃). **IR** (ATR): 2952, 2926, 1746, 1718, 1583, 1372, 1214, 1046, 765 cm⁻¹. **MS** (ESI): *m/z* (relative intensity): 575 (15) [M+Na]⁺, 553 (100) [M+H]⁺. **HR-MS** (ESI): *m/z* calcd for C₂₇H₂₉N₄O₉⁺ [M+H]⁺: 553.1929, found: 553.1922.

(2*R*,3*R*,4*R*,5*R*)-2-(acetoxymethyl)-5-(6-{2-[2-({[(1*R*,2*S*,5*R*)-2-isopropyl-5-methylcyclohexyl]oxy}carbonyl)allyl]phenyl}-9*H*-purin-9-yl)tetrahydrofuran-3,4-diyl diacetate (**260b**)

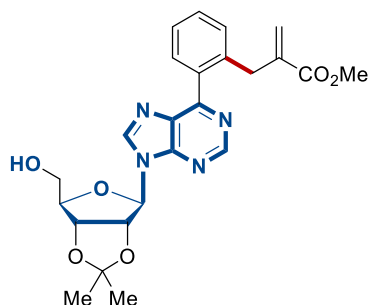


The general procedure **J** was followed using (2*R*,3*R*,4*R*,5*R*)-2-(acetoxymethyl)-5-(6-phenyl-9*H*-purin-9-yl)tetrahydrofuran-3,4-diyl diacetate **259a** (90.9 mg, 0.20 mmol), (1*R*,2*S*,5*R*)-2-isopropyl-5-methylcyclohexyl 2-[[*tert*-butoxycarbonyl]oxy]methyl]acrylate **253f** (136.2 mg, 0.40 mmol), MnBr(CO)₅ (5.5 mg, 10 mol %) and NaOAc (4.9 mg, 30 mol %) in 1,4-dioxane (1.0 mL). Purification by column chromatography on silica gel (*n*-hexane/EtOAc: 5/1 → 3/1) yielded **260b** (116.4 mg, 86%) as a colorless oil.

¹H NMR (600 MHz, CDCl₃): δ 9.00 (s, 1H), 8.23 (s, 1H), 7.77 (dd, *J* = 7.6, 1.6 Hz, 1H), 7.43 (ddd, *J* = 7.4, 7.4, 1.6 Hz, 1H), 7.39 (ddd, *J* = 7.6, 7.6, 1.4 Hz, 1H), 7.35 (dd, *J* = 7.6, 1.4 Hz, 1H), 6.29 (d, *J* = 5.4 Hz, 1H), 6.07 (ddd, *J* = 1.9, 1.9, 1.4 Hz, 1H), 5.99 (dd, *J* = 5.4, 5.4 Hz, 1H), 5.70 (dd, *J* = 5.4, 4.6 Hz, 1H), 5.20 (ddd, *J* = 2.2, 2.2, 1.4 Hz, 1H),

4.61 (ddd, $J = 10.9, 10.9, 4.4$ Hz, 1H), 4.51 – 4.44 (m, 2H), 4.42 – 4.38 (m, 1H), 3.97 (d, $J = 17.0$ Hz, 1H), 3.93 (d, $J = 17.0$ Hz, 1H), 2.16 (s, 3H), 2.12 (s, 3H), 2.10 (s, 3H), 1.86 (dtd, $J = 12.0, 3.8, 1.8$ Hz, 1H), 1.66 – 1.57 (m, 3H), 1.42 (tdd, $J = 12.0, 6.5, 3.3$ Hz, 1H), 1.27 (ddt, $J = 12.4, 10.9, 3.2$ Hz, 1H), 0.99 (qd, $J = 13.5, 12.9, 3.8$ Hz, 1H), 0.87 – 0.83 (s, 4H), 0.81 (dd, $J = 12.4, 1.5$ Hz, 1H), 0.78 (d, $J = 7.0$ Hz, 3H), 0.64 (d, $J = 7.0$ Hz, 3H). ^{13}C NMR (126 MHz, CDCl_3): δ 170.1 (C_q), 169.4 (C_q), 169.1 (C_q), 166.2 (C_q), 158.9 (C_q), 152.2 (CH), 151.3 (C_q), 142.6 (CH), 140.2 (C_q), 138.0 (C_q), 134.5 (C_q), 132.6 (C_q), 131.3 (CH), 130.7 (CH), 129.8 (CH), 126.4 (CH), 125.8 (CH_2), 86.3 (CH), 80.4 (CH), 74.5 (CH), 73.1 (CH), 70.6 (CH), 63.1 (CH_2), 46.9 (CH), 40.6 (CH_2), 35.3 (CH_2), 34.2 (CH_2), 31.4 (CH), 26.2 (CH), 23.5 (CH_2), 22.0 (CH_3), 20.8 (CH_3), 20.8 (CH_3), 20.6 (CH_3), 20.5 (CH_3), 16.4 (CH_3). IR (ATR): 2955, 2869, 1748, 1707, 1582, 1456, 1210, 911, 729 cm^{-1} . MS (ESI): m/z (relative intensity) 699 (12) $[\text{M}+\text{Na}]^+$, 677 (100) $[\text{M}+\text{H}]^+$. HR-MS (ESI): m/z calcd for $\text{C}_{36}\text{H}_{45}\text{N}_4\text{O}_9^+$ $[\text{M}+\text{H}]^+$: 677.3181, found: 677.3177.

Methyl 2-(2-{9-[(3aR,4R,6R,6aR)-6-(hydroxymethyl)-2,2-dimethyltetrahydrofuro[3,4-d][1,3]dioxol-4-yl]-9H-purin-6-yl}benzyl)acrylate (260c)



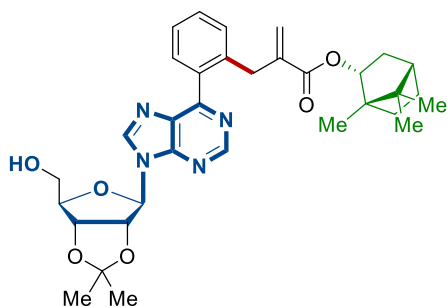
The general procedure **J** was followed using [(3aR,4R,6R,6aR)-2,2-dimethyl-6-(6-phenyl-9H-purin-9-yl)tetrahydrofuro[3,4-d][1,3]dioxol-4-yl]methanol **259b** (73.6 mg, 0.20 mmol), methyl 2-[(*tert*-butoxycarbonyl)oxy]methyl acrylate **253a** (86.5 mg, 0.40 mmol), $\text{MnBr}(\text{CO})_5$ (5.5 mg, 10 mol %) and NaOAc (4.9 mg, 30 mol %) in 1,4-dioxane (1.0 mL). Purification by column chromatography on silica gel (*n*-hexane/EtOAc: 2/1 \rightarrow 1/2) yielded **260c** (79.3 mg, 85%) as a colorless oil.

^1H NMR (300 MHz, CDCl_3): δ 8.96 (s, 1H), 8.18 (s, 1H), 7.72 (dd, $J = 7.0, 2.1$ Hz, 1H), 7.48 – 7.32 (m, 3H), 6.03 (ddd, $J = 1.8, 1.8, 1.3$ Hz, 1H), 5.99 (d, $J = 4.7$ Hz, 1H), 5.63 (dd, $J = 10.7, 2.2$ Hz, 1H), 5.28 (dd, $J = 5.9, 4.7$ Hz, 1H), 5.18 (ddd, $J = 2.3, 2.3, 1.3$ Hz, 1H), 5.13 (ddd, $J = 6.0, 1.5, 0.4$ Hz, 1H), 4.55 (q, $J = 1.8$ Hz, 1H), 4.02 – 3.89 (m,

5. Experimental Part

3H), 3.78 (ddd, $J = 12.7, 10.5, 2.1$ Hz, 1H), 3.59 (s, 3H), 1.65 (s, 3H), 1.38 (s, 3H). ^{13}C NMR (126 MHz, CDCl_3): δ 167.0 (C_q), 159.5 (C_q), 151.4 (CH), 150.4 (C_q), 144.1 (CH), 139.5 (C_q), 137.7 (C_q), 134.4 (C_q), 133.5 (C_q), 131.2 (CH), 131.0 (CH), 130.0 (CH), 126.5 (CH), 126.2 (CH_2), 114.2 (C_q), 93.9 (CH), 86.2 (CH), 83.0 (CH), 81.5 (CH), 63.2 (CH_2), 51.8 (CH_3), 35.1 (CH_2), 27.6 (CH_3), 25.3 (CH_3). IR (ATR): 2990, 2939, 2249, 1715, 1584, 1329, 1208, 1108, 1076, 725 cm^{-1} . MS (ESI): m/z (relative intensity) 956 (38) $[2\text{M}+\text{Na}]^+$, 489 (45) $[\text{M}+\text{Na}]^+$, 467 (100) $[\text{M}+\text{H}]^+$. HR-MS (ESI): m/z calcd for $\text{C}_{24}\text{H}_{27}\text{N}_4\text{O}_6^+$ $[\text{M}+\text{H}]^+$: 467.1925, found: 467.1931.

(1*S*,2*R*,4*S*)-1,7,7-Trimethylbicyclo[2.2.1]heptan-2-yl 2-(2-{9-[(3*aR*,4*R*,6*R*,6*aR*)-6-(hydroxymethyl)-2,2-dimethyltetrahydrofuro[3,4-*d*][1,3]dioxol-4-yl]-9*H*-purin-6-yl}benzyl)acrylate (260d)

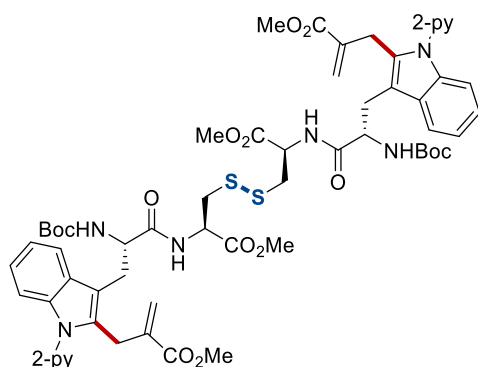


The general procedure **J** was followed using [(3*aR*,4*R*,6*R*,6*aR*)-2,2-dimethyl-6-(6-phenyl-9*H*-purin-9-yl)tetrahydrofuro[3,4-*d*][1,3]dioxol-4-yl]methanol **259b** (73.7 mg, 0.20 mmol), (1*S*,2*R*,4*S*)-1,7,7-trimethylbicyclo[2.2.1]heptan-2-yl 2-[[*tert*-butoxycarbonyl]oxy]methyl]acrylate **253i** (135.4 mg, 0.40 mmol), $\text{MnBr}(\text{CO})_5$ (5.5 mg, 10 mol %) and NaOAc (4.9 mg, 30 mol %) in 1,4-dioxane (1.0 mL). Purification by column chromatography on silica gel (*n*-hexane/EtOAc: 1/2 \rightarrow 0/1) yielded **260d** (82.4 mg, 70%) as a colorless oil.

^1H NMR (400 MHz, CDCl_3): δ 8.97 (s, 1H), 8.15 (s, 1H), 7.77 (dd, $J = 7.5, 1.5$ Hz, 1H), 7.50 – 7.34 (m, 3H), 6.08 (ddd, $J = 1.8, 1.8, 1.4$ Hz, 1H), 5.98 (d, $J = 4.8$ Hz, 1H), 5.63 (dd, $J = 11.0, 2.1$ Hz, 1H), 5.30 (dd, $J = 5.9, 4.8$ Hz, 1H), 5.18 (ddd, $J = 2.4, 2.4, 1.4$ Hz, 1H), 5.15 (dd, $J = 6.0, 1.4$ Hz, 1H), 4.82 (ddd, $J = 9.9, 3.5, 2.1$ Hz, 1H), 4.57 (t, $J = 1.8$ Hz, 1H), 4.09 – 3.91 (m, 3H), 3.82 (ddd, $J = 12.9, 11.1, 2.1$ Hz, 1H), 2.40 – 2.17 (m, 1H), 1.82 – 1.55 (m, 7H), 1.39 (s, 3H), 1.29 – 1.04 (m, 2H), 0.86 (s, 3H), 0.83 (s, 3H), 0.72 (s, 3H). ^{13}C NMR (101 MHz, CDCl_3): δ 167.1 (C_q), 159.7 (C_q), 151.5 (CH), 150.5 (C_q), 144.2 (CH), 140.1 (C_q), 138.1 (C_q), 134.4 (C_q), 133.8 (C_q), 131.4 (CH), 130.9 (CH), 130.2 (CH), 126.6 (CH), 126.1 (CH_2), 114.3 (C_q), 94.1 (CH), 86.2 (CH),

82.9 (CH), 81.6 (CH), 80.2 (CH), 63.3 (CH₂), 48.8 (C_q), 47.7 (C_q), 44.8 (CH), 36.6 (CH₂), 35.3 (CH₂), 27.9 (CH₂), 27.6 (CH₃), 27.1 (CH₂), 25.2 (CH₃), 19.6 (CH₃), 18.8 (CH₃), 13.4 (CH₃). IR (ATR): 2983, 2953, 2875, 1710, 1583, 1455, 1328, 1266, 1209, 946, 763 cm⁻¹. MS (ESI): *m/z* (relative intensity) 611 (18) [M+Na]⁺, 590 (100) [M+H]⁺. HR-MS (ESI): *m/z* calcd for C₃₃H₄₁N₄O₆⁺ [M+H]⁺: 589.3021, found: 589.3020.

(6*S*,9*R*,14*R*)-Methyl 14-[[*S*]-2-[(*tert*-butoxycarbonyl)amino]-3-{2-[2-{methoxycarbonyl}allyl]-1-[pyridin-2-yl]-1*H*-indol-3-yl]propanamido}-9-{methoxycarbonyl}-6-[[2-(2-(methoxycarbonyl)allyl)-1-[pyridin-2-yl]-1*H*-indol-3-yl]methyl]-2,2-dimethyl-4,7-dioxo-3-oxa-11,12-dithia-5,8-diazapentadecan-15-oate (S1**)**



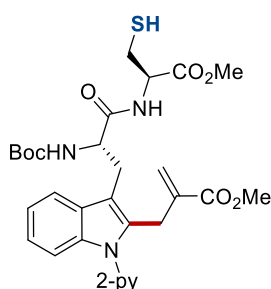
The general procedure I was followed using (6*S*,9*R*,14*R*)-methyl 14-[[*S*]-2-[(*tert*-butoxycarbonyl)amino]-3-[1-(pyridin-2-yl)-1*H*-indol-3-yl]propanamido]-9-[methoxycarbonyl]-2,2-dimethyl-4,7-dioxo-6-[[1-(pyridin-2-yl)-1*H*-indol-3-yl]methyl]-3-oxa-11,12-dithia-5,8-diazapentadecan-15-oate **261** (99.5 mg, 0.10 mmol), methyl 2-[[[(*tert*-butoxycarbonyl)oxy]methyl]acrylate **253A** (86.5 mg, 0.40 mmol), MnBr(CO)₅ (4.9 mg, 20 mol %) and NaOAc (2.5 mg, 30 mol %) in 1,4-dioxane (0.6 mL). Purification by column chromatography on silica gel (CH₂Cl₂/EtOAc: 4/1 → 3/1) yielded **S1** (115.6 mg, 97%) as a white solid.

M. p.: 136 – 138 °C. ¹H NMR (300 MHz, CDCl₃): δ 8.54 (ddd, *J* = 4.9, 1.9, 0.8 Hz, 2H), 7.80 (ddd, *J* = 7.7, 7.7, 1.9 Hz, 2H), 7.56 (ddd, *J* = 7.0, 3.5, 3.5 Hz, 2H), 7.36 (ddd, *J* = 7.9, 0.9, 0.9 Hz, 2H), 7.28 – 7.22 (m, 2H), 7.22 – 7.16 (m, 2H), 7.12 – 7.00 (m, 4H), 6.90 (t, *J* = 4.5 Hz, 2H), 5.85 (d, *J* = 1.3 Hz, 2H), 5.50 (d, *J* = 7.9 Hz, 2H), 5.04 (d, *J* = 1.3 Hz, 2H), 4.73 – 4.46 (m, 4H), 4.02 (d, *J* = 17.3 Hz, 2H), 3.94 (d, *J* = 17.3 Hz, 2H), 3.61 (s, 6H), 3.52 (s, 6H), 3.30 (dd, *J* = 14.3, 6.2 Hz, 2H), 3.15 (dd, *J* = 14.3, 7.9 Hz, 2H), 2.99 – 2.84 (m, 4H), 1.37 (s, 18H). ¹³C NMR (126 MHz, CDCl₃): δ 171.5 (C_q), 169.7 (C_q), 166.7 (C_q), 155.1 (C_q), 151.2 (C_q), 149.2 (CH), 138.1 (CH), 137.2 (C_q),

5. Experimental Part

136.8 (C_q), 134.2 (C_q), 128.3 (C_q), 126.2 (CH₂), 122.2 (CH), 122.1 (CH), 121.2 (CH), 120.5 (CH), 118.6 (CH), 110.7 (C_q), 109.8 (CH), 79.7 (C_q), 54.4 (CH), 52.4 (CH), 52.0 (CH₃), 51.6 (CH₃), 40.5 (CH₂), 28.3 (CH₃), 28.1 (CH₂), 27.7 (CH₂). **IR** (ATR): 3355, 2950, 1745, 1715, 1676, 1472, 1438, 1367, 1164, 738 cm⁻¹. **MS** (ESI): *m/z* (relative intensity): 2404 (21) [2M+Na]⁺, 1213 (74) [M+Na]⁺, 1191 (100) [M+H]⁺, 607 (27). **HR-MS** (ESI): *m/z* calcd for C₆₀H₇₁N₈O₁₄S₂⁺ [M+H]⁺: 1191.4526 found: 1191.4516.

Methyl 2-{{3-{{[S]-2-[(*tert*-butoxycarbonyl)amino]-3-{{[(*R*)-3-mercapto-1-methoxy-1-oxopropan-2-yl]amino}-3-oxopropyl]-1-{{pyridin-2-yl}-1*H*-indol-2-yl}methyl}acrylate (262)

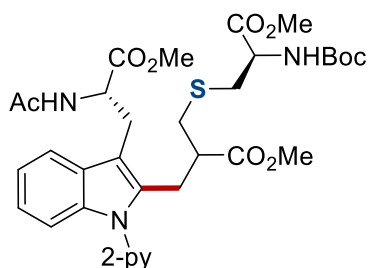


Following a modified literature procedure, the corresponding disulfide **S1** (64.4 mg, 0.054 mmol), PPh₃ (14.1 mg, 0.054 mmol), NaOAc (1.7 mg, 0.022 mmol) and HOAc (5.5 μL, 0.097 mmol) were dissolved in MeOH/H₂O (9 mL, 10/1). The mixture was heated to 60 °C for 16 h under N₂. After cooling to ambient temperature, H₂O (10 mL) were added and the mixture was extracted with CH₂Cl₂ (3 x 15 mL). The combined organic layers were dried over Na₂SO₄ and concentrated *in vacuo*. Purification by column chromatography on silica gel (CH₂Cl₂/EtOAc: 4/1) yielded **262** (47.1 mg, 73%) as colorless oil.

¹H NMR (400 MHz, CDCl₃): δ 8.56 (ddd, *J* = 4.9, 2.0, 0.8 Hz, 1H), 7.82 (ddd, *J* = 8.1, 7.5, 2.0 Hz, 1H), 7.62 – 7.52 (m, 1H), 7.39 (ddd, *J* = 8.1, 0.9, 0.9 Hz, 1H), 7.27 (ddd, *J* = 7.5, 4.9, 1.0 Hz, 1H), 7.23 – 7.17 (m, 1H), 7.14 – 7.06 (m, 2H), 6.77 (d, *J* = 6.7 Hz, 1H), 5.85 (td, *J* = 1.9, 1.3 Hz, 1H), 5.40 (d, *J* = 6.3 Hz, 1H), 5.05 (td, *J* = 2.5, 1.3 Hz, 1H), 4.62 (ddd, *J* = 7.6, 7.6, 7.6 Hz, 1H), 4.53 (ddd, *J* = 6.8, 4.2 Hz, 1H), 4.03 (d, *J* = 17.1 Hz, 1H), 3.98 (d, *J* = 17.1 Hz, 1H), 3.63 (s, 3H), 3.55 (s, 3H), 3.43 – 3.31 (m, 1H), 3.14 (dd, *J* = 14.4, 8.3 Hz, 1H), 2.90 (ddd, *J* = 13.0, 8.5, 4.2 Hz, 1H), 2.76 (ddd, *J* = 13.0, 8.5, 4.2 Hz, 1H), 1.42 (s, 9H), 1.23 (t, *J* = 8.5, 1H). **¹³C NMR** (101 MHz, CDCl₃): δ 171.6 (C_q), 169.5 (C_q), 166.8 (C_q), 155.2 (C_q), 151.3 (C_q), 149.4 (CH), 138.2 (CH), 137.3 (C_q), 137.0 (C_q), 134.3 (C_q), 128.4 (C_q), 126.4 (CH₂), 122.4 (CH), 122.3 (CH),

121.3 (CH), 120.7 (CH), 118.6 (CH), 110.6 (C_q), 109.8 (CH), 79.9 (C_q), 54.5 (CH), 53.8 (CH), 52.4 (CH₃), 52.0 (CH₃), 28.3 (CH₃), 27.9 (CH₂), 27.8 (CH₂), 26.8 (CH₂). IR (ATR): 3338, 2952, 2925, 1743, 1711, 1670, 1471, 1437, 1366, 1210, 1159, 736 cm⁻¹. MS (ESI): *m/z* (relative intensity) 619 (100) [M+Na]⁺, 597 (75) [M+H]⁺, 290 (38). HR-MS (ESI): *m/z* calcd for C₃₀H₃₇N₄O₇S⁺ [M+H]⁺: 597.2377, found: 597.2378.

Methyl (2S)-2-acetamido-3-(2-{2-[[[R]-2-[(*tert*-butoxycarbonyl)amino]-3-methoxy-3-oxopropyl]thio)methyl]-3-methoxy-3-oxopropyl}-1-{pyridin-2-yl}-1H-indol-3-yl)propanoate (264)



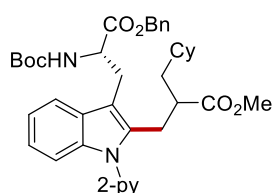
Following a modified literature procedure, a mixture of methyl (*S*)-2-[[3-(2-acetamido-3-methoxy-3-oxopropyl)-1-(pyridin-2-yl)-1*H*-indol-2-yl]methyl]acrylate **254a** (156.6 mg, 0.36 mmol), Boc-Cys-OMe **263** (127.1 mg, 0.54 mmol), Et₃N (54.6 mg, 0.54 mmol) in dry DMF (4.5 mL) was stirred at 60 °C under N₂ for 16 h. After cooling to ambient temperature, EtOAc (30 mL) was added and the mixture was washed with brine three times. The organic layer was dried over Na₂SO₄ and concentrated *in vacuo*. Purification by column chromatography on silica gel (*n*-hexane/EtOAc: 2/1 → 1/2) yielded **264** (172.3 mg, 71%, d.r. 1.6) as a white solid.

M. p.: 71 – 75 °C. ¹H NMR (300 MHz, CDCl₃): δ 8.73 – 8.47 (m, 1H), 8.00 – 7.81 (m, 1H), 7.60 – 7.47 (m, 1H), 7.50 – 7.39 (m, 1H), 7.39 – 7.27 (m, 1H), 7.28 – 7.22 (m, 1H), 7.18 – 7.06 (m, 2H), 6.32 (d, *J* = 7.5 Hz, 0.62H), 6.21 (d, *J* = 7.8 Hz, .38H), 5.37 (d, *J* = 8.2 Hz, 0.32H), 5.28 (d, *J* = 8.0 Hz, 0.62H), 5.00 – 4.81 (m, 1H), 4.46 – 4.28 (m, 1H), 3.67 – 3.65 (m, 4.13H), 3.64 (s, 1.87H), 3.47 (s, 1.87H), 3.46 (s, 1.13H), 3.38 – 3.12 (m, 4H), 2.82 – 2.29 (m, 5H), 1.94 (s, 3H), 1.40 (s, 5.61H), 1.39 (s, 3.39H). ¹³C NMR (126 MHz, CDCl₃): *Major diastereoisomer.* δ 173.6 (C_q), 172.4 (C_q), 171.0 (C_q), 169.7 (C_q), 154.9 (C_q), 151.0 (C_q), 149.7 (CH), 138.5 (CH), 136.7 (C_q), 134.5 (C_q), 128.2 (C_q), 122.6 (CH), 122.2 (CH), 120.9 (CH), 120.7 (CH), 118.6 (CH), 110.5 (C_q), 110.0 (CH), 80.1 (C_q), 53.0 (CH), 52.7 (CH), 52.4 (CH₃), 52.3 (CH₃), 51.9 (CH₃), 45.2 (CH), 34.8 (CH₂), 34.3 (CH₂), 28.3 (CH₃), 27.0 (CH₂), 26.9 (CH₂), 23.0 (CH₃). *Minor diastereoisomer.* δ 173.5 (C_q), 172.2 (C_q), 171.1 (C_q), 169.6 (C_q), 154.9 (C_q), 151.0

5. Experimental Part

(C_q), 149.6 (CH), 138.5 (CH), 136.7 (C_q), 134.6 (C_q), 128.4 (C_q), 122.5 (CH), 122.2 (CH), 121.0 (CH), 120.7 (CH), 118.5 (CH), 110.4 (C_q), 109.9 (CH), 80.0 (C_q), 53.3 (CH), 52.9 (CH), 52.4 (CH₃), 52.3 (CH₃), 51.8 (CH₃), 45.5 (CH), 34.8 (CH₂), 34.4 (CH₂), 28.3 (CH₃), 27.0 (CH₂), 26.9 (CH₂), 23.2 (CH₃). **IR** (ATR): 3368, 2977, 2952, 1735, 1663, 1471, 1458, 1437, 1367, 1215, 1163, 729cm⁻¹. **MS** (ESI): *m/z* (relative intensity) 693 (100) [M+Na]⁺, 671 (76) [M+H]⁺, 571 (24). **HR-MS** (ESI): *m/z* calcd for C₃₃H₄₃N₄O₉S⁺ [M+H]⁺: 671.2745, found: 671.2744.

Benzyl (2S)-2-[(*tert*-butoxycarbonyl)amino]-3-{2-[2-(cyclohexylmethyl)-3-methoxy-3-oxopropyl]-1-pyridin-2-yl]-1*H*-indol-3-yl}propanoate (265)

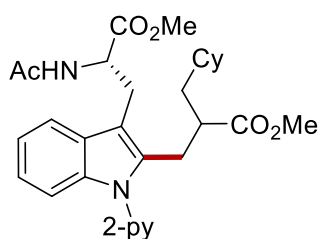


Following a modified literature procedure, a suspension of 1,3-dioxoisindolin-2-yl cyclohexanecarboxylate (54.6 mg, 0.20 mmol), methyl (*S*)-2-{{3-{{3-[benzyloxy]-2-[(*tert*-butoxycarbonyl)amino]-3-oxopropyl]-1-pyridin-2-yl]-1*H*-indol-2-yl}methyl}acrylate **254b** (227.5 mg, 0.40 mmol), Ni(acac)₂ (20.5 mg, 40.0 mol %), LiCl (25.4 mg, 0.60 mmol), Zn (26.1 mg, 0.40 mmol) in MeCN (1.0 mL) was stirred at 25 °C under N₂. After 16 h the mixture was diluted with CH₂Cl₂ (20 mL), filtered through a pad of Celite and concentrated *in vacuo*. Purification by column chromatography on silica gel afforded the desired product **265** (73.2 mg, 56%, d.r. 1.5) as a colorless oil.

¹H NMR (600 MHz, CDCl₃): δ 8.65 – 8.60 (m, 1H), 7.94 – 7.83 (m, 1H), 7.62 – 7.49 (m, 1H), 7.41 – 7.36 (m, 1H), 7.34 – 7.30 (m, 1H), 7.29 – 7.22 (m, 4H), 7.20 – 7.13 (m, 2H), 7.15 – 7.09 (m, 2H), 5.29 (d, *J* = 8.1 Hz, 0.60H), 5.13 (d, *J* = 8.1 Hz, 0.40H), 5.11 – 4.95 (m, 2H), 4.73 (ddd, *J* = 8.1, 7.0, 7.0 Hz, 0.60H), 4.66 (ddd, *J* = 8.1, 6.8, 6.8 Hz, 0.40H), 3.40 (s, 1.80H), 3.38 (s, 1.18H), 3.36 – 3.21 (m, 2H), 3.18 – 3.04 (m, 2H), 2.26 – 2.17 (m, 1H), 1.60 – 1.51 (m, 3H), 1.45 – 1.36 (m, 9H), 1.36 – 1.30 (m, 2H), 1.28 – 1.19 (m, 2H), 1.13 – 0.87 (m, 4H), 0.69 – 0.48 (m, 2H). **¹³C NMR** (126 MHz, CDCl₃): *Major diastereoisomer.* δ 175.8 (C_q), 172.3 (C_q), 155.1 (C_q), 151.4 (C_q), 149.6 (CH), 138.3 (CH), 136.8 (C_q), 135.8 (C_q), 135.2 (C_q), 128.6 (C_q), 128.3 (CH), 128.1 (CH), 128.1 (CH), 122.6 (CH), 122.1 (CH), 121.2 (CH), 120.5 (CH), 118.8 (CH), 110.1 (C_q), 109.7 (CH), 79.6 (C_q), 67.1 (CH₂), 54.0 (CH), 51.5 (CH₃), 42.4 (CH), 40.4 (CH₂), 35.2 (CH), 33.2 (CH₂), 32.7 (CH₂), 28.4 (CH₃), 28.0 (CH₂), 27.5 (CH₂), 26.4 (CH₂), 26.2

(CH₂), 26.1 (CH₂). *Minor diastereoisomer*: δ 175.6 (C_q), 172.1 (C_q), 155.0 (C_q), 151.3 (C_q), 149.6 (CH), 138.3 (CH), 136.8 (C_q), 135.8 (C_q), 135.2 (C_q), 128.6 (C_q), 128.3 (CH), 128.1 (CH), 128.0 (CH), 122.3 (CH), 122.0 (CH), 121.1 (CH), 120.5 (CH), 118. (CH), 110.1 (C_q), 109.8 (CH), 79.7 (C_q), 67.2 (CH₂), 54.4 (CH), 51.4 (CH₃), 42.5 (CH), 40.1 (CH₂), 35.3 (CH), 33.3 (CH₂), 32.6 (CH₂), 28.4 (CH₃), 28.1 (CH₂), 27.4 (CH₂), 26.4 (CH₂), 26.2 (CH₂), 26.1 (CH₂). **IR** (ATR): 2923, 2851, 1731, 1710, 1586, 1471, 1458, 1437, 1367, 1164, 735 cm⁻¹. **MS** (ESI): *m/z* (relative intensity) 676 (49) [M+Na]⁺, 654 (100) [M+H]⁺, 598 (17). **HR-MS** (ESI): *m/z* calcd for C₃₉H₄₈N₃O₆⁺ [M+H]⁺: 654.3538, found: 654.3532.

Methyl (2S)-2-acetamido-3-{2-[2-(cyclohexylmethyl)-3-methoxy-3-oxopropyl]-1-[pyridin-2-yl]-1H-indol-3-yl]propanoate (266)



Following a modified literature procedure, a suspension of 1,3-dioxoisindolin-2-yl cyclohexanecarboxylate (54.6 mg, 0.20 mmol), methyl (S)-2-[[3-(2-acetamido-3-methoxy-3-oxopropyl)-1-(pyridin-2-yl)-1H-indol-2-yl]methyl]acrylate **254a** (174.2 mg, 0.40 mmol), Ni(acac)₂ (20.5 mg, 40.0 mol %), LiCl (25.4 mg, 0.60 mmol), Zn (26.1 mg, 0.40 mmol) in MeCN (1.0 mL) was stirred at 25 °C under N₂. After 16 h the mixture was diluted with CH₂Cl₂ (20 mL), filtered through a pad of Celite and concentrated *in vacuo*. Purification by column chromatography on silica gel afforded the desired product **266** (53.9 mg, 52%, d.r. 1.3) as a colorless oil.

¹H NMR (300 MHz, CDCl₃): δ 8.70 – 8.63 (m, 1H), 8.04 – 7.89 (m, 1H), 7.68 – 7.44 (m, 2H), 7.42 – 7.34 (m, 1H), 7.32 – 7.25 (m, 1H), 7.20 – 7.11 (m, 2H), 6.45 (d, *J* = 7.2 Hz, 0.56H), 6.18 (d, *J* = 7.9 Hz, 0.44H), 5.05 – 4.90 (m, 1H), 3.74 (s, 1.68H), 3.71 (s, 1.32H), 3.68 – 3.61 (m, 1H), 3.47 (s, 1.68H), 3.45 (s, 1.32H), 3.42 – 3.06 (m, 4H), 1.99 (s, 1.68H), 1.97 (s, 1.32H), 1.67 – 1.38 (m, 5H), 1.35 – 0.89 (m, 6H), 0.79 – 0.50 (m, 2H). **¹³C NMR** (101 MHz, CDCl₃): *Major diastereoisomer*. δ 176.2 (C_q), 172.9 (C_q), 170.1 (C_q), 151.7 (C_q), 149.7 (CH), 138.6 (CH), 136.9 (C_q), 135.8 (C_q), 128.7 (C_q), 122.5 (CH), 122.3 (CH), 121.2 (CH), 120.7 (CH), 118.7 (CH), 110.1 (C_q), 109.7 (CH), 52.7 (CH), 52.3 (CH₃), 51.6 (CH₃), 42.1 (CH), 40.5 (CH₂), 35.2 (CH), 33.2 (CH₂), 32.7

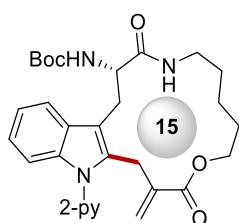
5. Experimental Part

(CH₂), 27.8 (CH₂), 26.9 (CH₂), 26.1 (CH₂), 23.0 (CH₃). *Minor diastereoisomer*: δ 175.8 (C_q), 172.5 (C_q), 169.8 (C_q), 151.4 (C_q), 149.7 (CH), 138.5 (CH), 136.8 (C_q), 135.9 (C_q), 128.3 (C_q), 122.4 (CH), 122.3 (CH), 121.2 (CH), 120.6 (CH), 118.6 (CH), 109.9 (C_q), 109.9 (CH), 52.9 (CH), 52.3 (CH₃), 51.5 (CH₃), 42.3 (CH), 40.3 (CH₂), 35.2 (CH), 33.3 (CH₂), 32.6 (CH₂), 28.0 (CH₂), 26.7 (CH₂), 26.1 (CH₂), 23.2 (CH₃). **IR** (ATR): 3355, 3292, 2924, 2851, 1734, 1656, 1471, 1437, 1212, 1174, 748 cm⁻¹. **MS** (ESI): *m/z* (relative intensity) 1062 (7) [2M+Na]⁺, 542 (100) [M+Na]⁺, 520 (60) [M+H]⁺. **HR-MS** (ESI): *m/z* calcd for C₃₀H₃₈N₃O₅⁺ [M+H]⁺: 520.2806, found: 520.2806.

tert-Butyl

(*S*)-[12-methylene-3,11-dioxo-14-(pyridin-2-yl)-

2,3,4,5,6,7,8,9,11,12,13,14-dodecahydro-1*H*-[1]oxa[7]azacyclopentadecino[12,11-*b*]indol-2-yl]carbamate (**268**)

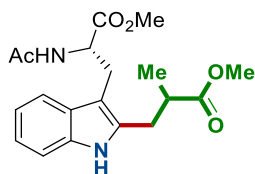


A suspension of peptide **267** (650.7 mg, 1.0 mmol), MnBr(CO)₅ (27.5 mg, 10 mol %) and NaOAc (24.6 mg, 30 mol %) in 1,4-dioxane (25 mL, 40 mM) was stirred at 80 °C for 16 h under N₂. After cooling to ambient temperature, CH₂Cl₂ (50 mL) was added and the mixture concentrated *in vacuo*. Purification by column chromatography on silica gel (*n*-hexane/EtOAc: 1/1) yielded **268** (330.0 mg, 62%) as a white solid.

M. p.: 245 °C (decomposition). **¹H NMR** (600 MHz, CDCl₃): δ 8.57 (dd, *J* = 5.2, 1.9 Hz, 1H), 7.85 (td, *J* = 7.7, 2.0 Hz, 1H), 7.59 – 7.54 (m, 1H), 7.32 – 7.26 (m, 2H), 7.24 (d, *J* = 7.5 Hz, 1H), 7.14 – 7.05 (m, 2H), 6.19 (brs, 1H), 5.57 – 5.48 (m, 2H), 5.13 (s, 1H), 4.70 – 4.60 (m, 2H), 4.22 (d, *J* = 16.2 Hz, 1H), 3.98 (d, *J* = 16.2 Hz, 1H), 3.81 – 4.67 (m, 1H), 3.33 – 3.23 (m, 1H), 3.08 (dd, *J* = 14.2, 9.8 Hz, 2H), 2.42 – 2.32 (m, 1H), 1.68 (tdd, *J* = 11.5, 6.0, 3.0 Hz, 1H), 1.42 (s, 9H), 1.40 – 1.20 (m, 4H), 0.87 – 0.76 (m, 1H). **¹³C NMR** (126 MHz, CDCl₃): δ 171.1 (C_q), 168.6 (C_q), 155.0 (C_q), 151.2 (C_q), 149.2 (CH), 138.4 (C_q), 137.9 (CH), 136.6 (C_q), 133.7 (C_q), 129.0 (C_q), 124.8 (CH₂), 122.4 (CH), 121.9 (CH), 120.8 (CH), 120.7 (CH), 119.2 (CH), 111.9 (C_q), 109.2 (CH), 79.4 (C_q), 62.1 (CH₂), 53.9 (CH), 38.4 (CH₂), 29.6 (CH₂), 29.1 (CH₂), 28.5 (CH₂), 28.4 (CH₃), 25.4 (CH₂), 20.1 (CH₂). **IR** (ATR): 3344, 3325, 3052, 2926, 2868, 1710, 1654, 1470, 1457, 1438, 1249, 733 cm⁻¹. **MS** (ESI): *m/z* (relative intensity) 555 (67) [M+Na]⁺, 533 (100) [M+H]⁺, 433 (29). **HR-MS** (ESI): *m/z* calcd for C₃₀H₃₇N₄O₅⁺ [M+H]⁺: 533.2758,

found: 533.2756.

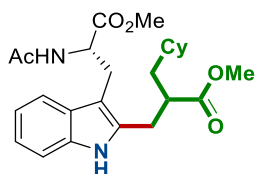
Methyl (S)-2-acetamido-3-[2-(3-methoxy-2-methyl-3-oxopropyl)-1H-indol-3-yl]propanoate (269a)



General procedure **K** was followed using **254a** (87.1 mg, 0.20 mmol). Purification by column chromatography on silica gel (*n*-hexane/EtOAc: 1/2) yielded **269a** (43.2 mg, 60%, d.r. 1.1) as a colorless oil.

¹H NMR (400 MHz, CDCl₃): δ 8.69 – 8.60 (m, 1H), 7.48 – 7.38 (m, 1H), 7.30 – 7.20 (m, 1H), 7.14 – 6.99 (m, 2H), 6.20 (d, *J* = 7.1 Hz, 0.48 H), 6.15 (d, *J* = 7.1 Hz, 0.52H), 4.94 – 4.73 (m, 1H), 3.73 – 3.57 (m, 6H), 3.29 – 3.15 (m, 2H), 3.13 – 2.93 (m, 1H), 2.89 – 2.74 (m, 2H), 1.92 (s, 1.55H), 1.91 (s, 1.45H), 1.29 – 1.13 (m, 3H). **¹³C NMR** (101 MHz, CDCl₃): *Major diastereoisomer*. δ 177.2 (C_q), 172.5 (C_q), 169.7 (C_q), 135.3 (C_q), 134.4 (C_q), 128.3 (C_q), 121.5 (CH), 119.3 (CH), 118.0 (CH), 110.7 (CH), 106.6 (C_q), 53.0 (CH), 52.3 (CH₃), 52.1 (CH₃), 39.9 (CH), 28.8 (CH₂), 26.8 (CH₂), 23.1 (CH₃), 17.4 (CH₃). *Minor diastereoisomer*. δ 177.2 (C_q), 172.6 (C_q), 169.8 (C_q), 135.3 (C_q), 134.3 (C_q), 128.2 (C_q), 121.5 (CH), 119.3 (CH), 118.0 (CH), 110.7 (CH), 106.6 (C_q), 53.0 (CH), 52.3 (CH₃), 52.1 (CH₃), 39.7 (CH), 28.7 (CH₂), 26.8 (CH₂), 23.0 (CH₃), 17.5 (CH₃). **IR** (ATR): 3374, 3297, 2953, 1732, 1655, 1529, 1436, 1208, 1177, 738 cm⁻¹. **MS** (ESI): *m/z* (relative intensity) 743 (11) [2M+Na]⁺, 383 (100) [M+Na]⁺, 361 (73) [M+H]⁺. **HR-MS** (ESI): *m/z* calcd for C₁₉H₂₅N₂O₅⁺ [M+H]⁺: 361.1758, found: 361.1760.

Methyl (2S)-2-acetamido-3-{2-[2-(cyclohexylmethyl)-3-methoxy-3-oxopropyl]-1H-indol-3-yl}propanoate (269b)



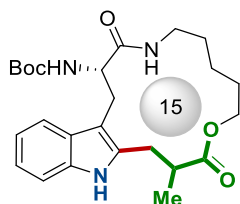
General procedure **K** was followed using **266** (103.8 mg, 0.20 mmol). Purification by column chromatography on silica gel (*n*-hexane/EtOAc: 1/1) yielded **269b** (46.8 mg, 53%, d.r. 1.3) as a colorless oil.

¹H NMR (600 MHz, CDCl₃): δ 8.49 – 8.43 (m, 1H), 7.44 (d, *J* = 7.9 Hz, 0.56H), 7.41 (d, *J* = 7.9 Hz, 0.44H), 7.28 – 7.21 (m, 1H), 7.14 – 7.06 (m, 1H), 7.08 – 7.01 (m, 1H), 6.18

5. Experimental Part

– 6.06 (m, 1H), 4.88 – 4.80 (m, 1H), 3.67 – 3.58 (m, 6H), 3.28 – 3.13 (m, 2H), 2.99 – 2.85 (m, 1H), 2.90 – 2.75 (m, 2H), 1.92 (s, 1.32H), 1.91 (s, 1.68H), 1.76 – 1.53 (m, 6H), 1.38 – 1.07 (m, 5H), 0.93 – 0.78 (m, 2H). ^{13}C NMR (126 MHz, CDCl_3): *Major diastereoisomer*. δ 177.2 (C_q), 172.5 (C_q), 169.7 (C_q), 135.4 (C_q), 134.2 (C_q), 128.3 (C_q), 121.5 (CH), 119.4 (CH), 118.1 (CH), 110.6 (CH), 106.6 (C_q), 53.0 (CH), 52.2 (CH₃), 52.0 (CH₃), 43.0 (CH), 40.3 (CH₂), 35.6 (CH), 33.3 (CH₂), 33.1 (CH₂), 27.9 (CH₂), 26.5 (CH₂), 26.2 (CH₂), 23.1 (CH₃). *Minor diastereoisomer*. δ 177.2 (C_q), 172.4 (C_q), 169.5 (C_q), 135.3 (C_q), 134.2 (C_q), 128.4 (C_q), 121.5 (CH), 119.3 (CH), 118.0 (CH), 110.6 (CH), 106.5 (C_q), 53.0 (CH), 52.2 (CH₃), 52.0 (CH₃), 43.0 (CH), 40.2 (CH₂), 35.6 (CH), 33.4 (CH₂), 33.0 (CH₂), 28.1 (CH₂), 26.9 (CH₂), 26.2 (CH₂), 23.2 (CH₃). IR (ATR): 3363, 3291, 2922, 2850, 1729, 1655, 1460, 1436, 1212, 1197, 1170, 909, 730 cm^{-1} . MS (ESI): m/z (relative intensity) 908 (39) $[2\text{M}+\text{Na}]^+$, 465 (100) $[\text{M}+\text{Na}]^+$, 443 (88) $[\text{M}+\text{H}]^+$. HR-MS (ESI): m/z calcd for $\text{C}_{25}\text{H}_{35}\text{N}_2\text{O}_5^+$ $[\text{M}+\text{H}]^+$: 443.2540, found: 443.2543.

tert-Butyl (S)-(12-methyl-3,11-dioxo-2,3,4,5,6,7,8,9,11,12,13,14-dodecahydro-1H-[1]oxa[7]azacyclopentadecino[12,11-*b*]indol-2-yl)carbamate (269c)

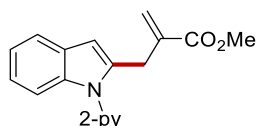


General procedure **K** was followed using **268** (53.2 mg, 0.10 mmol). Purification by column chromatography on silica gel (*n*-hexane/EtOAc: 1/1) yielded **269c** (28.3 mg, 62%, d.r. 1.1) as a colorless oil.

^1H NMR (300 MHz, CDCl_3): δ 8.13 (s, 0.47H), 8.05 (s, 0.53H), 7.61 – 7.47 (m, 1H), 7.24 – 7.17 (m, 1H), 7.15 – 6.99 (m, 2H), 5.65 (d, J = 8.2 Hz, 0.47H), 5.50 (d, J = 8.1 Hz, 0.53H), 5.18 (brs, 0.47H), 5.00 (t, J = 5.7 Hz, 0.53H), 4.68 – 4.44 (m, 1H), 4.44 – 4.22 (m, 0.53H), 4.19 – 3.92 (m, 0.94H), 3.68 (ddt, J = 10.2, 5.5, 2.8 Hz, 0.53H), 3.34 – 3.21 (m, 1H), 3.20 – 2.79 (m, 5H), 2.75 – 2.47 (m, 1H), 1.46 (s, 9H), 1.42 – 1.23 (m, 6H), 1.06 – 0.38 (m, 3H). ^{13}C NMR (126 MHz, CDCl_3): *Major diastereoisomer*. δ 177.8 (C_q), 171.0 (C_q), 155.2 (C_q), 135.1 (C_q), 133.2 (C_q), 128.0 (C_q), 121.7 (CH), 119.8 (CH), 118.5 (CH), 110.3 (CH), 107.7 (C_q), 79.5 (C_q), 63.9 (CH₂), 54.2 (CH), 41.1 (CH), 38.0 (CH₂), 31.3 (CH₂), 30.3 (CH₂), 29.2 (CH₂), 28.4 (CH₃), 25.6 (CH₂), 20.0 (CH₂), 18.6 (CH₃). *Minor diastereoisomer*. δ 177.0 (C_q), 170.9 (C_q), 155.2 (C_q), 135.3 (C_q), 133.4 (C_q), 128.4 (C_q), 121.8 (CH), 119.7 (CH), 118.5 (CH), 110.3 (CH), 107.4 (C_q), 79.6 (C_q),

63.3 (CH₂), 55.6 (CH), 40.4 (CH), 37.3 (CH₂), 31.3 (CH₂), 30.3 (CH₂), 28.9 (CH₂), 28.4 (CH₃), 25.7 (CH₂), 21.0 (CH₂), 18.2 (CH₃). **IR** (ATR): 3300, 2931, 1712, 1659, 1496, 1460, 1366, 1243, 1167, 733 cm⁻¹. **MS** (ESI): *m/z* (relative intensity) 937 (19) [2M+Na]⁺, 480 (100) [M+Na]⁺, 458 (50) [M+H]⁺, 402 (26). **HR-MS** (ESI): *m/z* calcd for C₂₅H₃₆N₃O₅⁺ [M+H]⁺: 458.2649, found: 458.2652.

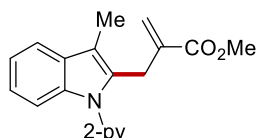
Methyl 2-[[1-(pyridin-2-yl)-1H-indol-2-yl]methyl]acrylate (**271a**)



The general procedure **J** was followed using 1-(pyridin-2-yl)-1*H*-indole **270a** (48.6 mg, 0.25 mmol), methyl 2-[[*tert*-butoxycarbonyl]oxy]methyl]acrylate **253a** (81.0 mg, 0.38 mmol), MnBr(CO)₅ (3.4 mg, 5.0 mol %), NaOAc (6.2 mg, 30 mol %) in 1,4-dioxane (1.0 mL). Purification by column chromatography on silica gel (*n*-hexane/EtOAc: 20/1 → 10/1) yielded **271a** (69.4 mg, 95%) as a colorless oil.

¹H NMR (600 MHz, CDCl₃): δ 8.62 (ddd, *J* = 5.0, 1.9, 0.9 Hz, 1H), 7.84 (ddd, *J* = 7.7, 7.7, 1.9 Hz, 1H), 7.65 – 7.51 (m, 1H), 7.44 (d, *J* = 8.0 Hz, 1H), 7.39 – 7.34 (m, 1H), 7.31 – 7.26 (m, 1H), 7.18 – 7.10 (m, 2H), 6.47 (d, *J* = 0.9 Hz, 1H), 6.15 (dt, *J* = 0.9, 0.9 Hz, 1H), 5.40 (dt, *J* = 1.6, 0.9 Hz, 1H), 3.99 – 3.86 (m, 2H), 3.69 (s, 3H). **¹³C NMR** (126 MHz, CDCl₃): δ 166.8 (C_q), 151.1 (C_q), 149.4 (CH), 138.1 (CH), 137.7 (C_q), 137.4 (C_q), 137.2 (C_q), 128.3 (C_q), 126.4 (CH₂), 121.9 (CH), 121.9 (CH), 120.8 (CH), 120.6 (CH), 120.1 (CH), 110.2 (CH), 104.2 (CH), 51.9 (CH₃), 29.9 (CH₂). **IR** (ATR): 3052, 2950, 1716, 1586, 1468, 1435, 1325, 1205, 1143, 735 cm⁻¹. **MS** (ESI): *m/z* (relative intensity) 315 (36) [M+Na]⁺, 293 (100) [M+H]⁺. **HR-MS** (ESI) *m/z* calcd for C₁₈H₁₇N₂O₂⁺ [M+H]⁺: 293.1285, found: 293.1285.

Methyl 2-[[3-methyl-1-(pyridin-2-yl)-1H-indol-2-yl]methyl]acrylate (**271b**)



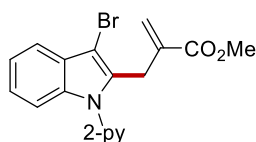
The general procedure **J** was followed using 3-methyl-1-(pyridin-2-yl)-1*H*-indole **270b** (52.1 mg, 0.25 mmol), methyl 2-[[*tert*-butoxycarbonyl]oxy]methyl]acrylate **253a** (81.0 mg, 0.38 mmol), MnBr(CO)₅ (3.4 mg, 5.0 mol %) and NaOAc (6.2 mg, 30 mol %) in 1,4-dioxane (1.0 mL). The reaction was performed at 80 °C. Purification by column

5. Experimental Part

chromatography on silica gel (*n*-hexane/EtOAc: 20/1 → 15/1) yielded **271b** (73.5 mg, 96%) as a white solid.

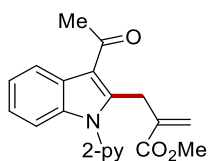
M.p.: 59 – 60 °C. **¹H NMR** (400 MHz, CDCl₃): δ 8.59 (ddd, *J* = 4.9, 2.0, 0.9 Hz, 1H), 7.81 (ddd, *J* = 8.1, 7.5, 2.0 Hz, 1H), 7.63 – 7.54 (m, 1H), 7.41 – 7.33 (m, 2H), 7.27 – 7.22 (m, 1H), 7.21 – 7.13 (m, 2H), 6.06 (td, *J* = 1.7, 1.2 Hz, 1H), 5.13 (td, *J* = 1.7, 1.2 Hz, 1H), 3.95 (dd, *J* = 1.7, 1.7 Hz, 2H), 3.70 (s, 3H), 2.30 (s, 3H). **¹³C NMR** (101 MHz, CDCl₃): δ 167.1 (C_q), 151.5 (C_q), 149.4 (CH), 138.1 (CH), 137.5 (C_q), 136.6 (C_q), 132.3 (C_q), 129.2 (C_q), 125.7 (CH₂), 122.2 (CH), 121.7 (CH), 120.6 (CH), 120.2 (CH), 118.4 (CH), 112.0 (C_q), 110.1 (CH), 51.8 (CH₃), 27.0 (CH₂), 8.7 (CH₃). **IR** (ATR): 3054, 2949, 1711, 1585, 1469, 1455, 1436, 1214, 746 cm⁻¹. **MS** (ESI): *m/z* (relative intensity) 635 (12) [2M+Na]⁺, 329 (100) [M+Na]⁺, 307 (52) [M+H]⁺. **HR-MS** (ESI): *m/z* calcd for C₁₉H₁₉N₂O₂⁺ [M+H]⁺: 307.1441, found: 307.1440.

Methyl 2-[[3-bromo-1-(pyridin-2-yl)-1*H*-indol-2-yl]methyl]acrylate (**271c**)



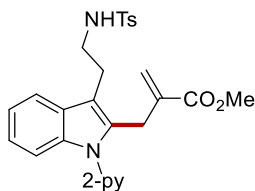
The general procedure **J** was followed using 3-bromo-1-(pyridin-2-yl)-1*H*-indole **270c** (68.3 mg, 0.25 mmol), methyl 2-[[*tert*-butoxycarbonyl]oxy]methyl]acrylate **253a** (81.0 mg, 0.375 mmol), MnBr(CO)₅ (3.4 mg, 5.0 mol %) and NaOAc (6.2 mg, 30 mol %) in 1,4-dioxane (1.0 mL). The reaction was performed at 80 °C. Purification by column chromatography on silica gel (*n*-hexane/EtOAc: 10/1) yielded **271c** (86.9 mg, 94%) as a pale yellow oil.

¹H NMR (400 MHz, CDCl₃): δ 8.59 (ddd, *J* = 4.9, 2.0, 0.9 Hz, 1H), 7.84 (ddd, *J* = 8.0, 7.5, 2.0 Hz, 1H), 7.63 – 7.55 (m, 1H), 7.37 – 7.33 (m, 2H), 7.30 (ddd, *J* = 7.5, 4.9, 0.9 Hz, 1H), 7.26 – 7.18 (m, 2H), 6.11 (td, *J* = 1.5, 1.0 Hz, 1H), 5.22 (td, *J* = 1.9, 1.0 Hz, 1H), 4.00 (dd, *J* = 1.9, 1.5 Hz, 2H), 3.70 (s, 3H). **¹³C NMR** (101 MHz, CDCl₃): δ 166.7 (C_q), 150.7 (C_q), 149.6 (CH), 138.4 (CH), 136.2 (C_q), 136.1 (C_q), 134.0 (C_q), 127.4 (C_q), 126.2 (CH₂), 123.4 (CH), 122.5 (CH), 121.5 (CH), 120.7 (CH), 119.0 (CH), 110.6 (CH), 95.8 (C_q), 51.9 (CH₃), 27.8 (CH₂). **IR** (ATR): 3056, 2949, 1717, 1632, 1587, 1498, 1452, 1436, 1345, 946, 785 cm⁻¹. **MS** (ESI): *m/z* (relative intensity) 393 (100) [M+Na]⁺, 371 (86) [M+H]⁺. **HR-MS** (ESI): *m/z* calcd for C₁₈H₁₆⁷⁹BrN₂O₂⁺ [M+H]⁺: 371.0390, found: 371.0386.

Methyl 2-[[3-acetyl-1-(pyridin-2-yl)-1*H*-indol-2-yl]methyl]acrylate (271d)

The general procedure **J** was followed using 1-[1-(pyridin-2-yl)-1*H*-indol-3-yl]ethanone **270d** (59.1 mg, 0.25 mmol), methyl 2-[[*tert*-butoxycarbonyloxy]methyl]acrylate **253a** (81.0 mg, 0.38 mmol), MnBr(CO)₅ (3.4 mg, 5.0 mol %) and NaOAc (6.2 mg, 30 mol %) in 1,4-dioxane (1.0 mL). The reaction was run at 80 °C. Purification by column chromatography on silica gel (*n*-hexane/EtOAc: 10/1 → 2/1) yielded **271d** (74.9 mg, 90%) as a pale yellow oil.

¹H NMR (300 MHz, CDCl₃): δ 8.65 (ddd, *J* = 4.9, 2.0, 0.8 Hz, 1H), 8.08 (ddd, *J* = 8.1, 1.1, 1.1 Hz, 1H), 7.90 (ddd, *J* = 7.6, 7.6, 2.0 Hz, 1H), 7.42 (ddd, *J* = 7.6, 4.9, 1.0 Hz, 1H), 7.36 (ddd, *J* = 7.6, 1.1, 1.1 Hz, 1H), 7.34 – 7.27 (m, 1H), 7.25 – 7.14 (m, 2H), 6.13 (td, *J* = 1.6, 1.0 Hz, 1H), 5.23 (td, *J* = 1.8, 1.0 Hz, 1H), 4.17 (dd, *J* = 1.8, 1.6 Hz, 2H), 3.69 (s, 3H), 2.71 (s, 3H). **¹³C NMR** (126 MHz, CDCl₃): δ 194.3 (C_q), 166.6 (C_q), 150.0 (CH), 149.6 (C_q), 143.6 (C_q), 138.6 (CH), 137.0 (C_q), 136.9 (C_q), 126.2 (C_q), 125.7 (CH₂), 123.7 (CH), 123.1 (CH), 122.7 (CH), 122.2 (CH), 121.0 (CH), 116.5 (C_q), 111.0 (CH), 52.0 (CH₃), 31.6 (CH₃), 28.6 (CH₂). **IR** (ATR): 2953, 2923, 2853, 1718, 1650, 1588, 1518, 1467, 1198, 1138, 792 cm⁻¹. **MS** (ESI): *m/z* (relative intensity) 691 (12) [2M+Na]⁺, 357 (100) [M+Na]⁺, 335 (11) [M+H]⁺. **HR-MS** (ESI): *m/z* calcd for C₂₀H₁₉N₂O₃⁺ [M+H]⁺: 335.1390, found: 335.1397.

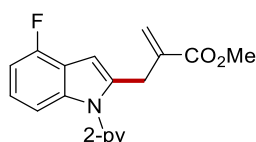
Methyl 2-[[3-[2-(4-methylphenylsulfonamido)ethyl]-1-(pyridin-2-yl)-1*H*-indol-2-yl]methyl]acrylate (271e)

The general procedure **J** was followed using 4-methyl-*N*-{2-[1-(pyridin-2-yl)-1*H*-indol-3-yl]ethyl}benzenesulfonamide **270e** (97.9 mg, 0.25 mmol), methyl 2-[[*tert*-butoxycarbonyloxy]methyl]acrylate **253a** (81.0 mg, 0.38 mmol), MnBr(CO)₅ (3.4 mg, 5.0 mol %) and NaOAc (6.2 mg, 30 mol %) in 1,4-dioxane (1.0 mL). The reaction was performed at 80 °C. Purification by column chromatography on silica gel (*n*-hexane/EtOAc: 2/1 → 1/2) yielded **271e** (114.4 mg, 93%) as a white solid.

5. Experimental Part

M.p.: 112 –114 °C. **¹H NMR** (500 MHz, CDCl₃): δ 8.56 (ddd, *J* = 4.9, 2.0, 0.8 Hz, 1H), 7.82 (ddd, *J* = 7.7, 7.7, 2.0 Hz, 1H), 7.65 (d, *J* = 8.1 Hz, 2H), 7.44 (ddd, *J* = 7.4, 0.9, 0.9 Hz, 1H), 7.33 (ddd, *J* = 8.0, 0.9, 0.9 Hz, 1H), 7.30 – 7.26 (m, 2H), 7.20 (d, *J* = 8.1 Hz, 2H), 7.16 – 7.05 (m, 2H), 5.91 (td, *J* = 2.1, 1.2 Hz, 1H), 5.06 – 4.84 (m, 2H), 3.91 – 3.89 (m, 2H), 3.65 (s, 3H), 3.22 (td, *J* = 7.0, 6.8 Hz, 2H), 2.96 (t, *J* = 7.0 Hz, 2H), 2.36 (s, 3H). **¹³C NMR** (126 MHz, CDCl₃): δ 166.6 (C_q), 151.0 (C_q), 149.4 (CH), 143.0 (C_q), 138.2 (CH), 137.4 (C_q), 136.8 (C_q), 136.7 (C_q), 133.6 (C_q), 129.4 (CH), 127.9 (C_q), 126.9 (CH), 125.9 (CH₂), 122.4 (CH), 122.1 (CH), 120.9 (CH), 120.6 (CH), 118.2 (CH), 111.8 (C_q), 110.1 (CH), 51.9 (CH₃), 43.2 (CH₂), 27.1 (CH₂), 25.0 (CH₂), 21.5 (CH₃). **IR** (ATR): 3053, 2950, 1712, 1586, 1469, 1454, 1435, 1348, 1337, 1266, 734 cm⁻¹. **MS** (ESI): *m/z* (relative intensity) 512 (78) [M+Na]⁺, 490 (100) [M+H]⁺. **HR-MS** (ESI): *m/z* calcd for C₂₇H₂₈N₃O₄S⁺ [M+H]⁺: 490.1795, found: 490.1796.

Methyl 2-[[4-fluoro-1-(pyridin-2-yl)-1*H*-indol-2-yl]methyl]acrylate (**271f**)

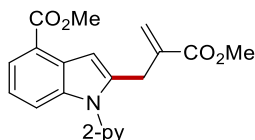


The general procedure **J** was followed using 4-fluoro-1-(pyridin-2-yl)-1*H*-indole **270f** (53.1 mg, 0.25 mmol), [(*tert*-butoxycarbonyl)oxy]methyl]acrylate **253a** (81.0 mg, 0.38 mmol), MnBr(CO)₅ (3.4 mg, 5.0 mol %) and NaOAc (6.2 mg, 30 mol %) in 1,4-dioxane (1.0 mL). Purification by column chromatography on silica gel (*n*-hexane/EtOAc: 20/1 → 10/1) yielded **271f** (66.7 mg, 86%) as a pale yellow oil.

¹H NMR (400 MHz, CDCl₃): δ 8.64 (ddd, *J* = 4.9, 2.0, 1.0 Hz, 1H), 7.88 (td, *J* = 7.7, 2.0 Hz, 1H), 7.45 (ddd, *J* = 8.0, 1.0, 1.0 Hz, 1H), 7.33 (ddd, *J* = 7.4, 4.9, 1.0 Hz, 1H), 7.12 (dd, *J* = 8.3, 0.8 Hz, 1H), 7.05 (ddd, *J* = 8.0, 8.0, 5.1 Hz, 1H), 6.81 (ddd, *J* = 10.1, 7.7, 0.9 Hz, 1H), 6.55 (td, *J* = 1.4, 1.1 Hz, 1H), 6.18 (td, *J* = 1.9, 1.1 Hz, 1H), 5.43 (dd, *J* = 1.9, 1.4 Hz, 1H), 3.91 (t, *J* = 1.2 Hz, 2H), 3.70 (s, 3H). **¹³C NMR** (101 MHz, CDCl₃): δ 166.9 (C_q), 155.8 (d, *J* = 246.5 Hz, C_q), 151.0 (C_q), 149.6 (CH), 139.8 (d, *J* = 11.1 Hz, C_q), 138.4 (CH), 137.7 (C_q), 137.5 (C_q), 126.9 (CH₂), 122.4 (CH), 122.4 (d, *J* = 7.7 Hz, CH), 121.0 (CH), 117.34 (d, *J* = 22.7 Hz, C_q), 106.40 (d, *J* = 3.5 Hz, CH), 105.64 (d, *J* = 19.0 Hz, CH), 99.8 (CH) 51.9 (CH₃), 29.8 (CH₂). **¹⁹F NMR** (376 MHz, CDCl₃): δ –122.7 (dd, *J* = 10.0, 5.1 Hz). **IR** (ATR): 2951, 1716, 1584, 1469, 1436, 1388, 1329, 1203, 1175, 853, 745 cm⁻¹. **MS** (ESI): *m/z* (relative intensity) 333 (39) [M+Na]⁺, 311

(100) $[M+H]^+$. **HR-MS** (ESI): m/z calcd for $C_{18}H_{16}FN_2O_2^+$ $[M+H]^+$: 311.1190, found: 311.1195.

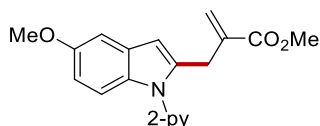
Methyl 2-[2-(methoxycarbonyl)allyl]-1-(pyridin-2-yl)-1H-indole-4-carboxylate (271g)



The general procedure **J** was followed using methyl 1-(pyridin-2-yl)-1H-indole-4-carboxylate **270g** (63.1 mg, 0.25 mmol), methyl 2-[[*tert*-butoxycarbonyl]oxy]methyl]acrylate **253a** (81.0 mg, 0.38 mmol), $MnBr(CO)_5$ (3.4 mg, 5.0 mol %) and NaOAc (6.2 mg, 30 mol %) in 1,4-dioxane (1.0 mL). Purification by column chromatography on silica gel (*n*-hexane/EtOAc: 10/1) yielded **271g** (86.3 mg, 98%) as a colorless oil.

1H NMR (400 MHz, $CDCl_3$): δ 8.62 (ddd, $J = 4.9, 2.0, 0.9$ Hz, 1H), 7.91 – 7.83 (m, 2H), 7.50 (ddd, $J = 8.2, 0.9, 0.9$ Hz, 1H), 7.39 (ddd, $J = 8.0, 0.9, 0.9$ Hz, 1H), 7.31 (ddd, $J = 7.5, 4.9, 0.9$ Hz, 1H), 7.15 (dd, $J = 8.2, 7.5$ Hz, 1H), 7.11 (d, $J = 0.8$ Hz, 1H), 6.17 (td, $J = 1.4, 1.2$ Hz, 1H), 5.43 (td, $J = 2.0, 1.2$ Hz, 1H), 3.96 (s, 3H), 3.93 – 3.88 (m, 2H), 3.67 (s, 3H). **^{13}C NMR** (101 MHz, $CDCl_3$): δ 167.8 (C_q), 166.8 (C_q), 150.7 (C_q), 149.6 (CH), 139.9 (C_q), 138.4 (CH), 138.2 (C_q), 137.3 (C_q), 128.1 (C_q), 127.0 (CH_2), 124.0 (CH), 122.5 (CH), 121.2 (CH), 121.1 (CH), 120.9 (C_q), 115.0 (CH), 105.1 (CH), 51.9 (CH_3), 51.7 (CH_3), 29.8 (CH_2). **IR** (ATR): 2951, 1710, 1633, 1585, 1469, 1437, 1285, 1262, 1192, 1135, 786 cm^{-1} . **MS** (ESI): m/z (relative intensity) 723 (9) $[2M+Na]^+$, 373 (100) $[M+Na]^+$, 351 (87) $[M+H]^+$. **HR-MS** (ESI): m/z calcd for $C_{20}H_{19}N_2O_4$ $[M+H]^+$: 351.1339, found: 351.1352.

Methyl 2-[[5-methoxy-1-(pyridin-2-yl)-1H-indol-2-yl]methyl]acrylate (271h)

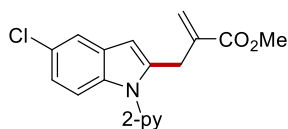


The general procedure **J** was followed using 5-methoxy-1-(pyridin-2-yl)-1H-indole **270h** (56.1 mg, 0.25 mmol), methyl 2-[[*tert*-butoxycarbonyl]oxy]methyl]acrylate **253a** (81.0 mg, 0.38 mmol), $MnBr(CO)_5$ (3.4 mg, 5.0 mol %) and NaOAc (6.2 mg, 30 mol %) in 1,4-dioxane (1.0 mL). Purification by column chromatography on silica gel (*n*-hexane/EtOAc: 10/1→5/1) yielded **271h** (76.1 mg, 94%) as a pale colorless oil.

5. Experimental Part

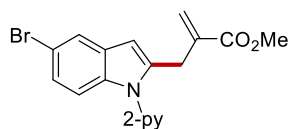
¹H NMR (300 MHz, CDCl₃): δ 8.59 (ddd, *J* = 4.9, 2.0, 0.9 Hz, 1H), 7.83 (ddd, *J* = 8.1, 7.5, 2.5 Hz, 1H), 7.40 (ddd, *J* = 8.0, 0.9, 0.9 Hz, 1H), 7.29 – 7.22 (m, 2H), 7.03 (dd, *J* = 2.5, 0.8 Hz, 1H), 6.78 (dd, *J* = 8.9, 2.5 Hz, 1H), 6.37 (d, *J* = 0.8 Hz, 1H), 6.13 (td, *J* = 1.5, 1.1 Hz, 1H), 5.38 (td, *J* = 2.1, 1.1 Hz, 1H), 3.93 – 3.88 (m, 2H), 3.83 (s, 3H), 3.68 (s, 3H). **¹³C NMR** (126 MHz, CDCl₃): δ 166.9 (C_q), 154.7 (C_q), 151.3 (C_q), 149.4 (CH), 138.2 (CH), 138.0 (C_q), 137.8 (C_q), 132.3 (C_q), 128.9 (C_q), 126.4 (CH₂), 121.7 (CH), 120.5 (CH), 111.6 (CH), 111.0 (CH), 104.1 (CH), 102.3 (CH), 55.9 (CH₃), 51.9 (CH₃), 30.1 (CH₂). **IR** (ATR): 2950, 2832, 1718, 1582, 1471, 1437, 1388, 1204, 1140, 1033, 746 cm⁻¹. **MS** (ESI): *m/z* (relative intensity) 345 (100) [M+Na]⁺, 323 (84) [M+H]⁺. **HR-MS** (ESI): *m/z* calcd for C₁₉H₁₉N₂O₃⁺ [M+H]⁺: 323.1390, found: 323.1392.

Methyl 2-[[5-chloro-1-(pyridin-2-yl)-1*H*-indol-2-yl]methyl]acrylate (**271i**)



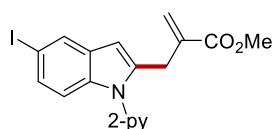
The general procedure **J** was followed using 5-chloro-1-(pyridin-2-yl)-1*H*-indole **270i** (57.2 mg, 0.25 mmol), methyl 2-[[*tert*-butoxycarbonyl]oxy]methyl]acrylate **253a** (81.0 mg, 0.38 mmol), MnBr(CO)₅ (3.4 mg, 5.0 mol %) and NaOAc (6.2 mg, 30 mol %) in 1,4-dioxane (1.0 mL). Purification by column chromatography on silica gel (*n*-hexane/EtOAc: 20/1 → 10/1) yielded **271i** (78.9 mg, 96%) as a white solid.

M.p.: 82 – 83 °C. **¹H NMR** (400 MHz, CDCl₃): δ 8.61 (ddd, *J* = 4.8, 2.0, 0.9 Hz, 1H), 7.86 (ddd, *J* = 8.0, 7.5, 2.0 Hz, 1H), 7.51 (dd, *J* = 2.1, 0.5 Hz, 1H), 7.39 (ddd, *J* = 8.1, 1.0, 0.9 Hz, 1H), 7.30 (ddd, *J* = 7.5, 4.9, 1.0 Hz, 1H), 7.24 (ddd, *J* = 8.7, 0.7, 0.7 Hz, 1H), 7.07 (dd, *J* = 8.8, 2.1 Hz, 1H), 6.38 (d, *J* = 0.9 Hz, 1H), 6.15 (d, *J* = 1.2 Hz, 1H), 5.39 (d, *J* = 1.2 Hz, 1H), 3.89 – 3.86 (m, 2H), 3.67 (s, 3H). **¹³C NMR** (101 MHz, CDCl₃): δ 166.9 (C_q), 150.8 (C_q), 149.6 (CH), 139.0(C_q), 138.5 (CH), 137.5 (C_q), 135.7 (C_q), 129.4 (C_q), 126.8 (CH₂), 126.3 (C_q), 122.4 (CH), 122.1 (CH), 120.8 (CH), 119.5 (CH), 111.3 (CH), 103.6 (CH), 51.9 (CH₃), 29.9 (CH₂). **IR** (ATR): 2950, 2924, 1716, 1587, 1435, 1384, 1281, 1205, 1135, 783 cm⁻¹. **MS** (ESI): *m/z* (relative intensity) 349 (52) [M+Na]⁺, 327 (100) [M+H]⁺. **HR-MS** (ESI): *m/z* calcd for C₁₈H₁₅³⁵ClN₂O₂⁺ [M+H]⁺: 327.0895, found: 327.0897.

Methyl 2-[[5-bromo-1-(pyridin-2-yl)-1H-indol-2-yl]methyl]acrylate (271j)

The general procedure **J** was followed using 5-bromo-1-(pyridin-2-yl)-1H-indole **270j** (52.1 mg, 0.25 mmol), methyl 2-[[*tert*-butoxycarbonyl]oxy]methyl]acrylate **253a** (81.0 mg, 0.38 mmol), MnBr(CO)₅ (3.4 mg, 5.0 mol %) and NaOAc (6.2 mg, 30 mol %) in 1,4-dioxane (1.0 mL). Purification by column chromatography on silica gel (*n*-hexane/EtOAc: 20/1 → 10/1) yielded **271j** (87.3 mg, 94%) as a white solid.

M.p.: 88 – 89 °C. **¹H NMR** (300 MHz, CDCl₃): δ 8.61 (ddd, *J* = 4.9, 2.0, 0.8 Hz, 1H), 7.92 – 7.80 (m, 1H), 7.67 (dd, *J* = 1.3, 1.3 Hz, 1H), 7.39 (ddd, *J* = 8.0, 1.0, 1.0 Hz, 1H), 7.31 (ddd, *J* = 7.5, 4.9, 1.0 Hz, 1H), 7.21 – 7.18 (m, 2H), 6.37 (s, 1H), 6.15 (d, *J* = 1.2 Hz, 1H), 5.38 (d, *J* = 1.2 Hz, 1H), 3.91 – 3.85 (m, 2H), 3.67 (s, 3H). **¹³C NMR** (126 MHz, CDCl₃): δ 166.7 (C_q), 150.7 (C_q), 149.5 (CH), 138.9 (C_q), 138.4 (CH), 137.4 (C_q), 135.9 (C_q), 130.0 (C_q), 126.7 (CH₂), 124.7 (CH), 122.6 (CH), 122.3 (CH), 120.8 (CH), 113.8 (C_q), 111.7 (CH), 103.4 (CH), 52.0 (CH₃), 30.0 (CH₂). **IR** (ATR): 2949, 2924, 1717, 1632, 1470, 1438, 1281, 1205, 1146, 784 cm⁻¹. **MS** (ESI): *m/z* (relative intensity) 393 (59) [M+Na]⁺, 371 (100) [M+H]⁺. **HR-MS** (ESI): *m/z* calcd for C₁₈H₁₅⁷⁹BrN₂O₂⁺ [M+H]⁺: 371.0390, found: 371.0395.

Methyl 2-[[5-iodo-1-(pyridin-2-yl)-1H-indol-2-yl]methyl]acrylate (271k)

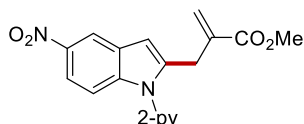
The general procedure **J** was followed using 5-iodo-1-(pyridin-2-yl)-1H-indole **270k** (80.0 mg, 0.25 mmol), methyl 2-[[*tert*-butoxycarbonyl]oxy]methyl]acrylate **253a** (81.0 mg, 0.38 mmol), MnBr(CO)₅ (3.4 mg, 5.0 mol %) and NaOAc (6.2 mg, 30 mol %) in 1,4-dioxane (1.0 mL). Purification by column chromatography on silica gel (*n*-hexane/EtOAc: 20/1 → 10/1) yielded **271k** (94.1 mg, 90%) as a white solid.

M.p.: 89 – 91 °C. **¹H NMR** (400 MHz, CDCl₃): δ 8.61 (ddd, *J* = 4.9, 2.0, 0.8 Hz, 1H), 7.92 – 7.81 (m, 2H), 7.42 – 7.34 (m, 2H), 7.30 (ddd, *J* = 7.4, 4.9, 1.0 Hz, 1H), 7.10 (ddd, *J* = 8.6, 0.7, 0.7 Hz, 1H), 6.36 (d, *J* = 0.7 Hz, 1H), 6.14 (dt, *J* = 0.9, 0.9 Hz, 1H), 5.37 (td, *J* = 1.4, 0.9 Hz, 1H), 3.88 (dd, *J* = 1.4, 0.9 Hz, 2H), 3.67 (s, 3H). **¹³C NMR** (126 MHz, CDCl₃): δ 166.7 (C_q), 150.6 (C_q), 149.5 (CH), 138.5 (C_q), 138.4 (CH), 137.4 (C_q), 136.4 (C_q), 130.8 (C_q), 130.2 (CH), 128.8 (CH), 126.7 (CH₂), 122.3 (CH), 120.8

5. Experimental Part

(CH), 112.2 (CH), 103.1 (CH), 84.2 (C_q), 52.0 (CH₃), 29.9 (CH₂). **IR** (ATR): 2948, 2922, 1718, 1632, 1586, 1470, 1438, 1280, 1205, 784 cm⁻¹. **MS** (ESI): *m/z* (relative intensity) 441 (48) [M+Na]⁺, 419 (100) [M+H]⁺. **HR-MS** (ESI): *m/z* calcd for C₁₈H₁₆IN₂O₂⁺ [M+H]⁺: 419.0251, found: 419.0255.

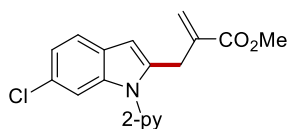
Methyl 2-[[5-nitro-1-(pyridin-2-yl)-1*H*-indol-2-yl]methyl]acrylate (**271l**)



The general procedure **J** was followed using 5-nitro-1-(pyridin-2-yl)-1*H*-indole **270l** (59.8 mg, 0.25 mmol), methyl 2-[[*tert*-butoxycarbonyl]oxy]methyl]acrylate **253a** (81.0 mg, 0.38 mmol), MnBr(CO)₅ (3.4 mg, 5.0 mol %) and NaOAc (6.2 mg, 30.0 mol %) in 1,4-dioxane (1.0 mL). Purification by column chromatography on silica gel (*n*-hexane/EtOAc: 4/1 → 2/1) yielded **271l** (73.4 mg, 87%) as a pale yellow solid.

M.p.: 125 – 126 °C. **¹H NMR** (300 MHz, CDCl₃): δ 8.66 (ddd, *J* = 4.0, 2.0, 0.8 Hz, 1H), 8.48 (d, *J* = 2.3 Hz, 1H), 8.01 (dd, *J* = 9.1, 2.3 Hz, 1H), 7.93 (ddd, *J* = 7.7, 7.7, 1.9 Hz, 1H), 7.47 – 7.36 (m, 2H), 7.30 (d, *J* = 9.1 Hz, 1H), 6.58 (d, *J* = 0.9 Hz, 1H), 6.19 (td, *J* = 1.6, 1.2 Hz, 1H), 5.43 (td, *J* = 2.1, 1.2 Hz, 1H), 3.88 – 3.85 (m, 2H), 3.68 (s, 3H). **¹³C NMR** (126 MHz, CDCl₃): δ 166.5 (C_q), 150.0 (C_q), 149.8 (CH), 142.4 (C_q), 141.3 (C_q), 140.1 (C_q), 138.7 (CH), 136.9 (C_q), 127.6 (C_q), 127.2 (CH₂), 123.2 (CH), 121.2 (CH), 117.6 (CH), 117.0 (CH), 110.2 (CH), 105.3 (CH), 52.1 (CH₃), 30.0 (CH₂). **IR** (ATR): 2951, 1718, 1587, 1511, 1470, 1437, 1326, 1145, 785 cm⁻¹. **MS** (ESI): *m/z* (relative intensity) 360 (55) [M+Na]⁺, 338 (100) [M+H]⁺. **HR-MS** (ESI): *m/z* calcd for C₁₈H₁₆N₃O₄⁺ [M+H]⁺: 338.1135, found: 338.1133.

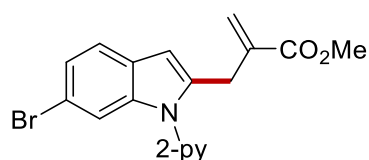
Methyl 2-[[6-chloro-1-(pyridin-2-yl)-1*H*-indol-2-yl]methyl]acrylate (**271m**)



The general procedure **J** was followed using 6-chloro-1-(pyridin-2-yl)-1*H*-indole **270m** (57.2 mg, 0.25 mmol), methyl 2-[[*tert*-butoxycarbonyl]oxy]methyl]acrylate **253a** (81.0 mg, 0.38 mmol), MnBr(CO)₅ (3.4 mg, 5.0 mol %) and NaOAc (6.2 mg, 30 mol %) in 1,4-dioxane (1.0 mL). Purification by column chromatography on silica gel (*n*-hexane/EtOAc: 20/1 → 10/1) yielded **271m** (79.2 mg, 97%) as a colorless oil.

¹H NMR (400 MHz, CDCl₃): δ 8.62 (ddd, *J* = 4.9, 2.0, 0.9 Hz, 1H), 7.87 (ddd, *J* = 8.0, 7.5, 2.0 Hz, 1H), 7.45 (dd, *J* = 8.4, 0.5 Hz, 1H), 7.40 (ddd, *J* = 8.0, 1.0, 1.0 Hz, 1H), 7.35 – 7.29 (m, 2H), 7.08 (dd, *J* = 8.4, 1.9 Hz, 1H), 6.41 (d, *J* = 0.9 Hz, 1H), 6.15 (dt, *J* = 1.4, 1.0 Hz, 1H), 5.38 (dt, *J* = 1.4, 1.4 Hz, 1H), 3.88 – 3.85 (m, 2H), 3.67 (s, 3H). **¹³C NMR** (101 MHz, CDCl₃): δ 166.9 (C_q), 150.7 (C_q), 149.7 (CH), 138.5 (CH), 138.4 (C_q), 137.7 (C_q), 137.5 (C_q), 127.9 (C_q), 126.9 (C_q), 126.8 (CH₂), 122.4 (CH), 121.3 (CH), 120.9 (CH), 120.8 (CH), 110.4 (CH), 104.0 (CH), 51.9 (CH₃), 29.9 (CH₂). **IR** (ATR): 2950, 2923, 1718, 1587, 1469, 1435, 1339, 1325, 1146, 814 cm⁻¹. **MS** (ESI): *m/z* (relative intensity) 349 (81) [M+Na]⁺, 327 (100) [M+H]⁺. **HR-MS** (ESI): *m/z* calcd for C₁₈H₁₆³⁵ClN₂O₂⁺ [M+H]⁺: 327.0895, found: 327.0899.

Methyl 2-[[6-bromo-1-(pyridin-2-yl)-1*H*-indol-2-yl]methyl]acrylate (**271n**)

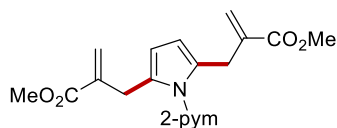


The general procedure **J** was followed using 6-bromo-1-(pyridin-2-yl)-1*H*-indole **270n** (68.3 mg, 0.25 mmol), [(*tert*-butoxycarbonyl)oxy]methyl]acrylate **253a** (81.0 mg, 0.38 mmol), MnBr(CO)₅ (3.4 mg, 5.0 mol %) and NaOAc (6.2 mg, 30 mol %) in 1,4-dioxane (1.0 mL). Purification by column chromatography on silica gel (*n*-hexane/EtOAc: 20/1 → 10/1) yielded **271n** (89.1 mg, 96%) as a pale yellow oil.

¹H NMR (300 MHz, CDCl₃): δ 8.62 (ddd, *J* = 4.9, 2.0, 0.8 Hz, 1H), 7.86 (ddd, *J* = 8.0, 7.5, 2.0 Hz, 1H), 7.48 (ddd, *J* = 1.5, 0.8 Hz, 1H), 7.43 – 7.36 (m, 2H), 7.31 (ddd, *J* = 7.5, 4.9, 1.0 Hz, 1H), 7.22 (dd, *J* = 8.4, 1.7 Hz, 1H), 6.41 (d, *J* = 0.9 Hz, 1H), 6.14 (td, *J* = 1.4, 1.2 Hz, 1H), 5.38 (dd, *J* = 2.0, 1.2 Hz, 1H), 3.86 (dd, *J* = 2.0, 1.2 Hz, 2H), 3.67 (s, 3H). **¹³C NMR** (126 MHz, CDCl₃): δ 166.7 (C_q), 150.5 (C_q), 149.6 (CH), 138.4 (CH), 138.2 (C_q), 138.0 (C_q), 137.4 (C_q), 127.1 (C_q), 126.7 (CH₂), 123.8 (CH), 122.4 (CH), 121.2 (CH), 120.8 (CH), 115.5 (C_q), 113.2 (CH), 104.0 (CH), 51.9 (CH₃), 29.9 (CH₂). **IR** (ATR): 2950, 1718, 1632, 1587, 1460, 1435, 1338, 1146, 955, 784 cm⁻¹. **MS** (ESI): *m/z* (relative intensity) 393 (44) [M+Na]⁺, 371 (100) [M+H]⁺. **HR-MS** (ESI): *m/z* calcd for C₁₈H₁₆⁷⁹BrN₂O₂⁺ [M+H]⁺: 371.0390, found: 371.0396.

5. Experimental Part

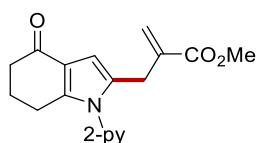
Dimethyl 2,2'-[[1-(pyrimidin-2-yl)-1*H*-pyrrole-2,5-diyl]bis(methylene)]diacrylate (271o)



The general procedure **J** was followed using 2-(1*H*-pyrrol-1-yl)pyrimidine **270o** (36.3 mg, 0.25 mmol), methyl 2-[[*tert*-butoxycarbonyl]oxy]methyl]acrylate **253a** (162.0 mg, 0.75 mmol), MnBr(CO)₅ (3.4 mg, 5.0 mol %) and NaOAc (6.2 mg, 30 mol %) in 1,4-dioxane (1.0 mL). The reaction was performed at 80 °C. Purification by column chromatography on silica gel (*n*-hexane/EtOAc: 10/1) yielded **271o** (70.0 mg, 82%) as a colorless oil.

¹H NMR (400 MHz, CDCl₃): δ 8.64 (d, *J* = 4.8 Hz, 2H), 7.10 (t, *J* = 4.8 Hz, 1H), 5.99 (td, *J* = 1.7, 1.4 Hz, 2H), 5.98 (s, 2H), 5.22 (td, *J* = 2.3, 1.4 Hz, 2H), 3.86 (dd, *J* = 2.3, 1.7 Hz, 4H), 3.66 (s, 6H). **¹³C NMR** (101 MHz, CDCl₃): δ 167.3 (C_q), 158.1 (CH), 157.7 (C_q), 139.1 (C_q), 131.1 (C_q), 125.4 (CH₂), 118.1 (CH), 110.3 (CH), 51.7 (CH₃), 30.3 (CH₂). **IR** (ATR): 2953, 2923, 1718, 1632, 1571, 1430, 1278, 1256, 1155, 816 cm⁻¹. **MS** (ESI): *m/z* (relative intensity) 364 (100) [M+Na]⁺, 342 (82) [M+H]⁺. **HR-MS** (ESI): *m/z* calcd for C₁₈H₂₀N₃O₄⁺ [M+H]⁺: 342.1448, found: 342.1440.

Methyl 2-[[4-oxo-1-(pyridin-2-yl)-4,5,6,7-tetrahydro-1*H*-indol-2-yl]methyl]acrylate (271p)

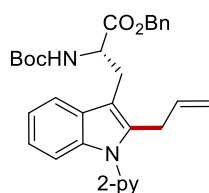


The general procedure **J** was followed using 1-(pyridin-2-yl)-6,7-dihydro-1*H*-indol-4(5*H*)-one **270p** (53.1 mg, 0.25 mmol), methyl 2-[[*tert*-butoxycarbonyl]oxy]methyl]acrylate **253a** (81.0 mg, 0.38 mmol), MnBr(CO)₅ (3.4 mg, 5.0 mol %) and NaOAc (6.2 mg, 30 mol %) in 1,4-dioxane (1.0 mL). The reaction was performed at 80 °C. Purification by column chromatography on silica gel (*n*-hexane/EtOAc: 5/1 → 2/1) yielded **271p** (76.3 mg, 96%) as a colorless oil.

¹H NMR (300 MHz, CDCl₃): δ 8.57 (ddd, *J* = 4.8, 1.9, 0.8 Hz, 1H), 7.87 – 7.80 (m, 1H), 7.39 – 7.30 (m, 1H), 7.28 – 7.23 (m, 1H), 6.41 – 6.35 (m, 1H), 6.10 (d, *J* = 1.1 Hz, 1H), 5.36 (td, *J* = 1.4, 1.1 Hz, 1H), 3.63 (s, 3H), 3.54 – 3.51 (m, 2H), 2.62 (t, *J* = 6.0 Hz, 2H), 2.51 – 2.38 (m, 2H), 2.05 (tt, *J* = 7.4, 6.0 Hz, 2H). **¹³C NMR** (75 MHz, CDCl₃): δ 194.4

(C_q), 166.8 (C_q), 150.0 (C_q), 149.6 (CH), 144.5 (C_q), 138.5 (CH), 137.4 (C_q), 131.9 (C_q), 126.7 (CH₂), 123.4 (CH), 121.4 (CH), 120.8 (C_q), 105.6 (CH), 51.9 (CH₃), 37.8 (CH₂), 29.0 (CH₂), 23.8 (CH₂), 22.9 (CH₂). **IR** (ATR): 2948, 1717, 1655, 1588, 1459, 1438, 1210, 1140, 1001, 783 cm⁻¹. **MS** (ESI): *m/z* (relative intensity) 333 (45) [M+Na]⁺, 311 (100) [M+H]⁺. **HR-MS** (ESI): *m/z* calcd for C₁₈H₁₉N₂O₃⁺ [M+H]⁺: 311.1390, found: 311.1394.

Benzyl **(S)-3-[2-allyl-1-(pyridin-2-yl)-1*H*-indol-3-yl]-2-[(*tert*-butoxycarbonyl)amino]propanoate (273a)**

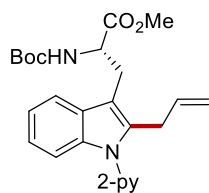


The general procedure **L** was followed using benzyl *N*-(*tert*-butoxycarbonyl)-1-(pyridin-2-yl)-L-tryptophanate **153** (70.7 mg, 0.15 mmol), allyl acetate **272** (30.0 mg, 0.30 mmol), [Cp*Co(MeCN)₃](SbF₆)₂ (5.9 mg, 5.0 mol %) and PivOH (1.5 mg, 10 mol %) in TFE (1.0 mL). Purification by column chromatography on silica gel (*n*-hexane/EtOAc: 4/1) yielded **273a** (55.3 mg, 72%) as a colorless oil. The reaction was also performed using H₂O (27.0 mg, 1.5 mmol, 10 equiv), and yielded **273a** (40.9 mg, 53%).

¹H NMR (300 MHz, CDCl₃): δ 8.63 (ddd, *J* = 4.9, 1.9, 0.6 Hz, 1H), 7.84 (ddd, *J* = 7.7, 7.7, 1.9 Hz, 1H), 7.59 – 7.53 (m, 1H), 7.35 – 7.28 (m, 6H), 7.20 – 7.11 (m, 4H), 5.67 (dddd, *J* = 16.3, 10.8, 5.8, 5.8 Hz, 1H), 5.19 (d, *J* = 8.1 Hz, 1H), 5.09 (d, *J* = 12.3 Hz, 1H), 5.00 (d, *J* = 12.3 Hz, 1H), 4.79 (d, *J* = 10.8 Hz, 1H), 4.72 – 4.66 (m, 2H), 3.66 (d, *J* = 5.8 Hz, 2H), 3.31 (d, *J* = 6.3 Hz, 2H), 1.41 (s, 9H). **¹³C NMR** (126 MHz, CDCl₃): δ 172.3 (C_q), 151.4 (C_q), 149.5 (CH), 138.1 (CH), 136.9 (C_q), 135.9 (C_q), 135.3 (C_q), 135.0 (CH), 133.7 (CH), 128.7 (C_q), 128.5 (CH), 128.3 (CH), 128.2 (CH), 122.3 (CH), 122.1 (CH), 121.4 (CH), 118.6 (C_q), 116.1 (CH₂), 113.9 (CH), 110.2 (CH), 109.4 (C_q), 79.9 (C_q), 67.4 (CH₂), 55.4 (CH), 29.3 (CH₂), 28.5 (CH₃), 27.8 (CH₂). **IR** (ATR): 3377, 3171, 2970, 1701, 1610, 1511, 1381, 1029, 710, 695 cm⁻¹. **MS** (ESI): *m/z* (relative intensity) 1045 (85) [2M+Na]⁺, 534 (100) [M+Na]⁺. **HR-MS** (ESI): *m/z* calcd for C₃₁H₃₃N₃O₄Na⁺ [M+Na]⁺: 534.2363; found: 534.2366.

5. Experimental Part

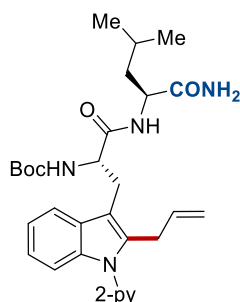
Methyl (S)-3-[2-allyl-1-(pyridin-2-yl)-1H-indol-3-yl]-2-[(*tert*-butoxycarbonyl)amino]propanoate (273b)



The general procedure **L** was followed using methyl *N*-(*tert*-butoxycarbonyl)-1-(pyridin-2-yl)-*L*-tryptophanate **153** (59.3 mg, 0.15 mmol), allyl acetate **272** (30.0 mg, 0.30 mmol), [Cp*Co(MeCN)₃](SbF₆)₂ (5.9 mg, 5.0 mol %) and PivOH (1.5 mg, 10 mol %) in TFE (1.0 mL). Purification by column chromatography on silica gel (*n*-hexane/EtOAc: 2/1) yielded **273b** (52.9 mg, 81%) as a colorless oil. The reaction was also performed using H₂O (27.0 mg, 1.5 mmol, 10 equiv), and yielded **273b** (40.9 mg, 69%).

¹H NMR (500 MHz, CDCl₃): δ 8.63 (ddd, *J* = 4.9, 2.0, 0.9 Hz, 1H), 7.85 (ddd, *J* = 7.9, 7.5, 2.0 Hz, 1H), 7.56 – 7.54 (m, 1H), 7.41 (ddd, *J* = 8.0, 1.0, 1.0 Hz, 1H), 7.33 – 7.28 (m, 2H), 7.18 – 7.10 (m, 2H), 5.70 – 5.65 (m, 1H), 5.16 (d, *J* = 8.0 Hz, 2H), 4.81 (d, *J* = 10.0 Hz, 1H), 4.72 (d, *J* = 17.0 Hz, 1H), 4.64 (ddd, *J* = 8.0, 5.9, 5.9 Hz, 1H), 3.69 (d, *J* = 5.9 Hz, 1H), 3.68 (s, 3H), 3.34– 3.25 (m, 2H), 1.41 (s, 9H). **¹³C NMR** (126 MHz, CDCl₃): δ = 173.0 (C_q), 155.2 (C_q), 151.5 (C_q), 149.6 (CH), 138.3 (CH), 136.9 (C_q), 136.0 (C_q), 135.0 (CH), 128.7 (C_q), 122.4 (CH), 122.2 (CH), 121.4 (CH), 120.7 (CH), 118.6 (CH), 116.1 (CH₂), 110.2 (CH), 109.4 (C_q), 79.9 (C_q), 54.2 (CH), 52.4 (CH₃), 29.2 (CH₂), 28.4 (CH₃), 27.6 (CH₂). **IR** (ATR): 3374, 2977, 1741, 1708, 1499, 1470, 1437, 1366, 1017, 735 cm⁻¹. **MS** (ESI): *m/z* (relative intensity) 893 (20) [2M+Na]⁺, 458 (100) [M+Na]⁺, 436 (35) [M+H]⁺. **HR-MS** (ESI): *m/z* calcd for C₂₅H₂₉N₃O₄Na⁺ [M+Na]⁺: 458.2050, found: 458.2053.

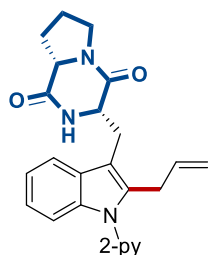
tert-Butyl {(S)-3-[2-allyl-1-(pyridin-2-yl)-1H-indol-3-yl]-1-[(S)-1-amino-4-methyl-1-oxopentan-2-yl]amino]-1-oxopropan-2-yl}carbamate (273c)



The general procedure **L** was followed using *tert*-butyl [(*S*)-1-{[(*S*)-1-amino-4-methyl-1-oxopentan-2-yl]amino}-1-oxo-3-[1-(pyridin-2-yl)-1*H*-indol-3-yl]propan-2-yl]carbamate **243k** (74.1 mg, 0.15 mmol), allyl acetate **272** (30.0 mg, 0.30 mmol), [Cp*Co(MeCN)₃](SbF₆)₂ (5.9 mg, 5.0 mol %) and PivOH (1.5 mg, 10 mol %) in TFE (1.0 mL). Purification by column chromatography on silica gel (*n*-hexane/EtOAc: 4/1) yielded **273c** (48.1 mg, 60%) as a colorless oil.

¹H NMR (300 MHz, CDCl₃): δ 8.70 – 8.58 (m, 1H), 7.90 (ddd, *J* = 7.6, 7.6, 1.9 Hz, 1H), 7.74 – 7.68 (m, 1H), 7.44 (d, *J* = 8.0 Hz, 1H), 7.37 (ddd, *J* = 7.6, 4.9, 1.0 Hz, 1H), 7.33 – 7.24 (m, 1H), 7.23 – 7.14 (m, 2H), 6.02 (d, *J* = 8.3 Hz, 1H), 5.88 – 5.60 (m, 2H), 5.50 (br s, 1H), 5.29 (d, *J* = 7.2 Hz, 1H), 4.88 (dd, *J* = 10.1, 1.6 Hz, 1H), 4.75 (dd, *J* = 17.1, 1.6 Hz, 1H), 4.50 (ddd, *J* = 7.2, 7.2, 7.2 Hz, 1H), 4.39 (ddd, *J* = 9.6, 8.3, 4.6 Hz, 1H), 3.67 (d, *J* = 6.2 Hz, 2H), 3.36 – 3.15 (m, 2H), 1.69 (ddd, *J* = 13.6, 9.6, 4.5 Hz, 1H), 1.62 – 1.50 (m, 1H), 1.45 (s, 9H), 1.38 – 1.25 (m, 1H), 0.88 (d, *J* = 6.5 Hz, 3H), 0.86 (d, *J* = 6.5 Hz, 3H). **¹³C NMR** (126 MHz, CDCl₃): δ = 173.6 (C_q), 171.7 (C_q), 155.6 (C_q), 150.9 (C_q), 149.5 (CH), 138.4 (CH), 136.7 (C_q), 135.7 (C_q), 134.8 (CH), 127.7 (C_q), 122.6 (CH), 122.5 (CH), 121.6 (CH), 120.9 (CH), 118.5 (CH), 116.0 (CH₂), 110.3 (CH), 109.1 (C_q), 80.4 (C_q), 55.4 (CH), 51.5 (CH), 40.1 (CH₂), 28.9 (CH₂), 28.3 (CH₃), 27.6 (CH₂), 24.7 (CH), 23.1 (CH₃), 21.6 (CH₃). **IR** (ATR): 3284, 3056, 2957, 1650, 1586, 1471, 1366, 1166, 782 cm⁻¹. **MS** (ESI): *m/z* (relative intensity) 556 (96) [M+Na]⁺, 534 (100) [M+H]⁺. **HR-MS** (ESI): *m/z* calcd for C₃₀H₄₀N₅O₄⁺ [M+H]⁺: 534.3075, found: 534.3079.

(3*S*,8*aS*)-3-[[2-allyl-1-(pyridin-2-yl)-1*H*-indol-3-yl]methyl]hexahydropyrrolo[1,2-*a*]pyrazine-1,4-dione (273d**)**



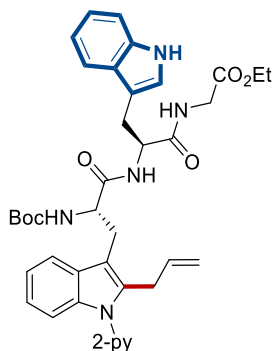
The general procedure **L** was followed using (3*S*,8*aS*)-3-[[1-(pyridin-2-yl)-1*H*-indol-3-yl]methyl]hexahydropyrrolo[1,2-*a*]pyrazine-1,4-dione **243c** (51.1 mg, 0.15 mmol), allyl acetate **272** (30.0 mg, 0.30 mmol), [Cp*Co(MeCN)₃](SbF₆)₂ (5.9 mg, 5.0 mol %) and PivOH (1.5 mg, 10 mol %) in TFE (1.0 mL). Purification by column chromatography on silica gel (*n*-hexane/EtOAc: 4/1) yielded **273d** (46.4 mg, 77%) as a white solid.

5. Experimental Part

M.p.: 89 – 91 °C. **¹H NMR** (400 MHz, CDCl₃): δ 8.62 (ddd, *J* = 4.9, 2.0, 0.9 Hz, 1H), 7.87 (ddd, *J* = 8.0, 7.5, 2.0 Hz, 1H), 7.57 – 7.51 (m, 1H), 7.43 (ddd, *J* = 8.0, 1.0, 1.0 Hz, 1H), 7.36 – 7.28 (m, 2H), 7.20 – 7.12 (m, 2H), 5.81 – 5.58 (m, 2H), 4.87 (dd, *J* = 10.1, 1.5 Hz, 1H), 4.75 (dtd, *J* = 17.1, 1.7, 1.5 Hz, 1H), 4.41 (ddd, *J* = 11.3, 3.8, 1.5 Hz, 1H), 4.04 (dd, *J* = 9.0, 6.9 Hz, 1H), 3.78 – 3.51 (m, 5H), 3.01 (dd, *J* = 15.1, 11.5 Hz, 1H), 2.40 – 2.24 (m, 1H), 2.12 – 1.96 (m, 2H), 1.94 – 1.81 (m, 1H). **¹³C NMR** (101 MHz, CDCl₃): δ 169.3 (C_q), 165.6 (C_q), 151.0 (C_q), 149.6 (CH), 138.3 (CH), 136.9 (C_q), 136.2 (C_q), 134.8 (CH), 127.8 (C_q), 122.8 (CH), 122.3 (CH), 121.2 (CH), 121.0 (CH), 118.0 (CH), 116.4 (CH₂), 110.5 (CH), 108.6 (C_q), 59.2 (CH), 54.7 (CH), 45.4 (CH₂), 29.1 (CH₂), 28.3 (CH₂), 25.7 (CH₂), 22.6 (CH₂). **IR** (ATR): 3056, 2953, 2924, 1659, 1587, 1469, 1458, 1436, 1370, 731 cm⁻¹. **MS** (ESI): *m/z* (relative intensity) 423 (100) [M+Na]⁺, 401 (77) [M+H]⁺. **HR-MS** (ESI): *m/z* calcd for C₂₄H₂₅N₄O₂⁺ [M+H]⁺: 401.1972, found: 401.1975.

Ethyl

{(S)-3-[2-allyl-1-(pyridin-2-yl)-1H-indol-3-yl]-2-[(*tert*-butoxycarbonyl)amino]propanoyl}-L-tryptophylglycinate (273e)

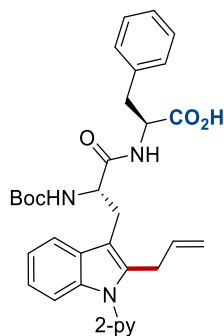


The general procedure **L** was followed using ethyl *N*-(*tert*-butoxycarbonyl)-1-(pyridin-2-yl)-*L*-tryptophyl-*L*-tryptophylglycinate **243q** (97.9 mg, 0.15 mmol), allyl acetate **272** (30.0 mg, 0.30 mmol), [Cp*Co(MeCN)₃](SbF₆)₂ (5.9 mg, 5.0 mol %) and PivOH (1.5 mg, 10 mol %) in TFE (1.0 mL). Purification by column chromatography on silica gel (*n*-hexane/EtOAc: 4/1) yielded **273e** (78.6 mg, 76%) as a white solid.

M.p.: 100 – 102 °C. **¹H NMR** (300 MHz, CDCl₃): δ 8.70 (s, 1H), 8.68 – 8.64 (m, 1H), 7.88 (ddd, *J* = 7.7, 7.7, 2.0 Hz, 1H), 7.70 – 7.50 (m, 1H), 7.43 (ddd, *J* = 8.0, 1.0, 1.0 Hz, 1H), 7.38 – 7.28 (m, 2H), 7.22 – 7.12 (m, 2H), 7.10 – 6.99 (m, 2H), 6.95 – 6.78 (m, 2H), 6.70 (d, *J* = 2.4 Hz, 1H), 6.38 (d, *J* = 7.8 Hz, 1H), 5.66 (ddt, *J* = 17.1, 10.0, 5.8 Hz, 1H), 4.93 (d, *J* = 5.9 Hz, 1H), 4.81 – 4.56 (m, 3H), 4.29 (ddd, *J* = 5.9, 5.9, 5.9 Hz, 1H), 4.10 (q, *J* = 7.1 Hz, 2H), 3.88 (dd, *J* = 17.7, 5.7 Hz, 1H), 3.80 – 3.54 (m, 3H), 3.38 –

3.23 (m, 2H), 3.14 (dd, $J = 14.8, 6.3$ Hz, 1H), 2.92 (dd, $J = 14.8, 6.0$ Hz, 1H), 1.22 (t, $J = 7.1$ Hz, 3H), 1.16 (s, 9H). $^{13}\text{C NMR}$ (126 MHz, CDCl_3): δ 171.8 (C_q), 171.4 (C_q), 169.2 (C_q), 155.7 (C_q), 151.0 (C_q), 149.3 (CH), 138.4 (CH), 136.8 (C_q), 135.9 (C_q), 135.9 (C_q), 134.7 (CH), 128.3 (C_q), 127.4 (C_q), 123.6 (CH), 122.6 (CH), 122.4 (CH), 121.8 (CH), 121.5 (CH), 120.9 (CH), 119.5 (CH), 118.7 (CH), 117.9 (CH), 116.3 (CH_2), 111.2 (CH), 110.1 (CH), 109.0 (C_q), 109.0 (C_q), 80.2 (C_q), 61.1 (CH_2), 55.7 (CH), 53.8 (CH), 41.4 (CH_2), 29.0 (CH_2), 28.0 (CH_3), 26.5 (CH_2), 26.3 (CH_2), 14.2 (CH_3). **IR** (ATR): 3315, 3056, 2977, 2867, 1744, 1655, 1508, 1471, 1438, 1200, 1166, 742 cm^{-1} . **MS** (ESI): m/z (relative intensity) 716 (100) $[\text{M}+\text{Na}]^+$, 693 (40) $[\text{M}+\text{H}]^+$. **HR-MS** (ESI): m/z calcd for $\text{C}_{39}\text{H}_{45}\text{N}_6\text{O}_6^+$ $[\text{M}+\text{H}]^+$: 693.3395, found: 693.3399.

(S)-2-{[S]-3-[2-allyl-1-(pyridin-2-yl)-1H-indol-3-yl]-2-[(*tert*-butoxycarbonyl)amino]propanamido}-3-phenylpropanoic acid (273f)



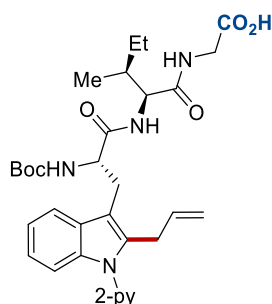
The general procedure **L** was followed using (S)-2-{[S]-2-[(*tert*-butoxycarbonyl)amino]-3-[1-(pyridin-2-yl)-1H-indol-3-yl]propanamido}-3-phenylpropanoic acid **243ab** (79.2 mg, 0.15 mmol), allyl acetate **272** (30.0 mg, 0.30 mmol), $[\text{Cp}^*\text{Co}(\text{MeCN})_3](\text{SbF}_6)_2$ (11.8 mg, 10 mol %) and PivOH (1.5 mg, 10 mol %) in TFE (1.0 mL) Purification by column chromatography on silica gel ($\text{CH}_2\text{Cl}_2/\text{MeOH}$: 9/1, + 1% AcOH) yielded **273f** (52.0 mg, 61%) as a colorless oil.

$^1\text{H NMR}$ (400 MHz, CDCl_3): δ 10.10 (br s, 1H), 8.71 – 8.61 (m, 1H) 8.01 (ddd, $J = 7.8, 7.8, 2.0$ Hz, 1H), 7.93 – 7.81 (m, 1H), 7.54 – 7.44 (m, 2H), 7.39 – 6.83 (m, 9H), 5.66 – 5.43 (m, 2H), 4.92 – 4.70 (m, 2H), 4.68 – 4.45 (m, 2H), 3.77 – 3.26 (m, 3H), 3.10 – 2.64 (m, 3H), 1.49 (s, 9H). $^{13}\text{C NMR}$ (101 MHz, CDCl_3): δ 172.1 (C_q), 171.0 (C_q), 155.1 (C_q), 150.6 (C_q), 148.5 (CH), 139.8 (CH), 137.3 (C_q), 136.1 (C_q), 135.9 (C_q), 134.5 (CH), 129.0 (CH), 128.4 (CH), 127.7 (C_q), 126.7 (CH), 123.3 (CH), 123.3 (CH), 122.6 (CH), 121.0 (CH), 118.8 (CH), 115.9 (CH_2), 109.8 (CH), 109.6 (C_q), 79.8 (C_q), 54.6 (CH), 53.7 (CH), 37.6 (CH_2), 28.8 (CH_2), 28.6 (CH_2), 28.3 (CH_3). **IR** (ATR): 3406, 3309,

5. Experimental Part

2977, 2930, 1712, 1693, 1497, 1472, 1438, 1367, 1166, 733 cm^{-1} . **MS** (ESI): m/z (relative intensity) 1159 (40) $[2\text{M}+\text{Na}]^+$, 1137 (40) $[2\text{M}+\text{H}]^+$, 583 (50) $[\text{M}+\text{Na}]^+$, 569 (100) $[\text{M}+\text{H}]^+$, 469 (45). **HR-MS** (ESI): m/z calcd for $\text{C}_{33}\text{H}_{37}\text{N}_5\text{O}_6^+$ $[\text{M}+\text{H}]^+$: 569.2758, found: 569.2759.

(6*S*,9*S*)-6-[[2-Allyl-1-(pyridin-2-yl)-1*H*-indol-3-yl]methyl]-9-[(*S*)-*sec*-butyl]-2,2-dimethyl-4,7,10-trioxo-3-oxa-5,8,11-triazatridecan-13-oic acid (**273g**)

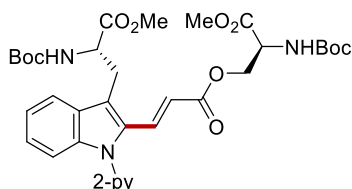


The general procedure **L** was followed using (6*S*,9*S*)-9-[(*S*)-*sec*-butyl]-2,2-dimethyl-4,7,10-trioxo-6-[(1-(pyridin-2-yl)-1*H*-indol-3-yl)methyl]-3-oxa-5,8,11-triazatridecan-13-oic acid **243ac** (82.7 mg, 0.15 mmol), allyl acetate **272** (30.0 mg, 0.30 mmol), $[\text{Cp}^*\text{Co}(\text{MeCN})_3](\text{SbF}_6)_2$ (11.8 mg, 10 mol %) and PivOH (1.5 mg, 10 mol %) in TFE (1.0 mL). Purification by column chromatography on silica gel ($\text{CH}_2\text{Cl}_2/\text{MeOH}$: 85/15, + 1% AcOH) yielded **273g** (47.0 mg, 53%) as a white solid.

M.p.: 166 – 168 °C. **$^1\text{H NMR}$** (300 MHz, $\text{DMSO}-d_6$): δ 8.64 (d, $J = 4.7$ Hz, 1H), 8.08 – 7.81 (m, 3H), 7.74 – 7.62 (m, 1H), 7.56 – 7.37 (m, 2H), 7.30 – 7.17 (m, 1H), 7.18 – 6.97 (m, 2H), 5.64 (dddd, $J = 14.4, 10.8, 5.5, 4.7$ Hz, 1H), 4.73 (d, $J = 10.0$ Hz, 1H), 4.63 (d, $J = 17.1$ Hz, 1H), 4.40 – 4.15 (m, 2H), 3.79 – 3.40 (m, 5H), 3.16 (dd, $J = 13.8, 4.4$ Hz, 1H), 2.99 (dd, $J = 13.8, 9.3$ Hz, 1H), 1.82 – 1.65 (m, 1H), 1.57 – 1.38 (m, 1H), 1.25 (s, 9H), 1.14 – 1.06 (m, 1H), 0.92 – 0.78 (m, 6H). **$^{13}\text{C NMR}$** (101 MHz, $\text{DMSO}-d_6$): δ 171.8 (C_q), 171.7 (C_q), 170.7 (C_q), 155.5 (C_q), 151.1 (C_q), 149.7 (CH), 139.4 (CH), 136.6 (C_q), 135.8 (C_q), 135.8 (CH), 128.7 (C_q), 123.0 (CH), 122.2 (CH), 121.7 (CH), 120.5 (CH), 119.2 (CH), 115.9 (CH_2), 111.0 (C_q), 110.3 (CH), 78.6 (C_q), 70.2 (CH_2), 57.2 (CH), 56.2 (CH), 37.8 (CH), 29.1 (CH_2), 28.5 (CH_3), 27.3 (CH_2), 24.7 (CH_2), 15.7 (CH_3), 11.6 (CH_3). **IR** (ATR): 3306, 2967, 2931, 1692, 1645, 1526, 1473, 1438, 1367, 1222, 1169, 742 cm^{-1} . **MS** (ESI): m/z (relative intensity) 614 (100) $[\text{M}+\text{Na}]^+$, 592 (85) $[\text{M}+\text{H}]^+$, 287 (83). **HR-MS** (ESI): m/z calcd for $\text{C}_{32}\text{H}_{42}\text{N}_5\text{O}_6^+$ $[\text{M}+\text{H}]^+$: 592.3130, found: 592.3124.

5.7. Manganese(I)-Catalyzed Peptide C–H Ligation and Macrocyclization

5.7.1. Characterization Data

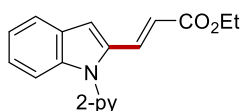
(S)-2-[(*tert*-butoxycarbonyl)amino]-3-methoxy-3-oxopropyl (E)-3-(3-[(S)-2-[(*tert*-butoxycarbonyl)amino]-3-methoxy-3-oxopropyl]-1-(pyridin-2-yl)-1*H*-indol-2-yl)acrylate (274b)

The general procedure **M** was followed using methyl *N*^B-(*tert*-butoxycarbonyl)-1-(pyridin-2-yl)-L-tryptophanate **153** (59.3 mg, 0.15 mmol), (S)-2-[(*tert*-butoxycarbonyl)amino]-3-methoxy-3-oxopropyl propiolate **211b** (61.0 mg, 0.23 mmol), MnBr(CO)₅ (4.1 mg, 10 mol %) and NaOAc (3.7 mg, 30 mol %) in 1,4-dioxane (0.6 mL). Purification by column chromatography on silica gel (*n*-hexane/EtOAc: 6/1 → 3/1) yielded **274b** (95.0 mg, 95%, *E/Z* = 97:3) as a white solid.

M. p.: 83 – 85 °C. **¹H NMR** (400 MHz, DMSO-*d*₆): δ 8.71 (dd, *J* = 5.0, 1.8 Hz, 1H), 8.10 (ddd, *J* = 7.7, 7.7, 1.9 Hz, 1H), 7.80 (d, *J* = 8.0 Hz, 1H), 7.68 (d, *J* = 16.2 Hz, 1H), 7.56 (dd, *J* = 7.5, 4.9 Hz, 1H), 7.50 – 7.42 (m, 2H), 7.38 (d, *J* = 7.5 Hz, 1H), 7.31 – 7.23 (m, 2H), 7.23 – 7.16 (m, 1H), 5.59 (d, *J* = 16.2 Hz, 1H), 4.51 – 4.11 (m, 4H), 3.63 (s, 3H), 3.59 (s, 3H), 3.45 – 3.34 (m, 2H), 1.37 (s, 9H), 1.30 (s, 9H). **¹³C NMR** (101 MHz, DMSO-*d*₆): δ 172.5 (C_q), 170.7 (C_q), 166.0 (C_q), 155.7 (C_q), 150.9 (C_q), 150.3 (CH), 140.0 (CH), 139.0 (C_q), 133.1 (CH), 131.5 (C_q), 128.4 (C_q), 125.8 (CH), 124.0 (CH), 122.6 (CH), 121.7 (CH), 120.7 (CH), 119.9 (C_q), 117.7 (CH), 111.2 (CH), 79.0 (C_q), 78.8 (C_q), 63.5 (CH₂), 54.9 (CH), 53.0 (CH), 52.6 (CH₃), 52.4 (CH₃), 28.6 (CH₃), 28.5 (CH₃), 27.0 (CH₂). (One C_q of the Boc group is missing due to overlap, the overlap was verified by HSQC and HMBC analysis, showing that the peaks at 155.7 ppm correspond to two carbons). **IR** (ATR): 2978, 1706, 1625, 1588, 1503, 1470, 1366, 1212, 1158, 1060, 852, 731 cm⁻¹. **MS** (ESI) *m/z* (relative intensity): 689 (100) [M+Na]⁺, 667 (12) [M+H]⁺. **HR-MS** (ESI): *m/z* calcd for C₃₄H₄₃N₄O₁₀⁺ [M+H]⁺: 667.2974, found: 667.2960.

5. Experimental Part

Ethyl (*E*)-3-[1-(pyridin-2-yl)-1*H*-indol-2-yl]acrylate (**S2**)

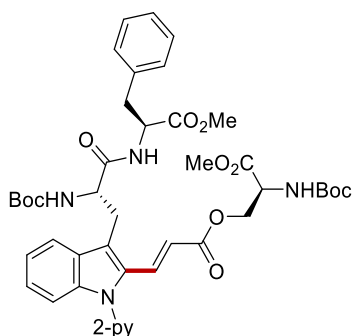


The general procedure **M** was followed using 1-(pyridin-2-yl)-1*H*-indole (48.6 mg, 0.25 mmol), ethyl propiolate (**1a**) (36.8 mg, 0.38 mmol), $\text{MnBr}(\text{CO})_5$ (6.9 mg, 10 mol %) and NaOAc (6.1 mg, 30 mol %) in 1,4-dioxane (1.0 mL). Purification by column chromatography on silica gel (*n*-hexane/EtOAc: 20/1) yielded **S3** (70.8 mg, 97%) as colorless oil.

¹H NMR (400 MHz, CDCl_3): δ 8.69 (ddd, $J = 5.0, 2.0, 0.9$ Hz, 1H), 7.90 (ddd, $J = 7.7, 7.7, 1.9$ Hz, 1H), 7.68 (dd, $J = 15.9, 0.7$ Hz, 1H), 7.66 – 7.62 (m, 1H), 7.45 (d, $J = 8.2$ Hz, 1H), 7.40 – 7.32 (m, 2H), 7.27 – 7.20 (m, 1H), 7.17 (ddd, $J = 8.2, 7.0, 1.1$ Hz, 1H), 7.11 (d, $J = 0.7$ Hz, 1H), 6.34 (d, $J = 15.9$ Hz, 1H), 4.21 (q, $J = 7.1$ Hz, 2H), 1.28 (t, $J = 7.1$ Hz, 3H). **¹³C NMR** (101 MHz, CDCl_3): δ 166.8 (C_q), 150.5 (C_q), 149.9 (CH), 138.6 (C_q), 138.5 (CH), 134.8 (C_q), 133.8 (CH), 128.0 (C_q), 124.5 (CH), 122.5 (CH), 121.7 (CH), 121.4 (CH), 121.4 (CH), 118.5 (CH), 111.0 (CH), 106.5 (CH), 60.4 (CH_2), 14.3 (CH_3). **IR** (ATR): 3053, 2979, 1703, 1627, 1467, 1214, 1170, 738 cm^{-1} . **MS** (ESI) *m/z* (relative intensity): 315 (60) $[\text{M}+\text{Na}]^+$, 293 (100) $[\text{M}+\text{H}]^+$. **HR-MS** (ESI): *m/z* calcd for $\text{C}_{18}\text{H}_{17}\text{N}_2\text{O}_2^+$ $[\text{M}+\text{H}]^+$: 293.1285, found: 293.1285.

The data is in accordance with those previously reported.

(*S*)-2-[(*tert*-Butoxycarbonyl)amino]-3-methoxy-3-oxopropyl (*E*)-3-[3-({*S*}-2-[(*tert*-butoxycarbonyl)amino]-3-[(*S*)-1-methoxy-1-oxo-3-phenylpropan-2-yl]amino)-3-oxopropyl]-1-(pyridin-2-yl)-1*H*-indol-2-yl]acrylate (**275b**)

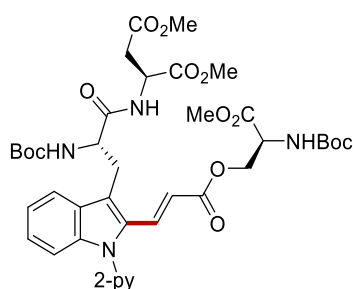


The general procedure **M** was followed using methyl *N*^a-(*tert*-butoxycarbonyl)-1-(pyridin-2-yl)-*L*-tryptophyl-*L*-phenylalaninate **243m** (81.3 mg, 0.15 mmol), (*S*)-2-[(*tert*-butoxycarbonyl)amino]-3-methoxy-3-oxopropyl propiolate **211b** (61.0 mg, 0.23 mmol), $\text{MnBr}(\text{CO})_5$ (4.1 mg, 10 mol %) and NaOAc (3.7 mg, 30 mol %) in 1,4-dioxane (0.6 mL).

Purification by column chromatography on silica gel (*n*-hexane/EtOAc: 2/1 → 1/1) yielded **275b** (106.2 mg, 87%, *E/Z* = 95:5) as a white solid.

M. p. 89 – 93 °C. **¹H NMR** (400 MHz, CDCl₃): δ 8.64 (ddd, *J* = 5.0, 2.0, 0.8 Hz, 1H), 7.87 (ddd, *J* = 7.7, 7.7, 1.9 Hz, 1H), 7.77 – 7.67 (m, 2H), 7.39 – 7.31 (m, 2H), 7.27 (d, *J* = 8.2 Hz, 1H), 7.26 – 7.21 (m, 1H), 7.20 – 7.11 (m, 4H), 6.98 – 6.84 (m, 2H), 6.10 (brs, 1H), 5.92 (d, *J* = 10.4 Hz, 1H), 5.43 (d, *J* = 16.3 Hz, 1H), 5.35 (brs, 1H), 4.66 – 4.58 (m, 2H), 4.52 (dd, *J* = 11.2, 3.6 Hz, 1H), 4.47 – 4.36 (m, 1H), 4.33 (dd, *J* = 11.2, 3.3 Hz, 1H), 3.74 (s, 3H), 3.58 – 3.40 (m, 4H), 3.32 (dd, *J* = 14.0, 8.5 Hz, 1H), 3.00 (dd, *J* = 13.7, 5.9 Hz, 1H), 2.93 (dd, *J* = 13.7, 5.0 Hz, 1H), 1.43 (s, 9H), 1.40 (s, 9H). **¹³C NMR** (101 MHz, CDCl₃): δ 170.9 (C_q), 170.5 (C_q), 170.3 (C_q), 165.9 (C_q), 155.4 (C_q), 155.0 (C_q), 151.1 (C_q), 149.9 (CH), 139.4 (C_q), 138.6 (CH), 135.5 (C_q), 132.9 (CH), 131.5 (C_q), 129.2 (CH), 128.4 (CH), 128.0 (C_q), 127.0 (CH), 125.7 (CH), 123.0 (CH), 122.1 (CH), 121.7 (CH), 120.1 (CH), 119.4 (C_q), 117.1 (CH), 110.8 (CH), 80.1 (C_q), 80.0 (C_q), 64.6 (CH₂), 55.0 (CH), 53.5 (CH), 53.0 (CH), 52.7 (CH₃), 52.1 (CH₃), 38.0 (CH₂), 28.7 (CH₂), 28.3 (CH₃), 28.3 (CH₃). **IR** (ATR): 3345, 2976, 2927, 1744, 1711, 1510, 1454, 1438, 1214, 1164, 745 cm⁻¹. **MS** (ESI) *m/z* (relative intensity): 836 (100) [M+Na]⁺, 814 (26) [M+H]⁺. **HR-MS** (ESI): *m/z* calcd for C₄₃H₅₂N₅O₁₁⁺ [M+H]⁺: 814.3658, found: 814.3648.

Dimethyl **{[S]-2-[(*tert*-butoxycarbonyl)amino]-3-[2-({*E*}-3-{{[S]-2-[(*tert*-butoxycarbonyl)amino]-3-methoxy-3-oxopropoxy}-3-oxoprop-1-en-1-yl)-1-(pyridin-2-yl)-1*H*-indol-3-yl]propanoyl]-L-aspartate (275c)**

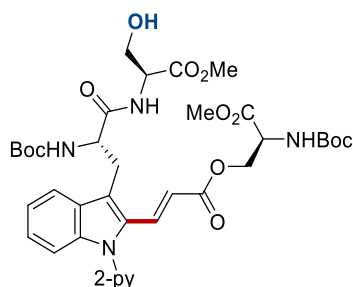


The general procedure **M** was followed using dimethyl *N*^a-(*tert*-butoxycarbonyl)-1-(pyridin-2-yl)-L-tryptophyl-L-aspartate **243ab** (78.6 mg, 0.15 mmol), (*S*)-2-[(*tert*-butoxycarbonyl)amino]-3-methoxy-3-oxopropyl propiolate **211b** (61.0 mg, 0.23 mmol), MnBr(CO)₅ (4.1 mg, 10 mol %) and NaOAc (3.7 mg, 30 mol %) in 1,4-dioxane (0.6 mL). Purification by column chromatography on silica gel (*n*-hexane/EtOAc: 2/1 → 1/1) yielded **275c** (100.2 mg, 84%, *E/Z* = 95:5) as a white solid.

5. Experimental Part

M. p. 70 – 73 °C. **¹H NMR** (400 MHz, CDCl₃): δ 8.70 (d, *J* = 5.4 Hz, 1H), 7.93 (ddd, *J* = 7.7, 7.7, 1.9 Hz, 1H), 7.83 – 7.71 (m, 2H), 7.47 – 7.39 (m, 2H), 7.35 (d, *J* = 8.2 Hz, 1H), 7.32 – 7.29 (m, 1H), 7.26 – 7.19 (m, 1H), 6.61 (brs, 1H), 5.90 (d, *J* = 8.6 Hz, 1H), 5.51 (d, *J* = 16.2 Hz, 1H), 5.34 (brs, 1H), 4.79 – 4.44 (m, 4H), 4.36 (dd, *J* = 11.3, 3.2 Hz, 1H), 3.89 – 3.73 (m, 3H), 3.71 – 3.32 (m, 8H), 2.93 (dd, *J* = 17.3, 3.7 Hz, 1H), 2.83 (dd, *J* = 17.3, 4.6 Hz, 1H), 1.48 (s, 9H), 1.43 (s, 9H). **¹³C NMR** (101 MHz, CDCl₃): δ 171.0 (C_q), 170.7 (C_q), 170.5 (C_q), 170.3 (C_q), 166.0 (C_q), 155.4 (C_q), 155.0 (C_q), 151.2 (C_q), 149.9 (CH), 139.5 (C_q), 138.6 (CH), 133.0 (CH), 131.6 (C_q), 128.1 (C_q), 125.8 (CH), 123.0 (CH), 122.2 (CH), 121.8 (CH), 120.1 (CH), 119.3 (C_q), 117.2 (CH), 110.9 (CH), 80.2 (C_q), 80.1 (C_q), 64.6 (CH₂), 55.0 (CH), 53.0 (CH), 52.7 (CH₃), 52.6 (CH₃), 51.9 (CH₃), 48.9 (CH), 36.1 (CH₂), 28.6 (CH₂), 28.3 (CH₃), 28.3 (CH₃). **IR** (ATR): 3344, 2954, 2926, 1711, 1503, 1454, 1366, 1246, 1213, 1160, 744 cm⁻¹. **MS** (ESI) *m/z* (relative intensity): 818 (100) [M+Na]⁺, 796 (23) [M+H]⁺. **HR-MS** (ESI): *m/z* calcd for C₃₉H₅₀N₅O₁₃⁺ [M+H]⁺: 796.3400, found: 796.3384.

(*S*)-2-[(*tert*-Butoxycarbonyl)amino]-3-methoxy-3-oxopropyl (*E*)-3-[3-({*S*)-2-[(*tert*-butoxycarbonyl)amino]-3-[(*S*)-3-hydroxy-1-methoxy-1-oxopropan-2-yl]amino]-3-oxopropyl)-1-(pyridin-2-yl)-1*H*-indol-2-yl]acrylate (**275d**)

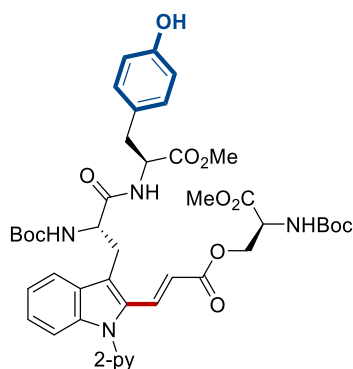


The general procedure **M** was followed using methyl *N*^a-(*tert*-butoxycarbonyl)-1-(pyridin-2-yl)-L-tryptophyl-L-serinate **243n** (72.3 mg, 0.15 mmol), (*S*)-2-[(*tert*-butoxycarbonyl)amino]-3-methoxy-3-oxopropyl propiolate **211b** (61.0 mg, 0.23 mmol), MnBr(CO)₅ (4.1 mg, 10 mol %) and NaOAc (3.7 mg, 30 mol %) in 1,4-dioxane (1.0 mL). Purification by column chromatography on silica gel (*n*-hexane/EtOAc: 1/2) yielded **275d** (78.1 mg, 69%, *E/Z* = 98:2) as a white solid.

M. p. 82 – 86 °C. **¹H NMR** (400 MHz, CDCl₃): δ 8.62 (d, *J* = 4.2 Hz, 1H), 8.08 – 7.89 (m, 2H), 7.73 (d, *J* = 7.8 Hz, 1H), 7.55 (d, *J* = 8.0 Hz, 1H), 7.50 – 7.41 (m, 1H), 7.36 – 7.29 (m, 2H), 7.26 – 7.21 (m, 2H), 6.96 – 6.80 (m, 1H), 6.48 (d, *J* = 8.9 Hz, 1H), 5.22 – 5.06 (m, 2H), 4.70 – 4.55 (d, *J* = 11.3 Hz, 1H), 4.63 (d, *J* = 9.2 Hz, 3H), 4.34 – 4.19

(m, 1H), 4.14 (s, 1H), 3.89 – 3.80 (m, 2H), 3.78 (s, 3H), 3.72 (s, 3H), 3.40 (dd, $J = 14.6$, 6.5 Hz, 1H), 1.47 (s, 9H), 1.45 (s, 9H). $^{13}\text{C NMR}$ (101 MHz, CDCl_3): δ 170.8 (C_q), 170.6 (C_q), 170.5 (C_q), 165.6 (C_q), 155.8 (C_q), 155.1 (C_q), 150.7 (C_q), 150.0 (CH), 139.7 (C_q), 139.4 (CH), 133.2 (CH), 131.8 (C_q), 128.4 (C_q), 126.1 (CH), 123.5 (CH), 122.1 (CH), 122.1 (CH), 119.8 (CH), 119.6 (C_q), 117.4 (CH), 110.7 (CH), 80.5 (C_q), 80.0 (C_q), 64.3 (CH_2), 62.3 (CH_2), 55.4 (CH), 54.9 (CH), 53.2 (CH), 52.7 (CH_3), 52.6 (CH_3), 28.3 (CH_3), 28.3 (CH_3), 27.0 (CH_2). **IR** (ATR): 3344, 2977, 2954, 1743, 1708, 1505, 1454, 1366, 1214, 1160, 731 cm^{-1} . **MS** (ESI) m/z (relative intensity): 776 (100) $[\text{M}+\text{Na}]^+$, 754 (16) $[\text{M}+\text{H}]^+$. **HR-MS** (ESI): m/z calcd for $\text{C}_{37}\text{H}_{48}\text{N}_5\text{O}_{12}^+$ $[\text{M}+\text{H}]^+$: 754.3294, found: 754.3291.

(S)-2-[(*tert*-butoxycarbonyl)amino]-3-methoxy-3-oxopropyl (*E*)-3-[3-({S}-2-[(*tert*-butoxycarbonyl)amino]-3-[[*S*]-3-(4-hydroxyphenyl)-1-methoxy-1-oxopropan-2-yl]amino]-3-oxopropyl)-1-(pyridin-2-yl)-1*H*-indol-2-yl]acrylate (275e)



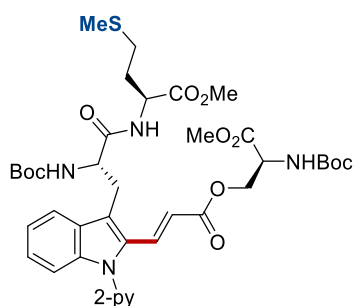
The general procedure **M** was followed using methyl *N*^a-(*tert*-butoxycarbonyl)-1-(pyridin-2-yl)-L-tryptophyl-L-tyrosinate **243o** (83.9 mg, 0.15 mmol), (*S*)-2-[(*tert*-butoxycarbonyl)amino]-3-methoxy-3-oxopropyl propiolate **211b** (61.0 mg, 0.23 mmol), $\text{MnBr}(\text{CO})_5$ (4.1 mg, 10 mol %) and NaOAc (3.7 mg, 30 mol %) in 1,4-dioxane (0.6 mL). Purification by column chromatography on silica gel (*n*-hexane/EtOAc: 1/1 \rightarrow 1/2) yielded **275e** (83.4 mg, 67%, *E/Z* = 98:2) as a white solid.

M. p. 90 – 92 °C. $^1\text{H NMR}$ (400 MHz, CDCl_3): δ 8.69 (dd, $J = 5.0$, 1.9 Hz, 1H), 7.92 (ddd, $J = 7.7$, 7.7, 1.9 Hz, 1H), 7.83 – 7.70 (m, 2H), 7.42 (ddd, $J = 7.6$, 4.9, 1.1 Hz, 1H), 7.34 (d, $J = 8.0$ Hz, 1H), 7.27 – 7.22 (m, 2H), 7.19 (ddd, $J = 8.0$, 6.1, 1.9 Hz, 1H), 6.90 – 6.71 (m, 3H), 6.62 (d, $J = 7.8$ Hz, 2H), 6.30 (brs, 1H), 5.94 (brs, 1H), 5.38 (d, $J = 16.2$ Hz, 1H), 5.22 (brs, 1H), 4.81 – 4.44 (m, 4H), 4.34 (dd, $J = 11.2$, 3.3 Hz, 1H), 3.72 (s, 3H), 3.59 (s, 3H), 3.51 – 3.34 (s, 2H), 3.10 – 2.97 (m, 1H), 2.88 (dd, $J = 14.0$, 6.0 Hz, 1H), 1.47 (s, 9H), 1.40 (s, 9H). $^{13}\text{C NMR}$ (101 MHz, CDCl_3): δ 171.3 (C_q), 170.6 (C_q), 170.5 (C_q), 166.0 (C_q), 155.6 (C_q), 155.4 (C_q), 155.1 (C_q), 151.2 (C_q), 149.8 (CH), 139.7

5. Experimental Part

(C_q), 138.9 (CH), 133.0 (CH), 131.6 (C_q), 130.3 (CH), 128.0 (C_q), 126.9 (C_q), 125.9 (CH), 123.1 (CH), 122.4 (CH), 121.8 (CH), 120.2 (CH), 120.0 (C_q), 117.0 (CH), 115.6 (CH), 110.8 (CH), 80.4 (C_q), 80.2 (C_q), 64.5 (CH₂), 55.0 (CH), 53.4 (CH), 53.0 (CH), 52.8 (CH₃), 52.2 (CH₃), 37.0 (CH₂), 28.3 (CH₃), 28.2 (CH₃), 28.1 (CH₂). **IR** (ATR): 3337, 2976, 1741, 1710, 1515, 1366, 1246, 1215, 1163, 744 cm⁻¹. **MS** (ESI) m/z (relative intensity): 852 (100) [M+Na]⁺, 830 (55) [M+H]⁺. **HR-MS** (ESI): m/z calcd for C₄₃H₅₂N₅O₁₂ [M+H]⁺: 830.3607, found: 830.3600.

Methyl {[S]-2-[(*tert*-butoxycarbonyl)amino]-3-[2-({*E*}-3-[[S]-2-[(*tert*-butoxycarbonyl)amino]-3-methoxy-3-oxopropoxy]-3-oxoprop-1-en-1-yl)-1-(pyridin-2-yl)-1*H*-indol-3-yl]propanoyl]-L-methioninate (**275f**)

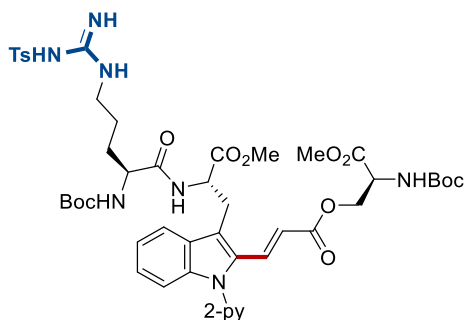


The general procedure **M** was followed using methyl *N*^a-(*tert*-butoxycarbonyl)-1-(pyridin-2-yl)-L-tryptophyl-L-methioninate **243ac** (78.9 mg, 0.15 mmol), (*S*)-2-[(*tert*-butoxycarbonyl)amino]-3-methoxy-3-oxopropyl propiolate **211b** (61.0 mg, 0.23 mmol), MnBr(CO)₅ (4.1 mg, 10 mol %) and NaOAc (3.7 mg, 30 mol %) in 1,4-dioxane (0.9 mL). Purification by column chromatography on silica gel (*n*-hexane/EtOAc: 1/1) yielded **275f** (105.6 mg, 88%, *E/Z* = 97:3) as a pale yellow solid.

M. p. 131 – 133 °C. **¹H NMR** (400 MHz, CDCl₃): δ 8.70 (d, *J* = 4.7 Hz, 1H), 7.93 (t, *J* = 7.6 Hz, 1H), 7.83 – 7.71 (m, 2H), 7.45 – 7.38 (m, 2H), 7.32 (d, *J* = 9.9 Hz, 1H), 7.26–7.22 (m, 1H), 7.22 (t, *J* = 7.4 Hz, 1H), 6.30 (d, *J* = 7.5 Hz, 1H), 5.89 (d, *J* = 8.6 Hz, 1H), 5.52 (d, *J* = 16.2 Hz, 1H), 5.38 (d, *J* = 8.2 Hz, 1H), 4.72 – 4.44 (m, 4H), 4.41 – 4.33 (m, 1H), 3.78 (s, 3H), 3.67 – 3.48 (m, 4H), 3.38 (dd, *J* = 11.4, 8.5 Hz, 1H), 2.47 – 2.27 (m, 2H), 2.10 – 1.98 (m, 4H), 1.94 – 1.79 (m, 1H), 1.47 (s, 9H), 1.44 (s, 9H). **¹³C NMR** (101 MHz, CDCl₃): δ 171.4 (C_q), 170.7 (C_q), 170.5 (C_q), 165.9 (C_q), 155.4 (C_q), 155.1 (C_q), 151.1 (C_q), 149.9 (CH), 139.4 (C_q), 138.6 (CH), 132.9 (CH), 131.5 (C_q), 128.1 (C_q), 125.8 (CH), 123.0 (CH), 122.2 (CH), 121.8 (CH), 120.0 (CH), 119.2 (C_q), 117.3 (CH), 110.9 (CH), 80.1 (C_q), 64.6 (CH₂), 55.1 (CH), 53.1 (CH), 52.7 (CH), 52.4 (CH₃), 51.7 (CH₃), 31.9 (CH₂), 29.5 (CH₂), 28.5 (CH₂), 28.3 (CH₃), 28.3 (CH₃), 15.3 (CH₃). (One C_q

of the Boc group is missing due to overlap, the overlap was verified by HMBC and HSQC analysis, showing that the peak at 80.1 ppm corresponds to two carbons). **IR** (ATR): 3335, 2976, 2927, 1741, 1708, 1524, 1366, 1247, 1214, 1163, 739 cm^{-1} . **MS** (ESI) m/z (relative intensity): 820 (100) $[\text{M}+\text{Na}]^+$. **HR-MS** (ESI): m/z calcd for $\text{C}_{39}\text{H}_{51}\text{N}_5\text{O}_{11}\text{SNa}^+$ $[\text{M}+\text{Na}]^+$: 820.3198, found: 820.3192.

(S)-2-[(*tert*-Butoxycarbonyl)amino]-3-methoxy-3-oxopropyl (*E*)-3-[3-({*S*}-2-[[*S*]-2-[(*tert*-butoxycarbonyl)amino]-5-[3-tosylguanidino]pentanamido)-3-methoxy-3-oxopropyl]-1-(pyridin-2-yl)-1*H*-indol-2-yl]acrylate (275g**)**



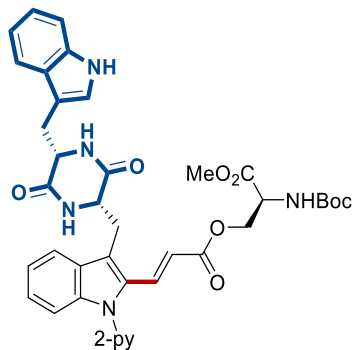
The general procedure **M** was followed using methyl *N*^a-(*N*²-(*tert*-butoxycarbonyl)-*N*^ω-tosyl-L-arginyl)-1-(pyridin-2-yl)-L-tryptophanate **243ad** (105.9 mg, 0.15 mmol), (*S*)-2-[(*tert*-butoxycarbonyl)amino]-3-methoxy-3-oxopropyl propiolate **211b** (61.0 mg, 0.23 mmol), $\text{MnBr}(\text{CO})_5$ (4.1 mg, 10 mol %) and NaOAc (3.7 mg, 30 mol %) in 1,4-dioxane (0.6 mL). Purification by column chromatography on silica gel (*n*-hexane/EtOAc: 1/1 → 1/2) yielded **275g** (124.5 mg, 85%, *E/Z* = 86:14) as a yellow solid.

M. p. 98 – 101 °C. **¹H NMR** (400 MHz, $\text{DMSO-}d_6$): δ 8.70 (dd, $J = 4.8, 1.9$ Hz, 1H), 8.46 (d, $J = 7.7$ Hz, 1H), 8.09 (ddd, $J = 7.8, 7.8, 2.0$ Hz, 1H), 7.76 (d, $J = 7.8$ Hz, 1H), 7.71 – 7.61 (m, 3H), 7.57 (dd, $J = 7.4, 4.8$ Hz, 1H), 7.47 (d, $J = 7.8$ Hz, 1H), 7.37 (d, $J = 8.2$ Hz, 1H), 7.32 – 6.94 (m, 6H), 6.83 – 6.69 (m, 2H), 6.56 (s, 1H), 5.48 (d, $J = 16.3$ Hz, 1H), 4.62 (ddd, $J = 7.5, 7.5, 7.5$ Hz, 1H), 4.42 – 4.17 (m, 3H), 3.98 – 3.90 (m, 1H), 3.62 (s, 3H), 3.54 – 3.50 (m, 5H), 3.08 – 2.90 (m, 2H), 2.33 (s, 3H), 1.49 – 1.15 (m, 22H). **¹³C NMR** (101 MHz, $\text{DMSO-}d_6$): δ 172.3 (C_q), 171.6 (C_q), 170.3 (C_q), 165.6 (C_q), 156.7 (C_q), 155.4 (C_q), 155.3 (C_q), 155.3 (C_q), 150.5 (C_q), 149.9 (CH), 141.2 (C_q), 139.7 (CH), 138.8 (C_q), 132.6 (CH), 131.3 (C_q), 129.1 (CH), 127.7 (C_q), 125.7 (CH), 125.6 (CH), 123.7 (CH), 122.3 (CH), 121.5 (CH), 120.2 (CH), 119.0 (C_q), 117.4 (CH), 110.9 (CH), 78.8 (C_q), 78.3 (C_q), 63.1 (CH₂), 53.9 (CH), 52.8 (CH), 52.6 (CH), 52.3 (CH₃), 52.1 (CH₃), 40.1 (CH₂), 29.5 (CH₂), 28.2 (CH₃), 28.2 (CH₃), 28.0 (CH₂), 26.9 (CH₂), 21.0 (CH₃). **IR** (ATR): 3336, 2967, 2929, 1738, 1709, 1547, 1228, 1160, 1131, 729 cm^{-1} .

5. Experimental Part

MS (ESI) m/z (relative intensity): 999 (100) $[M+Na]^+$, 977 (67) $[M+H]^+$. **HR-MS** (ESI): m/z calcd for $C_{47}H_{61}N_8O_{13}S^+$ $[M+H]^+$: 977.4073, found: 977.4071.

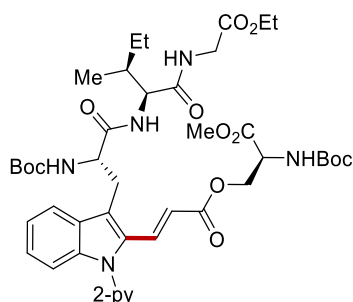
(S)-2-[(*tert*-Butoxycarbonyl)amino]-3-methoxy-3-oxopropyl (E)-3-[3-({[2S,5S]-5-[(1*H*-indol-3-yl)methyl]-3,6-dioxopiperazin-2-yl)methyl]-1-(pyridin-2-yl)-1*H*-indol-2-yl]acrylate (277b)



The general procedure **M** was followed using (3*S*,6*S*)-3-[(1*H*-indol-3-yl)methyl]-6-[[1-(pyridin-2-yl)-1*H*-indol-3-yl]methyl]piperazine-2,5-dione **276b** (67.4 mg, 0.15 mmol), (S)-2-[(*tert*-butoxycarbonyl)amino]-3-methoxy-3-oxopropyl propiolate **211b** (61.0 mg, 0.23 mmol), $MnBr(CO)_5$ (4.1 mg, 10 mol %) and NaOAc (3.7 mg, 30 mol %) in 1,4-dioxane (0.9 mL). Purification by column chromatography on silica gel ($CH_2Cl_2/MeOH$: 95/5 \rightarrow 90/10) yielded **277b** (77.7 mg, 72%) as a white solid.

M. p. 151 – 154 °C. **1H NMR** (400 MHz, $CDCl_3$): δ 8.65 (dd, $J = 4.9, 2.1$ Hz, 1H), 8.22 (brs, 1H), 7.91 – 7.82 (m, 2H), 7.74 (dd, $J = 16.3$ Hz, 1H), 7.54 (d, $J = 3.0$ Hz, 1H), 7.43 – 7.28 (m, 5H), 7.26 – 7.23 (m, $J = 9.2$ Hz, 2H), 7.23 – 7.12 (m, 2H), 7.02 (t, $J = 7.5$ Hz, 1H), 5.84 (brs, 1H), 5.57 (brs, 1H), 5.11 (d, $J = 16.3$ Hz, 1H), 4.76 – 4.65 (m, 2H), 4.59 – 4.42 (m, 2H), 4.34 (dd, $J = 11.4, 3.5$ Hz, 1H), 3.94 (d, $J = 10.8$ Hz, 1H), 3.88 (s, 3H), 3.70 (dd, $J = 14.8, 4.5$ Hz, 1H), 3.32 – 3.17 (m, 2H), 1.45 (s, 9H). **^{13}C NMR** (101 MHz, $CDCl_3$): δ 173.1 (C_q), 166.4 (C_q), 166.0 (C_q), 165.0 (C_q), 156.2 (C_q), 150.9 (C_q), 150.3 (CH), 139.9 (C_q), 139.0 (CH), 136.3 (C_q), 132.7 (C_q), 131.9 (CH), 128.2 (C_q), 126.4 (C_q), 126.1 (CH), 123.6 (CH), 123.6 (CH), 122.3 (CH), 122.1 (CH), 121.9 (CH), 121.2 (CH), 119.8 (CH), 118.4 (C_q), 118.3 (CH), 117.4 (CH), 111.2 (CH), 110.6 (CH), 109.1 (C_q), 79.8 (C_q), 64.5 (CH_2), 55.9 (CH), 55.4 (CH), 53.5 (CH), 53.0 (CH_3), 30.4 (CH_2), 29.7 (CH_2), 28.3 (CH_3). **IR** (ATR): 3288, 2954, 2925, 1706, 16721454, 1438, 1163, 741 cm^{-1} . **MS** (ESI): m/z (relative intensity): 743 (100) $[M+Na]^+$, 721 (24) $[M+H]^+$. **HR-MS** (ESI): m/z calcd for $C_{39}H_{41}N_6O_8^+$ $[M+H]^+$: 721.2980, found: 721.2965.

Ethyl (6*S*,9*S*)-6-{{2-({*E*}-3-{{[*S*]-2-[(*tert*-butoxycarbonyl)amino]-3-methoxy-3-oxopropoxy}-3-oxoprop-1-en-1-yl)-1-(pyridin-2-yl)-1*H*-indol-3-yl]methyl}-9-((*S*)-*sec*-butyl)-2,2-dimethyl-4,7,10-trioxo-3-oxa-5,8,11-triazatridecan-13-oate (276h)

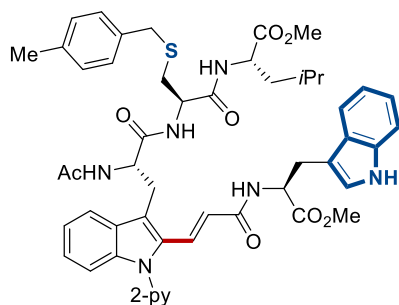


The general procedure **M** was followed using ethyl *N*²-(*tert*-butoxycarbonyl)-1-(pyridin-2-yl)-*L*-tryptophyl-*L*-isoleucylglycinate **243ae** (86.9 mg, 0.15 mmol), (*S*)-2-[(*tert*-butoxycarbonyl)amino]-3-methoxy-3-oxopropyl propiolate **211b** (61.0 mg, 0.23 mmol), MnBr(CO)₅ (4.1 mg, 10 mol %) and NaOAc (3.7 mg, 30 mol %) in 1,4-dioxane (1.2 mL). Purification by column chromatography on silica gel (*n*-hexane/EtOAc: 1/1) yielded **276h** (110.9 mg, 87%, *E/Z* = 98:2) as a white solid.

M. p. 146 – 148 °C. **¹H NMR** (400 MHz, CDCl₃): δ 8.70 (dd, *J* = 5.0, 1.9 Hz, 1H), 8.01 – 7.91 (m, 1H), 7.88 (d, *J* = 7.6 Hz, 1H), 7.73 (d, *J* = 16.4 Hz, 1H), 7.52 (d, *J* = 8.0 Hz, 1H), 7.42 (dd, *J* = 7.5, 4.9 Hz, 1H), 7.33 – 7.26 (m, 2H), 7.23 (ddd, *J* = 8.0, 6.3, 1.9 Hz, 1H), 6.72 (d, *J* = 5.7 Hz, 1H), 6.19 (d, *J* = 8.5 Hz, 1H), 6.04 (d, *J* = 8.0 Hz, 1H), 5.52 (d, *J* = 16.4 Hz, 1H), 5.44 (d, *J* = 7.7 Hz, 1H), 4.68 – 4.56 (m, 2H), 4.54 – 4.34 (m, 3H), 4.29 (t, *J* = 7.5 Hz, 1H), 4.15 (q, *J* = 7.1 Hz, 2H), 3.85 (s, 3H), 3.78 (dd, *J* = 18.0, 5.3 Hz, 1H), 3.55 (dd, *J* = 14.2, 4.8 Hz, 1H), 3.35 (dd, *J* = 14.2, 9.2 Hz, 1H), 1.80 – 1.65 (m, 1H), 1.50 – 1.39 (m, 18H), 1.32 – 1.23 (m, 4H), 1.12 – 0.95 (m, 1H), 0.92 – 0.76 (m, 6H). **¹³C NMR** (101 MHz, CDCl₃): δ 171.1 (C_q), 170.7 (C_q), 170.5 (C_q), 169.5 (C_q), 166.4 (C_q), 155.4 (C_q), 155.2 (C_q), 151.1 (C_q), 149.8 (CH), 139.3 (C_q), 138.6 (CH), 133.3 (CH), 131.6 (C_q), 128.0 (C_q), 125.8 (CH), 123.0 (CH), 122.6 (CH), 121.8 (CH), 120.2 (CH), 118.9 (C_q), 116.8 (CH), 111.0 (CH), 80.2 (C_q), 80.1 (C_q), 64.3 (CH₂), 61.4 (CH₂), 57.4 (CH), 55.3 (CH), 53.6 (CH), 53.0 (CH₃), 41.2 (CH₂), 37.9 (CH), 28.6 (CH₂), 28.3 (CH₃), 24.6 (CH₂), 15.0 (CH₃), 14.1 (CH₃), 11.4 (CH₃). (One CH₃ of the Boc group is missing due to overlap, the overlap was verified by HSQC, showing that the peaks at 28.3 ppm corresponds to two carbons). **IR** (ATR): 3314, 2969, 2931, 1708, 1651, 1521, 1366, 1247, 1161, 1022, 739 cm⁻¹. **MS** (ESI) *m/z* (relative intensity): 873 (100) [M+Na]⁺, 851 (8) [M+H]⁺. **HR-MS** (ESI): *m/z* calcd for C₄₃H₅₉N₆O₁₂⁺ [M+H]⁺: 851.1485, found: 851.4165.

5. Experimental Part

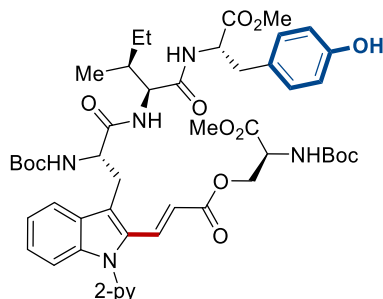
Methyl *N*-{[*S*]-3-[2-({*E*}-3-{{[*S*]-3-(1*H*-indol-3-yl)-1-methoxy-1-oxopropan-2-yl]amino}-3-oxoprop-1-en-1-yl)-1-(pyridin-2-yl)-1*H*-indol-3-yl]-2-acetamidopropionyl}-*S*-(4-methylbenzyl)-*L*-cysteinyl-*L*-leucinate (**276i**)



The general procedure **M** was followed using methyl *N*-[*N*^ε-acetyl-1-(pyridin-2-yl)-*L*-tryptophyl]-*S*-(4-methylbenzyl)-*L*-cysteinyl-*L*-leucinate **243h** (98.6 mg, 0.15 mmol), methyl propioloyl-*L*-tryptophanate **211c** (60.8 mg, 0.23 mmol), MnBr(CO)₅ (4.1 mg, 10 mol %) and NaOAc (3.7 mg, 30 mol %) in 1,4-dioxane (0.6 mL). Purification by column chromatography on silica gel (*n*-hexane/EtOAc: 1/4 → 1/9) yielded **276i** (109.9 mg, 79%) as a pale yellow solid.

M. p. 117 – 119 °C. ¹H NMR (300 MHz, CDCl₃): δ 8.68 (dd, *J* = 5.0, 1.8 Hz, 1H), 8.41 (brs, 1H), 7.89 (ddd, *J* = 7.7, 7.7, 2.0 Hz, 1H), 7.63 – 7.50 (m, 3H), 7.44 (d, *J* = 8.0 Hz, 1H), 7.42 – 7.31 (m, 3H), 7.27 – 7.06 (m, 10H), 6.78 (d, *J* = 16.2 Hz, 1H), 6.59 (d, *J* = 7.5 Hz, 1H), 6.55 – 6.46 (m, 2H), 4.98 (ddd, *J* = 6.4, 6.4, 6.4 Hz, 1H), 4.59 (ddd, *J* = 7.5, 7.5, 6.1 Hz, 1H), 4.31 – 3.97 (m, 2H), 3.78 – 3.70 (m, 2H), 3.69 (s, 3H), 3.64 (s, 3H), 3.55 – 3.43 (m, 1H), 3.42 – 3.27 (m, 3H), 2.85 (dd, *J* = 14.0, 4.6 Hz, 1H), 2.57 (dd, *J* = 14.0, 8.0 Hz, 1H), 2.36 (s, 3H), 1.99 (s, 3H), 1.55 – 1.41 (m, 2H), 1.39 – 1.30 (m, 1H), 0.90 (d, *J* = 5.6 Hz, 3H), 0.85 (d, *J* = 5.6 Hz, 3H). ¹³C NMR (101 MHz, CDCl₃): δ 172.8 (C_q), 172.8 (C_q), 170.7 (C_q), 170.3 (C_q), 169.3 (C_q), 165.8 (C_q), 150.8 (C_q), 149.9 (CH), 138.7 (CH), 137.8 (C_q), 137.1 (C_q), 136.3 (C_q), 135.3 (C_q), 132.6 (C_q), 129.5 (CH), 129.0 (CH), 129.0 (C_q), 128.9 (CH), 127.7 (C_q), 124.6 (CH), 123.6 (CH), 123.5 (CH), 122.8 (CH), 122.4 (CH), 122.1 (CH), 121.5 (CH), 119.5 (CH), 118.8 (CH), 118.7 (CH), 114.5 (C_q), 111.5 (CH), 111.3 (CH), 110.2 (C_q), 54.5 (CH), 53.2 (CH), 52.6 (CH), 52.4 (CH), 52.3 (CH₃), 51.5 (CH₃), 40.8 (CH₂), 36.6 (CH₂), 34.2 (CH₂), 29.3 (CH₂), 27.8 (CH₂), 24.9 (CH), 23.4 (CH₃), 22.7 (CH₃), 22.2 (CH₃), 21.3 (CH₃). IR (ATR): 3282, 2955, 1740, 1645, 1532, 1514, 1437, 1206, 735 cm⁻¹. MS (ESI) *m/z* (relative intensity): 950 (85) [M+Na]⁺, 928 (35) [M+H]⁺. HR-MS (ESI): *m/z* calcd for C₅₁H₅₈N₇O₈S⁺ [M+H]⁺: 928.4062, found: 928.4070.

Methyl (6*S*,9*S*,12*S*)-6-[[2-({*E*}-3-{{*S*}-2-[(*tert*-butoxycarbonyl)amino]-3-methoxy-3-oxopropoxy}-3-oxoprop-1-en-1-yl)-1-(pyridin-2-yl)-1*H*-indol-3-yl]methyl]-9-[(*S*)-*sec*-butyl]-12-(4-hydroxybenzyl)-2,2-dimethyl-4,7,10-trioxo-3-oxa-5,8,11-triazatridecan-13-oate (276j)

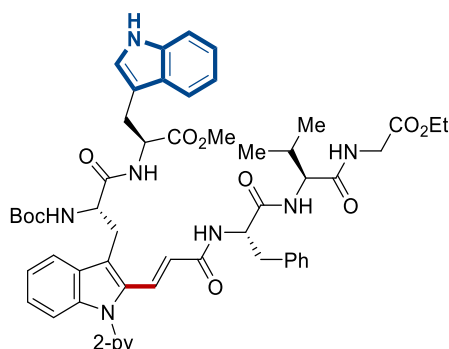


The general procedure **M** was followed using methyl *N*^a-(*tert*-butoxycarbonyl)-1-(pyridin-2-yl)-*L*-tryptophyl-*L*-isoleucyl-*L*-tyrosinate **243af** (100.8 mg, 0.15 mmol), (*S*)-2-[(*tert*-butoxycarbonyl)amino]-3-methoxy-3-oxopropyl propiolate **211b** (61.0 mg, 0.23 mmol), MnBr(CO)₅ (4.1 mg, 10 mol %) and NaOAc (3.7 mg, 30 mol %) in 1,4-dioxane (0.6 mL). Purification by column chromatography on silica gel (CH₂Cl₂/acetone: 7/3 → 6/4) yielded **276j** (96.7 mg, 68%) as a white solid.

M. p. 155 – 157 °C. ¹H NMR (400 MHz, DMSO-*d*₆): δ 9.22 (s, 1H), 8.79 – 8.65 (m, 1H), 8.50 (d, *J* = 6.7 Hz, 1H), 8.08 (ddd, *J* = 8.0, 8.0 1.9 Hz, 1H), 7.84 (d, *J* = 8.0 Hz, 1H), 7.72 (d, *J* = 16.2 Hz, 1H), 7.65 – 7.53 (m, 2H), 7.47 (d, *J* = 8.0 Hz, 1H), 7.36 (d, *J* = 7.5 Hz, 1H), 7.31 – 7.13 (m, 4H), 6.97 (d, *J* = 7.9 Hz, 2H), 6.72 – 6.62 (m, 2H), 5.55 (d, *J* = 16.2 Hz, 1H), 4.45 – 4.26 (m, 5H), 4.26 – 4.15 (m, 1H), 3.62 (s, 3H), 3.51 (s, 3H), 3.43 – 3.37 (m, 1H), 3.21 (dd, *J* = 14.4, 9.4 Hz, 1H), 2.84 (d, *J* = 7.4 Hz, 2H), 1.79 – 1.65 (m, 1H), 1.37 (s, 9H), 1.21 (s, 9H), 1.14 – 0.97 (m, 2H), 0.91 – 0.74 (m, 6H). ¹³C NMR (101 MHz, DMSO-*d*₆): δ 171.8 (C_q), 170.9 (C_q), 170.6 (C_q), 170.3 (C_q), 165.7 (C_q), 156.0 (C_q), 155.3 (C_q), 154.9 (C_q), 150.6 (C_q), 149.8 (CH), 139.4 (CH), 138.7 (C_q), 133.0 (CH), 131.1 (C_q), 129.9 (CH), 128.1 (C_q), 126.8 (C_q), 125.3 (CH), 123.5 (CH), 122.3 (CH), 121.0 (CH), 120.5 (CH), 120.2 (C_q), 117.0 (CH), 115.1 (CH), 110.7 (CH), 78.6 (C_q), 78.4 (C_q), 62.9 (CH₂), 56.1 (CH), 55.6 (CH), 54.2 (CH), 52.6 (CH), 52.1 (CH₃), 51.5 (CH₃), 37.6 (CH), 35.9 (CH₂), 28.1 (CH₃), 27.9 (CH₃), 27.6 (CH₂), 23.9 (CH₂), 15.0 (CH₃), 11.1 (CH₃). IR (ATR): 3310, 2965, 2930, 1744, 1712, 1650, 1516, 1367, 1248, 1165, 747 cm⁻¹. MS (ESI) *m/z* (relative intensity): 965 (95) [M+Na]⁺, 944 (35) [M+H]⁺, 772 (65). HR-MS (ESI): *m/z* calcd for C₄₉H₆₃N₆O₁₃⁺ [M+H]⁺: 943.4448, found: 943.4426.

5. Experimental Part

Ethyl (S)-4-({S}-2-{{E}-3-[3-({S}-3-{{(S)-3-(1*H*-indol-3-yl)-1-methoxy-1-oxopropan-2-yl]amino}-2-{{*tert*-butoxycarbonyl]amino}-3-oxopropyl)-1-(pyridin-2-yl)-1*H*-indol-2-yl]acrylamido}-3-phenylpropanamido)-5-methyl-3-oxohexanoate (**276k**)

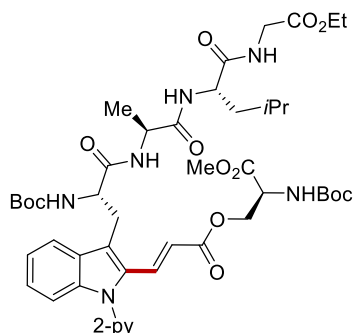


The general procedure **M** was followed using methyl *N*^a-(*tert*-butoxycarbonyl)-1-(pyridin-2-yl)-L-tryptophyl-L-tryptophanate **243ag** (87.2 mg, 0.15 mmol), ethyl propioloyl-L-phenylalanyl-L-valylglycinate **211e** (90.3 mg, 0.23 mmol), MnBr(CO)₅ (4.1 mg, 10 mol %) and NaOAc (3.7 mg, 30 mol %) in 1,4-dioxane (0.6 mL). Purification by column chromatography on silica gel (*n*-hexane/EtOAc: 1/3 → 0/1) yielded **276k** (129.7 mg, 88%) as a pale yellow solid.

M. p. 147 – 148 °C. ¹H NMR (400 MHz, CDCl₃): δ 8.61 (dd, *J* = 4.8, 1.8 Hz, 1H), 8.43 (s, 1H), 7.79 (dd, *J* = 7.9, 7.9 Hz, 1H), 7.54 – 7.38 (m, 3H), 7.36 – 7.30 (m, 2H), 7.30 – 7.25 (m, 2H), 7.24 – 7.20 (m, 4H), 7.18 – 7.05 (m, 5H), 6.98 (t, *J* = 7.5 Hz, 1H), 6.91 (d, *J* = 16.2 Hz, 1H), 6.82 (d, *J* = 8.6 Hz, 1H), 6.62 (d, *J* = 2.4 Hz, 1H), 6.39 (t, *J* = 5.5 Hz, 1H), 5.89 – 5.73 (m, 2H), 4.69 (ddd, *J* = 7.6, 7.6, 7.2 Hz, 1H), 4.46 (ddd, *J* = 6.6, 5.4, 5.4 Hz, 1H), 4.33 – 4.19 (m, 2H), 4.11 (q, *J* = 7.1 Hz, 2H), 3.89 (dd, *J* = 18.2, 5.4 Hz, 1H), 3.82 (dd, *J* = 18.2, 5.4 Hz, 1H), 3.43 – 3.24 (m, 3H), 3.23 – 3.13 (m, 4H), 3.12 – 2.93 (m, 2H), 2.17 (hept, *J* = 6.8 Hz, 1H), 1.51 (s, 9H), 1.21 (t, *J* = 7.1 Hz, 3H), 0.83 (d, *J* = 6.8 Hz, 3H), 0.78 (d, *J* = 6.8 Hz, 3H). ¹³C NMR (101 MHz, CDCl₃): δ 171.4 (C_q), 170.9 (C_q), 170.3 (C_q), 170.0 (C_q), 169.4 (C_q), 166.8 (C_q), 155.4 (C_q), 150.5 (C_q), 149.7 (CH), 138.6 (CH), 137.3 (C_q), 137.1 (C_q), 136.0 (C_q), 132.2 (C_q), 129.3 (CH), 129.1 (CH), 129.1 (CH), 128.7 (C_q), 128.6 (CH), 127.4 (C_q), 126.7 (CH), 124.4 (CH), 122.9 (CH), 122.5 (CH), 121.9 (CH), 121.7 (CH), 121.5 (CH), 119.3 (CH), 118.4 (CH), 114.7 (C_q), 111.2 (CH), 110.8 (CH), 109.3 (C_q), 80.3 (C_q), 61.4 (CH₂), 58.4 (CH), 55.4 (CH), 54.5 (CH), 53.4 (CH), 52.1 (CH₃), 41.2 (CH₂), 37.0 (CH₂), 30.7 (CH₂), 30.1 (CH), 28.5 (CH₃), 27.6 (CH₂), 19.1 (CH₃), 17.3 (CH₃), 14.0 (CH₃). (One aromatic CH is missing due to overlap, the overlap was verified by HSQC, showing that the peak at 122.8 ppm corresponds to two carbons). IR (ATR): 3287, 2967, 2929, 1738/, 1650, 1521, 1469,

1436, 1199, 1165, 741 cm^{-1} . **MS** (ESI) m/z (relative intensity): 1006 (100) $[\text{M}+\text{Na}]^+$, 983 (25) $[\text{M}+\text{H}]^+$. **HR-MS** (ESI): m/z calcd for $\text{C}_{54}\text{H}_{63}\text{N}_8\text{O}_{10}^+$ $[\text{M}+\text{H}]^+$: 983.4662, found: 983.4638.

Ethyl (6S,9S,12S)-6-{{2-({E}-3-{{[S]-2-[(*tert*-butoxycarbonyl)amino]-3-methoxy-3-oxopropoxy}-3-oxoprop-1-en-1-yl)-1-(pyridin-2-yl)-1*H*-indol-3-yl]methyl}-12-isobutyl-2,2,9-trimethyl-4,7,10,13-tetraoxo-3-oxa-5,8,11,14-tetraazahexadecan-16-oate (276I)



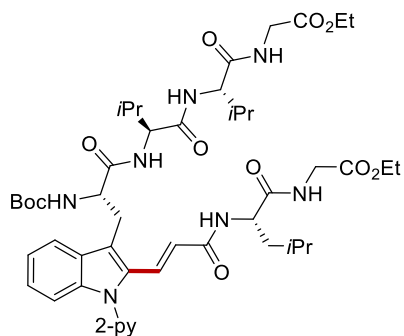
The general procedure **M** was followed using ethyl *N*²-(*tert*-butoxycarbonyl)-1-(pyridin-2-yl)-L-tryptophyl-L-alanyl-L-leucylglycinate **243ah** (97.6 mg, 0.15 mmol), (*S*)-2-[(*tert*-butoxycarbonyl)amino]-3-methoxy-3-oxopropyl propiolate **211b** (61.0 mg, 0.23 mmol), $\text{MnBr}(\text{CO})_5$ (4.1 mg, 10 mol %) and NaOAc (3.7 mg, 30 mol %) in 1,4-dioxane (1.2 mL). Purification by column chromatography on silica gel (*n*-hexane/EtOAc: 1/3) yielded **276I** (110.8 mg, 80%) as a white solid.

M. p. 137 – 141 °C. **¹H NMR** (400 MHz, CDCl_3): δ 8.66 (ddd, $J = 4.9, 1.9, 0.8$ Hz, 1H), 7.90 (ddd, $J = 7.7, 7.7, 1.9$ Hz, 1H), 7.79 – 7.66 (m, 2H), 7.38 (ddd, $J = 7.7, 4.9, 1.0$ Hz, 1H), 7.30 (dt, $J = 8.0, 1.0$ Hz, 1H), 7.28 – 7.25 (m, 1H), 7.25 – 7.21 (m, 1H), 7.17 (ddd, $J = 8.0, 6.6, 1.5$ Hz, 1H), 7.08 (brs, 1H), 6.94 (d, $J = 8.0$ Hz, 1H), 6.75 (d, $J = 6.3$ Hz, 1H), 5.81 (d, $J = 7.9$ Hz, 1H), 5.42 (d, $J = 16.2$ Hz, 1H), 5.15 (d, $J = 6.6$ Hz, 1H), 4.66 – 4.47 (m, 3H), 4.42 (m, 1H), 4.38 – 4.29 (m, 2H), 4.14 (q, $J = 7.2$ Hz, 2H), 4.07 – 3.88 (m, 2H), 3.74 (s, 3H), 3.50 – 3.32 (m, 2H), 1.84 – 1.67 (m, 1H), 1.64 – 1.45 (m, 2H), 1.42 (s, 9H), 1.32 (s, 9H), 1.26 (d, $J = 7.2$ Hz, 3H), 1.22 (t, $J = 7.2$ Hz, 3H), 0.87 (d, $J = 6.5$ Hz, 3H), 0.84 (d, $J = 6.5$ Hz, 3H). **¹³C NMR** (101 MHz, CDCl_3): δ 172.3 (C_q), 172.1 (C_q), 171.7 (C_q), 170.9 (C_q), 169.8 (C_q), 166.1 (C_q), 155.7 (C_q), 155.5 (C_q), 151.2 (C_q), 150.1 (CH), 139.6 (C_q), 139.0 (CH), 132.9 (CH), 131.8 (C_q), 128.3 (C_q), 126.1 (CH), 123.3 (CH), 122.3 (CH), 122.0 (CH), 120.1 (CH), 119.2 (C_q), 117.6 (CH), 111.1 (CH), 80.7 (C_q), 80.4 (C_q), 64.7 (CH_2), 61.4 (CH_2), 55.5 (CH), 53.2 (CH), 53.0 (CH), 51.9 (CH_3), 49.9 (CH), 41.4 (CH_2), 40.5 (CH_2), 28.4 (CH_3), 28.3 (CH_3), 27.7 (CH_2), 24.9

5. Experimental Part

(CH), 22.9 (CH₃), 22.0 (CH₃), 18.3 (CH₃), 14.3 (CH₃). **IR** (ATR): 3295, 2958, 2926, 1742, 1707, 1645, 1523, 1366, 1197, 1158, 1022, 734 cm⁻¹. **MS** (ESI) m/z (relative intensity): 944 (100) [M+Na]⁺, 922 (18) [M+H]⁺. **HR-MS** (ESI): m/z calcd for C₄₆H₆₄N₇O₁₃⁺ [M+H]⁺: 922.4557, found: 922.4544.

Ethyl **({S}-2-{{tert-butoxycarbonyl}amino}-3-{2-[(E)-3-({S}-1-[(2-methoxy-2-oxoethyl)amino]-4-methyl-1-oxopentan-2-yl)amino]-3-oxoprop-1-en-1-yl]-1-[pyridin-2-yl]-1H-indol-3-yl}propanoyl)-L-valyl-L-valylglycinate (276m)**

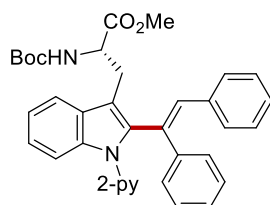


The general procedure **M** was followed using ethyl *N*^a-(*tert*-butoxycarbonyl)-1-(pyridin-2-yl)-L-tryptophyl-L-valyl-L-valylglycinate **243x** (99.7 mg, 0.15 mmol), methyl propionyl-L-leucylglycinate **211f** (57.2 mg, 0.23 mmol), MnBr(CO)₅ (4.1 mg, 10 mol %) and NaOAc (3.7 mg, 30 mol %) in 1,4-dioxane (0.6 mL). Purification by column chromatography on silica gel (EtOAc) yielded **276m** (91.0 mg, 66%, *E/Z* = 97:3) as a pale yellow solid.

M. p. 146 – 148 °C. **¹H NMR** (400 MHz, CDCl₃): δ 8.67 (dd, *J* = 4.9, 1.9 Hz, 1H), 7.89 (ddd, *J* = 7.7, 7.7, 2.0 Hz, 1H), 7.69 (d, *J* = 7.7 Hz, 1H), 7.58 (d, *J* = 16.1 Hz, 1H), 7.41 – 7.27 (m, 4H), 7.22 – 7.05 (m, 3H), 6.84 (brs, 1H), 6.74 (brs, 1H), 6.60 (brs, 1H), 6.48 (d, *J* = 16.1 Hz, 1H), 5.64 (d, *J* = 7.6 Hz, 1H), 4.55 (ddd, *J* = 8.5, 6.9, 5.3 Hz, 1H), 4.46 (dd, *J* = 7.6, 7.6 Hz, 1H), 4.24 – 4.13 (m, 3H), 4.13 – 4.00 (m, 1H), 4.01 – 3.86 (m, 4H), 3.69 (s, 3H), 3.39 (d, *J* = 6.9 Hz, 2H), 2.00 – 1.91 (m, 2H), 1.84 – 1.68 (m, 2H), 1.69 – 1.60 (m, 1H), 1.37 (s, 9H), 1.23 (t, *J* = 7.1 Hz, 3H), 0.99 – 0.70 (m, 18H). **¹³C NMR** (101 MHz, CDCl₃): δ 172.8 (C_q), 171.7 (C_q), 171.2 (C_q), 170.6 (C_q), 170.4 (C_q), 169.7 (C_q), 166.7 (C_q), 155.6 (C_q), 151.0 (C_q), 150.0 (CH), 138.8 (CH), 138.0 (C_q), 132.1 (C_q), 129.6 (CH), 129.1 (C_q), 125.0 (CH), 122.8 (CH), 122.3 (CH), 122.1 (CH), 121.6 (CH), 119.7 (CH), 116.1 (C_q), 111.1 (CH), 80.3 (C_q), 61.6 (CH₂), 58.9 (CH), 58.9 (CH), 55.1 (CH), 52.5 (CH₃), 52.1 (CH), 41.4 (CH₂), 41.3 (CH₂), 40.2 (CH₂), 31.5 (CH), 30.7 (CH), 29.4 (CH₂), 28.4 (CH₃), 24.9 (CH), 23.1 (CH₃), 22.1 (CH₃), 19.1 (CH₃), 19.0 (CH₃), 18.5 (CH₃), 18.1 (CH₃), 14.3 (CH₃). **IR** (ATR): 3292, 2960, 1748, 1642, 1523, 1438, 1201,

1166, 1020, 736 cm^{-1} . **MS** (ESI) m/z (relative intensity): 941 (85) $[\text{M}+\text{Na}]^+$, 920 (100) $[\text{M}+\text{H}]^+$. **HR-MS** (ESI): m/z calcd for $\text{C}_{47}\text{H}_{67}\text{N}_8\text{O}_{11}$ $[\text{M}+\text{H}]^+$: 919.4924, found: 919.4926.

Methyl (S,E)-2-[(tert-butoxycarbonyl)amino]-3-[2-(1,2-diphenylvinyl)-1-(pyridin-2-yl)-1H-indol-3-yl]propanoate (277a)

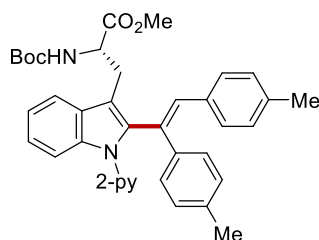


The general procedure **M** was followed using methyl *N*^B-(*tert*-butoxycarbonyl)-1-(pyridin-2-yl)-L-tryptophanate **153** (59.3 mg, 0.15 mmol), 1,2-diphenylethyne **82a** (40.1 mg, 0.23 mmol), $\text{MnBr}(\text{CO})_5$ (4.1 mg, 10 mol %) and NaOAc (3.7 mg, 30 mol %) in 1,4-dioxane (0.6 mL). Purification by column chromatography on silica gel (*n*-hexane/EtOAc: 10/1) yielded **277a** (79.1 mg, 92%) as a colorless oil.

¹H NMR (400 MHz, CDCl_3): δ 8.41 (dd, $J = 4.9, 1.9$ Hz, 1H), 7.69 (ddd, $J = 6.8, 3.4, 3.4$ Hz, 1H), 7.56 (ddd, $J = 7.8, 7.8, 2.0$ Hz, 1H), 7.41 (dd, $J = 6.2, 3.1$ Hz, 1H), 7.24 – 7.19 (m, 2H), 7.19 – 7.10 (m, 6H), 7.08 – 7.03 (m, 2H), 7.02 – 6.96 (m, 4H), 6.89 (s, 1H), 5.08 (d, $J = 8.3$ Hz, 1H), 4.62 (ddd, $J = 8.3, 7.7, 5.5$ Hz, 1H), 3.62 (s, 3H), 3.31 (dd, $J = 14.5, 5.5$ Hz, 1H), 3.24 (dd, $J = 14.5, 7.7$ Hz, 1H), 1.36 (s, 9H). **¹³C NMR** (101 MHz, CDCl_3): δ 173.0 (C_q), 155.2 (C_q), 151.4 (C_q), 149.0 (CH), 139.9 (C_q), 138.3 (C_q), 137.5 (CH), 137.0 (C_q), 136.5 (C_q), 133.3 (CH), 132.9 (C_q), 130.1 (CH), 129.4 (CH), 128.4 (C_q), 128.0 (CH), 127.8 (CH), 127.3 (CH), 127.2 (CH), 123.5 (CH), 121.4 (CH), 121.4 (CH), 121.0 (CH), 119.2 (CH), 112.9 (C_q), 110.8 (CH), 79.7 (C_q), 54.4 (CH), 52.2 (CH_3), 28.2 (CH_2), 27.6 (CH_3). **IR** (ATR): 3055, 2977, 2927, 1742, 1711, 1469, 1437, 1366, 1165, 907, 728 cm^{-1} . **MS** (ESI) m/z (relative intensity): 596 (35) $[\text{M}+\text{Na}]^+$, 574 (100) $[\text{M}+\text{H}]^+$. **HR-MS** (ESI): m/z calcd for $\text{C}_{36}\text{H}_{36}\text{N}_3\text{O}_4^+$ $[\text{M}+\text{H}]^+$: 574.2700, found: 574.2703.

5. Experimental Part

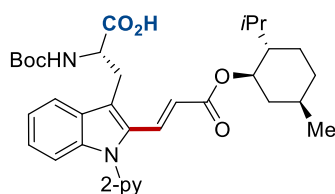
Methyl (*S,E*)-2-[(*tert*-butoxycarbonyl)amino]-3-[2-(1,2-di-*p*-tolylvinyl)-1-(pyridin-2-yl)-1*H*-indol-3-yl]propanoate (**277b**)



The general procedure **M** was followed using methyl *N*^a-(*tert*-butoxycarbonyl)-1-(pyridin-2-yl)-L-tryptophanate **153** (59.3 mg, 0.15 mmol), 1,2-di-*p*-tolylethyne **82b** (46.4 mg, 0.23 mmol), MnBr(CO)₅ (4.1 mg, 10 mol %) and NaOAc (3.7 mg, 30 mol %) in 1,4-dioxane (0.6 mL). Purification by column chromatography on silica gel (*n*-hexane/EtOAc: 10/1) yielded **277b** (76.7 mg, 85%, *E/Z* = 95:5) as a colorless oil. ()

¹H NMR (400 MHz, CDCl₃): δ 8.45 (dd, *J* = 4.6, 2.2 Hz, 1H), 7.70 (ddd, *J* = 5.7, 2.4, 2.4 Hz, 1H), 7.59 (ddd, *J* = 7.7, 7.7, 2.0 Hz, 1H), 7.51 – 7.40 (m, 1H), 7.26 – 7.17 (m, 3H), 7.11 – 7.02 (m, 3H), 7.01 – 6.95 (m, 2H), 6.93 (d, *J* = 8.2 Hz, 2H), 6.87 – 6.82 (m, 2H), 6.79 (s, 1H), 5.10 (d, *J* = 8.2 Hz, 1H), 4.61 (ddd, *J* = 8.2, 6.9, 6.9 Hz, 1H), 3.63 (s, 3H), 3.35 – 3.14 (m, 2H), 2.30 (s, 3H), 2.25 (s, 3H), 1.39 (s, 9H). **¹³C NMR** (101 MHz, CDCl₃): δ 173.0 (C_q), 155.2 (C_q), 151.6 (C_q), 148.8 (CH), 140.2 (C_q), 137.4 (CH), 137.0 (C_q), 137.0 (C_q), 135.4 (C_q), 133.7 (C_q), 133.2 (C_q), 133.1 (CH), 131.8 (C_q), 131.3 (CH), 129.9 (CH), 129.3 (CH), 128.7 (CH), 128.6 (C_q), 123.3 (CH), 121.4 (CH), 121.4 (CH), 120.9 (CH), 119.1 (CH), 112.6 (C_q), 110.9 (CH), 79.6 (C_q), 54.4 (CH), 52.2 (CH₃), 28.2 (CH₃), 27.5 (CH₂), 21.2 (CH₃), 21.2 (CH₃). **IR** (ATR): 2975, 2925, 1743, 1714, 1588, 1506, 1469, 1436, 1365, 1165, 738 cm⁻¹. **MS** (ESI) *m/z* (relative intensity): 624 (50) [M+Na]⁺, 602 (100) [M+H]⁺. **HR-MS** (ESI): *m/z* calcd for C₃₈H₄₀N₃O₄⁺ [M+H]⁺: 602.3013, found: 602.3012.

(*S*)-2-[(*tert*-Butoxycarbonyl)amino]-3-[2-({*E*}-3-[(1*R*,2*S*,5*R*)-2-isopropyl-5-methylcyclohexyl]oxy}-3-oxoprop-1-en-1-yl)-1-(pyridin-2-yl)-1*H*-indol-3-yl]propanoic acid (**279a**)

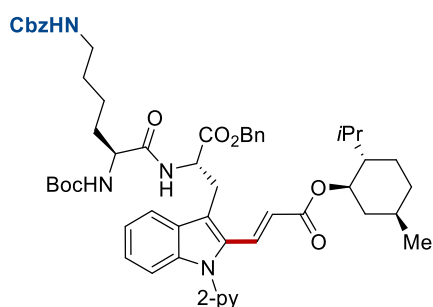


The general procedure **M** was followed using *N*^a-(*tert*-butoxycarbonyl)-1-(pyridin-2-yl)-L-tryptophan **243j** (57.2 mg, 0.15 mmol), (1*R*,2*S*,5*R*)-2-isopropyl-5-methylcyclohexyl

propiolate **211g** (46.8 mg, 0.23 mmol), MnBr(CO)₅ (8.2 mg, 20 mol %) and NaOAc (7.4 mg, 60 mol %) in 1,4-dioxane (1.0 mL). Purification by column chromatography on silica gel (*n*-hexane/EtOAc/HOAc: 1/1/0.01) yielded **279a** (63.4 mg, 72%, *E/Z* = 97:3) as a pale yellow solid.

M. p. 59 – 63 °C. **¹H NMR** (400 MHz, DMSO-*d*₆): δ 12.74 (brs, 1H), 8.69 (dd, *J* = 5.1, 1.8 Hz, 1H), 8.17 – 8.02 (m, 1H), 7.82 (d, *J* = 8.0 Hz, 1H), 7.67 (d, *J* = 16.2 Hz, 1H), 7.59 – 7.52 (m, 1H), 7.48 (d, *J* = 8.0 Hz, 1H), 7.29 – 7.14 (m, 4H), 5.64 (d, *J* = 16.2 Hz, 1H), 4.60 (ddd, *J* = 10.8, 10.8, 4.3 Hz, 1H), 4.22 (ddd, *J* = 8.7, 7.4, 5.7 Hz, 1H), 3.40 (dd, *J* = 14.4, 5.7 Hz, 1H), 3.31 (dd, *J* = 14.4, 8.7 Hz, 1H), 1.92 – 1.82 (m, 1H), 1.78 – 1.56 (m, 3H), 1.50 – 1.41 (m, 1H), 1.27 (s, 9H), 1.09 – 0.90 (m, 2H), 0.91 – 0.76 (m, 8H), 0.69 (d, *J* = 7.0 Hz, 3H). **¹³C NMR** (101 MHz, DMSO-*d*₆): δ 173.2 (C_q), 165.4 (C_q), 155.3 (C_q), 150.5 (C_q), 149.7 (CH), 139.4 (CH), 138.3 (C_q), 132.2 (CH), 131.1 (C_q), 128.1 (C_q), 125.1 (CH), 123.4 (CH), 122.2 (CH), 121.1 (CH), 120.3 (CH), 119.5 (C_q), 118.3 (CH), 110.6 (CH), 78.1 (C_q), 73.5 (CH), 54.3 (CH), 46.4 (CH), 40.5 (CH₂), 33.7 (CH₂), 30.8 (CH), 28.1 (CH₃), 26.8 (CH₂), 26.2 (CH), 23.4 (CH₂), 21.9 (CH₃), 20.3 (CH₃), 16.7 (CH₃). **IR** (ATR): 3441, 2925, 2868, 1699, 1624, 1468, 1437, 1254, 1151, 1008, 980, 744 cm⁻¹. **MS** (ESI) *m/z* (relative intensity): 612 (42) [M+Na]⁺, 590 (100) [M+H]⁺. **HR-MS** (ESI): *m/z* calcd for C₃₄H₄₄N₃O₆⁺ [M+H]⁺: 590.3225, found: 590.3224.

(1*R*,2*S*,5*R*)-2-Isopropyl-5-methylcyclohexyl (E)-3-{3-[(*S*)-3-(benzyloxy)-2-({*S*}-6-[(benzyloxy)carbonyl]amino)-2-[[*tert*-butoxycarbonyl]amino]hexanamido)-3-oxopropyl]-1-[pyridin-2-yl]-1*H*-indol-2-yl}acrylate (279b**)**

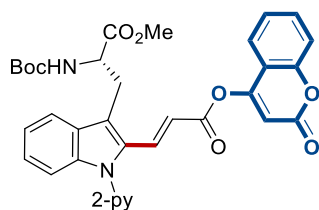


The general procedure **M** was followed using benzyl *N*^a-{*N*⁶-[(benzyloxy)carbonyl]-*N*²-[[*tert*-butoxycarbonyl]-L-lysyl]-1-(pyridin-2-yl)-L-tryptophanate **243k** (110.1 mg, 0.15 mmol), (1*R*,2*S*,5*R*)-2-isopropyl-5-methylcyclohexyl propiolate **211g** (46.9 mg, 0.23 mmol), MnBr(CO)₅ (4.1 mg, 10 mol %) and NaOAc (3.7 mg, 30 mol %) in 1,4-dioxane (0.6 mL). Purification by column chromatography on silica gel (*n*-hexane/EtOAc: 1/1 → 1/2) yielded **279b** (120.6 mg, 85%) as pale yellow solid.

5. Experimental Part

M. p. 98 – 101 °C. **¹H NMR** (400 MHz, CDCl₃): δ 8.65 (dd, *J* = 5.1, 1.9 Hz, 1H), 7.83 (ddd, *J* = 7.7, 7.7, 2.0 Hz, 1H), 7.72 – 7.60 (m, 2H), 7.38 – 7.29 (m, 6H), 7.27 – 7.24 (m, 4H), 7.21 (dd, *J* = 8.2, 1.3 Hz, 1H), 7.19 – 7.10 (m, 4H), 6.70 (d, *J* = 7.8 Hz, 1H), 5.60 (d, *J* = 16.2 Hz, 1H), 5.20 – 5.02 (m, 4H), 5.01 – 4.86 (m, 3H), 4.69 (td, *J* = 10.8, 4.3 Hz, 1H), 4.12 – 3.94 (m, 1H), 3.48 (d, *J* = 6.7 Hz, 2H), 3.09 (dt, *J* = 6.6, 6.6 Hz, 2H), 1.99 – 1.91 (m, 1H), 1.85 – 1.71 (m, 2H), 1.68 – 1.57 (m, 2H), 1.51 – 1.39 (m, 4H), 1.38 (s, 9H), 1.36 – 1.29 (m, 2H), 1.28 – 1.18 (m, 2H), 1.10 – 0.92 (m, 2H), 0.86 (d, *J* = 6.6 Hz, 3H), 0.83 (d, *J* = 7.0 Hz, 3H), 0.71 (d, *J* = 7.0 Hz, 3H). **¹³C NMR** (101 MHz, CDCl₃): δ 171.6 (C_q), 171.2 (C_q), 166.4 (C_q), 156.4 (C_q), 155.6 (C_q), 151.2 (C_q), 149.7 (CH), 139.0 (C_q), 138.5 (CH), 136.6 (C_q), 134.9 (C_q), 131.9 (C_q), 131.7 (CH), 128.4 (CH), 128.4 (CH), 128.4 (C_q), 128.2 (CH), 128.2 (CH), 128.0 (CH), 128.0 (CH), 125.4 (CH), 122.7 (CH), 122.1 (CH), 121.6 (CH), 119.7 (CH), 117.8 (C_q), 111.1 (CH), 79.9 (C_q), 74.4 (CH), 67.4 (CH₂), 66.5 (CH₂), 54.1 (CH), 52.7 (CH), 46.9 (CH), 40.9 (CH₂), 40.4 (CH₂), 34.2 (CH₂), 31.8 (CH₂), 31.3 (CH), 29.2 (CH₂), 28.2 (CH₃), 27.9 (CH₂), 26.4 (CH), 23.7 (CH₂), 22.3 (CH₂), 22.0 (CH₃), 20.6 (CH₃), 16.6 (CH₃). (One aromatic CH is missing due to overlap, the overlap was verified by HSQC, showing that the peak at 119.7 ppm corresponds to two carbons). **IR** (ATR): 3313, 2950, 2927, 1707, 1522, 1453, 1247, 1169, 736 cm⁻¹. **MS** (ESI) *m/z* (relative intensity): 965 (45) [M+Na]⁺, 943 (100) [M+H]⁺. **HR-MS** (ESI): *m/z* calcd for C₅₅H₆₈N₅O₉⁺ [M+H]⁺: 942.5012, found: 942.5008.

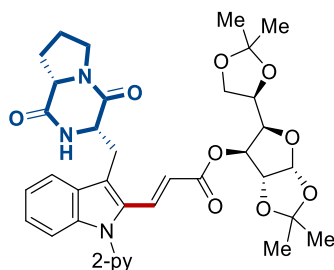
4-Oxo-4*H*-chromen-2-yl (*S,E*)-3-(3-(2-[(*tert*-butoxycarbonyl)amino]-3-methoxy-3-oxopropyl)-1-(pyridin-2-yl)-1*H*-indol-2-yl)acrylate (**279c**)



The general procedure **M** was followed using methyl *N*^B-(*tert*-butoxycarbonyl)-1-(pyridin-2-yl)-L-tryptophanate **153** (59.3 mg, 0.15 mmol), 2-oxo-2*H*-chromen-4-yl propiolate **211h** (48.1 mg, 0.23 mmol), MnBr(CO)₅ (4.1 mg, 10 mol %) and NaOAc (3.7 mg, 30 mol %) in 1,4-dioxane (0.6 mL). Purification by column chromatography on silica gel (*n*-hexane/EtOAc: 6/4) yielded **279c** (86.8 mg, 95%, *E/Z* = 96:4) as a pale yellow solid.

M. p. 109 – 112 °C. **¹H NMR** (400 MHz, CDCl₃): δ 8.75 (dd, *J* = 5.0, 1.8 Hz, 1H), 8.02 – 7.90 (m, 2H), 7.74 – 7.68 (m, 2H), 7.49 (d, *J* = 8.5 Hz, 1H), 7.46 (ddd, *J* = 7.5, 4.9, 1.1 Hz, 1H), 7.40 (d, *J* = 7.9 Hz, 1H), 7.37 – 7.29 (m, 2H), 7.23 (ddd, *J* = 8.1, 6.6, 1.5 Hz, 1H), 7.16 (d, *J* = 2.2 Hz, 1H), 7.10 (dd, *J* = 8.4, 2.2 Hz, 1H), 6.40 (d, *J* = 9.6 Hz, 1H), 5.73 (d, *J* = 16.1 Hz, 1H), 5.22 (d, *J* = 8.4 Hz, 1H), 4.77 (q, *J* = 6.6 Hz, 1H), 3.69 (s, 3H), 3.64 – 3.48 (m, 2H), 1.41 (s, 9H). **¹³C NMR** (101 MHz, CDCl₃): δ 172.1 (C_q), 164.5 (C_q), 160.4 (C_q), 155.0 (C_q), 154.9 (C_q), 154.6 (C_q), 153.4 (C_q), 151.2 (C_q), 150.1 (CH), 142.9 (CH), 139.7 (C_q), 138.9 (CH), 134.5 (CH), 131.5 (C_q), 128.5 (C_q), 128.5 (CH), 126.2 (CH), 123.2 (CH), 122.3 (CH), 121.8 (CH), 120.3 (CH), 118.4 (CH), 116.5 (C_q), 116.2 (CH), 115.9 (CH), 111.0 (CH), 110.4 (CH), 80.0 (C_q), 54.1 (CH), 52.6 (CH₃), 28.4 (CH₂), 28.3 (CH₃). **IR** (ATR): 3280, 2968, 2927, 1739, 1650, 1615, 1521, 1470, 1437, 1164, 740 cm⁻¹. **MS** (ESI) *m/z* (relative intensity): 632 (100) [M+Na]⁺, 610 (12) [M+H]⁺. **HR-MS** (ESI): *m/z* calcd for C₃₄H₃₂N₃O₈⁺ [M+H]⁺: 610.2184, found: 610.2175.

(3*aR*,5*R*,6*S*,6*aR*)-5-[(*R*)-2,2-Dimethyl-1,3-dioxolan-4-yl]-2,2-dimethyltetrahydrofuro[2,3-*d*][1,3]dioxol-6-yl (E)-3-(3-[(3*S*,8*aS*)-1,4-dioxooctahydropyrrolo[1,2-*a*]pyrazin-3-yl]methyl)-1-(pyridin-2-yl)-1*H*-indol-2-yl)acrylate (279e**)**



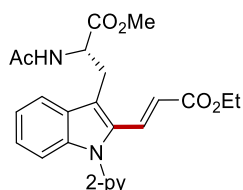
The general procedure **M** was followed using (3*S*,8*aS*)-3-[[1-(pyridin-2-yl)-1*H*-indol-3-yl]methyl]hexahydropyrrolo[1,2-*a*]pyrazine-1,4-dione **243c** (54.0 mg, 0.15 mmol), (3*aR*,5*R*,6*S*,6*aR*)-5-[(*R*)-2,2-dimethyl-1,3-dioxolan-4-yl]-2,2-dimethyltetrahydrofuro[2,3-*d*][1,3]dioxol-6-yl propiolate **211j** (70.2 mg, 0.23 mmol), MnBr(CO)₅ (4.1 mg, 10 mol %) and NaOAc (3.7 mg, 30 mol %) in 1,4-dioxane (0.6 mL). Purification by column chromatography on silica gel (*n*-hexane/EtOAc: 2/1 → 1/1) yielded **279e** (75.4 mg, 75%, *E/Z* = 97:3) as a white solid.

M. p. 121 – 124 °C. **¹H NMR** (600 MHz, CDCl₃): δ 8.69 (ddd, *J* = 4.8, 1.9, 0.8 Hz, 1H), 7.94 (ddd, *J* = 7.7, 7.7, 2.0 Hz, 1H), 7.76 (d, *J* = 16.2 Hz, 1H), 7.64 (ddd, *J* = 8.0, 1.0, 1.0 Hz, 1H), 7.42 (ddd, *J* = 7.5, 4.9, 1.0 Hz, 1H), 7.38 (ddd, *J* = 7.9, 0.9, 0.9 Hz, 1H), 7.34 (dt, *J* = 8.4, 1.0 Hz, 1H), 7.29 (ddd, *J* = 8.4, 6.9, 1.1 Hz, 1H), 7.21 (ddd, *J* = 7.9,

5. Experimental Part

6.9, 1.1 Hz, 1H), 5.83 (d, $J = 3.7$ Hz, 1H), 5.62 (d, $J = 16.2$ Hz, 1H), 5.51 (s, 1H), 5.24 (dd, $J = 3.0, 0.6$ Hz, 1H), 4.50 (d, $J = 3.7$ Hz, 1H), 4.48 – 4.42 (m, 1H), 4.23 (dd, $J = 7.3, 3.0$ Hz, 1H), 4.15 – 4.02 (m, 2H), 3.98 – 3.90 (m, 3H), 3.69 (dt, $J = 12.5, 8.2$ Hz, 1H), 3.59 (ddd, $J = 11.9, 8.9, 3.0$ Hz, 1H), 3.26 (dd, $J = 15.2, 11.4$ Hz, 1H), 2.38 – 2.28 (m, 1H), 2.13 – 1.98 (m, 2H), 1.96 – 1.83 (m, 1H), 1.49 (s, 3H), 1.38 (s, 3H), 1.28 (s, 3H), 1.27 (s, 3H). ^{13}C NMR (151 MHz, CDCl_3): δ 169.6 (C_q), 165.2 (C_q), 165.1 (C_q), 150.9 (C_q), 150.2 (CH), 139.4 (C_q), 139.0 (CH), 133.0 (CH), 132.0 (C_q), 127.7 (C_q), 126.4 (CH), 123.4 (CH), 122.3 (CH), 122.2 (CH), 119.6 (CH), 118.6 (CH), 117.8 (C_q), 112.4 (C_q), 111.5 (CH), 109.3 (C_q), 105.1 (CH), 83.3 (CH), 79.8 (CH), 76.5 (CH), 72.6 (CH), 66.9 (CH_2), 59.4 (CH), 55.0 (CH), 45.7 (CH_2), 28.5 (CH_2), 26.9 (CH_3), 26.8 (CH_3), 26.3 (CH_3), 26.3 (CH_2), 25.4 (CH_3), 22.8 (CH_2). IR (ATR): 2987, 2889, 1662, 1587, 1469, 1436, 1211, 1158, 1158, 1068, 1016, 726 cm^{-1} . MS (ESI) m/z (relative intensity): 695 (67) $[\text{M}+\text{Na}]^+$, 673 (100) $[\text{M}+\text{H}]^+$. HR-MS (ESI): m/z calcd for $\text{C}_{36}\text{H}_{41}\text{N}_4\text{O}_9^+$ $[\text{M}+\text{H}]^+$: 673.2868, found: 673.2864.

Ethyl (*S,E*)-3-[3-(2-acetamido-3-methoxy-3-oxopropyl)-1-(pyridin-2-yl)-1*H*-indol-2-yl]acrylate (**274c**).

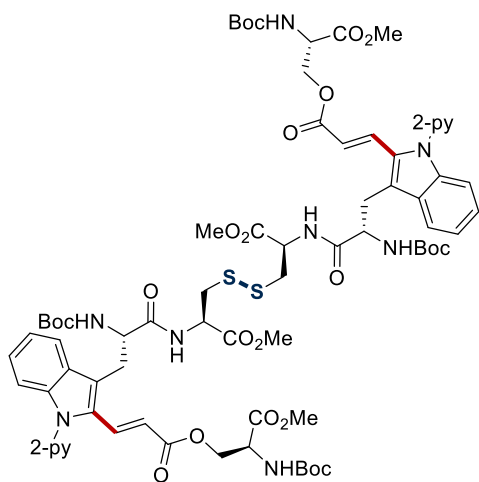


The general procedure **M** was followed using methyl *N*^a-acetyl-1-(pyridin-2-yl)-L-tryptophanate **241a** (1.688 g, 5.0 mmol), ethyl propiolate **211a** (736 mg, 7.50 mmol), $\text{MnBr}(\text{CO})_5$ (137.4 mg, 10 mol %) and NaOAc (123.5 mg, 30 mol %) in 1,4-dioxane (20.0 mL). Purification by column chromatography on silica gel (*n*-hexane/EtOAc: 1/2) yielded **274c** (2.13 g, 98%) as a white foam.

M. p. 61 – 63 °C. ^1H NMR (400 MHz, CDCl_3): δ 8.73 (dd, $J = 4.6, 2.0$ Hz, 1H), 7.93 (ddd, $J = 7.7, 7.7, 2.0$ Hz, 1H), 7.70 (d, $J = 16.2$ Hz, 1H), 7.65 (d, $J = 8.2$ Hz, 1H), 7.47 – 7.38 (m, 1H), 7.38 – 7.25 (m, 3H), 7.25 – 7.16 (m, 1H), 6.04 (d, $J = 7.8$ Hz, 1H), 5.52 (d, $J = 16.2$ Hz, 1H), 5.04 (ddd, $J = 7.8, 5.5, 5.5$ Hz, 1H), 4.20 (q, $J = 7.1$ Hz, 2H), 3.68 (s, 3H), 3.58 (d, $J = 5.5$, Hz, 2H), 1.96 (s, 3H), 1.30 (t, $J = 7.1$ Hz, 3H). ^{13}C NMR (101 MHz, CDCl_3): δ 172.0 (C_q), 169.8 (C_q), 166.8 (C_q), 151.5 (C_q), 150.1 (CH), 139.6 (C_q), 138.8 (CH), 132.2 (C_q), 131.7 (CH), 128.7 (C_q), 125.7 (CH), 123.2 (CH), 122.4 (CH), 121.7 (CH), 119.9 (CH), 119.2 (CH), 118.4 (C_q), 111.2 (CH), 60.7 (CH_2), 52.8 (CH),

52.7 (CH₃), 27.5 (CH₂), 23.3 (CH₃), 14.5 (CH₃). **IR** (ATR): 3285, 2980, 2929, 1742, 1703, 1623, 1468, 1435, 1171, 743 cm⁻¹. **MS** (ESI) m/z (relative intensity): 458 (100) [M+Na]⁺, 436 (45) [M+H]⁺. **HR-MS** (ESI): m/z calcd for C₂₄H₂₆N₃O₅⁺ [M+H]⁺: 436.1867, found: 436.1872.

Methyl (6*S*,9*R*,14*R*)-14-[[*S*]-2-[(*tert*-butoxycarbonyl)amino]-3-[2-({*E*}-3-[[*S*]-2-[(*tert*-butoxycarbonyl)amino]-3-methoxy-3-oxopropoxy}-3-oxoprop-1-en-1-yl)-1-(pyridin-2-yl)-1*H*-indol-3-yl]propanamido]-6-[[2-({*E*}-3-[[*S*]-2-[(*tert*-butoxycarbonyl)amino]-3-methoxy-3-oxopropoxy}-3-oxoprop-1-en-1-yl)-1-(pyridin-2-yl)-1*H*-indol-3-yl]methyl]-9-(methoxycarbonyl)-2,2-dimethyl-4,7-dioxo-3-oxa-11,12-dithia-5,8-diazapentadecan-15-oate (S4**)**



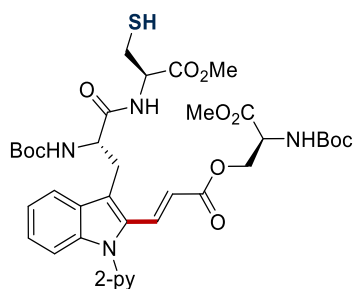
The general procedure **M** was followed using methyl (6*S*,9*R*,14*R*)-14-[[*S*]-2-[(*tert*-butoxycarbonyl)amino]-3-[1-(pyridin-2-yl)-1*H*-indol-3-yl]propanamido]-9-{methoxycarbonyl}-2,2-dimethyl-4,7-dioxo-6-[[1-(pyridin-2-yl)-1*H*-indol-3-yl]methyl]-3-oxa-11,12-dithia-5,8-diazapentadecan-15-oate **261** (149.1 mg, 0.15 mmol), (*S*)-2-[(*tert*-butoxycarbonyl)amino]-3-methoxy-3-oxopropyl propiolate **211b** (122.1 mg, 0.45 mmol), MnBr(CO)₅ (8.2 mg, 20 mol %) and NaOAc (7.4 mg, 30 mol %) in 1,4-dioxane (1.2 mL). Purification by column chromatography on silica gel (CH₂Cl₂/MeOH: 50/1) yielded **S4** (209.9 mg, 91%) as pale brown solid.

M. p. 108 – 110 °C. **¹H NMR** (400 MHz, CDCl₃): δ 8.67 (dd, *J* = 5.2, 1.8 Hz, 2H), 7.89 (ddd, *J* = 7.7, 7.7, 1.9 Hz, 2H), 7.83 – 7.67 (m, 4H), 7.38 (dd, *J* = 7.7, 4.9 Hz, 2H), 7.35 – 7.29 (m, 2H), 7.26 – 7.21 (m, 4H), 7.15 (t, *J* = 7.4 Hz, 2H), 6.89 (d, *J* = 7.3 Hz, 2H), 5.80 (d, *J* = 7.5 Hz, 2H), 5.57 (d, *J* = 8.7 Hz, 2H), 5.49 (d, *J* = 16.3 Hz, 2H), 4.83 – 4.67 (m, 2H), 4.66 – 4.46 (m, 6H), 4.35 (dd, *J* = 11.2, 3.4 Hz, 2H), 3.76 (s, 6H), 3.62 (s, 6H), 3.54 – 3.31 (m, 4H), 3.07 (dd, *J* = 13.8, 4.9 Hz, 2H), 2.98 (dd, *J* = 13.8, 5.0 Hz, 2H),

5. Experimental Part

1.46 (s, 18H), 1.36 (s, 18H). ^{13}C NMR (101 MHz, CDCl_3): δ 171.1 (C_q), 170.4 (C_q), 170.0 (C_q), 166.0 (C_q), 155.4 (C_q), 155.2 (C_q), 151.2 (C_q), 149.8 (CH), 139.4 (C_q), 138.6 (CH), 133.1 (CH), 131.6 (C_q), 128.3 (C_q), 125.7 (CH), 122.9 (CH), 122.1 (CH), 121.6 (CH), 120.2 (CH), 119.7 (C_q), 117.2 (CH), 110.9 (CH), 80.1 (C_q), 80.0 (C_q), 64.5 (CH_2), 54.9 (CH), 53.0 (CH), 52.7 (CH_3), 52.7 (CH_3), 51.9 (CH), 40.5 (CH_2), 28.3 (CH_3), 28.2 (CH_3). (One CH_2 is missing due to overlap, the overlap was verified by HSQC analysis, showing that the peaks at 28.2 ppm corresponds to two carbons). IR (ATR): 2977, 1706, 1624, 1588, 1470, 1366, 1438, 1366, 1158, 1058, 730, 647 cm^{-1} . MS (ESI) m/z (relative intensity): 1556 (100) $[\text{M}+\text{Na}]^+$, 1538 (80) $[\text{M}+\text{H}]^+$. HR-MS (ESI): m/z calcd for $\text{C}_{74}\text{H}_{93}\text{N}_{10}\text{O}_{22}\text{S}_2^+$ $[\text{M}+\text{H}]^+$: 1537.5902, found: 1537.5916.

(S)-2-[(*tert*-Butoxycarbonyl)amino]-3-methoxy-3-oxopropyl (*E*)-3-[3-({S}-2-[(*tert*-butoxycarbonyl)amino]-3-[(*R*)-3-mercapto-1-methoxy-1-oxopropan-2-yl]amino)-3-oxopropyl)-1-(pyridin-2-yl)-1*H*-indol-2-yl]acrylate (**280**)

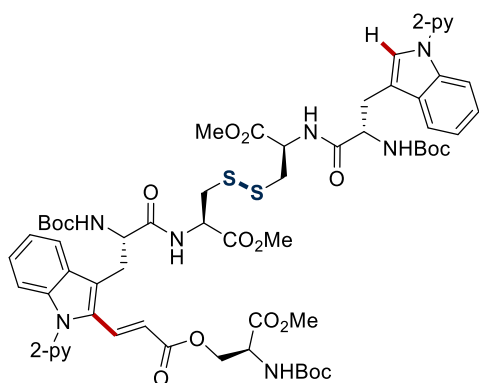


Following a modified literature procedure, the corresponding disulfide **S4** (60.1 mg, 39.0 μmol mmol), PPh_3 (10.4 mg, 39.0 μmol), NaOAc (1.3 mg, 15.6 μmol) and HOAc (4.0 μL , 70.2 μmol) were dissolved in $\text{MeOH}/\text{H}_2\text{O}$ (7 mL, 10/1). The mixture was heated at 60 $^\circ\text{C}$ for 16 h under N_2 . After cooling to ambient temperature, H_2O (10 mL) was added and the mixture was extracted with CH_2Cl_2 (3 x 15 mL). The combined organic layers were dried over Na_2SO_4 and concentrated *in vacuo*. Purification by column chromatography on silica gel (*n*-hexane/ EtOAc : 8/2 \rightarrow 7/3) yielded **280** (40.4 mg, 67%, *E/Z* = 95:5) as colorless oil.

^1H NMR (400 MHz, CDCl_3): δ 8.74 – 8.62 (m, 1H), 7.92 (ddd, J = 7.7, 7.7, 1.9 Hz, 1H), 7.89 – 7.66 (m, 2H), 7.46 – 7.36 (m, 2H), 7.33 – 7.24 (m, 2H), 7.21 (ddd, J = 8.0, 6.5, 1.6 Hz, 1H), 6.53 (s, 1H), 5.89 (d, J = 8.6 Hz, 1H), 5.46 (d, J = 15.8 Hz, 1H), 5.40 – 5.29 (m, 1H), 4.71 – 4.59 (m, 2H), 4.57 – 4.48 (m, 2H), 4.33 (dd, J = 11.1, 3.2 Hz, 1H), 3.77 (s, 3H), 3.62 (s, 3H), 3.61 – 3.52 (m, 1H), 3.39 (dd, J = 13.9, 8.3 Hz, 1H), 3.03 – 2.89 (m, 1H), 2.89 – 2.78 (m, 1H), 1.45 (s, 9H), 1.42 (s, 9H), 1.28 (t, J = 8.3 Hz, 1H).

^{13}C NMR (101 MHz, CDCl_3): δ 170.9 (C_q), 170.6 (C_q), 169.8 (C_q), 166.0 (C_q), 155.5 (C_q), 155.2 (C_q), 151.2 (C_q), 150.1 (CH), 139.6 (C_q), 138.8 (CH), 133.0 (CH), 131.7 (C_q), 128.21 (C_q), 126.0 (CH), 123.2 (CH), 122.3 (CH), 121.9 (CH), 120.1 (CH), 119.3 (C_q), 117.4 (CH), 111.1 (CH), 80.4 (C_q), 80.3 (C_q), 64.7 (CH_2), 55.2 (CH), 54.2 (CH), 53.2 (CH), 52.9 (CH_3), 52.8 (CH_3), 28.5 (CH_3), 28.4 (CH_3), 26.8 (CH_2). (One CH_2 is missing due to overlap, the overlap was verified by HSQC analysis, showing that the peaks at 28.4 ppm corresponds to two carbons). **IR** (ATR): 2978, 1705, 1625, 1588, 1470, 1366, 1213, 1157, 1057, 782, 647 cm^{-1} . **MS** (ESI) m/z (relative intensity): 792 (100) $[\text{M}+\text{Na}]^+$. **HR-MS** (ESI): m/z calcd for $\text{C}_{37}\text{H}_{47}\text{N}_5\text{O}_{11}\text{SNa}^+$ $[\text{M}+\text{Na}]^+$: 792.2885, found: 792.2885.

Methyl (6*S*,9*R*,14*R*)-14-{[*S*]-2-[(*tert*-butoxycarbonyl)amino]-3-[1-(pyridin-2-yl)-1*H*-indol-3-yl]propanamido}-6-{{2-({*E*}-3-[[*S*]-2-[(*tert*-butoxycarbonyl)amino]-3-methoxy-3-oxopropoxy}-3-oxoprop-1-en-1-yl)-1-(pyridin-2-yl)-1*H*-indol-3-yl]methyl}-9-(methoxycarbonyl)-2,2-dimethyl-4,7-dioxo-3-oxa-11,12-dithia-5,8-diazapentadecan-15-oate (S5)



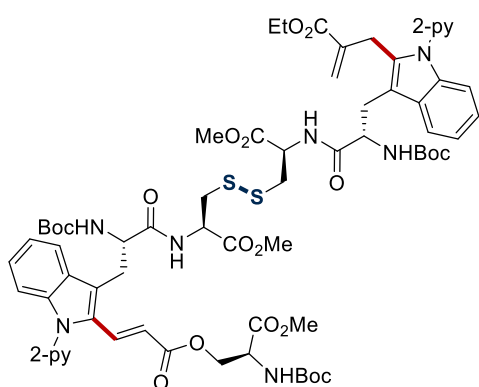
The general procedure **A** was followed using methyl (6*S*,9*R*,14*R*)-14-{[*S*]-2-[(*tert*-butoxycarbonyl)amino]-3-[1-(pyridin-2-yl)-1*H*-indol-3-yl]propanamido}-9-{methoxycarbonyl}-2,2-dimethyl-4,7-dioxo-6-[[1-(pyridin-2-yl)-1*H*-indol-3-yl]methyl]-3-oxa-11,12-dithia-5,8-diazapentadecan-15-oate **260** (398.1 mg, 0.40 mmol), (*S*)-2-[(*tert*-butoxycarbonyl)amino]-3-methoxy-3-oxopropyl propiolate **211b** (54.2 mg, 0.20 mmol), $\text{MnBr}(\text{CO})_5$ (5.4 mg, 10 mol %) and NaOAc (4.9 mg, 30 mol %) in 1,4-dioxane (1.0 mL). Purification by column chromatography on silica gel ($\text{CH}_2\text{Cl}_2/\text{MeOH}$: 60/1 \rightarrow 30/1) yielded **S5** (172.2 mg, 68%) as a white solid.

M. p. 109 – 112 $^\circ\text{C}$. **^1H NMR** (400 MHz, CDCl_3): δ 8.68 (dd, $J = 4.9, 1.9$ Hz, 1H), 8.51 (dd, $J = 4.9, 1.9$ Hz, 1H), 8.23 (d, $J = 8.3$ Hz, 1H), 7.88 (ddd, $J = 7.7, 7.7, 2.0$ Hz, 1H), 7.84 – 7.72 (m, 3H), 7.70 – 7.58 (m, 2H), 7.47 – 7.35 (m, 2H), 7.34 – 7.28 (m, 3H), 7.27 – 7.02 (m, 5H), 6.96 (d, $J = 7.3$ Hz, 1H), 5.77 (d, $J = 8.5$ Hz, 1H), 5.65 (s, 1H),

5. Experimental Part

5.59 – 5.40 (m, 2H), 4.86 – 4.46 (m, 6H), 4.36 (dd, $J = 11.2, 3.4$ Hz, 1H), 3.76 (s, 3H), 3.68 – 3.59 (m, 6H), 3.56 – 3.39 (m, 2H), 3.38 – 3.18 (m, 2H), 3.09 (dd, $J = 14.1, 5.4$ Hz, 1H), 3.04 – 2.89 (m, 3H), 1.47 (s, 9H), 1.41 (s, 9H), 1.35 (s, 9H). ^{13}C NMR (101 MHz, CDCl_3): δ 171.8 (C_q), 171.2 (C_q), 170.4 (C_q), 170.2 (C_q), 170.1 (C_q), 166.1 (C_q), 155.6 (C_q), 155.4 (C_q), 155.3 (C_q), 152.4 (C_q), 151.2 (C_q), 149.8 (CH), 148.8 (CH), 139.4 (C_q), 138.6 (CH), 138.3 (CH), 135.3 (C_q), 133.2 (CH), 131.6 (C_q), 130.1 (C_q), 128.3 (C_q), 125.7 (CH), 124.9 (CH), 123.4 (CH), 122.9 (CH), 122.1 (CH), 121.6 (CH), 121.2 (CH), 120.2 (CH), 119.7 (CH), 119.6 (C_q), 119.1 (CH), 117.2 (CH), 114.2 (CH), 113.7 (C_q), 113.4 (CH), 110.9 (CH), 80.1 (C_q), 80.1 (C_q), 80.0 (C_q), 64.4 (CH_2), 54.9 (CH), 54.8 (CH), 53.1 (CH), 52.7 (CH_3), 52.7 (CH_3), 51.9 (CH), 51.9 (CH), 40.5 (CH_2), 40.2 (CH_2), 28.3 (CH_3), 28.3 (CH_3), 28.2 (CH_3), 28.1 (CH_2), 28.1 (CH_2). (One CH_3 is missing due to overlap, the overlap was verified by HSQC analysis, showing that the peaks at 52.7 ppm correspond to two carbons). IR (ATR): 3338, 2979, 1743, 1710, 1676, 1472, 1438, 1367, 1165, 745 cm^{-1} . MS (ESI) m/z (relative intensity): 1288 (100) $[\text{M}+\text{Na}]^+$, 1266 (22) $[\text{M}+\text{H}]^+$. HR-MS (ESI): m/z calcd for $\text{C}_{62}\text{H}_{76}\text{N}_9\text{O}_{16}\text{S}_2^+$ $[\text{M}+\text{H}]^+$: 1266.4846, found: 1266.4835.

Methyl (6S,9R,14R)-14-[[S]-2-[(*tert*-butoxycarbonyl)amino]-3-[2-({*E*}-3-[[S]-2-[[*tert*-butoxycarbonyl)amino]-3-methoxy-3-oxopropoxy]-3-oxoprop-1-en-1-yl)-1-(pyridin-2-yl)-1*H*-indol-3-yl]propanamido]-6-[[2-(2-{ethoxycarbonyl}allyl)-1-(pyridin-2-yl)-1*H*-indol-3-yl]methyl]-9-(methoxycarbonyl)-2,2-dimethyl-4,7-dioxo-3-oxa-11,12-dithia-5,8-diazapentadecan-15-oate (281).

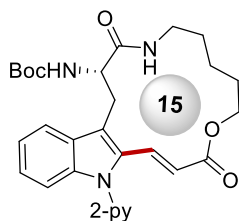


Following a modified literature procedure, a suspension of **S4** (141.2 mg, 0.122 mmol), ethyl 2-[[(*tert*-butoxycarbonyl)oxy]methyl]acrylate **253a** (51.3 mg, 0.244 mmol), $\text{MnBr}(\text{CO})_5$ (3.1 mg, 10 mol %) and NaOAc (2.7 mg, 30 mol %) in 1,4-dioxane (2.0 mL) was stirred at 80 °C for 16 h. After cooling to ambient temperature, CH_2Cl_2 (10 mL) was added and the mixture concentrated *in vacuo*. Purification by column

chromatography on silica gel (CH₂Cl₂/MeOH: 60/1 → 30/1) yielded **281** (152.3 mg, 99%) as a pale yellow solid.

M. p. 111 – 114 °C. **¹H NMR** (400 MHz, CDCl₃): δ 8.67 (dd, *J* = 5.0, 1.9 Hz, 1H), 8.58 (dd, *J* = 5.0, 1.9 Hz, 1H), 7.98 – 7.70 (m, 4H), 7.66 – 7.54 (m, 1H), 7.47 – 7.05 (m, 10H), 6.95 (d, *J* = 7.2 Hz, 1H), 6.81 (d, *J* = 7.1 Hz, 1H), 5.91 (s, 1H), 5.83 (d, *J* = 8.6 Hz, 1H), 5.64 – 5.38 (m, 3H), 5.06 (s, 1H), 4.80 – 4.46 (m, 6H), 4.35 (dd, *J* = 11.2, 3.3 Hz, 1H), 4.11 (q, *J* = 7.1 Hz, 2H), 4.03 (d, *J* = 17.6 Hz, 1H), 3.97 (d, *J* = 17.6 Hz, 1H), 3.76 (s, 3H), 3.61 (s, 3H), 3.56 (s, 3H), 3.49 – 3.38 (m, 2H), 3.36 – 3.12 (m, 2H), 3.11 – 2.82 (m, 4H), 1.46 (s, 9H), 1.41 (s, 9H), 1.38 (s, 9H), 1.21 (t, *J* = 7.1 Hz, 3H). **¹³C NMR** (101 MHz, CDCl₃): δ 171.8 (C_q), 170.9 (C_q), 170.4 (C_q), 170.0 (C_q), 169.9 (C_q), 166.4 (C_q), 166.0 (C_q), 155.4 (C_q), 155.3 (C_q), 155.2 (C_q), 151.4 (C_q), 151.2 (C_q), 149.9 (CH), 149.4 (CH), 139.4 (C_q), 138.6 (CH), 138.2 (CH), 137.6 (C_q), 136.9 (C_q), 134.4 (C_q), 133.1 (CH), 131.6 (C_q), 128.5 (C_q), 128.2 (C_q), 126.1 (CH₂), 125.7 (CH), 122.9 (CH), 122.3 (CH), 122.2 (CH), 121.6 (CH), 121.3 (CH), 120.6 (CH), 120.2 (CH), 119.5 (C_q), 118.7 (CH), 117.2 (CH), 110.9 (CH), 110.9 (CH), 110.8 (C_q), 109.9 (CH), 80.1 (C_q), 80.0 (C_q), 79.7 (C_q), 64.5 (CH₂), 60.9 (CH₂), 54.9 (CH), 54.6 (CH), 53.1 (CH), 52.7 (CH₃), 52.6 (CH₃), 52.5 (CH₃), 51.8 (CH), 51.7 (CH), 40.6 (CH₂), 40.4 (CH₂), 28.6 (CH₂), 28.3 (CH₃), 28.3 (CH₃), 28.3 (CH₃), 27.9 (CH₂), 27.5 (CH₂), 14.1 (CH₃). **IR** (ATR): 3336, 2977, 1743, 1713, 1676, 1471, 1438, 1367, 1250, 1165, 741 cm⁻¹. **MS** (ESI): *m/z* (relative intensity): 1401 (100) [M+Na]⁺, 1376 (15) [M+H]⁺, 712 (96) [M+2Na]²⁺. **HR-MS** (ESI): *m/z* calcd for C₆₈H₈₄N₉O₁₈S₂⁺ [M+H]⁺: 1378.5370, found: 1378.5345.

***tert*-Butyl (S,E)-(3,11-dioxo-14-[pyridin-2-yl]-2,3,4,5,6,7,8,9,11,14-decahydro-1*H*-[1]oxa[7]azacyclopentadecino[12,11-*b*]indol-2-yl]carbamate (283)**

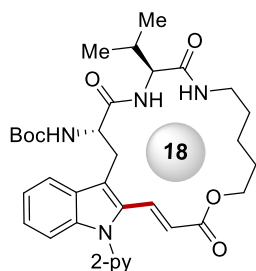


The general procedure **N** was followed using (*S*)-5-{2-[(*tert*-butoxycarbonyl)amino]-3-[1-(pyridin-2-yl)-1*H*-indol-3-yl]propanamido)pentyl propiolate **282** (77.8 mg, 0.15 mmol), MnBr(CO)₅ (8.2 mg, 20 mol %) and NaOAc (7.3 mg, 60 mol %) in 1,4-dioxane (30 mL). Purification by column chromatography on silica gel (CH₂Cl₂/acetone: 9/1) yielded **283** (50.0 mg, 64%, *E/Z* = 94:6) as a pale yellow solid.

5. Experimental Part

M. p. 265 – 268 °C. **¹H NMR** (400 MHz, CDCl₃) δ 8.68 (d, *J* = 4.8 Hz, 1H), 7.88 (dd, *J* = 7.8, 7.8 Hz, 1H), 7.78 – 7.54 (m, 2H), 7.38 (dd, *J* = 6.2, 6.2 Hz, 1H), 7.33 – 7.20 (m, 3H), 7.15 (dd, *J* = 7.5, 7.5 Hz, 1H), 6.29 (brs, 1H), 5.45 (d, *J* = 8.5 Hz, 1H), 5.16 (d, *J* = 16.1 Hz, 1H), 4.61 – 4.45 (m, 1H), 4.45 – 4.30 (m, 1H), 4.08 (t, *J* = 8.5 Hz, 1H), 3.70 – 3.48 (m, 2H), 3.25 (dd, *J* = 15.1, 4.7 Hz, 1H), 3.15 – 2.90 (m, 1H), 1.94 – 1.57 (m, 6H), 1.40 (s, 9H). **¹³C NMR** (101 MHz, CDCl₃) δ 171.5 (C_q), 165.8 (C_q), 155.4 (C_q), 151.5 (C_q), 149.9 (CH), 139.8 (C_q), 138.7 (CH), 131.6 (C_q), 131.0 (CH), 129.1 (C_q), 125.6 (CH), 123.0 (CH), 122.3 (CH), 121.5 (CH), 120.7 (C_q), 120.3 (CH), 119.0 (CH), 110.8 (CH), 79.9 (C_q), 63.7 (CH₂), 55.1 (CH), 38.4 (CH₂), 28.4 (CH₂), 28.3 (CH₃), 27.7 (CH₂), 26.5 (CH₂), 22.8 (CH₂). **IR** (ATR): 3329, 2928, 1698, 1656, 1468, 1438, 1365, 1246, 1167, 733 cm⁻¹. **MS** (ESI) *m/z* (relative intensity): 541 (100) [M+Na]⁺, 519 (35) [M+H]⁺. **HR-MS** (ESI): *m/z* calcd for C₂₉H₃₅N₄O₅⁺ [M+H]⁺: 519.2602, found: 516.2598.

tert-Butyl [(2*S*,5*S*,*E*)-5-isopropyl-3,6,14-trioxo-17-(pyridin-2-yl)-1,2,3,4,5,6,7,8,9,10,11,12,14,17-tetradecahydro-[1]oxa[7,10]diazacyclooctadecino[15,14-*b*]indol-2-yl]carbamate (**285a**)

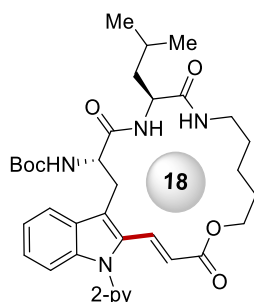


The general procedure **N** was followed using (6*S*,9*S*)-9-isopropyl-2,2-dimethyl-4,7,10-trioxo-6-[[1-(pyridin-2-yl)-1*H*-indol-3-yl]methyl]-3-oxa-5,8,11-triazahexadecan-16-yl propiolate **284a** (92.6 mg, 0.15 mmol), MnBr(CO)₅ (8.2 mg, 20 mol %) and NaOAc (7.3 mg, 60 mol %) in 1,4-dioxane (30 mL). Purification by column chromatography on silica gel (CH₂Cl₂/EtOAc: 7/3) yielded **285a** (49.0 mg, 53%, *E/Z* = 95:5) as a pale yellow solid.

M. p. 245 °C (decomposition). **¹H NMR** (400 MHz, CDCl₃): δ 8.70 (dd, *J* = 4.7, 1.7 Hz, 1H), 7.90 (ddd, *J* = 7.5, 7.5, 1.9 Hz, 1H), 7.72 – 7.62 (m, 2H), 7.43 (d, *J* = 8.3 Hz, 1H), 7.38 (dd, *J* = 7.5, 5.0 Hz, 1H), 7.34 – 7.23 (m, 2H), 7.19 (dd, *J* = 7.5, 7.5 Hz, 1H), 6.87 (d, *J* = 8.5 Hz, 1H), 6.41 (brs, 1H), 6.00 (d, *J* = 16.4 Hz, 1H), 5.10 (d, *J* = 7.8 Hz, 1H), 4.39 – 4.25 (m, 2H), 4.19 (dd, *J* = 7.8, 7.8 Hz, 1H), 4.08 (dt, *J* = 10.6, 4.8 Hz, 1H), 3.72 (dd, *J* = 15.1, 3.4 Hz, 1H), 3.64 – 3.48 (m, 2H), 3.18 – 3.06 (m, 1H), 2.35 – 2.17 (m, 1H), 1.74 – 1.47 (m, 6H), 1.34 (s, 9H), 0.98 (d, *J* = 6.8 Hz, 3H), 0.95 (d, *J* = 6.9 Hz,

3H). **¹³C NMR** (101 MHz, CDCl₃): δ 171.4 (C_q), 170.9 (C_q), 166.5 (C_q), 155.7 (C_q), 150.8 (C_q), 149.8 (CH), 138.7 (CH), 138.2 (C_q), 132.4 (CH), 130.8 (C_q), 129.2 (C_q), 125.3 (CH), 122.7 (CH), 121.9 (CH), 121.6 (CH), 119.5 (CH), 119.4 (CH), 118.7 (C_q), 111.2 (CH), 80.6 (C_q), 64.2 (CH₂), 59.5 (CH), 54.9 (CH), 38.9 (CH₂), 29.3 (CH), 29.1 (CH₂), 28.3 (CH₂), 28.1 (CH₃), 25.3 (CH₂), 23.7 (CH₂), 19.5 (CH₃), 17.8 (CH₃). **IR** (ATR): 3296, 2965, 2928, 1711, 1650, 1524, 1366, 166, 756 cm⁻¹. **MS** (ESI) m/z (relative intensity): 634 (81) [M+Na]⁺, 618 (100) [M+H]⁺. **HR-MS** (ESI): m/z calcd for C₃₄H₄₄N₅O₆⁺ [M+H]⁺: 618.3286, found: 618.3273.

tert-Butyl [(2*S*,5*S*,*E*)-5-isobutyl-3,6,14-trioxo-17-(pyridin-2-yl)-1,2,3,4,5,6,7,8,9,10,11,12,14,17-tetradecahydro-[1]oxa[7,10]diazacyclooctadecino[15,14-*b*]indol-2-yl]carbamate (**285b**)



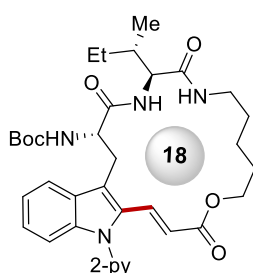
The general procedure **N** was followed using (6*S*,9*S*)-9-isobutyl-2,2-dimethyl-4,7,10-trioxo-6-[[1-(pyridin-2-yl)-1*H*-indol-3-yl]methyl]-3-oxa-5,8,11-triazahexadecan-16-yl propiolate **284b** (94.8 mg, 0.15 mmol), MnBr(CO)₅ (8.2 mg, 20 mol %) and NaOAc (7.3 mg, 60 mol %) in 1,4-dioxane (30 mL). Purification by column chromatography on silica gel (CH₂Cl₂/EtOAc: 7/3 → 6/4) yielded **285b** (61.7 mg, 65%, *E/Z* = 98:2) as a white solid.

M. p. 259 °C (decomposition). **¹H NMR** (600 MHz, DMSO-*d*₆, 80 °C) δ 8.71 (dd, *J* = 4.9, 1.9 Hz, 1H), 8.09 (ddd, *J* = 7.7, 7.7, 2.0 Hz, 1H), 7.85 (d, *J* = 8.0 Hz, 1H), 7.61 (d, *J* = 16.3 Hz, 1H), 7.57 – 7.51 (m, 2H), 7.48 – 7.41 (m, 2H), 7.28 (d, *J* = 8.3 Hz, 1H), 7.24 (dd, *J* = 7.7, 7.7 Hz, 1H), 7.16 (dd, *J* = 7.7, 7.7 Hz, 1H), 6.97 (brs, 1H), 5.85 (d, *J* = 16.3 Hz, 1H), 4.30 (ddd, *J* = 7.7, 7.7, 3.1 Hz, 1H), 4.26 – 4.15 (m, 2H), 4.00 (dt, *J* = 10.6, 5.0 Hz, 1H), 3.52 (dd, *J* = 14.9, 3.1 Hz, 1H), 3.48 – 3.37 (m, 1H), 3.28 – 3.18 (m, 1H), 3.06 – 2.99 (m, 1H), 1.72 – 1.57 (m, 3H), 1.55 – 1.39 (m, 6H), 1.22 (s, 9H), 0.91 (d, *J* = 6.6 Hz, 3H), 0.89 (d, *J* = 6.6 Hz, 3H). **¹³C NMR** (151 MHz, DMSO-*d*₆): δ 171.8 (C_q), 170.7 (C_q), 166.0 (C_q), 155.2 (C_q), 150.2 (C_q), 149.8 (CH), 139.4 (CH), 137.7 (C_q), 132.3 (CH), 130.2 (C_q), 129.1 (C_q), 125.0 (CH), 123.3 (CH), 122.0 (CH), 121.0 (CH),

5. Experimental Part

120.5 (CH), 120.5 (C_q), 118.0 (CH), 110.6 (CH), 78.2 (C_q), 63.9 (CH₂), 54.2 (CH), 51.8 (CH), 40.5 (CH₂), 37.9 (CH₂), 29.0 (CH₂), 28.0 (CH₂), 27.9 (CH₃), 24.8 (CH₂), 23.9 (CH), 23.2 (CH₂), 23.1 (CH₃), 21.4 (CH₃). **IR** (ATR): 3323, 2956, 2926, 1697, 1684, 1641, 1523, 1268, 1246, 1163, 658 cm⁻¹. **MS** (ESI) m/z (relative intensity): 654 (55) [M+Na]⁺, 632 (17) [M+H]⁺. **HR-MS** (ESI): m/z calcd for C₃₅H₄₆N₅O₆⁺ [M+H]⁺: 632.3443, found: 632.3429.

tert-Butyl **{[2S,5S,E]-5-[(S)-sec-butyl]-3,6,14-trioxo-17-[pyridin-2-yl]-1,2,3,4,5,6,7,8,9,10,11,12,14,17-tetradecahydro-[1]oxa[7,10]diazacyclooctadecino[15,14-b]indol-2-yl}carbamate (285c)**

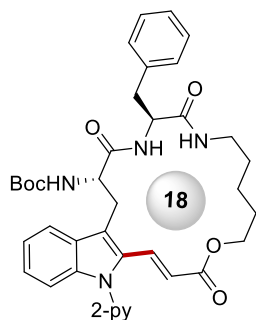


The general procedure **N** was followed using (6S,9S)-9-[(S)-sec-butyl]-2,2-dimethyl-4,7,10-trioxo-6-[[1-(pyridin-2-yl)-1*H*-indol-3-yl]methyl]-3-oxa-5,8,11-triazahexadecan-16-yl propiolate **284c** (94.8 mg, 0.15 mmol), MnBr(CO)₅ (8.2 mg, 20 mol %) and NaOAc (7.3 mg, 60 mol %) in 1,4-dioxane (30 mL). Purification by column chromatography on silica gel (CH₂Cl₂/acetone: 7/3) yielded **285c** (51.2 mg, 54%, *E/Z* = 96:4) as a white solid.

M. p. 261 – 262 °C. **¹H NMR** (400 MHz, DMSO-*d*₆): δ 8.71 (dd, *J* = 5.3, 1.3 Hz, 1H), 8.11 (ddd, *J* = 7.7, 7.7, 2.0 Hz, 1H), 7.93 (dd, *J* = 6.8, 4.8 Hz, 1H), 7.86 (d, *J* = 8.0 Hz, 1H), 7.60 – 7.53 (m, 2H), 7.51 (ddd, *J* = 8.1, 1.2, 1.2 Hz, 1H), 7.41 (d, *J* = 9.1 Hz, 1H), 7.35 (d, *J* = 8.4 Hz, 1H), 7.31 (d, *J* = 8.4 Hz, 1H), 7.25 (ddd, *J* = 8.1, 6.8, 1.2 Hz, 1H), 7.16 (ddd, *J* = 8.1, 6.8, 1.2 Hz, 1H), 5.97 (d, *J* = 16.3 Hz, 1H), 4.18 (dt, *J* = 11.3, 5.7 Hz, 1H), 4.11 (t, *J* = 8.5 Hz, 2H), 4.02 – 3.90 (m, 1H), 3.57 – 3.38 (m, 2H), 3.31 – 3.20 (m, 1H), 3.06 – 2.94 (m, 1H), 1.81 – 1.67 (m, 1H), 1.64 – 1.53 (m, 2H), 1.53 – 1.42 (m, 2H), 1.40 – 1.30 (m, 2H), 1.22 (s, 9H), 1.11 – 0.98 (m, 2H), 0.90 – 0.77 (m, 6H). **¹³C NMR** (101 MHz, DMSO-*d*₆): δ 171.3 (C_q), 171.1 (C_q), 166.5 (C_q), 155.9 (C_q), 150.6 (C_q), 150.2 (CH), 139.9 (CH), 138.0 (C_q), 132.9 (CH), 130.5 (C_q), 129.6 (C_q), 125.5 (CH), 123.7 (CH), 122.5 (CH), 121.5 (CH), 121.1 (CH), 120.8 (C_q), 118.4 (CH), 111.1 (CH), 78.7 (C_q), 64.4 (CH₂), 58.2 (CH), 54.6 (CH), 38.2 (CH₂), 36.4 (CH), 29.4 (CH₂), 28.4 (CH₂), 28.4 (CH₃), 25.1 (CH₂), 24.8 (CH₂), 23.5 (CH₂), 15.9 (CH₃), 11.3 (CH₃). **IR**

(ATR): 3318, 2959, 2928, 1692, 1642, 1530, 1437, 1167, 741 cm^{-1} . **MS** (ESI) m/z (relative intensity): 654 (80) $[\text{M}+\text{Na}]^+$, 632 (100) $[\text{M}+\text{H}]^+$. **HR-MS** (ESI): m/z calcd for $\text{C}_{35}\text{H}_{45}\text{N}_5\text{O}_6\text{Na}$ $[\text{M}+\text{Na}]^+$: 632.3443, found: 632.3439.

tert-Butyl [(2*S*,5*S*,*E*)-5-benzyl-3,6,14-trioxo-17-(pyridin-2-yl) 1,2,3,4,5,6,7,8,9,10,11,12,14,17-tetradecahydro-[1]oxa[7,10]diazacyclooctadecino[15,14-*b*]indol-2-yl]carbamate (285d)



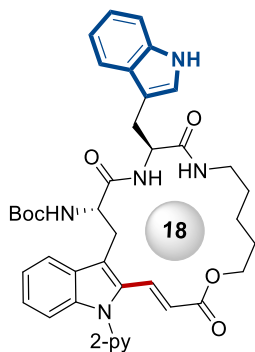
The general procedure **N** was followed using (6*S*,9*S*)-9-benzyl-2,2-dimethyl-4,7,10-trioxo-6-[[1-(pyridin-2-yl)-1*H*-indol-3-yl]methyl]-3-oxa-5,8,11-triazahexadecan-16-yl propiolate **284d** (99.8 mg, 0.15 mmol), $\text{MnBr}(\text{CO})_5$ (8.2 mg, 20 mol %) and NaOAc (7.3 mg, 60 mol %) in 1,4-dioxane (30 mL). Purification by column chromatography on silica gel ($\text{CH}_2\text{Cl}_2/\text{EtOAc}$: 7/3 \rightarrow 5/5) yielded **285d** (74.9 mg, 75%, *E/Z* = 97:3) as a pale yellow solid.

M. p. 192 $^\circ\text{C}$ (decomposition). **$^1\text{H NMR}$** (400 MHz, CDCl_3): δ 8.69 (dd, $J = 5.0, 1.8$ Hz, 1H), 7.90 (ddd, $J = 7.8, 7.8, 1.9$ Hz, 1H), 7.73 – 7.64 (m, 2H), 7.43 (d, $J = 8.3$ Hz, 1H), 7.38 (dd, $J = 7.5, 4.9$ Hz, 1H), 7.31 (d, $J = 9.1$ Hz, 1H), 7.27 – 7.12 (m, 7H), 6.68 (d, $J = 7.7$ Hz, 1H), 6.48 (brs, 1H), 5.88 (d, $J = 16.3$ Hz, 1H), 5.06 (d, $J = 8.0$ Hz, 1H), 4.61 (ddd, $J = 7.7, 7.7, 7.7$ Hz, 1H), 4.42 (ddd, $J = 9.2, 8.6, 4.1$ Hz, 1H), 4.27 (dt, $J = 10.8, 5.3$ Hz, 1H), 4.08 (dt, $J = 10.8, 5.1$ Hz, 1H), 3.62 (dd, $J = 15.0, 4.2$ Hz, 1H), 3.56 – 3.49 (m, 1H), 3.41 (dd, $J = 15.0, 10.0$ Hz, 1H), 3.14 (dd, $J = 13.8, 7.0$ Hz, 1H), 3.10 – 2.95 (m, 2H), 1.73 – 1.62 (m, 2H), 1.59 – 1.41 (m, 4H), 1.27 (s, 9H). **$^{13}\text{C NMR}$** (100 MHz, CDCl_3): δ 171.4 (C_q), 170.4 (C_q), 166.6 (C_q), 155.6 (C_q), 151.1 (C_q), 150.0 (CH), 138.8 (CH), 138.7 (C_q), 136.7 (C_q), 132.4 (CH), 131.4 (C_q), 129.3 (CH), 128.9 (C_q), 128.8 (CH), 127.1 (CH), 125.4 (CH), 122.9 (CH), 122.1 (CH), 121.8 (CH), 119.8 (CH), 119.8 (CH), 118.6 (C_q), 111.4 (CH), 80.6 (C_q), 64.4 (CH_2), 55.1 (CH), 54.8 (CH), 39.1 (CH_2), 37.2 (CH_2), 29.1 (CH_2), 28.3 (CH_2), 28.2 (CH_3), 26.7 (CH_2), 23.8 (CH_2). **IR** (ATR): 3305, 3263, 2935, 1698, 1682, 1644, 1519, 1245, 1161, 743 cm^{-1} . **MS** (ESI) m/z (relative

5. Experimental Part

intensity): 1353 (25) [2M+Na]⁺, 688 (100) [M+Na]⁺, 666 (35) [M+H]⁺. **HR-MS** (ESI): *m/z* calcd for C₃₈H₄₄N₅O₆ [M+H]⁺: 666.3286, found: 666.3268.

tert-Butyl **{[2*S*,5*S*,*E*]-5-[(1*H*-indol-3-yl)methyl]-3,6,14-trioxo-17-[pyridin-2-yl]-1,2,3,4,5,6,7,8,9,10,11,12,14,17-tetradecahydro-[1]oxa[7,10]diazacyclooctadecino[15,14-*b*]indol-2-yl}carbamate (285e)**

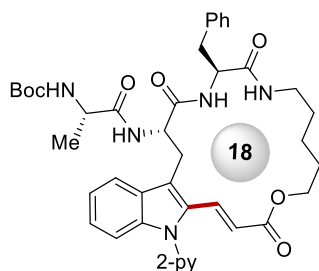


The general procedure **N** was followed using {[6*S*,9*S*]-9-[(1*H*-indol-3-yl)methyl]-2,2-dimethyl-4,7,10-trioxo-6-[(1-(pyridin-2-yl)-1*H*-indol-3-yl)methyl]-3-oxa-5,8,11-triazahexadecan-16-yl propiolate **284e** (105.7 mg, 0.15 mmol), MnBr(CO)₅ (8.2 mg, 20 mol %) and NaOAc (7.3 mg, 60 mol %) in 1,4-dioxane (30 mL). Purification by column chromatography on silica gel (CH₂Cl₂/acetone: 8/2) yielded **285e** (39.6 mg, 37%, *E/Z* = 94:6) as a white solid.

M. p. 250 °C (decomposition). **¹H NMR** (300 MHz, DMSO-*d*₆): δ 10.86 (d, *J* = 2.4 Hz, 1H), 8.72 (dd, *J* = 4.9, 1.9 Hz, 1H), 8.11 (ddd, *J* = 7.7, 7.7, 2.0 Hz, 1H), 7.92 – 7.82 (m, 2H), 7.71 (d, *J* = 7.8 Hz, 1H), 7.62 – 7.53 (m, 3H), 7.45 (d, *J* = 8.1 Hz, 1H), 7.36 – 7.32 (m, 1H), 7.32 – 7.21 (m, 2H), 7.21 – 7.12 (m, 3H), 7.07 (ddd, *J* = 8.1, 6.9, 1.2 Hz, 1H), 7.02 – 6.93 (m, 1H), 5.90 (d, *J* = 16.4 Hz, 1H), 4.57 – 4.42 (m, 1H), 4.31 – 4.09 (m, 2H), 4.07 – 3.88 (m, 1H), 3.50 (d, *J* = 14.5 Hz, 1H), 3.33 – 3.28 (s, 1H), 3.26 – 3.14 (m, 1H), 3.14 – 3.04 (m, 2H), 3.03 – 2.88 (m, 1H), 1.63 – 1.52 (m, 2H), 1.50 – 1.38 (m, 3H), 1.36 – 1.29 (m, 1H), 1.13 (s, 9H). **¹³C NMR** (126 MHz, DMSO-*d*₆): δ 171.1 (C_q), 170.9 (C_q), 166.0 (C_q), 155.3 (C_q), 150.4 (C_q), 149.8 (CH), 139.5 (CH), 137.8 (C_q), 136.1 (C_q), 132.2 (CH), 130.3 (C_q), 128.9 (C_q), 127.4 (C_q), 124.9 (CH), 123.5 (CH), 123.3 (CH), 122.0 (CH), 120.9 (CH), 120.7 (CH), 120.4 (C_q), 118.4 (CH), 118.3 (CH), 118.2 (CH), 111.3 (CH), 110.6 (CH), 109.9 (C_q), 78.1 (C_q), 63.9 (CH₂), 54.4 (CH), 54.2 (CH), 38.1 (CH₂), 29.0 (CH₂), 27.8 (CH₃), 27.3 (CH₂), 25.8 (CH₂), 23.3 (CH₂), 22.1 (CH₂). (One aromatic CH is missing due to overlap, the overlap was verified by HSQC analysis, showing that the peaks at 132.2 ppm correspond to two carbons). **IR** (ATR):

3332, 2961, 2930, 1682, 1651, 1520, 1438, 1251, 1164, 741 cm^{-1} . **MS** (ESI): m/z (relative intensity) 727 (100) $[\text{M}+\text{Na}]^+$, 705 (18) $[\text{M}+\text{H}]^+$. **HR-MS** (ESI): m/z calcd for $\text{C}_{40}\text{H}_{45}\text{N}_6\text{O}_6^+$ $[\text{M}+\text{H}]^+$: 705.3395, found: 705.3382.

tert-Butyl **({S}-1-[(2S,5S,E)-5-benzyl-3,6,14-trioxo-17-(pyridin-2-yl)-1,2,3,4,5,6,7,8,9,10,11,12,14,17-tetradecahydro-[1]oxa[7,10]diazacyclooctadecino[15,14-b]indol-2-yl]amino}-1-oxopropan-2-yl)carbamate (287a)**



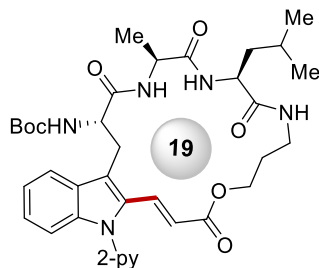
The general procedure **N** was followed using (6S,9S,12S)-12-benzyl-2,2,6-trimethyl-4,7,10,13-tetraoxo-9-[[1-(pyridin-2-yl)-1*H*-indol-3-yl]methyl]-3-oxa-5,8,11,14-tetraazanonadecan-19-yl propiolate **286a** (110.5 mg, 0.15 mmol), $\text{MnBr}(\text{CO})_5$ (8.2 mg, 20 mol %) and NaOAc (7.3 mg, 60 mol %) in 1,4-dioxane (30 mL). Purification by column chromatography on silica gel (CH_2Cl_2 /acetone: 8/2) yielded **287a** (72.1 mg, 65%, *E/Z* = 94:6) as a pale yellow solid.

M. p. 259 °C (decomposition). **$^1\text{H NMR}$** (400 MHz, $\text{DMSO}-d_6$): δ 8.71 (dd, $J = 5.0, 1.9$ Hz, 1H), 8.17 (d, $J = 8.2$ Hz, 1H), 8.08 (ddd, $J = 7.7, 7.7, 2.0$ Hz, 1H), 7.96 (ddd, $J = 7.7, 2.0, 2.0$ Hz, 1H), 7.91 – 7.79 (m, 2H), 7.59 (d, $J = 16.3$ Hz, 1H), 7.57 – 7.50 (m, 2H), 7.29 (d, $J = 8.2$ Hz, 1H), 7.26 – 7.20 (m, 3H), 7.20 – 7.12 (m, 4H), 6.80 (d, $J = 7.3$ Hz, 1H), 5.79 (d, $J = 16.3$ Hz, 1H), 4.57 – 4.29 (m, 2H), 4.13 (dt, $J = 10.8, 5.2$ Hz, 1H), 4.04 (dt, $J = 10.8, 4.8$ Hz, 1H), 3.83 (dq, $J = 7.3, 7.1$ Hz, 1H), 3.51 – 3.35 (m, 2H), 3.34 – 3.26 (m, 1H), 3.02 – 2.67 (m, 3H), 1.65 – 1.53 (m, 2H), 1.55 – 1.43 (m, 2H), 1.43 – 1.25 (m, 11H), 0.95 (d, $J = 7.1$ Hz, 3H). **$^{13}\text{C NMR}$** (101 MHz, $\text{DMSO}-d_6$): δ 172.2 (C_q), 170.4 (C_q), 170.3 (C_q), 165.9 (C_q), 154.9 (C_q), 150.5 (C_q), 149.7 (CH), 139.4 (CH), 138.0 (C_q), 137.8 (C_q), 132.2 (CH), 130.6 (C_q), 129.1 (CH), 128.7 (C_q), 128.1 (CH), 126.2 (CH), 125.0 (CH), 123.3 (CH), 122.2 (CH), 121.1 (CH), 120.6 (CH), 119.9 (C_q), 118.5 (CH), 110.7 (CH), 78.3 (C_q), 64.0 (CH_2), 55.1 (CH), 53.4 (CH), 49.9 (CH), 38.1 (CH_2), 37.3 (CH_2), 29.0 (CH_2), 28.2 (CH_3), 27.9 (CH_2), 25.7 (CH_2), 23.3 (CH_2), 18.0 (CH_3). **IR** (ATR): 3055, 2977, 2927, 1742, 1711, 1469, 1437, 1366, 1165, 907, 728 cm^{-1} .

5. Experimental Part

1. **MS** (ESI): m/z (relative intensity): 759 (100) $[M+Na]^+$, 737 (50) $[M+H]^+$. **HR-MS** (ESI): m/z calcd for $C_{41}H_{49}N_6O_7^+$ $[M+H]^+$: 737.3657, found: 737.3647.

tert-Butyl **{(2*S*,5*S*,8*S*,*E*)-8-isobutyl-5-methyl-3,6,9,15-tetraoxo-18-(pyridin-2-yl)-2,3,4,5,6,7,8,9,10,11,12,13,15,18-tetradecahydro-1*H*-[1]oxa[5,8,11]triazacyclononadecino[16,15-*b*]indol-2-yl}carbamate (287b)**

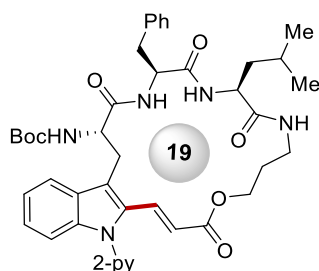


The general procedure **N** was followed using (6*S*,9*S*,12*S*)-12-isobutyl-2,2,9-trimethyl-4,7,10,13-tetraoxo-6-[[1-(pyridin-2-yl)-1*H*-indol-3-yl]methyl]-3-oxa-5,8,11,14-tetraazaheptadecan-17-yl propiolate **286b** (101.2 mg, 0.15 mmol), $MnBr(CO)_5$ (8.2 mg, 20 mol %) and NaOAc (7.3 mg, 60 mol %) in 1,4-dioxane (30 mL). Purification by column chromatography on silica gel ($CH_2Cl_2/MeOH$: 25/1) yielded **287b** (57.6 mg, 57%) as a white solid.

M. p. 113 – 116 °C. **1H NMR** (400 MHz, $CDCl_3$): δ 8.72 (dd, $J = 4.9, 2.1$ Hz, 1H), 8.01 – 7.90 (m, 2H), 7.69 (d, $J = 7.8$ Hz, 1H), 7.48 – 7.37 (m, 3H), 7.36 – 7.20 (m, 3H), 6.98 (d, $J = 8.0$ Hz, 1H), 6.76 (d, $J = 4.5$ Hz, 1H), 5.98 (d, $J = 16.4$ Hz, 1H), 5.08 (d, $J = 3.8$ Hz, 1H), 4.53 – 4.36 (m, 2H), 4.36 – 4.21 (m, 2H), 4.15 – 4.03 (m, 1H), 3.77 (d, $J = 15.2$ Hz, 1H), 3.58 – 3.46 (m, 1H), 3.43 – 3.22 (m, 2H), 2.11 – 1.97 (m, 2H), 1.91 – 1.87 (m, 1H), 1.71 – 1.53 (m, 2H), 1.49 (d, $J = 7.3$ Hz, 3H), 1.39 (s, 9H), 0.96 – 0.90 (m, 6H). **^{13}C NMR** (101 MHz, $CDCl_3$): δ 173.0 (C_q), 172.5 (C_q), 171.8 (C_q), 166.5 (C_q), 156.6 (C_q), 150.6 (C_q), 150.0 (CH), 138.9 (CH), 138.5 (C_q), 131.8 (CH), 131.3 (C_q), 128.6 (C_q), 125.5 (CH), 123.3 (CH), 122.0 (CH), 120.0 (CH), 118.3 (CH), 117.3 (C_q), 111.4 (CH), 81.8 (C_q), 62.3 (CH_2), 56.9 (CH), 52.3 (CH), 51.5 (CH), 40.1 (CH_2), 36.4 (CH_2), 28.2 (CH_2), 28.0 (CH_3), 26.3 (CH_2), 25.0 (CH), 23.2 (CH_3), 20.9 (CH_3), 17.4 (CH_3). (One aromatic CH is missing due to overlap, the overlap was verified by HSQC analysis, showing that the peak at 122.0 ppm corresponds to two carbons). **IR** (ATR): 3288, 2956, 2928, 1716, 1640, 1546, 1473, 1454, 1229, 746 cm^{-1} . **MS** (ESI): m/z (relative intensity) 697 (55) $[M+Na]^+$, 675 (35) $[M+H]^+$. **HR-MS** (ESI): m/z calcd for $C_{36}H_{47}N_6O_7^+$ $[M+H]^+$: 675.3501, found: 675.3494.

tert-Butyl [(2*S*,5*S*,8*S*,*E*)-5-benzyl-8-isobutyl-3,6,9,15-tetraoxo-18-(pyridin-2-yl)-2,3,4,5,6,7,8,9,10,11,12,13,15,18-tetradecahydro-1*H*-

[1]oxa[5,8,11]triazacyclononadecino[16,15-*b*]indol-2-yl]carbamate (287c)



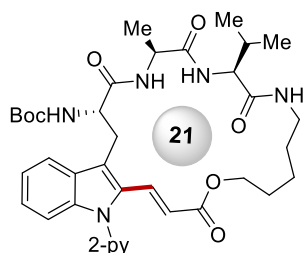
The general procedure **N** was followed using (6*S*,9*S*,12*S*)-9-benzyl-12-isobutyl-2,2-dimethyl-4,7,10,13-tetraoxo-6-[[1-(pyridin-2-yl)-1*H*-indol-3-yl]methyl]-3-oxa-5,8,11,14-tetraazaheptadecan-17-yl propiolate **286c** (112.6 mg, 0.15 mmol), MnBr(CO)₅ (8.2 mg, 20 mol %) and NaOAc (7.3 mg, 60 mol %) in 1,4-dioxane (30 mL). Purification by column chromatography on silica gel (CH₂Cl₂/acetone: 8/2 → 6/4) yielded **287c** (83.5 mg, 74%, *E/Z* = 95:5) as a white solid.

M. p. 106 – 108 °C. **¹H NMR** (400 MHz, DMSO-*d*₆): δ 8.71 (dd, *J* = 4.9, 1.9 Hz, 1H), 8.09 (ddd, *J* = 7.7, 7.7, 2.0 Hz, 1H), 7.92 – 7.78 (m, 4H), 7.68 (dd, *J* = 5.9, 5.9 Hz, 1H), 7.62 – 7.53 (m, 1H), 7.40 (d, *J* = 7.9 Hz, 1H), 7.32 – 7.08 (m, 9H), 5.32 (d, *J* = 16.2 Hz, 1H), 4.35 (ddd, *J* = 11.0, 10.3, 3.2 Hz, 1H), 4.26 – 3.89 (m, 4H), 3.56 (dd, *J* = 14.7, 3.2 Hz, 1H), 3.29 – 3.14 (m, 3H), 3.06 (dd, *J* = 13.8, 8.2 Hz, 1H), 2.97 (dd, *J* = 13.8, 5.7 Hz, 1H), 1.87 – 1.65 (m, 2H), 1.58 – 1.47 (m, 2H), 1.47 – 1.37 (m, 1H), 1.12 (s, 9H), 0.92 – 0.74 (m, 6H). **¹³C NMR** (101 MHz, DMSO-*d*₆): δ 172.0 (C_q), 171.8 (C_q), 170.9 (C_q), 165.7 (C_q), 155.1 (C_q), 150.8 (C_q), 149.8 (CH), 139.5 (CH), 138.8 (C_q), 137.2 (C_q), 132.0 (CH), 130.7 (C_q), 129.0 (CH), 128.6 (C_q), 128.3 (CH), 126.5 (CH), 125.1 (CH), 123.4 (CH), 122.1 (CH), 121.3 (C_q), 120.9 (CH), 120.8 (CH), 117.7 (CH), 110.4 (CH), 78.0 (C_q), 60.8 (CH₂), 56.2 (CH), 55.2 (CH), 51.3 (CH), 40.2 (CH₂), 36.4 (CH₂), 35.2 (CH₂), 27.8 (CH₃), 27.5 (CH₂), 26.1 (CH₂), 24.1 (CH), 23.2 (CH₃), 21.2 (CH₃). **IR** (ATR): 3265, 2955, 2928, 1653, 1522, 1470, 1454, 1153, 1004, 745 cm⁻¹. **MS** (ESI) *m/z* (relative intensity): 773 (100) [M+Na]⁺, 751 (20) [M+H]⁺. **HR-MS** (ESI): *m/z* calcd for C₄₂H₅₀N₆O₇Na⁺ [M+Na]⁺: 773.3633, found: 773.3623.

5. Experimental Part

***tert*-Butyl [(2*S*,5*S*,8*S*,*E*)-8-isopropyl-5-methyl-3,6,9,17-tetraoxo-20-(pyridin-2-yl)-2,3,4,5,6,7,8,9,10,11,12,13,14,15,17,20-hexadecahydro-1*H*-**

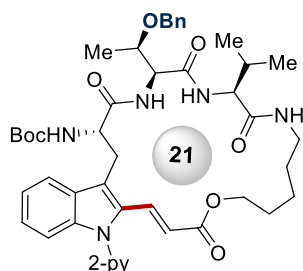
[1]oxa[7,10,13]triazacyclohenicosino[18,17-*b*]indol-2-yl]carbamate (287d**)**



The general procedure **N** was followed using (6*S*,9*S*,12*S*)-12-isopropyl-2,2,9-trimethyl-4,7,10,13-tetraoxo-6-[[1-(pyridin-2-yl)-1*H*-indol-3-yl]methyl]-3-oxa-5,8,11,14-tetraazanonadecan-19-yl propiolate **286d** (103.3 mg, 0.15 mmol), MnBr(CO)₅ (8.2 mg, 20 mol %) and NaOAc (7.3 mg, 60 mol %) in 1,4-dioxane (30 mL). Purification by column chromatography on silica gel (CH₂Cl₂/EtOAc/MeOH: 5/5/0.1 → 5/5/0.5) yielded **287d** (69.3 mg, 67%) as a pale yellow solid. (*E/Z* = 94:6)

M. p. 181 – 183 °C. **¹H NMR** (400 MHz, DMSO-*d*₆): δ 8.72 (dd, *J* = 5.0, 1.9 Hz, 1H), 8.20 – 8.08 (m, 2H), 7.96 (d, *J* = 7.9 Hz, 1H), 7.67 (dd, *J* = 5.8, 5.8 Hz, 1H), 7.62 – 7.52 (m, 3H), 7.47 (d, *J* = 8.0 Hz, 1H), 7.35 – 7.16 (m, 3H), 7.13 (d, *J* = 8.8 Hz, 1H), 6.23 (d, *J* = 16.3 Hz, 1H), 4.36 (ddd, *J* = 9.4, 8.8 4.4 Hz, 1H), 4.20 (dd, *J* = 6.7, 6.7 Hz, 1H), 4.08 (t, *J* = 5.4 Hz, 2H), 3.95 (t, *J* = 7.8 Hz, 1H), 3.50 (dd, *J* = 14.6, 4.4 Hz, 1H), 3.32 – 3.12 (m, 2H), 3.00 – 2.75 (m, 1H), 2.02 (hept, *J* = 7.1 Hz, 1H), 1.62 – 1.53 (m, 2H), 1.50 – 1.35 (m, 4H), 1.32 (d, *J* = 8.9 Hz, 3H), 1.21 (s, 9H), 0.90 – 0.76 (m, 6H). **¹³C NMR** (101 MHz, DMSO-*d*₆): δ 172.1 (C_q), 171.8 (C_q), 170.6 (C_q), 166.6 (C_q), 155.1 (C_q), 150.2 (C_q), 149.8 (CH), 139.4 (CH), 137.6 (C_q), 132.5 (CH), 130.7 (C_q), 128.6 (C_q), 124.9 (CH), 123.3 (CH), 122.1 (CH), 121.0 (CH), 120.8 (CH), 118.7 (C_q), 118.5 (CH), 110.6 (CH), 78.2 (C_q), 64.7 (CH₂), 58.8 (CH), 55.3 (CH), 49.2 (CH), 38.3 (CH₂), 29.3 (CH), 29.0 (CH₂), 28.1 (CH₂), 27.9 (CH₃), 27.4 (CH₂), 23.9 (CH₂), 19.2 (CH₃), 18.3 (CH₃), 17.4 (CH₃). **IR** (ATR): 3341, 2963, 2933, 1705, 1654, 1634, 1508, 1468, 1246, 1163, 1025, 746 cm⁻¹. **MS** (ESI) *m/z* (relative intensity): 711 (100) [M+Na]⁺, 689 (17) [M+H]⁺. **HR-MS** (ESI): *m/z* calcd for C₃₇H₄₉N₆O₇⁺ [M+H]⁺: 689.3657, found: 689.3640.

tert-Butyl {[2S,5S,8S,E]-5-[(R)-1-(benzyloxy)ethyl]-8-isopropyl-3,6,9,17-tetraoxo-20-[pyridin-2-yl]-2,3,4,5,6,7,8,9,10,11,12,13,14,15,17,20-hexadecahydro-1H-[1]oxa[7,10,13]triazacyclohenicosino[18,17-b]indol-2-yl}carbamate (287e)

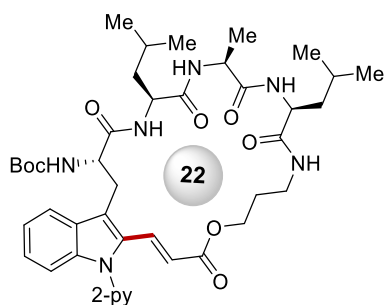


The general procedure **N** was followed using (6S,9S,12S)-9-[(R)-1-(benzyloxy)ethyl]-12-isopropyl-2,2-dimethyl-4,7,10,13-tetraoxo-6-[[1-(pyridin-2-yl)-1H-indol-3-yl]methyl]-3-oxa-5,8,11,14-tetraazanonadecan-19-yl propionate **286e** (121.3 mg, 0.15 mmol), MnBr(CO)₅ (8.2 mg, 20 mol %) and NaOAc (7.3 mg, 60 mol %) in 1,4-dioxane (30 mL). Purification by column chromatography on silica gel (CH₂Cl₂/acetone: 8/2 → 5/5) yielded **287e** (74.9 mg, 74%, *E/Z* = 91:9) as a pale yellow solid.

M. p. 148 °C (decomposition). **¹H NMR** (400 MHz, DMSO-*d*₆): δ 8.71 (dd, *J* = 5.0, 1.8 Hz, 1H), 8.11 (ddd, *J* = 7.7, 7.7, 2.0 Hz, 1H), 8.02 (d, *J* = 8.0 Hz, 1H), 7.79 (d, *J* = 6.8 Hz, 1H), 7.62 (d, *J* = 16.4 Hz, 1H), 7.59 – 7.54 (m, 2H), 7.50 (d, *J* = 8.0 Hz, 1H), 7.42 – 7.10 (m, 10H), 6.23 (d, *J* = 16.4 Hz, 1H), 4.59 (d, *J* = 11.8 Hz, 1H), 4.50 – 4.37 (m, 2H), 4.30 – 4.21 (m, 2H), 4.20 – 3.99 (m, 3H), 3.58 – 3.45 (m, 1H), 3.40 – 3.22 (m, 2H), 2.96 – 2.81 (m, 1H), 2.06 (hept, *J* = 6.7 Hz, 1H), 1.65 – 1.56 (m, 1H), 1.57 – 1.47 (m, 1H), 1.47 – 1.38 (m, 2H), 1.30 (d, *J* = 6.3 Hz, 3H), 1.23 – 1.19 (m, 2H), 1.15 (s, 9H), 0.88 – 0.77 (m, 6H). **¹³C NMR** (101 MHz, DMSO-*d*₆): δ 173.2 (C_q), 170.1 (C_q), 169.6 (C_q), 166.4 (C_q), 155.4 (C_q), 150.1 (C_q), 149.8 (CH), 139.5 (CH), 138.2 (C_q), 137.5 (C_q), 132.6 (CH), 130.6 (C_q), 128.7 (C_q), 128.1 (CH), 127.5 (CH), 127.4 (CH), 125.0 (CH), 123.4 (CH), 122.2 (CH), 121.0 (CH), 120.8 (CH), 118.9 (C_q), 118.3 (CH), 110.7 (CH), 78.6 (C_q), 73.7 (CH), 70.5 (CH₂), 64.9 (CH₂), 58.6 (CH), 55.7 (CH), 38.7 (CH₂), 29.7 (CH), 28.9 (CH₂), 27.9 (CH₃), 27.6 (CH₂), 26.9 (CH₂), 24.3 (CH₂), 19.1 (CH₃), 17.8 (CH₃), 16.5 (CH₃). (One aliphatic CH is missing due to overlap, the overlap was verified by HSQC analysis, showing that the peak at 58.6 ppm corresponds to two carbons). **IR** (ATR): 3313, 2961, 2935, 1693, 1643, 1518, 1436, 1248, 1162, 742 cm⁻¹. **MS** (ESI) *m/z* (relative intensity): 831 (100) [M+Na]⁺, 809 (89) [M+H]⁺. **HR-MS** (ESI): *m/z* calcd for C₄₅H₅₇N₆O₈⁺ [M+H]⁺: 809.4232, found: 809.4227.

5. Experimental Part

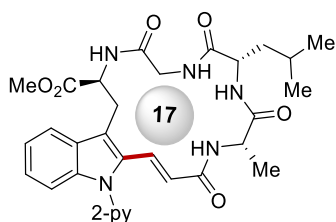
tert-Butyl [(2S,5S,8S,11S,E)-5,11-diisobutyl-8-methyl-3,6,9,12,18-pentaoxo-21-(pyridin-2-yl)-1,2,3,4,5,6,7,8,9,10,11,12,13,14,15,16,18,21-octadecahydro-[1]oxa[5,8,11,14]tetraazacyclodocosino[19,18-b]indol-2-yl]carbamate (287f)



The general procedure **N** was followed using (6S,9S,12S,15S)-9,15-diisobutyl-2,2,12-trimethyl-4,7,10,13,16-pentaoxo-6-[[1-(pyridin-2-yl)-1H-indol-3-yl]methyl]-3-oxa-5,8,11,14,17-pentaazaicosan-20-yl propiolate **286f** (118.2 mg, 0.15 mmol), $\text{MnBr}(\text{CO})_5$ (8.2 mg, 20 mol %) and NaOAc (7.3 mg, 60 mol %) in 1,4-dioxane (30 mL). Purification by column chromatography on silica gel ($\text{CH}_2\text{Cl}_2/\text{acetone}$: 9/1 \rightarrow 6/4) yielded **287f** (61.4 mg, 52%, *E/Z* = 98:2) as a pale yellow solid.

M. p. 160-163 °C. **$^1\text{H NMR}$** (400 MHz, $\text{DMSO}-d_6$): δ 8.71 (dd, J = 4.9, 1.9 Hz, 1H), 8.31 – 8.16 (m, 2H), 8.11 (ddd, J = 7.8, 7.8, 2.0 Hz, 1H), 7.96 (d, J = 7.8 Hz, 1H), 7.70 (d, J = 16.2 Hz, 1H), 7.64 – 7.53 (m, 3H), 7.42 (d, J = 7.8 Hz, 1H), 7.30 – 7.15 (m, 3H), 7.09 (d, J = 9.1 Hz, 1H), 5.39 (d, J = 16.2 Hz, 1H), 4.36 (ddd, J = 8.5, 8.5, 5.5 Hz, 1H), 4.23 (ddd, J = 9.1, 6.1, 6.1 Hz, 1H), 4.16 – 3.94 (m, 4H), 3.34 – 3.27 (m, 2H), 3.26 – 3.18 (m, 2H), 1.82 – 1.65 (m, 3H), 1.64 – 1.48 (m, 5H), 1.28 (d, J = 7.4 Hz, 3H), 1.21 (s, 9H), 0.96 – 0.75 (m, 12H). **$^{13}\text{C NMR}$** (101 MHz, $\text{DMSO}-d_6$): δ 173.2 (C_q), 172.3 (C_q), 171.8 (C_q), 171.5 (C_q), 165.7 (C_q), 155.1 (C_q), 150.8 (C_q), 149.8 (CH), 139.5 (CH), 138.8 (C_q), 131.8 (CH), 131.2 (C_q), 128.6 (C_q), 125.1 (CH), 123.5 (CH), 122.2 (CH), 121.0 (CH), 120.9 (CH), 120.3 (C_q), 118.3 (CH), 110.4 (CH), 78.1 (C_q), 61.3 (CH_2), 55.7 (CH), 52.1 (CH), 51.5 (CH), 50.4 (CH), 35.3 (CH_2), 27.9 (CH_3), 27.8 (CH_2), 27.5 (CH_2), 27.2 (CH_2), 24.3 (CH), 24.1 (CH), 23.1 (CH_3), 23.0 (CH_3), 21.4 (CH_3), 21.4 (CH_3), 17.0 (CH_3). (One aliphatic CH_2 is missing due to overlap with the $\text{DMSO}-d_6$, the overlap was verified by HSQC analysis). **IR** (ATR): 3258, 2956, 2927, 1711, 1652, 1521, 1468, 1436, 1278, 735, 694 cm^{-1} . **MS** (ESI): m/z (relative intensity) 810 (100) $[\text{M}+\text{Na}]^+$, 788 (29) $[\text{M}+\text{H}]^+$. **HR-MS** (ESI): m/z calcd for $\text{C}_{42}\text{H}_{58}\text{N}_7\text{O}_8^+$ $[\text{M}+\text{H}]^+$: 788.4341, found: 788.4333.

Methyl (2*S*,8*S*,11*S*,*E*)-8-isobutyl-11-methyl-4,7,10,13-tetraoxo-16-(pyridin-2-yl)-1,2,3,4,5,6,7,8,9,10,11,12,13,16-tetradecahydro-[1,4,7,10]tetraazacycloheptadecino[14,13-*b*]indole-2-carboxylate (289a)

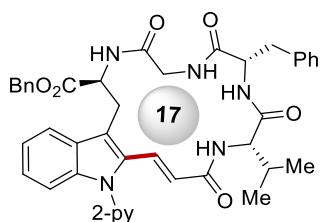


The general procedure **N** was followed using methyl *N*^a-propioloyl-*L*-alanyl-*L*-leucylglycyl-1-(pyridin-2-yl)-*L*-tryptophanate **288a** (88.2 mg, 0.15 mmol), MnBr(CO)₅ (8.2 mg, 20 mol %) and NaOAc (7.3 mg, 60 mol %) in 1,4-dioxane (90 mL) for 48 h. Purification by column chromatography on silica gel (CH₂Cl₂/acetone: 8/2 → 7/3) yielded **289a** (53.2 mg, 60%, *E/Z* = 97:3) as a pale yellow solid.

M. p. 198-201 °C. **¹H NMR** (400 MHz, DMSO-*d*₆): δ 8.73 (dd, *J* = 5.0, 1.8 Hz, 1H), 8.58 – 8.52 (m, 2H), 8.07 (ddd, *J* = 7.7, 7.7, 1.9 Hz, 1H), 7.75 (d, *J* = 8.8 Hz, 1H), 7.71 (d, *J* = 7.7 Hz, 1H), 7.62 – 7.54 (m, 2H), 7.42 – 7.33 (m, 3H), 7.29 – 7.23 (m, 1H), 7.23 – 7.17 (m, 1H), 5.51 (d, *J* = 15.9 Hz, 1H), 4.18 (ddd, *J* = 9.9, 9.0, 4.2 Hz, 1H), 4.00 (ddd, *J* = 7.5, 7.5, 2.7 Hz, 1H), 3.96 – 3.90 (m, 1H), 3.89 – 3.81 (m, 1H), 3.76 (dd, *J* = 15.0, 2.8 Hz, 1H), 3.69 (s, 3H), 3.63 – 3.50 (m, 1H), 3.31 – 3.28 (m, 1H), 1.72 – 1.58 (m, 1H), 1.56 – 1.39 (m, 2H), 1.22 (d, *J* = 7.2 Hz, 3H), 0.84 (d, *J* = 6.4 Hz, 3H), 0.81 (d, *J* = 6.4 Hz, 3H). **¹³C NMR** (150 MHz, DMSO-*d*₆): δ 172.6 (C_q), 171.8 (C_q), 171.2 (C_q), 168.7 (C_q), 166.7 (C_q), 150.9 (C_q), 149.5 (CH), 139.3 (CH), 139.0 (C_q), 132.5 (C_q), 127.8 (CH), 127.3 (C_q), 125.1 (CH), 123.2 (CH), 121.8 (CH), 121.3 (C_q), 121.2 (CH), 120.7 (CH), 119.4 (CH), 110.9 (CH), 54.1 (CH), 52.2 (CH₃), 51.7 (CH), 50.5 (CH), 41.9 (CH₂), 39.0 (CH₂), 25.8 (CH₂), 24.4 (CH), 23.2 (CH₃), 21.1 (CH₃), 16.3 (CH₃). **IR** (ATR): 3337, 3309, 2929, 1730, 1648, 1523, 1281, 1149, 805 cm⁻¹. **MS** (ESI) *m/z* (relative intensity) 1199 (10) [2M+Na]⁺, 611 (55) [M+Na]⁺, 589 (100) [M+H]⁺. **HR-MS** (ESI): *m/z* calcd for C₃₁H₃₇N₆O₆⁺ [M+H]⁺: 589.2769, found: 589.2768.

5. Experimental Part

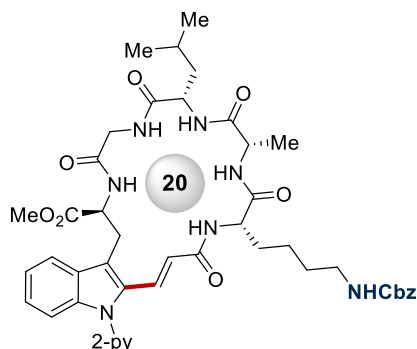
Benzyl (2*S*,8*S*,11*S*,*E*)-8-benzyl-11-isopropyl-4,7,10,13-tetraoxo-16-(pyridin-2-yl)-1,2,3,4,5,6,7,8,9,10,11,12,13,16-tetradecahydro-[1,4,7,10]tetraazacycloheptadecino[14,13-*b*]indole-2-carboxylate (**289b**)



The general procedure **N** was followed using benzyl *N*^a-propioloyl-L-valyl-L-phenylalanylglycyl-1-(pyridin-2-yl)-L-tryptophanate **288b** (109.0 mg, 0.15 mmol), MnBr(CO)₅ (8.2 mg, 20 mol %) and NaOAc (7.3 mg, 60 mol %) in 1,4-dioxane (90 mL) for 48 h. Purification by column chromatography on silica gel (CH₂Cl₂/acetone: 8/2 → 6/4) yielded **289b** (52.3 mg, 48%, *E/Z* = 87:13) as a pale yellow solid.

M. p. 310-312 °C. **¹H NMR** (400 MHz, DMSO-*d*₆): δ 8.73 (dd, *J* = 4.9, 1.8 Hz, 1H), 8.64 (d, *J* = 7.5 Hz, 1H), 8.32 (d, *J* = 5.5 Hz, 1H), 8.05 (ddd, *J* = 7.7, 7.7, 2.0 Hz, 1H), 7.93 (d, *J* = 8.2 Hz, 1H), 7.67 (d, *J* = 8.2 Hz, 1H), 7.61 (d, *J* = 15.9 Hz, 1H), 7.56 (dd, *J* = 7.5, 4.9 Hz, 1H), 7.44 – 7.34 (m, 7H), 7.31 – 7.11 (m, 8H), 5.64 (d, *J* = 15.9 Hz, 1H), 5.19 (s, 2H), 4.42 (ddd, *J* = 12.1, 8.2, 4.0 Hz, 1H), 4.13 (ddd, *J* = 7.9, 7.9, 3.1 Hz, 1H), 3.78 – 3.66 (m, 3H), 3.58 (dd, *J* = 8.2, 5.5 Hz, 1H), 3.42 (dd, *J* = 14.6, 8.2 Hz, 1H), 3.35 – 3.29 (m, 1H), 2.86 (dd, *J* = 14.6, 11.0 Hz, 1H), 1.74 (h, *J* = 6.8 Hz, 1H), 0.73 (d, *J* = 6.8 Hz, 3H), 0.52 (d, *J* = 6.8 Hz, 3H). **¹³C NMR** (101 MHz, DMSO-*d*₆): δ 171.1 (C_q), 170.9 (C_q), 170.6 (C_q), 168.7 (C_q), 167.0 (C_q), 150.9 (C_q), 149.5 (CH), 139.3 (CH), 139.1 (C_q), 138.7 (C_q), 135.9 (C_q), 132.8 (C_q), 129.0 (CH), 128.4 (CH), 128.0 (CH), 128.0 (CH), 127.9 (CH), 127.7 (CH), 127.4 (C_q), 126.0 (CH), 125.1 (CH), 123.2 (CH), 121.8 (CH), 121.2 (CH), 120.9 (C_q), 120.8 (CH), 119.5 (CH), 111.0 (CH), 66.4 (CH₂), 62.1 (CH), 54.1 (CH), 54.0 (CH), 42.0 (CH₂), 35.6 (CH₂), 28.2 (CH), 25.6 (CH₂), 19.4 (CH₃), 18.7 (CH₃). **IR** (ATR): 3255, 2966, 2925, 1712, 1653, 1522, 1468, 1209, 734, 696 cm⁻¹. **MS** (ESI) *m/z* (relative intensity): 749 (100) [M+Na]⁺, 727 (27) [M+H]⁺. **HR-MS** (ESI): *m/z* calcd for C₄₂H₄₃N₆O₆⁺ [M+H]⁺: 727.3239, found: 727.3223.

Methyl (2S,8S,11S,14S,E)-14-(4-(((benzyloxy)carbonyl)amino)butyl)-8-isobutyl-11-methyl-4,7,10,13,16-pentaoxo-19-(pyridin-2-yl)-2,3,4,5,6,7,8,9,10,11,12,13,14,15,16,19-hexadecahydro-1H-[1,4,7,10,13]pentaazacycloicosino[17,16-b]indole-2-carboxylate (289c)

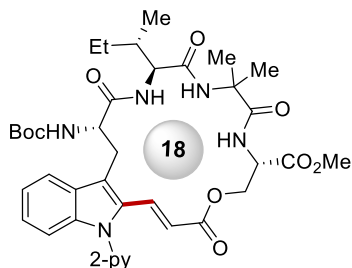


The general procedure **N** was followed using methyl *N*^a-*N*⁶-((benzyloxy)carbonyl)-*N*²-propioloyl-L-lysyl-L-alanyl-L-leucylglycyl-1-(pyridin-2-yl)-L-tryptophanate **288c** (127.6 mg, 0.15 mmol), MnBr(CO)₅ (8.2 mg, 20 mol %) and NaOAc (7.3 mg, 60 mol %) in 1,4-dioxane (90 mL) for 48h. Purification by column chromatography on silica gel (CH₂Cl₂/acetone: 8/2 → 5/5) yielded **289c** (72.7 mg, 57%) as a pale yellow solid.

M. p. 244 – 246 °C. **¹H NMR** (400 MHz, DMSO-*d*₆): δ 8.71 (dd, *J* = 5.4, 1.6 Hz, 1H), 8.43 (d, *J* = 8.3 Hz, 1H), 8.24 (d, *J* = 7.5 Hz, 1H), 8.14 (d, *J* = 6.8 Hz, 1H), 8.08 (ddd, *J* = 7.8, 7.8, 1.9 Hz, 1H), 7.82 (d, *J* = 7.5 Hz, 1H), 7.59 (dd, *J* = 7.0, 4.6 Hz, 1H), 7.57 – 7.52 (m, 2H), 7.49 (d, *J* = 8.0 Hz, 1H), 7.39 – 7.27 (m, 7H), 7.26 – 7.16 (m, 3H), 6.12 (d, *J* = 16.0 Hz, 1H), 5.00 (s, 2H), 4.69 (ddd, *J* = 7.6, 7.4, 5.3 Hz, 1H), 4.14 – 3.98 (m, 3H), 3.91 (dd, *J* = 17.1, 7.2 Hz, 1H), 3.69 – 3.60 (m, 1H), 3.55 (s, 3H), 3.49 (dd, *J* = 14.5, 7.4 Hz, 1H), 3.39 – 3.34 (m, 1H), 3.05 – 2.93 (m, 2H), 1.86 – 1.74 (m, 1H), 1.74 – 1.55 (m, 4H), 1.46 – 1.39 (m, 2H), 1.30 (d, *J* = 7.2 Hz, 3H), 1.28 – 1.16 (m, 2H), 0.89 (d, *J* = 5.5 Hz, 3H), 0.83 (d, *J* = 5.5 Hz, 3H). **¹³C NMR** (101 MHz, DMSO-*d*₆): δ 172.6 (C_q), 172.5 (C_q), 171.9 (C_q), 171.7 (C_q), 169.4 (C_q), 165.7 (C_q), 156.5 (C_q), 151.1 (C_q), 150.0 (CH), 139.7 (CH), 138.3 (C_q), 137.7 (C_q), 133.4 (C_q), 128.8 (CH), 128.3 (C_q), 128.2 (CH), 128.1 (CH), 127.8 (CH), 125.0 (CH), 124.3 (CH), 123.6 (CH), 122.4 (CH), 121.5 (CH), 119.6 (CH), 116.2 (C_q), 111.4 (CH), 65.6 (CH₂), 63.3 (CH₂), 54.0 (CH), 53.1 (CH), 52.6 (CH₃), 52.4 (CH), 50.7 (CH), 42.3 (CH₂), 40.7 (CH₂), 31.0 (CH₂), 29.5 (CH₂), 27.7 (CH₂), 24.7 (CH), 23.5 (CH₃), 23.4 (CH₂), 21.7 (CH₃), 17.5 (CH₃). **IR** (ATR): 3306, 2952, 2927, 1739, 1654, 1528, 1455, 1252, 1005, 744 cm⁻¹. **MS** (ESI): *m/z* (relative intensity) 873 (100) [M+Na]⁺, 851 (16) [M+H]⁺. **HR-MS** (ESI): *m/z* calcd for C₄₅H₅₅N₈O₉⁺ [M+H]⁺: 851.4087, found: 851.4071.

5. Experimental Part

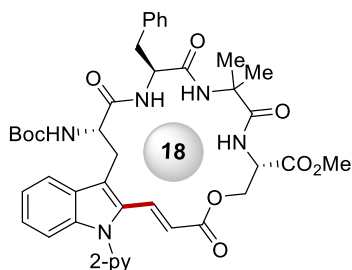
Methyl (2S,5S,11S,E)-2-[(*tert*-butoxycarbonyl)amino]-5-[(*S*)-*sec*-butyl]-8,8-dimethyl-3,6,9,14-tetraoxo-17-(pyridin-2-yl)-1,2,3,4,5,6,7,8,9,10,11,12,14,17-tetradecahydro-[1]oxa[4,7,10]triazacyclooctadecino[15,14-*b*]indole-11-carboxylate (289d**).**



The general procedure **N** was followed using methyl (6*S*,9*S*,15*S*)-9-[(*S*)-*sec*-butyl]-2,2,12,12-tetramethyl-4,7,10,13-tetraoxo-15-[(propionylloxy)methyl]-6-[[1-(pyridin-2-yl)-1*H*-indol-3-yl]methyl]-3-oxa-5,8,11,14-tetraazahexadecan-16-oate **288d** (109.9 mg, 0.15 mmol), MnBr(CO)₅ (8.2 mg, 20 mol %) and NaOAc (7.3 mg, 60 mol %) in 1,4-dioxane (30 mL). Purification by column chromatography on silica gel (CH₂Cl₂/acetone 9/1 → 6/4) yielded **289d** (56.2 mg, 51%, *E/Z* = 93:7) as a white solid.

M. p. 241 °C (decomposition). **¹H NMR** (600 MHz, CD₂Cl₂): δ 8.66 (dd, *J* = 5.0, 1.8 Hz, 1H), 7.89 (ddd, *J* = 7.8, 4.5, 4.5 Hz, 1H), 7.77 – 7.63 (m, 2H), 7.42 (d, *J* = 8.3 Hz, 1H), 7.40 – 7.36 (m, 2H), 7.31 – 7.24 (m, 2H), 7.19 (dd, *J* = 7.5, 7.5 Hz, 1H), 6.86 (d, *J* = 6.2 Hz, 1H), 6.77 (s, 1H), 6.30 (d, *J* = 16.4 Hz, 1H), 5.37 (d, *J* = 6.5 Hz, 1H), 4.97 (ddd, *J* = 10.2, 6.5, 2.8 Hz, 1H), 4.60 (dd, *J* = 11.1, 2.5 Hz, 1H), 4.43 (ddd, *J* = 7.7, 6.9, 3.5 Hz, 1H), 4.32 – 4.22 (m, 2H), 3.74 (s, 3H), 3.71 – 3.61 (m, 1H), 3.33 (dd, *J* = 15.5, 10.2 Hz, 1H), 1.95 – 1.83 (m, 1H), 1.53 (s, 3H), 1.46 (s, 3H), 1.32 (s, 9H), 1.19 – 1.07 (m, 2H), 0.97 (d, *J* = 6.7 Hz, 3H), 0.91 (t, *J* = 7.4 Hz, 3H). **¹³C NMR** (151 MHz, CD₂Cl₂): δ 174.4 (C_q), 172.7 (C_q), 170.5 (C_q), 170.5 (C_q), 166.6 (C_q), 156.4 (C_q), 151.1 (C_q), 150.3 (CH), 139.2 (CH), 138.3 (C_q), 134.3 (CH), 131.5 (C_q), 129.5 (CH), 125.6 (CH), 123.2 (CH), 122.1 (CH), 119.9 (CH), 119.8 (CH), 118.9 (C_q), 111.8 (CH), 81.2 (C_q), 64.9 (CH₂), 59.6 (CH), 57.9 (C_q), 55.7 (CH), 53.1 (CH), 52.0 (CH₃), 37.6 (CH), 30.2 (CH₂), 28.5 (CH₃), 27.4 (CH₂), 26.3 (CH₃), 25.9 (CH₃), 15.8 (CH₃), 11.9 (CH₃). (One aromatic C_q is missing due to overlap, the overlap was verified by HSQC and HMBC analysis, showing that the peaks at 122.1 ppm correspond to two carbons). **IR** (ATR): 3332, 2961, 2925, 1749, 1686, 1630, 1517, 1438, 1365, 1166, 742 cm⁻¹. **MS** (ESI) *m/z* (relative intensity): 755 (100) [M+Na]⁺, 733 (15) [M+H]⁺. **HR-MS** (ESI): *m/z* calcd for C₃₈H₄₉N₆O₉⁺ [M+H]⁺: 733.3556, found: 733.3541.

Methyl (2*S*,5*S*,11*S*,*E*)-5-benzyl-2-[(*tert*-butoxycarbonyl)amino]-8,8-dimethyl-3,6,9,14-tetraoxo-17-(pyridin-2-yl)-1,2,3,4,5,6,7,8,9,10,11,12,14,17-tetradecahydro-[1]oxa[4,7,10]triazacyclooctadecino[15,14-*b*]indole-11-carboxylate (289e**)**

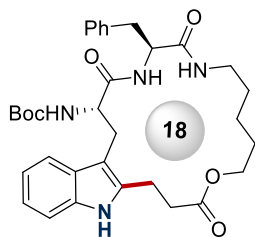


The general procedure **N** was followed using methyl (6*S*,9*S*,15*S*)-9-benzyl-2,2,12,12-tetramethyl-4,7,10,13-tetraoxo-15-[(propiolyloxy)methyl]-6-[(1-(pyridin-2-yl)-1*H*-indol-3-yl)methyl]-3-oxa-5,8,11,14-tetraazahexadecan-16-oate **288e** (115.0 mg, 0.15 mmol), MnBr(CO)₅ (8.2 mg, 20 mol %) and NaOAc (7.3 mg, 60 mol %) in 1,4-dioxane (30 mL). Purification by column chromatography on silica gel (CH₂Cl₂/acetone: 8/2→6/4) yielded **289e** (74.9 mg, 65%, *E/Z* = 90:10) as a pale yellow semisolid.

¹H NMR (400 MHz, DMSO-*d*₆): δ 8.71 (dd, *J* = 4.8, 1.8 Hz, 1H), 8.20 (brs, 1H), 8.14 – 8.05 (m, 1H), 7.95 (d, *J* = 7.8 Hz, 1H), 7.82 (d, *J* = 7.3 Hz, 1H), 7.75 (d, *J* = 8.1 Hz, 1H), 7.64 (d, *J* = 16.4 Hz, 1H), 7.58 – 7.47 (m, 2H), 7.36 (d, *J* = 8.4 Hz, 1H), 7.31 – 7.10 (m, 8H), 5.95 (d, *J* = 16.4 Hz, 1H), 4.76 (ddd, *J* = 8.0, 3.5, 3.5 Hz, 1H), 4.54 (ddd, *J* = 8.1, 7.8, 7.0 Hz, 1H), 4.46 (dd, *J* = 11.3, 4.9 Hz, 1H), 4.27 – 4.08 (m, 2H), 3.67 (s, 3H), 3.43 (dd, *J* = 14.8, 3.3 Hz, 1H), 3.33 – 3.22 (m, 1H), 2.96 (dd, *J* = 13.7, 5.8 Hz, 1H), 2.86 (dd, *J* = 13.7, 8.1 Hz, 1H), 1.35 – 1.09 (m, 15H). **¹³C NMR** (101 MHz, DMSO-*d*₆): δ 174.4 (C_q), 171.5 (C_q), 170.6 (C_q), 170.1 (C_q), 166.2 (C_q), 155.7 (C_q), 150.6 (C_q), 150.2 (CH), 139.9 (CH), 138.0 (C_q), 137.7 (C_q), 134.1 (CH), 130.7 (C_q), 129.8 (CH), 129.2 (C_q), 128.4 (CH), 126.7 (CH), 125.6 (CH), 123.6 (CH), 122.3 (CH), 121.5 (CH), 121.3 (CH), 120.7 (C_q), 117.8 (CH), 111.1 (CH), 78.6 (C_q), 63.7 (CH₂), 56.6 (C_q), 55.0 (CH), 54.9 (CH), 52.9 (CH₃), 51.9 (CH), 37.9 (CH₂), 28.5 (CH₃), 27.4 (CH₃), 27.0 (CH₂), 23.5 (CH₃). **IR** (ATR): 3327, 2980, 2929, 1741, 1700, 1653, 1504, 1437, 1165, 1023, 741 cm⁻¹. **MS** (ESI): *m/z* (relative intensity) 789 (100) [M+Na]⁺, 767 (22) [M+H]⁺. **HR-MS** (ESI): *m/z* calcd for C₄₁H₄₇N₆O₉⁺ [M+H]⁺: 767.3399, found: 767.3390.

5. Experimental Part

tert-Butyl [(2*S*,5*S*)-5-benzyl-3,6,14-trioxo-1,2,3,4,5,6,7,8,9,10,11,12,14,15,16,17-hexadecahydro-[1]oxa[7,10]diazacyclooctadecino[15,14-*b*]indol-2-yl]carbamate (290)



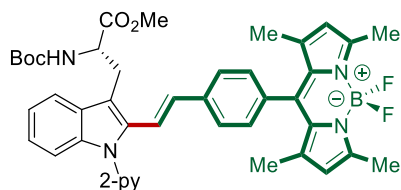
To a stirred solution of **285d** (99.8 mg, 0.15 mmol) in CH₂Cl₂ (0.6 mL) methyl trifluoromethanesulfonate (24.6 mg, 0.15 mmol) was added at 0 °C. After 30 min, the mixture was allowed to warm up to 25 °C and stirred for 18 h. The crude mixture was concentrated under reduced pressure to afford a bright yellow solid. In a sealed-tube, the crude product, Pd(OH)₂/C (10.5 mg, 5.0 mol %, 20 wt%), and ammonium formate (141.5 mg, 15.0 equiv) were dissolved in methanol (1.0 mL), and stirred at 60 °C for 16 hours. The mixture was filtered through a short plug of celite, concentrated under reduced pressure and purified by column chromatography on silica gel (CH₂Cl₂/EtOAc: 7/3 → 5/5), yielding **290** (50.5 mg, 57%) as a white solid.

M. p. 212 – 215°C. **¹H NMR** (400 MHz, DMSO-*d*₆, 80 °C): δ 10.51 (s, 1H), 7.85 (d, *J* = 7.9 Hz, 1H), 7.58 (dd, *J* = 7.9, 1.1 Hz, 1H), 7.32 (dd, *J* = 5.8, 5.8 Hz, 1H), 7.25 – 7.19 (m, 3H), 7.19 – 7.13 (m, 3H), 6.99 (ddd, *J* = 7.9, 7.0, 1.2 Hz, 1H), 6.92 (ddd, *J* = 7.9, 7.0, 1.1 Hz, 1H), 6.09 (brs, 1H), 4.46 (ddd, *J* = 7.9, 7.9, 5.9 Hz, 1H), 4.24 (ddd, *J* = 7.9, 7.9, 5.3 Hz, 1H), 4.06 (t, *J* = 5.5 Hz, 2H), 3.29 (p, *J* = 6.9, 6.5 Hz, 1H), 3.12 – 3.06 (m, 1H), 3.05 – 2.96 (m, 3H), 2.97 – 2.79 (m, 3H), 2.73 – 2.58 (m, 2H) 1.58 (qt, *J* = 5.1, 2.1 Hz, 2H), 1.50 – 1.33 (m, 4H), 1.25 (s, 9H). **¹³C NMR** (100 MHz, DMSO-*d*₆): δ 171.9 (C_q), 171.5 (C_q), 170.3 (C_q), 154.9 (C_q), 138.0 (C_q), 135.3 (C_q), 135.2 (C_q), 129.1 (CH), 128.5 (C_q), 128.0 (CH), 126.2 (CH), 120.2 (CH), 118.7 (CH), 118.0 (CH), 110.3 (CH), 106.8 (C_q), 77.8 (C_q), 64.1 (CH₂), 55.0 (CH), 54.7 (CH), 38.1 (CH₂), 37.2 (CH₂), 34.7 (CH₂), 28.8 (CH₂), 28.1 (CH₃), 27.9 (CH₂), 26.7 (CH₂), 23.4 (CH₂), 21.6 (CH₂). **IR** (ATR): 3335, 2929, 1726, 1677, 1646, 1523, 1243, 1151, 1044, 10014, 700 cm⁻¹. **MS** (ESI): *m/z* (relative intensity) 1203 (15) [2M+Na]⁺, 613 (100) [M+Na]⁺, 591 (18) [M+H]⁺. **HR-MS** (ESI): *m/z* calcd for C₃₃H₄₂N₄O₆Na⁺ [M+Na]⁺: 613.2997, found: 613.2983.

5.7. Manganese(I)-Catalyzed C–H BODIPY-Labeling of Tryptophan-Containing Peptides

5.7.1. Characterization Data

Methyl (S,E)-2-[(*tert*-butoxycarbonyl)amino]-3-{2-[4-(5,5-difluoro-1,3,7,9-tetramethyl-5*H*-4 λ ,5 λ -dipyrrolo[1,2-*c*:2',1'-*f*][1,3,2]diazaborinin-10-yl)styryl]-1-(pyridin-2-yl)-1*H*-indol-3-yl}propanoate (292a**)**



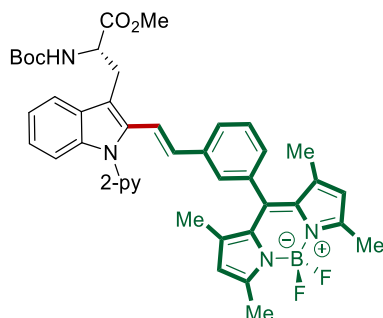
The general procedure **O** was followed using methyl *N*_a-(*tert*-butoxycarbonyl)-1-(pyridin-2-yl)-L-tryptophanate **153** (39.5 mg, 0.10 mmol), 10-(4-ethynylphenyl)-5,5-difluoro-1,3,7,9-tetramethyl-5*H*-4 λ ,5 λ -dipyrrolo[1,2-*c*:2',1'-*f*][1,3,2]diazaborinine **294a** (38.3 mg, 0.11 mmol), MnBr(CO)₅ (5.5 mg, 20 mol %) and (1-Ad)CO₂H (7.2 mg, 40 mol %) in 1,4-dioxane (1.0 mL). Purification by column chromatography on silica gel (CH₂Cl₂/MeOH: 100/0.2) yielded **292a** (65.4 mg, 88%) as an orange solid. The obtained solid was analyzed by inductively coupled plasma mass spectrometry (ICP-MS) analysis, showing 24.5 ppm of residual manganese.

M. p. 149 – 152 °C. **¹H NMR** (300 MHz, CDCl₃): δ 8.76 (d, *J* = 3.7 Hz, 1H), 7.93 (dd, *J* = 7.2, 7.1 Hz, 1H), 7.62 (d, *J* = 7.1 Hz, 1H), 7.49 (d, *J* = 7.7 Hz, 2H), 7.50 – 7.47 (m, 2H), 7.35 (d, *J* = 16.7 Hz, 1H), 7.28 – 7.21 (m, 5H), 6.54 (d, *J* = 16.7 Hz, 1H), 6.00 (s, 2H), 5.26 (d, *J* = 7.6 Hz, 1H), 4.78 (ddd, *J* = 7.6, 5.4, 5.3 Hz, 1H), 3.57 – 3.54 (m, 5H), 2.58 (s, 6H), 1.44 (s, 9H), 1.43 (s, 6H). **¹³C NMR** (75 MHz, CDCl₃): δ 172.7 (C_q), 155.4 (C_q), 155.0 (C_q), 152.0 (C_q), 149.7 (CH), 143.0 (C_q), 141.4 (C_q), 138.4 (CH), 138.2 (C_q), 137.9 (C_q), 134.2 (C_q), 134.1 (C_q), 131.3 (C_q), 130.5 (CH), 129.1 (C_q), 128.3 (CH), 126.9 (CH), 123.9 (CH), 122.4 (CH), 122.3 (CH), 121.2 (CH), 119.0 (CH), 118.0 (CH), 113.5 (C_q), 110.7 (CH), 79.9 (C_q), 54.3 (CH), 52.3 (CH₃), 28.6 (CH₂), 28.3 (CH₃), 14.7 (CH₃), 14.6 (CH₃). (One aromatic CH is missing due to overlap, the overlap was verified by HSQC analysis, showing that the peak at 121.2 corresponds to two carbons). **¹⁹F NMR** (282 MHz, CDCl₃): δ –146.2 (q, ¹*J*_{B-F} = 31.9 Hz). **IR** (ATR): 3425, 3054, 2975, 2928, 2864, 1741, 1710, 1541, 1508, 1455 cm⁻¹. **MS** (ESI): *m/z* (relative intensity) 766

5. Experimental Part

(55) $[M+Na]^+$, 744 (100) $[M+H]^+$. **HR-MS** (ESI): m/z calcd for $C_{43}H_{44}BF_2N_5O_4Na^+$ $[M+Na]^+$:766.3354, found: 766.3343.

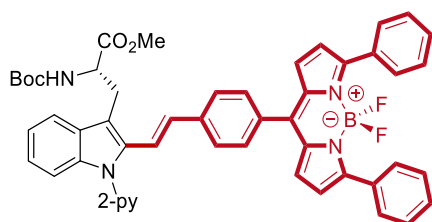
Methyl (S,E)-2-[(tert-butoxycarbonyl)amino]-3-{2-[3-(5,5-difluoro-1,3,7,9-tetramethyl-5H-4 λ ,5 λ -dipyrrolo[1,2-c:2',1'-f][1,3,2]diazaborinin-10-yl)styryl]-1-[pyridin-2-yl]-1H-indol-3-yl}propanoate (292b)



The general procedure **O** was followed using methyl N_α -(tert-butoxycarbonyl)-1-(pyridin-2-yl)-L-tryptophanate **153** (39.5 mg, 0.10 mmol), 10-(3-ethynylphenyl)-5,5-difluoro-1,3,7,9-tetramethyl-5H-4 λ ,5 λ -dipyrrolo[1,2-c:2',1'-f][1,3,2]diazaborinine **294b** (38.3 mg, 0.11 mmol), $MnBr(CO)_5$ (5.5 mg, 20 mol %) and 1-AdCO₂H (7.2 mg, 40 mol %) in 1,4-dioxane (1.0 mL). Purification by column chromatography on silica gel (CH₂Cl₂/MeOH: 100/0.3) yielded **292b** (57.2 mg, 77%) as an orange solid.

M. p.: 116 – 118 °C. **¹H NMR** (400 MHz, CDCl₃): δ 8.71 (d, J = 3.4 Hz, 1H), 7.88 (ddd, J = 7.8, 7.8, 1.5 Hz, 1H), 7.66 – 7.51 (m, 2H), 7.50 – 7.32 (m, 4H), 7.25 – 7.10 (m, 5H), 6.46 (d, J = 16.7 Hz, 1H), 6.00 (s, 2H), 5.24 (d, J = 8.3 Hz, 1H), 4.73 (ddd, J = 8.3, 7.0, 7.0 Hz, 1H), 3.70 – 3.35 (m, 5H), 2.58 (s, 6H), 1.45 – 1.34 (m, 15H). **¹³C NMR** (101 MHz, CDCl₃): δ 172.7 (C_q), 155.5 (C_q), 155.0 (C_q), 152.0 (C_q), 149.7 (CH), 143.0 (C_q), 141.3 (C_q), 138.3 (CH), 138.3 (C_q), 135.4 (C_q), 135.4 (C_q), 134.2 (C_q), 131.3 (C_q), 130.7 (CH), 129.4 (CH), 129.0 (C_q), 127.1 (CH), 126.3 (CH), 123.9 (CH), 122.5 (CH), 122.2 (CH), 121.2 (CH), 119.0 (CH), 117.8 (CH), 113.6 (C_q), 110.7 (CH), 79.9 (C_q), 54.4 (CH), 52.4 (CH₃), 28.8 (CH₂), 28.2 (CH₃), 14.6 (CH₃), 14.6 (CH₃). (Two aromatic CH are missing due to overlap, the overlap was verified by HSQC analysis, showing that the peaks at 126.3 and 121.2 ppm correspond to two carbons). **¹⁹F NMR** (282 MHz, CDCl₃): δ -146.30 (q, $^1J_{B-F}$ = 32.0 Hz). **IR** (ATR): 2971, 2921, 1738, 1706, 1541, 1505, 1468, 1435, 1190, 1153, 973, 728 cm⁻¹. **MS** (ESI) m/z (relative intensity): 766 (100) $[M+Na]^+$, 744 (5) $[M+H]^+$. **HR-MS** (ESI): m/z calcd for $C_{43}H_{46}BF_2N_5O_4^+$ $[M+H]^+$: 744.3535, found: 744.3525.

Methyl (S,E)-2-[(*tert*-butoxycarbonyl)amino]-3-{2-[4-(5,5-difluoro-3,7-diphenyl-5*H*-4 λ ₄,5 λ ₄-dipyrrolo[1,2-*c*:2',1'-*f*][1,3,2]diazaborinin-10-yl)styryl]-1-[pyridin-2-yl]-1*H*-indol-3-yl}propanoate (292c**)**

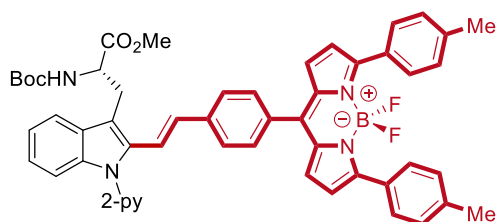


The general procedure **O** was followed using methyl *N*_α-(*tert*-butoxycarbonyl)-1-(pyridin-2-yl)-L-tryptophanate **153** (39.5 mg, 0.10 mmol), 10-(4-ethynylphenyl)-5,5-difluoro-3,7-diphenyl-5*H*-4 λ ₄,5 λ ₄-dipyrrolo[1,2-*c*:2',1'-*f*][1,3,2]diazaborinine **294c** (48.9 mg, 0.11 mmol), MnBr(CO)₅ (5.5 mg, 20 mol %) and 1-AdCO₂H (7.2 mg, 40 mol %) in 1,4-dioxane (1.0 mL). Purification by column chromatography on silica gel (CH₂Cl₂/MeOH: 99/1) yielded **292c** (45.3 mg, 54%) as a purple solid.

M. p.: 128 – 130 °C. **¹H NMR** (300 MHz, CDCl₃): δ 8.78 (d, *J* = 4.8 Hz, 1H), 7.99 – 7.85 (m, 5H), 7.64 (d, *J* = 6.7 Hz, 1H), 7.60 – 7.52 (m, 4H), 7.51 – 7.35 (m, 9H), 7.33 – 7.29 (m, 1H), 7.28 – 7.17 (m, 2H), 6.94 (d, *J* = 4.3 Hz, 2H), 6.66 (d, *J* = 4.3 Hz, 2H), 6.57 (d, *J* = 16.7 Hz, 1H), 5.27 (d, *J* = 8.4 Hz, 1H), 4.80 (ddd, *J* = 8.4, 6.9, 6.9 Hz, 1H), 3.69 – 3.40 (m, 5H), 1.42 (s, 9H). **¹³C NMR** (75 MHz, CDCl₃): δ 172.7 (C_q), 158.8 (C_q), 155.1 (C_q), 152.1 (C_q), 149.7 (CH), 143.8 (C_q), 139.4 (C_q), 138.5 (CH), 138.4 (C_q), 136.2 (C_q), 134.4 (C_q), 133.6 (C_q), 132.6 (C_q), 131.2 (CH), 130.7 (CH), 129.5 (CH), 129.5 (CH), 129.4 (CH), 129.0 (C_q), 128.2 (CH), 126.2 (CH), 124.2 (CH), 122.4 (CH), 122.3 (CH), 121.4 (CH), 120.9 (CH), 119.1 (CH), 118.9 (CH), 114.1 (C_q), 110.9 (CH), 79.9 (C_q), 54.3 (CH), 52.5 (CH₃), 28.7 (CH₃), 28.3 (CH₂). **¹⁹F NMR** (282 MHz, CDCl₃): δ – 132.45 (q, ¹*J*_{B-F} = 31.7 Hz). **IR** (ATR): 3439, 2923, 1739, 1707, 1561, 1537, 1466, 1435, 1135, 1066, 728 cm⁻¹. **MS** (ESI): *m/z* (relative intensity): 862 (100) [M+Na]⁺, 840 (71) [M+H]⁺. **HR-MS** (ESI): *m/z* calcd for C₅₁H₄₅BF₂N₅O₄ [M+H]⁺: 840.3536, found: 840.3517.

5. Experimental Part

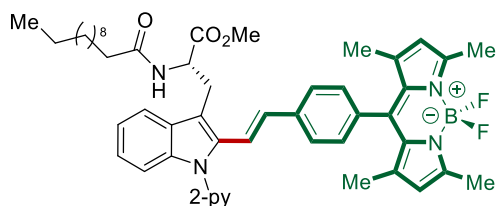
Methyl (S,E)-2-[(*tert*-butoxycarbonyl)amino]-3-{2-[4-(5,5-difluoro-3,7-di-*p*-tolyl-5*H*-4 λ ₄,5 λ ₄-dipyrrolo[1,2-*c*:2',1'-*f*][1,3,2]diazaborinin-10-yl)styryl]-1-[pyridin-2-yl]-1*H*-indol-3-yl}propanoate (**292d**)



The general procedure **O** was followed using methyl *N*_α-(*tert*-butoxycarbonyl)-1-(pyridin-2-yl)-L-tryptophanate **153** (39.5 mg, 0.10 mmol), 10-(4-ethynylphenyl)-5,5-difluoro-3,7-di-*p*-tolyl-5*H*-4 λ ₄,5 λ ₄-dipyrrolo[1,2-*c*:2',1'-*f*][1,3,2]diazaborinine **294d** (51.9 mg, 0.11 mmol), MnBr(CO)₅ (5.5 mg, 20 mol %) and (1-Ad)CO₂H (7.2 mg, 40 mol %) in 1,4-dioxane (1.0 mL). Purification by column chromatography on silica gel (CH₂Cl₂/MeOH: 99/1) yielded **292d** (63.3 mg, 73%) as a purple solid.

M. p.: 158 – 160 °C. **¹H NMR** (400 MHz, CDCl₃): δ 8.79 (d, *J* = 4.7 Hz, 1H), 7.93 (dd, *J* = 7.8, 7.8 Hz, 1H), 7.83 (d, *J* = 7.7 Hz, 4H), 7.65 (d, *J* = 7.5 Hz, 1H), 7.59 – 7.48 (m, 5H), 7.44 – 7.39 (m, 2H), 7.34 (d, *J* = 16.6 Hz, 1H), 7.29 – 7.24 (m, 6H), 6.91 (d, *J* = 4.3 Hz, 2H), 6.65 (d, *J* = 4.3 Hz, 2H), 6.58 (d, *J* = 16.6 Hz, 1H), 5.28 (d, *J* = 8.4 Hz, 1H), 4.81 (ddd, *J* = 8.4, 7.3, 7.3 Hz, 1H), 3.81 – 3.45 (m, 5H), 2.42 (s, 6H), 1.43 (s, 9H). **¹³C NMR** (101 MHz, CDCl₃): δ 172.6 (C_q), 158.7 (C_q), 155.0 (C_q), 152.0 (C_q), 149.6 (CH), 142.9 (C_q), 139.6 (C_q), 139.1 (C_q), 138.4 (CH), 138.3 (C_q), 136.1 (C_q), 134.3 (C_q), 133.7 (C_q), 131.1 (CH), 130.6 (CH), 130.3 (CH), 129.8 (C_q), 129.3 (CH), 129.0 (CH), 129.0 (C_q), 126.1 (CH), 124.1 (CH), 122.3 (CH), 122.2 (CH), 121.3 (CH), 120.6 (CH), 119.0 (CH), 118.7 (CH), 113.9 (C_q), 110.9 (CH), 79.8 (C_q), 54.3 (CH), 52.4 (CH₃), 28.6 (CH₂), 28.2 (CH₃), 21.4 (CH₃). **¹⁹F NMR** (376 MHz, CDCl₃): δ – 132.59 (q, ¹*J*_{B-F} = 32.1 Hz). **IR** (ATR): 2920, 1740, 1707, 1561, 1537, 1465, 1432, 1279, 1137, 1055, 727 cm⁻¹. **MS** (ESI): *m/z* (relative intensity) 890 (100) [M+Na]⁺, 868 (58) [M+H]⁺. **HR-MS** (ESI): *m/z* calcd for C₅₃H₄₉BF₂N₅O₄ [M+H]⁺: 868.3849, found: 868.3834.

Methyl (S,E)-3-{2-[4-(5,5-difluoro-1,3,7,9-tetramethyl-5*H*-4 λ ₄,5 λ ₄-dipyrrolo[1,2-*c*:2',1'-*f*][1,3,2]diazaborinin-10-yl)styryl]-1-[pyridin-2-yl]-1*H*-indol-3-yl]-2-dodecanamidopropanoate (296a)

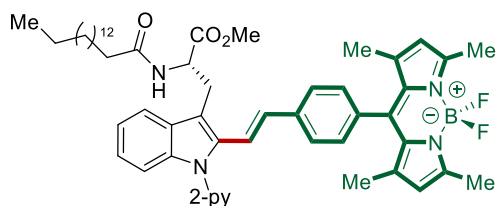


The general procedure **O** was followed using methyl *N_a*-dodecanoyl-1-(pyridin-2-yl)-L-tryptophanate **295a** (47.8 mg, 0.10 mmol), 10-(4-ethynylphenyl)-5,5-difluoro-1,3,7,9-tetramethyl-5*H*-4 λ ₄,5 λ ₄-dipyrrolo[1,2-*c*:2',1'-*f*][1,3,2]diazaborinine **294a** (38.3 mg, 0.11 mmol), MnBr(CO)₅ (5.5 mg, 20 mol %) and 1-AdCO₂H (7.2 mg, 40 mol %) in 1,4-dioxane (1.0 mL). Purification by column chromatography on silica gel (*n*-hexane/EtOAc: 8/2) yielded **296a** (54.6 mg, 66%) as an orange solid.

M. p. 114 – 117 °C. **¹H NMR** (600 MHz, CDCl₃): δ 8.72 (ddd, *J* = 4.9, 2.0, 0.9 Hz, 1H), 7.89 (ddd, *J* = 7.7, 7.7, 2.0 Hz, 1H), 7.55 (ddd, *J* = 7.7, 0.9, 0.9 Hz, 1H), 7.43 (d, *J* = 8.2 Hz, 2H), 7.40 – 7.35 (m, 3H), 7.21 – 7.13 (m, 5H), 6.46 (d, *J* = 16.8 Hz, 1H), 6.08 (d, *J* = 7.9 Hz, 1H), 5.95 (s, 2H), 5.00 (ddd, *J* = 7.9, 7.1, 5.1 Hz, 1H), 3.58 (dd, *J* = 14.6, 5.1 Hz, 1H), 3.55 – 3.52 (dd, *J* = 14.6, 7.1 Hz, 1H), 3.51 (s, 3H), 2.53 (s, 6H), 2.10 – 2.04 (m, 2H), 1.56 – 1.46 (m, 2H), 1.39 (s, 6H), 1.28 – 1.16 (m, 16H), 0.85 (t, *J* = 7.1 Hz, 3H). **¹³C NMR** (151 MHz, CDCl₃): δ 172.7 (C_q), 172.4 (C_q), 155.5 (C_q), 151.9 (C_q), 149.7 (CH), 142.9 (C_q), 141.3 (C_q), 138.4 (CH), 138.3 (C_q), 137.8 (C_q), 134.3 (C_q), 134.2 (C_q), 131.3 (C_q), 130.4 (CH), 129.0 (C_q), 128.4 (CH), 126.8 (CH), 124.0 (CH), 122.5 (CH), 122.3 (CH), 121.2 (CH), 121.2 (CH), 118.8 (CH), 117.8 (CH), 113.3 (C_q), 110.8 (CH), 52.7 (CH), 52.4 (CH₃), 36.5 (CH₂), 31.9 (CH₂), 29.6 (CH₂), 29.5 (CH₂), 29.4 (CH₂), 29.3 (CH₂), 29.3 (CH₂), 29.2 (CH₂), 27.8 (CH₂), 25.3 (CH₂), 22.6 (CH₂), 14.6 (CH₃), 14.5 (CH₃), 14.1 (CH₃). **¹⁹F NMR** (282 MHz, CDCl₃): δ – 146.28 (q, ¹*J*_{B-F} = 32.2 Hz). **IR** (ATR): 2921, 2851, 1740, 1653, 1540, 1508, 1466, 1191, 1154, 1081, 973, 741 cm⁻¹. **MS** (ESI): *m/z* (relative intensity) 848 (41) [M+Na]⁺, 826 (100) [M+H]⁺. **HR-MS** (ESI): *m/z* calcd for C₅₀H₅₉BF₂N₅O₃⁺ [M+H]⁺: 826.4682, found: 826.4660.

5. Experimental Part

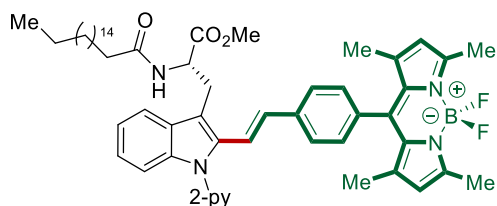
Methyl (S,E)-3-{2-[4-(5,5-difluoro-1,3,7,9-tetramethyl-5H-4 λ ₄,5 λ ₄-dipyrrolo[1,2-c:2',1'-f][1,3,2]diazaborinin-10-yl)styryl]-1-[pyridin-2-yl]-1H-indol-3-yl}-2-palmitamidopropanoate (**296b**)



The general procedure **O** was followed using methyl *N_a*-palmitoyl-1-(pyridin-2-yl)-L-tryptophanate **295b** (53.3 mg, 0.10 mmol), 10-(4-ethynylphenyl)-5,5-difluoro-1,3,7,9-tetramethyl-5H-4 λ ₄,5 λ ₄-dipyrrolo[1,2-c:2',1'-f][1,3,2]diazaborinine **294a** (38.3 mg, 0.11 mmol), MnBr(CO)₅ (5.5 mg, 20 mol %) and 1-AdCO₂H (7.2 mg, 40 mol %) in 1,4-dioxane (1.0 mL). Purification by column chromatography on silica gel (*n*-hexane/EtOAc: 8/2) yielded **296b** (59.9 mg, 68%) as an orange solid.

M. p. 122 – 124 °C. **¹H NMR** (400 MHz, CDCl₃): δ 8.77 (dd, *J* = 5.0, 1.8 Hz, 1H), 7.94 (ddd, *J* = 7.8, 7.8, 2.0 Hz, 1H), 7.59 (dd, *J* = 7.0, 1.7 Hz, 1H), 7.47 (d, *J* = 8.0 Hz, 2H), 7.45 – 7.39 (m, 3H), 7.27 – 7.16 (m, 5H), 6.50 (d, *J* = 16.8 Hz, 1H), 6.11 (d, *J* = 7.8 Hz, 1H), 5.99 (s, 2H), 5.05 (ddd, *J* = 7.8, 7.1, 5.2 Hz, 1H), 3.63 (dd, *J* = 14.6, 5.2 Hz, 1H), 3.59 (dd, *J* = 14.6, 7.1 Hz, 1H), 3.55 (s, 3H), 2.57 (s, 6H), 2.11 (t, *J* = 7.7 Hz, 2H), 1.63 – 1.49 (m, 2H), 1.43 (s, 6H), 1.31 – 1.17 (m, 24H), 0.90 (t, *J* = 6.7 Hz, 3H). **¹³C NMR** (101 MHz, CDCl₃): δ 172.7 (C_q), 172.4 (C_q), 155.5 (C_q), 152.0 (C_q), 149.7 (CH), 142.9 (C_q), 141.3 (C_q), 138.4 (CH), 138.3 (C_q), 137.8 (C_q), 134.3 (C_q), 134.3 (C_q), 131.3 (C_q), 130.4 (CH), 129.0 (C_q), 128.4 (CH), 126.8 (CH), 124.0 (CH), 122.5 (CH), 122.4 (CH), 121.3 (CH), 121.2 (CH), 118.8 (CH), 117.8 (CH), 113.3 (C_q), 110.8 (CH), 52.7 (CH), 52.4 (CH₃), 36.6 (CH₂), 31.9 (CH₂), 29.7 (CH₂), 29.7 (CH₂), 29.6 (CH₂), 29.6 (CH₂), 29.6 (CH₂), 29.4 (CH₂), 29.3 (CH₂), 29.3 (CH₂), 29.2 (CH₂), 27.8 (CH₂), 25.4 (CH₂), 22.7 (CH₂), 14.6 (CH₃), 14.6 (CH₃), 14.1 (CH₃). (One aliphatic CH₂ is missing due to overlap). **¹⁹F NMR** (376 MHz, CDCl₃): δ – 146.29 (q, ¹*J*_{B-F} = 32.1 Hz). **IR** (ATR): 2924, 1739, 1541, 1509, 1468, 1435, 1193, 982, 741 cm⁻¹. **MS** (ESI): *m/z* (relative intensity) 904 (38) [M+Na]⁺, 882 (100) [M+H]⁺. **HR-MS** (ESI): *m/z* calcd for C₅₄H₆₇BF₂N₅O₃⁺ [M+H]⁺: 882.5309, found: 882.5273.

Methyl (S,E)-3-{2-[4-(5,5-difluoro-1,3,7,9-tetramethyl-5H-4λ₄,5λ₄-dipyrrolo[1,2-c:2',1'-f][1,3,2]diazaborinin-10-yl)styryl)-1-[pyridin-2-yl]-1H-indol-3-yl]-2-stearamidopropanoate (296c)

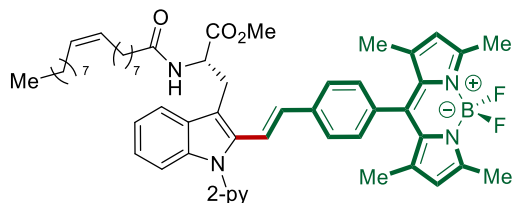


The general procedure **O** was followed using methyl 1-(pyridin-2-yl)-*N*_α-stearyl-L-tryptophanate **295c** (56.1 mg, 0.10 mmol), 10-(4-ethynylphenyl)-5,5-difluoro-1,3,7,9-tetramethyl-5H-4λ₄,5λ₄-dipyrrolo[1,2-c:2',1'-f][1,3,2]diazaborinine **294a** (38.3 mg, 0.11 mmol), MnBr(CO)₅ (5.5 mg, 20 mol %) and 1-AdCO₂H (7.2 mg, 40 mol %) in 1,4-dioxane (1.0 mL). Purification by column chromatography on silica gel (*n*-hexane/EtOAc: 8/2) yielded **296c** (60.0 mg, 66%) as an orange solid.

M. p. 125 – 127 °C. **¹H NMR** (400 MHz, CDCl₃): δ 8.77 (dd, *J* = 5.0, 1.8 Hz, 1H), 7.94 (td, *J* = 7.7, 1.9 Hz, 1H), 7.62 – 7.55 (m, 1H), 7.50 – 7.45 (m, 2H), 7.45 – 7.38 (m, 3H), 7.26 – 7.17 (m, 5H), 6.50 (d, *J* = 16.7 Hz, 1H), 6.12 (d, *J* = 7.8 Hz, 1H), 5.99 (s, 2H), 5.05 (ddd, *J* = 7.2, 7.2, 5.1 Hz, 1H), 3.63 (dd, *J* = 14.6, 5.2 Hz, 1H), 3.60 – 3.57 (m, 1H), 3.55 (s, 3H), 2.57 (s, 6H), 2.11 (dd, *J* = 8.5, 6.9 Hz, 2H), 1.55 (t, *J* = 7.3 Hz, 2H), 1.43 (s, 6H), 1.33 – 1.18 (m, 28H), 0.89 (t, *J* = 7.1 Hz, 3H). **¹³C NMR** (101 MHz, CDCl₃): δ 172.7 (C_q), 172.4 (C_q), 155.5 (C_q), 152.0 (C_q), 149.7 (CH), 142.9 (C_q), 141.3 (C_q), 138.4 (CH), 138.3 (C_q), 137.8 (C_q), 134.3 (C_q), 134.3 (C_q), 131.3 (C_q), 130.5 (CH), 129.0 (C_q), 128.4 (CH), 126.8 (CH), 124.0 (CH), 122.5 (CH), 122.4 (CH), 121.3 (CH), 121.2 (CH), 118.8 (CH), 117.8 (CH), 113.3 (C_q), 110.8 (CH), 52.7 (CH), 52.4 (CH₃), 38.7 (CH₂), 36.6 (CH₂), 36.4 (CH₂), 31.9 (CH₂), 29.7 (CH₂), 29.7 (CH₂), 29.6 (CH₂), 29.6 (CH₂), 29.6 (CH₂), 29.4 (CH₂), 29.3 (CH₂), 29.3 (CH₂), 29.2 (CH₂), 27.8 (CH₂), 25.4 (CH₂), 22.7 (CH₂), 14.6 (CH₃), 14.6 (CH₃), 14.1 (CH₃). (One aliphatic CH₂ is missing due to overlap). **¹⁹F NMR** (376 MHz, CDCl₃): δ – 146.30 (q, ¹*J*_{B-F} = 32.2 Hz). **IR** (ATR): 2921, 2850, 1740, 1712, 1541, 1508, 1456, 1435, 1192, 975, 742 cm⁻¹. **MS** (ESI): *m/z* (relative intensity) 932 (100) [M+Na]⁺, 910 (57) [M+H]⁺. **HR-MS** (ESI): *m/z* calcd for C₅₆H₇₁BF₂N₅O₃ [M+H]⁺: 910.5622, found: 910.5592.

5. Experimental Part

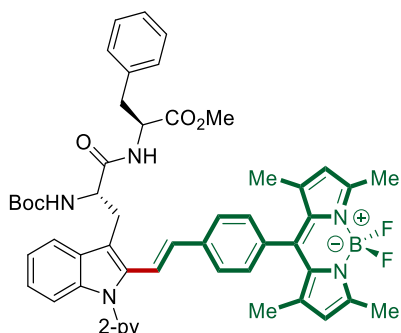
Methyl (S)-3-{2-[(E)-4-(5,5-difluoro-1,3,7,9-tetramethyl-5H-4λ₄,5λ₄-dipyrrolo[1,2-c:2',1'-f][1,3,2]diazaborinin-10-yl)styryl]-1-[pyridin-2-yl]-1H-indol-3-yl}-2-oleamidopropanoate (296d)



The general procedure **O** was followed using methyl *N_a*-oleoyl-1-(pyridin-2-yl)-L-tryptophanate **295d** (56.0 mg, 0.10 mmol), 10-(4-ethynylphenyl)-5,5-difluoro-1,3,7,9-tetramethyl-5H-4λ₄,5λ₄-dipyrrolo[1,2-c:2',1'-f][1,3,2]diazaborinine **294a** (38.3 mg, 0.11 mmol), MnBr(CO)₅ (5.5 mg, 20 mol %) and 1-AdCO₂H (7.2 mg, 40 mol %) in 1,4-dioxane (1.0 mL). Purification by column chromatography on silica gel (*n*-hexane/EtOAc: 8/2) yielded **296d** (48.1 mg, 53%) as an orange solid.

M. p. 116 – 118 °C. **¹H NMR** (400 MHz, CDCl₃): δ 8.77 (d, *J* = 4.7 Hz, 1H), 7.94 (ddd, *J* = 7.9, 7.9 1.6 Hz, 1H), 7.60 (d, *J* = 7.4 Hz, 1H), 7.48 (d, *J* = 7.7 Hz, 2H), 7.46 – 7.38 (m, 3H), 7.28 – 7.16 (m, 5H), 6.50 (d, *J* = 16.7 Hz, 1H), 6.11 (d, *J* = 7.8 Hz, 1H), 6.00 (s, 2H), 5.43 – 5.28 (m, 2H), 5.05 (ddd, *J* = 7.8, 7.1, 5.2 Hz, 1H), 3.64 (dd, *J* = 14.7, 5.2 Hz, 1H), 3.59 (dd, *J* = 14.7, 7.1 Hz, 1H), 3.56 (s, 3H), 2.58 (s, 6H), 2.17 – 1.90 (m, 6H), 1.62 – 1.49 (m, 2H), 1.43 (s, 6H), 1.36 – 1.21 (m, 20H), 0.90 (t, *J* = 6.6 Hz, 3H). **¹³C NMR** (101 MHz, CDCl₃): δ 172.7 (C_q), 172.4 (C_q), 155.5 (C_q), 152.0 (C_q), 149.7 (CH), 142.9 (C_q), 141.3 (C_q), 138.4 (CH), 138.3 (C_q), 137.8 (C_q), 134.3 (C_q), 134.3 (C_q), 131.3 (C_q), 130.5 (CH), 130.0 (CH), 129.7 (CH), 129.0 (C_q), 128.4 (CH), 126.8 (CH), 124.0 (CH), 122.5 (CH), 122.4 (CH), 121.3 (CH), 121.2 (CH), 118.8 (CH), 117.8 (CH), 113.3 (C_q), 110.8 (CH), 52.7 (CH), 52.4 (CH₃), 36.6 (CH₂), 31.9 (CH₂), 29.7 (CH₂), 29.7 (CH₂), 29.5 (CH₂), 29.3 (CH₂), 29.3 (CH₂), 29.2 (CH₂), 29.2 (CH₂), 29.1 (CH₂), 27.8 (CH₂), 27.2 (CH₂), 27.2 (CH₂), 25.4 (CH₂), 22.7 (CH₂), 14.6 (CH₃), 14.6 (CH₃), 14.1 (CH₃). **¹⁹F NMR** (377 MHz, CDCl₃): δ – 146.30 (q, ¹*J*_{B-F} = 32.2 Hz). **IR** (ATR): 2922, 2850, 1736, 1666, 1650, 1541, 1509, 1305, 1193, 951, 705 cm⁻¹. **MS** (ESI): *m/z* (relative intensity) 931 (100) [M+Na]⁺, 909 (56) [M+H]⁺. **HR-MS** (ESI): *m/z* calcd for C₅₆H₆₈BF₂N₅O₃Na⁺ [M+Na]⁺: 930.5285, found: 930.5263.

Methyl ((S)-2-[[*tert*-butoxycarbonyl]amino]-3-{2-[(*E*)-4-(5,5-difluoro-1,3,7,9-tetramethyl-5*H*-4 λ ₄,5 λ ₄-dipyrrolo[1,2-*c*:2',1'-*f*][1,3,2]diazaborinin-10-yl)styryl]-1-[pyridin-2-yl]-1*H*-indol-3-yl}propanoyl)-L-phenylalaninate (297a)

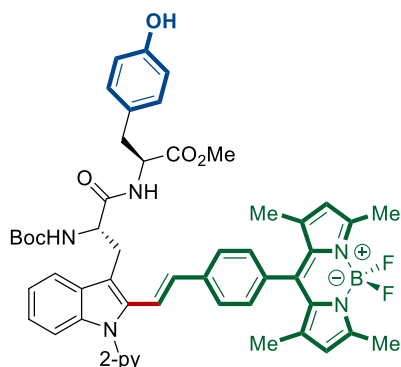


The general procedure **O** was followed using methyl *N*_α-(*tert*-butoxycarbonyl)-1-(pyridin-2-yl)-L-tryptophyl-L-phenylalaninate **243m** (54.3 mg, 0.10 mmol), 10-(4-ethynylphenyl)-5,5-difluoro-1,3,7,9-tetramethyl-5*H*-4 λ ₄,5 λ ₄-dipyrrolo[1,2-*c*:2',1'-*f*][1,3,2]diazaborinine **294a** (38.3 mg, 0.11 mmol), MnBr(CO)₅ (5.5 mg, 20 mol %) and (1-Ad)CO₂H (7.2 mg, 40 mol %) in 1,4-dioxane (1.0 mL). Purification by column chromatography on silica gel (CH₂Cl₂/MeOH: 100/0.2) yielded **297a** (48.3 mg, 54%) as an orange solid. The reaction was also performed at 60 °C, using **294a** (69.6 mg, 0.11 mmol), and yielded **297a** (46.6 mg, 52%).

M. p. 129 – 133 °C. **¹H NMR** (400 MHz, CDCl₃): δ 8.72 (d, *J* = 3.6 Hz, 1H), 7.89 (dd, *J* = 7.7, 7.7, 1.8 Hz, 1H), 7.66 – 7.60 (m, 1H), 7.52 (d, *J* = 7.8 Hz, 2H), 7.43 (d, *J* = 7.7 Hz, 1H), 7.38 (dd, *J* = 7.7, 3.6 Hz, 1H), 7.35 – 7.33 (m, 1H), 7.30 (d, *J* = 16.7 Hz, 1H), 7.18 (d, *J* = 7.8 Hz, 2H), 7.17 – 7.14 (m, 5H), 6.87 – 6.85 (m, 2H), 6.67 (d, *J* = 16.7 Hz, 1H), 5.98 (brs, 1H), 5.96 (s, 2H), 5.45 (brs, 1H), 4.60 – 4.40 (m, 2H), 3.57 – 3.50 (m, 1H), 3.38 (s, 3H), 3.36 – 3.32 (m, 1H), 2.95 (dd, *J* = 13.7, 5.9 Hz, 1H), 2.87 (dd, *J* = 13.7, 5.0 Hz, 1H), 2.54 (s, 6H), 1.43 (s, 6H), 1.41 (s, 9H). **¹³C NMR** (101 MHz, CDCl₃): δ 170.7 (C_q), 170.4 (C_q), 155.3 (C_q), 155.1 (C_q), 151.7 (C_q), 149.6 (CH), 143.0 (C_q), 141.5 (C_q), 138.3 (CH), 138.0 (C_q), 135.4 (C_q), 134.1 (C_q), 134.0 (C_q), 131.3 (C_q), 130.5 (CH), 129.1 (CH), 128.9 (C_q), 128.8 (C_q), 128.3 (CH), 128.2 (CH), 127.0 (CH), 126.9 (CH), 123.8 (CH), 122.4 (CH), 122.3 (CH), 121.3 (CH), 121.1 (CH), 118.8 (CH), 117.9 (CH), 113.1 (C_q), 110.6 (CH), 79.9 (C_q), 55.4 (CH), 53.5 (CH), 52.0 (CH₃), 37.9 (CH₂), 29.1 (CH₂), 28.2 (CH₃), 14.6 (CH₃), 14.5 (CH₃). **¹⁹F NMR** (376 MHz, CDCl₃): δ – 146.3 (q, ¹*J*_{B-F} = 32.1 Hz). **IR** (ATR): 3397, 3316, 3057, 2975, 2928, 1741, 1707, 1672, 1541, 1508 cm⁻¹. **MS** (ESI): *m/z* (relative intensity) 913 (100) [M+Na]⁺, 891 (85) [M+H]⁺. **HR-MS** (ESI) *m/z* calcd for C₅₂H₅₃BF₂N₆O₅Na [M+Na]⁺: 913.4036, found: 913.4037.

5. Experimental Part

Methyl ((S)-2-[[*tert*-butoxycarbonyl]amino]-3-{2-[(*E*)-4-(5,5-difluoro-1,3,7,9-tetramethyl-5*H*-4 λ ₄,5 λ ₄-dipyrrolo[1,2-*c*:2',1'-*f*][1,3,2]diazaborinin-10-yl)styryl]-1-[pyridin-2-yl]-1*H*-indol-3-yl]propanoyl)-L-tyrosinate (**297b**)

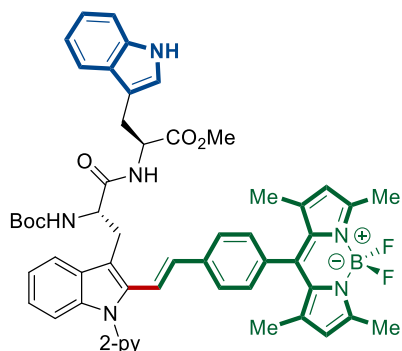


The general procedure **O** was followed using methyl *N*_α-(*tert*-butoxycarbonyl)-1-(pyridin-2-yl)-L-tryptophyl-L-tyrosinate **243o** (55.7 mg, 0.10 mmol), 10-(4-ethynylphenyl)-5,5-difluoro-1,3,7,9-tetramethyl-5*H*-4 λ ₄,5 λ ₄-dipyrrolo[1,2-*c*:2',1'-*f*][1,3,2]diazaborinine **294a** (38.3 mg, 0.11 mmol), MnBr(CO)₅ (5.5 mg, 20 mol %) and (1-Ad)CO₂H (7.2 mg, 40 mol %) in 1,4-dioxane (1.0 mL). Purification by column chromatography on silica gel (CH₂Cl₂/MeOH: 100/0.7) yielded **297b** (61.1 mg, 67%) as an orange solid.

M. p. 158 – 162 °C. **¹H NMR** (400 MHz, CDCl₃): δ 8.77 (dd, *J* = 4.8, 1.9 Hz, 1H), 7.94 (ddd, *J* = 7.7, 7.7, 1.9 Hz, 1H), 7.64 (dd, *J* = 7.7, 1.9 Hz, 1H), 7.53 (d, *J* = 7.7 Hz, 2H), 7.48 – 7.41 (m, 2H), 7.35 (dd, *J* = 7.7, 4.8 Hz, 1H), 7.34 (d, *J* = 18.2 Hz, 1H), 7.21 (d, *J* = 7.7 Hz, 2H), 7.19 – 7.15 (m, 2H), 6.65 (d, *J* = 8.4 Hz, 2H), 6.56 (d, *J* = 8.4 Hz, 2H), 6.52 (d, *J* = 18.2 Hz, 1H), 6.45 (brs, 1H), 6.06 (brs, 1H), 5.99 (s, 2H), 5.39 (brs, 1H), 4.60 – 4.53 (m, 1H), 4.49 (ddd, *J* = 5.8, 5.8, 5.7 Hz, 1H), 3.62 (d, *J* = 12.4 Hz, 1H), 3.47 (s, 3H), 3.35 (dd, *J* = 12.4, 9.3 Hz, 1H), 2.90 (dd, *J* = 13.9, 5.7 Hz, 1H), 2.80 (dd, *J* = 13.9, 5.8 Hz, 1H), 2.57 (s, 6H), 1.46 (s, 9H), 1.44 (s, 6H). **¹³C NMR** (101 MHz, CDCl₃): δ 170.9 (C_q), 170.7 (C_q), 155.4 (C_q), 155.2 (C_q), 155.0 (C_q), 151.9 (C_q), 149.4 (CH), 143.1 (C_q), 141.5 (C_q), 138.7 (CH), 138.3 (C_q), 137.9 (C_q), 134.3 (C_q), 134.1 (C_q), 131.3 (C_q), 130.5 (CH), 130.1 (CH), 128.8 (C_q), 128.2 (CH), 127.1 (CH), 127.0 (C_q), 123.9 (CH), 122.8 (CH), 122.7 (CH), 121.4 (CH), 121.1 (CH), 119.1 (CH), 117.8 (CH), 115.6 (CH), 113.4 (C_q), 110.5 (CH), 80.1 (C_q), 55.3 (CH), 53.5 (CH), 52.1 (CH₃), 36.9 (CH₂), 28.5 (CH₂), 28.3 (CH₃), 14.7 (CH₃), 14.6 (CH₃). **¹⁹F NMR** (376 MHz, CDCl₃): δ – 146.24 (q, ¹*J*_{B-F} = 31.7 Hz). **IR** (ATR): 3388, 3300, 2971, 2926, 2856, 1741, 1709, 1670, 1542,

1509 cm^{-1} . **MS** (ESI): m/z (relative intensity): 929 (100) $[\text{M}+\text{Na}]^+$, 907 (90) $[\text{M}+\text{H}]^+$. **HR-MS** (ESI): m/z calcd for $\text{C}_{52}\text{H}_{53}\text{BF}_2\text{N}_6\text{O}_6\text{Na}$ $[\text{M}+\text{Na}]^+$:929.3989, found: 929.3982.

Methyl ((*S*)-2-[(*tert*-butoxycarbonyl)amino]-3-{2-[(*E*)-4-(5,5-difluoro-1,3,7,9-tetramethyl-5*H*-4 λ ,5 λ -dipyrrolo[1,2-*c*:2',1'-*f*][1,3,2]diazaborinin-10-yl)styryl]-1-[pyridin-2-yl]-1*H*-indol-3-yl}propanoyl)-*L*-tryptophanate (**297c**)



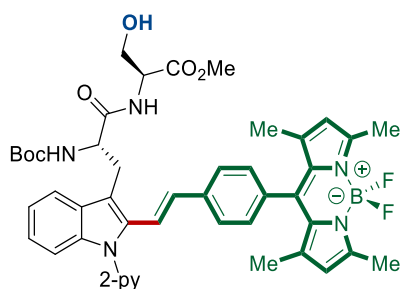
The general procedure **O** was followed using methyl *N*_a-(*tert*-butoxycarbonyl)-1-(pyridin-2-yl)-*L*-tryptophyl-*L*-tryptophanate **243ag** (52.5 mg, 0.10 mmol), 10-(4-ethynylphenyl)-5,5-difluoro-1,3,7,9-tetramethyl-5*H*-4 λ ,5 λ -dipyrrolo[1,2-*c*:2',1'-*f*][1,3,2]diazaborinine **294a** (38.3 mg, 0.11 mmol), $\text{MnBr}(\text{CO})_5$ (5.5 mg, 20 mol %) and 1-AdCO₂H (7.2 mg, 40 mol %) in 1,4-dioxane (1.0 mL). Purification by column chromatography on silica gel (*n*-hexane/CH₂C: 10/1) yielded **297c** (67.8 mg, 73%) as an orange solid.

M. p. 160 – 162 °C. **¹H NMR** (400 MHz, CDCl₃): δ 8.79 (dd, $J = 4.9, 1.9$ Hz, 1H), 8.56 (d, $J = 2.4$ Hz, 1H), 7.90 (ddd, $J = 7.7, 7.7, 2.0$ Hz, 1H), 7.74 – 7.65 (m, 1H), 7.51 – 7.40 (m, 3H), 7.39 – 7.28 (m, 4H), 7.24 (d, $J = 8.2$ Hz, 1H), 7.22 – 7.15 (m, 4H), 7.08 (dd, $J = 7.7, 7.7$ Hz, 1H), 6.94 (dd, $J = 7.5, 7.5$ Hz, 1H), 6.49 (d, $J = 2.4$ Hz, 1H), 6.41 (d, $J = 16.8$ Hz, 1H), 6.09 (d, $J = 6.9$ Hz, 1H), 5.97 (s, 2H), 5.36 (d, $J = 7.5$ Hz, 1H), 4.71 – 4.46 (m, 2H), 3.71 – 3.56 (m, 1H), 3.43 (s, 3H), 3.36 (dd, $J = 14.4, 9.1$ Hz, 1H), 3.11 (dd, $J = 14.8, 5.4$ Hz, 1H), 3.04 (dd, $J = 14.8, 5.6$ Hz, 1H), 2.55 (s, 6H), 1.48 – 1.36 (m, 15H). **¹³C NMR** (101 MHz, CDCl₃): δ 171.2 (C_q), 170.8 (C_q), 155.4 (C_q), 155.2 (C_q), 152.0 (C_q), 149.5 (CH), 143.1 (C_q), 141.6 (C_q), 138.7 (CH), 138.4 (C_q), 137.9 (C_q), 135.9 (C_q), 134.3 (C_q), 134.1 (C_q), 131.4 (C_q), 130.6 (CH), 128.9 (C_q), 128.2 (CH), 127.3 (C_q), 127.1 (CH), 124.0 (CH), 123.0 (CH), 122.8 (CH), 121.9 (CH), 121.4 (CH), 121.1 (CH), 119.4 (CH), 119.3 (CH), 118.3 (CH), 117.9 (CH), 113.4 (C_q), 111.1 (CH), 110.6 (CH), 109.3 (C_q), 80.0 (C_q), 55.3 (CH), 53.0 (CH), 52.1 (CH₃), 28.5 (CH₂), 28.3 (CH₃), 27.3 (CH₂), 14.6 (CH₃), 14.6 (CH₃). (One aromatic CH is missing due to overlap,

5. Experimental Part

the overlap was verified by HSQC analysis, showing that the peak at 111.1 corresponds to two carbons). ^{19}F NMR (376 MHz, CDCl_3): δ – 146.26 (q, $^1J_{\text{B-F}} = 32.0$ Hz). IR (ATR): 1670, 1509, 1455, 1195, 1156, 904, 723, 647 cm^{-1} . MS (ESI): m/z (relative intensity) 952 (100) $[\text{M}+\text{Na}]^+$, 930 (45) $[\text{M}+\text{H}]^+$. HR-MS (ESI) m/z calcd for $\text{C}_{54}\text{H}_{55}\text{BF}_2\text{N}_7\text{O}_5$ $[\text{M}+\text{H}]^+$:930.4329, found: 930.4330.

Methyl ((S)-2-[(*tert*-butoxycarbonyl)amino]-3-{2-[(*E*)-4-(5,5-difluoro-1,3,7,9-tetramethyl-5*H*-4 λ ,5 λ -dipyrrolo[1,2-*c*:2',1'-*f*][1,3,2]diazaborinin-10-yl)styryl]-1-[pyridin-2-yl]-1*H*-indol-3-yl]propanoyl)-L-serinate (297d)

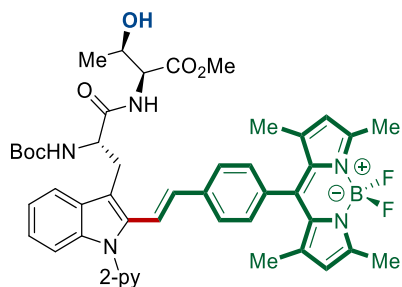


The general procedure **O** was followed using methyl *N*_α-(*tert*-butoxycarbonyl)-1-(pyridin-2-yl)-L-tryptophyl-L-serinate **243n** (48.2 mg, 0.10 mmol), 10-(4-ethynylphenyl)-5,5-difluoro-1,3,7,9-tetramethyl-5*H*-4 λ ,5 λ -dipyrrolo[1,2-*c*:2',1'-*f*][1,3,2]diazaborinine **294a** (69.7 mg, 0.20 mmol), $\text{MnBr}(\text{CO})_5$ (5.5 mg, 20 mol %) and 1-AdCO₂H (7.2 mg, 40 mol %) in 1,4-dioxane (1.0 mL). Purification by column chromatography on silica gel ($\text{CH}_2\text{Cl}_2/\text{EtOAc}$: 7/3) yielded **297d** (65.6 mg, 79%) as an orange solid.

M. p. 158 – 160 °C. ^1H NMR (400 MHz, CDCl_3): δ 8.68 (dd, $J = 4.8, 2.0$ Hz, 1H), 8.05 (ddd, $J = 7.7, 7.7, 1.9$ Hz, 1H), 7.72 – 7.66 (m, 1H), 7.63 (d, $J = 7.9$ Hz, 1H), 7.52 – 7.36 (m, 4H), 7.34 – 7.29 (m, 1H), 7.27 – 7.18 (m, 4H), 6.75 (d, $J = 6.6$ Hz, 1H), 6.27 (d, $J = 16.7$ Hz, 1H), 6.00 (s, 2H), 5.36 (d, $J = 7.7$ Hz, 1H), 4.66 (ddd, $J = 7.7, 7.4, 4.2$ Hz, 1H), 4.51 – 4.41 (m, 1H), 3.91 – 3.82 (m, 2H), 3.81 – 3.71 (m, 2H), 3.64 (s, 3H), 3.42 (dd, $J = 14.6, 7.4$ Hz, 1H), 2.57 (s, 6H), 1.47 (s, 9H), 1.44 (s, 6H). ^{13}C NMR (101 MHz, CDCl_3): δ 171.6 (C_q), 170.1 (C_q), 155.5 (C_q), 155.3 (C_q), 151.7 (C_q), 149.8 (CH), 143.1 (C_q), 141.5 (C_q), 139.1 (CH), 138.6 (C_q), 137.9 (C_q), 134.4 (C_q), 134.3 (C_q), 131.4 (C_q), 130.4 (CH), 129.0 (C_q), 128.4 (CH), 127.0 (CH), 124.3 (CH), 123.0 (CH), 122.4 (CH), 121.7 (CH), 121.2 (CH), 118.8 (CH), 117.9 (CH), 113.9 (C_q), 110.4 (CH), 80.4 (C_q), 62.3 (CH₂), 55.8 (CH), 55.2 (CH), 52.6 (CH₃), 28.3 (CH₃), 27.5 (CH₂), 14.6 (CH₃), 14.6 (CH₃). ^{19}F NMR (376 MHz, CDCl_3): δ – 146.3 (q, $^1J_{\text{B-F}} = 32.1$ Hz). IR (ATR): 3410, 2955, 2925, 1744, 1705, 1674, 1542, 1470, 1195, 1157, 982 cm^{-1} . MS (ESI): m/z

(relative intensity) 853 (65) $[M+Na]^+$, 831 (100) $[M+H]^+$. **HR-MS** (ESI): m/z calcd for $C_{46}H_{50}BF_2N_6O_6^+$ $[M+H]^+$:831.3855, found: 831.3842.

Methyl ((S)-2-[(*tert*-butoxycarbonyl)amino]-3-{2-[(*E*)-4-(5,5-difluoro-1,3,7,9-tetramethyl-5*H*-4 λ ₄,5 λ ₄-dipyrrolo[1,2-*c*:2',1'-*f*][1,3,2]diazaborinin-10-yl)styryl]-1-[pyridin-2-yl]-1*H*-indol-3-yl}propanoyl)-L-threoninate (297e)



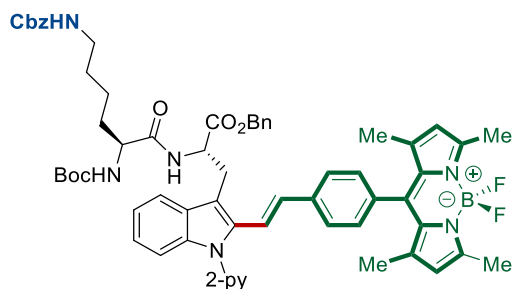
The general procedure **O** was followed using methyl *N*_a-(*tert*-butoxycarbonyl)-1-(pyridin-2-yl)-L-tryptophyl-L-threoninate **243ag** (49.6 mg, 0.10 mmol), 10-(4-ethynylphenyl)-5,5-difluoro-1,3,7,9-tetramethyl-5*H*-4 λ ₄,5 λ ₄-dipyrrolo[1,2-*c*:2',1'-*f*][1,3,2]diazaborinine **294a** (69.7 mg, 0.20 mmol), $MnBr(CO)_5$ (5.5 mg, 20 mol %) and 1-AdCO₂H (7.2 mg, 40 mol %) in 1,4-dioxane (1.0 mL). Purification by column chromatography on silica gel (CH₂Cl₂/EtOAc: 7/3) yielded **297e** (70.0 mg, 83%) as an orange solid.

M. p. 157 – 160 °C. **¹H NMR** (400 MHz, CDCl₃): δ 8.71 (dd, $J = 5.0, 1.9$ Hz, 1H), 7.96 (ddd, $J = 7.7, 7.7, 2.0$ Hz, 1H), 7.76 – 7.63 (m, 1H), 7.56 – 7.48 (m, 3H), 7.45 – 7.39 (m, 1H), 7.36 – 7.28 (m, 2H), 7.23 – 7.15 (m, 4H), 6.57 (d, $J = 16.7$ Hz, 1H), 6.42 (d, $J = 7.6$ Hz, 1H), 5.97 (s, 2H), 5.48 (d, $J = 7.0$ Hz, 1H), 4.58 (ddd, $J = 8.0, 7.0, 5.3$ Hz, 1H), 4.30 (dd, $J = 7.6, 3.5$ Hz, 1H), 4.12 – 3.99 (m, 1H), 3.59 (dd, $J = 14.3, 5.3$ Hz, 1H), 3.52 – 3.37 (m, 4H), 2.79 (d, $J = 6.0$ Hz, 1H), 2.55 (s, 6H), 1.44 (s, 9H), 1.42 (s, 6H), 1.06 (d, $J = 6.4$ Hz, 3H). **¹³C NMR** (101 MHz, CDCl₃): δ 171.8 (C_q), 170.2 (C_q), 155.5 (C_q), 155.3 (C_q), 151.9 (C_q), 149.7 (CH), 143.1 (C_q), 141.6 (C_q), 138.7 (CH), 138.3 (C_q), 138.0 (C_q), 134.3 (C_q), 134.2 (C_q), 131.4 (C_q), 130.7 (CH), 128.8 (C_q), 128.3 (CH), 127.1 (CH), 124.0 (CH), 122.7 (CH), 122.5 (CH), 121.4 (CH), 121.2 (CH), 119.1 (CH), 118.0 (CH), 113.6 (C_q), 110.5 (CH), 80.2 (C_q), 68.3 (CH), 57.8 (CH), 55.5 (CH), 52.4 (CH₃), 28.7 (CH₂), 28.3 (CH₃), 19.9 (CH₃), 14.7 (CH₃), 14.6 (CH₃). **¹⁹F NMR** (376 MHz, CDCl₃): δ – 146.3 (q, $^1J_{B-F} = 32.3$ Hz). **IR** (ATR): 3423, 2976, 2926, 1742, 1706, 1671, 1542, 1469, 1155, 906, 727 cm⁻¹. **MS** (ESI): m/z (relative intensity) 867 (55) $[M+Na]^+$,

5. Experimental Part

845 (100) [M+H]⁺. **HR-MS** (ESI): *m/z* calcd for C₄₇H₅₂BF₂N₆O₆ [M+H]⁺:845.4012, found: 845.3995.

Benzyl (S)-2-({S}-6-{[(benzyloxy)carbonyl]amino}-2-{{tert-butoxycarbonyl}amino}hexanamido)-3-{2-[(E)-4-(5,5-difluoro-1,3,7,9-tetramethyl-5H-4λ₄,5λ₄-dipyrrolo[1,2-c:2',1'-f][1,3,2]diazaborinin-10-yl)styryl]-1-[pyridin-2-yl]-1H-indol-3-yl}propanoate (**297f**)

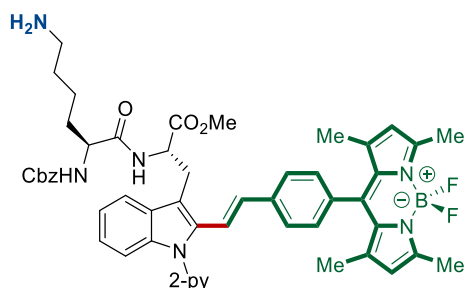


The general procedure **O** was followed using benzyl *N*_a-(*N*₆-((benzyloxy)carbonyl)-*N*₂-(*tert*-butoxycarbonyl)-L-lysyl)-1-(pyridin-2-yl)-L-tryptophanate **243k** (73.4 mg, 0.10 mmol), 10-(4-ethynylphenyl)-5,5-difluoro-1,3,7,9-tetramethyl-5H-4λ₄,5λ₄-dipyrrolo[1,2-c:2',1'-f][1,3,2]diazaborinine **294a** (69.6 mg, 0.20 mmol), MnBr(CO)₅ (5.5 mg, 20 mol %) and 1-AdCO₂H (7.2 mg, 40 mol %) in 1,4-dioxane (1.0 mL). Purification by column chromatography on silica gel (CH₂Cl₂/EtOAc: 10/1 → 10/2) yielded **297f** (63.8 mg, 59%) as an orange solid.

M. p. 132 – 134 °C. **¹H NMR** (400 MHz, CDCl₃): δ 8.75 (dd, *J* = 5.0, 1.9 Hz, 1H), 7.91 (ddd, *J* = 7.7, 7.7, 2.0 Hz, 1H), 7.68 – 7.57 (m, 1H), 7.46 – 7.38 (m, 4H), 7.38 – 7.29 (m, 6H), 7.27 – 7.21 (m, 5H), 7.21 – 7.16 (m, 3H), 7.11 – 6.99 (m, 2H), 6.80 (d, *J* = 7.7 Hz, 1H), 6.66 (d, *J* = 16.7 Hz, 1H), 5.99 (s, 2H), 5.19 – 5.01 (m, 5H), 5.02 – 4.94 (m, 1H), 4.87 (d, *J* = 12.2 Hz, 1H), 4.19 – 3.99 (m, 1H), 3.66 – 3.43 (m, 2H), 3.19 – 3.01 (m, 2H), 2.57 (s, 6H), 1.76 – 1.68 (m, 1H), 1.55 – 1.35 (m, 18H), 1.33 – 1.16 (m, 2H). **¹³C NMR** (101 MHz, CDCl₃): δ 171.8 (C_q), 171.7 (C_q), 156.5 (C_q), 155.6 (C_q), 155.4 (C_q), 151.7 (C_q), 149.7 (CH), 143.0 (C_q), 141.4 (C_q), 138.4 (CH), 137.9 (C_q), 137.8 (C_q), 136.6 (C_q), 134.7 (C_q), 134.2 (C_q), 134.2 (C_q), 131.3 (C_q), 130.7 (CH), 129.0 (C_q), 128.5 (CH), 128.4 (CH), 128.3 (CH), 128.3 (CH), 128.2 (CH), 128.1 (CH), 128.0 (CH), 126.9 (CH), 124.0 (CH), 122.5 (CH), 122.1 (CH), 121.4 (CH), 121.2 (CH), 118.6 (CH), 117.9 (CH), 112.8 (C_q), 110.9 (CH), 80.1 (C_q), 67.6 (CH₂), 66.6 (CH₂), 54.3 (CH), 53.0 (CH), 40.3 (CH₂), 31.7 (CH₂), 29.3 (CH₂), 28.4 (CH₂), 28.2 (CH₃), 22.1 (CH₂), 14.6 (CH₃), 14.6 (CH₃). **¹⁹F NMR** (376 MHz, CDCl₃): δ – 146.26 (q, ¹*J*_{B-F} = 31.7 Hz). **IR** (ATR): 3334, 2929, 1699, 1540, 1507, 1468, 1191, 1154, 972, 740 cm⁻¹. **MS** (ESI): *m/z*

(relative intensity) 1104 (100) $[M+Na]^+$, 1082 (24) $[M+H]^+$. **HR-MS** (ESI): m/z calcd for $C_{63}H_{67}BF_2N_7O_7$ $[M+H]^+$: 1082.5168, found: 1082.5149.

Methyl (S)-2-((S)-6-amino-2-(((benzyloxy)carbonyl)amino)hexanamido)-3-{2-[(E)-4-(5,5-difluoro-1,3,7,9-tetramethyl-5H-4 λ ,5 λ -dipyrrolo[1,2-c:2',1'-f][1,3,2]diazaborinin-10-yl)styryl]-1-[pyridin-2-yl]-1H-indol-3-yl]propanoate (297g)



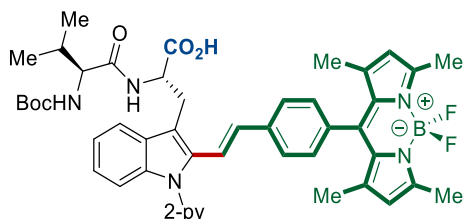
The general procedure **O** was followed using methyl N_α -{[(benzyloxy)carbonyl]-L-lysyl}-1-(pyridin-2-yl)-L-tryptophanate **243ak** (55.7 mg, 0.10 mmol), 10-(4-ethynylphenyl)-5,5-difluoro-1,3,7,9-tetramethyl-5H-4 λ ,5 λ -dipyrrolo[1,2-c:2',1'-f][1,3,2]diazaborinine **294a** (69.7 mg, 0.20 mmol), $MnBr(CO)_5$ (27.4 mg, 100 mol %) and 1-AdCO₂H (25.3 mg, 140 mol %) in 1,4-dioxane (2.0 mL). Purification by column chromatography on silica gel ($CH_2Cl_2/MeOH$: 98/2 \rightarrow 95/5 + 3% NEt_3) yielded **297g** (59.9 mg, 66%) as an orange solid.

M. p. 92 – 94 °C. **¹H NMR** (400 MHz, DMSO- d_6): δ 8.73 (d, J = 5.1 Hz, 1H), 8.60 (d, J = 7.9 Hz, 1H), 8.05 (ddd, J = 7.8, 7.8, 2.0 Hz, 1H), 7.70 – 7.61 (m, 1H), 7.61 – 7.48 (m, 4H), 7.40 – 7.22 (m, 10H), 7.20 – 7.13 (m, 2H), 6.42 (d, J = 16.7 Hz, 1H), 6.17 (s, 2H), 5.02 (d, J = 12.6 Hz, 1H), 4.95 (d, J = 12.6 Hz, 1H), 4.69 (dt, J = 7.9, 7.4 Hz, 1H), 4.06 (ddd, J = 8.6, 8.6, 5.0 Hz, 1H), 3.56 – 3.38 (m, 9H), 2.45 (s, 6H), 1.68 – 1.42 (m, 3H), 1.37 (s, 6H), 1.34 – 1.17 (m, 3H). **¹³C NMR** (101 MHz, DMSO- d_6): δ 172.2 (C_q), 172.0 (C_q), 155.8 (C_q), 154.9 (C_q), 151.1 (C_q), 149.6 (CH), 142.6 (C_q), 141.7 (C_q), 139.2 (CH), 137.7 (C_q), 137.6 (C_q), 136.9 (C_q), 134.0 (C_q), 133.2 (C_q), 130.6 (C_q), 130.0 (CH), 128.2 (CH), 128.2 (C_q), 127.7 (CH), 127.6 (CH), 126.9 (CH), 123.6 (CH), 123.1 (CH), 122.2 (CH), 121.3 (CH), 120.9 (CH), 118.9 (CH), 118.3 (CH), 113.7 (C_q), 110.6 (CH), 69.8 (CH₂), 65.4 (CH₂), 54.6 (CH), 52.9 (CH), 51.9 (CH₃), 40.7 (CH₂), 31.7 (CH₂), 31.4 (CH₂), 27.2 (CH₂), 14.2 (CH₃), 14.2 (CH₃). (One aromatic CH is missing due to overlap, the overlap was verified by HSQC analysis, showing that the peak at 128.2 corresponds to two CH carbons) **¹⁹F NMR** (376 MHz, CDCl₃): δ – 143.7 (q, $^1J_{B-F}$ = 30.8 Hz). **IR** (ATR): 3260, 3248, 3032, 2927, 2859, 1716, 1669, 1540, 1468, 1435, 1193,

5. Experimental Part

1155, 1024, 982, 741 cm^{-1} . **MS** (ESI): m/z (relative intensity) 906 (60) $[\text{M}+\text{H}]^+$. **HR-MS** (ESI): m/z calcd for $\text{C}_{52}\text{H}_{55}\text{BF}_2\text{N}_7\text{O}_5^+$ $[\text{M}+\text{H}]^+$:906.4329, found: 906.4352.

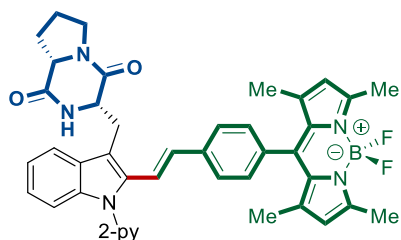
(S)-2-{[S]-2-[(*tert*-butoxycarbonyl)amino]-3-methylbutanamido}-3-{2-[(*E*)-4-(5,5-difluoro-1,3,7,9-tetramethyl-5*H*-4 λ_4 ,5 λ_4 -dipyrrolo[1,2-*c*:2',1'-*f*][1,3,2]diazaborinin-10-yl)styryl]-1-[pyridin-2-yl]-1*H*-indol-3-yl}propanoic acid (297h)



The general procedure **O** was followed using N_α -[(*tert*-butoxycarbonyl)-L-valyl]-1-(pyridin-2-yl)-L-tryptophan **243al** (48.0 mg, 0.10 mmol), 10-(4-ethynylphenyl)-5,5-difluoro-1,3,7,9-tetramethyl-5*H*-4 λ_4 ,5 λ_4 -dipyrrolo[1,2-*c*:2',1'-*f*][1,3,2]diazaborinine **294a** (69.7 mg, 0.20 mmol), $\text{MnBr}(\text{CO})_5$ (5.5 mg, 20 mol %) and 1-AdCO₂H (7.2 mg, 40 mol %) in 1,4-dioxane (1.0 mL). Purification by column chromatography on silica gel ($\text{CH}_2\text{Cl}_2/\text{EtOAc}$: 9/1 \rightarrow 7/3 +1% AcOH) yielded **297h** (42.1 mg, 51%) as an orange solid.

M. p. 105 – 107 °C. **¹H NMR** (400 MHz, DMSO-*d*₆): δ 12.88 (brs, 1H), 8.73 (dd, J = 5.0, 1.8 Hz, 1H), 8.36 (d, J = 8.3 Hz, 1H), 8.08 (ddd, J = 7.7, 7.7, 1.9 Hz, 1H), 7.78 – 7.69 (m, 1H), 7.60 – 7.53 (m, 3H), 7.50 (d, J = 8.0 Hz, 1H), 7.37 (d, J = 16.7 Hz, 1H), 7.34 – 7.27 (m, 3H), 7.23 – 7.12 (m, 2H), 6.56 (d, J = 9.2 Hz, 1H), 6.48 (d, J = 16.7 Hz, 1H), 6.18 (s, 2H), 4.72 (ddd, J = 8.0, 7.3, 6.8 Hz, 1H), 3.83 (dd, J = 9.2, 7.0 Hz, 1H), 3.48 (dd, J = 14.3, 6.8 Hz, 1H), 3.28 (dd, J = 14.3, 7.3 Hz, 1H), 2.45 (s, 6H), 1.90 (h, J = 6.9 Hz, 1H), 1.40 (s, 6H), 1.35 (s, 9H), 0.82 – 0.65 (m, 6H). **¹³C NMR** (101 MHz, DMSO-*d*₆): δ 173.6 (C_q), 171.8 (C_q), 155.7 (C_q), 155.3 (C_q), 151.6 (C_q), 150.1 (CH), 143.1 (C_q), 142.2 (C_q), 139.7 (CH), 138.3 (C_q), 138.2 (C_q), 134.5 (C_q), 133.6 (C_q), 131.1 (C_q), 130.3 (CH), 128.8 (C_q), 128.7 (CH), 127.4 (CH), 124.0 (CH), 123.6 (CH), 122.7 (CH), 121.8 (CH), 121.3 (CH), 119.6 (CH), 118.8 (CH), 114.7 (C_q), 111.0 (CH), 78.5 (C_q), 60.3 (CH), 53.2 (CH), 31.1 (CH), 28.6 (CH₃), 28.1 (CH₂), 19.6 (CH₃), 18.5 (CH₃), 14.7 (CH₃), 14.7 (CH₃). **¹⁹F NMR** (376 MHz, DMSO-*d*₆): δ – 143.7 (q, $^1J_{\text{B-F}}$ = 30.6 Hz). **IR** (ATR): 2960, 2925, 1713, 1672, 1543, 1470, 1195, 1157, 984 cm^{-1} . **MS** (ESI): m/z (relative intensity) 851 (60) $[\text{M}+\text{Na}]^+$, 829 (100) $[\text{M}+\text{H}]^+$. **HR-MS** (ESI): m/z calcd for $\text{C}_{47}\text{H}_{52}\text{BF}_2\text{N}_6\text{O}_5$ $[\text{M}+\text{H}]^+$:829.4063, found: 829.4044.

(3*S*,8_a*S*)-3-({2-[(*E*)-4-(5,5-difluoro-1,3,7,9-tetramethyl-5*H*-4 λ ₄,5 λ ₄-dipyrrolo[1,2-*c*:2',1'-*f*][1,3,2]diazaborinin-10-yl)styryl]-1-pyridin-2-yl]-1*H*-indol-3-yl)methyl)hexahydropyrrolo[1,2-*a*]pyrazine-1,4-dione (298a)

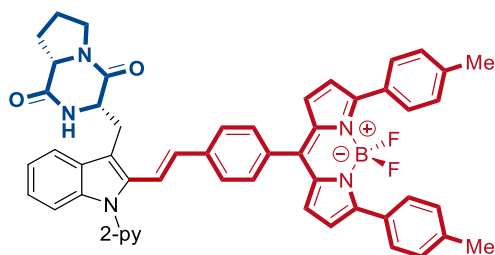


The general procedure **O** was followed using (3*S*,8_a*S*)-3-{{1-(pyridin-2-yl)-1*H*-indol-3-yl)methyl}hexahydropyrrolo[1,2-*a*]pyrazine-1,4-dione **276a** (36.1 mg, 0.10 mmol), 10-(4-ethynylphenyl)-5,5-difluoro-1,3,7,9-tetramethyl-5*H*-4 λ ₄,5 λ ₄-dipyrrolo[1,2-*c*:2',1'-*f*][1,3,2]diazaborinine **294a** (38.3 mg, 0.11 mmol), MnBr(CO)₅ (5.5 mg, 20 mol %) and 1-AdCO₂H (7.2 mg, 40 mol %) in 1,4-dioxane (1.0 mL). Purification by column chromatography on silica gel (CH₂Cl₂/EtOAc: 10/1) yielded **298a** (52.4 mg, 74%) as an orange solid.

M. p. 178 °C (decomposition). **¹H NMR** (400 MHz, CDCl₃): δ 8.74 (dd, *J* = 5.1, 1.8 Hz, 1H), 7.95 (ddd, *J* = 7.7, 7.7, 2.0 Hz, 1H), 7.68 – 7.59 (m, 1H), 7.47 (d, *J* = 8.0 Hz, 1H), 7.44 – 7.38 (m, 4H), 7.28 (dd, *J* = 7.2, 1.3 Hz, 1H), 7.25 (dd, *J* = 1.7, 1.7 Hz, 1H), 7.23 – 7.16 (m, 3H), 6.58 (d, *J* = 16.7 Hz, 1H), 5.98 (s, 2H), 5.72 (s, 1H), 4.56 (dd, *J* = 11.5, 2.1 Hz, 1H), 4.10 (ddd, *J* = 7.4, 7.4, 3.6 Hz, 1H), 4.01 (dd, *J* = 15.2, 3.6 Hz, 1H), 3.78 – 3.58 (m, 2H), 3.34 (dd, *J* = 15.2, 11.5 Hz, 1H), 2.55 (s, 6H), 2.35 (ddd, *J* = 9.9, 8.4, 5.8 Hz, 1H), 2.16 – 2.02 (m, 2H), 1.99 – 1.85 (m, 1H), 1.42 (s, 6H). **¹³C NMR** (101 MHz, CDCl₃): δ 169.4 (C_q), 165.5 (C_q), 155.5 (C_q), 151.4 (C_q), 149.8 (CH), 143.0 (C_q), 141.2 (C_q), 138.5 (CH), 138.1 (C_q), 137.4 (C_q), 134.6 (C_q), 134.6 (C_q), 131.9 (CH), 131.3 (C_q), 128.4 (CH), 128.2 (C_q), 127.1 (CH), 124.4 (CH), 122.7 (CH), 122.1 (CH), 121.7 (CH), 121.2 (CH), 118.5 (CH), 117.7 (CH), 111.8 (C_q), 111.1 (CH), 59.3 (CH), 54.9 (CH), 45.5 (CH₂), 28.3 (CH₂), 26.2 (CH₂), 22.7 (CH₂), 14.7 (CH₃), 14.6 (CH₃). **¹⁹F NMR** (282 MHz, CDCl₃): δ – 146.33 (q, ¹*J*_{B-F} = 32.7 Hz). **IR** (ATR): 3259, 2923, 1701, 1666, 1542, 1468, 1436, 1144, 1070, 760 cm⁻¹. **MS** (ESI): *m/z* (relative intensity) 731 (100) [M+Na]⁺, 709 (63) [M+H]⁺. **HR-MS** (ESI): *m/z* calcd for C₄₂H₄₀BF₂N₆O₃ [M+H]⁺: 709.3276, found: 709.3260.

5. Experimental Part

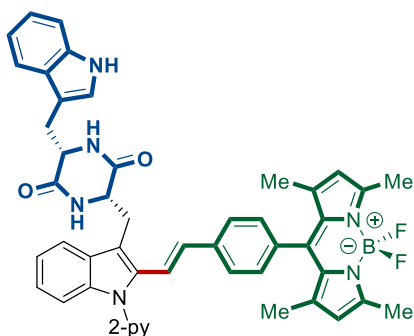
(3*S*,8*aS*)-3-({2-[(*E*)-4-(5,5-Difluoro-3,7-di-*p*-tolyl-5*H*-4 λ ₄,5 λ ₄-dipyrrolo[1,2-*c*:2',1'-*f*][1,3,2]diazaborinin-10-yl)styryl]-1-[pyridin-2-yl]-1*H*-indol-3-yl)methyl}hexahydropyrrolo[1,2-*a*]pyrazine-1,4-dione (**298b**)



The general procedure **O** was followed using (3*S*,8*aS*)-3-{{1-(pyridin-2-yl)-1*H*-indol-3-yl)methyl}hexahydropyrrolo[1,2-*a*]pyrazine-1,4-dione **276a** (36.1 mg, 0.10 mmol), 10-(4-ethynylphenyl)-5,5-difluoro-3,7-di-*p*-tolyl-5*H*-4 λ ₄,5 λ ₄-dipyrrolo[1,2-*c*:2',1'-*f*][1,3,2]diazaborinine **294c** (51.9 mg, 0.11 mmol), MnBr(CO)₅ (5.5 mg, 20 mol %) and (1-Ad)CO₂H (7.2 mg, 40 mol %) in 1,4-dioxane (1.0 mL). Purification by column chromatography on silica gel (CH₂Cl₂/MeOH: 98/2) yielded **298b** (55.7 mg, 67%) as a purple solid.

M. p. 191 – 194 °C. **¹H NMR** (400 MHz, CDCl₃): δ 8.78 (d, *J* = 5.0 Hz, 1H), 7.97 (ddd, *J* = 7.7, 7.7, 2.0 Hz, 1H), 7.81 (d, *J* = 8.0 Hz, 4H), 7.72 – 7.65 (m, 1H), 7.56 (d, *J* = 8.0 Hz, 2H), 7.52 – 7.46 (m, 4H), 7.44 (dd, *J* = 7.5, 5.0 Hz, 1H), 7.34 – 7.29 (m, 2H), 7.27 – 7.20 (m, 5H), 6.90 (d, *J* = 4.3 Hz, 2H), 6.68 (d, *J* = 16.8 Hz, 1H), 6.64 (d, *J* = 4.3 Hz, 2H), 5.73 (s, 1H), 4.64 – 4.47 (m, 1H), 4.17 – 3.99 (m, 2H), 3.73 (dt, *J* = 11.6, 7.9 Hz, 1H), 3.64 (ddd, *J* = 11.6, 8.8, 2.9 Hz, 1H), 3.38 (dd, *J* = 15.2, 11.6 Hz, 1H), 2.45 – 2.32 (m, 7H), 2.18 – 2.01 (m, 2H), 2.01 – 1.86 (m, 1H). **¹³C NMR** (101 MHz, CDCl₃): δ 169.3 (C_q), 165.4 (C_q), 158.8 (C_q), 151.4 (C_q), 149.8 (CH), 142.7 (C_q), 139.7 (C_q), 138.6 (C_q), 138.5 (CH), 138.1 (C_q), 136.1 (C_q), 134.6 (C_q), 134.1 (C_q), 132.0 (CH), 131.1 (CH), 130.4 (CH), 129.8 (C_q), 129.4 (CH), 129.0 (CH), 128.2 (C_q), 126.2 (CH), 124.5 (CH), 122.6 (CH), 122.0 (CH), 121.8 (CH), 120.7 (CH), 118.5 (CH), 118.4 (CH), 112.2 (C_q), 111.2 (CH), 59.2 (CH), 55.0 (CH), 45.5 (CH₂), 28.3 (CH₂), 26.1 (CH₂), 22.6 (CH₂), 21.4 (CH₃). **¹⁹F NMR** (377 MHz, CDCl₃): δ – 132.63 (q, ¹*J*_{B-F} = 31.8 Hz). **IR** (ATR): 3372, 1660, 1561, 1537, 1464, 1429, 1278, 1137, 1068, 1055, 738 cm⁻¹. **MS** (ESI): *m/z* (relative intensity): 855 (66) [M+Na]⁺, 833 (100) [M+H]⁺. **HR-MS** (ESI): *m/z* calcd for C₅₂H₄₄BF₂N₆O₂⁺ [M+H]⁺: 833.3590, found: 833.3573.

(3*S*,6*S*)-3-((1*H*-Indol-3-yl)methyl)-6-((2-[(*E*)-4-(5,5-difluoro-1,3,7,9-tetramethyl-5*H*-4 λ ₄,5 λ ₄-dipyrrolo[1,2-*c*:2',1'-*f*][1,3,2]diazaborinin-10-yl)styryl]-1-[pyridin-2-yl]-1*H*-indol-3-yl)methyl)piperazine-2,5-dione (298c)

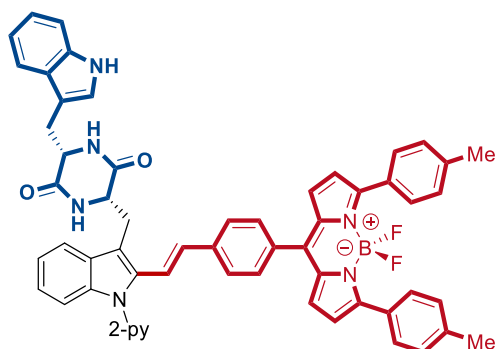


The general procedure **O** was followed using (3*S*,6*S*)-3-[(1*H*-indol-3-yl)methyl]-6-[[1-(pyridin-2-yl)-1*H*-indol-3-yl]methyl]piperazine-2,5-dione **276b** (44.9 mg, 0.10 mmol), 10-(4-ethynylphenyl)-5,5-difluoro-1,3,7,9-tetramethyl-5*H*-4 λ ₄,5 λ ₄-dipyrrolo[1,2-*c*:2',1'-*f*][1,3,2]diazaborinine **294a** (38.3 mg, 0.11 mmol), MnBr(CO)₅ (5.5 mg, 20 mol %) and 1-AdCO₂H (7.2 mg, 40 mol %) in 1,4-dioxane (1.0 mL). Purification by column chromatography on silica gel (CH₂Cl₂/MeOH: 96/4) yielded **298c** (44.7 mg, 56%) as an orange solid.

M. p. 202 °C (decomposition). **¹H NMR** (400 MHz, CDCl₃): δ 8.73 (dd, *J* = 4.9, 1.8 Hz, 1H), 8.28 (s, 1H), 7.94 (ddd, *J* = 7.7, 7.7, 1.9 Hz, 1H), 7.69 – 7.60 (m, 1H), 7.49 (d, *J* = 7.9 Hz, 2H), 7.46 – 7.38 (m, 3H), 7.38 – 7.34 (m, 1H), 7.27 – 7.14 (m, 8H), 6.88 – 6.82 (m, 1H), 6.78 (d, *J* = 16.7 Hz, 1H), 6.07 (s, 1H), 5.98 (s, 2H), 5.92 (s, 1H), 4.36 (d, *J* = 9.1 Hz, 1H), 4.29 (d, *J* = 7.4 Hz, 1H), 3.69 (dd, *J* = 14.8, 3.0 Hz, 1H), 3.41 (dd, *J* = 14.8, 3.4 Hz, 1H), 2.98 – 2.81 (m, 2H), 2.57 (s, 6H), 1.41 (s, 6H). **¹³C NMR** (101 MHz, CDCl₃): δ 167.2 (C_q), 166.7 (C_q), 155.5 (C_q), 151.4 (C_q), 149.8 (CH), 143.0 (C_q), 141.3 (C_q), 138.6 (CH), 137.7 (C_q), 137.6 (C_q), 136.3 (C_q), 134.5 (C_q), 134.4 (C_q), 131.7 (CH), 131.3 (C_q), 128.6 (C_q), 128.4 (CH), 127.1 (CH), 126.8 (C_q), 124.1 (CH), 123.9 (CH), 122.7 (CH), 122.7 (CH), 122.1 (CH), 121.9 (CH), 121.2 (CH), 120.1 (CH), 118.9 (CH), 118.9 (CH), 118.1 (CH), 112.0 (C_q), 111.4 (CH), 110.8 (CH), 109.2 (C_q), 56.1 (CH), 55.3 (CH), 30.4 (CH₂), 30.0 (CH₂), 14.6 (CH₃), 14.6 (CH₃). **¹⁹F NMR** (376 MHz, CDCl₃): δ – 146.17 (q, ¹*J*_{B-F} = 31.9 Hz). **IR** (ATR): 3229, 1666, 1541, 1506, 1454, 1434, 1153, 973, 739 cm⁻¹. **MS** (ESI): *m/z* (relative intensity) 820 (100) [M+Na]⁺, 798 (65) [M+H]⁺. **HR-MS** (ESI): *m/z* calcd for C₄₈H₄₃BF₂N₇O₂⁺ [M+H]⁺: 798.3542, found: 798.3527.

5. Experimental Part

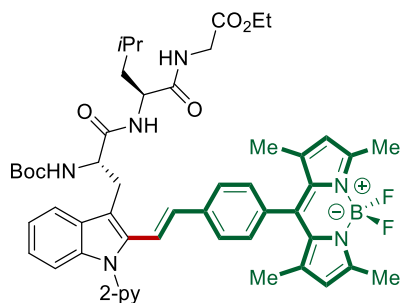
(3*S*,6*S*)-3-[(1*H*-indol-3-yl)methyl]-6-({2-[(*E*)-4-(5,5-difluoro-1,3,7,9-tetramethyl-5*H*-4 λ ₄,5 λ ₄-dipyrrolo[1,2-*c*:2',1'-*f*][1,3,2]diazaborinin-10-yl)styryl]-1-[pyridin-2-yl]-1*H*-indol-3-yl)methyl)piperazine-2,5-dione (**298d**)



The general procedure **O** was followed using (3*S*,6*S*)-3-[(1*H*-indol-3-yl)methyl]-6-[[1-(pyridin-2-yl)-1*H*-indol-3-yl)methyl]piperazine-2,5-dione **276b** (44.9 mg, 0.10 mmol), 10-(4-ethynylphenyl)-5,5-difluoro-3,7-di-*p*-tolyl-5*H*-4 λ ₄,5 λ ₄-dipyrrolo[1,2-*c*:2',1'-*f*][1,3,2]diazaborinine **294c** (51.9 mg, 0.11 mmol), MnBr(CO)₅ (5.5 mg, 20 mol %) and 1-AdCO₂H (7.2 mg, 40 mol %) in 1,4-dioxane (1.0 mL). Purification by column chromatography on silica gel (CH₂Cl₂/MeOH: 95/5) yielded **298d** (58.9 mg, 64%) as a purple solid.

M. p. 189 – 191 °C. **¹H NMR** (400 MHz, CDCl₃): δ 8.72 (d, J = 3.9 Hz, 1H), 8.27 (brs, 1H), 7.90 (ddd, J = 7.9, 5.8, 2.0 Hz, 1H), 7.83 – 7.75 (m, 4H), 7.66 – 7.56 (m, 1H), 7.52 – 7.41 (m, 5H), 7.39 (dd, J = 7.8, 3.8 Hz, 2H), 7.36 – 7.12 (m, 11H), 6.83 (d, J = 4.0 Hz, 2H), 6.74 – 6.61 (m, 2H), 6.57 (d, J = 4.0 Hz, 2H), 6.09 (d, J = 9.1 Hz, 2H), 4.28 (d, J = 7.3 Hz, 1H), 4.20 (d, J = 8.5 Hz, 1H), 3.61 – 3.48 (m, 1H), 3.44 – 3.23 (m, 1H), 2.98 (ddd, J = 19.0, 5.8, 5.8 Hz, 1H), 2.73 – 2.54 (m, 1H), 2.38 (s, 6H). **¹³C NMR** (101 MHz, CDCl₃): δ 167.2 (C_q), 166.7 (C_q), 158.8 (C_q), 151.5 (C_q), 149.7 (CH), 142.8 (C_q), 139.7 (C_q), 138.9 (C_q), 138.6 (CH), 137.8 (C_q), 136.3 (C_q), 136.0 (C_q), 134.7 (C_q), 133.9 (C_q), 131.7 (CH), 131.1 (CH), 130.5 (CH), 129.8 (C_q), 129.4 (CH), 129.4 (CH), 129.0 (CH), 128.6 (C_q), 126.7 (C_q), 126.2 (CH), 124.2 (CH), 123.9 (CH), 122.6 (CH), 122.0 (CH), 121.9 (CH), 120.7 (CH), 120.0 (CH), 119.2 (CH), 118.9 (CH), 118.8 (CH), 112.5 (CH), 111.4 (C_q), 110.9 (C_q), 109.2 (CH), 56.1 (CH), 55.2 (CH), 30.5 (CH₂), 29.8 (CH₂), 21.4 (CH₃). **¹⁹F NMR** (376 MHz, CDCl₃): δ – 132.26 (q, $^1J_{B-F}$ = 31.9 Hz). **IR** (ATR): 2919, 1669, 1562, 1539, 1465, 1433, 1279, 1139, 1056, 1018, 739 cm⁻¹. **MS** (ESI): m/z (relative intensity) 944 (60) [M+Na]⁺, 922 (100) [M+H]⁺. **HR-MS** (ESI): m/z calcd for C₅₈H₄₆BF₂N₇O₂Na [M+Na]⁺: 944.3676, found: 944.3650.

Ethyl ((S)-2-[[*tert*-butoxycarbonyl]amino]-3-{2-[(*E*)-4-(5,5-difluoro-1,3,7,9-tetramethyl-5*H*-4 λ ₄,5 λ ₄-dipyrrolo[1,2-*c*:2',1'-*f*][1,3,2]diazaborinin-10-yl)styryl]-1-[pyridin-2-yl]-1*H*-indol-3-yl]propanoyl)-L-leucylglycinate (297i)



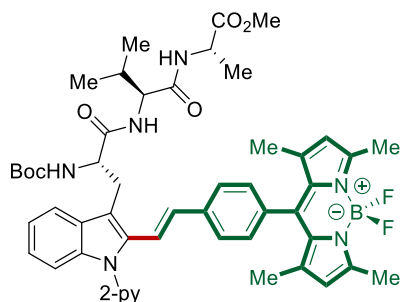
The general procedure **O** was followed using ethyl *N*_α-(*tert*-butoxycarbonyl)-1-(pyridin-2-yl)-L-tryptophyl-L-leucylglycinate **243ae** (58.0 mg, 0.10 mmol), 10-(4-ethynylphenyl)-5,5-difluoro-1,3,7,9-tetramethyl-5*H*-4 λ ₄,5 λ ₄-dipyrrolo[1,2-*c*:2',1'-*f*][1,3,2]diazaborinine **294a** (69.6 mg, 0.20 mmol), MnBr(CO)₅ (5.5 mg, 20 mol %) and 1-AdCO₂H (7.2 mg, 40 mol %) in 1,4-dioxane (1.0 mL). Purification by column chromatography on silica gel (CH₂Cl₂/EtOAc: 20/1→10/1) yielded **297i** (65.9 mg, 71%) as an orange solid.

M. p. 156 – 158 °C. **¹H NMR** (400 MHz, CDCl₃): δ 8.76 (dd, *J* = 5.0, 1.9 Hz, 1H), 7.96 (ddd, *J* = 7.7, 7.7, 1.9 Hz, 1H), 7.72 – 7.67 (m, 1H), 7.54 (d, *J* = 7.9 Hz, 2H), 7.50 (d, *J* = 8.0 Hz, 1H), 7.44 (dd, *J* = 7.5, 4.9 Hz, 1H), 7.40 – 7.36 (m, 1H), 7.31 (d, *J* = 16.9 Hz, 1H), 7.26 – 7.16 (m, 4H), 6.70 (d, *J* = 16.7 Hz, 1H), 6.31 – 6.14 (m, 2H), 5.99 (s, 2H), 5.45 – 5.29 (m, 1H), 4.57 (ddd, *J* = 7.2, 7.2, 7.2 Hz, 1H), 4.39 (ddd, *J* = 8.6, 8.6, 5.5 Hz, 1H), 4.14 (q, *J* = 7.2 Hz, 2H), 3.81 – 3.65 (m, 2H), 3.65 – 3.42 (m, 2H), 2.57 (s, 6H), 1.69 – 1.50 (m, 2H), 1.49 – 1.36 (m, 16H), 1.25 (t, *J* = 7.2 Hz, 3H), 0.87 (d, *J* = 6.4 Hz, 6H). **¹³C NMR** (101 MHz, CDCl₃): δ 171.4 (C_q), 171.3 (C_q), 169.4 (C_q), 155.6 (C_q), 155.4 (C_q), 151.7 (C_q), 149.7 (CH), 143.0 (C_q), 141.4 (C_q), 138.5 (CH), 138.0 (C_q), 137.9 (C_q), 134.3 (C_q), 134.2 (C_q), 131.3 (C_q), 130.9 (CH), 128.7 (C_q), 128.3 (CH), 127.1 (CH), 123.9 (CH), 122.6 (CH), 122.4 (CH), 121.4 (CH), 121.1 (CH), 118.9 (CH), 117.9 (CH), 112.8 (C_q), 110.7 (CH), 80.4 (C_q), 61.3 (CH₂), 55.8 (CH), 51.7 (CH), 41.2 (CH₂), 41.1 (CH₂), 28.2 (CH₃), 24.6 (CH), 22.8 (CH₃), 22.0 (CH₃), 14.6 (CH₃), 14.5 (CH₃), 14.1 (CH₃). (One aliphatic CH₂ is missing due to overlap, the overlap was verified by HSQC analysis, showing that the peak at 28.2 corresponds to two carbons, the CH₂ of the Trp side chain and the CH₃ of the Boc group). **¹⁹F NMR** (376 MHz, CDCl₃): δ – 146.28 (q, ¹*J*_{B-F} = 31.8 Hz). **IR** (ATR): 3302, 2959, 2930, 1740, 1656, 1507, 1468, 1436, 1191, 1154, 974, 741 cm⁻¹. **MS** (ESI): *m/z* (relative intensity) 950 (100)

5. Experimental Part

[M+Na]⁺, 928 (29) [M+H]⁺. **HR-MS** (ESI) *m/z* calcd for C₅₂H₆₁BF₂N₇O₆⁺ [M+H]⁺: 928.4748, found: 928.4739.

Methyl ((*S*)-2-[(*tert*-butoxycarbonyl)amino]-3-{2-[(*E*)-4-(5,5-difluoro-1,3,7,9-tetramethyl-5*H*-4λ₄,5λ₄-dipyrrolo[1,2-*c*:2',1'-*f*][1,3,2]diazaborinin-10-yl)styryl]-1-[pyridin-2-yl]-1*H*-indol-3-yl}propanoyl)-L-valyl-L-alaninate (**297j**)

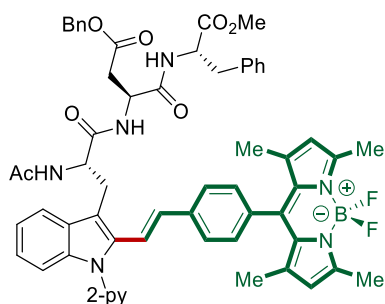


The general procedure **O** was followed using methyl *N*_α-(*tert*-butoxycarbonyl)-1-(pyridin-2-yl)-L-tryptophyl-L-valyl-L-alaninate **243a** (56.5 mg, 0.10 mmol), 10-(4-ethynylphenyl)-5,5-difluoro-1,3,7,9-tetramethyl-5*H*-4λ₄,5λ₄-dipyrrolo[1,2-*c*:2',1'-*f*][1,3,2]diazaborinine **294a** (69.6 mg, 0.11 mmol), MnBr(CO)₅ (5.5 mg, 20 mol %) and 1-AdCO₂H (7.2 mg, 40 mol %) in 1,4-dioxane (1.0 mL). Purification by column chromatography on silica gel (CH₂Cl₂/EtOAc: 20/1→10/1) yielded **297j** (57.5 mg, 63%) as an orange solid. The reaction was also performed at 60 °C, and yielded **297j** (53.9 mg, 59%).

M. p. 192 – 194 °C. **¹H NMR** (400 MHz, CDCl₃): δ 8.78 – 8.70 (m, 1H), 7.93 (ddd, *J* = 7.7, 7.7, 2.1 Hz, 1H), 7.72 – 7.62 (m, 1H), 7.55 – 7.47 (m, 3H), 7.45 – 7.26 (m, 3H), 7.24 – 7.11 (m, 4H), 6.68 (d, *J* = 16.7 Hz, 1H), 6.41 (d, *J* = 8.1 Hz, 1H), 6.17 (d, *J* = 7.1 Hz, 1H), 5.97 (s, 2H), 5.40 (d, *J* = 7.4 Hz, 1H), 4.56 (dd, *J* = 7.1, 7.1 Hz, 1H), 4.29 (ddd, *J* = 8.2, 7.4, 5.6 Hz, 1H), 4.12 (dd, *J* = 8.1, 7.1 Hz, 1H), 3.69 (s, 3H), 3.57 (dd, *J* = 14.6, 5.6 Hz, 1H), 3.46 (dd, *J* = 14.6, 8.2 Hz, 1H), 2.54 (s, 6H), 2.08 – 1.96 (m, 1H), 1.51 – 1.34 (m, 15H), 1.25 (d, *J* = 7.1 Hz, 3H), 0.87 – 0.77 (m, 6H). **¹³C NMR** (101 MHz, CDCl₃): δ 172.8 (C_q), 171.3 (C_q), 169.6 (C_q), 155.4 (C_q), 151.8 (C_q), 149.6 (CH), 143.0 (C_q), 141.5 (C_q), 138.4 (CH), 138.1 (C_q), 138.0 (C_q), 134.2 (C_q), 134.1 (C_q), 131.3 (C_q), 130.7 (CH), 128.8 (C_q), 128.3 (CH), 127.0 (CH), 123.8 (CH), 122.6 (CH), 122.5 (CH), 121.2 (CH), 121.1 (CH), 118.9 (CH), 118.0 (CH), 112.9 (C_q), 110.7 (CH), 80.2 (C_q), 58.1 (CH), 55.6 (CH), 52.3 (CH₃), 48.0 (CH), 31.2 (CH), 28.2 (CH₃), 18.7 (CH₃), 17.8 (CH₃), 17.7 (CH₃), 14.6 (CH₃), 14.5 (CH₃). (One aromatic C_q and one aliphatic CH₂ is missing due to overlap, the overlap was verified by HSQC and HMBC analysis,

showing that the peak at 155.4 correspond to two C_q carbons and the peak at 28.2 corresponds to two carbons, the CH₂ of the Trp side chain and the CH₃ of the Boc group). **¹⁹F NMR** (376 MHz, CDCl₃): δ – 146.27 (q, ¹J_{B-F} = 31.8 Hz). **IR** (ATR): 1670, 1542, 1509, 1456, 1195, 1157, 904, 723, 647 cm⁻¹. **MS** (ESI): *m/z* (relative intensity) 936 (25) [M+Na]⁺, 914 (100) [M+H]⁺. **HR-MS** (ESI): *m/z* calcd for C₅₁H₅₉BF₂N₇O₆ [M+H]⁺: 914.4591, found: 914.4606.

Benzyl (S)-3-({S}-2-acetamido-3-{2-[(E)-4-(5,5-difluoro-1,3,7,9-tetramethyl-5H-4λ₄,5λ₄-dipyrrolo[1,2-c:2',1'-f][1,3,2]diazaborinin-10-yl)styryl]-1-[pyridin-2-yl]-1H-indol-3-yl}propanamido)-4-[(S)-1-methoxy-1-oxo-3-phenylpropan-2-yl]amino}-4-oxobutanoate (297k)



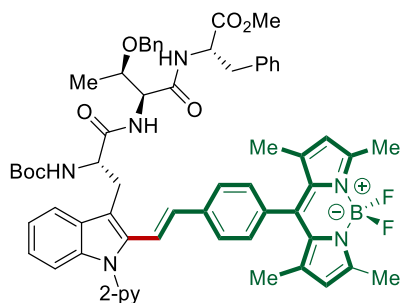
The general procedure **O** was followed using benzyl (S)-3-[(S)-2-acetamido-3-[1-(pyridin-2-yl)-1H-indol-3-yl]propanamido}-4-[(S)-1-methoxy-1-oxo-3-phenylpropan-2-yl]amino}-4-oxobutanoate **243i** (68.9 mg, 0.10 mmol), 10-(4-ethynylphenyl)-5,5-difluoro-1,3,7,9-tetramethyl-5H-4λ₄,5λ₄-dipyrrolo[1,2-c:2',1'-f][1,3,2]diazaborinine **294a** (69.6 mg, 0.20 mmol), MnBr(CO)₅ (5.5 mg, 20 mol %) and 1-AdCO₂H (7.2 mg, 40 mol %) in 1,4-dioxane (1.0 mL). Purification by column chromatography on silica gel (CH₂Cl₂/Acetone: 10/1) yielded **297k** (70.5 mg, 68%) as an orange solid.

M. p. 151 – 153 °C. **¹H NMR** (400 MHz, CDCl₃): δ 8.75 (d, *J* = 4.8 Hz, 1H), 7.94 (ddd, *J* = 7.8, 7.8, 1.9 Hz, 1H), 7.59 (d, *J* = 5.0 Hz, 1H), 7.57 – 7.49 (m, 3H), 7.44 (dd, *J* = 7.4, 4.9 Hz, 1H), 7.37 – 7.20 (m, 12H), 7.17 – 7.05 (m, 4H), 6.85 (d, *J* = 7.4 Hz, 1H), 6.82 – 6.71 (m, 2H), 6.37 (d, *J* = 6.9 Hz, 1H), 5.99 (s, 2H), 5.03 (s, 2H), 4.77 (ddd, *J* = 8.4, 6.9, 5.4 Hz, 1H), 4.60 – 4.33 (m, 2H), 3.70 (dd, *J* = 14.4, 5.4 Hz, 1H), 3.61 (s, 3H), 3.39 (dd, *J* = 14.4, 8.4 Hz, 1H), 3.00 (dd, *J* = 13.9, 5.9 Hz, 1H), 2.93 (dd, *J* = 13.9, 7.2 Hz, 1H), 2.84 (dd, *J* = 17.4, 3.6 Hz, 1H), 2.57 (s, 6H), 2.42 (dd, *J* = 17.4, 8.1 Hz, 1H), 1.94 (s, 3H), 1.43 (s, 6H). **¹³C NMR** (101 MHz, CDCl₃): δ 171.8 (C_q), 171.2 (C_q), 170.6 (C_q), 170.2 (C_q), 169.1 (C_q), 155.4 (C_q), 151.7 (C_q), 149.7 (CH), 143.0 (C_q), 141.4 (C_q), 138.5 (CH), 138.1 (C_q), 137.8 (C_q), 135.8 (C_q), 135.2 (C_q), 134.3 (C_q), 134.1 (C_q), 131.3

5. Experimental Part

(C_q), 130.8 (CH), 129.1 (CH), 128.8 (C_q), 128.6 (CH), 128.5 (CH), 128.4 (CH), 128.3 (CH), 128.2 (CH), 127.1 (CH), 127.0 (CH), 124.0 (CH), 122.7 (CH), 122.6 (CH), 121.4 (CH), 121.2 (CH), 118.5 (CH), 117.7 (CH), 112.6 (C_q), 110.7 (CH), 66.8 (CH₂), 54.3 (CH), 53.8 (CH), 52.2 (CH₃), 48.8 (CH), 37.4 (CH₂), 35.9 (CH₂), 27.7 (CH₂), 23.1 (CH₃), 14.6 (CH₃), 14.6 (CH₃). **¹⁹F NMR** (376 MHz, CDCl₃): δ - 146.26 (q, ¹J_{B-F} = 31.4 Hz). **IR** (ATR): 3286, 3032, 1732, 1632, 1540, 1507, 1453, 1304, 1191, 972, 711 cm⁻¹. **MS** (ESI): *m/z* (relative intensity) 1060 (100) [M+Na]⁺, 1038 (55) [M+H]⁺. **HR-MS** (ESI): *m/z* calcd for C₆₀H₅₉BF₂N₇O₇ [M+H]⁺: 1038.4541, found: 1038.4527.

Methyl *O*-benzyl-*N*-({*S*}-2-[[*tert*-butoxycarbonyl]amino]-3-{2-[(*E*)-4-(5,5-difluoro-1,3,7,9-tetramethyl-5*H*-4λ₄,5λ₄-dipyrrolo[1,2-*c*:2',1'-*f*][1,3,2]diazaborinin-10-yl)styryl]-1-[pyridin-2-yl]-1*H*-indol-3-yl]propanoyl)-*L*-threonyl-*L*-phenylalaninate (**297I**)

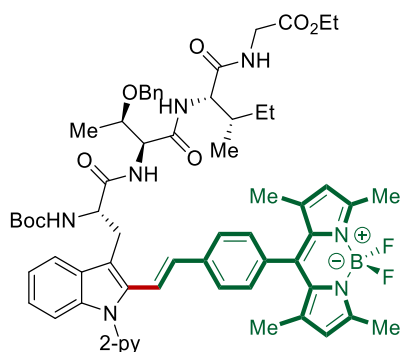


The general procedure **O** was followed using ethyl *N*_α-(*tert*-butoxycarbonyl)-1-(pyridin-2-yl)-*L*-tryptophyl-*L*-leucylglycinate **243an** (73.4 mg, 0.10 mmol), 10-(4-ethynylphenyl)-5,5-difluoro-1,3,7,9-tetramethyl-5*H*-4λ₄,5λ₄-dipyrrolo[1,2-*c*:2',1'-*f*][1,3,2]diazaborinine **294a** (69.6 mg, 0.20 mmol), MnBr(CO)₅ (5.5 mg, 20 mol %) and 1-AdCO₂H (7.2 mg, 40 mol %) in 1,4-dioxane (1.0 mL). Purification by column chromatography on silica gel (CH₂Cl₂/EtOAc: 10/1→10/2) yielded **297I** (59.5 mg, 55%) as an orange solid.

M. p. 147 – 149 °C. **¹H NMR** (400 MHz, CDCl₃): δ 8.77 (d, *J* = 5.0 Hz, 1H), 7.95 (ddd, *J* = 7.7, 7.7, 2.0 Hz, 1H), 7.62 – 7.53 (m, 4H), 7.44 (dd, *J* = 7.7, 5.0 Hz, 1H), 7.37 – 7.26 (m, 8H), 7.24 – 7.20 (m, 4H), 7.14 – 7.02 (m, 2H), 7.00 – 6.90 (m, 3H), 6.82 (d, *J* = 16.8 Hz, 1H), 6.62 (d, *J* = 5.4 Hz, 1H), 5.99 (s, 2H), 5.44 (d, *J* = 7.4 Hz, 1H), 4.72 – 4.35 (m, 4H), 4.25 – 4.09 (m, 1H), 4.03 (qd, *J* = 6.3, 3.4 Hz, 1H), 3.71 – 3.64 (m, 1H), 3.62 (s, 3H), 3.42 (dd, *J* = 14.3, 8.4 Hz, 1H), 2.96 (dd, *J* = 13.9, 5.8 Hz, 1H), 2.85 (dd, *J* = 13.9, 7.1 Hz, 1H), 2.58 (s, 6H), 1.47 – 1.38 (m, 15H), 0.92 (d, *J* = 6.3 Hz, 3H). **¹³C NMR** (101 MHz, CDCl₃): δ 171.4 (C_q), 171.4 (C_q), 168.0 (C_q), 155.4 (C_q), 155.2 (C_q), 151.8 (C_q), 149.6 (CH), 143.1 (C_q), 141.6 (C_q), 138.4 (CH), 138.2 (C_q), 138.1 (C_q),

137.8 (C_q), 135.7 (C_q), 134.1 (C_q), 134.0 (C_q), 131.4 (C_q), 130.6 (CH), 128.9 (CH), 128.8 (C_q), 128.5 (CH), 128.4 (CH), 128.2 (CH), 127.8 (CH), 127.7 (CH), 127.1 (CH), 127.0 (CH), 123.8 (CH), 122.7 (CH), 122.5 (CH), 121.1 (CH), 121.1 (CH), 118.8 (CH), 118.0 (CH), 112.8 (C_q), 110.5 (CH), 80.1 (C_q), 73.8 (CH), 71.2 (CH₂), 55.5 (CH), 55.4 (CH), 53.6 (CH), 52.0 (CH₃), 37.7 (CH₂), 28.7 (CH₂), 28.3 (CH₃), 14.6 (CH₃), 14.5 (CH₃), 13.9 (CH₃). ¹⁹F NMR (376 MHz, CDCl₃): δ – 146.29 (q, ¹J_{B-F} = 31.8 Hz). IR (ATR): 3343, 2973, 2928, 1744, 1667, 1541, 1507, 1454, 1192, 1154, 973, 733 cm⁻¹. MS (ESI): *m/z* (relative intensity) 1104 (100) [M+Na]⁺, 1083 (41) [M+H]⁺. HR-MS (ESI): *m/z* calcd for C₆₃H₆₇BF₂N₇O₇⁺ [M+H]⁺: 1082.5168, found: 1082.5147.

Ethyl O-benzyl-N-({S}-2-[[*tert*-butoxycarbonyl]amino]-3-{2-[(*E*)-4-(5,5-difluoro-1,3,7,9-tetramethyl-5H-4λ₄,5λ₄-dipyrrolo[1,2-c:2',1'-f][1,3,2]diazaborinin-10-yl)styryl]-1-[pyridin-2-yl]-1*H*-indol-3-yl]propanoyl)-L-threonyl-L-isoleucylglycinate (297m)



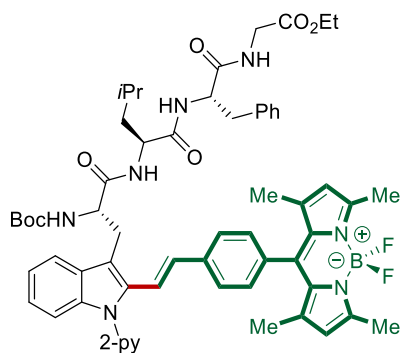
The general procedure **O** was followed using ethyl O-benzyl-N-(*N*_α-(*tert*-butoxycarbonyl)-1-(pyridin-2-yl)-L-tryptophyl)-L-threonyl-L-isoleucylglycinate **243ao** (77.1 mg, 0.10 mmol), 10-(4-ethynylphenyl)-5,5-difluoro-1,3,7,9-tetramethyl-5*H*-4λ₄,5λ₄-dipyrrolo[1,2-c:2',1'-f][1,3,2]diazaborinine **294a** (69.6 mg, 0.20 mmol), MnBr(CO)₅ (5.5 mg, 20 mol %) and 1-AdCO₂H (7.2 mg, 40 mol %) in 1,4-dioxane (1.0 mL). Purification by column chromatography on silica gel (CH₂Cl₂/EtOAc: 10/2→10/4) yielded **297m** (97.3 mg, 87%) as an orange solid. The reaction was also performed at 60 °C and yielded **297m** (69.6 mg, 62%).

M. p. 152 – 154 °C. ¹H NMR (400 MHz, CDCl₃): δ 8.78 (dd, *J* = 5.3, 2.0 Hz, 1H), 7.97 (ddd, *J* = 7.7, 7.7, 1.9 Hz, 1H), 7.73 – 7.61 (m, 1H), 7.52 – 7.43 (m, 4H), 7.40 (dd, *J* = 7.6, 1.4 Hz, 1H), 7.34 – 7.27 (m, 4H), 7.26 – 7.18 (m, 6H), 7.11 (brs, 1H), 7.04 (d, *J* = 8.3 Hz, 1H), 6.83 (s, 1H), 6.66 (d, *J* = 16.7 Hz, 1H), 5.99 (s, 2H), 5.29 (d, *J* = 4.7 Hz, 1H), 4.61 – 4.46 (m, 3H), 4.39 (d, *J* = 11.4 Hz, 1H), 4.24 – 4.13 (m, 4H), 4.07 (dd, *J* =

5. Experimental Part

17.9, 5.8 Hz, 1H), 3.92 (dd, $J = 17.9, 5.3$ Hz, 1H), 3.66 (dd, $J = 14.8, 5.8$ Hz, 1H), 3.56 (dd, $J = 14.8, 6.4$ Hz, 1H), 2.57 (s, 6H), 1.84 – 1.70 (m, 1H), 1.62 – 1.46 (m, 2H), 1.43 (s, 6H), 1.32 – 1.21 (m, 12H), 0.92 – 0.80 (m, 9H). $^{13}\text{C NMR}$ (101 MHz, CDCl_3): δ 173.0 (C_q), 172.4 (C_q), 169.6 (C_q), 169.6 (C_q), 156.1 (C_q), 155.6 (C_q), 151.7 (C_q), 149.7 (CH), 143.0 (C_q), 141.2 (C_q), 138.6 (CH), 138.2 (C_q), 137.6 (C_q), 137.6 (C_q), 134.6 (C_q), 134.4 (C_q), 131.5 (CH), 131.3 (C_q), 128.7 (C_q), 128.5 (CH), 128.4 (CH), 127.9 (CH), 127.8 (CH), 127.0 (CH), 124.3 (CH), 122.8 (CH), 122.5 (CH), 121.7 (CH), 121.3 (CH), 118.8 (CH), 117.6 (CH), 112.5 (C_q), 110.9 (CH), 80.9 (C_q), 73.6 (CH), 71.7 (CH_2), 61.1 (CH_2), 58.3 (CH), 56.4 (CH), 51.9 (CH), 41.3 (CH_2), 40.0 (CH_2), 28.0 (CH_3), 27.1 (CH_2), 24.5 (CH), 23.1 (CH_3), 21.2 (CH_3), 15.9 (CH_3), 14.6 (CH_3), 14.6 (CH_3), 14.1 (CH_3). $^{19}\text{F NMR}$ (376 MHz, CDCl_3): δ – 146.30 (q, $^1J_{\text{B-F}} = 31.8$ Hz). **IR** (ATR): 3311, 3272, 2969, 2924, 1749, 1669, 1640, 1541, 1507, 1191, 1154, 974, 739 cm^{-1} . **MS** (ESI): m/z (relative intensity) 1142 (100) $[\text{M}+\text{Na}]^+$, 1120 (11) $[\text{M}+\text{H}]^+$. **HR-MS** (ESI): m/z calcd for $\text{C}_{63}\text{H}_{74}\text{BF}_2\text{N}_8\text{O}_8^+$ $[\text{M}+\text{H}]^+$: 1119.5695, found: 1119.5684.

Ethyl **((S)-2-[[*tert*-butoxycarbonyl]amino]-3-{2-[(*E*)-4-(5,5-difluoro-1,3,7,9-tetramethyl-5*H*-4 λ_4 ,5 λ_4 -dipyrrolo[1,2-*c*:2',1'-*f*][1,3,2]diazaborinin-10-yl)styryl]-1-[pyridin-2-yl]-1*H*-indol-3-yl]propanoyl)-L-leucyl-L-phenylalanyl-glycinate (297n)**

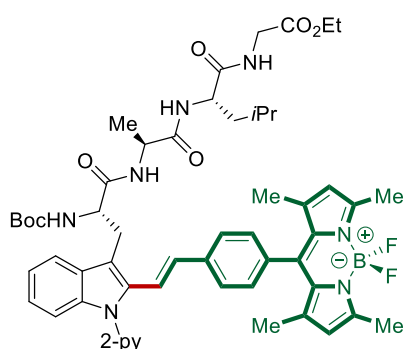


The general procedure **O** was followed using ethyl *N*_a-(*tert*-butoxycarbonyl)-1-(pyridin-2-yl)-L-tryptophyl-L-leucyl-L-phenylalanyl-glycinate **243ap** (72.7 mg, 0.10 mmol), 10-(4-ethynylphenyl)-5,5-difluoro-1,3,7,9-tetramethyl-5*H*-4 λ_4 ,5 λ_4 -dipyrrolo[1,2-*c*:2',1'-*f*][1,3,2]diazaborinine **294a** (69.6 mg, 0.20 mmol), $\text{MnBr}(\text{CO})_5$ (5.5 mg, 20 mol %) and 1-AdCO₂H (7.2 mg, 40 mol %) in 1,4-dioxane (1.0 mL). Purification by column chromatography on silica gel ($\text{CH}_2\text{Cl}_2/\text{EtOAc}$: 10/1→10/2) yielded **297n** (81.7 mg, 76%) as an orange solid.

M. p. 168 – 170 °C. $^1\text{H NMR}$ (400 MHz, CDCl_3): δ 8.78 – 8.69 (m, 1H), 7.94 (ddd, $J = 7.7, 7.7, 1.9$ Hz, 1H), 7.74 – 7.61 (m, 1H), 7.50 (d, $J = 8.0$ Hz, 2H), 7.46 – 7.37 (m, 3H),

7.32 (d, $J = 16.8$ Hz, 1H), 7.27 – 7.10 (m, 9H), 6.75 (brs, 1H), 6.65 (d, $J = 8.3$ Hz, 1H), 6.60 (d, $J = 16.8$ Hz, 1H), 6.39 (d, $J = 6.3$ Hz, 1H), 5.99 (s, 2H), 5.28 (d, $J = 6.1$ Hz, 1H), 4.69 – 4.53 (m, 2H), 4.30 – 4.04 (m, 4H), 3.85 (dd, $J = 18.0, 4.8$ Hz, 1H), 3.70 – 3.47 (m, 2H), 3.25 (dd, $J = 14.4, 5.9$ Hz, 1H), 2.89 (dd, $J = 14.4, 8.6$ Hz, 1H), 2.57 (s, 6H), 1.43 (s, 6H), 1.41 – 1.34 (m, 11H), 1.26 (t, $J = 7.1$ Hz, 3H), 1.23 – 1.17 (m, 1H), 0.82 – 0.69 (m, 6H). ^{13}C NMR (101 MHz, CDCl_3): δ 172.4 (C_q), 171.3 (C_q), 170.9 (C_q), 169.5 (C_q), 155.9 (C_q), 155.5 (C_q), 151.8 (C_q), 149.8 (CH), 143.0 (C_q), 141.3 (C_q), 138.6 (CH), 138.2 (C_q), 137.7 (C_q), 137.1 (C_q), 134.5 (C_q), 131.3 (C_q), 131.3 (CH), 129.0 (CH), 128.7 (C_q), 128.5 (CH), 128.5 (CH), 127.1 (CH), 126.7 (CH), 124.2 (CH), 122.7 (CH), 122.3 (CH), 121.6 (CH), 121.2 (CH), 118.9 (CH), 117.8 (CH), 112.9 (C_q), 110.9 (CH), 80.7 (C_q), 61.4 (CH_2), 55.8 (CH), 54.1 (CH), 52.9 (CH), 41.3 (CH_2), 40.6 (CH_2), 37.2 (CH_2), 28.2 (CH_3), 27.3 (CH_2), 24.6 (CH), 22.7 (CH_3), 22.1 (CH_3), 14.7 (CH_3), 14.6 (CH_3), 14.1 (CH_3). (One aromatic C_q is missing due to overlap, the overlap was verified by HSQC and HMBC analysis, showing that the peak at 134.5 corresponds to two carbons). ^{19}F NMR (376 MHz, CDCl_3): δ -146.29 (q, $^1J_{\text{B-F}} = 31.9$ Hz). IR (ATR): 3305, 2959, 2930, 1749, 1667, 1641, 1541, 1508, 1468, 1191, 975, 739 cm^{-1} . MS (ESI): m/z (relative intensity) 1098 (100) $[\text{M}+\text{Na}]^+$, 1076 (18) $[\text{M}+\text{H}]^+$. HR-MS (ESI): m/z calcd for $\text{C}_{61}\text{H}_{70}\text{BF}_2\text{N}_8\text{O}_7^+$ $[\text{M}+\text{H}]^+$: 1075.5433, found: 1075.5410.

Ethyl (*S*)-2-[[*tert*-butoxycarbonyl]amino]-3-{2-[(*E*)-4-(5,5-difluoro-1,3,7,9-tetramethyl-5*H*-4 λ ₄,5 λ ₄-dipyrrolo[1,2-*c*:2',1'-*f*][1,3,2]diazaborinin-10-yl)styryl]-1-[pyridin-2-yl]-1*H*-indol-3-yl]propanoyl}-L-alanyl-L-leucylglycinate (**297o**)



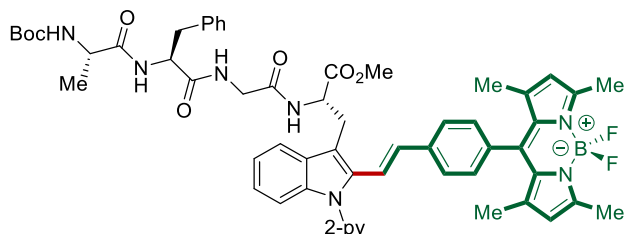
The general procedure **O** was followed using ethyl *N*_a-(*tert*-butoxycarbonyl)-1-(pyridin-2-yl)-L-tryptophyl-L-alanyl-L-leucylglycinate **243aq** (65.0 mg, 0.10 mmol), 10-(4-ethynylphenyl)-5,5-difluoro-1,3,7,9-tetramethyl-5*H*-4 λ ₄,5 λ ₄-dipyrrolo[1,2-*c*:2',1'-*f*][1,3,2]diazaborinine **294a** (69.6 mg, 0.20 mmol), $\text{MnBr}(\text{CO})_5$ (5.5 mg, 20 mol %) and 1-AdCO₂H (7.2 mg, 40 mol %) in 1,4-dioxane (1.0 mL). Purification by column

5. Experimental Part

chromatography on silica gel (CH₂Cl₂/EtOAc: 6/4) yielded **297o** (73.9 mg, 74%) as an orange solid.

M. p. 166 – 169 °C. **¹H NMR** (400 MHz, CDCl₃): δ 8.78 (d, *J* = 4.8 Hz, 1H), 7.95 (dd, *J* = 6.8, 6.8 Hz, 1H), 7.65 (d, *J* = 7.4 Hz, 1H), 7.53 – 7.37 (m, 5H), 7.31 – 7.27 (m, 1H), 7.27 – 7.19 (m, 4H), 7.03 (brs, 1H), 6.84 (d, *J* = 8.4 Hz, 1H), 6.60 (d, *J* = 16.7 Hz, 1H), 6.44 (brs, 1H), 5.99 (s, 2H), 5.29 (d, *J* = 5.0 Hz, 1H), 4.55 (ddd, *J* = 5.8, 5.5, 4.8 Hz, 1H), 4.42 (ddd, *J* = 7.6, 7.6, 6.4 Hz, 1H), 4.25 – 4.14 (m, 3H), 4.08 (dd, *J* = 18.1, 5.5 Hz, 1H), 3.94 (dd, *J* = 18.1, 4.8 Hz, 1H), 3.66 – 3.49 (m, 2H), 2.56 (s, 6H), 1.86 – 1.75 (m, 1H), 1.67 – 1.50 (m, 2H), 1.43 (s, 6H), 1.37 (s, 9H), 1.26 (t, *J* = 7.1 Hz, 3H), 1.19 (d, *J* = 6.9 Hz, 3H), 0.90 (d, *J* = 6.3 Hz, 3H), 0.87 (d, *J* = 6.3 Hz, 3H). **¹³C NMR** (101 MHz, CDCl₃): δ 172.4 (C_q), 172.2 (C_q), 171.7 (C_q), 169.6 (C_q), 155.8 (C_q), 155.5 (C_q), 151.7 (C_q), 149.7 (CH), 142.9 (C_q), 141.2 (C_q), 138.6 (CH), 138.1 (C_q), 137.5 (C_q), 134.5 (C_q), 134.4 (C_q), 131.6 (CH), 131.3 (C_q), 128.7 (C_q), 128.4 (CH), 127.0 (CH), 124.3 (CH), 122.7 (CH), 122.4 (CH), 121.6 (CH), 121.2 (CH), 118.7 (CH), 117.5 (CH), 112.7 (C_q), 110.9 (CH), 80.8 (C_q), 61.2 (CH₂), 56.1 (CH), 51.7 (CH), 50.0 (CH), 41.3 (CH₂), 40.2 (CH₂), 28.1 (CH₃), 27.1 (CH₂), 24.8 (CH), 22.9 (CH₃), 21.5 (CH₃), 17.6 (CH₃), 14.6 (CH₃), 14.5 (CH₃), 14.1 (CH₃). **¹⁹F NMR** (376 MHz, CDCl₃): δ – 146.27 (q, ¹*J*_{B-F} = 31.7 Hz). **IR** (ATR): 3275, 2966, 1700, 1633, 1541, 1507, 1453, 1191, 975, 709 cm⁻¹. **MS** (ESI): *m/z* (relative intensity) 1021 (100) [M+Na]⁺, 999 (25) [M+H]⁺. **HR-MS** (ESI): *m/z* calcd for C₅₅H₆₆BF₂N₈O₇ [M+H]⁺: 999.5119, found: 999.5100.

Methyl (6*S*,9*S*,15*S*)-9-benzyl-15-((2-[(*E*)-4-(5,5-difluoro-1,3,7,9-tetramethyl-5*H*-4*λ*₄,5*λ*₄-dipyrrolo[1,2-*c*:2',1'-*f*][1,3,2]diazaborinin-10-yl)styryl]-1-[pyridin-2-yl]-1*H*-indol-3-yl)methyl)-2,2,6-trimethyl-4,7,10,13-tetraoxo-3-oxa-5,8,11,14-tetraazahexadecan-16-oate (297p)

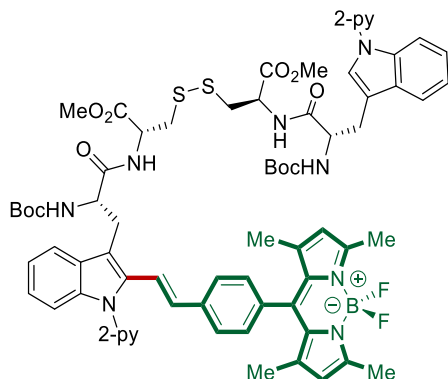


The general procedure **O** was followed using methyl *N*_α-(*tert*-butoxycarbonyl)-L-alanyl-L-phenylalanyl-glycyl-1-(pyridin-2-yl)-L-tryptophanate **243w** (67.1 mg, 0.10 mmol), 10-(4-ethynylphenyl)-5,5-difluoro-1,3,7,9-tetramethyl-5*H*-4*λ*₄,5*λ*₄-dipyrrolo[1,2-*c*:2',1'-*f*][1,3,2]diazaborinine **294a** (69.6 mg, 0.20 mmol), MnBr(CO)₅ (5.5 mg, 20 mol %) and

1-AdCO₂H (7.2 mg, 40 mol %) in 1,4-dioxane (1.0 mL). Purification by column chromatography on silica gel (CH₂Cl₂/EtOAc: 1/1) yielded **297p** (57.1 mg, 56%) as an orange solid.

M. p. 167 – 169 °C. **¹H NMR** (400 MHz, CDCl₃): δ 8.66 (dd, *J* = 5.0, 2.0 Hz, 1H), 7.95 (ddd, *J* = 7.7, 7.7, 2.0 Hz, 1H), 7.62 – 7.56 (m, 1H), 7.51 (d, *J* = 8.2 Hz, 2H), 7.46 (d, *J* = 8.0 Hz, 1H), 7.43 – 7.36 (m, 2H), 7.28 – 7.18 (m, 8H), 7.16 – 7.10 (m, 2H), 7.09 – 6.97 (m, 2H), 6.91 (d, *J* = 7.5 Hz, 1H), 6.55 (d, *J* = 16.7 Hz, 1H), 5.99 (s, 2H), 5.12 – 4.88 (m, 2H), 4.61 (ddd, *J* = 7.0, 7.0, 7.0 Hz, 1H), 4.03 (dq, *J* = 7.5, 6.9 Hz, 1H), 3.96 – 3.77 (m, 2H), 3.58 (d, *J* = 6.6 Hz, 2H), 3.55 (s, 3H), 3.09 (d, *J* = 6.7 Hz, 2H), 2.57 (s, 6H), 1.43 (s, 6H), 1.39 (s, 9H), 1.19 (d, *J* = 6.9 Hz, 3H). **¹³C NMR** (101 MHz, CDCl₃): δ 173.0 (C_q), 172.0 (C_q), 171.2 (C_q), 168.5 (C_q), 155.7 (C_q), 155.4 (C_q), 151.8 (C_q), 149.7 (CH), 143.0 (C_q), 141.4 (C_q), 138.6 (CH), 138.1 (C_q), 137.8 (C_q), 136.4 (C_q), 134.3 (C_q), 134.3 (C_q), 131.3 (C_q), 130.7 (CH), 129.1 (CH), 128.9 (C_q), 128.7 (CH), 128.4 (CH), 127.0 (CH), 126.9 (CH), 124.0 (CH), 122.6 (CH), 122.3 (CH), 121.3 (CH), 121.2 (CH), 118.9 (CH), 117.9 (CH), 113.2 (C_q), 110.7 (CH), 80.5 (C_q), 54.3 (CH), 52.9 (CH), 52.5 (CH₃), 50.7 (CH), 43.2 (CH₂), 37.1 (CH₂), 28.2 (CH₃), 27.9 (CH₂), 17.8 (CH₃), 14.6 (CH₃), 14.6 (CH₃). **¹⁹F NMR** (376 MHz, CDCl₃): δ – 146.26 (q, ¹*J*_{B-F} = 31.8 Hz). **IR** (ATR): 3297, 3279, 2952, 1738, 1667, 1639, 1540, 1507, 1436, 1192, 975 cm⁻¹. **MS** (ESI): *m/z* (relative intensity) 1041 (100) [M+Na]⁺, 1019 (18) [M+H]⁺. **HR-MS** (ESI): *m/z* calcd for C₅₇H₆₂BF₂N₈O₇ [M+H]⁺: 1019.4806, found: 1019.4789.

Methyl *N*-[*N*_α-(*tert*-butoxycarbonyl)-1-(pyridin-2-yl)-L-tryptophyl]-*S*-{[(*R*)-2-({*S*)-2-{{*tert*-butoxycarbonyl}amino}-3-{2-[(*E*)-4-(5,5-difluoro-1,3,7,9-tetramethyl-5*H*-4*λ*₄,5*λ*₄-dipyrrolo[1,2-*c*:2',1'-*f*][1,3,2]diazaborinin-10-yl)styryl]-1-[pyridin-2-yl]-1*H*-indol-3-yl]propanamido)-3-methoxy-3-oxopropyl]thio}-L-cysteinate (297q)



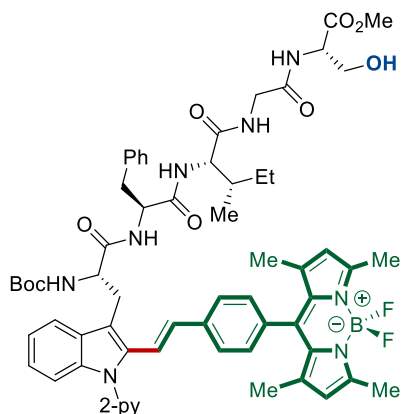
The general procedure **O** was followed using methyl (6*S*,9*R*,14*R*)-14-[[*S*]-2-[(*tert*-butoxycarbonyl)amino]-3-[1-(pyridin-2-yl)-1*H*-indol-3-yl]propanamido]-9-

5. Experimental Part

(methoxycarbonyl)-2,2-dimethyl-4,7-dioxo-6-[[1-(pyridin-2-yl)-1*H*-indol-3-yl]methyl]-3-oxa-11,12-dithia-5,8-diazapentadecan-15-oate **261** (99.5 mg, 0.10 mmol), 10-(4-ethynylphenyl)-5,5-difluoro-1,3,7,9-tetramethyl-5*H*-4 λ ₄,5 λ ₄-dipyrrolo[1,2-*c*:2',1'-*f*][1,3,2]diazaborinine **294a** (139.2 mg, 0.40 mmol), MnBr(CO)₅ (5.5 mg, 20 mol %) and 1-AdCO₂H (7.2 mg, 40 mol %) in 1,4-dioxane (1.0 mL). Purification by column chromatography on silica gel (CH₂Cl₂/EtOAc: 6/4) yielded **297q** (67.2 mg, 50%) as an orange solid.

M. p. 150 – 152 °C. **¹H NMR** (400 MHz, CDCl₃): δ 8.73 (d, *J* = 5.2 Hz, 1H), 8.50 (d, *J* = 5.3 Hz, 1H), 8.24 (d, *J* = 8.3 Hz, 1H), 7.88 (ddd, *J* = 7.7, 7.7, 2.0 Hz, 1H), 7.75 (dd, *J* = 7.9, 7.9 Hz, 1H), 7.69 – 7.60 (m, 3H), 7.55 (d, *J* = 7.7 Hz, 2H), 7.47 – 7.33 (m, 4H), 7.33 – 7.29 (m, 1H), 7.28 – 7.25 (m, 1H), 7.25 – 6.99 (m, 7H), 6.80 (d, *J* = 7.1 Hz, 1H), 6.69 (d, *J* = 16.8 Hz, 1H), 5.99 (s, 2H), 5.77 (d, *J* = 8.0 Hz, 1H), 5.48 (brs, 1H), 4.76 (ddd, *J* = 8.0, 6.0, 5.2 Hz, 1H), 4.73 – 4.56 (m, 3H), 3.68 – 3.46 (m, 8H), 3.40 – 3.21 (m, 2H), 3.08 (dd, *J* = 14.3, 5.2 Hz, 1H), 3.00 – 2.86 (m, 3H), 2.57 (s, 6H), 1.50 – 1.32 (m, 24H). **¹³C NMR** (101 MHz, CDCl₃): δ 171.7 (C_q), 171.6 (C_q), 170.2 (C_q), 169.8 (C_q), 155.6 (C_q), 155.5 (C_q), 155.4 (C_q), 152.3 (C_q), 151.9 (C_q), 149.6 (CH), 148.7 (CH), 143.1 (C_q), 141.6 (C_q), 138.4 (CH), 138.3 (CH), 138.1 (C_q), 138.1 (C_q), 135.4 (C_q), 134.2 (C_q), 134.1 (C_q), 131.4 (C_q), 130.6 (CH), 130.1 (C_q), 129.1 (C_q), 128.3 (CH), 127.1 (CH), 124.9 (CH), 123.8 (CH), 123.4 (CH), 122.4 (CH), 122.4 (CH), 121.3 (CH), 121.2 (CH), 121.2 (CH), 119.7 (CH), 119.1 (CH), 119.0 (CH), 118.1 (CH), 114.2 (CH), 113.6 (C_q), 113.6 (C_q), 113.4 (CH), 110.7 (CH), 80.1 (C_q), 80.0 (C_q), 55.5 (CH), 54.8 (CH), 52.7 (CH₃), 52.6 (CH₃), 52.0 (CH), 51.8 (CH), 40.5 (CH₂), 40.3 (CH₂), 29.0 (CH₂), 28.3 (CH₃), 28.3 (CH₃), 28.1 (CH₂), 14.7 (CH₃), 14.6 (CH₃). **¹⁹F NMR** (376 MHz, CDCl₃): δ – 146.28 (q, ¹*J*_{B-F} = 31.2 Hz). **IR** (ATR): 1746, 1680, 1507, 1470, 1435, 1192, 1154, 974, 740 cm⁻¹. **MS** (ESI): *m/z* (relative intensity) 1366 (75) [M+Na]⁺, 1344 (100) [M+H]⁺. **HR-MS** (ESI): *m/z* calcd for C₇₁H₇₈BF₂N₁₀O₁₀S⁺ [M+H]⁺: 1343.5411, found: 1343.5395.

Methyl ((S)-2-[[*tert*-butoxycarbonyl)amino]-3-{2-[(*E*)-4-(5,5-difluoro-1,3,7,9-tetramethyl-5*H*-4 λ ₄,5 λ ₄-dipyrrolo[1,2-*c*:2',1'-*f*][1,3,2]diazaborinin-10-yl)styryl]-1-[pyridin-2-yl]-1*H*-indol-3-yl}propanoyl)-L-phenylalanyl-L-isoleucylglycyl-L-serinate (297r)



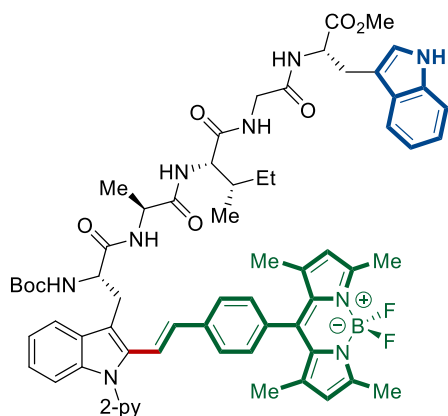
The general procedure **O** was followed using methyl *N*_a-(*tert*-butoxycarbonyl)-1-(pyridin-2-yl)-L-tryptophyl-L-phenylalanyl-L-isoleucylglycyl-L-serinate **243ar** (80.0 mg, 0.10 mmol), 10-(4-ethynylphenyl)-5,5-difluoro-1,3,7,9-tetramethyl-5*H*-4 λ ₄,5 λ ₄-dipyrrolo[1,2-*c*:2',1'-*f*][1,3,2]diazaborinine **294a** (69.7 mg, 0.20 mmol), MnBr(CO)₅ (5.5 mg, 20 mol %) and 1-AdCO₂H (7.2 mg, 40 mol %) in 1,4-dioxane (1.0 mL). Purification by column chromatography on silica gel (CH₂Cl₂/Acetone: 8/2→6/4) yielded **297r** (79.0 mg, 69%) as an orange solid.

M. p. 97 °C (decomposition). ¹H NMR (400 MHz, DMSO-*d*₆): δ 8.73 (dd, *J* = 5.0, 1.7 Hz, 1H), 8.24 – 8.14 (m, 3H), 8.09 (dd, *J* = 7.9, 7.9 Hz, 1H), 7.92 (d, *J* = 8.3 Hz, 1H), 7.79 – 7.71 (m, 1H), 7.62 – 7.53 (m, 3H), 7.48 (d, *J* = 8.0 Hz, 1H), 7.40 – 7.31 (m, 3H), 7.31 – 7.09 (m, 9H), 6.47 (d, *J* = 16.7 Hz, 1H), 6.18 (s, 2H), 4.79 (td, *J* = 8.3, 4.8 Hz, 1H), 4.50 – 4.35 (m, 2H), 4.30 (td, *J* = 9.3, 4.0 Hz, 1H), 4.22 (t, *J* = 7.9 Hz, 1H), 3.91 – 3.67 (m, 3H), 3.66 – 3.55 (m, 4H), 3.22 – 3.00 (m, 3H), 2.87 (dd, *J* = 13.8, 8.7 Hz, 1H), 2.45 (s, 6H), 1.81 – 1.67 (m, 1H), 1.50 – 1.43 (m, 1H), 1.40 (s, 6H), 1.18 (s, 9H), 1.12 – 1.02 (m, 1H), 0.85 (d, *J* = 6.6 Hz, 3H), 0.79 (t, *J* = 7.4 Hz, 3H). ¹³C NMR (101 MHz, DMSO-*d*₆): δ 171.7 (C_q), 171.4 (C_q), 171.4 (C_q), 171.1 (C_q), 169.3 (C_q), 155.4 (C_q), 155.3 (C_q), 151.7 (C_q), 150.1 (CH), 143.1 (C_q), 142.2 (C_q), 139.7 (CH), 138.3 (C_q), 138.2 (C_q), 137.9 (C_q), 134.1 (C_q), 133.6 (C_q), 131.1 (C_q), 130.0 (CH), 129.9 (CH), 129.0 (C_q), 128.7 (CH), 128.3 (CH), 127.3 (CH), 126.6 (CH), 124.0 (CH), 123.6 (CH), 122.8 (CH), 121.8 (CH), 121.1 (CH), 119.9 (CH), 118.8 (CH), 115.7 (C_q), 110.8 (CH), 78.7 (C_q), 61.7 (CH₂), 57.5 (CH), 56.6 (CH), 55.1 (CH), 53.7 (CH), 52.3 (CH₃), 42.1 (CH₂), 38.3 (CH₂), 37.1 (CH), 28.5 (CH₂), 28.4 (CH₃), 24.8 (CH₂), 15.7 (CH₃), 14.7

5. Experimental Part

(CH₃), 14.7 (CH₃), 11.5 (CH₃). **¹⁹F NMR** (376 MHz, DMSO-*d*₆): δ – 143.7 (q, ¹J_{B-F} = 31.3 Hz). **IR** (ATR): 3280, 2962, 2926, 1745, 1656, 1542, 1509, 1195, 1025, 1007, 983 cm⁻¹. **MS** (ESI): *m/z* (relative intensity) 1171 (100) [M+Na]⁺, 1149 (10) [M+H]⁺. **HR-MS** (ESI) *m/z* calcd for C₆₃H₇₂BF₂N₉O₉Na⁺ [M+Na]⁺: 1170.5417, found: 1170.5374.

Methyl ((S)-2-[(*tert*-butoxycarbonyl)amino]-3-{2-[(*E*)-4-(5,5-difluoro-1,3,7,9-tetramethyl-5*H*-4λ₄,5λ₄-dipyrrolo[1,2-*c*:2',1'-*f*][1,3,2]diazaborinin-10-yl)styryl]-1-[pyridin-2-yl]-1*H*-indol-3-yl}propanoyl)-L-alanyl-L-isoleucylglycyl-L-tryptophanate (243s)

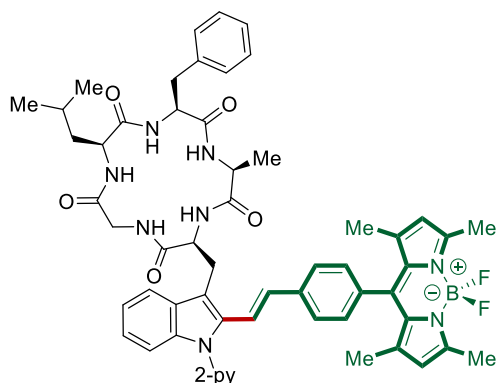


The general procedure **O** was followed using methyl *N*_α-(*tert*-butoxycarbonyl)-1-(pyridin-2-yl)-L-tryptophyl-L-alanyl-L-isoleucylglycyl-L-tryptophanate **243as** (82.6 mg, 0.10 mmol), 10-(4-ethynylphenyl)-5,5-difluoro-1,3,7,9-tetramethyl-5*H*-4λ₄,5λ₄-dipyrrolo[1,2-*c*:2',1'-*f*][1,3,2]diazaborinine **294a** (69.2 mg, 0.40 mmol), MnBr(CO)₅ (5.5 mg, 20 mol %) and 1-AdCO₂H (7.2 mg, 40 mol %) in 1,4-dioxane (1.0 mL). Purification by column chromatography on silica gel (CH₂Cl₂/EtOAc: 6/4) yielded **297s** (66.7 mg, 57%) as an orange solid.

M. p. 179 – 181 °C. **¹H NMR** (400 MHz, CD₃OD): δ 8.69 (d, *J* = 5.5 Hz, 1H), 8.06 (dd, *J* = 8.0, 8.0 Hz, 1H), 7.73 (d, *J* = 7.4 Hz, 1H), 7.58 – 7.41 (m, 5H), 7.39 – 7.26 (m, 2H), 7.25 – 7.11 (m, 5H), 7.09 – 6.92 (m, 3H), 6.39 (d, *J* = 16.7 Hz, 1H), 6.03 (s, 2H), 4.71 (dd, *J* = 6.5, 6.5 Hz, 1H), 4.58 (dd, *J* = 6.9, 6.9 Hz, 1H), 4.32 (d, *J* = 7.8 Hz, 1H), 4.11 (d, *J* = 7.1 Hz, 1H), 3.93 (d, *J* = 16.6 Hz, 1H), 3.79 (d, *J* = 16.9 Hz, 1H), 3.65 – 3.46 (m, 4H), 3.44 – 3.35 (m, 1H), 3.29 – 3.10 (m, 2H), 2.49 (s, 6H), 1.87 – 1.75 (m, 1H), 1.60 – 1.46 (m, 1H), 1.40 (s, 6H), 1.31 (s, 9H), 1.24 – 1.08 (m, 4H), 0.90 (d, *J* = 7.8 Hz, 3H), 0.86 (d, *J* = 7.3 Hz, 3H). **¹³C NMR** (101 MHz, CD₃OD): δ 174.7 (C_q), 174.1 (C_q), 174.0 (C_q), 173.6 (C_q), 171.2 (C_q), 157.4 (C_q), 156.7 (C_q), 153.4 (C_q), 150.5 (CH), 144.4 (C_q), 143.2 (C_q), 140.9 (CH), 140.2 (C_q), 139.5 (C_q), 137.9 (C_q), 135.8 (C_q), 135.4 (C_q), 132.5

(C_q), 131.7 (CH), 130.3 (C_q), 129.7 (CH), 128.7 (C_q), 128.2 (CH), 125.1 (CH), 124.5 (CH), 124.5 (CH), 122.4 (CH), 122.3 (CH), 122.2 (CH), 120.4 (CH), 119.9 (CH), 119.2 (CH), 119.1 (CH), 115.8 (C_q), 112.3 (CH), 111.4 (CH), 111.4 (CH), 110.5 (C_q), 80.8 (C_q), 59.8 (CH), 57.0 (CH), 54.8 (CH), 52.7 (CH₃), 50.5 (CH), 43.3 (CH₂), 37.7 (CH), 28.8 (CH₂), 28.6 (CH₃), 28.4 (CH₂), 26.2 (CH₂), 17.9 (CH₃), 15.9 (CH₃), 14.9 (CH₃), 14.6 (CH₃), 11.6 (CH₃). ¹⁹F NMR (376 MHz, CD₃OD): δ – 146.95 (q, ¹J_{B-F} = 31.2 Hz). IR (ATR): 3292, 2962, 2929, 1742, 1712, 1628, 1541, 1454, 1409, 1192, 1154, 973, 739 cm⁻¹. MS (ESI): *m/z* (relative intensity) 1194 (100) [M+Na]⁺, 1172 (8) [M+H]⁺. HR-MS (ESI): *m/z* calcd for C₆₅H₇₄BF₂N₁₀O₈⁺ [M+H]⁺: 1171.5757, found: 1171.5739.

(3*S*,6*S*,9*S*,12*S*)-6-Benzyl-12-({2-[(*E*)-4-(5,5-difluoro-1,3,7,9-tetramethyl-5*H*-4λ₄,5λ₄-dipyrrolo[1,2-*c*:2',1'-*f*][1,3,2]diazaborinin-10-yl)styryl]-1-[pyridin-2-yl]-1*H*-indol-3-yl)methyl)-3-isobutyl-9-methyl-1,4,7,10,13-pentaazacyclopentadecane-2,5,8,11,14-pentaone (300a)



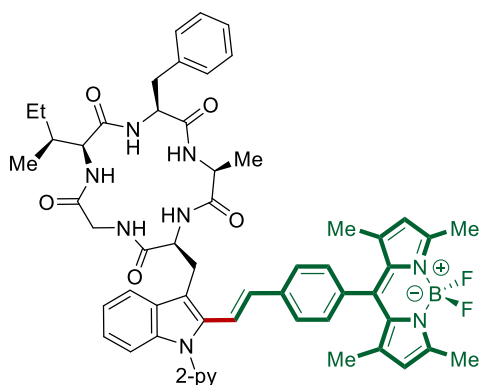
The general procedure **O** was followed using (3*S*,6*S*,9*S*,12*S*)-6-benzyl-3-isobutyl-9-methyl-12-{{1-(pyridin-2-yl)-1*H*-indol-3-yl)methyl}-1,4,7,10,13-pentaazacyclopentadecane-2,5,8,11,14-pentaone **299a** (65.2 mg, 0.10 mmol), 10-(4-ethynylphenyl)-5,5-difluoro-1,3,7,9-tetramethyl-5*H*-4λ₄,5λ₄-dipyrrolo[1,2-*c*:2',1'-*f*][1,3,2]diazaborinine **294a** (69.2 mg, 0.40 mmol), MnBr(CO)₅ (5.5 mg, 20 mol %) and 1-AdCO₂H (7.2 mg, 40 mol %) in 1,4-dioxane (1.0 mL). Purification by column chromatography on silica gel (CH₂Cl₂/MeOH: 96/4) yielded **300a** (66.9 mg, 67%) as an orange solid.

M. p. 217 – 219 °C. ¹H NMR (400 MHz, DMSO-*d*₆): δ 8.84 (dd, *J* = 5.9, 5.9 Hz, 1H), 8.73 (dd, *J* = 4.9, 1.9 Hz, 1H), 8.51 (d, *J* = 8.6 Hz, 1H), 8.20 (d, *J* = 7.6 Hz, 1H), 8.08 (ddd, *J* = 7.7, 7.7, 2.0 Hz, 1H), 8.02 (d, *J* = 8.1 Hz, 1H), 7.95 (d, *J* = 8.4 Hz, 1H), 7.87 – 7.79 (m, 1H), 7.62 – 7.49 (m, 4H), 7.42 (d, *J* = 16.7 Hz, 1H), 7.36 – 7.30 (m, 2H), 7.29 – 7.23 (m, 3H), 7.23 – 7.13 (m, 5H), 6.51 (d, *J* = 16.7 Hz, 1H), 6.17 (s, 2H), 4.53

5. Experimental Part

(ddd, $J = 8.4, 8.4, 5.5$ Hz, 1H), 4.32 – 4.19 (m, 1H), 4.17 – 3.98 (m, 2H), 3.84 (dd, $J = 14.2, 5.9$ Hz, 1H), 3.57 (dd, $J = 14.2, 5.3$ Hz, 1H), 3.31 – 3.27 (m, 1H), 3.25 – 3.12 (m, 2H), 3.07 (dd, $J = 13.6, 6.2$ Hz, 1H), 2.45 (s, 6H), 1.53 – 1.46 (m, 2H), 1.38 (s, 6H), 1.26 – 1.17 (m, 4H), 0.89 (d, $J = 5.9$ Hz, 3H), 0.85 (d, $J = 5.8$ Hz, 3H). $^{13}\text{C NMR}$ (101 MHz, DMSO- d_6): δ 173.5 (C_q), 172.1 (C_q), 171.6 (C_q), 171.0 (C_q), 169.8 (C_q), 155.4 (C_q), 151.7 (C_q), 150.1 (CH), 143.1 (C_q), 142.2 (C_q), 139.7 (CH), 138.3 (C_q), 138.2 (C_q), 138.2 (C_q), 134.2 (C_q), 133.6 (C_q), 131.1 (C_q), 130.0 (CH), 129.5 (CH), 128.8 (C_q), 128.7 (CH), 128.6 (CH), 127.3 (CH), 126.9 (CH), 124.1 (CH), 123.6 (CH), 122.9 (CH), 121.8 (CH), 121.3 (CH), 119.8 (CH), 118.8 (CH), 115.5 (C_q), 111.0 (CH), 58.3 (CH), 55.6 (CH), 51.5 (CH), 50.1 (CH), 44.2 (CH₂), 41.2 (CH₂), 36.3 (CH₂), 27.3 (CH₂), 24.9 (CH), 23.4 (CH₃), 22.2 (CH₃), 17.3 (CH₃), 14.7 (CH₃), 14.6 (CH₃). $^{19}\text{F NMR}$ (376 MHz, DMSO- d_6): δ – 143.67 (q, $^1J_{\text{B-F}} = 28.7$ Hz). **IR** (ATR): 3306, 2954, 2900, 1655, 1514, 1454, 1437, 1289, 1148, 1080, 740 cm^{-1} . **MS** (ESI): m/z (relative intensity) 1022 (100) [M+Na]⁺, 1000 (75) [M+H]⁺. **HR-MS** (ESI): m/z calcd for C₅₇H₆₀BF₂N₉O₅Na⁺ [M+Na]⁺: 1022.4680, found: 1022.4659.

(3S,6S,9S,12S)-6-Benzyl-3-[(S)-sec-butyl]-12-({2-[(E)-4-(5,5-difluoro-1,3,7,9-tetramethyl-5H-4 λ_4 ,5 λ_4 -dipyrrolo[1,2-c:2',1'-f][1,3,2]diazaborinin-10-yl)styryl]-1-[pyridin-2-yl]-1H-indol-3-yl)methyl)-9-methyl-1,4,7,10,13-pentaazacyclopentadecane-2,5,8,11,14-pentaone (300b)

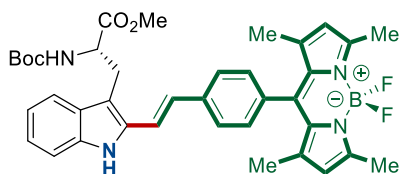


The general procedure **O** was followed using (3S,6S,9S,12S)-6-benzyl-3-[(S)-sec-butyl]-9-methyl-12-[[1-(pyridin-2-yl)-1H-indol-3-yl)methyl]-1,4,7,10,13-pentaazacyclopentadecane-2,5,8,11,14-pentaone **299b** (65.2 mg, 0.10 mmol), 10-(4-ethynylphenyl)-5,5-difluoro-1,3,7,9-tetramethyl-5H-4 λ_4 ,5 λ_4 -dipyrrolo[1,2-c:2',1'-f][1,3,2]diazaborinine **294a** (69.2 mg, 0.40 mmol), MnBr(CO)₅ (5.5 mg, 20 mol %) and 1-AdCO₂H (7.2 mg, 40 mol %) in 1,4-dioxane (1.0 mL). Purification by column

chromatography on silica gel (CH₂Cl₂/MeOH: 95/5) yielded **300b** (57.9 mg, 58%) as an orange solid.

M. p. 207 –209 °C. **¹H NMR** (400 MHz, DMSO-*d*₆): δ 9.05 (t, *J* = 5.9 Hz, 1H), 8.83 (d, *J* = 8.9 Hz, 1H), 8.73 (dd, *J* = 5.0, 1.9 Hz, 1H), 8.37 (d, *J* = 7.3 Hz, 1H), 8.08 (ddd, *J* = 7.7, 7.7, 2.0 Hz, 1H), 7.90 – 7.77 (m, 3H), 7.59 (d, *J* = 8.1 Hz, 2H), 7.58 – 7.50 (m, 2H), 7.44 (d, *J* = 16.8 Hz, 1H), 7.33 (d, *J* = 8.1 Hz, 2H), 7.30 – 7.13 (m, 8H), 6.55 (d, *J* = 16.8 Hz, 1H), 6.16 (s, 2H), 4.52 (ddd, *J* = 9.2, 8.9, 4.2 Hz, 1H), 4.26 (dq, *J* = 7.0, 6.8 Hz, 1H), 4.12 (dd, *J* = 9.1, 7.4 Hz, 1H), 3.95 (ddd, *J* = 9.6, 6.4, 4.1 Hz, 1H), 3.80 (dd, *J* = 13.7, 5.7 Hz, 1H), 3.61 (dd, *J* = 14.4, 4.1 Hz, 1H), 3.31 – 3.21 (m, 2H), 3.17 – 3.06 (m, 2H), 2.45 (s, 6H), 1.75 – 1.59 (m, 1H), 1.47 – 1.40 (m, 1H), 1.38 (s, 6H), 1.25 (d, *J* = 6.8 Hz, 3H), 1.11 – 0.97 (m, 1H), 0.91 – 0.78 (m, 6H). **¹³C NMR** (101 MHz, DMSO-*d*₆): δ 172.9 (C_q), 171.6 (C_q), 171.4 (C_q), 170.4 (C_q), 169.3 (C_q), 154.9 (C_q), 151.2 (C_q), 149.6 (CH), 142.6 (C_q), 141.7 (C_q), 139.2 (CH), 137.8 (C_q), 137.8 (C_q), 133.6 (C_q), 133.1 (C_q), 130.6 (C_q), 129.6 (CH), 128.9 (CH), 128.4 (C_q), 128.2 (CH), 128.2 (CH), 126.8 (CH), 126.4 (CH), 123.6 (CH), 123.1 (CH), 122.4 (CH), 121.3 (CH), 120.8 (CH), 119.3 (CH), 118.3 (CH), 115.5 (C_q), 110.5 (CH), 59.1 (CH), 56.5 (CH), 55.1 (CH), 49.2 (CH), 44.0 (CH₂), 37.1 (CH), 35.6 (CH₂), 26.8 (CH₂), 24.4 (CH₂), 16.8 (CH₃), 15.5 (CH₃), 14.2 (CH₃), 11.0 (CH₃). (One aromatic C_q and one CH₃ are missing due to overlap, the overlap was verified by HSQC and HMBC analysis, showing that the peak at 137.8 corresponds to two carbons and the peak at 14.2 corresponds to the two CH₃). **¹⁹F NMR** (376 MHz, DMSO-*d*₆) δ – 143.67 (q, ¹*J*_{B-F} = 30.1 Hz). **IR** (ATR): 3313, 3288, 2914, 1658, 1513, 1468, 1150, 1081, 975 cm⁻¹. **MS** (ESI): *m/z* (relative intensity) 1022 (100) [M+Na]⁺, 1000 (80) [M+H]⁺. **HR-MS** (ESI): *m/z* calcd for C₅₇H₆₁BF₂N₉O₅⁺ [M+H]⁺: 1000.4861, found: 1000.4836.

Methyl (S,E)-2-[(*tert*-butoxycarbonyl)amino]-3-{2-[4-(5,5-difluoro-1,3,7,9-tetramethyl-5*H*-4λ₄,5λ₄-dipyrrolo[1,2-*c*:2',1'-*f*][1,3,2]diazaborinin-10-yl)styryl]-1*H*-indol-3-yl}propanoate (301)



To a stirred solution of methyl (S,E)-2-[(*tert*-butoxycarbonyl)amino]-3-{2-[4-(5,5-difluoro-1,3,7,9-tetramethyl-5*H*-4λ₄,5λ₄-dipyrrolo[1,2-*c*:2',1'-*f*][1,3,2]diazaborinin-10-yl)styryl]-1-(pyridin-2-yl)-1*H*-indol-3-yl}propanoate **292a** (111.5 mg, 0.15 mmol) in

5. Experimental Part

CH₂Cl₂ (1.0 mL) methyl trifluoromethanesulfonate (73.8 mg, 0.45 mmol) was added at 0 °C. After 30 min, the mixture was allowed to warm up to 25 °C and stirred for 18 h. The crude mixture was concentrated under reduced pressure to afford an orange solid. In a sealed-tube, the crude product, Pd(OH)₂/C (20 wt%, containing 50% water) (9.2 mg, 5.0 mol %), and ammonium formate (141.9 mg, 15.0 equiv) were dissolved in methanol (2.0 mL), and stirred at 60 °C for 16 hours. The mixture was filtered through a short plug of celite, concentrated under reduced pressure and purified by column chromatography on silica gel (*n*-Hexane/EtOAc: 8/2 → 7/3), yielding **300** (46.9 mg, 47%) as an orange solid.

M. p. 168 – 170 °C. **¹H NMR** (400 MHz, CDCl₃): δ 8.36 (brs, 1H), 7.66 (d, *J* = 7.8 Hz, 2H), 7.52 (d, *J* = 7.4 Hz, 1H), 7.35 – 7.26 (m, 4H), 7.21 (dd, *J* = 7.4 Hz, 1H), 7.10 (dd, *J* = 7.4 Hz, 1H), 6.89 (d, *J* = 16.5 Hz, 1H), 6.00 (s, 2H), 5.18 (d, *J* = 8.2 Hz, 1H), 4.71 (ddd, *J* = 8.2, 6.9, 4.4 Hz, 1H), 3.57 (s, 3H), 3.46 (dd, *J* = 14.9, 4.4 Hz, 1H), 3.41 (dd, *J* = 14.9, 6.9 Hz, 1H), 2.57 (s, 6H), 1.46 (s, 6H), 1.41 (s, 9H). **¹³C NMR** (101 MHz, CDCl₃): δ 172.5 (C_q), 155.7 (C_q), 155.2 (C_q), 143.1 (C_q), 141.5 (C_q), 137.8 (C_q), 136.7 (C_q), 134.3 (C_q), 133.7 (C_q), 131.5 (C_q), 129.3 (C_q), 128.7 (CH), 127.1 (CH), 125.7 (CH), 123.8 (CH), 121.4 (CH), 120.2 (CH), 119.3 (CH), 118.0 (CH), 111.8 (C_q), 110.8 (CH), 80.0 (C_q), 54.6 (CH), 52.4 (CH₃), 28.5 (CH₃), 27.7 (CH₂), 14.8 (CH₃), 14.7 (CH₃). **¹⁹F NMR** (376 MHz, CDCl₃): δ – 146.1 (q, ¹*J*_{B-F} = 32.2 Hz). **IR** (ATR): 3401, 2970, 2952, 1707, 1541, 1506, 1191, 1153, 973, 710 cm⁻¹. **MS** (ESI): *m/z* (relative intensity) 689 (100) [M+Na]⁺, 667 (60) [M+H]⁺, 647 (45) [M-F]⁺. **HR-MS** (ESI) *m/z* calcd for C₃₈H₄₂BF₂N₄O₄ [M+H]⁺:667.3268, found: 667.3248.

5.7.2 Manganese(I)-Catalyzed C–H Labeling in Flow

A 5 mL oven-dried pear-shaped flask was charged with methyl *N*_α-(*tert*-butoxycarbonyl)-1-(pyridin-2-yl)-L-tryptophanate **153** (39.5 mg, 0.10 mmol), 10-(4-ethynylphenyl)-5,5-difluoro-1,3,7,9-tetramethyl-5*H*-4*λ*₄,5*λ*₄-dipyrrolo[1,2-*c*:2',1'-*f*][1,3,2]diazaborinine **294a** (38.3 mg, 0.11 mmol), MnBr(CO)₅ (5.5 mg, 20 mol %) and 1-AdCO₂H (7.2 mg, 40 mol %) and 1,4-dioxane (2.0 mL) under air. Subsequently, the reaction media was connected to the inlet of the 10 mL standard heated reactor connected with a column reactor (Ø = 8 mm) packed with 250 mg of QuadraPure™ IDA over 2 g of sand. The syringe pump was operated at a flow rate of 100 μL / min (100 min residence time). The temperature of the standard heated reactor was set at

100 °C. By using the Flow Wizard system, the solution was collected automatically. To ensure full transfer of the crude mixture to the collection flask EtOAc (20 mL) was pumped through the reactor at ambient temperature. Next, the mixture was concentrated *in vacuo*. Purification by column chromatography on silica gel (CH₂Cl₂/MeOH: 100/0.2) yielded **3** (46.0 mg, 62%) as an orange solid.

6. References

6. References

- [1] a) P. T. Anastas, M. M. Kirchhoff, *Acc. Chem. Res.* **2002**, *35*, 686-694; b) P. T. Anastas, J. C. Warner, *Green Chemistry: Theory and Practice*, Oxford University Press, New York, **1998**.
- [2] a) P. Gandeepan, L. H. Finger, T. H. Meyer, L. Ackermann, *Chem. Soc. Rev.* **2020**, *49*, 4254-4272; b) T. H. Meyer, L. H. Finger, P. Gandeepan, L. Ackermann, *Trends Chem.* **2019**, *1*, 63-76; c) B. Trost, *Science* **1991**, *254*, 1471-1477.
- [3] a) A. Fürstner, *Angew. Chem. Int. Ed.* **2013**, *52*, 2794-2819; b) K. C. Nicolaou, P. G. Bulger, D. Sarlah, *Angew. Chem. Int. Ed.* **2005**, *44*, 4490-4527.
- [4] K. C. Nicolaou, P. G. Bulger, D. Sarlah, *Angew. Chem. Int. Ed.* **2005**, *44*, 4442-4489.
- [5] E.-i. Negishi, A. de Meijere, *Handbook of Organopalladium Chemistry for Organic Synthesis*, Wiley, New York, **2002**.
- [6] a) K. Tamao, K. Sumitani, M. Kumada, *J. Am. Chem. Soc.* **1972**, *94*, 4374-4376; b) R. J. P. Corriu, J. P. Masse, *J. Chem. Soc., Chem. Commun.* **1972**, 144a-144a.
- [7] a) A. O. King, N. Okukado, E.-i. Negishi, *J. Chem. Soc., Chem. Commun.* **1977**, 683-684; b) E. Negishi, A. O. King, N. Okukado, *J. Org. Chem.* **1977**, *42*, 1821-1823; c) E. Negishi, *Acc. Chem. Res.* **1982**, *15*, 340-348; d) E. Negishi, T. Takahashi, S. Baba, D. E. Van Horn, N. Okukado, *J. Am. Chem. Soc.* **1987**, *109*, 2393-2401.
- [8] a) M. Kosugi, K. Sasazawa, Y. Shimizu, T. Migita, *Chem. Lett.* **1977**, *6*, 301-302; b) M. Kosugi, Y. Shimizu, T. Migita, *Chem. Lett.* **1977**, *6*, 1423-1424; c) D. Milstein, J. K. Stille, *J. Am. Chem. Soc.* **1978**, *100*, 3636-3638; d) D. Milstein, J. K. Stille, *J. Am. Chem. Soc.* **1979**, *101*, 4992-4998; e) J. K. Stille, *Angew. Chem. Int. Ed.* **1986**, *25*, 508-524.
- [9] a) N. Miyaura, A. Suzuki, *J. Chem. Soc., Chem. Commun.* **1979**, 866-867; b) N. Miyaura, K. Yamada, A. Suzuki, *Tetrahedron Lett.* **1979**, *20*, 3437-3440; c) A. Suzuki, *Acc. Chem. Res.* **1982**, *15*, 178-184; d) N. Miyaura, A. Suzuki, *Chem. Rev.* **1995**, *95*, 2457-2483.
- [10] a) Y. Hatanaka, T. Hiyama, *J. Org. Chem.* **1988**, *53*, 918-920; b) T. Hiyama, *J. Organomet. Chem.* **2002**, *653*, 58-61.

- [11] a) H. A. Dieck, R. F. Heck, *J. Am. Chem. Soc.* **1974**, *96*, 1133-1136; b) H. A. Dieck, R. F. Heck, *J. Org. Chem.* **1975**, *40*, 1083-1090; c) R. F. Heck, J. P. Nolley, *J. Org. Chem.* **1972**, *37*, 2320-2322; d) T. Mizoroki, K. Mori, A. Ozaki, *Bull. Chem. Soc. Jpn.* **1971**, *44*, 581-581.
- [12] a) L. Cassar, *J. Organomet. Chem.* **1975**, *93*, 253-257; b) H. A. Dieck, F. R. Heck, *J. Organomet. Chem.* **1975**, *93*, 259-263; c) K. Sonogashira, Y. Tohda, N. Hagihara, *Tetrahedron Lett.* **1975**, *16*, 4467-4470; d) K. Sonogashira, *J. Organomet. Chem.* **2002**, *653*, 46-49.
- [13] a) J. Tsuji, H. Takahashi, M. Morikawa, *Tetrahedron Lett.* **1965**, *6*, 4387-4388; b) B. M. Trost, T. J. Fullerton, *J. Am. Chem. Soc.* **1973**, *95*, 292-294; c) B. M. Trost, *Acc. Chem. Res.* **1980**, *13*, 385-393; d) J. Tsuji, *Tetrahedron* **1986**, *42*, 4361-4401.
- [14] The Nobel Prize in Chemistry 2010 - Press Release: https://www.nobelprize.org/nobel_prizes/chemistry/laureates/2010/press.html (accessed on 10.04.2021).
- [15] a) A. de Meijere, S. Bräse, M. Oestreich, *Metal-Catalyzed Cross-Coupling Reactions and More*, Wiley-VCH, Weinheim, **2014**; b) L. Ackermann, *Modern Arylation Methods*, Wiley-VCH, Weinheim, **2009**; c) C. C. C. Johansson Seechurn, M. O. Kitching, T. J. Colacot, V. Snieckus, *Angew. Chem. Int. Ed.* **2012**, *51*, 5062-5085.
- [16] a) S. Rej, Y. Ano, N. Chatani, *Chem. Rev.* **2020**, *120*, 1788-1887; b) A. Dey, S. K. Sinha, T. K. Achar, D. Maiti, *Angew. Chem. Int. Ed.* **2019**, *58*, 10820-10843; c) C. Sambriago, D. Schönbauer, R. Blicke, T. Dao-Huy, G. Pototschnig, P. Schaaf, T. Wiesinger, M. F. Zia, J. Wencel-Delord, T. Besset, B. U. W. Maes, M. Schnürch, *Chem. Soc. Rev.* **2018**, *47*, 6603-6743; d) Y. Park, Y. Kim, S. Chang, *Chem. Rev.* **2017**, *117*, 9247-9301; e) J. He, M. Wasa, K. S. L. Chan, Q. Shao, J.-Q. Yu, *Chem. Rev.* **2017**, *117*, 8754-8786; f) T. Gensch, M. N. Hopkinson, F. Glorius, J. Wencel-Delord, *Chem. Soc. Rev.* **2016**, *45*, 2900-2936; g) O. Daugulis, J. Roane, L. D. Tran, *Acc. Chem. Res.* **2015**, *48*, 1053-1064; h) J. Wencel-Delord, F. Glorius, *Nat. Chem.* **2013**, *5*, 369-375; i) D. C. Powers, T. Ritter, *Acc. Chem. Res.* **2012**, *45*, 840-850; j) C. S. Yeung, V. M. Dong, *Chem. Rev.* **2011**, *111*, 1215-1292; k) I. A. I. Mkhaliid, J. H. Barnard, T. B. Marder, J. M. Murphy, J. F. Hartwig, *Chem. Rev.* **2010**, *110*, 890-931; l) T. W. Lyons, M. S. Sanford, *Chem. Rev.* **2010**, *110*, 1147-1169; m) D. A. Colby,

6. References

- R. G. Bergman, J. A. Ellman, *Chem. Rev.* **2010**, *110*, 624-655; n) R. G. Bergman, *Nature* **2007**, *446*, 391-393; o) L. Ackermann, *Synlett* **2007**, 507-526.
- [17] a) L. Ackermann, *Chem. Rev.* **2011**, *111*, 1315-1345; b) D. Balcells, E. Clot, O. Eisenstein, *Chem. Rev.* **2010**, *110*, 749-823; c) M. Albrecht, *Chem. Rev.* **2010**, *110*, 576-623.
- [18] T. Rogge, J. C. A. Oliveira, R. Kuniyil, L. Hu, L. Ackermann, *ACS Catal.* **2020**, *10*, 10551-10558.
- [19] B. Biswas, M. Sugimoto, S. Sakaki, *Organometallics* **2000**, *19*, 3895-3908.
- [20] a) D. Lapointe, K. Fagnou, *Chem. Lett.* **2010**, *39*, 1118-1126; b) S. I. Gorelsky, D. Lapointe, K. Fagnou, *J. Am. Chem. Soc.* **2008**, *130*, 10848-10849.
- [21] a) Y. Boutadla, D. L. Davies, S. A. Macgregor, A. I. Poblador-Bahamonde, *Dalton Trans.* **2009**, 5820-5831; b) Y. Boutadla, D. L. Davies, S. A. Macgregor, A. I. Poblador-Bahamonde, *Dalton Trans.* **2009**, 5887-5893.
- [22] a) D. Zell, M. Bursch, V. Müller, S. Grimme, L. Ackermann, *Angew. Chem. Int. Ed.* **2017**, *56*, 10378-10382; b) R. Mei, H. Wang, S. Warratz, S. A. Macgregor, L. Ackermann, *Chem. Eur. J.* **2016**, *22*, 6759-6763; c) W. Ma, R. Mei, G. Tenti, L. Ackermann, *Chem. Eur. J.* **2014**, *20*, 15248-15251.
- [23] a) D. J. Abrams, P. A. Provencher, E. J. Sorensen, *Chem. Soc. Rev.* **2018**, *47*, 8925-8967; b) W. R. Gutekunst, P. S. Baran, *Chem. Soc. Rev.* **2011**, *40*, 1976-1991; c) J. Yamaguchi, A. D. Yamaguchi, K. Itami, *Angew. Chem. Int. Ed.* **2012**, *51*, 8960-9009.
- [24] J.-R. Pouliot, F. Grenier, J. T. Blaskovits, S. Beaupré, M. Leclerc, *Chem. Rev.* **2016**, *116*, 14225-14274.
- [25] a) J. Börgel, T. Ritter, *Chem* **2020**, *6*, 1877-1887; b) W. Wang, M. M. Lorion, J. Shah, A. R. Kapdi, L. Ackermann, *Angew. Chem. Int. Ed.* **2018**, *57*, 14700-14717; c) D. C. Blakemore, L. Castro, I. Churcher, D. C. Rees, A. W. Thomas, D. M. Wilson, A. Wood, *Nat. Chem.* **2018**, *10*, 383-394; d) M. Seki, *Org. Process Res. Dev.* **2016**, *20*, 867-877; e) T. Cernak, K. D. Dykstra, S. Tyagarajan, P. Vachal, S. W. Krska, *Chem. Soc. Rev.* **2016**, *45*, 546-576; f) L. Ackermann, *Org. Process Res. Dev.* **2015**, *19*, 260-269; g) A. F. M. Noisier, M. A. Brimble, *Chem. Rev.* **2014**, *114*, 8775-8806.
- [26] P. Gandeepan, T. Müller, D. Zell, G. Cera, S. Warratz, L. Ackermann, *Chem. Rev.* **2019**, *119*, 2192-2452.
- [27] T. J. Potter, J. A. Ellman, *Org. Lett.* **2017**, *19*, 2985-2988.

- [28] L. M. Chapman, J. C. Beck, L. Wu, S. E. Reisman, *J. Am. Chem. Soc.* **2016**, *138*, 9803-9806.
- [29] Y. Feng, D. Holte, J. Zoller, S. Umemiya, L. R. Simke, P. S. Baran, *J. Am. Chem. Soc.* **2015**, *137*, 10160-10163.
- [30] a) A. Fürstner, *J. Am. Chem. Soc.* **2019**, *141*, 11-24; b) O. M. Ogba, N. C. Warner, D. J. O'Leary, R. H. Grubbs, *Chem. Soc. Rev.* **2018**, *47*, 4510-4544; c) P. H. Dixneuf, *Catal. Lett.* **2015**, *145*, 360-372; d) B. M. Trost, F. D. Toste, A. B. Pinkerton, *Chem. Rev.* **2001**, *101*, 2067-2096.
- [31] L. N. Lewis, J. F. Smith, *J. Am. Chem. Soc.* **1986**, *108*, 2728-2735.
- [32] J. Chatt, J. M. Davidson, *J. Chem. Soc.* **1965**, 843-855.
- [33] a) M. I. Lapuh, S. Mazeh, T. Besset, *ACS Catal.* **2020**, *10*, 12898-12919; b) J. I. Higham, J. A. Bull, *Org. Biomol. Chem.* **2020**, *18*, 7291-7315; c) P. Gandeepan, L. Ackermann, *Chem* **2018**, *4*, 199-222; d) H. Sun, N. Guimond, Y. Huang, *Org. Biomol. Chem.* **2016**, *14*, 8389-8397.
- [34] S. Murai, F. Kakiuchi, S. Sekine, Y. Tanaka, A. Kamatani, M. Sonoda, N. Chatani, *Nature* **1993**, *366*, 529-531.
- [35] a) K. Korvorapun, J. Struwe, R. Kuniyil, A. Zangarelli, A. Casnati, M. Waeterschoot, L. Ackermann, *Angew. Chem. Int. Ed.* **2020**, *59*, 18103-18109; b) S. R. Yetra, T. Rogge, S. Warratz, J. Struwe, W. Peng, P. Vana, L. Ackermann, *Angew. Chem. Int. Ed.* **2019**, *58*, 7490-7494; c) T. Rogge, L. Ackermann, *Angew. Chem. Int. Ed.* **2019**, *58*, 15640-15645; d) M. Simonetti, D. M. Cannas, X. Just-Baringo, I. J. Vitorica-Yrezabal, I. Larrosa, *Nat. Chem.* **2018**, *10*, 724-731; e) M. Simonetti, D. M. Cannas, A. Panigrahi, S. Kujawa, M. Kryjewski, P. Xie, I. Larrosa, *Chem. Eur. J.* **2017**, *23*, 549-553; f) J. Hubrich, T. Himmler, L. Rodefeld, L. Ackermann, *ACS Catal.* **2015**, *5*, 4089-4093; g) L. Ackermann, E. Diers, A. Manvar, *Org. Lett.* **2012**, *14*, 1154-1157; h) I. Özdemir, S. Demir, B. Çetinkaya, C. Gourlaouen, F. Maseras, C. Bruneau, P. H. Dixneuf, *J. Am. Chem. Soc.* **2008**, *130*, 1156-1157; i) L. Ackermann, A. Althammer, R. Born, *Angew. Chem. Int. Ed.* **2006**, *45*, 2619-2622.
- [36] a) G.-W. Wang, M. Wheatley, M. Simonetti, D. M. Cannas, I. Larrosa, *Chem* **2020**, *6*, 1459-1468; b) L. Ackermann, N. Hofmann, R. Vicente, *Org. Lett.* **2011**, *13*, 1875-1877; c) L. Ackermann, P. Novák, R. Vicente, N. Hofmann, *Angew. Chem. Int. Ed.* **2009**, *48*, 6045-6048; d) L. Ackermann, P. Novák, *Org. Lett.* **2009**, *11*, 4966-4969.

6. References

- [37] a) K. Raghuvanshi, D. Zell, K. Rauch, L. Ackermann, *ACS Catal.* **2016**, *6*, 3172-3175; b) J. Kim, J. Kim, S. Chang, *Chem. Eur. J.* **2013**, *19*, 7328-7333.
- [38] a) L. Massignan, X. Tan, T. H. Meyer, R. Kuniyil, A. M. Messinis, L. Ackermann, *Angew. Chem. Int. Ed.* **2020**, *59*, 3184-3189; b) Q. Bu, R. Kuniyil, Z. Shen, E. Gońka, L. Ackermann, *Chem. Eur. J.* **2020**, *26*, 16450-16454; c) G. G. Dias, T. Rogge, R. Kuniyil, C. Jacob, R. F. S. Menna-Barreto, E. N. da Silva Júnior, L. Ackermann, *Chem. Commun.* **2018**, *54*, 12840-12843; d) Y.-H. Sun, T.-Y. Sun, Y.-D. Wu, X. Zhang, Y. Rao, *Chem. Sci.* **2016**, *7*, 2229-2238; e) F. Yang, K. Rauch, K. Kettelhoit, L. Ackermann, *Angew. Chem. Int. Ed.* **2014**, *53*, 11285-11288; f) X. Yang, G. Shan, Y. Rao, *Org. Lett.* **2013**, *15*, 2334-2337; g) F. Yang, L. Ackermann, *Org. Lett.* **2013**, *15*, 718-720.
- [39] a) Z. Dong, Z. Ren, S. J. Thompson, Y. Xu, G. Dong, *Chem. Rev.* **2017**, *117*, 9333-9403; b)
- [40] a) I. Choi, A. M. Messinis, L. Ackermann, *Angew. Chem. Int. Ed.* **2020**, *59*, 12534-12540; b) Q. Bu, T. Rogge, V. Kotek, L. Ackermann, *Angew. Chem. Int. Ed.* **2018**, *57*, 765-768; c) K. Padala, M. Jeganmohan, *Org. Lett.* **2012**, *14*, 1134-1137; d) B. Li, K. Devaraj, C. Darcel, P. H. Dixneuf, *Green Chem.* **2012**, *14*, 2706-2709; e) Y. Hashimoto, T. Ortloff, K. Hirano, T. Satoh, C. Bolm, M. Miura, *Chem. Lett.* **2012**, *41*, 151-153; f) K. Graczyk, W. Ma, L. Ackermann, *Org. Lett.* **2012**, *14*, 4110-4113; g) Y. Hashimoto, T. Ueyama, T. Fukutani, K. Hirano, T. Satoh, M. Miura, *Chem. Lett.* **2011**, *40*, 1165-1166.
- [41] a) A. Bechtoldt, M. E. Baumert, L. Vaccaro, L. Ackermann, *Green Chem.* **2018**, *20*, 398-402; b) A. Bechtoldt, C. Tirler, K. Raghuvanshi, S. Warratz, C. Kornhaaß, L. Ackermann, *Angew. Chem. Int. Ed.* **2016**, *55*, 264-267; c) S. Warratz, C. Kornhaaß, A. Cajaraville, B. Niepötter, D. Stalke, L. Ackermann, *Angew. Chem. Int. Ed.* **2015**, *54*, 5513-5517.
- [42] a) X. Tan, X. Hou, T. Rogge, L. Ackermann, *Angew. Chem. Int. Ed.* **2021**, *60*, 4619-4624; b) L. Yang, R. Steinbock, A. Scheremetjew, R. Kuniyil, L. H. Finger, A. M. Messinis, L. Ackermann, *Angew. Chem. Int. Ed.* **2020**, *59*, 11130-11135; c) M.-J. Luo, T.-T. Zhang, F.-J. Cai, J.-H. Li, D.-L. He, *Chem. Commun.* **2019**, *55*, 7251-7254; d) F. Xu, Y.-J. Li, C. Huang, H.-C. Xu, *ACS Catal.* **2018**, *8*, 3820-3824; e) Y. Qiu, C. Tian, L. Massignan, T. Rogge, L. Ackermann, *Angew. Chem. Int. Ed.* **2018**, *57*, 5818-5822; f) R. Mei, J. Koeller, L. Ackermann, *Chem. Commun.* **2018**, *54*, 12879-12882.

- [43] J. Li, L. Ackermann, *Org. Chem. Front.* **2015**, *2*, 1035-1039.
- [44] F. Li, Y. Zhou, H. Yang, D. Liu, B. Sun, F.-L. Zhang, *Org. Lett.* **2018**, *20*, 146-149.
- [45] K. Ghosh, R. K. Rit, E. Ramesh, A. K. Sahoo, *Angew. Chem. Int. Ed.* **2016**, *55*, 7821-7825.
- [46] M. Schinkel, I. Marek, L. Ackermann, *Angew. Chem. Int. Ed.* **2013**, *52*, 3977-3980.
- [47] M. Schinkel, L. Wang, K. Bielefeld, L. Ackermann, *Org. Lett.* **2014**, *16*, 1876-1879.
- [48] G. Meng, N. Y. S. Lam, E. L. Lucas, T. G. Saint-Denis, P. Verma, N. Chekshin, J.-Q. Yu, *J. Am. Chem. Soc.* **2020**, *142*, 10571-10591.
- [49] a) J. Ye, M. Lautens, *Nat. Chem.* **2015**, *7*, 863-870; b) X.-C. Wang, W. Gong, L.-Z. Fang, R.-Y. Zhu, S. Li, K. M. Engle, J.-Q. Yu, *Nature* **2015**, *519*, 334-338; c) L. Jiao, E. Herdtweck, T. Bach, *J. Am. Chem. Soc.* **2012**, *134*, 14563-14572; d) M. Catellani, E. Motti, N. Della Ca', *Acc. Chem. Res.* **2008**, *41*, 1512-1522.
- [50] a) S. Bag, T. Patra, A. Modak, A. Deb, S. Maity, U. Dutta, A. Dey, R. Kancherla, A. Maji, A. Hazra, M. Bera, D. Maiti, *J. Am. Chem. Soc.* **2015**, *137*, 11888-11891; b) D. Leow, G. Li, T.-S. Mei, J.-Q. Yu, *Nature* **2012**, *486*, 518-522; c) S. Das, C. D. Incarvito, R. H. Crabtree, G. W. Brudvig, *Science* **2006**, *312*, 1941-1943; d) R. Breslow, *Acc. Chem. Res.* **1980**, *13*, 170-177.
- [51] K. Korvorapun, M. Moselage, J. Struwe, T. Rogge, A. M. Messinis, L. Ackermann, *Angew. Chem. Int. Ed.* **2020**, *59*, 18795-18803.
- [52] N. Hofmann, L. Ackermann, *J. Am. Chem. Soc.* **2013**, *135*, 5877-5884.
- [53] J. Li, S. Warratz, D. Zell, S. De Sarkar, E. E. Ishikawa, L. Ackermann, *J. Am. Chem. Soc.* **2015**, *137*, 13894-13901.
- [54] A. J. Paterson, S. St John-Campbell, M. F. Mahon, N. J. Press, C. G. Frost, *Chem. Commun.* **2015**, *51*, 12807-12810.
- [55] a) J. Wang, M. Sánchez-Roselló, J. L. Aceña, C. del Pozo, A. E. Sorochinsky, S. Fustero, V. A. Soloshonok, H. Liu, *Chem. Rev.* **2014**, *114*, 2432-2506; b) H. Egami, M. Sodeoka, *Angew. Chem. Int. Ed.* **2014**, *53*, 8294-8308; c) T. Besset, T. Poisson, X. Pannecoucke, *Chem. Eur. J.* **2014**, *20*, 16830-16845.
- [56] Z. Ruan, S.-K. Zhang, C. Zhu, P. N. Ruth, D. Stalke, L. Ackermann, *Angew. Chem. Int. Ed.* **2017**, *56*, 2045-2049.

6. References

- [57] Z.-Y. Li, L. Li, Q.-L. Li, K. Jing, H. Xu, G.-W. Wang, *Chem. Eur. J.* **2017**, *23*, 3285-3290.
- [58] K. Korvorapun, R. Kuniyil, L. Ackermann, *ACS Catal.* **2020**, *10*, 435-440.
- [59] a) G. Li, D. Li, J. Zhang, D.-Q. Shi, Y. Zhao, *ACS Catal.* **2017**, *7*, 4138-4143; b) B. Li, S.-L. Fang, D.-Y. Huang, B.-F. Shi, *Org. Lett.* **2017**, *19*, 3950-3953.
- [60] J. Li, K. Korvorapun, S. De Sarkar, T. Rogge, D. J. Burns, S. Warratz, L. Ackermann, *Nat. Commun.* **2017**, *8*, 15430.
- [61] F. Fumagalli, S. Warratz, S.-K. Zhang, T. Rogge, C. Zhu, A. C. Stückl, L. Ackermann, *Chem. Eur. J.* **2018**, *24*, 3984-3988.
- [62] O. Saidi, J. Marafie, A. E. W. Ledger, P. M. Liu, M. F. Mahon, G. Kociok-Köhn, M. K. Whittlesey, C. G. Frost, *J. Am. Chem. Soc.* **2011**, *133*, 19298-19301.
- [63] P. Marcé, A. J. Paterson, M. F. Mahon, C. G. Frost, *Catal. Sci. Technol.* **2016**, *6*, 7068-7076.
- [64] S. Warratz, D. J. Burns, C. Zhu, K. Korvorapun, T. Rogge, J. Scholz, C. Jooss, D. Gelman, L. Ackermann, *Angew. Chem. Int. Ed.* **2017**, *56*, 1557-1560.
- [65] I. Choi, V. Müller, Y. Wang, K. Xue, R. Kuniyil, L. B. Andreas, V. Karius, J. G. Alauzun, L. Ackermann, *Chem. Eur. J.* **2020**, *26*, 15290-15297.
- [66] Z. Fan, H. Lu, Z. Cheng, A. Zhang, *Chem. Commun.* **2018**, *54*, 6008-6011.
- [67] a) Y. Kuninobu, S. Sueki, N. Kaplaneris, L. Ackermann, in *Catalysis with Earth-abundant Elements*, (Eds. U. Schneider, S. Thomas), The Royal Society of Chemistry, Cambridge, **2020**, pp 139–230; b) Y. Hu, B. Zhou, C. Wang, *Acc. Chem. Res.* **2018**, *51*, 816-827; c) W. Liu, L. Ackermann, *ACS Catal.* **2016**, *6*, 3743-3752.
- [68] M. I. Bruce, M. Z. Iqbal, F. G. A. Stone, *J. Chem. Soc. A* **1970**, 3204-3209.
- [69] a) L. H. P. Gommans, L. Main, B. K. Nicholson, *J. Chem. Soc., Chem. Commun.* **1987**, 761-762; b) W. Tully, L. Main, B. K. Nicholson, *J. Organomet. Chem.* **1995**, *503*, 75-92; c) G. J. Depree, L. Main, B. K. Nicholson, *J. Organomet. Chem.* **1998**, *551*, 281-291.
- [70] a) R. C. Cambie, M. R. Metzler, P. S. Rutledge, P. D. Woodgate, *J. Organomet. Chem.* **1990**, *381*, C26-C30; b) R. C. Cambie, M. R. Metzler, P. S. Rutledge, P. D. Woodgate, *J. Organomet. Chem.* **1990**, *398*, C22-C24; c) R. C. Cambie, M. R. Metzler, P. S. Rutledge, P. D. Woodgate, *J. Organomet. Chem.* **1992**, *429*, 41-57.

- [71] L. S. Liebeskind, J. R. Gasdaska, J. S. McCallum, S. J. Tremont, *J. Org. Chem.* **1989**, *54*, 669-677.
- [72] Y. Kuninobu, Y. Nishina, T. Takeuchi, K. Takai, *Angew. Chem. Int. Ed.* **2007**, *46*, 6518-6520.
- [73] J. R. Hummel, J. A. Boerth, J. A. Ellman, *Chem. Rev.* **2017**, *117*, 9163-9227.
- [74] B. Zhou, Y. Hu, C. Wang, *Angew. Chem. Int. Ed.* **2015**, *54*, 13659-13663.
- [75] Y.-F. Liang, L. Massignan, L. Ackermann, *ChemCatChem* **2018**, *10*, 2768-2772.
- [76] C. Zhu, T. Pinkert, S. Greßies, F. Glorius, *ACS Catal.* **2018**, *8*, 10036-10042.
- [77] W. Liu, J. Bang, Y. Zhang, L. Ackermann, *Angew. Chem. Int. Ed.* **2015**, *54*, 14137-14140.
- [78] B. Zhou, Y. Hu, T. Liu, C. Wang, *Nat. Commun.* **2017**, *8*, 1169.
- [79] B. Zhou, H. Chen, C. Wang, *J. Am. Chem. Soc.* **2013**, *135*, 1264-1267.
- [80] L. Shi, X. Zhong, H. She, Z. Lei, F. Li, *Chem. Commun.* **2015**, *51*, 7136-7139.
- [81] X. Yang, X. Jin, C. Wang, *Adv. Synth. Catal.* **2016**, *358*, 2436-2442.
- [82] H. Wang, F. Pesciaoli, J. C. A. Oliveira, S. Warratz, L. Ackermann, *Angew. Chem. Int. Ed.* **2017**, *56*, 15063-15067.
- [83] Q. Lu, S. Greßies, F. J. R. Klauck, F. Glorius, *Angew. Chem. Int. Ed.* **2017**, *56*, 6660-6664.
- [84] B. Zhou, P. Ma, H. Chen, C. Wang, *Chem. Commun.* **2014**, *50*, 14558-14561.
- [85] S. L. Liu, Y. Li, J. R. Guo, G. C. Yang, X. H. Li, J. F. Gong, M. P. Song, *Org. Lett.* **2017**, *19*, 4042-4045.
- [86] Q. Lu, S. Mondal, S. Cembellín, F. Glorius, *Angew. Chem. Int. Ed.* **2018**, *57*, 10732-10736.
- [87] S.-Y. Chen, Q. Li, H. Wang, *J. Org. Chem.* **2017**, *82*, 11173-11181.
- [88] W. Liu, S. C. Richter, Y. Zhang, L. Ackermann, *Angew. Chem. Int. Ed.* **2016**, *55*, 7747-7750.
- [89] H. Wang, M. M. Lorion, L. Ackermann, *Angew. Chem. Int. Ed.* **2017**, *56*, 6339-6342.
- [90] J. Ni, H. Zhao, A. Zhang, *Org. Lett.* **2017**, *19*, 3159-3162.
- [91] S. Ali, J. Huo, C. Wang, *Org. Lett.* **2019**, *21*, 6961-6965.
- [92] C. Zhu, J. L. Schwarz, S. Cembellín, S. Greßies, F. Glorius, *Angew. Chem. Int. Ed.* **2018**, *57*, 437-441.
- [93] W. Liu, S. C. Richter, R. Mei, M. Feldt, L. Ackermann, *Chem. Eur. J.* **2016**, *22*, 17958-17961.

6. References

- [94] a) H.-M. Huang, M. H. Garduño-Castro, C. Morrill, D. J. Procter, *Chem. Soc. Rev.* **2019**, *48*, 4626-4638; b) H. Pellissier, *Chem. Rev.* **2013**, *113*, 442-524; c) K. C. Nicolaou, J. S. Chen, *Chem. Soc. Rev.* **2009**, *38*, 2993-3009; d) K. C. Nicolaou, D. J. Edmonds, P. G. Bulger, *Angew. Chem. Int. Ed.* **2006**, *45*, 7134-7186; e) L. F. Tietze, *Chem. Rev.* **1996**, *96*, 115-136; f) L. F. Tietze, *Domino Reactions: Concepts for Efficient Organic Synthesis*, Wiley-VCH, Weinheim, **2014**
- [95] W. Liu, D. Zell, M. John, L. Ackermann, *Angew. Chem. Int. Ed.* **2015**, *54*, 4092-4096.
- [96] C. Lei, L. Peng, K. Ding, *Adv. Synth. Catal.* **2018**, *360*, 2952-2958.
- [97] Y.-F. Liang, V. Müller, W. Liu, A. Münch, D. Stalke, L. Ackermann, *Angew. Chem. Int. Ed.* **2017**, *56*, 9415-9419.
- [98] S.-Y. Chen, Q. Li, X.-G. Liu, J.-Q. Wu, S.-S. Zhang, H. Wang, *ChemSusChem* **2017**, *10*, 2360-2364.
- [99] B. Liu, Y. Yuan, P. Hu, G. Zheng, D. Bai, J. Chang, X. Li, *Chem. Commun.* **2019**, *55*, 10764-10767.
- [100] C. Wang, A. Wang, M. Rueping, *Angew. Chem. Int. Ed.* **2017**, *56*, 9935-9938.
- [101] S.-Y. Chen, X.-L. Han, J.-Q. Wu, Q. Li, Y. Chen, H. Wang, *Angew. Chem. Int. Ed.* **2017**, *56*, 9939-9943.
- [102] X. Zhou, Z. Li, Z. Zhang, P. Lu, Y. Wang, *Org. Lett.* **2018**, *20*, 1426-1429.
- [103] Z. Xu, Y. Wang, Y. Zheng, Z. Huang, L. Ackermann, Z. Ruan, *Org. Chem. Front.* **2020**, *7*, 3709-3714.
- [104] C. Zhu, R. Kuniyil, L. Ackermann, *Angew. Chem. Int. Ed.* **2019**, *58*, 5338-5342.
- [105] G. Zheng, J. Sun, Y. Xu, S. Zhai, X. Li, *Angew. Chem. Int. Ed.* **2019**, *58*, 5090-5094.
- [106] B. V. S. Reddy, L. R. Reddy, E. J. Corey, *Org. Lett.* **2006**, *8*, 3391-3394.
- [107] L. D. Tran, O. Daugulis, *Angew. Chem. Int. Ed.* **2012**, *51*, 5188-5191.
- [108] J. He, S. Li, Y. Deng, H. Fu, B. N. Laforteza, J. E. Spangler, A. Homs, J.-Q. Yu, *Science* **2014**, *343*, 1216-1220.
- [109] G. Chen, Z. Zhuang, G.-C. Li, T. G. Saint-Denis, Y. Hsiao, C. L. Joe, J.-Q. Yu, *Angew. Chem. Int. Ed.* **2017**, *56*, 1506-1509.
- [110] Q. Zhang, X.-S. Yin, K. Chen, S.-Q. Zhang, B.-F. Shi, *J. Am. Chem. Soc.* **2015**, *137*, 8219-8226.
- [111] Y. Feng, G. Chen, *Angew. Chem. Int. Ed.* **2010**, *49*, 958-961.

- [112] T. Kinsinger, U. Kazmaier, *Org. Lett.* **2018**, *20*, 7726-7730.
- [113] a) Y. Hamada, T. Shioiri, *Chem. Rev.* **2005**, *105*, 4441-4482; b) F. von Nussbaum, M. Brands, B. Hinzen, S. Weigand, D. Häbich, *Angew. Chem. Int. Ed.* **2006**, *45*, 5072-5129.
- [114] T. H. Meyer, W. Liu, M. Feldt, A. Wuttke, R. A. Mata, L. Ackermann, *Chem. Eur. J.* **2017**, *23*, 5443-5447.
- [115] J. Ruiz-Rodríguez, F. Albericio, R. Lavilla, *Chem. Eur. J.* **2010**, *16*, 1124-1127.
- [116] S. Preciado, L. Mendive-Tapia, C. Torres-García, R. Zamudio-Vázquez, V. Soto-Cerrato, R. Pérez-Tomás, F. Albericio, E. Nicolás, R. Lavilla, *Med. Chem. Commun.* **2013**, *4*, 1171-1174.
- [117] Y. Zhu, M. Bauer, L. Ackermann, *Chem. Eur. J.* **2015**, *21*, 9980-9983.
- [118] A. J. Reay, L. A. Hammarback, J. T. W. Bray, T. Sheridan, D. Turnbull, A. C. Whitwood, I. J. S. Fairlamb, *ACS Catal.* **2017**, *7*, 5174-5179.
- [119] A. J. Reay, T. J. Williams, I. J. S. Fairlamb, *Org. Biomol. Chem.* **2015**, *13*, 8298-8309.
- [120] A. Schischko, H. Ren, N. Kaplaneris, L. Ackermann, *Angew. Chem. Int. Ed.* **2017**, *56*, 1576-1580.
- [121] L. Ackermann, A. V. Lygin, *Org. Lett.* **2011**, *13*, 3332-3335.
- [122] W. Wang, J. Wu, R. Kuniyil, A. Kopp, R. N. Lima, L. Ackermann, *Chem* **2020**, *6*, 3428-3439.
- [123] Z. Ruan, N. Sauermann, E. Manoni, L. Ackermann, *Angew. Chem. Int. Ed.* **2017**, *56*, 3172-3176.
- [124] W. Gong, G. Zhang, T. Liu, R. Giri, J.-Q. Yu, *J. Am. Chem. Soc.* **2014**, *136*, 16940-16946.
- [125] Y. Weng, X. Ding, J. C. A. Oliveira, X. Xu, N. Kaplaneris, M. Zhu, H. Chen, Z. Chen, L. Ackermann, *Chem. Sci.* **2020**, *11*, 9290-9295.
- [126] T. Kinsinger, U. Kazmaier, *Org. Biomol. Chem.* **2019**, *17*, 5595-5600.
- [127] L. Karmann, K. Schultz, J. Herrmann, R. Müller, U. Kazmaier, *Angew. Chem. Int. Ed.* **2015**, *54*, 4502-4507.
- [128] D. P. Affron, O. A. Davis, J. A. Bull, *Org. Lett.* **2014**, *16*, 4956-4959.
- [129] B. Mondal, B. Roy, U. Kazmaier, *J. Org. Chem.* **2016**, *81*, 11646-11655.
- [130] B.-B. Zhan, Y. Li, J.-W. Xu, X.-L. Nie, J. Fan, L. Jin, B.-F. Shi, *Angew. Chem. Int. Ed.* **2018**, *57*, 5858-5862.

6. References

- [131] M. Bauer, W. Wang, M. M. Lorion, C. Dong, L. Ackermann, *Angew. Chem. Int. Ed.* **2018**, *57*, 203-207.
- [132] a) D. S. Pedersen, A. Abell, *Eur. J. Org. Chem.* **2011**, *2011*, 2399-2411; b) I. Avan, C. D. Hall, A. R. Katritzky, *Chem. Soc. Rev.* **2014**, *43*, 3575-3594.
- [133] a) M. Breugst, H.-U. Reissig, *Angew. Chem. Int. Ed.* **2020**, *59*, 12293-12307; b) J. E. Moses, A. D. Moorhouse, *Chem. Soc. Rev.* **2007**, *36*, 1249-1262; c) H. C. Kolb, M. G. Finn, K. B. Sharpless, *Angew. Chem. Int. Ed.* **2001**, *40*, 2004-2021.
- [134] W. Wang, M. M. Lorion, O. Martinazzoli, L. Ackermann, *Angew. Chem. Int. Ed.* **2018**, *57*, 10554-10558.
- [135] H. Dong, C. Limberakis, S. Liras, D. Price, K. James, *Chem. Commun.* **2012**, *48*, 11644-11646.
- [136] a) L. Mendive-Tapia, A. Bertran, J. García, G. Acosta, F. Albericio, R. Lavilla, *Chem. Eur. J.* **2016**, *22*, 13114-13119; b) L. Mendive-Tapia, S. Preciado, J. García, R. Ramón, N. Kielland, F. Albericio, R. Lavilla, *Nat. Commun.* **2015**, *6*, 7160.
- [137] a) S. H. Reisberg, Y. Gao, A. S. Walker, E. J. N. Helfrich, J. Clardy, P. S. Baran, *Science* **2020**, *367*, 458-463; b) M. J. Moore, S. Qu, C. Tan, Y. Cai, Y. Mogi, D. Jamin Keith, D. L. Boger, *J. Am. Chem. Soc.* **2020**, *142*, 16039-16050.
- [138] Z. Bai, C. Cai, Z. Yu, H. Wang, *Angew. Chem. Int. Ed.* **2018**, *57*, 13912-13916.
- [139] Z. Bai, C. Cai, W. Sheng, Y. Ren, H. Wang, *Angew. Chem. Int. Ed.* **2020**, *59*, 14686-14692.
- [140] A. F. M. Noisier, J. García, I. A. Ionuț, F. Albericio, *Angew. Chem. Int. Ed.* **2017**, *56*, 314-318.
- [141] J. Tang, Y. He, H. Chen, W. Sheng, H. Wang, *Chem. Sci.* **2017**, *8*, 4565-4570.
- [142] X. Zhang, G. Lu, M. Sun, M. Mahankali, Y. Ma, M. Zhang, W. Hua, Y. Hu, Q. Wang, J. Chen, G. He, X. Qi, W. Shen, P. Liu, G. Chen, *Nat. Chem.* **2018**, *10*, 540-548.
- [143] L. Grigorjeva, O. Daugulis, *Org. Lett.* **2014**, *16*, 4684-4687.
- [144] B. Li, X. Li, B. Han, Z. Chen, X. Zhang, G. He, G. Chen, *J. Am. Chem. Soc.* **2019**, *141*, 9401-9407.
- [145] D. Y.-K. Chen, S. W. Youn, *Chem. Eur. J.* **2012**, *18*, 9452-9474.
- [146] a) Ł. Woźniak, N. Cramer, *Trends Chem.* **2019**, *1*, 471-484; b) J. Loup, U. Dhawa, F. Pesciaoli, J. Wencel-Delord, L. Ackermann, *Angew. Chem. Int. Ed.* **2019**, *58*, 12803-12818.

- [147] H.-R. Tong, B. Li, G. Li, G. He, G. Chen, *CCS Chemistry* **2021**, *3*, 1797-1820.
- [148] a) N. Y. P. Kumar, T. Rogge, S. R. Yetra, A. Bechtoldt, E. Clot, L. Ackermann, *Chem. Eur. J.* **2017**, *23*, 17449-17453; b) J. Zhang, R. Shrestha, J. F. Hartwig, P. Zhao, *Nat. Chem.* **2016**, *8*, 1144-1151; c) N. Y. P. Kumar, A. Bechtoldt, K. Raghuvanshi, L. Ackermann, *Angew. Chem. Int. Ed.* **2016**, *55*, 6929-6932.
- [149] a) M. T. Mihai, B. D. Williams, R. J. Phipps, *J. Am. Chem. Soc.* **2019**, *141*, 15477-15482; b) X. Lu, Y. Yoshigoe, H. Ida, M. Nishi, M. Kanai, Y. Kuninobu, *ACS Catal.* **2019**, *9*, 1705-1709; c) H. J. Davis, M. T. Mihai, R. J. Phipps, *J. Am. Chem. Soc.* **2016**, *138*, 12759-12762; d) Y. Kuninobu, H. Ida, M. Nishi, M. Kanai, *Nat. Chem.* **2015**, *7*, 712-717.
- [150] M. Murai, K. Takai, *Synthesis* **2019**, *51*, 40-54.
- [151] L. Ackermann, R. Vicente, in *C-H Activation* (Eds.: J.-Q. Yu, Z. Shi), Springer Berlin Heidelberg, Berlin, Heidelberg, **2010**, pp. 211-229.
- [152] a) P. Valverde, A. Ardá, N.-C. Reichardt, J. Jiménez-Barbero, A. Gimeno, *Med. Chem. Commun.* **2019**, *10*, 1678-1691; b) S. A. W. Gruner, E. Locardi, E. Lohof, H. Kessler, *Chem. Rev.* **2002**, *102*, 491-514.
- [153] M. S. Butler, K. A. Hansford, M. A. T. Blaskovich, R. Halai, M. A. Cooper, *J. Antibiot.* **2014**, *67*, 631-644.
- [154] N. Probst, G. Grelier, S. Dahaoui, M. Alami, V. Gandon, S. Messaoudi, *ACS Catal.* **2018**, *8*, 7781-7786.
- [155] M. Liu, Y. Niu, Y.-F. Wu, X.-S. Ye, *Org. Lett.* **2016**, *18*, 1836-1839.
- [156] Q. Wang, S. An, Z. Deng, W. Zhu, Z. Huang, G. He, G. Chen, *Nat. Catal.* **2019**, *2*, 793-800.
- [157] W. Wang, P. Subramanian, O. Martinazzoli, J. Wu, L. Ackermann, *Chem. Eur. J.* **2019**, *25*, 10585-10589.
- [158] Y.-J. Liu, Y.-H. Liu, Z.-Z. Zhang, S.-Y. Yan, K. Chen, B.-F. Shi, *Angew. Chem. Int. Ed.* **2016**, *55*, 13859-13862.
- [159] a) T. Xiao, Z.-T. Chen, L.-F. Deng, D. Zhang, X.-Y. Liu, H. Song, Y. Qin, *Chem. Commun.* **2017**, *53*, 12665-12667; b) S.-Y. Zhang, Q. Li, G. He, W. A. Nack, G. Chen, *J. Am. Chem. Soc.* **2013**, *135*, 12135-12141.
- [160] a) A. Çapcı, M. M. Lorion, H. Wang, N. Simon, M. Leidenberger, M. C. Borges Silva, D. R. M. Moreira, Y. Zhu, Y. Meng, J. Y. Chen, Y. M. Lee, O. Friedrich, B. Kappes, J. Wang, L. Ackermann, S. B. Tsogoeva, *Angew. Chem. Int. Ed.* **2019**, *58*, 13066-13079; b) K. Gademann, *Chimia* **2006**, *60*, 841-845; c) B. Meunier,

6. References

- Acc. Chem. Res.* **2008**, *41*, 69-77; d) L. F. Tietze, H. P. Bell, S. Chandrasekhar, *Angew. Chem. Int. Ed.* **2003**, *42*, 3996-4028.
- [161] a) W. Zhang, J. Wei, S. Fu, D. Lin, H. Jiang, W. Zeng, *Org. Lett.* **2015**, *17*, 1349-1352; b) R. Manikandan, M. Jeganmohan, *Org. Lett.* **2014**, *16*, 912-915; c) L. Liang, S. Fu, D. Lin, X.-Q. Zhang, Y. Deng, H. Jiang, W. Zeng, *J. Org. Chem.* **2014**, *79*, 9472-9480; d) M. C. Reddy, M. Jeganmohan, *Chem. Commun.* **2013**, *49*, 481-483; e) Y. Hashimoto, K. Hirano, T. Satoh, F. Kakiuchi, M. Miura, *J. Org. Chem.* **2013**, *78*, 638-646; f) P. Zhao, R. Niu, F. Wang, K. Han, X. Li, *Org. Lett.* **2012**, *14*, 4166-4169; g) Y. Hashimoto, K. Hirano, T. Satoh, F. Kakiuchi, M. Miura, *Org. Lett.* **2012**, *14*, 2058-2061.
- [162] a) L. Song, X. Zhang, X. Tang, L. Van Meervelt, J. Van der Eycken, J. N. Harvey, E. V. Van der Eycken, *Chem. Sci.* **2020**, *11*, 11562-11569; b) E. N. da Silva Júnior, R. L. de Carvalho, R. G. Almeida, L. G. Rosa, F. Fantuzzi, T. Rogge, P. M. S. Costa, C. Pessoa, C. Jacob, L. Ackermann, *Chem. Eur. J.* **2020**, *26*, 10981-10986; c) E. Gońka, L. Yang, R. Steinbock, F. Pesciaioli, R. Kuniyil, L. Ackermann, *Chem. Eur. J.* **2019**, *25*, 16246-16250; d) M. Shankar, K. Ghosh, K. Mukherjee, R. K. Rit, A. K. Sahoo, *Org. Lett.* **2018**, *20*, 5144-5148; e) P. P. Kaishap, G. Duarah, B. Sarma, D. Chetia, S. Gogoi, *Angew. Chem. Int. Ed.* **2018**, *57*, 456-460; f) G. Duarah, P. P. Kaishap, B. Sarma, S. Gogoi, *Chem. Eur. J.* **2018**, *24*, 10196-10200; g) M. Shankar, T. Guntreddi, E. Ramesh, A. K. Sahoo, *Org. Lett.* **2017**, *19*, 5665-5668.
- [163] a) D. J. Drucker, *Nat. Rev. Drug Discov.* **2020**, *19*, 277-289; b) A. Henninot, J. C. Collins, J. M. Nuss, *J. Med. Chem.* **2018**, *61*, 1382-1414.
- [164] a) E. A. Hoyt, P. M. S. D. Cal, B. L. Oliveira, G. J. L. Bernardes, *Nat. Rev. Chem.* **2019**, *3*, 147-171; b) C. Bottecchia, T. Noël, *Chem. Eur. J.* **2019**, *25*, 26-42; c) J. N. deGruyter, L. R. Malins, P. S. Baran, *Biochemistry* **2017**, *56*, 3863-3873; d) O. Boutoureira, G. J. L. Bernardes, *Chem. Rev.* **2015**, *115*, 2174-2195; e) C. D. Spicer, B. G. Davis, *Nat. Commun.* **2014**, *5*, 4740.
- [165] M. Jbara, S. K. Maity, A. Brik, *Angew. Chem. Int. Ed.* **2017**, *56*, 10644-10655.
- [166] B.-B. Zhan, M.-X. Jiang, B.-F. Shi, *Chem. Commun.* **2020**, *56*, 13950-13958.
- [167] J. Dadová, S. R. G. Galan, B. G. Davis, *Curr. Opin. Chem. Biol.* **2018**, *46*, 71-81.

- [168] a) C. G. Lima–Junior, M. L. A. A. Vasconcellos, *Biorg. Med. Chem.* **2012**, *20*, 3954-3971; b) D. Basavaiah, A. J. Rao, T. Satyanarayana, *Chem. Rev.* **2003**, *103*, 811-892.
- [169] A. D. Borthwick, *Chem. Rev.* **2012**, *112*, 3641-3716.
- [170] T. Qin, L. R. Malins, J. T. Edwards, R. R. Merchant, A. J. E. Novak, J. Z. Zhong, R. B. Mills, M. Yan, C. Yuan, M. D. Eastgate, P. S. Baran, *Angew. Chem. Int. Ed.* **2017**, *56*, 260-265.
- [171] a) S. M. Ujwaldev, N. A. Harry, M. A. Divakar, G. Anilkumar, *Catal. Sci. Technol.* **2018**, *8*, 5983-6018; b) T. Yoshino, S. Matsunaga, *Adv. Synth. Catal.* **2017**, *359*, 1245-1262; c) M. Moselage, J. Li, L. Ackermann, *ACS Catal.* **2016**, *6*, 498-525.
- [172] a) H. Wang, M. M. Lorion, L. Ackermann, *ACS Catal.* **2017**, *7*, 3430-3433; b) M. Moselage, N. Sauermann, J. Koeller, W. Liu, D. Gelman, L. Ackermann, *Synlett* **2015**, *26*, 1596-1600; c) D.-G. Yu, T. Gensch, F. de Azambuja, S. Vásquez-Céspedes, F. Glorius, *J. Am. Chem. Soc.* **2014**, *136*, 17722-17725.
- [173] J. L. Lau, M. K. Dunn, *Biorg. Med. Chem.* **2018**, *26*, 2700-2707.
- [174] A. F. B. Räder, M. Weinmüller, F. Reichart, A. Schumacher-Klinger, S. Merzbach, C. Gilon, A. Hoffman, H. Kessler, *Angew. Chem. Int. Ed.* **2018**, *57*, 14414-14438.
- [175] a) R. Behrendt, P. White, J. Offer, *J. Pept. Chem.* **2016**, *22*, 4-27; b) J. M. Palomo, *RSC Adv.* **2014**, *4*, 32658-32672; c) A. El-Faham, F. Albericio, *Chem. Rev.* **2011**, *111*, 6557-6602.
- [176] S. S. Kulkarni, J. Sayers, B. Premdjee, R. J. Payne, *Nat. Rev. Chem.* **2018**, *2*, 0122.
- [177] a) V. Sarojini, A. J. Cameron, K. G. Varnava, W. A. Denny, G. Sanjayan, *Chem. Rev.* **2019**, *119*, 10318-10359; b) H. Itoh, M. Inoue, *Chem. Rev.* **2019**, *119*, 10002-10031; c) Y. Huang, M. M. Wiedmann, H. Suga, *Chem. Rev.* **2019**, *119*, 10360-10391.
- [178] a) G. E. Keck, E. P. Boden, M. R. Wiley, *J. Org. Chem.* **1989**, *54*, 896-906; b) J. Inanaga, K. Hirata, H. Saeki, T. Katsuki, M. Yamaguchi, *Bull. Chem. Soc. Jpn.* **1979**, *52*, 1989-1993; c) K. Narasaka, K. Maruyama, T. Mukaiyama, *Chem. Lett.* **1978**, *7*, 885-888; d) S. Masamune, C. U. Kim, K. E. Wilson, G. O. Spessard, P. E. Georghiou, G. S. Bates, *J. Am. Chem. Soc.* **1975**, *97*, 3512-3513; e) E. J. Corey, K. C. Nicolaou, *J. Am. Chem. Soc.* **1974**, *96*, 5614-5616.

6. References

- [179] V. Martí-Centelles, M. D. Pandey, M. I. Burguete, S. V. Luis, *Chem. Rev.* **2015**, *115*, 8736-8834.
- [180] C. J. White, A. K. Yudin, *Nat. Chem.* **2011**, *3*, 509-524.
- [181] a) S. Sengupta, G. Mehta, *Org. Biomol. Chem.* **2020**, *18*, 1851-1876; b) D. G. Rivera, G. M. Ojeda-Carralero, L. Reguera, E. V. Van der Eycken, *Chem. Soc. Rev.* **2020**, *49*, 2039-2059; c) J. Iegre, J. S. Gaynord, N. S. Robertson, H. F. Sore, M. Hyvönen, D. R. Spring, *Adv. Ther.* **2018**, *1*, 1800052; d) Y. H. Lau, P. de Andrade, Y. Wu, D. R. Spring, *Chem. Soc. Rev.* **2015**, *44*, 91-102; e) L. D. Walensky, G. H. Bird, *J. Med. Chem.* **2014**, *57*, 6275-6288.
- [182] a) Z. Cheng, E. Kuru, A. Sachdeva, M. Vendrell, *Nat. Rev. Chem.* **2020**, *4*, 275-290; b) S. Lee, J. Xie, X. Chen, *Biochemistry* **2010**, *49*, 1364-1376.
- [183] a) P. Kaur, K. Singh, *J. Mat. Chem. C* **2019**, *7*, 11361-11405; b) T. Kowada, H. Maeda, K. Kikuchi, *Chem. Soc. Rev.* **2015**, *44*, 4953-4972; c) Y. Ni, J. Wu, *Org. Biomol. Chem.* **2014**, *12*, 3774-3791.
- [184] A. Loudet, K. Burgess, *Chem. Rev.* **2007**, *107*, 4891-4932.
- [185] a) L. J. Patalag, J. A. Ulrichs, P. G. Jones, D. B. Werz, *Org. Lett.* **2017**, *19*, 2090-2093; b) L. J. Patalag, L. P. Ho, P. G. Jones, D. B. Werz, *J. Am. Chem. Soc.* **2017**, *139*, 15104-15113; c) R. Lincoln, L. E. Greene, W. Zhang, S. Louisia, G. Cosa, *J. Am. Chem. Soc.* **2017**, *139*, 16273-16281; d) S. Bose, A. H. Ngo, L. H. Do, *J. Am. Chem. Soc.* **2017**, *139*, 8792-8795; e) L. J. Patalag, P. G. Jones, D. B. Werz, *Angew. Chem. Int. Ed.* **2016**, *55*, 13340-13344; f) A. Vázquez-Romero, N. Kielland, M. J. Arévalo, S. Preciado, R. J. Mellanby, Y. Feng, R. Lavilla, M. Vendrell, *J. Am. Chem. Soc.* **2013**, *135*, 16018-16021; g) L.-G. Milroy, S. Rizzo, A. Calderon, B. Ellinger, S. Erdmann, J. Mondry, P. Verveer, P. Bastiaens, H. Waldmann, L. Dehmelt, H.-D. Arndt, *J. Am. Chem. Soc.* **2012**, *134*, 8480-8486.
- [186] a) M. Virelli, W. Wang, R. Kuniyil, J. Wu, G. Zanoni, A. Fernandez, J. Scott, M. Vendrell, L. Ackermann, *Chem. Eur. J.* **2019**, *25*, 12712-12718; b) L. Mendive-Tapia, R. Subiros-Funosas, C. Zhao, F. Albericio, N. D. Read, R. Lavilla, M. Vendrell, *Nat. Protoc.* **2017**, *12*, 1588-1619.
- [187] a) Y.-P. Hsu, E. Hall, G. Booher, B. Murphy, A. D. Radkov, J. Yablonowski, C. Mulcahey, L. Alvarez, F. Cava, Y. V. Brun, E. Kuru, M. S. VanNieuwenhze, *Nat. Chem.* **2019**, *11*, 335-341; b) F. Zhou, J. Shao, Y. Yang, J. Zhao, H. Guo, X. Li, S. Ji, Z. Zhang, *Eur. J. Org. Chem.* **2011**, *2011*, 4773-4787.

-
- [188] S. Santoro, F. Ferlin, L. Ackermann, L. Vaccaro, *Chem. Soc. Rev.* **2019**, *48*, 2767-2782.
- [189] a) J. Schwan, M. Christmann, *Chem. Soc. Rev.* **2018**, *47*, 7985-7995; b) C. A. Kuttruff, M. D. Eastgate, P. S. Baran, *Nat. Prod. Rep.* **2014**, *31*, 419-432.
- [190] K. Korvorapun, N. Kaplaneris, T. Rogge, S. Warratz, A. C. Stückl, L. Ackermann, *ACS Catal.* **2018**, *8*, 886-892.
- [191] J. Wu, N. Kaplaneris, S. Ni, F. Kaltenhäuser, L. Ackermann, *Chem. Sci.* **2020**, *11*, 6521-6526.
- [192] A. Schischko, N. Kaplaneris, T. Rogge, G. Sirvinskaite, J. Son, L. Ackermann, *Nat. Commun.* **2019**, *10*, 3553.
- [193] N. Kaplaneris, T. Rogge, R. Yin, H. Wang, G. Sirvinskaite, L. Ackermann, *Angew. Chem. Int. Ed.* **2019**, *58*, 3476-3480.
- [194] M. M. Lorion, N. Kaplaneris, J. Son, R. Kuniyil, L. Ackermann, *Angew. Chem. Int. Ed.* **2019**, *58*, 1684-1688.
- [195] N. Kaplaneris, F. Kaltenhäuser, G. Sirvinskaite, S. Fan, T. De Oliveira, L.-C. Conradi, L. Ackermann, *Sci. Adv.* **2021**, *7*, eabe6202.
- [196] N. Kaplaneris, J. Son, L. Mendive-Tapia, A. Kopp, N. D. Barth, I. Maksso, M. Vendrell, L. Ackermann, *Nat. Commun.* **2021**, *11*, 3389.
- [197] a) K. Schwekendiek, F. Glorius, *Synthesis* **2006**, 2996-3002; b) N. Mori, H. Togo, *Tetrahedron* **2005**, *61*, 5915-5925.
- [198] B. Jiang, M. Zhao, S.-S. Li, Y.-H. Xu, T.-P. Loh, *Angew. Chem. Int. Ed.* **2018**, *57*, 555-559.

7. Acknowledgements

7. Acknowledgements

First, I would like to express my sincere and warm gratitude to my PhD mentor Prof. Dr. Lutz Ackermann, who five years ago gave me the opportunity to carry out my PhD studies under his supervision, where I had the chance to work on some emerging aspects of organic chemistry. His constant encouragement and support for my experimental and academic growth have been instrumental. His insightful suggestions, in many ways, have shaped my research attitude and greatly influenced the my overall development as a scientist. He leads his group by example, he does not show us the correct, sometimes difficult, road but he goes along with us. The mentorship I got in this group is the best thing I have ever received in my short academic career.

Besides my advisor, I would like to thank Prof. Dr. Konrad Koszinowski for accepting to be my second supervisor. Valuable suggestions from him helped significantly to improve my work. Furthermore, his advice for my future career is highly appreciated.

I also would like to thank Prof. Dr. Dr. h.c.mult. Lutz F. Tietze, Prof. Dr. Ricardo Mata, Dr. Daniel Janßen-Müller and Dr. Michael John for agreeing to take part in my defense. I am thankful to the Institut für Organische und Biomolekulare Chemie, Georg-August-Universität Göttingen for the excellent facilities, that enabled me to conduct efficiently my research.

Financial assistance from the Onassis Foundation (Onassis Scholarship [Scholarship ID: F ZM 036/1 (2016-2017)]), University of Göttingen and Prof. Dr. Lutz Ackermann is gratefully acknowledged.

I deeply indebted to Ms. Gabriele Keil-Knepel and Ms. Bianca Spitalieri for their kind and prompt assistance regarding administrative work. I sincerely thank Mr. Stefan Beußhausen for taking care of all the instruments in our research group, especially the LC-MS, the glovebox and the GPC, which I used very often during the period of my PhD studies in the last five years. I sincerely thank Mr. Karsten Rauch for his kind support and guidance regarding experimental work.

My sincere thanks also goes to my fellow labmates, and all the members of our lab, past and present, for great work atmosphere, teamwork and companionship. I sincerely thank Dr. Hui Wang, Dr. Korakit Korvorapun, Dr. Torben Rogge, Dr. Jongwoo Son, Dr. Wei Wang, Dr. Alexandra Schischko, Dr. Mélanie Lorion, Dr. Gandeepan Parthasarathy, Dr Svenja Warratz, Dr. Joao Carlos Agostinho de Oliveira, Dr. Antonis Messinis, Dr. Ramesh Chandra Samanta, Dr. Shaofei Ni, Dr. Rositha Kuniyil, Dr. Uttam

7. Acknowledgements

Dhawa, Dr. Fabio Pesciaioli, Dr. Marc Moselage, Jun Wu, Adelina Kopp, Isaac Choi, Isaac Maksso, Giedre Sirvinskaite, Felix Kaltenhäuser, Rongxin Yin for their valuable help on my PhD projects both experimentally and intellectually.

I would like to thank whole Ackermann family and special thank to all members in Lab 306 and Lab 302: Dr. Hui Wang, Dr. Fabio Pesciaioli, Dr. Marc Moselage, Dr. Mélanie Lorion, Dr. Santhi Vardhana Yetra, Dr. Wei Wang, Dr. Gandeepan Parthasarathy, Dr. Ramesh Chandra Samanta Dr. Elżbieta Gońka, Isaac Choi Jun Wu, Adelina Kopp, Alexej Scheremetjew, Giedre Sirvinskaite, Felix Kaltenhäuser, Rongxin Yin.

Many thanks to Dr. Ramesh Chandra Samanta, Dr Uttam Dhawa, Isaac Choi, Maximilian Stangier, Julia Struwe, Nate Ang for their instructive comments during the correction of this thesis. I sincerely would like to thank all the people who previously corrected manuscripts, supporting information, posters, abstracts and proposals in very short notice: Dr. Uttam Dhawa, Dr. Hui Wang, Dr. Korkit Korvorapun, Dr. Torben Rogge, Dr. Wei Wang, Dr. Mélanie Lorion, Dr. Gandeepan Parthasarathy, Dr Svenja Warratz, Dr. João Carlos Agostinho de Oliveira, Dr. Ramesh Chandra Samanta, Isaac Choi, Maximilian Stangier.

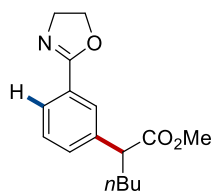
Moreover, I am thankful to Dr. Michael John for helping me in analyzing some NMR spectroscopic data. His assistance in elucidating two structures was crucial for two of my projects. I am thankful to the instrument operators, and staff of NMR and mass spectrometry departments at the IOBC for their continuous support to our research work.

I also would like to express my gratitude to my former supervisor, Prof. Dr. Christoforos G. Kokotos, for teaching me organic chemistry and giving me the opportunity to conduct research within his laboratory.

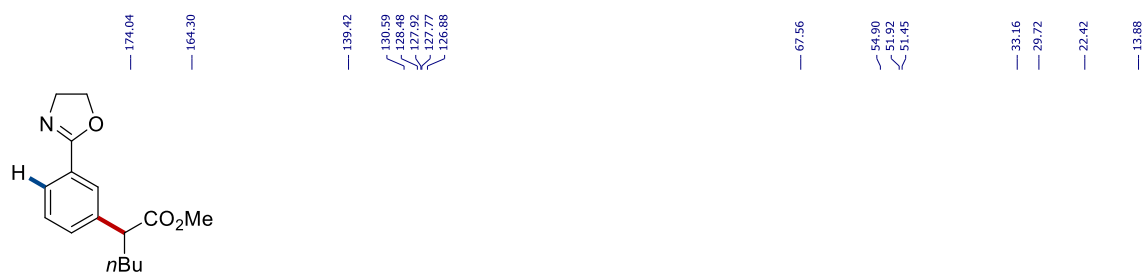
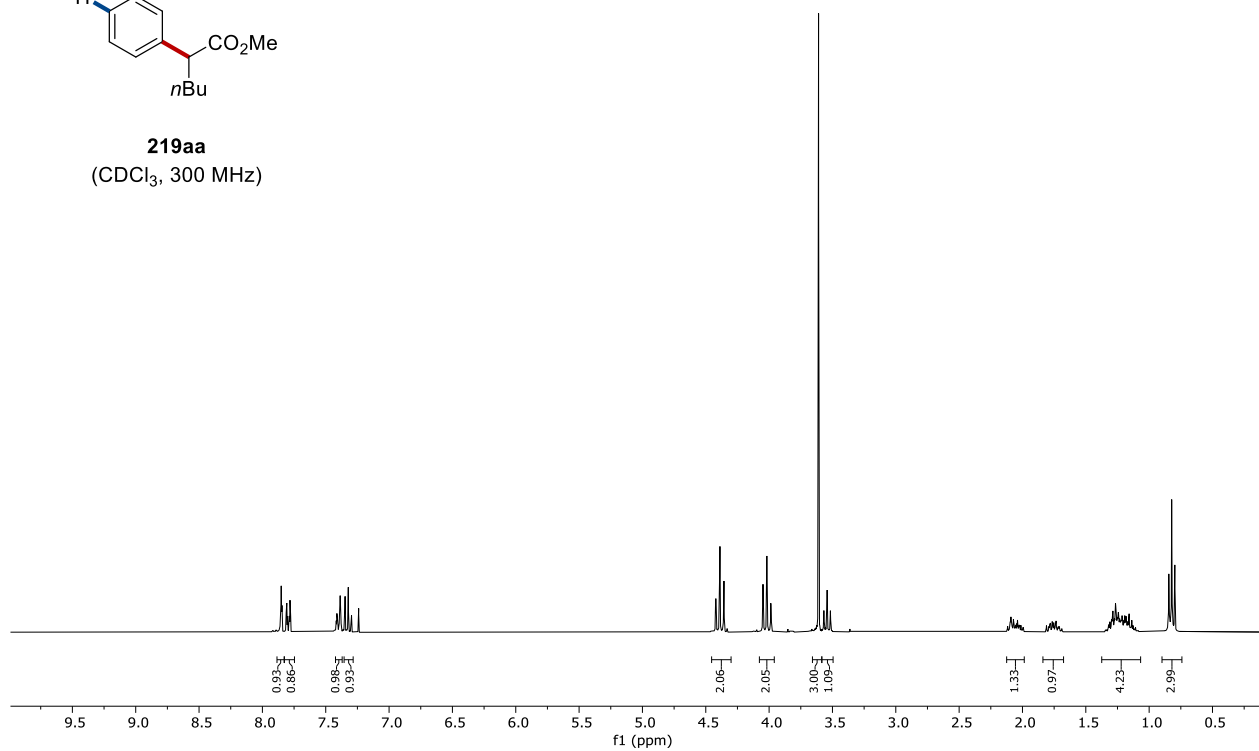
Lastly, I want to thank Θέμης, Βιβή and Μαρία for their unconditional and pure support in my every step. It is because of them I succeeded, knowing that they are always looking after me. Without a doubt I would not be here without you. Σας ευχαριστώ για όλα.

8. NMR Spectra

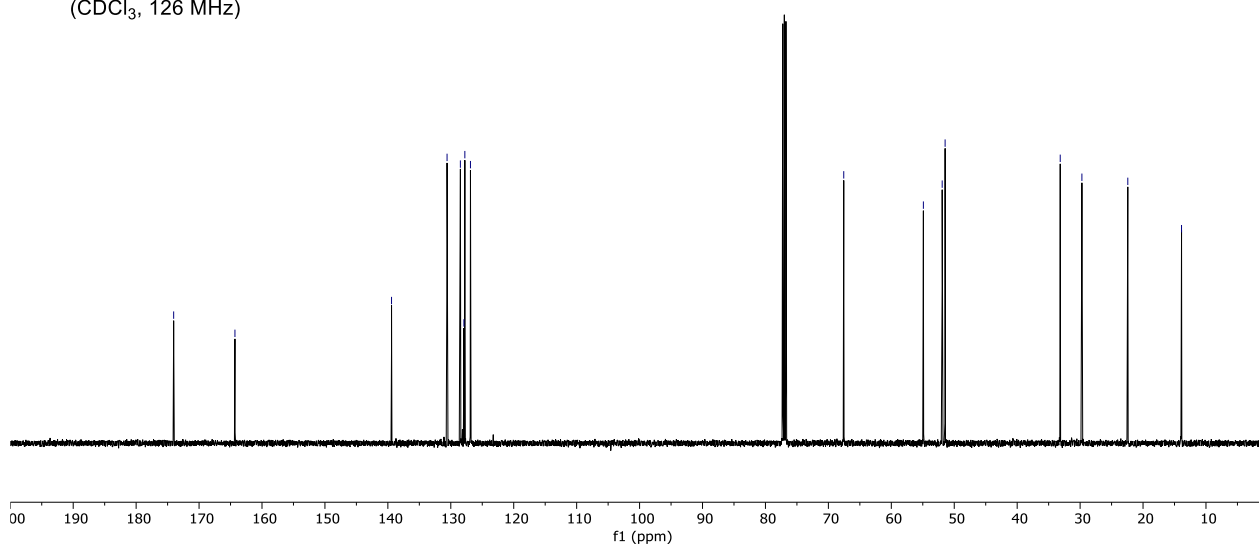
8. NMR Spectra

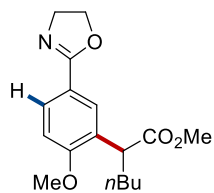


219aa
(CDCl₃, 300 MHz)

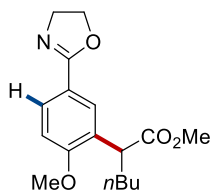
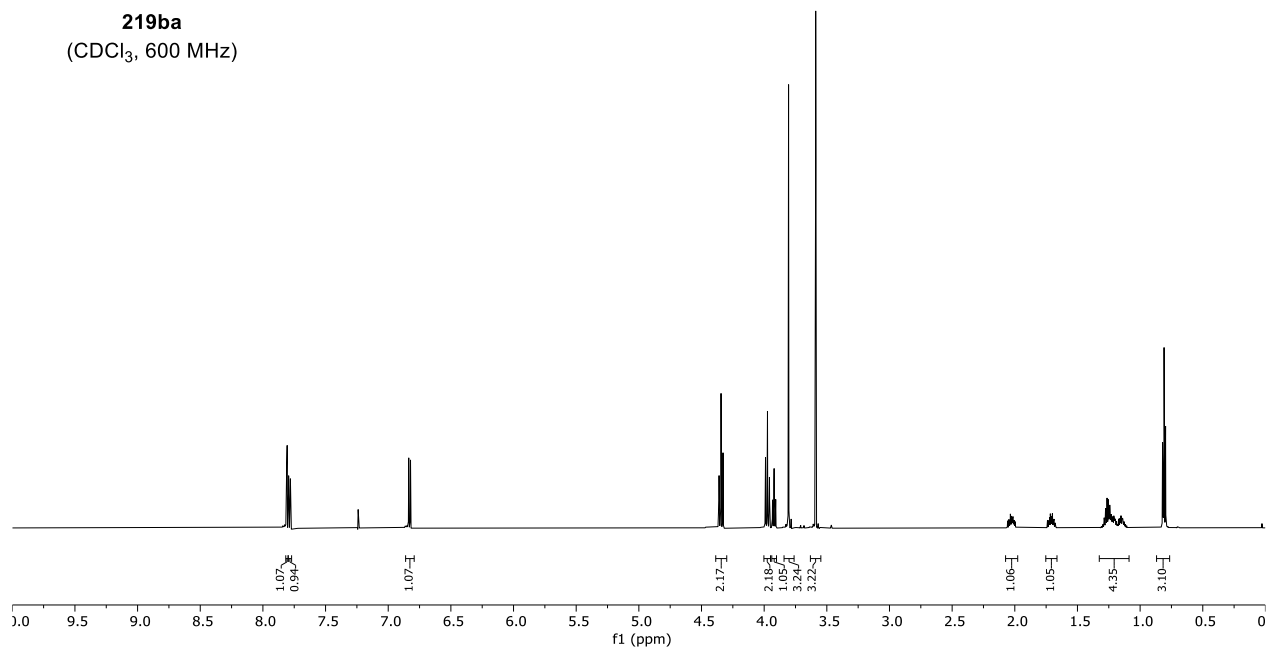


219aa
(CDCl₃, 126 MHz)

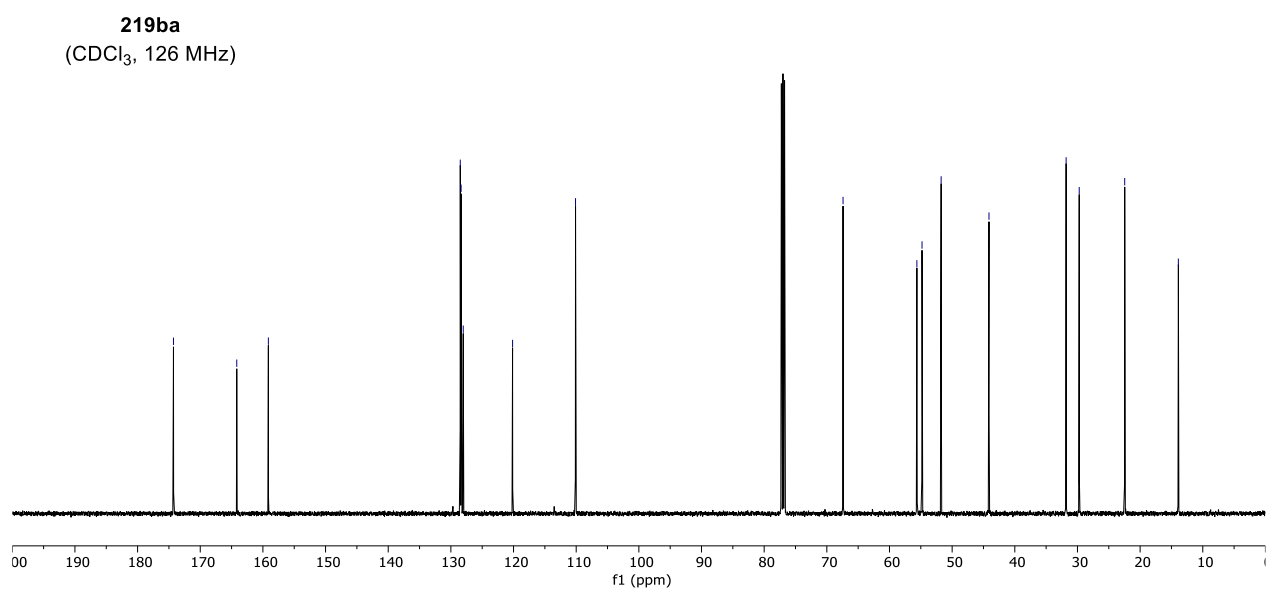




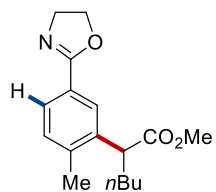
219ba
(CDCl₃, 600 MHz)



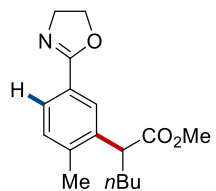
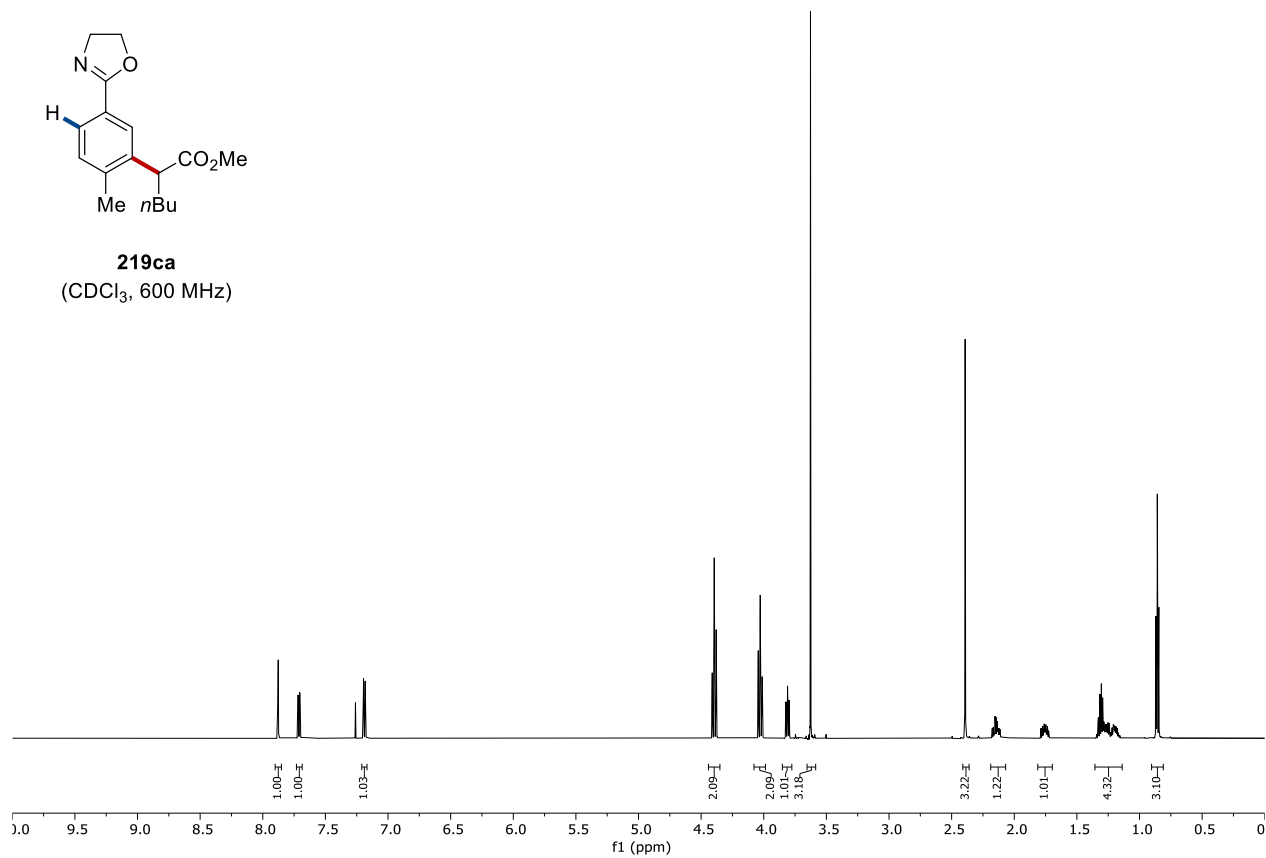
219ba
(CDCl₃, 126 MHz)



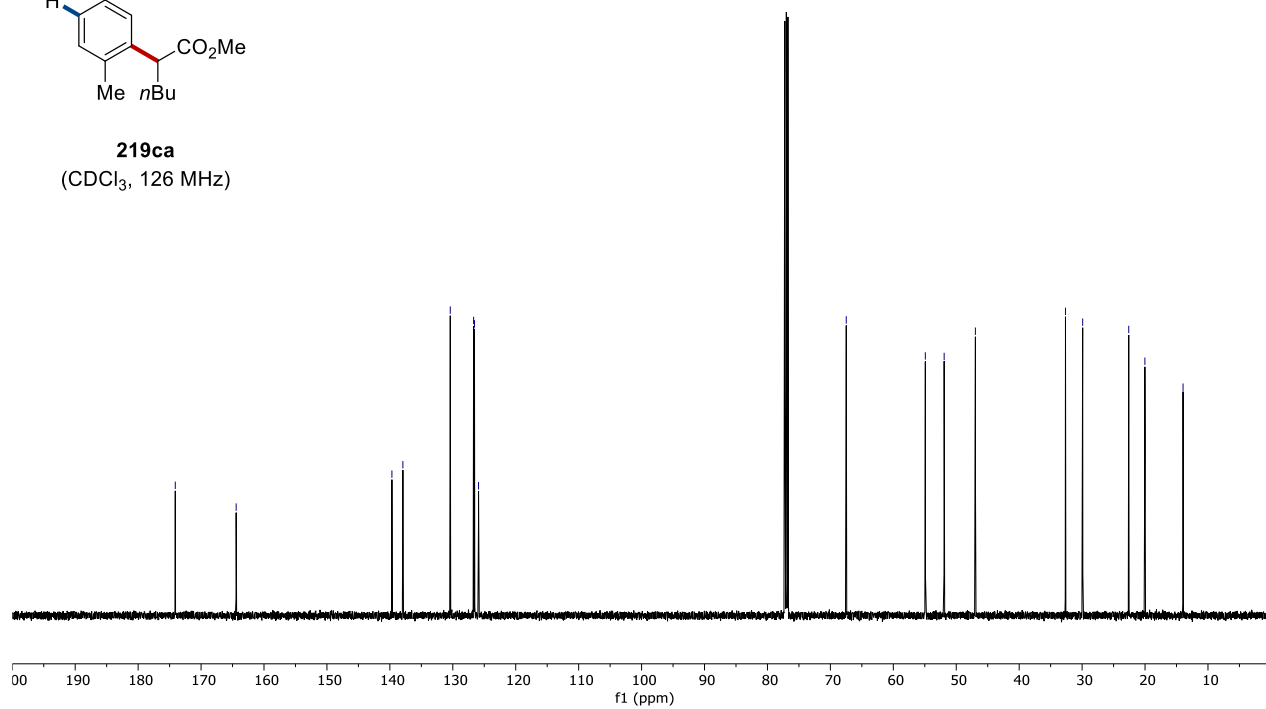
8. NMR Spectra



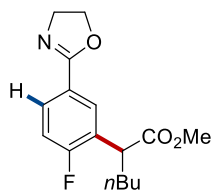
219ca
(CDCl₃, 600 MHz)



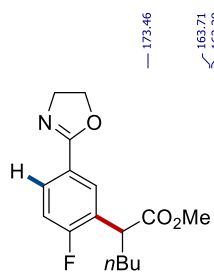
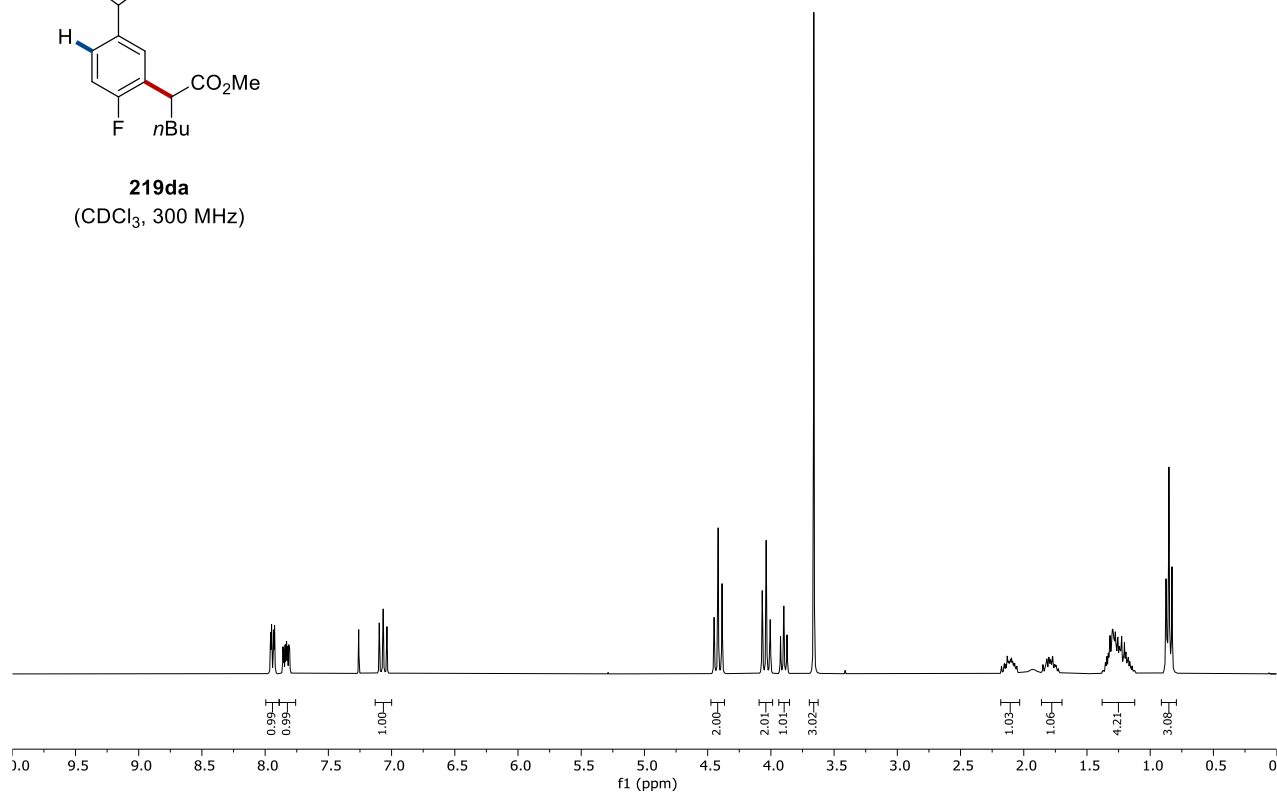
219ca
(CDCl₃, 126 MHz)



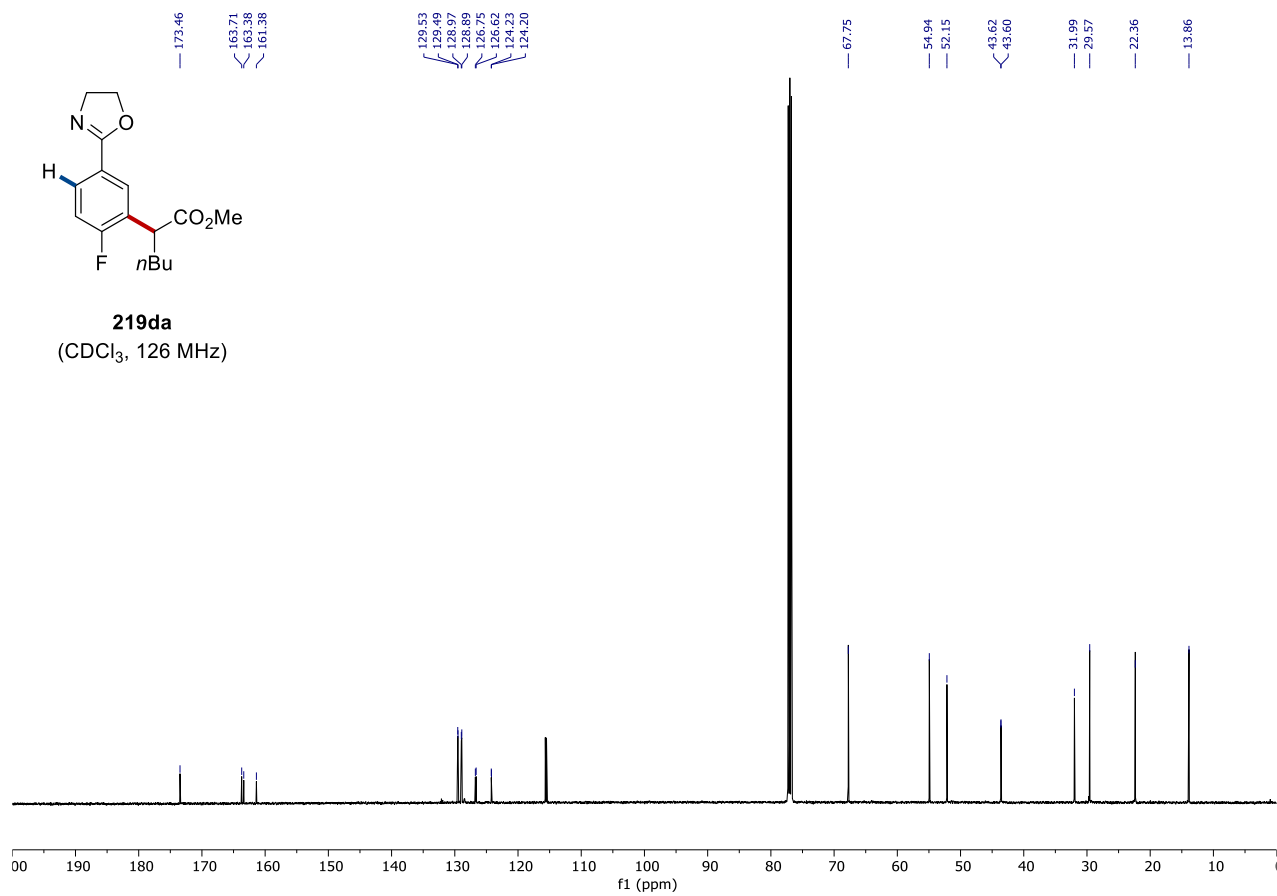
8. NMR Spectra



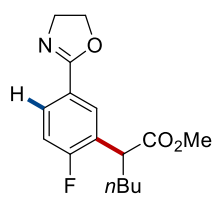
219da
(CDCl₃, 300 MHz)



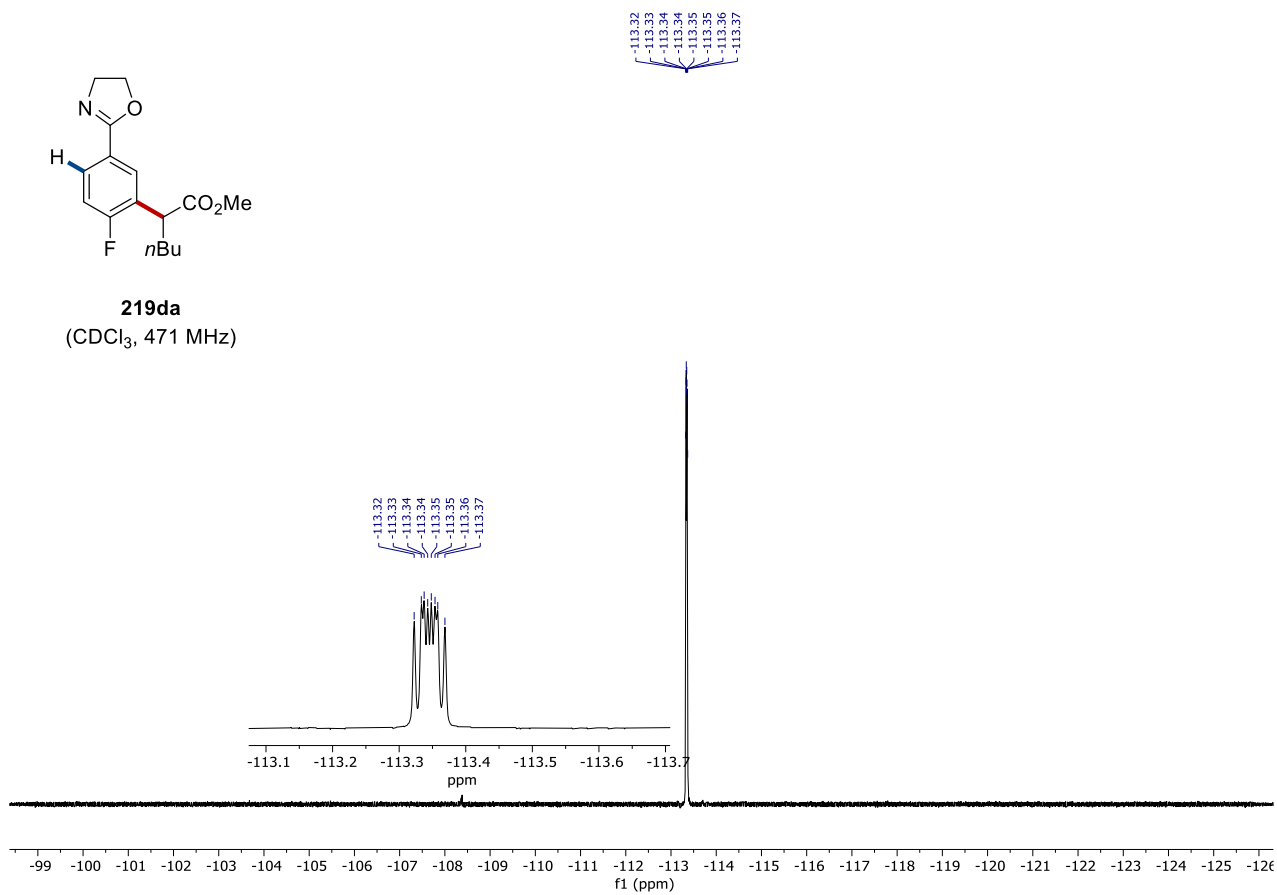
219da
(CDCl₃, 126 MHz)



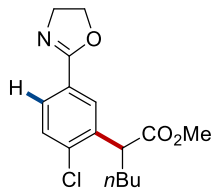
8. NMR Spectra



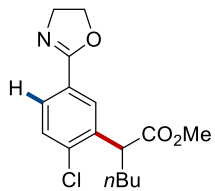
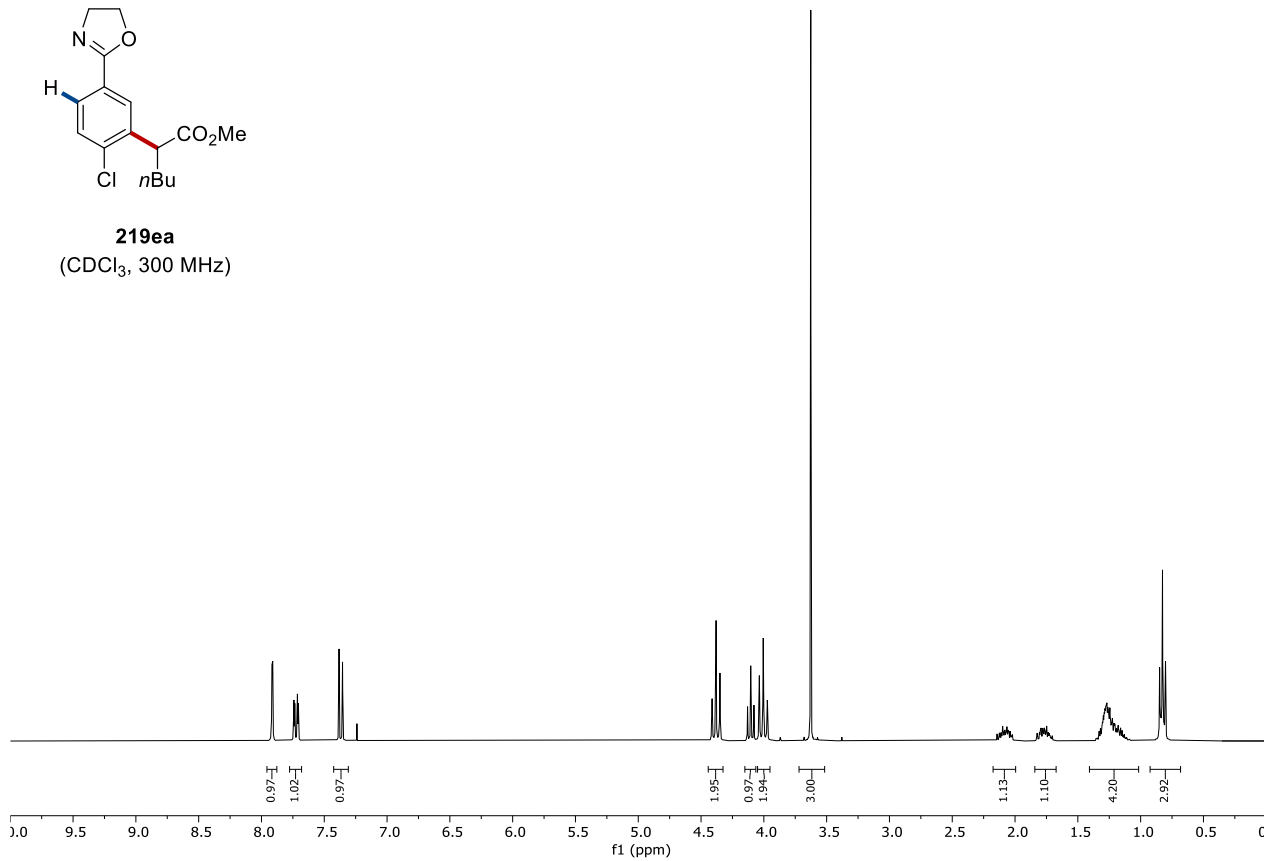
219da
(CDCl₃, 471 MHz)



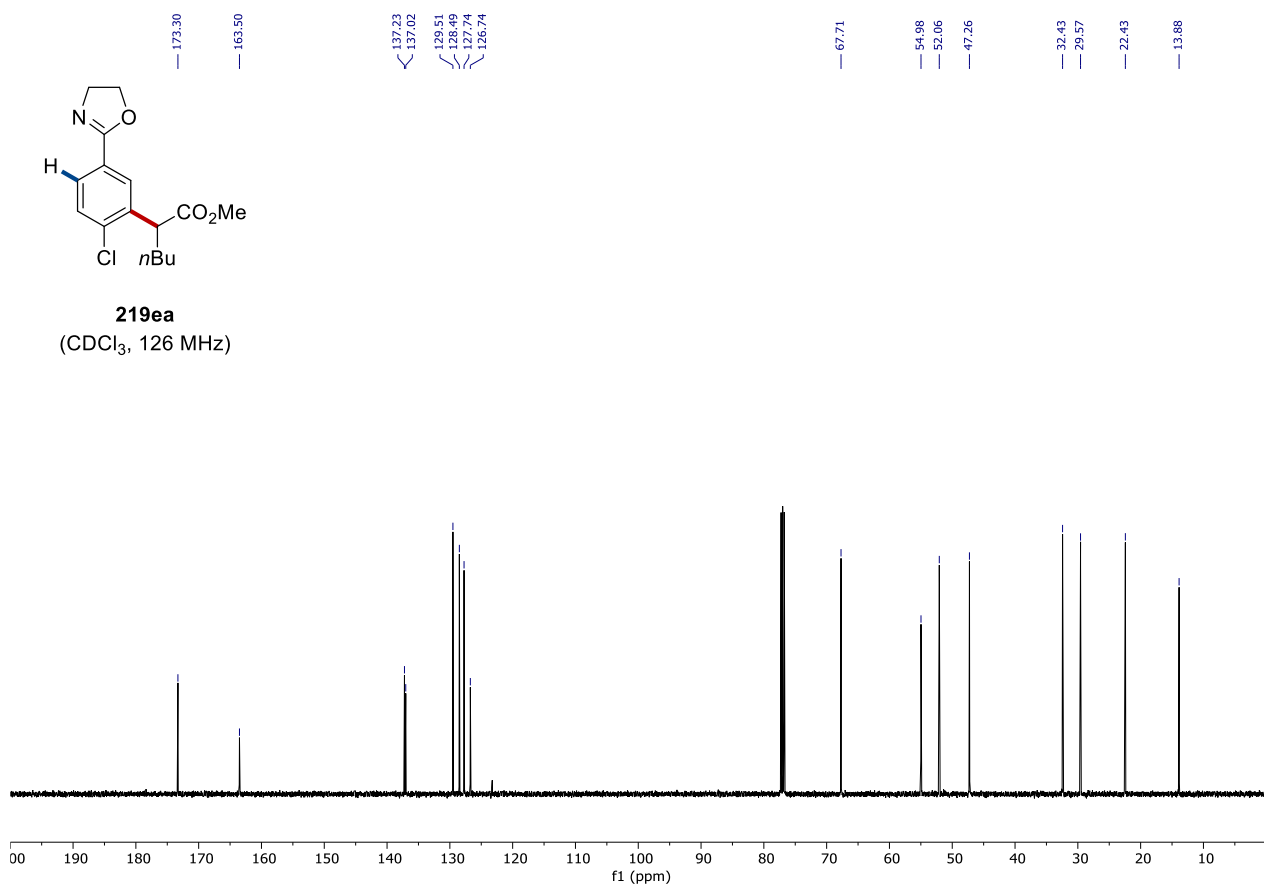
8. NMR Spectra



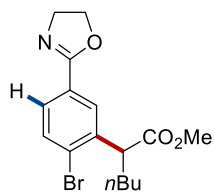
219ea
(CDCl₃, 300 MHz)



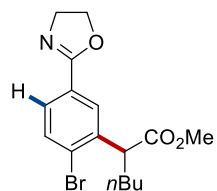
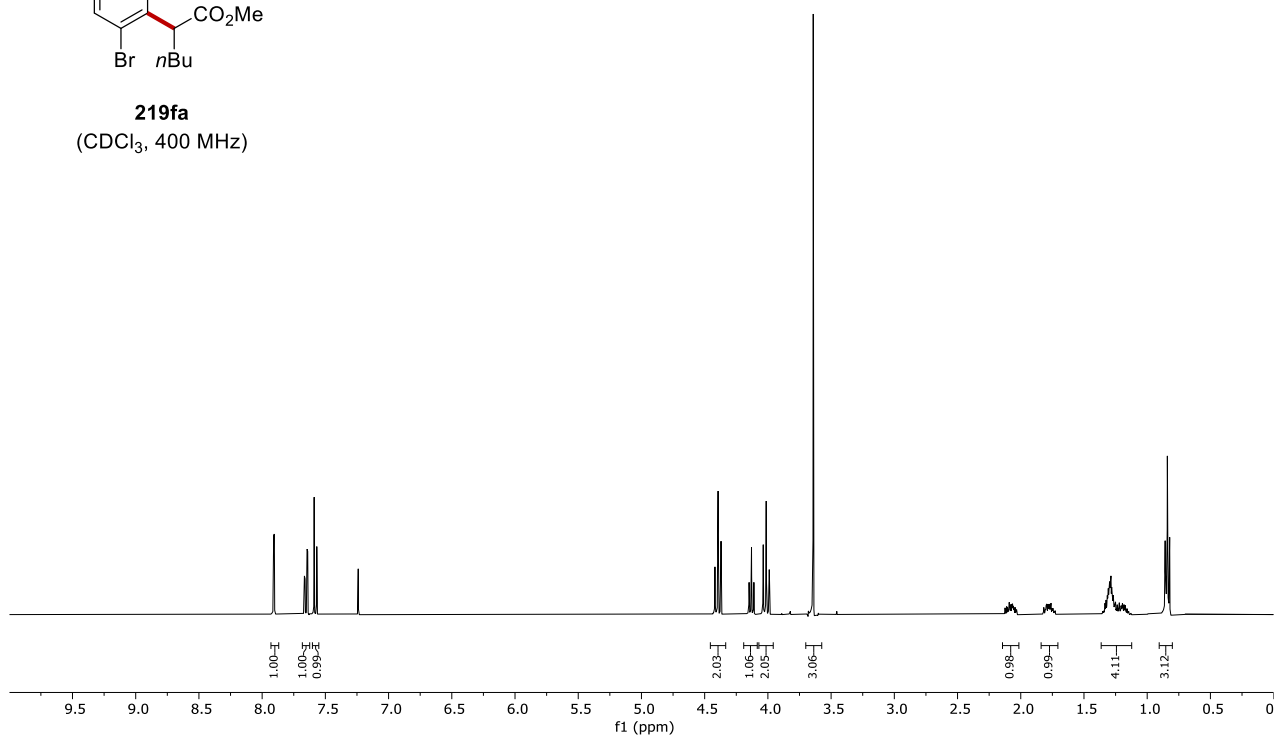
219ea
(CDCl₃, 126 MHz)



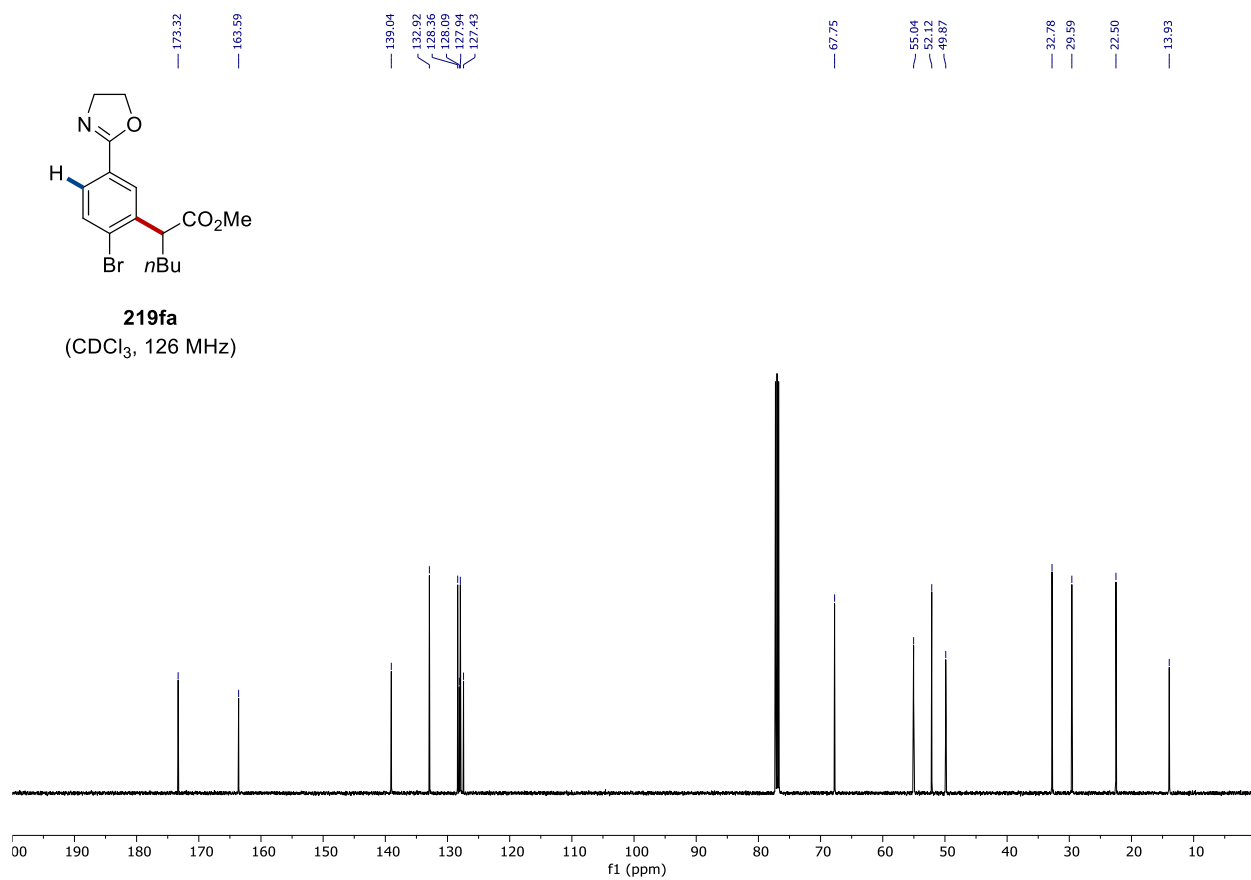
8. NMR Spectra

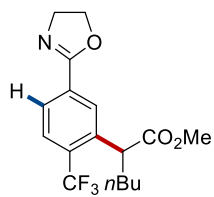


219fa
(CDCl₃, 400 MHz)

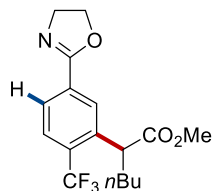
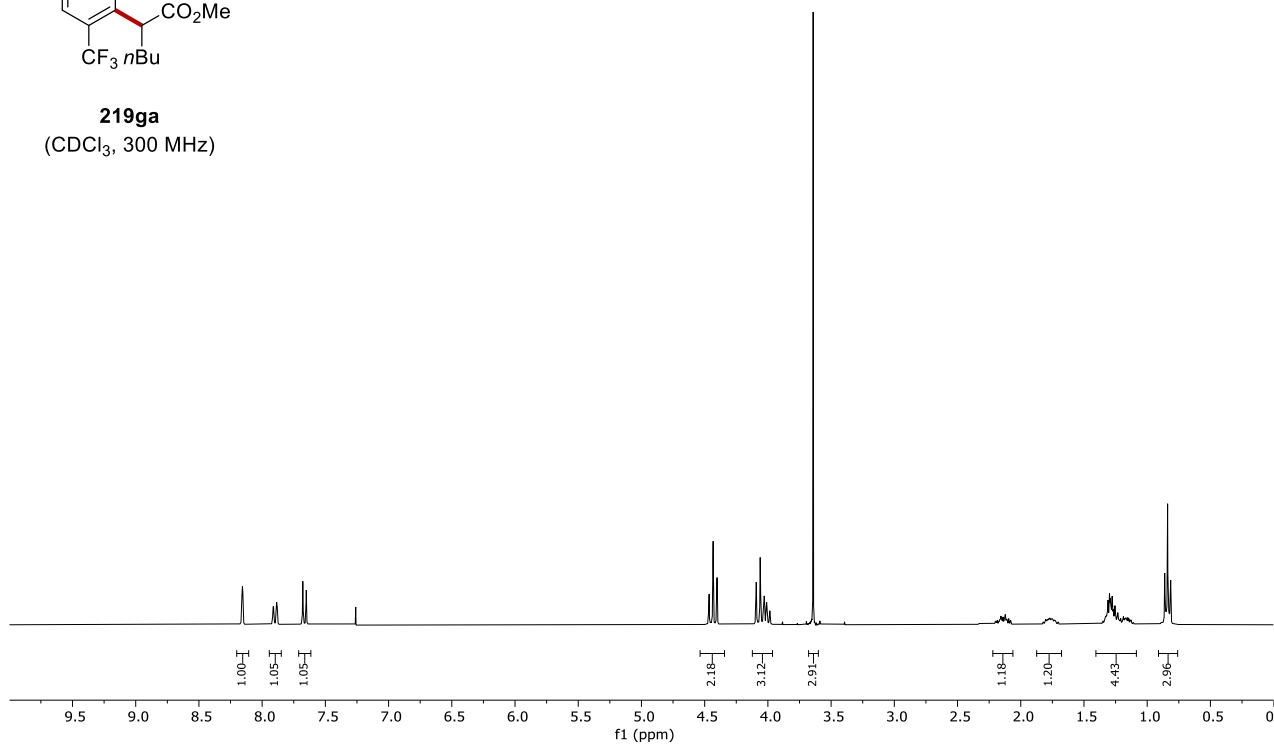


219fa
(CDCl₃, 126 MHz)

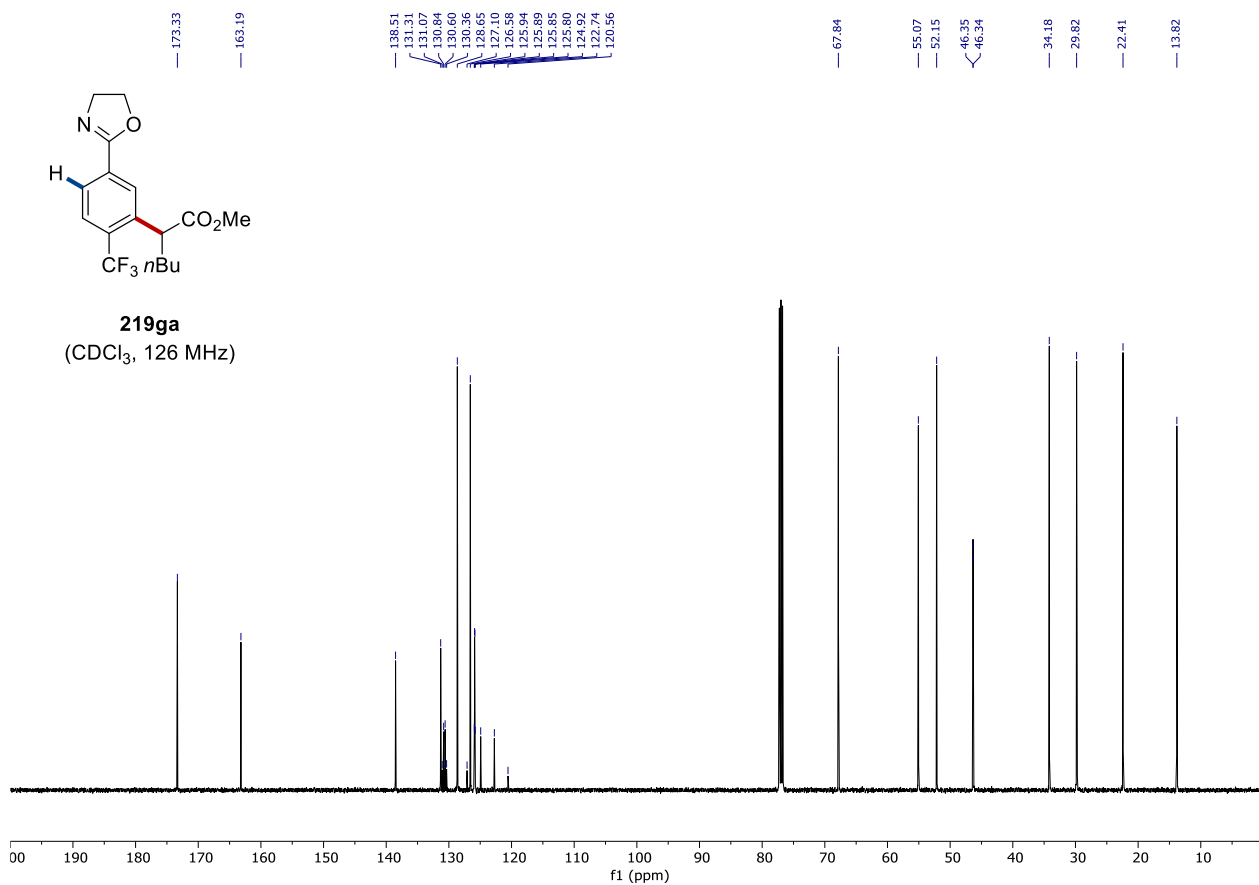




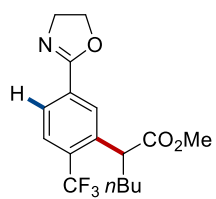
219ga
(CDCl₃, 300 MHz)



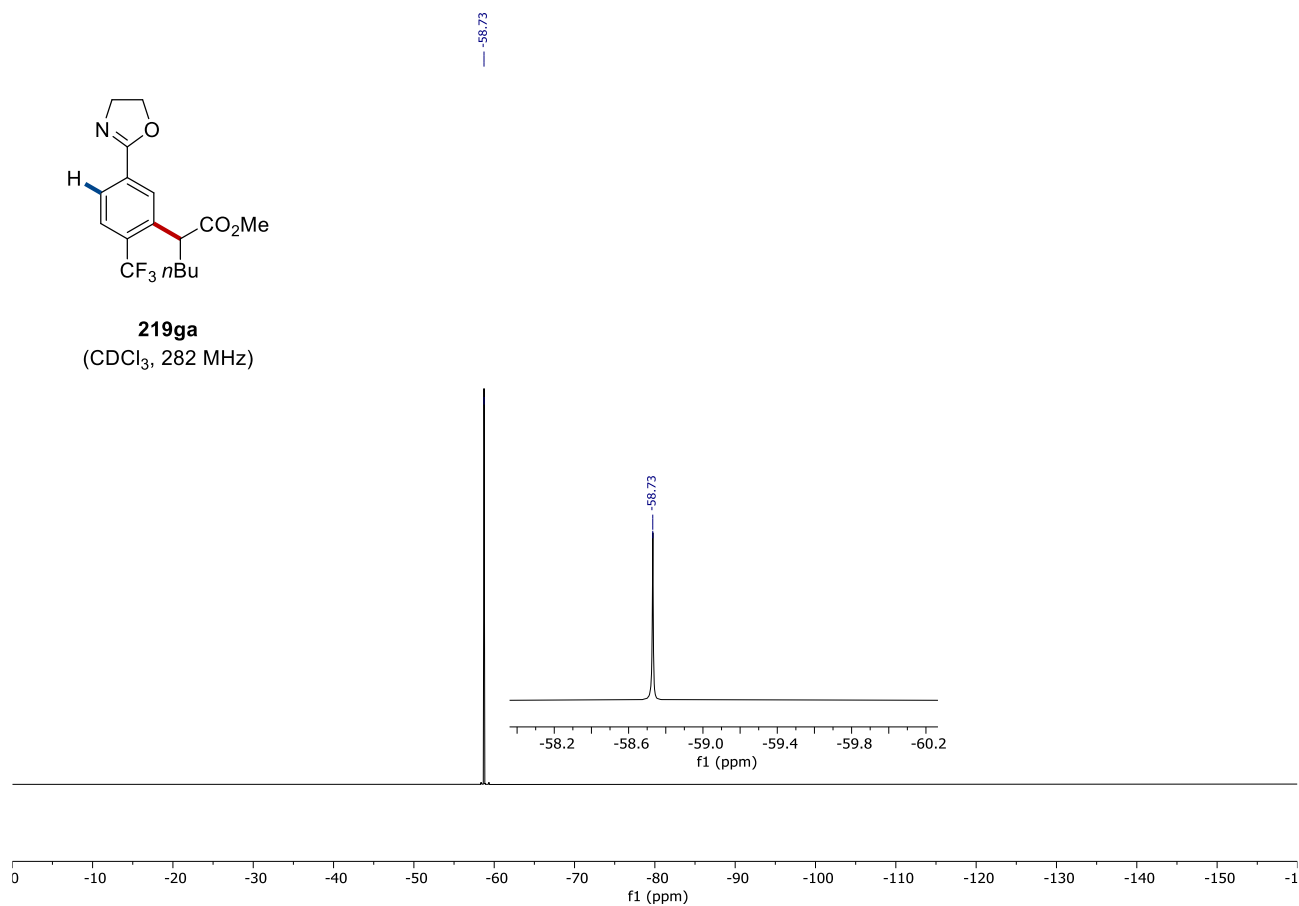
219ga
(CDCl₃, 126 MHz)

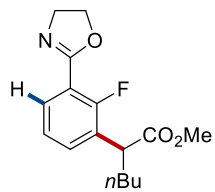


8. NMR Spectra

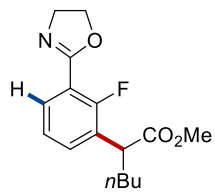
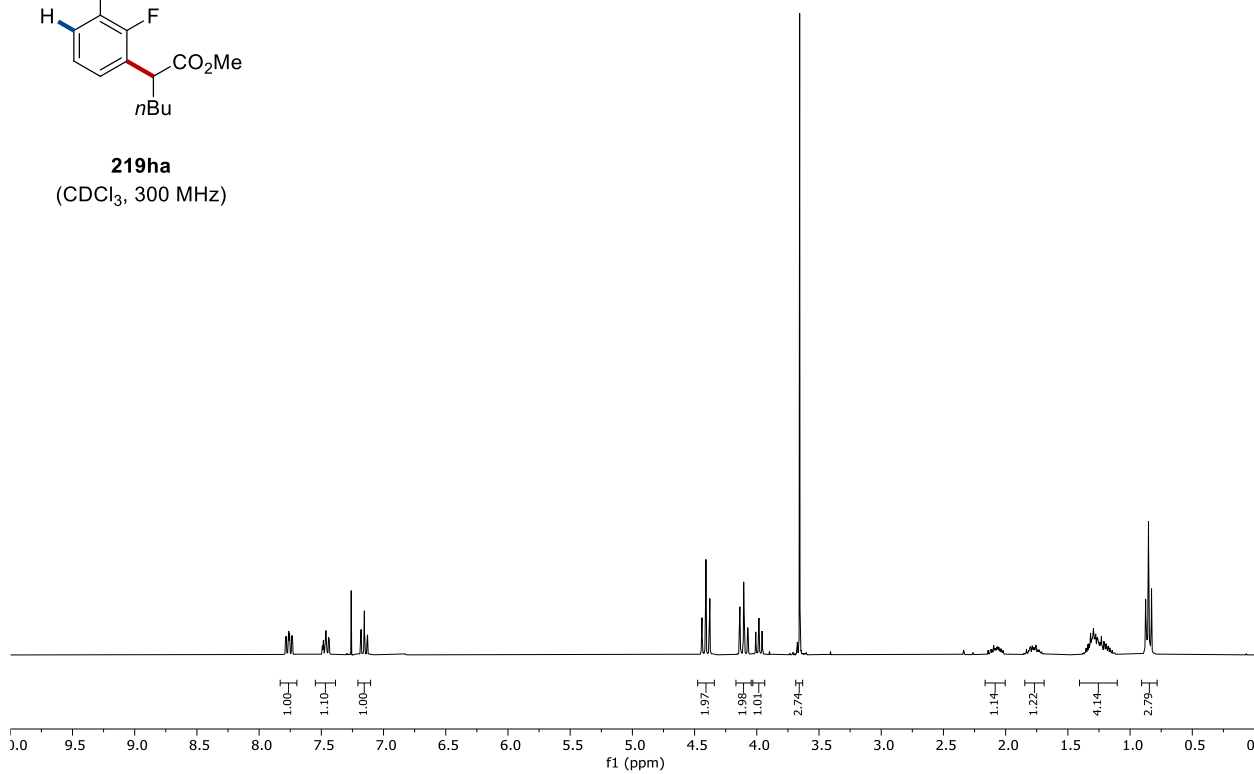


219ga
(CDCl₃, 282 MHz)

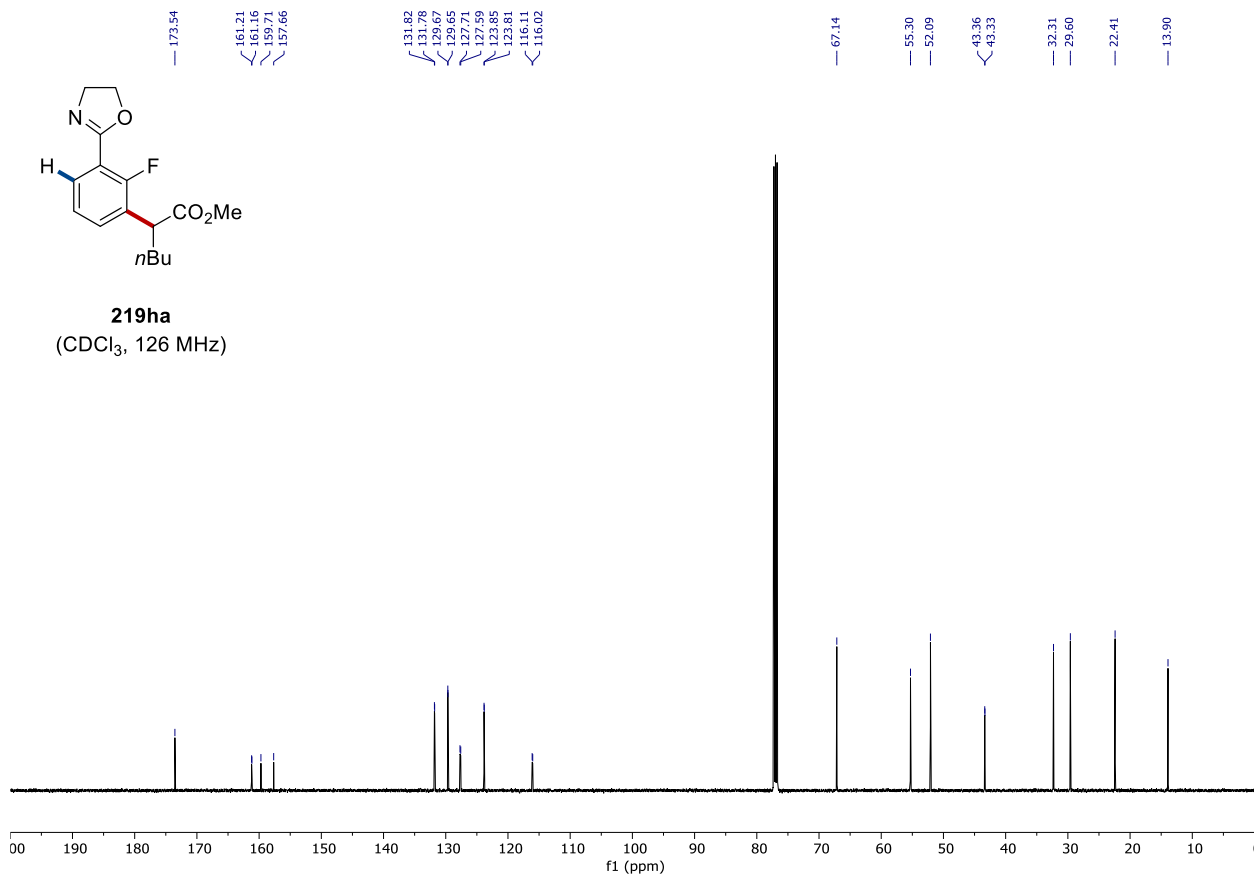




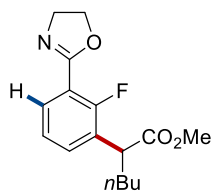
219ha
(CDCl₃, 300 MHz)



219ha
(CDCl₃, 126 MHz)

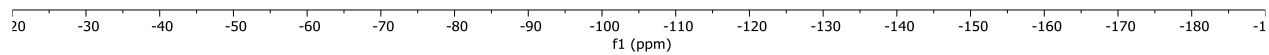
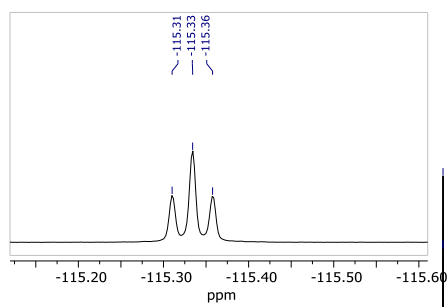


8. NMR Spectra

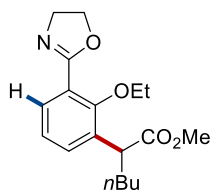


219ha
(CDCl₃, 282 MHz)

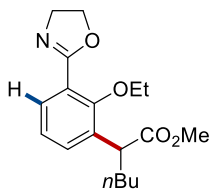
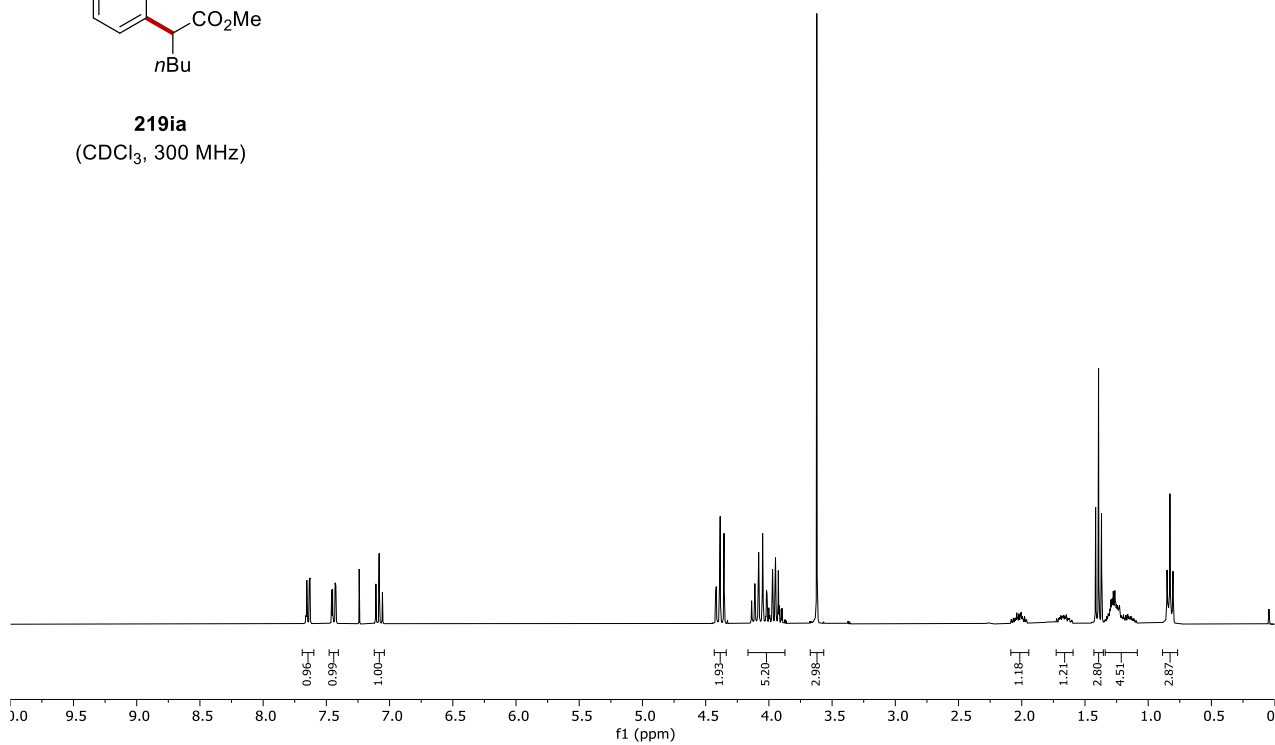
-115.31
-115.33
-115.36



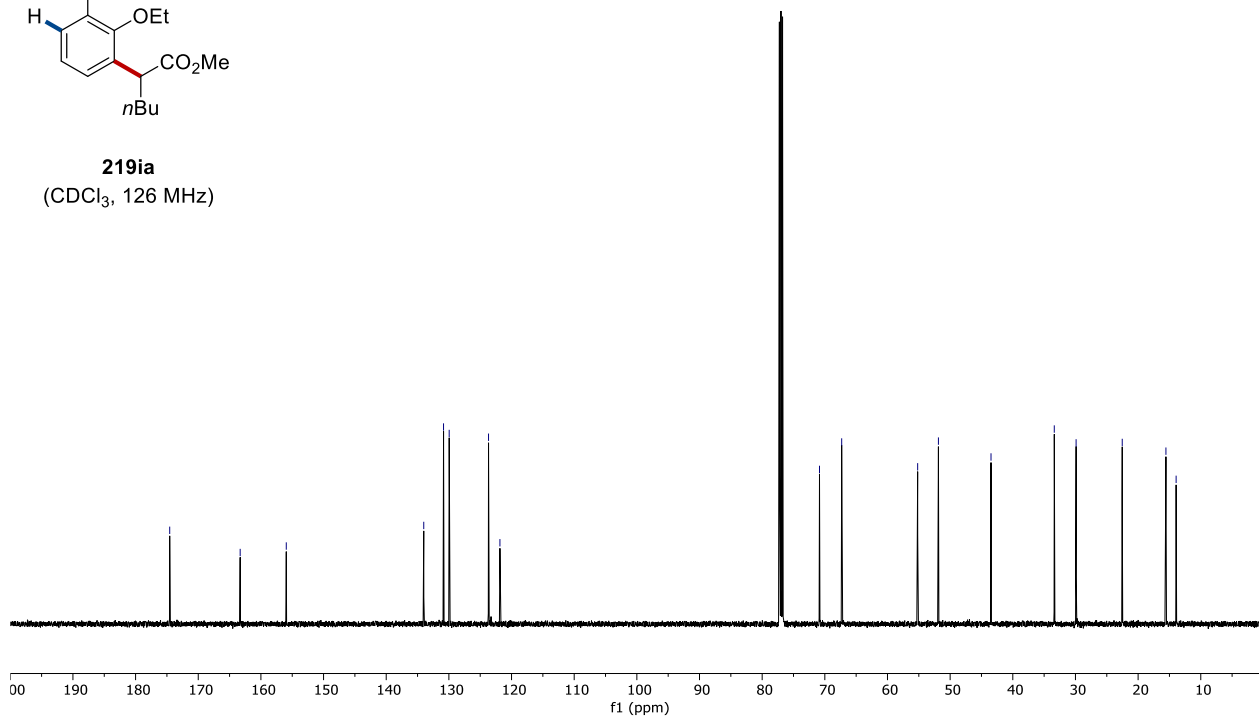
8. NMR Spectra



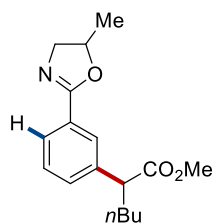
219ia
(CDCl₃, 300 MHz)



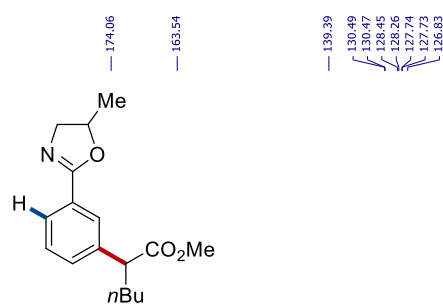
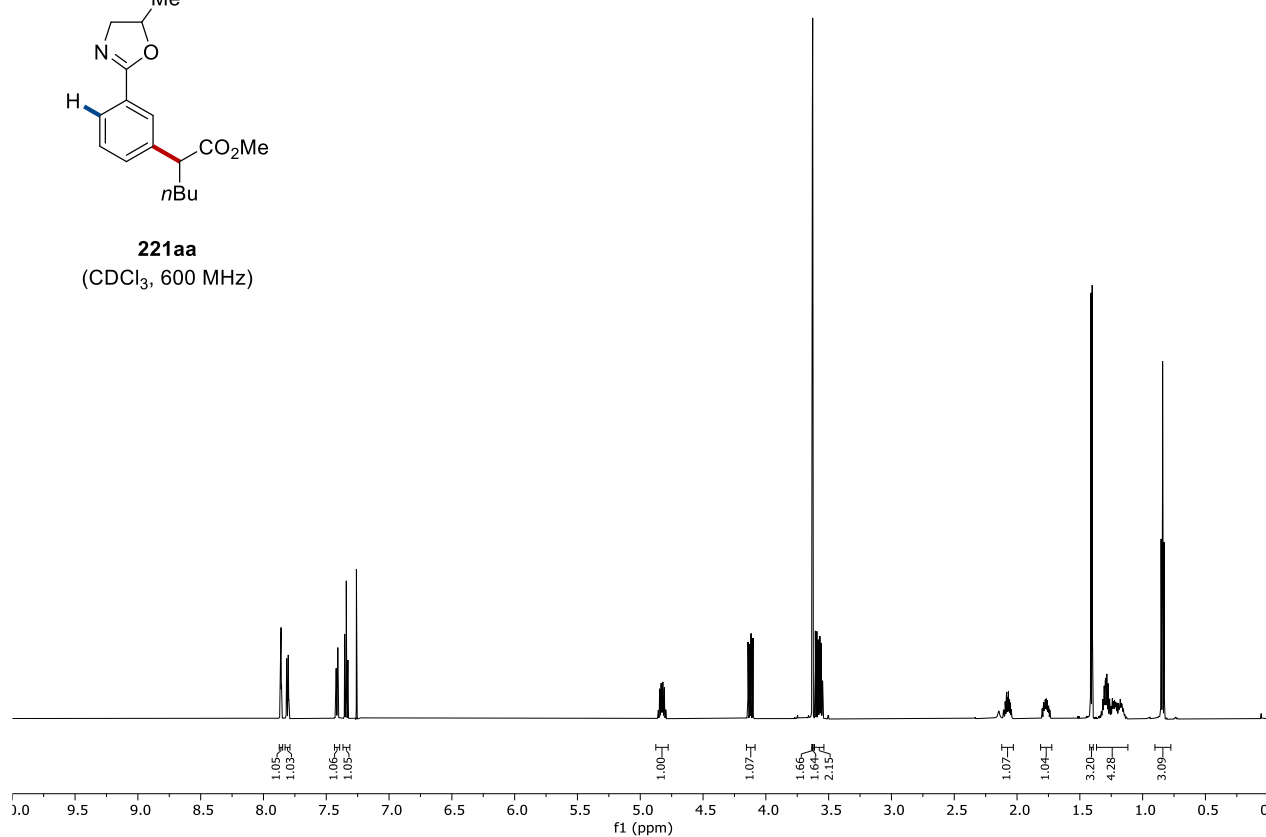
219ia
(CDCl₃, 126 MHz)



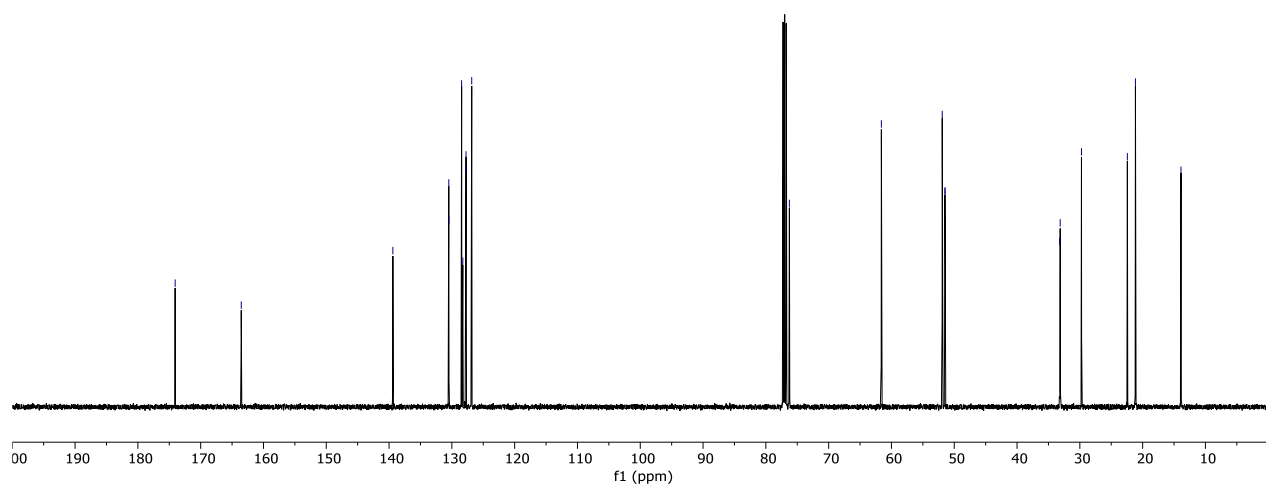
8. NMR Spectra

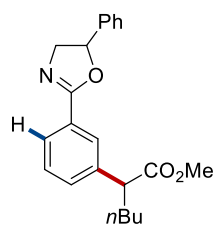


221aa
(CDCl₃, 600 MHz)

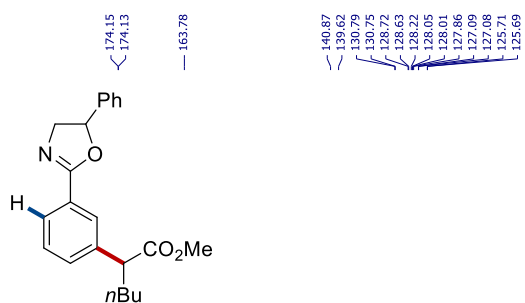
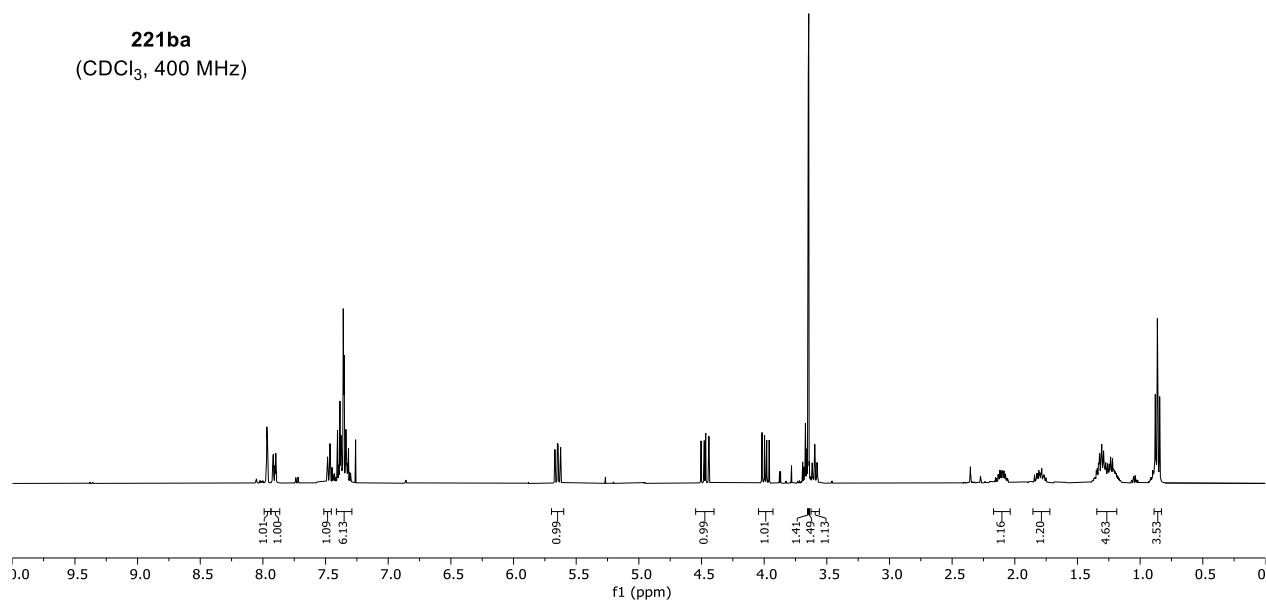


221aa
(CDCl₃, 126 MHz)

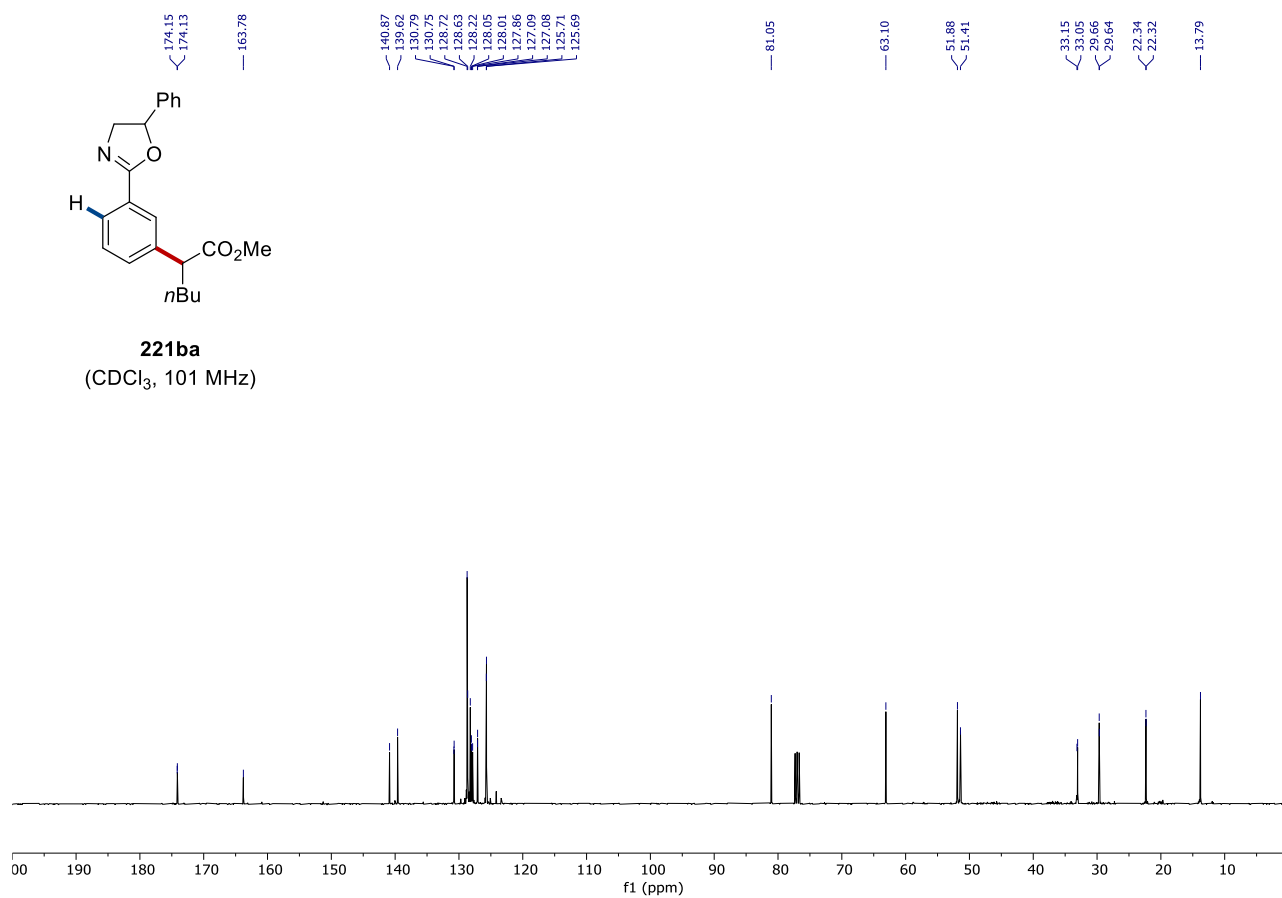




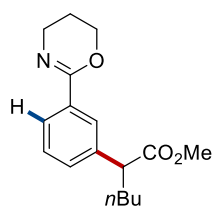
221ba
(CDCl₃, 400 MHz)



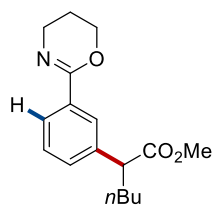
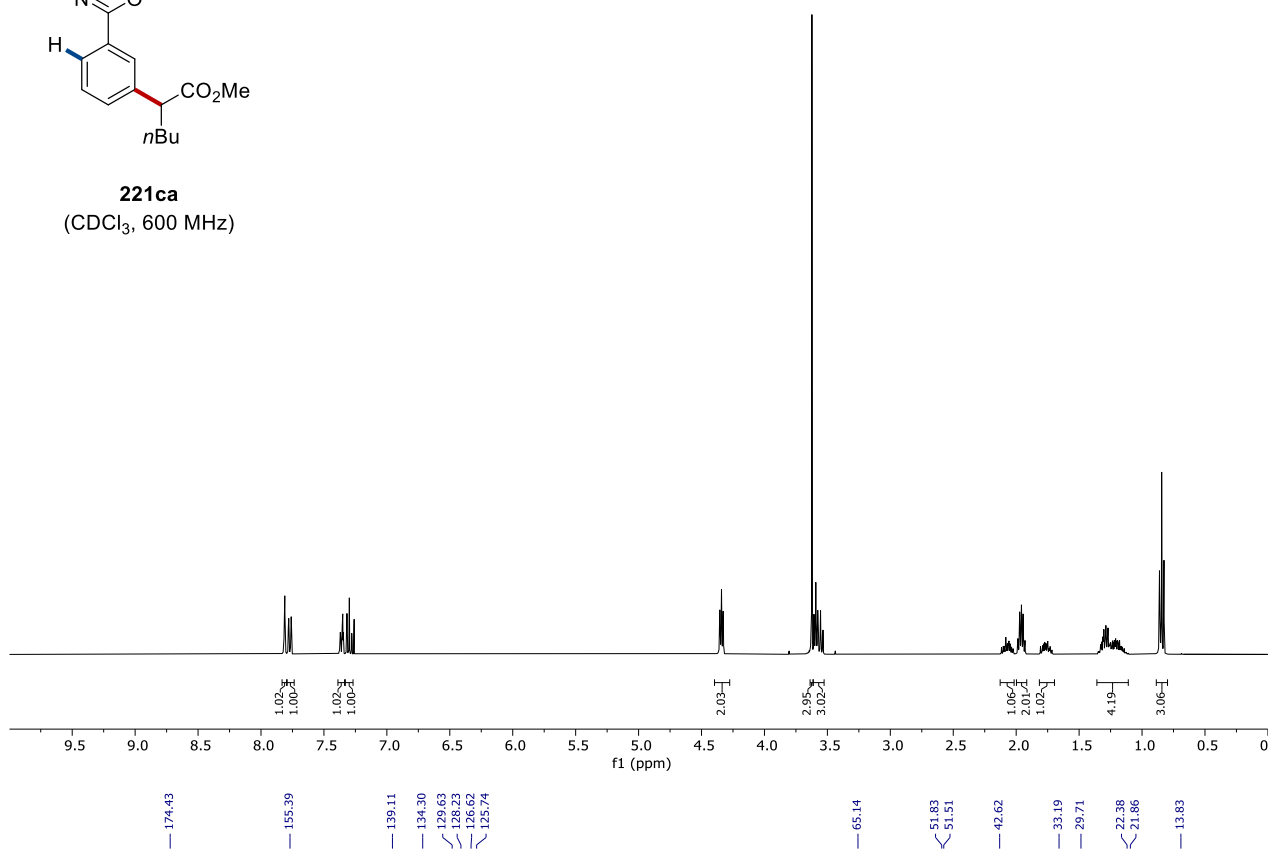
221ba
(CDCl₃, 101 MHz)



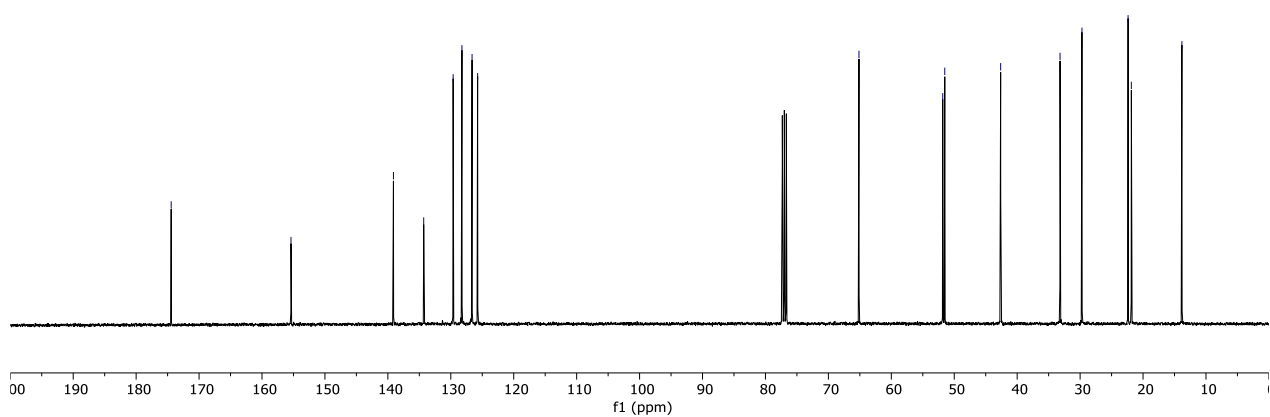
8. NMR Spectra

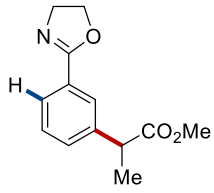


221ca
(CDCl₃, 600 MHz)

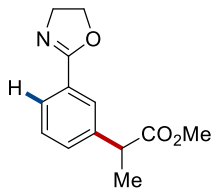
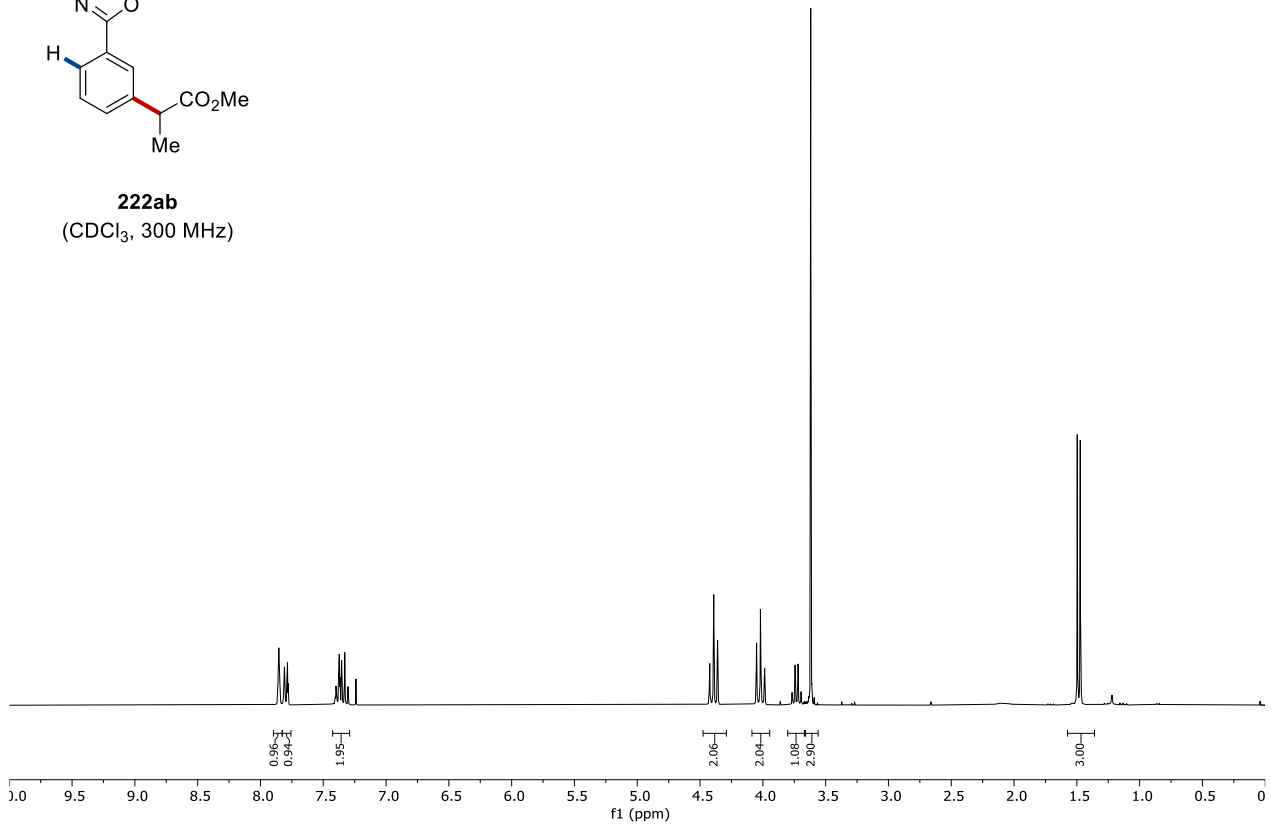


221ca
(CDCl₃, 101 MHz)

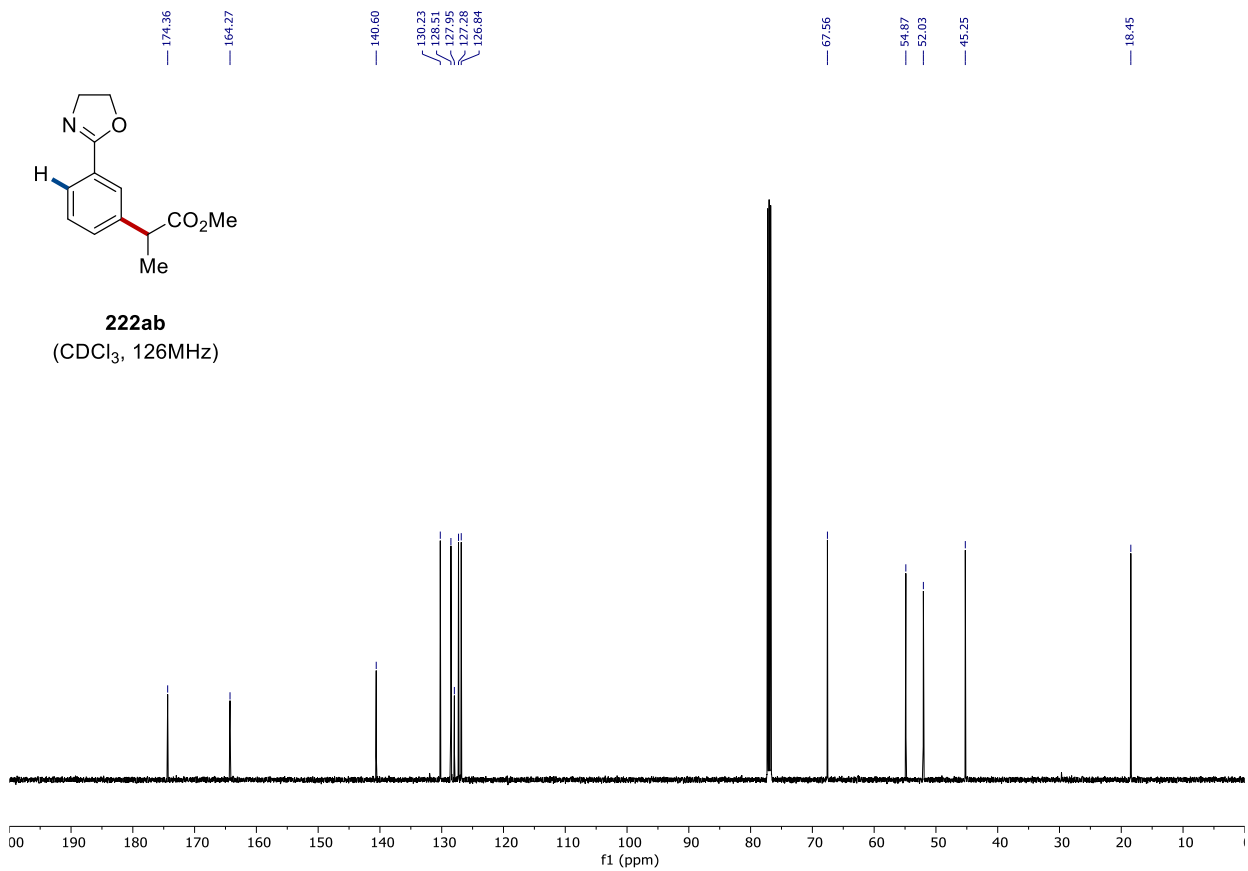




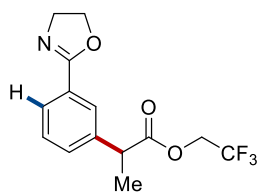
222ab
(CDCl₃, 300 MHz)



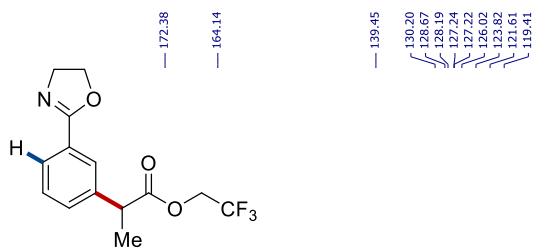
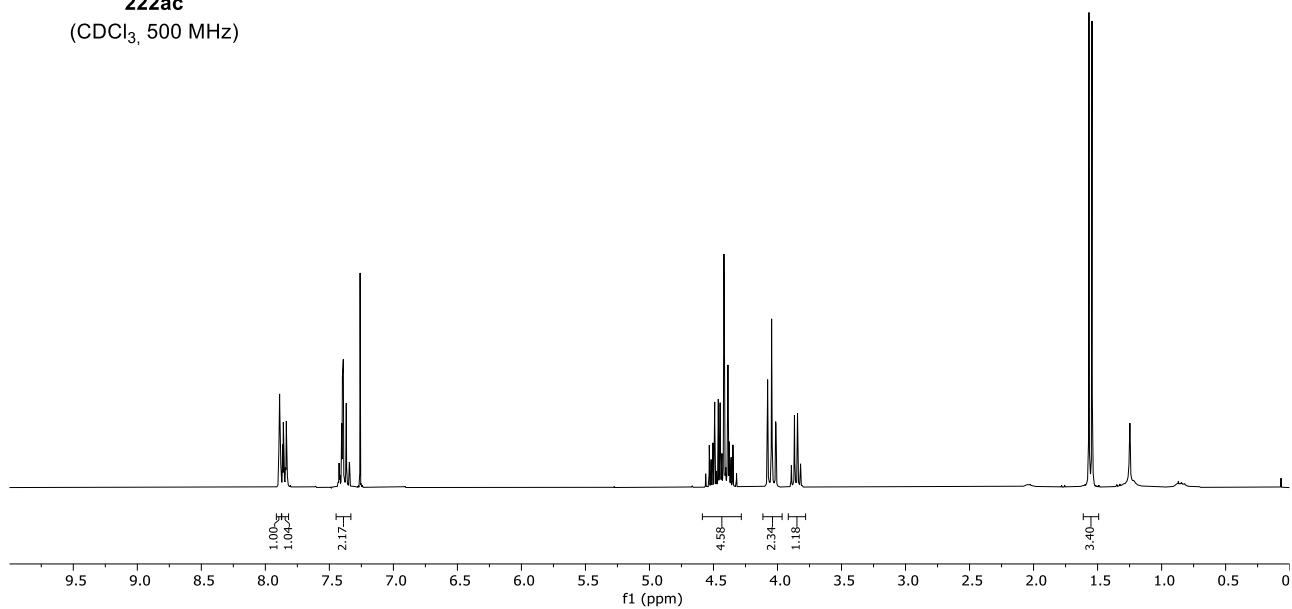
222ab
(CDCl₃, 126 MHz)



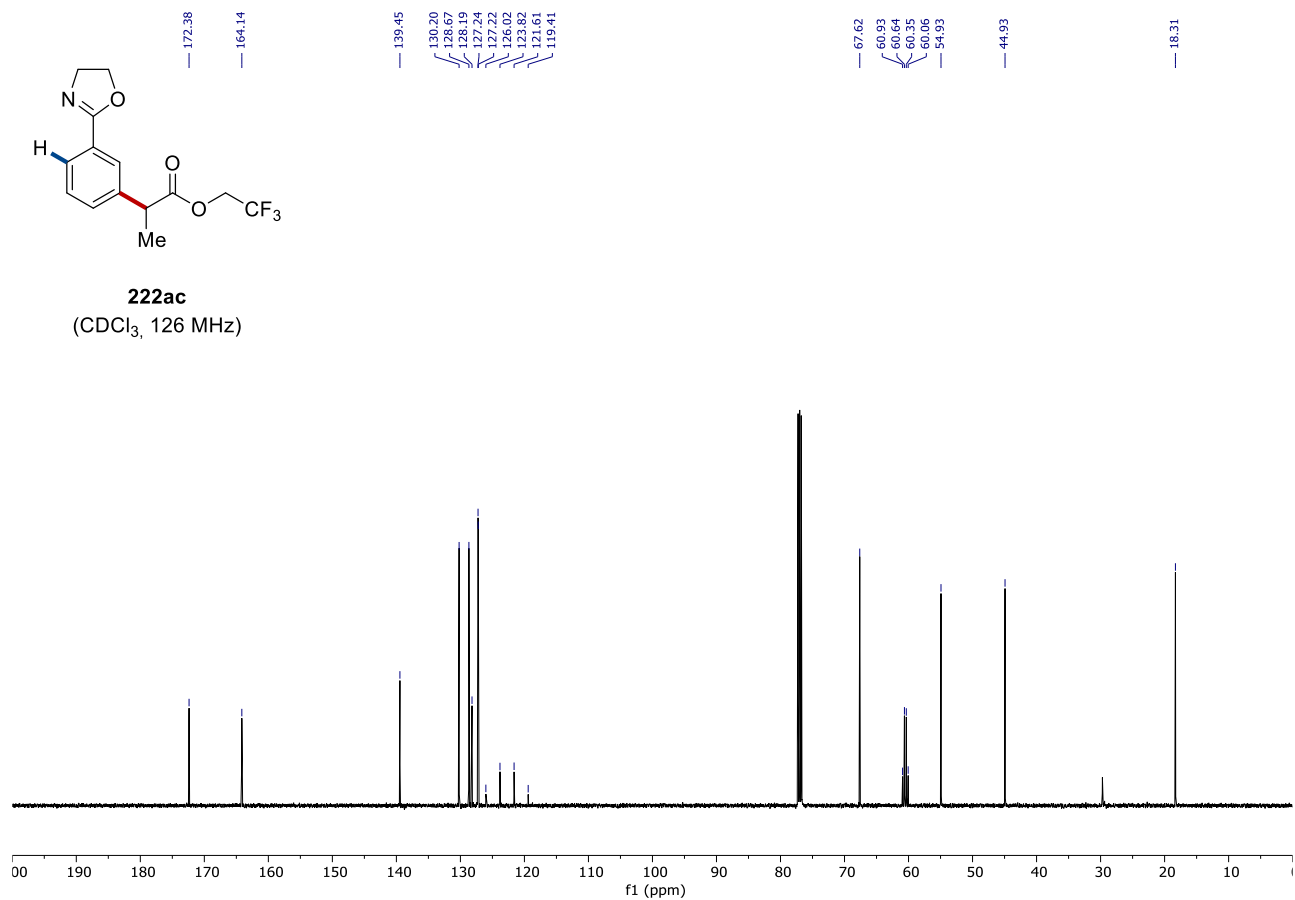
8. NMR Spectra

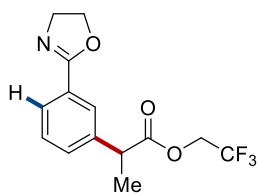


222ac
(CDCl₃, 500 MHz)



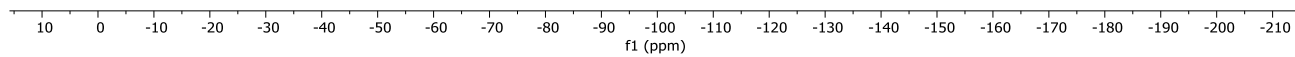
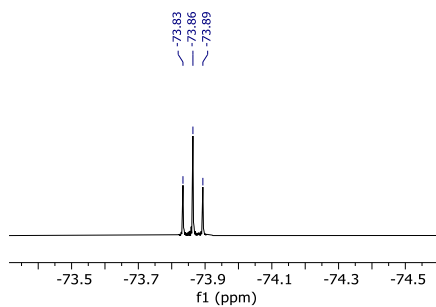
222ac
(CDCl₃, 126 MHz)



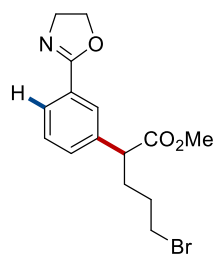


222ac
(CDCl₃, 282 MHz)

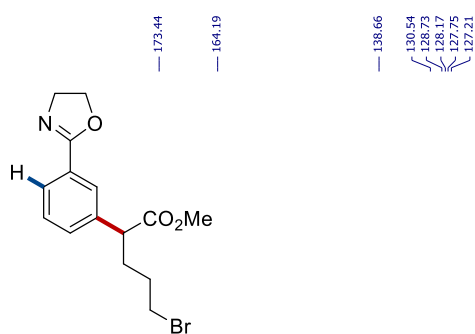
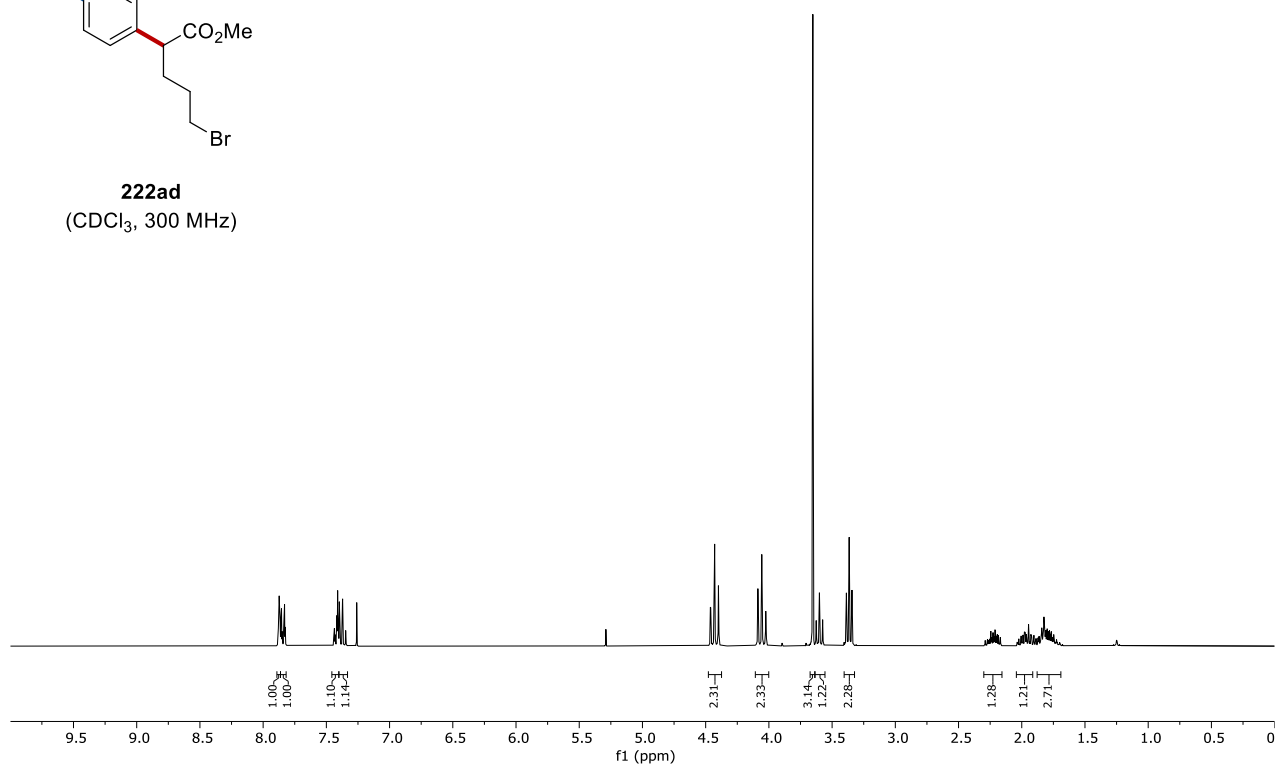
-73.83
-73.86
-73.89



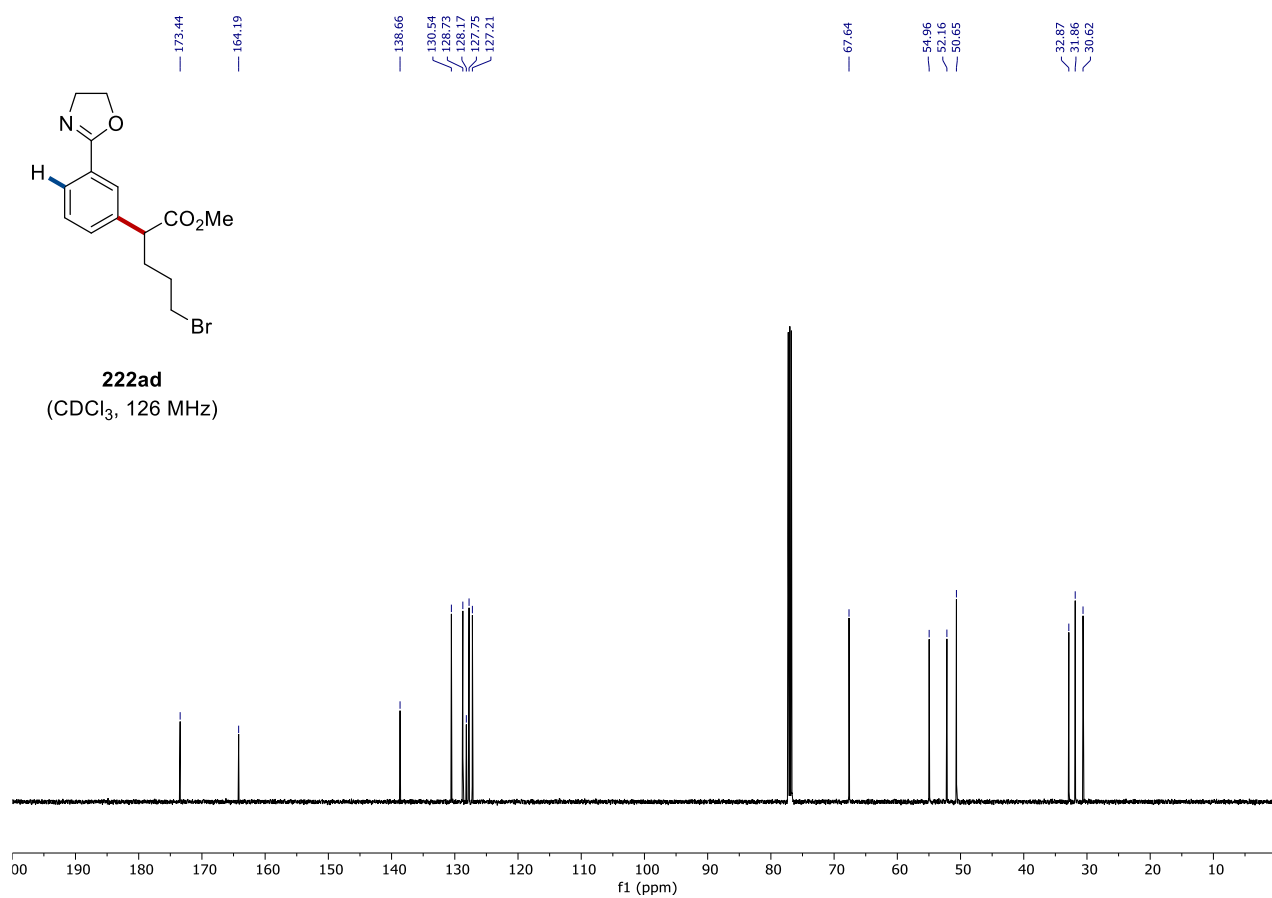
8. NMR Spectra



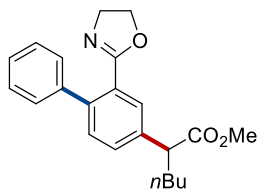
222ad
(CDCl₃, 300 MHz)



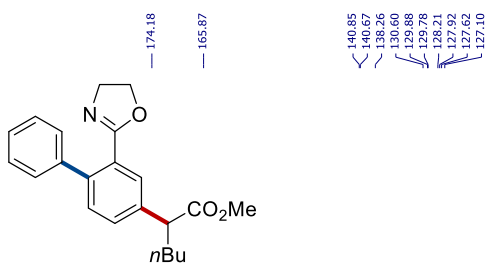
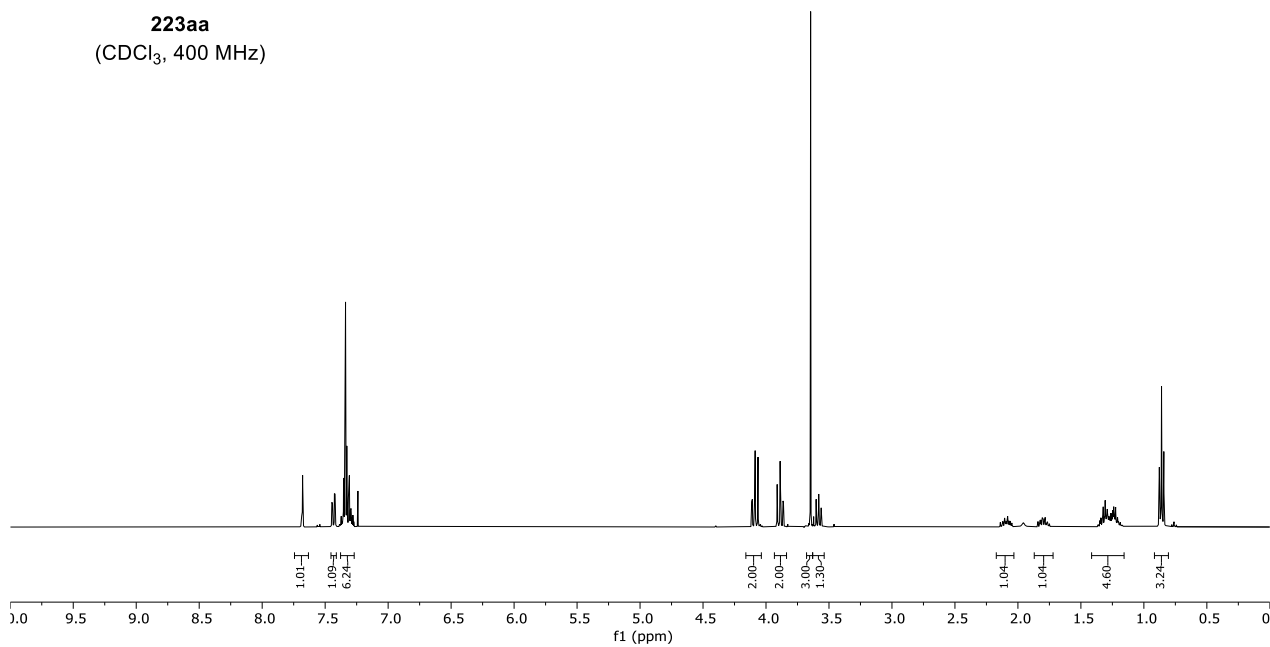
222ad
(CDCl₃, 126 MHz)



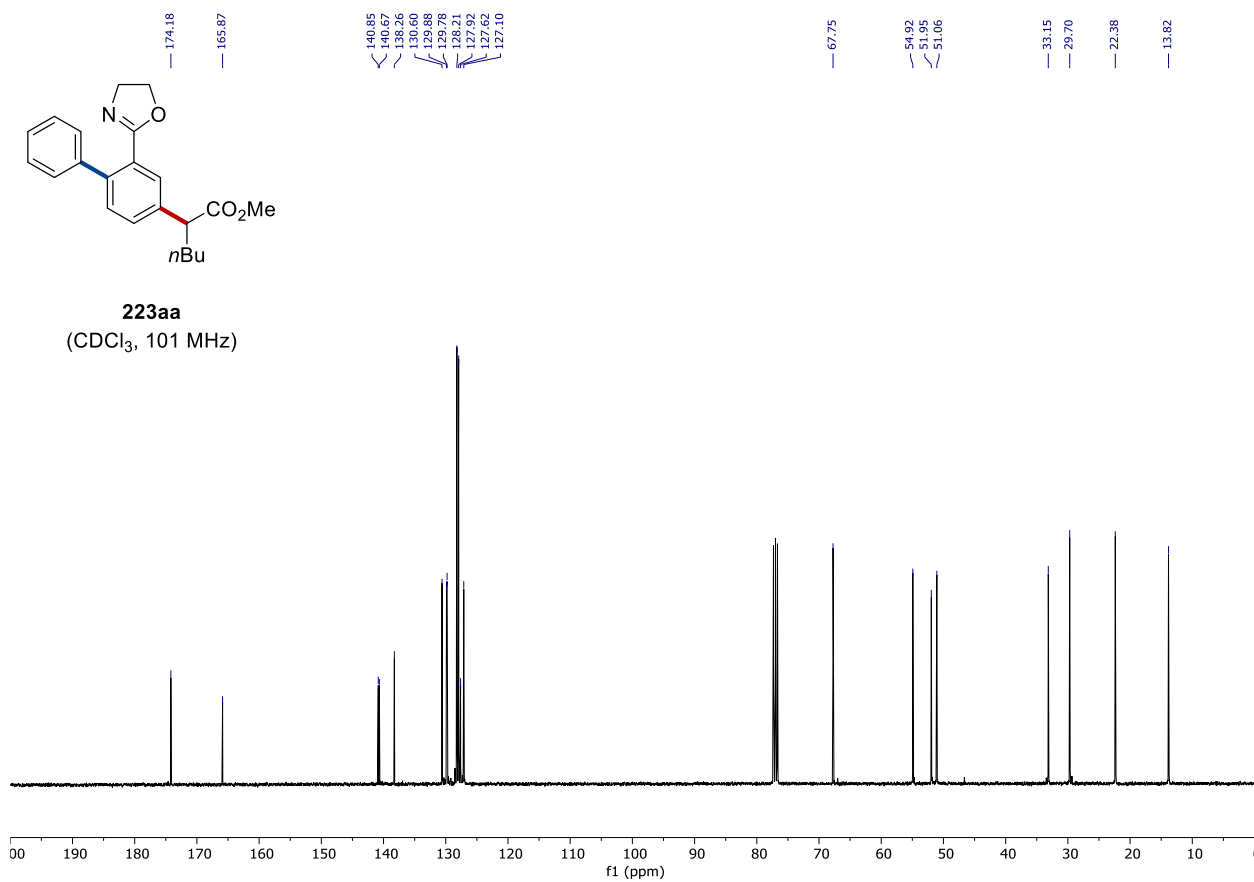
8. NMR Spectra



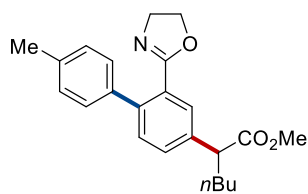
223aa
(CDCl₃, 400 MHz)



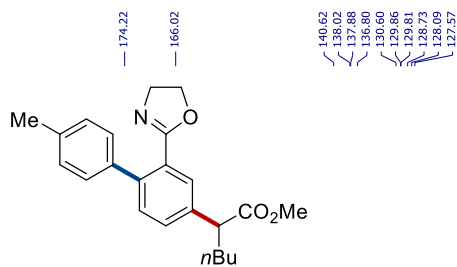
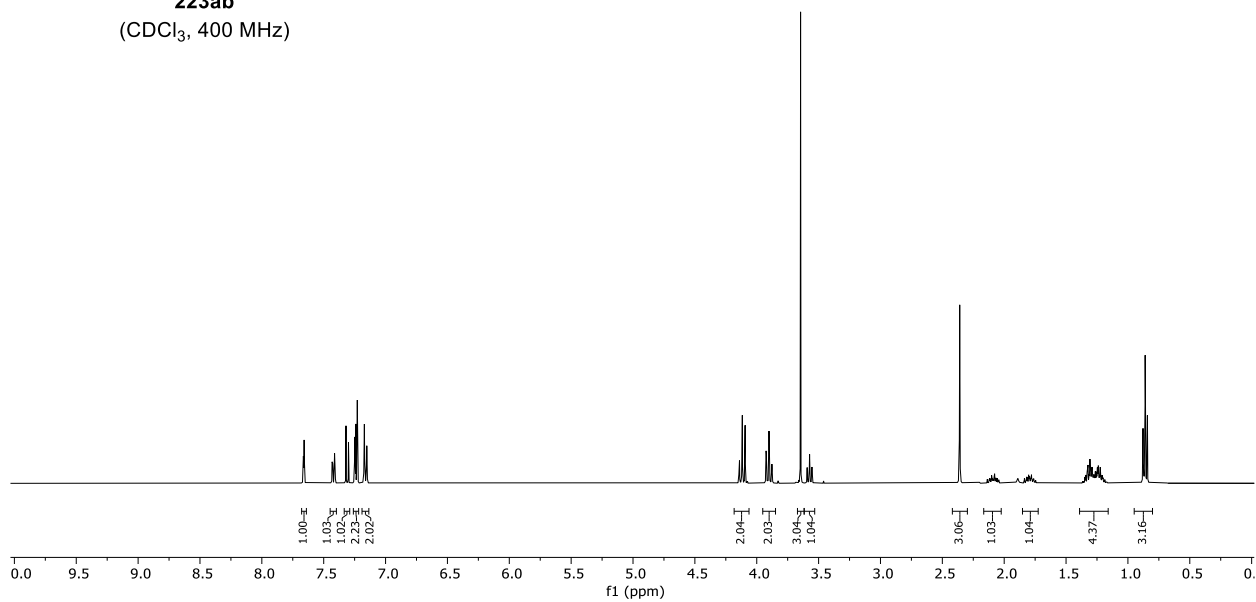
223aa
(CDCl₃, 101 MHz)



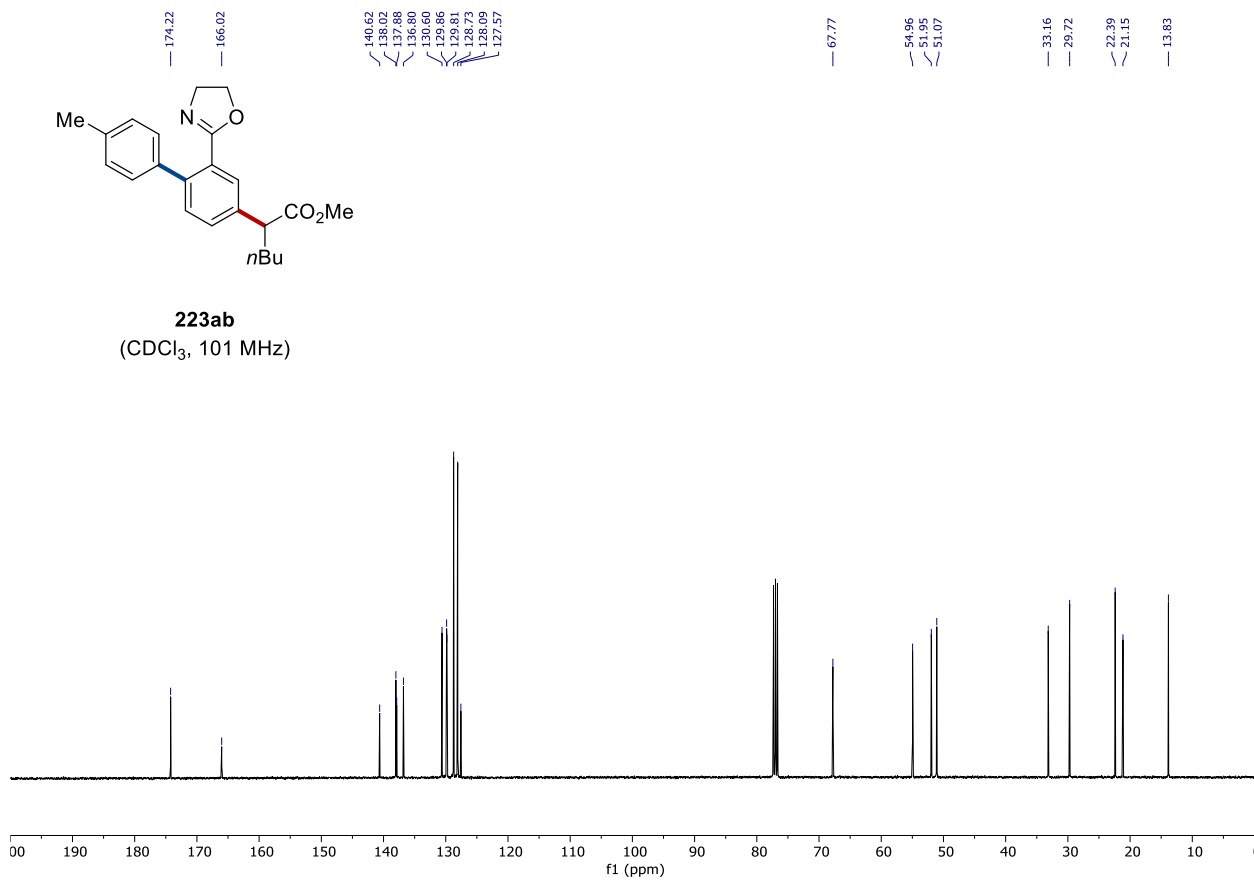
8. NMR Spectra



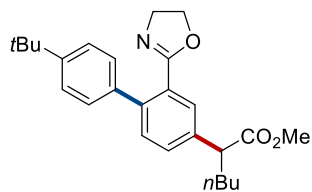
223ab
(CDCl₃, 400 MHz)



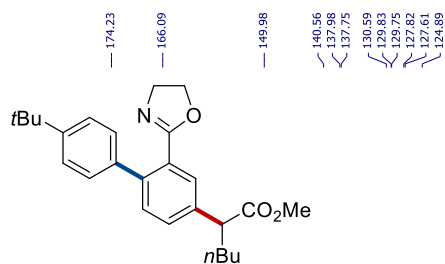
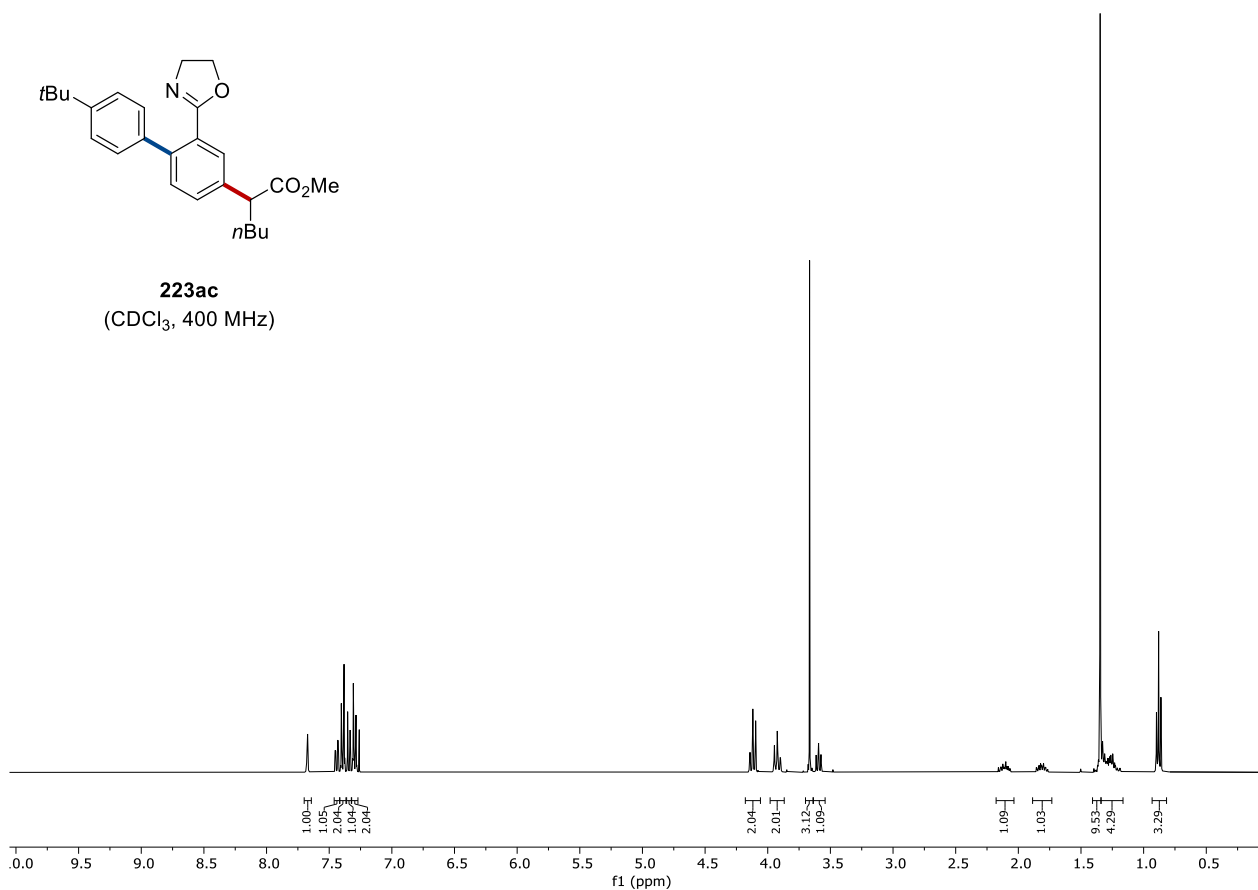
223ab
(CDCl₃, 101 MHz)



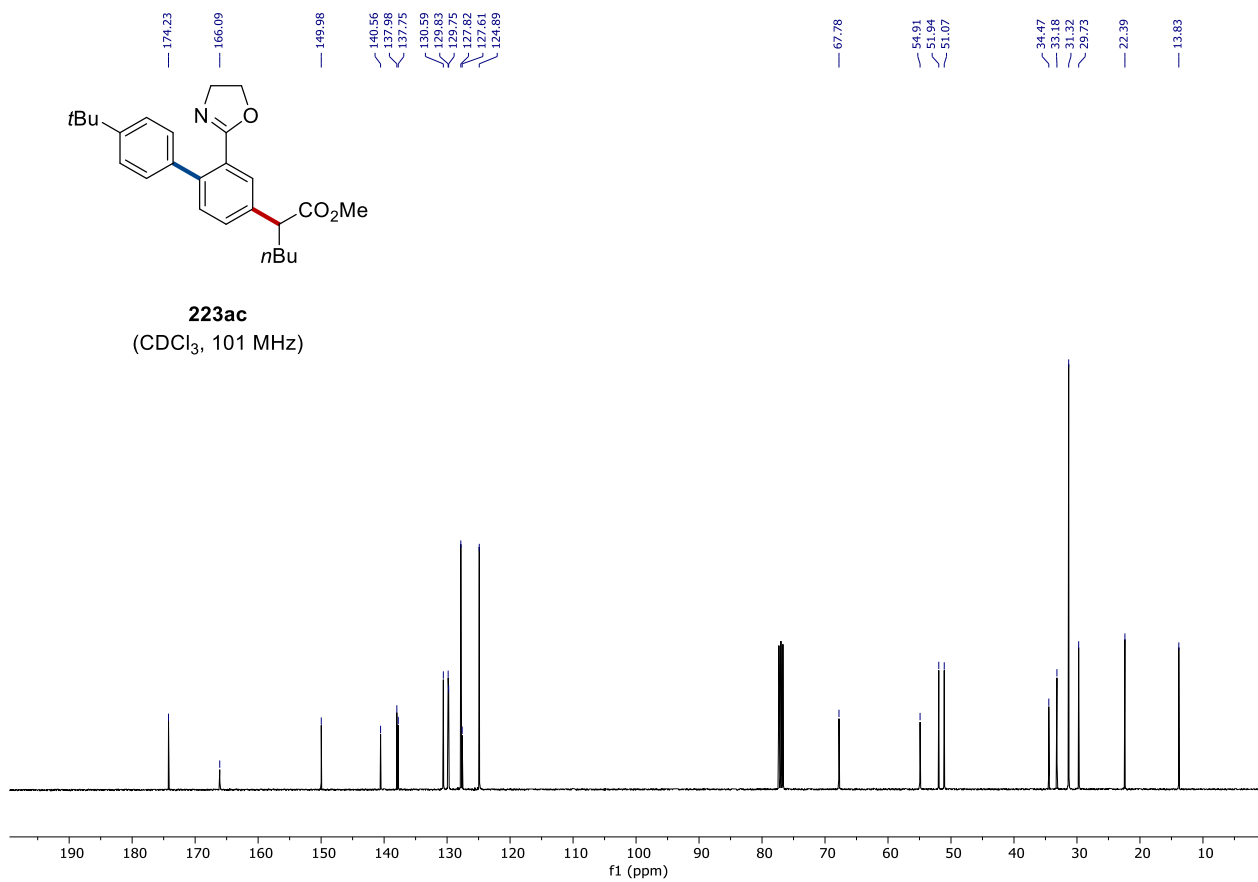
8. NMR Spectra



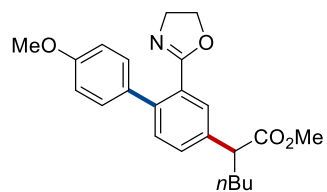
223ac
(CDCl₃, 400 MHz)



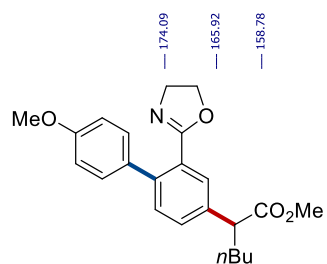
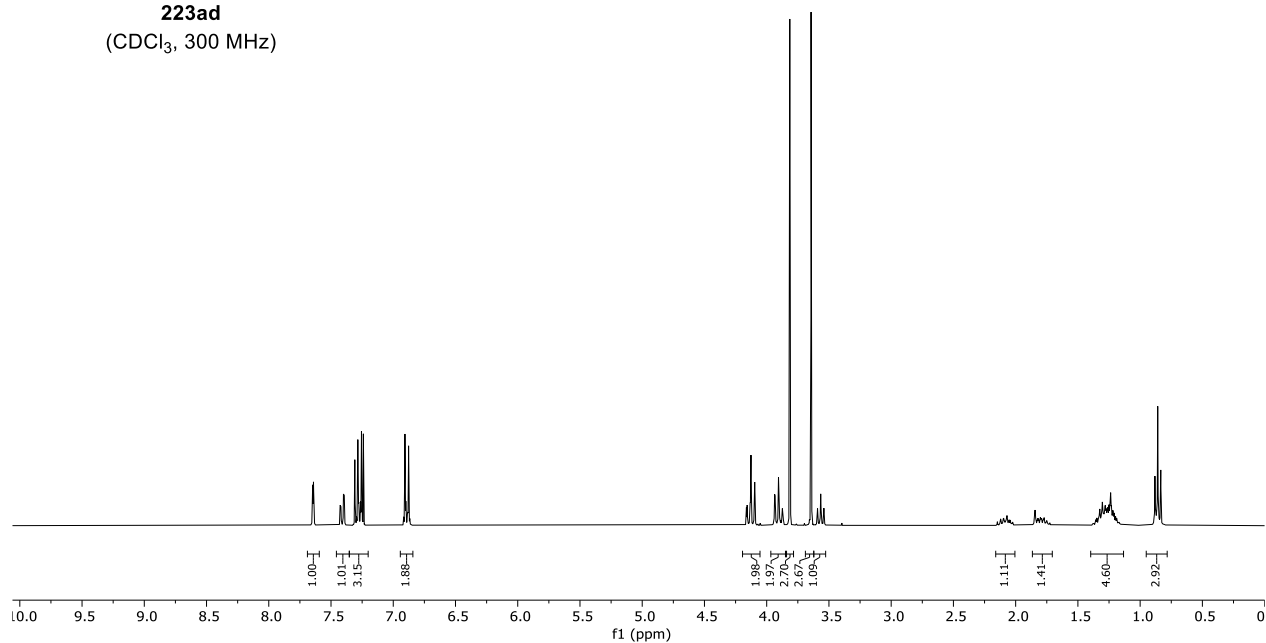
223ac
(CDCl₃, 101 MHz)



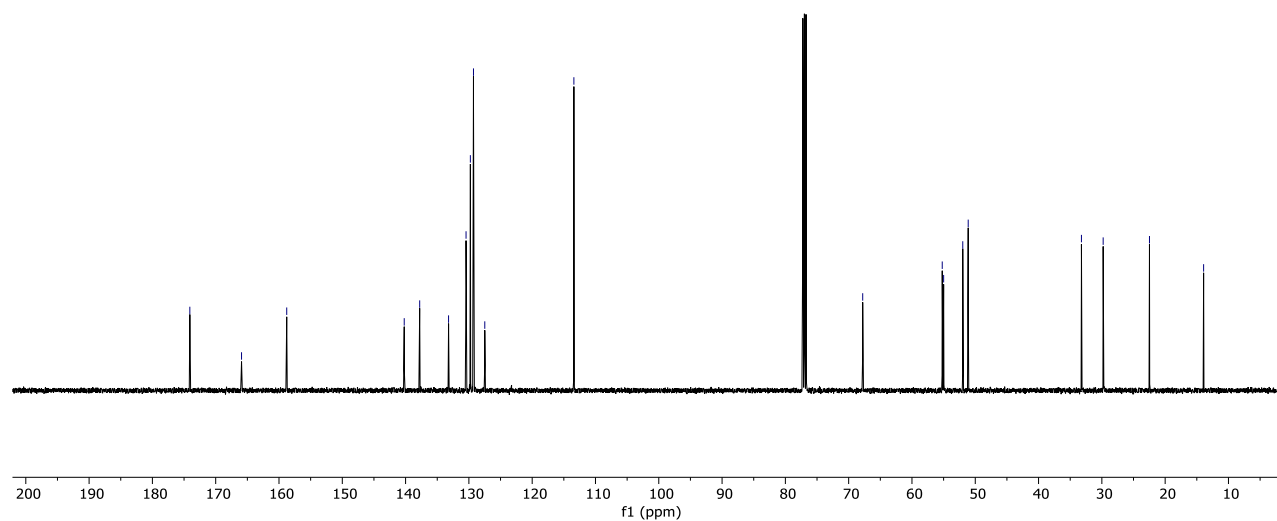
8. NMR Spectra

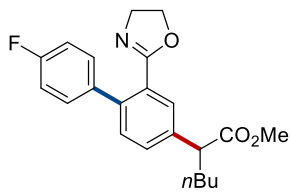


223ad
(CDCl₃, 300 MHz)

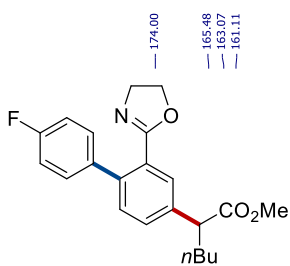
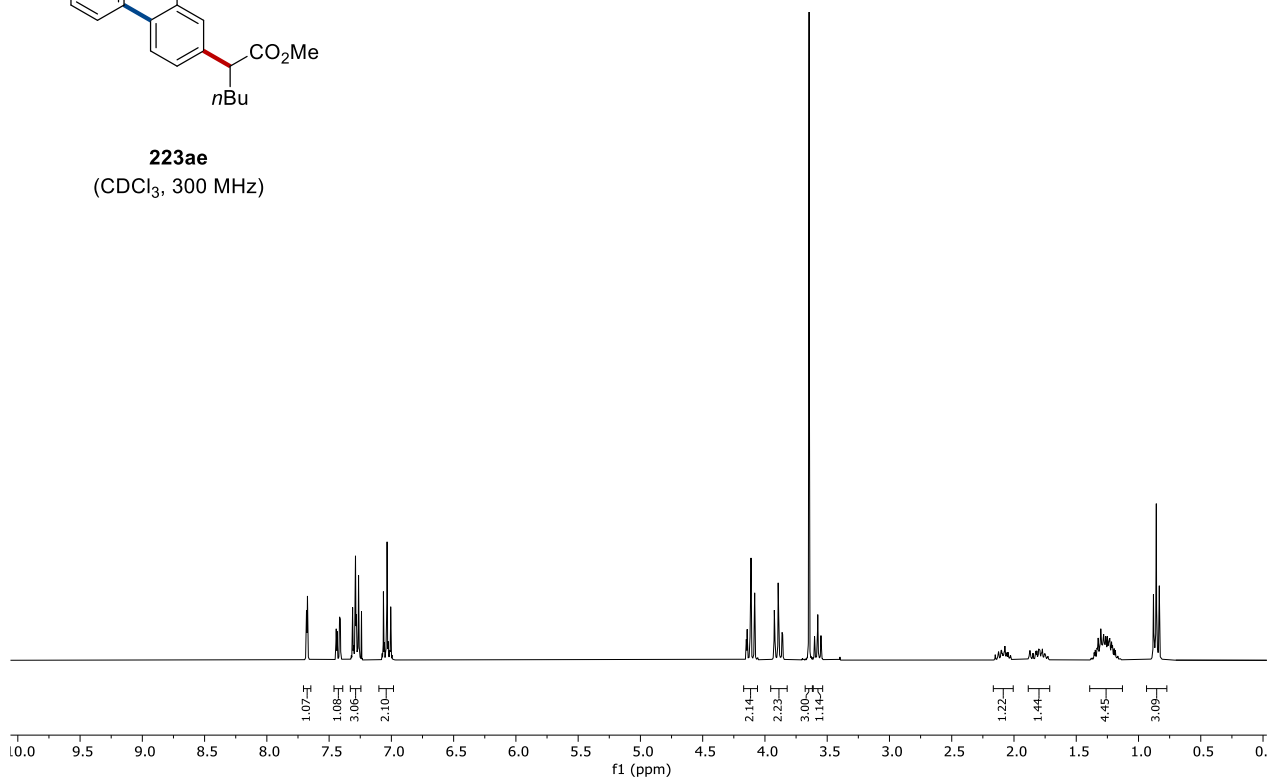


223ad
(CDCl₃, 126 MHz)

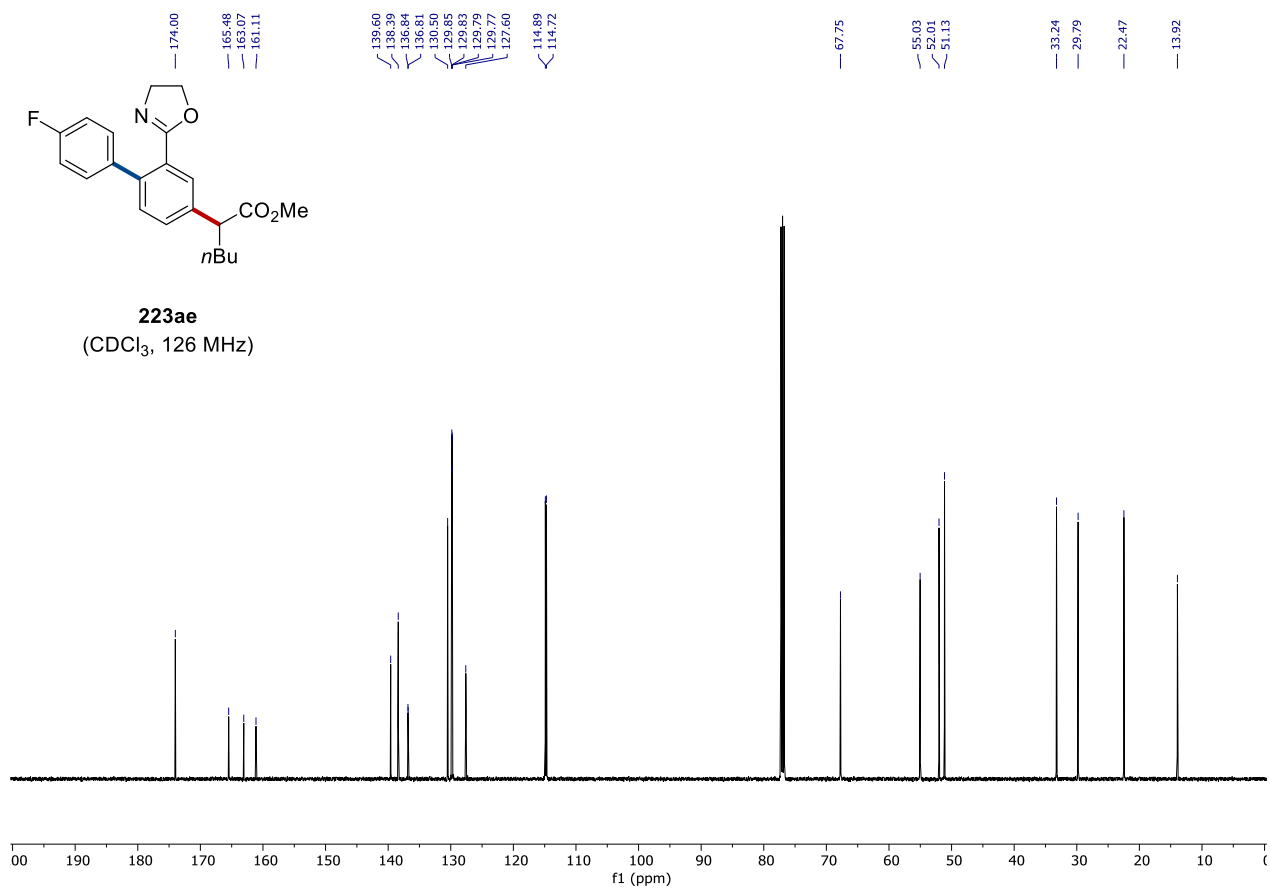




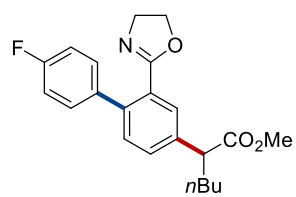
223ae
(CDCl₃, 300 MHz)



223ae
(CDCl₃, 126 MHz)

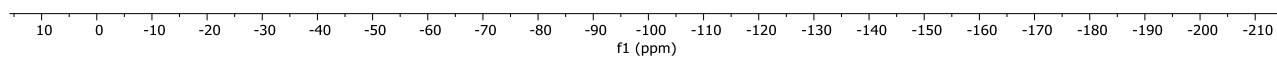
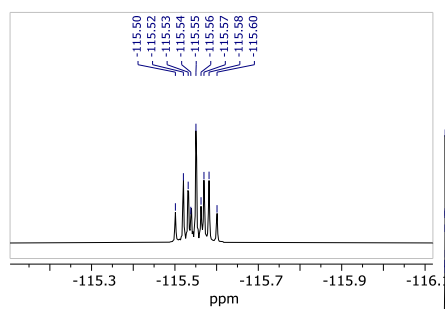


8. NMR Spectra

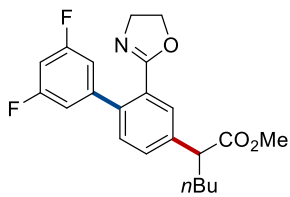


223ae
(CDCl₃, 282 MHz)

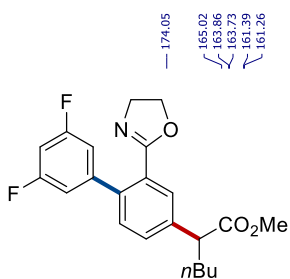
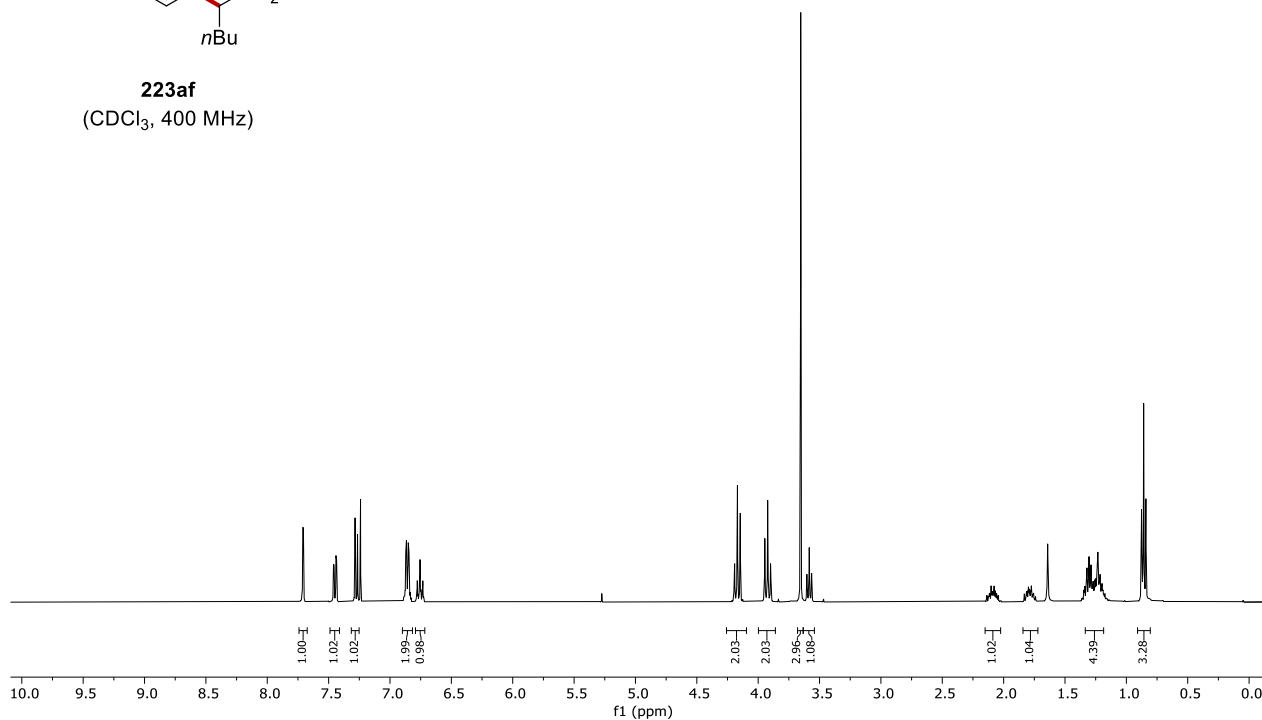
-115.50
-115.52
-115.53
-115.54
-115.55
-115.56
-115.57
-115.58
-115.60



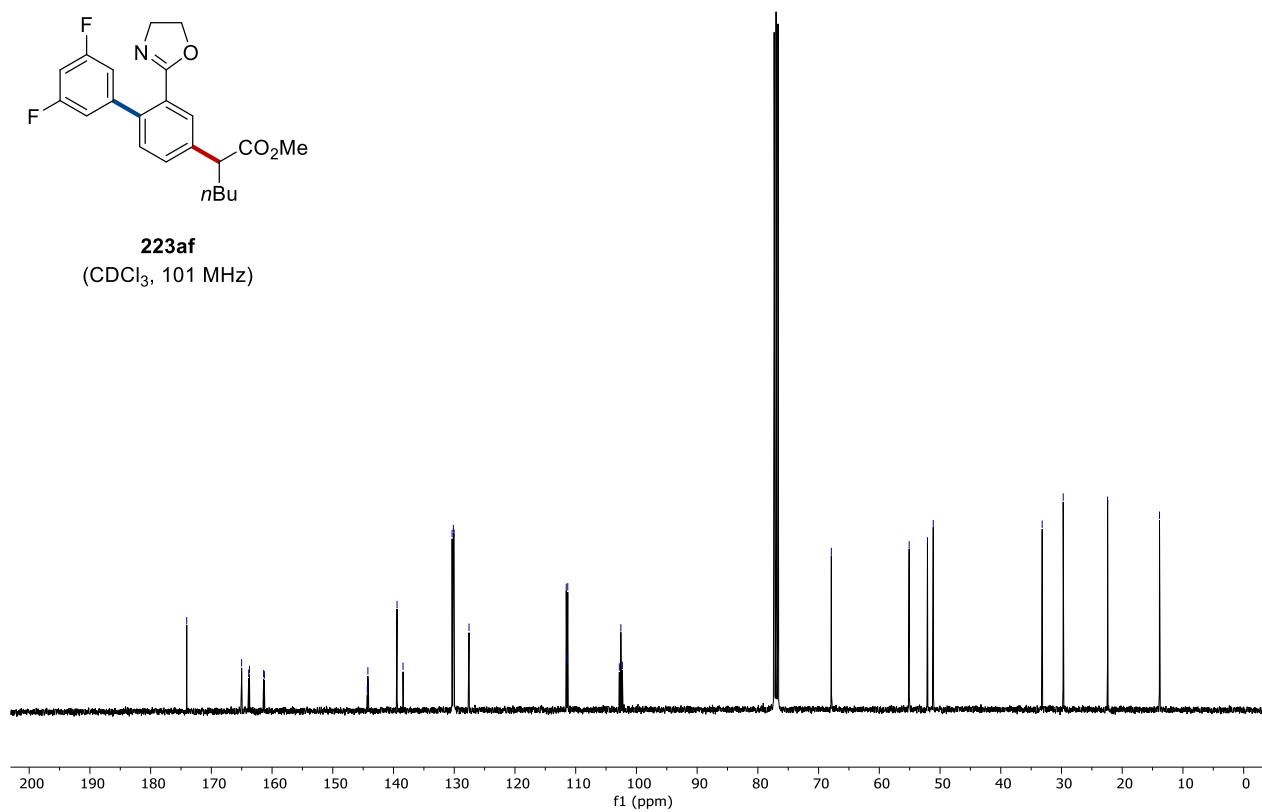
8. NMR Spectra



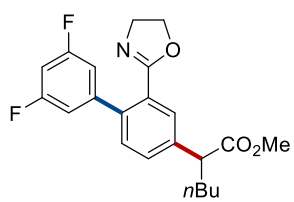
223af
(CDCl₃, 400 MHz)



223af
(CDCl₃, 101 MHz)

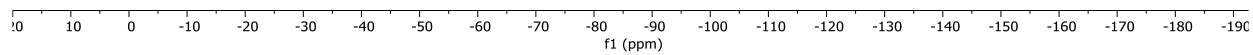
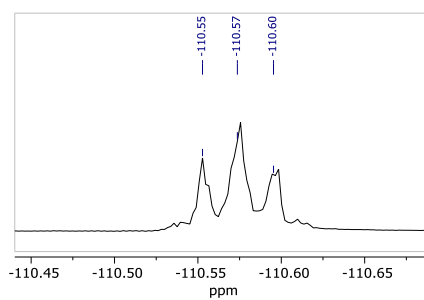


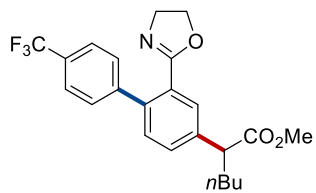
8. NMR Spectra



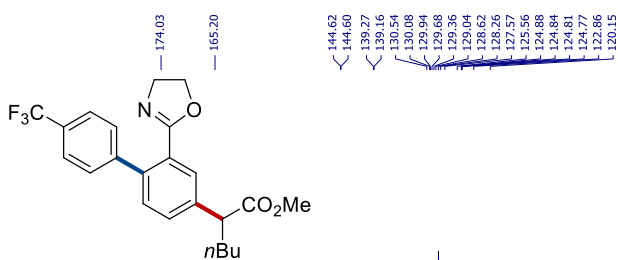
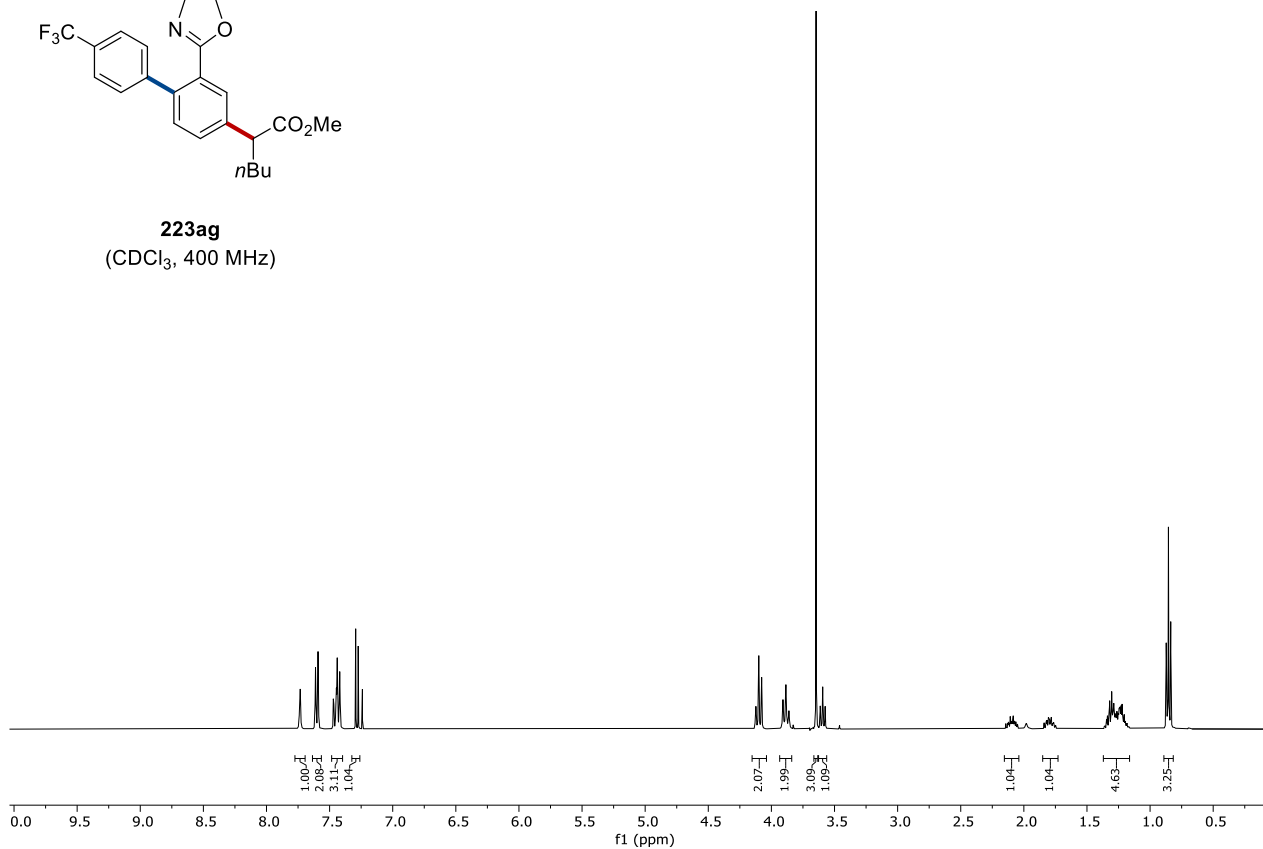
223af
(CDCl₃, 376 MHz)

-110.55
-110.57
-110.60

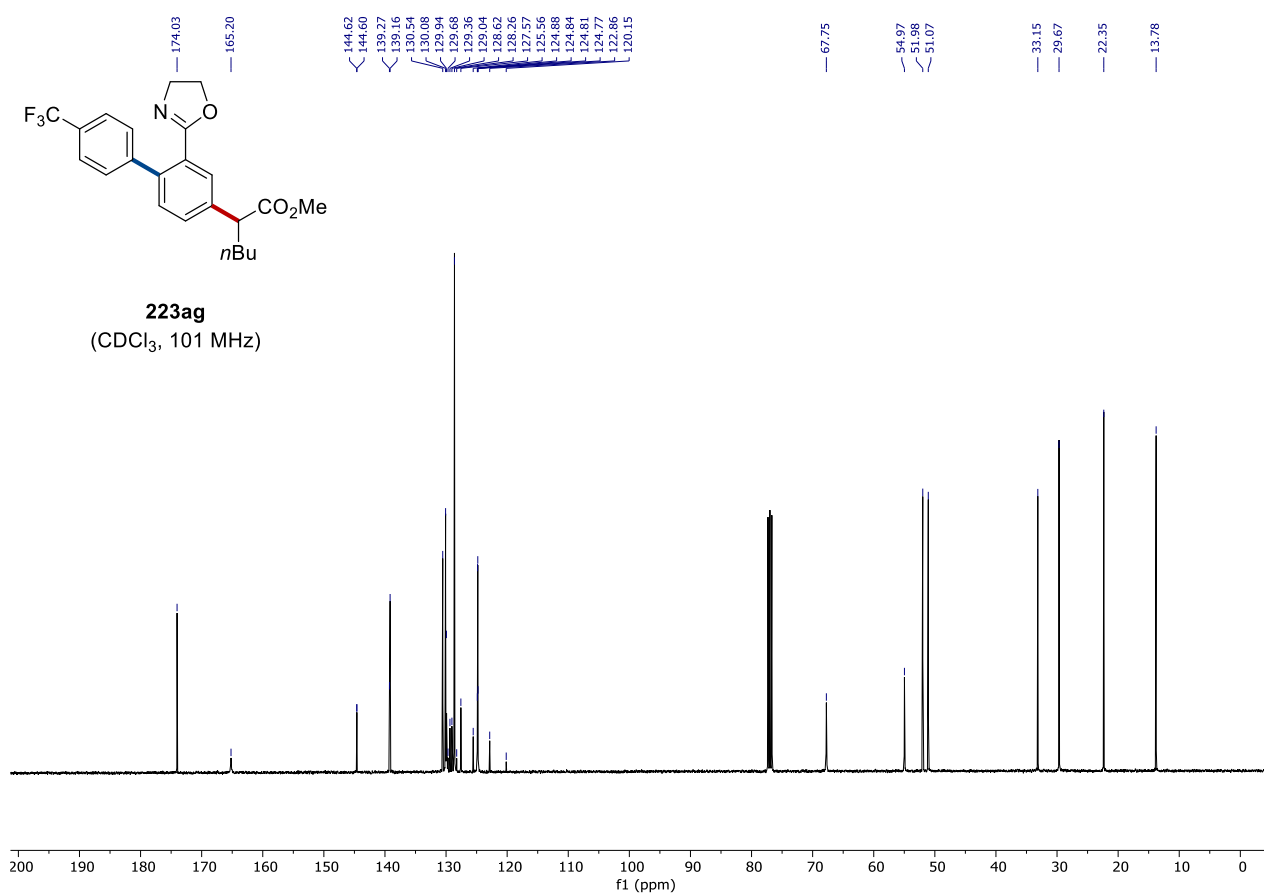




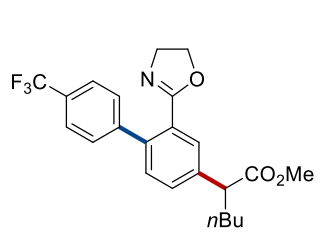
223ag
(CDCl₃, 400 MHz)



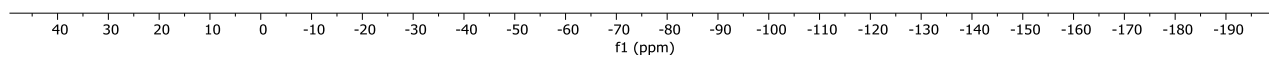
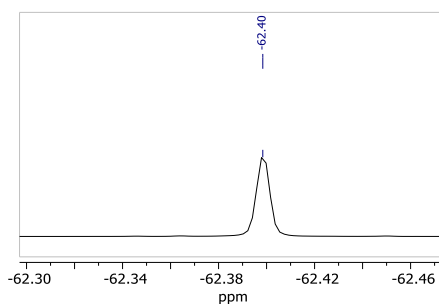
223ag
(CDCl₃, 101 MHz)

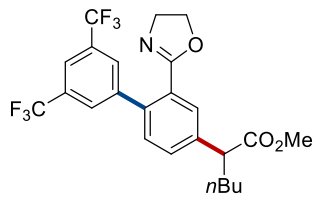


8. NMR Spectra

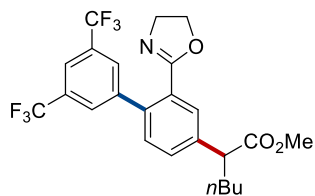
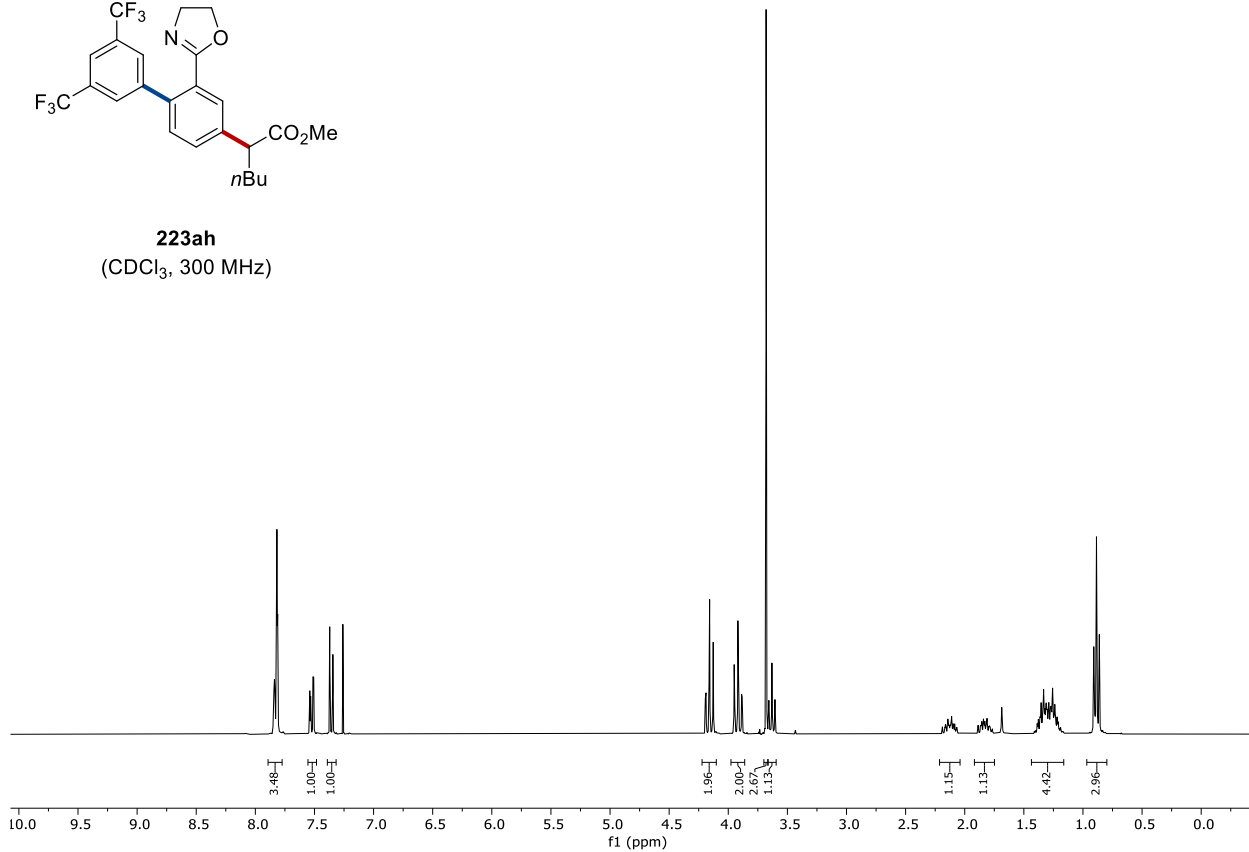


223ag
(CDCl₃, 376 MHz)

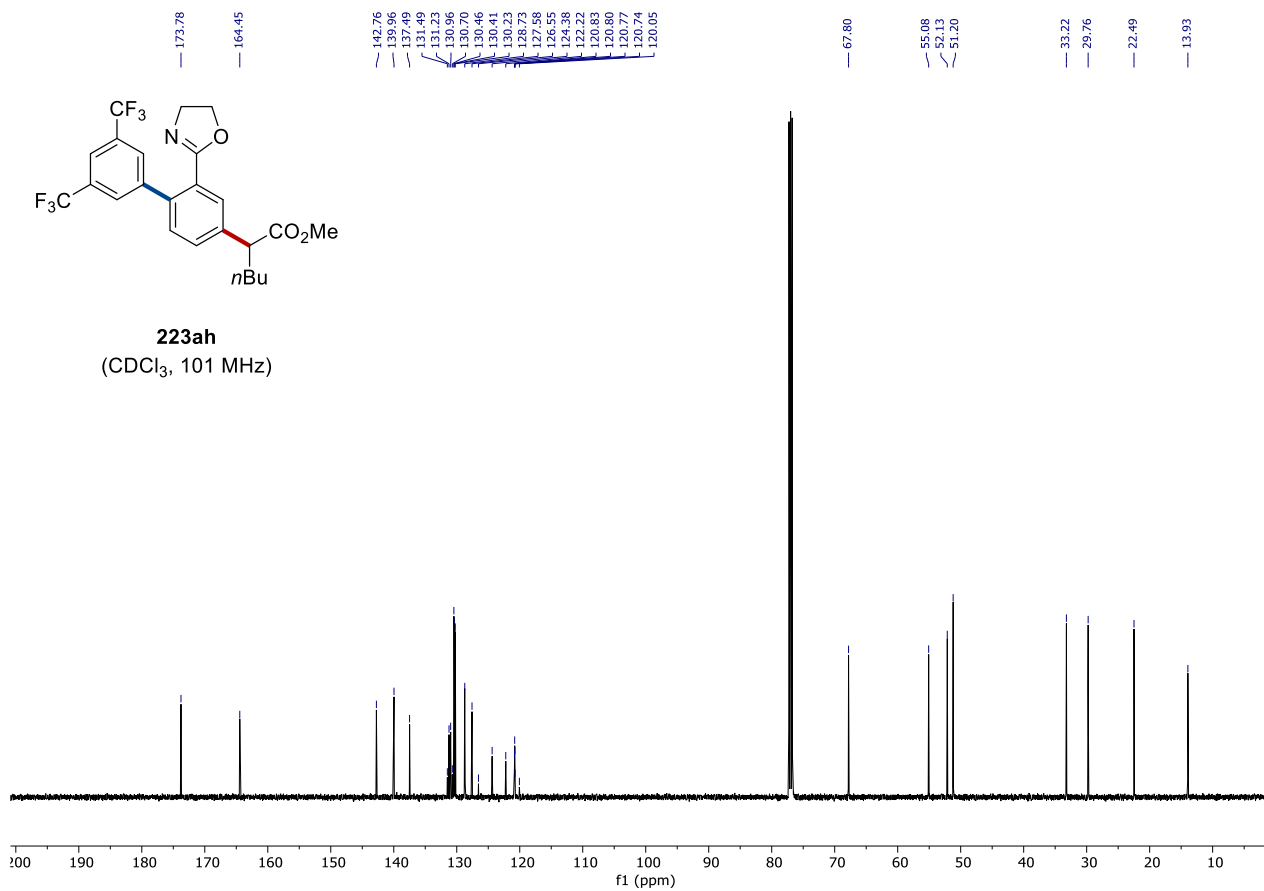




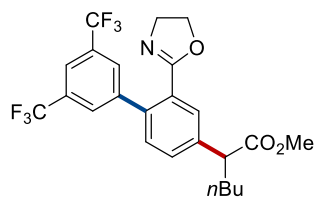
223ah
(CDCl₃, 300 MHz)



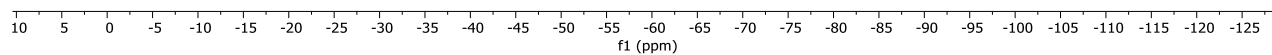
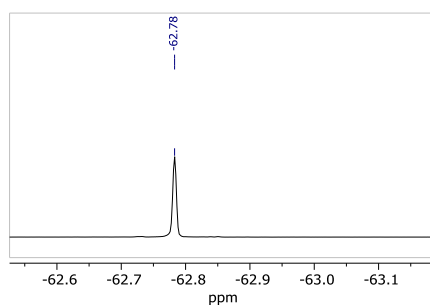
223ah
(CDCl₃, 101 MHz)

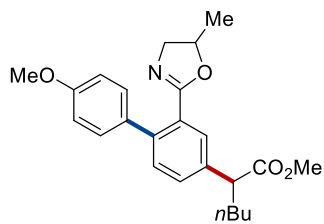


8. NMR Spectra

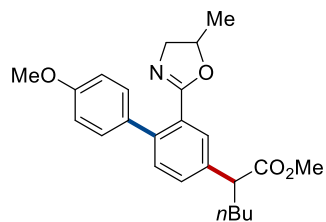
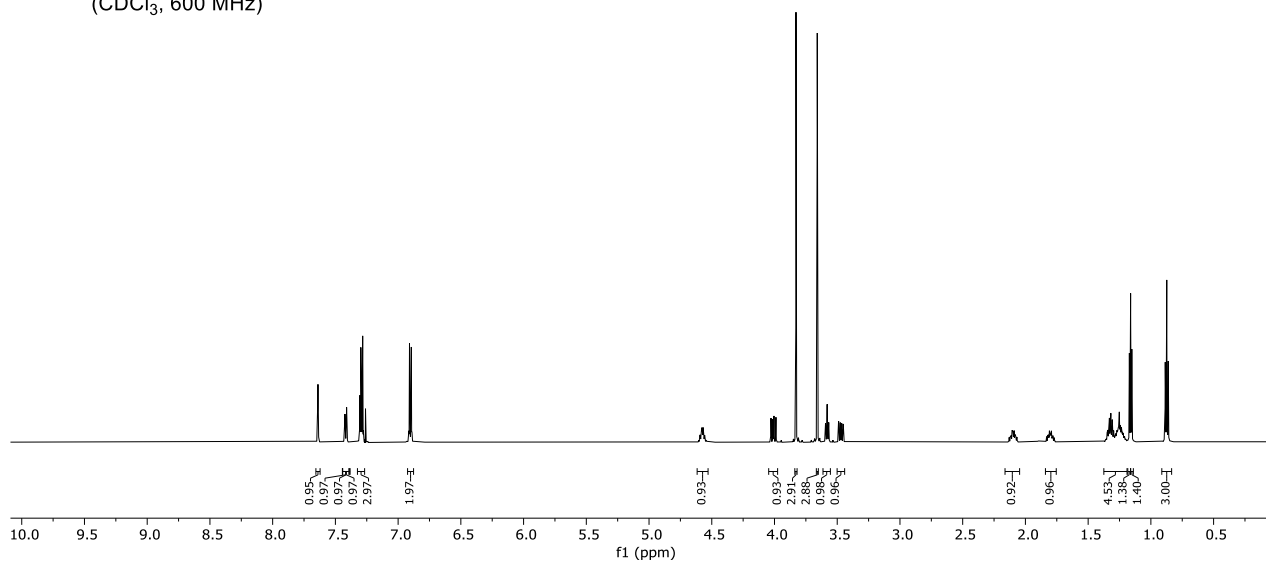


223ah
(CDCl₃, 282 MHz)

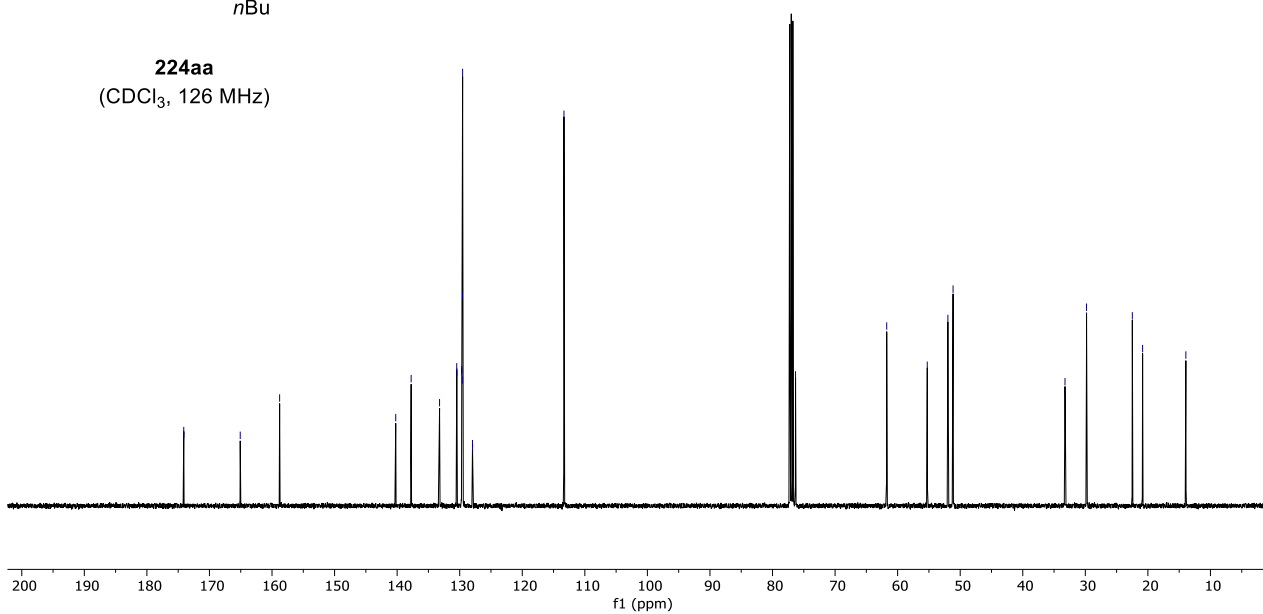




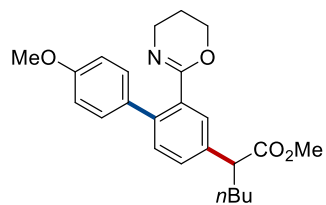
224aa
(CDCl₃, 600 MHz)



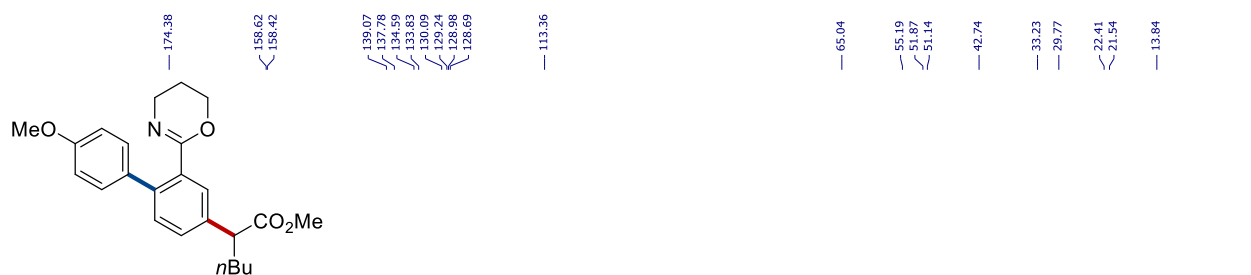
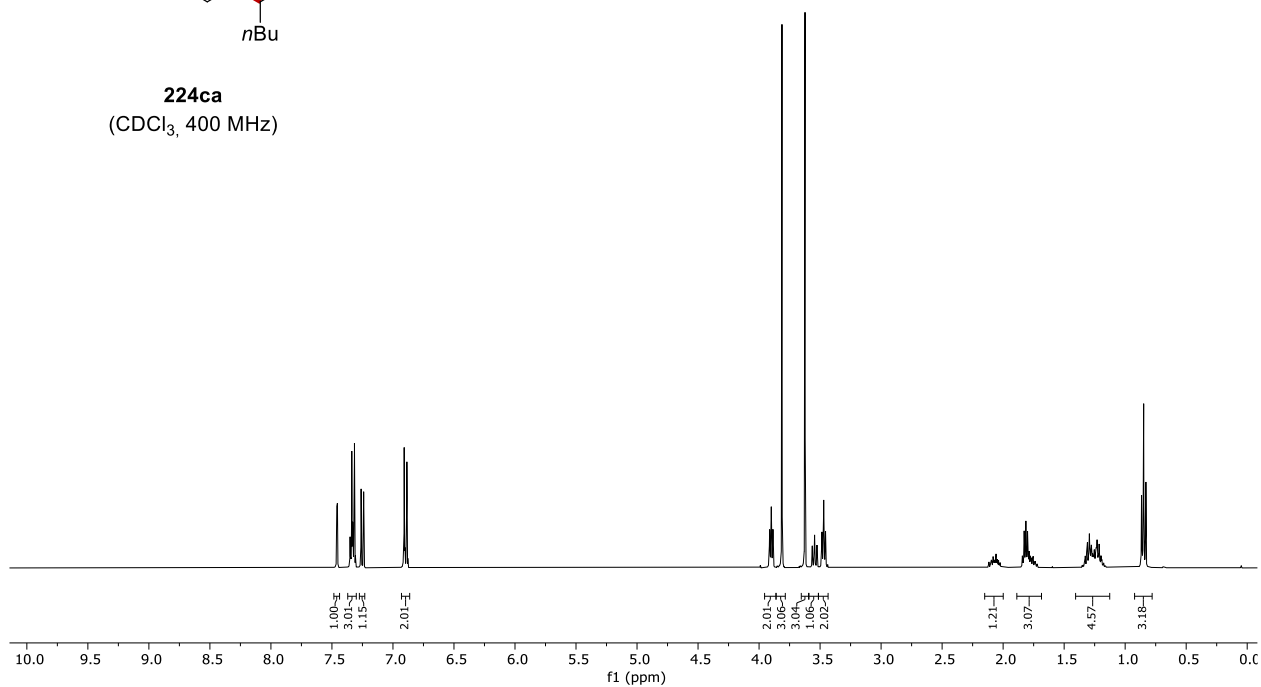
224aa
(CDCl₃, 126 MHz)



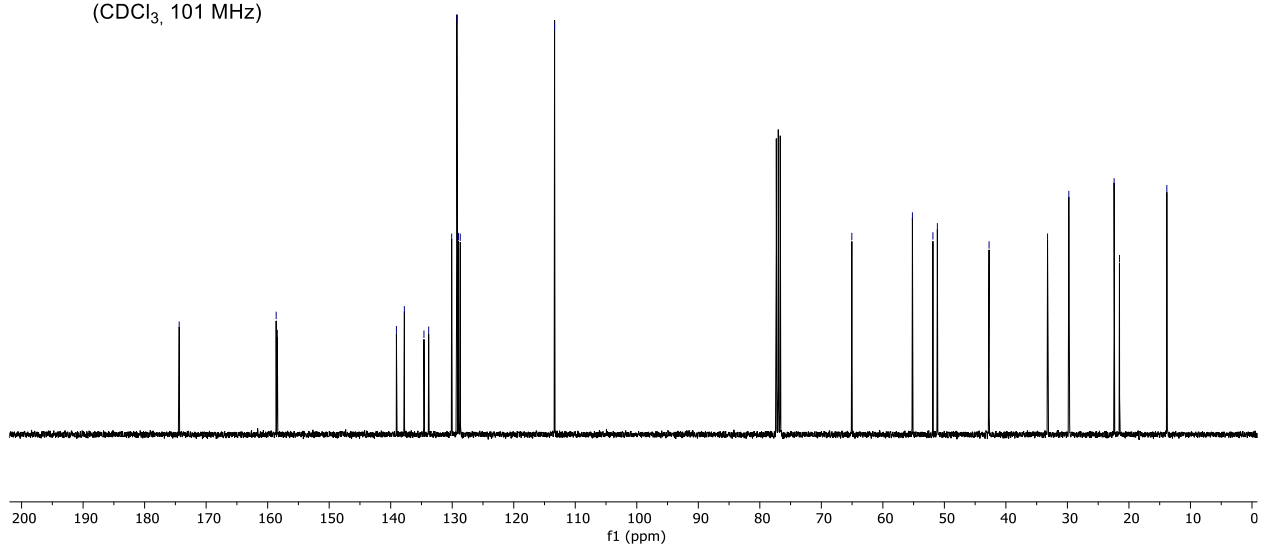
8. NMR Spectra

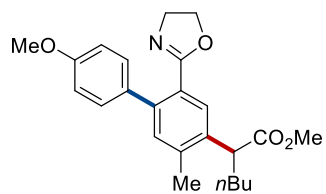


224ca
(CDCl₃, 400 MHz)

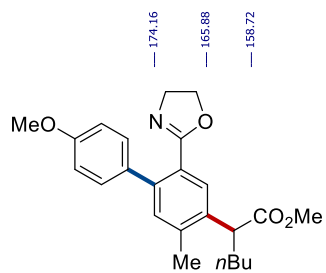
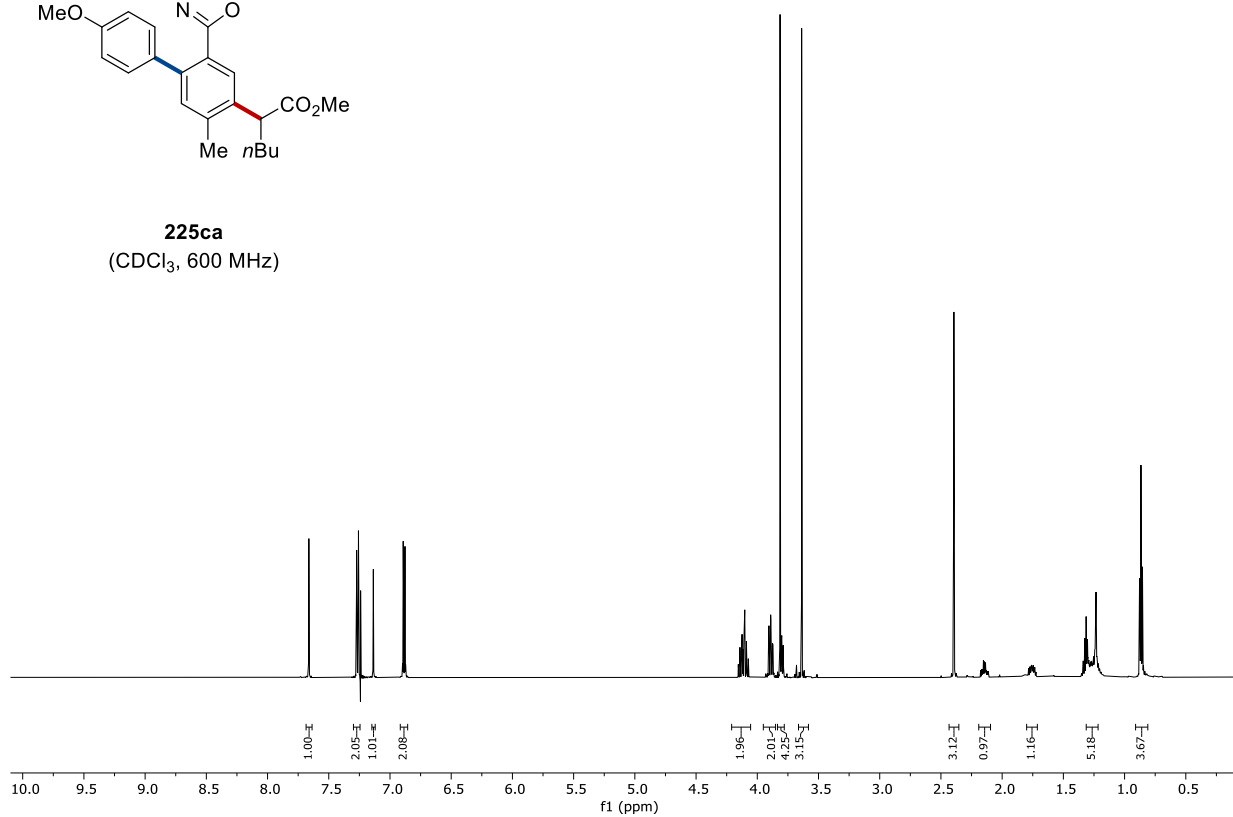


224ca
(CDCl₃, 101 MHz)

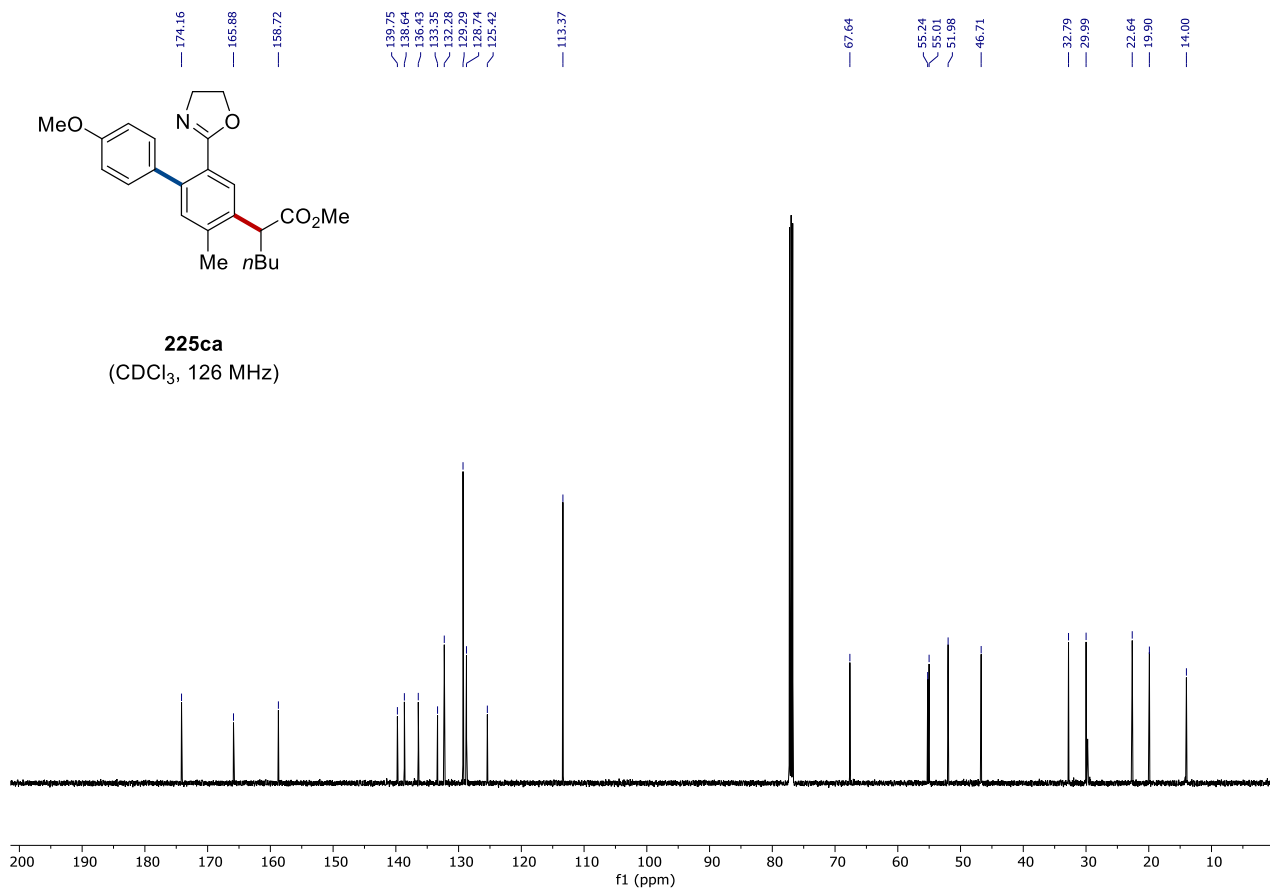




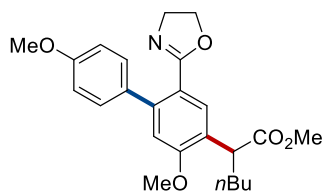
225ca
(CDCl₃, 600 MHz)



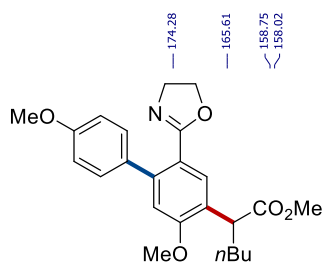
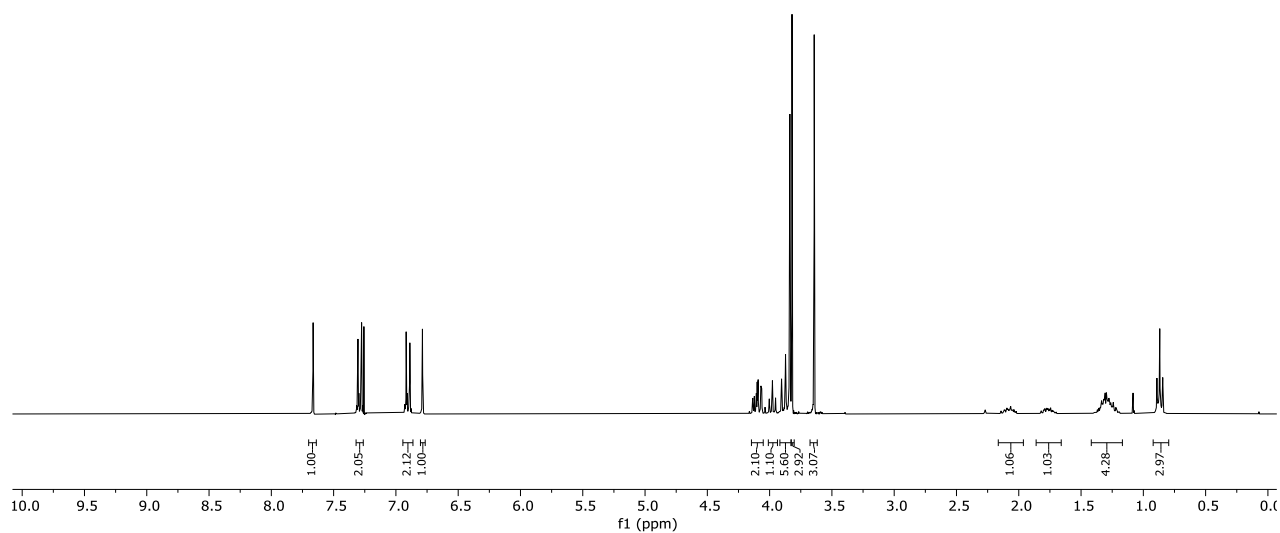
225ca
(CDCl₃, 126 MHz)



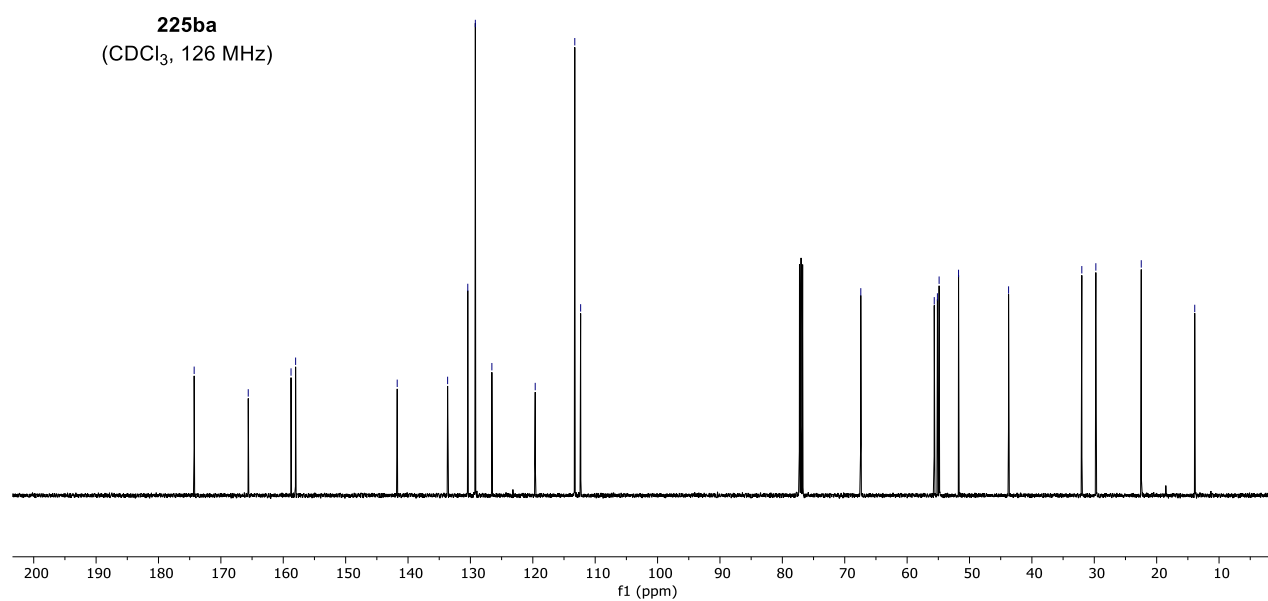
8. NMR Spectra

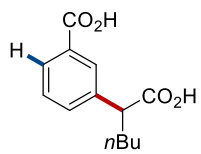


225ba
(CDCl₃, 300 MHz)

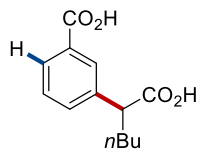
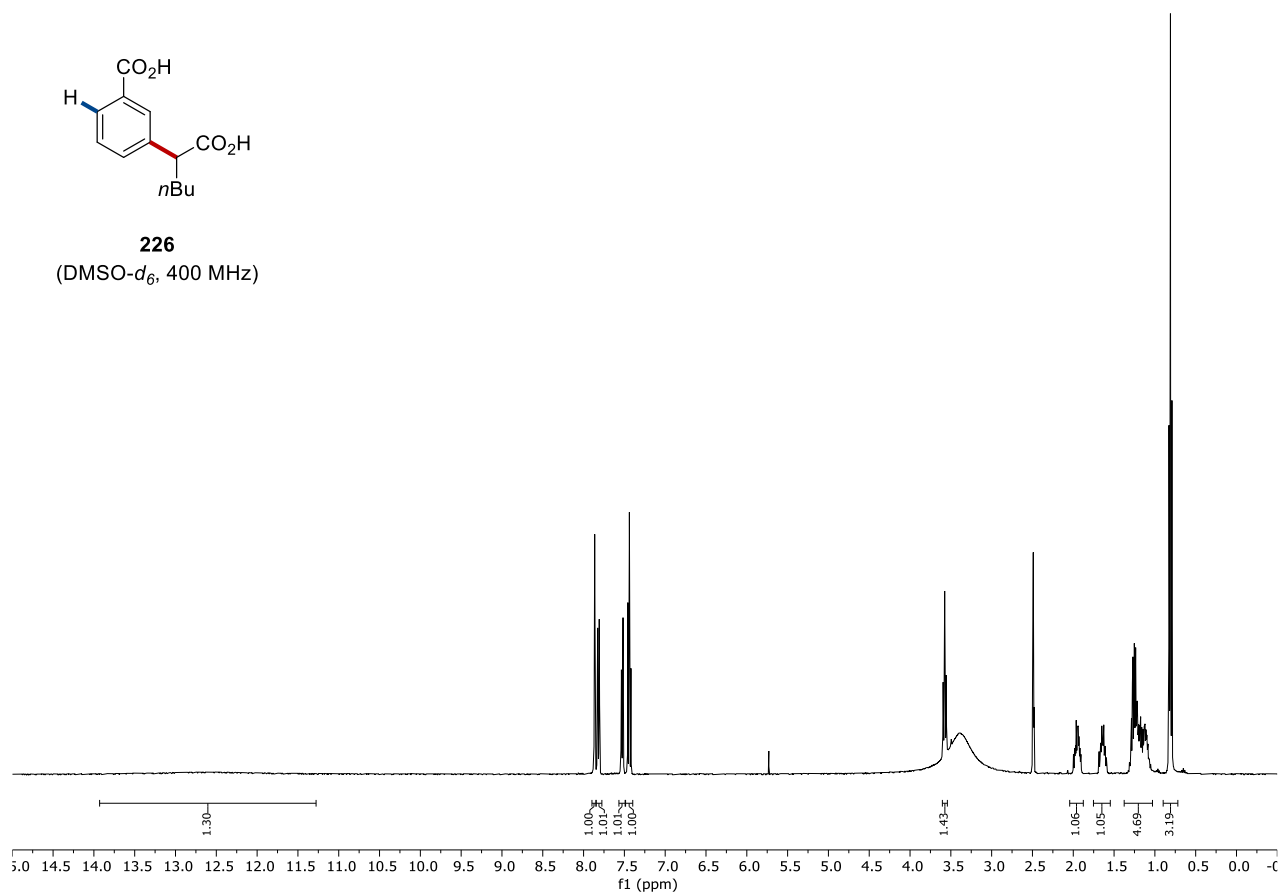


225ba
(CDCl₃, 126 MHz)

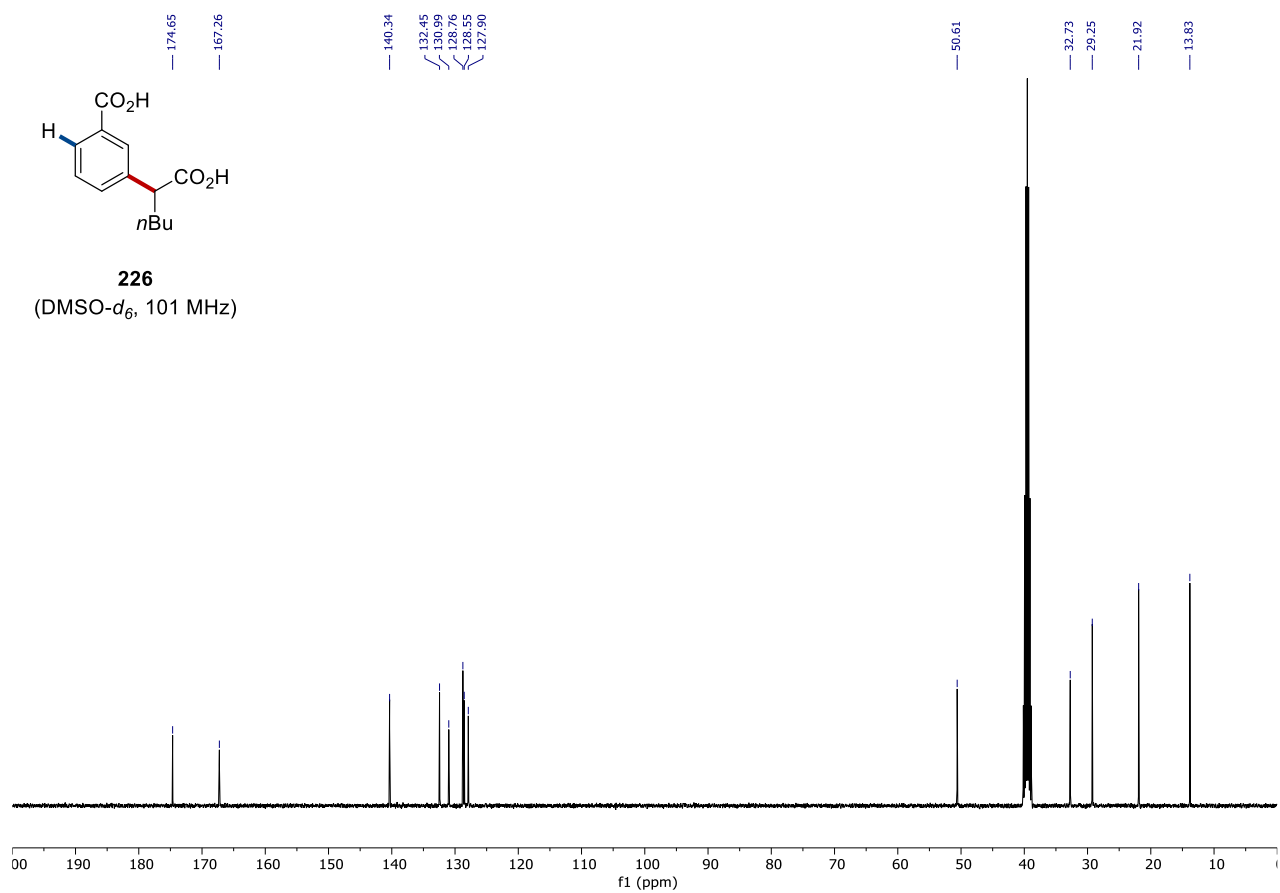




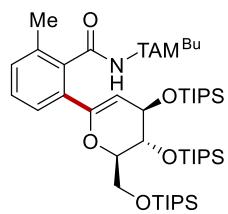
226
(DMSO- d_6 , 400 MHz)



226
(DMSO- d_6 , 101 MHz)

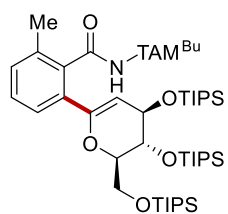
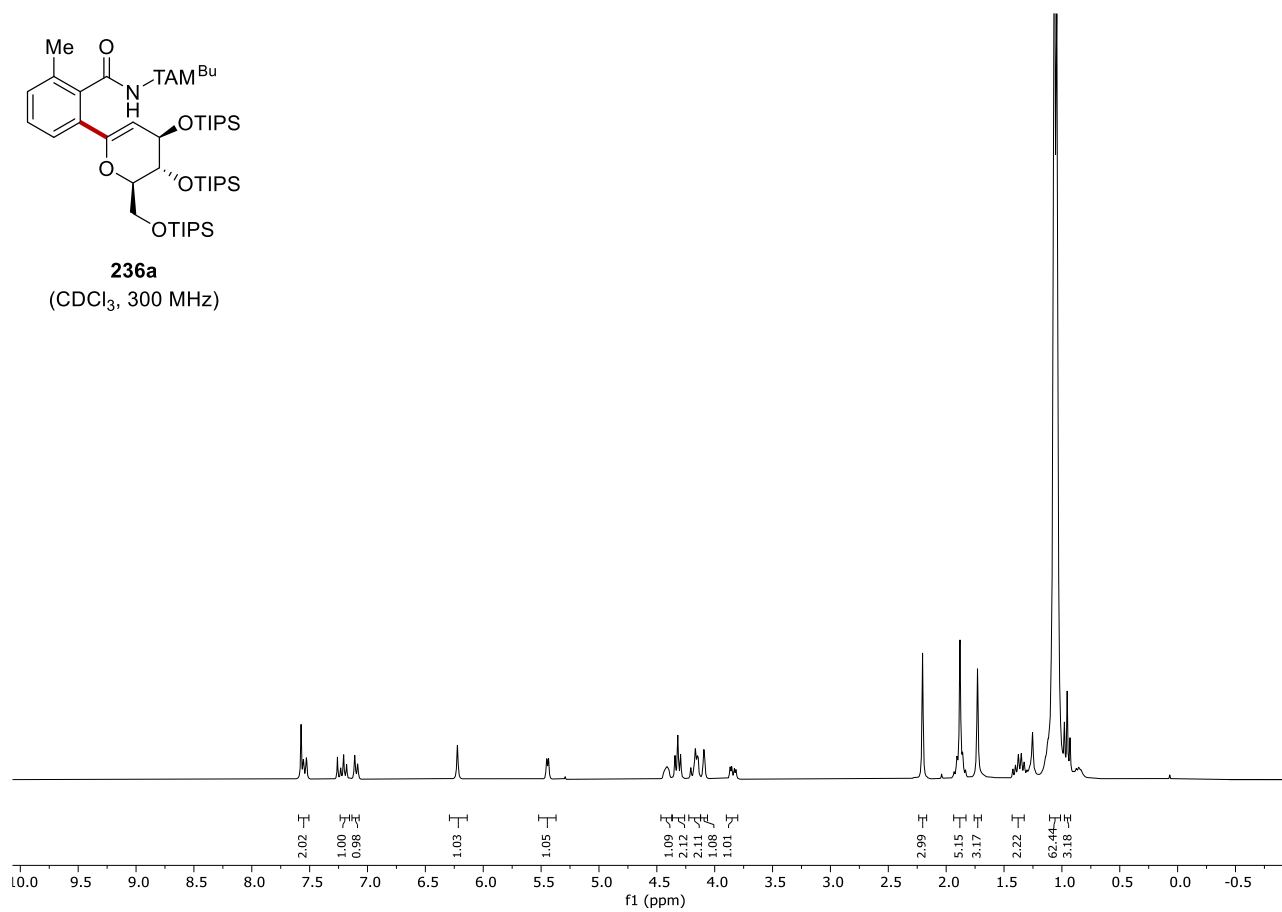


8. NMR Spectra



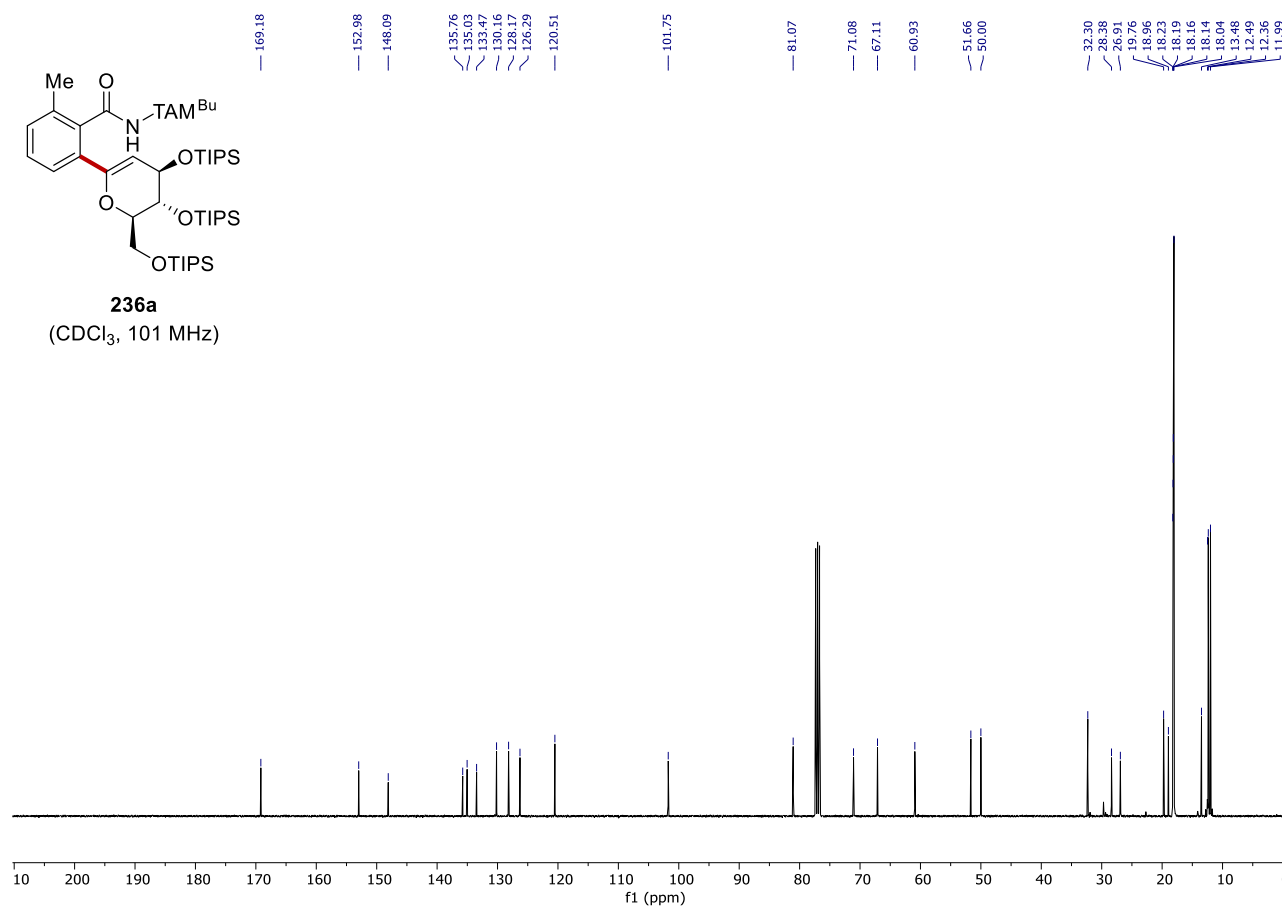
236a

(CDCl₃, 300 MHz)

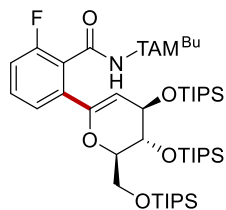


236a

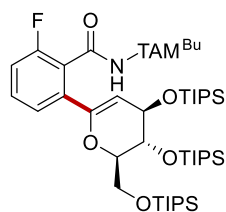
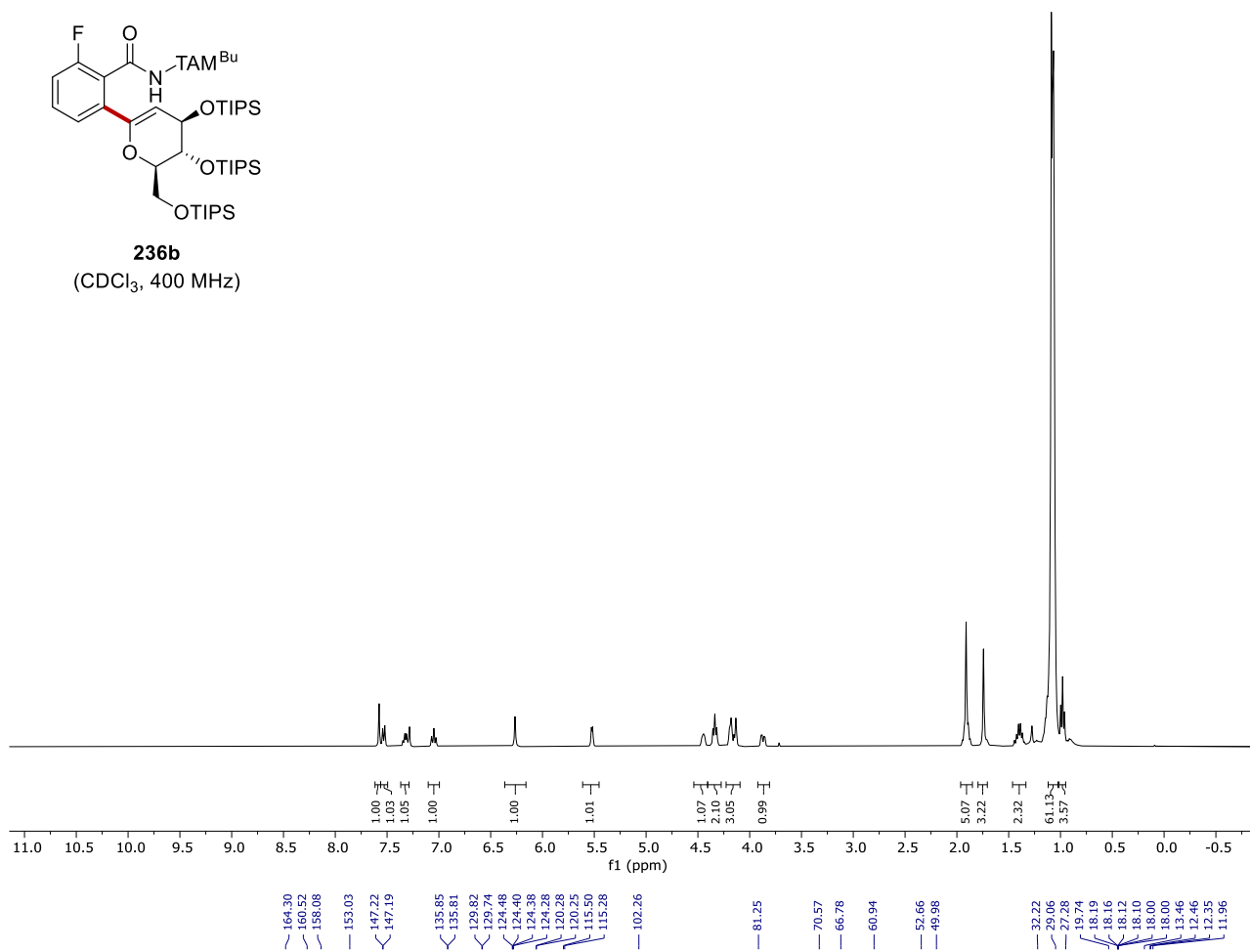
(CDCl₃, 101 MHz)



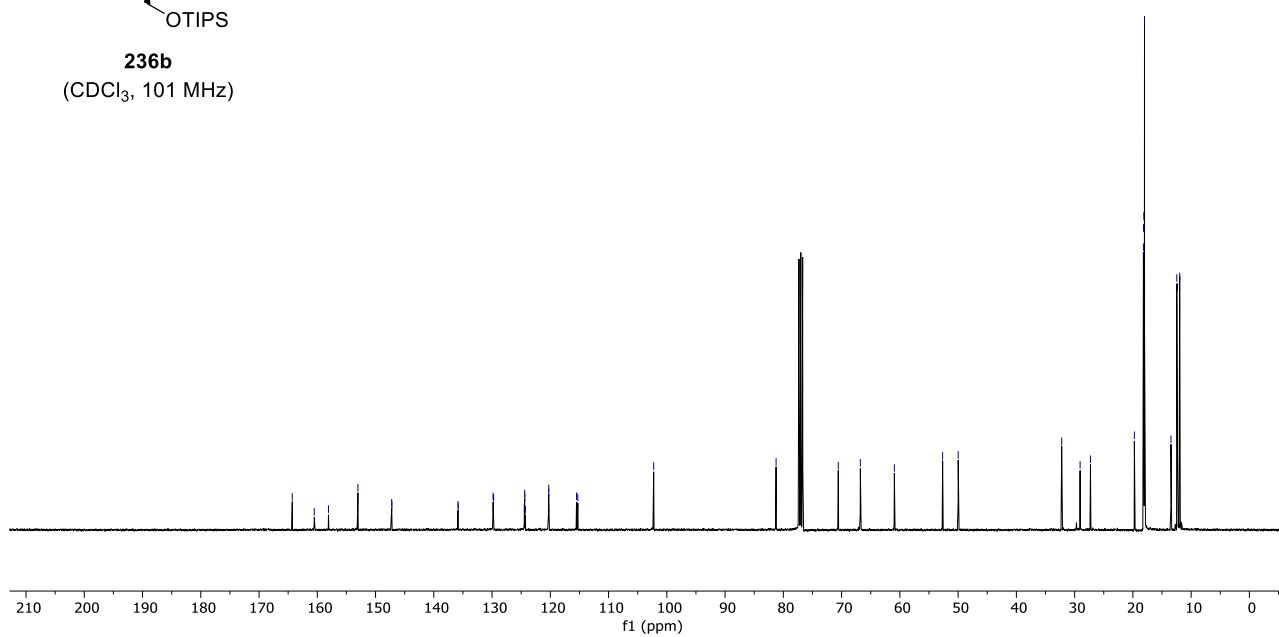
8. NMR Spectra



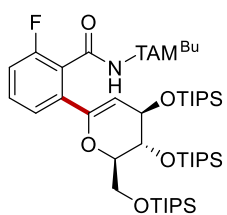
236b
(CDCl₃, 400 MHz)



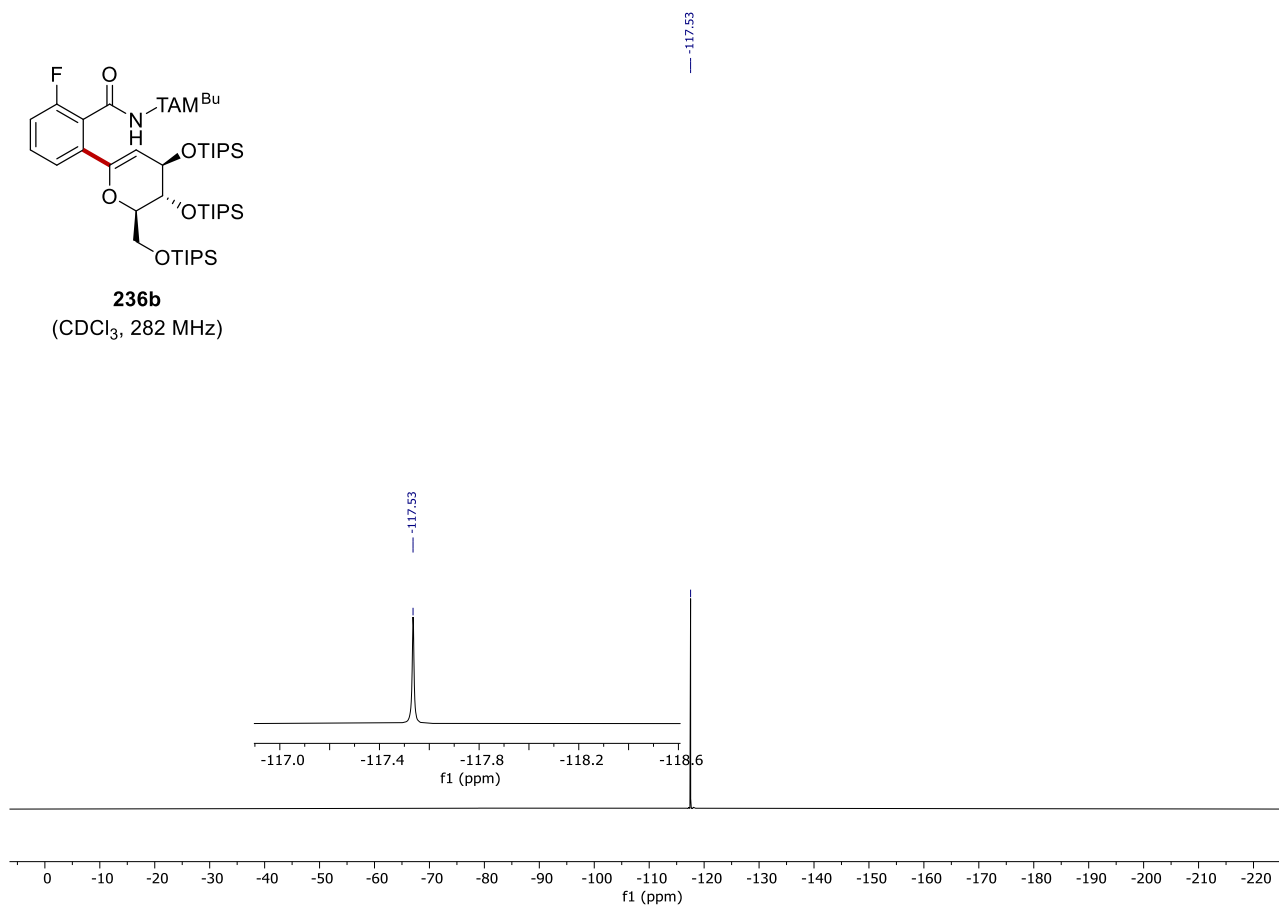
236b
(CDCl₃, 101 MHz)



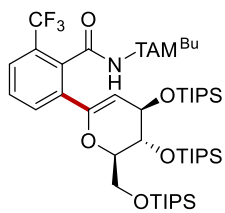
8. NMR Spectra



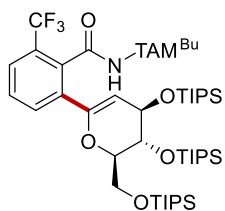
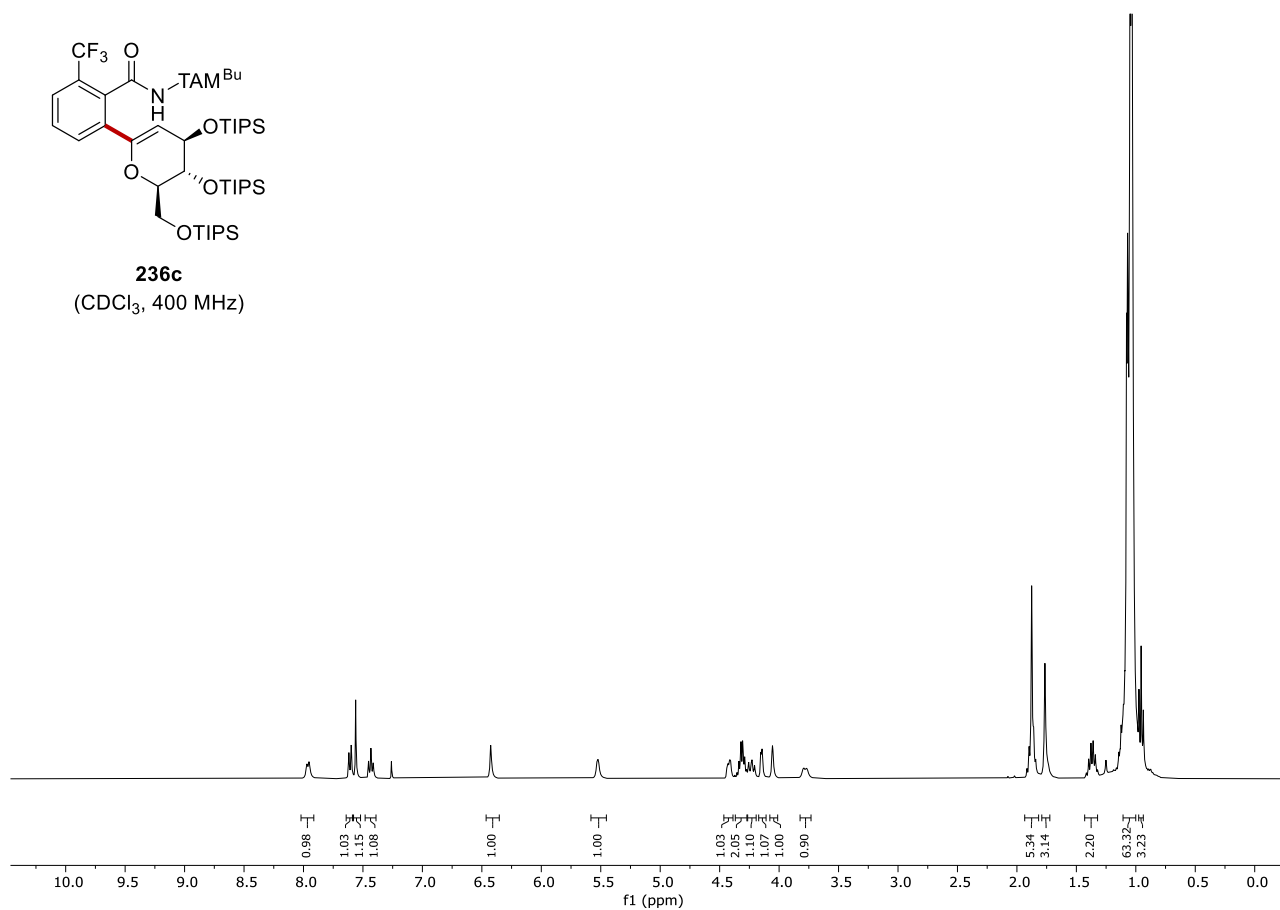
236b
(CDCl₃, 282 MHz)



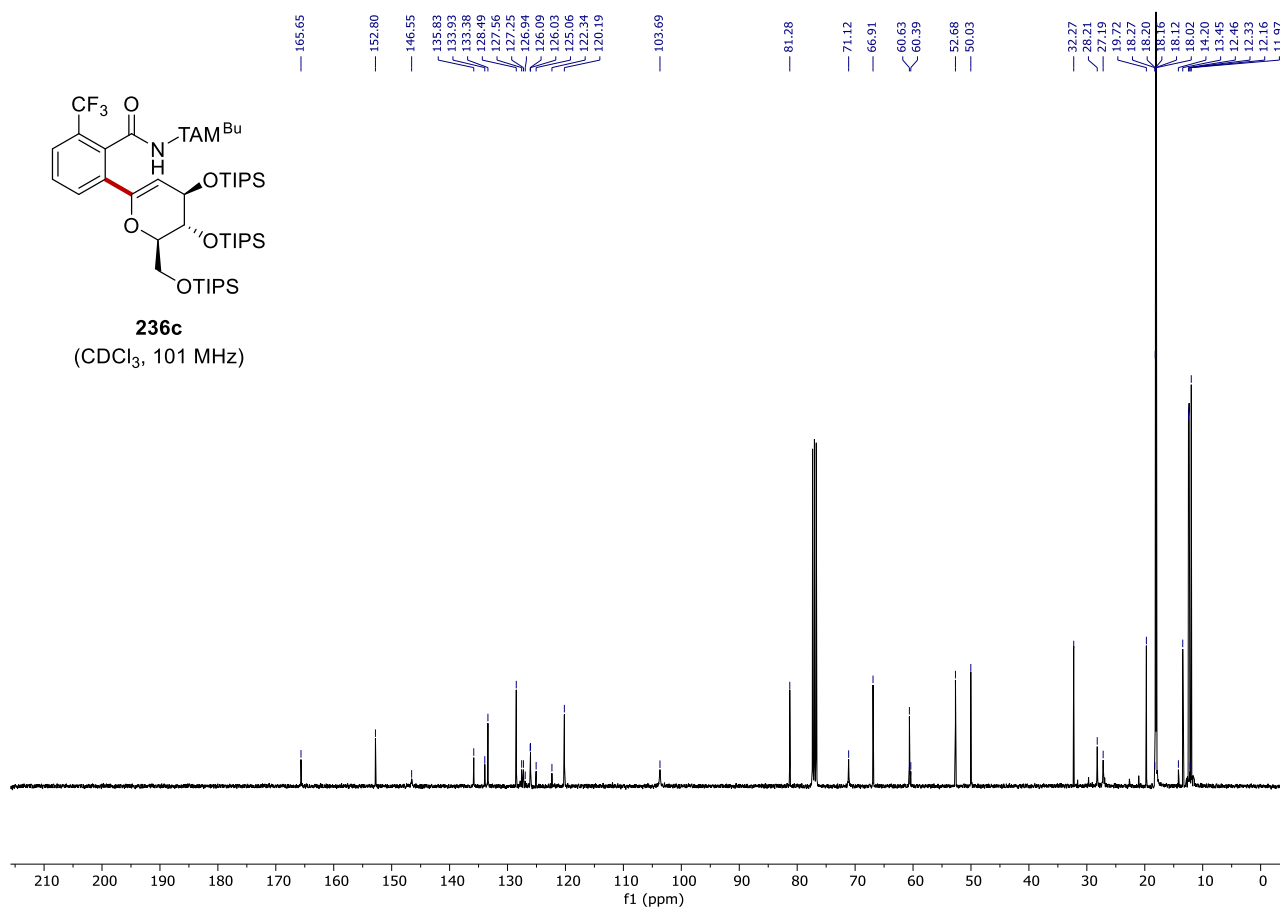
8. NMR Spectra



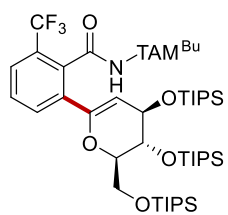
236c
(CDCl₃, 400 MHz)



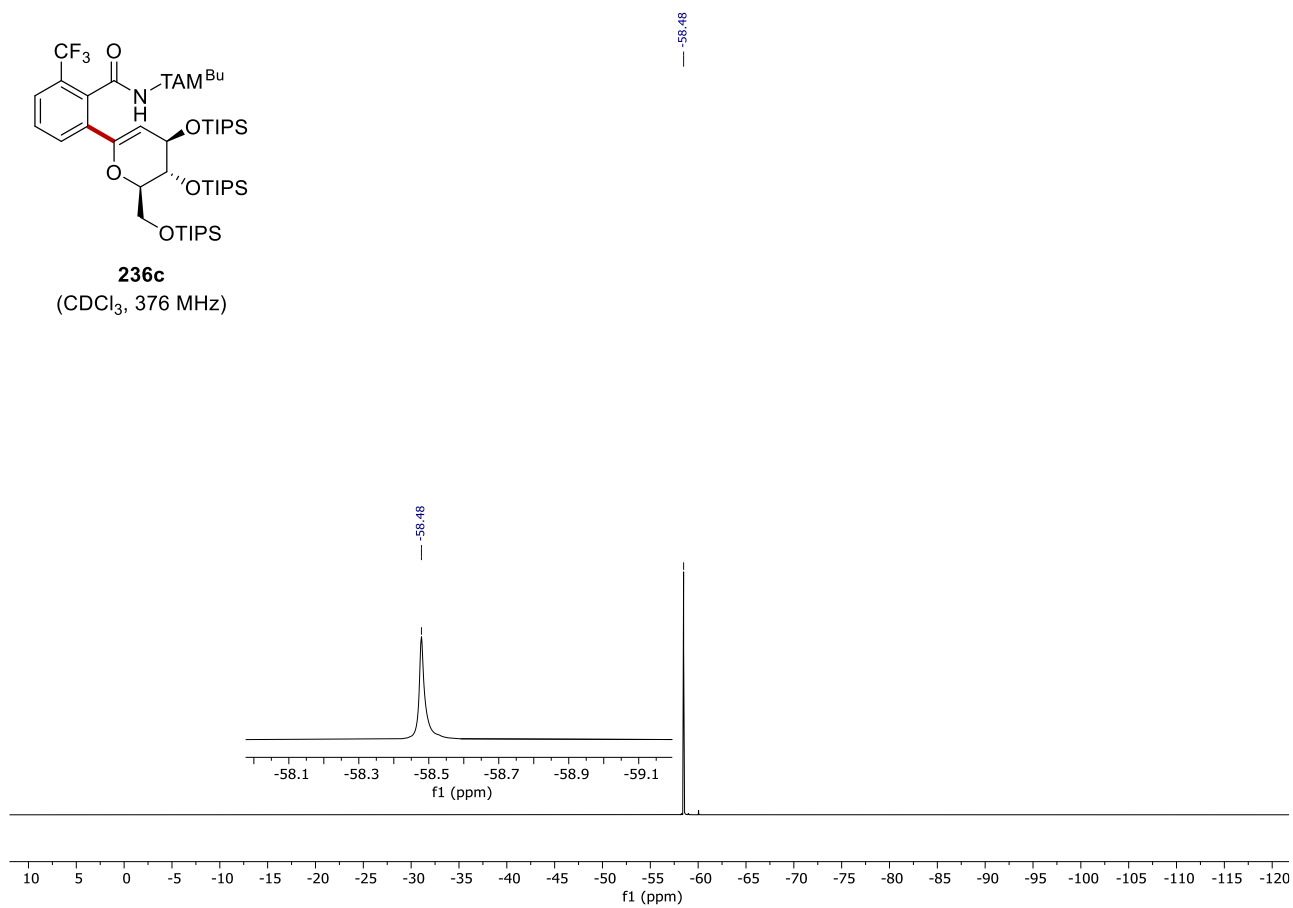
236c
(CDCl₃, 101 MHz)



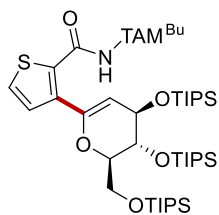
8. NMR Spectra



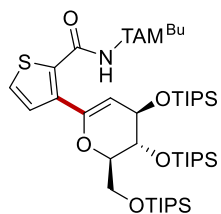
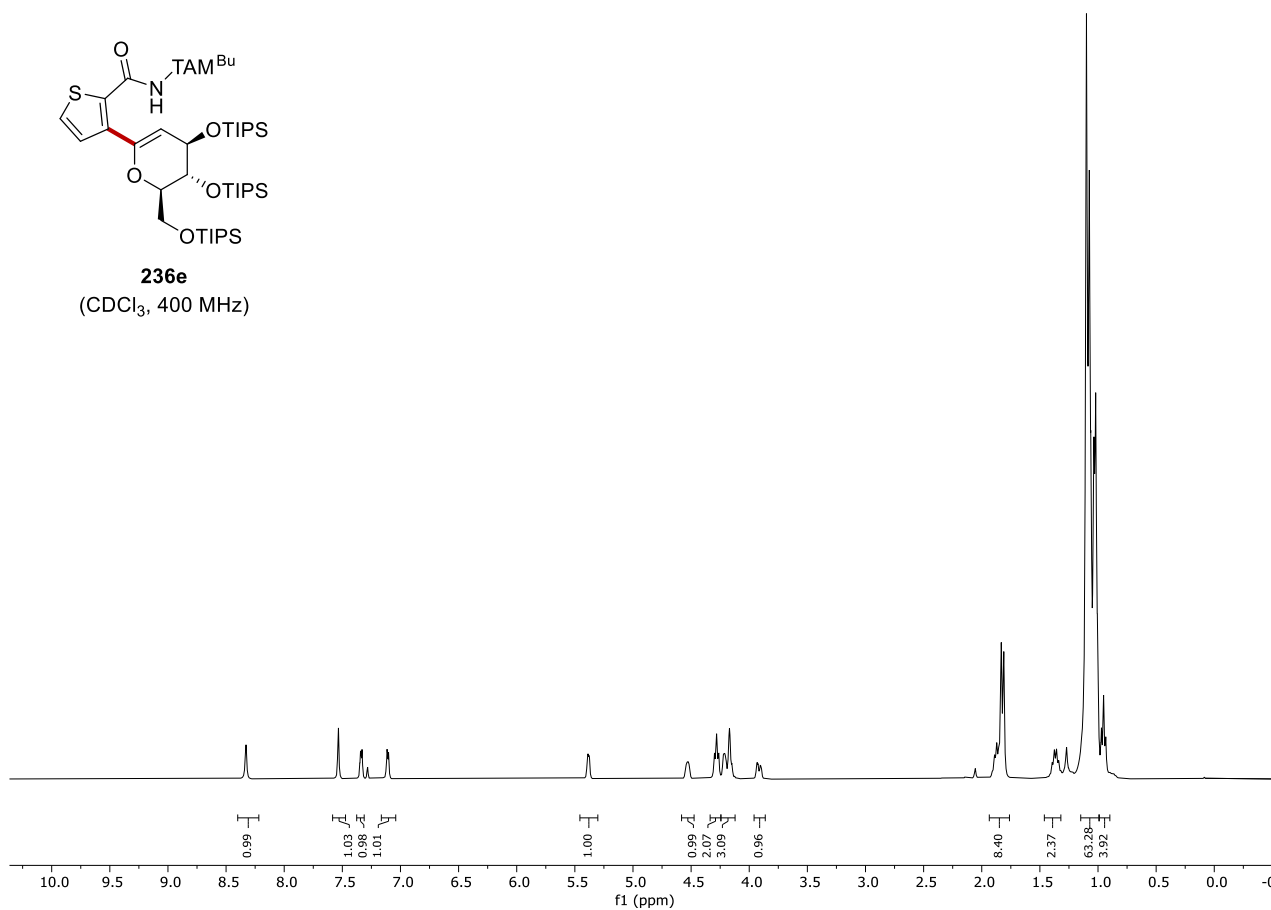
236c
(CDCl₃, 376 MHz)



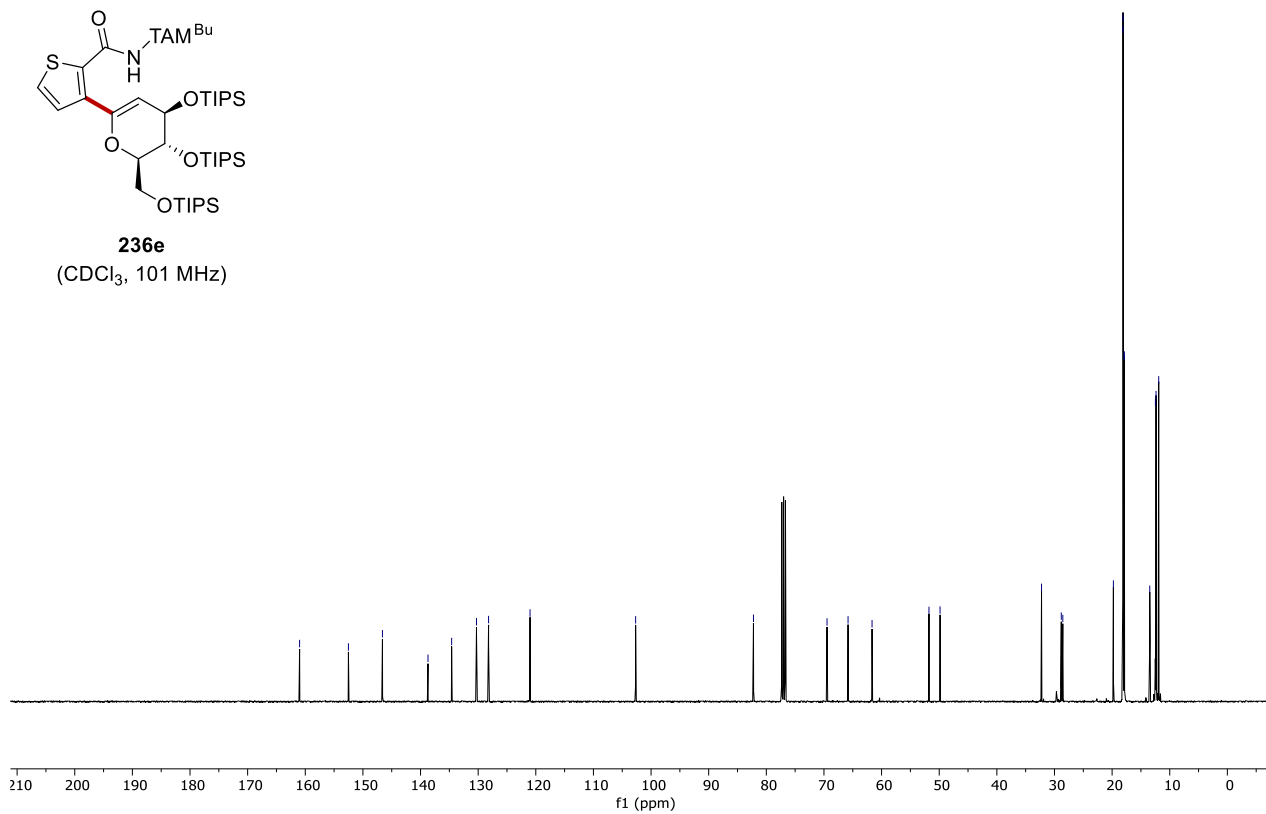
8. NMR Spectra



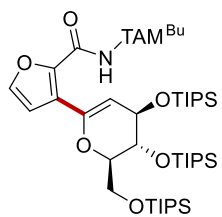
236e
(CDCl₃, 400 MHz)



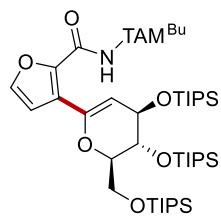
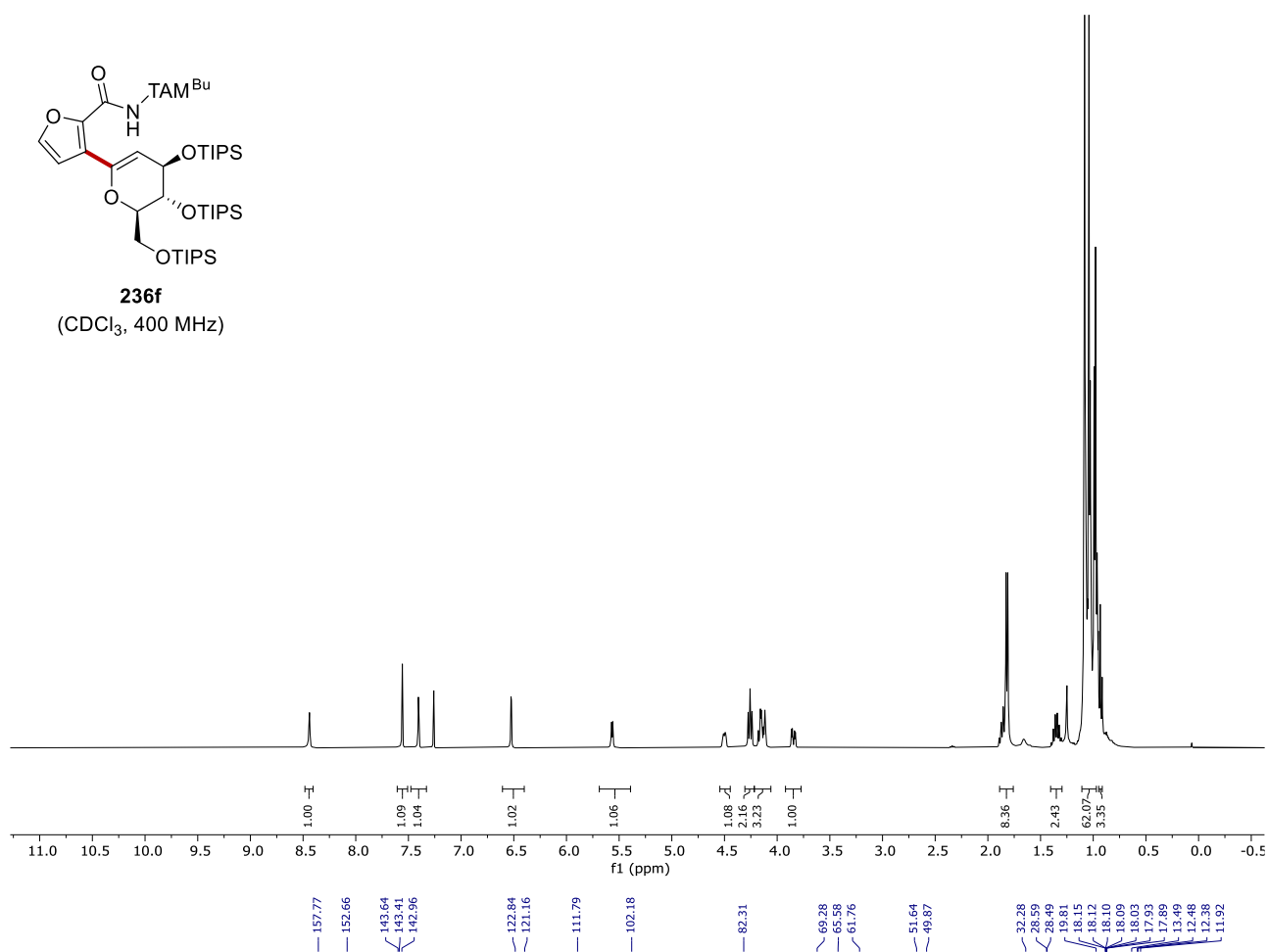
236e
(CDCl₃, 101 MHz)



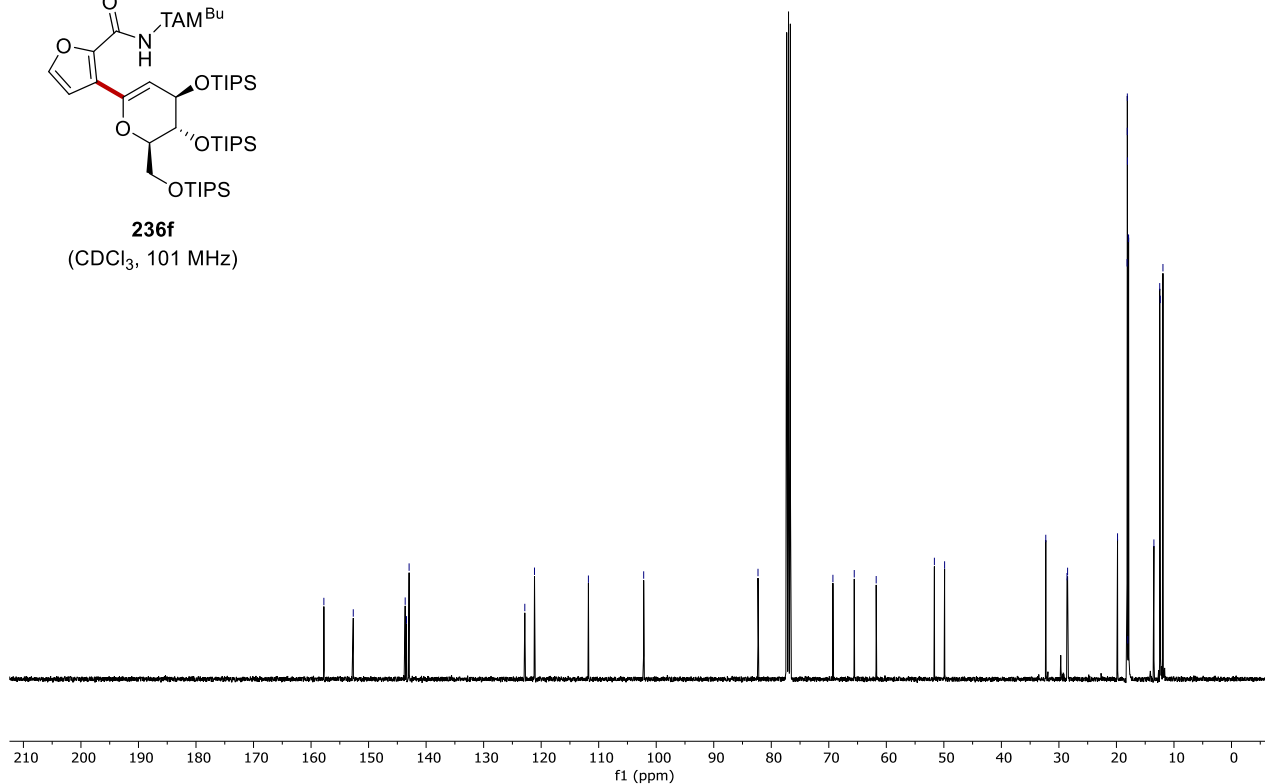
8. NMR Spectra

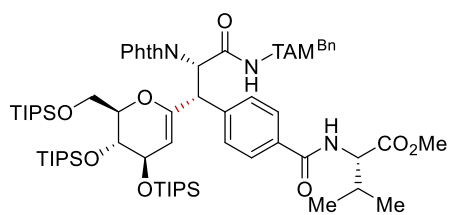


236f
(CDCl₃, 400 MHz)

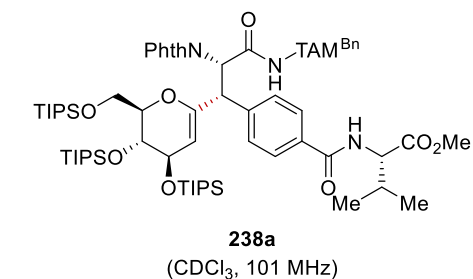
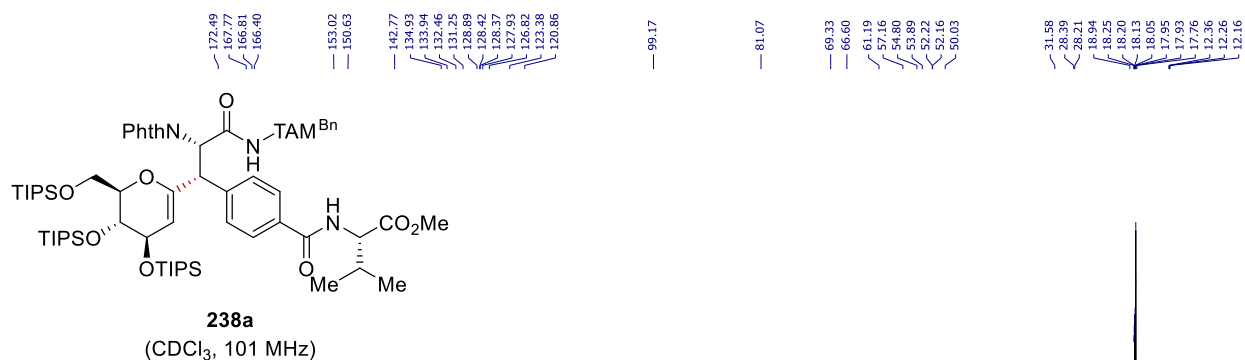
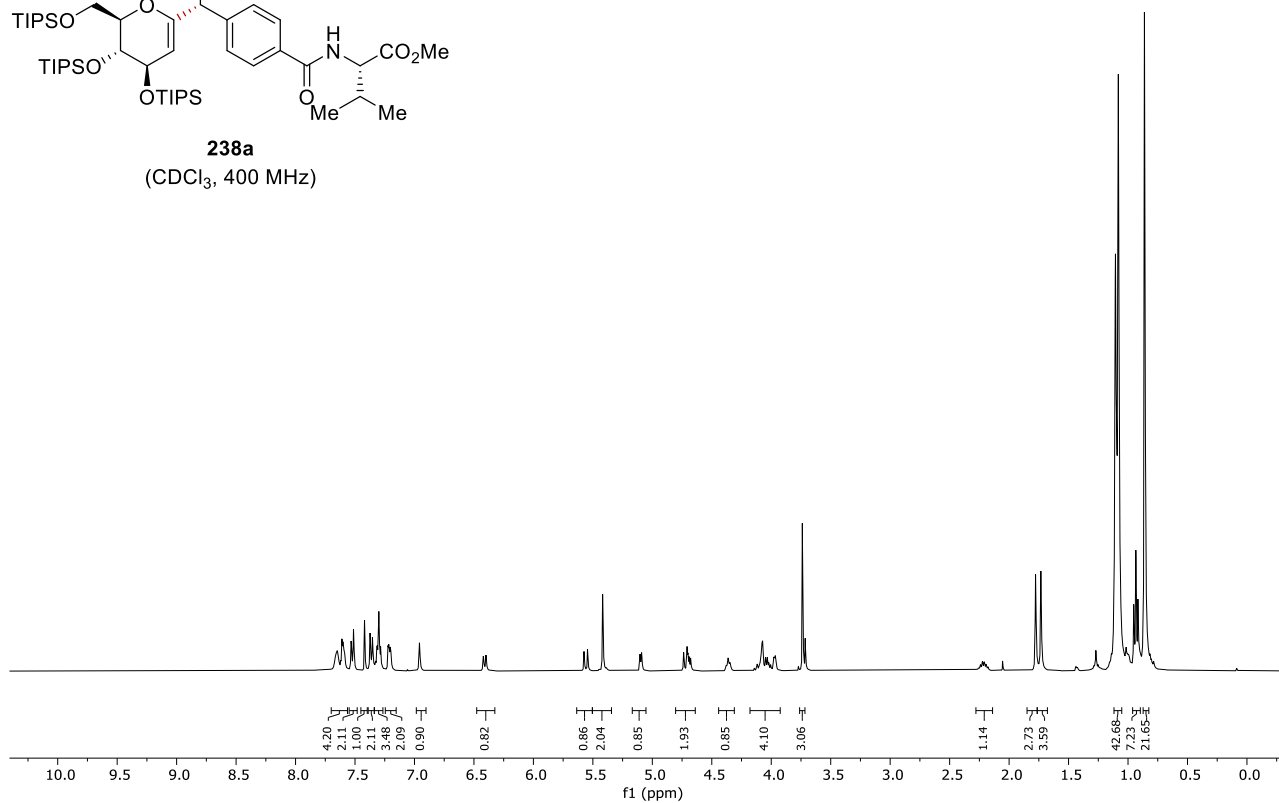


236f
(CDCl₃, 101 MHz)

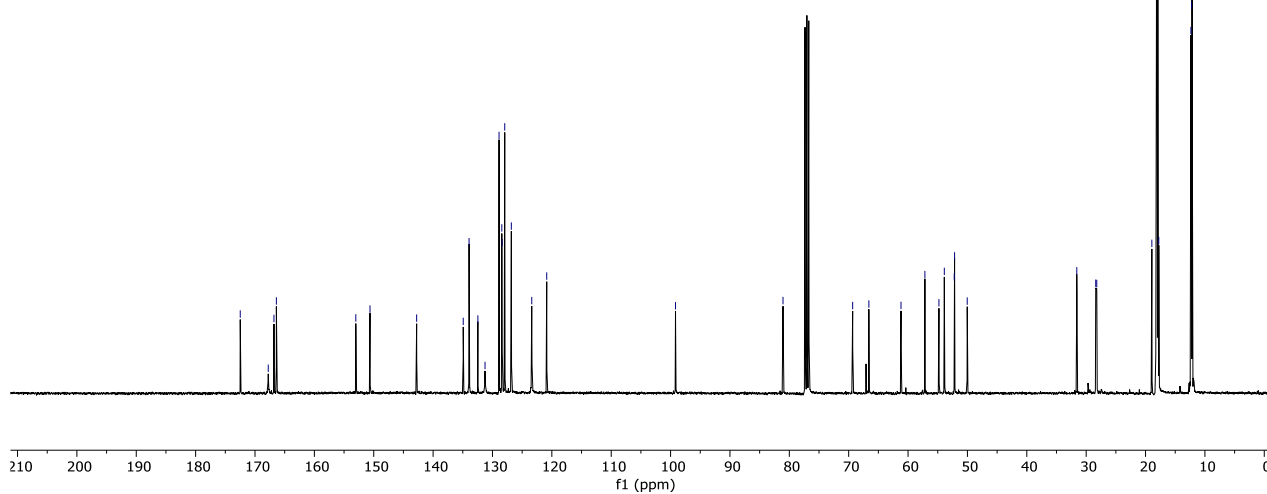




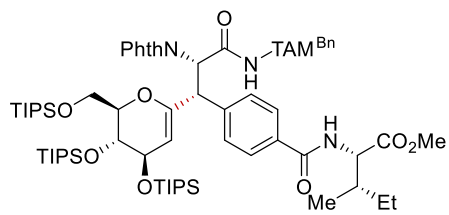
238a
(CDCl₃, 400 MHz)



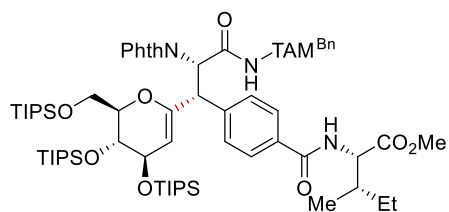
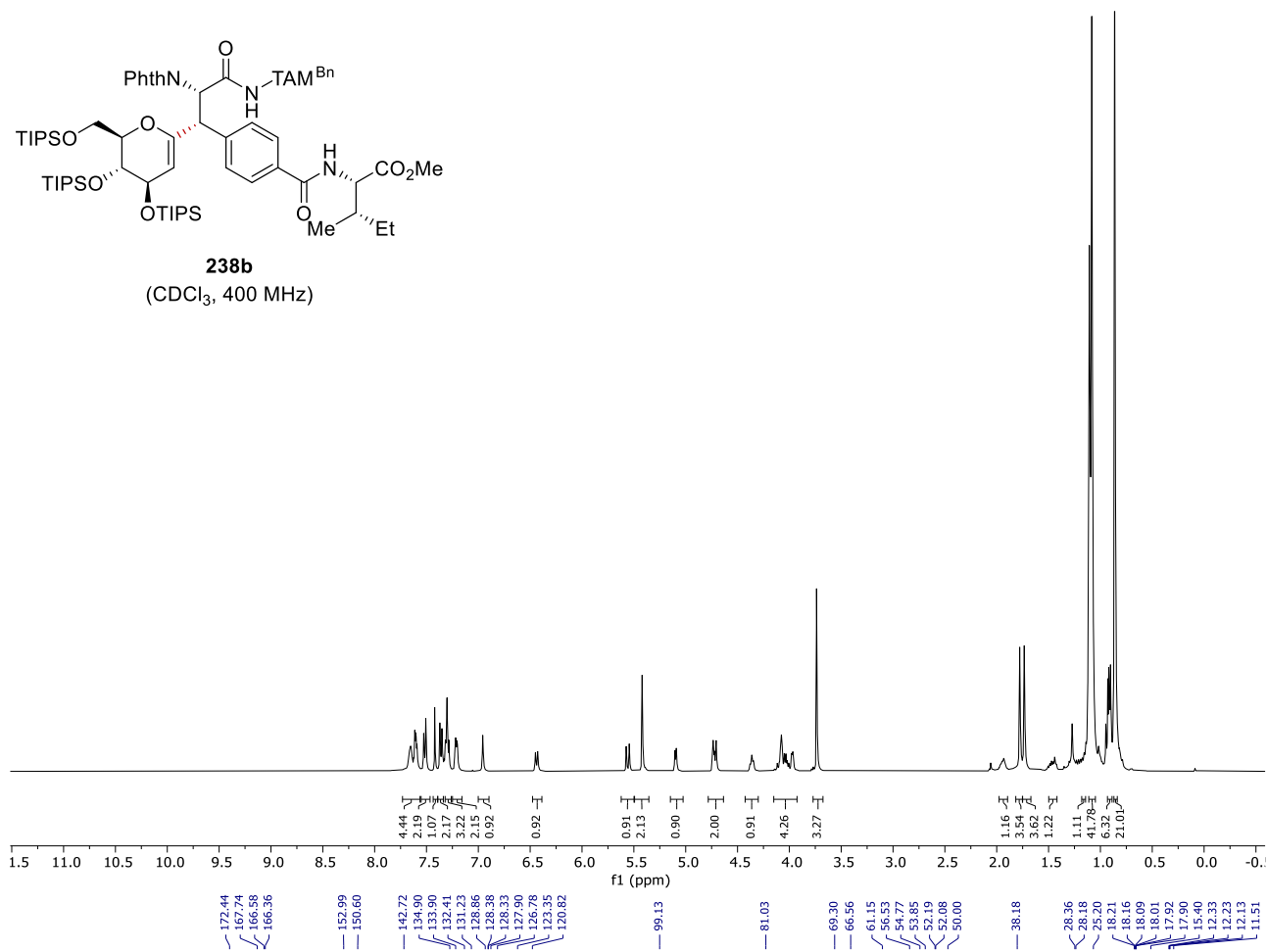
238a
(CDCl₃, 101 MHz)



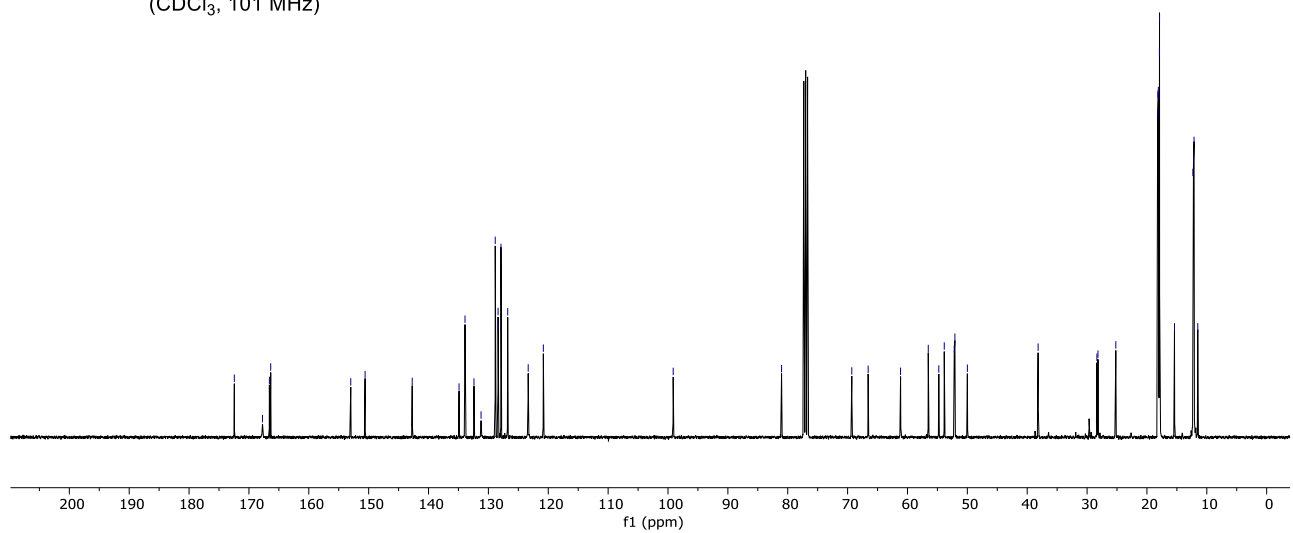
8. NMR Spectra



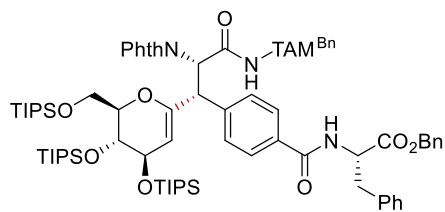
238b
(CDCl₃, 400 MHz)



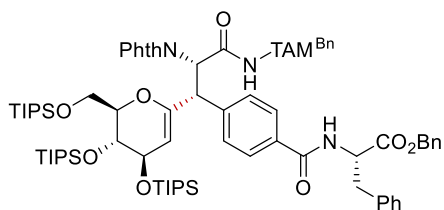
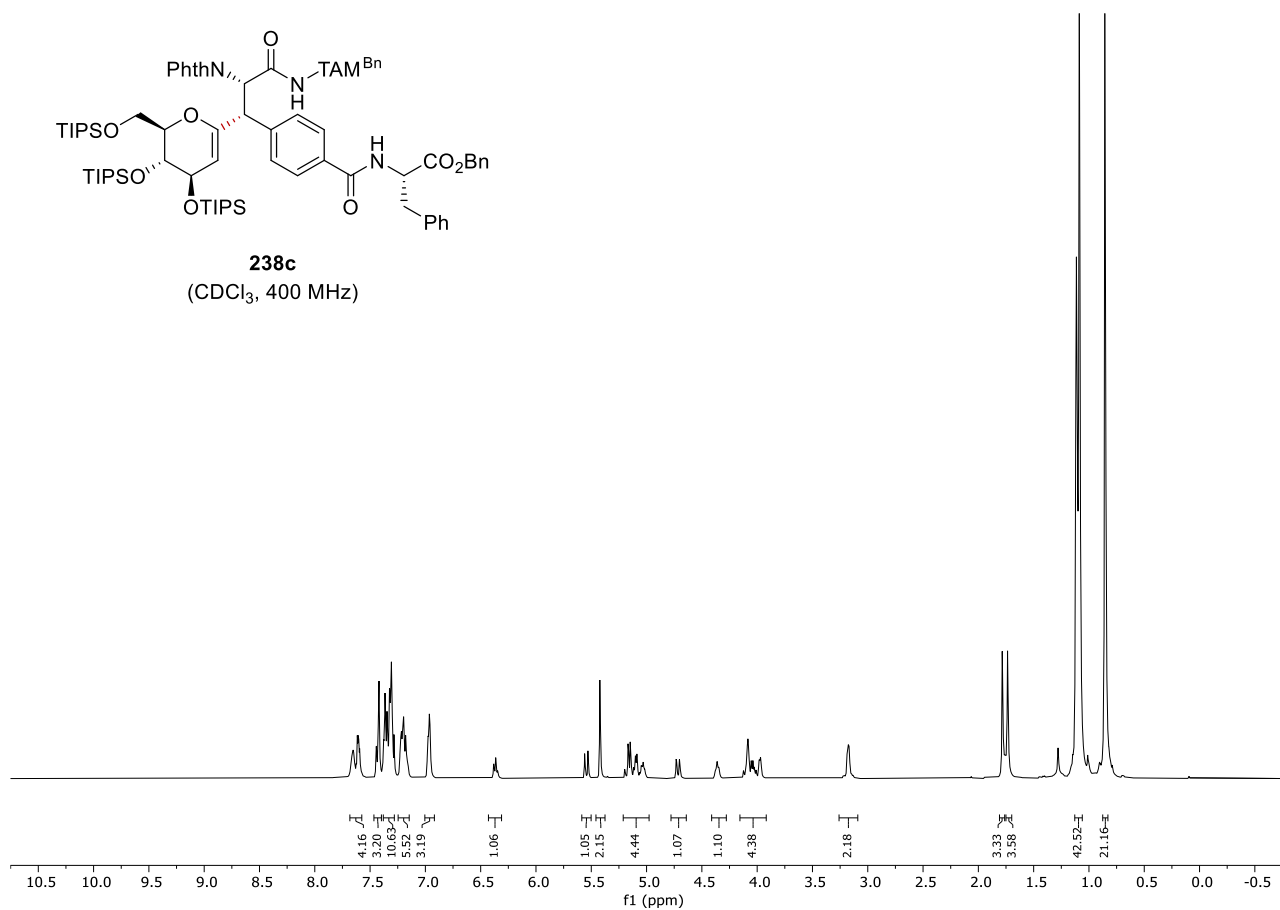
238b
(CDCl₃, 101 MHz)



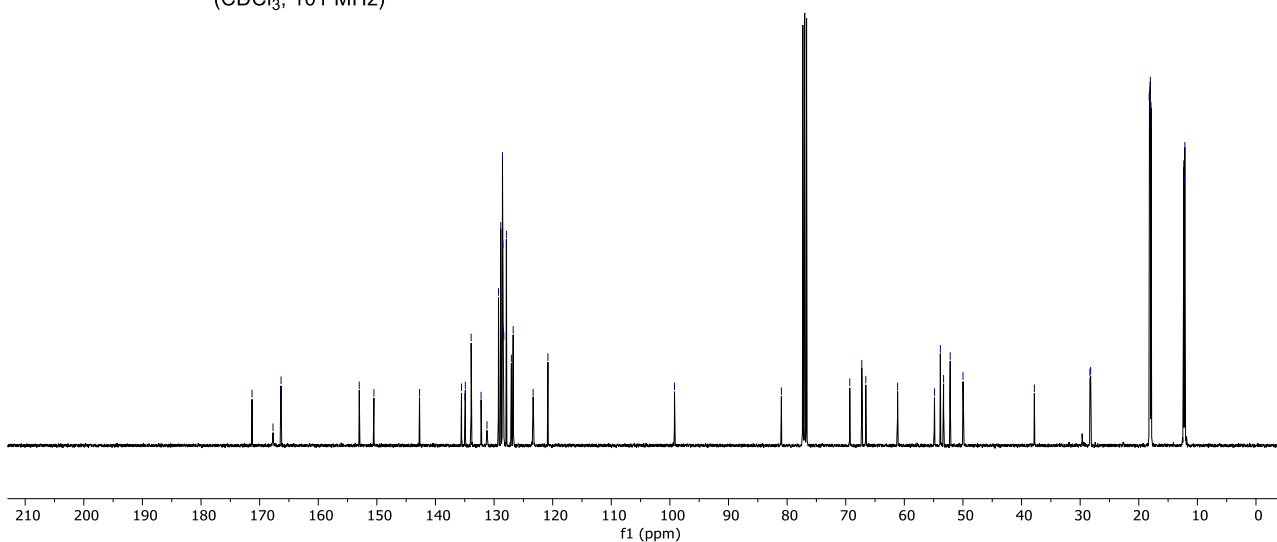
8. NMR Spectra



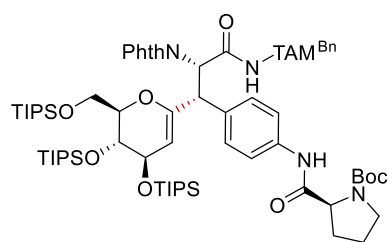
238c
(CDCl₃, 400 MHz)



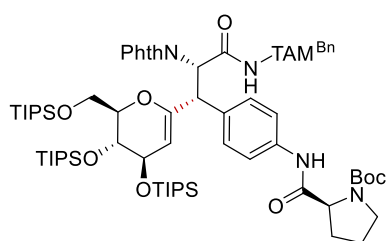
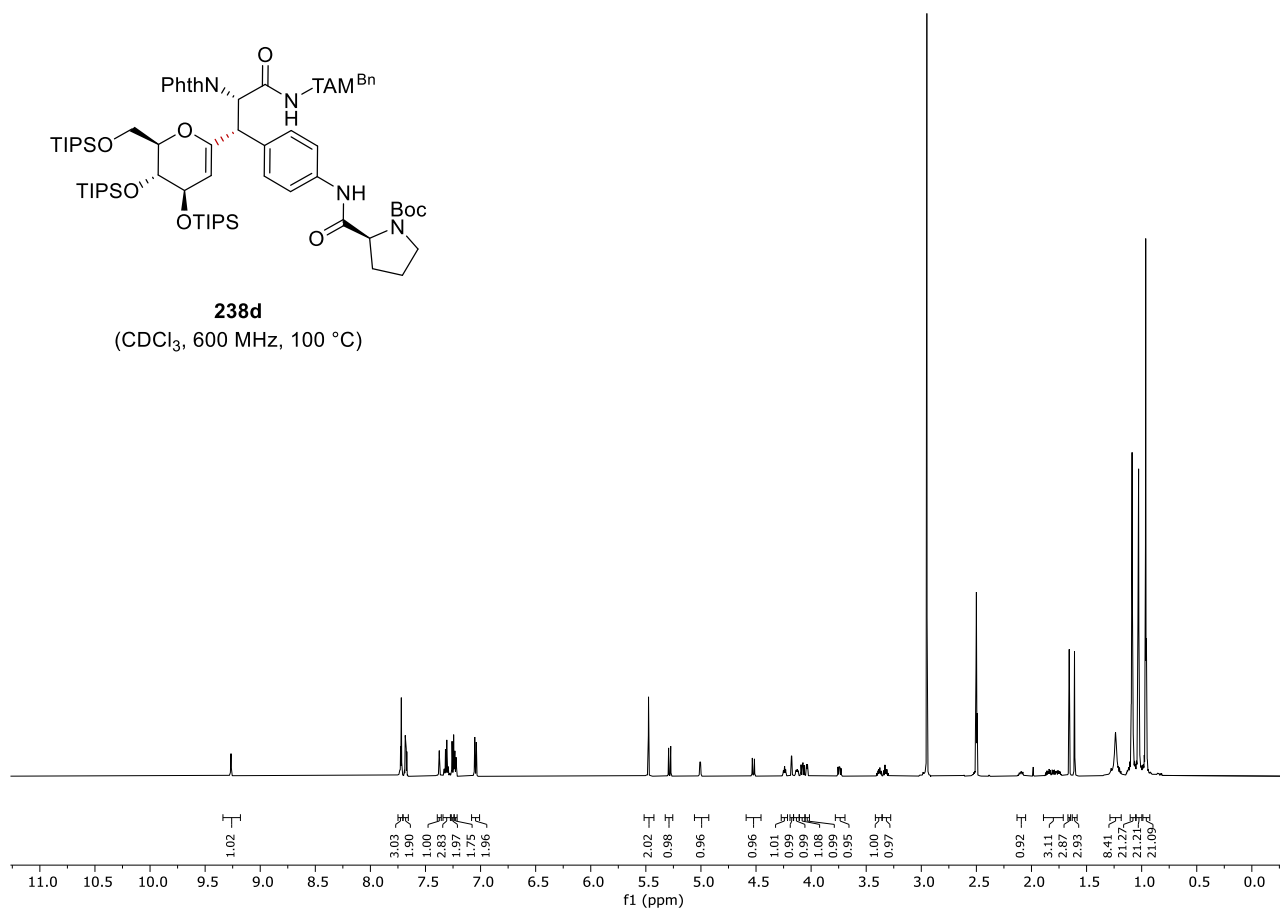
238c
(CDCl₃, 101 MHz)



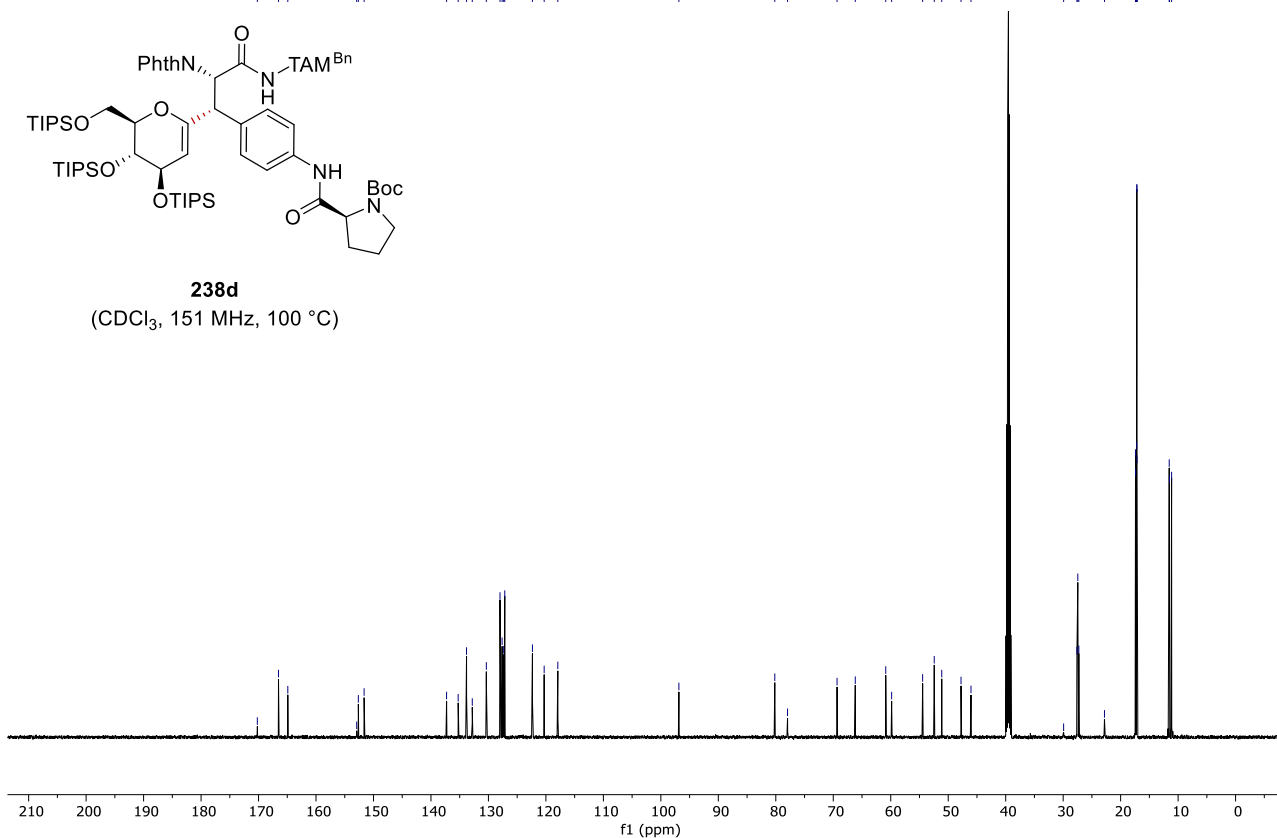
8. NMR Spectra



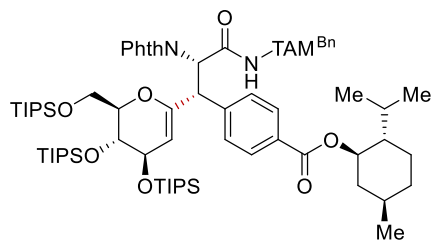
238d
(CDCl₃, 600 MHz, 100 °C)



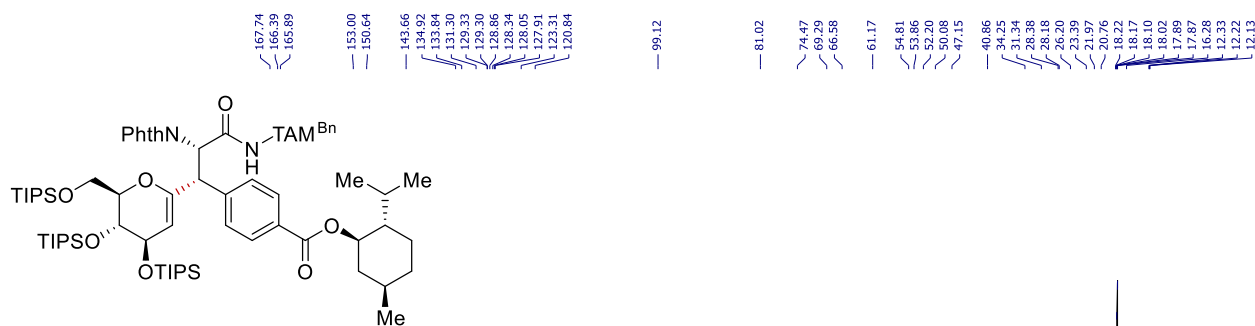
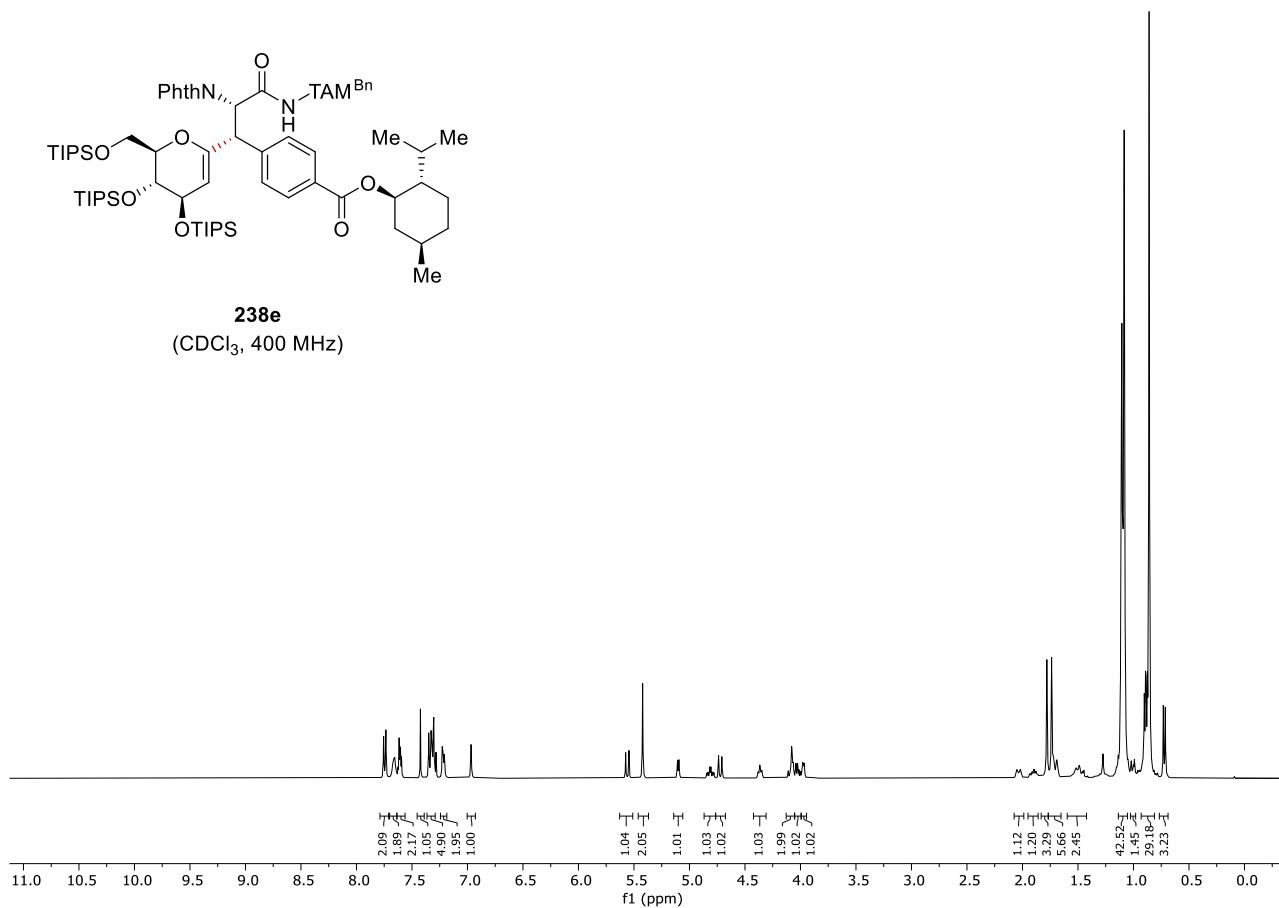
238d
(CDCl₃, 151 MHz, 100 °C)



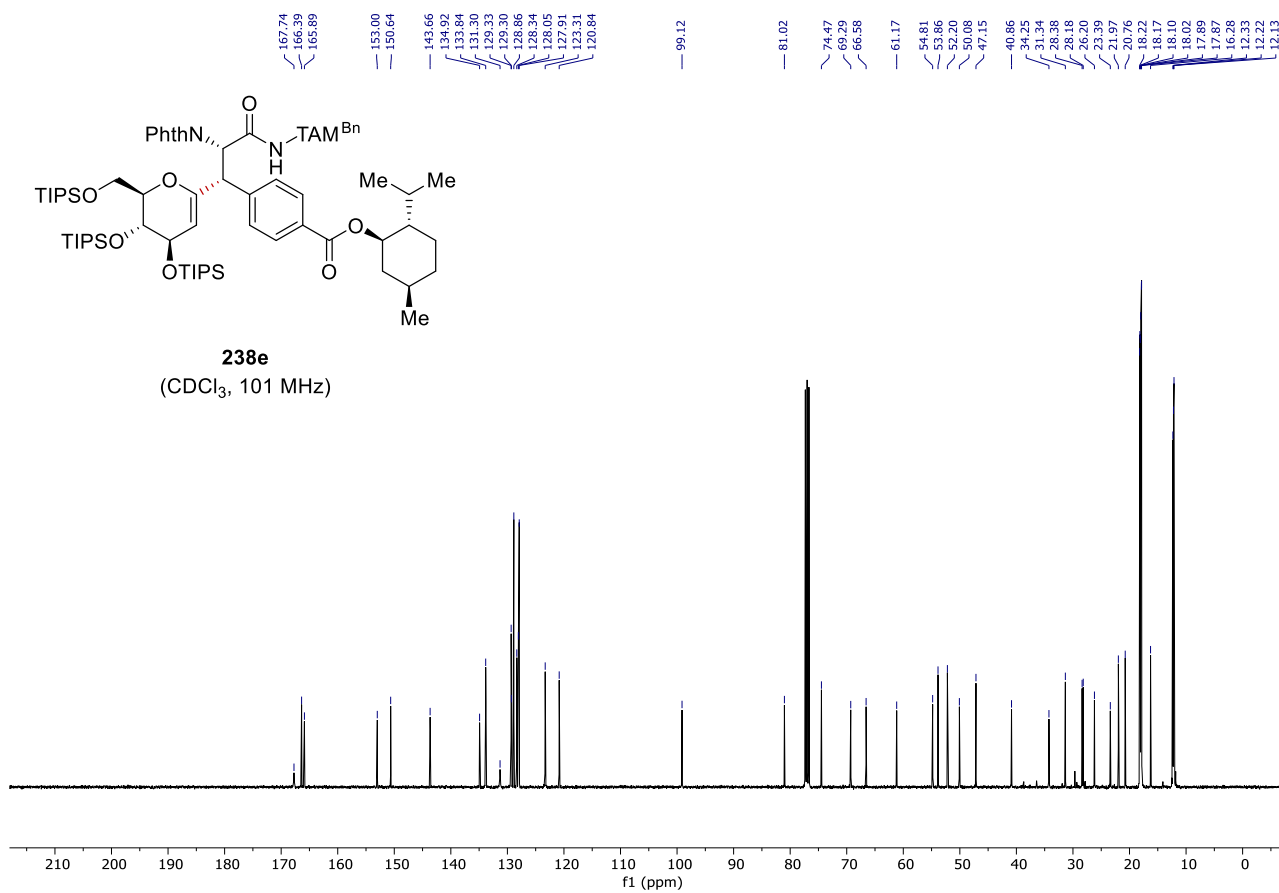
8. NMR Spectra



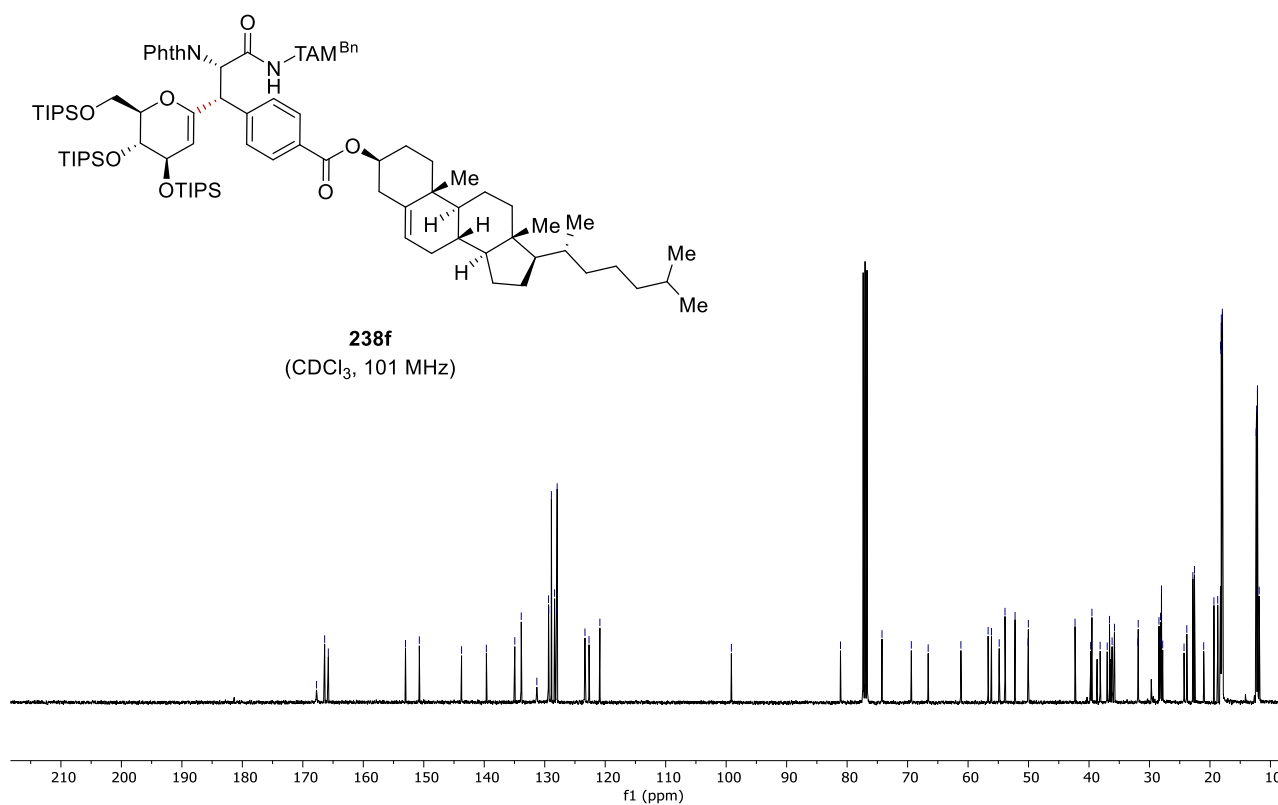
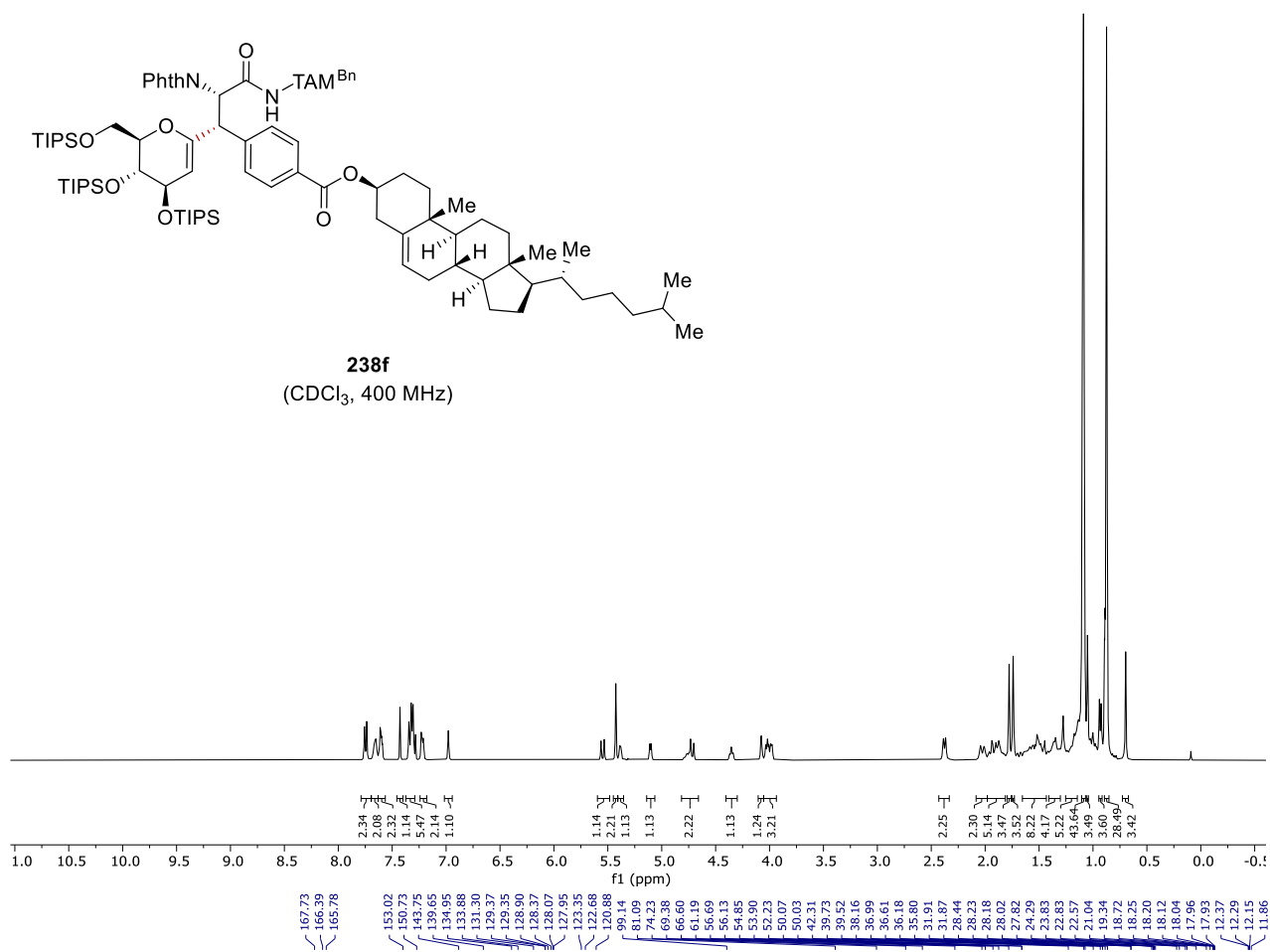
238e
(CDCl₃, 400 MHz)

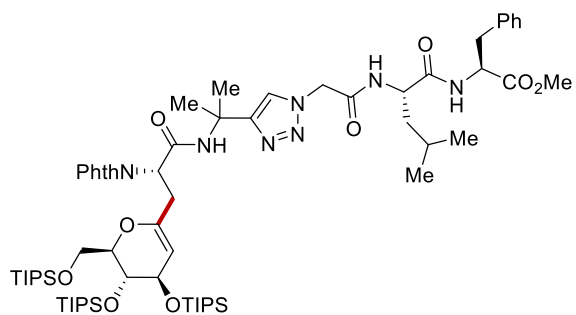


238e
(CDCl₃, 101 MHz)

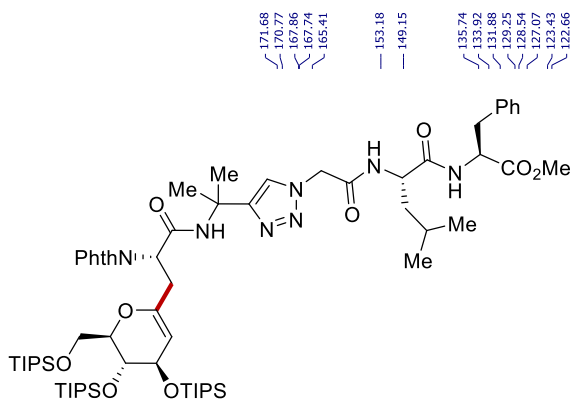
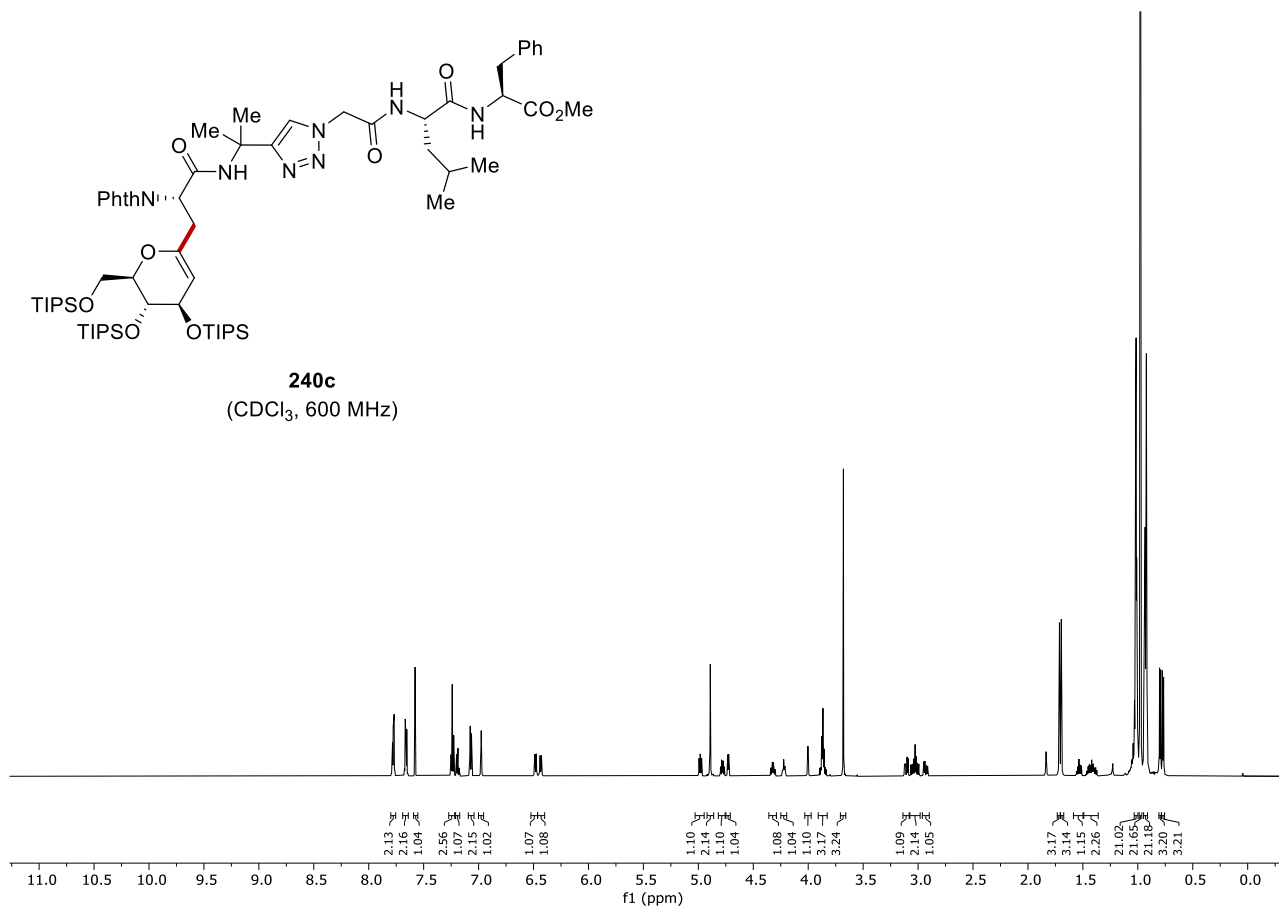


8. NMR Spectra

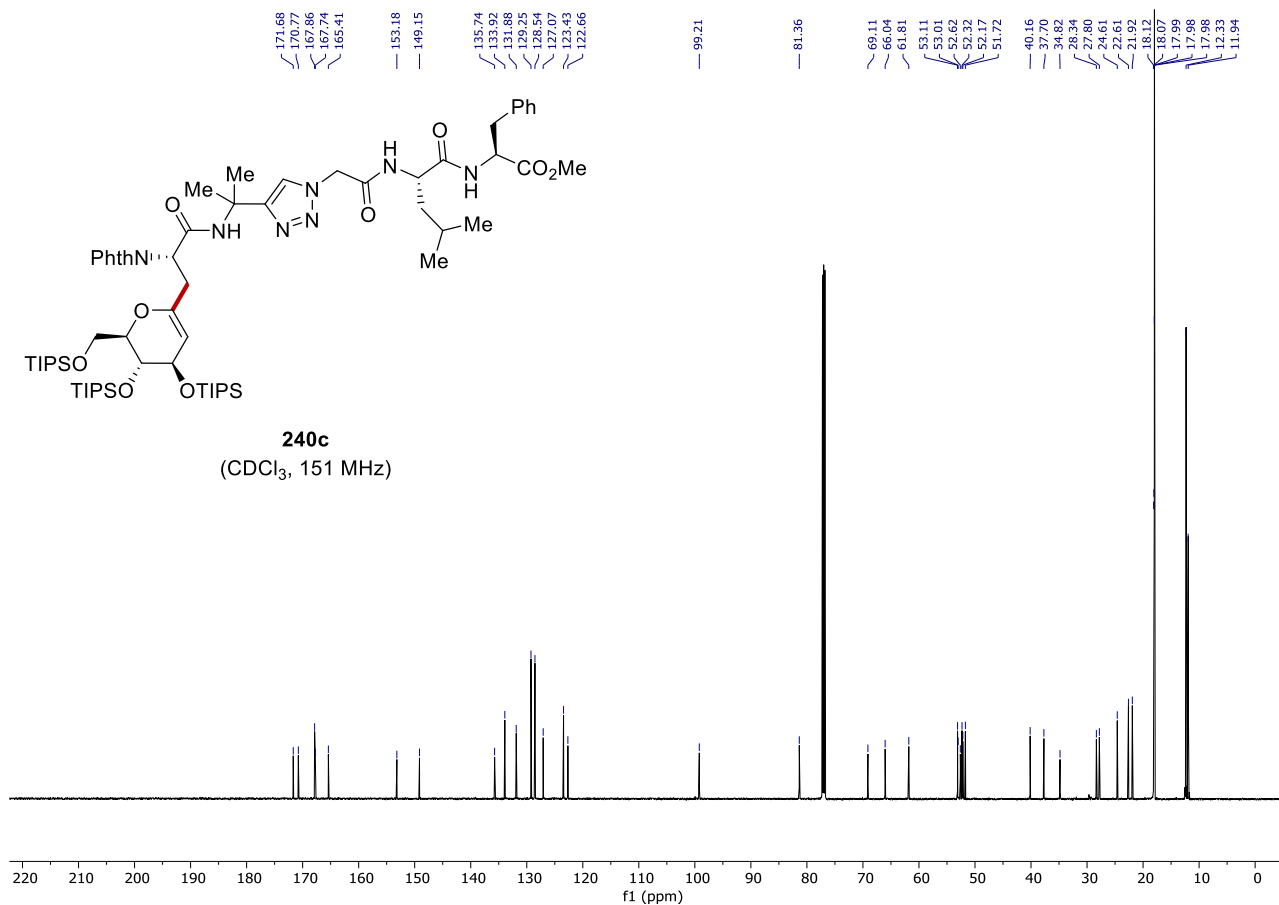




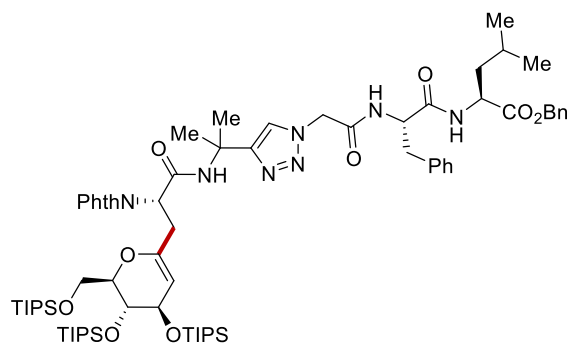
240c
(CDCl₃, 600 MHz)



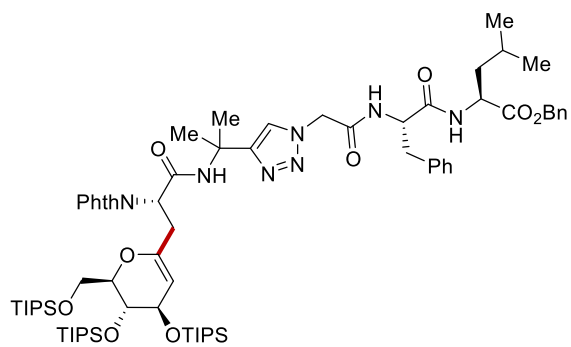
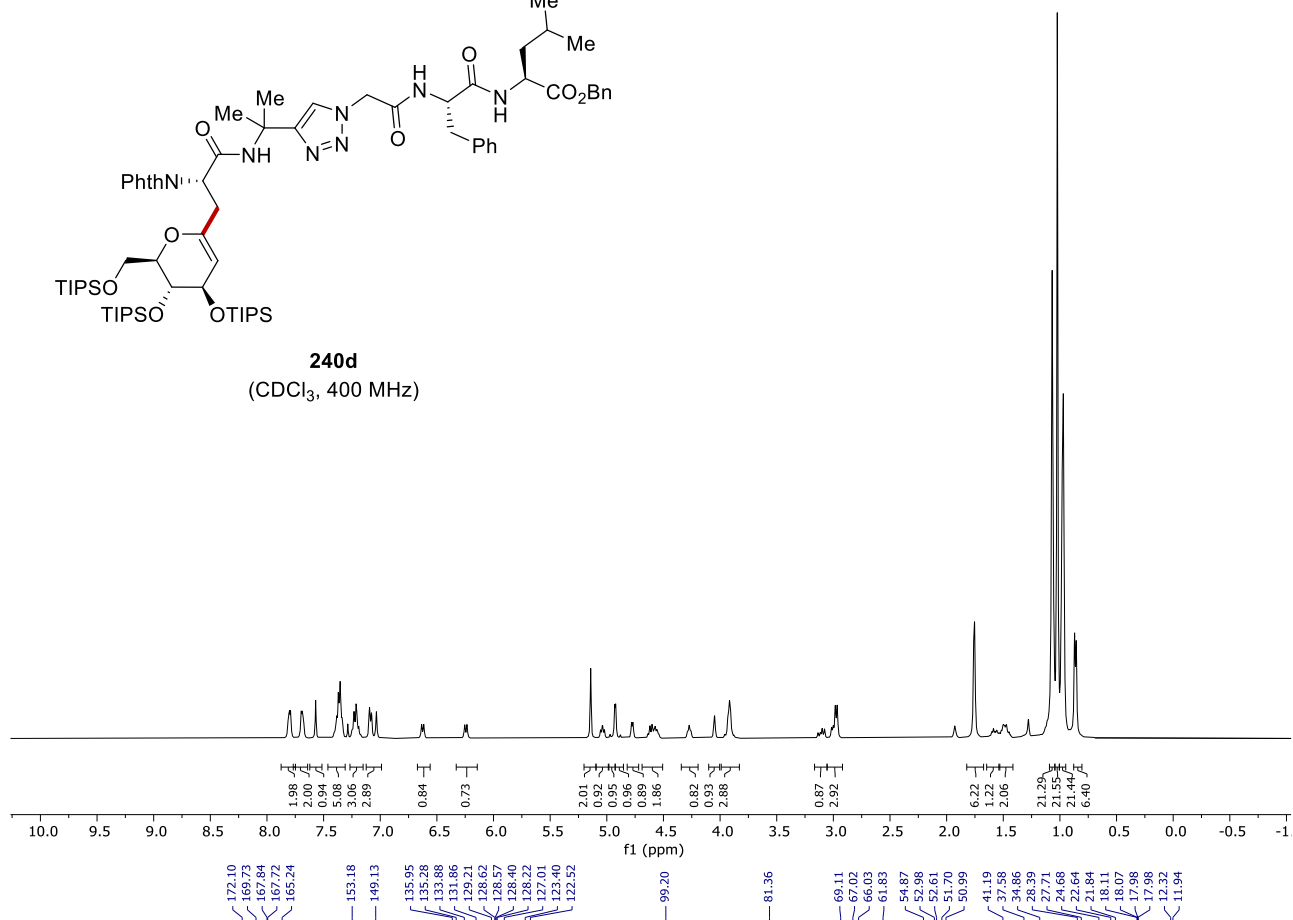
240c
(CDCl₃, 151 MHz)



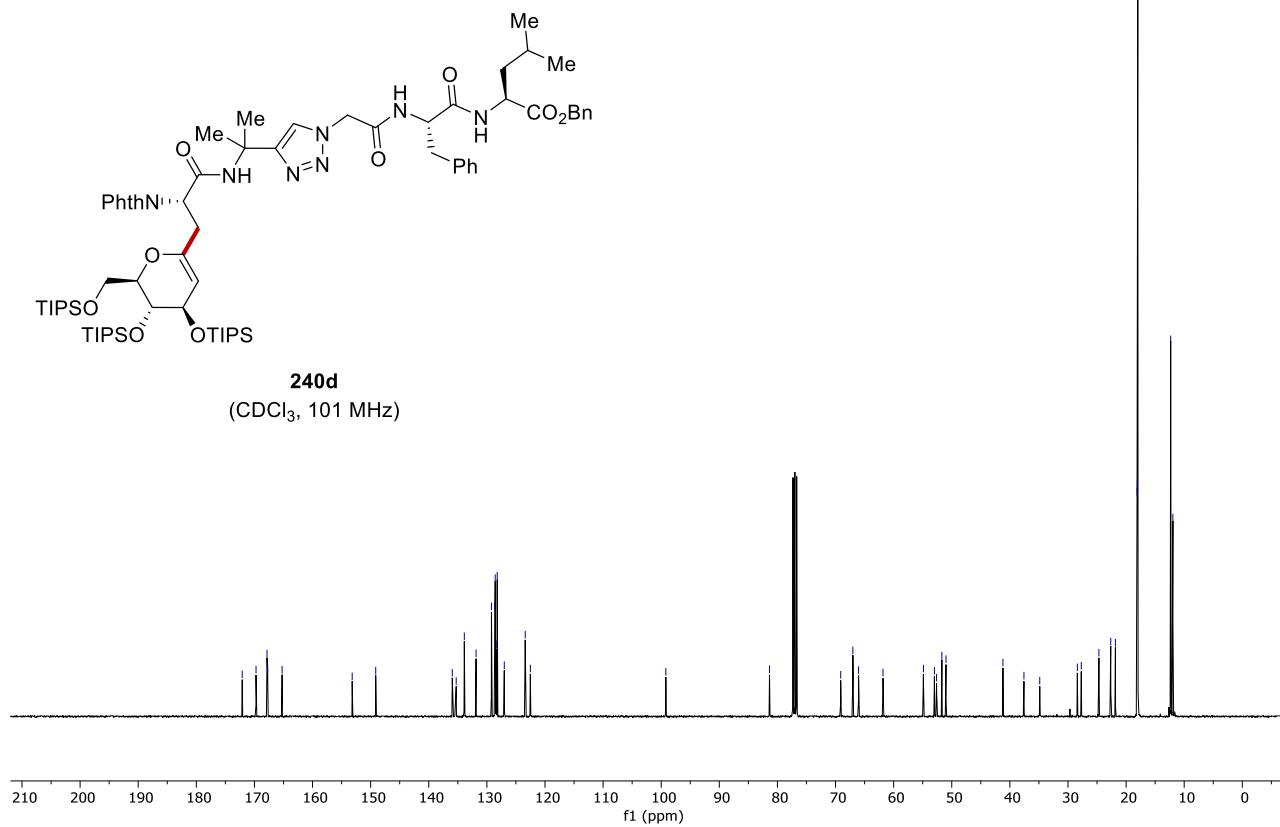
8. NMR Spectra



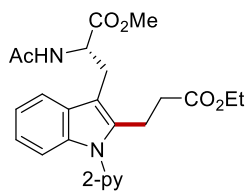
240d
(CDCl₃, 400 MHz)



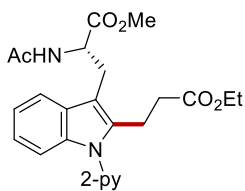
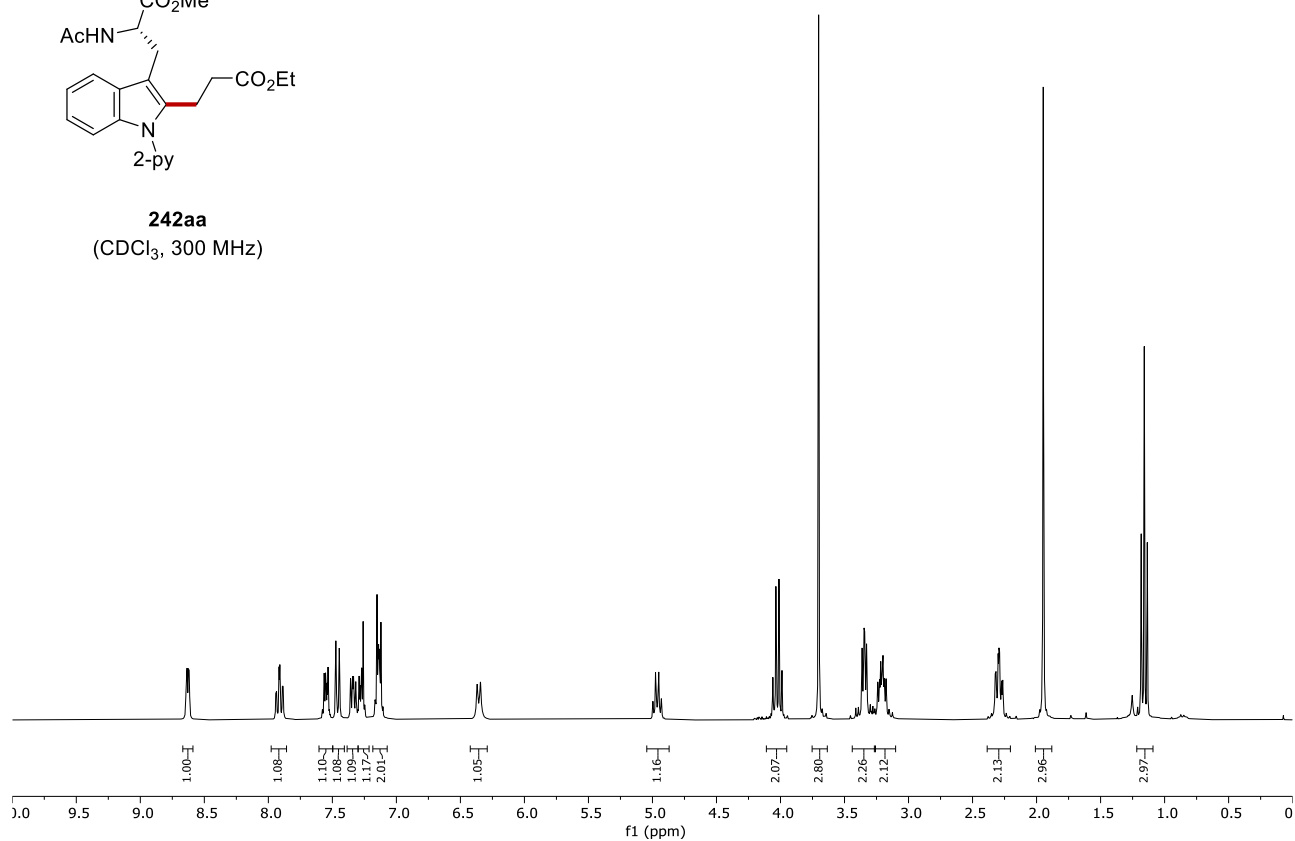
240d
(CDCl₃, 101 MHz)



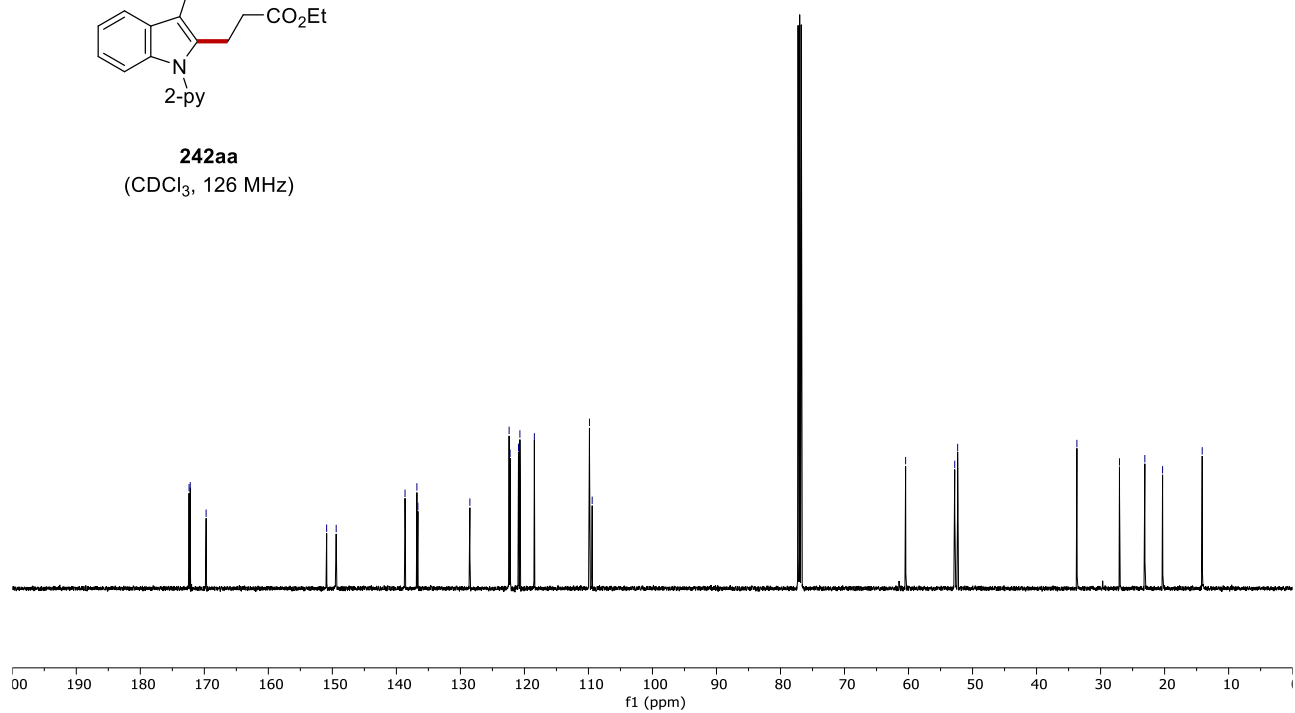
8. NMR Spectra



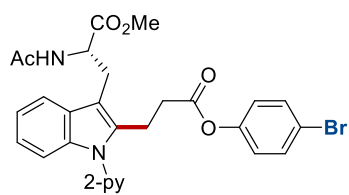
242aa
(CDCl₃, 300 MHz)



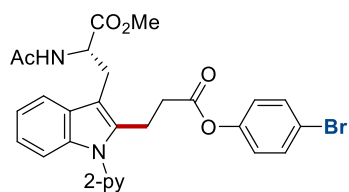
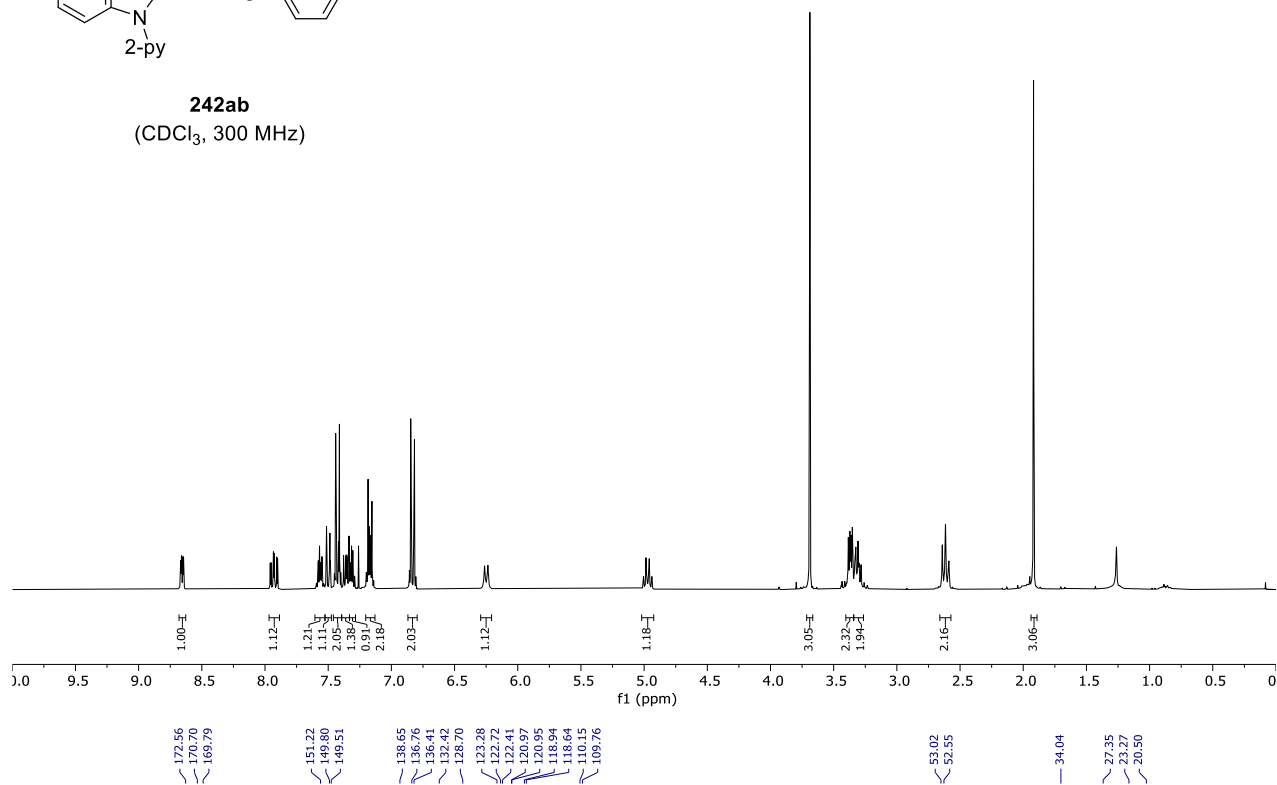
242aa
(CDCl₃, 126 MHz)



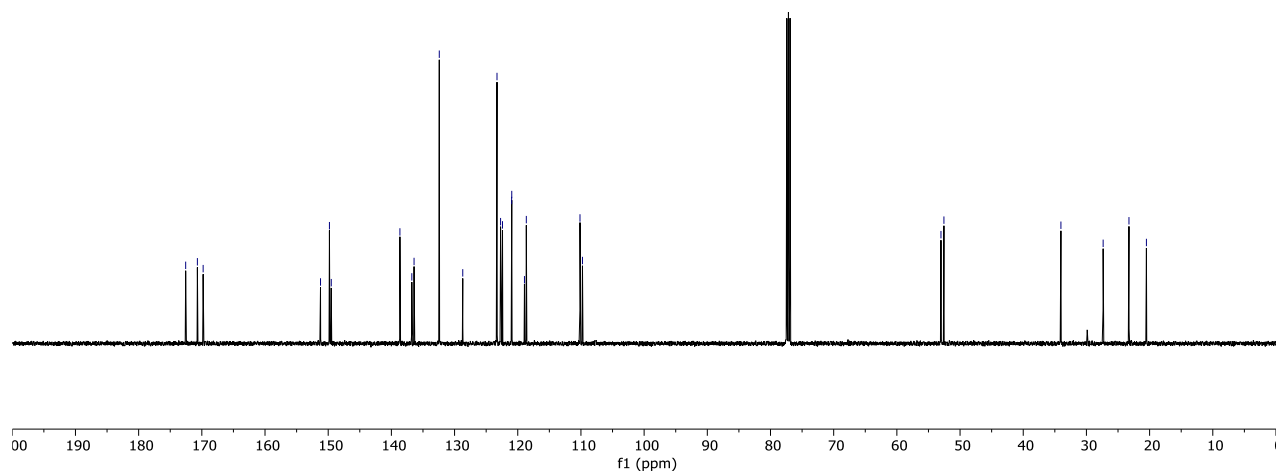
8. NMR Spectra



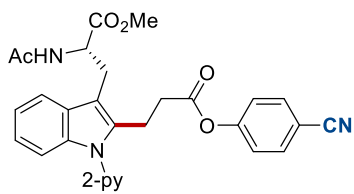
242ab
(CDCl₃, 300 MHz)



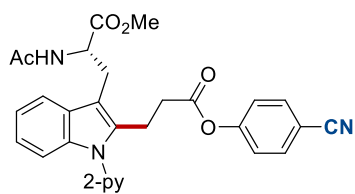
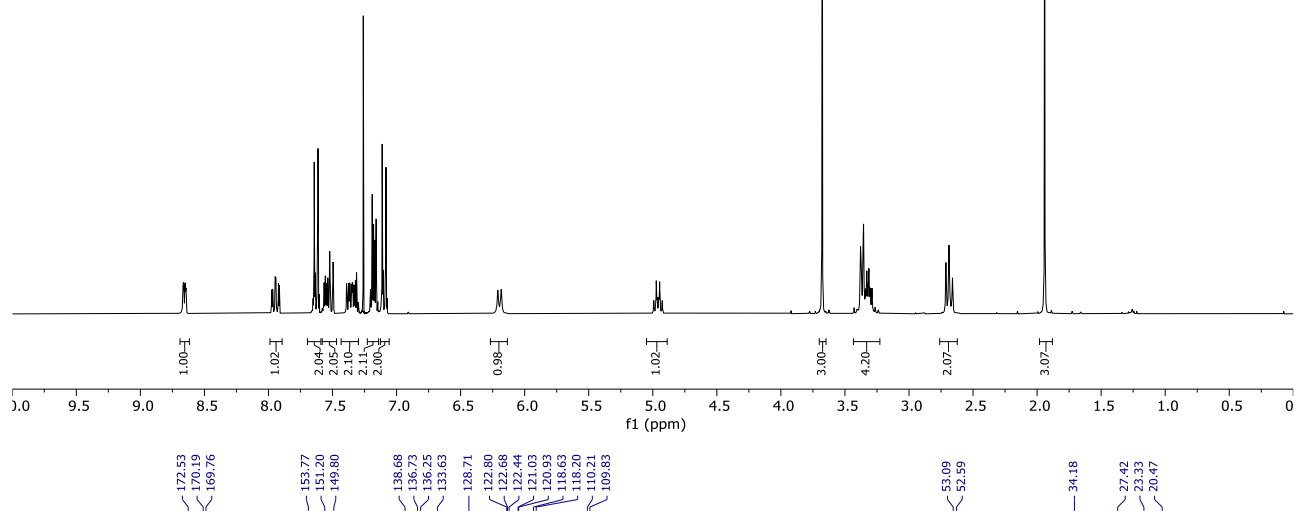
242ab
(CDCl₃, 126 MHz)



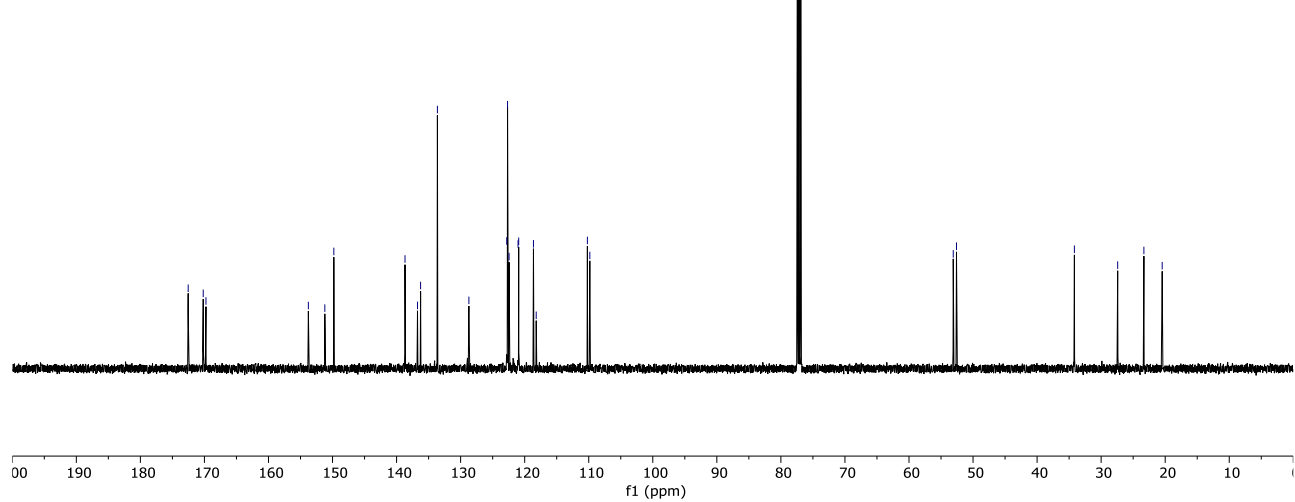
8. NMR Spectra



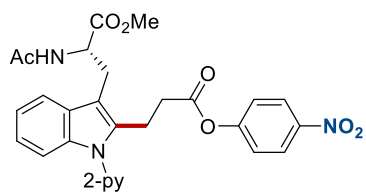
242ac
(CDCl₃, 300 MHz)



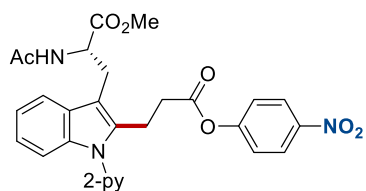
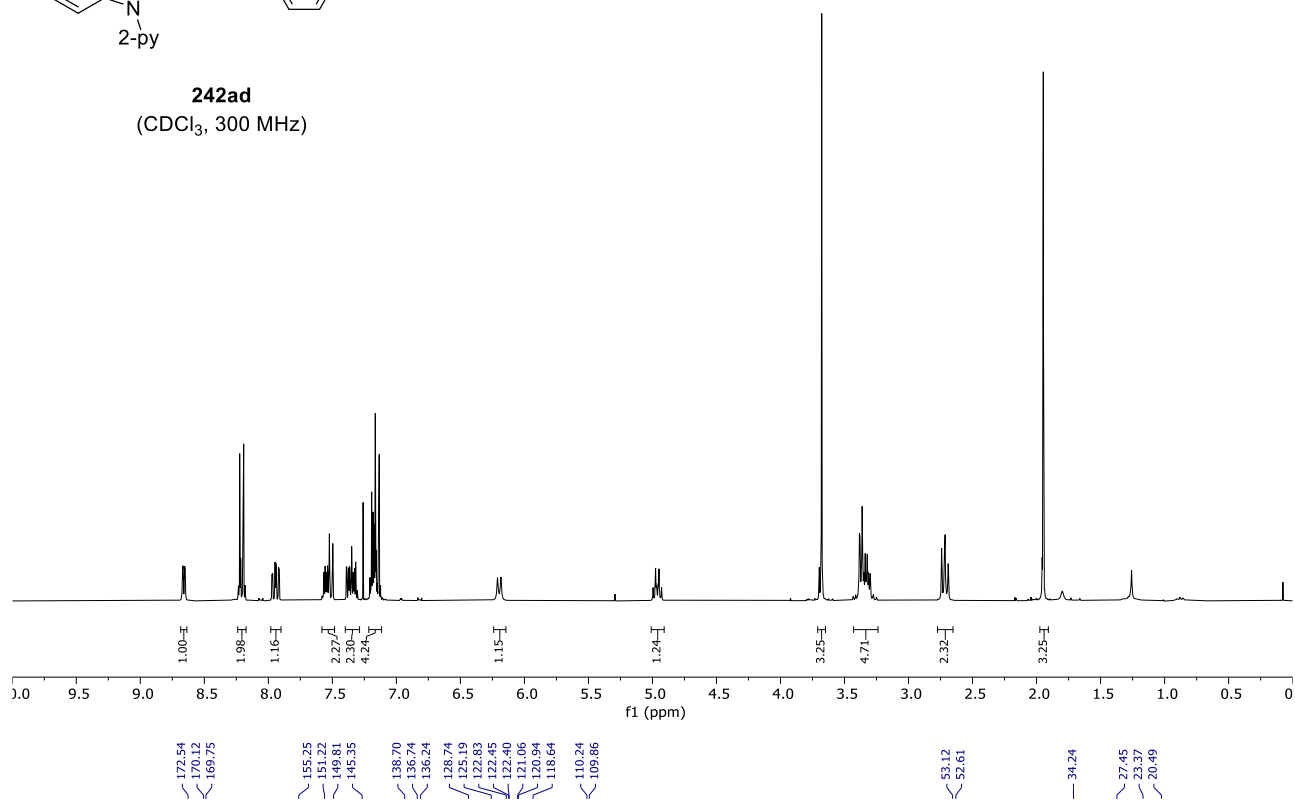
242ac
(CDCl₃, 126 MHz)



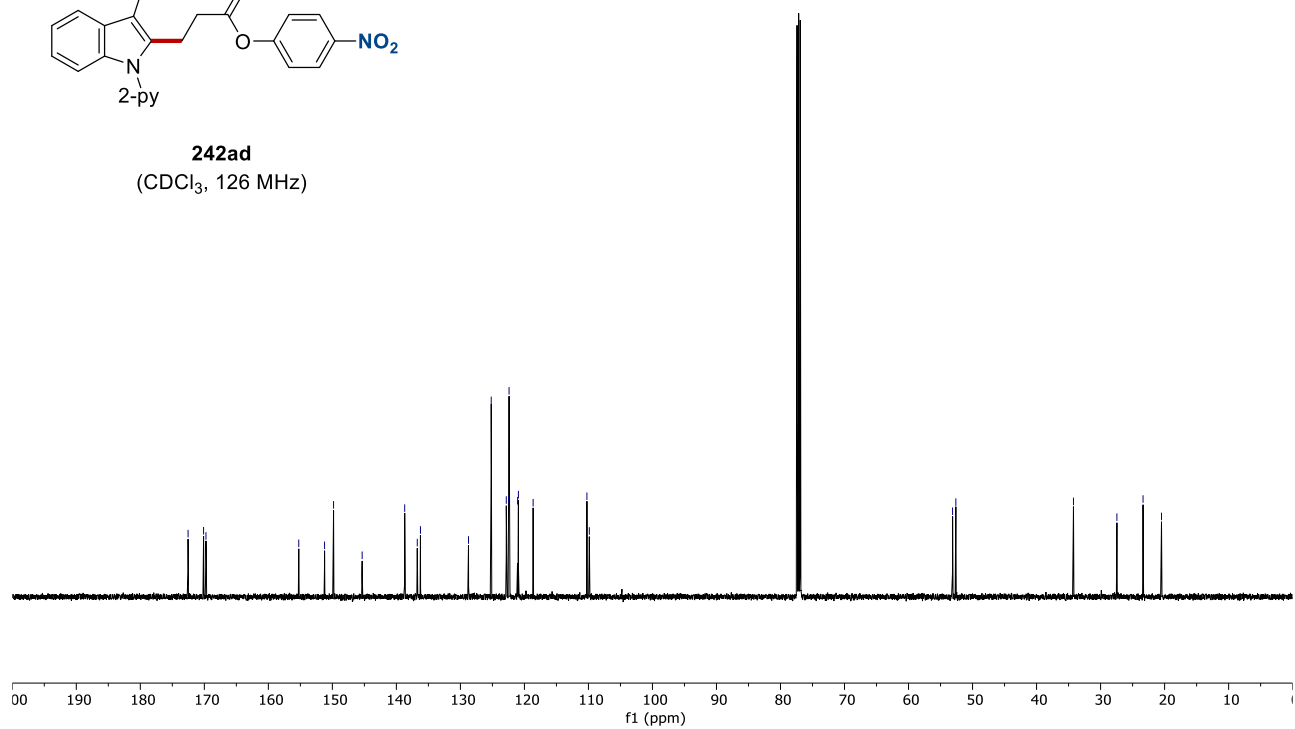
8. NMR Spectra

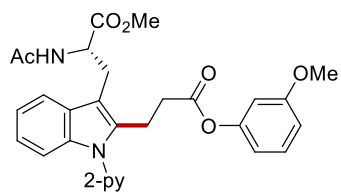


242ad
(CDCl₃, 300 MHz)

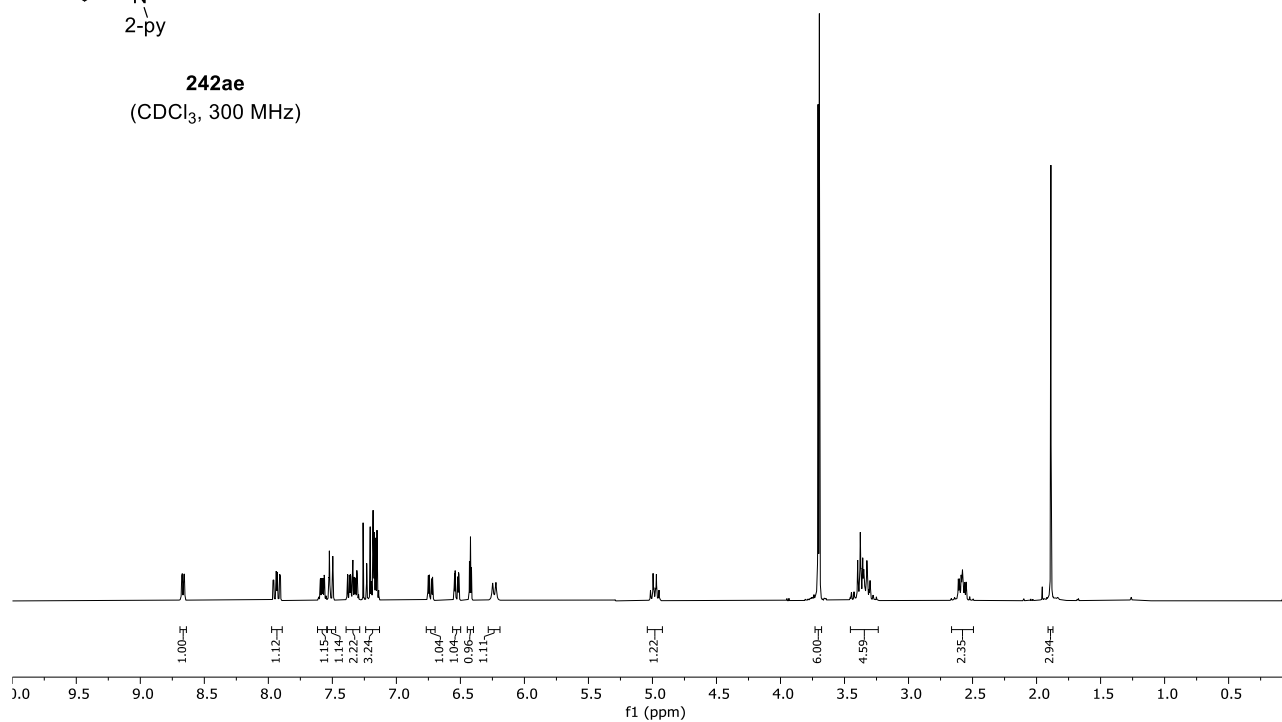


242ad
(CDCl₃, 126 MHz)



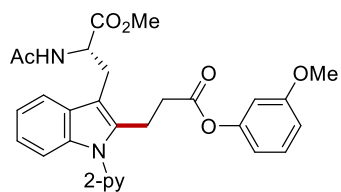


242ae
(CDCl₃, 300 MHz)

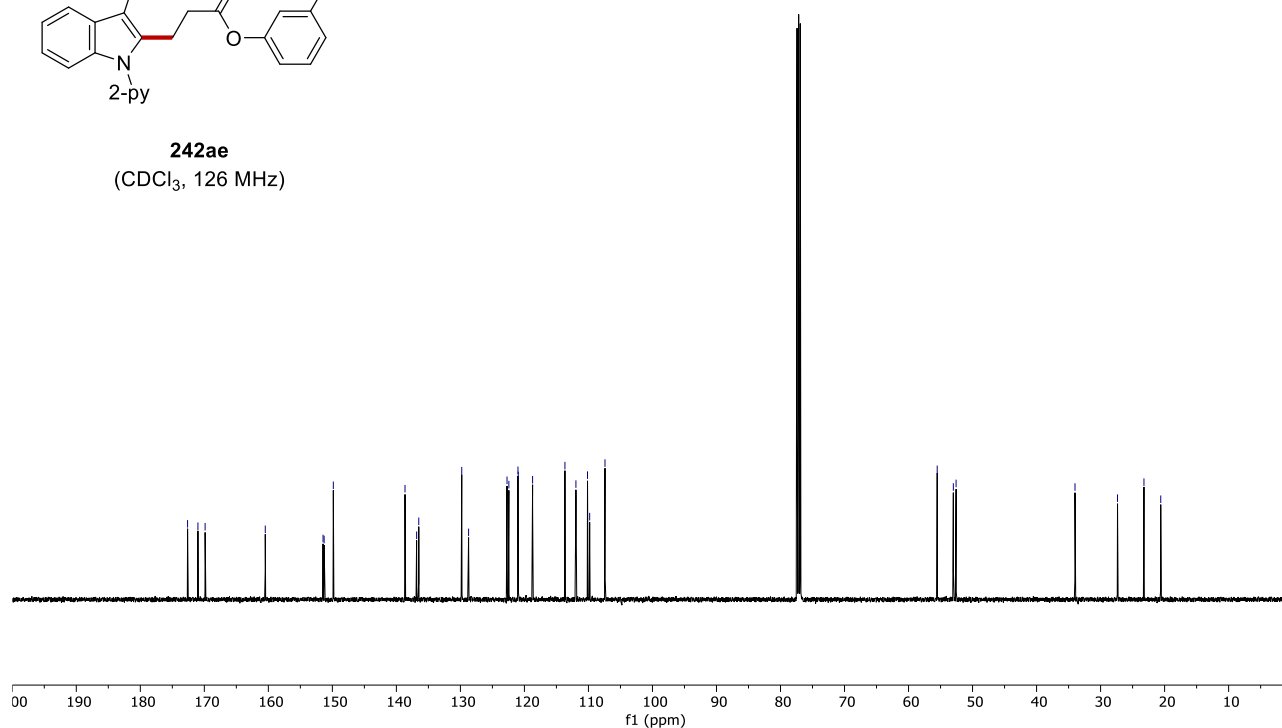


172.62
171.67
169.88
160.48
151.46
151.29
149.85
138.65
136.84
136.50
129.79
128.72
127.72
127.43
121.01
120.96
118.72
113.67
111.95
110.14
109.81
107.41

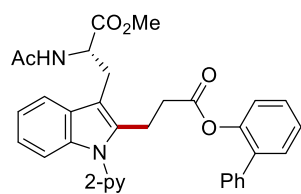
55.52
53.00
52.57
34.00
27.36
23.23
20.60



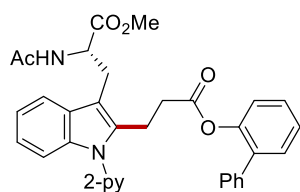
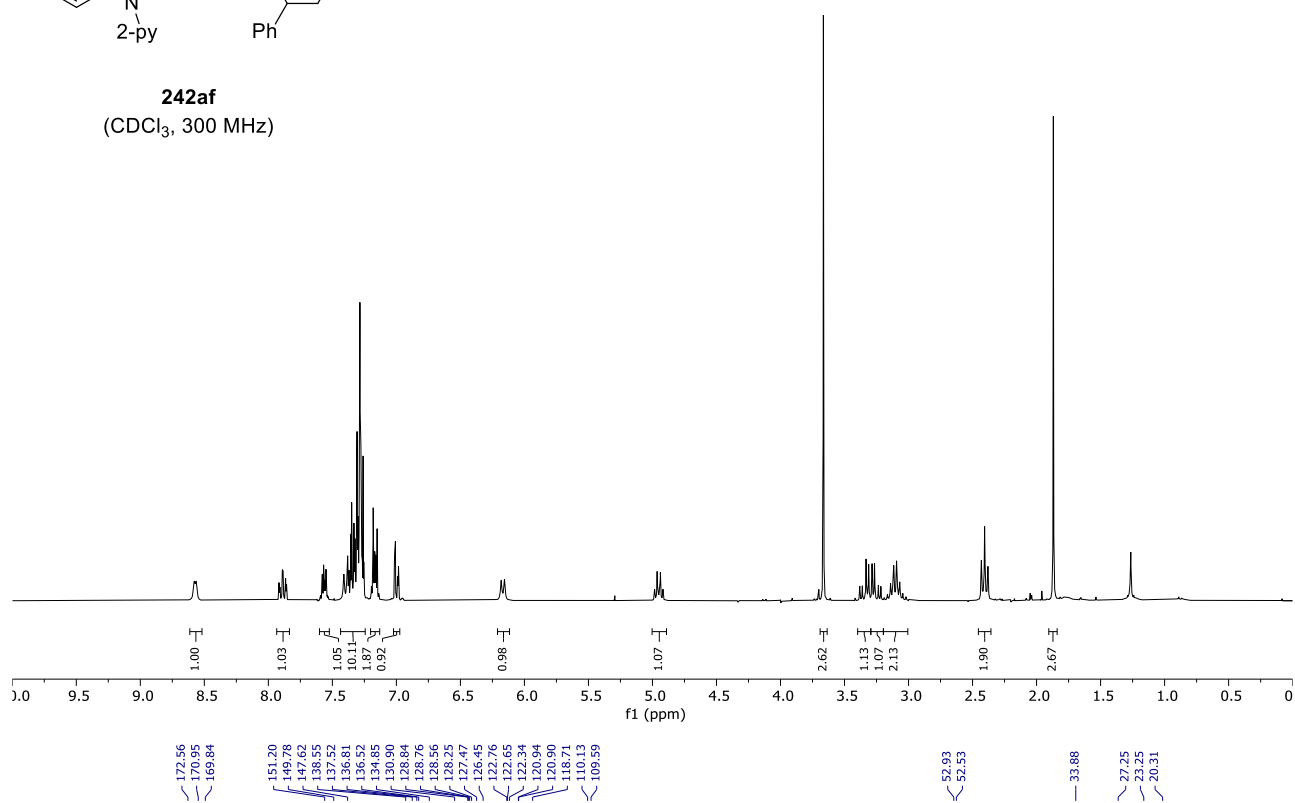
242ae
(CDCl₃, 126 MHz)



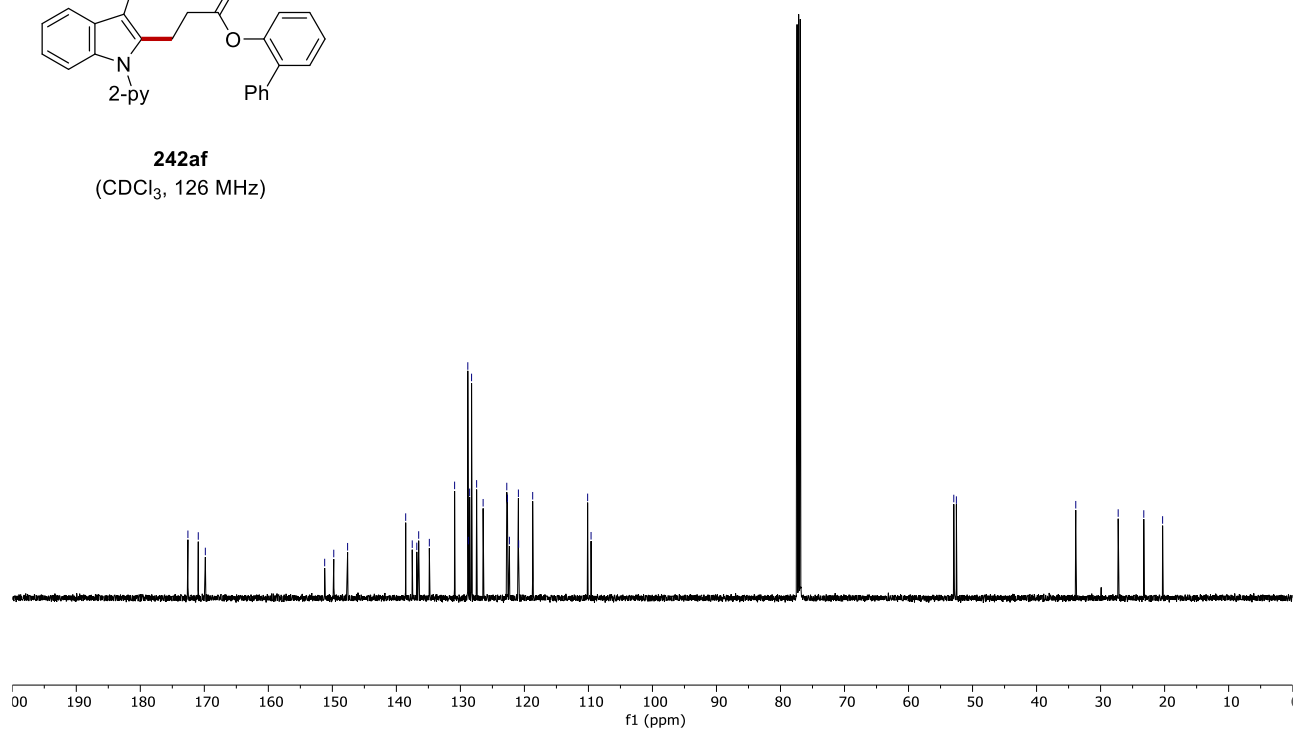
8. NMR Spectra

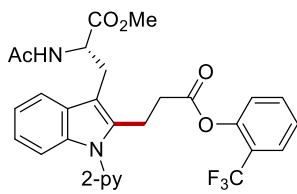


242af
(CDCl₃, 300 MHz)

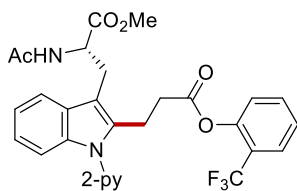
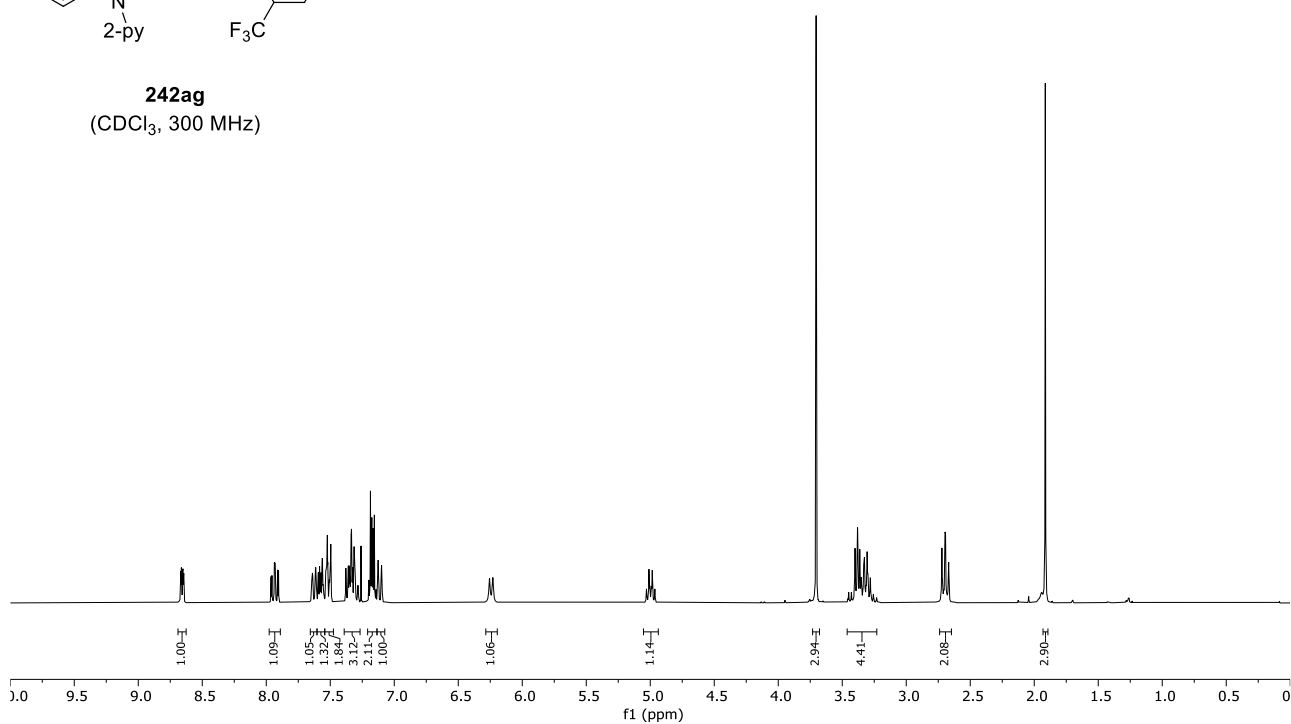


242af
(CDCl₃, 126 MHz)

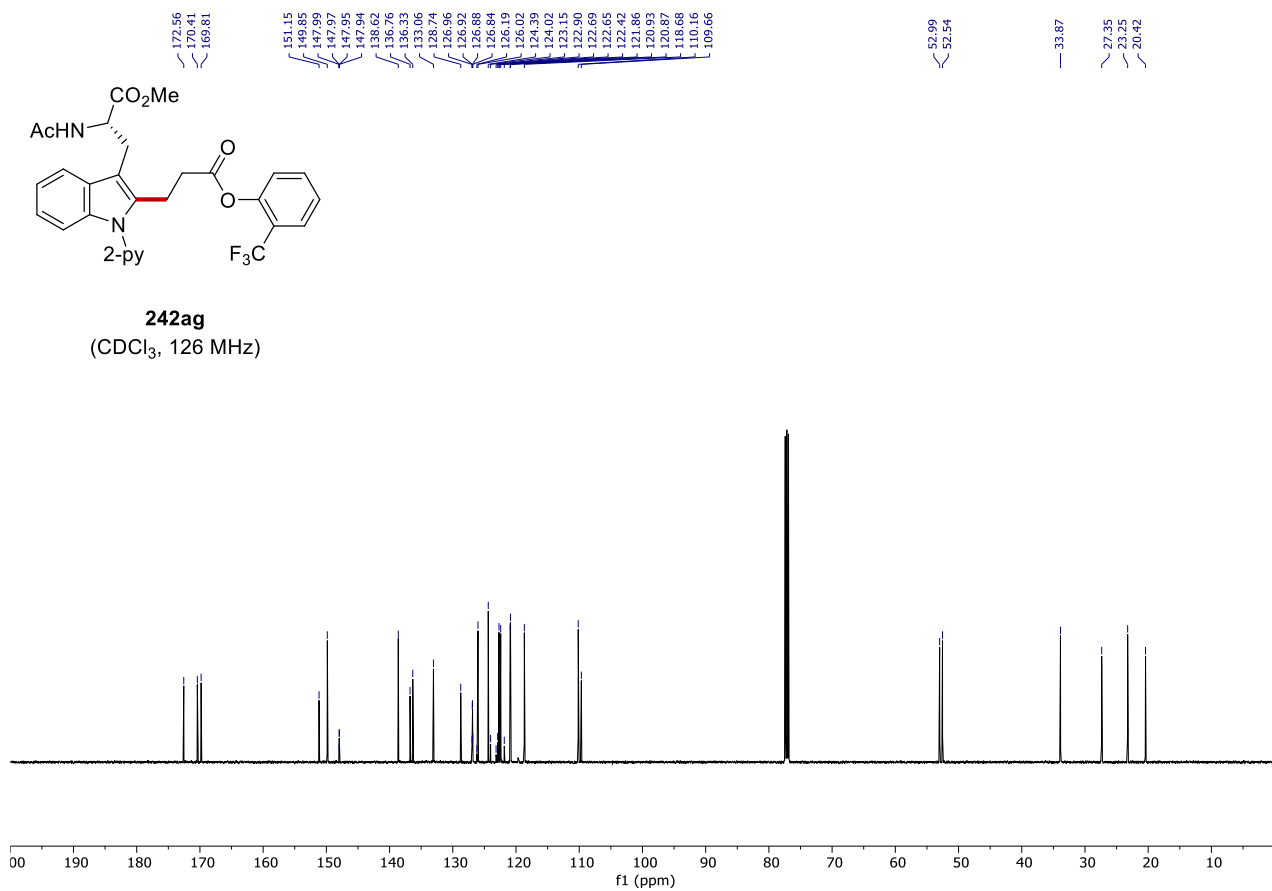




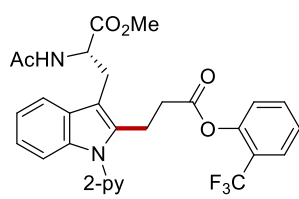
242ag
(CDCl₃, 300 MHz)



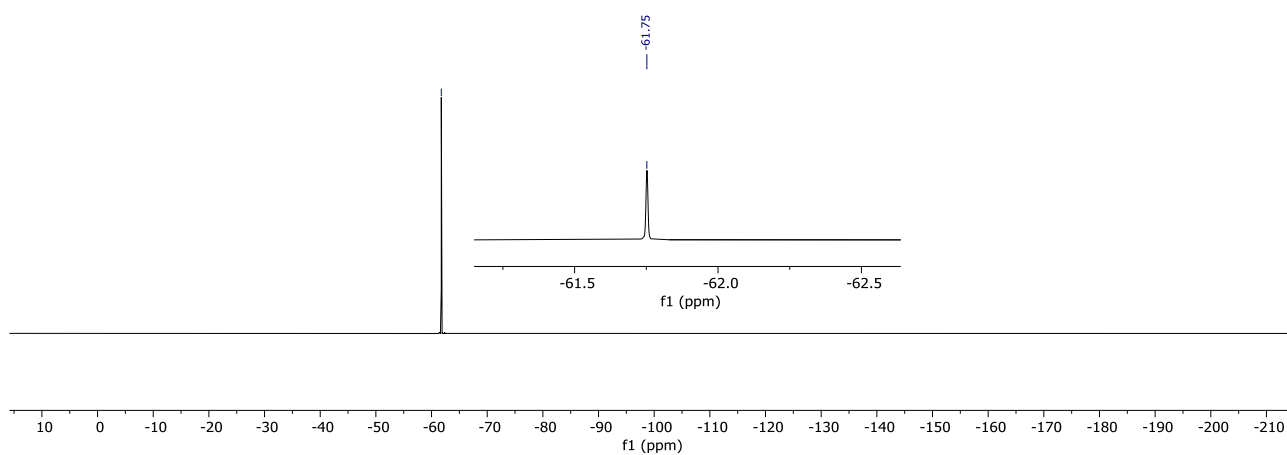
242ag
(CDCl₃, 126 MHz)

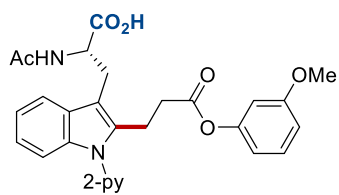


8. NMR Spectra

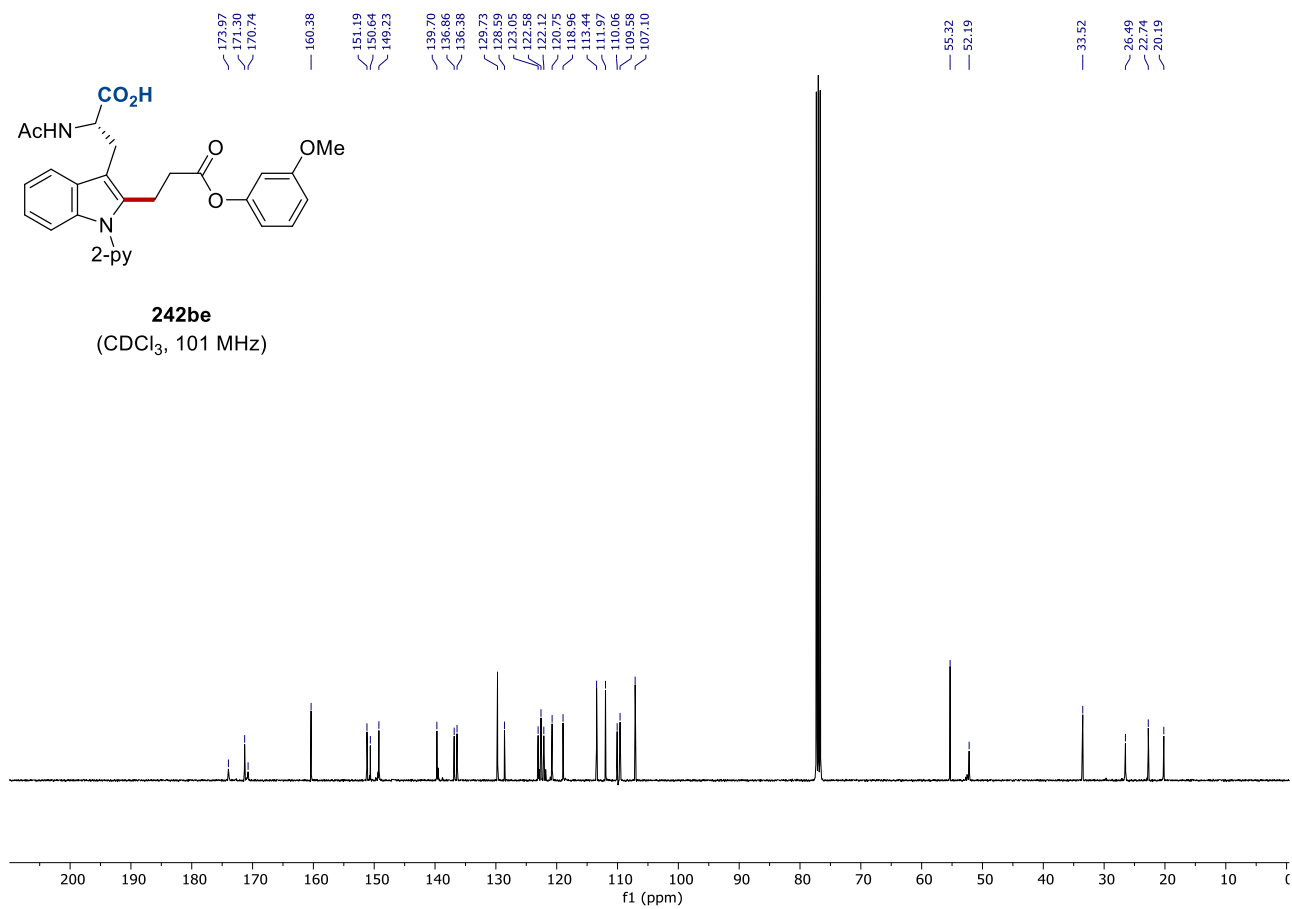
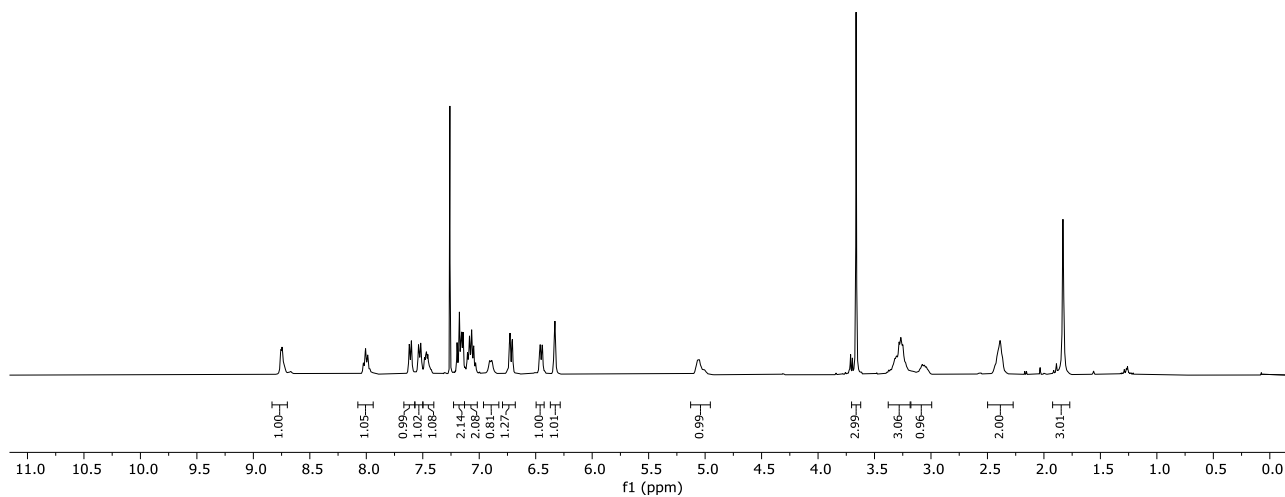


242ag
(CDCl₃, 282 MHz)

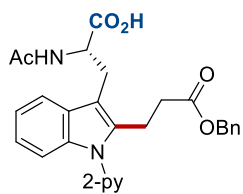




242be
(CDCl₃, 400 MHz)

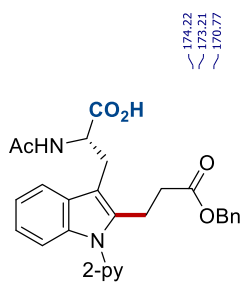
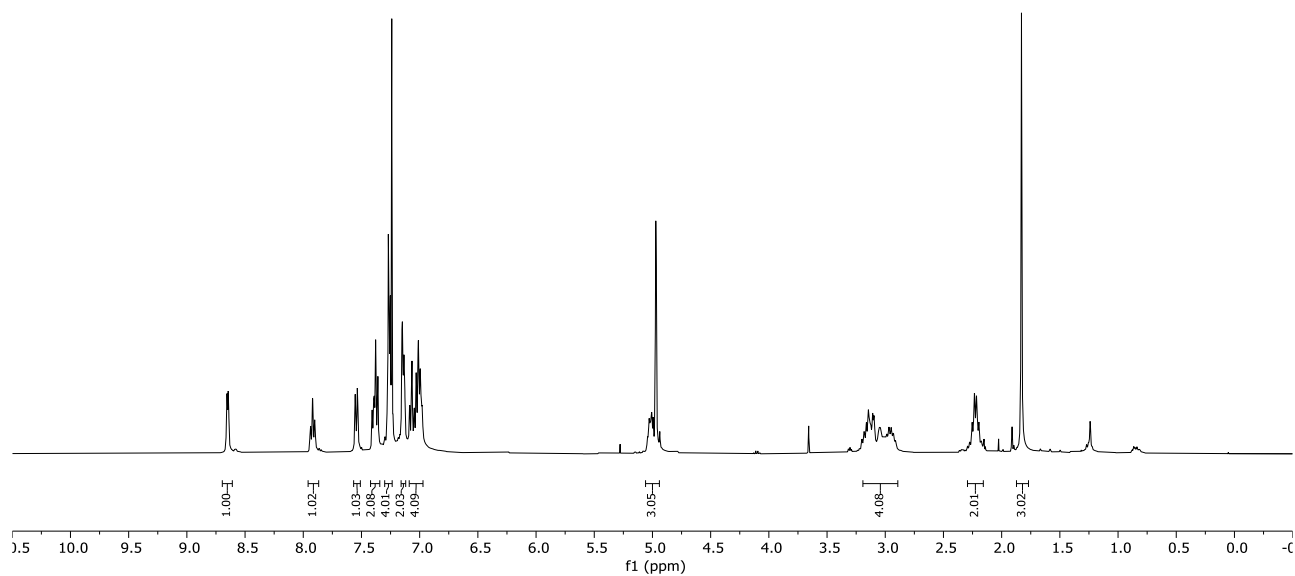


8. NMR Spectra



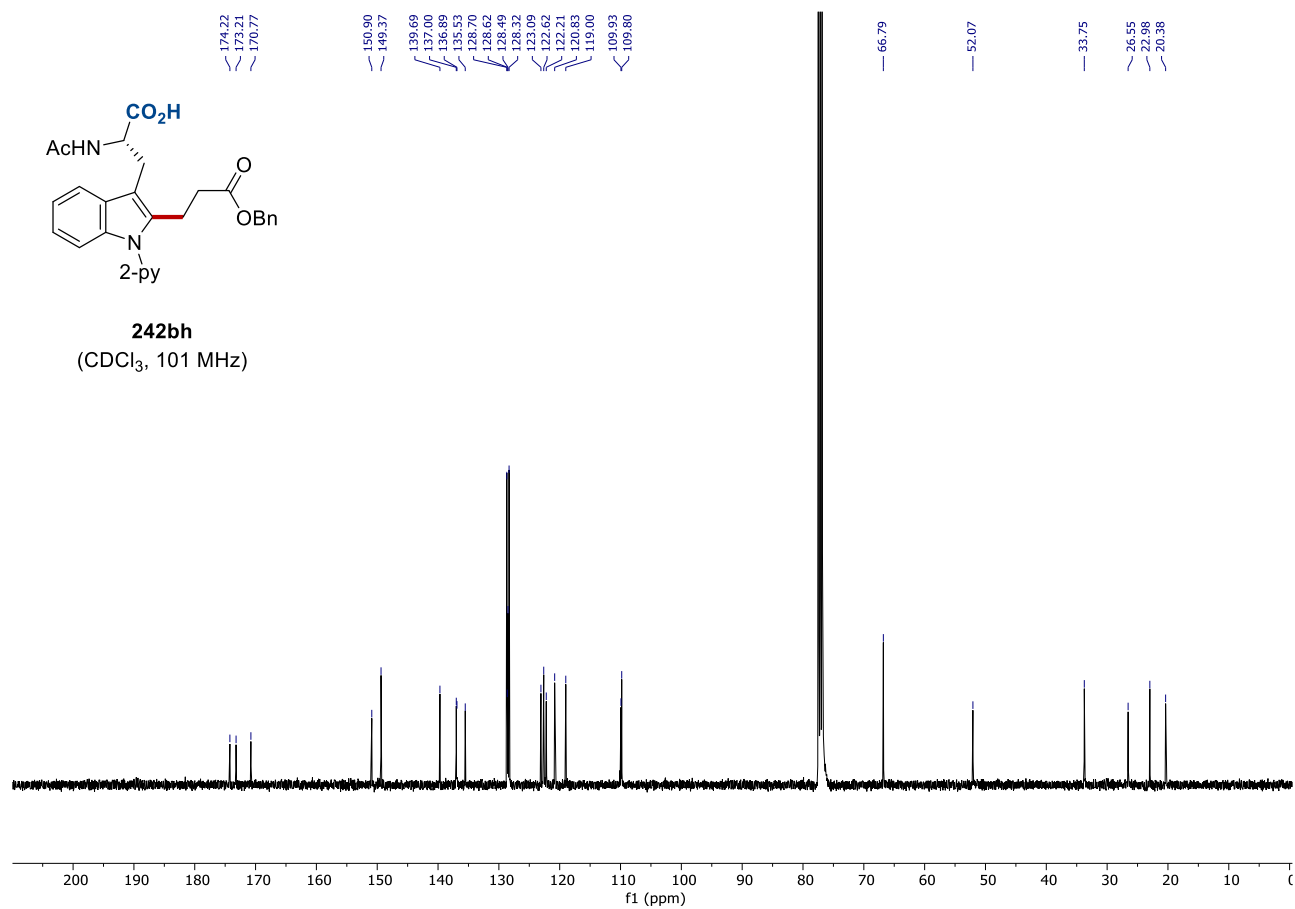
242bh

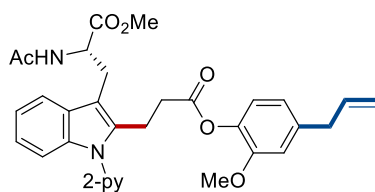
(CDCl₃, 400 MHz)



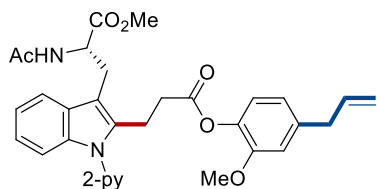
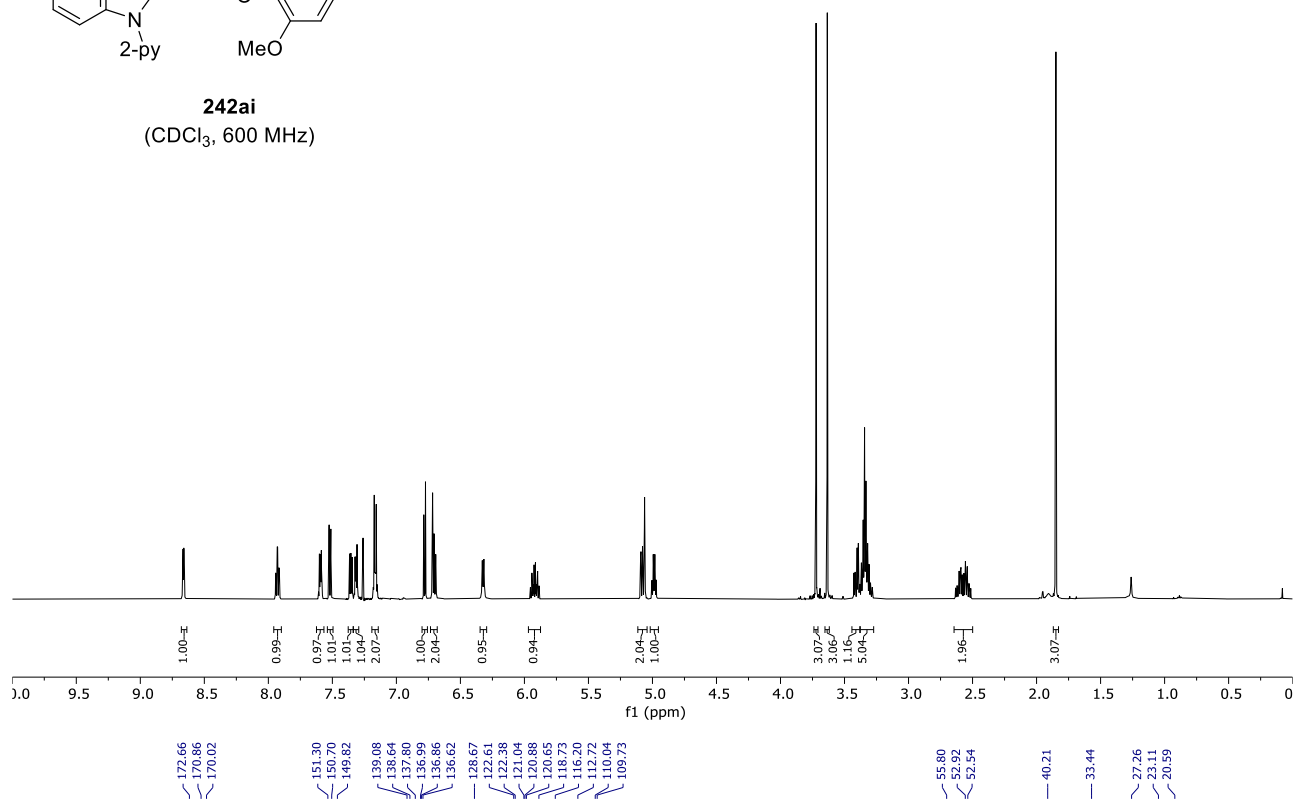
242bh

(CDCl₃, 101 MHz)

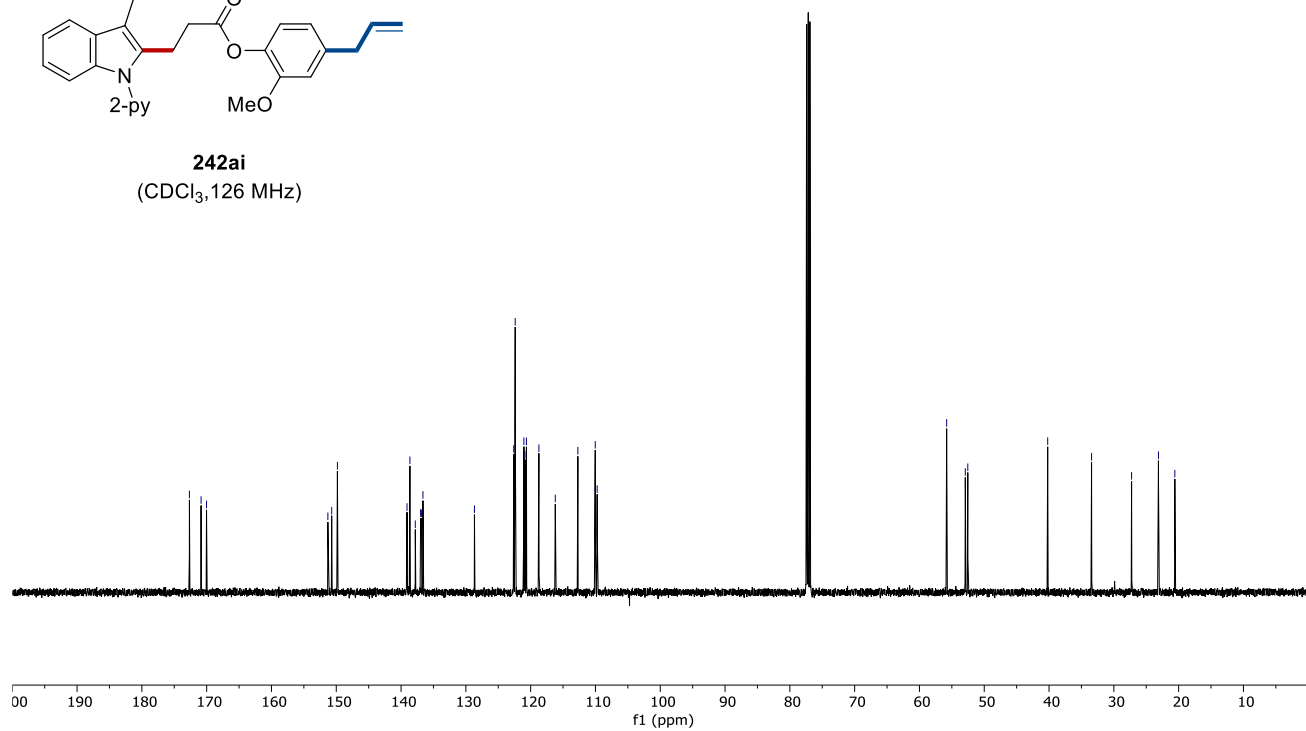




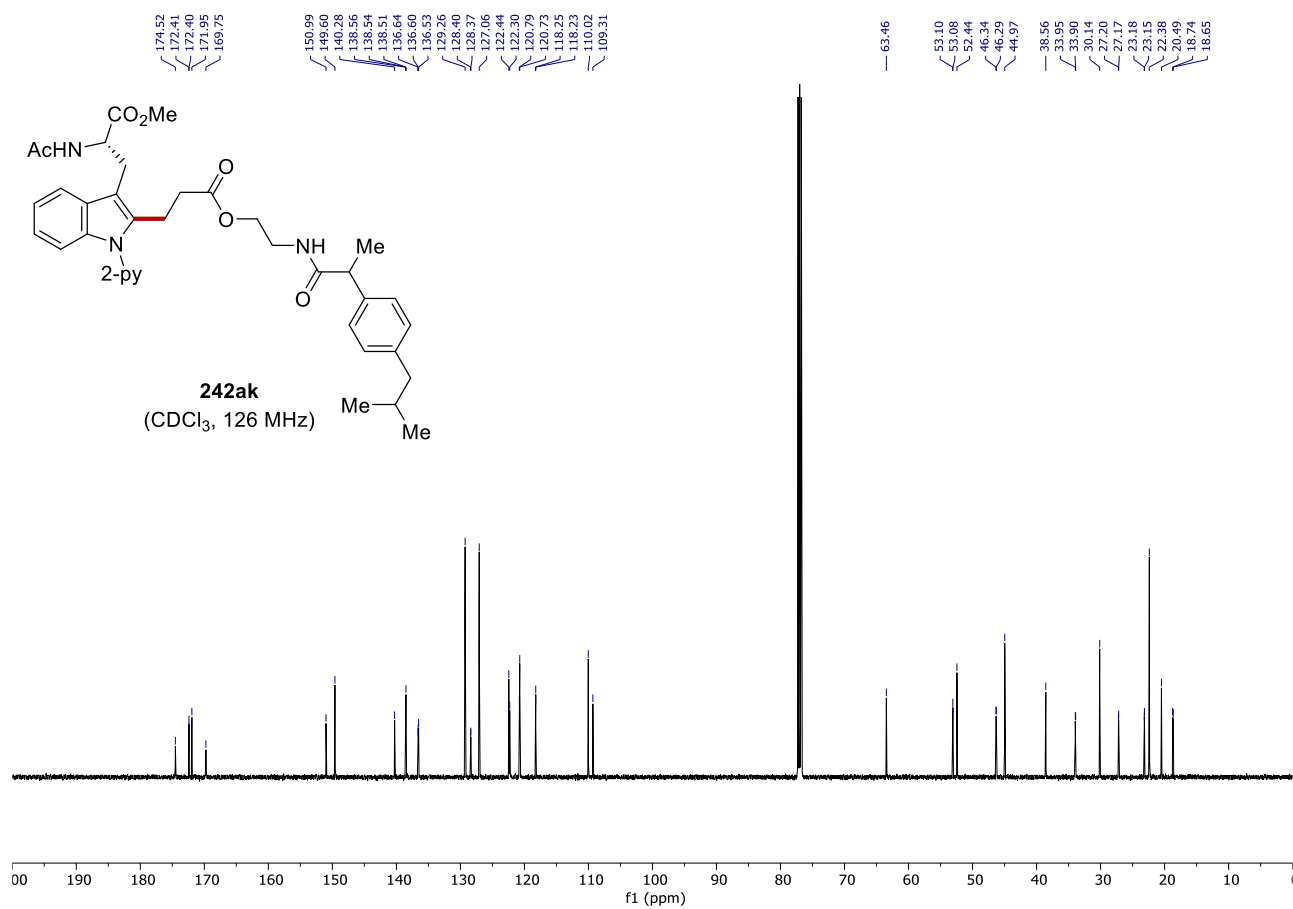
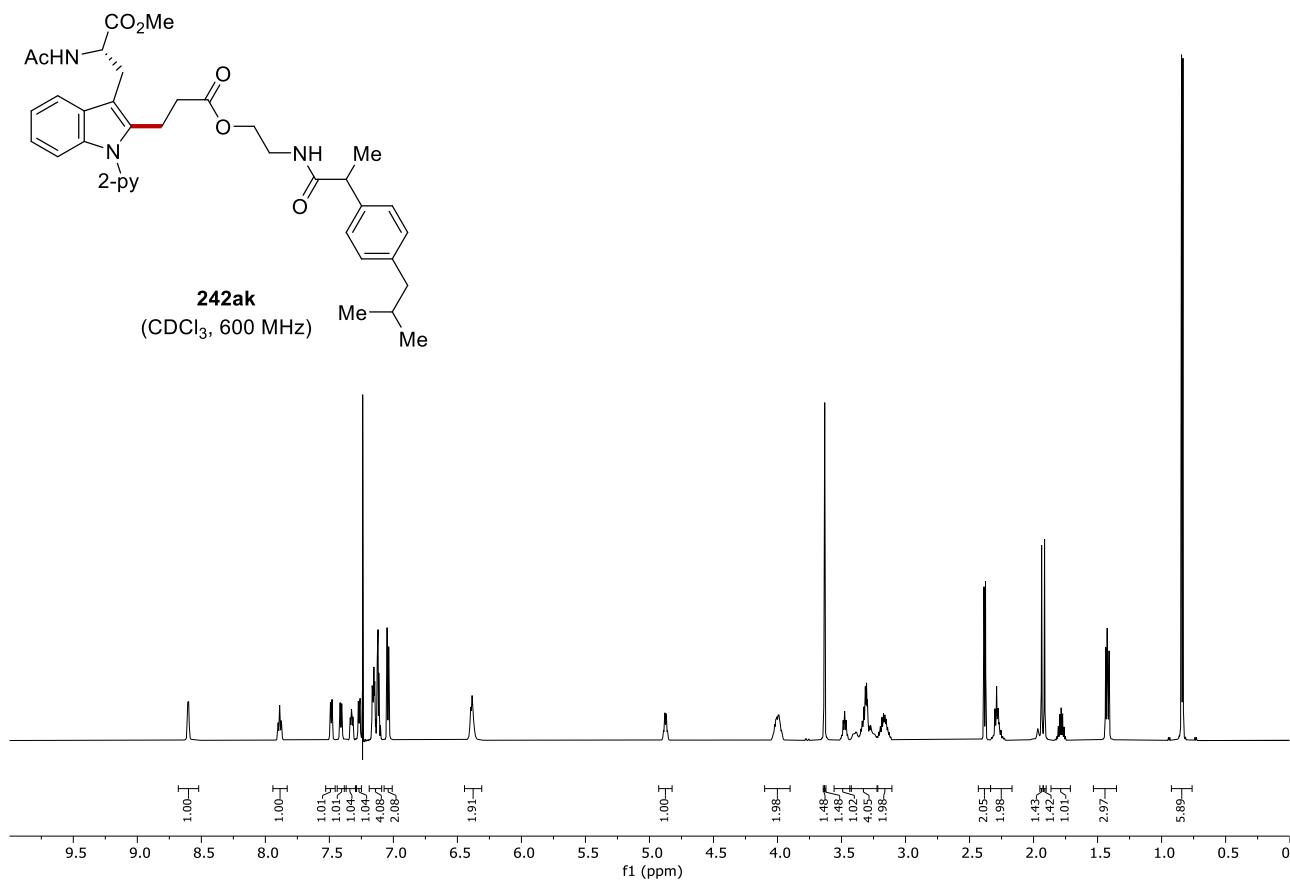
242ai
(CDCl₃, 600 MHz)



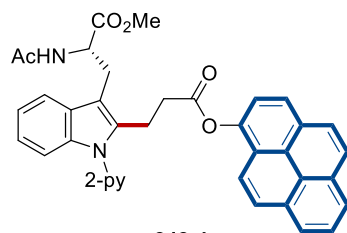
242ai
(CDCl₃, 126 MHz)



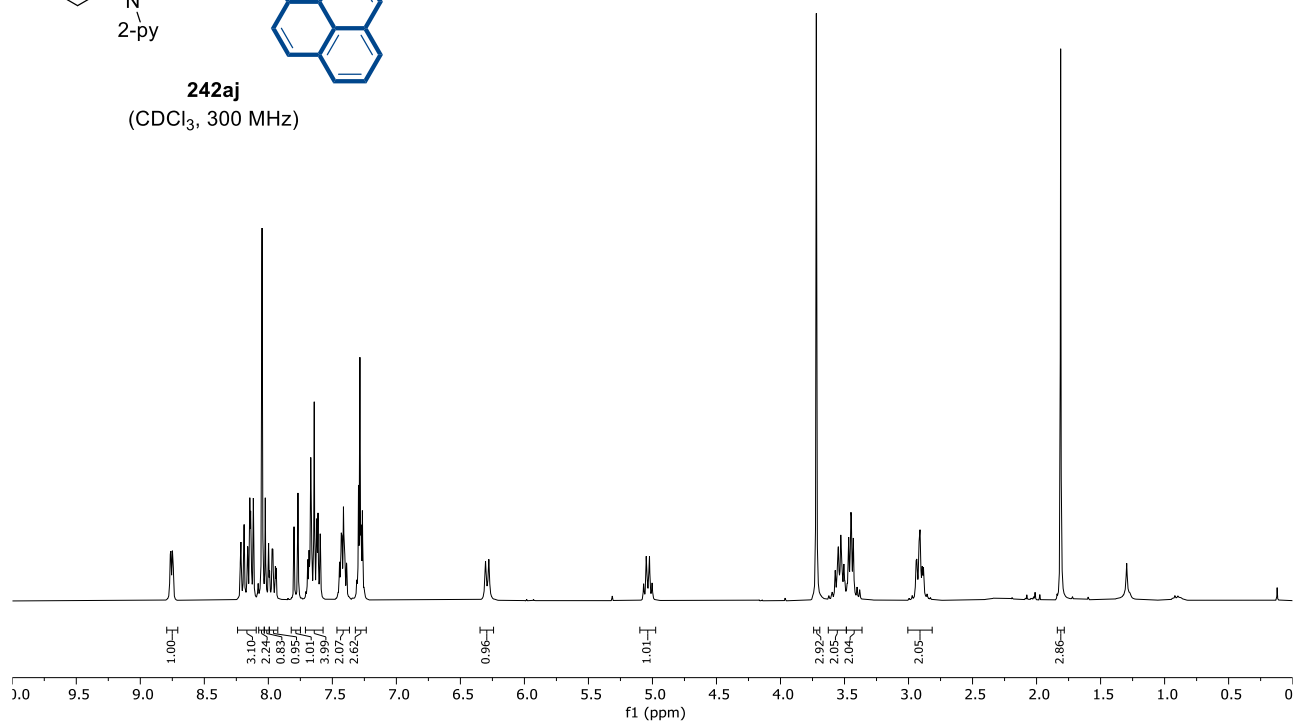
8. NMR Spectra



8. NMR Spectra



242aj
(CDCl₃, 300 MHz)



172.81
171.78
170.11
151.32
149.84
144.15
139.05
137.01
136.50
130.88
130.88
129.48
128.93
128.29
127.30
127.14
126.46
125.65
125.60
125.42
125.05
124.54
124.54
123.97
122.62
121.24
121.19
120.10
119.64
119.00
110.34
110.25

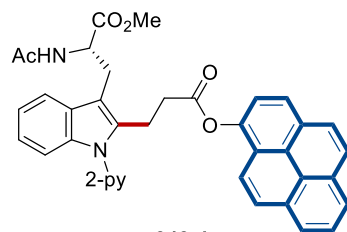
52.95
52.60

33.97

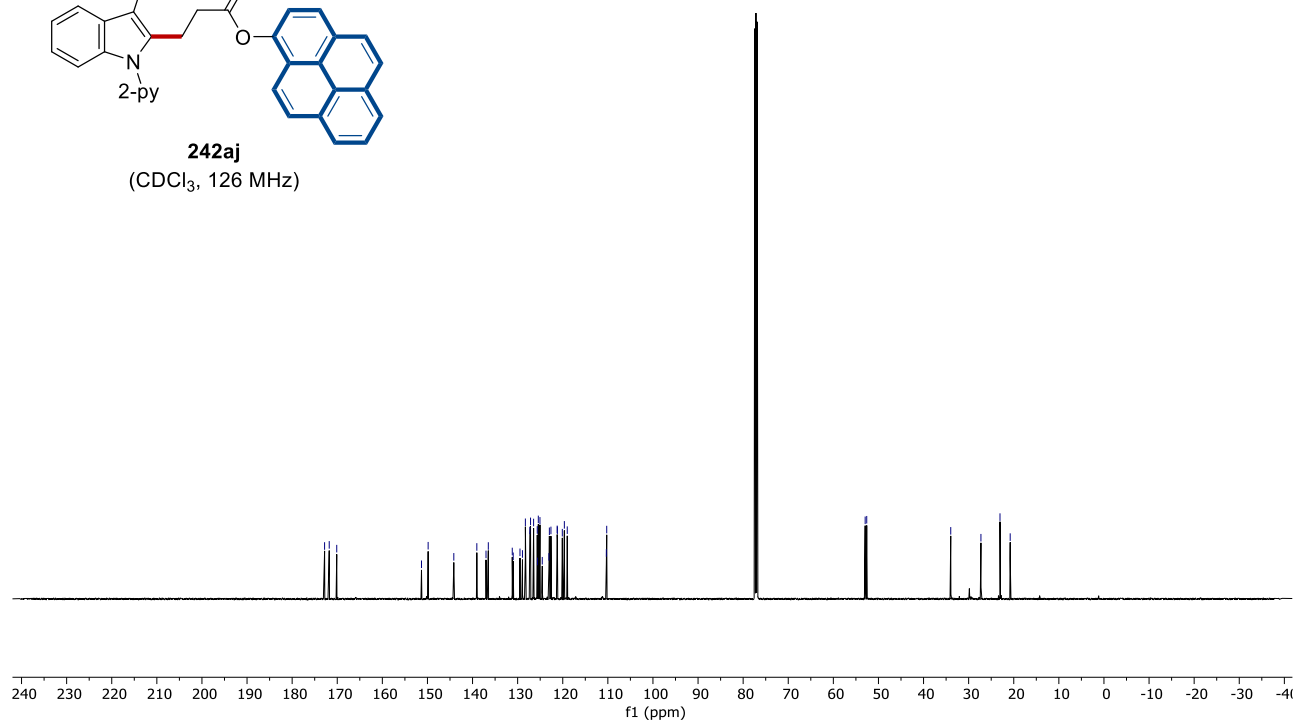
27.28

23.05

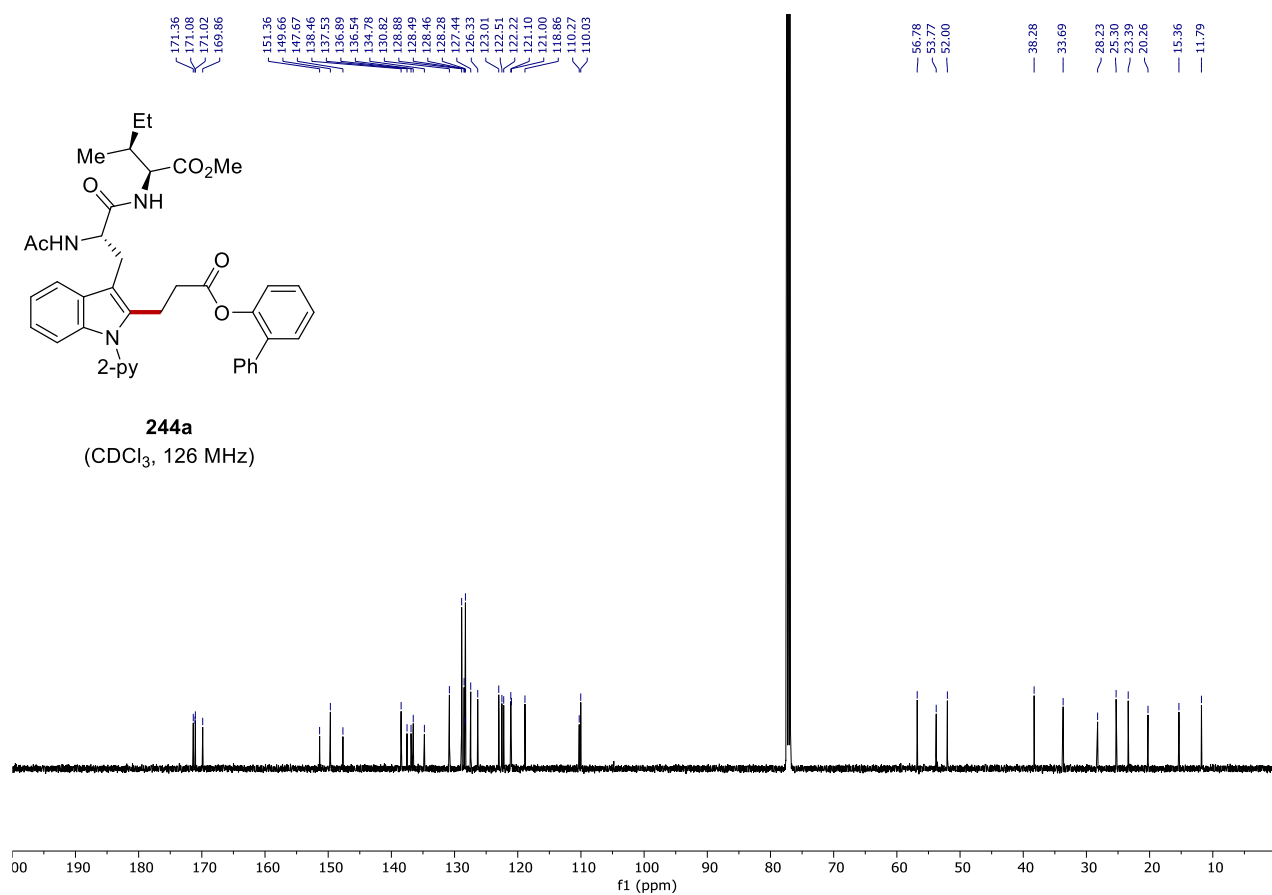
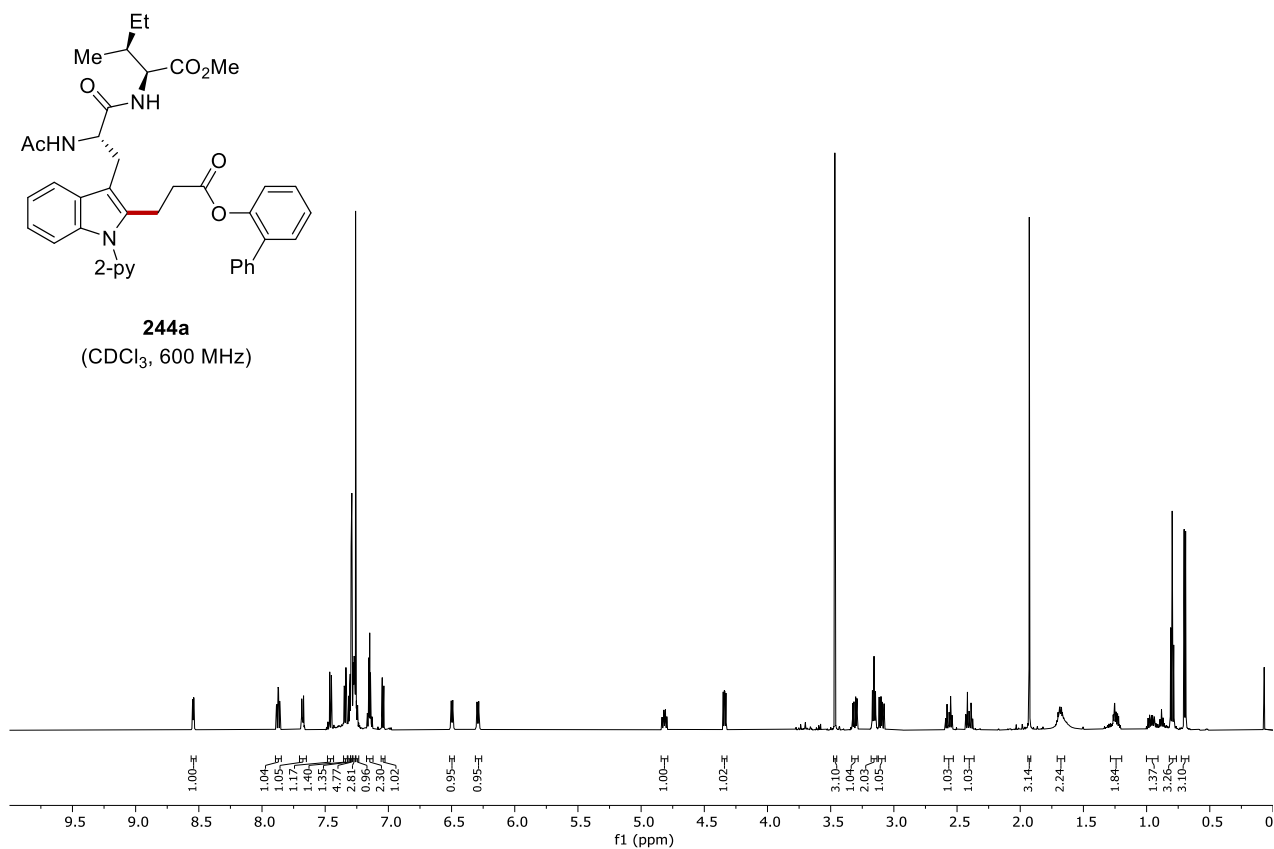
20.79

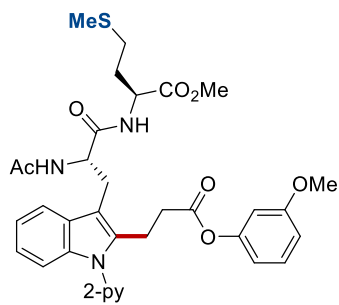


242aj
(CDCl₃, 126 MHz)

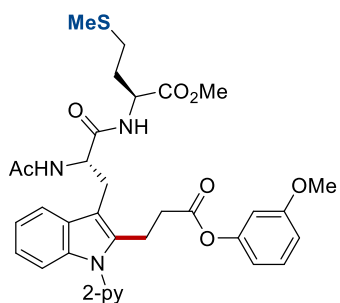
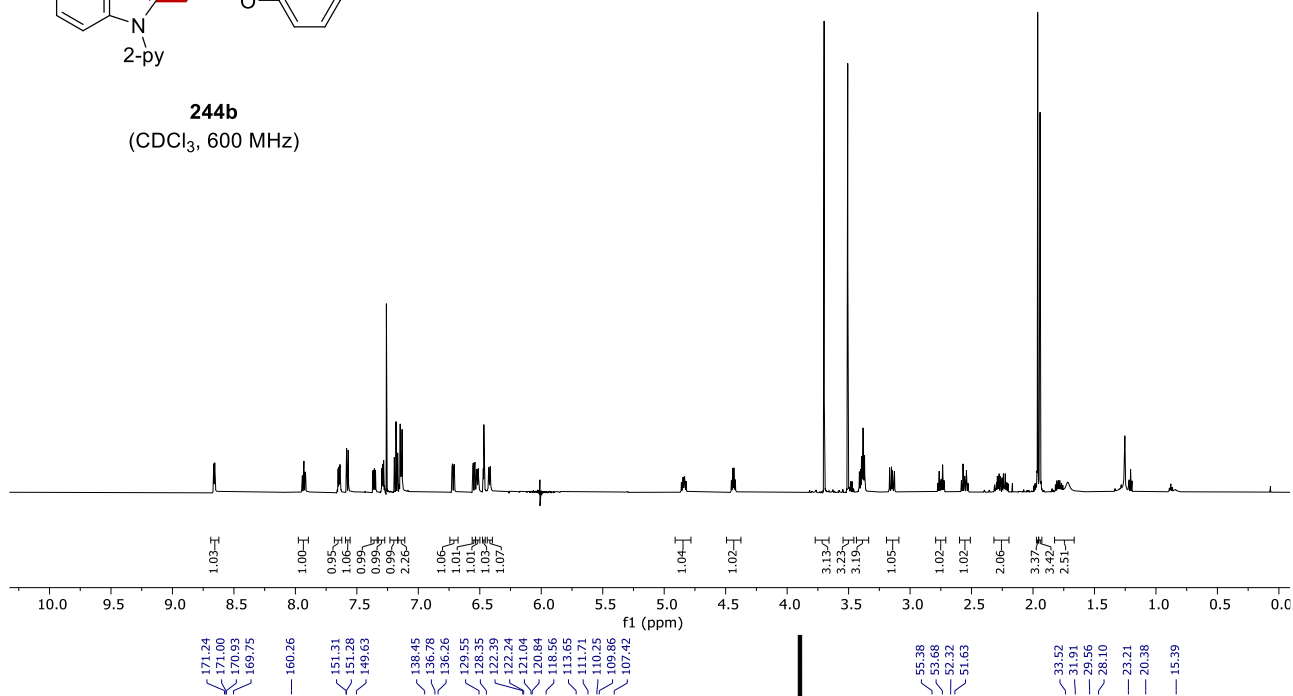


8. NMR Spectra

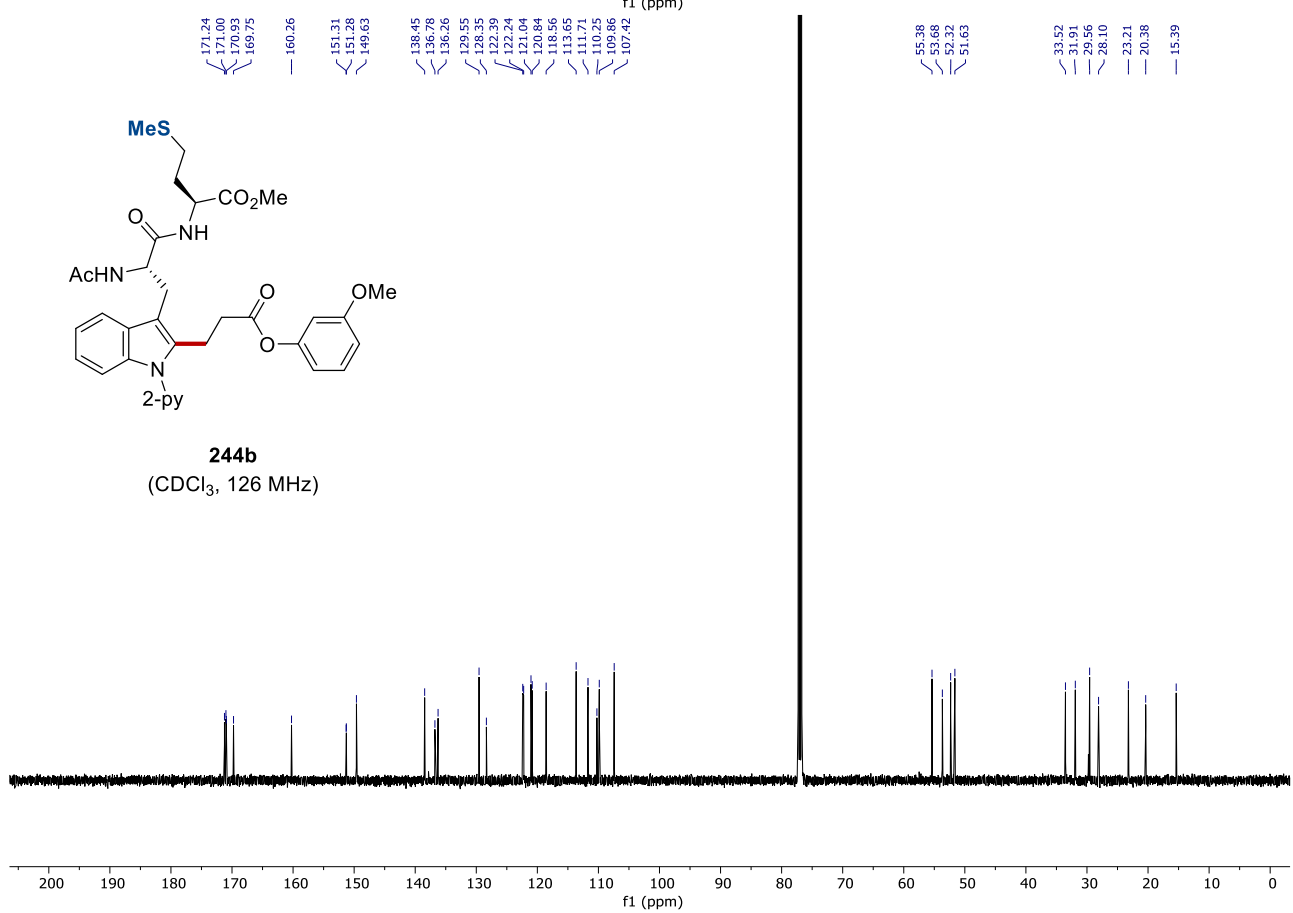




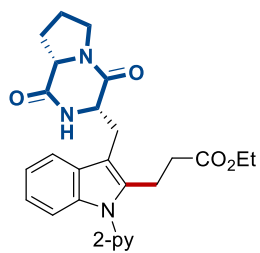
244b
(CDCl₃, 600 MHz)



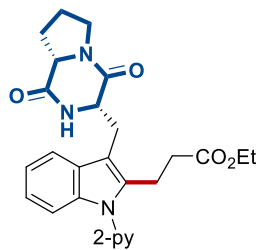
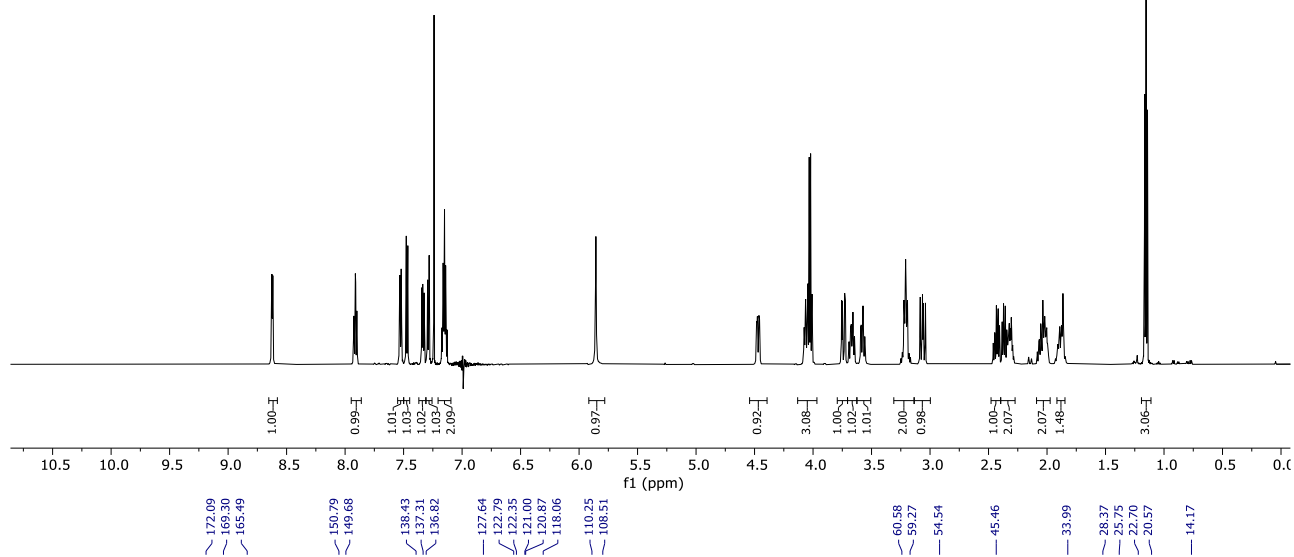
244b
(CDCl₃, 126 MHz)



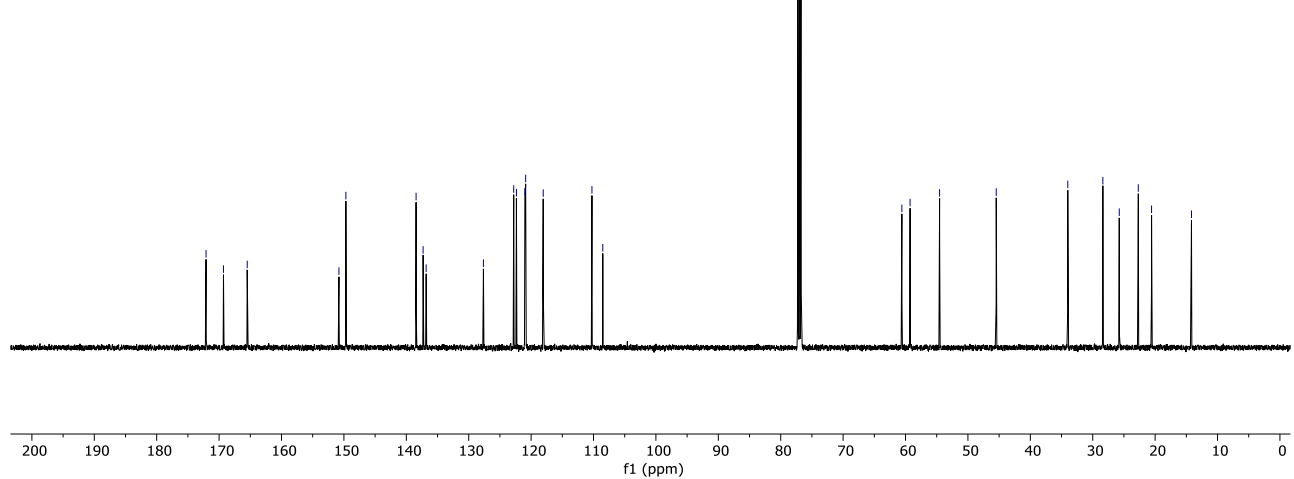
8. NMR Spectra

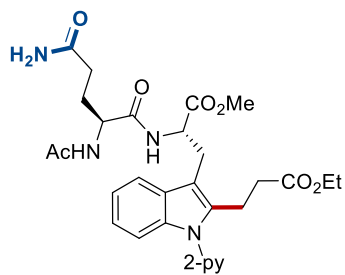


244c
(CDCl₃, 600 MHz)

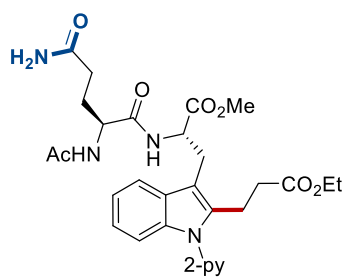
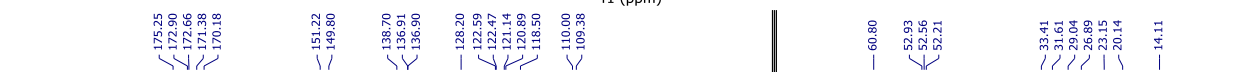
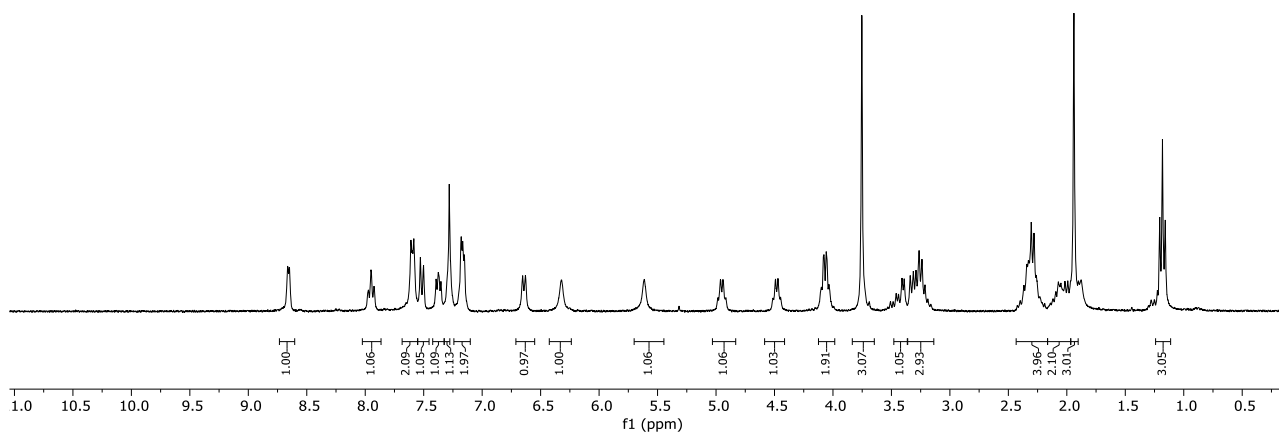


244c
(CDCl₃, 126 MHz)

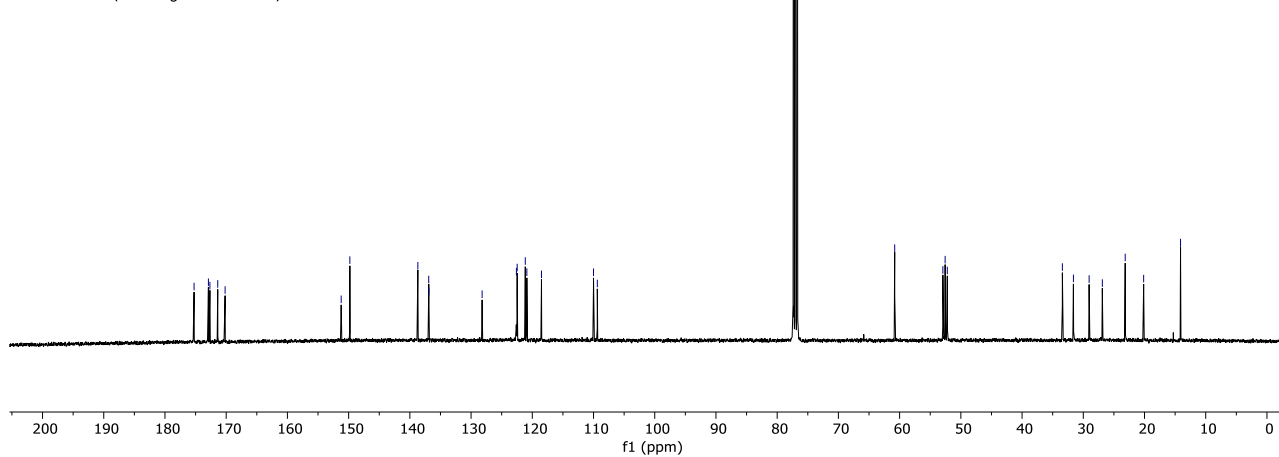




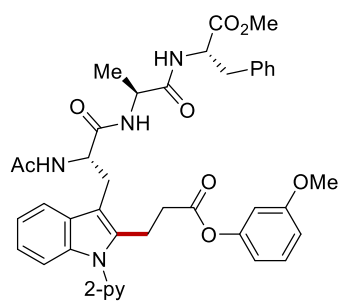
244d
(CDCl₃, 300 MHz)



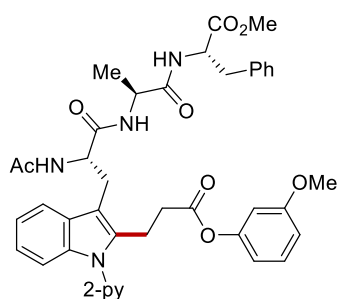
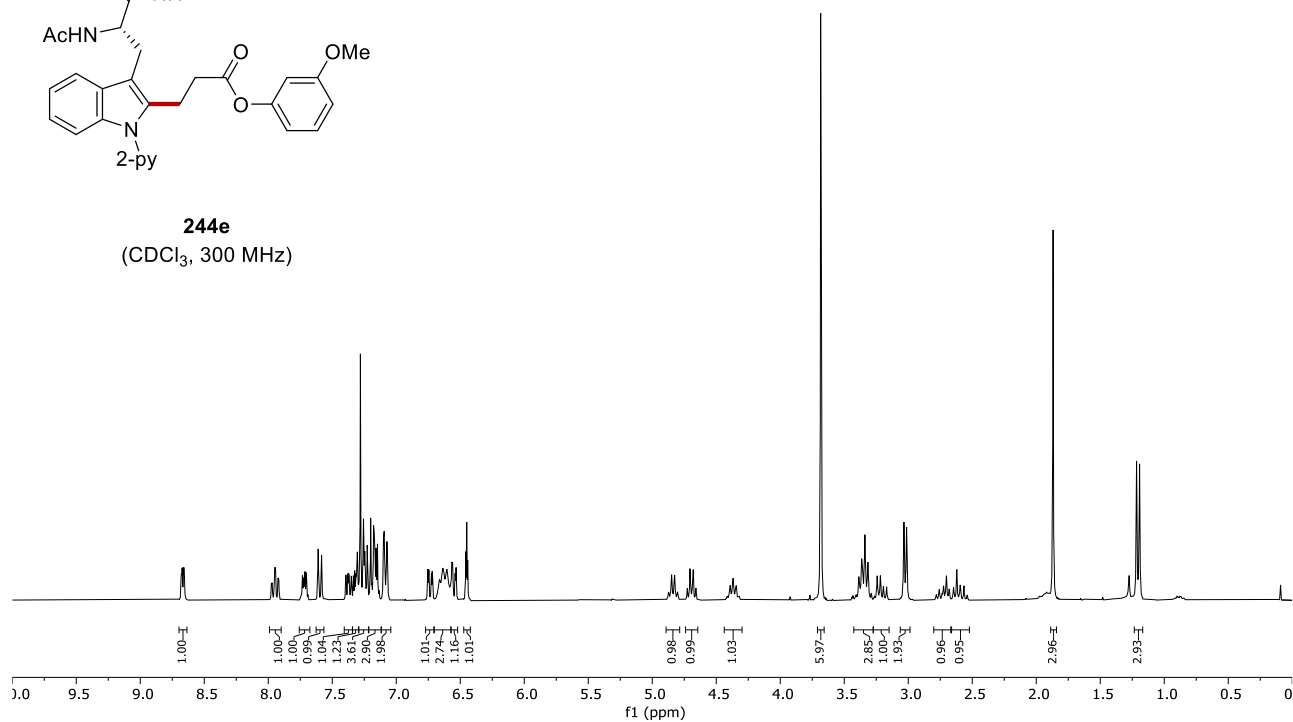
244d
(CDCl₃, 101 MHz)



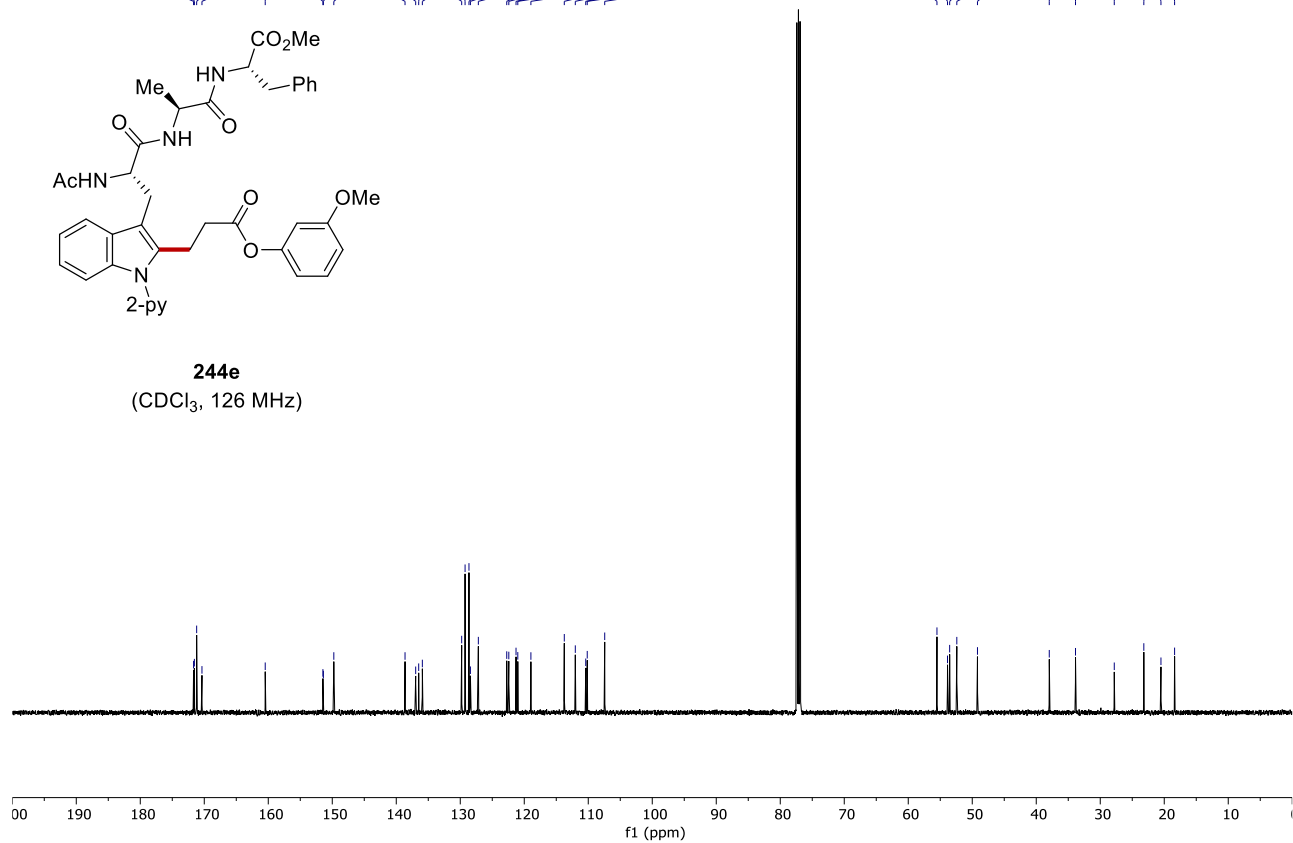
8. NMR Spectra

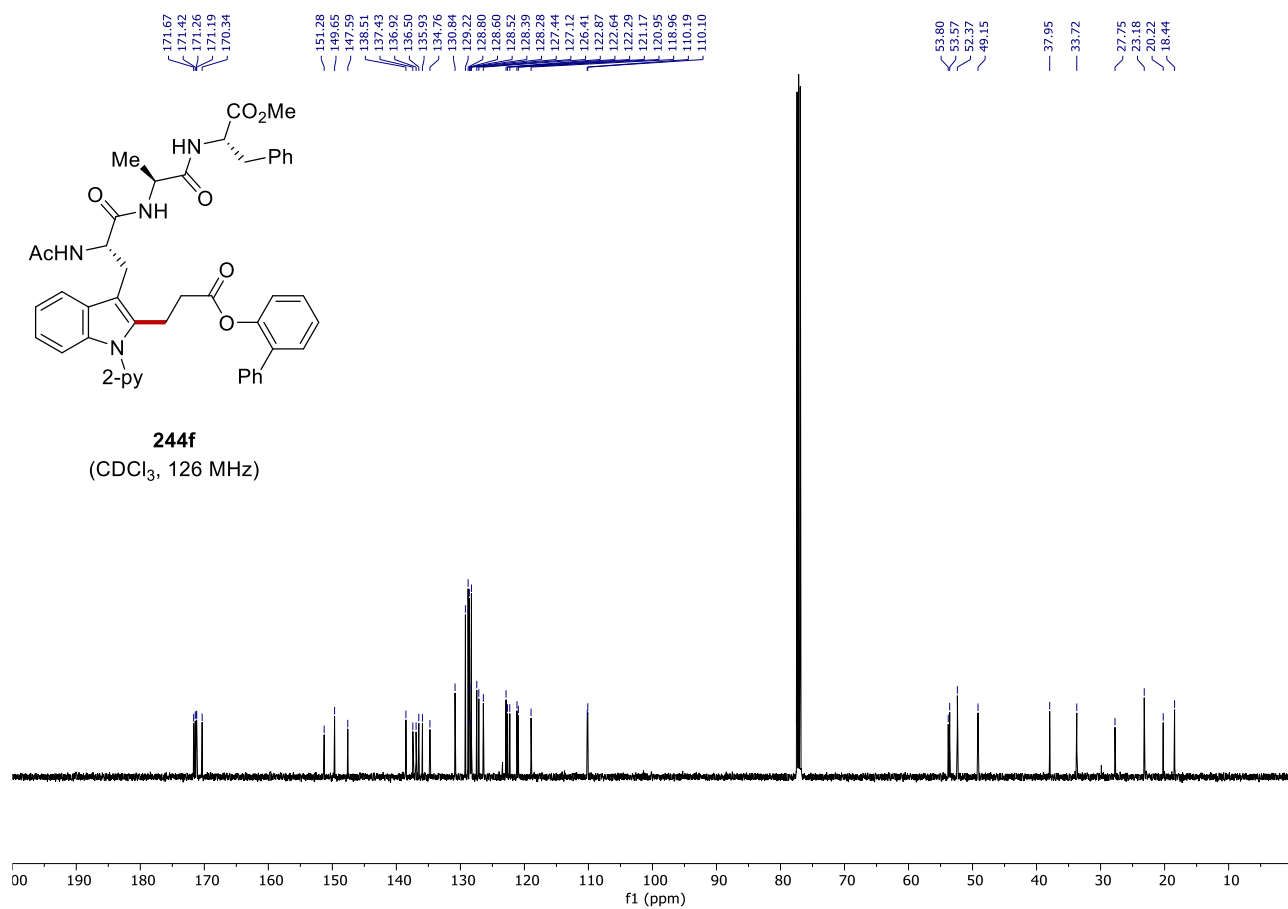
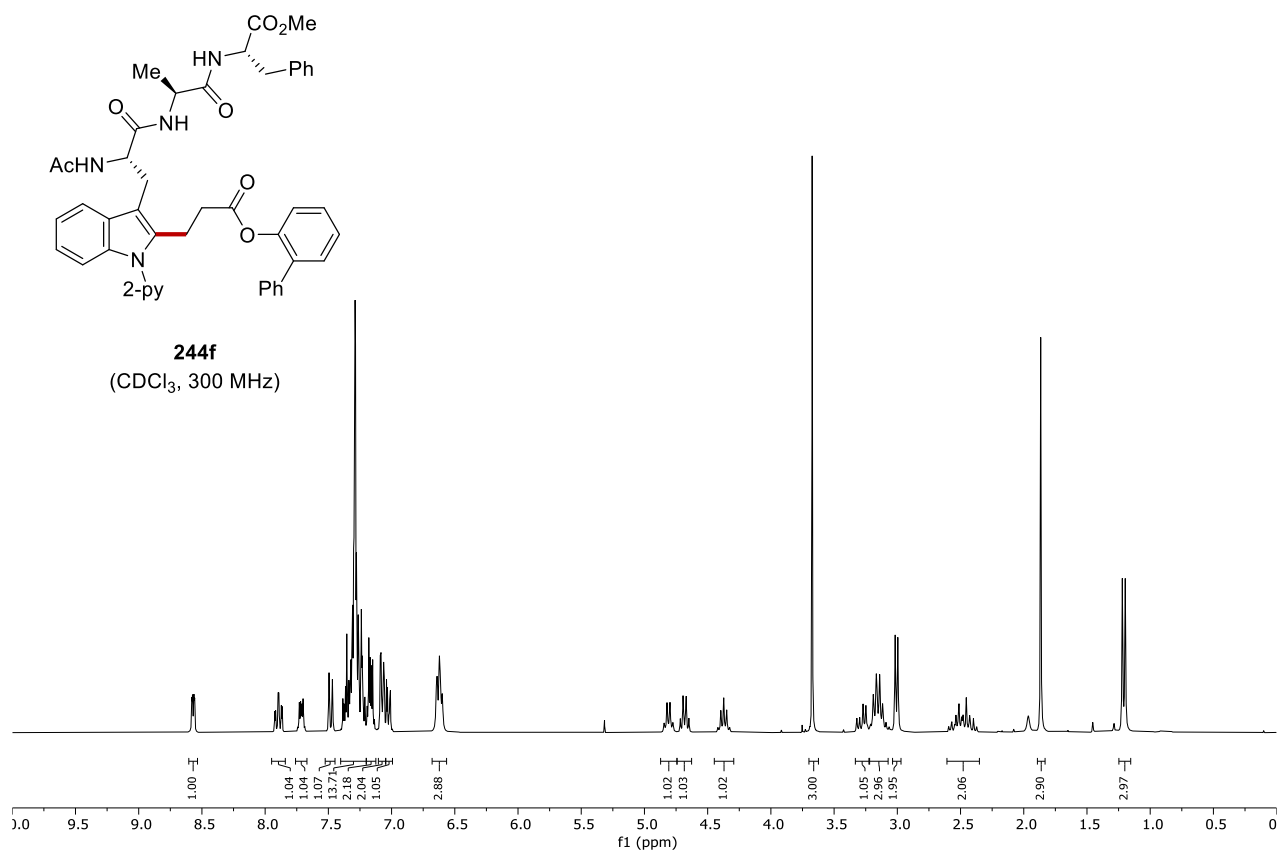


244e
(CDCl₃, 300 MHz)

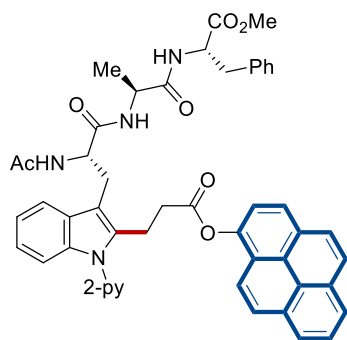


244e
(CDCl₃, 126 MHz)

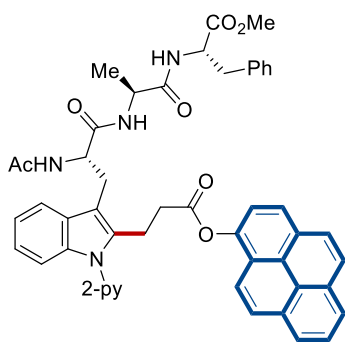
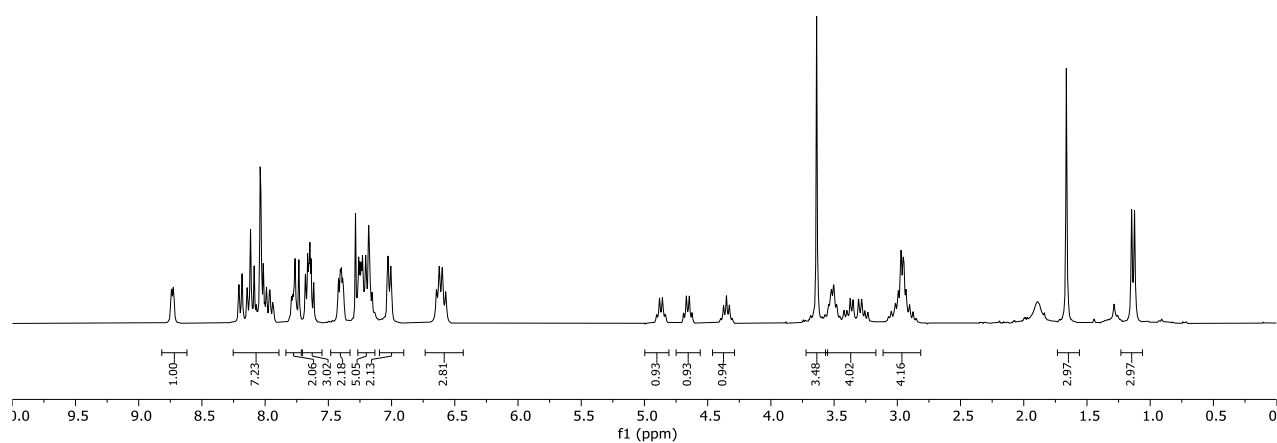




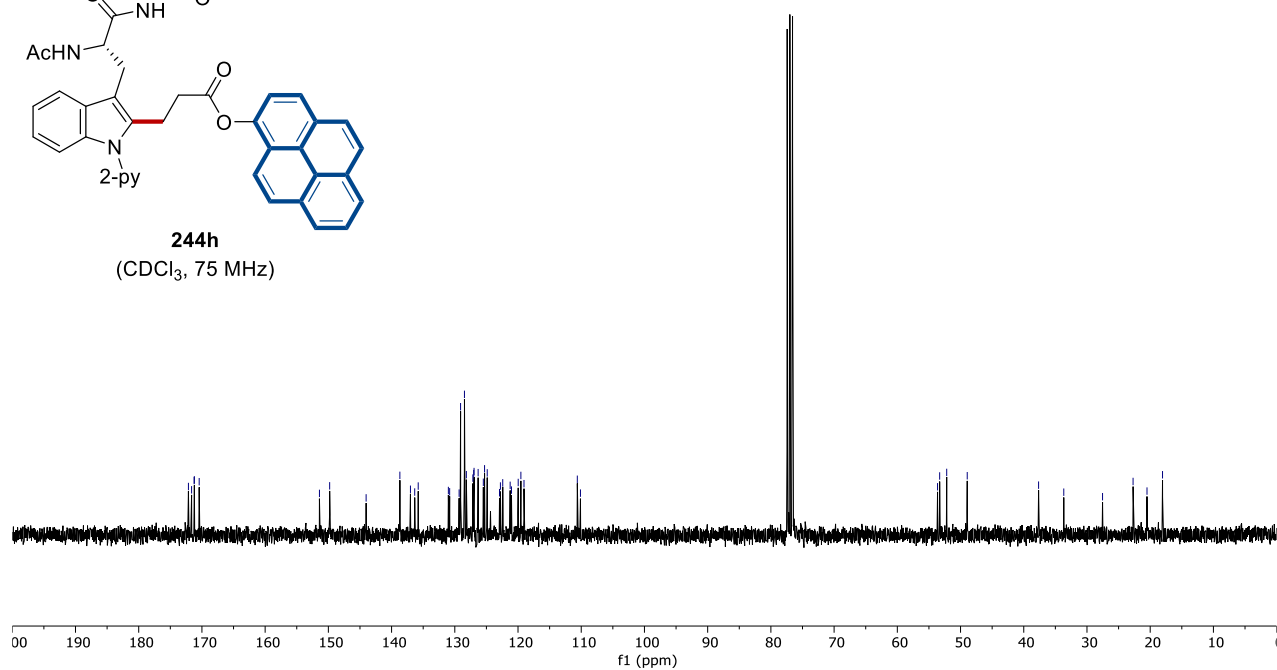
8. NMR Spectra

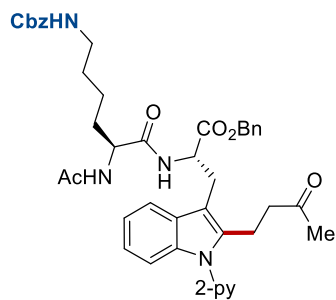


244h
(CDCl₃, 300 MHz)

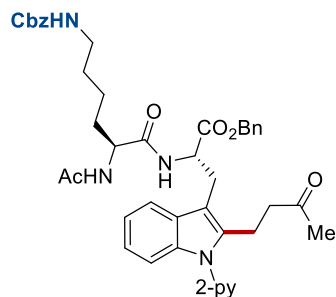
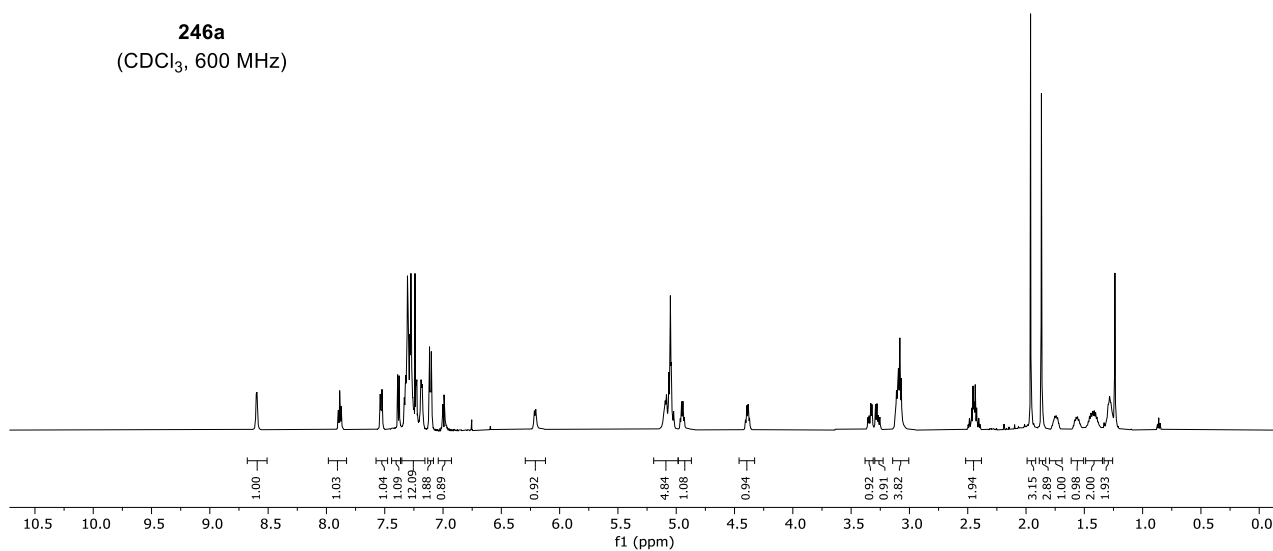


244h
(CDCl₃, 75 MHz)

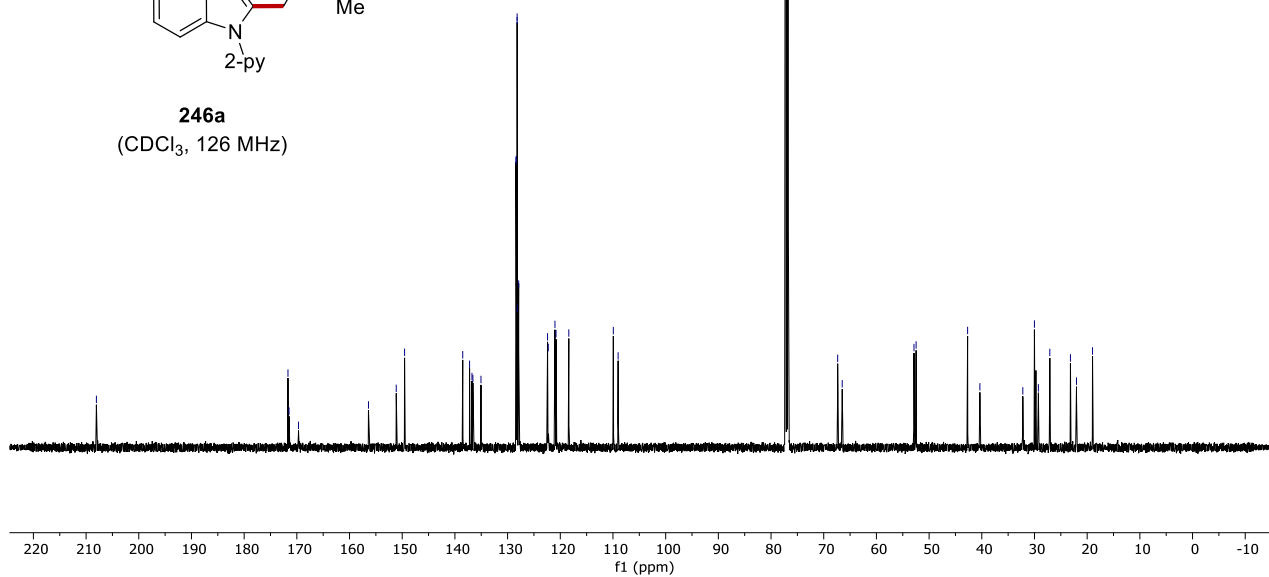




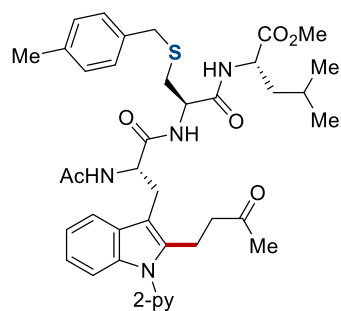
246a
(CDCl₃, 600 MHz)



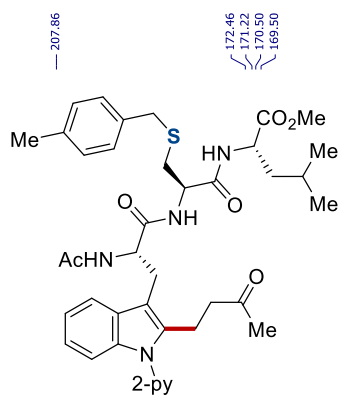
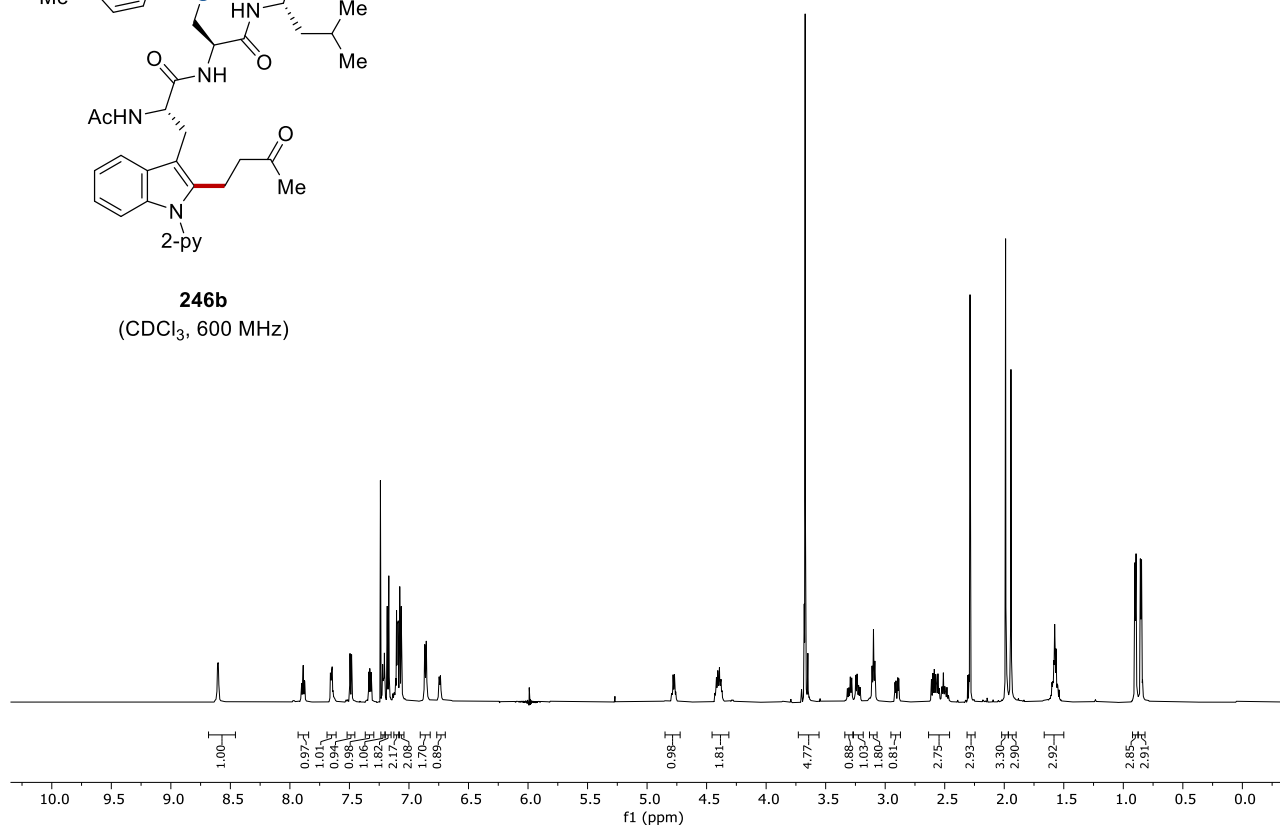
246a
(CDCl₃, 126 MHz)



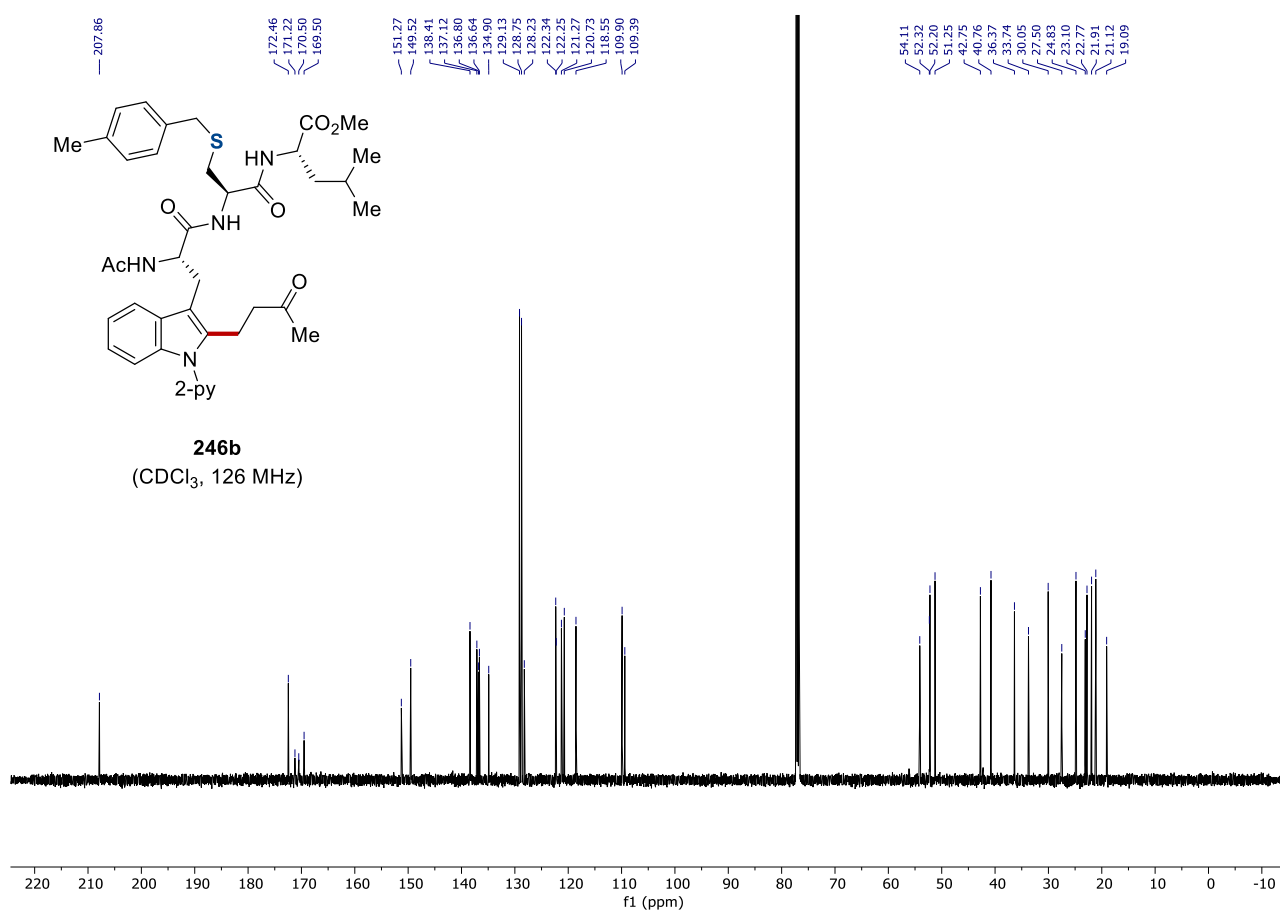
8. NMR Spectra

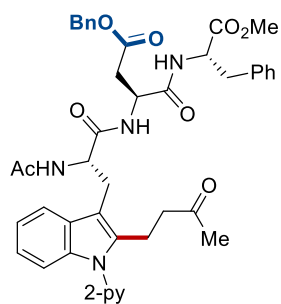


246b
(CDCl₃, 600 MHz)

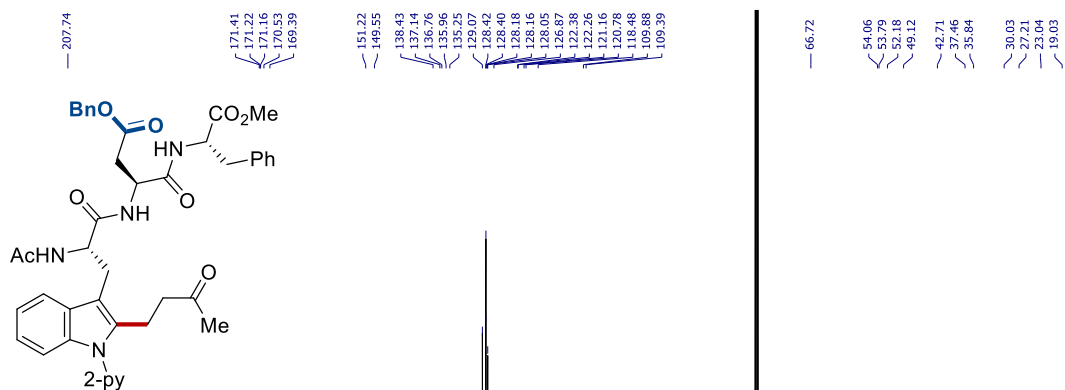
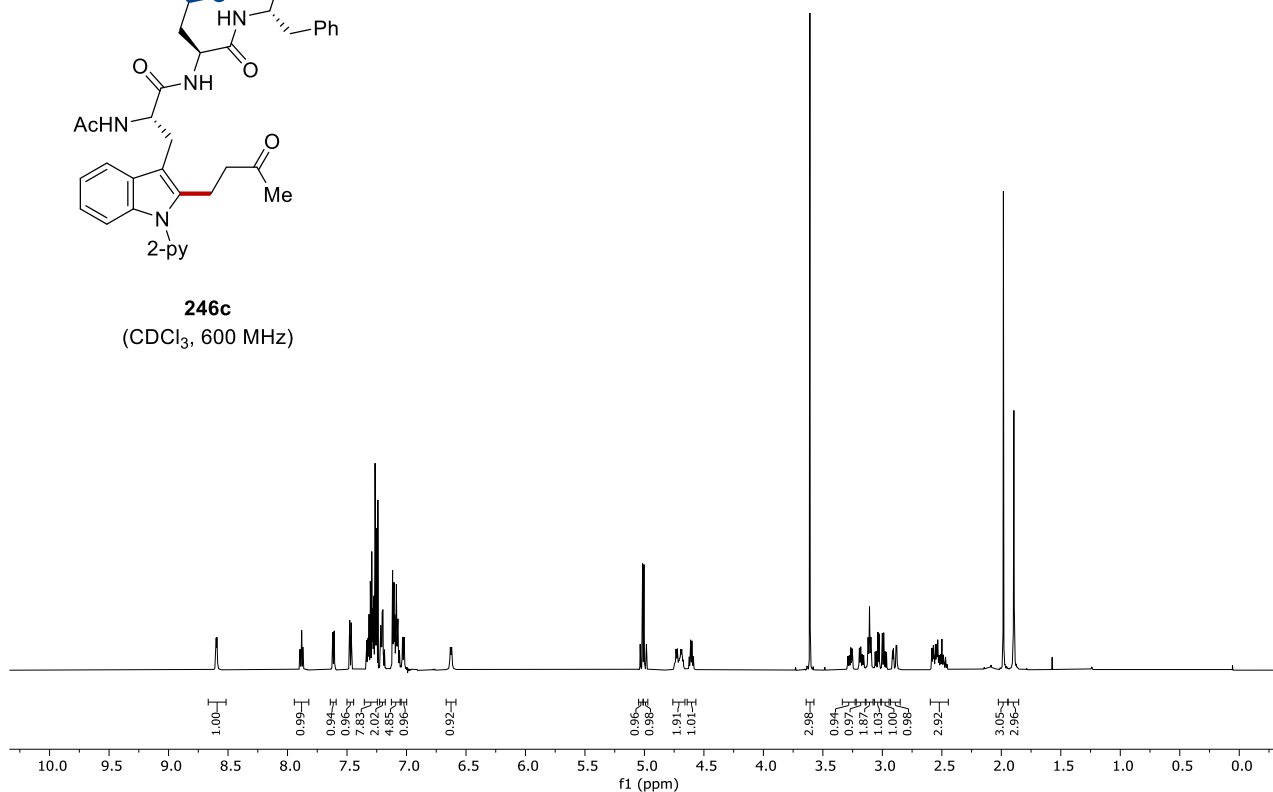


246b
(CDCl₃, 126 MHz)

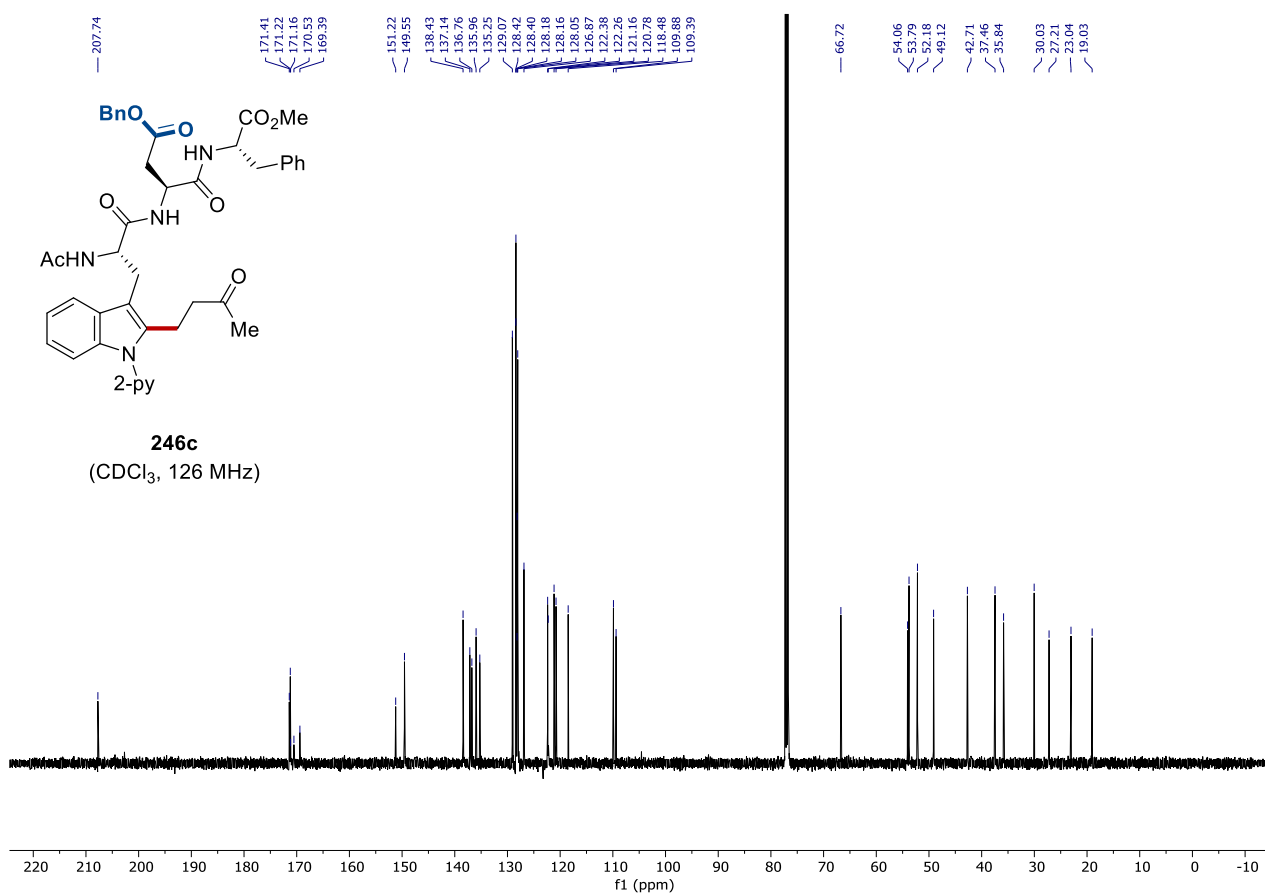




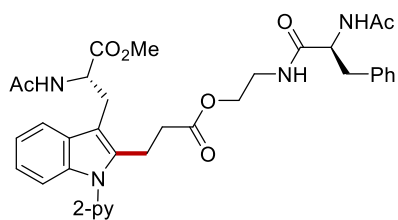
246c
(CDCl₃, 600 MHz)



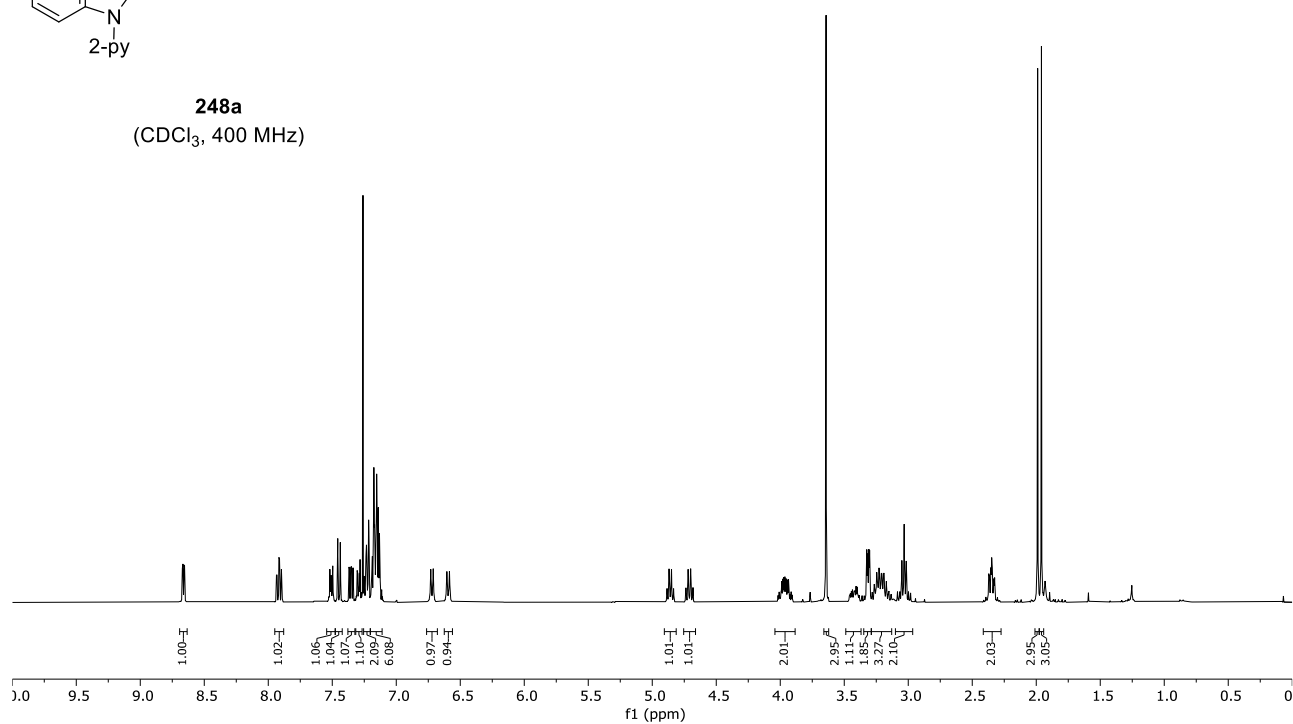
246c
(CDCl₃, 126 MHz)



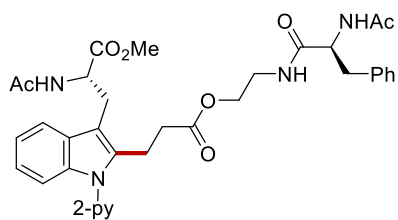
8. NMR Spectra



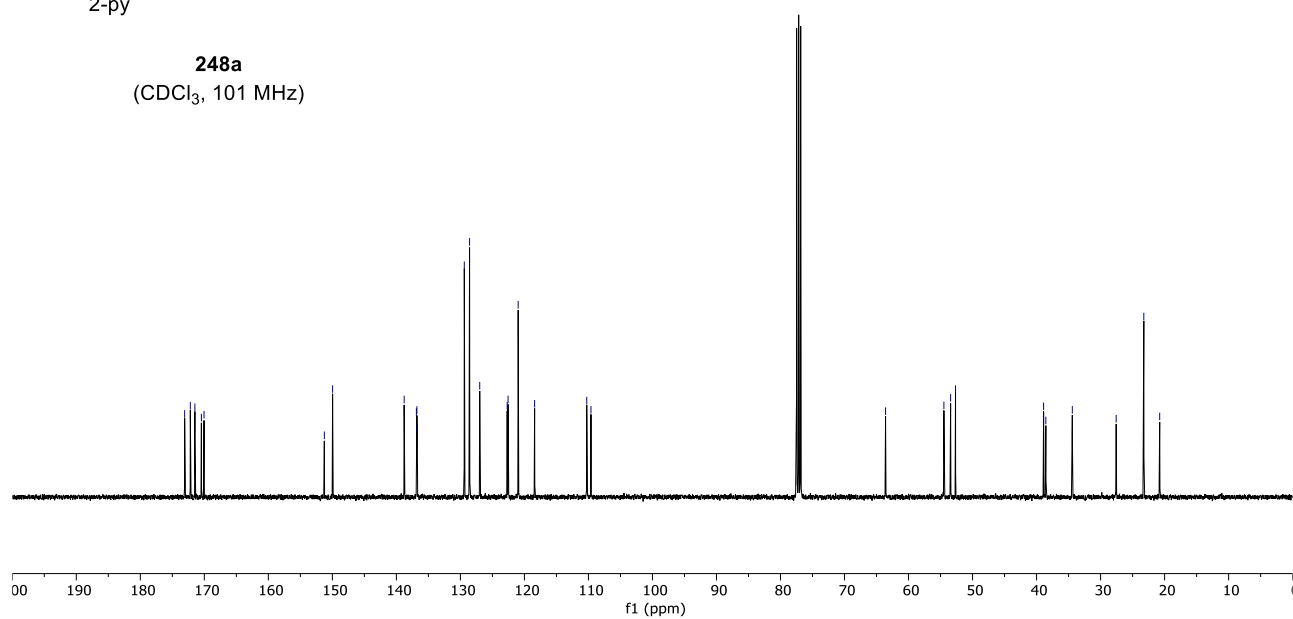
248a
(CDCl₃, 400 MHz)

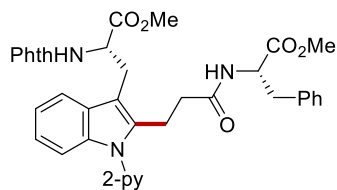


173.07, 172.19, 171.47, 170.04, 151.25, 149.96, 138.79, 136.79, 136.75, 129.39, 128.57, 126.98, 122.69, 122.65, 121.98, 118.41, 110.27, 109.61, 63.59, 54.48, 53.43, 52.66, 38.90, 38.55, 34.42, 27.57, 23.25, 20.77.

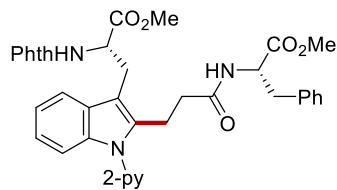
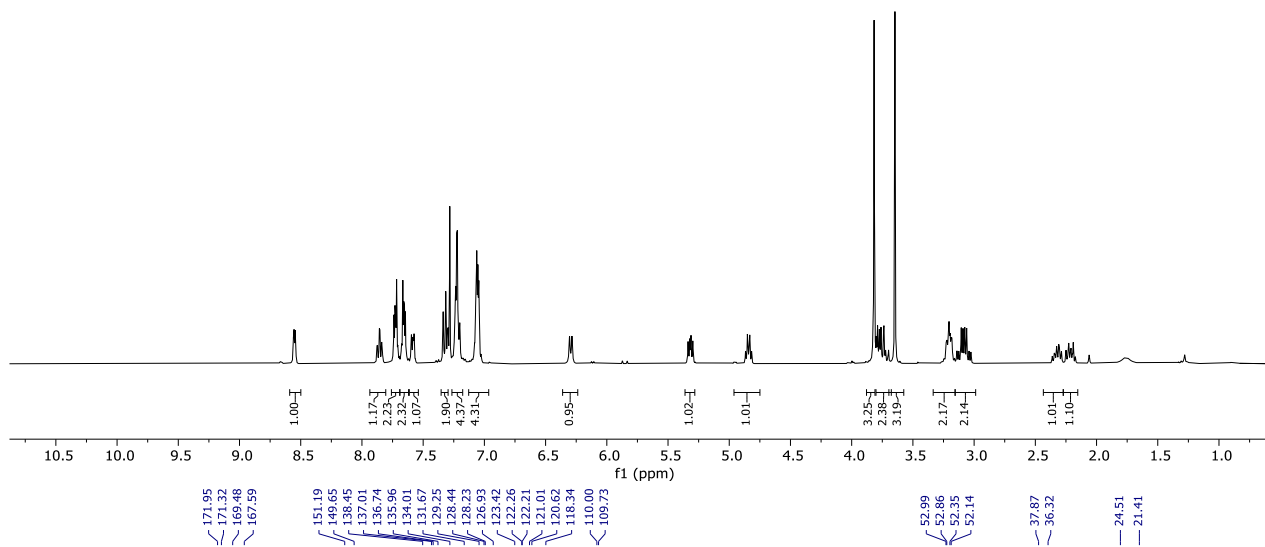


248a
(CDCl₃, 101 MHz)

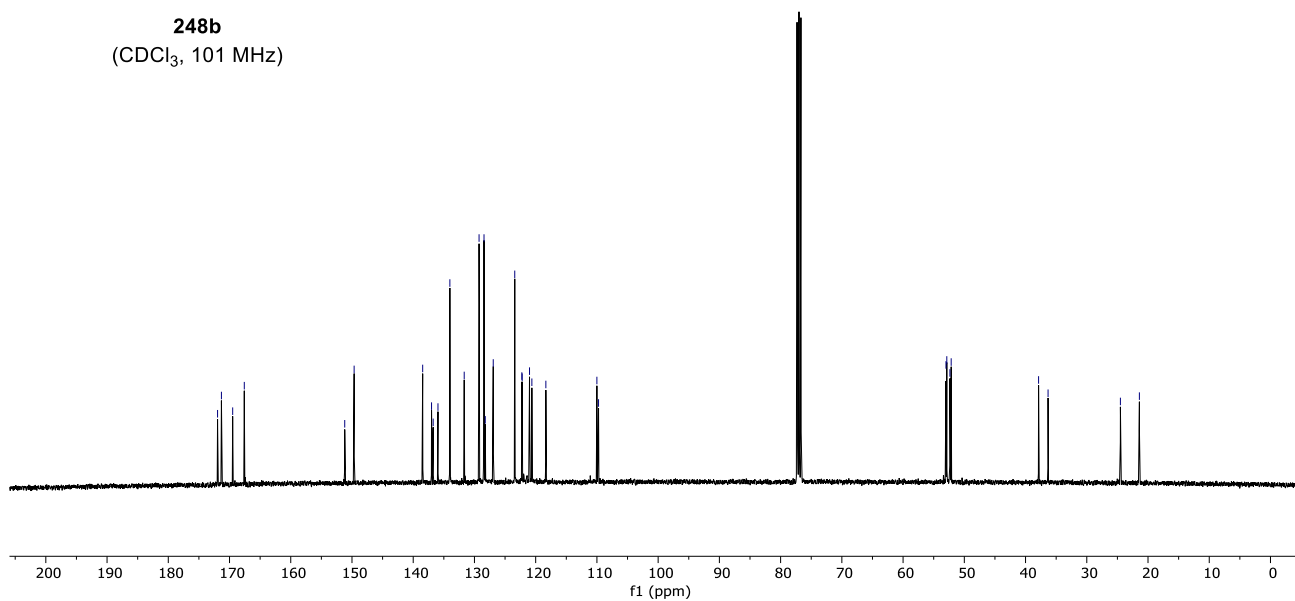




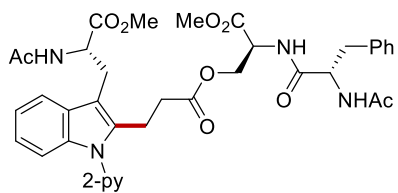
248b
(CDCl₃, 400 MHz)



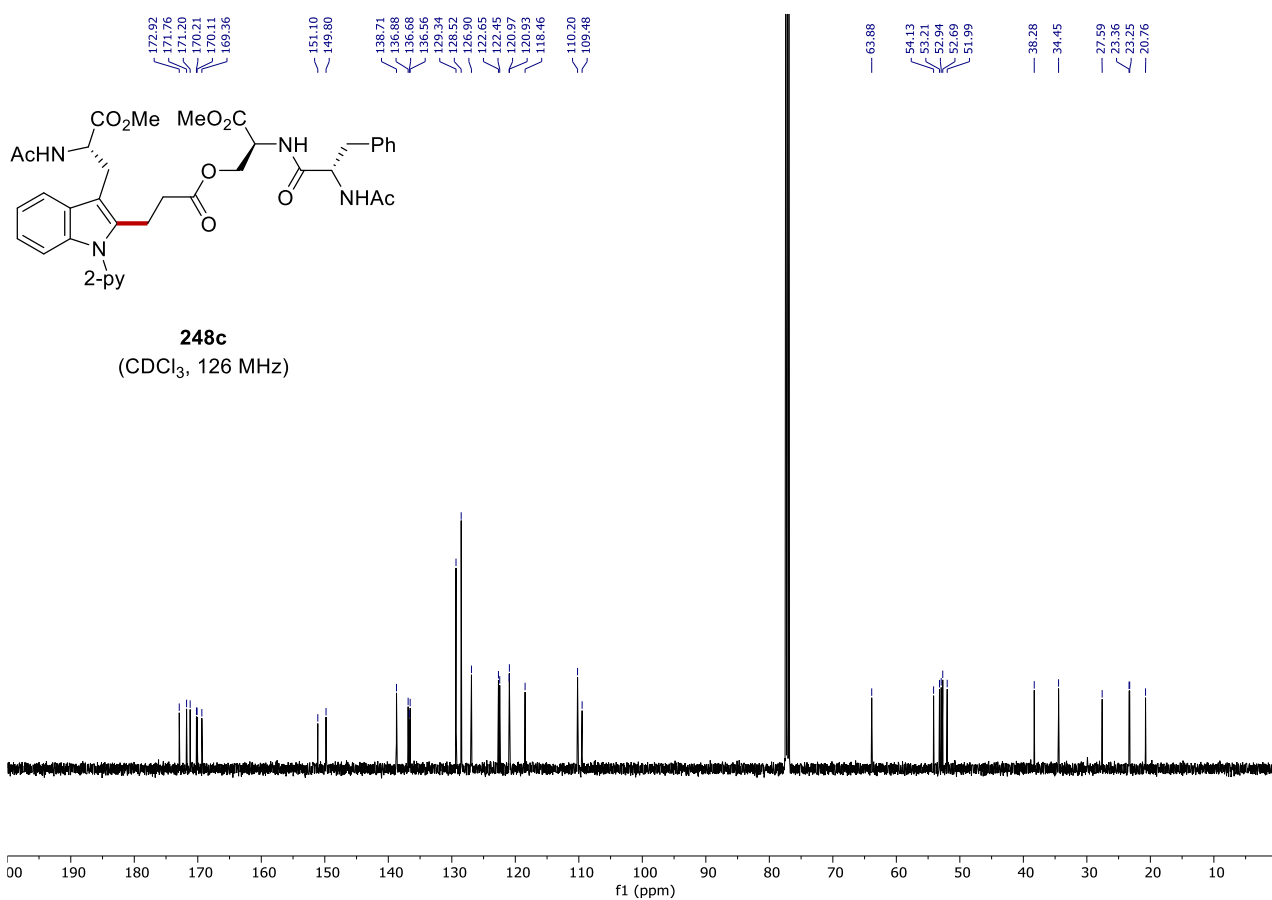
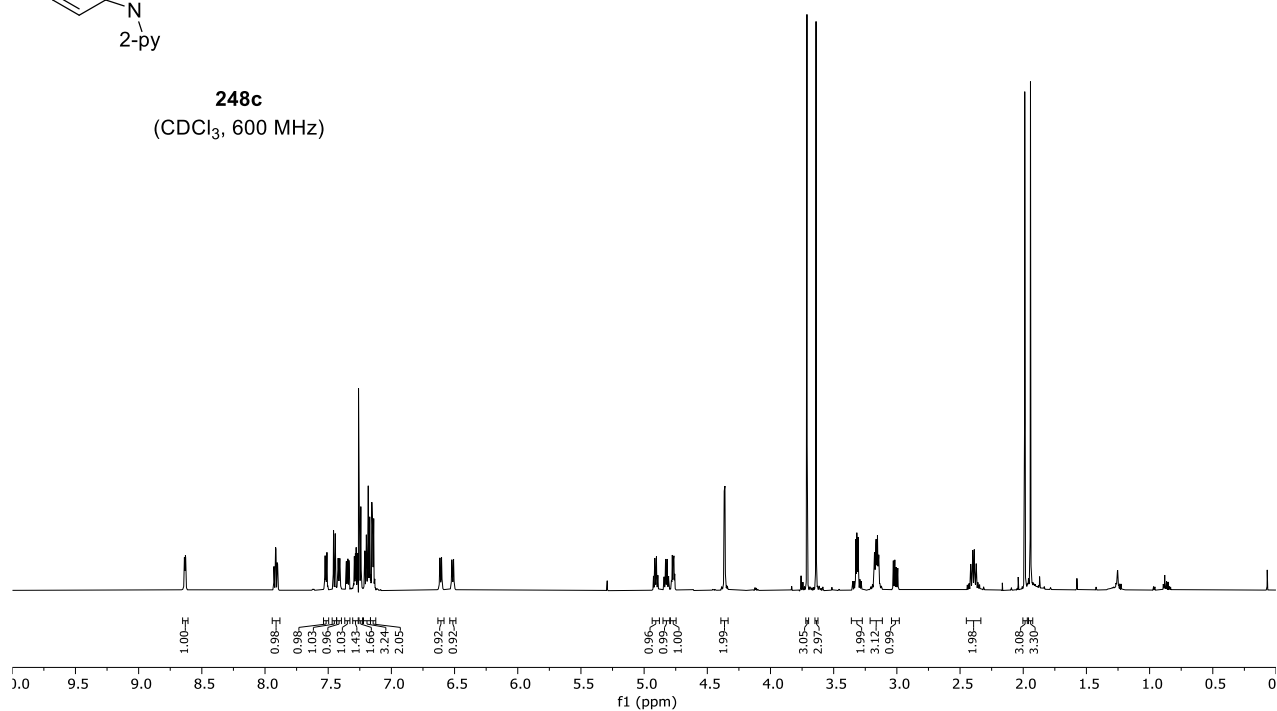
248b
(CDCl₃, 101 MHz)

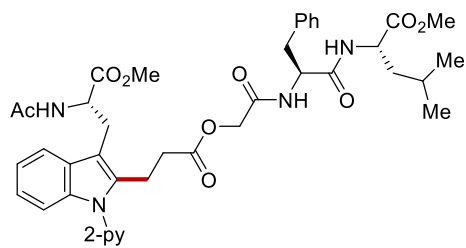


8. NMR Spectra

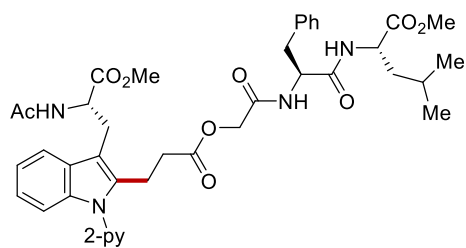
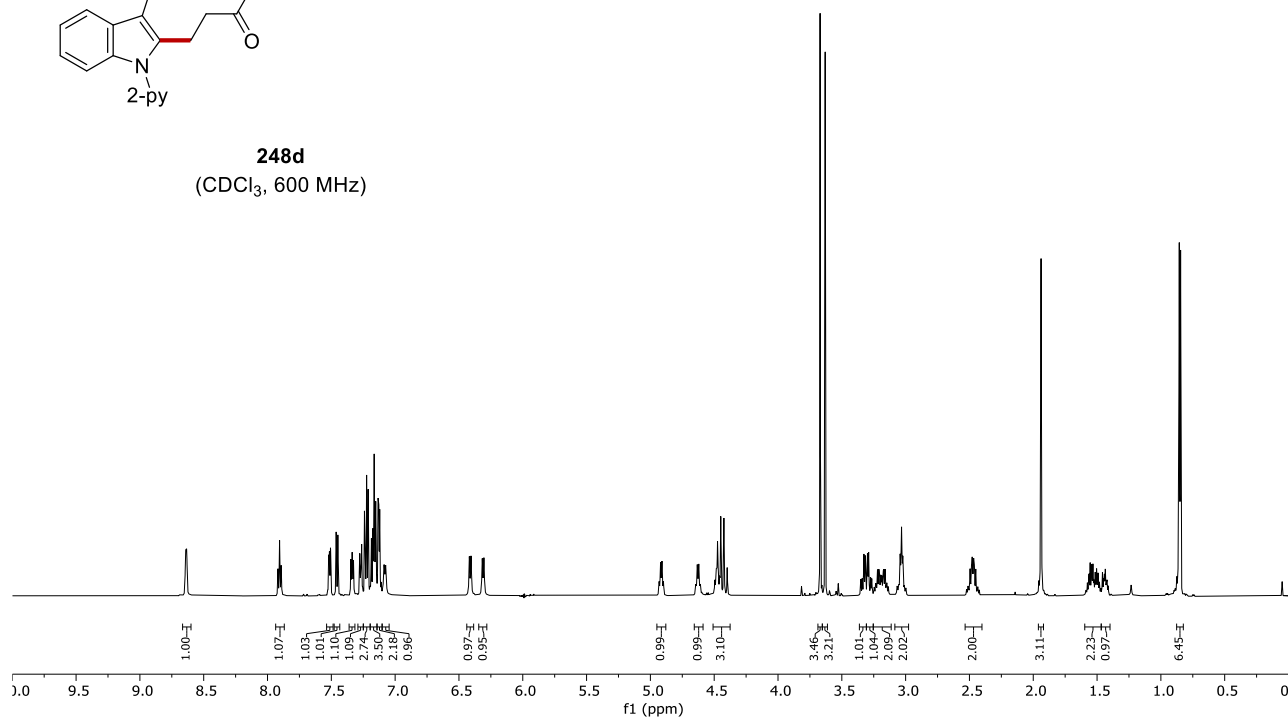


248c
(CDCl₃, 600 MHz)

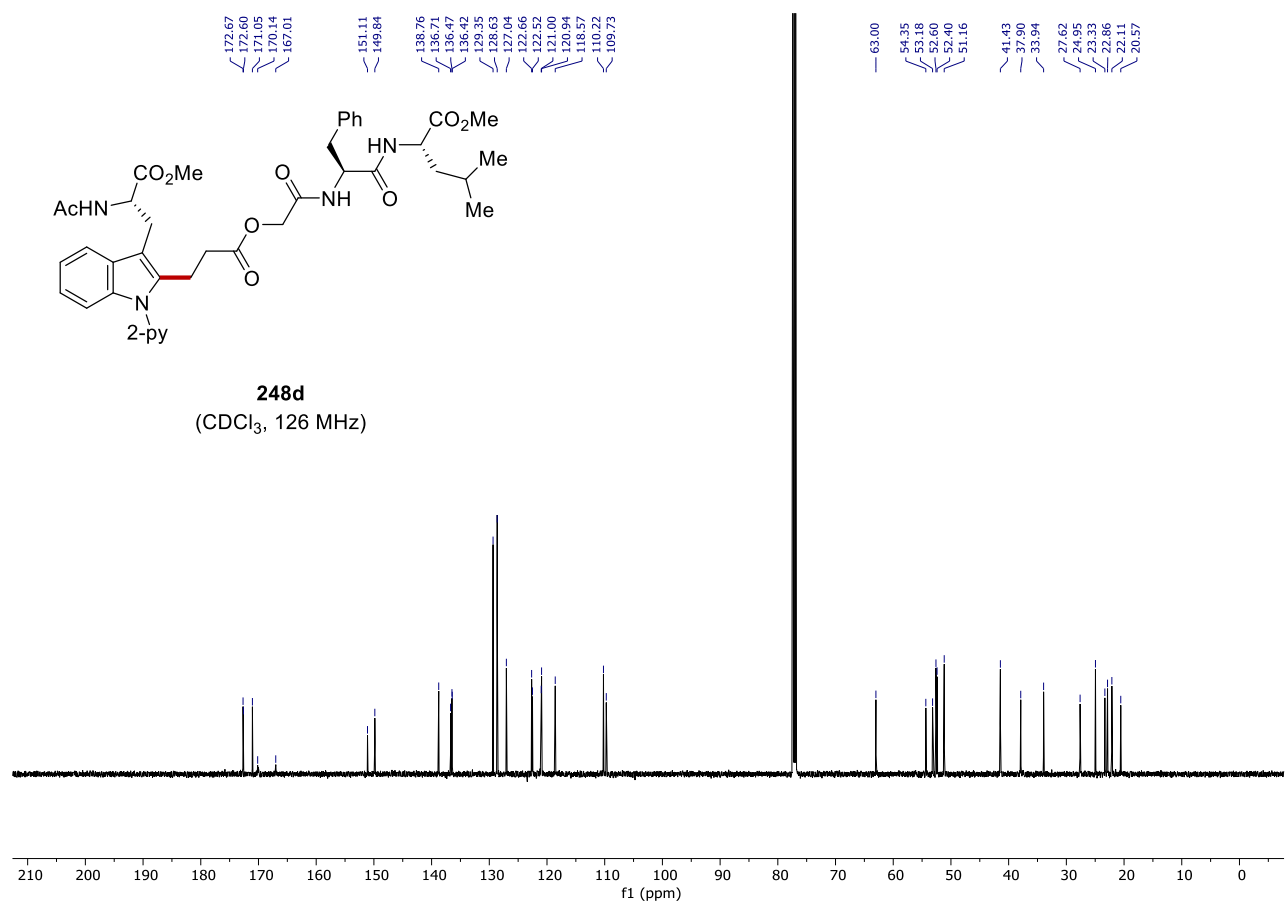




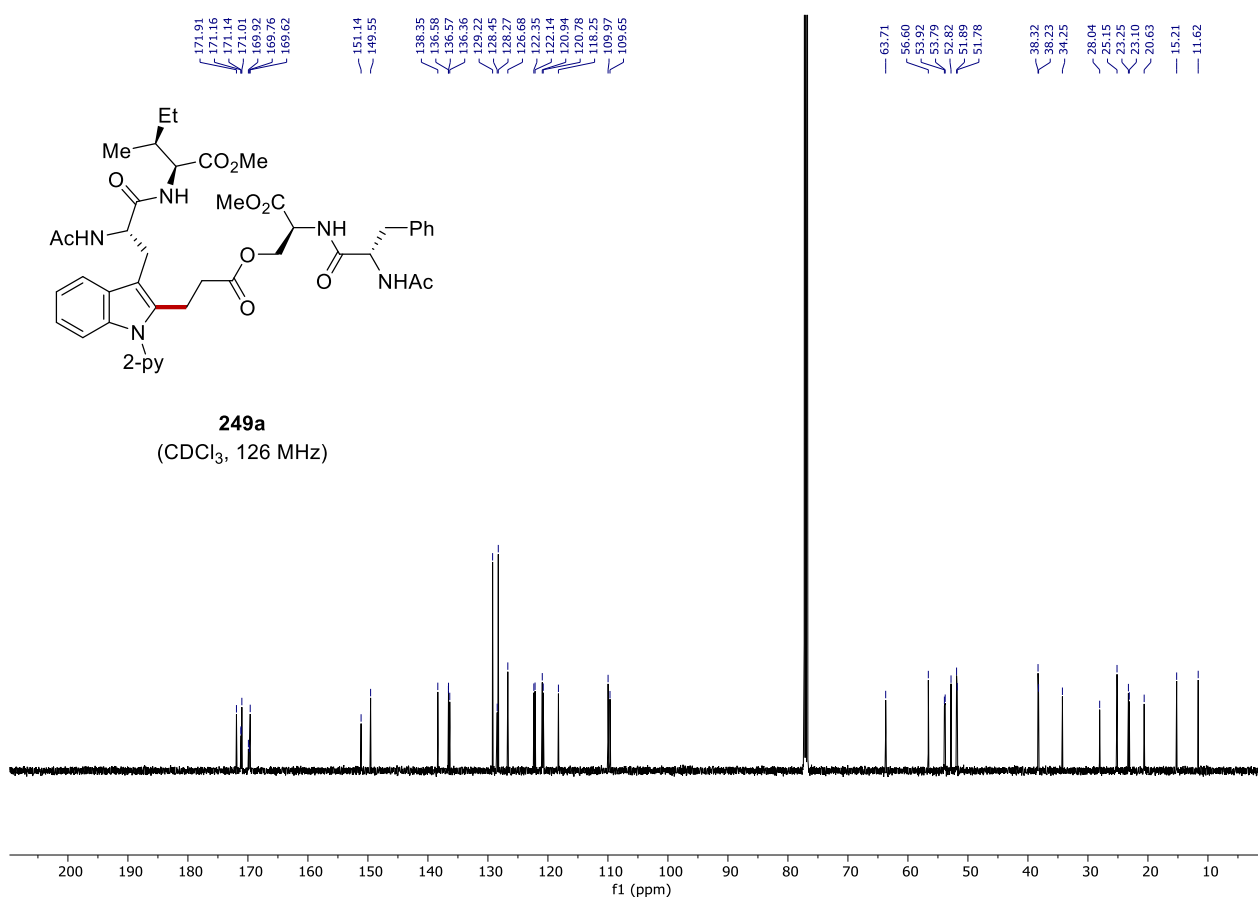
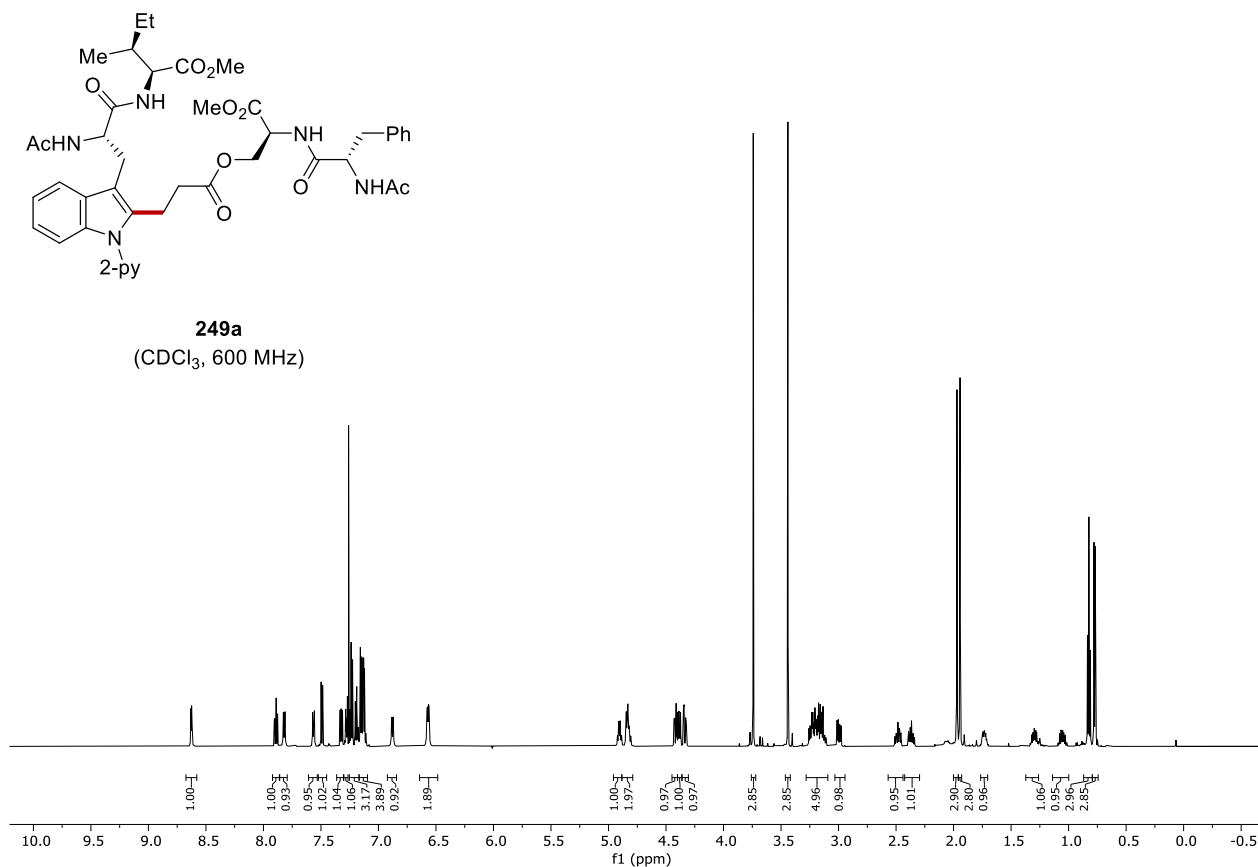
248d
(CDCl₃, 600 MHz)

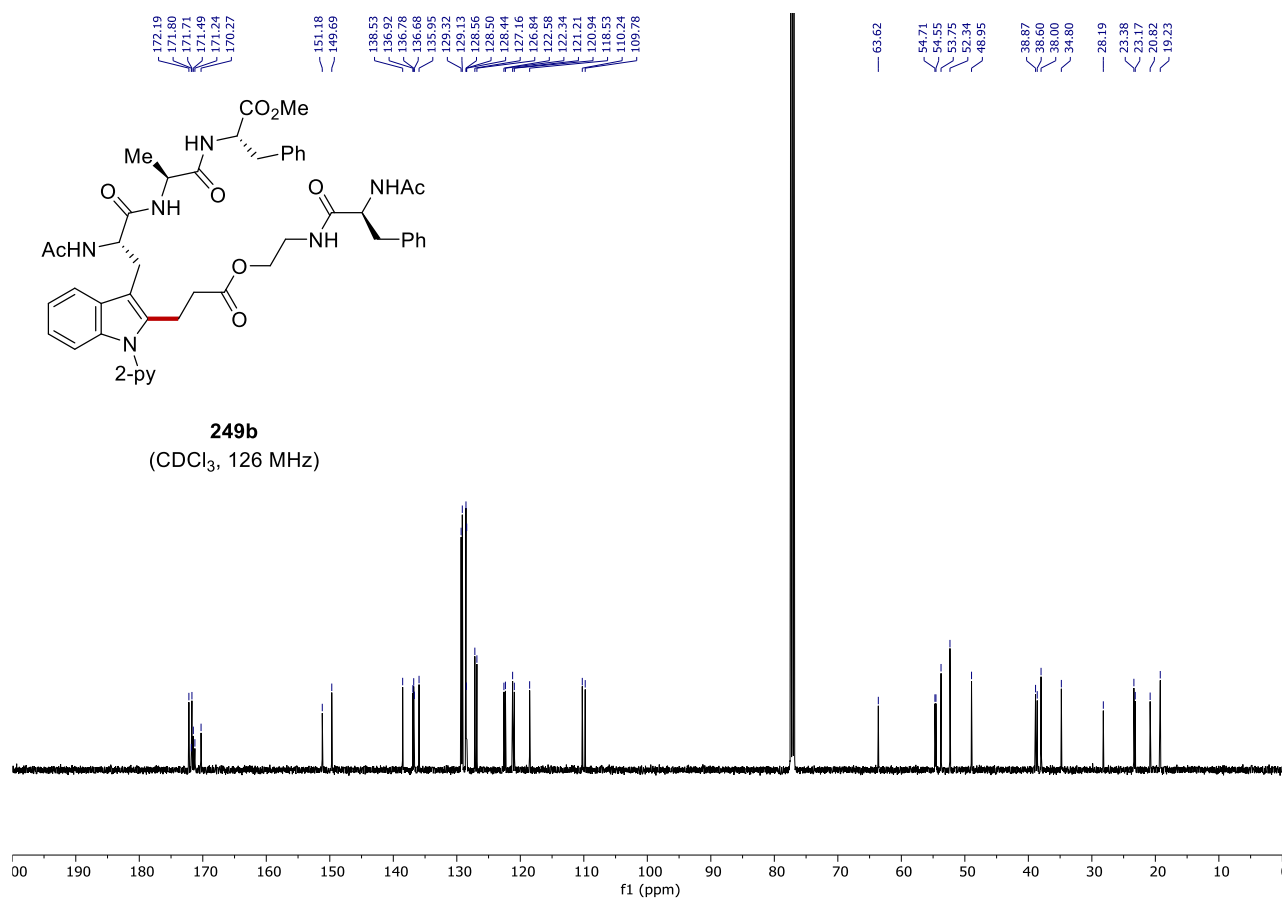
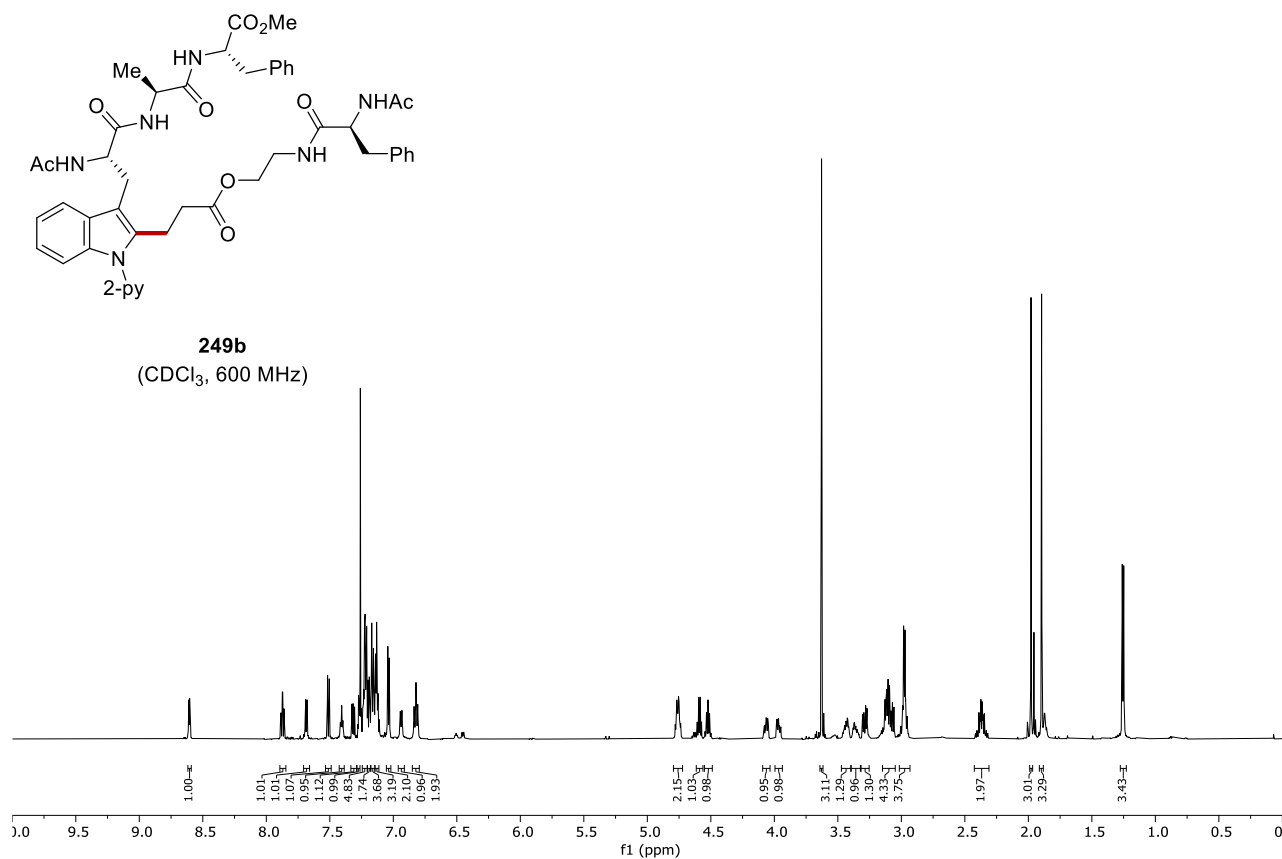


248d
(CDCl₃, 126 MHz)

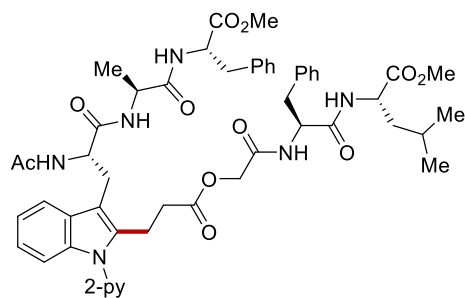


8. NMR Spectra

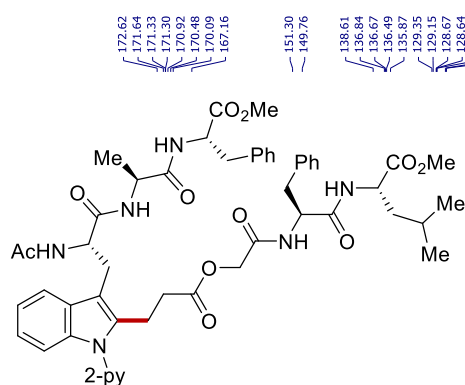
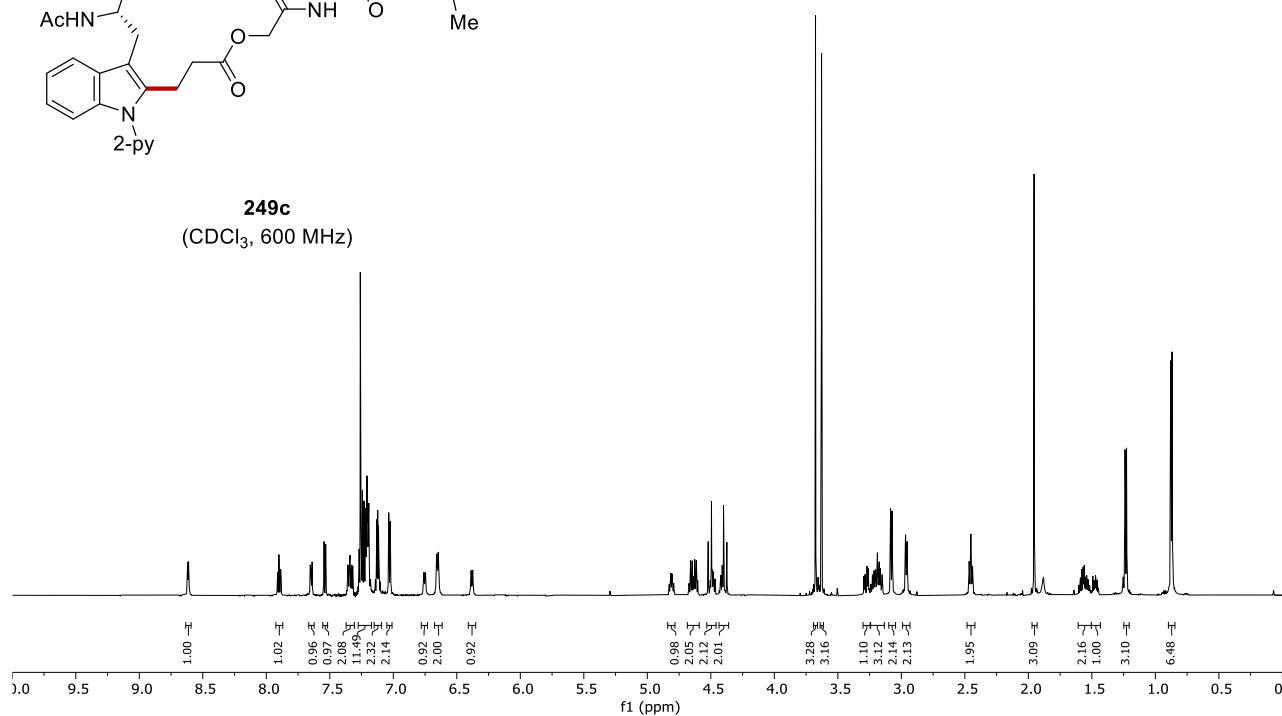




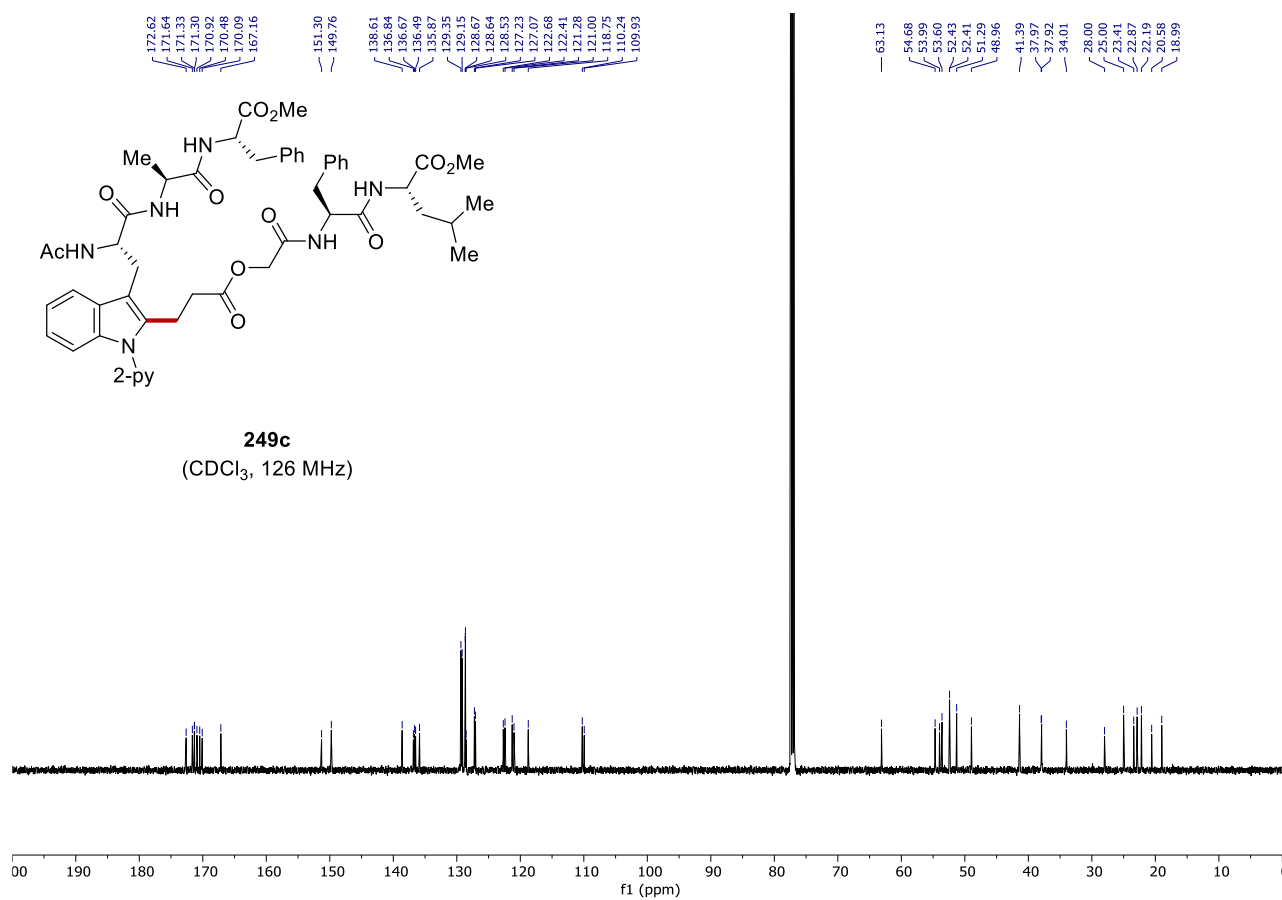
8. NMR Spectra



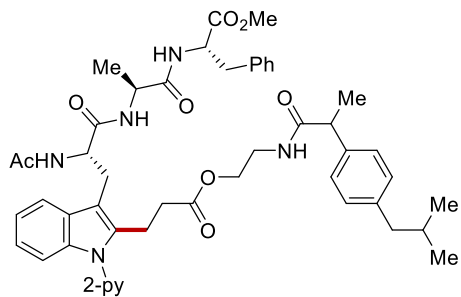
249c
(CDCl₃, 600 MHz)



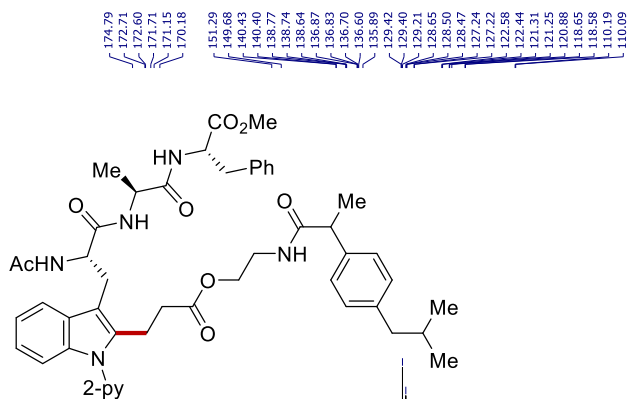
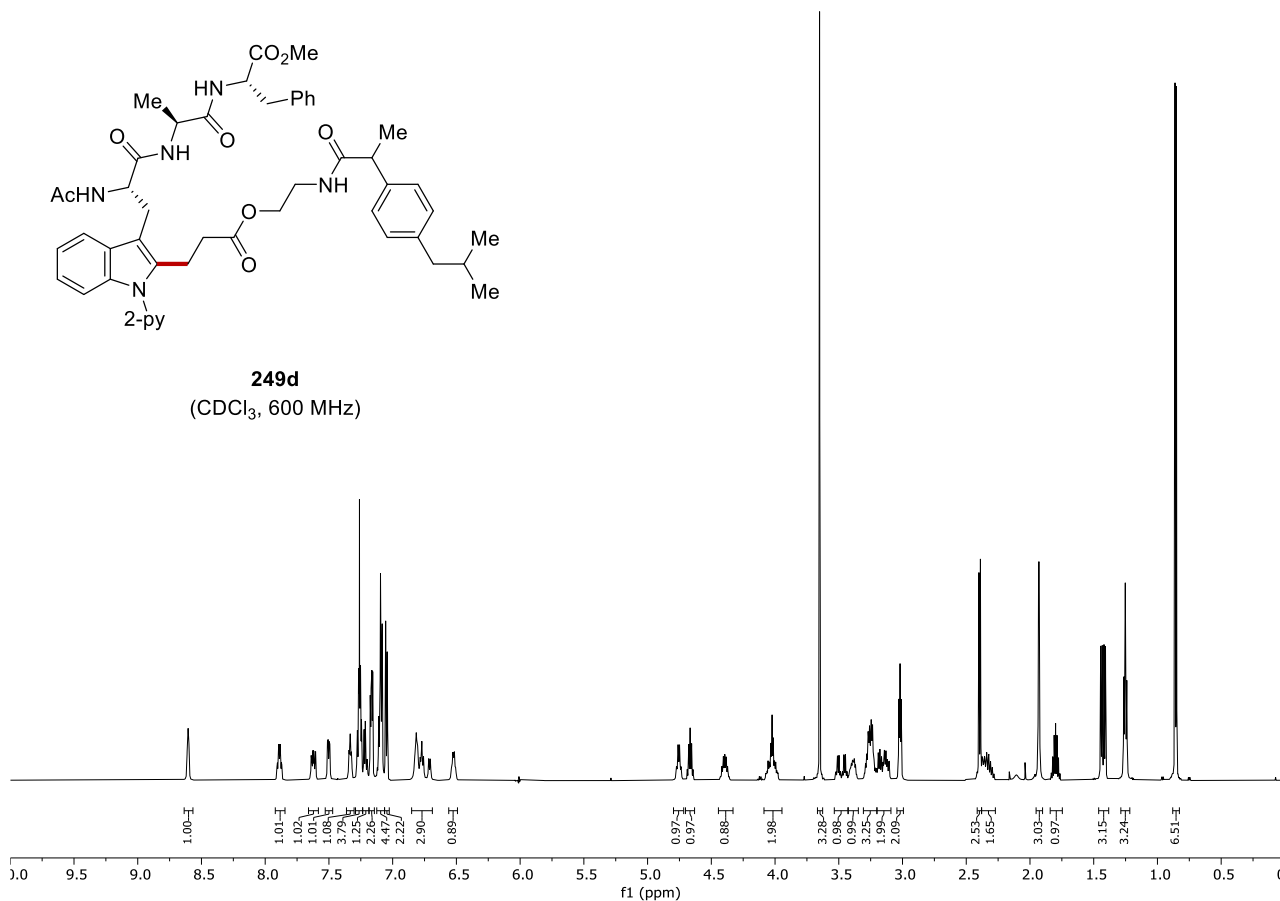
249c
(CDCl₃, 126 MHz)



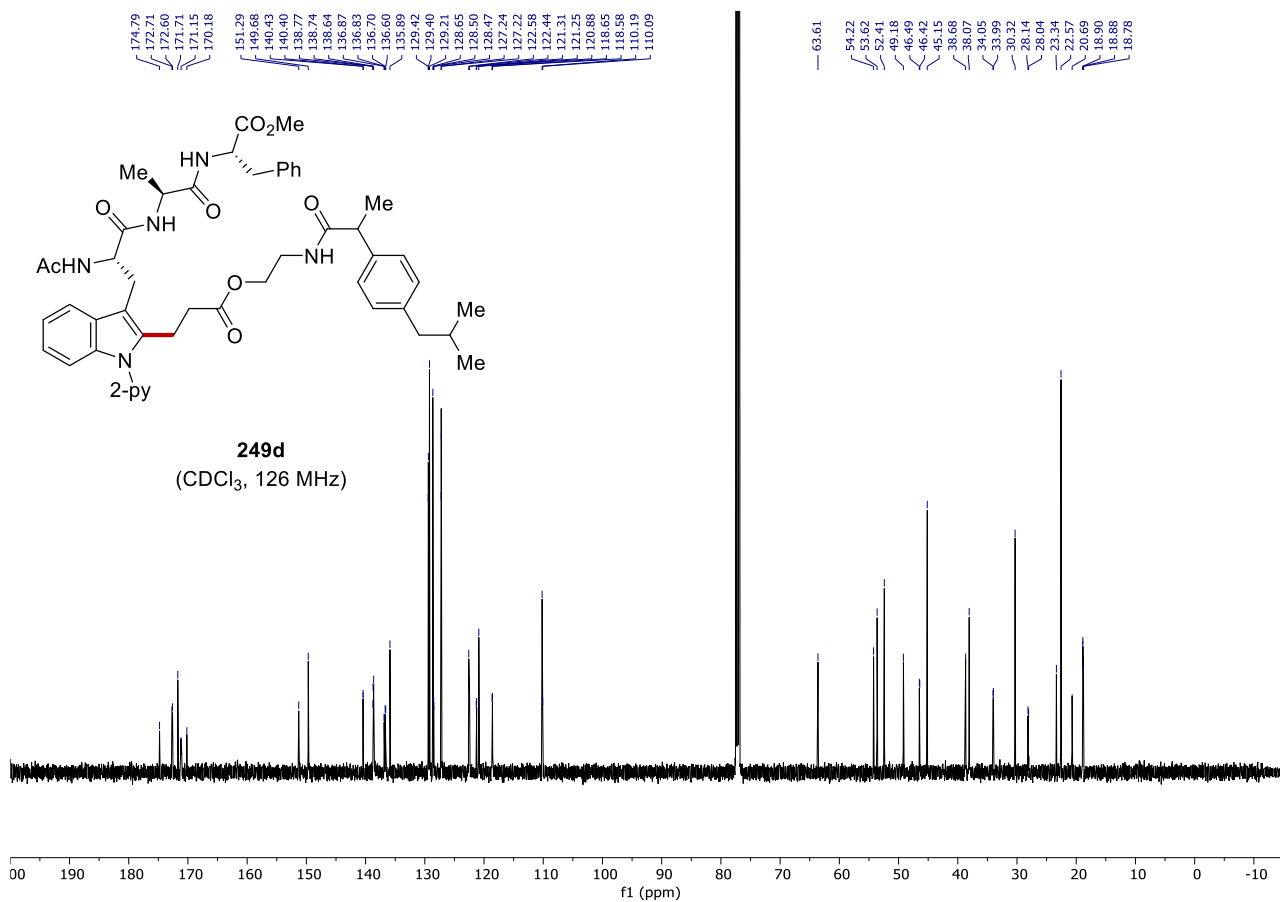
8. NMR Spectra



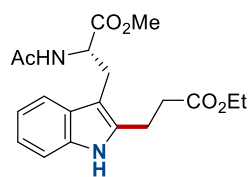
249d
(CDCl₃, 600 MHz)



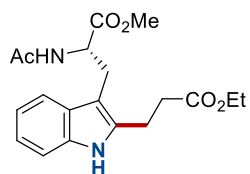
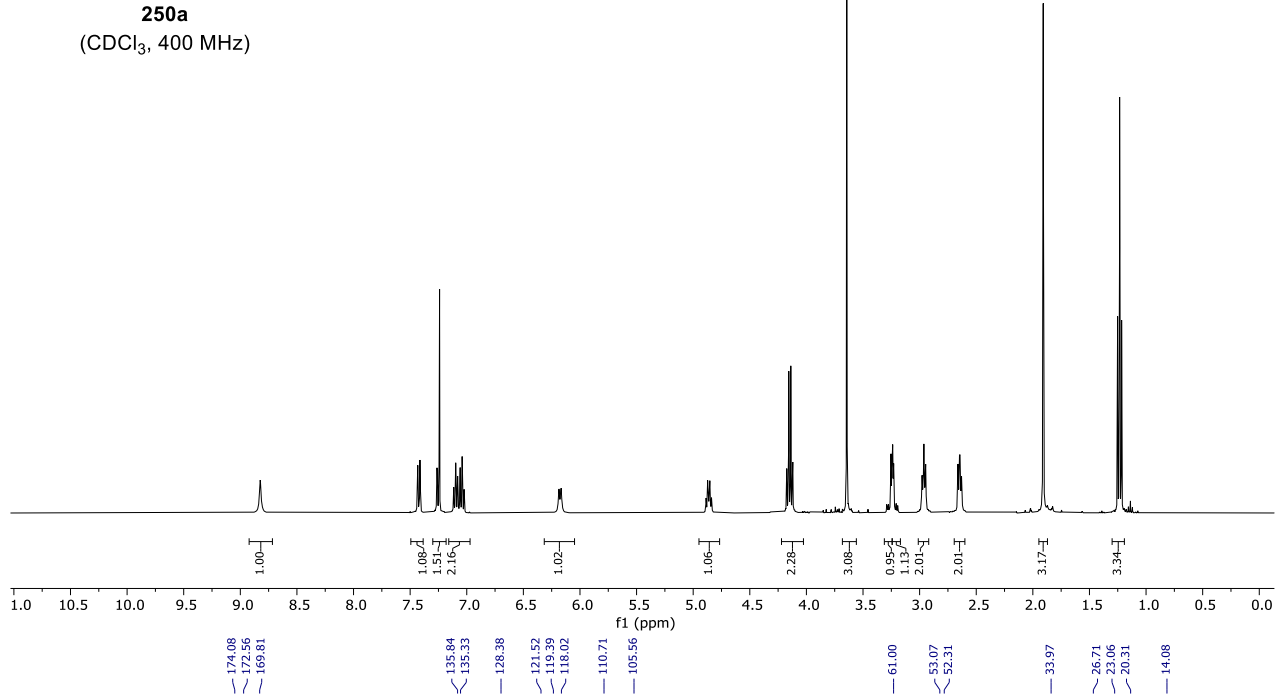
249d
(CDCl₃, 126 MHz)



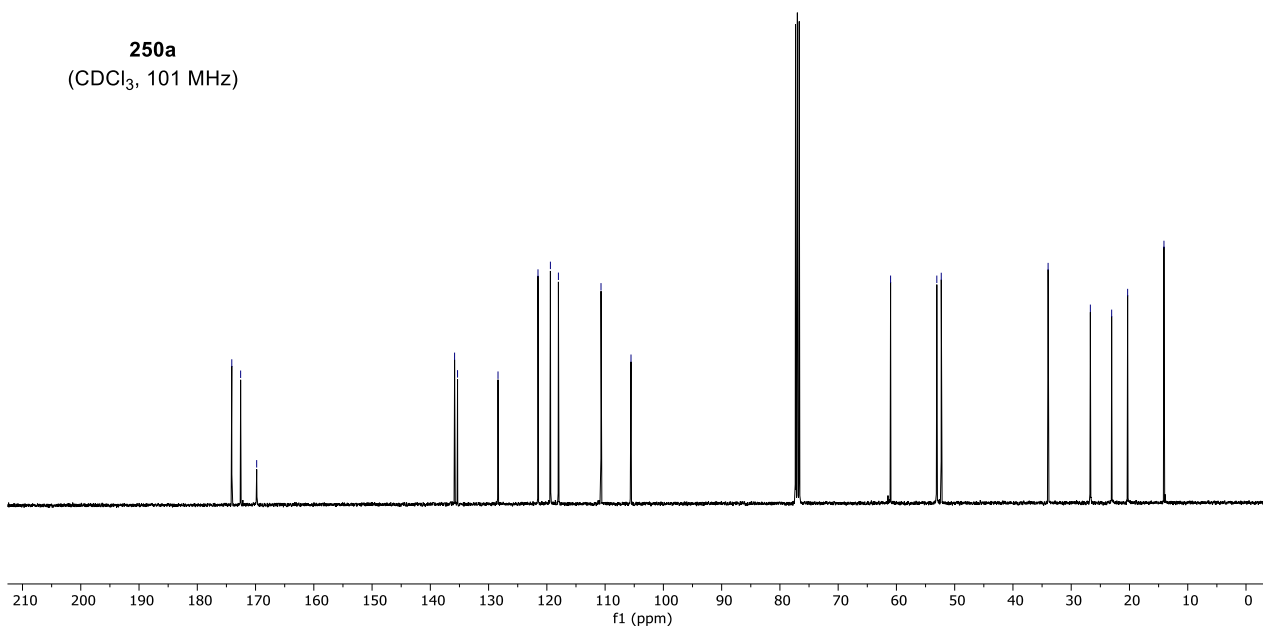
8. NMR Spectra

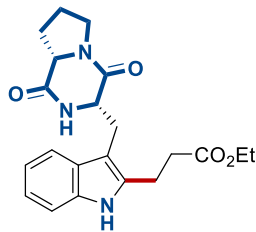


250a
(CDCl₃, 400 MHz)

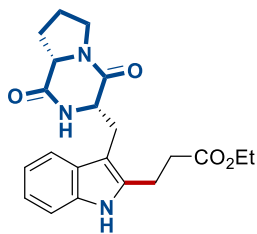
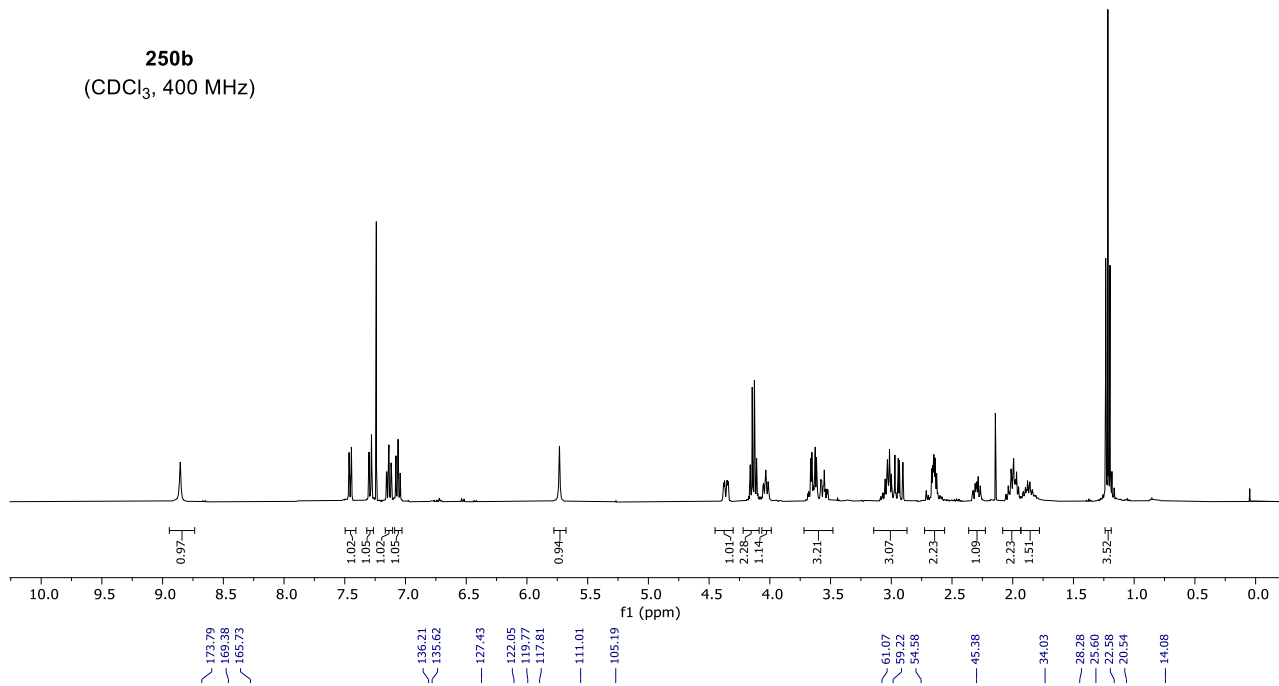


250a
(CDCl₃, 101 MHz)

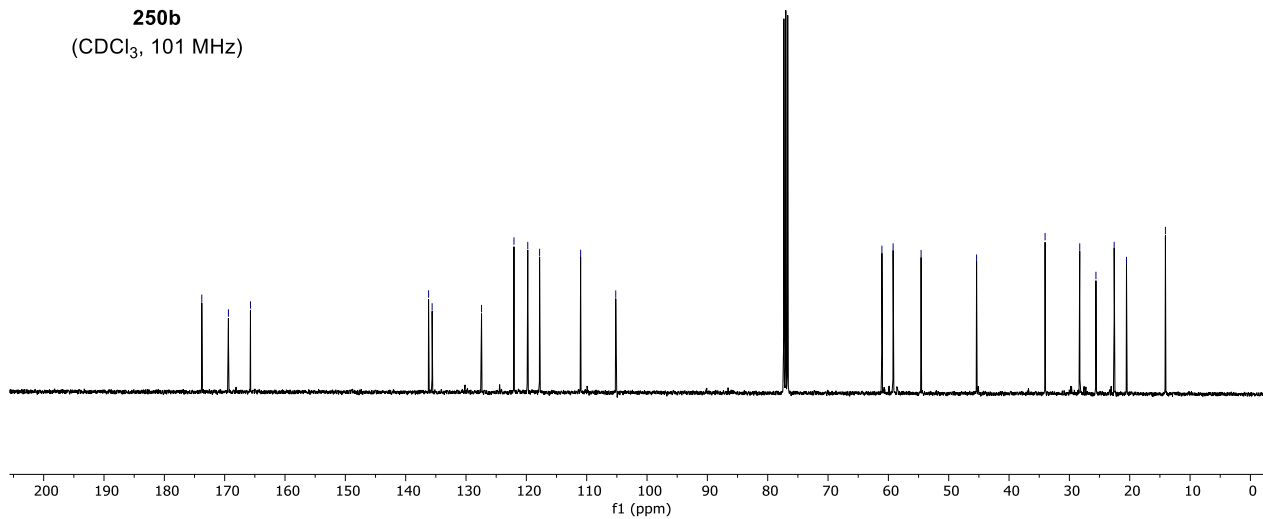




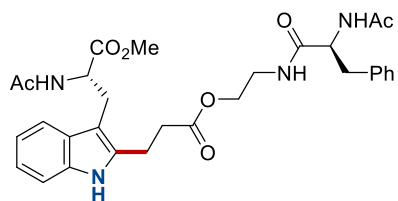
250b
(CDCl₃, 400 MHz)



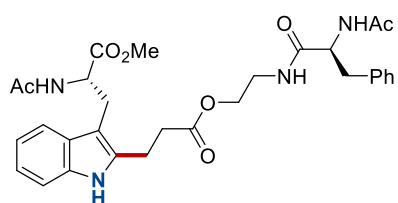
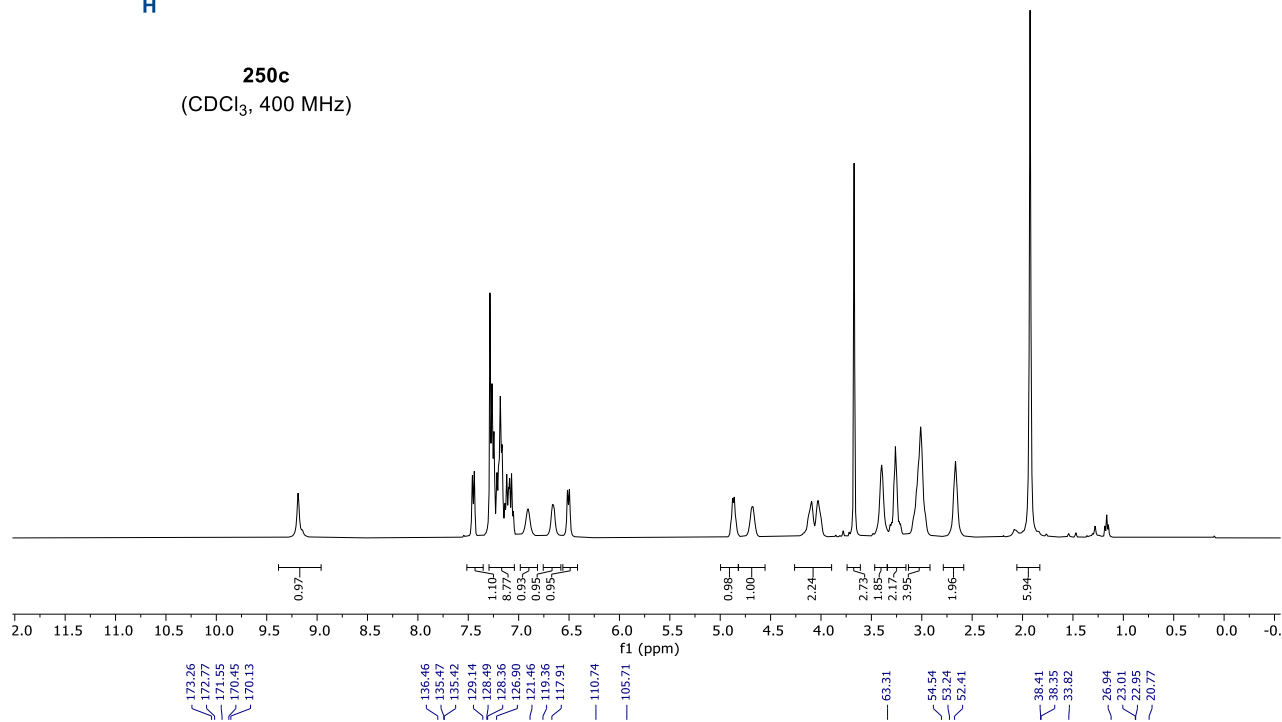
250b
(CDCl₃, 101 MHz)



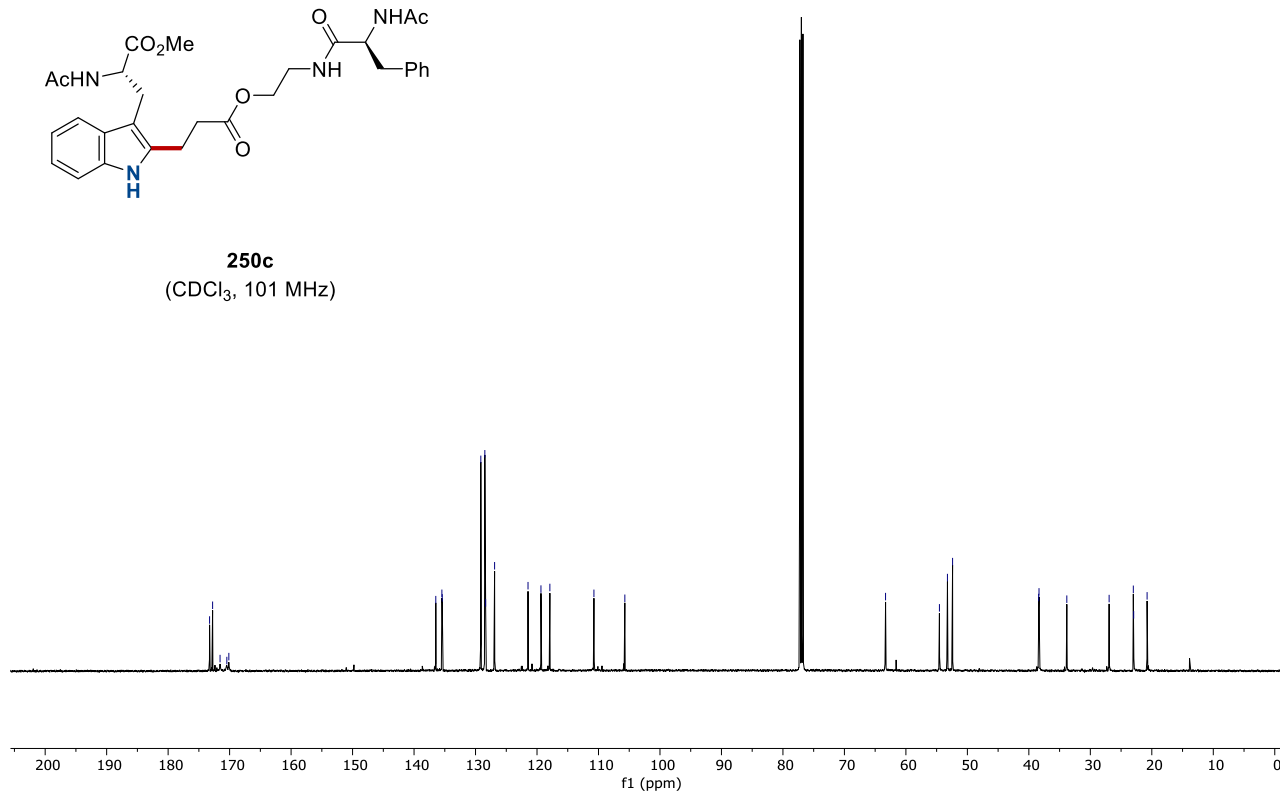
8. NMR Spectra

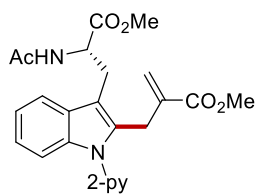
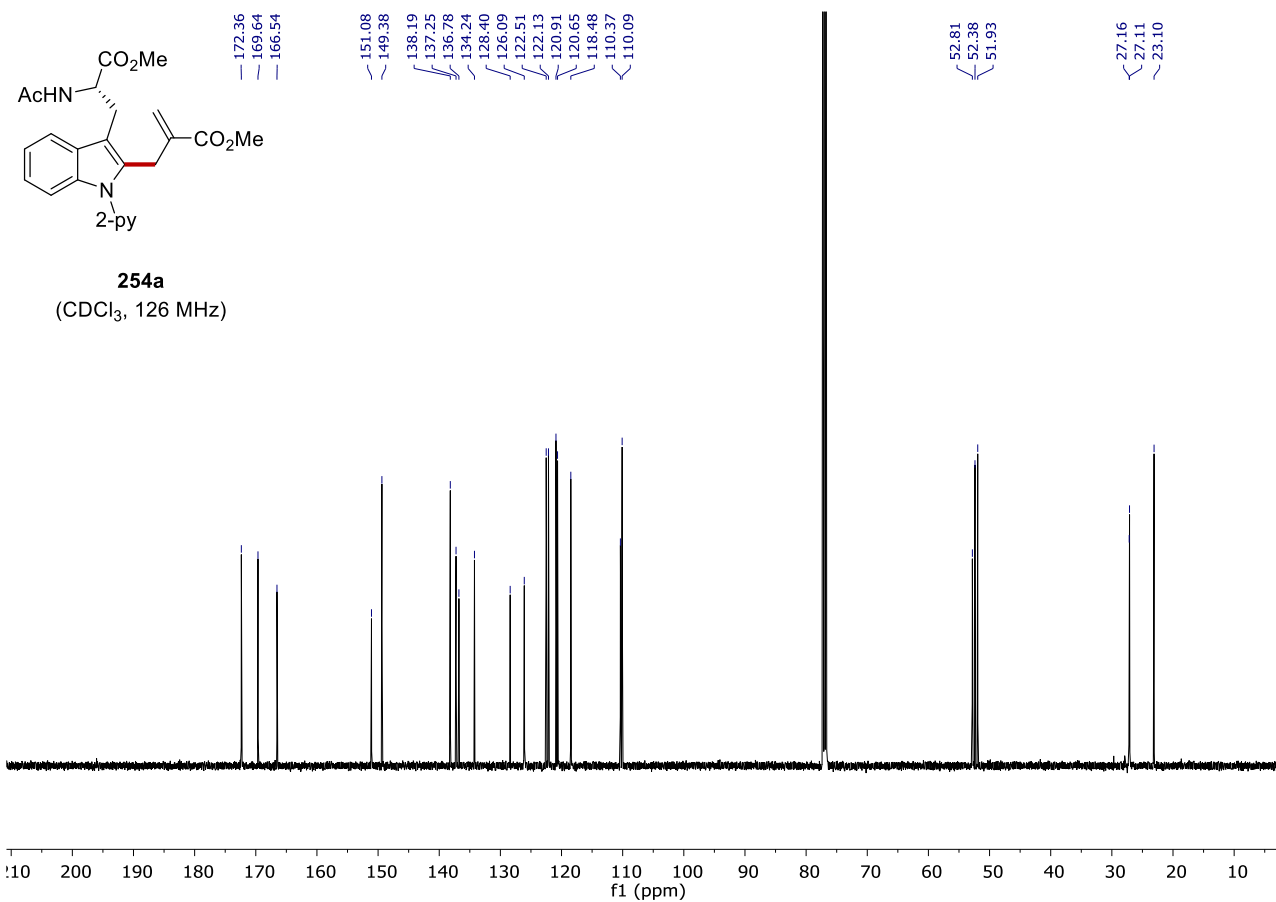
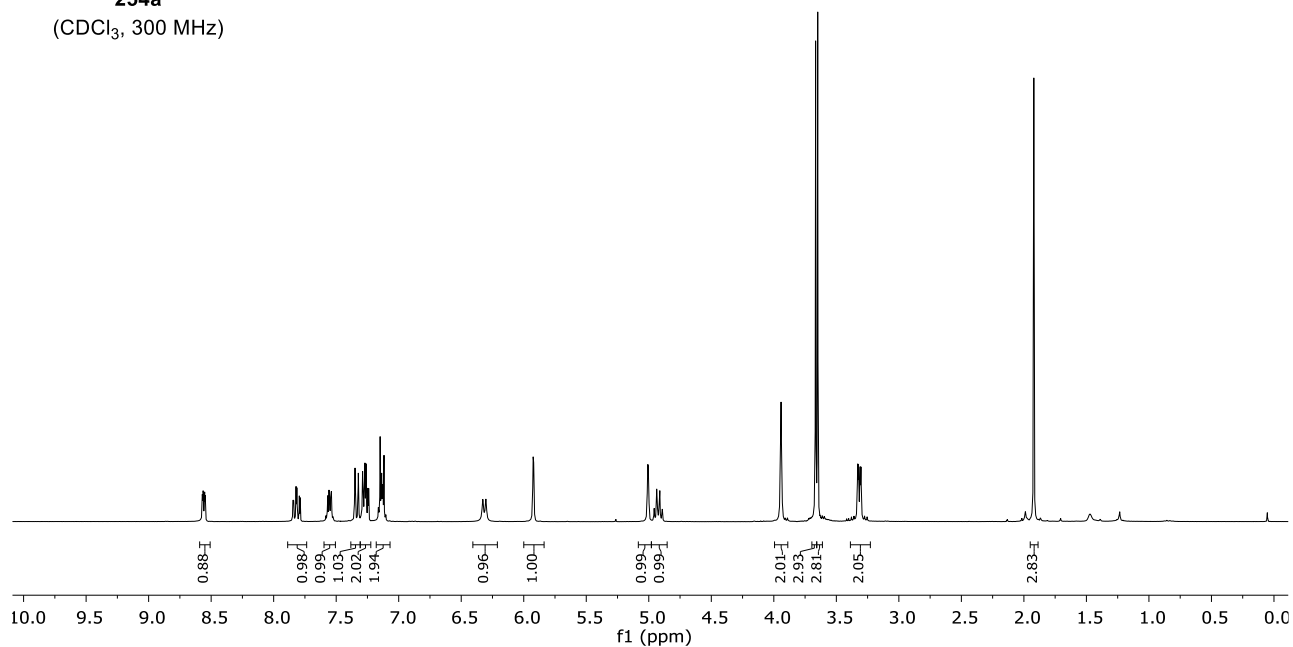


250c
(CDCl₃, 400 MHz)

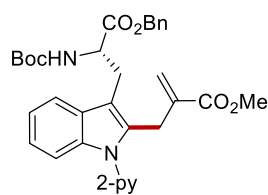


250c
(CDCl₃, 101 MHz)

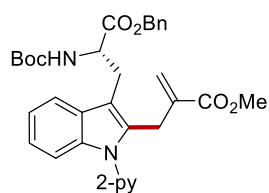
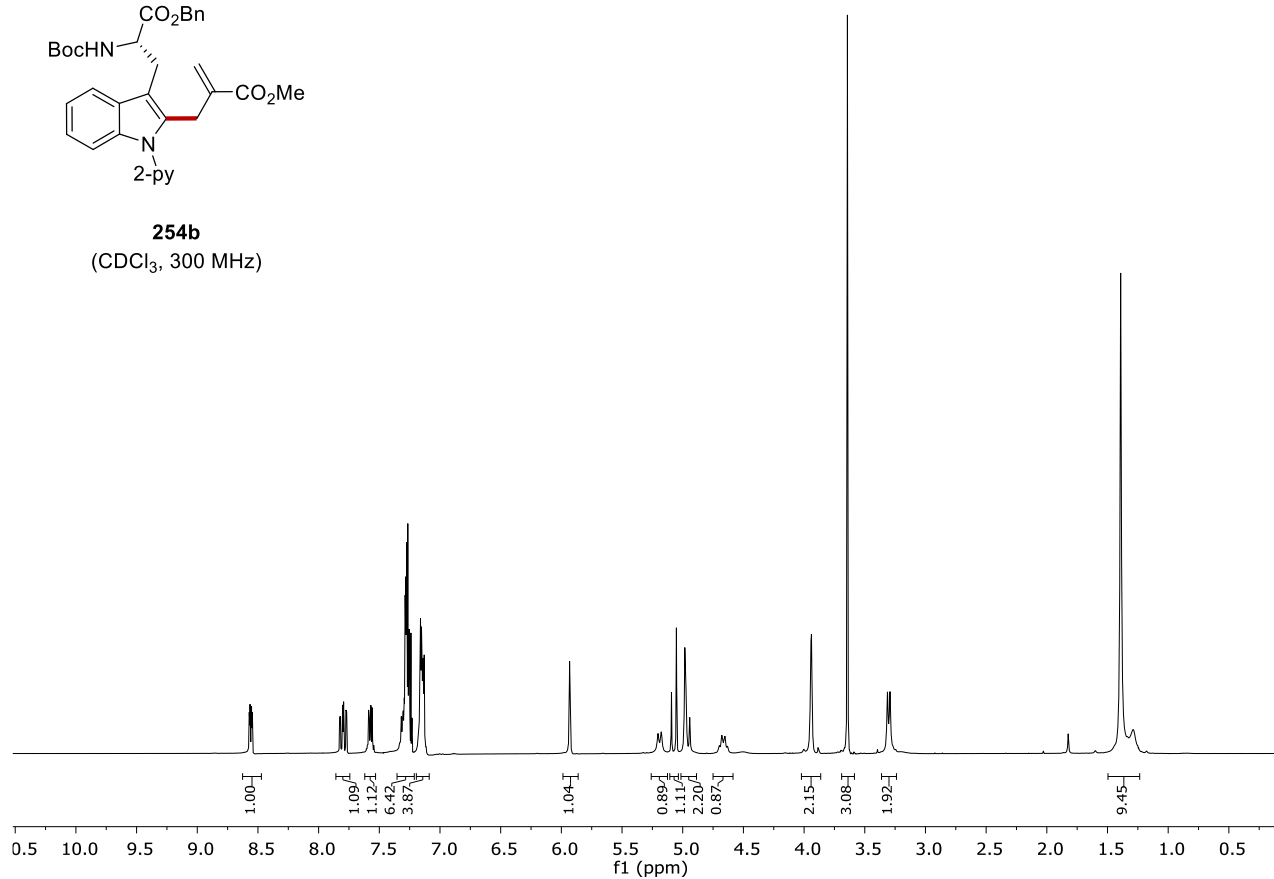


**254a**(CDCl₃, 300 MHz)**254a**(CDCl₃, 126 MHz)

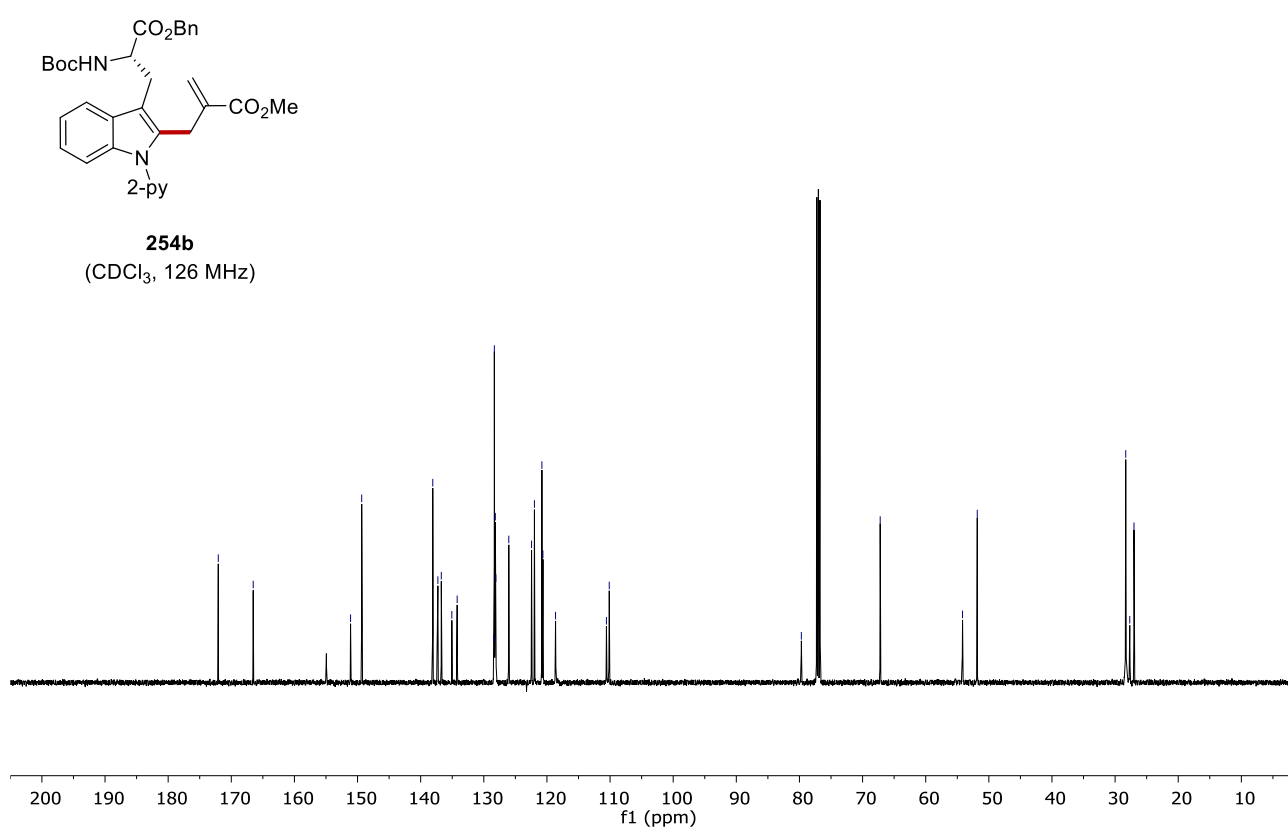
8. NMR Spectra

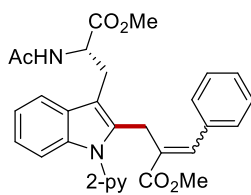


254b
(CDCl₃, 300 MHz)

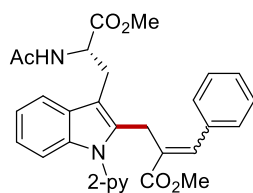
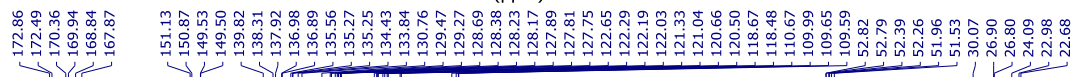
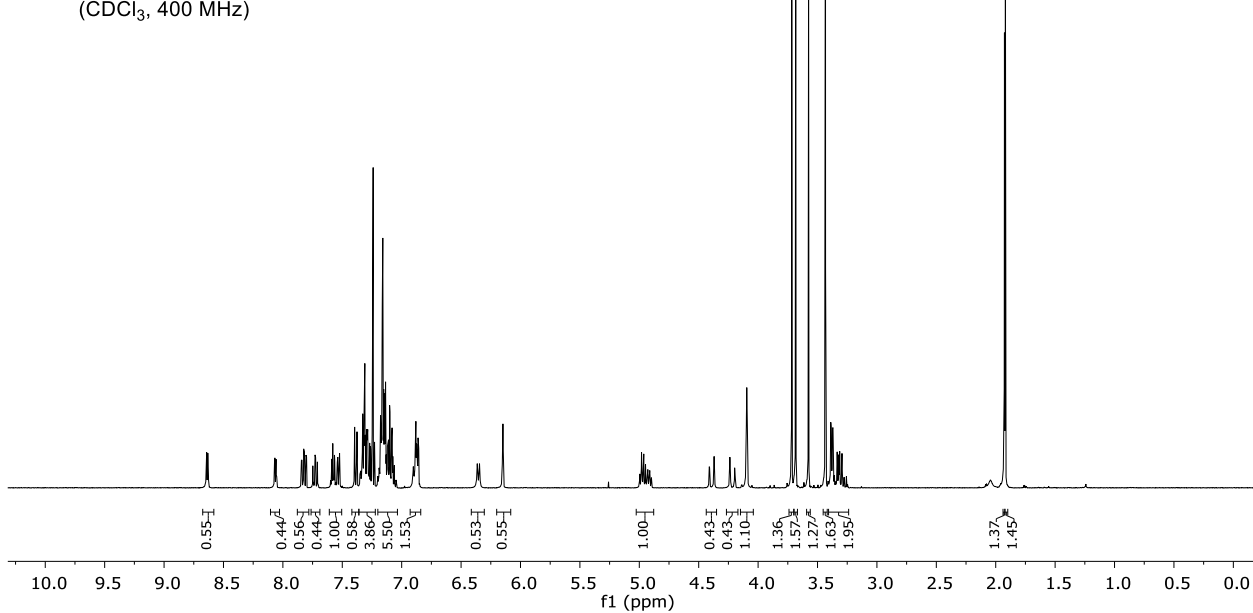


254b
(CDCl₃, 126 MHz)

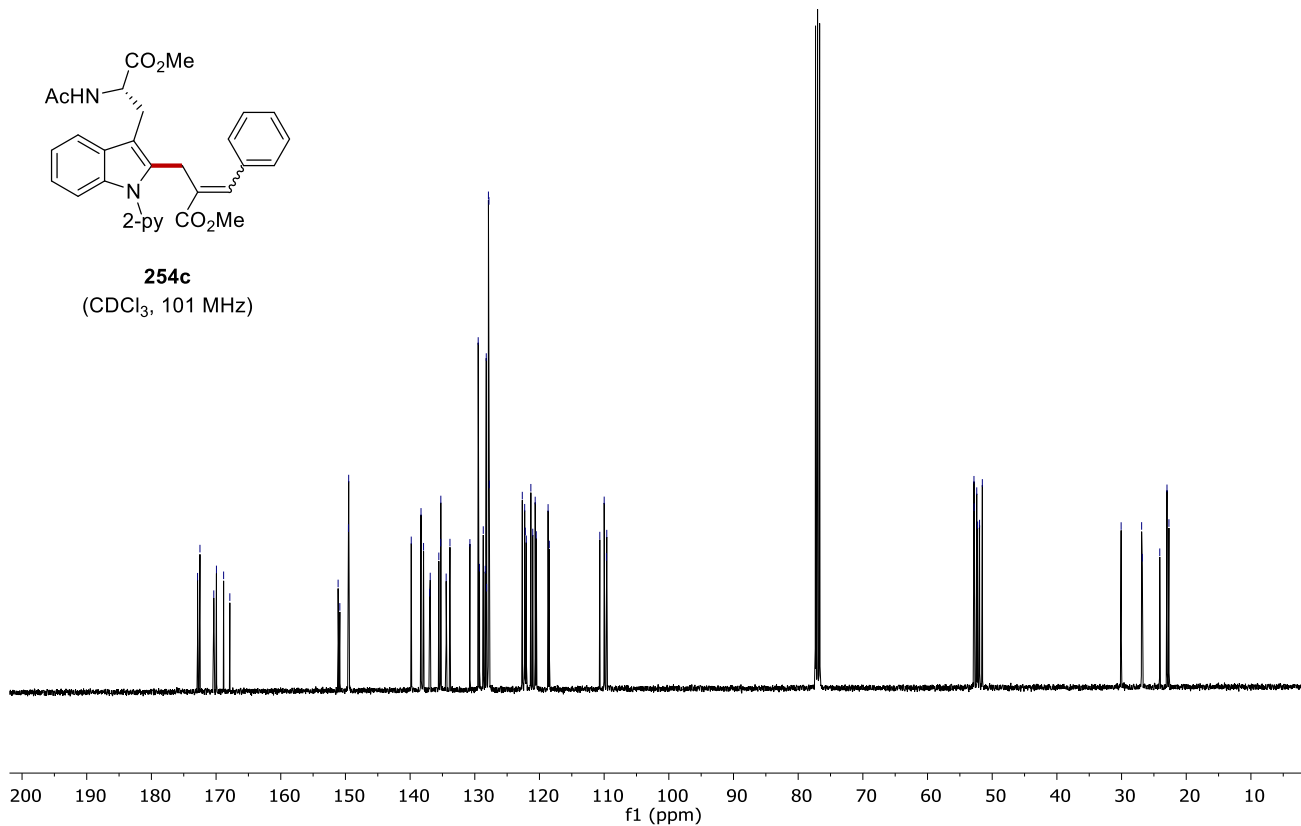




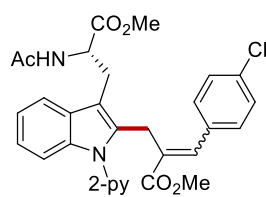
254c
(CDCl₃, 400 MHz)



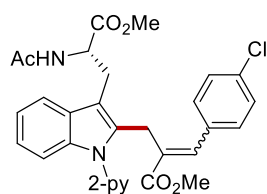
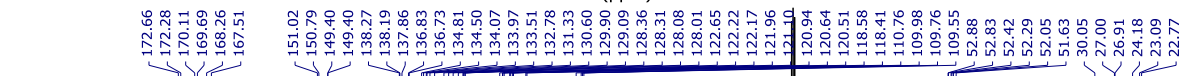
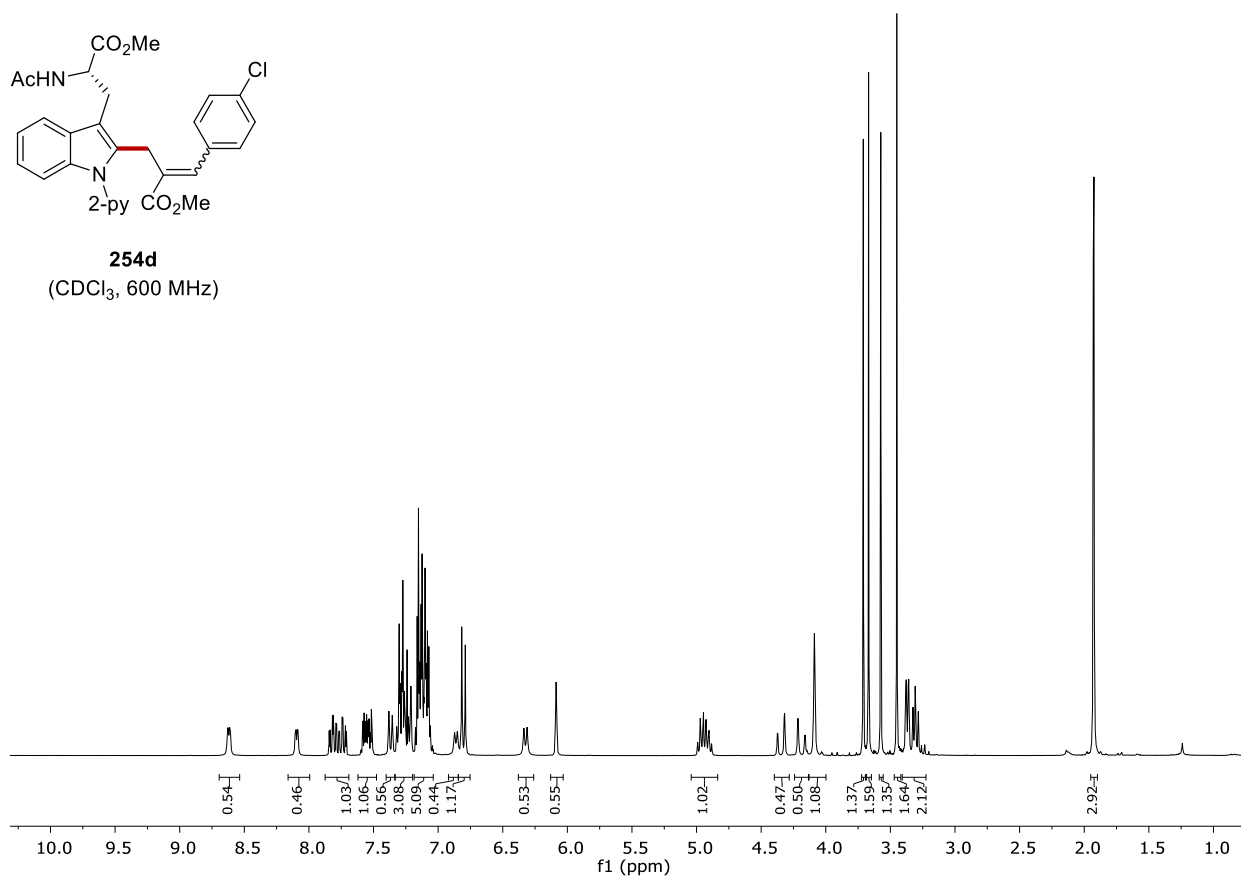
254c
(CDCl₃, 101 MHz)



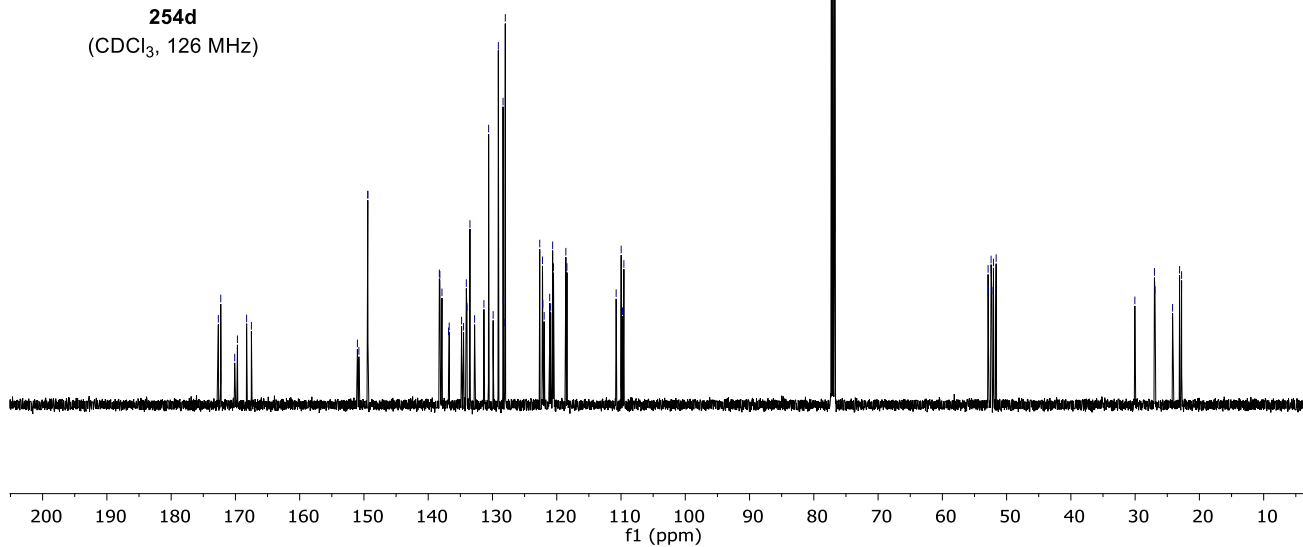
8. NMR Spectra



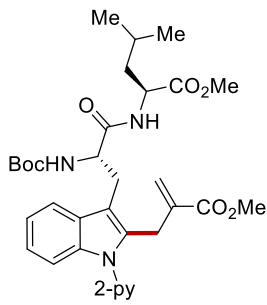
254d
(CDCl₃, 600 MHz)



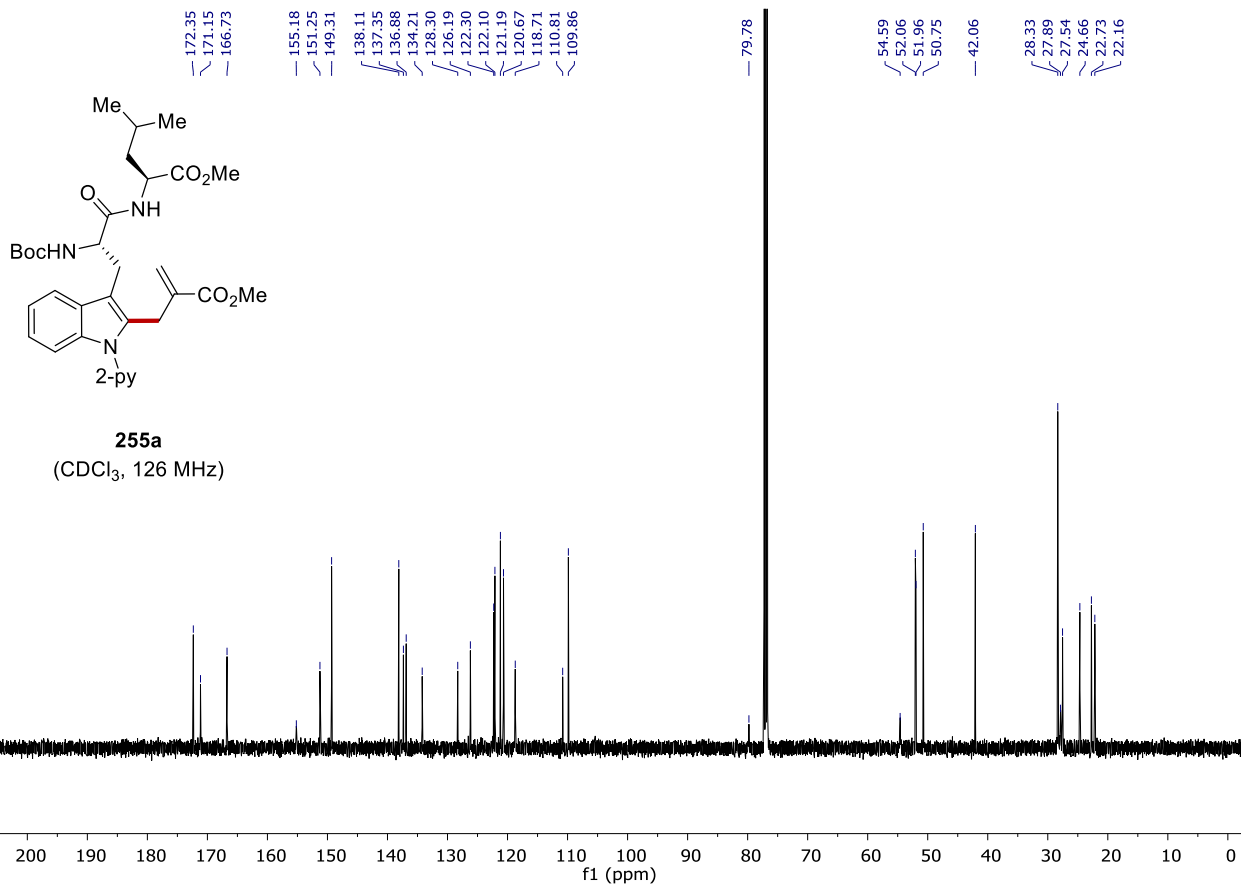
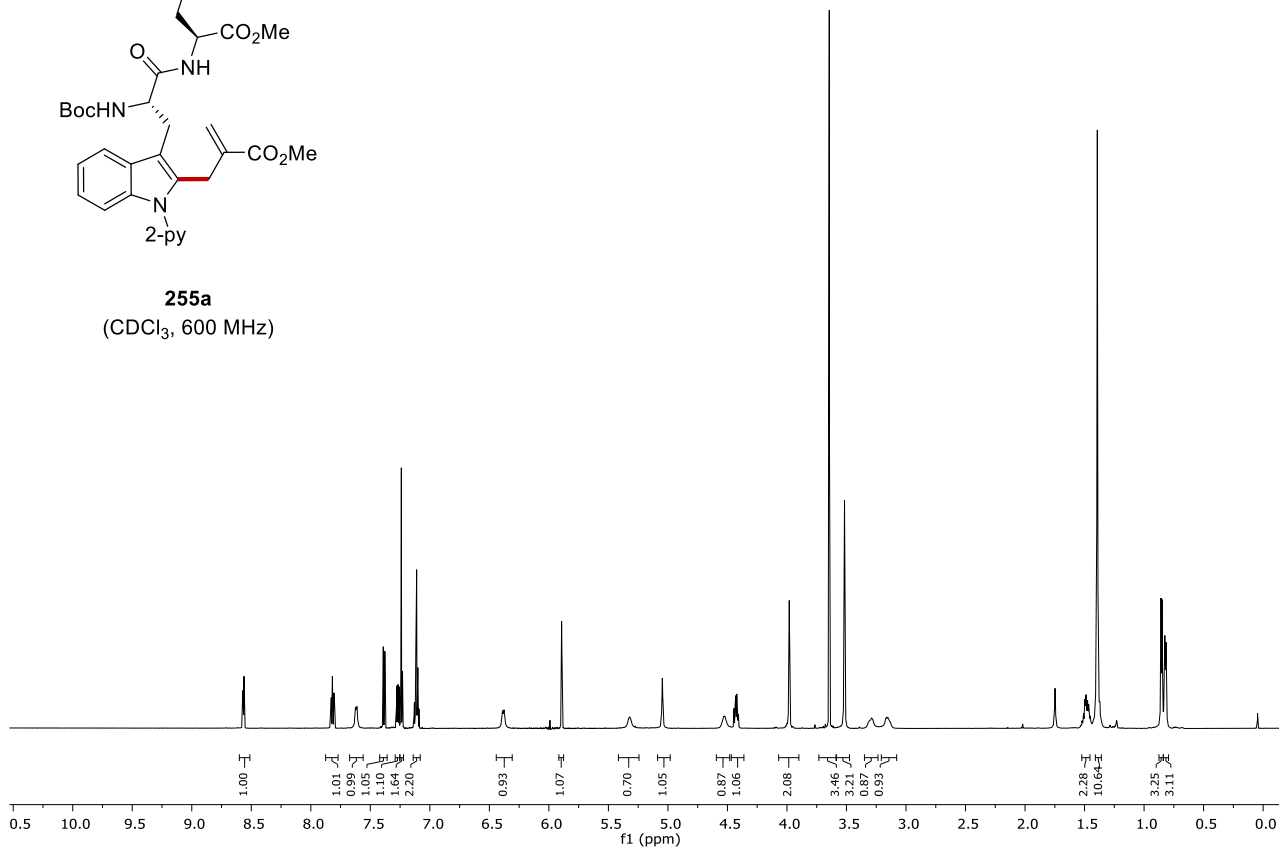
254d
(CDCl₃, 126 MHz)



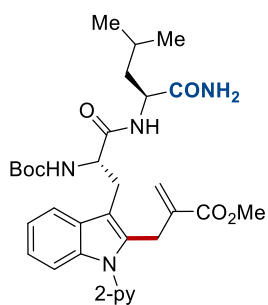
8. NMR Spectra



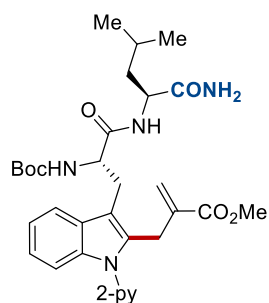
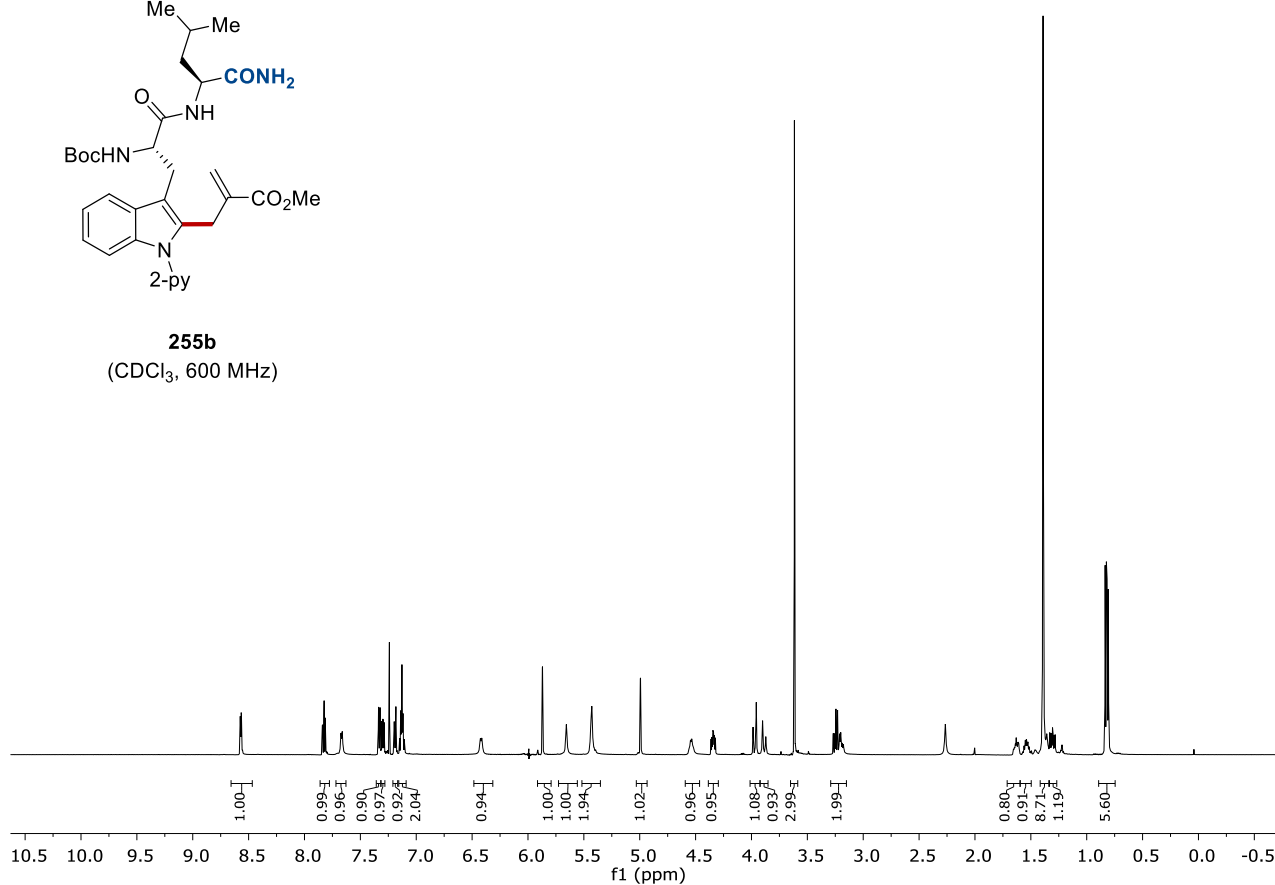
255a
(CDCl₃, 600 MHz)



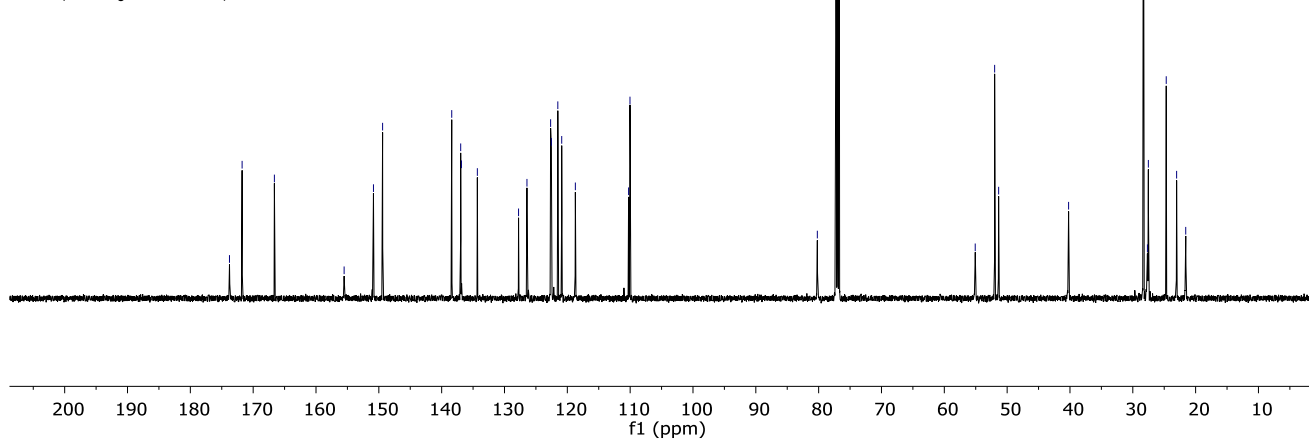
8. NMR Spectra

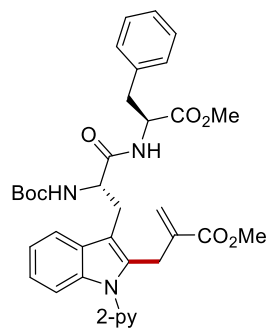


255b
(CDCl₃, 600 MHz)

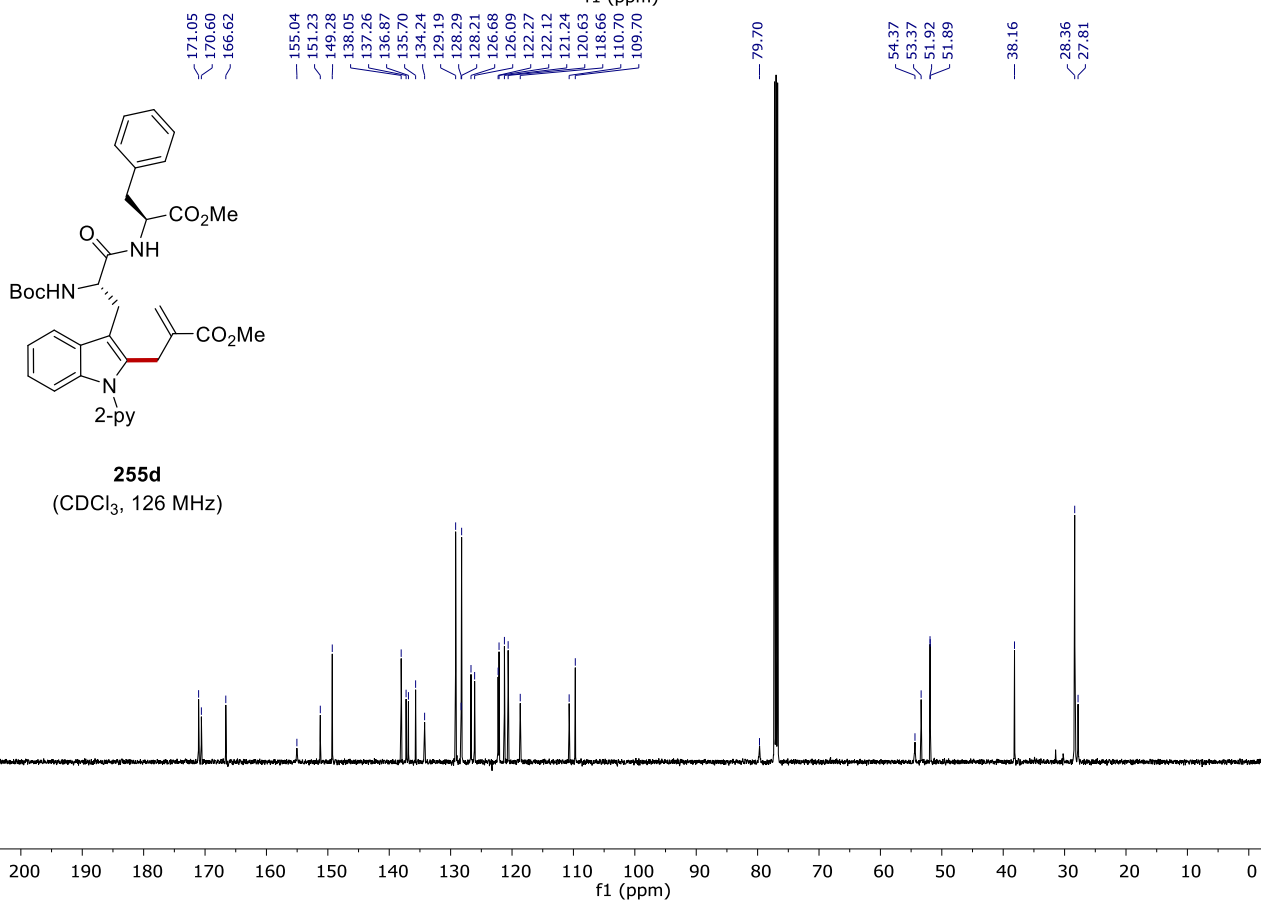
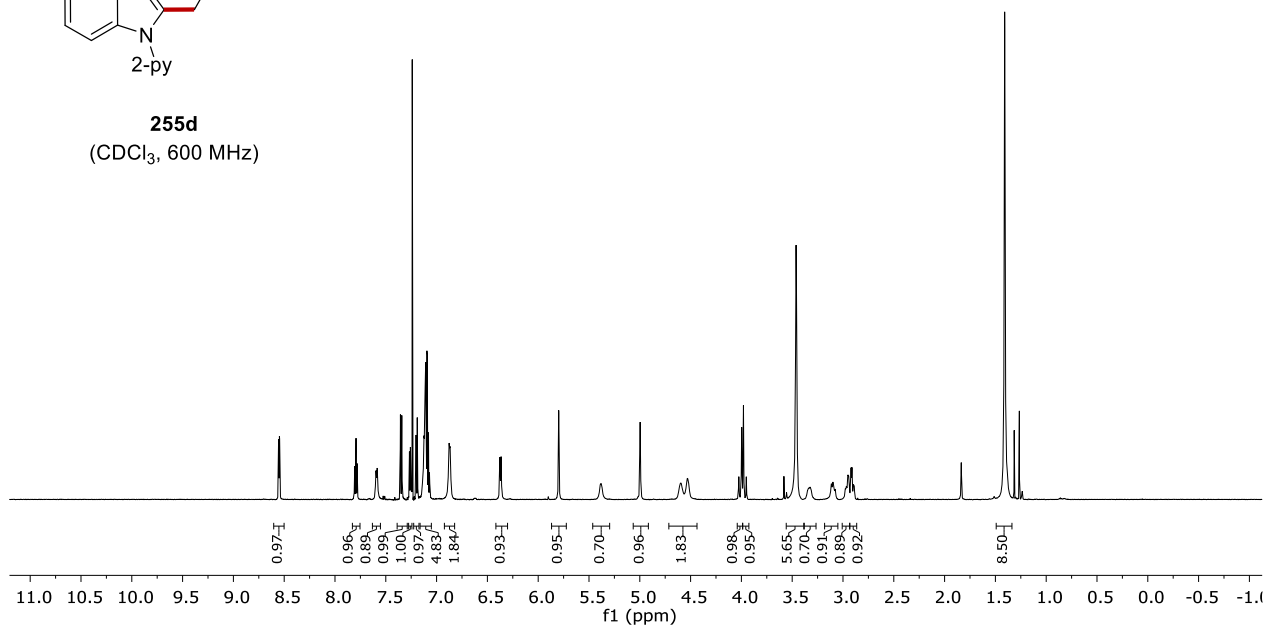


255b
(CDCl₃, 126 MHz)

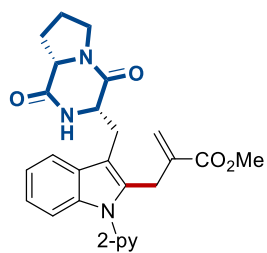




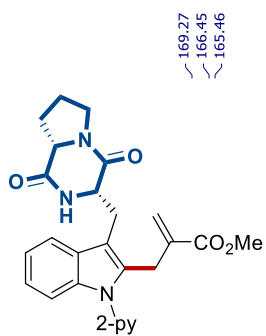
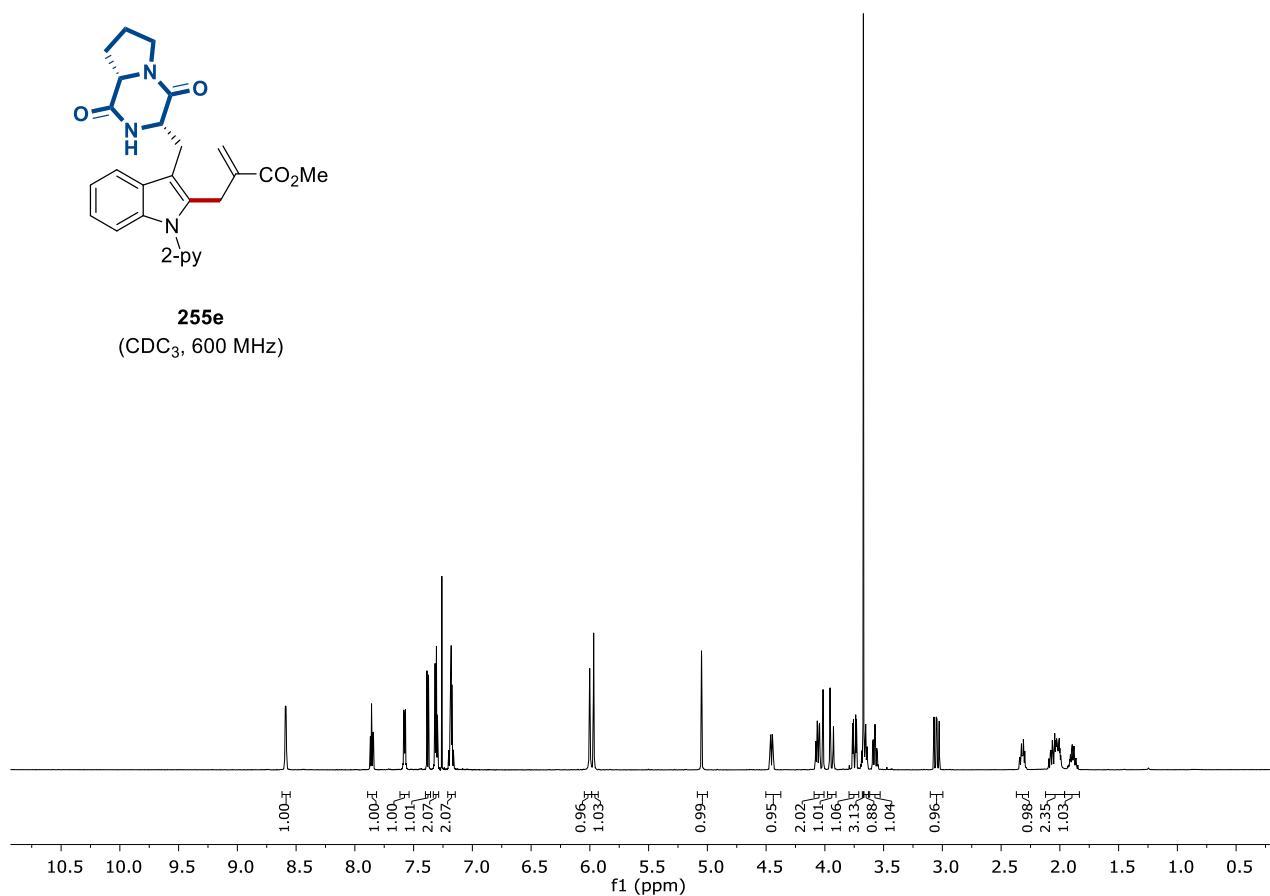
255d
(CDCl_3 , 600 MHz)



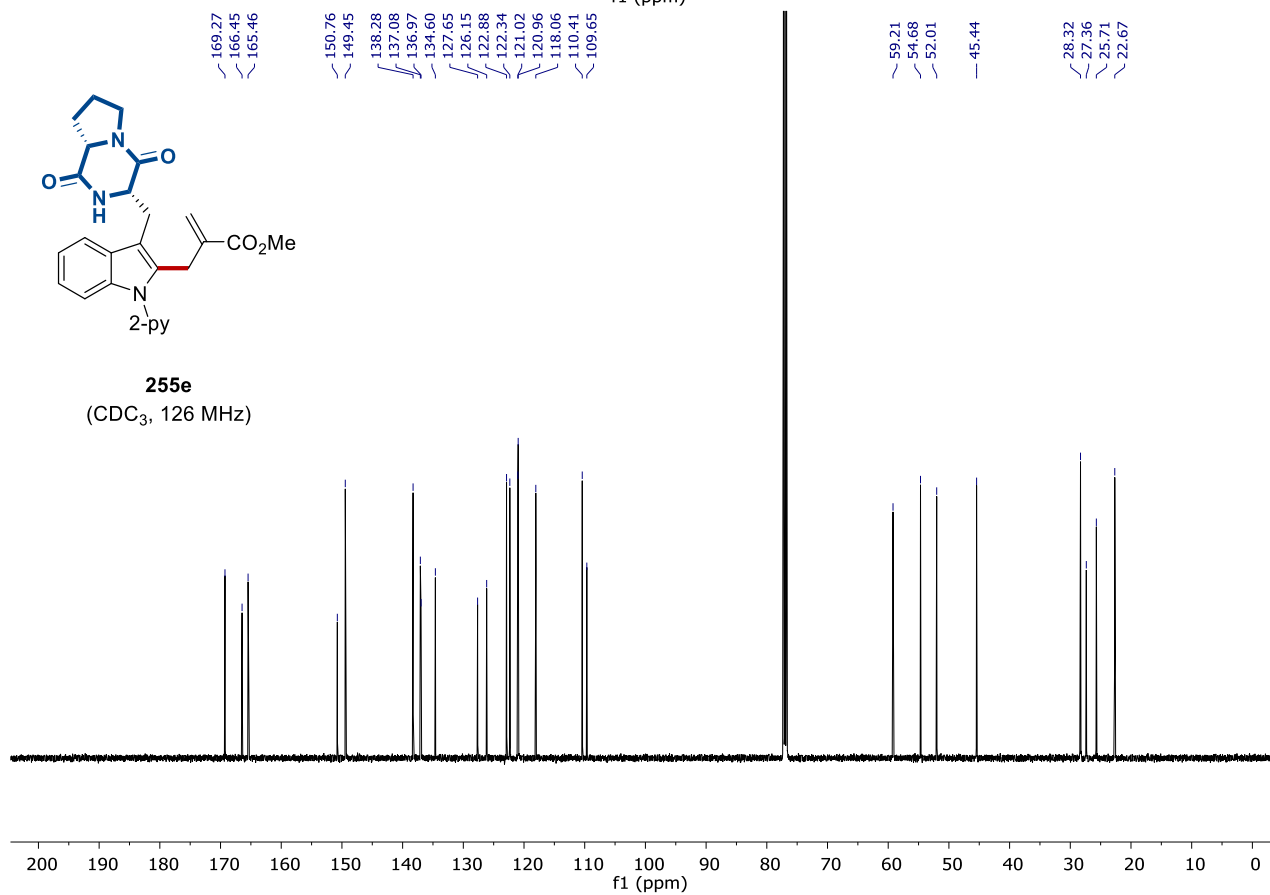
8. NMR Spectra

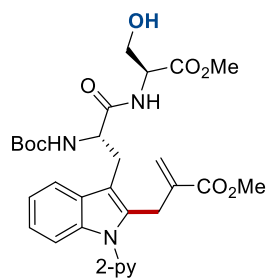


255e
(CDCl₃, 600 MHz)

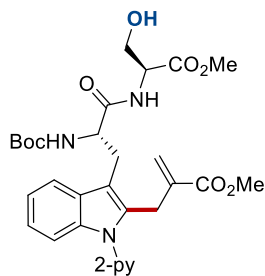
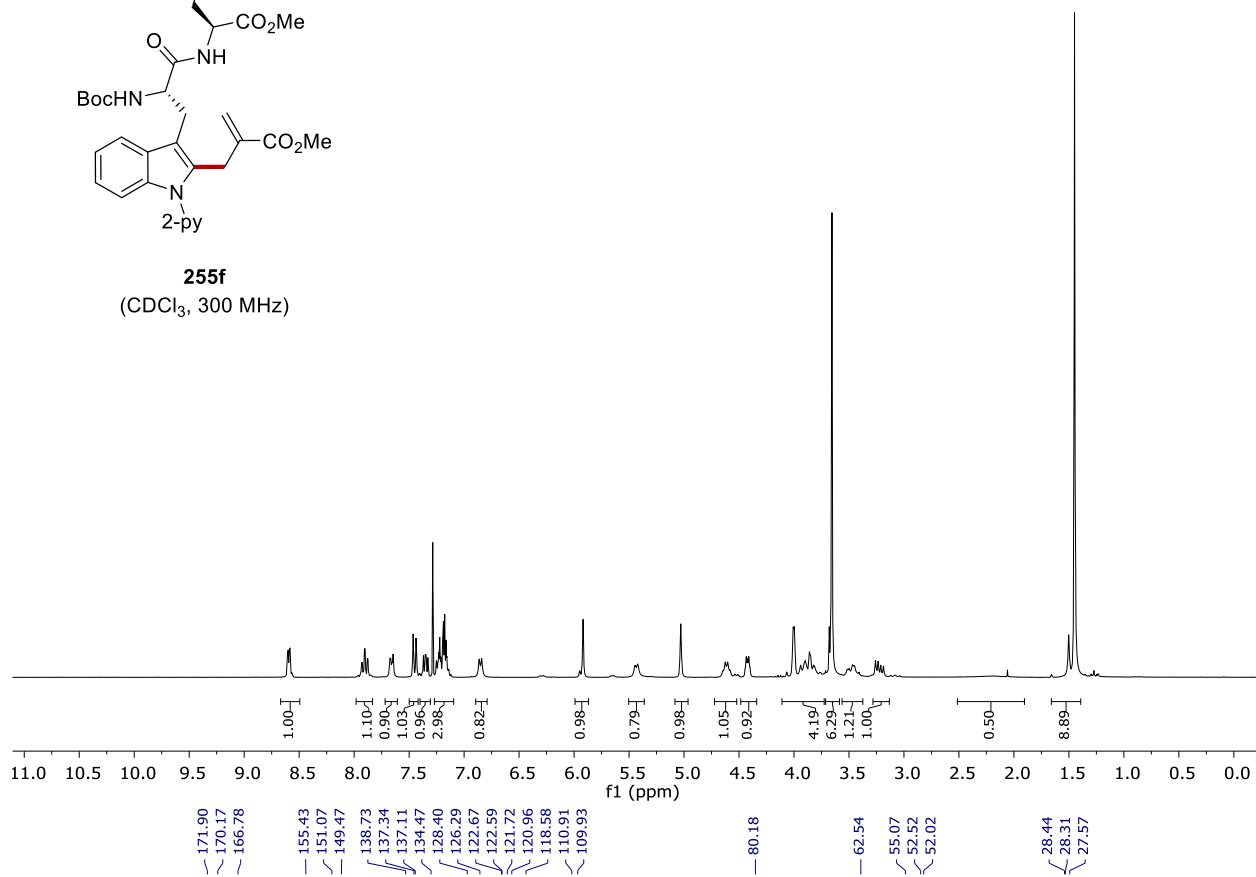


255e
(CDCl₃, 126 MHz)

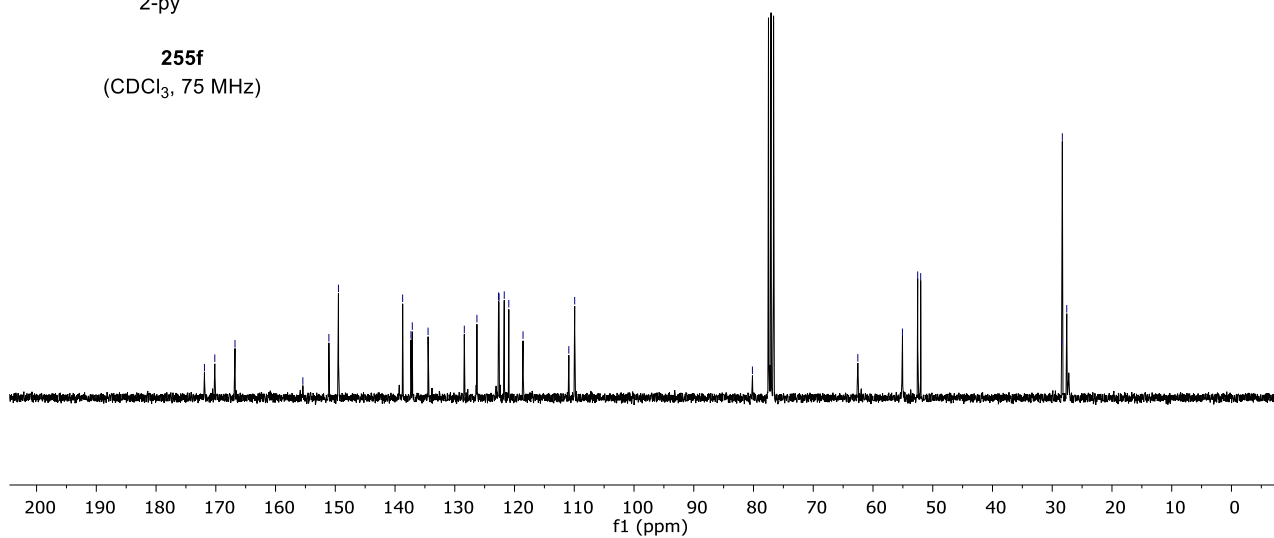




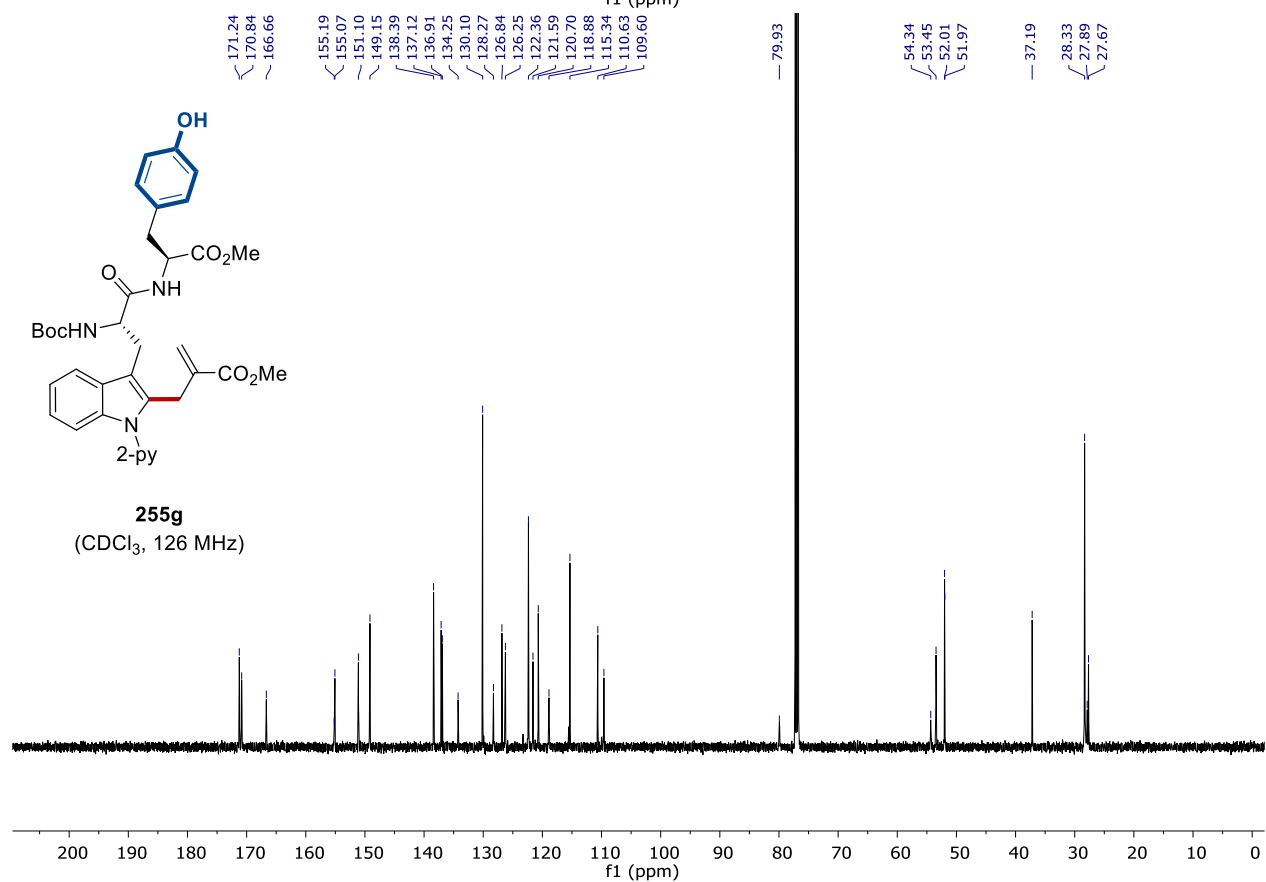
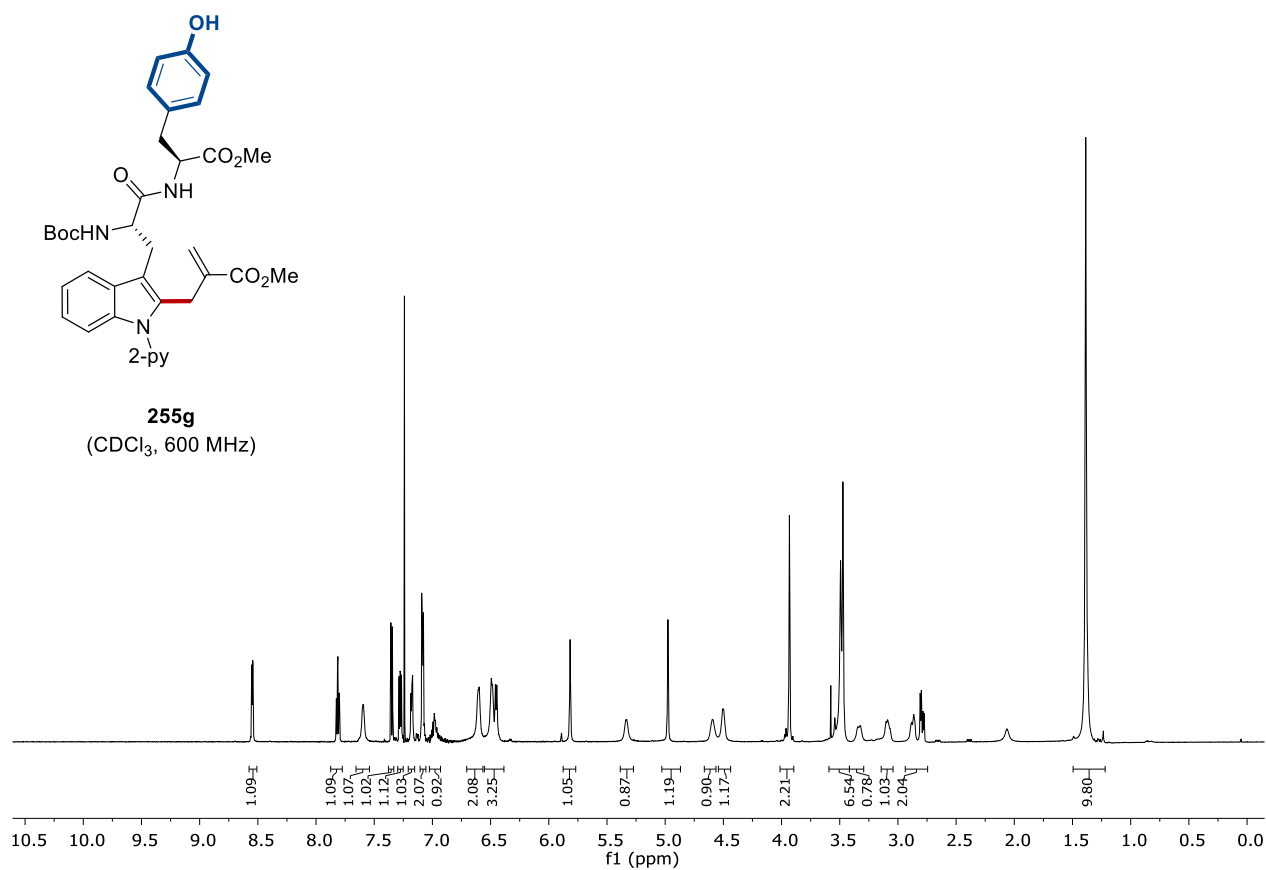
255f
(CDCl₃, 300 MHz)



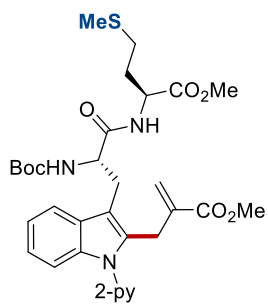
255f
(CDCl₃, 75 MHz)



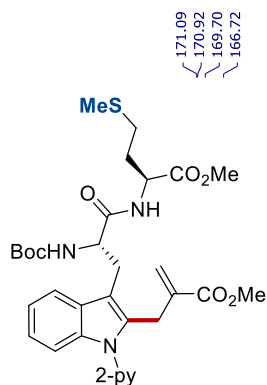
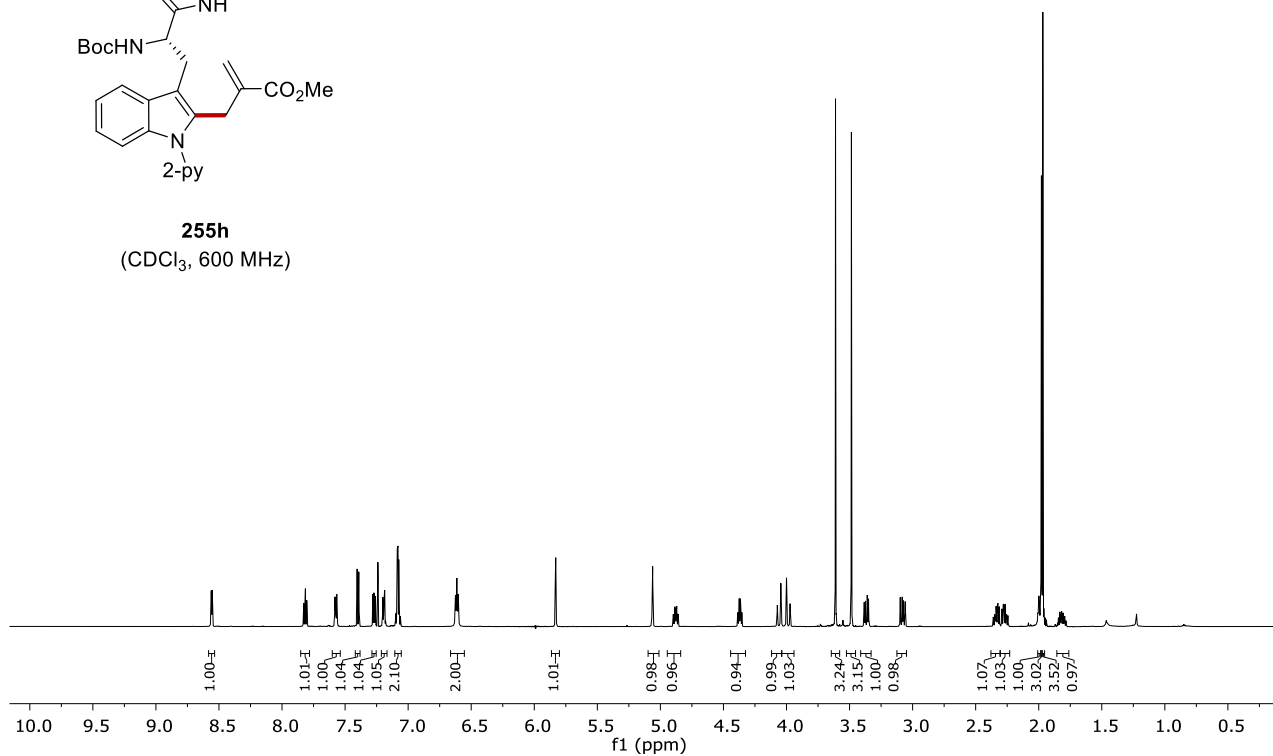
8. NMR Spectra



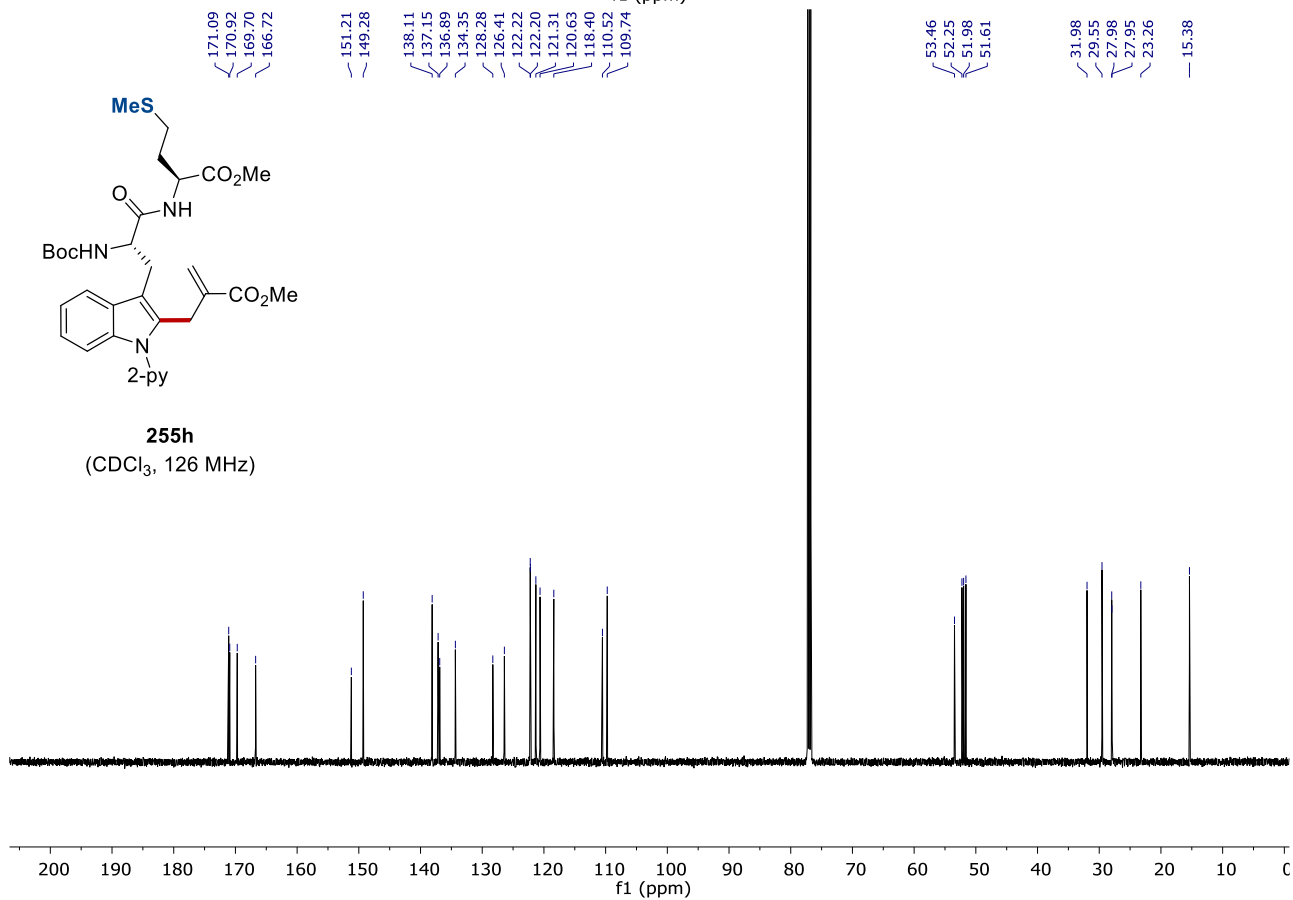
8. NMR Spectra



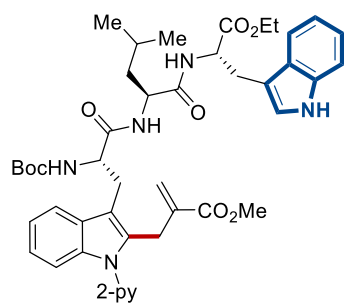
255h
(CDCl₃, 600 MHz)



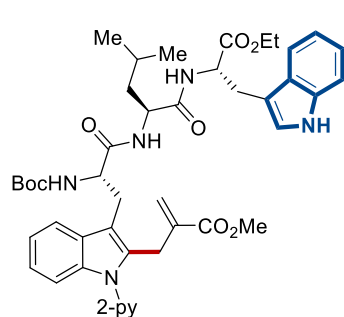
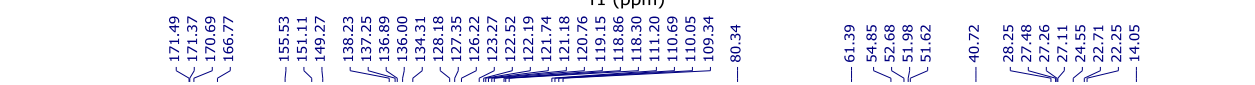
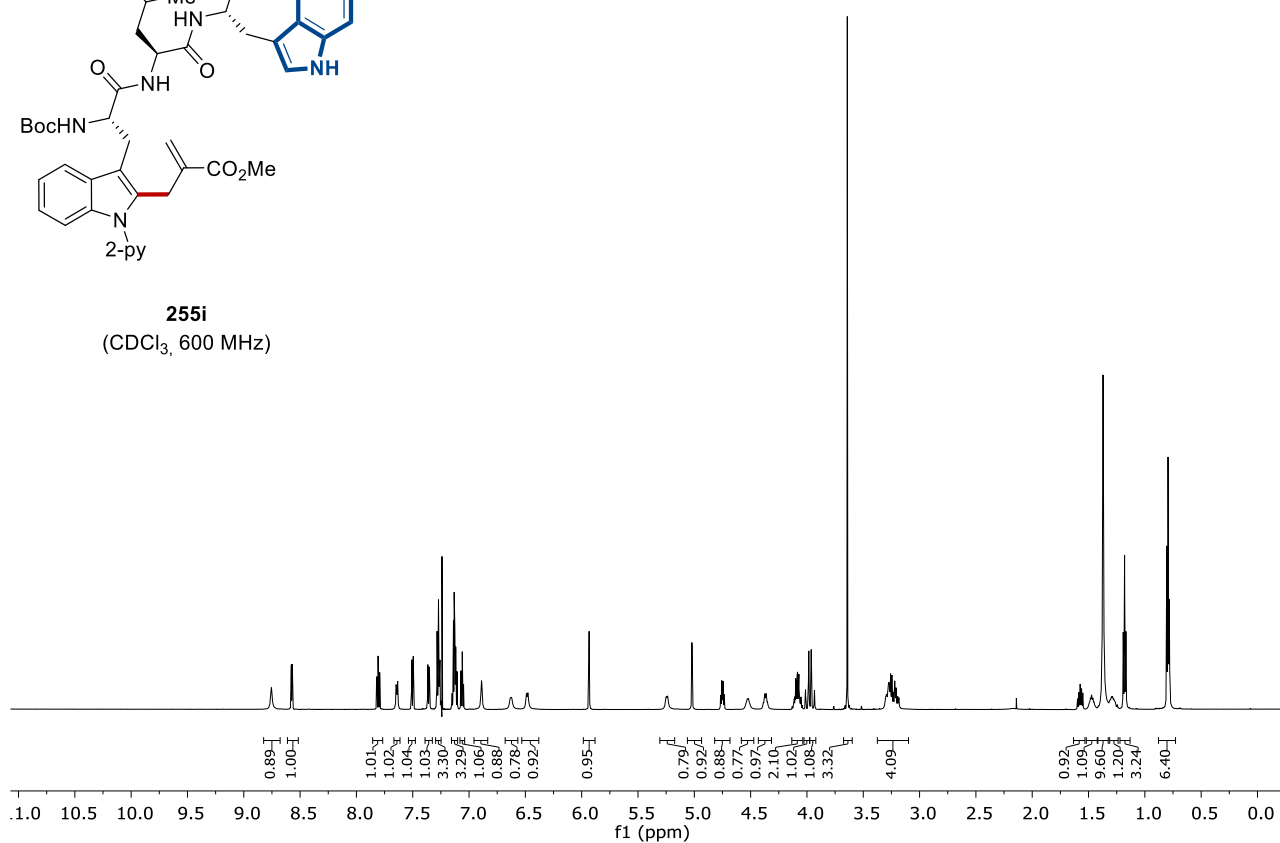
255h
(CDCl₃, 126 MHz)



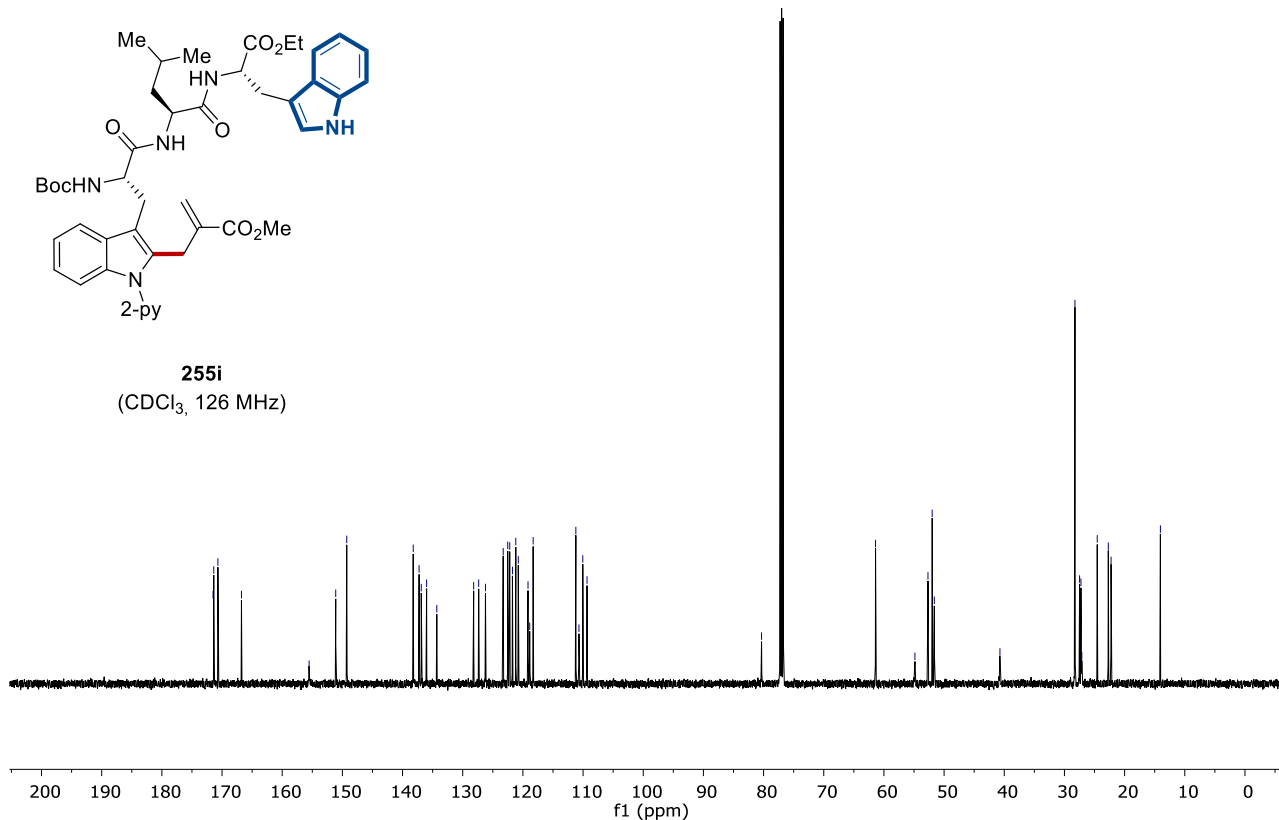
8. NMR Spectra

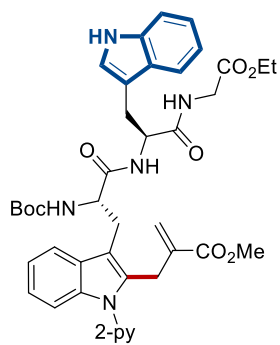


255i
(CDCl₃, 600 MHz)

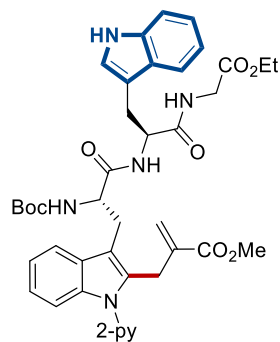
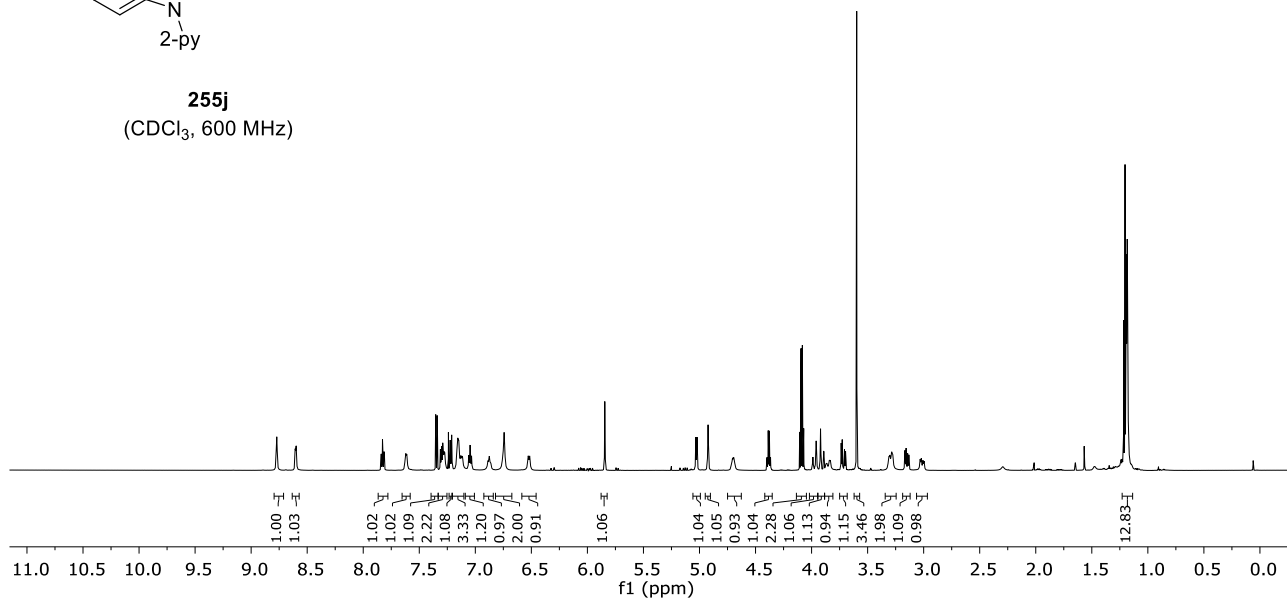


255i
(CDCl₃, 126 MHz)

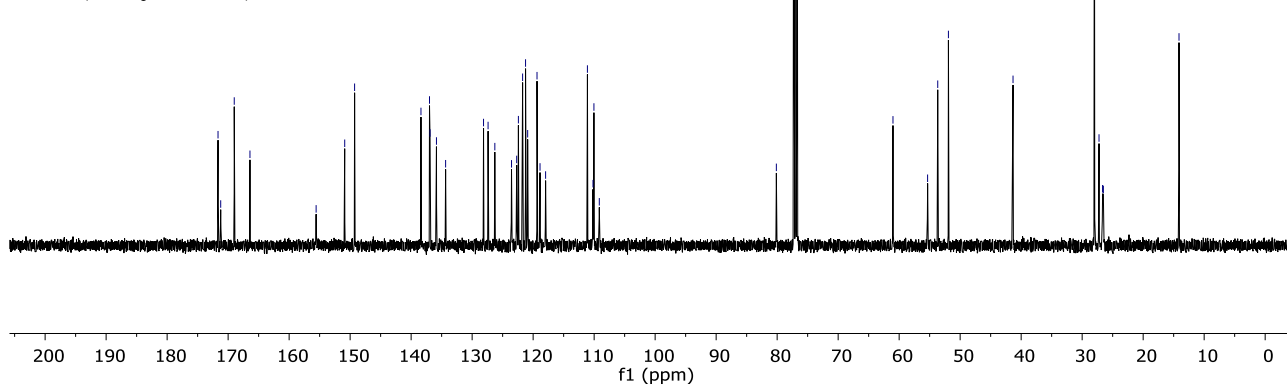




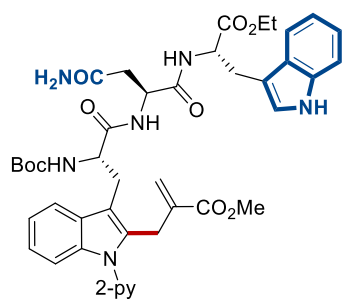
255j
(CDCl₃, 600 MHz)



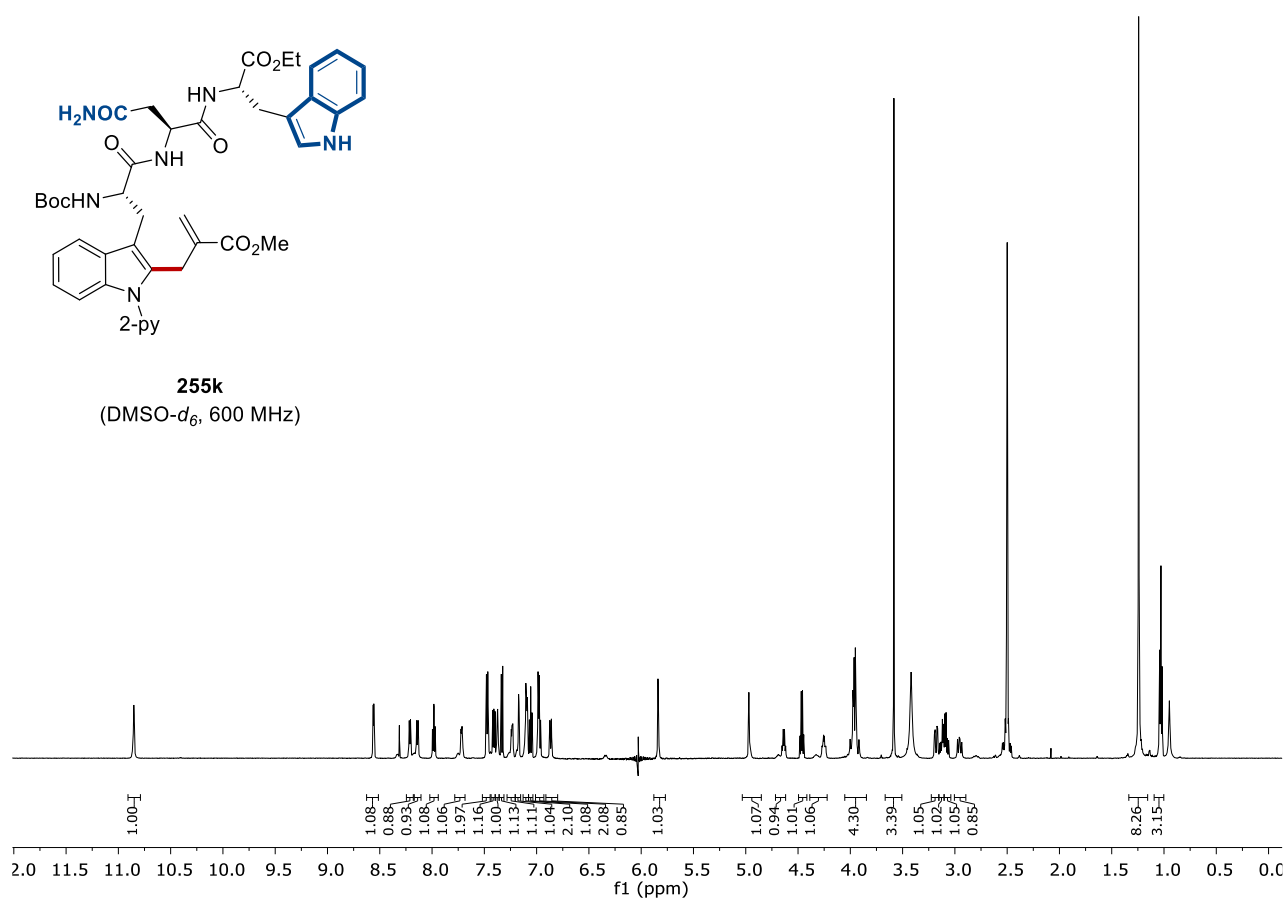
255j
(CDCl₃, 126 MHz)



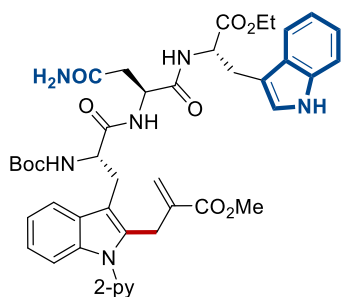
8. NMR Spectra



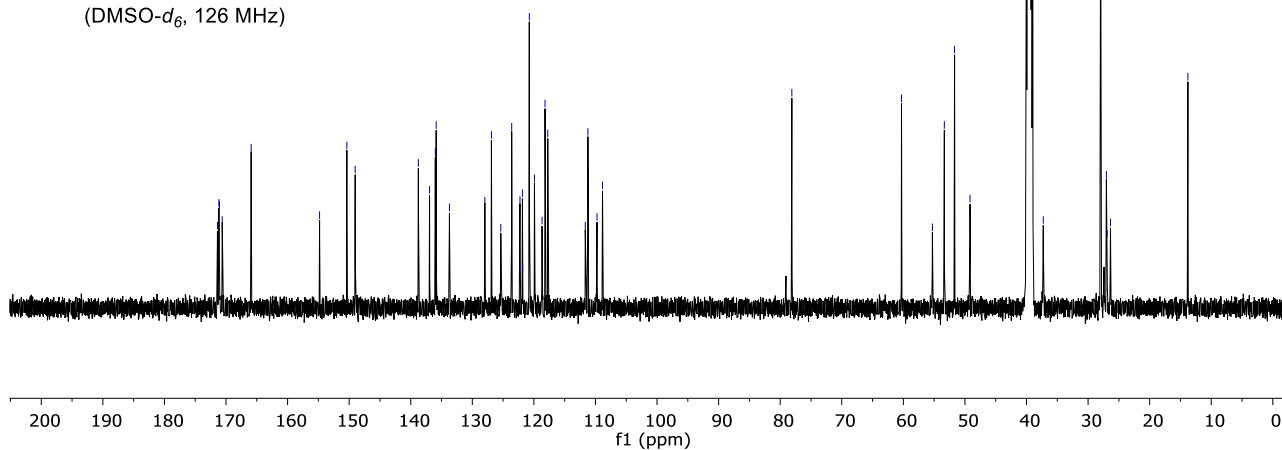
255k
(DMSO-*d*₆, 600 MHz)

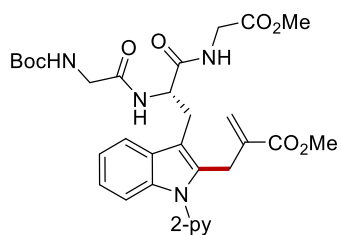


171.38, 171.15, 171.07, 170.61, 165.91, 154.80, 150.37, 149.02, 138.76, 136.94, 136.01, 135.87, 133.71, 127.96, 126.89, 125.38, 123.60, 122.26, 121.86, 121.83, 120.74, 119.91, 118.68, 118.19, 117.75, 111.66, 111.23, 109.75, 108.86, 78.11, 60.30, 55.28, 53.34, 51.68, 49.17, 40.00, 37.28, 27.95, 27.03, 26.91, 26.36, 13.79

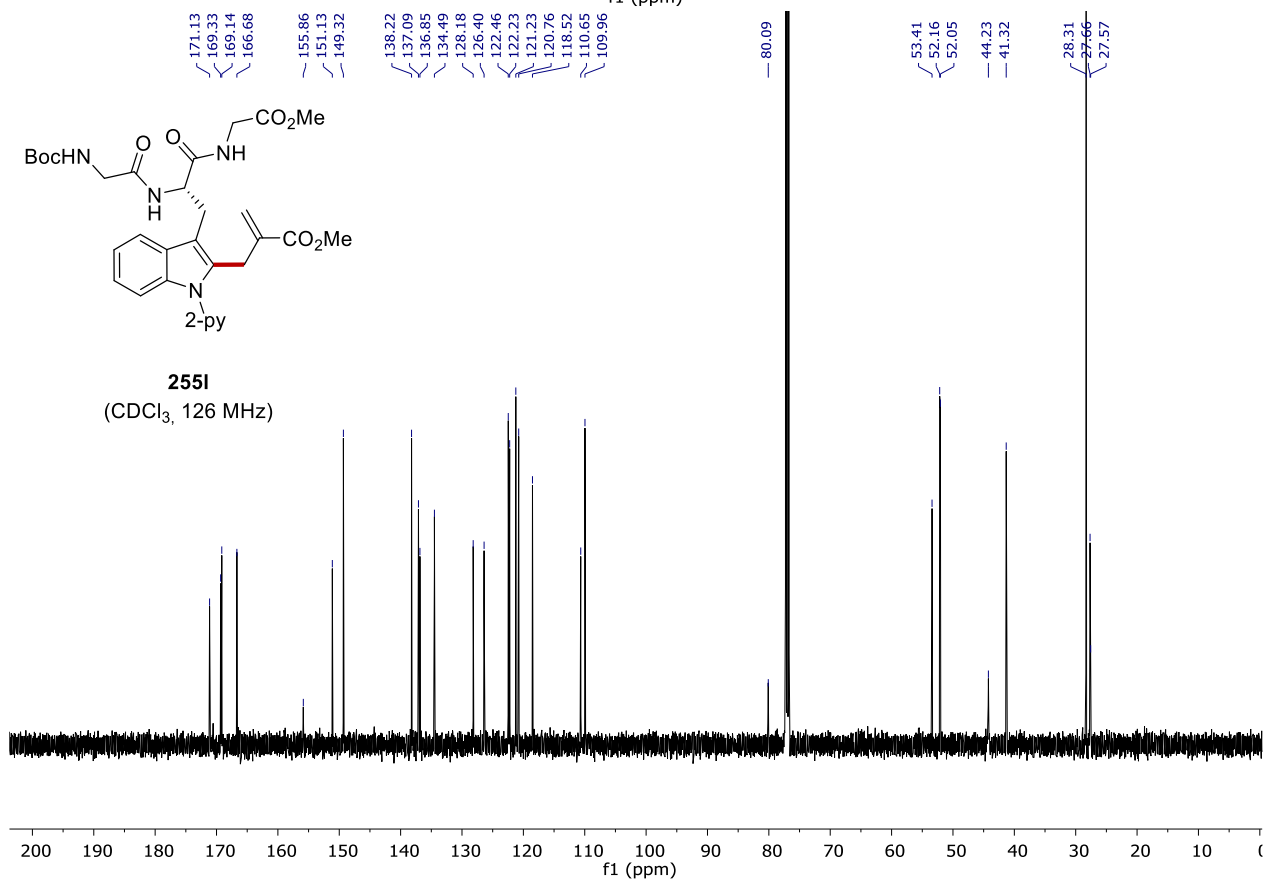
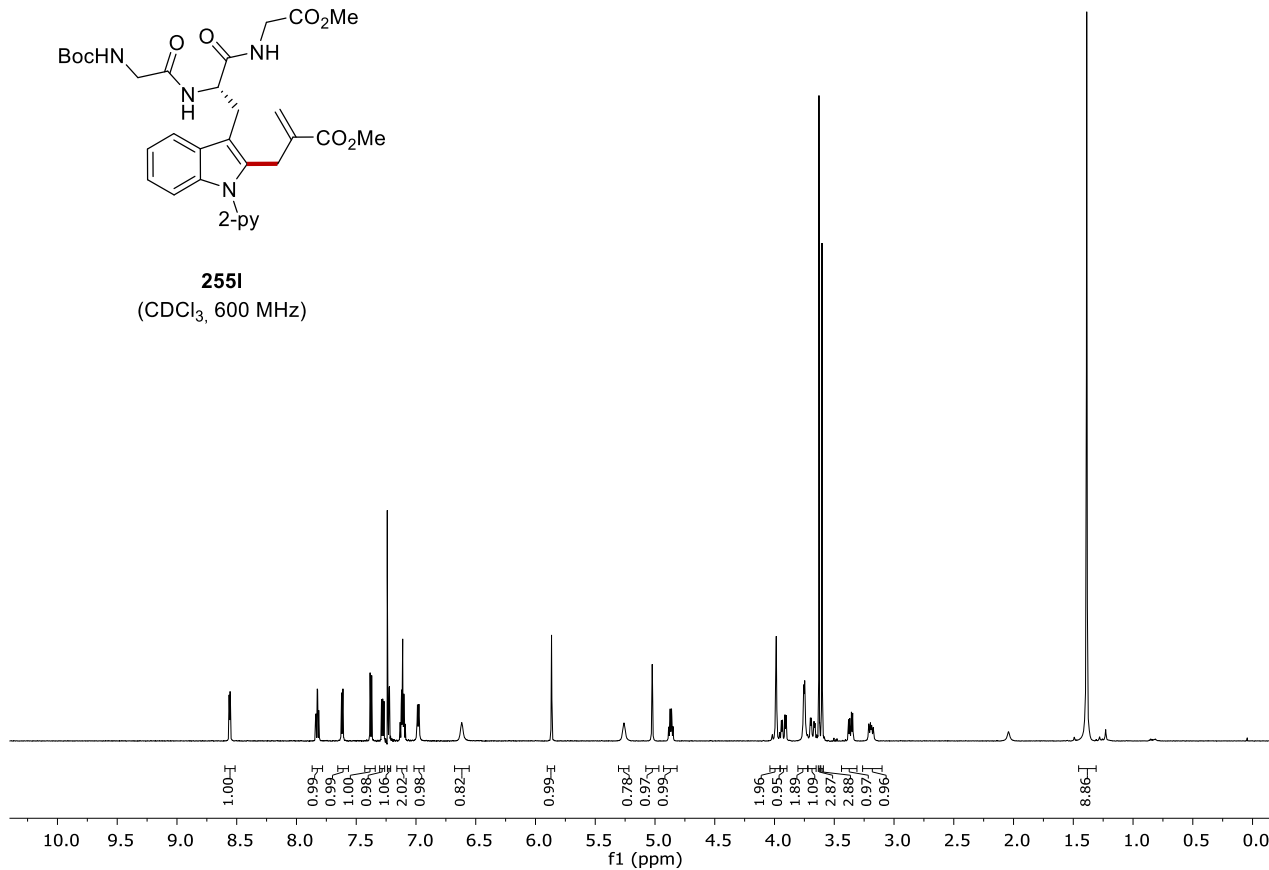


255k
(DMSO-*d*₆, 126 MHz)

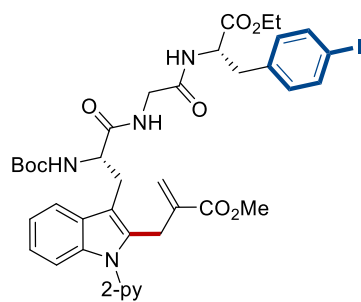




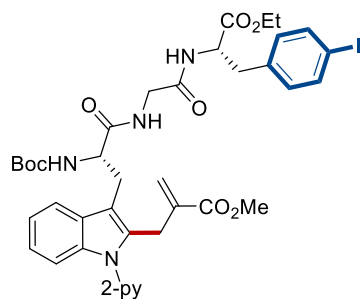
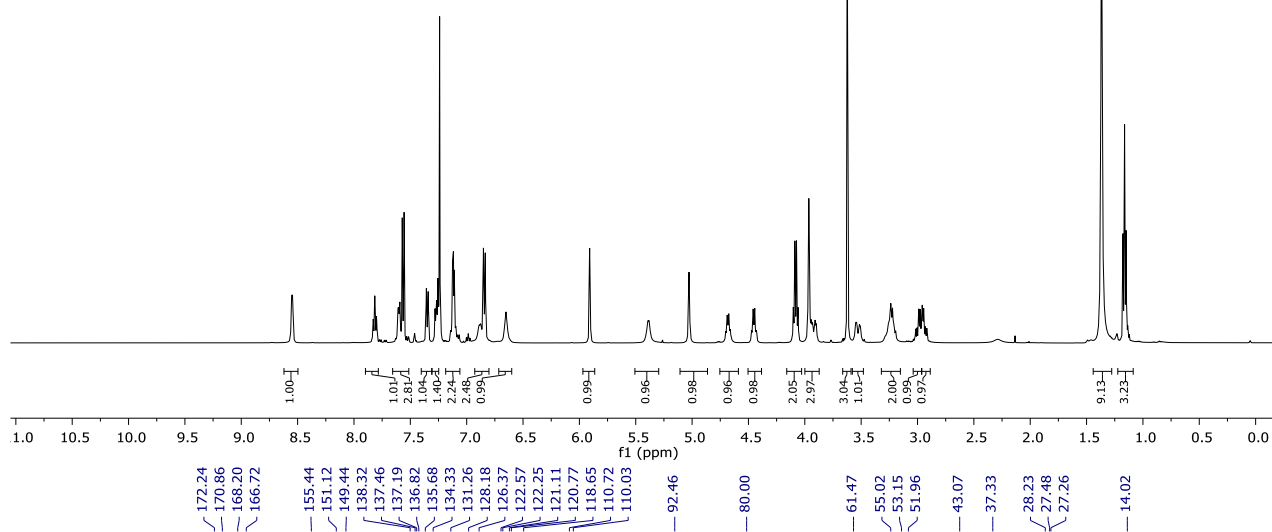
255I
(CDCl₃, 600 MHz)



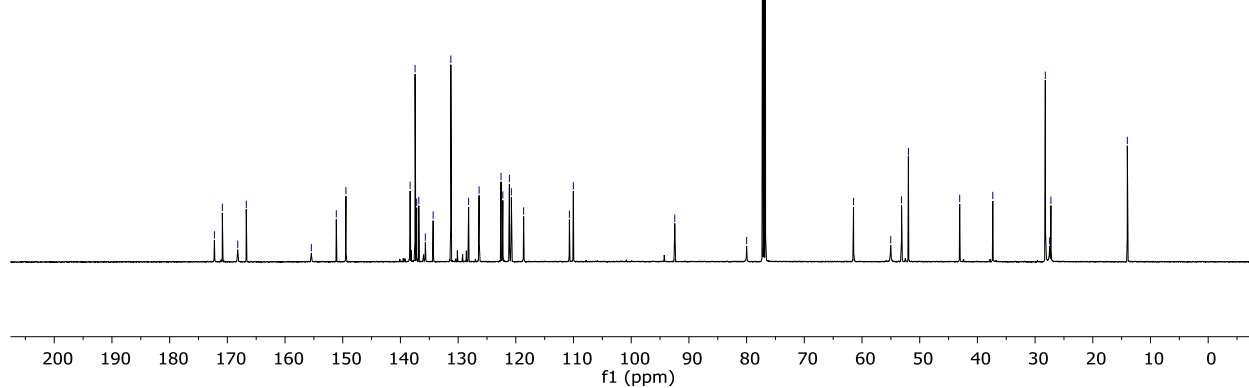
8. NMR Spectra



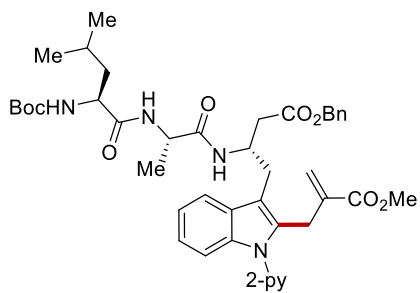
255m
(CDCl₃, 500 MHz)



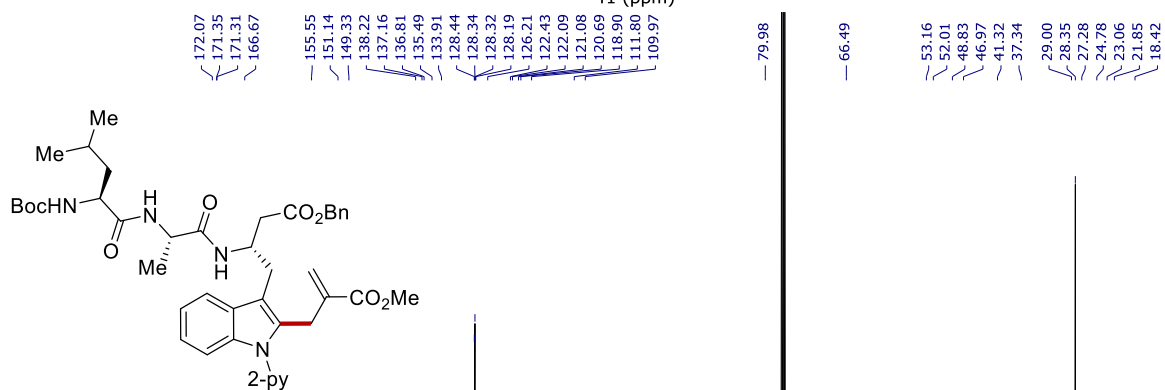
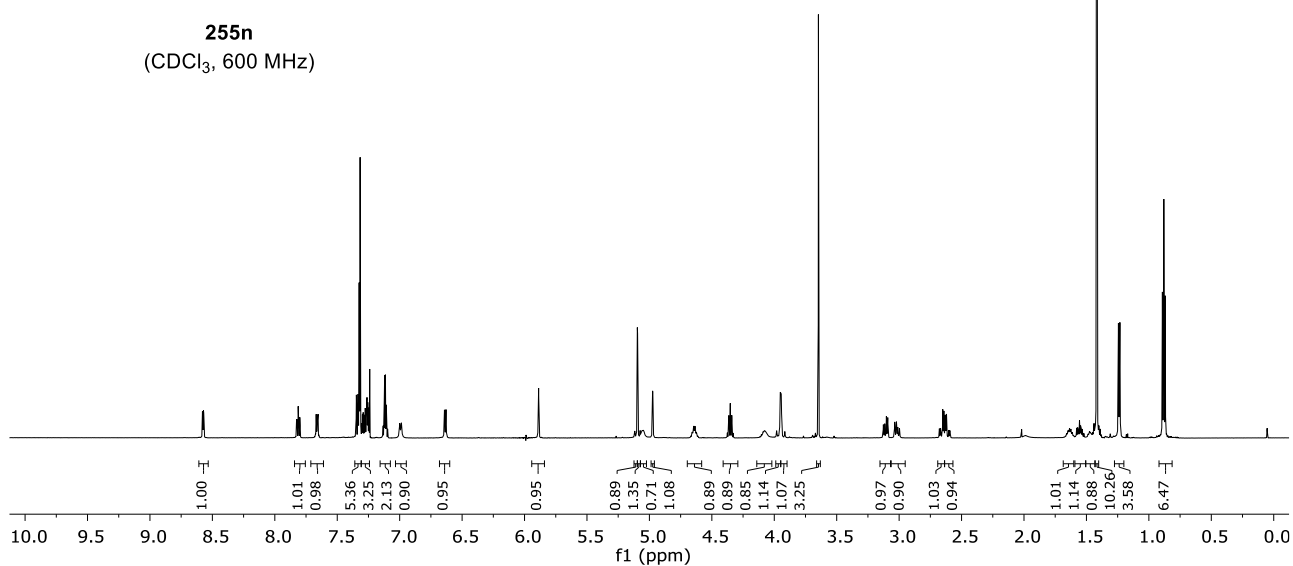
255m
(CDCl₃, 126 MHz)



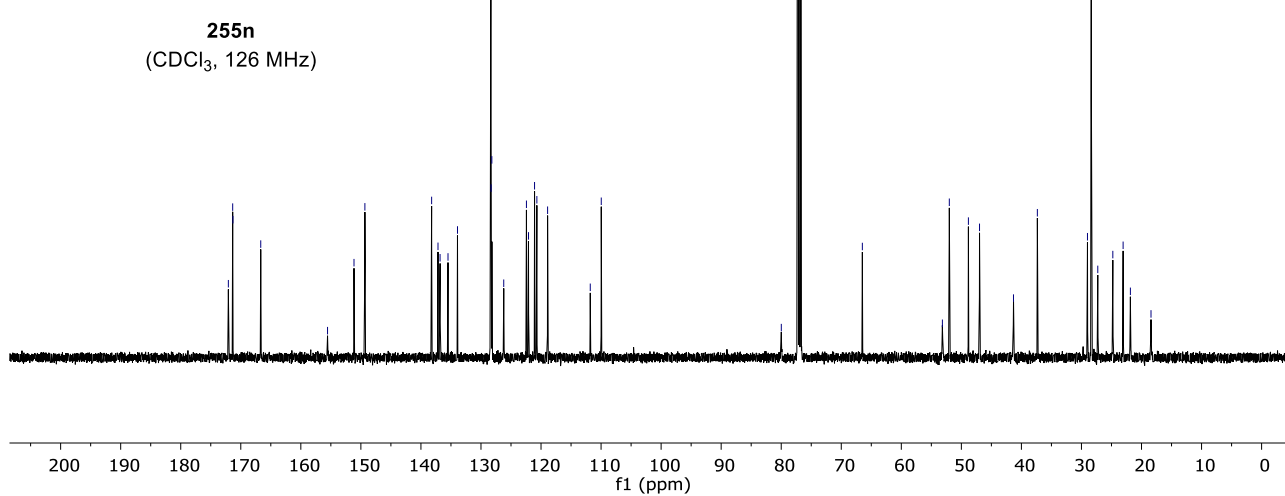
8. NMR Spectra



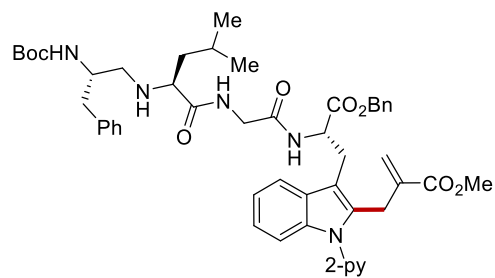
255n
(CDCl₃, 600 MHz)



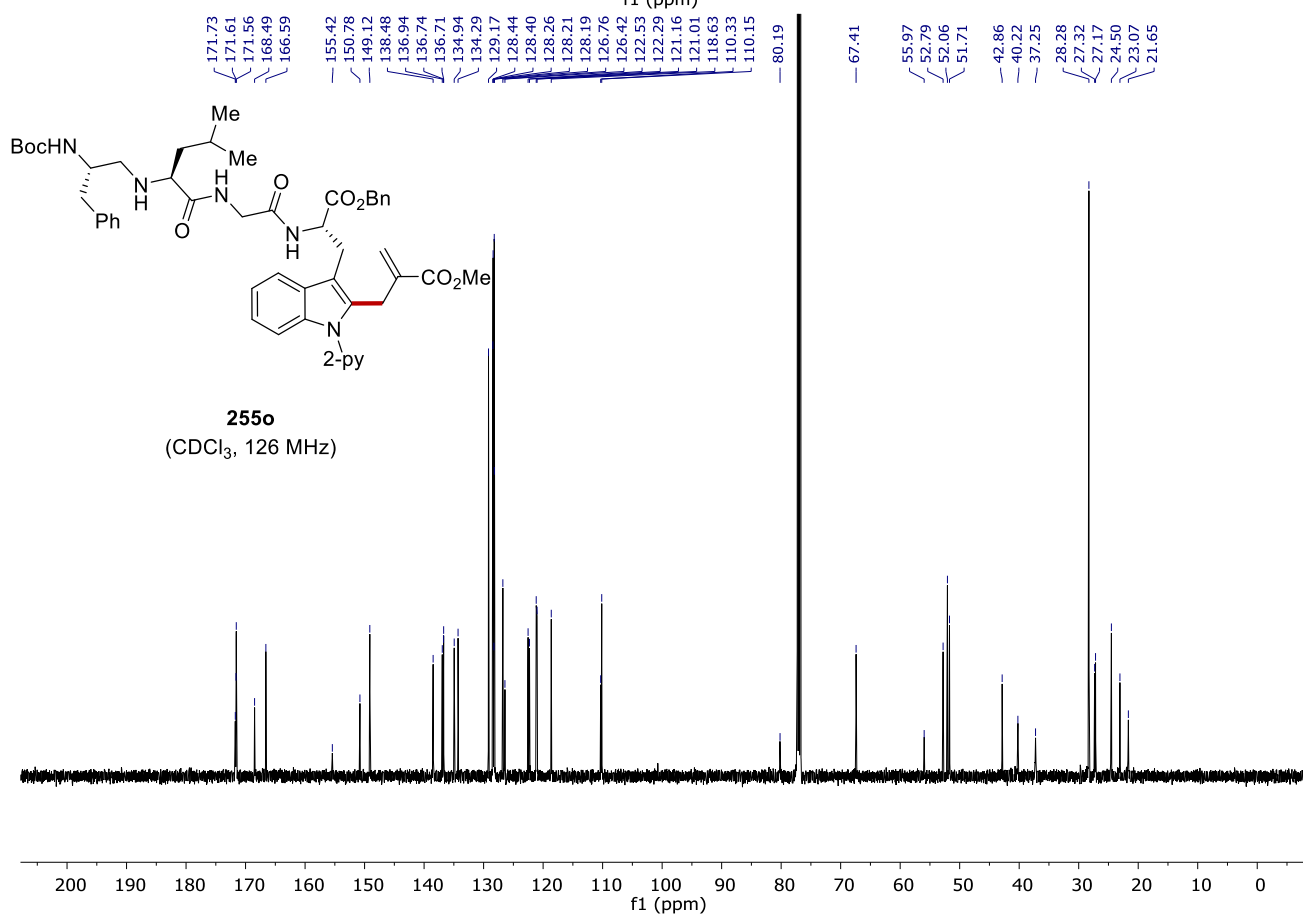
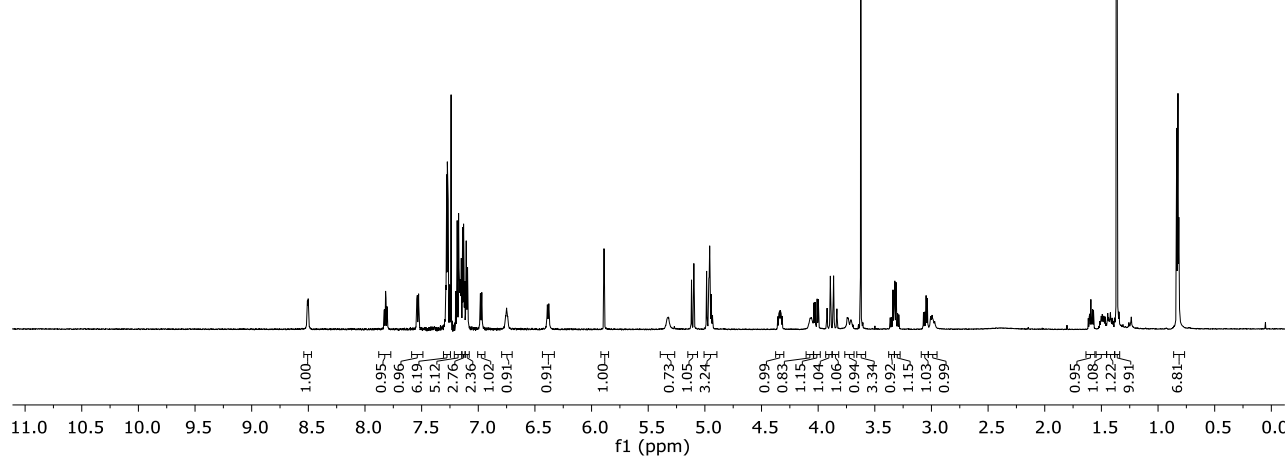
255n
(CDCl₃, 126 MHz)

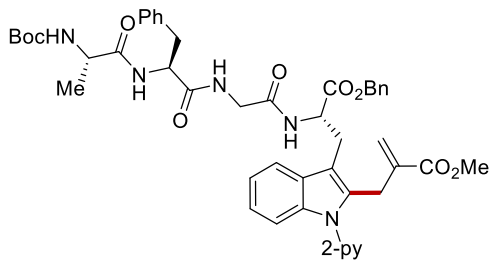


8. NMR Spectra

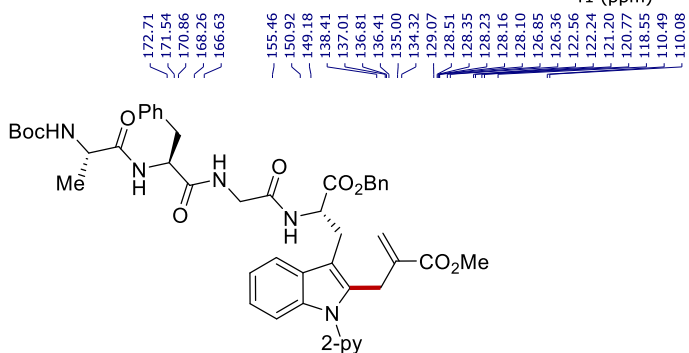
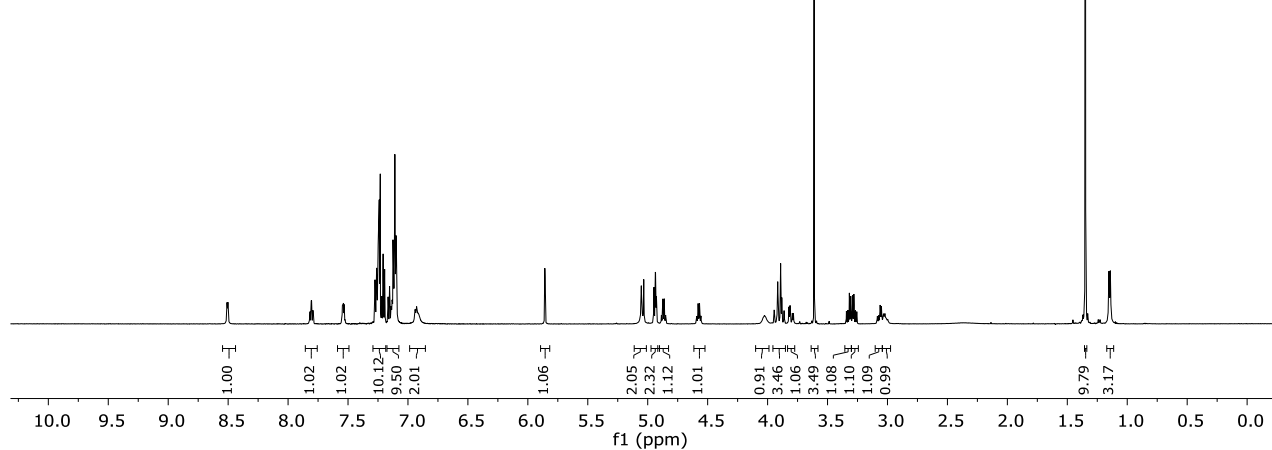


255o
(CDCl₃, 600 MHz)

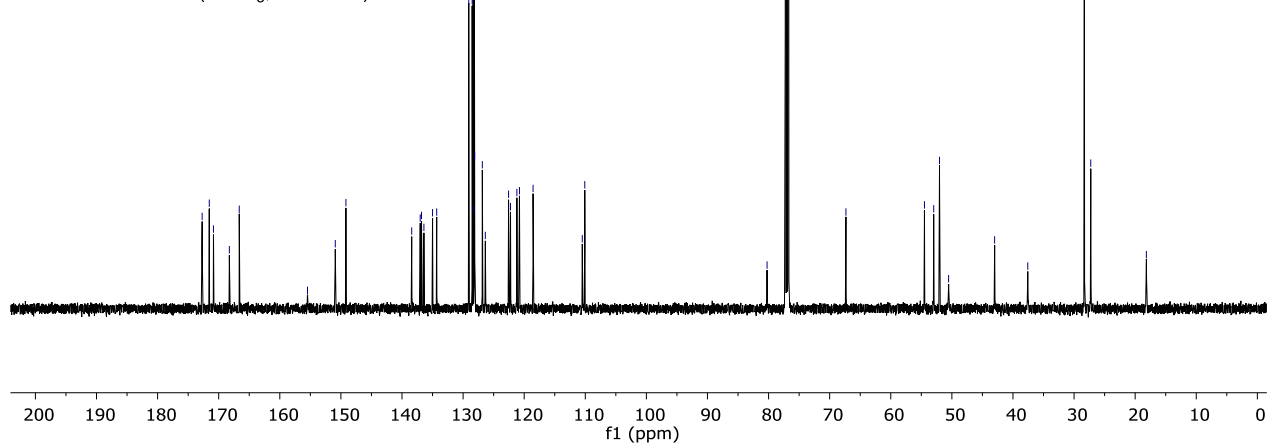




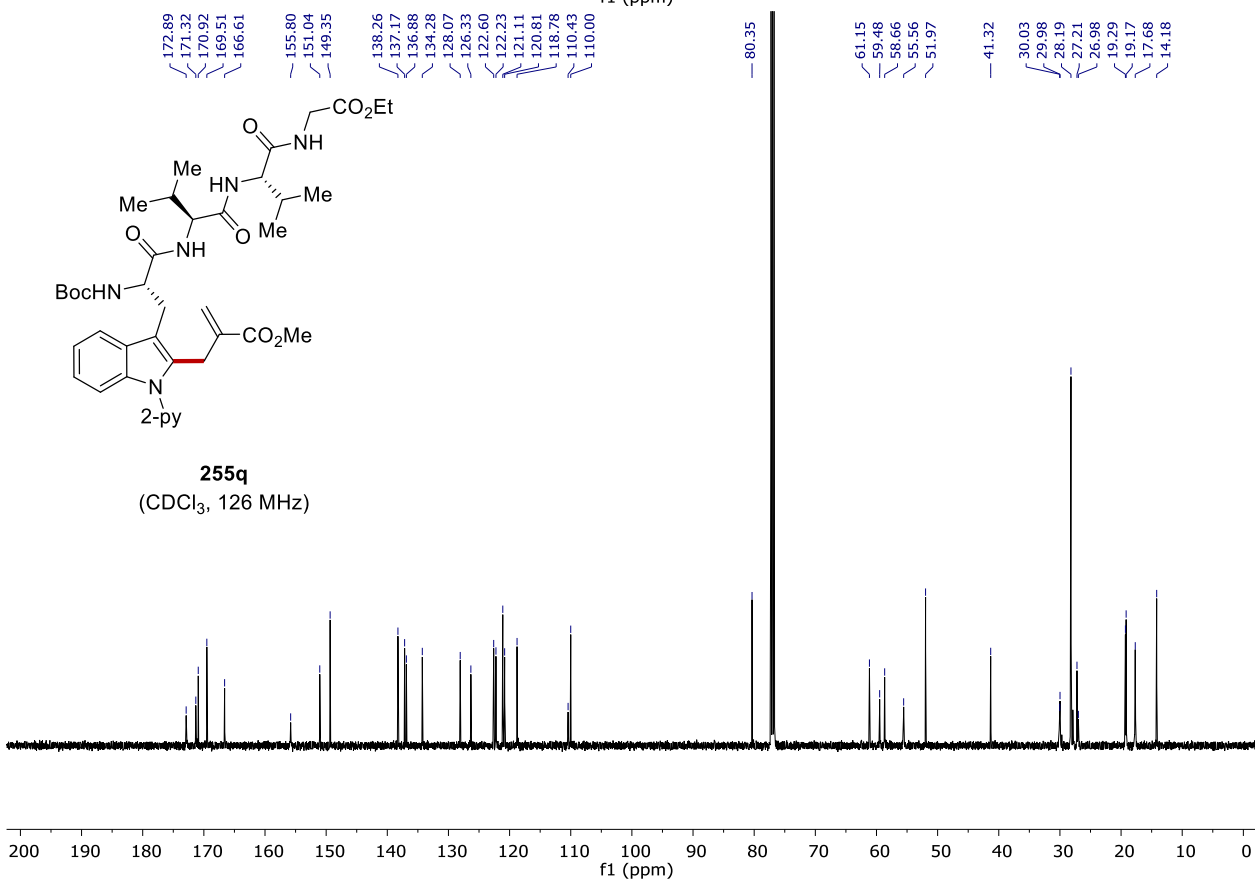
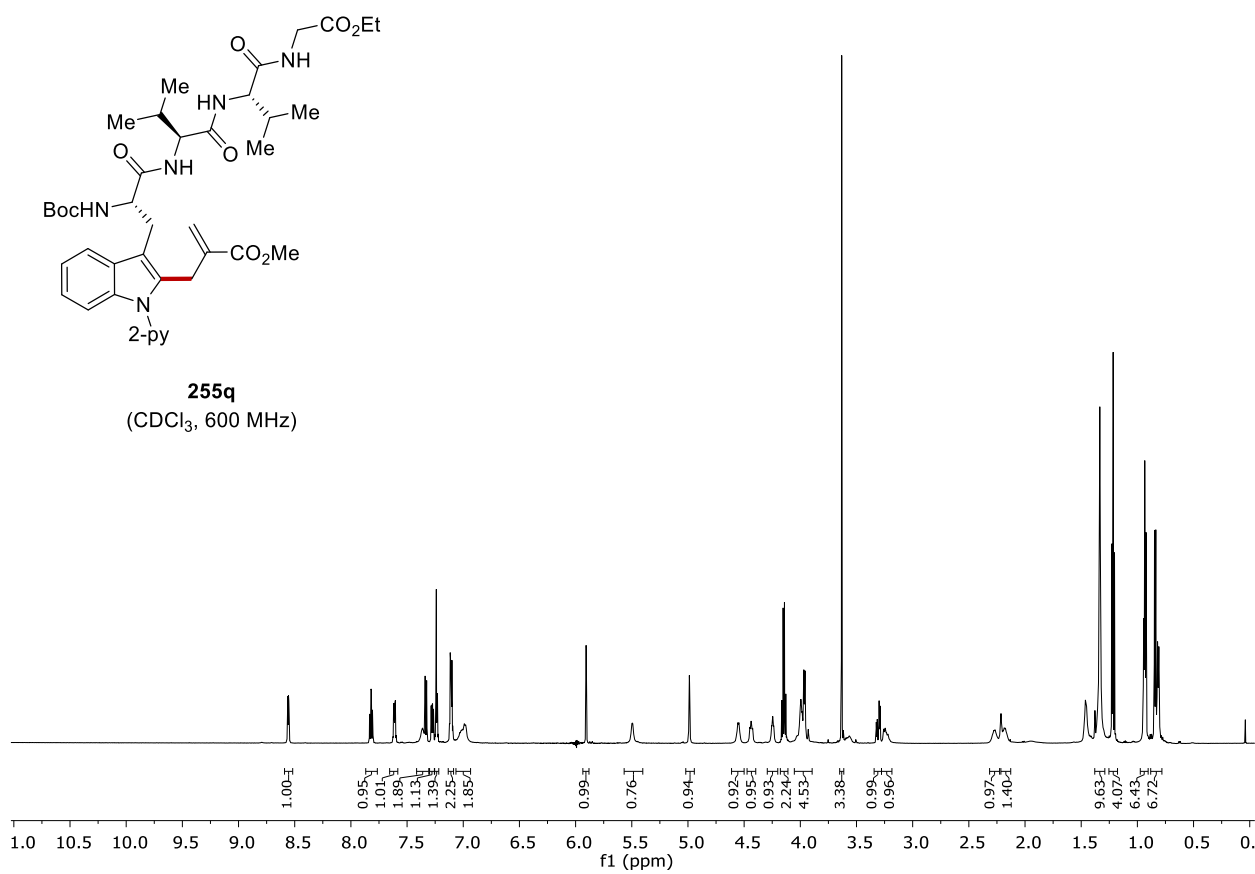
255p
(CDCl₃, 600 MHz)

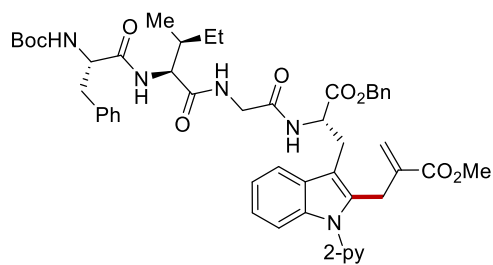


255p
(CDCl₃, 126 MHz)

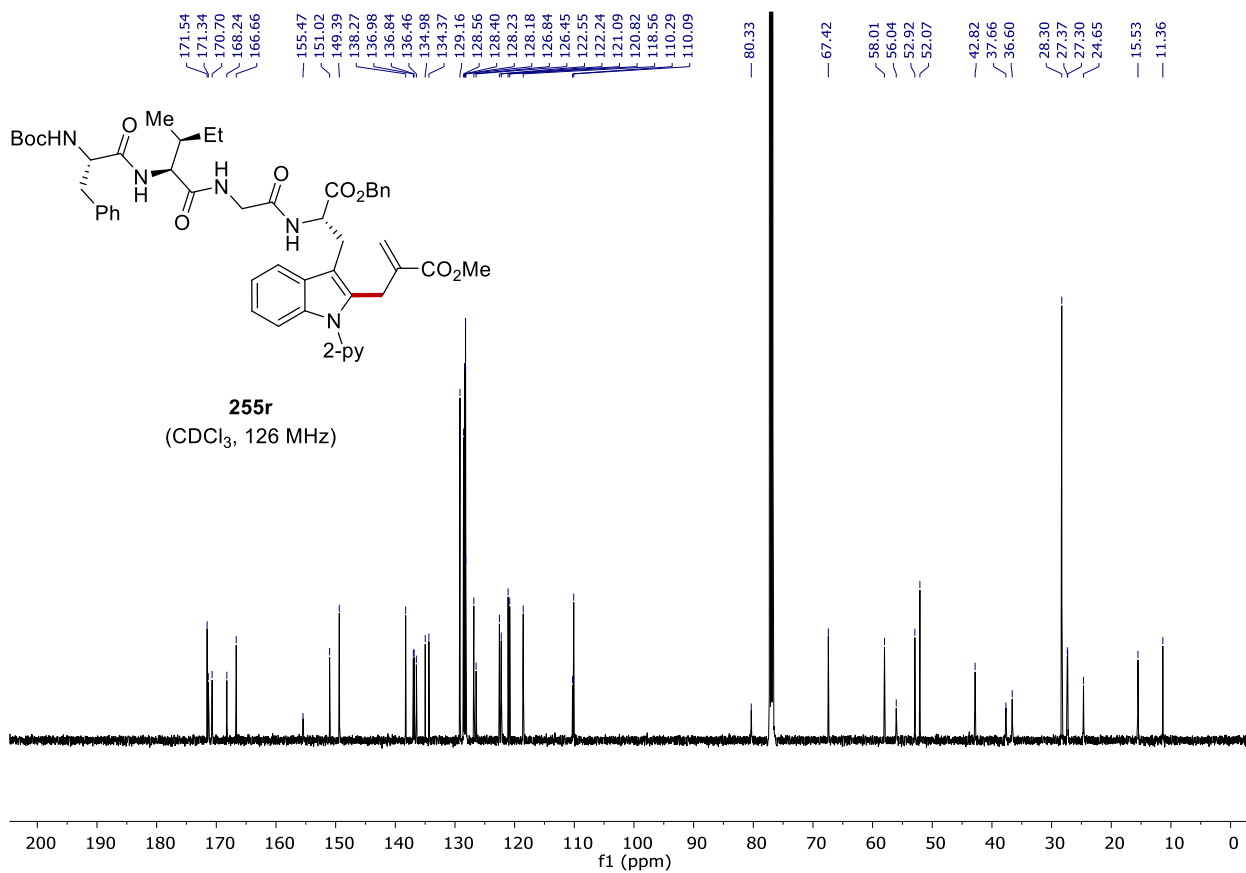
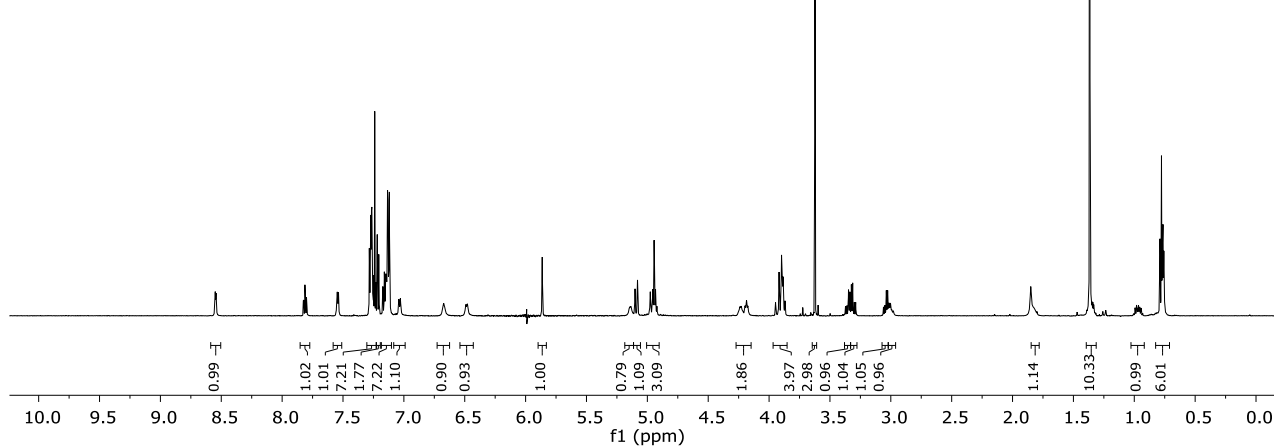


8. NMR Spectra

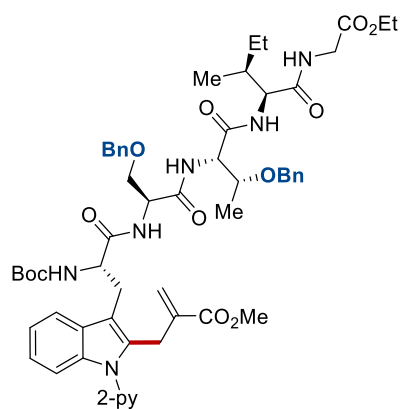




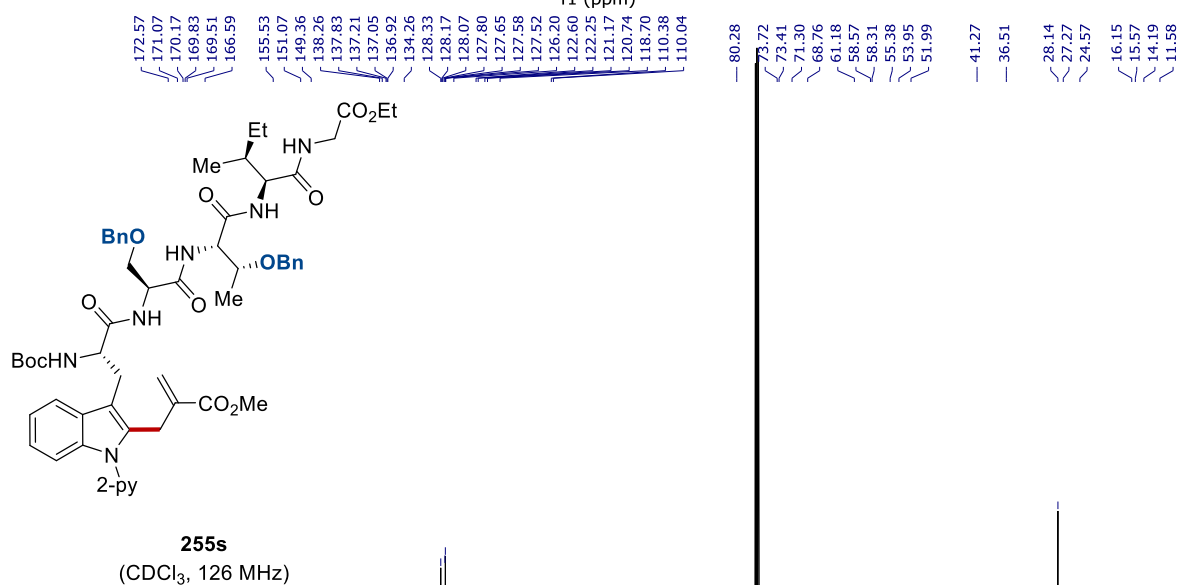
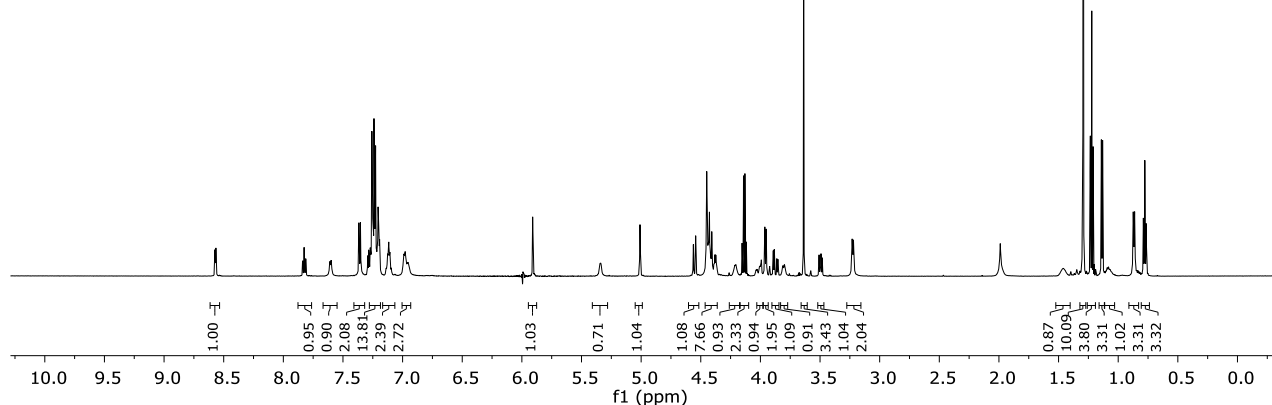
255r
(CDCl₃, 600 MHz)



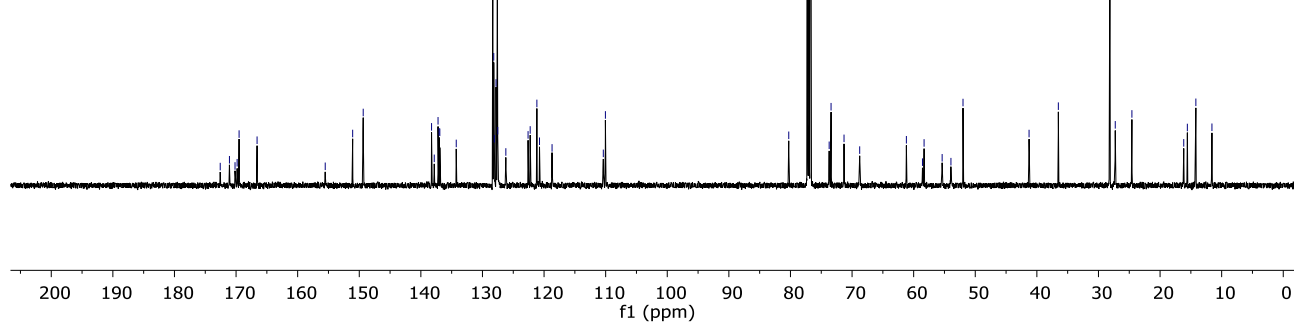
8. NMR Spectra

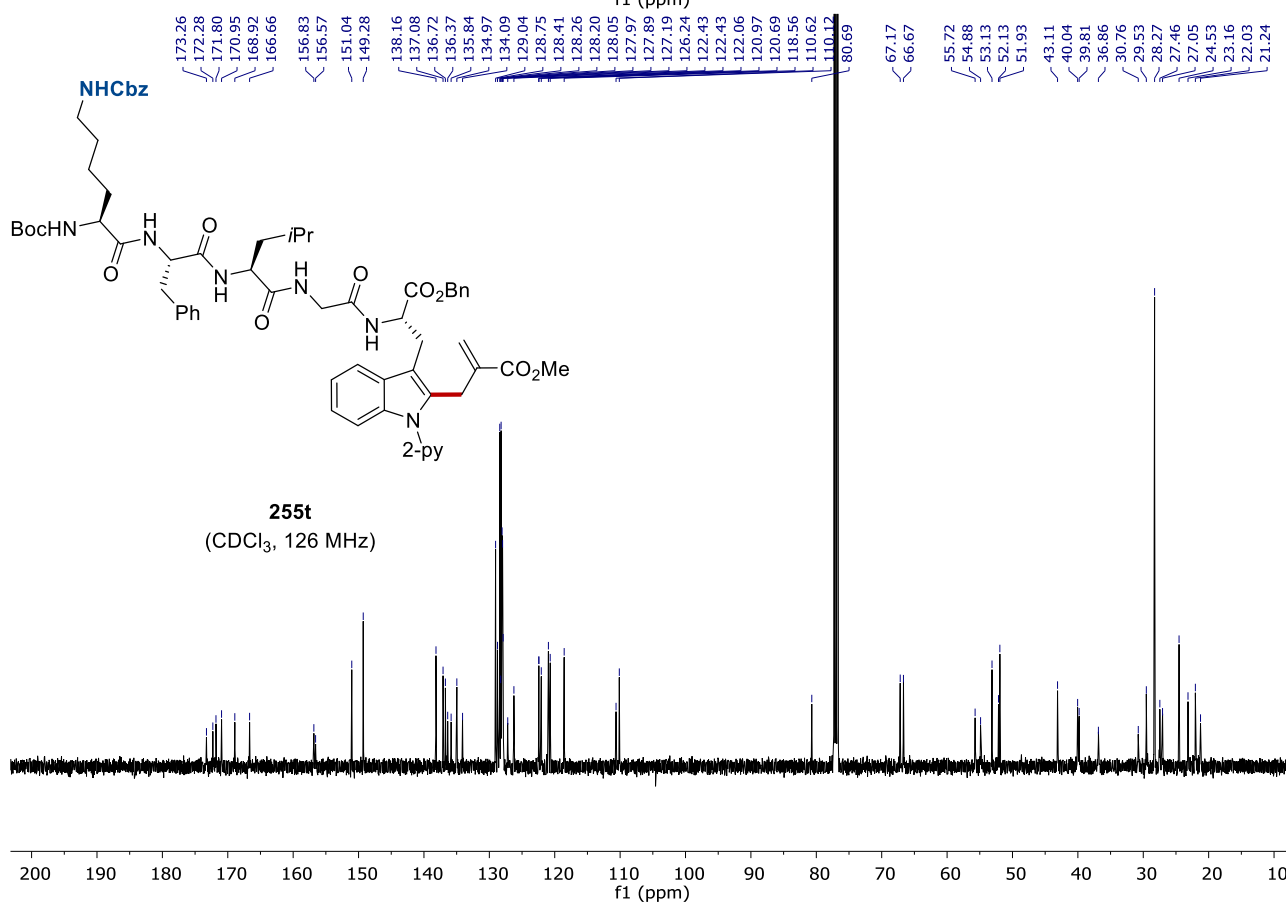
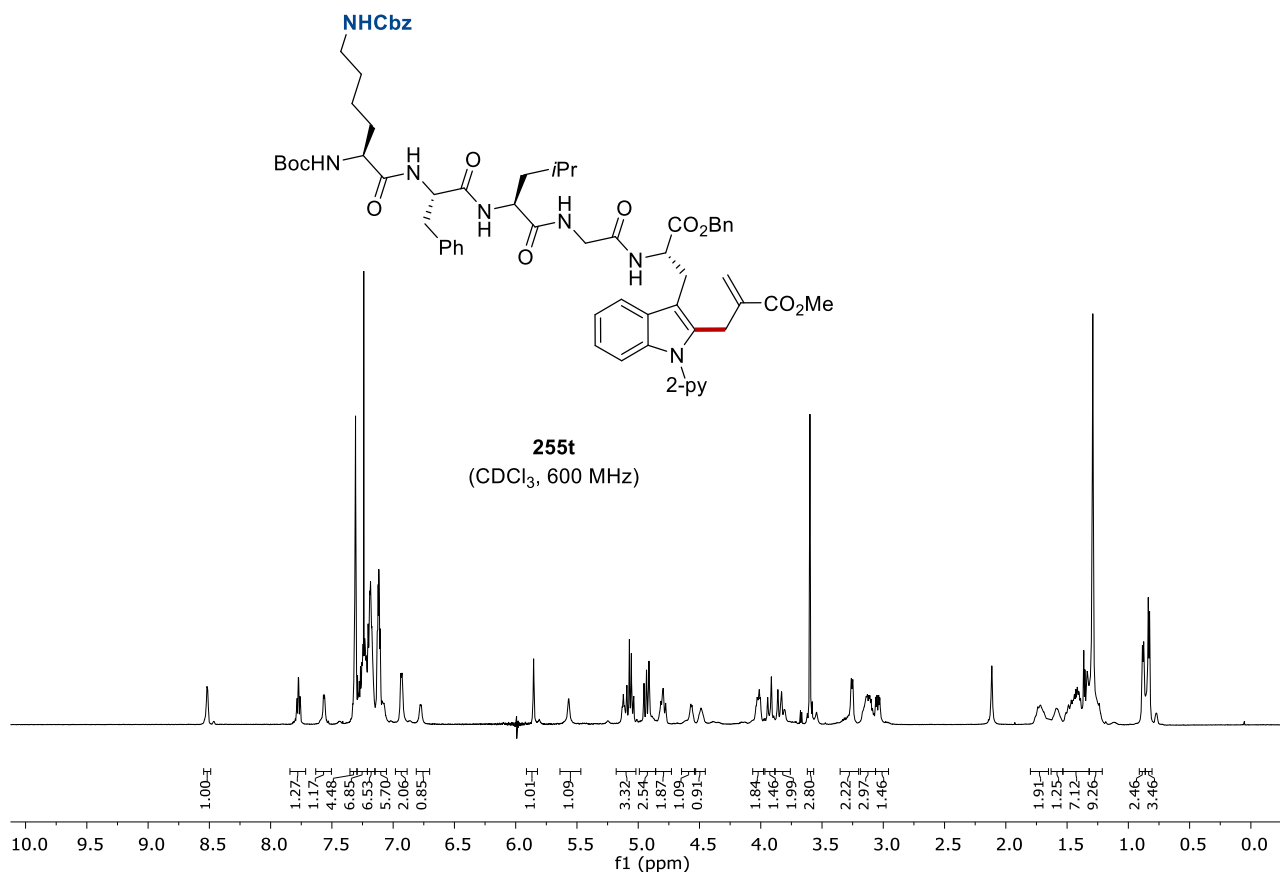


255s
(CDCl₃, 600 MHz)

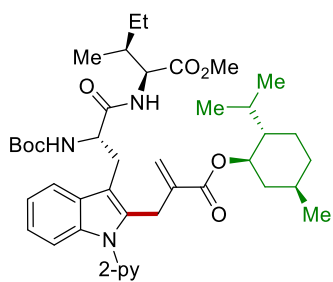


255s
(CDCl₃, 126 MHz)

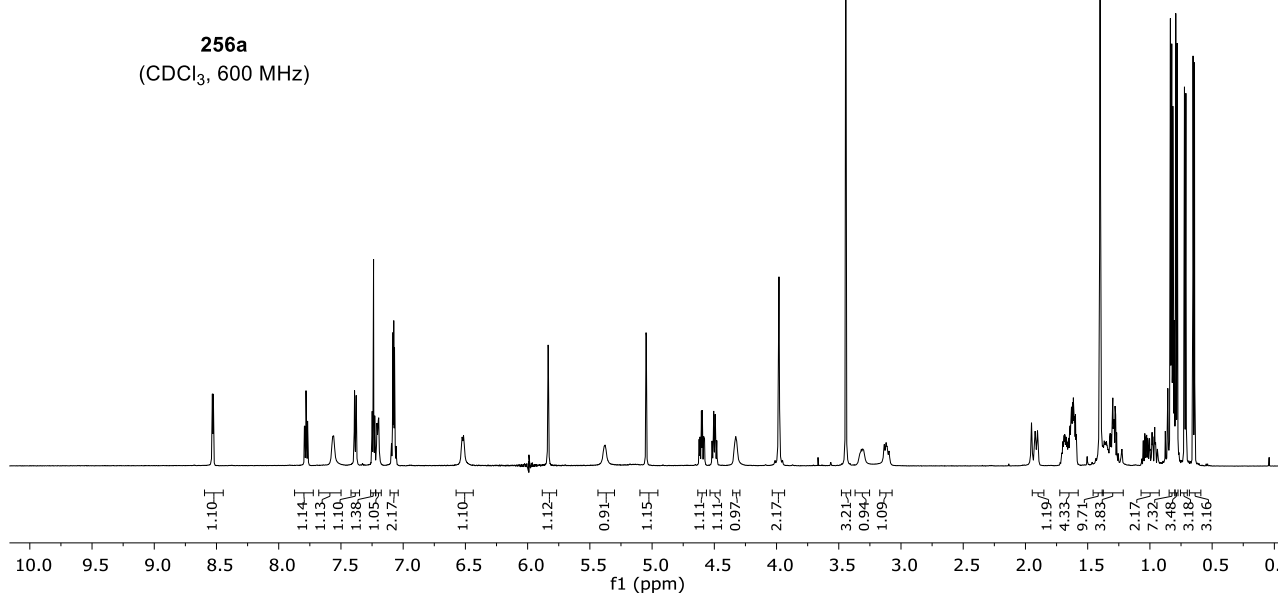




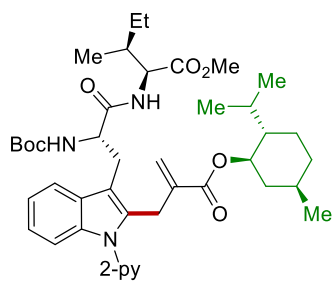
8. NMR Spectra



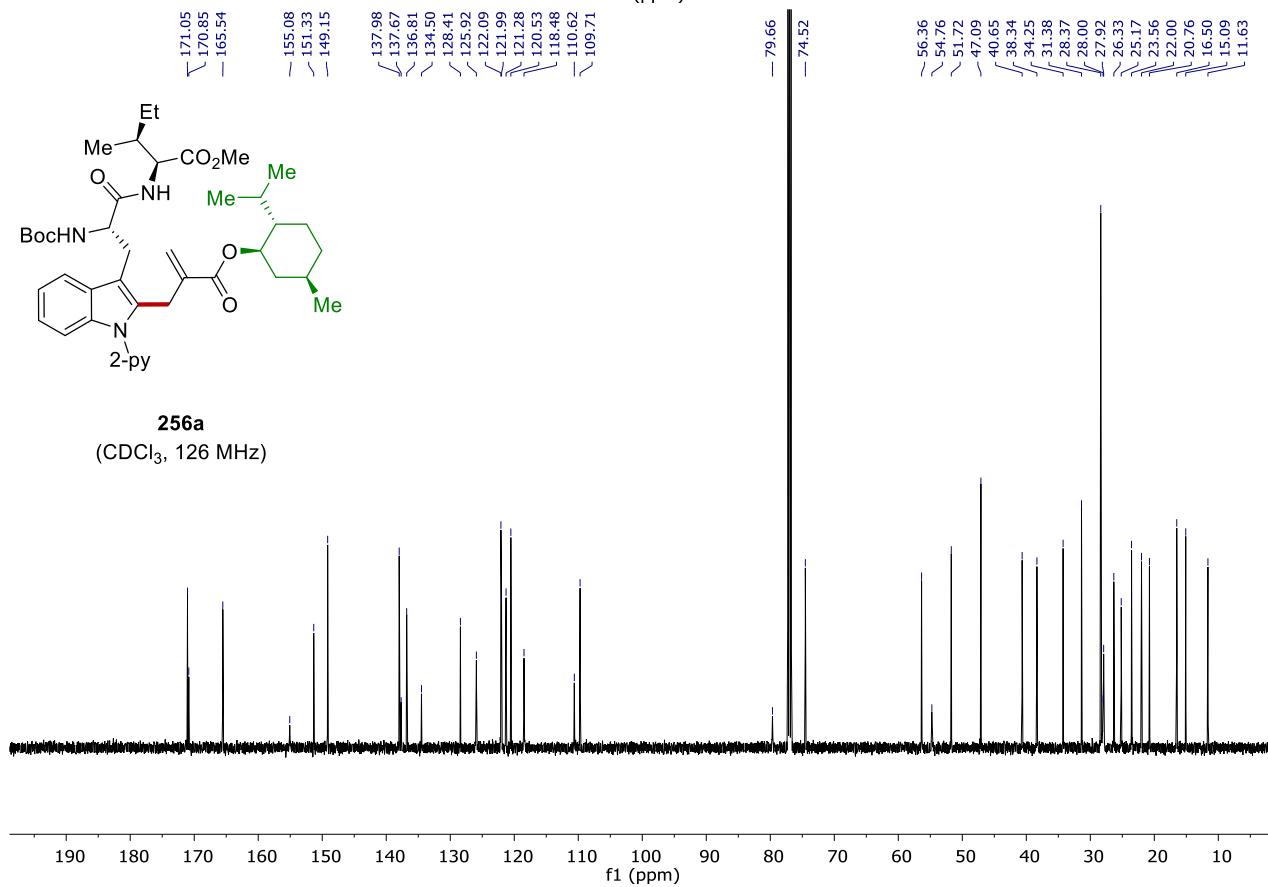
256a
(CDCl₃, 600 MHz)

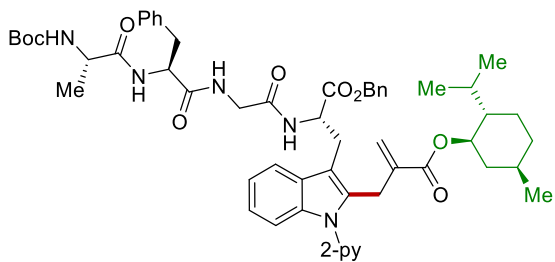


171.05
170.85
165.54
155.08
151.33
149.15
137.98
137.67
136.81
134.50
128.41
125.92
122.09
121.99
121.28
120.53
118.48
110.62
109.71

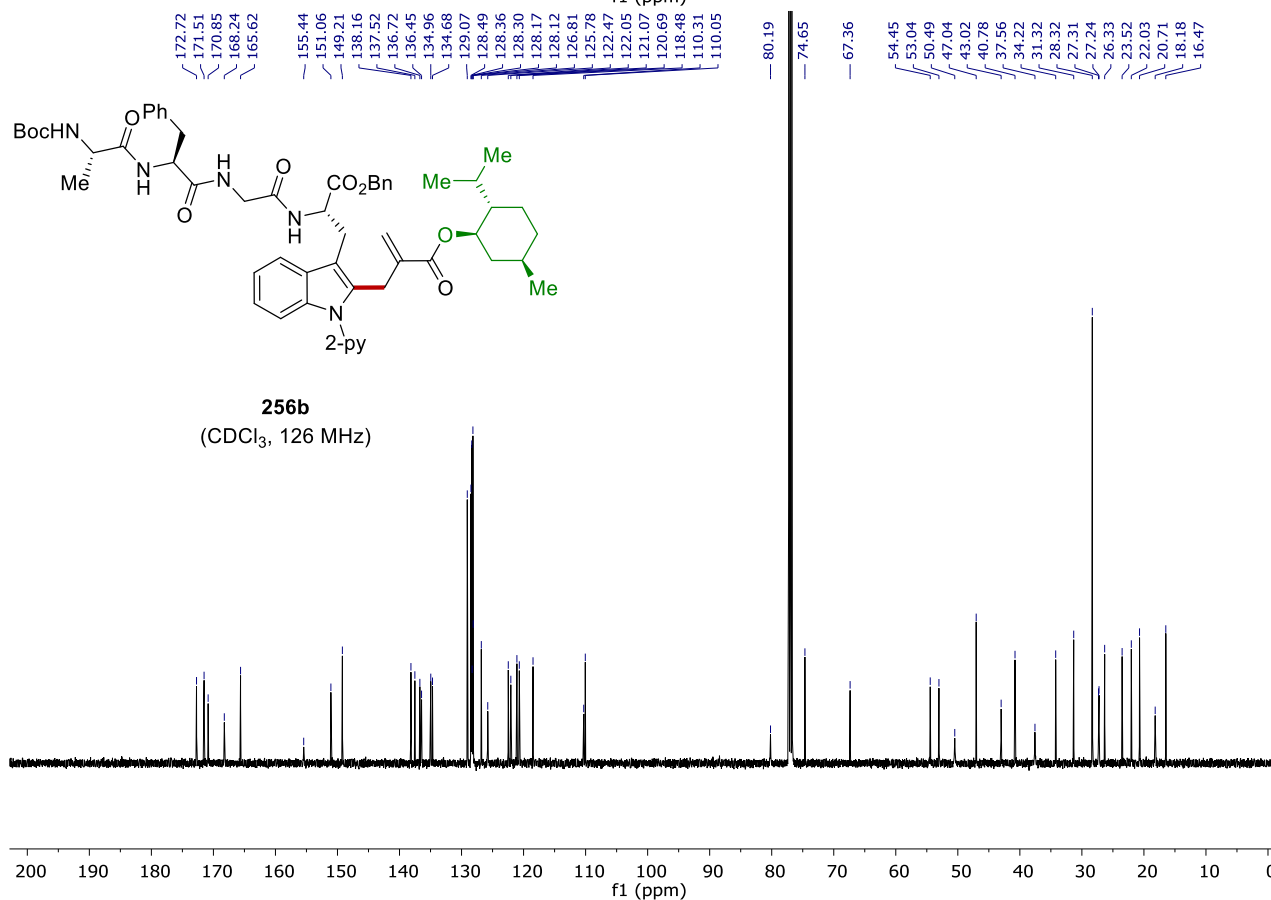
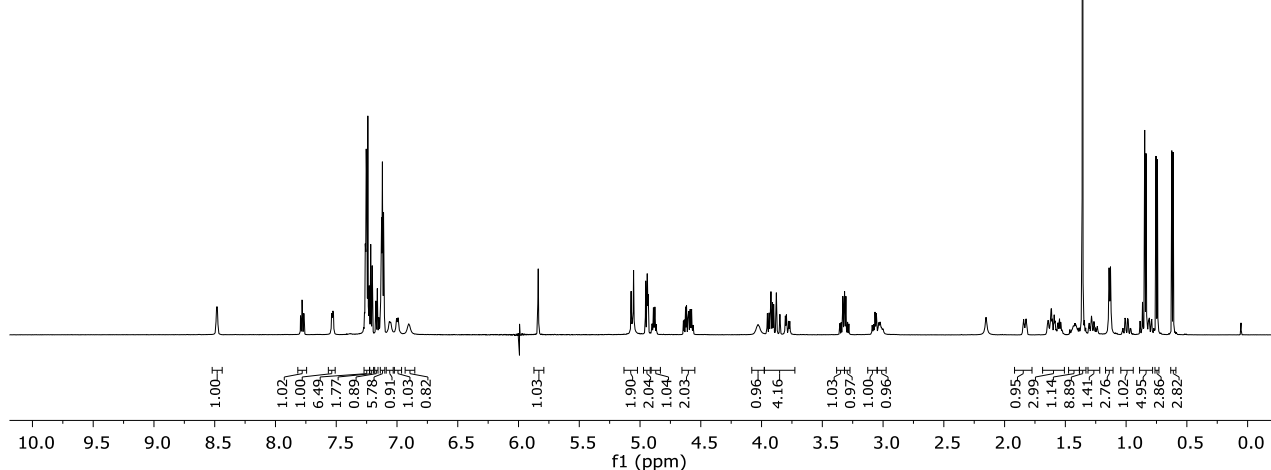


256a
(CDCl₃, 126 MHz)

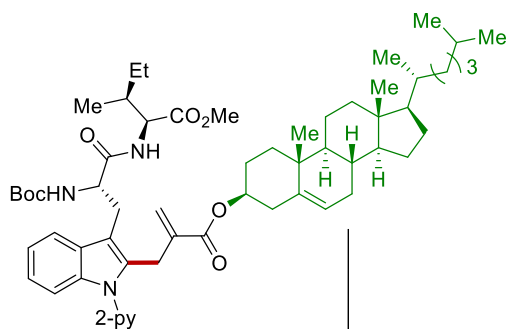




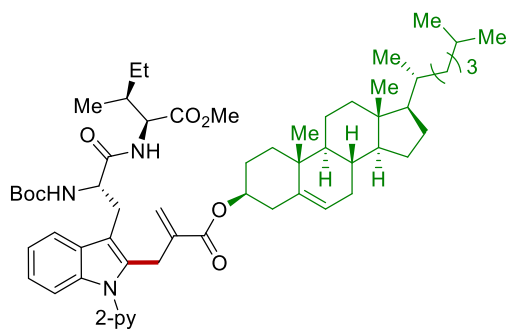
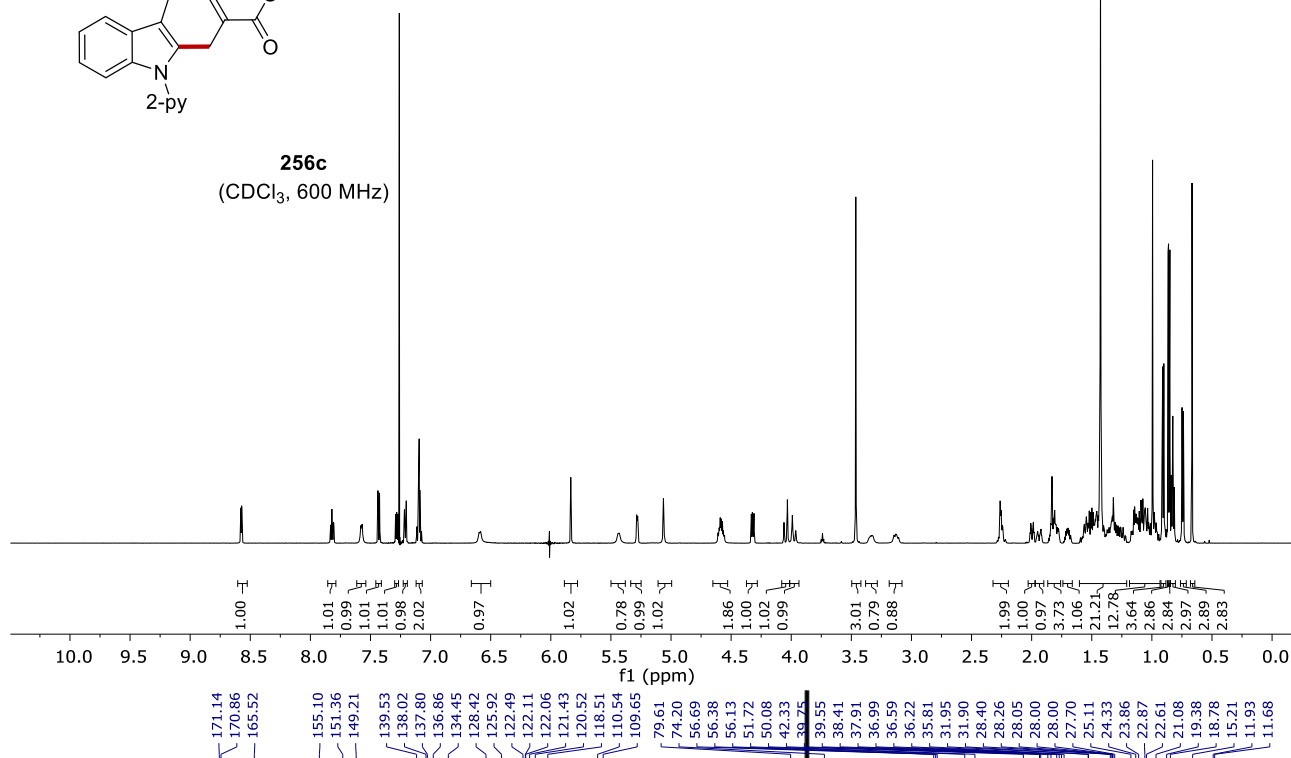
256b
(CDCl₃, 600 MHz)



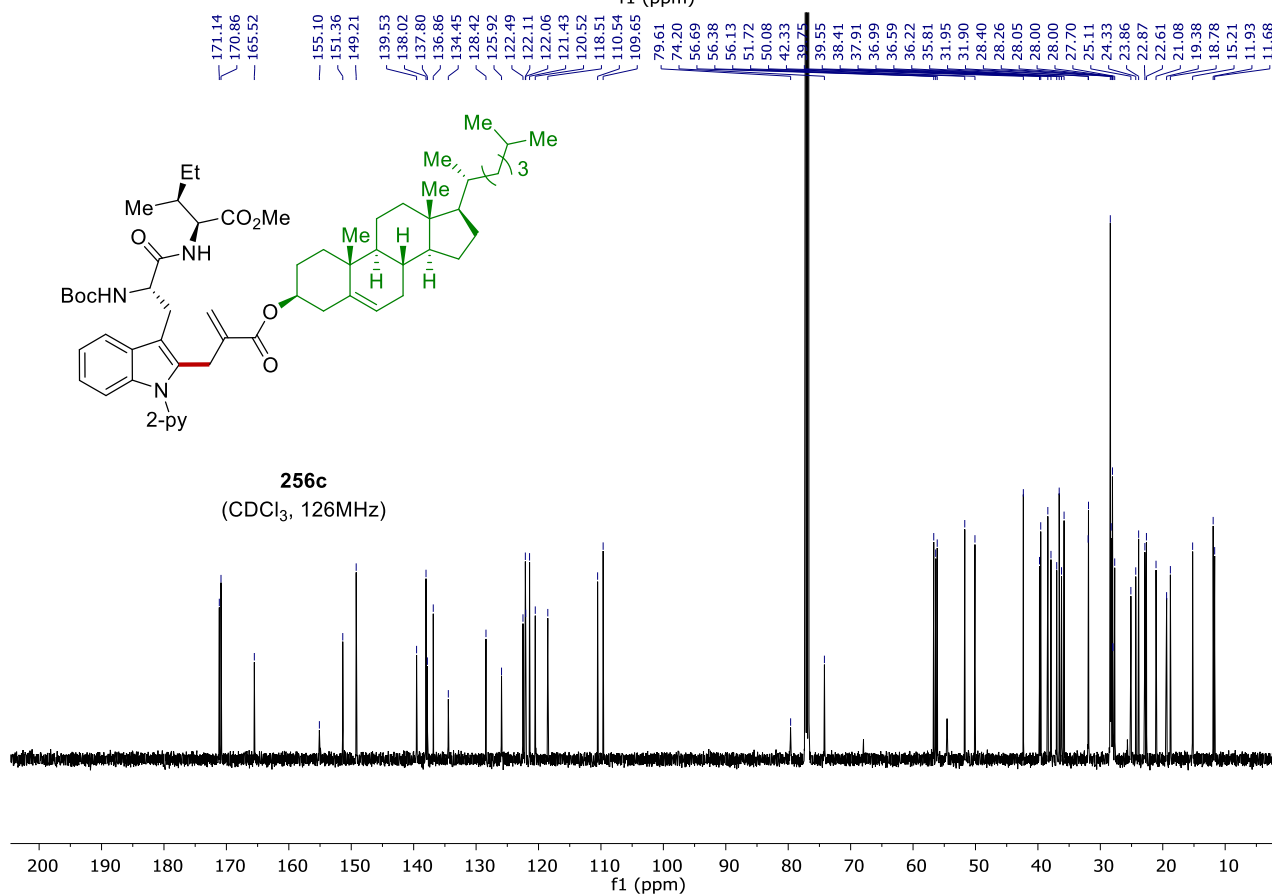
8. NMR Spectra



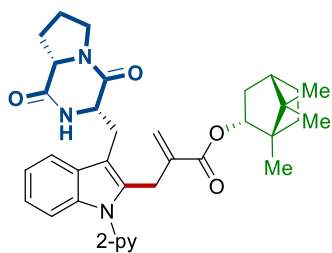
256c
(CDCl₃, 600 MHz)



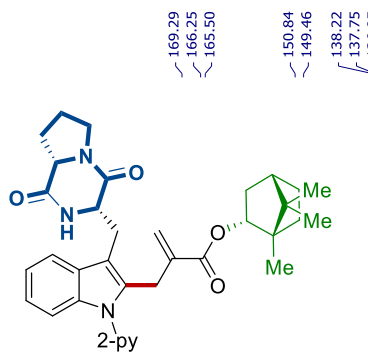
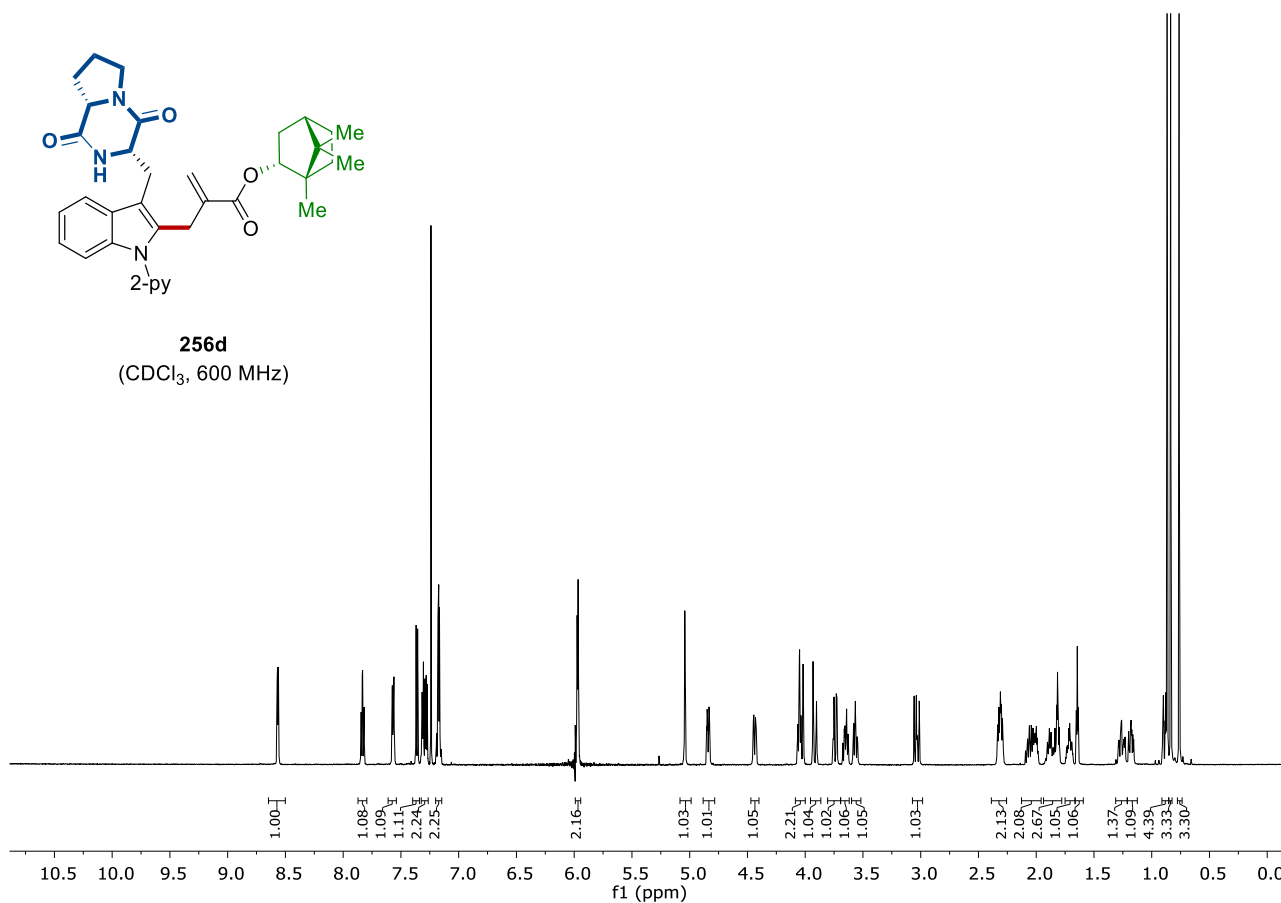
256c
(CDCl₃, 126MHz)



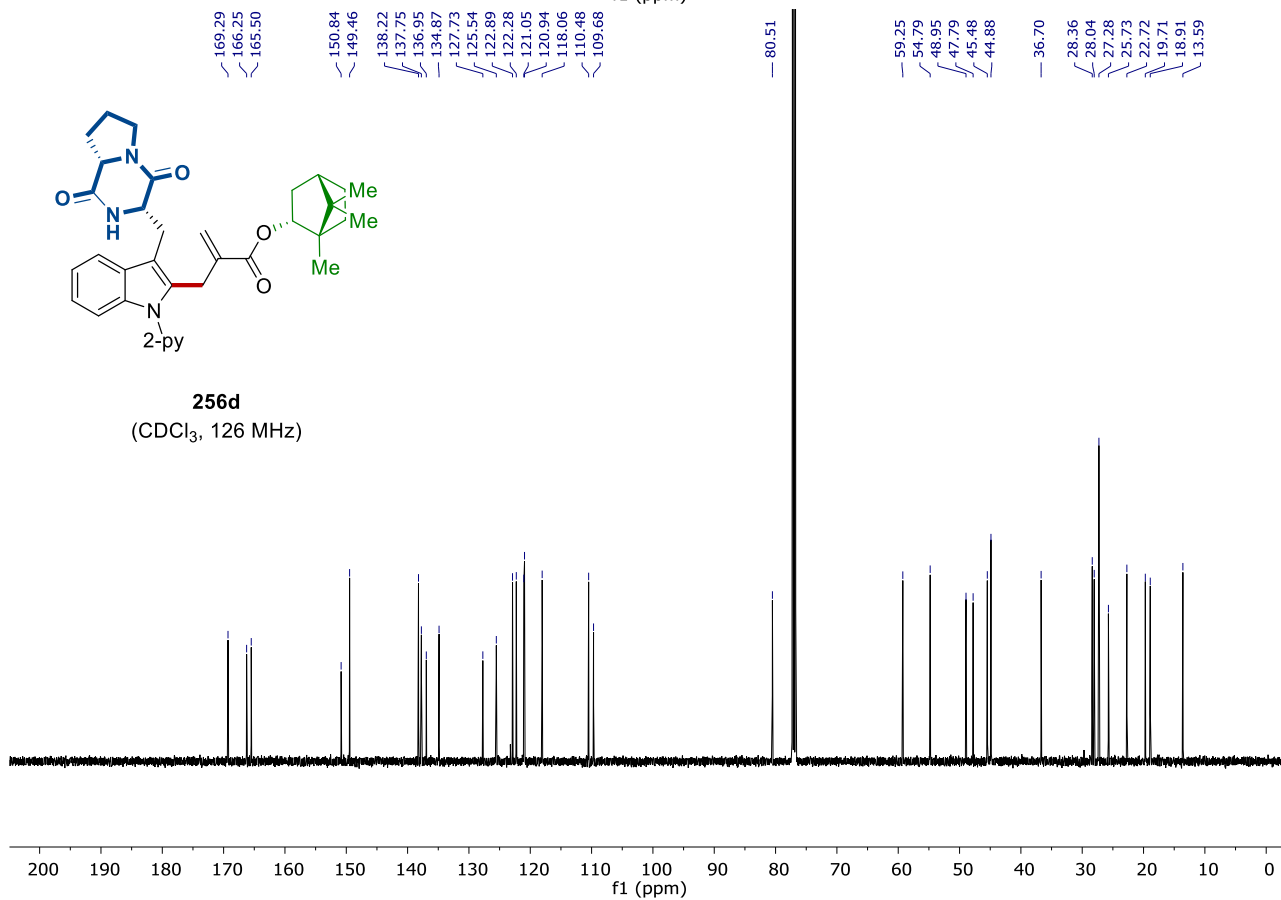
8. NMR Spectra



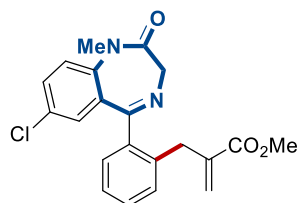
256d
(CDCl₃, 600 MHz)



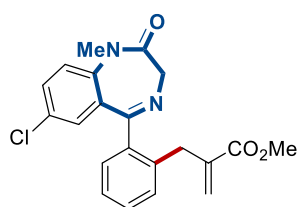
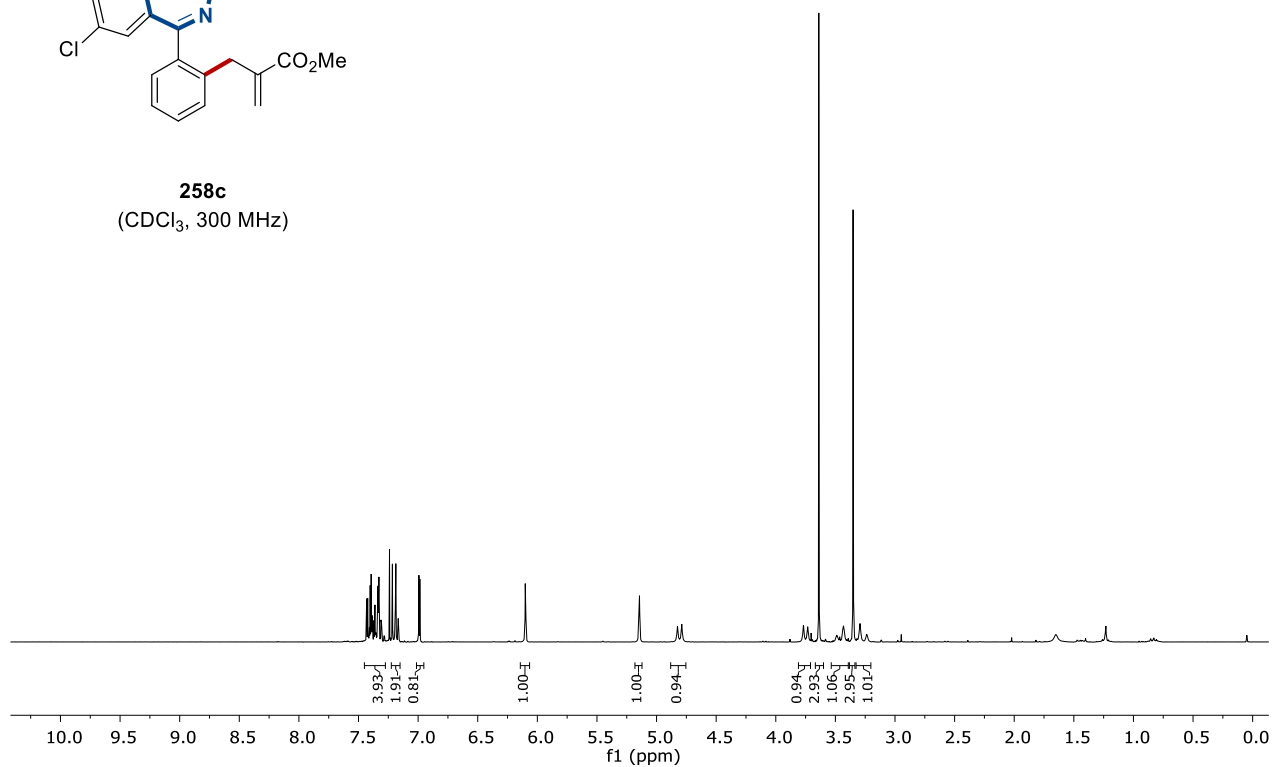
256d
(CDCl₃, 126 MHz)



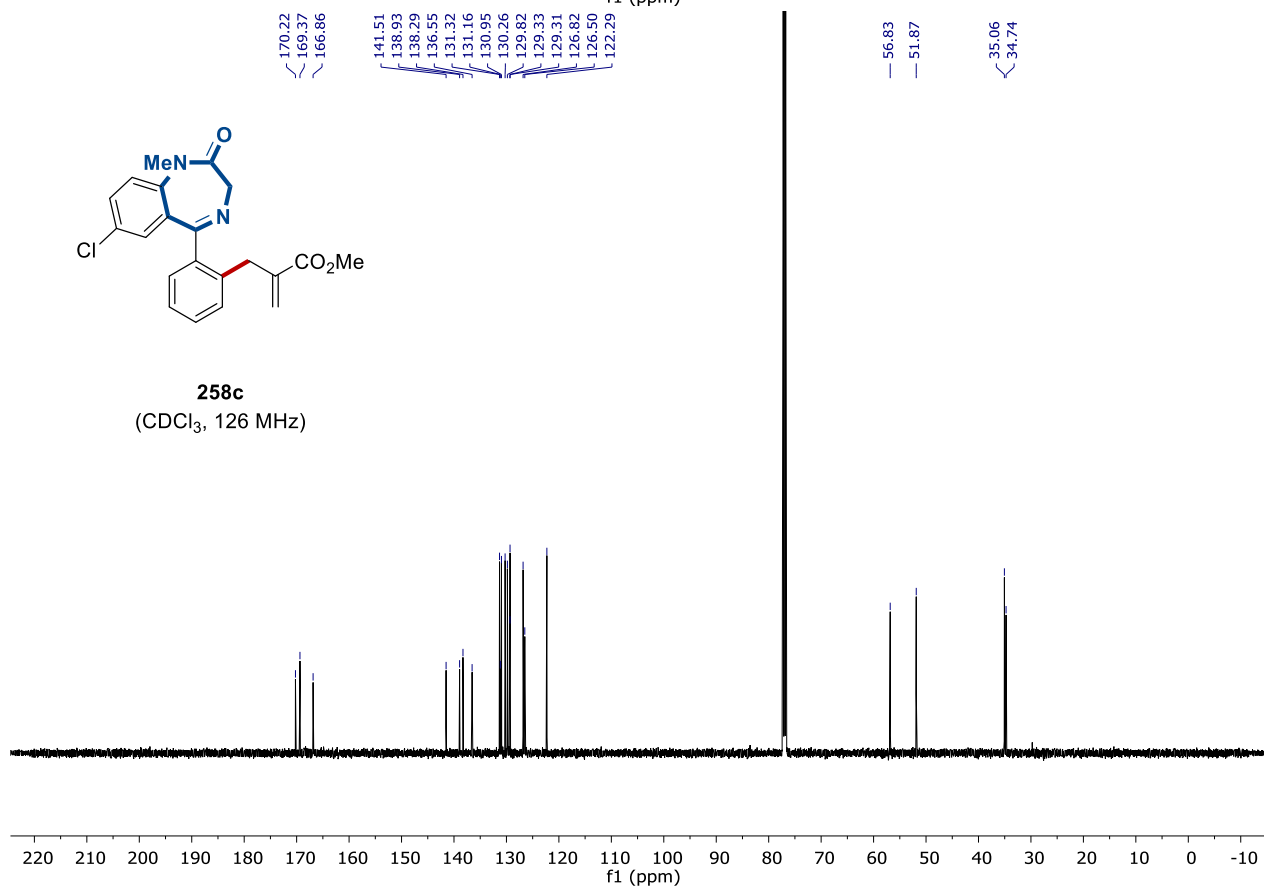
8. NMR Spectra

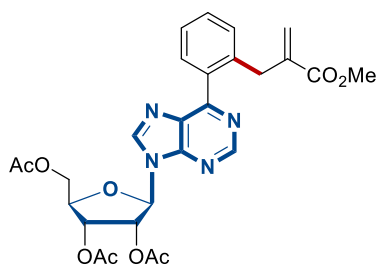


258c
(CDCl₃, 300 MHz)

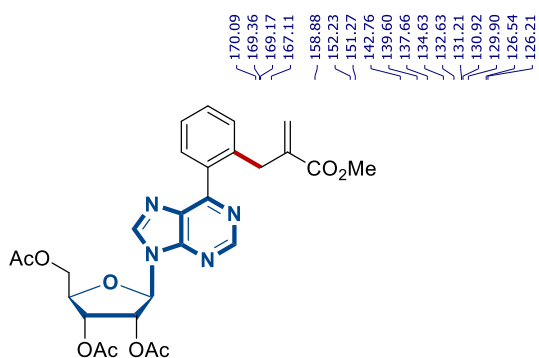
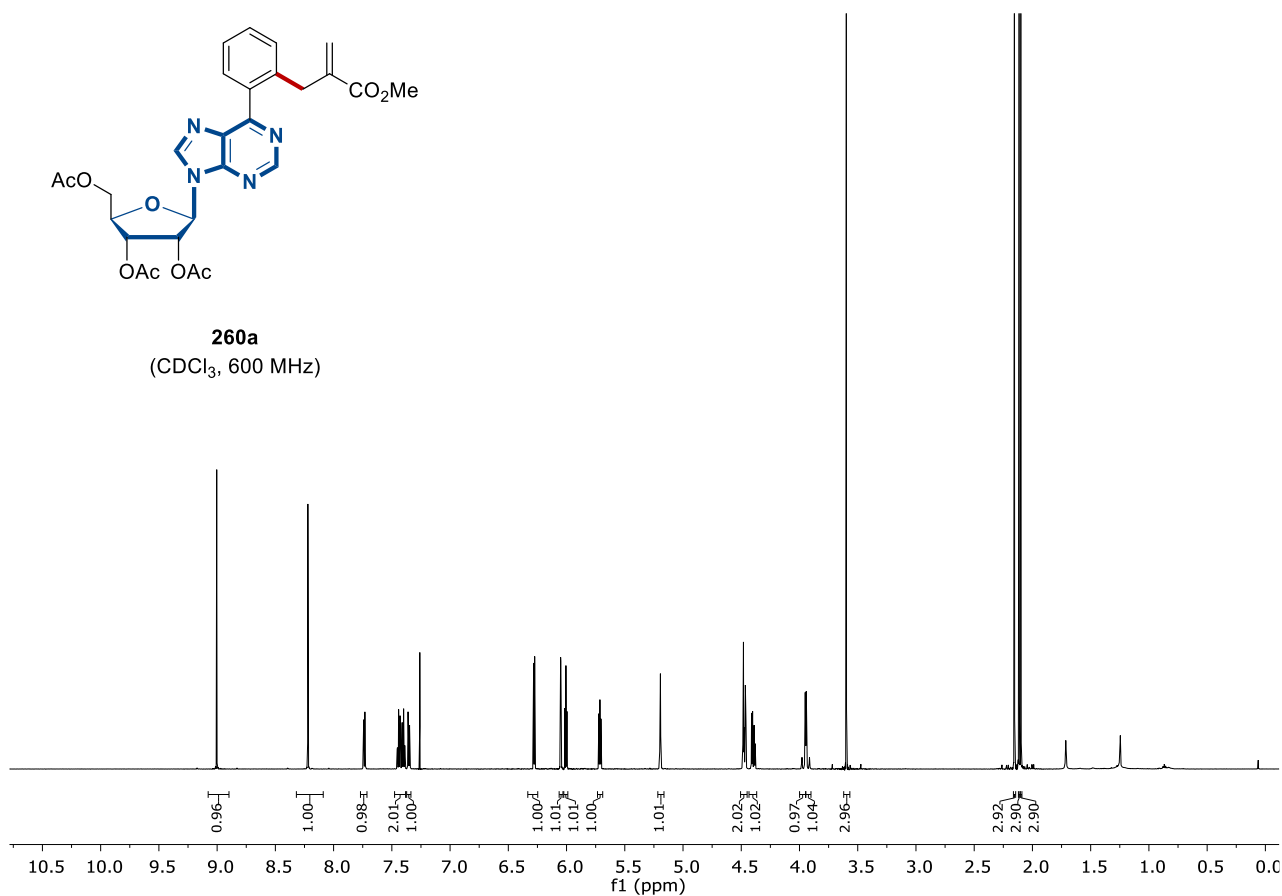


258c
(CDCl₃, 126 MHz)

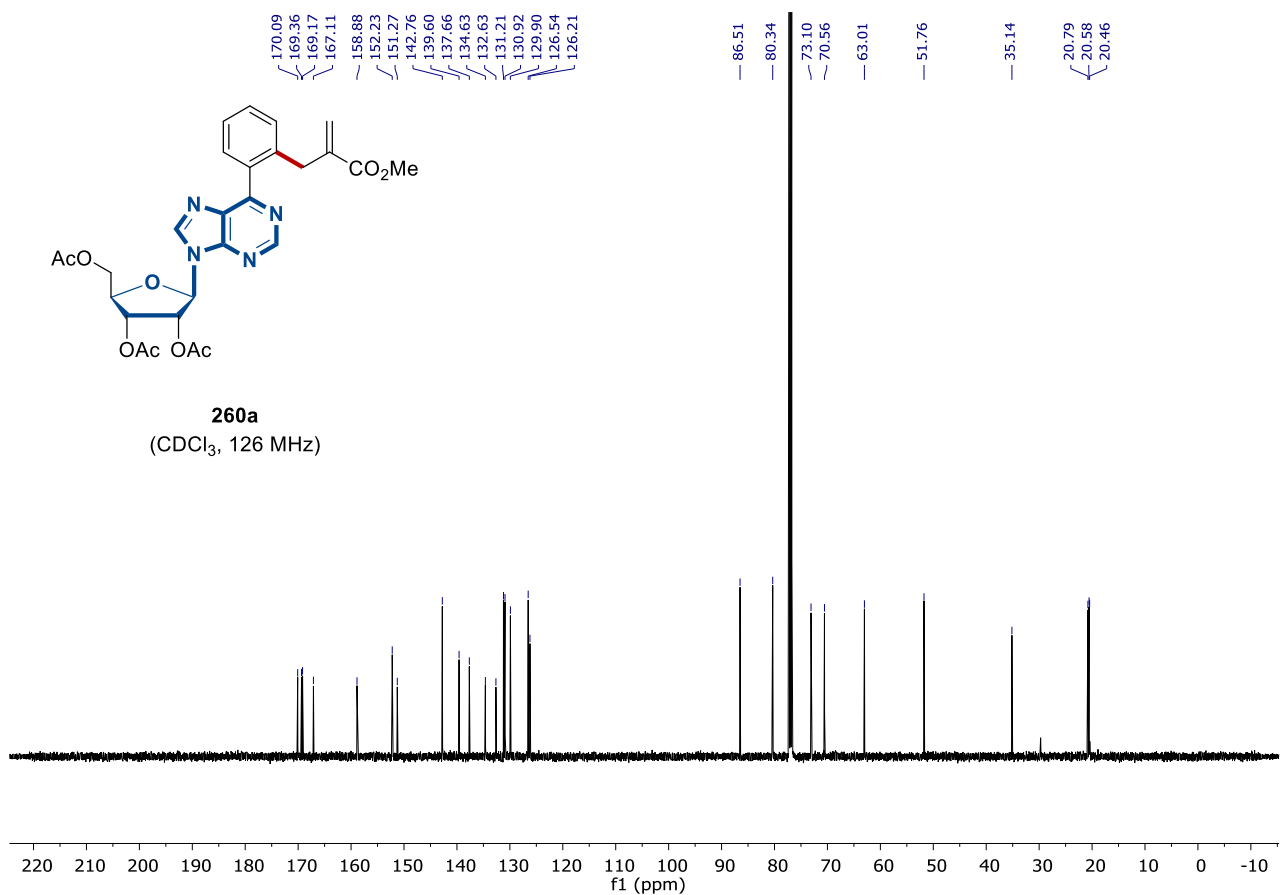




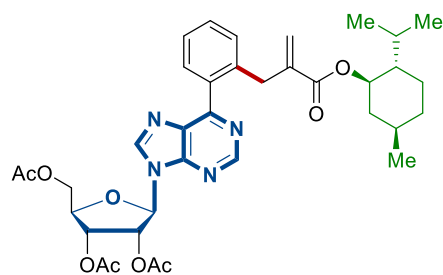
260a
(CDCl₃, 600 MHz)



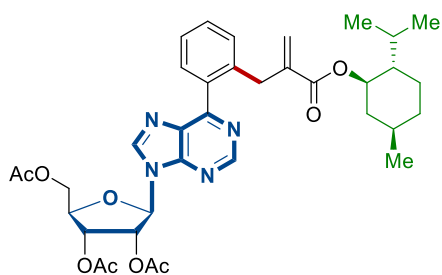
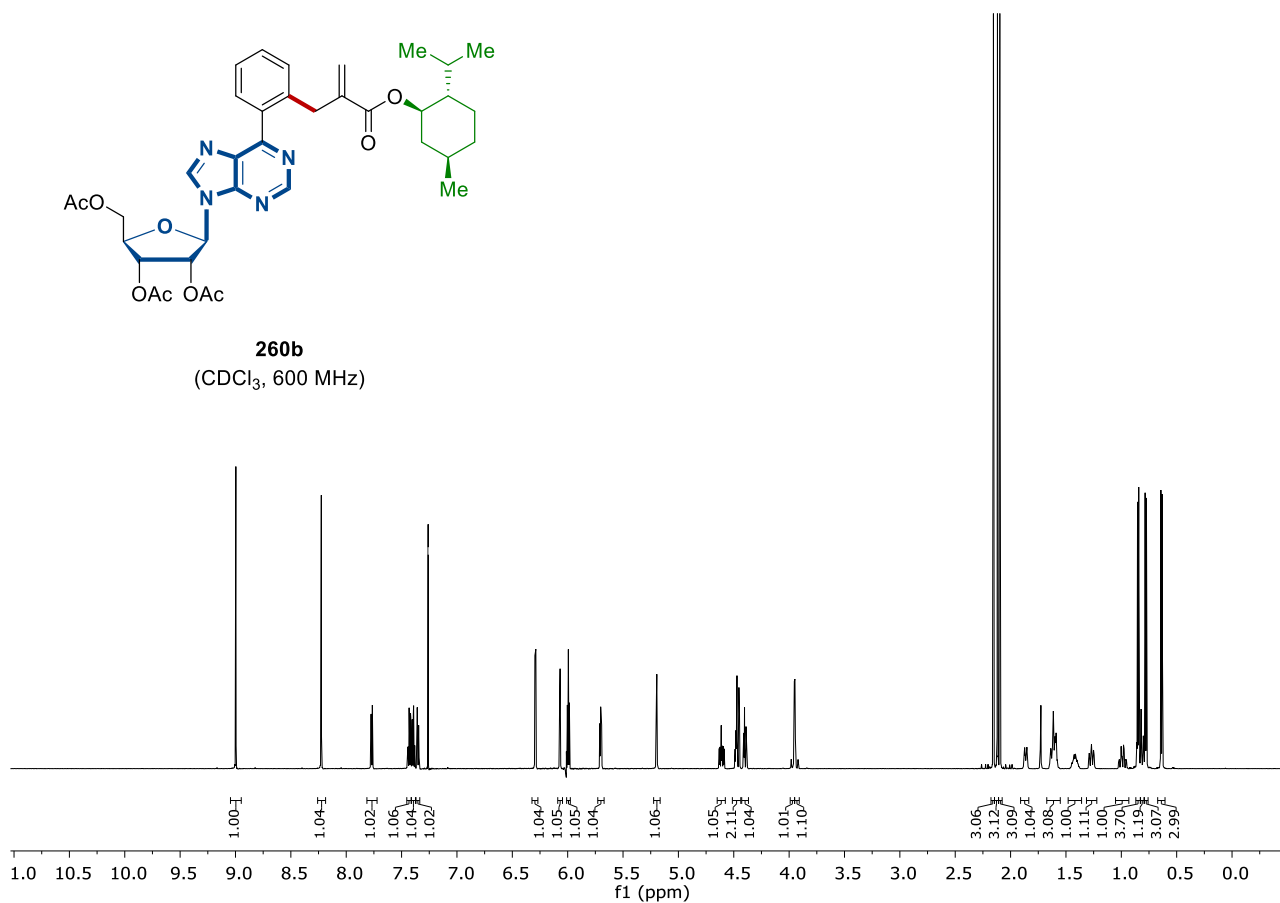
260a
(CDCl₃, 126 MHz)



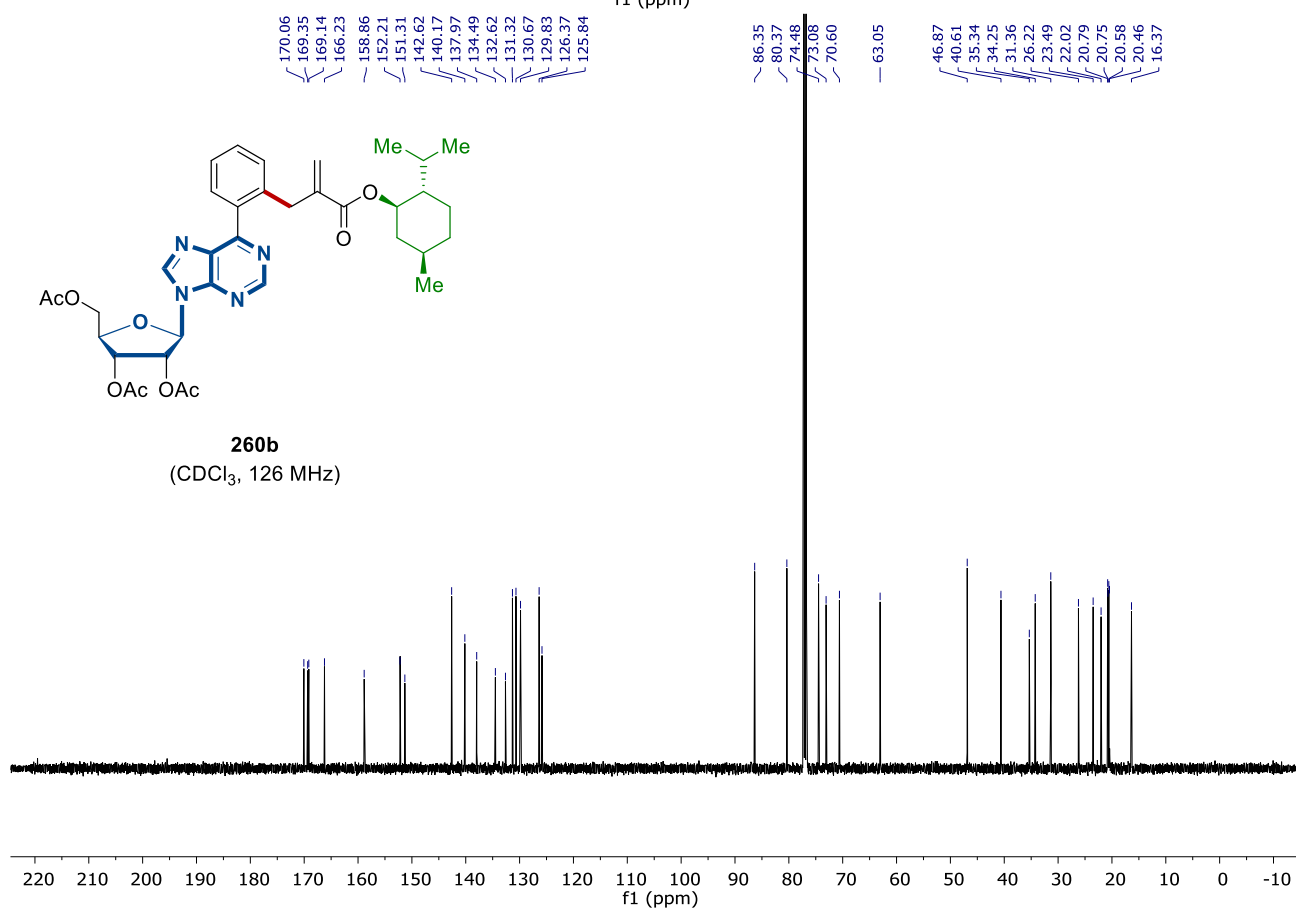
8. NMR Spectra

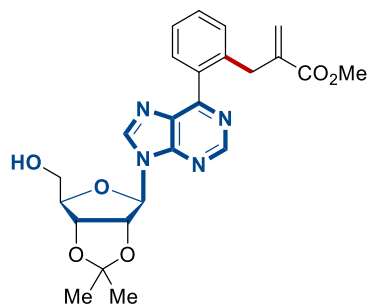


260b
(CDCl₃, 600 MHz)

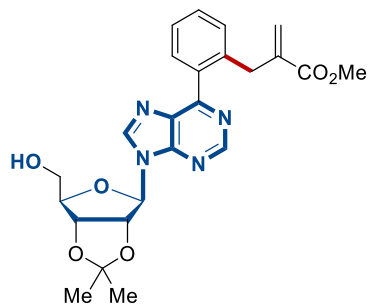
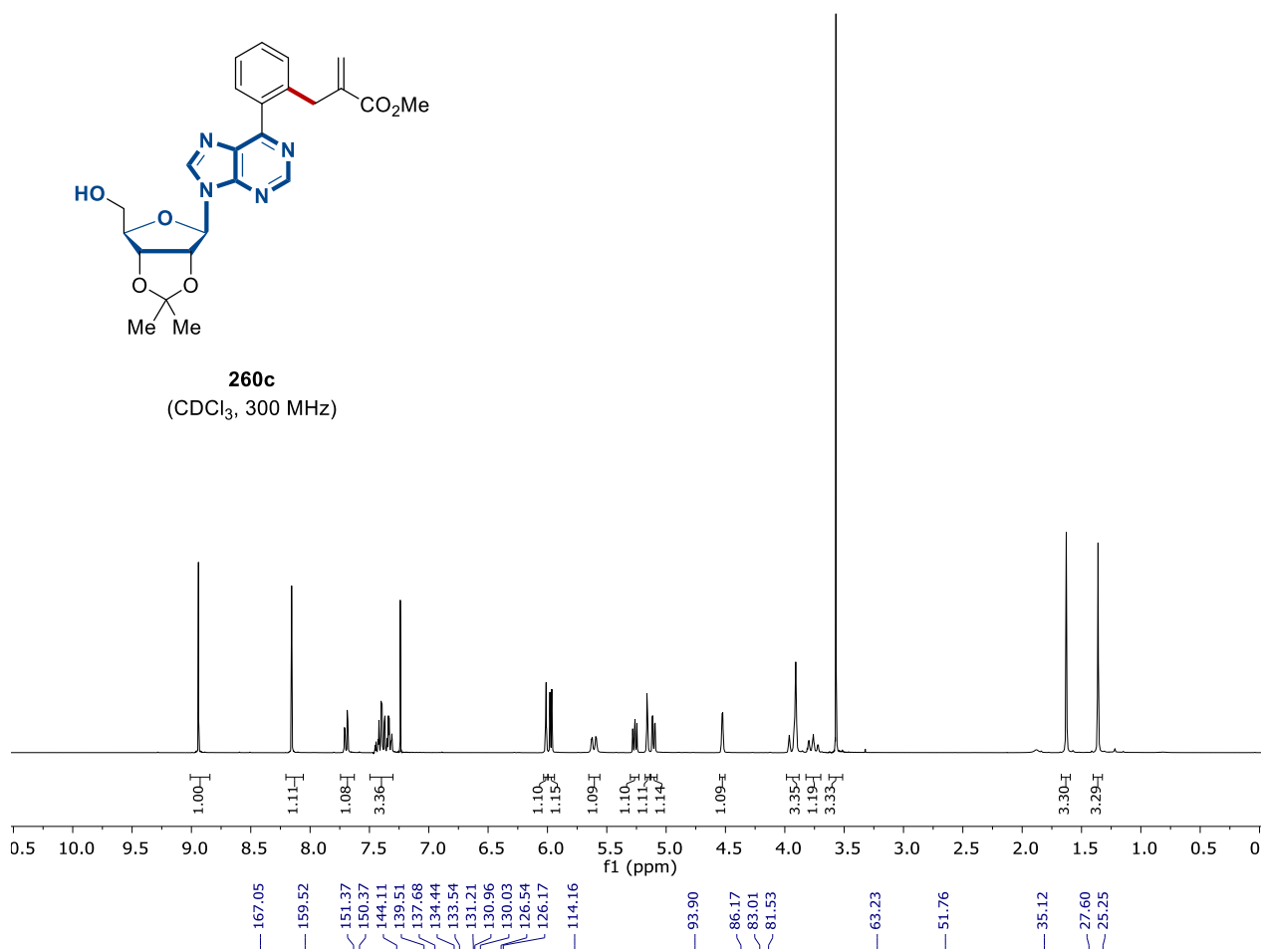


260b
(CDCl₃, 126 MHz)

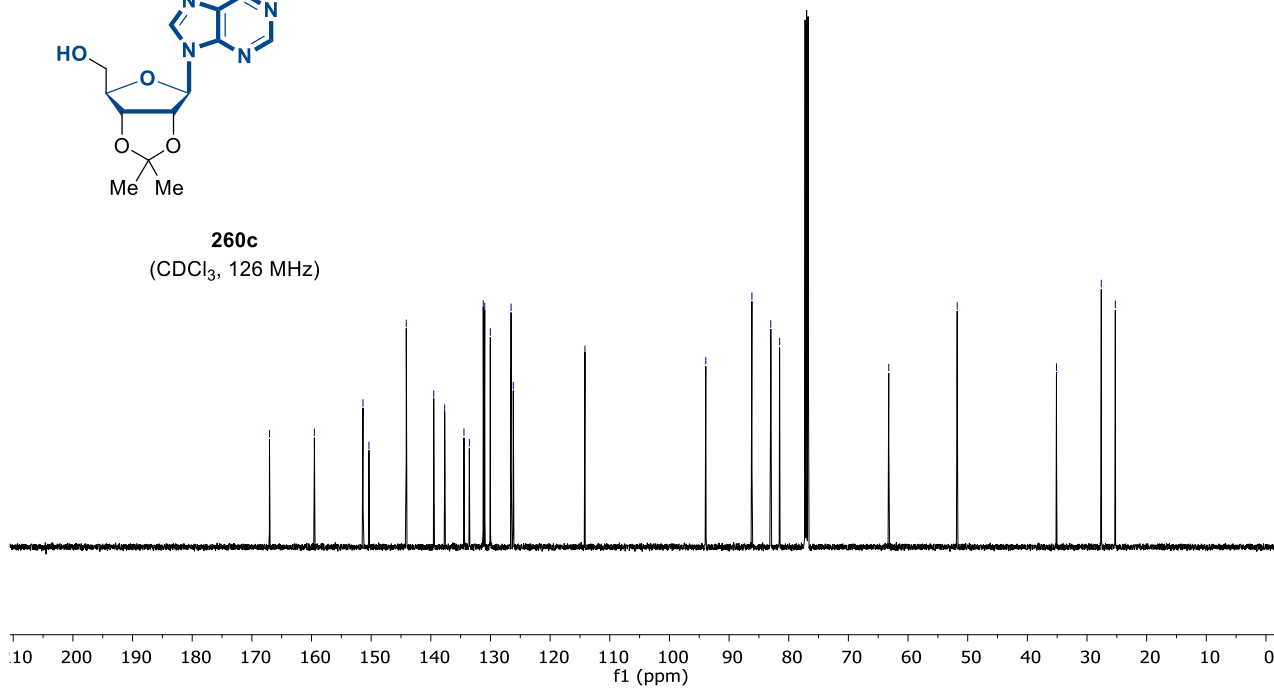




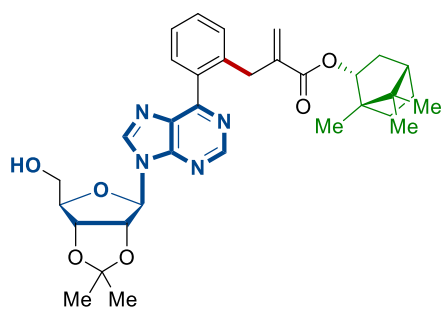
260c
(CDCl₃, 300 MHz)



260c
(CDCl₃, 126 MHz)

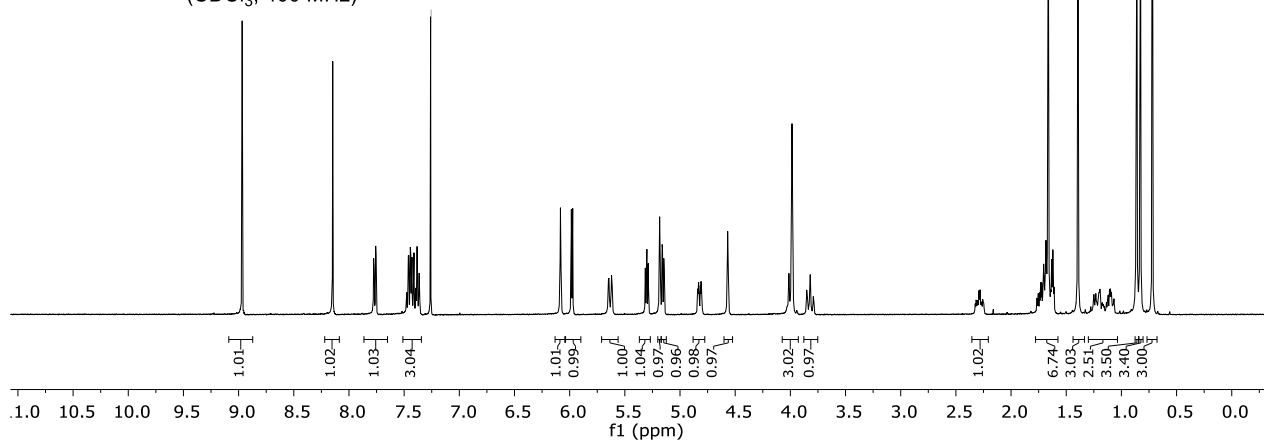


8. NMR Spectra



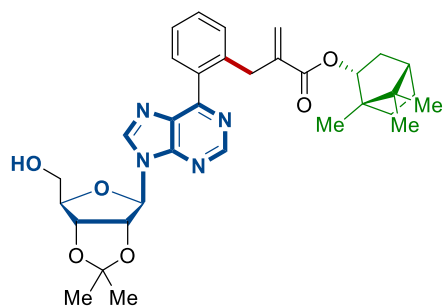
260d

(CDCl₃, 400 MHz)



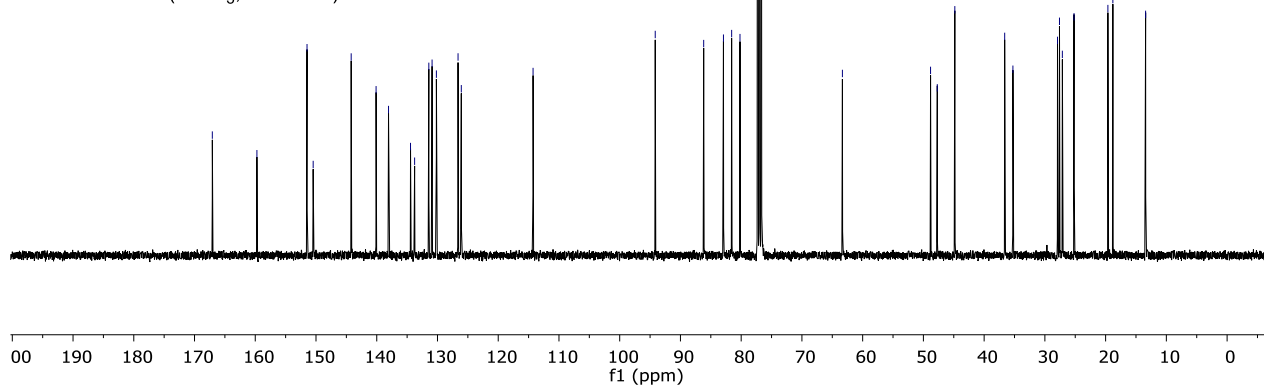
f1 (ppm)

167.07
159.73
151.48
150.47
144.21
140.11
138.06
134.44
133.76
131.43
130.89
130.18
126.61
126.08
114.26
94.15
86.17
82.92
81.57
80.20
63.33
48.82
47.72
44.83
36.62
35.26
27.92
27.59
27.12
25.20
19.63
18.81
13.42

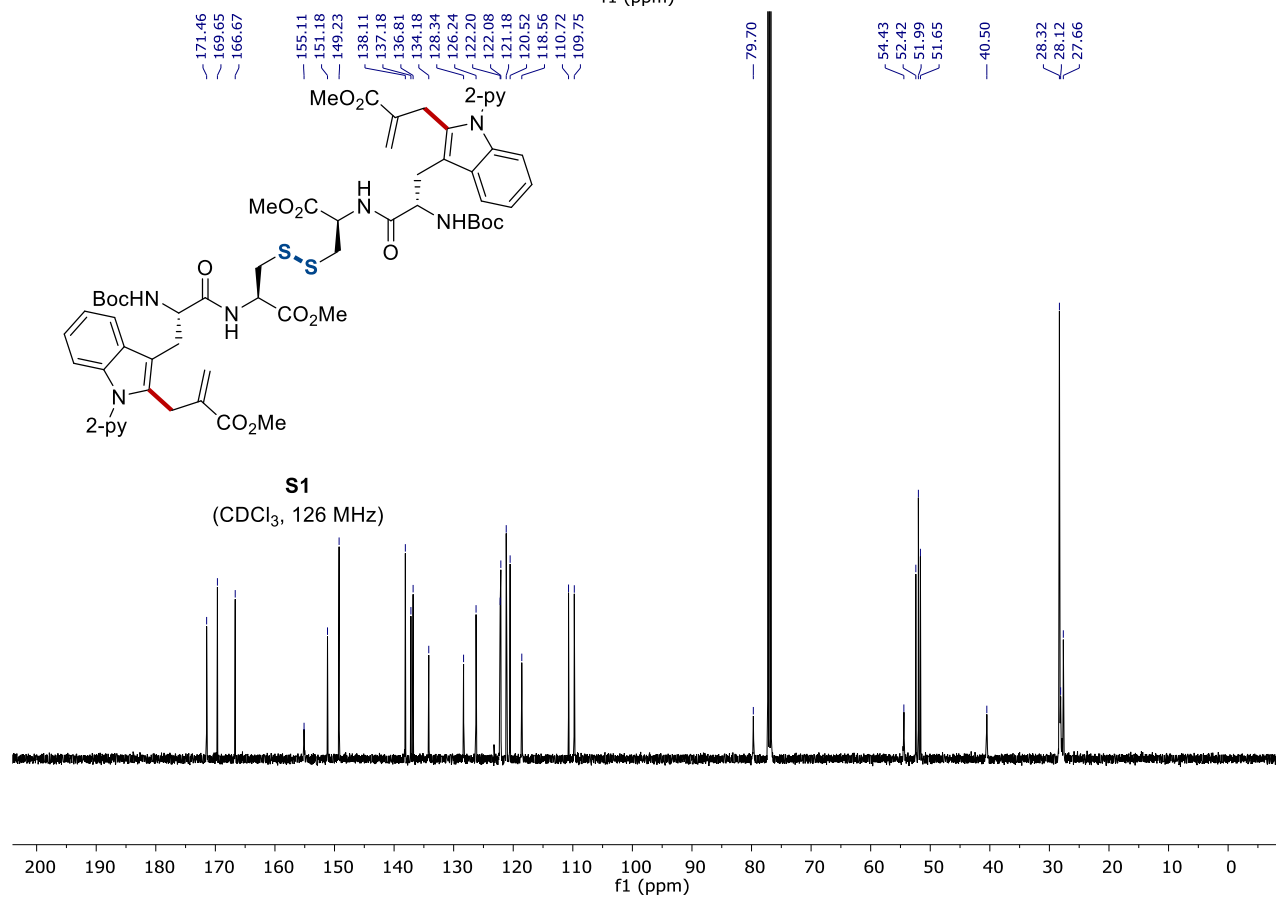
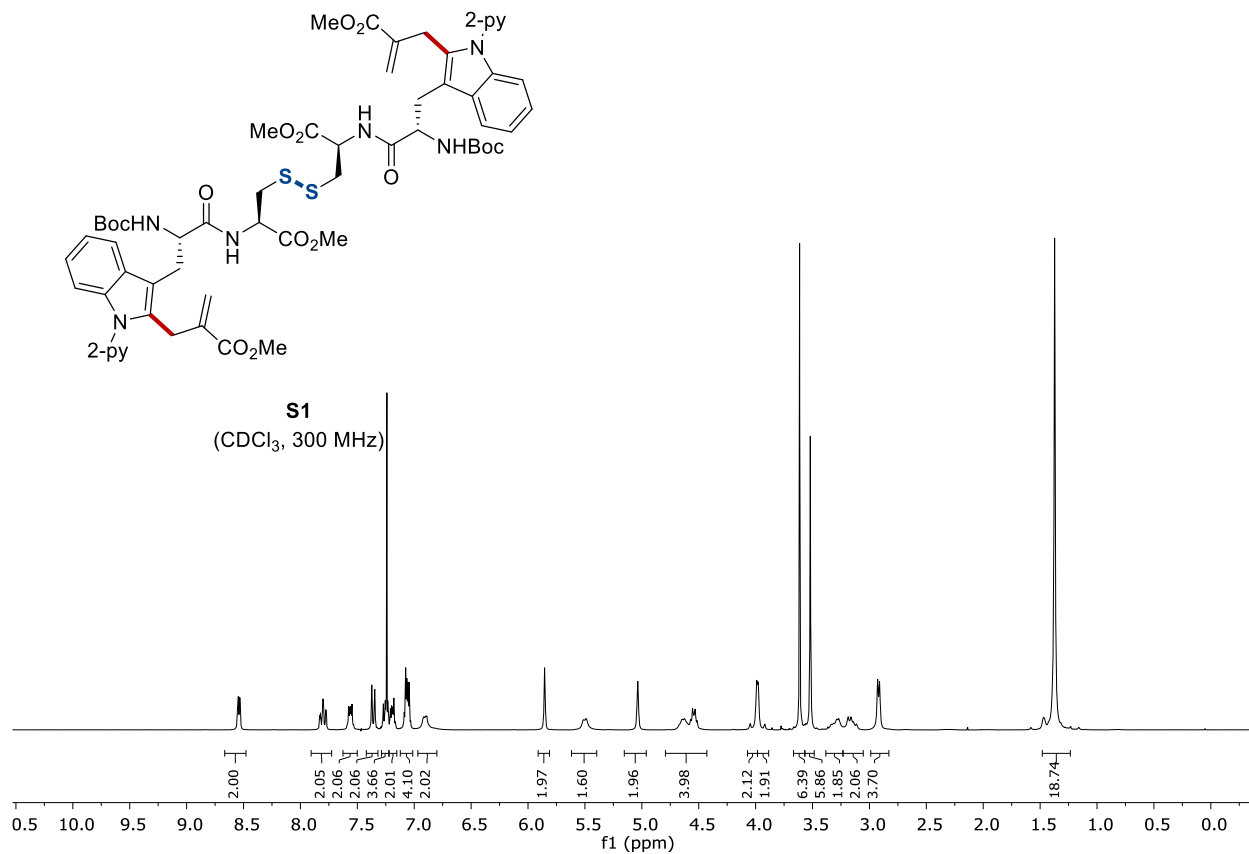


260d

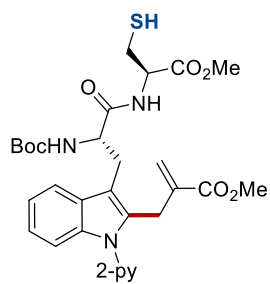
(CDCl₃, 101 MHz)



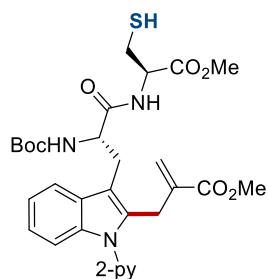
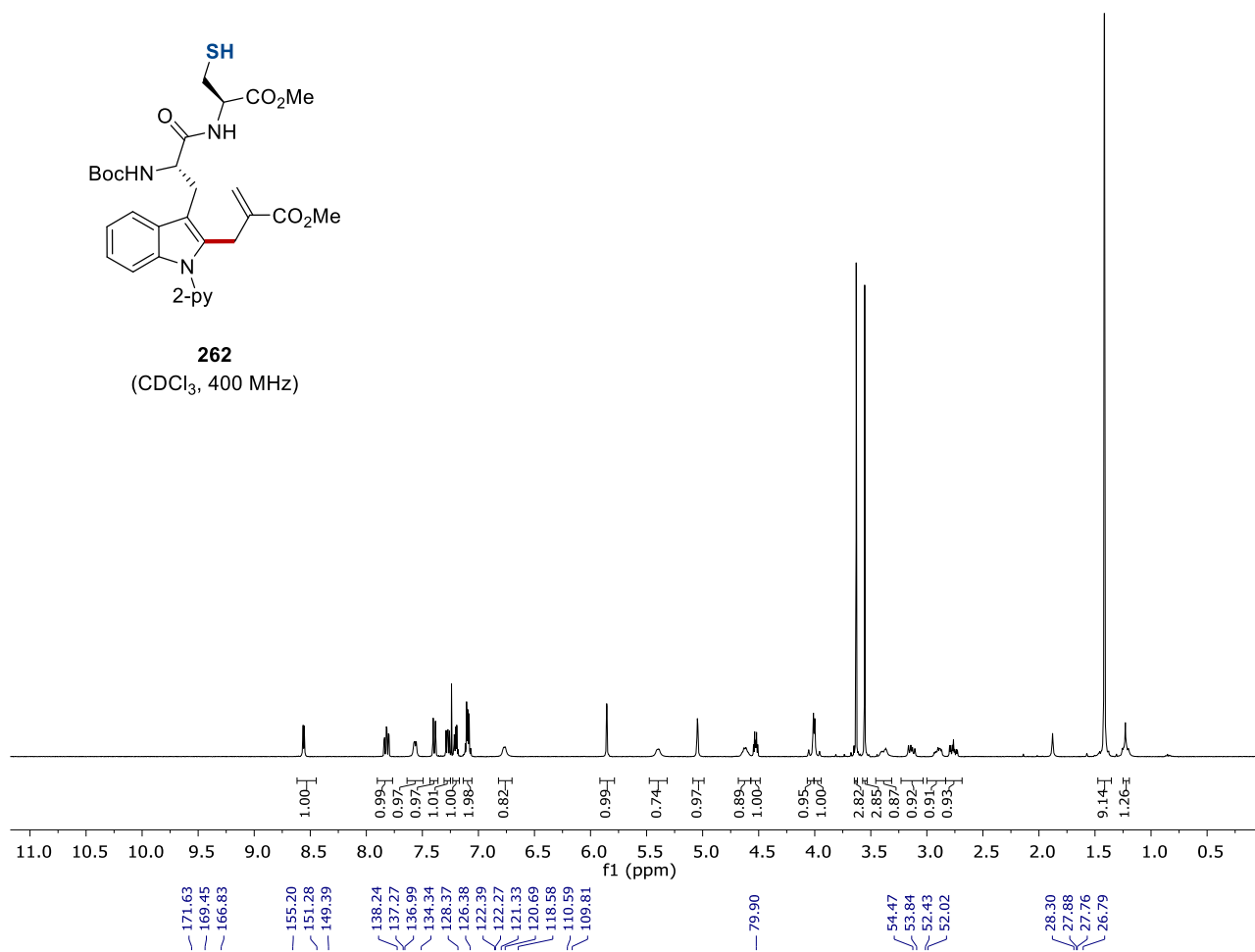
f1 (ppm)



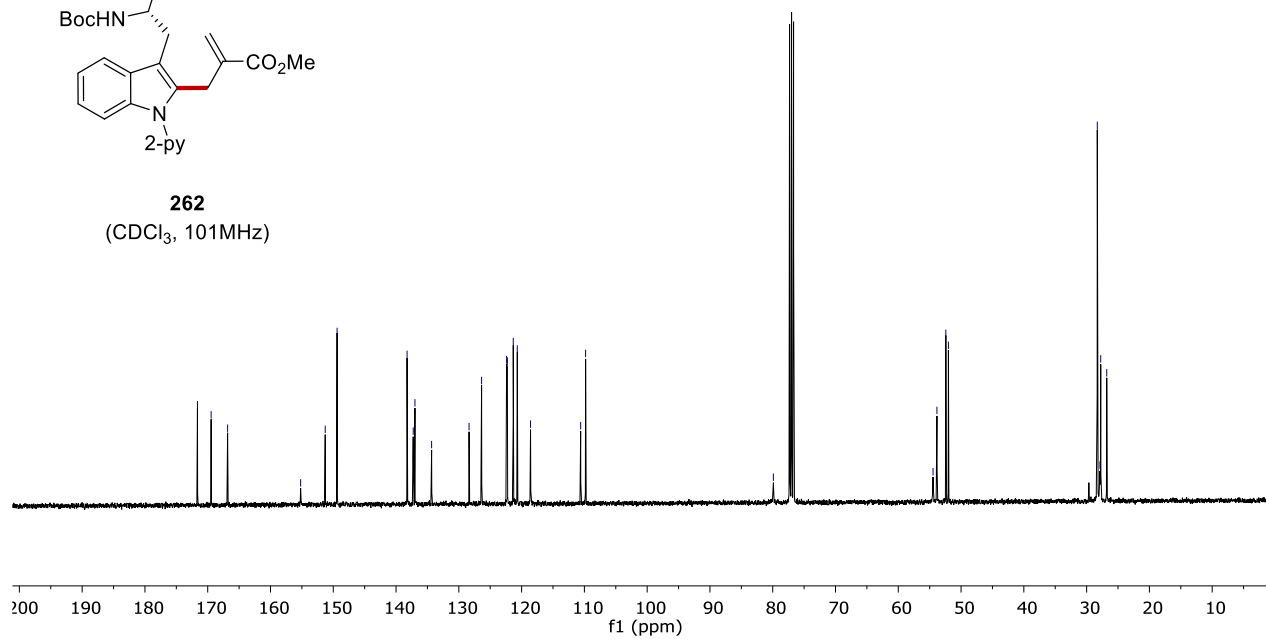
8. NMR Spectra

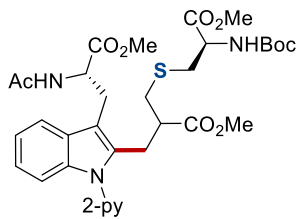


262
(CDCl₃, 400 MHz)

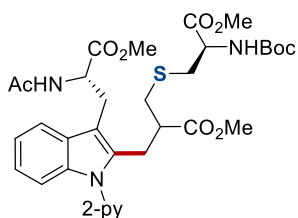
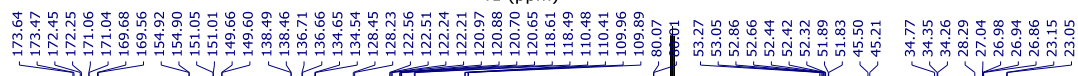
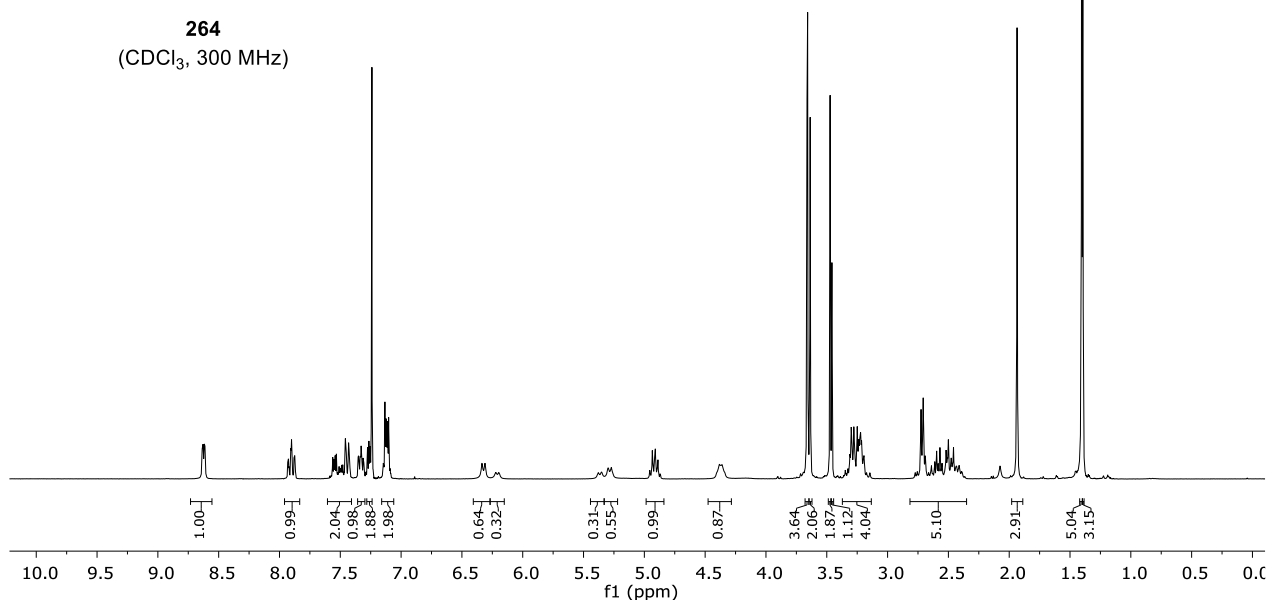


262
(CDCl₃, 101MHz)

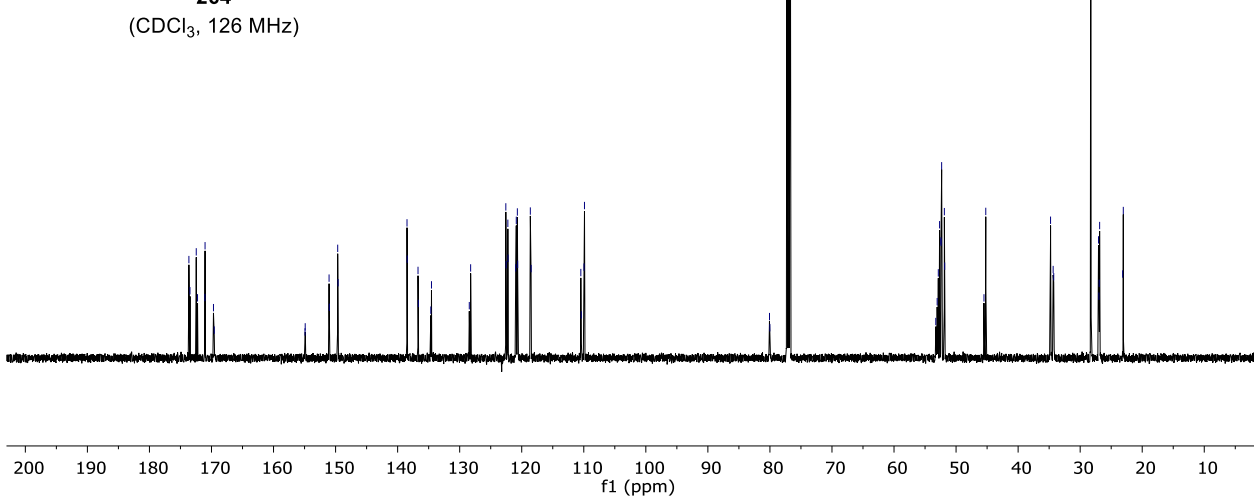




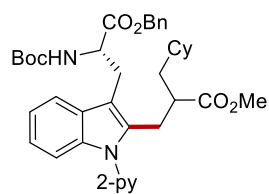
264
(CDCl₃, 300 MHz)



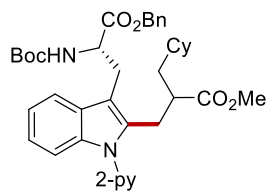
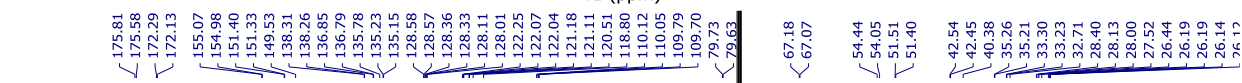
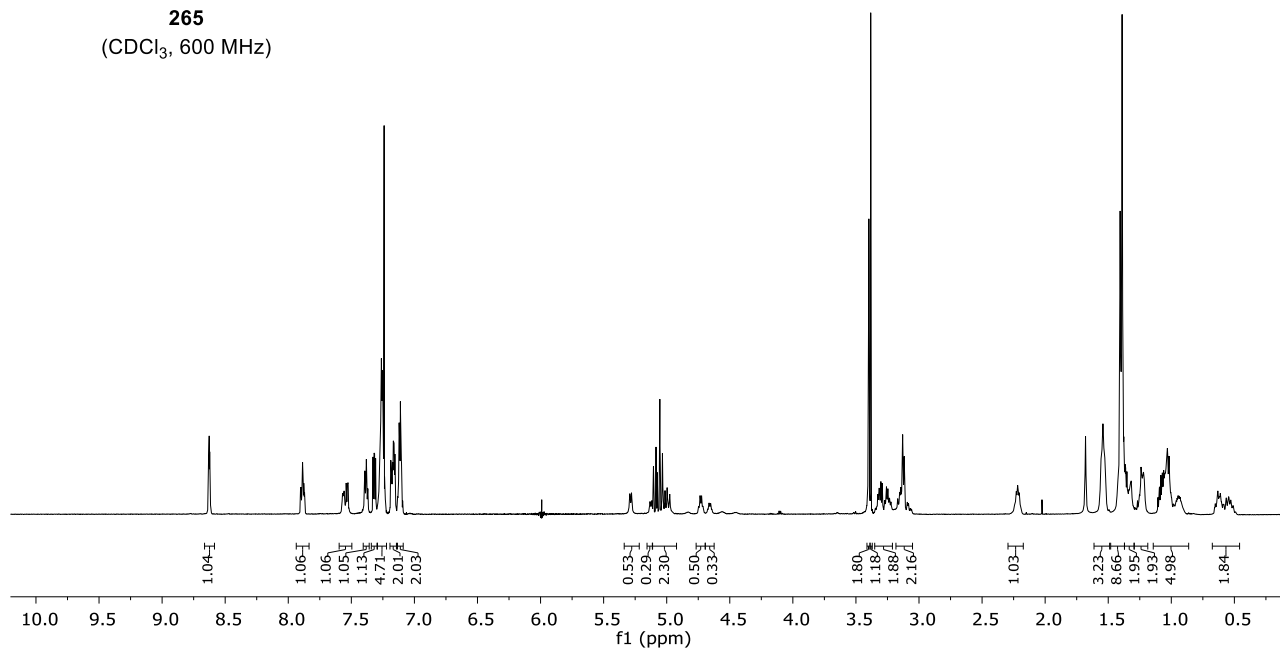
264
(CDCl₃, 126 MHz)



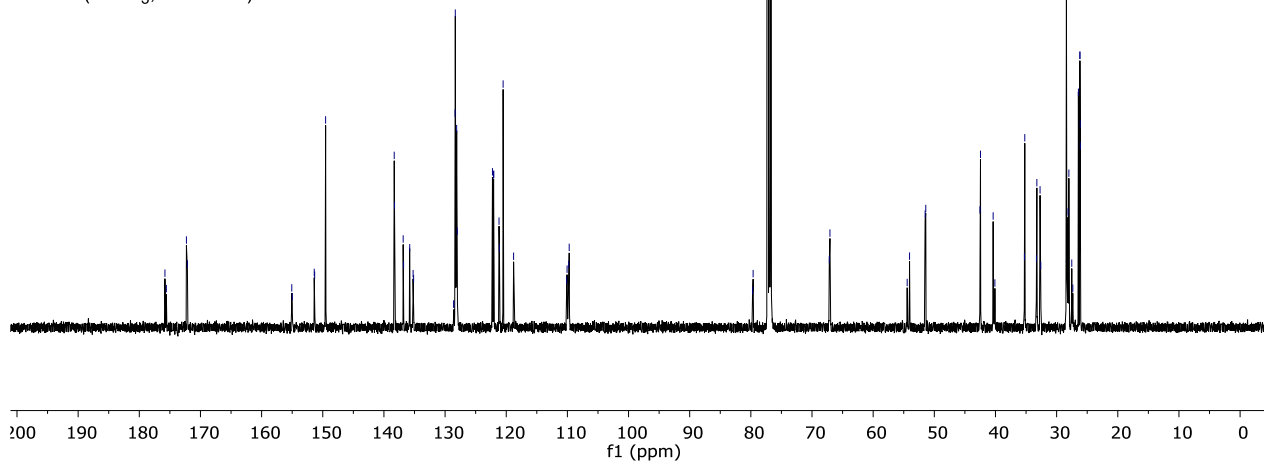
8. NMR Spectra

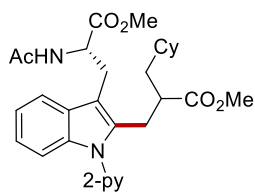


265
(CDCl₃, 600 MHz)

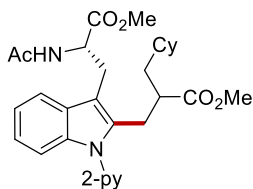
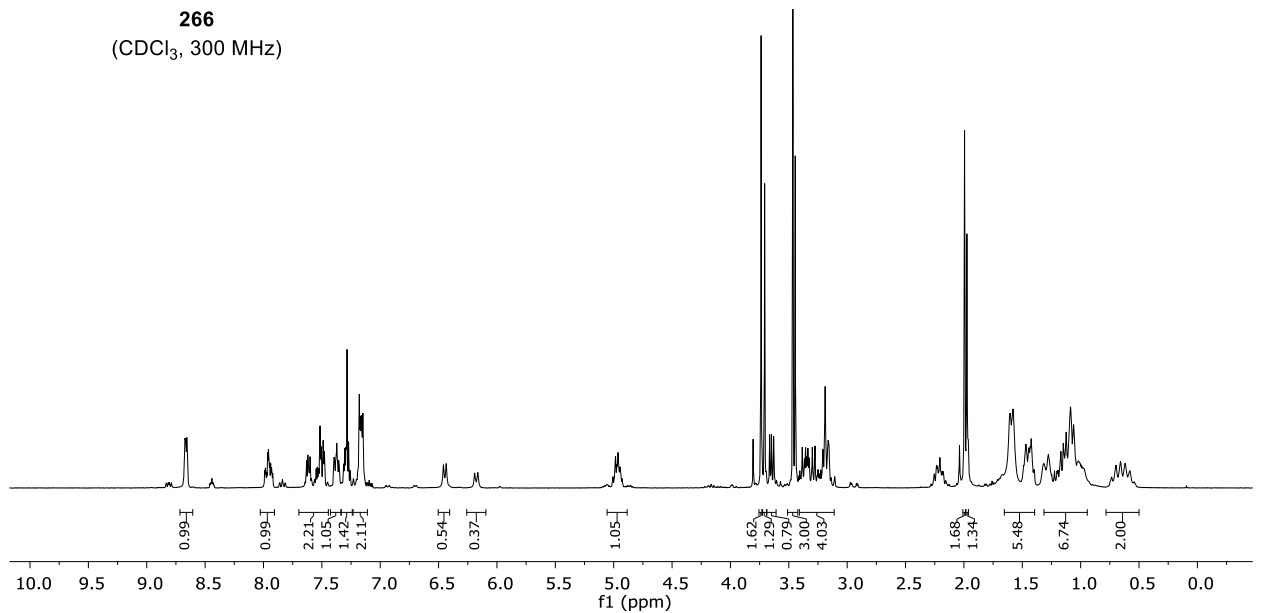


265
(CDCl₃, 126 MHz)

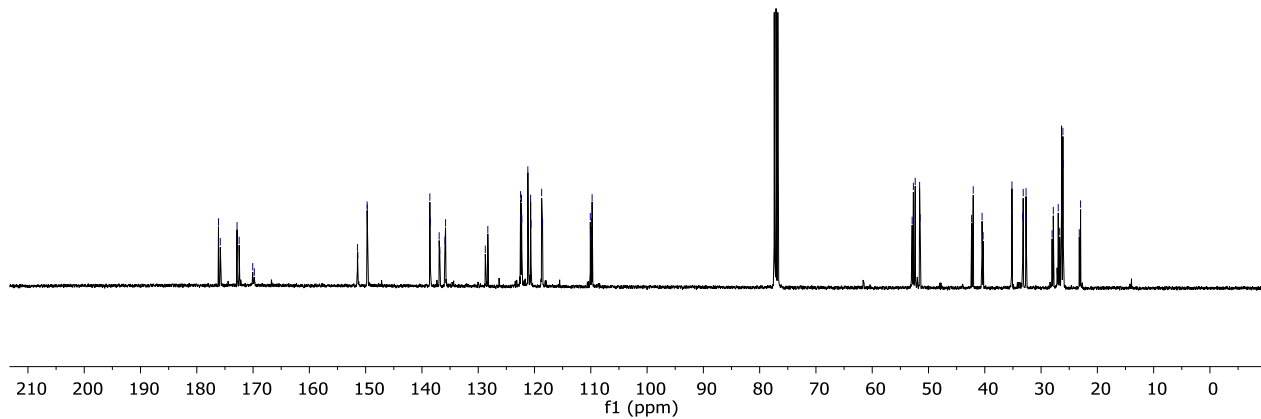




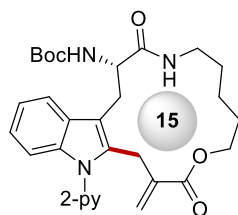
266
(CDCl₃, 300 MHz)



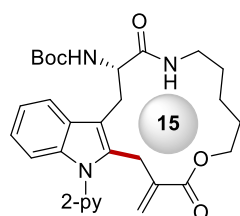
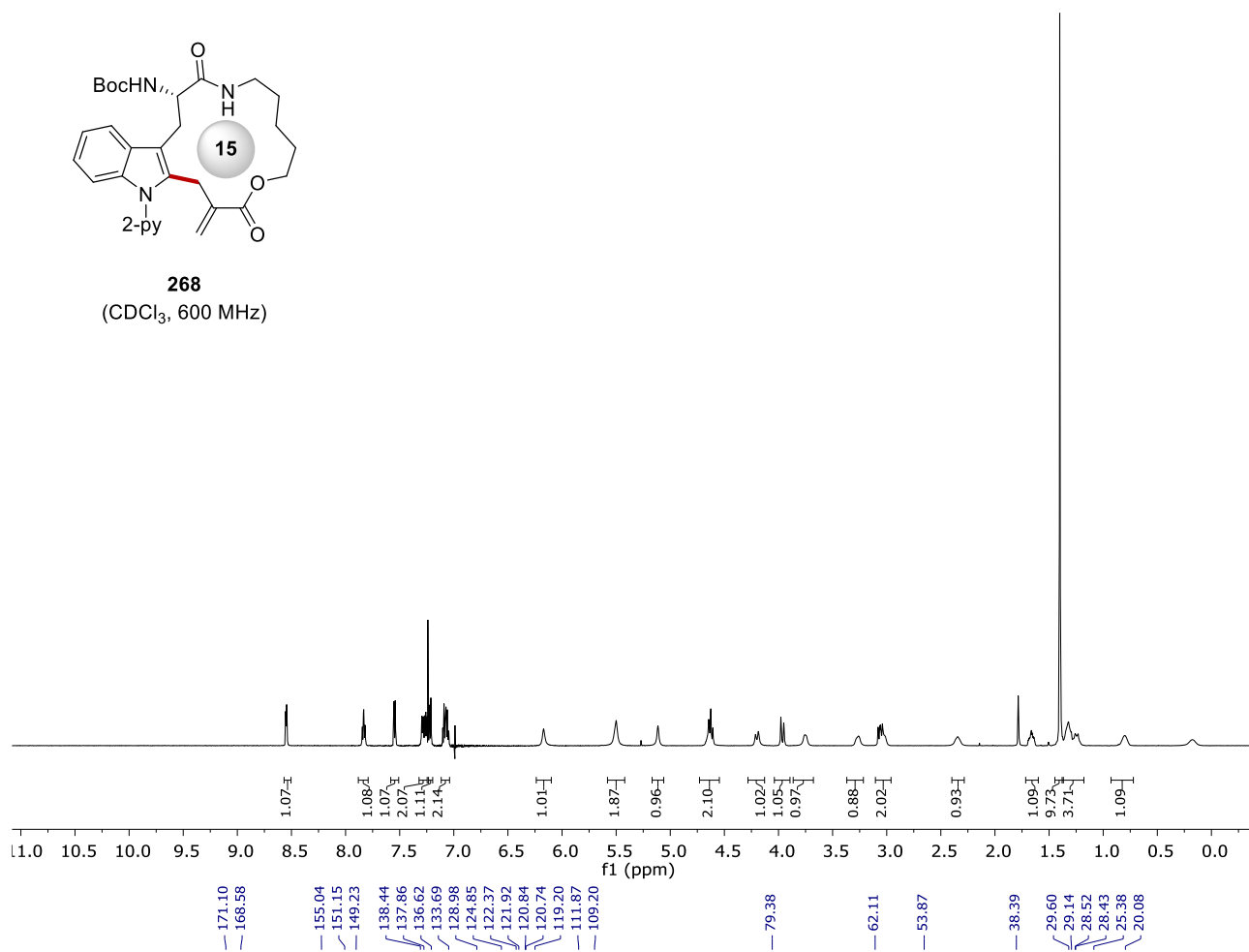
266
(CDCl₃, 101 MHz)



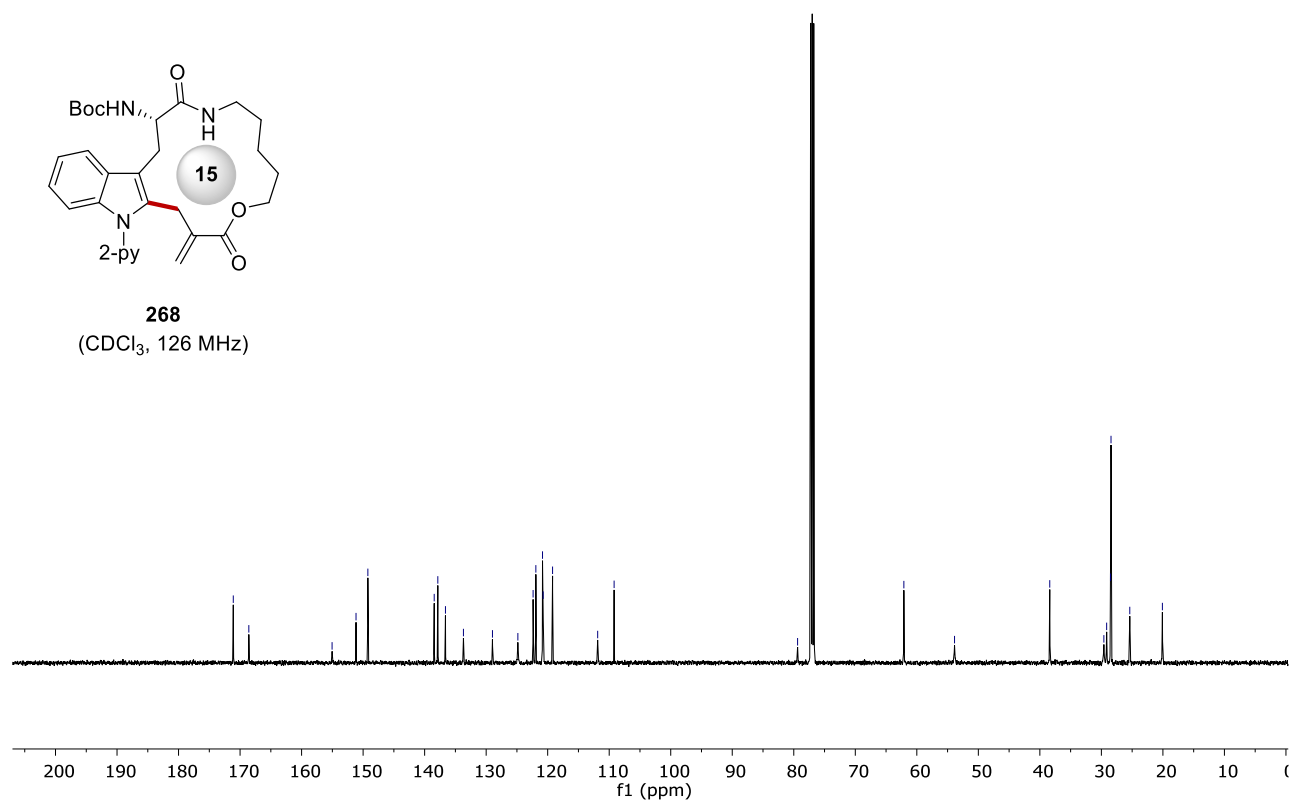
8. NMR Spectra



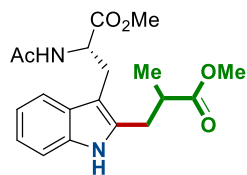
268
(CDCl₃, 600 MHz)



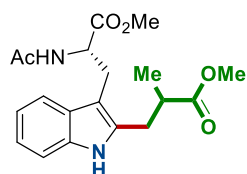
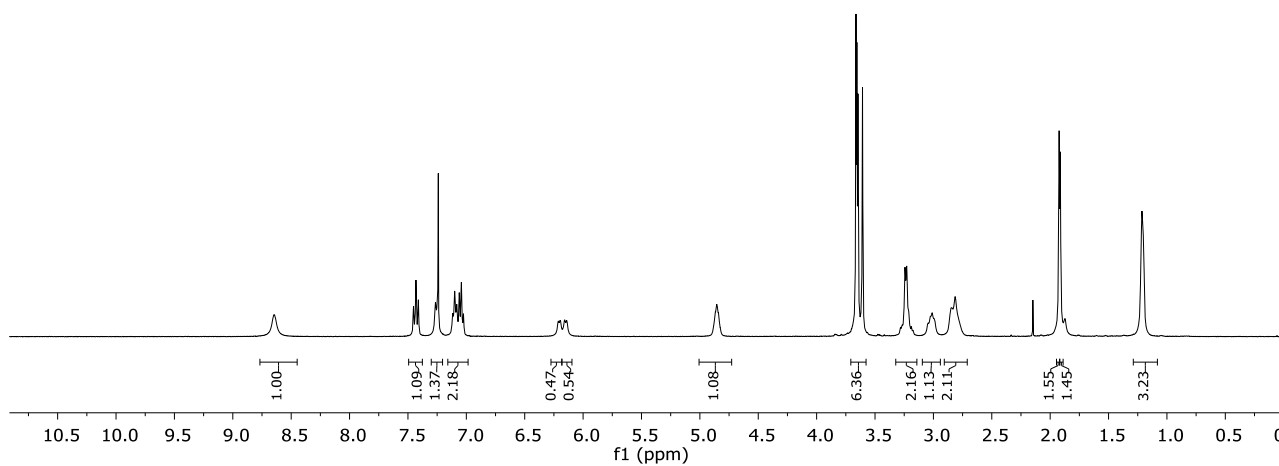
268
(CDCl₃, 126 MHz)



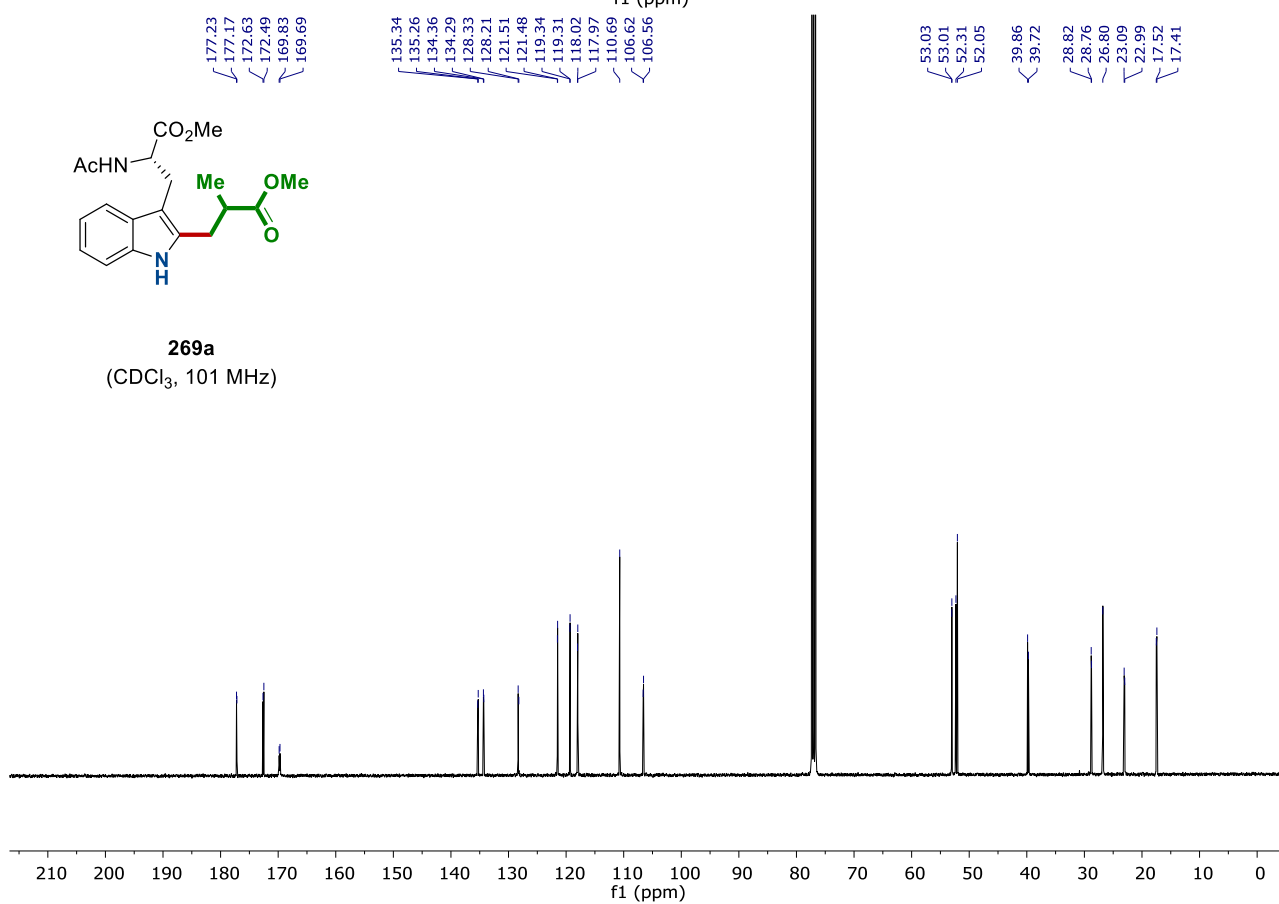
8. NMR Spectra



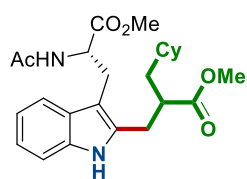
269a
(CDCl₃, 400 MHz)



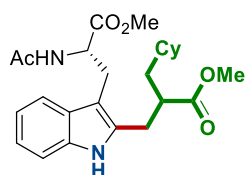
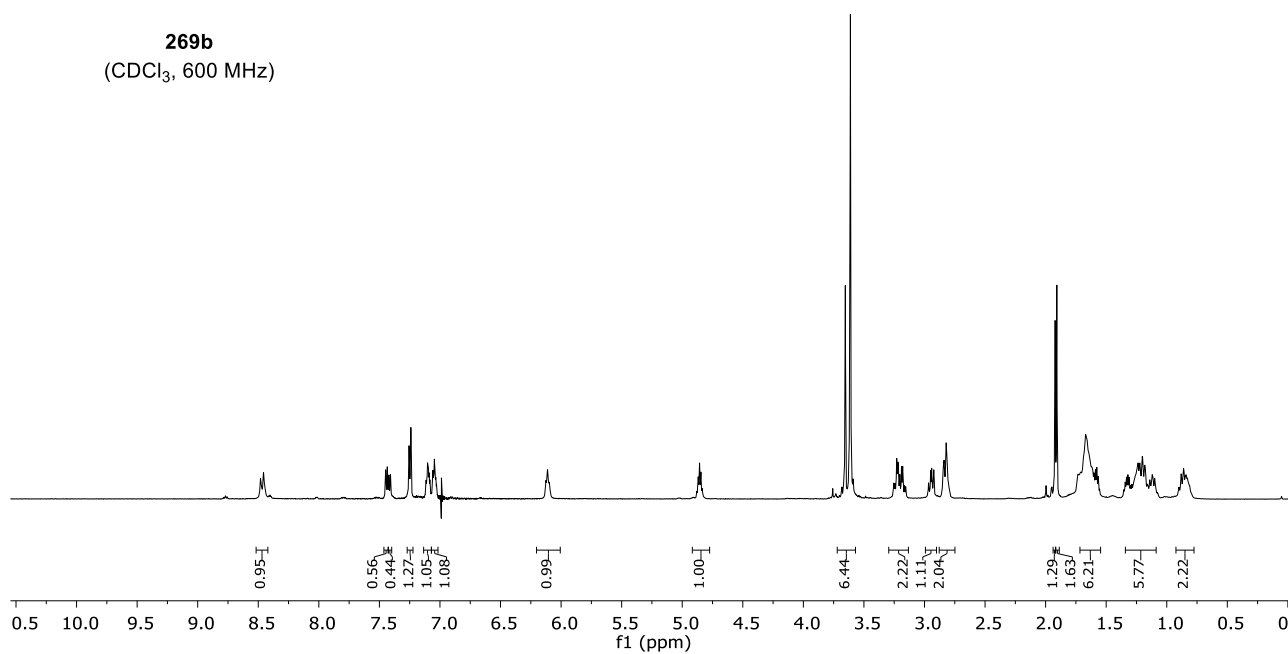
269a
(CDCl₃, 101 MHz)



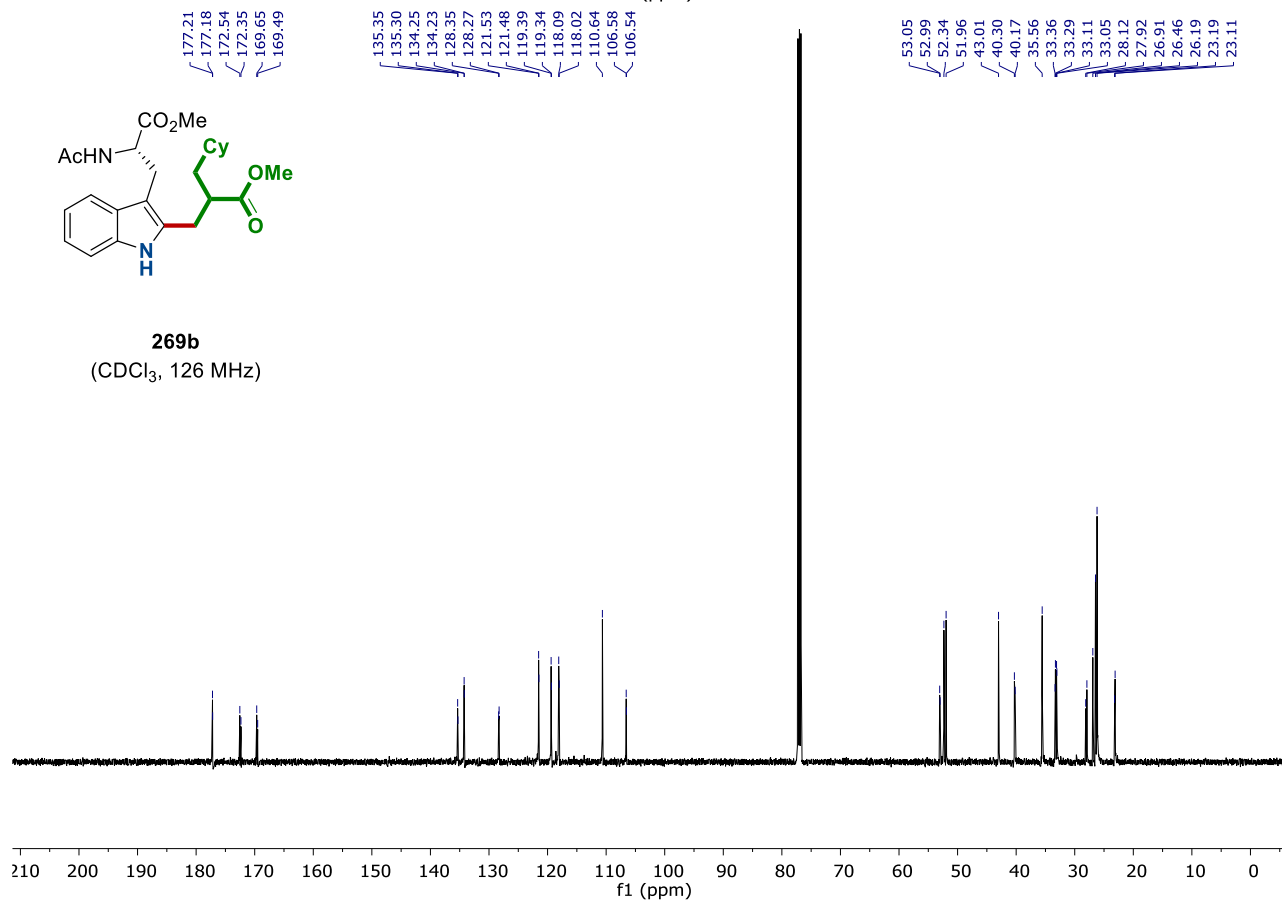
8. NMR Spectra

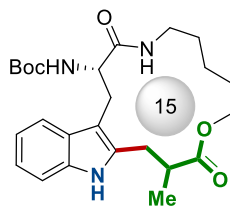


269b
(CDCl₃, 600 MHz)

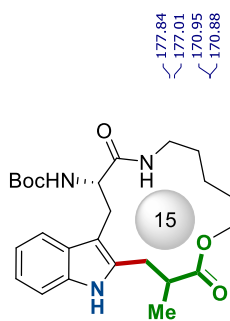
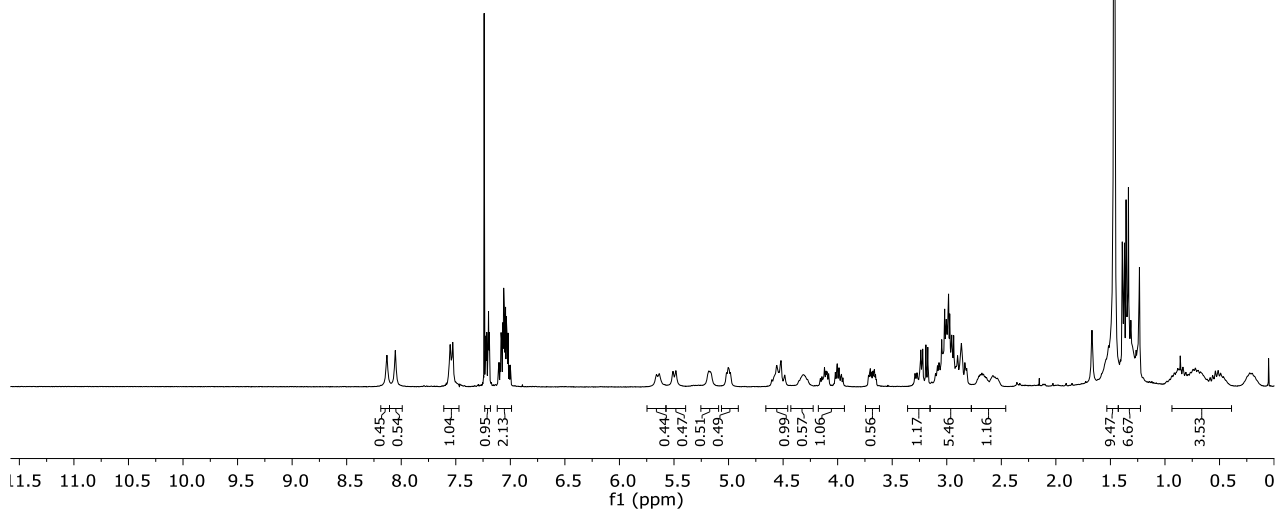


269b
(CDCl₃, 126 MHz)

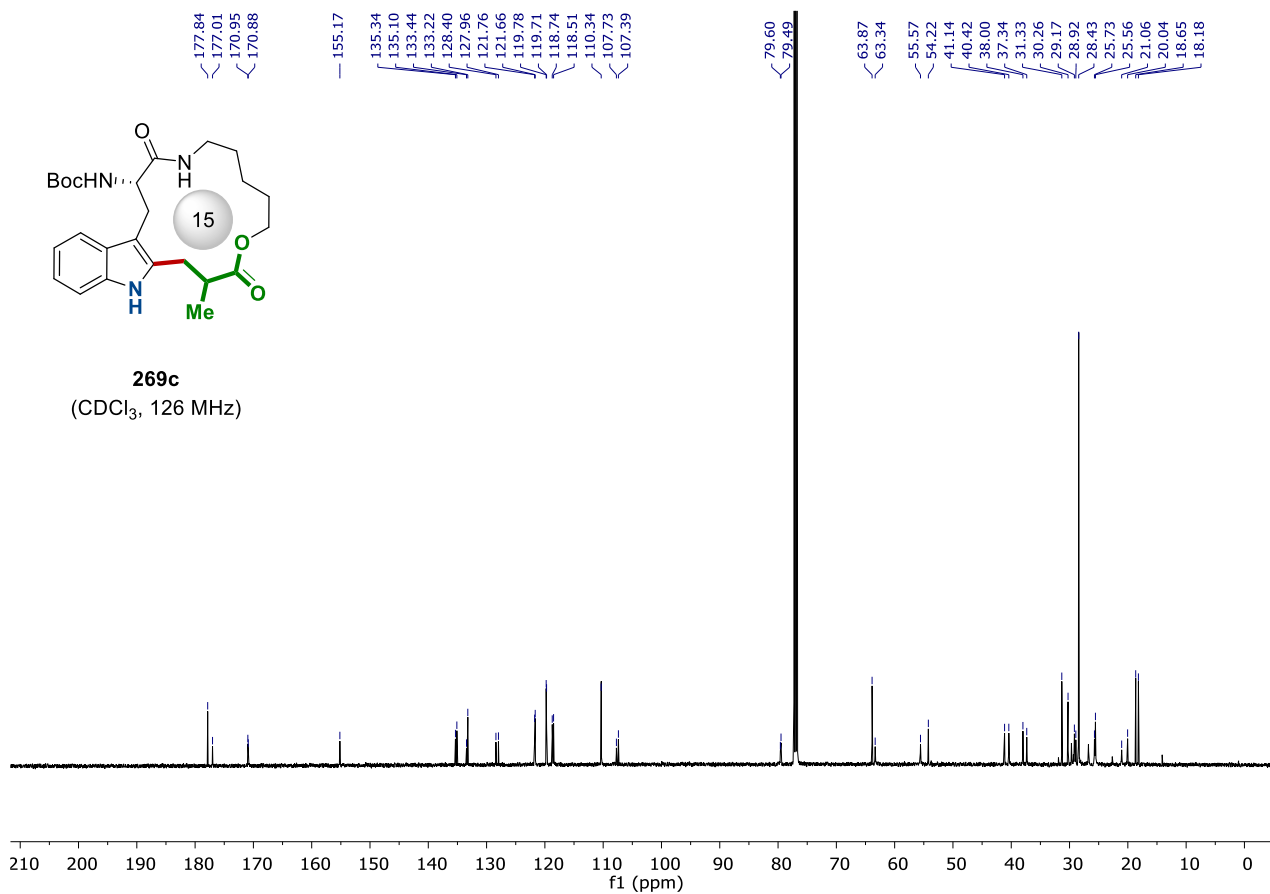




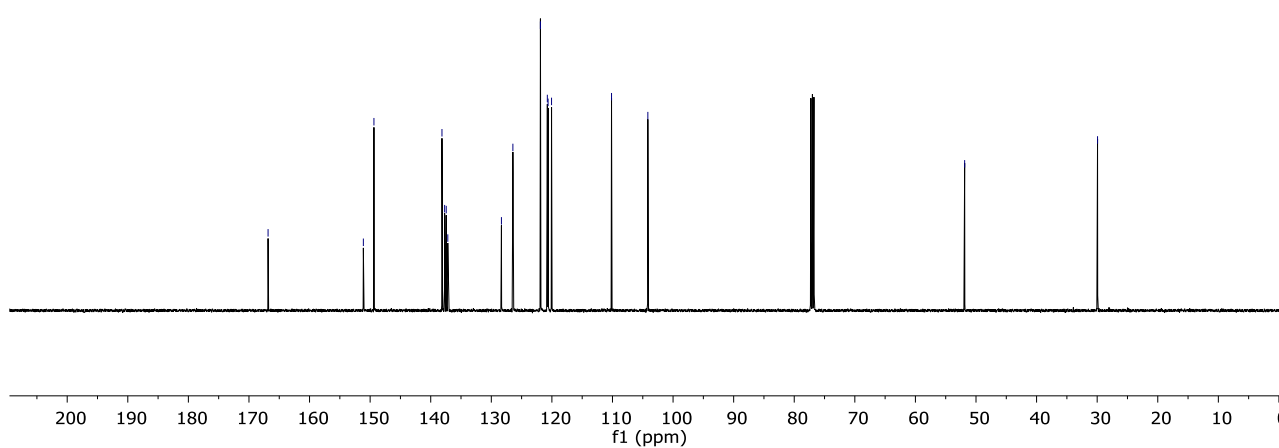
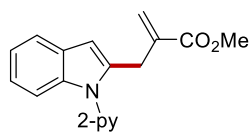
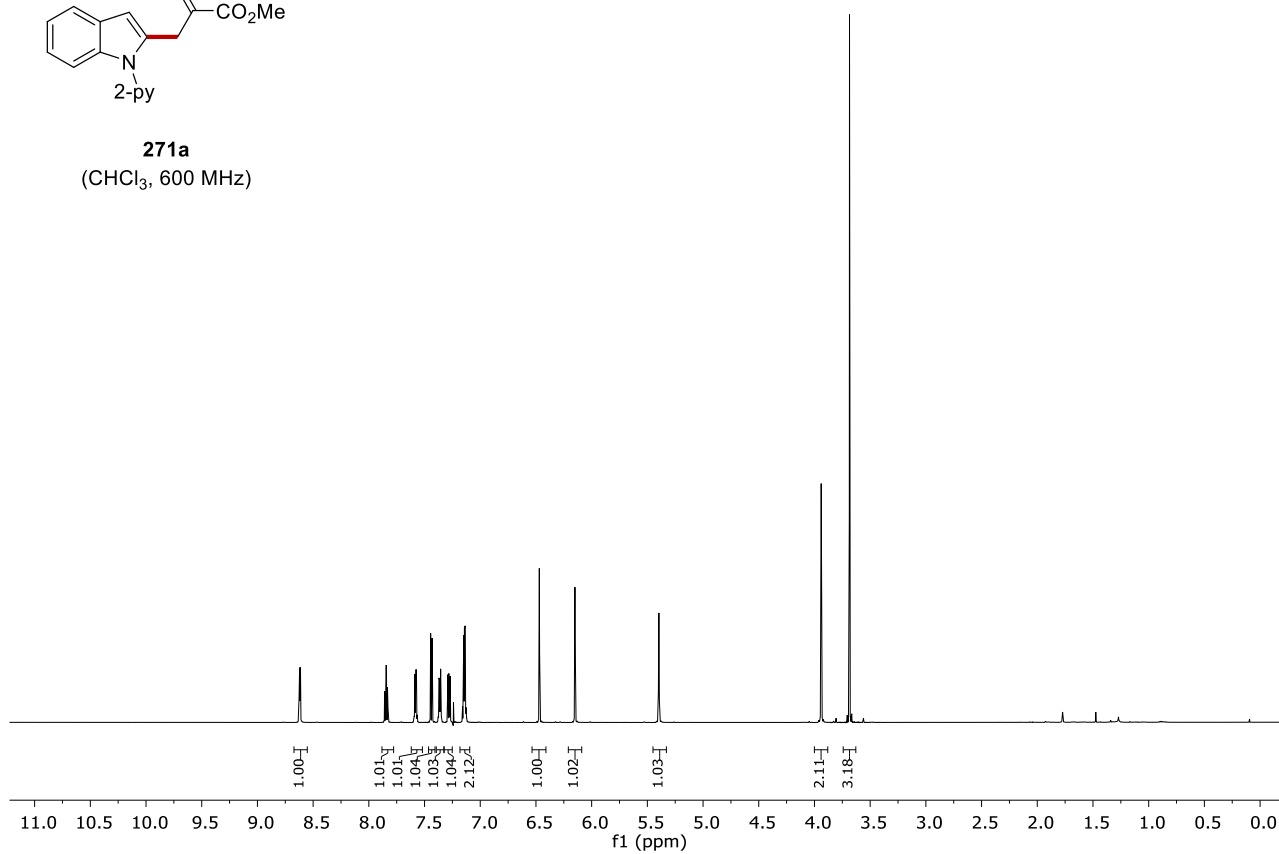
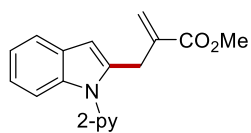
269c
(CDCl₃, 300 MHz)

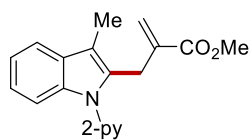


269c
(CDCl₃, 126 MHz)

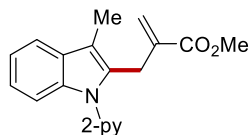
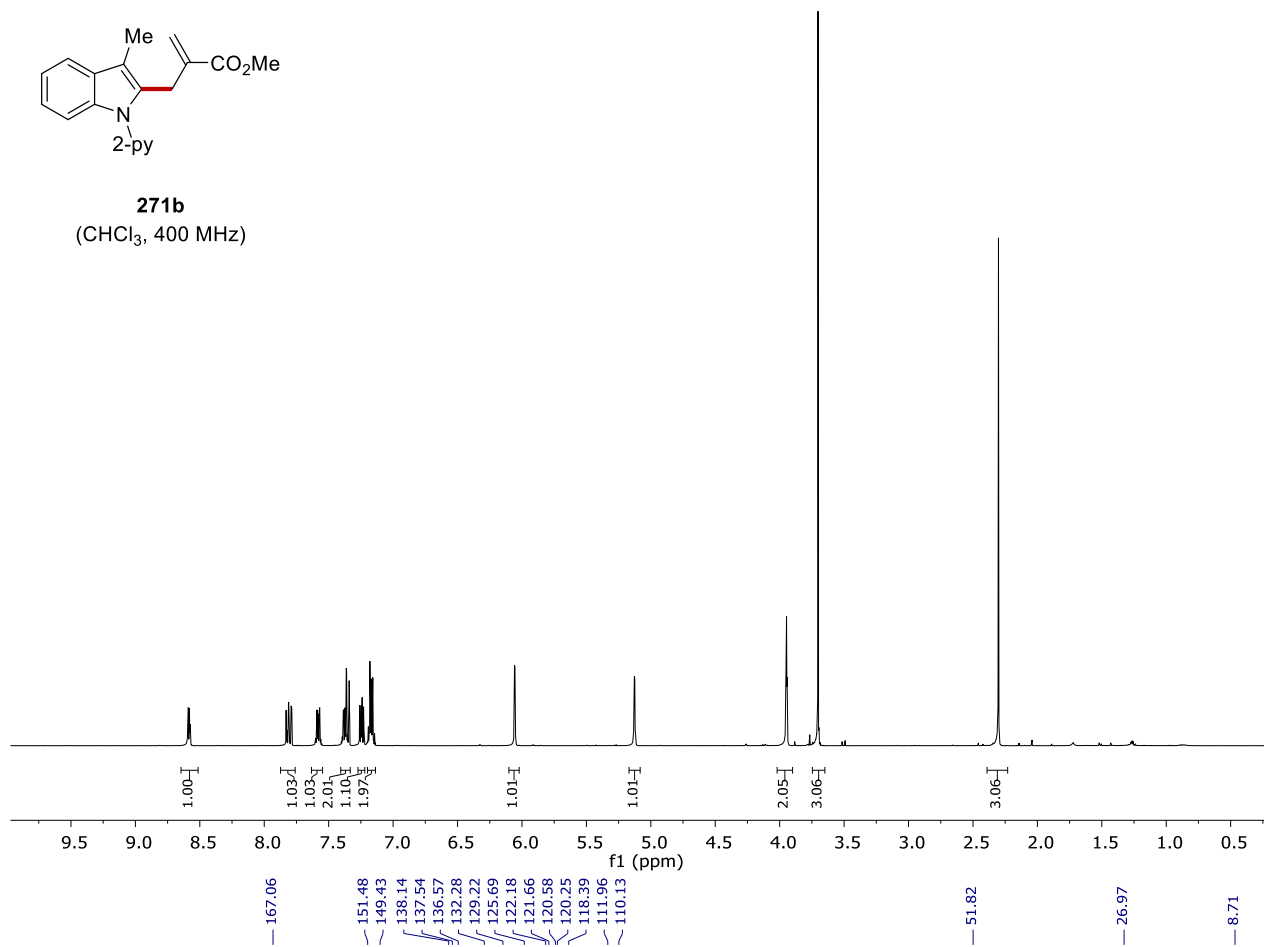


8. NMR Spectra

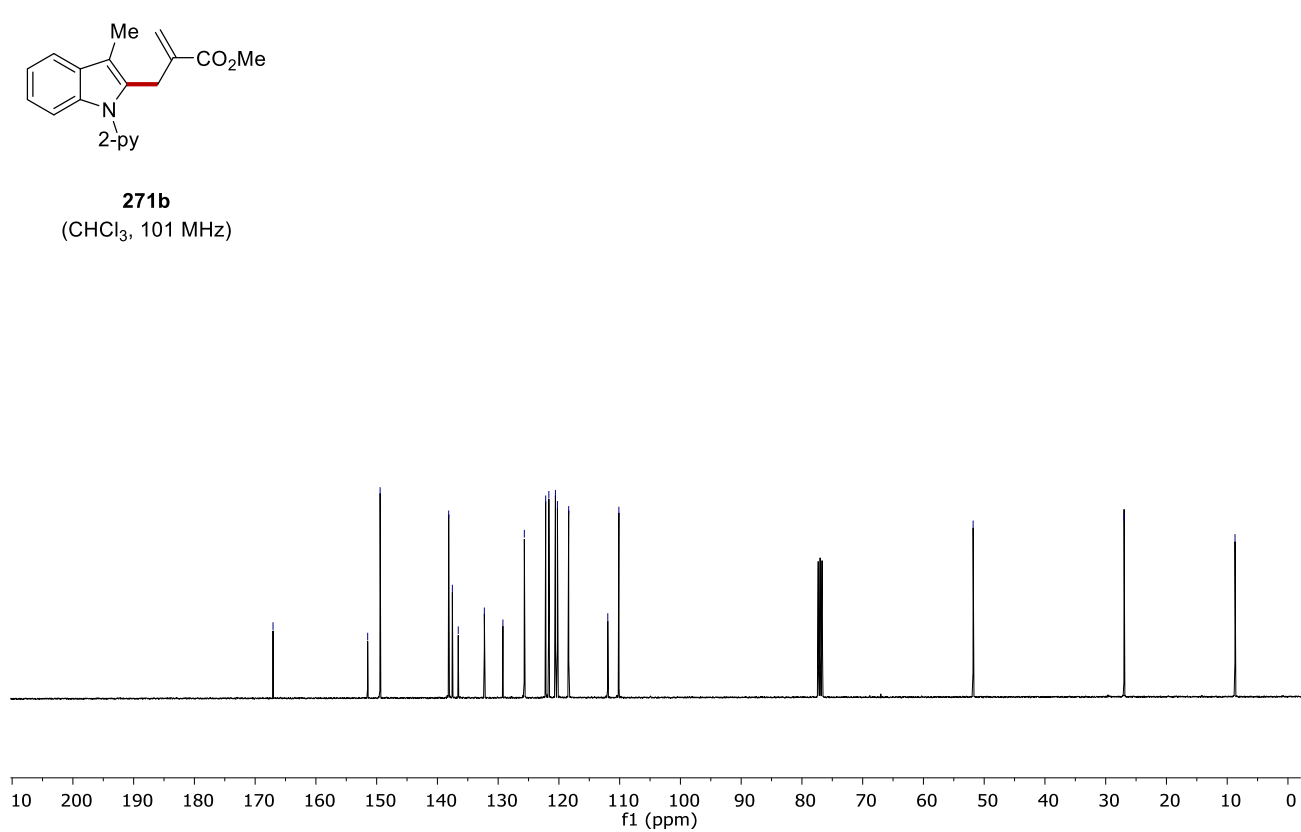




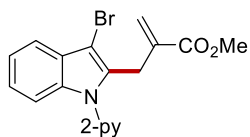
271b
(CHCl₃, 400 MHz)



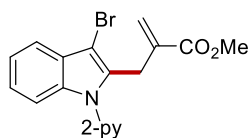
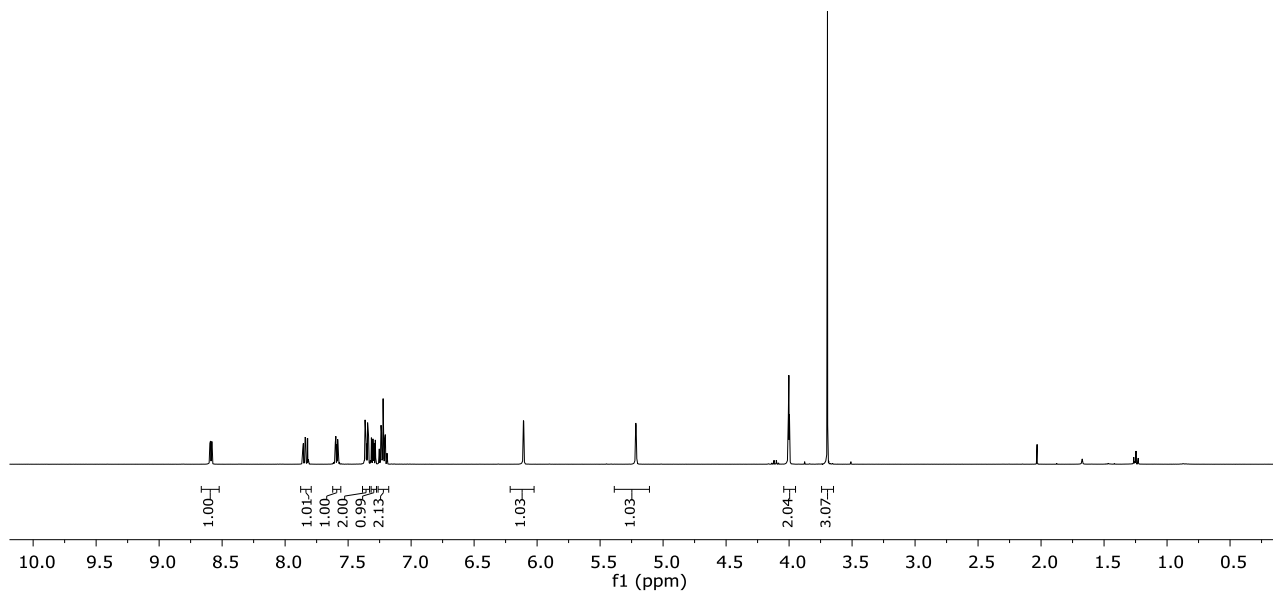
271b
(CHCl₃, 101 MHz)



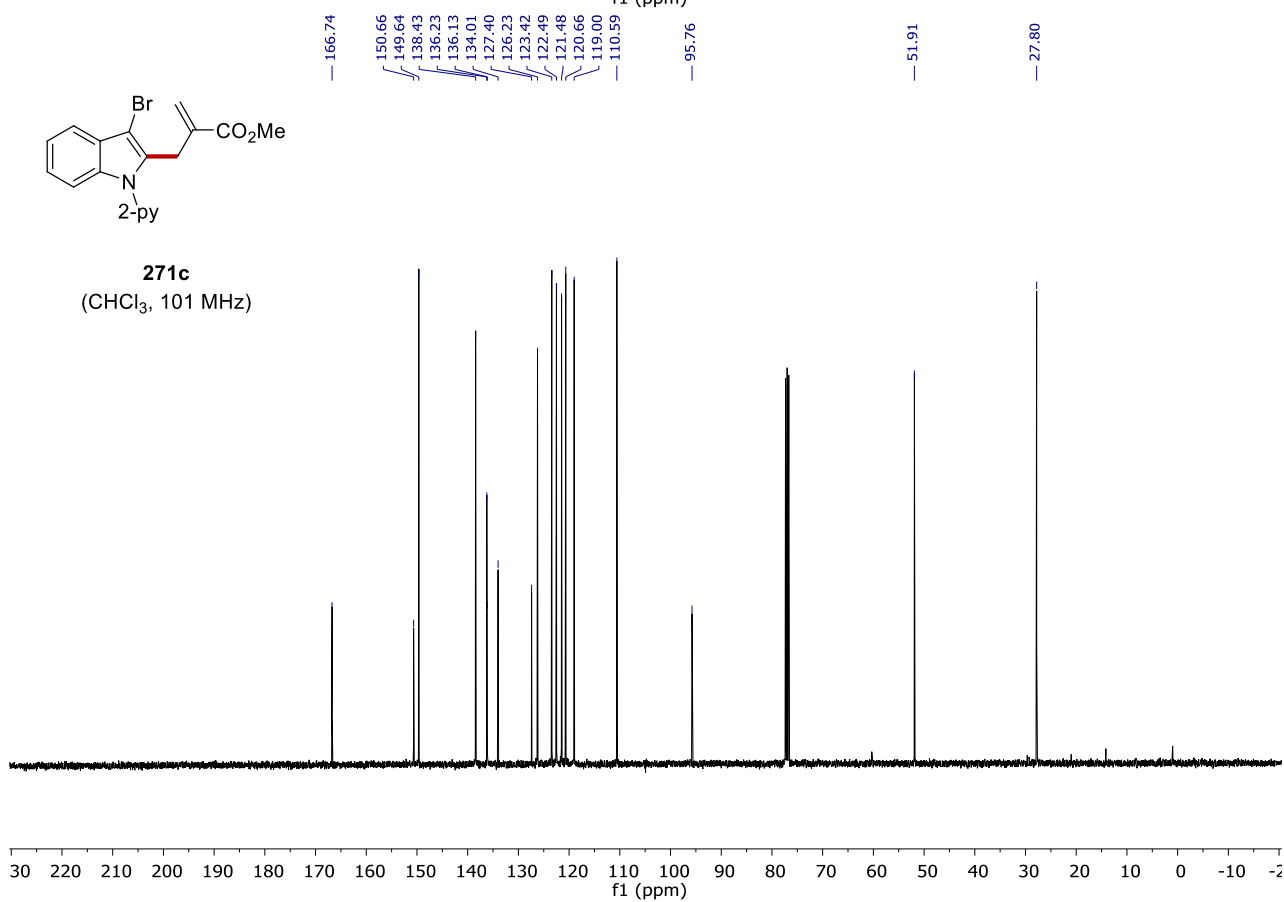
8. NMR Spectra



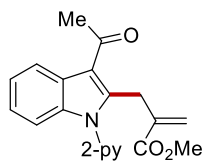
271c
(CHCl₃, 400 MHz)



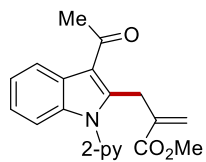
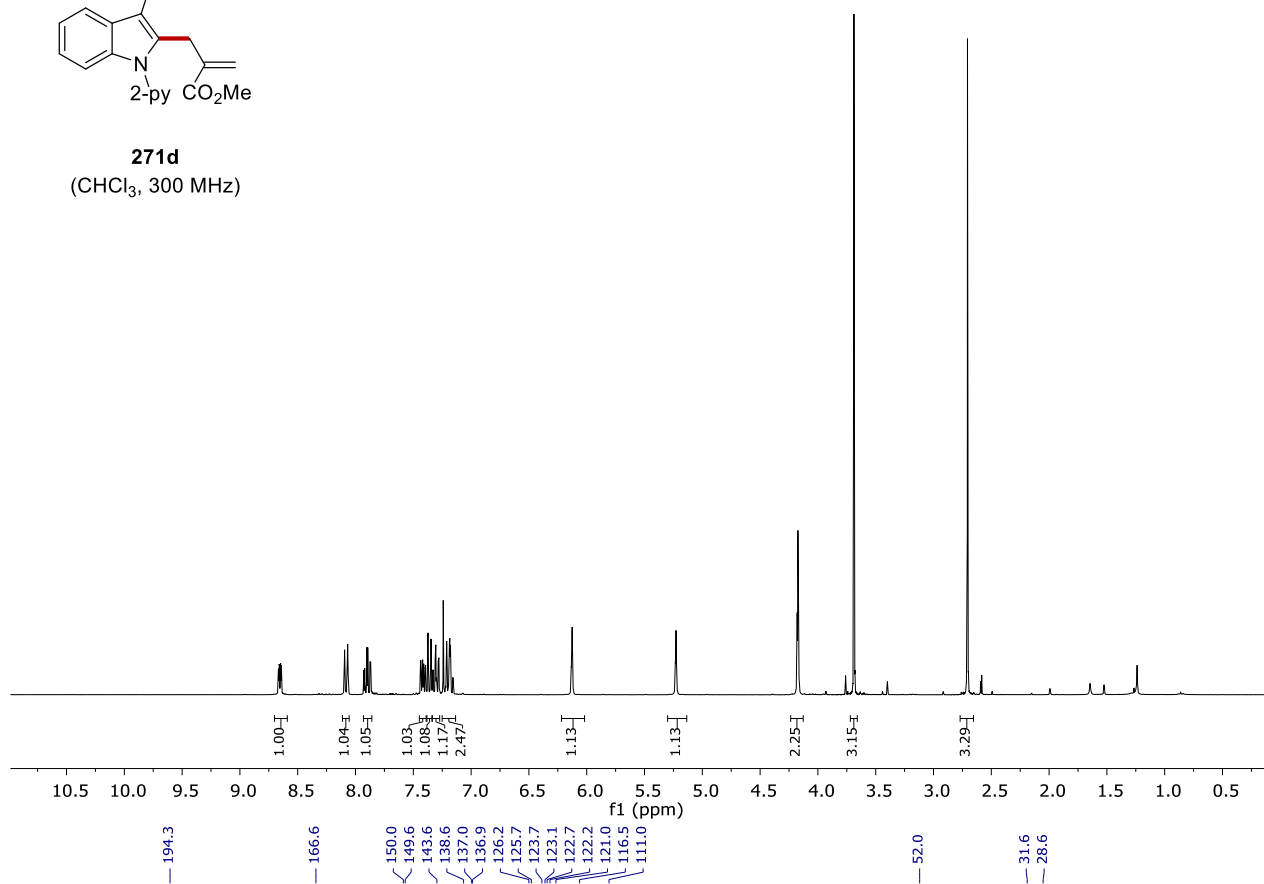
271c
(CHCl₃, 101 MHz)



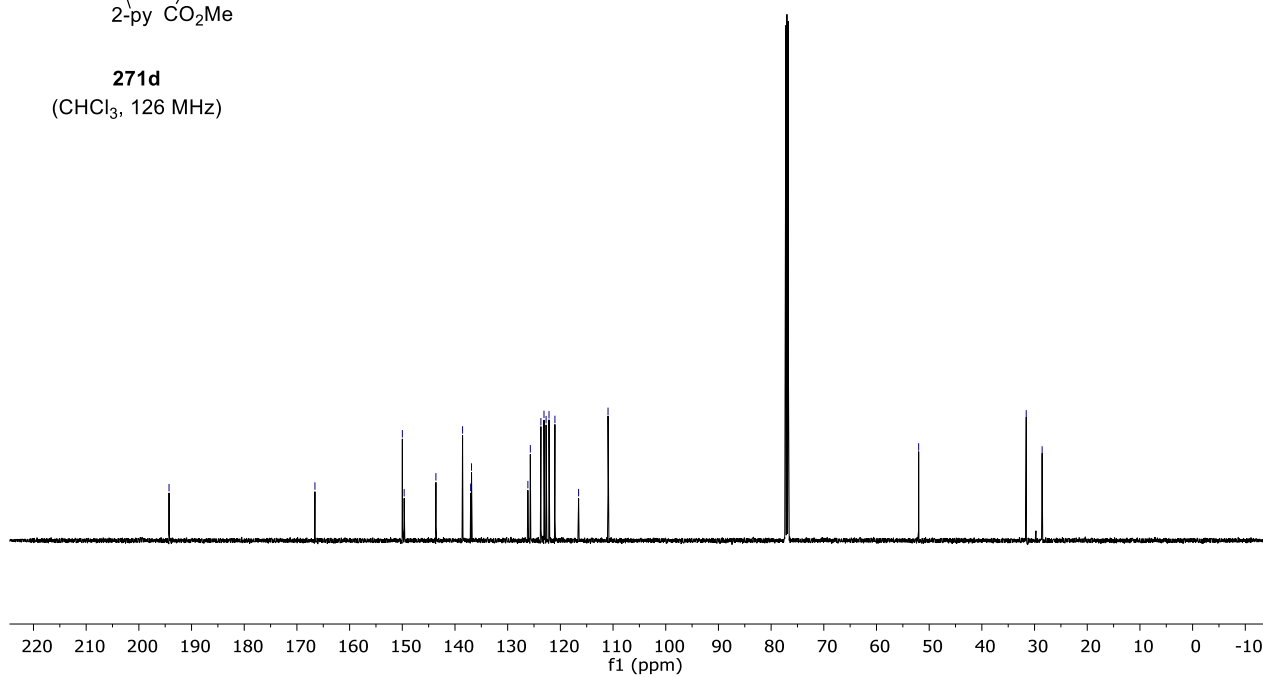
8. NMR Spectra



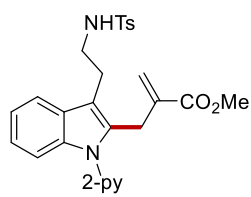
271d
(CHCl₃, 300 MHz)



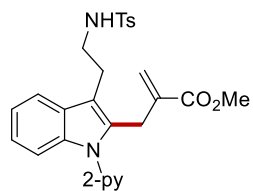
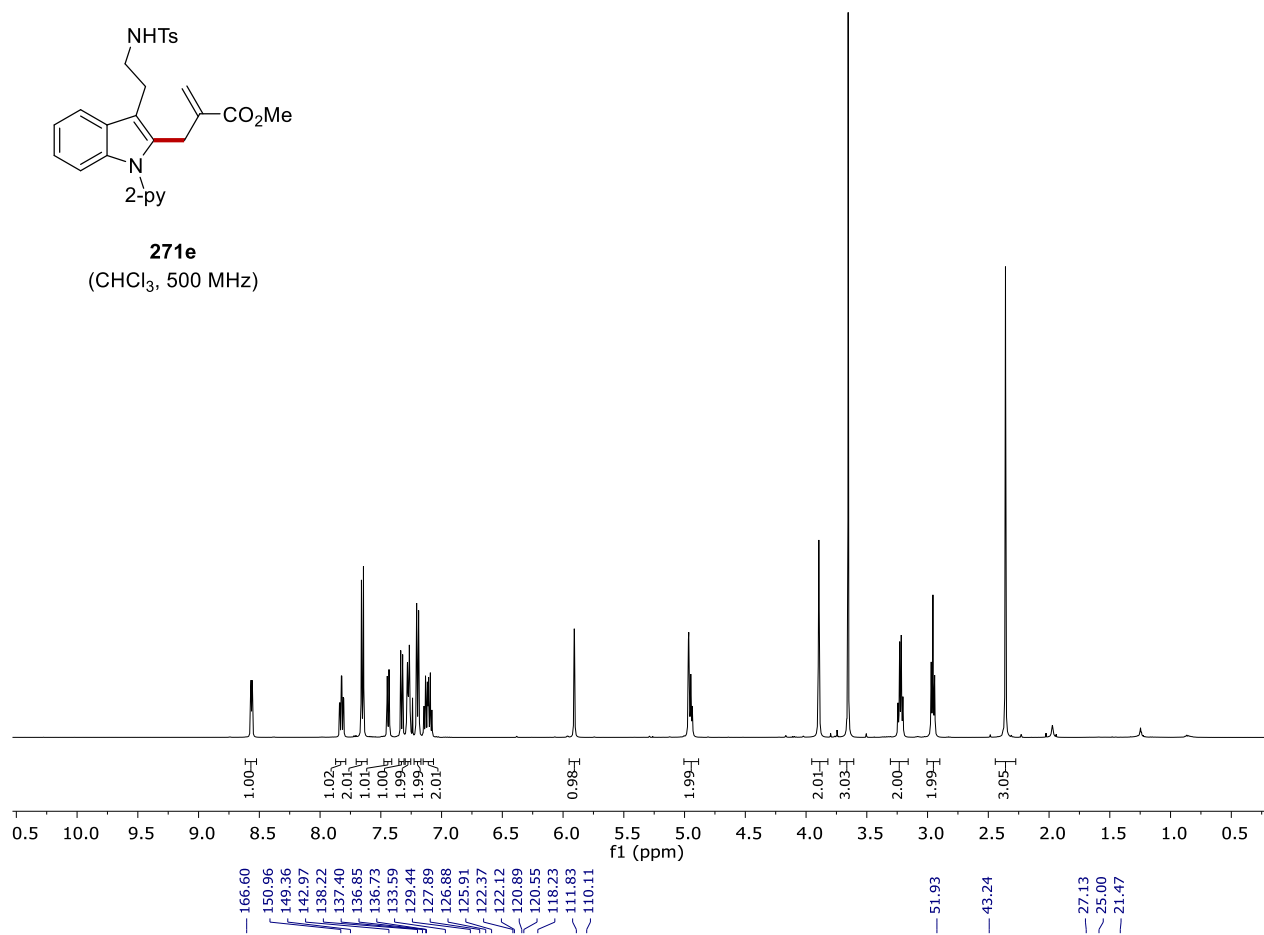
271d
(CHCl₃, 126 MHz)



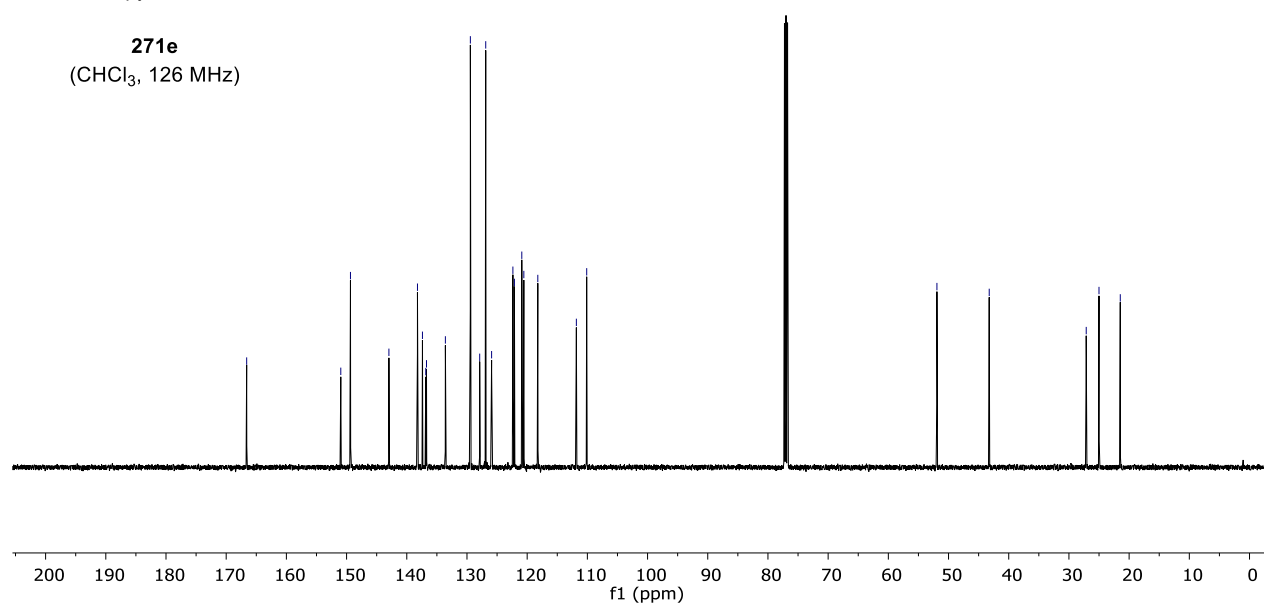
8. NMR Spectra

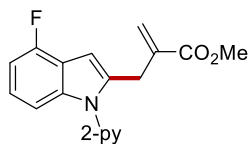


271e
(CHCl₃, 500 MHz)

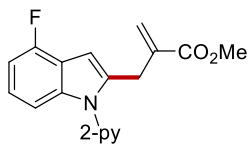
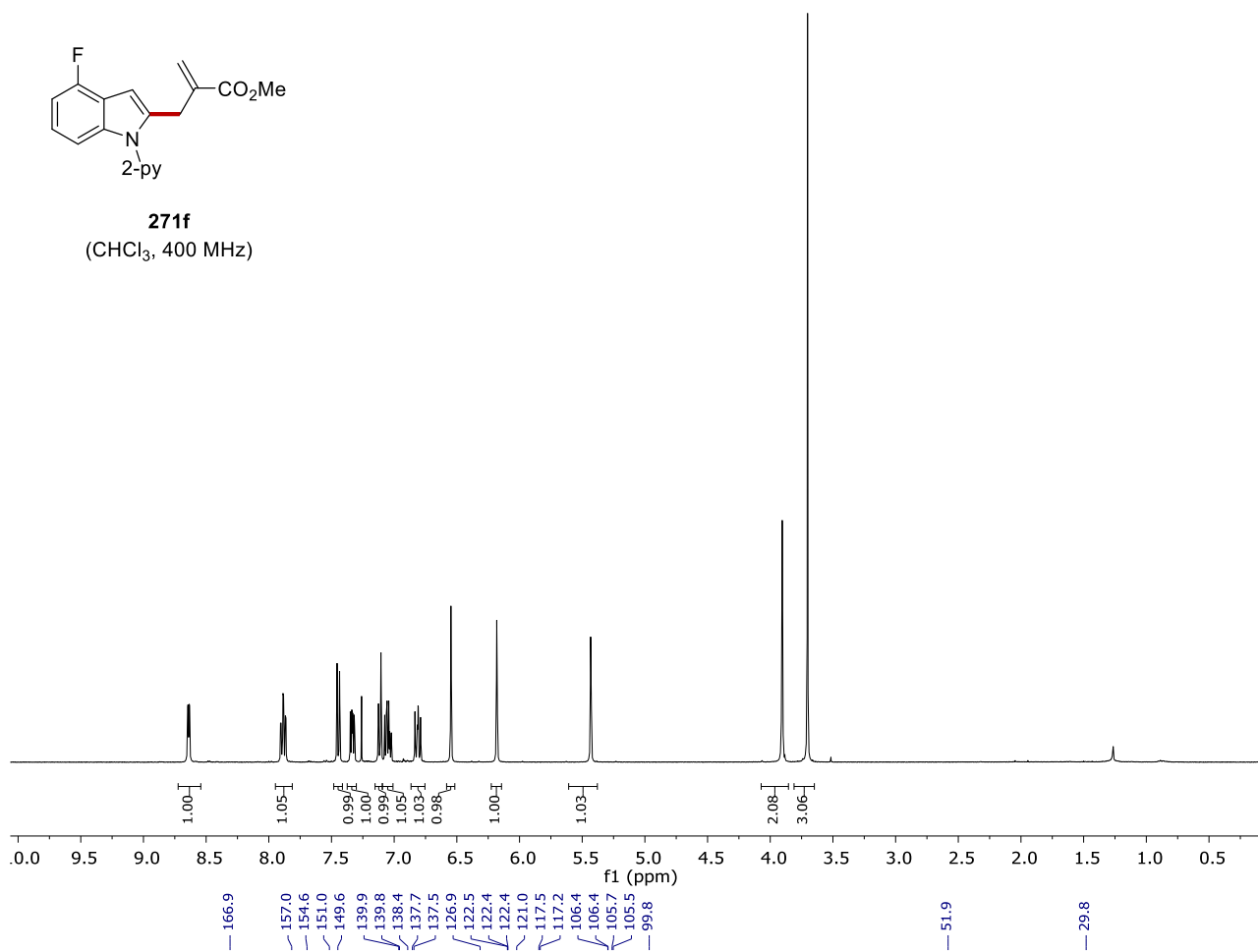


271e
(CHCl₃, 126 MHz)

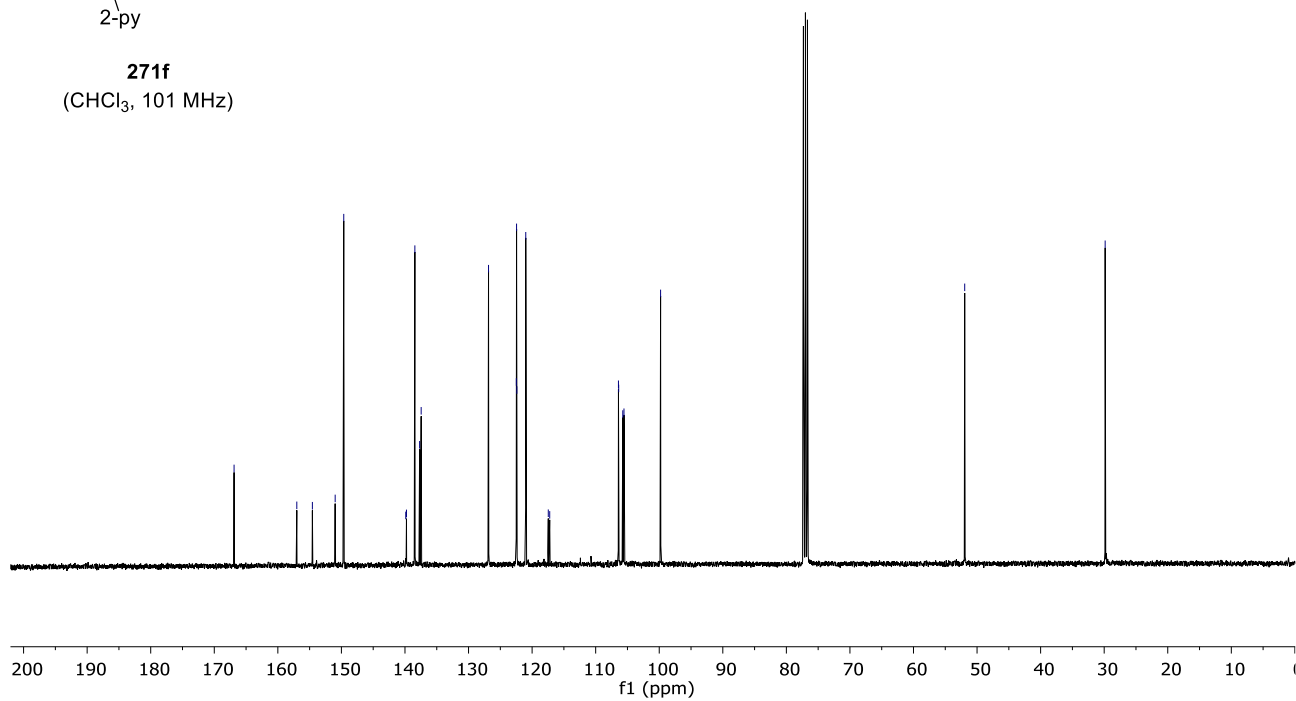




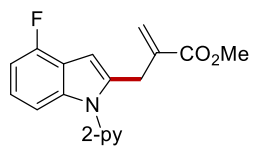
271f
(CHCl₃, 400 MHz)



271f
(CHCl₃, 101 MHz)



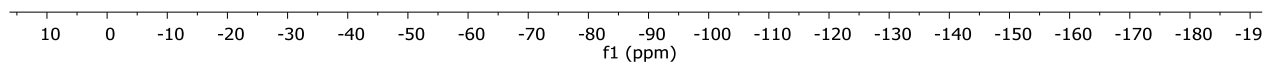
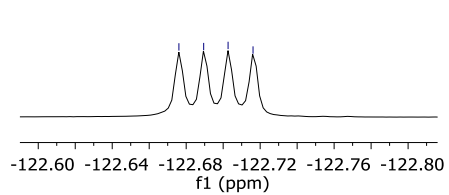
8. NMR Spectra



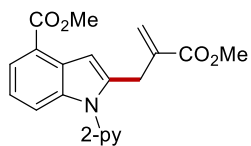
271f
(CHCl₃, 376 MHz)

-122.7
-122.7
-122.7

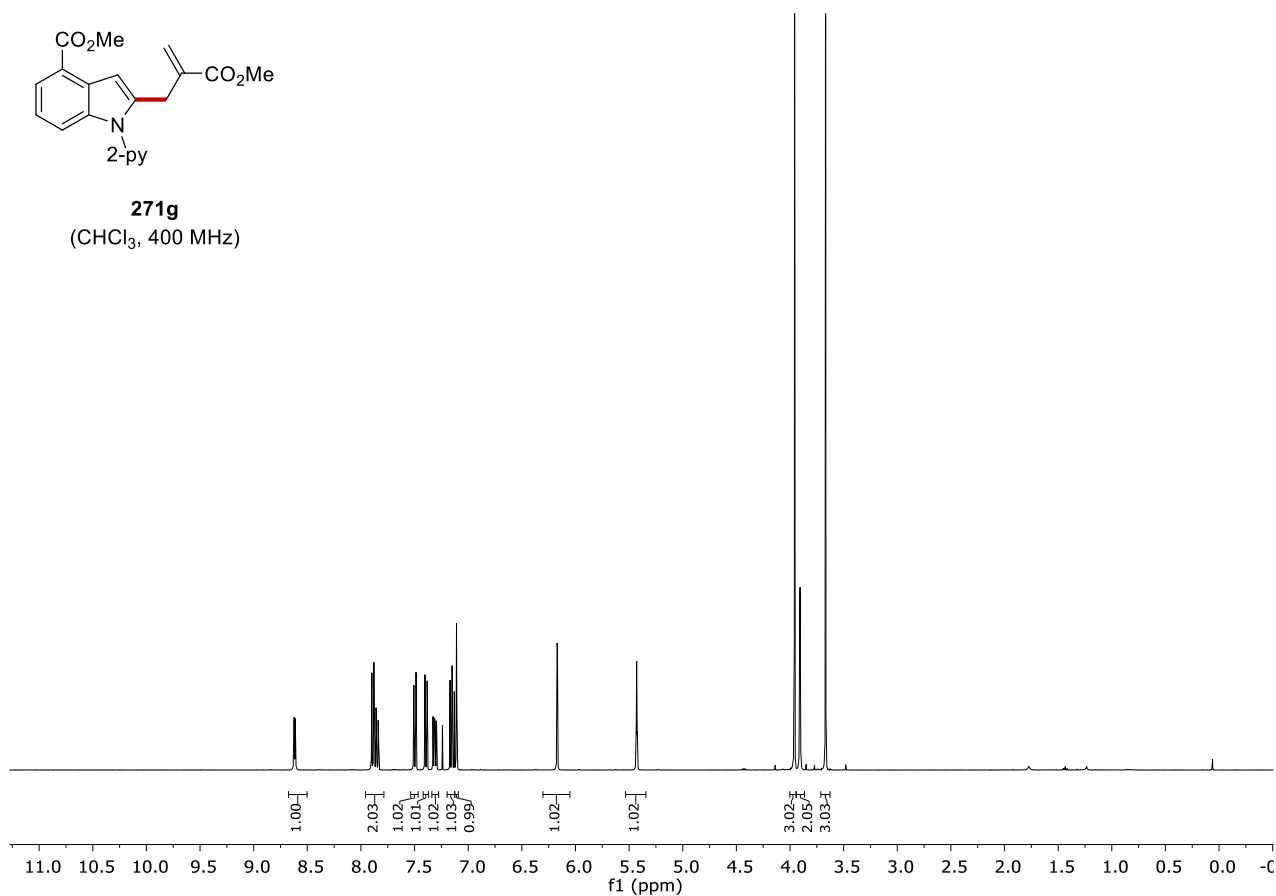
-122.7
-122.7
-122.7



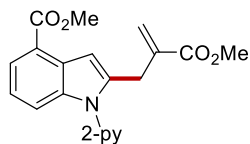
8. NMR Spectra



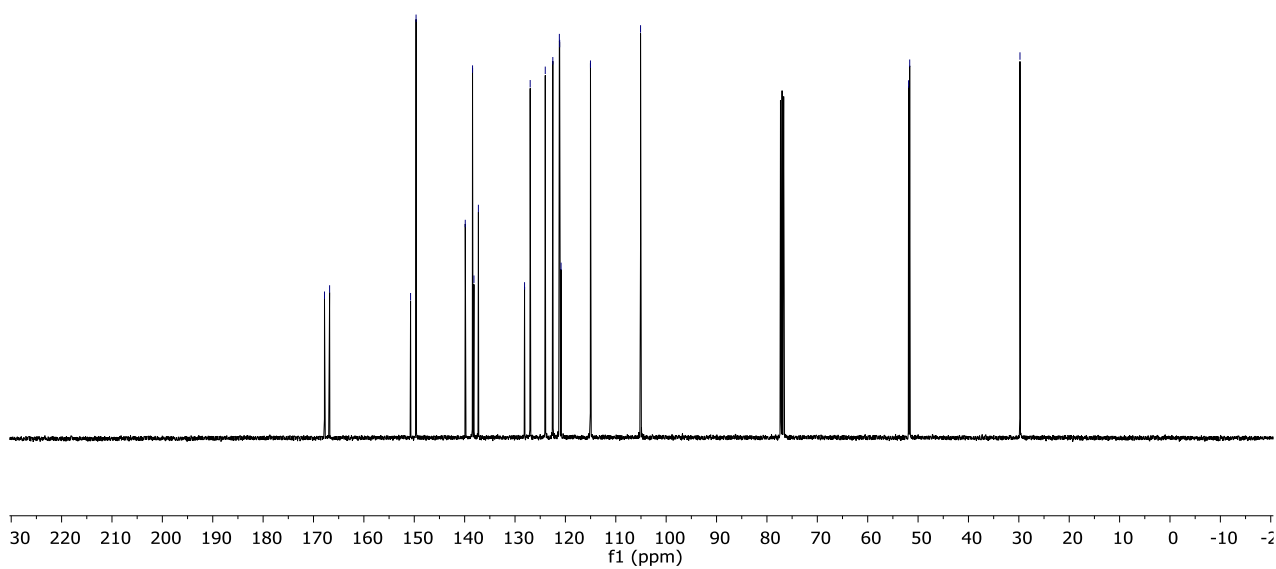
271g
(CHCl₃, 400 MHz)



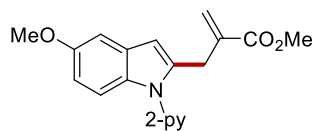
167.82
166.80
150.73
149.64
139.88
138.43
138.16
137.27
128.11
126.99
124.00
122.50
121.20
121.14
120.86
115.03
105.08
51.89
51.66
29.77



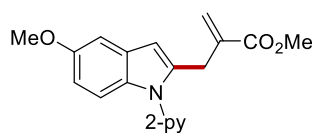
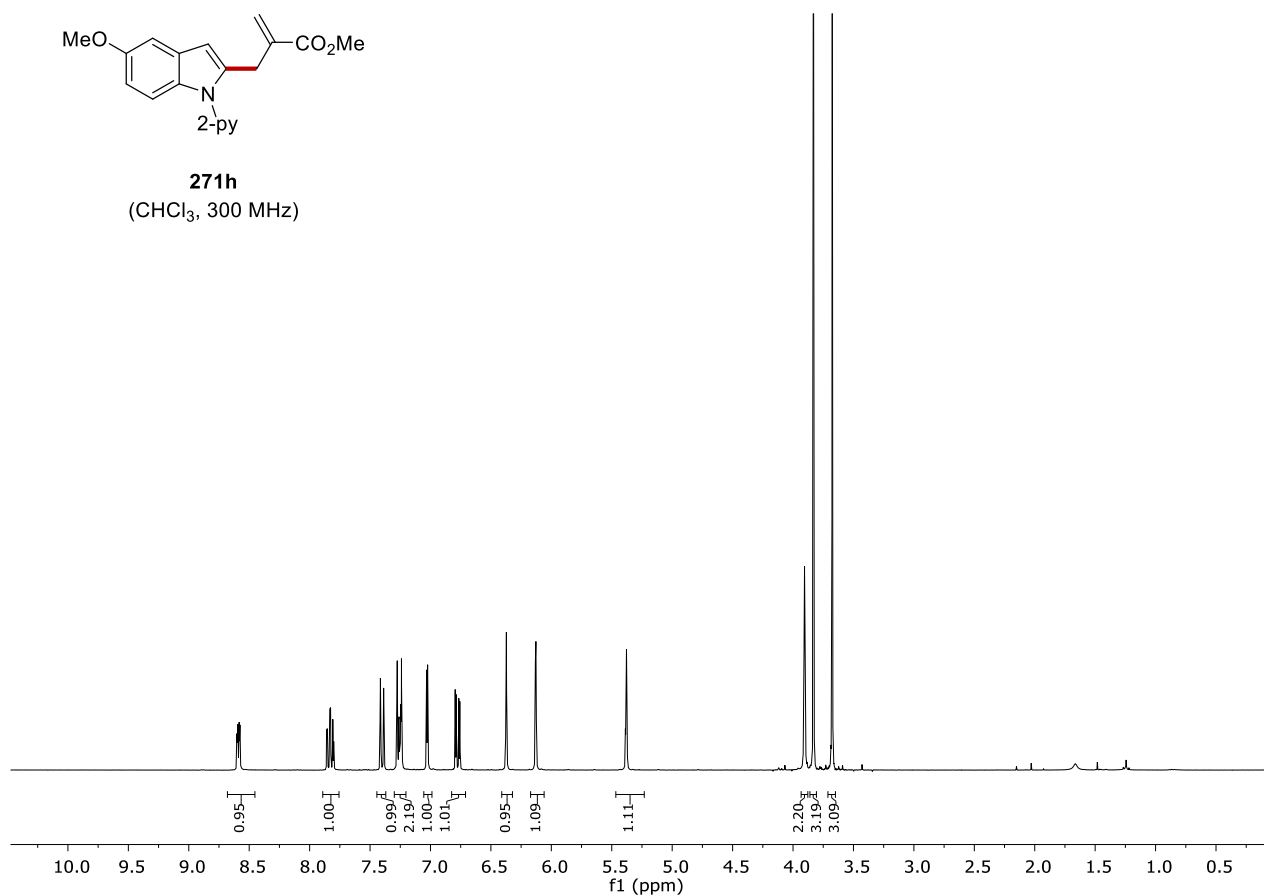
271g
(CHCl₃, 101 MHz)



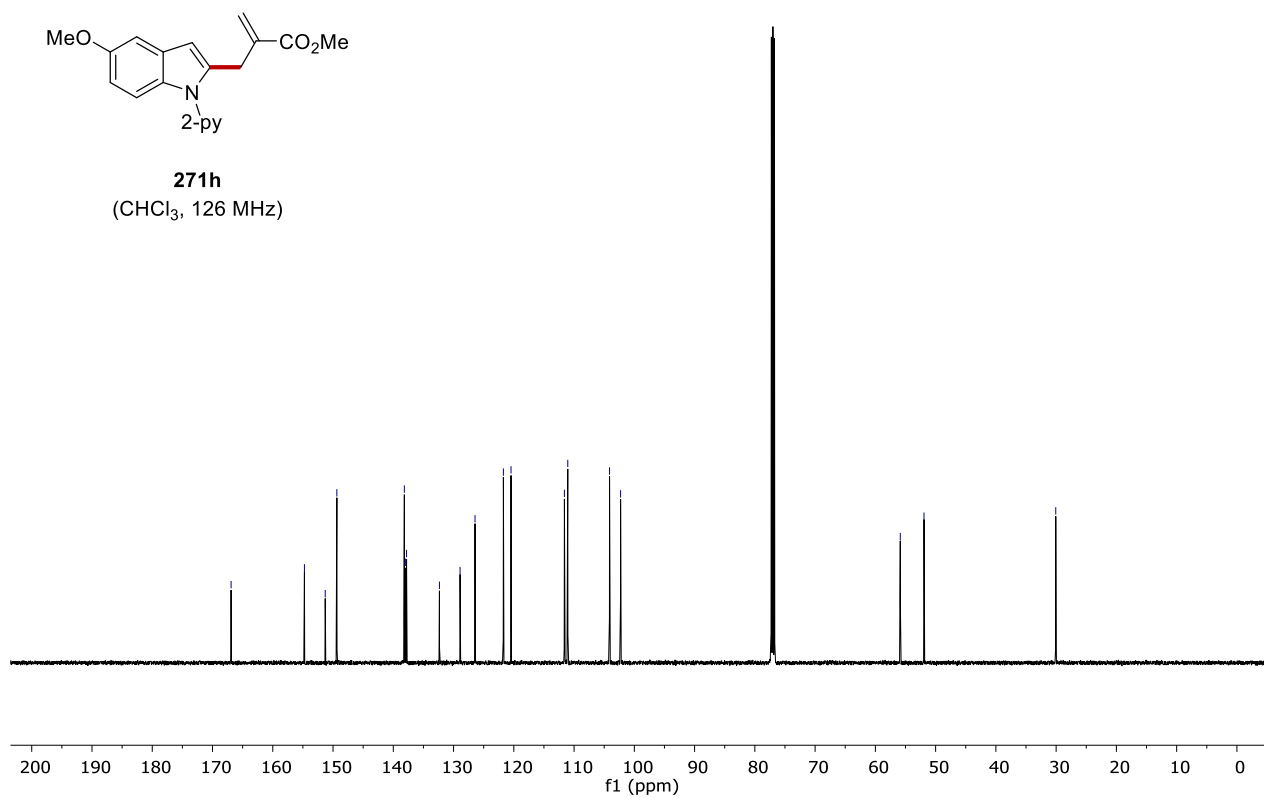
8. NMR Spectra

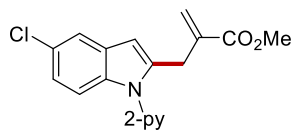


271h
(CHCl₃, 300 MHz)

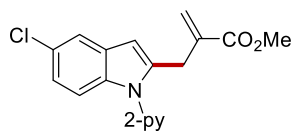
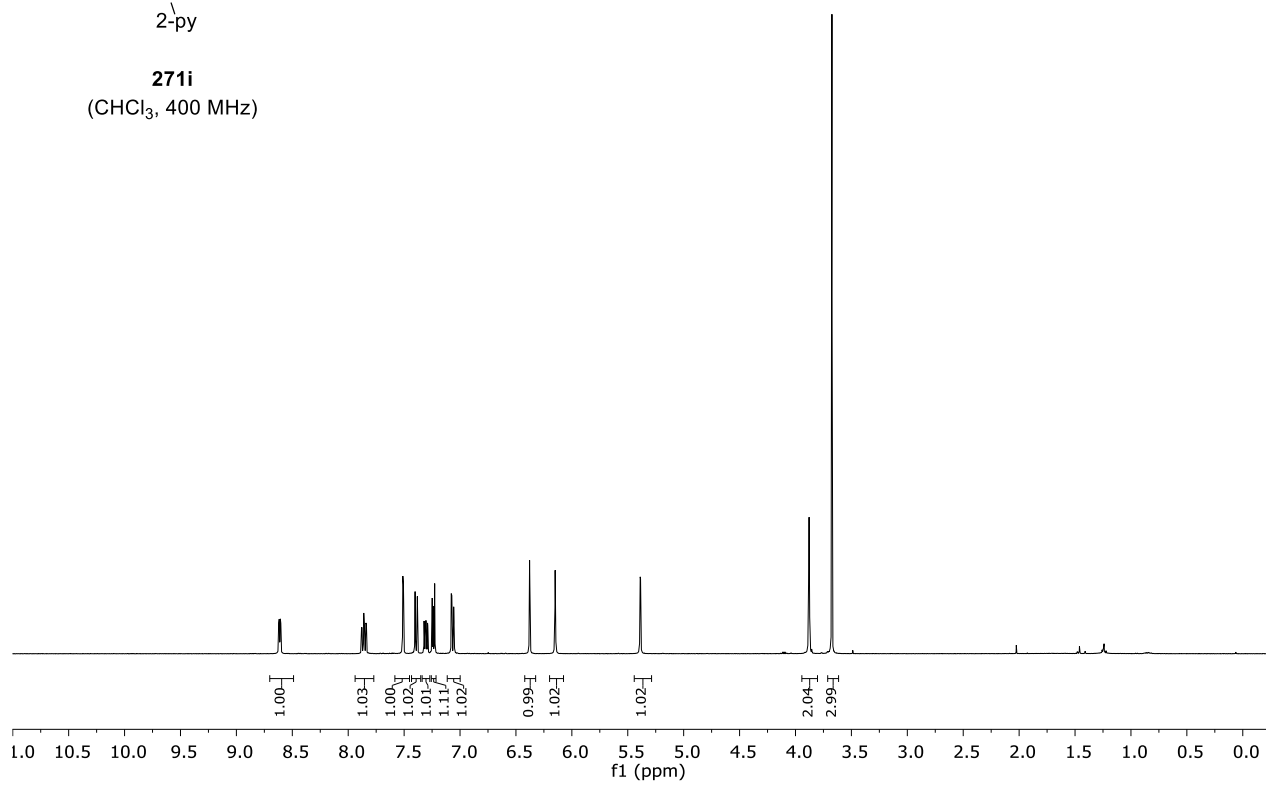


271h
(CHCl₃, 126 MHz)

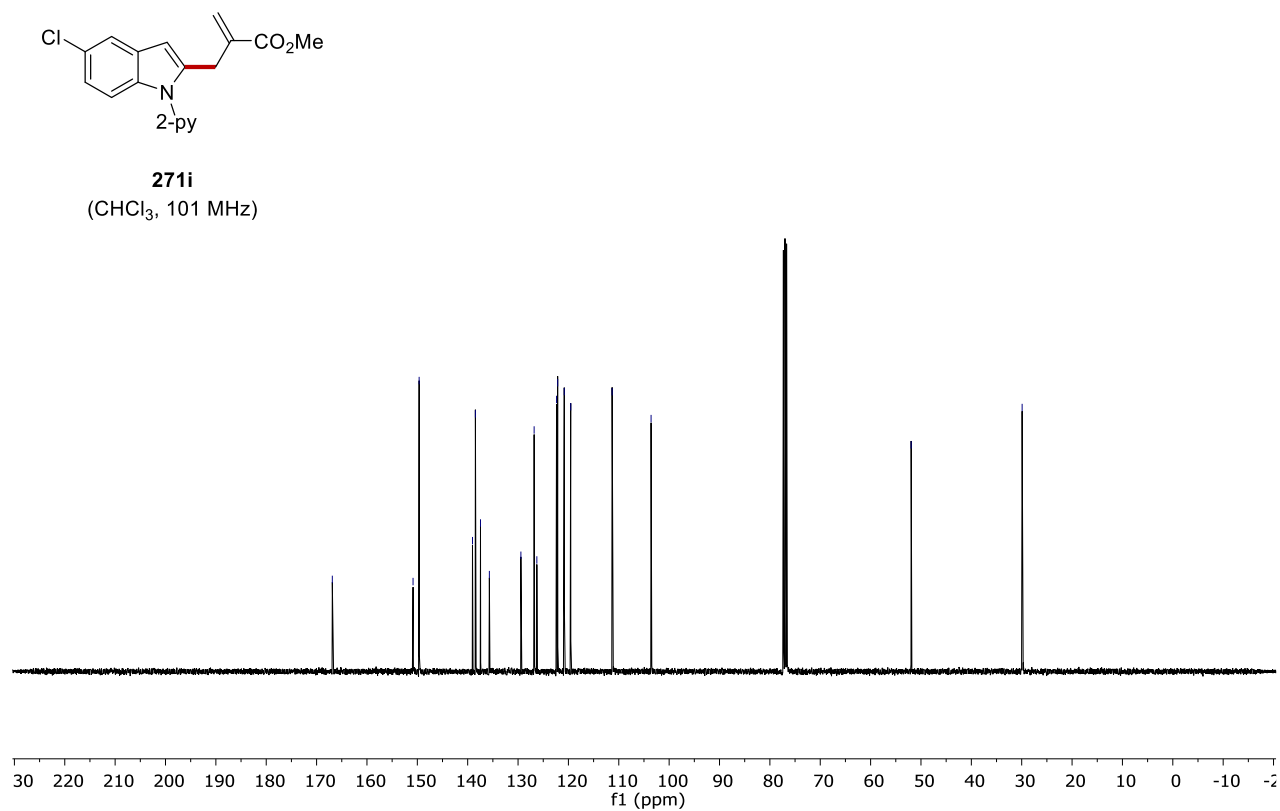




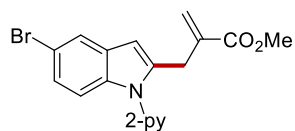
271i
(CHCl₃, 400 MHz)



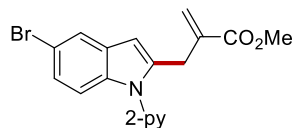
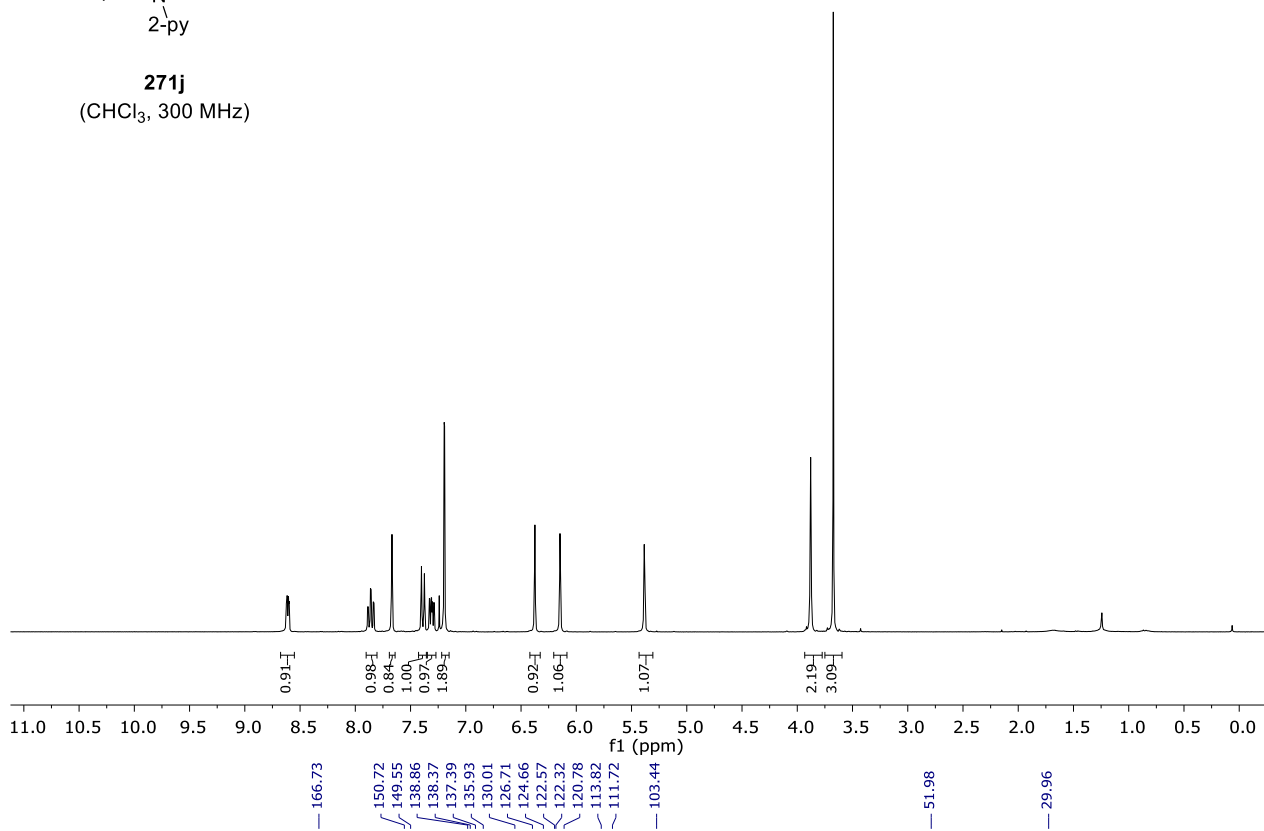
271i
(CHCl₃, 101 MHz)



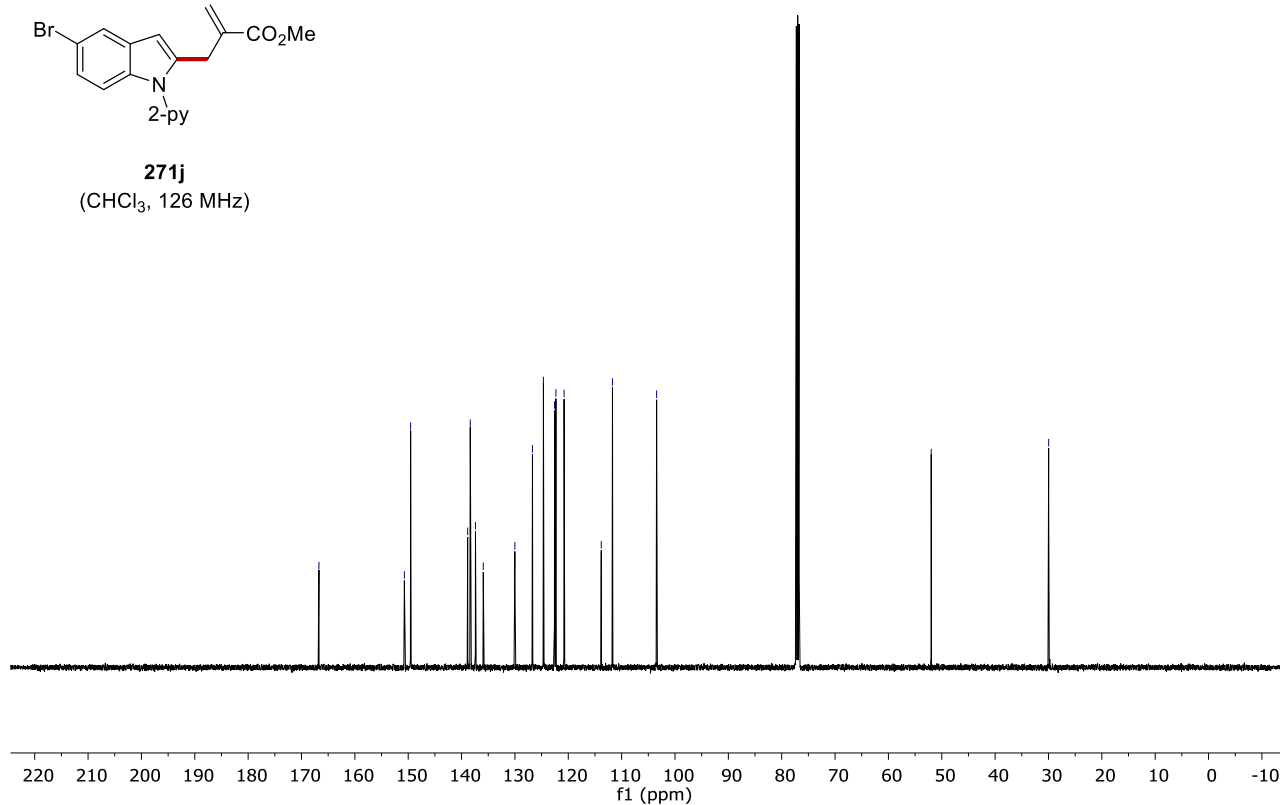
8. NMR Spectra

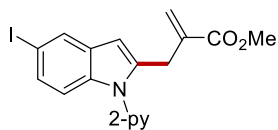


271j
(CHCl₃, 300 MHz)

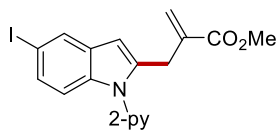
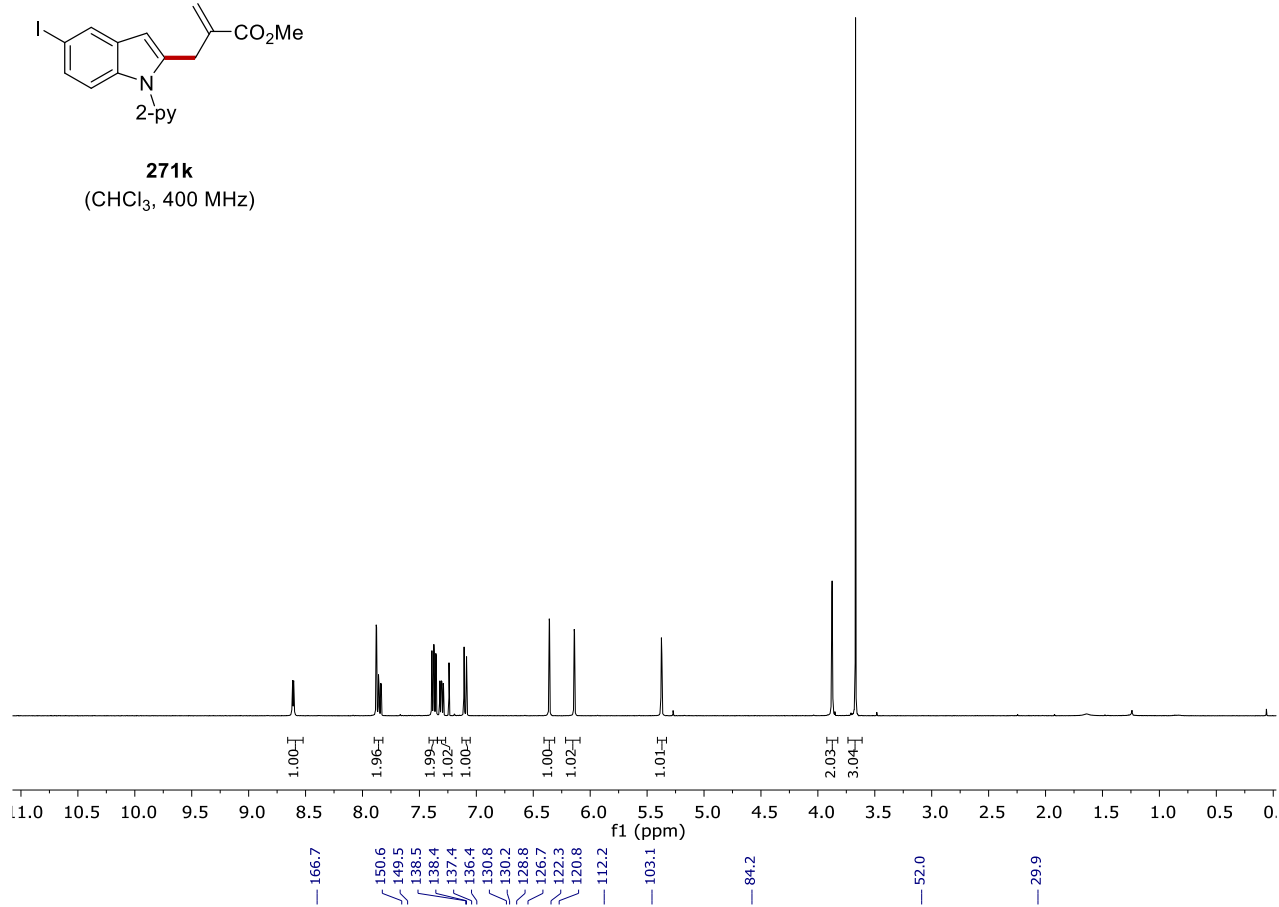


271j
(CHCl₃, 126 MHz)

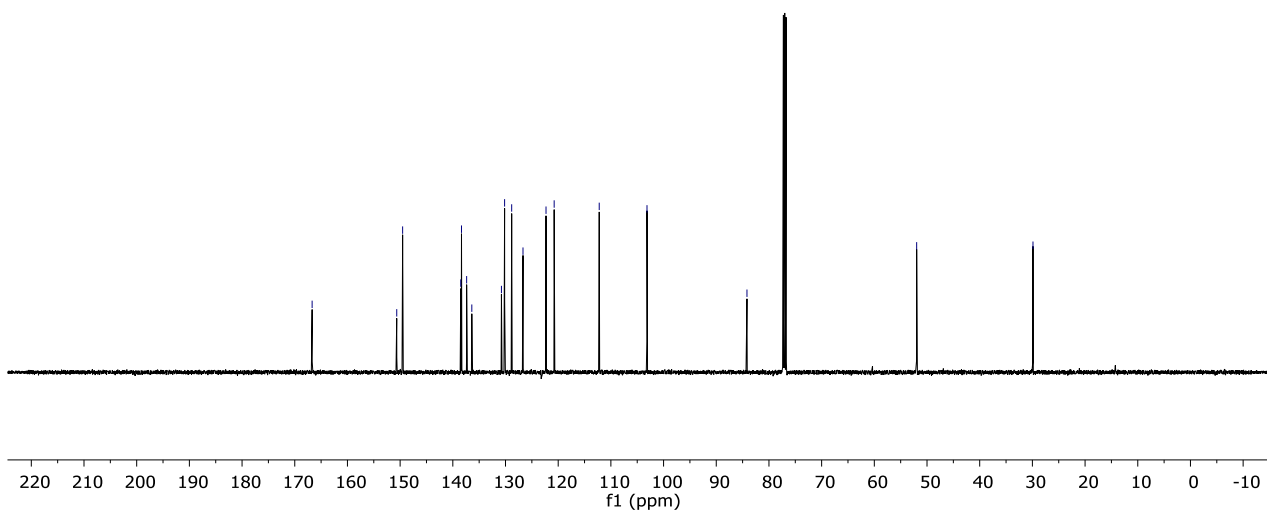




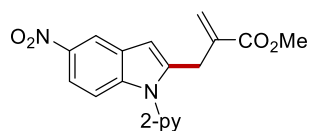
271k
(CHCl₃, 400 MHz)



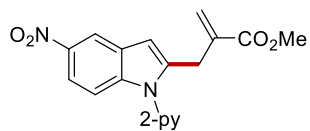
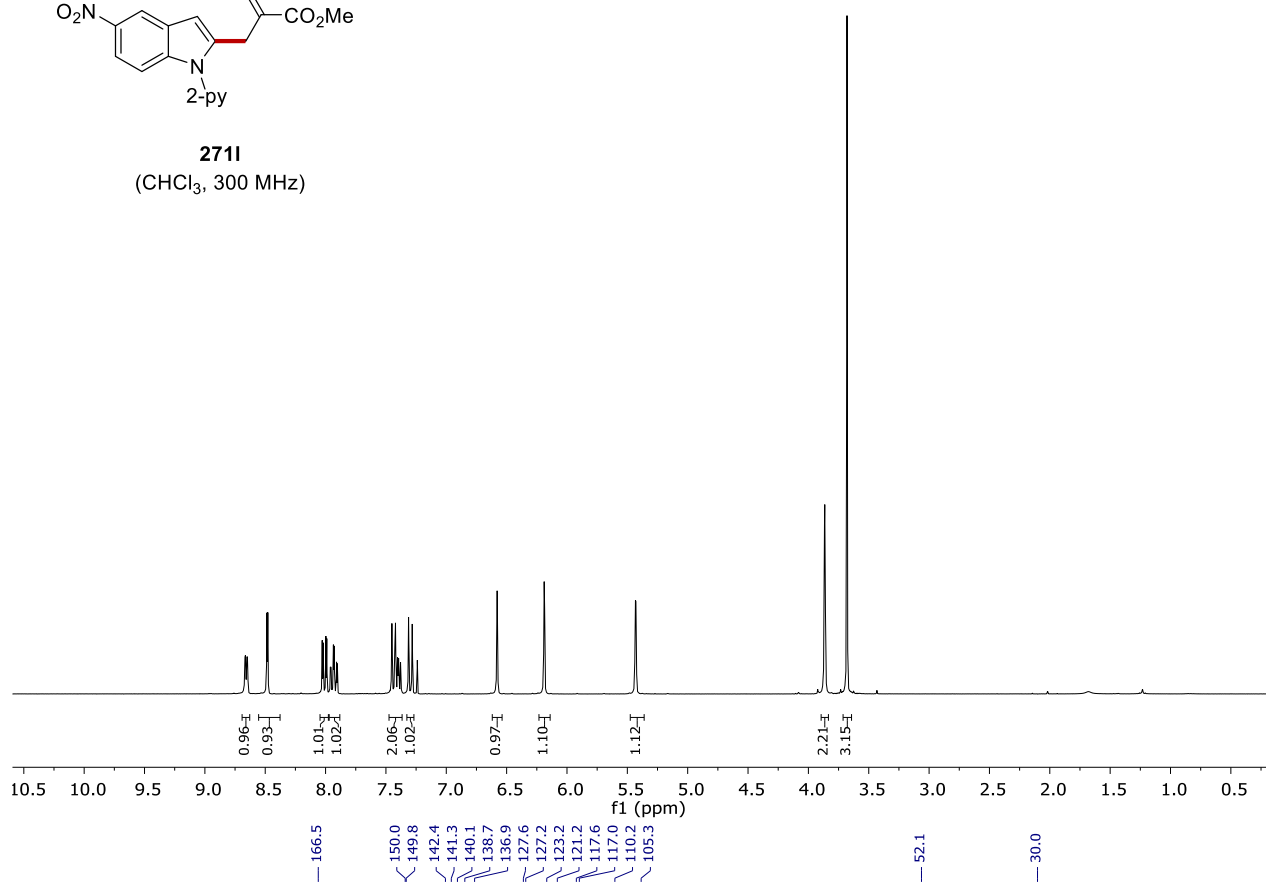
271k
(CHCl₃, 126 MHz)



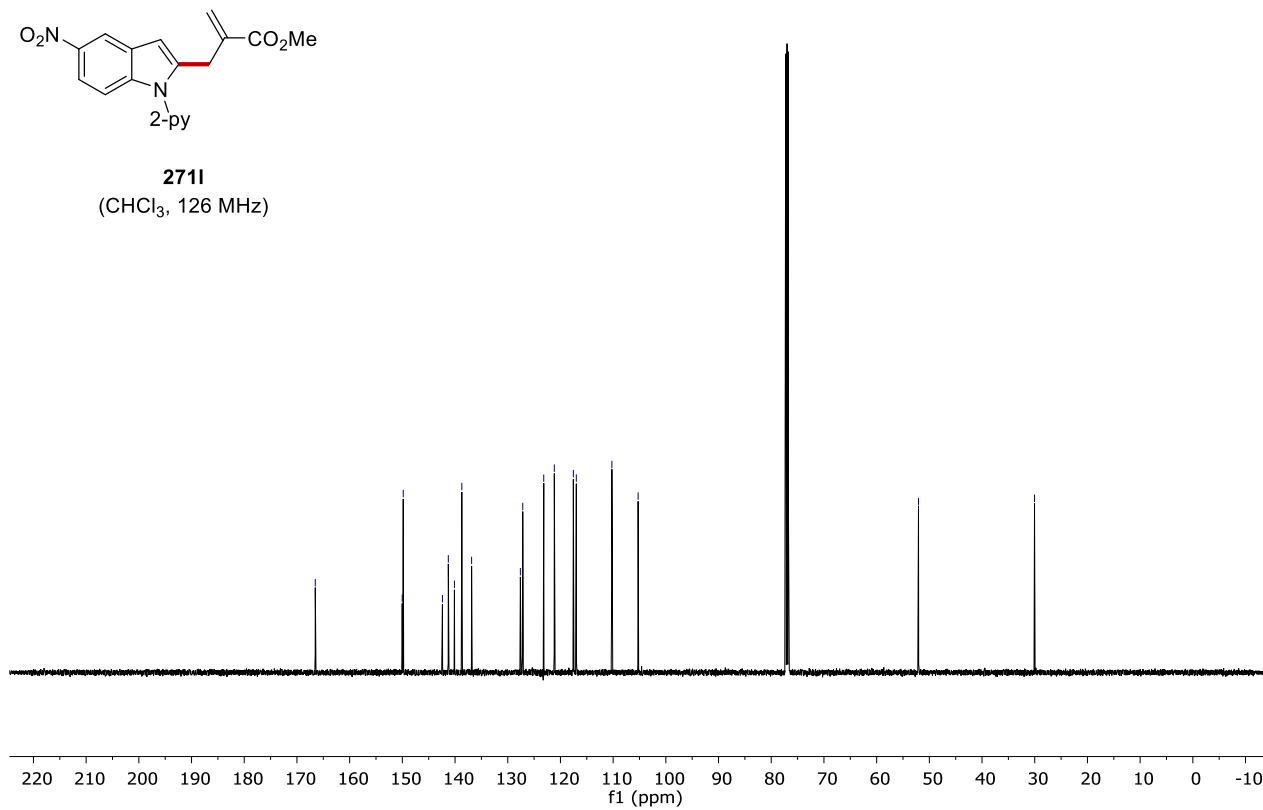
8. NMR Spectra

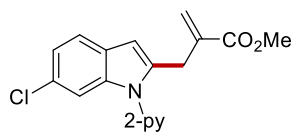


2711
(CHCl₃, 300 MHz)

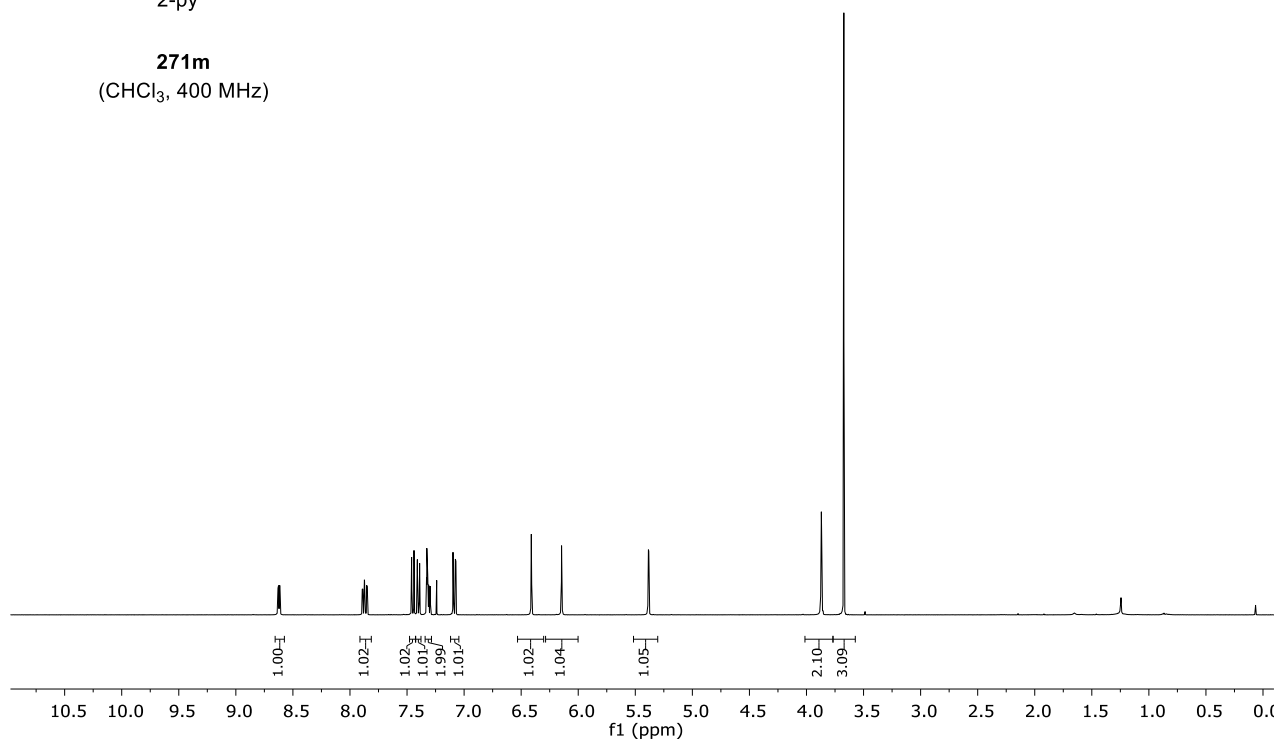


2711
(CHCl₃, 126 MHz)

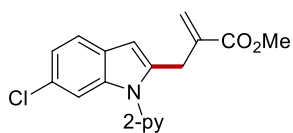




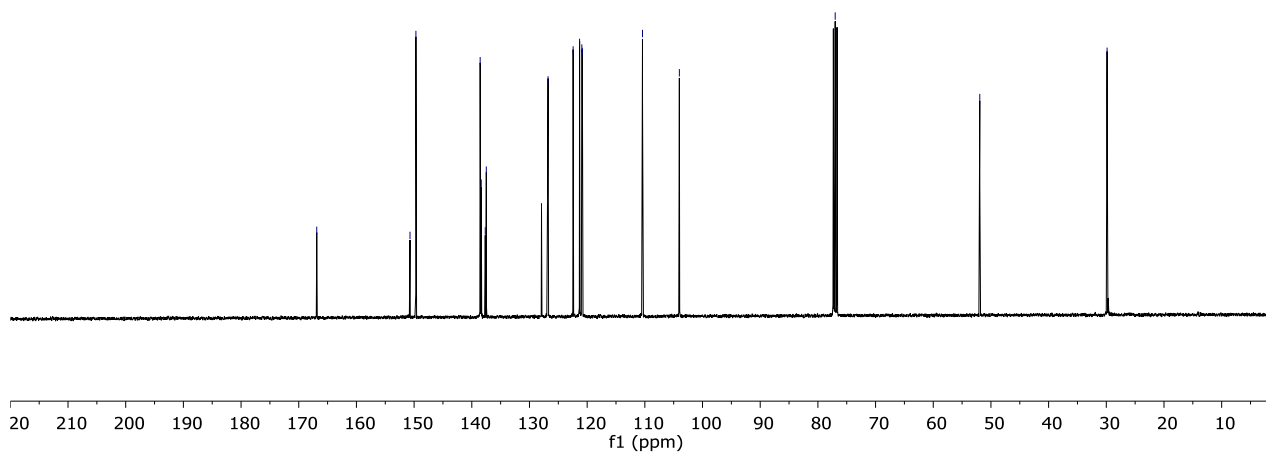
271m
(CHCl₃, 400 MHz)



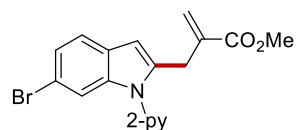
166.88
150.71
149.69
138.55
138.36
137.67
137.49
127.92
126.88
126.78
122.43
121.31
120.92
120.84
110.41
104.02
77.00
51.93
29.86



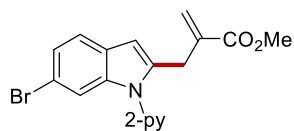
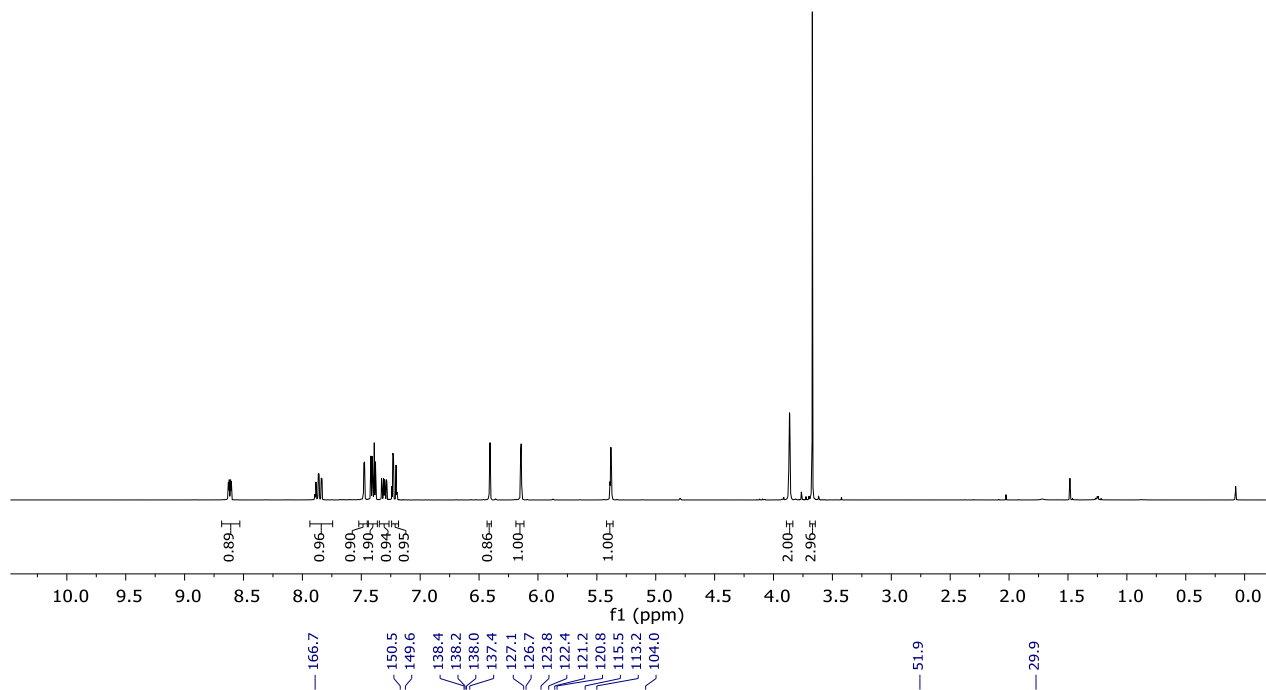
271m
(CHCl₃, 101 MHz)



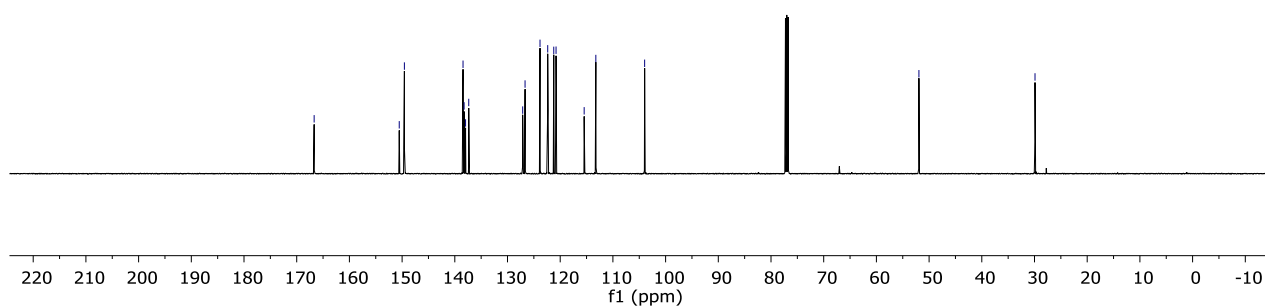
8. NMR Spectra

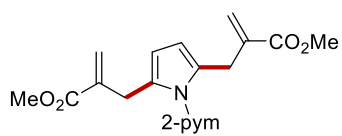


271n
(CHCl₃, 300 MHz)

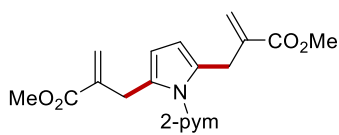
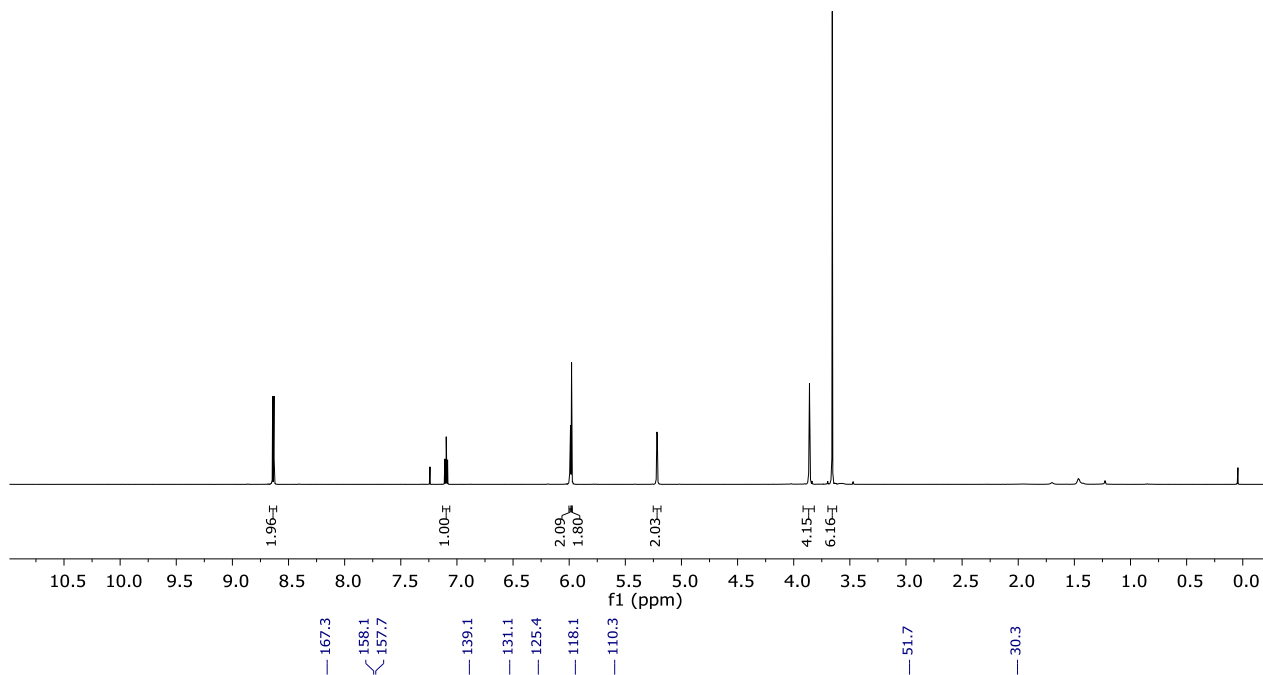


271n
(CHCl₃, 126 MHz)

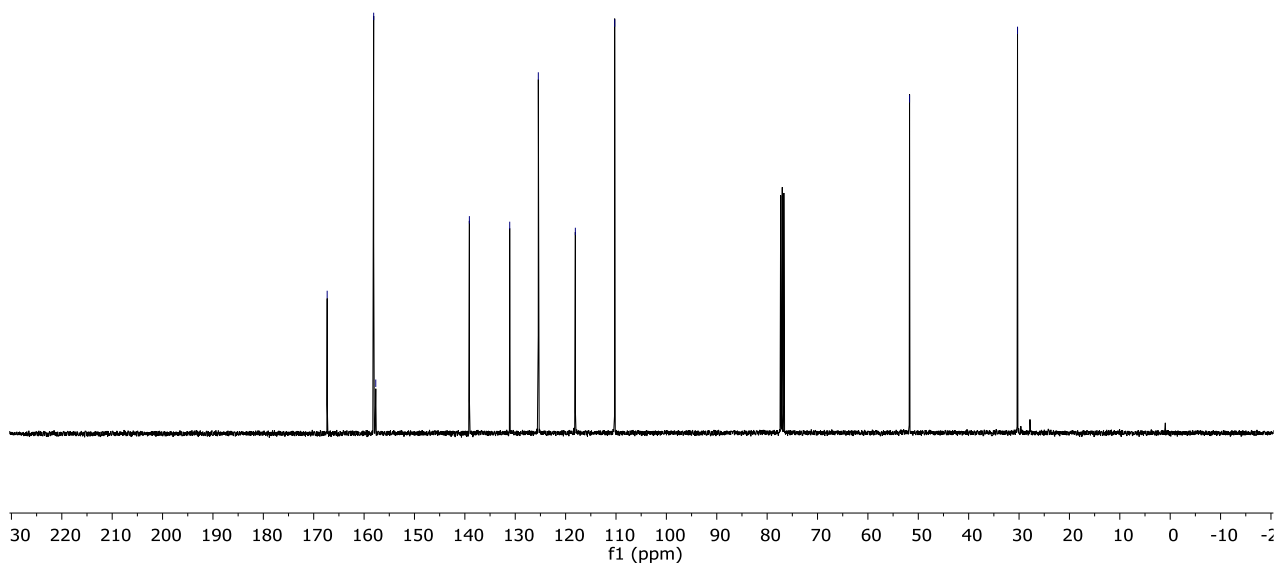




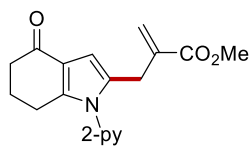
271o
(CHCl₃, 400 MHz)



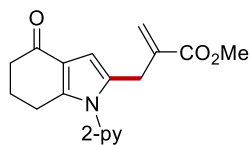
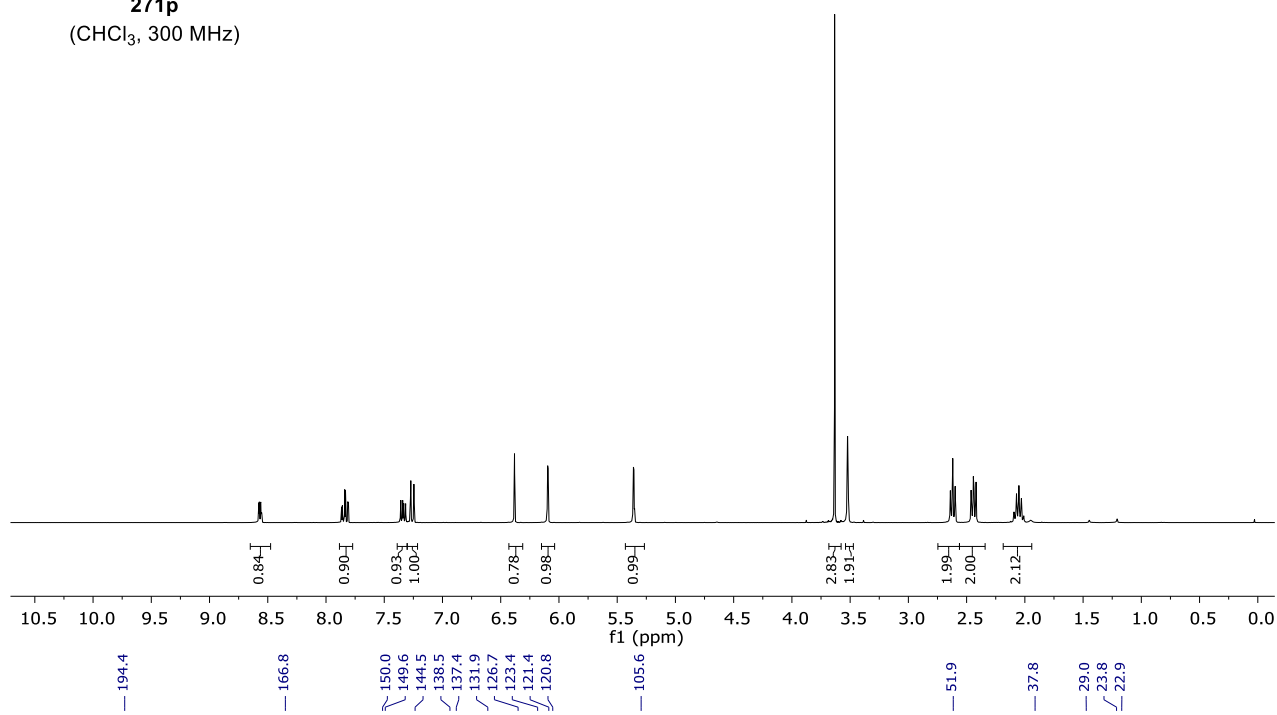
271o
(CHCl₃, 101 MHz)



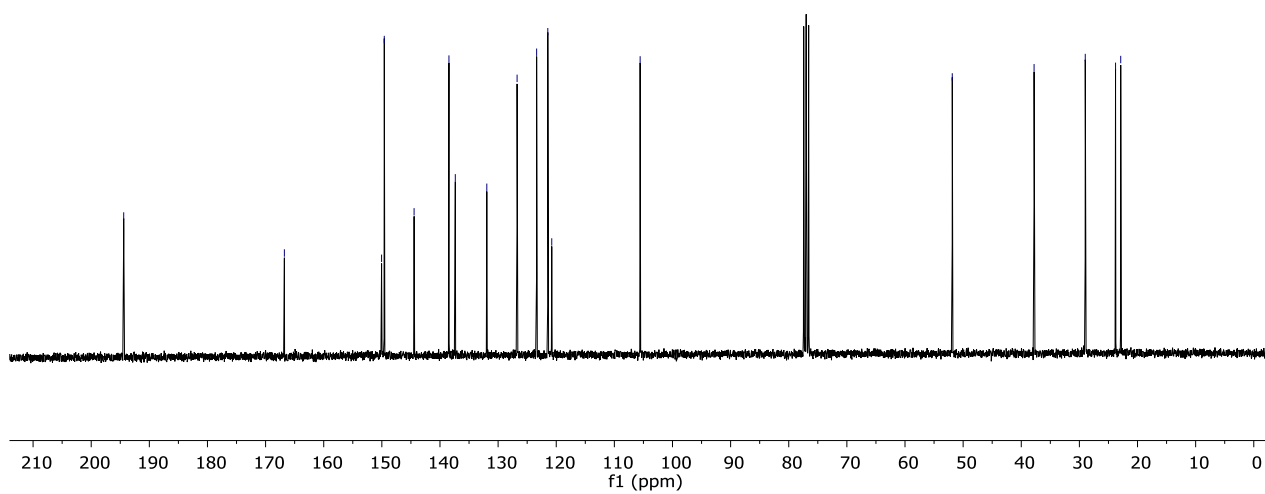
8. NMR Spectra

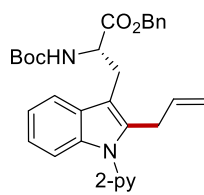


271p
(CHCl₃, 300 MHz)

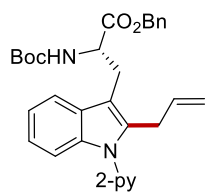
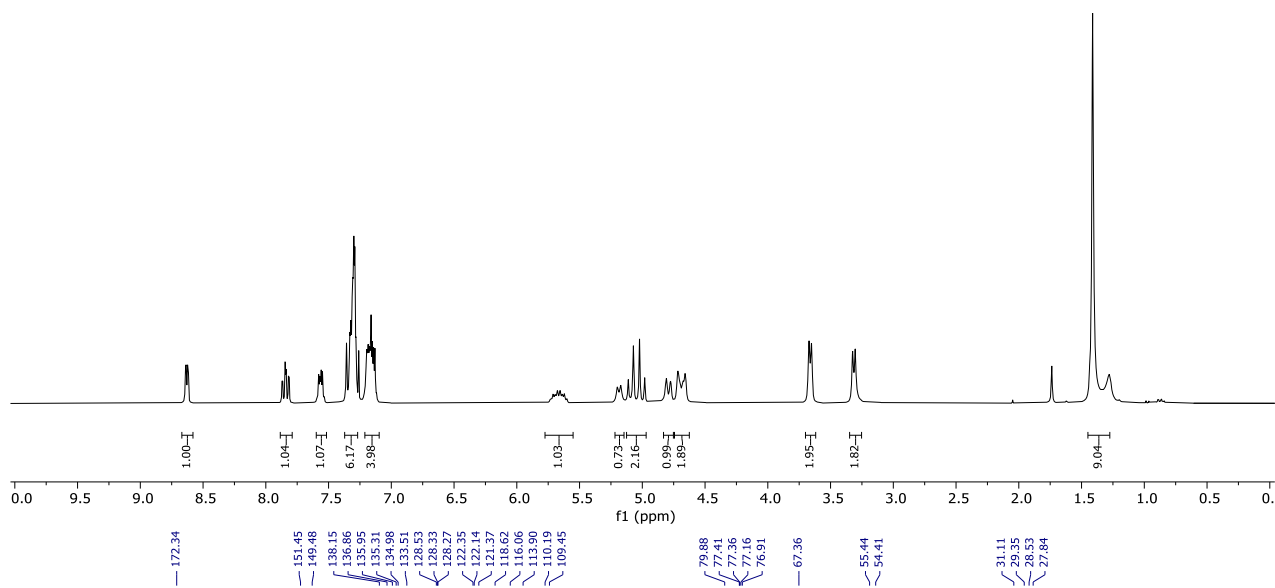


271p
(CHCl₃, 75 MHz)

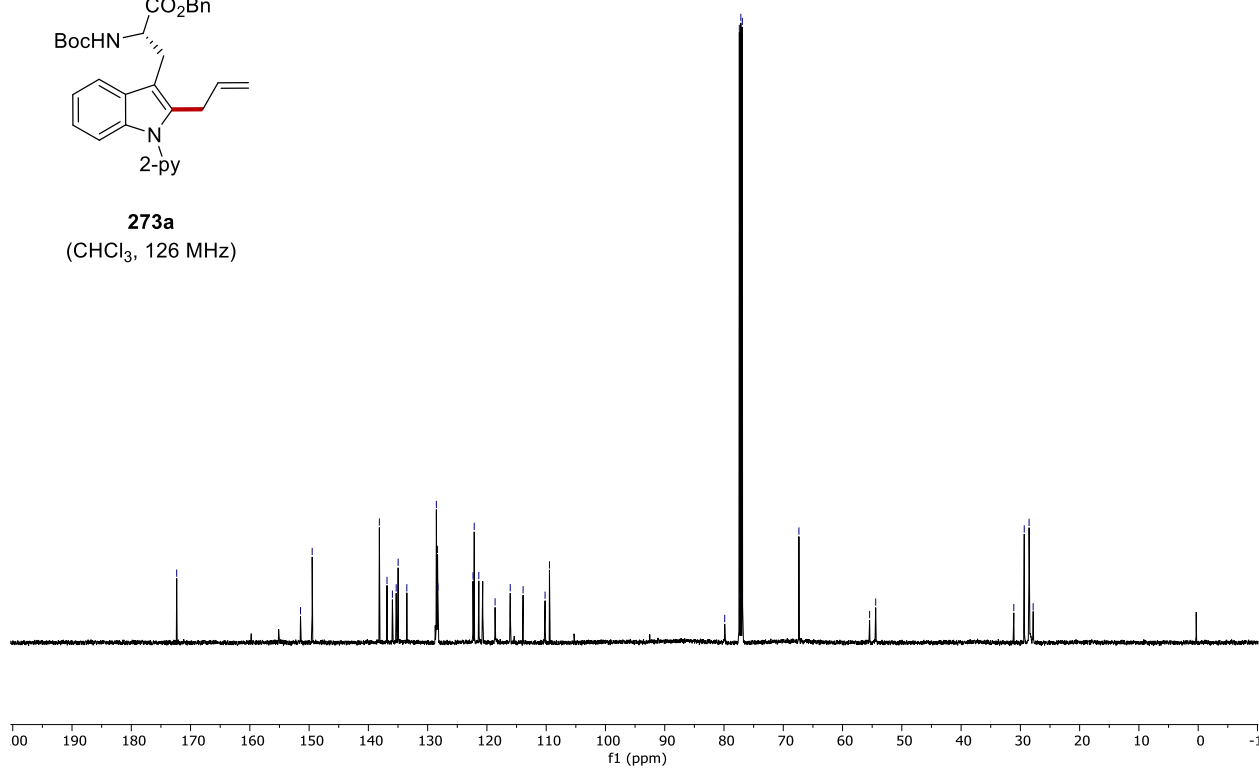




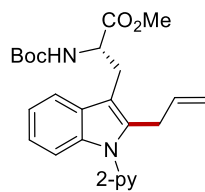
273a
(CHCl₃, 300 MHz)



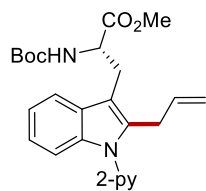
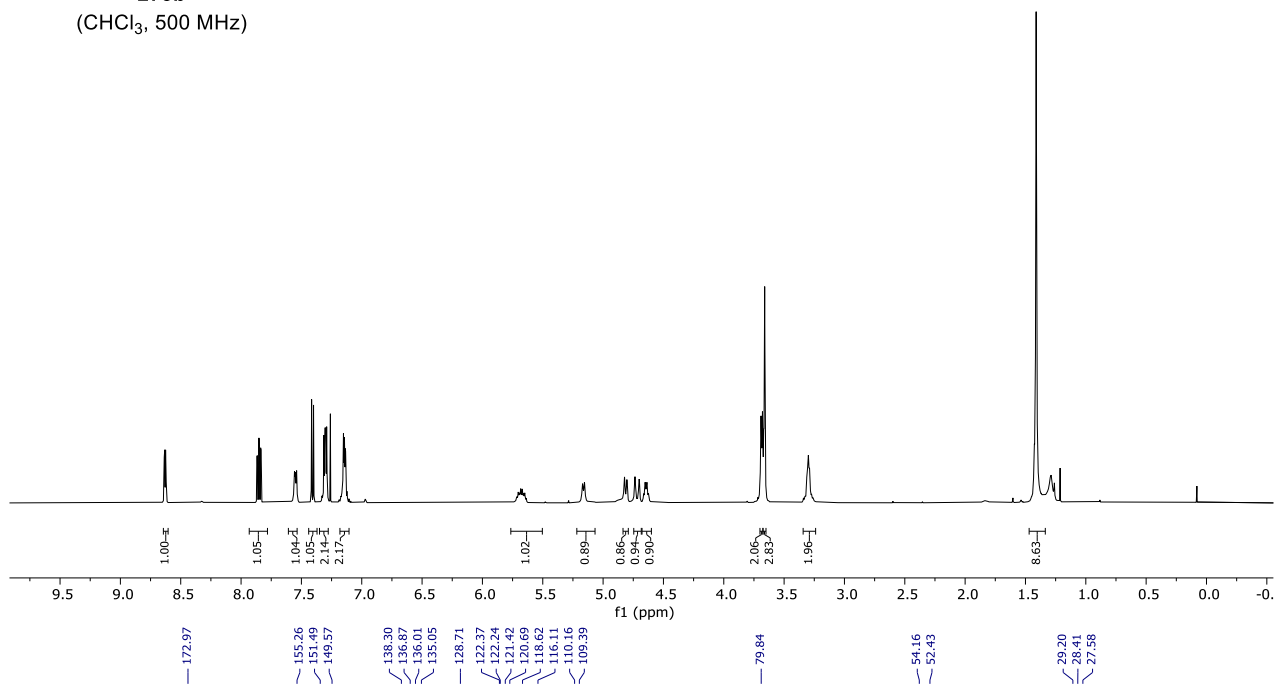
273a
(CHCl₃, 126 MHz)



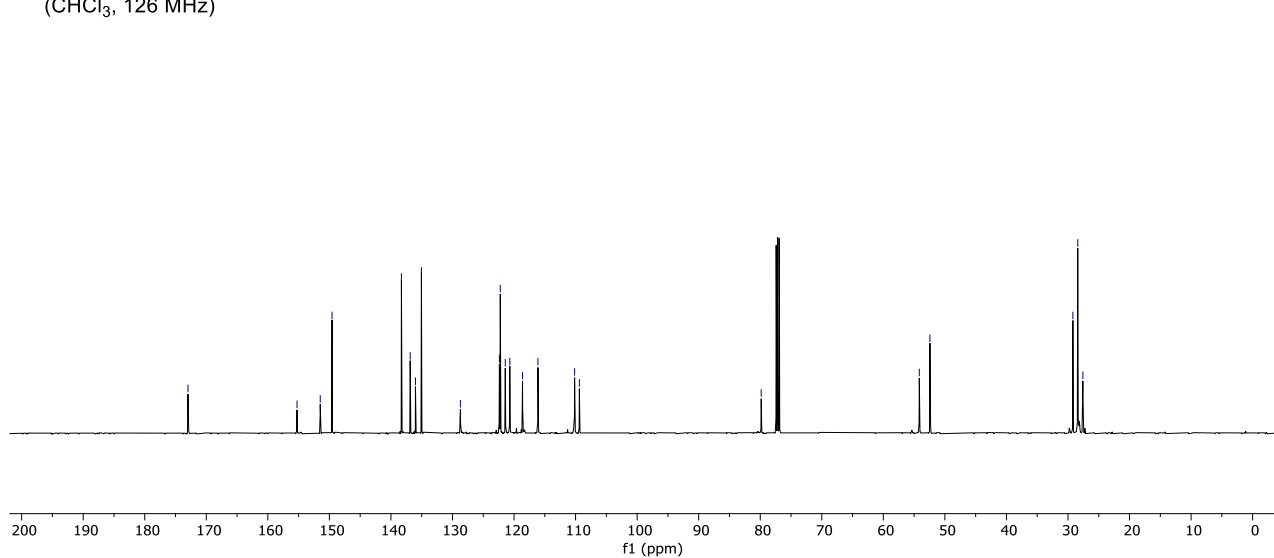
8. NMR Spectra



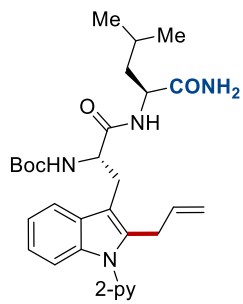
273b
(CHCl₃, 500 MHz)



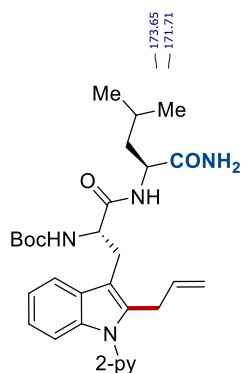
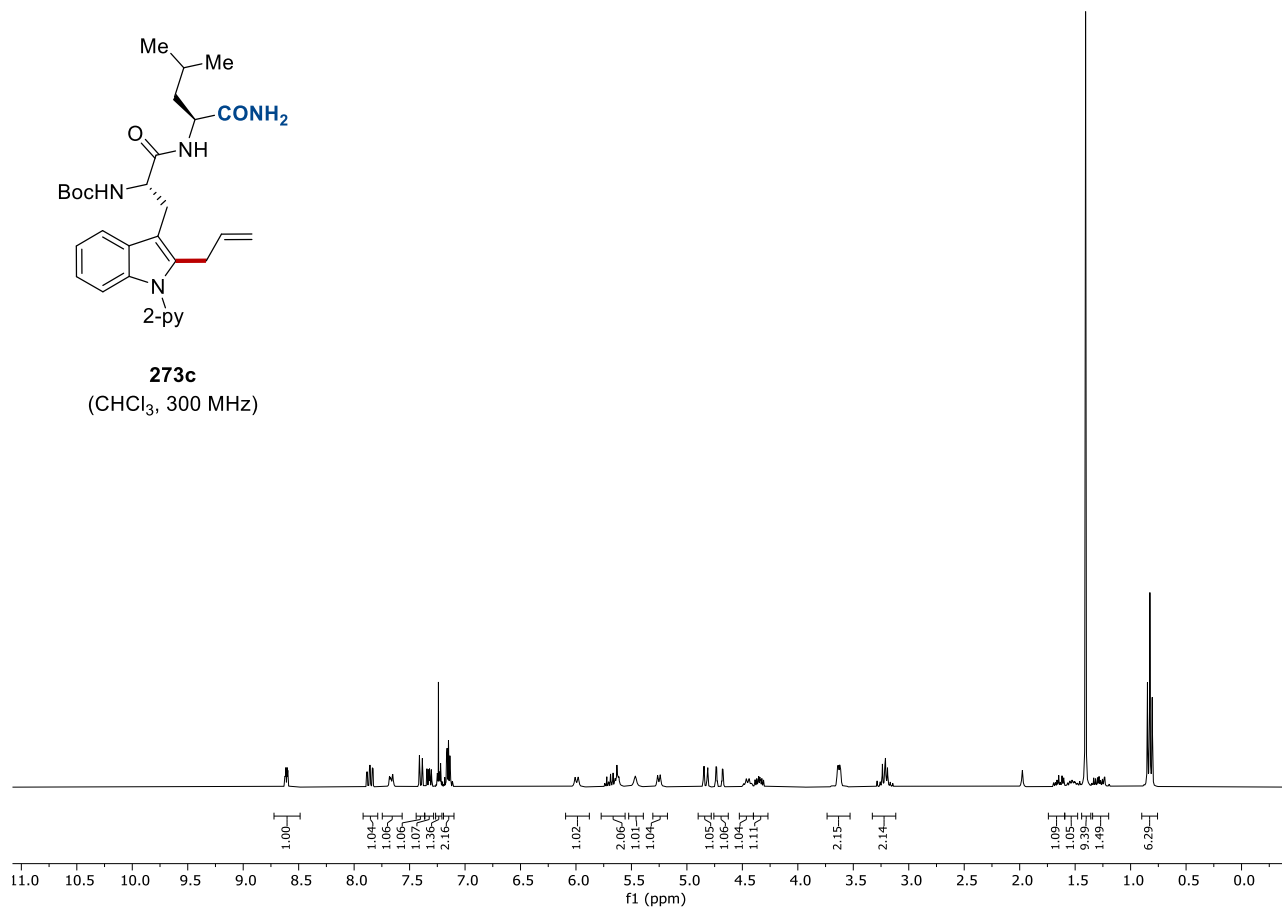
273b
(CHCl₃, 126 MHz)



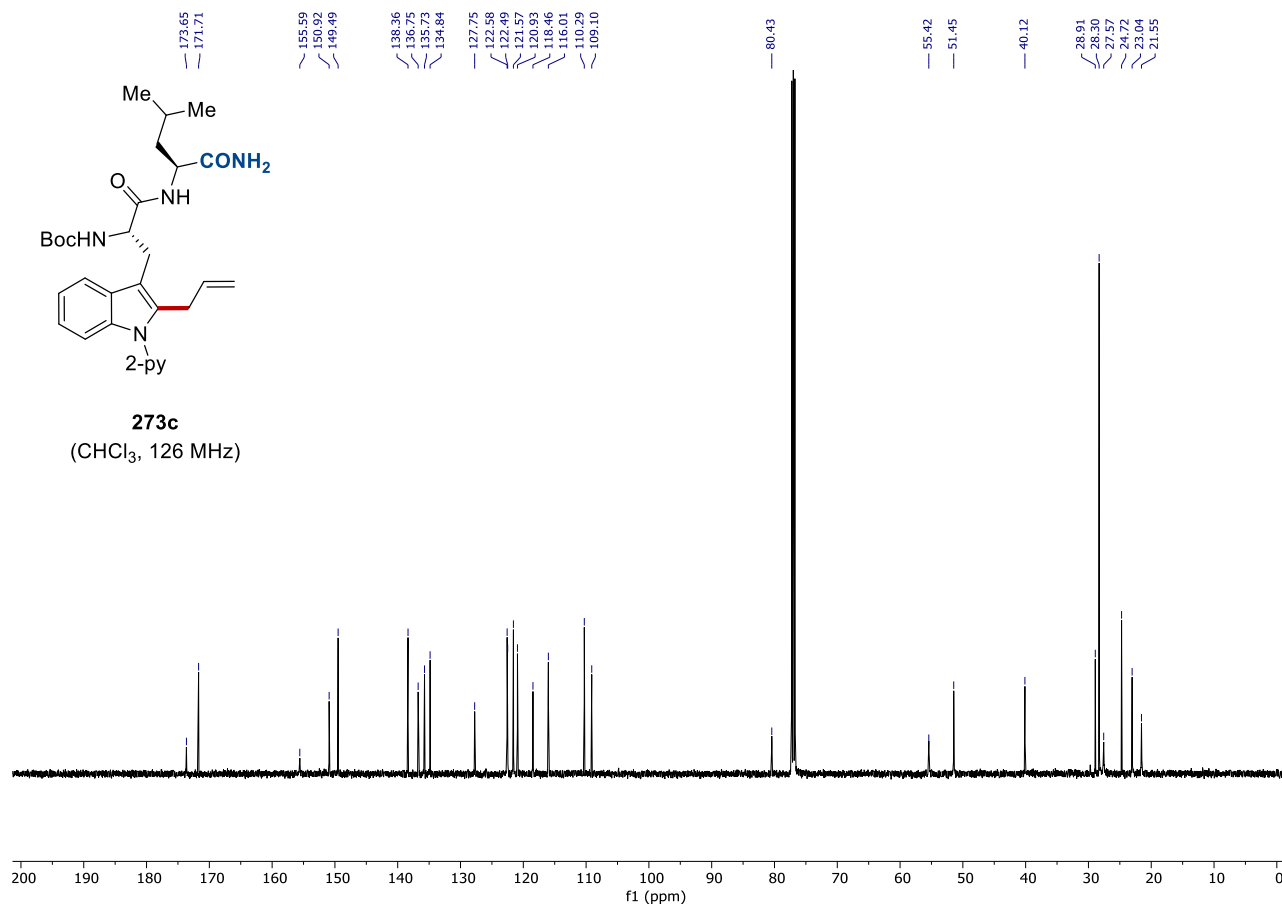
8. NMR Spectra



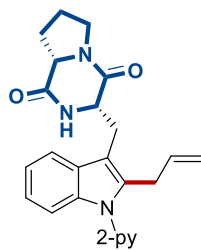
273c
(CHCl₃, 300 MHz)



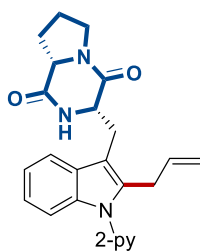
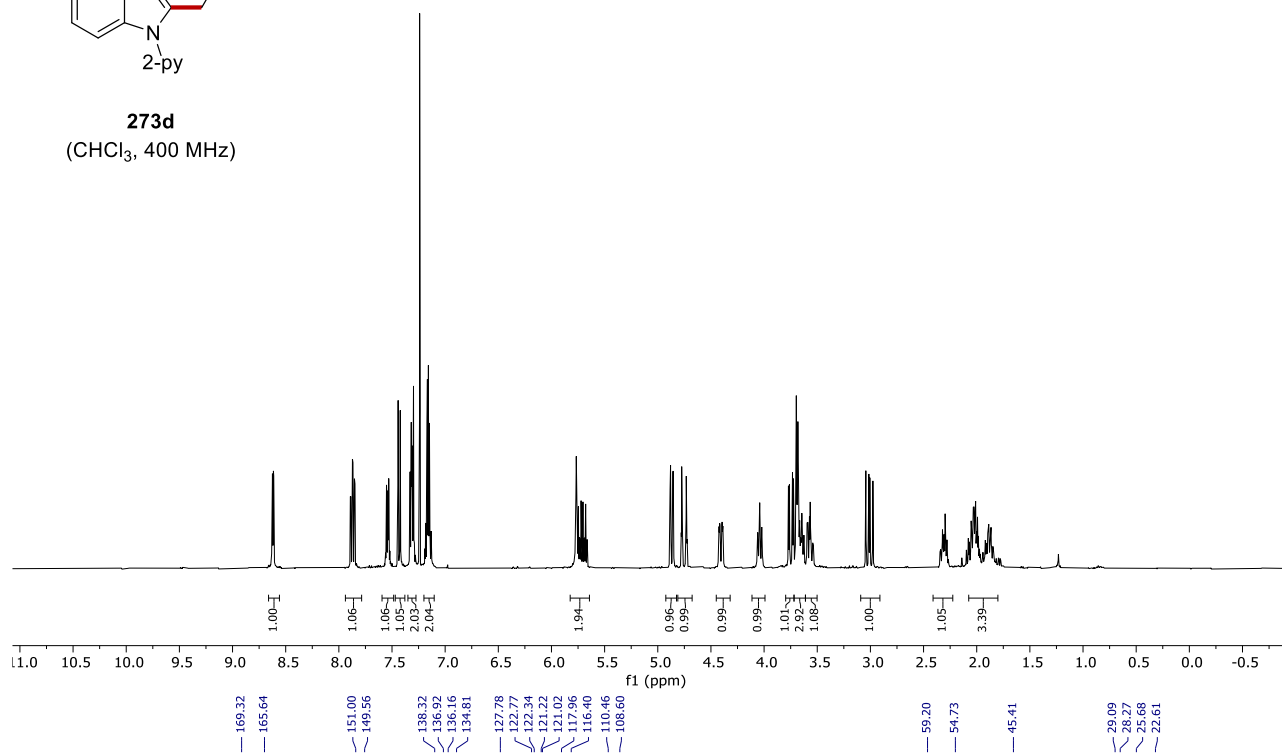
273c
(CHCl₃, 126 MHz)



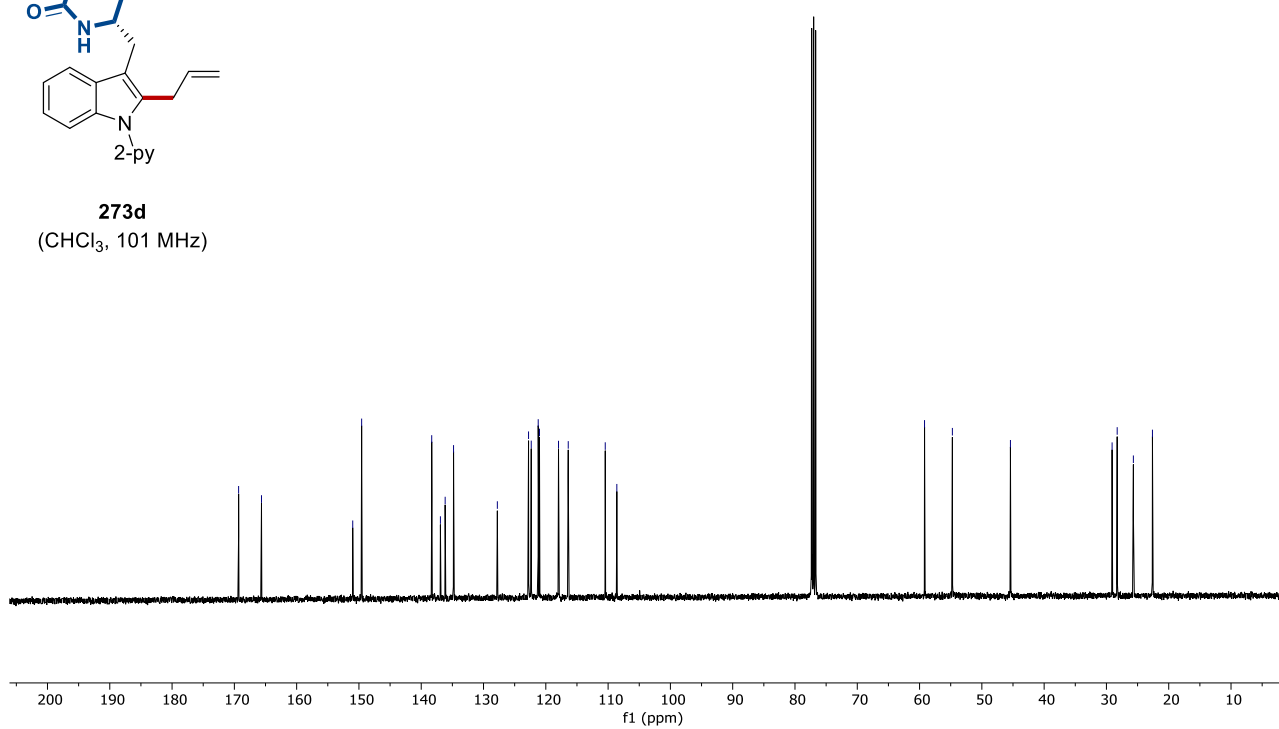
8. NMR Spectra

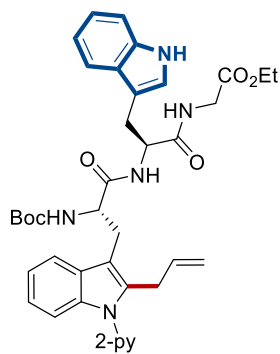


273d
(CHCl₃, 400 MHz)

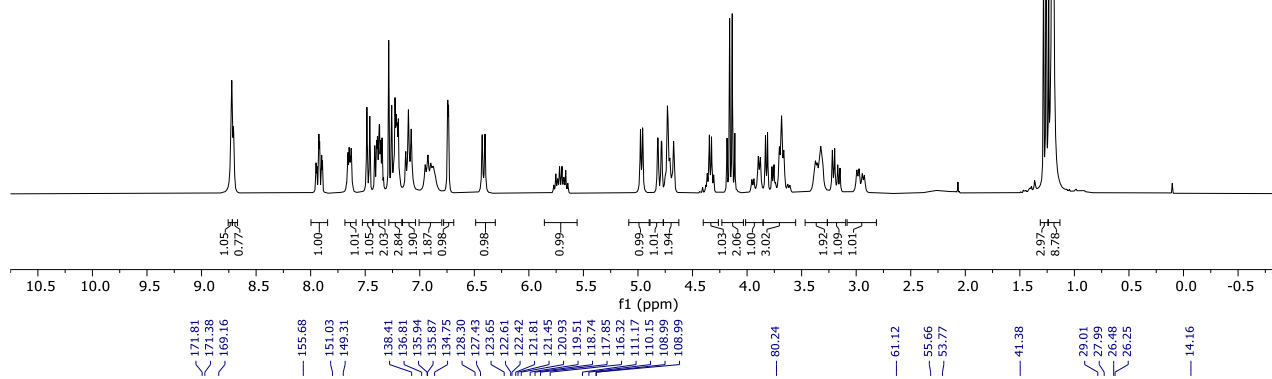


273d
(CHCl₃, 101 MHz)



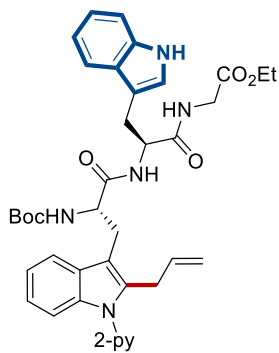


XX
(CHCl₃, 300 MHz)

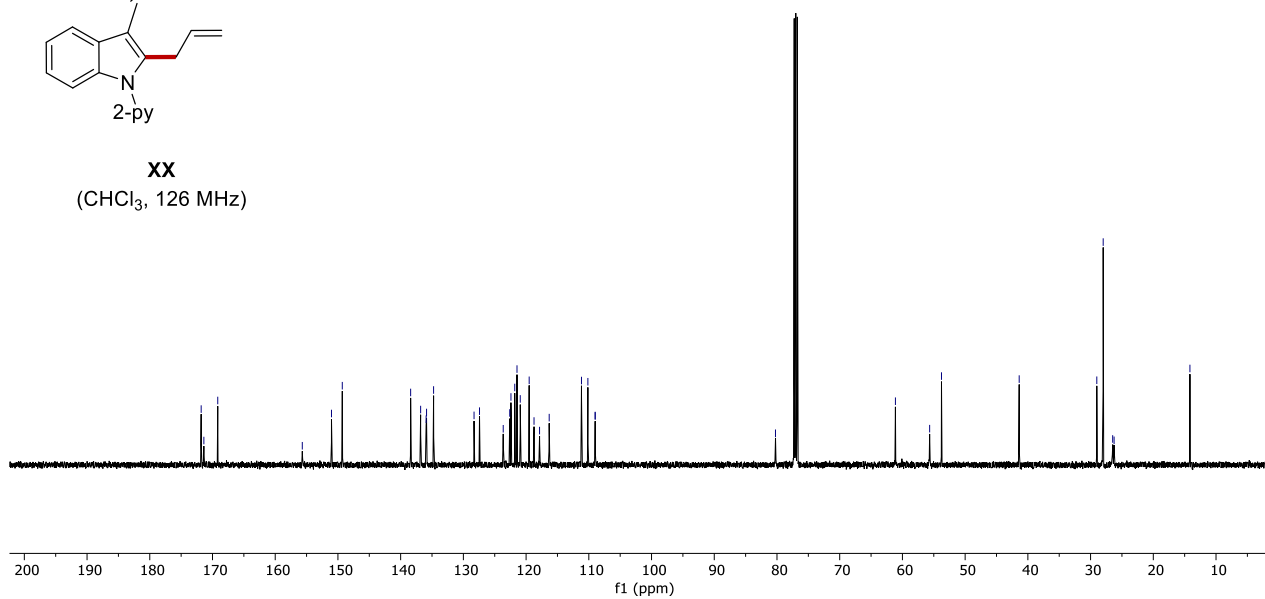


f1 (ppm)

171.81
171.38
169.16
155.68
151.03
149.31
138.41
136.81
135.94
135.97
133.56
128.30
127.43
123.65
122.61
122.42
121.81
121.45
120.93
119.51
118.74
116.95
116.85
111.17
110.15
108.99
108.99
80.24
61.12
55.66
53.77
41.38
29.01
27.09
26.48
26.25
14.16

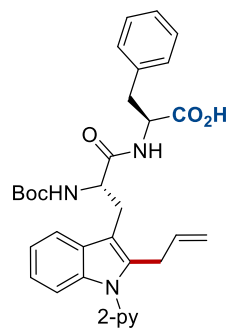


XX
(CHCl₃, 126 MHz)

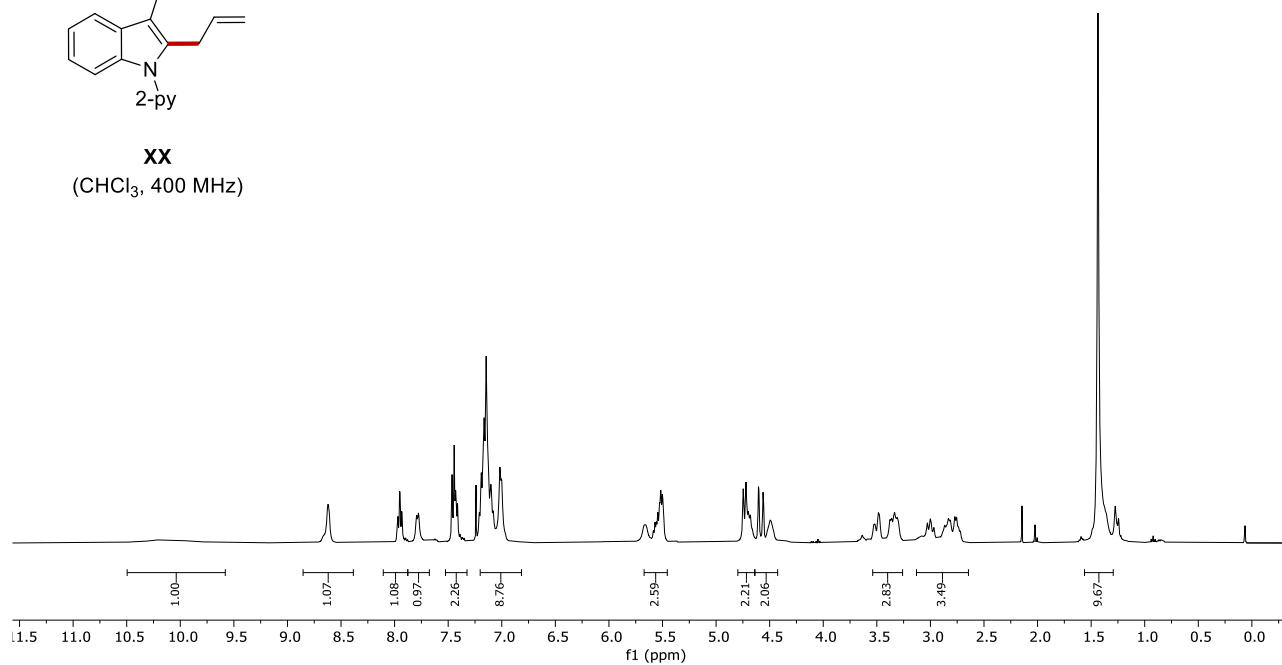


f1 (ppm)

8. NMR Spectra



XX
(CHCl₃, 400 MHz)



172.08
170.88

155.15
150.61
148.53

139.82
137.29
136.06
135.94

134.53
129.04
128.35

127.68
126.77
126.73

123.90
121.62
121.03

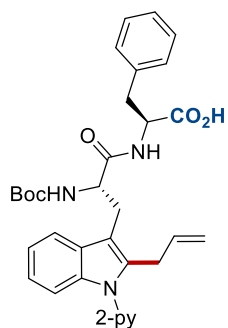
118.77
115.86
109.81
109.59

79.80

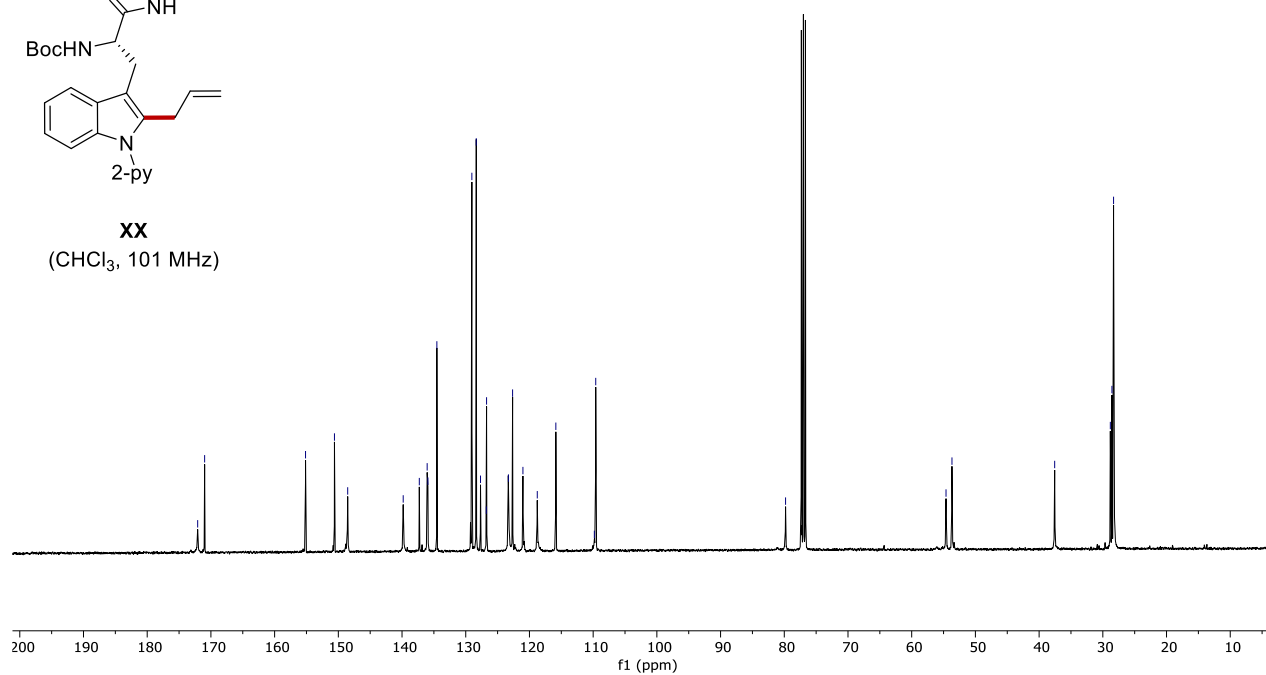
54.61
53.68

37.56

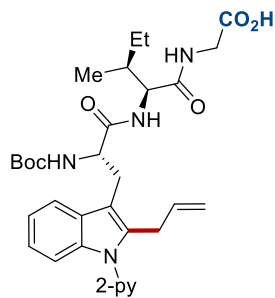
28.82
28.57
28.31



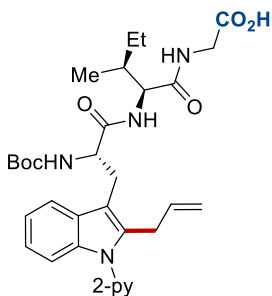
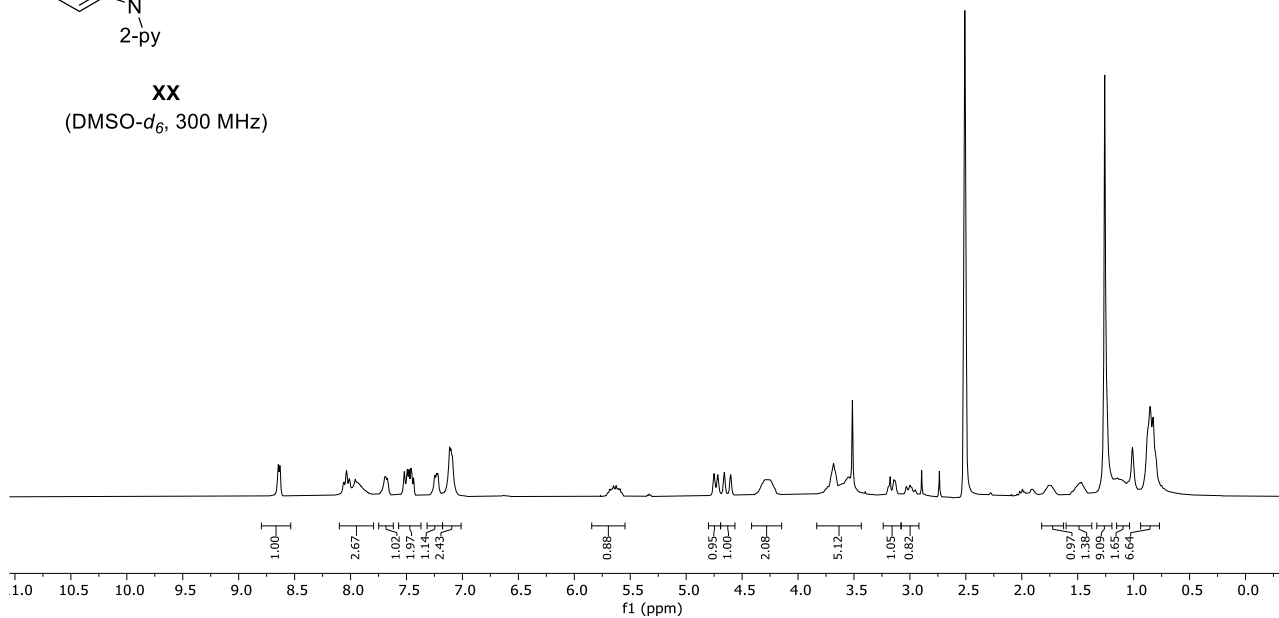
XX
(CHCl₃, 101 MHz)



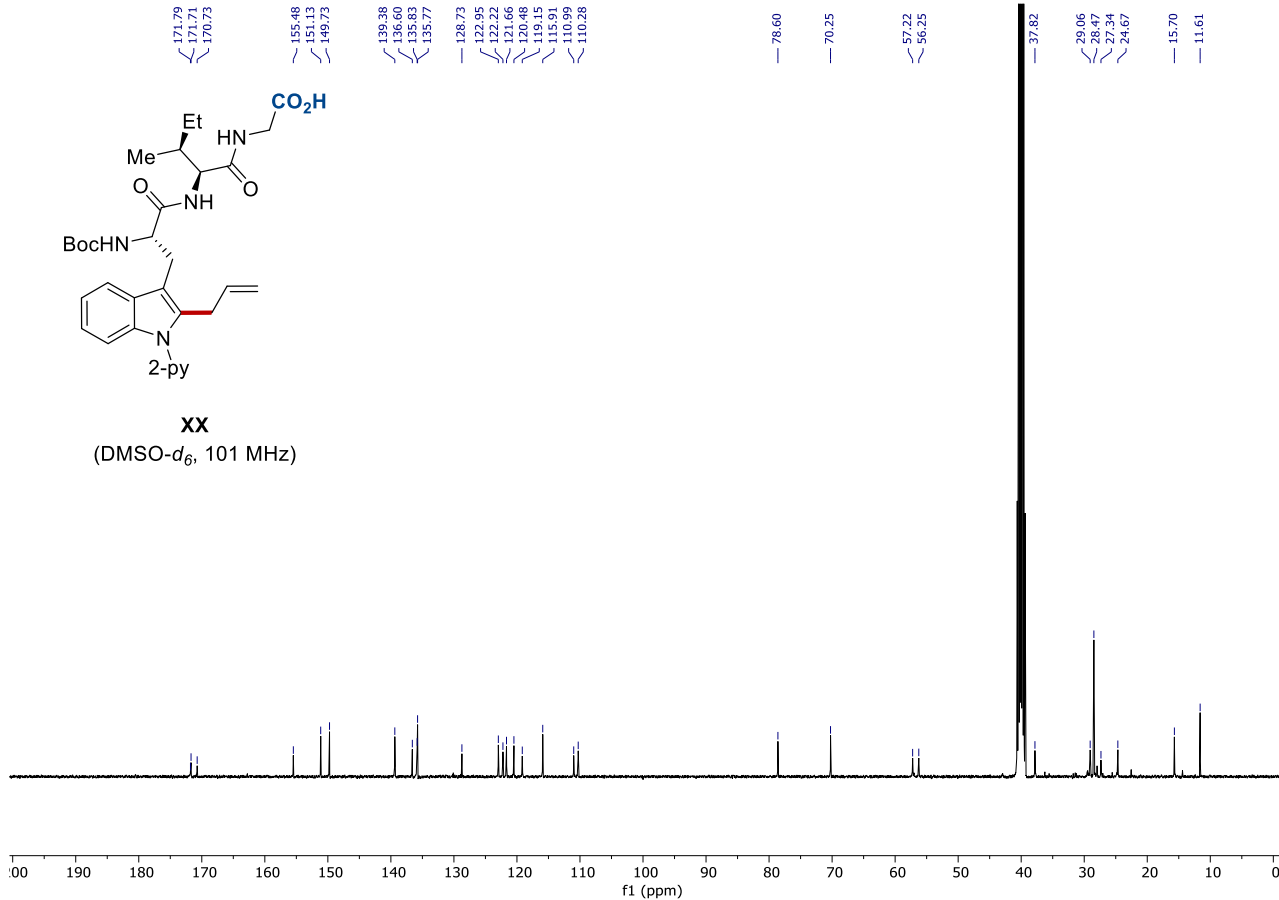
8. NMR Spectra



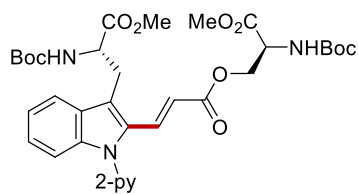
XX
(DMSO- d_6 , 300 MHz)



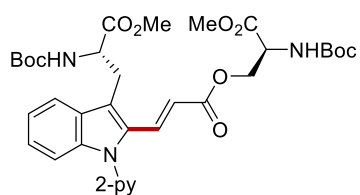
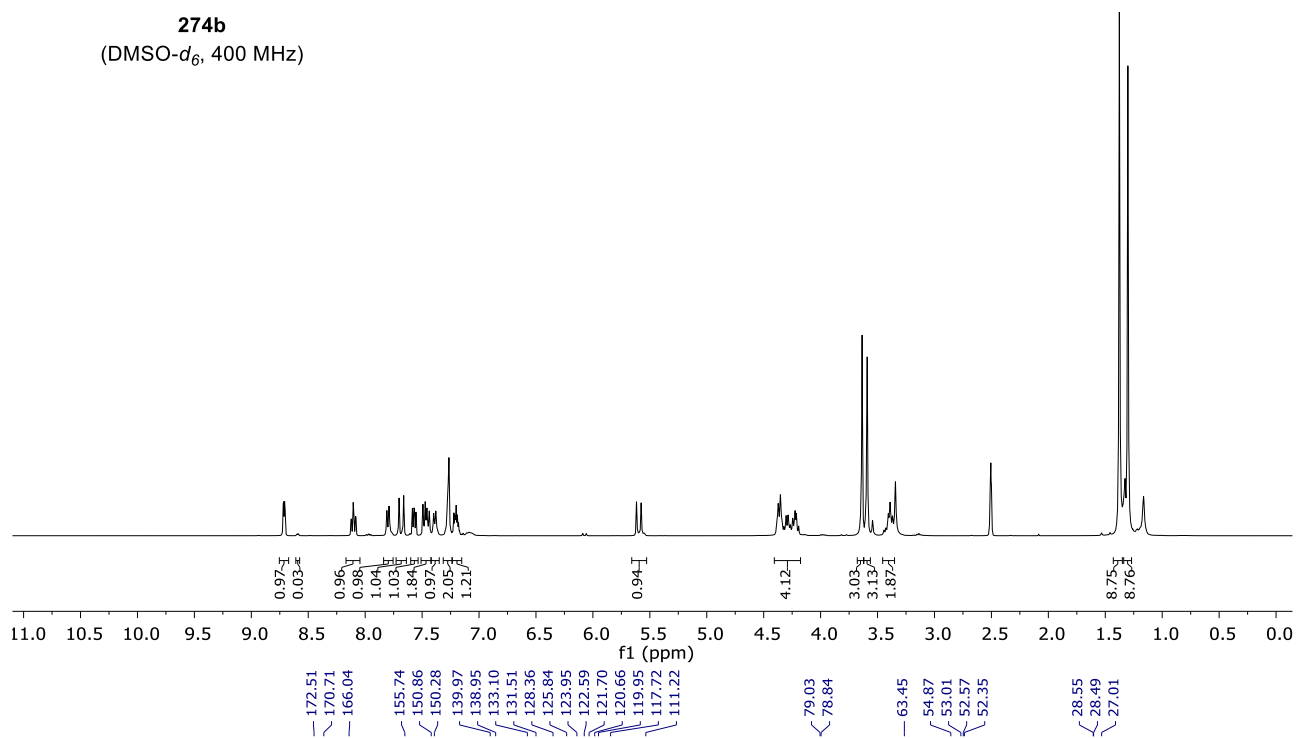
XX
(DMSO- d_6 , 101 MHz)



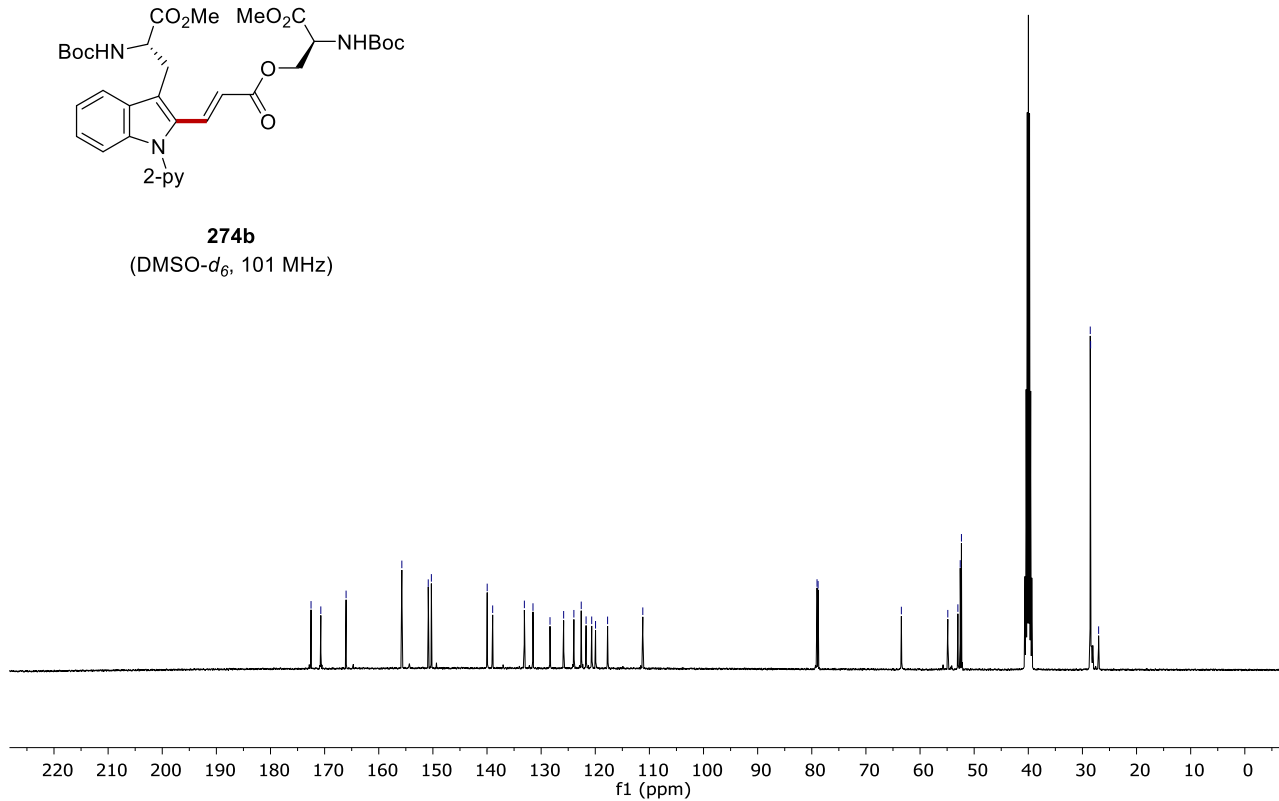
8. NMR Spectra

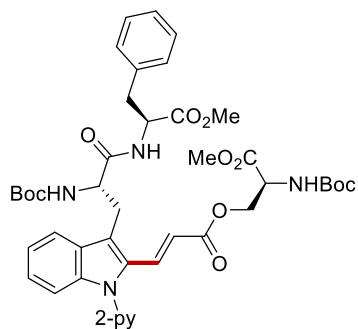


274b
(DMSO-*d*₆, 400 MHz)

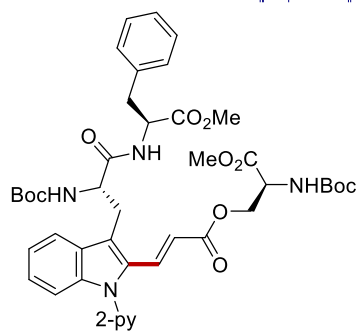
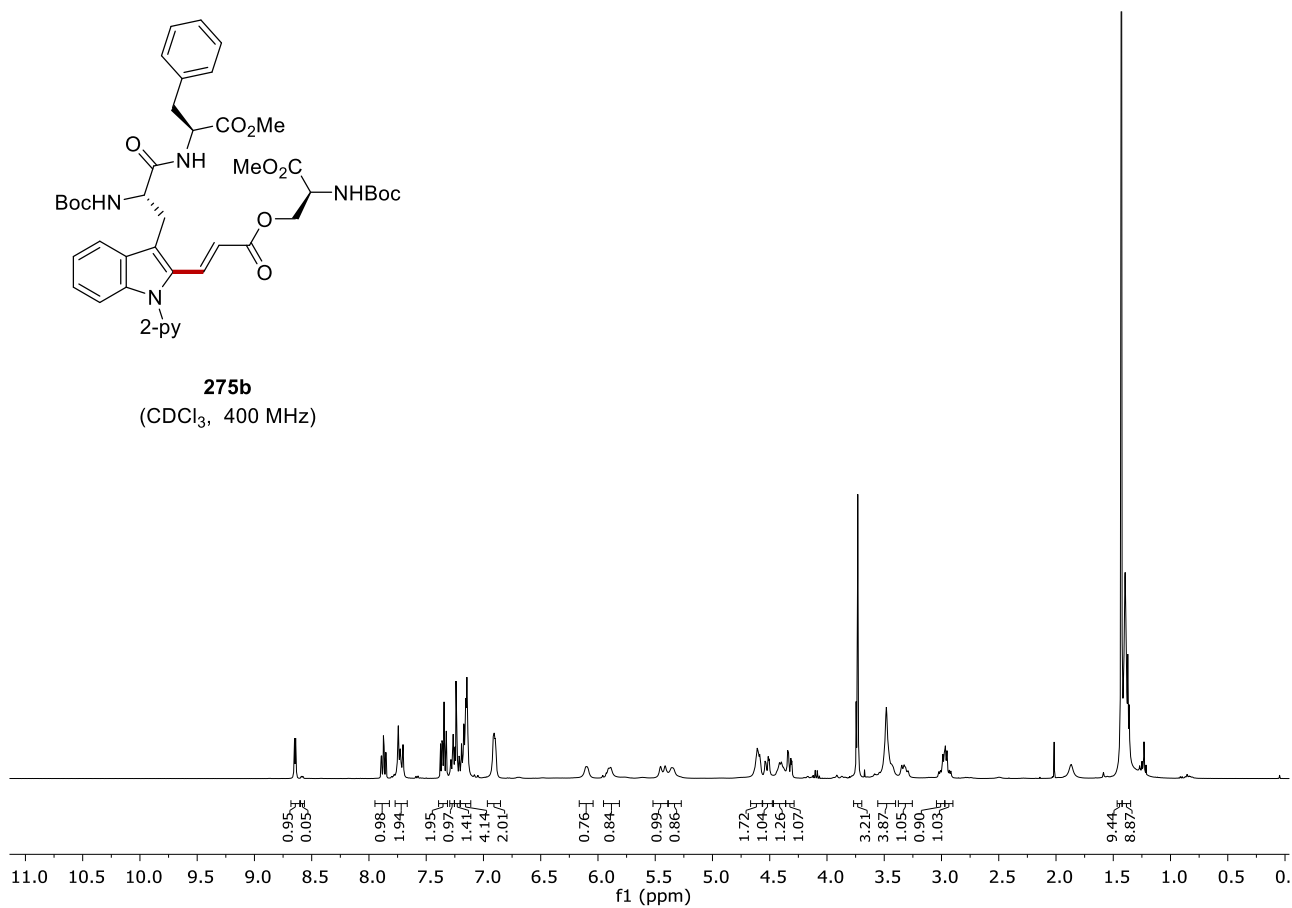


274b
(DMSO-*d*₆, 101 MHz)

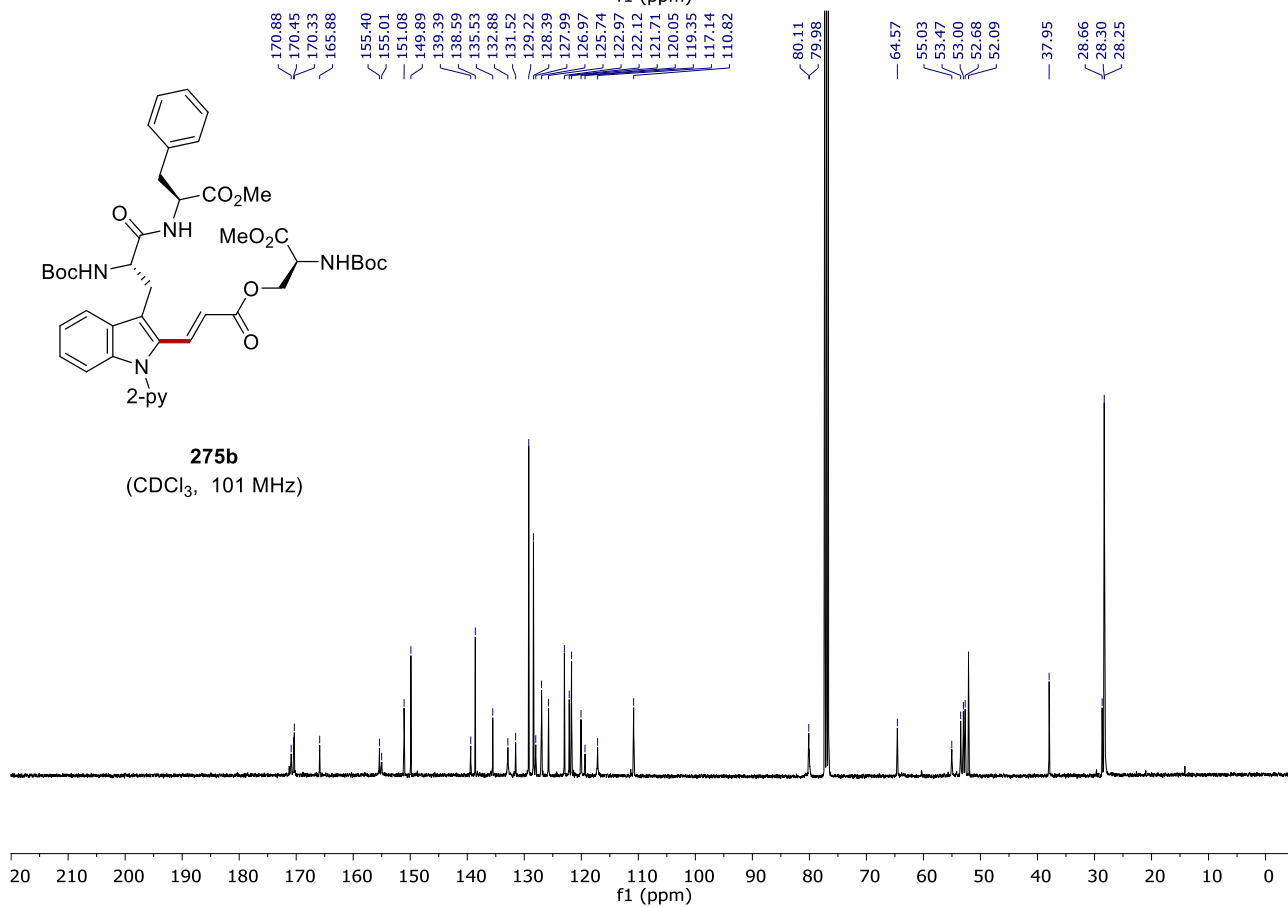




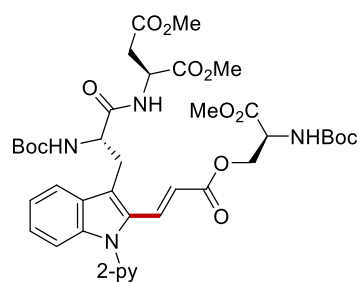
275b
(CDCl₃, 400 MHz)



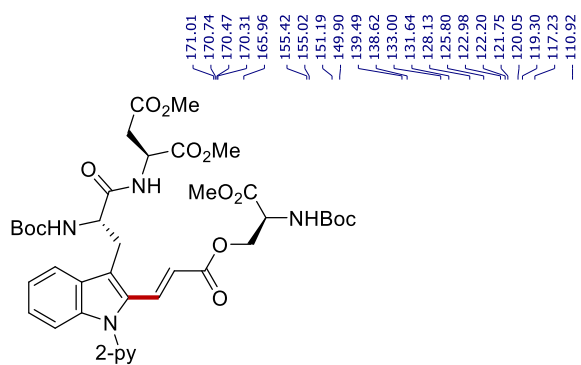
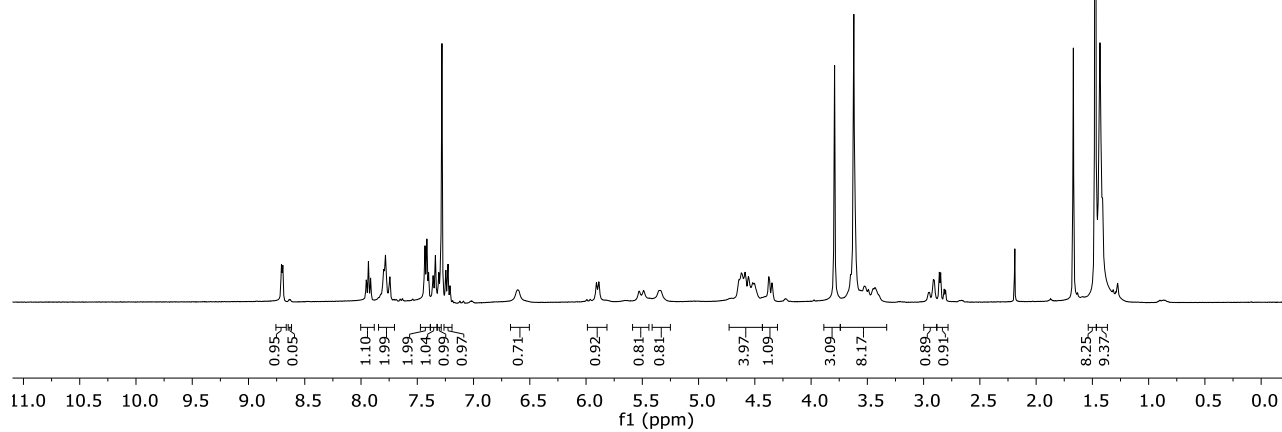
275b
(CDCl₃, 101 MHz)



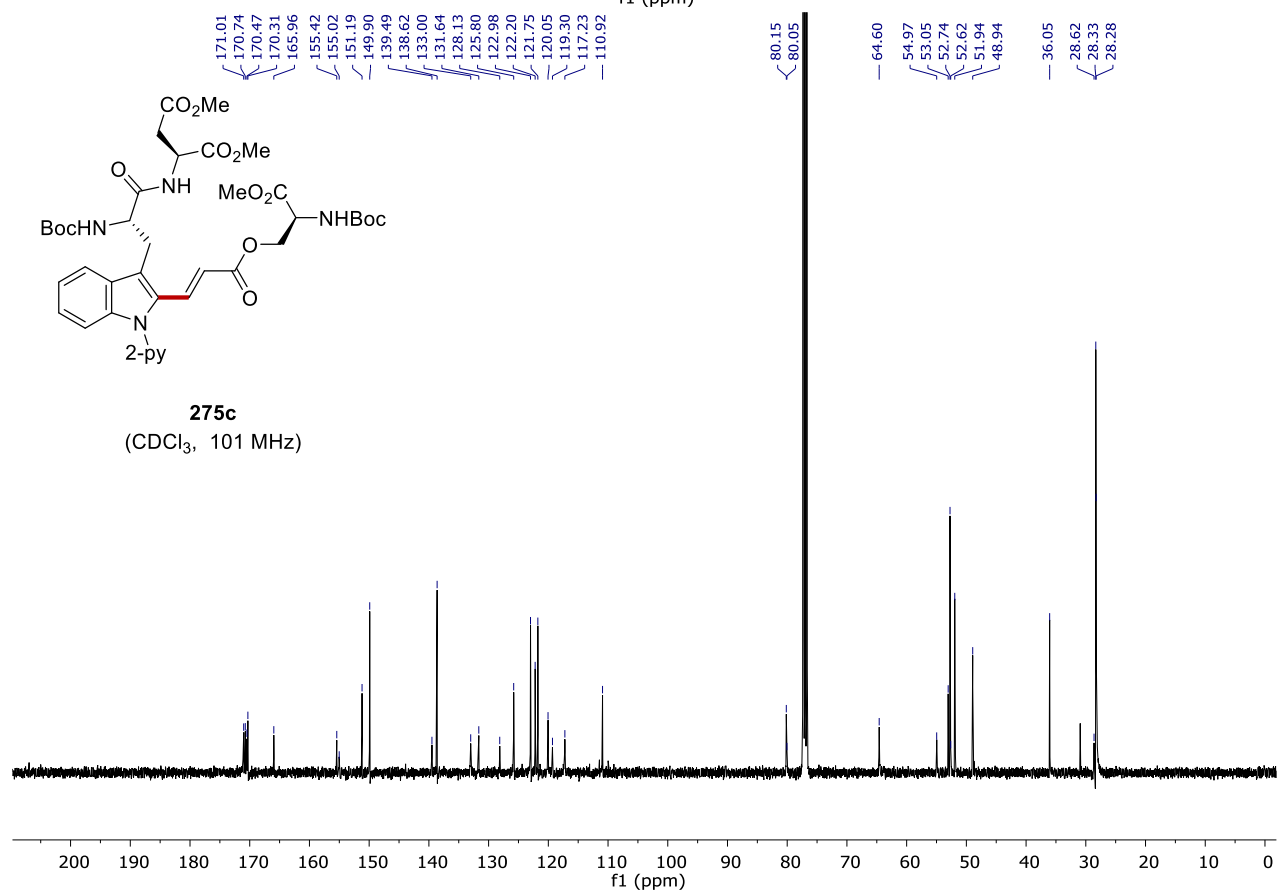
8. NMR Spectra



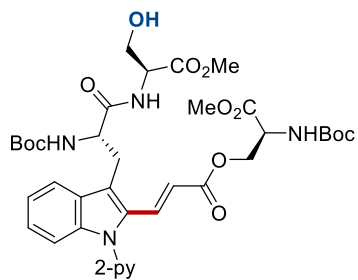
275c
(CDCl₃, 400 MHz)



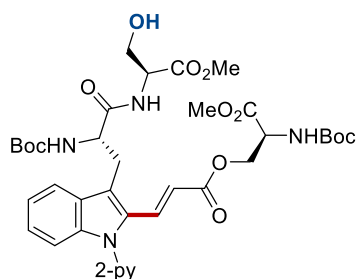
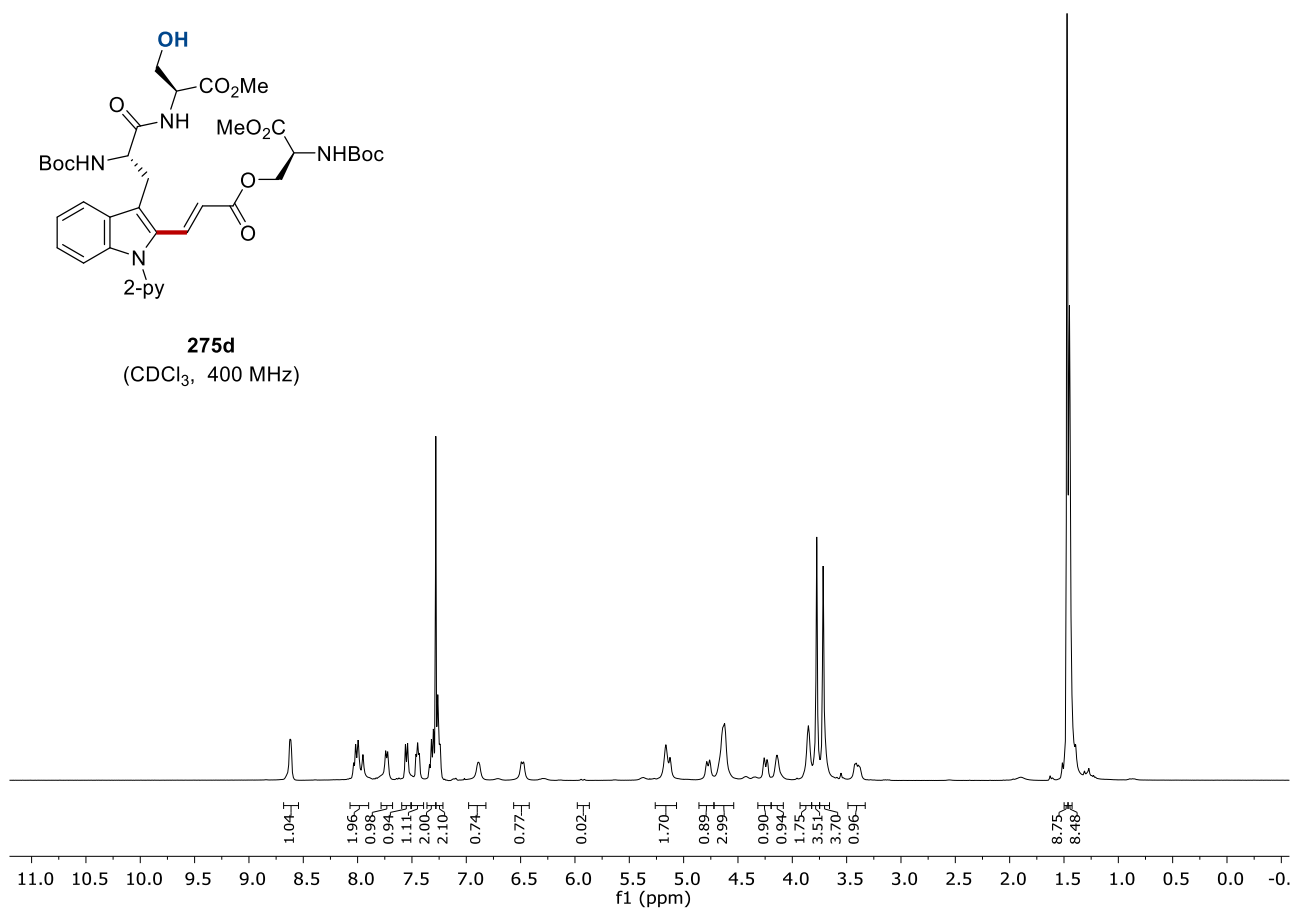
275c
(CDCl₃, 101 MHz)



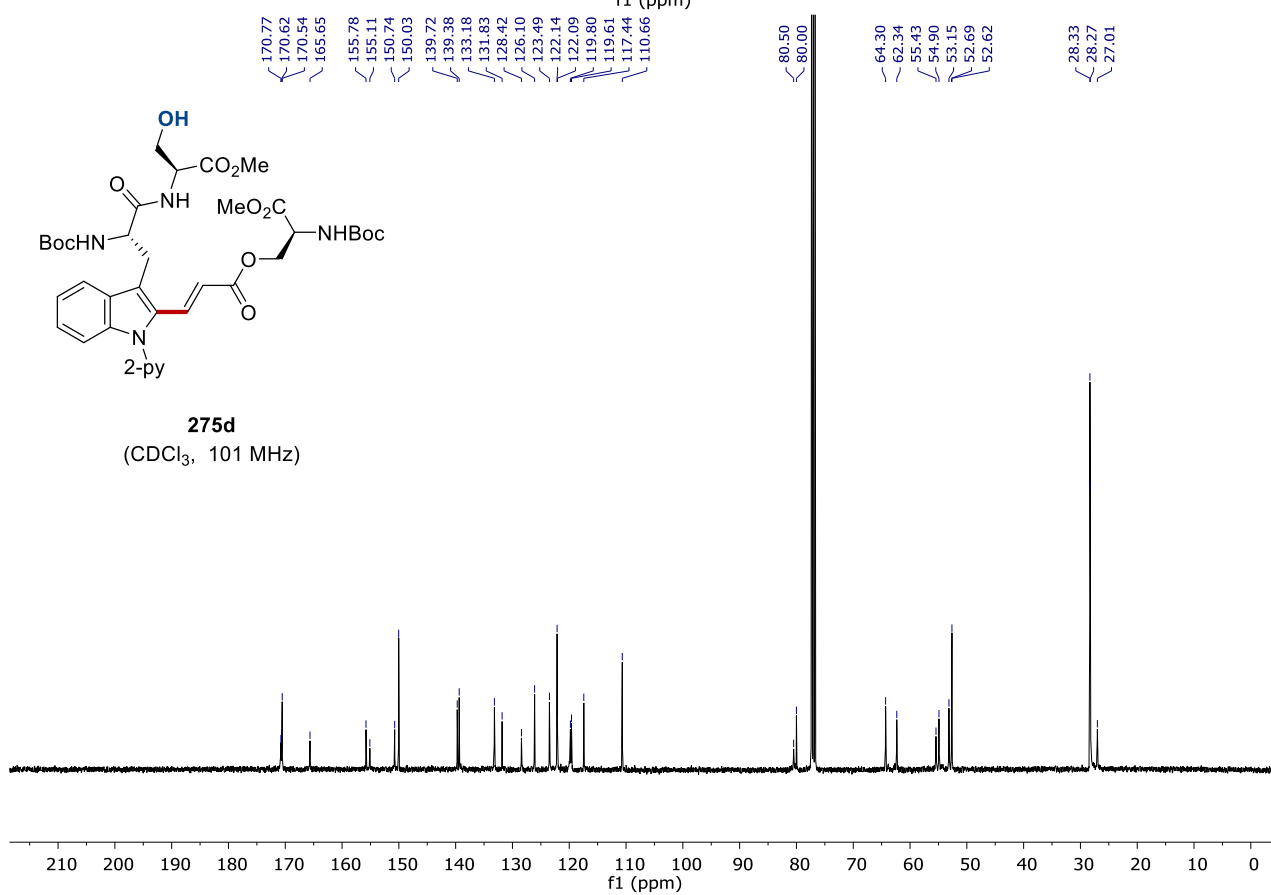
8. NMR Spectra



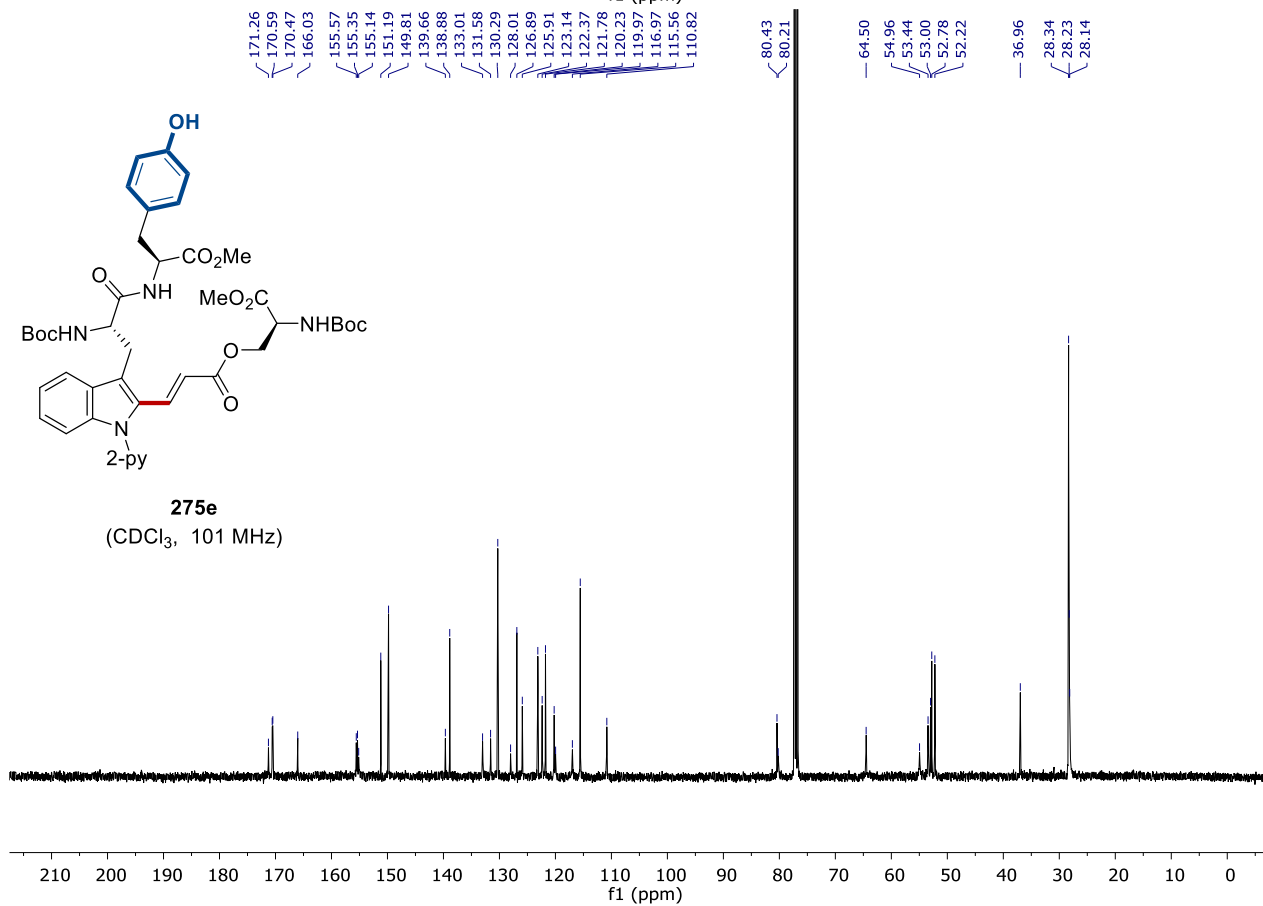
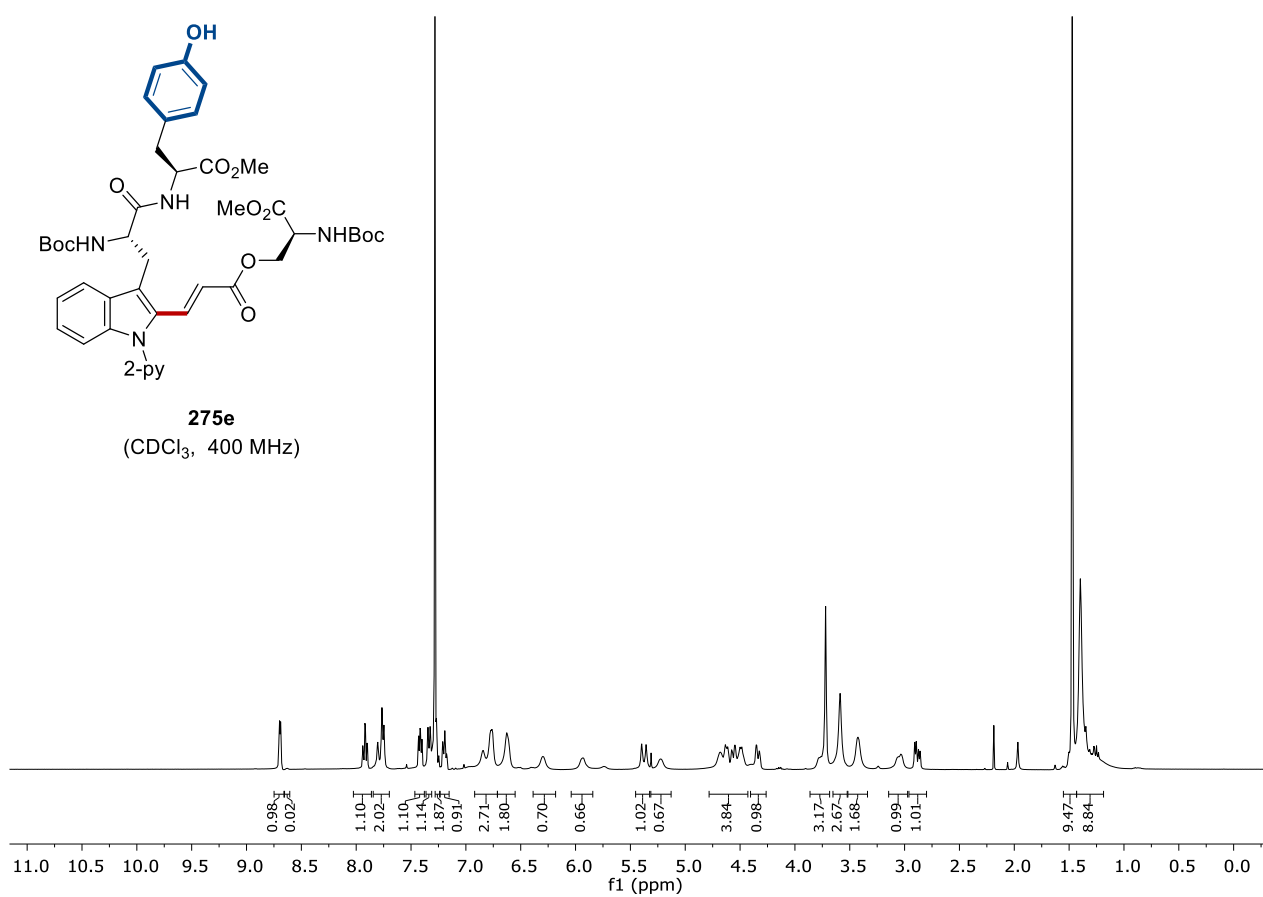
275d
(CDCl₃, 400 MHz)

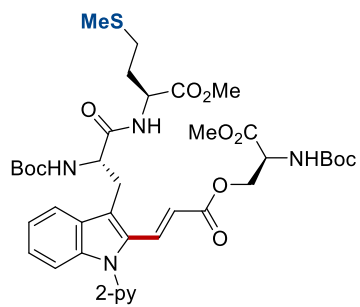


275d
(CDCl₃, 101 MHz)

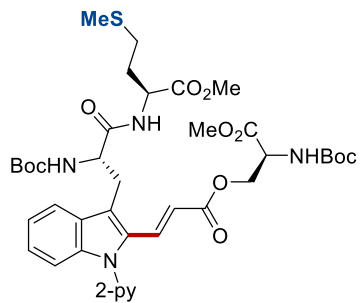
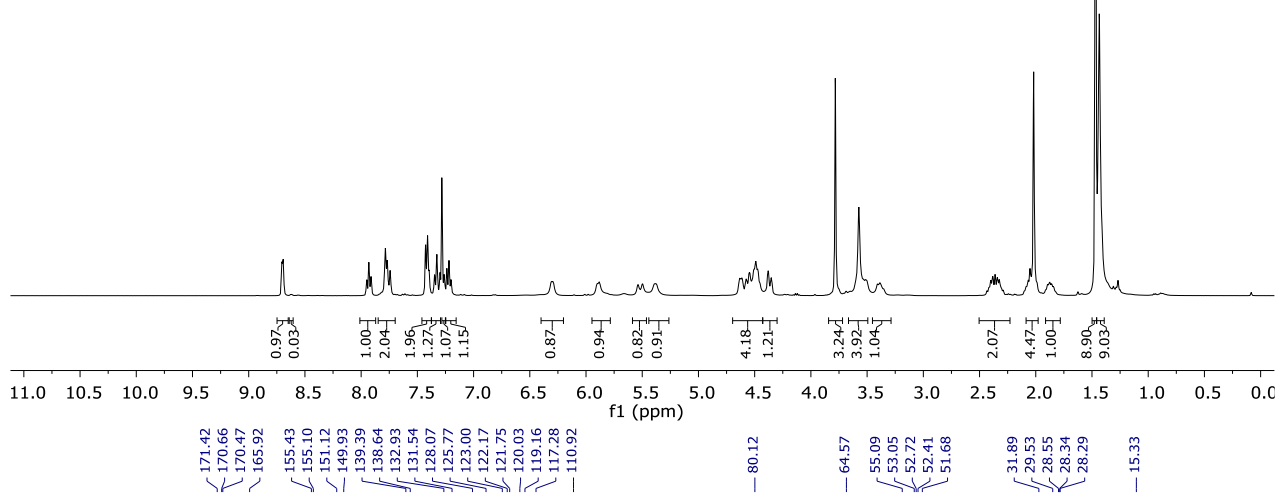


8. NMR Spectra

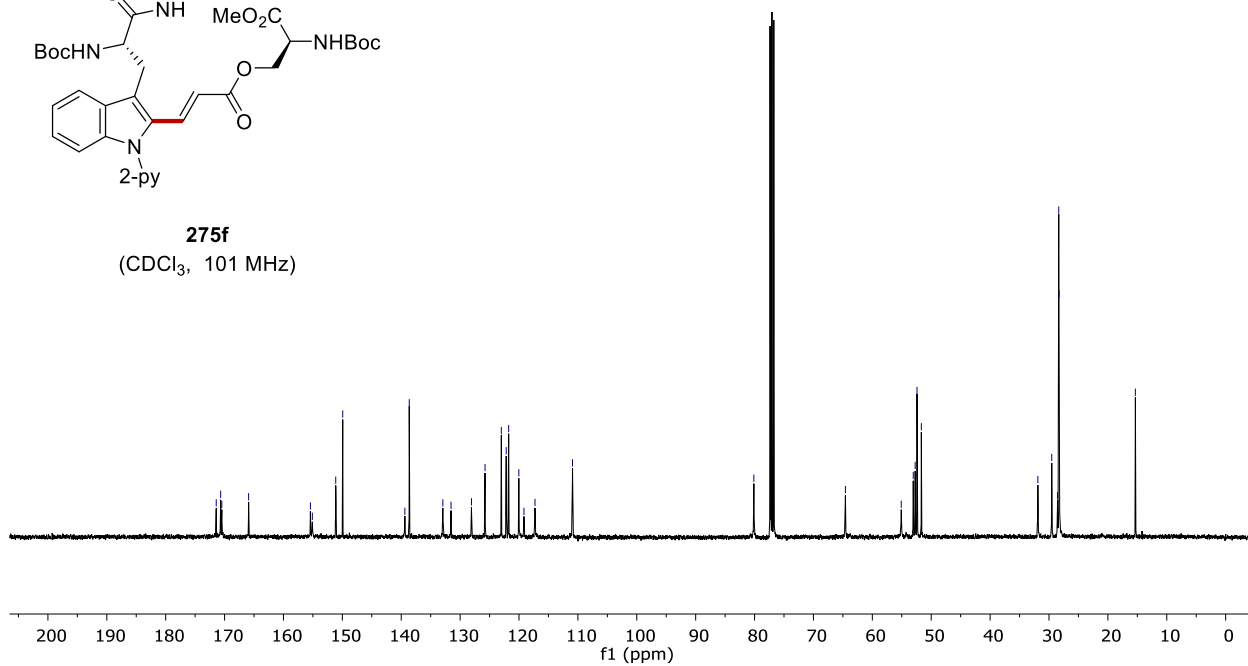




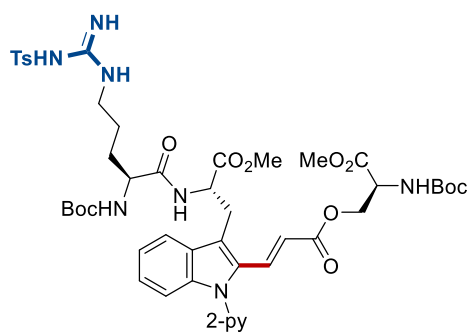
275f
(CDCl₃, 400 MHz)



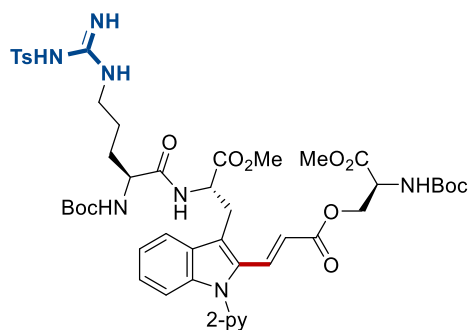
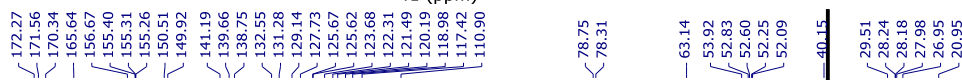
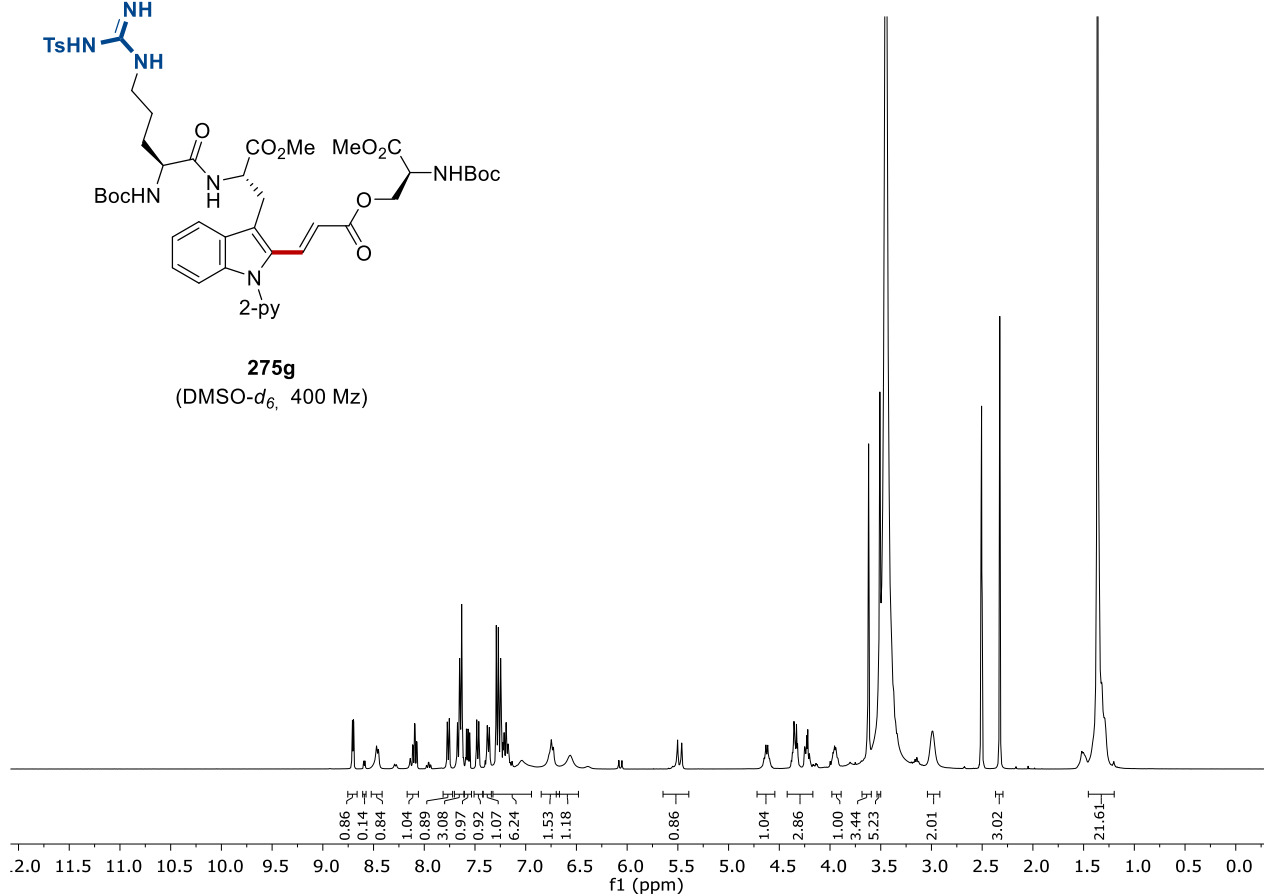
275f
(CDCl₃, 101 MHz)



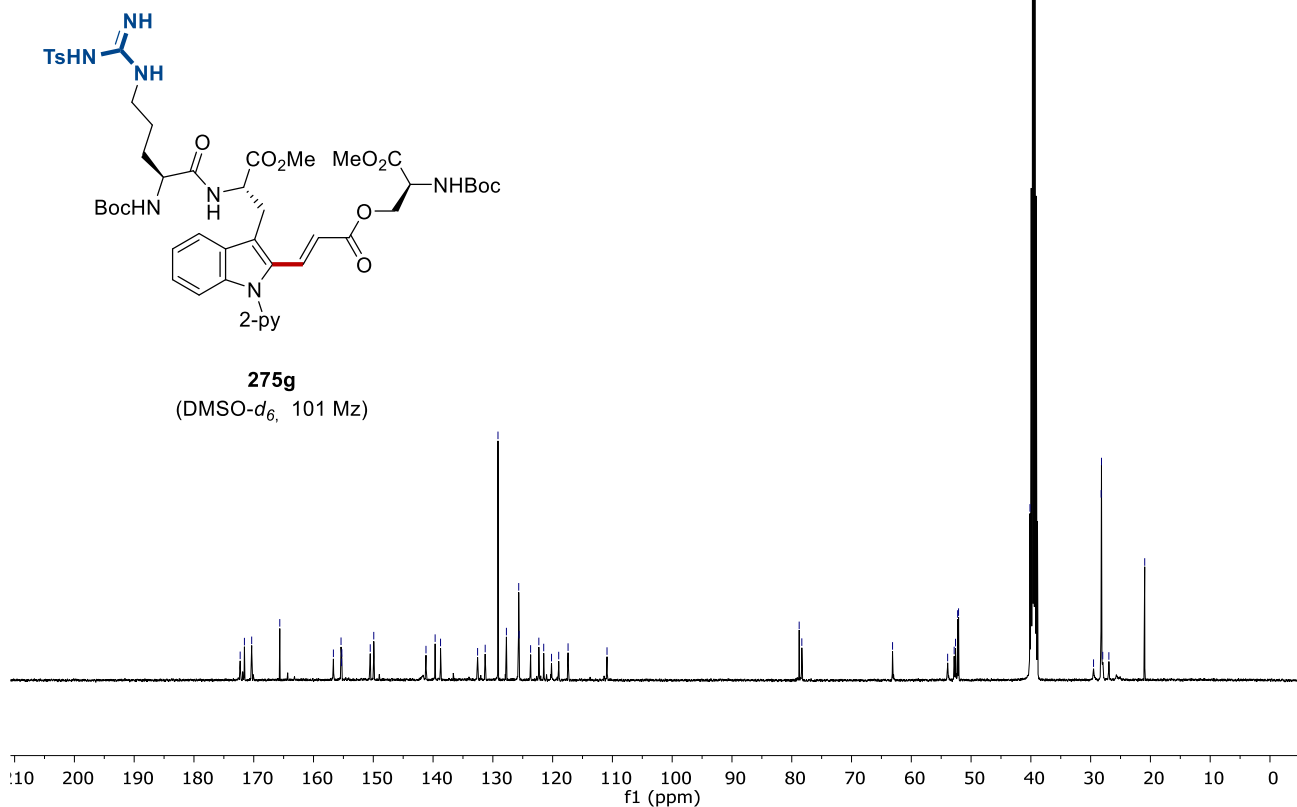
8. NMR Spectra

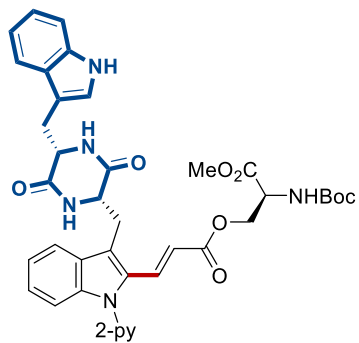


275g
(DMSO- d_6 , 400 Mz)

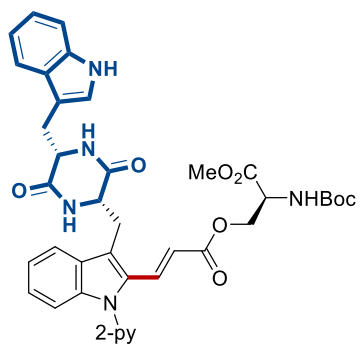
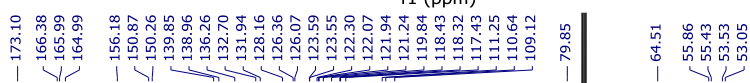
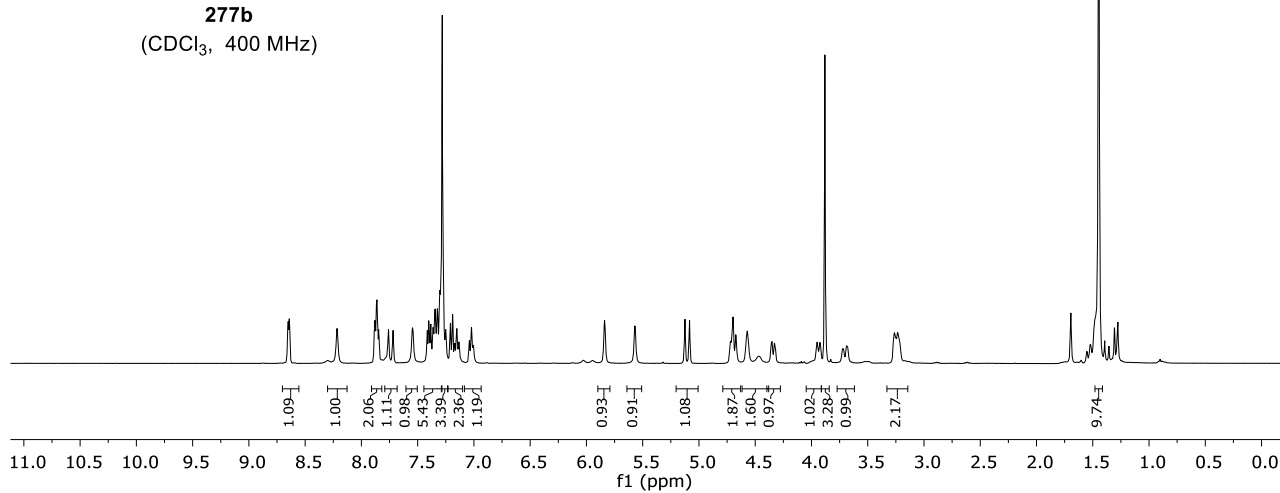


275g
(DMSO- d_6 , 101 Mz)

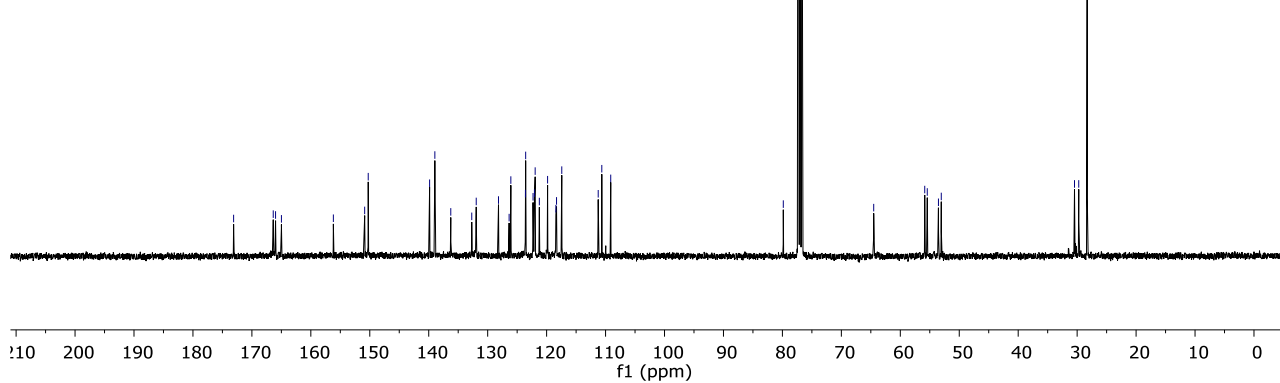




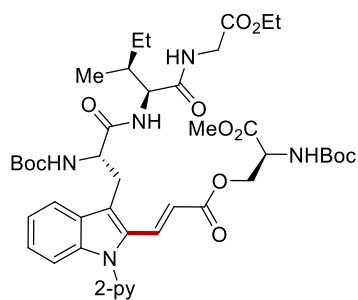
277b
(CDCl₃, 400 MHz)



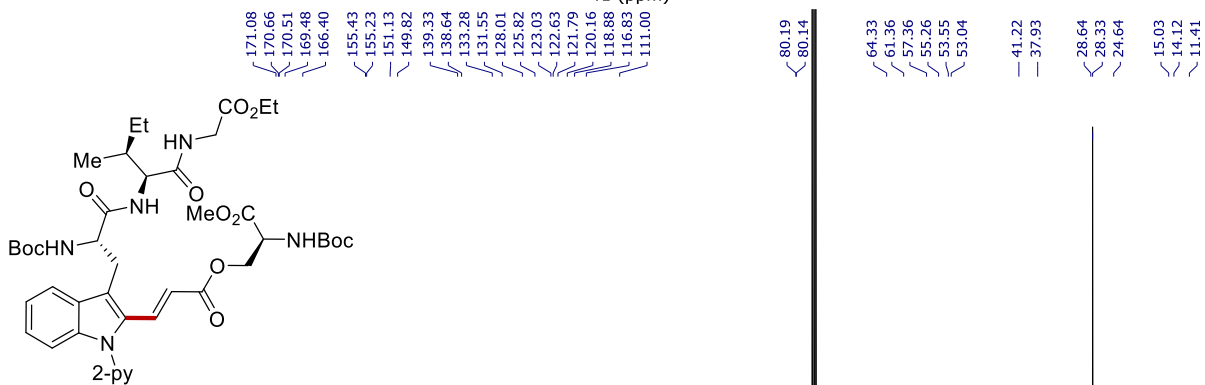
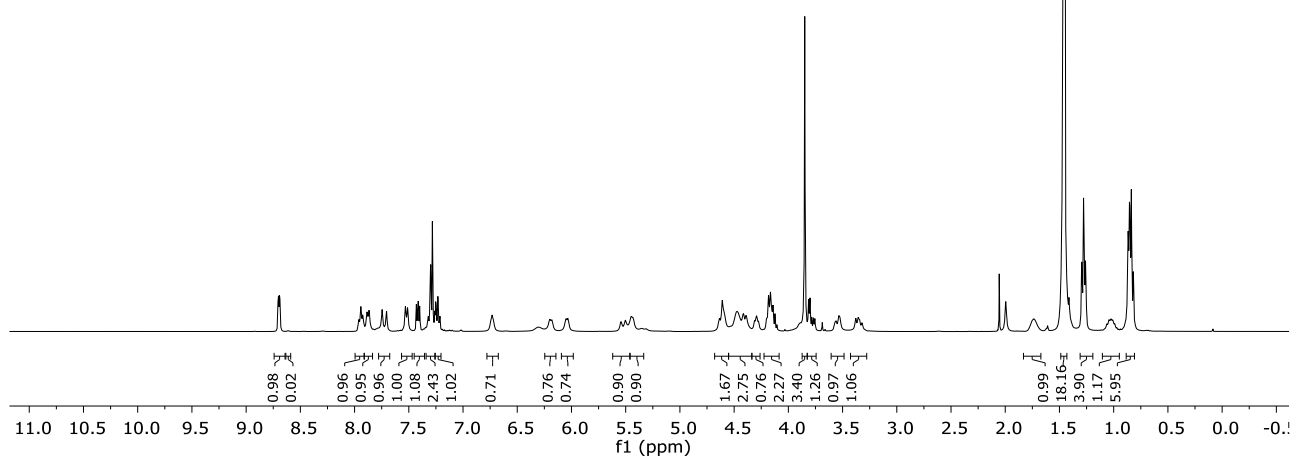
277b
(CDCl₃, 101 MHz)



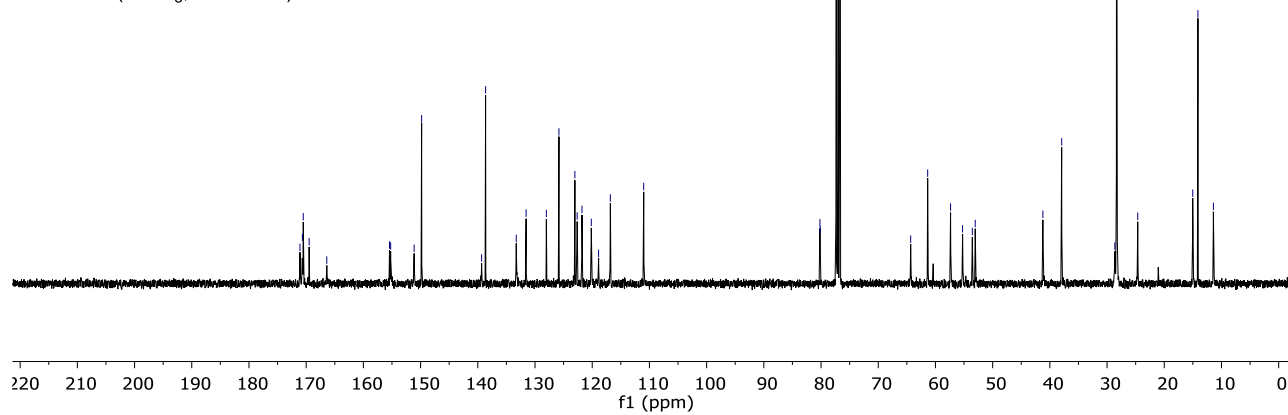
8. NMR Spectra

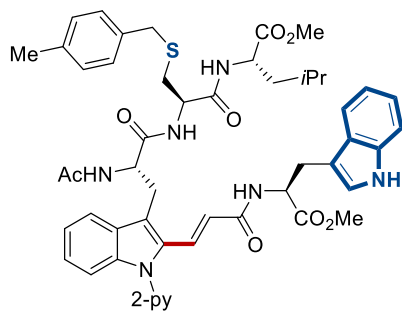


276h
(CDCl₃, 400 MHz)

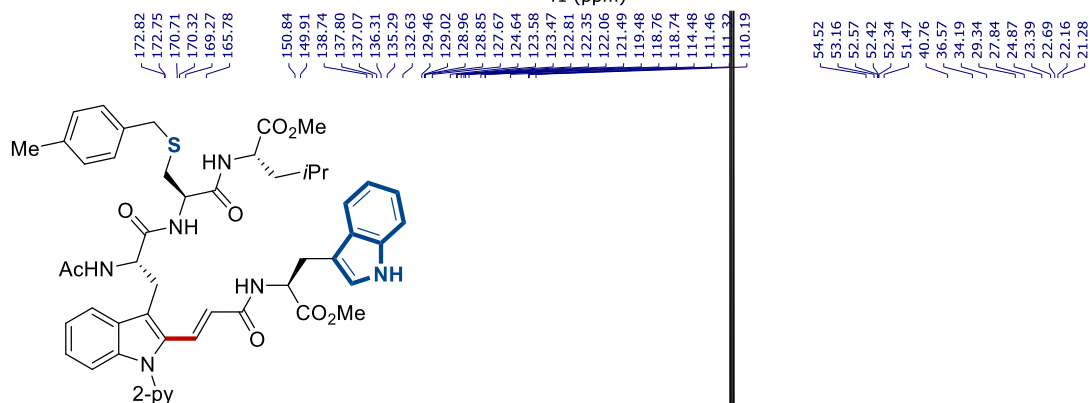
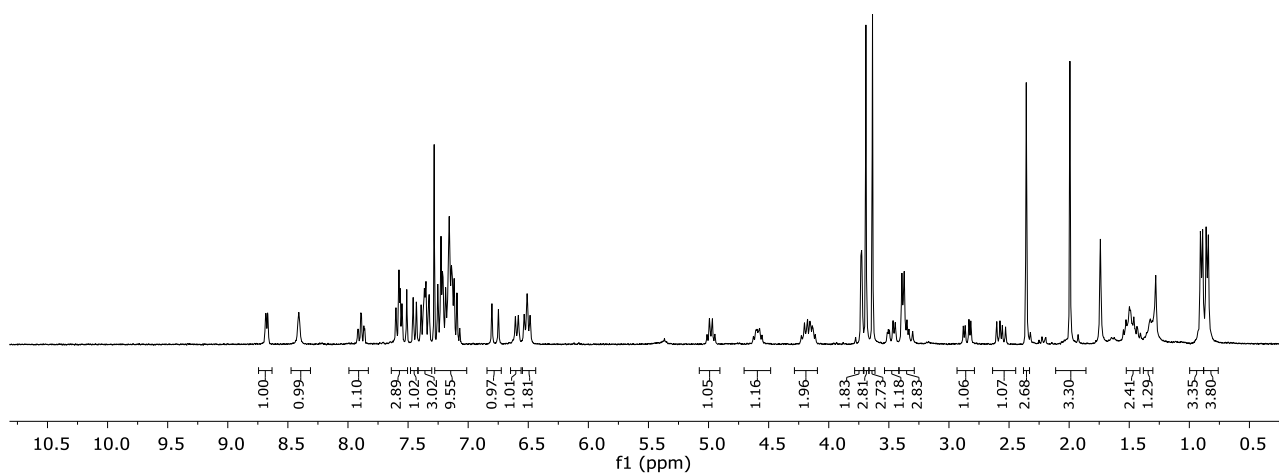


276h
(CDCl₃, 101 MHz)

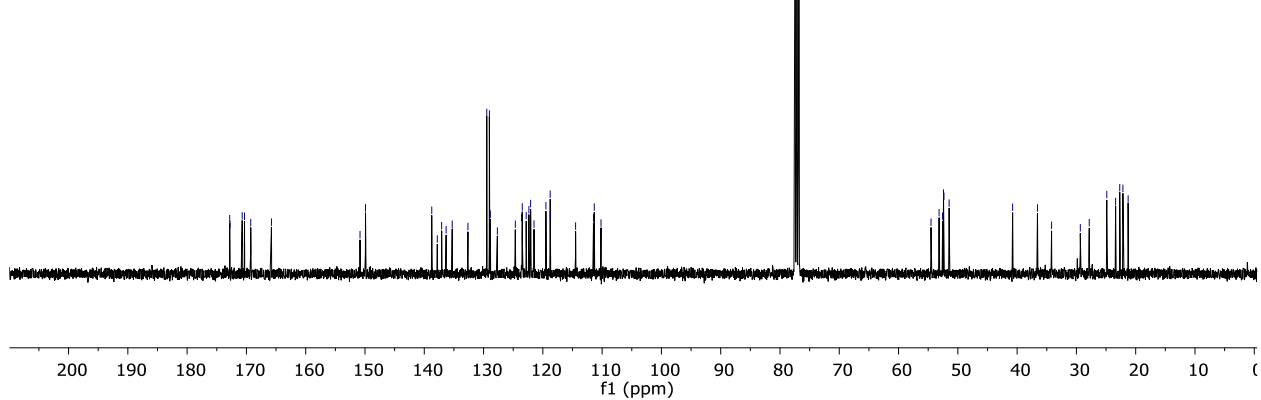




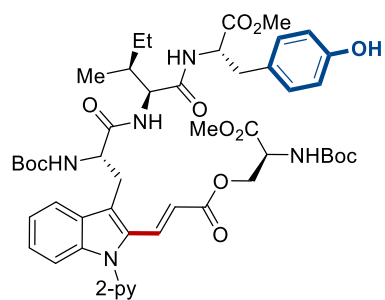
276i
(CDCl₃, 300 MHz)



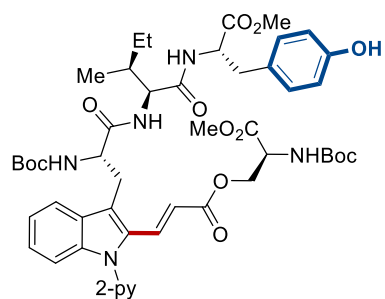
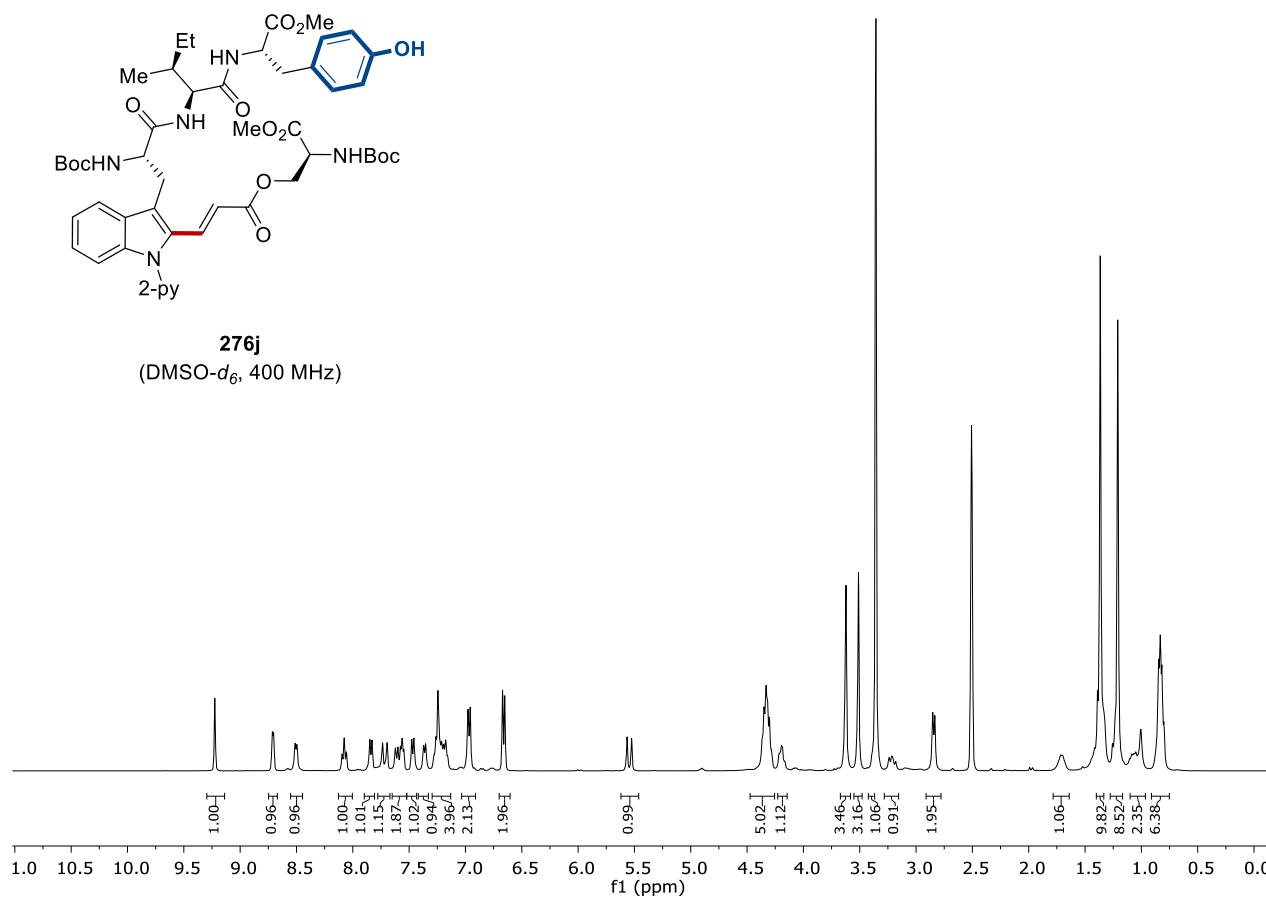
276i
(CDCl₃, 101 MHz)



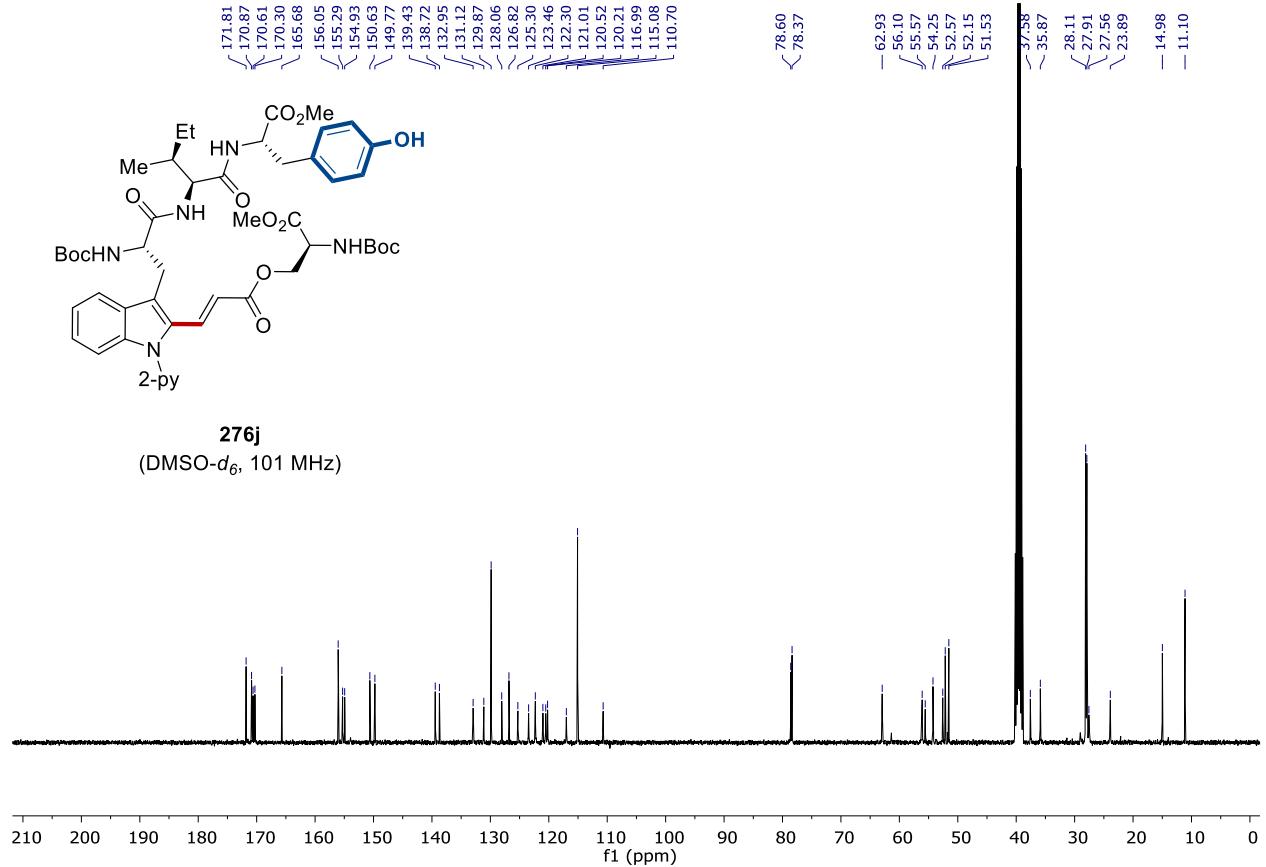
8. NMR Spectra

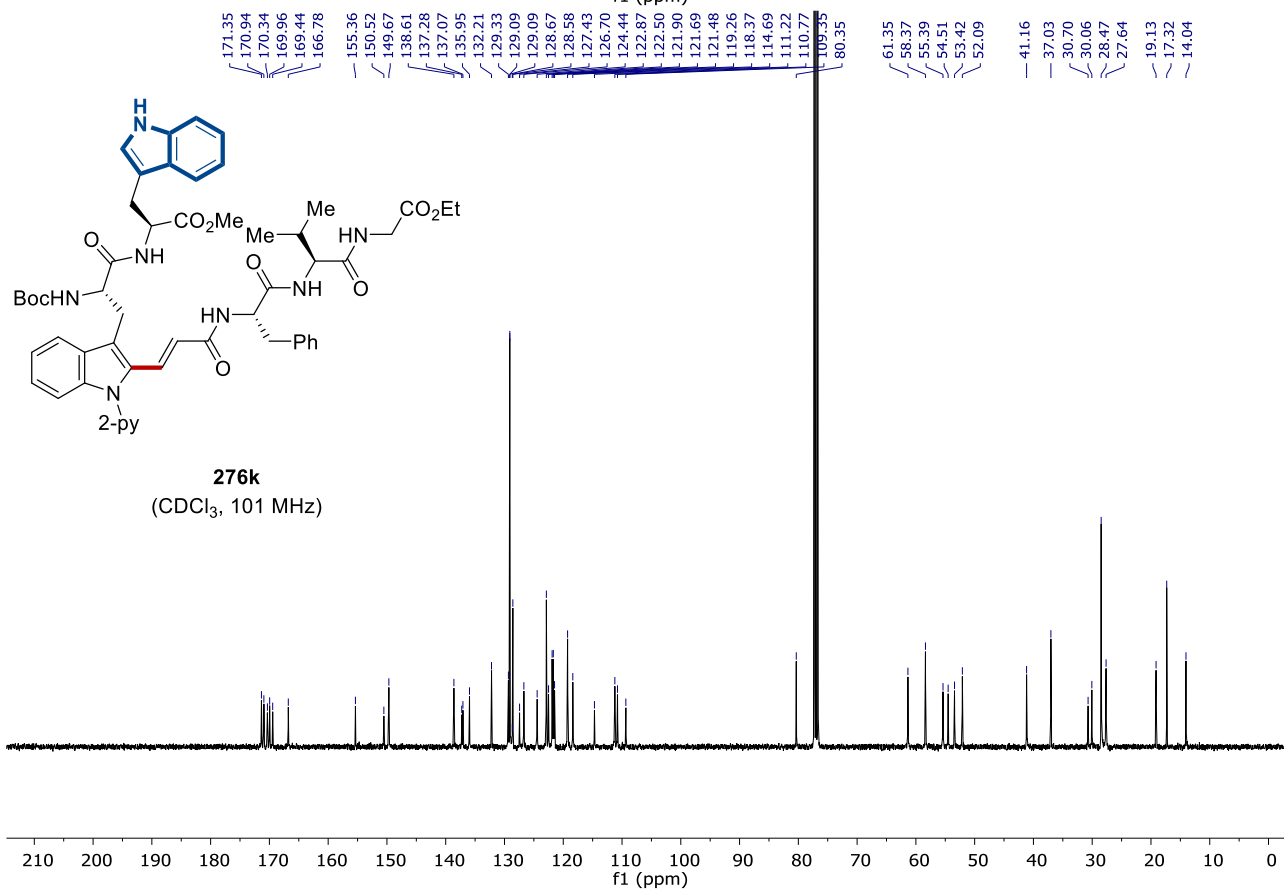
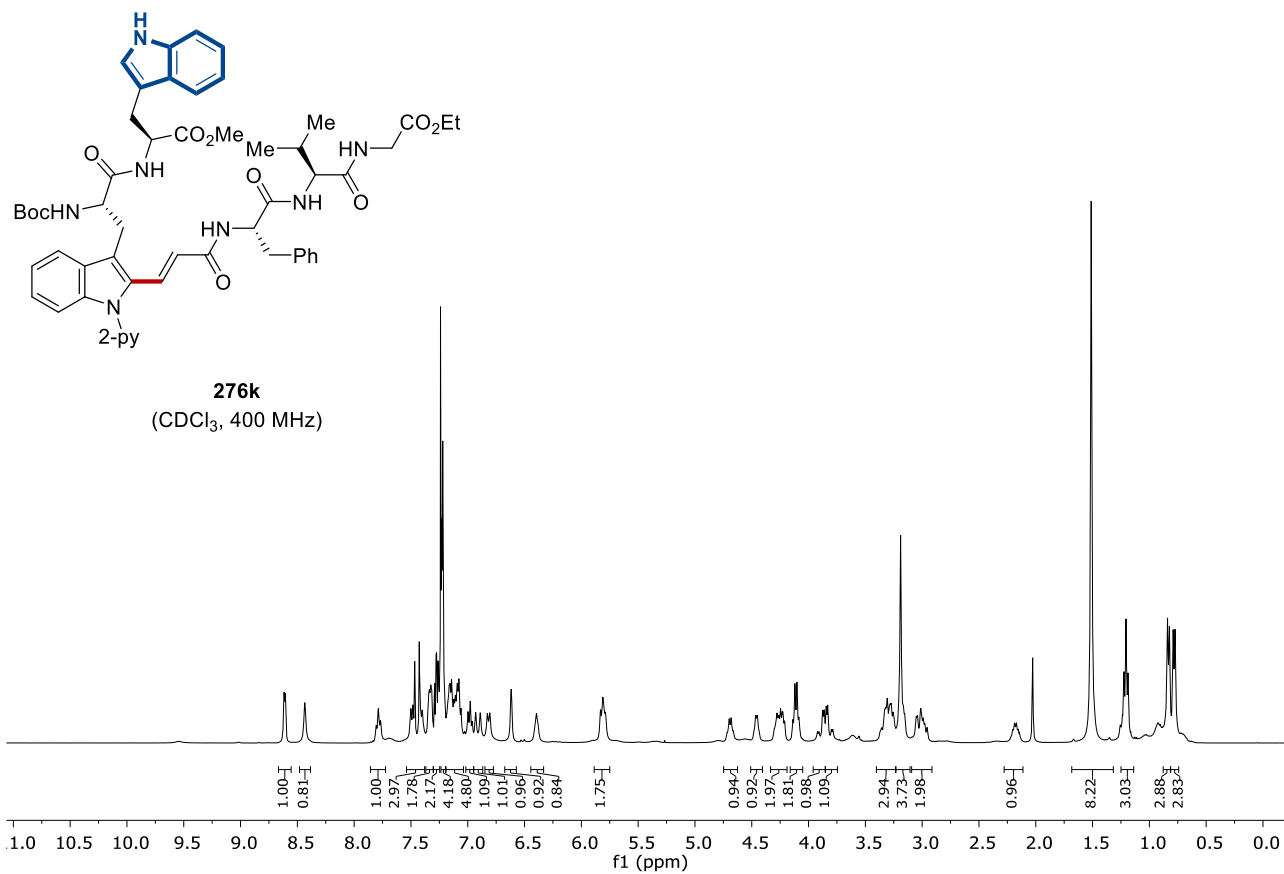


276j
(DMSO-*d*₆, 400 MHz)

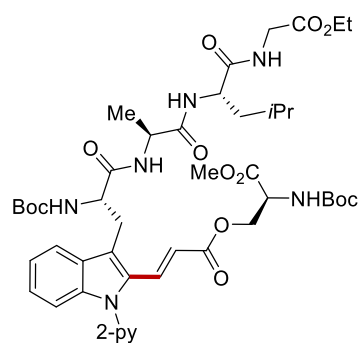


276j
(DMSO-*d*₆, 101 MHz)

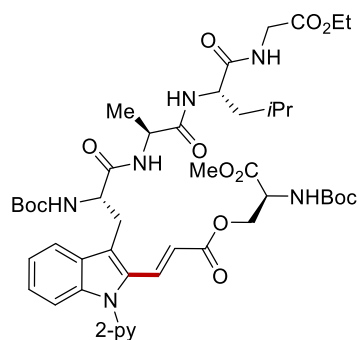
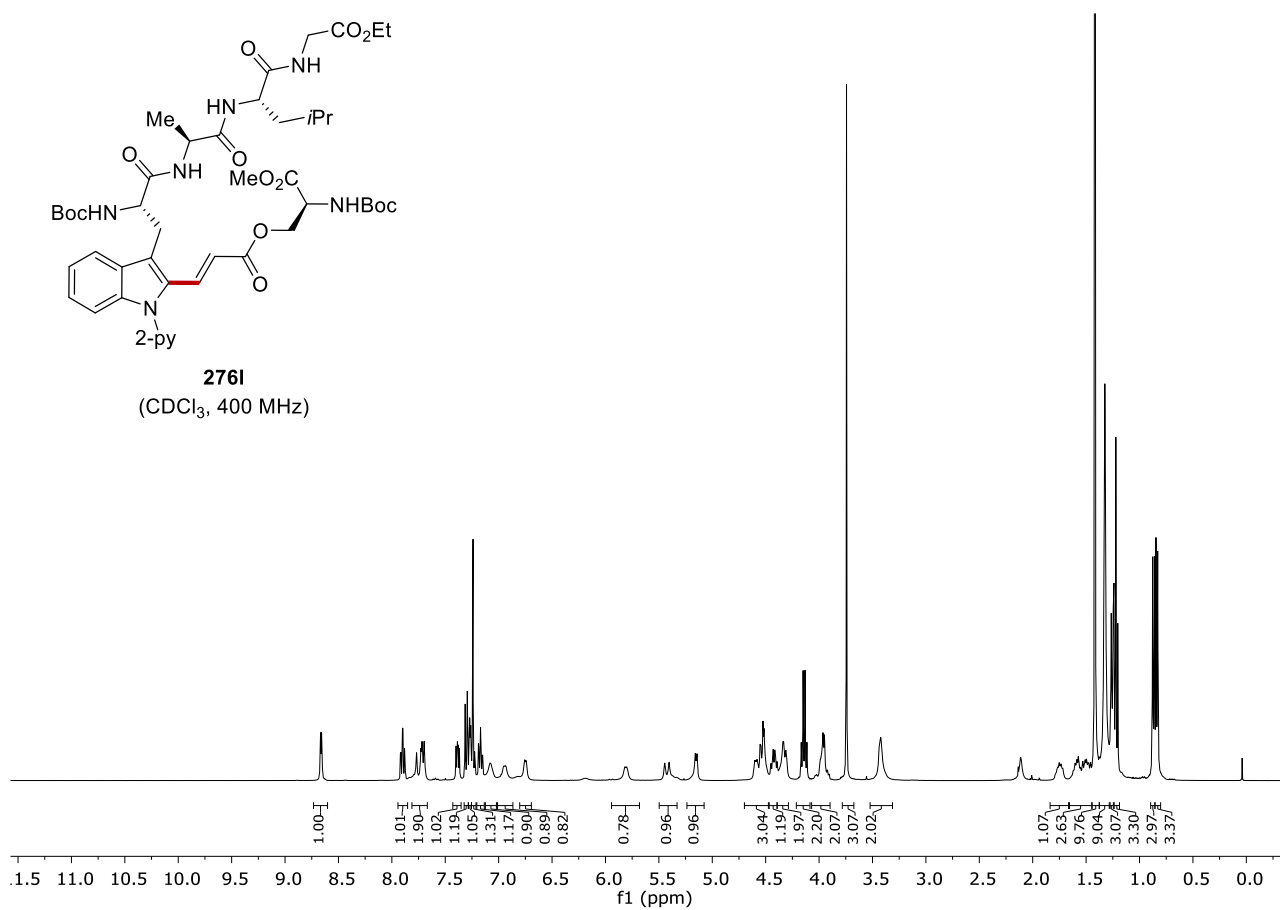




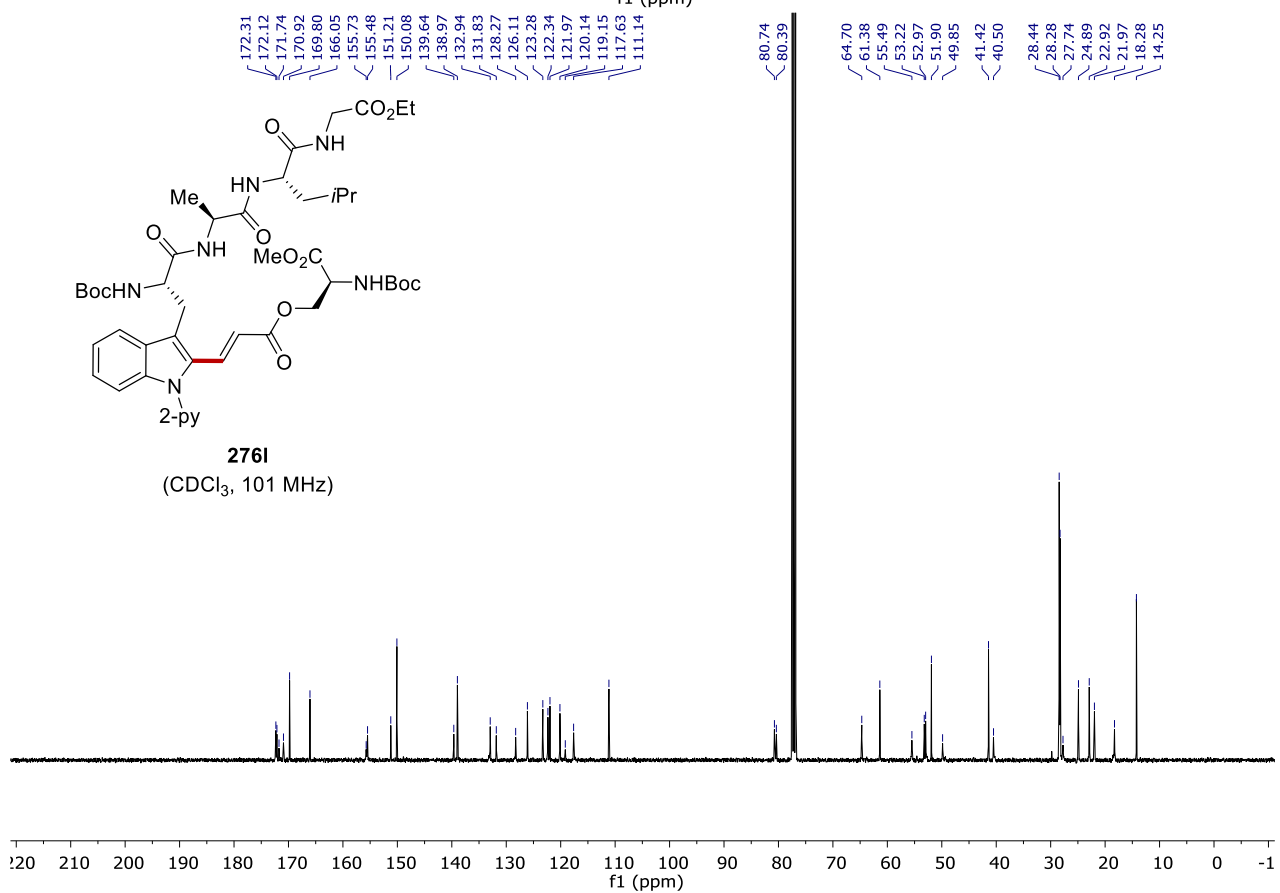
8. NMR Spectra

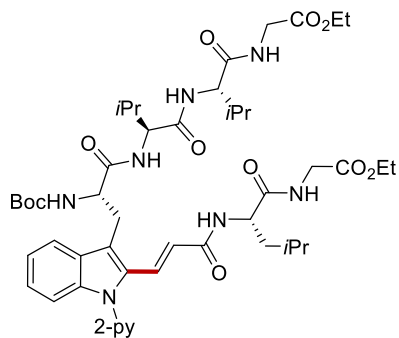


276I
(CDCl₃, 400 MHz)

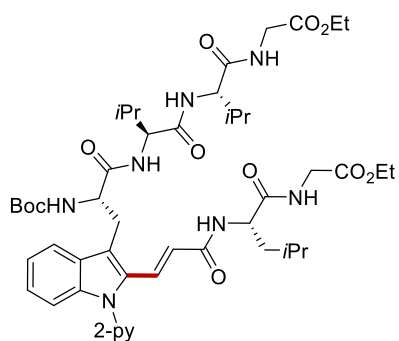
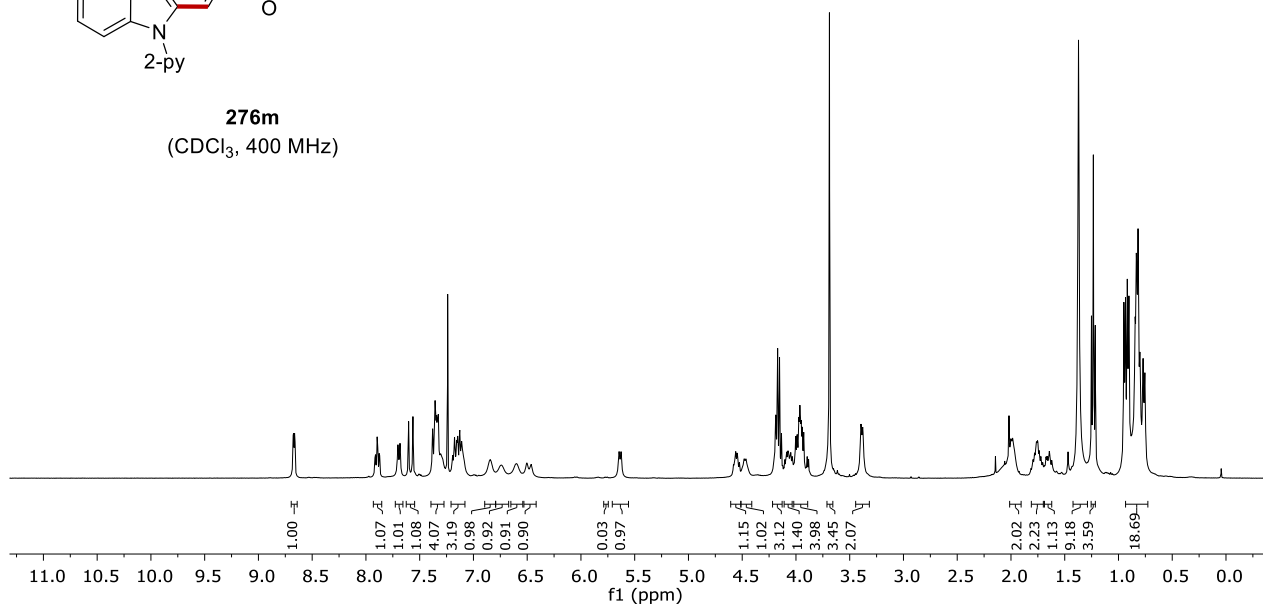


276I
(CDCl₃, 101 MHz)

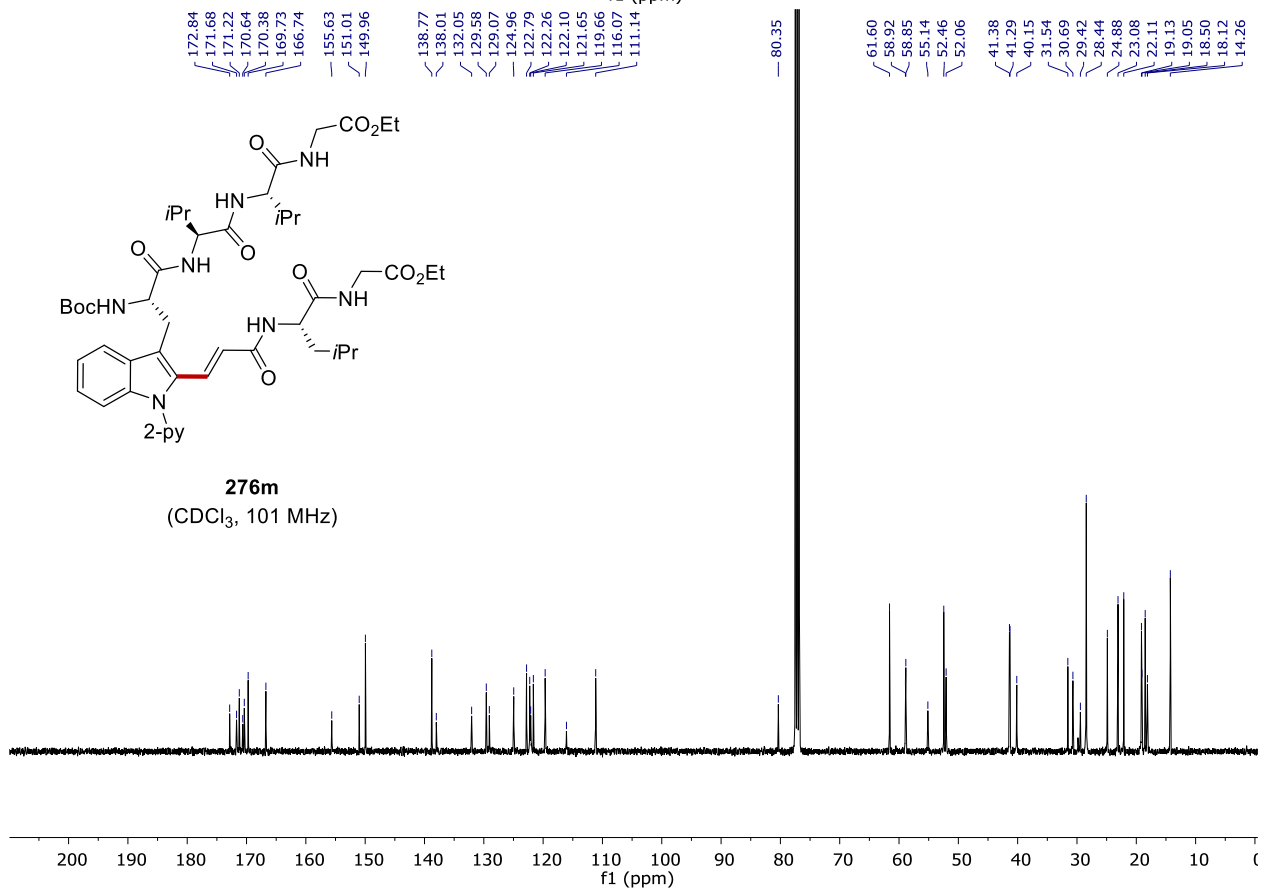




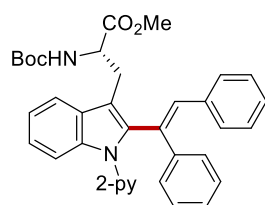
276m
(CDCl₃, 400 MHz)



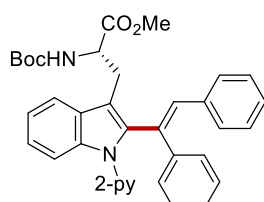
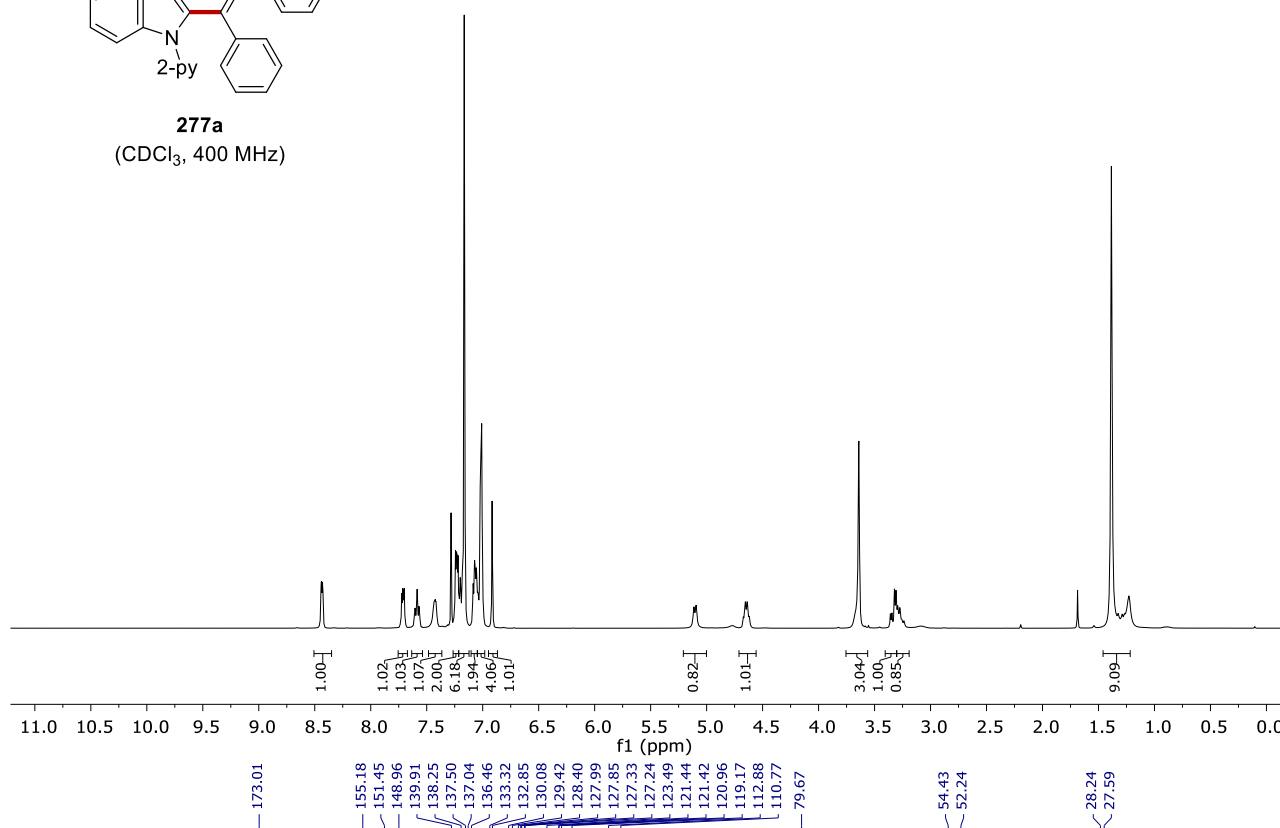
276m
(CDCl₃, 101 MHz)



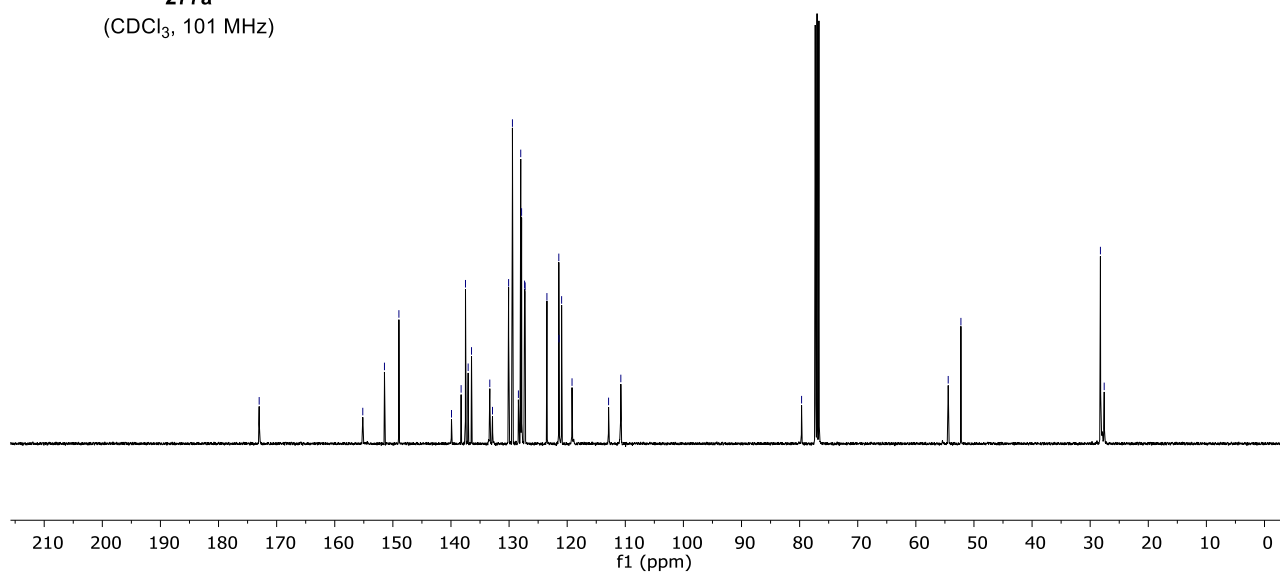
8. NMR Spectra

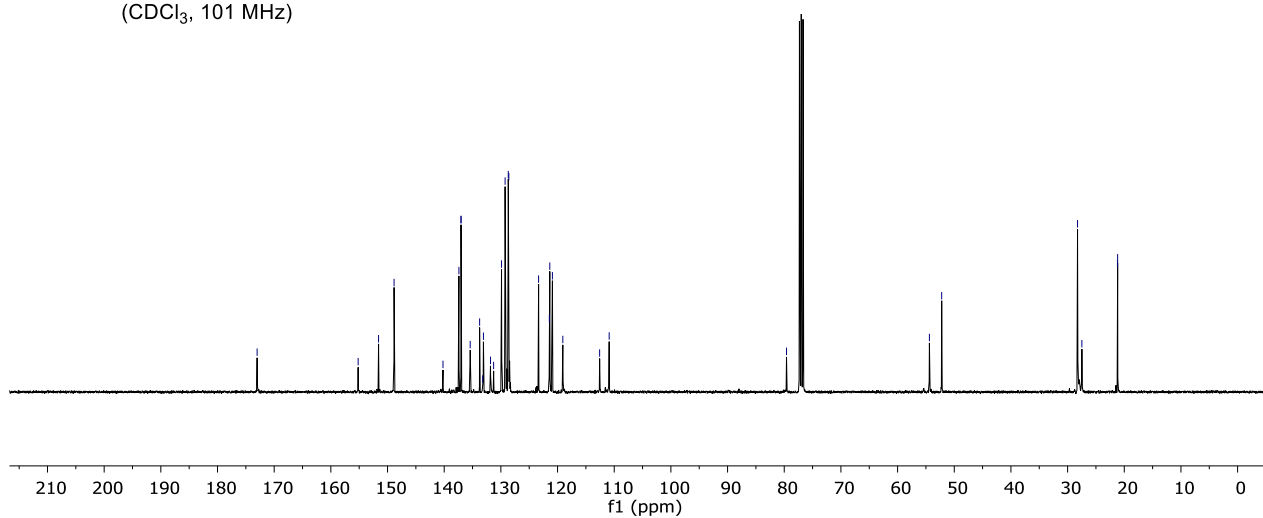
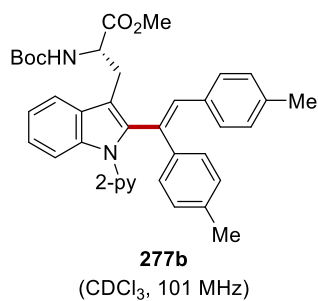
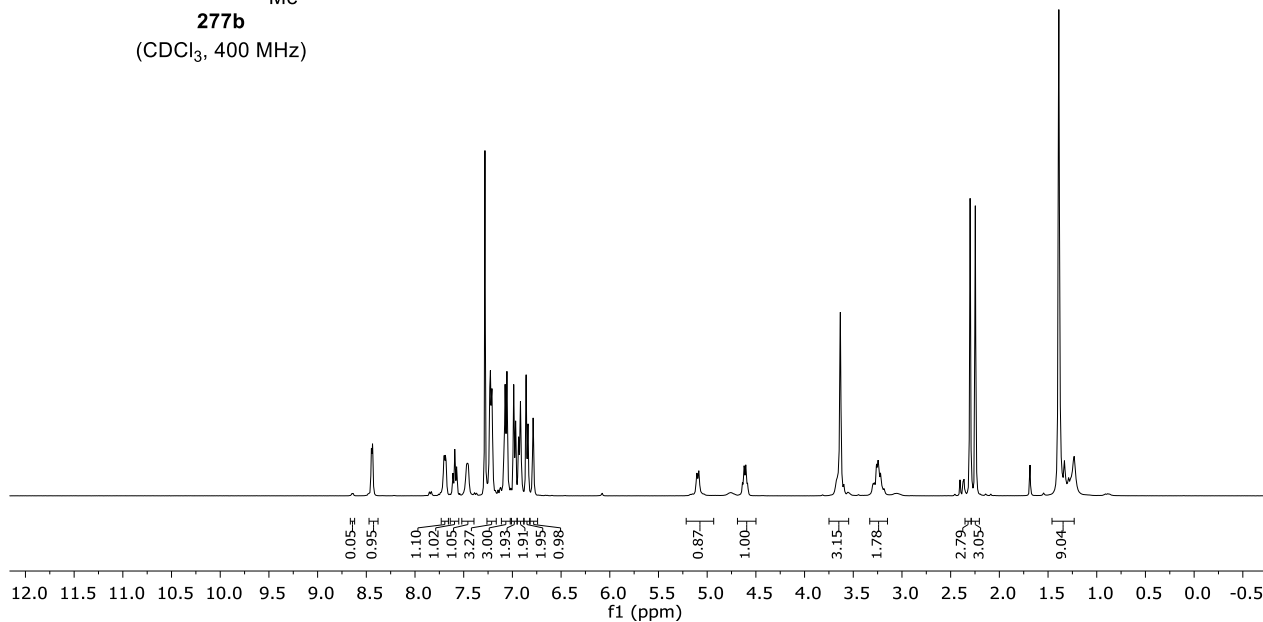
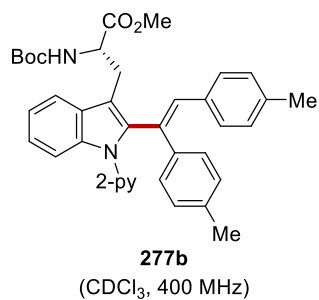


277a
(CDCl₃, 400 MHz)

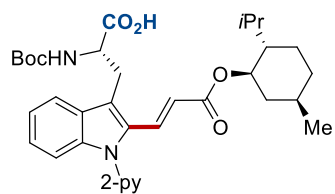


277a
(CDCl₃, 101 MHz)

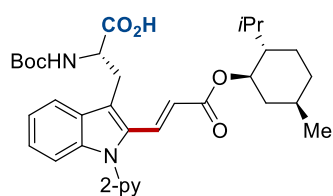
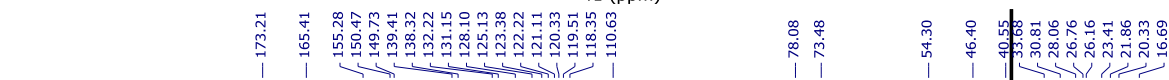
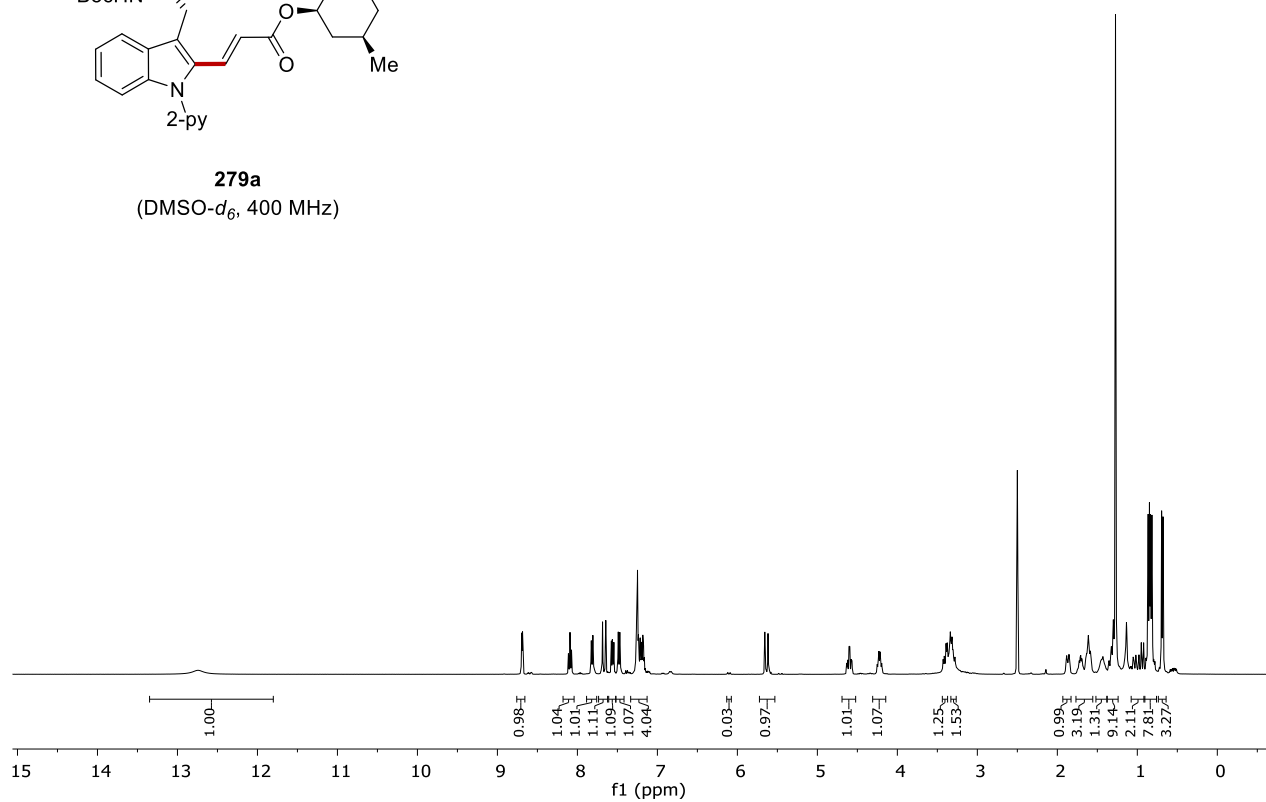




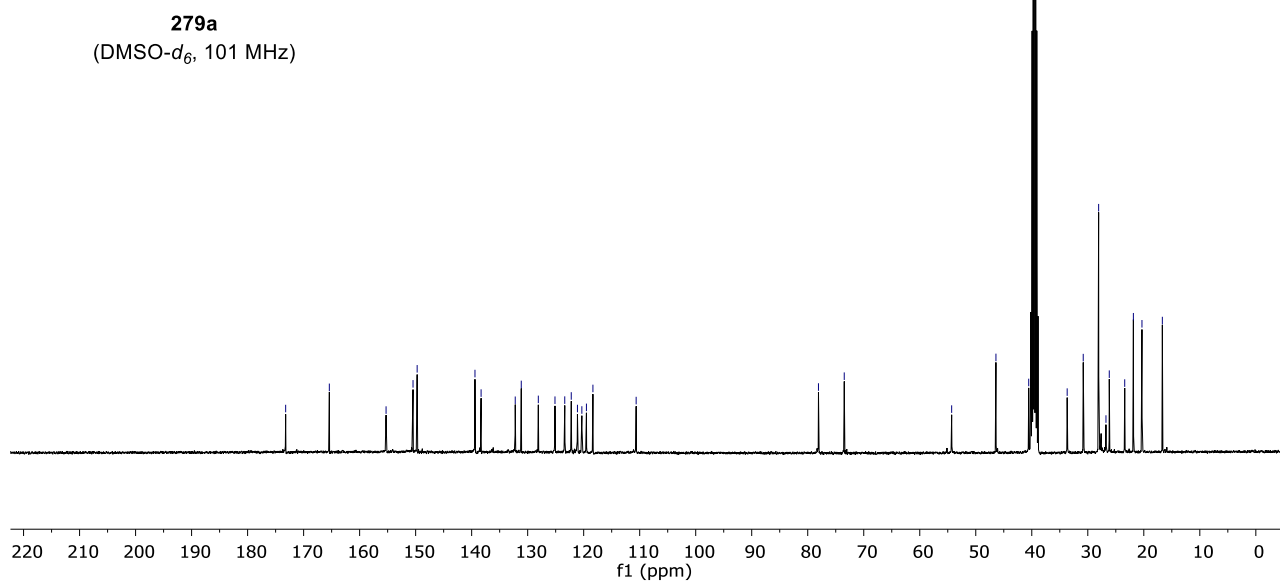
8. NMR Spectra

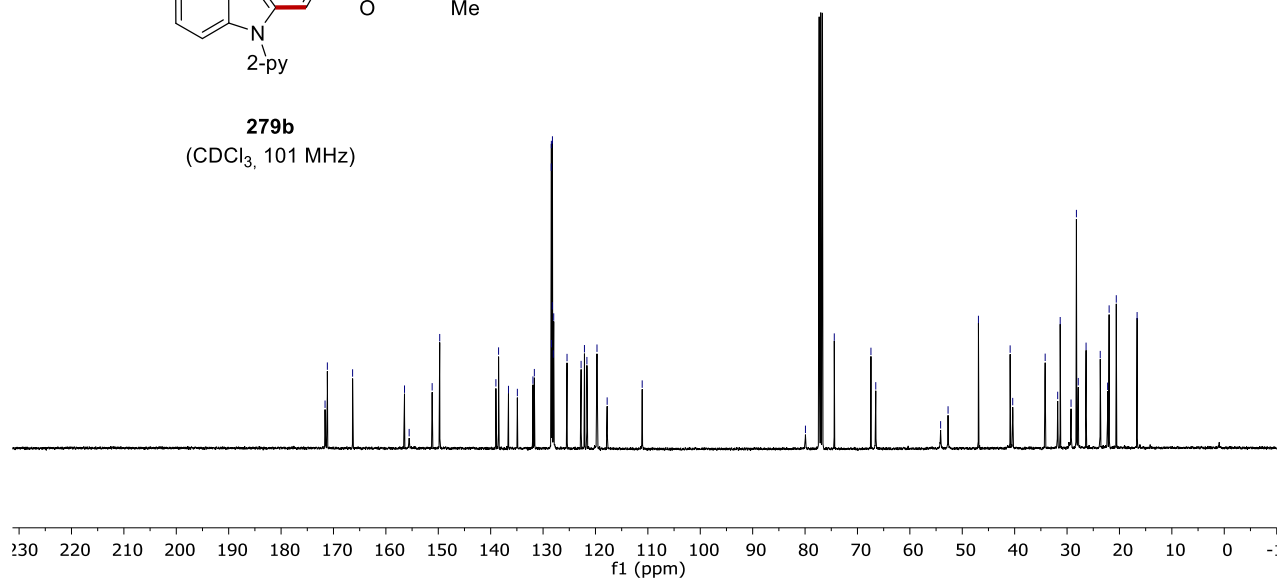
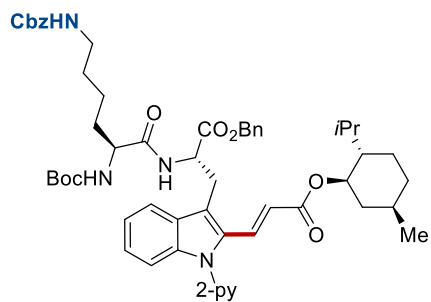
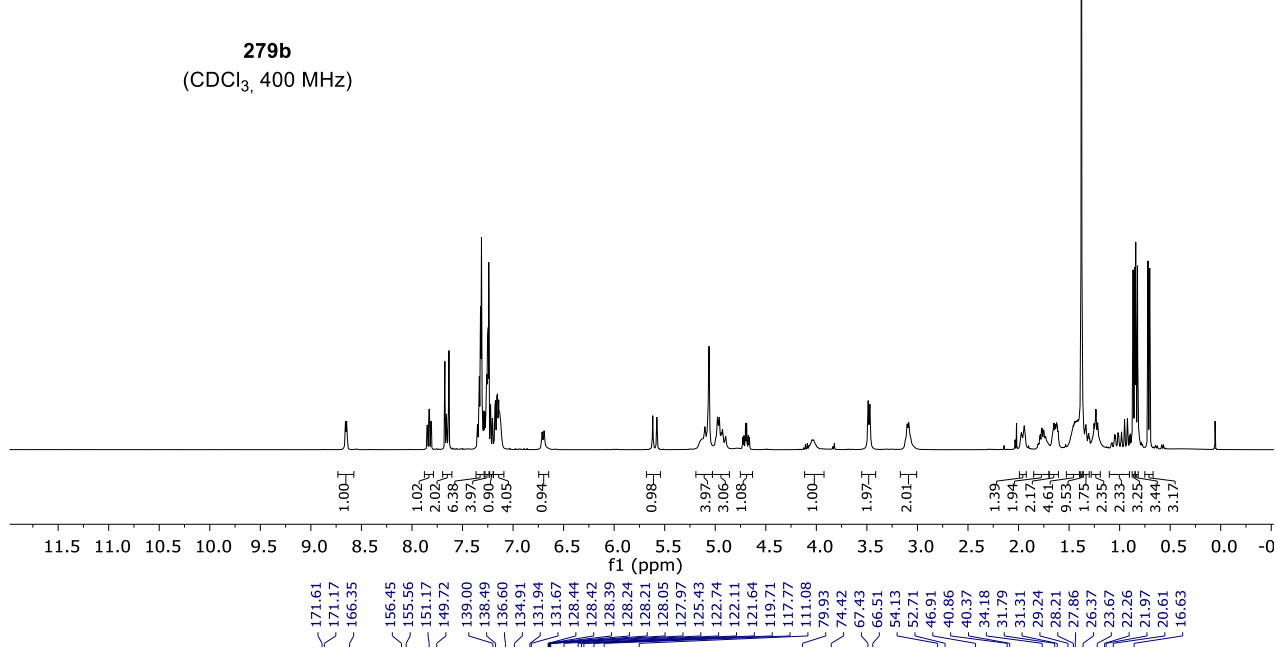
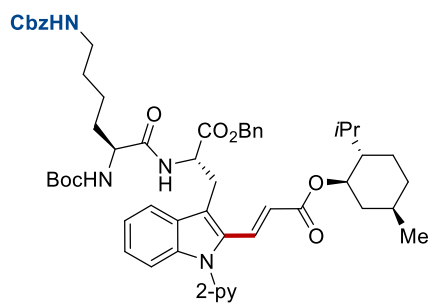


279a
(DMSO- d_6 , 400 MHz)

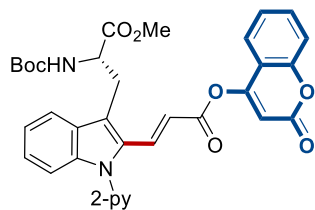


279a
(DMSO- d_6 , 101 MHz)

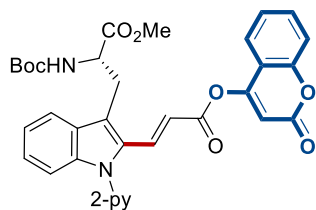
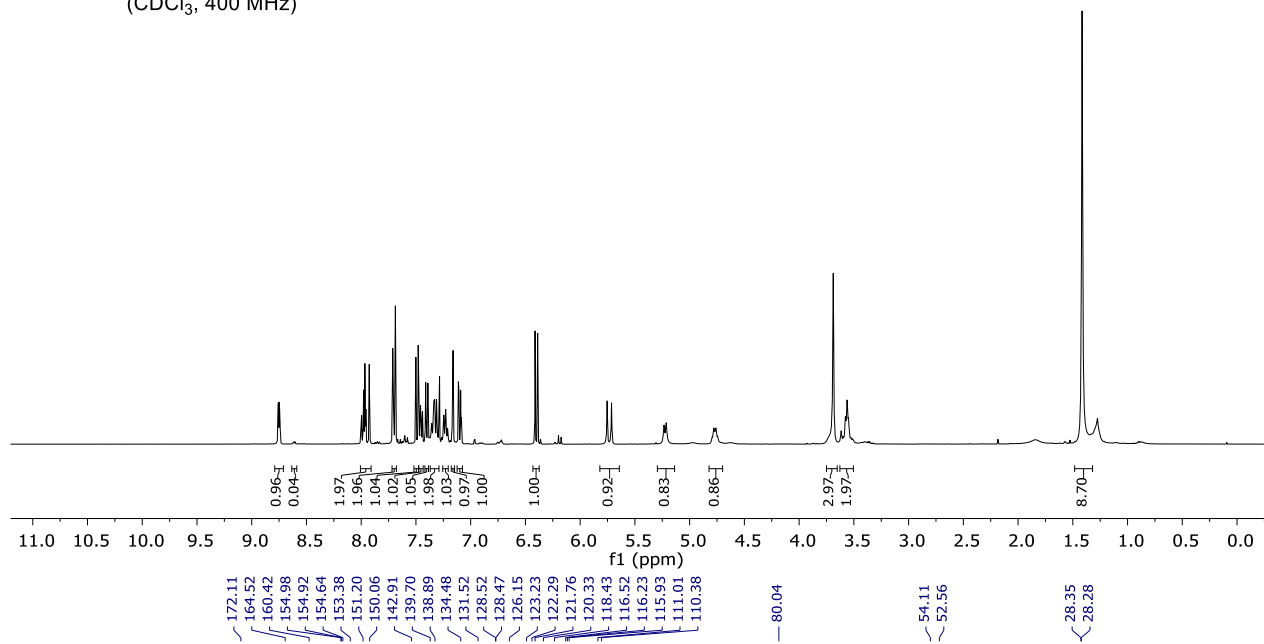




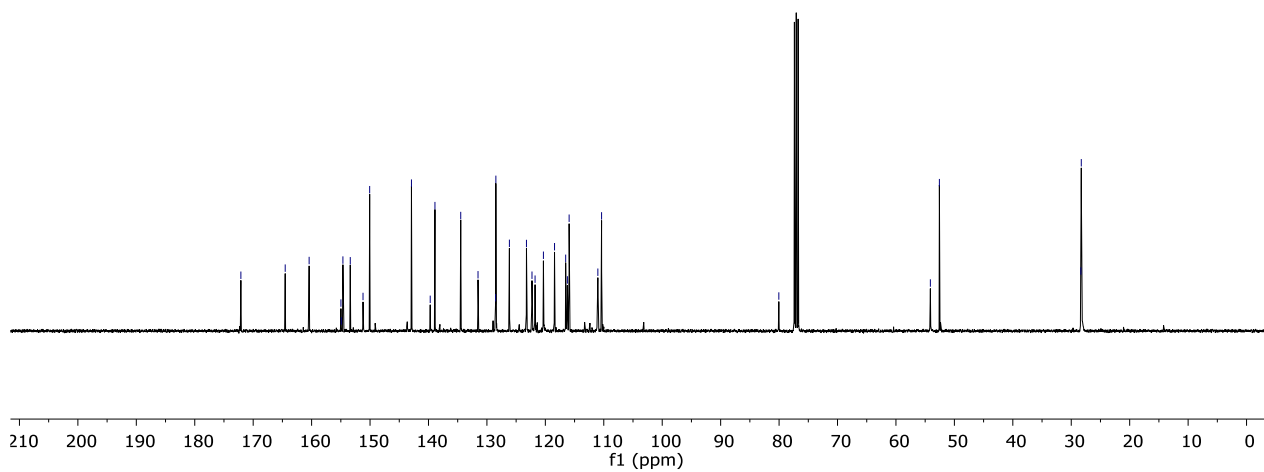
8. NMR Spectra

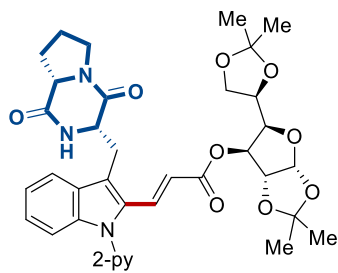


279c
(CDCl₃, 400 MHz)

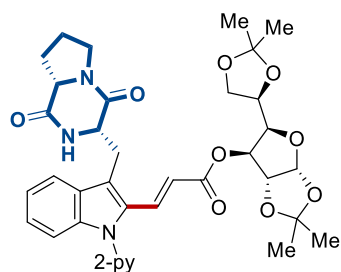
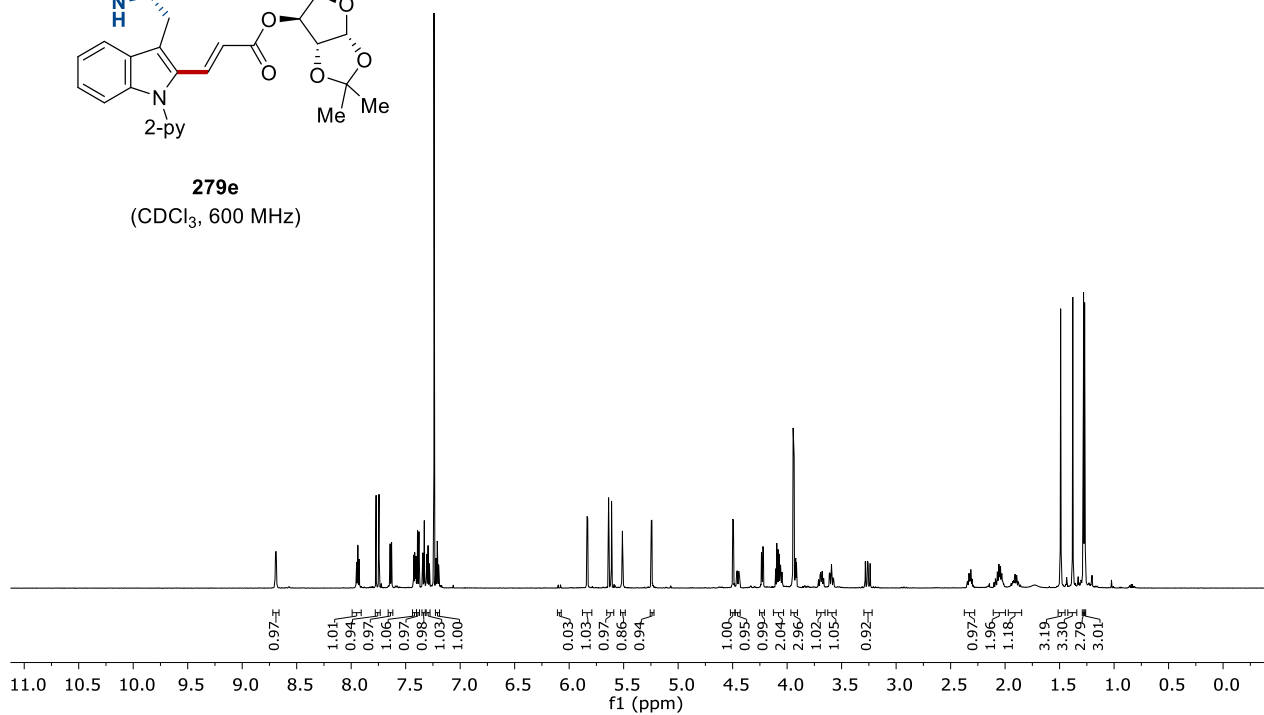


279d
(CDCl₃, 101 MHz)

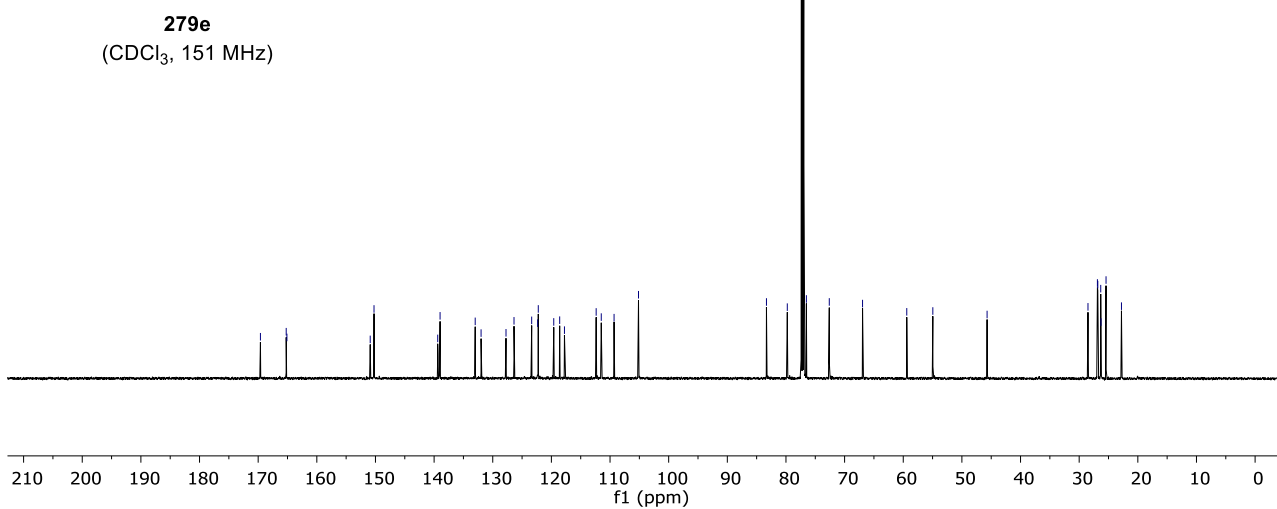




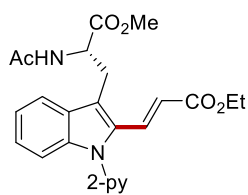
279e
(CDCl₃, 600 MHz)



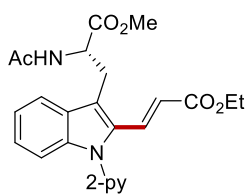
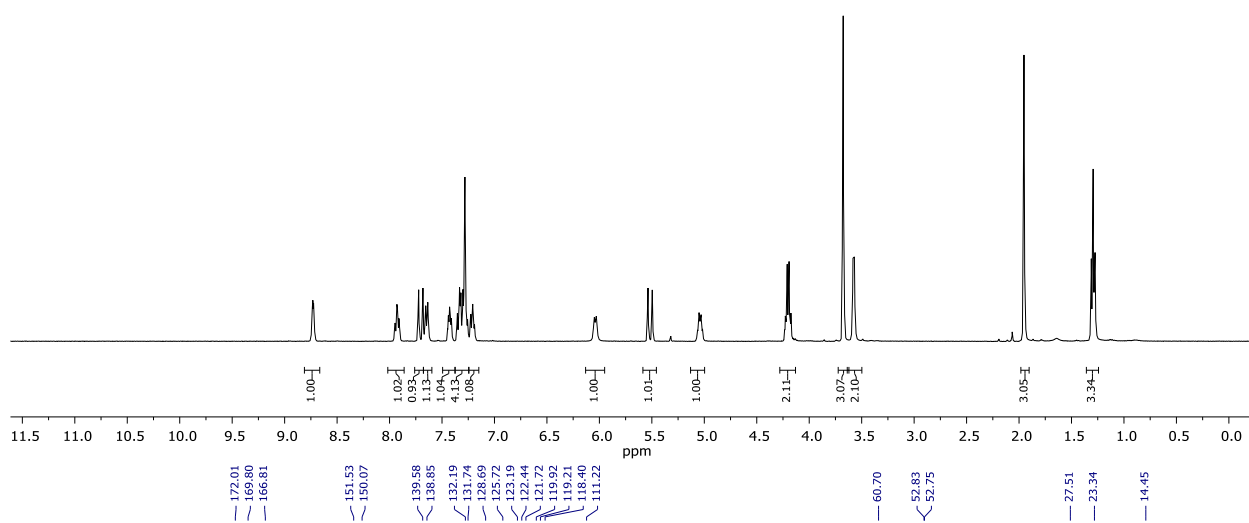
279e
(CDCl₃, 151 MHz)



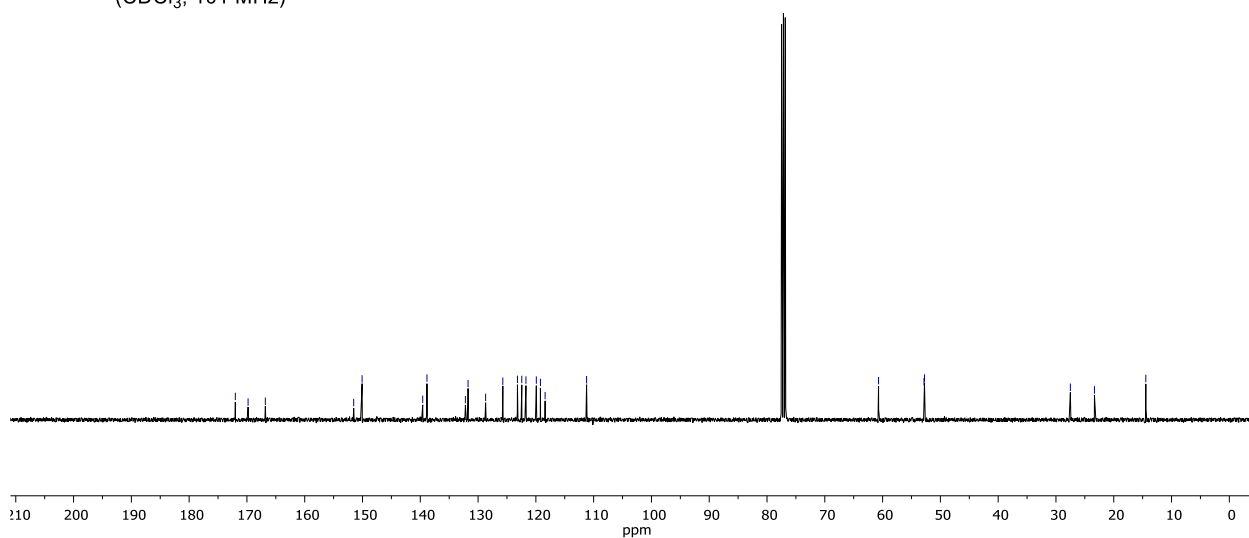
8. NMR Spectra



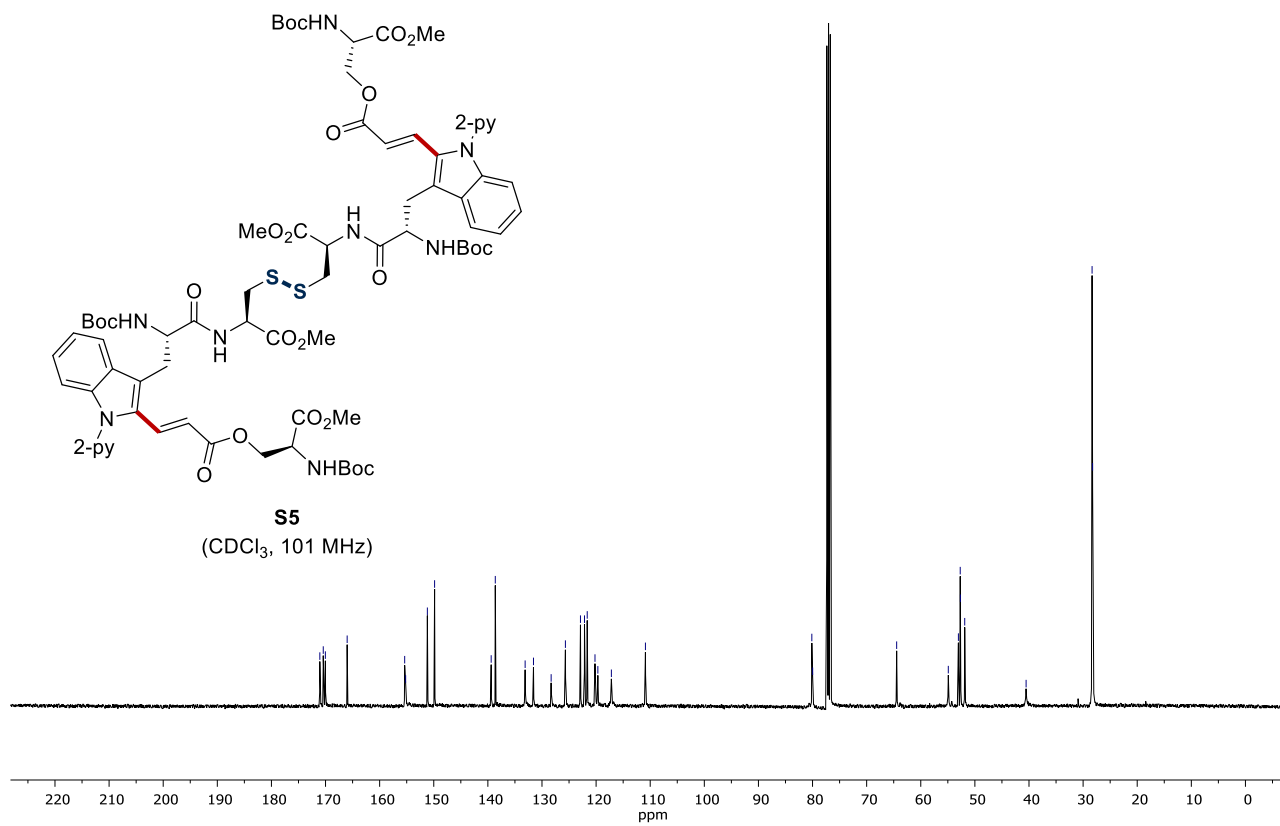
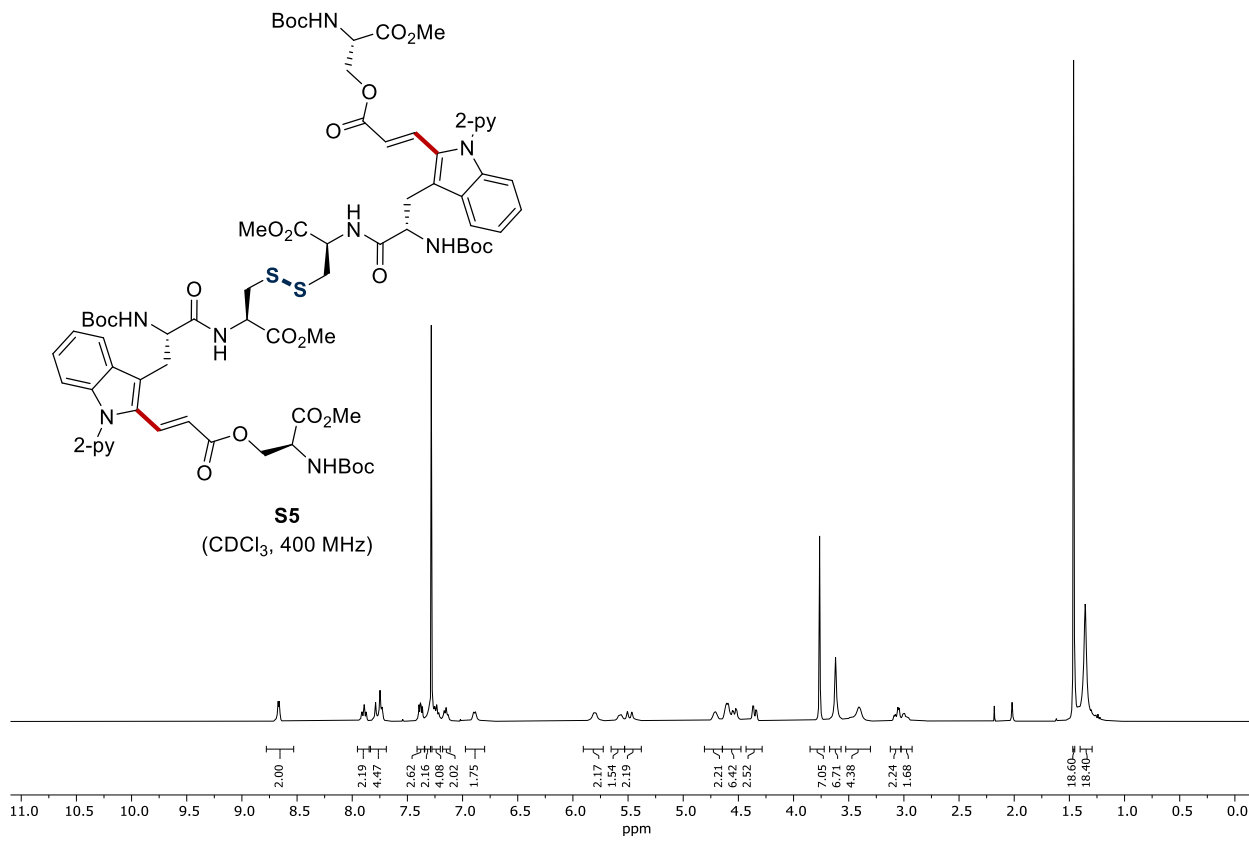
274e
(CDCl₃, 400 MHz)



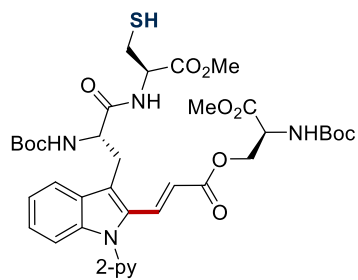
274e
(CDCl₃, 101 MHz)



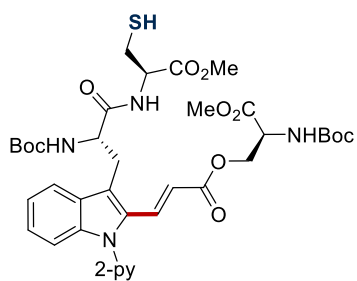
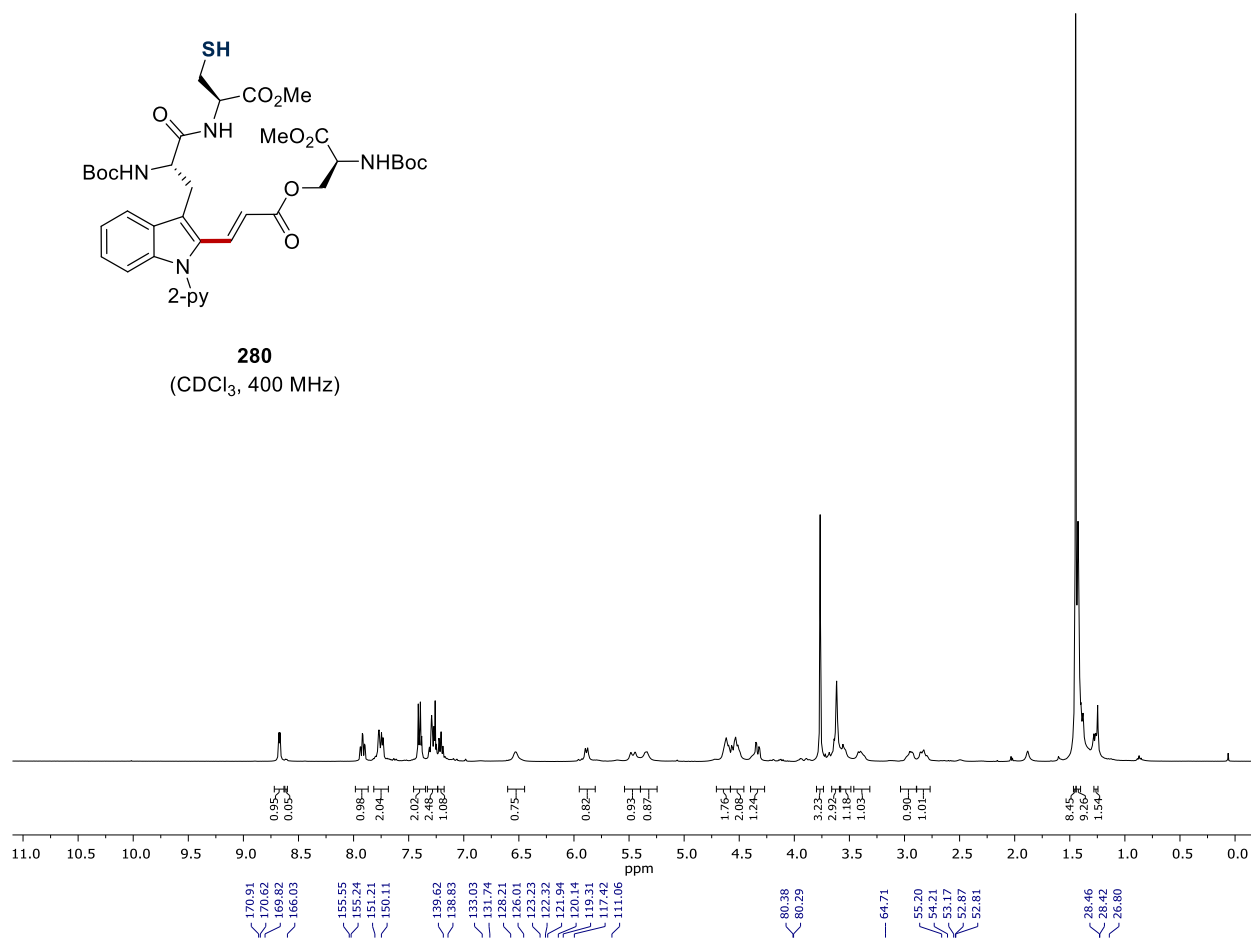
8. NMR Spectra



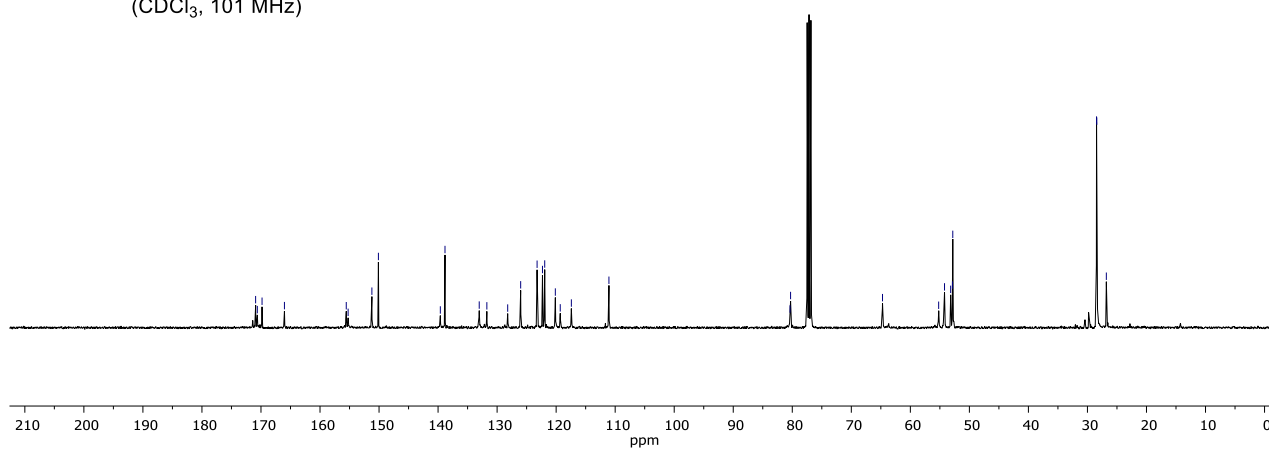
8. NMR Spectra



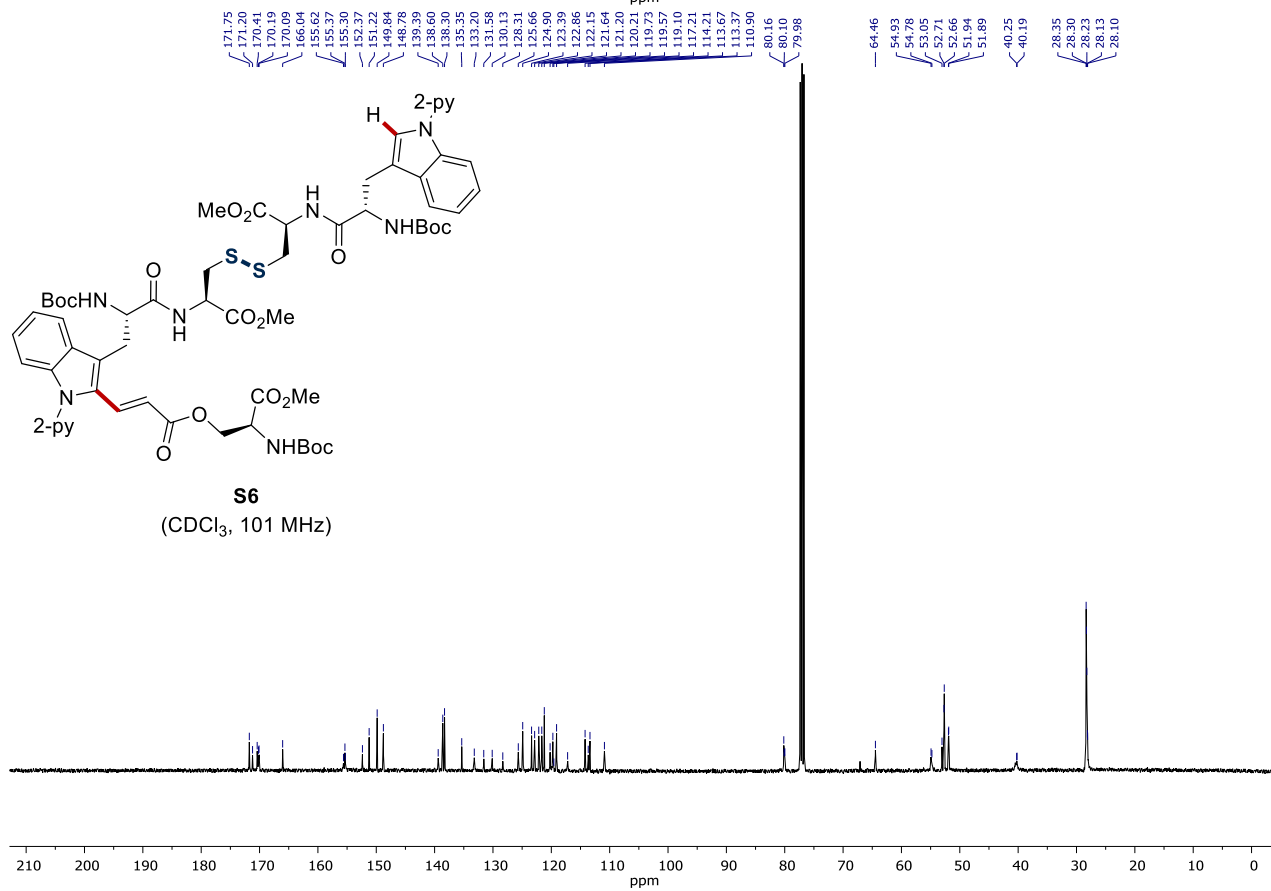
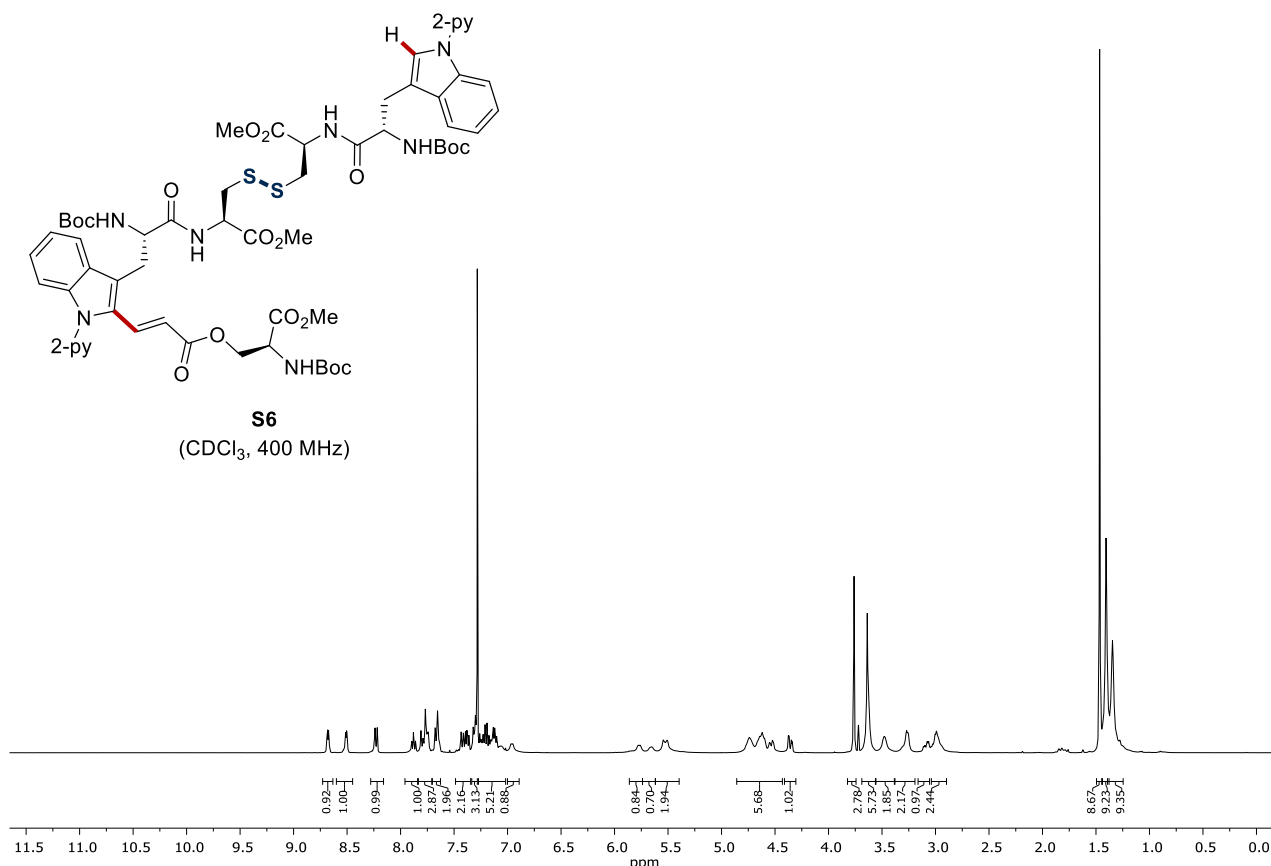
280
(CDCl₃, 400 MHz)



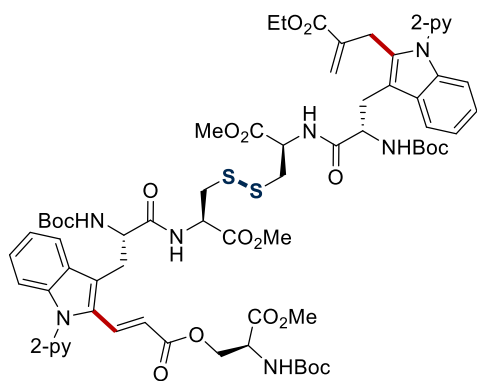
280
(CDCl₃, 101 MHz)



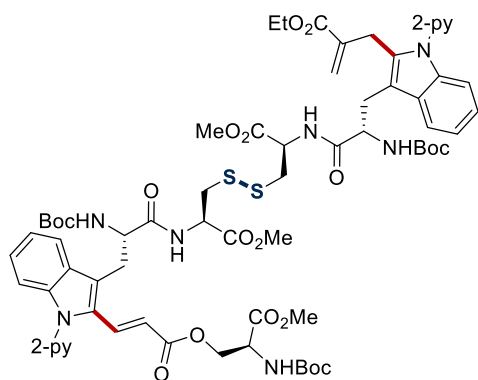
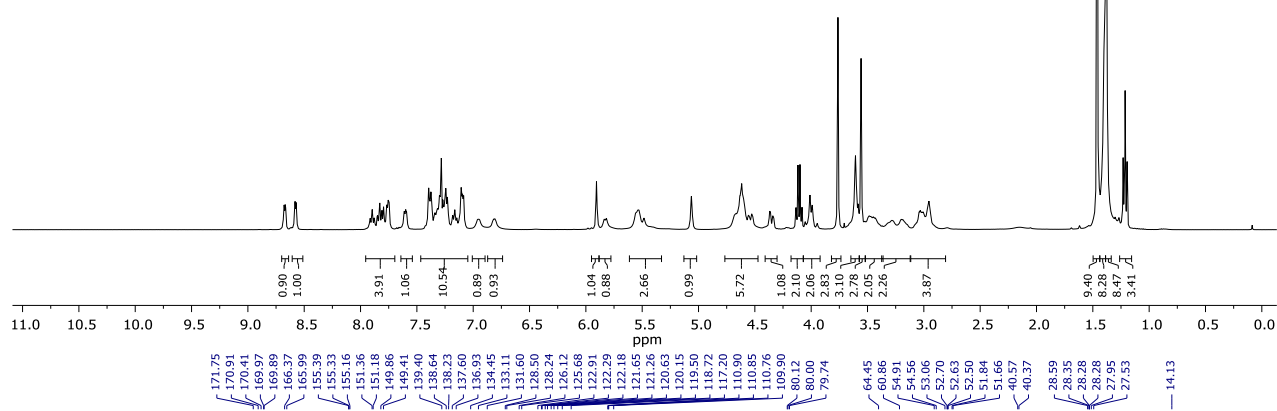
8. NMR Spectra



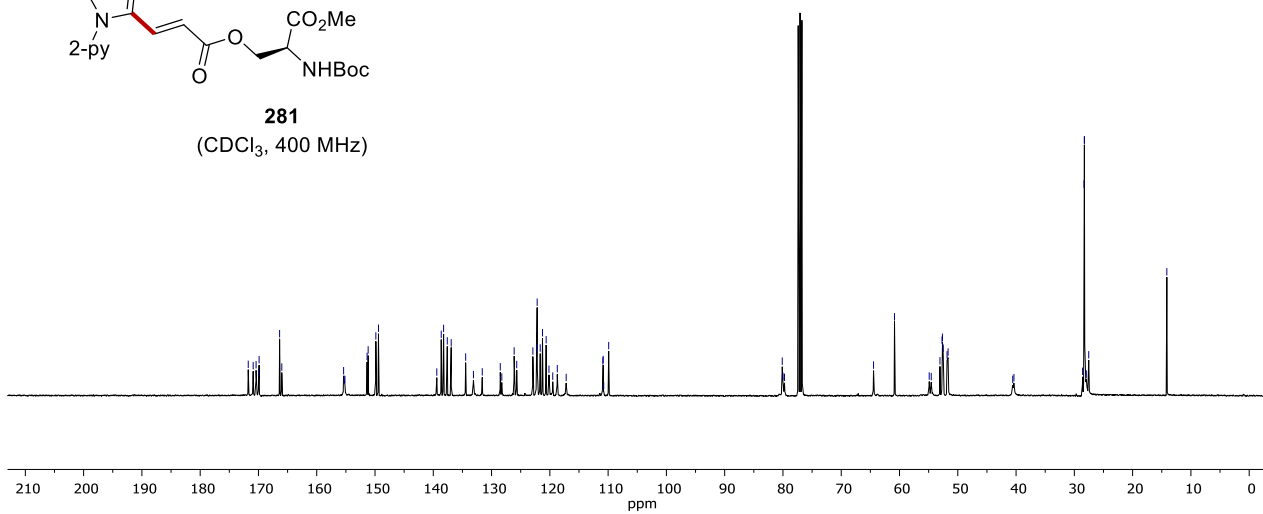
8. NMR Spectra

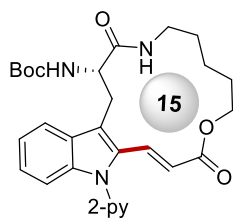


281
(CDCl₃, 400 MHz)

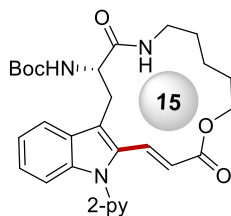
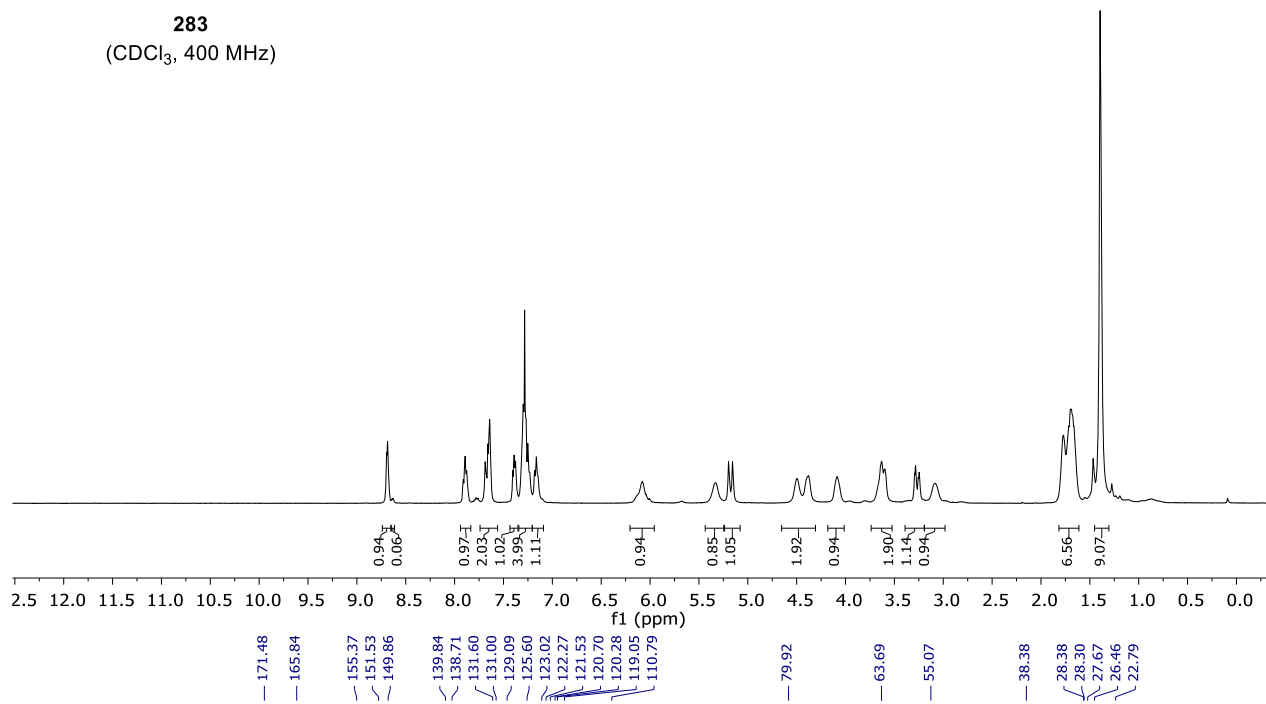


281
(CDCl₃, 400 MHz)

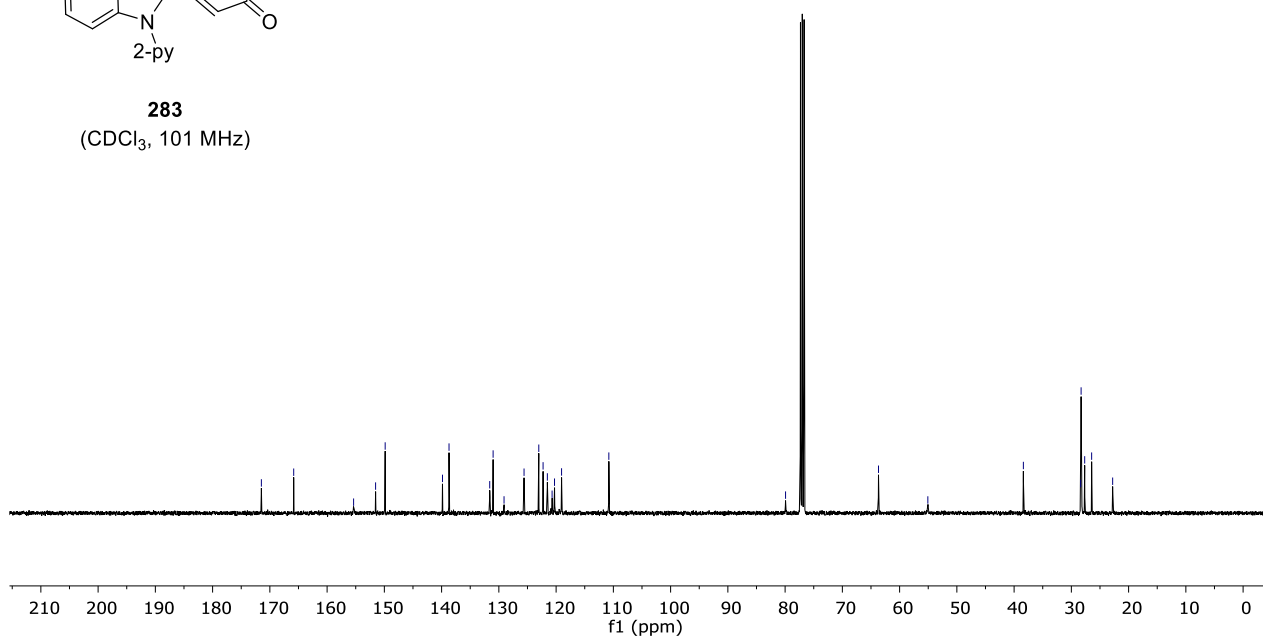




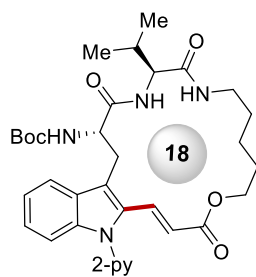
283
(CDCl₃, 400 MHz)



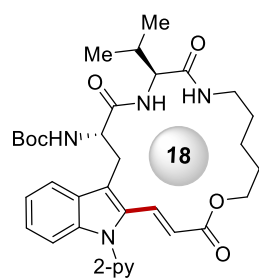
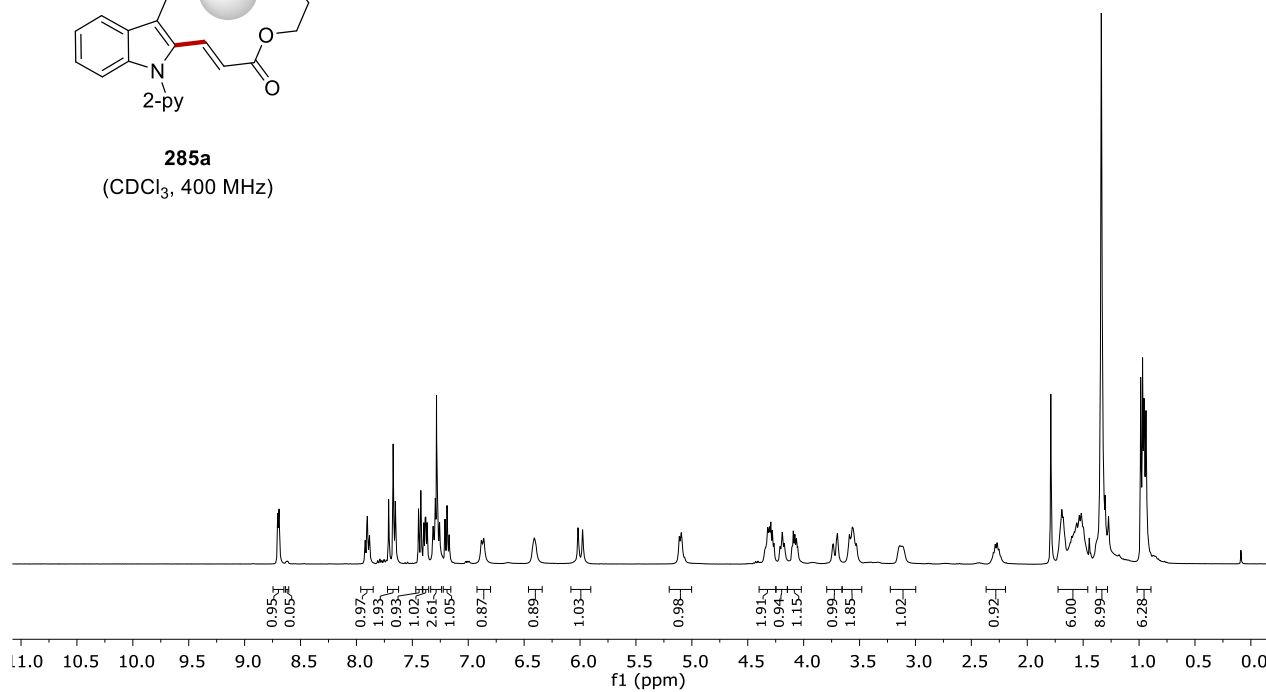
283
(CDCl₃, 101 MHz)



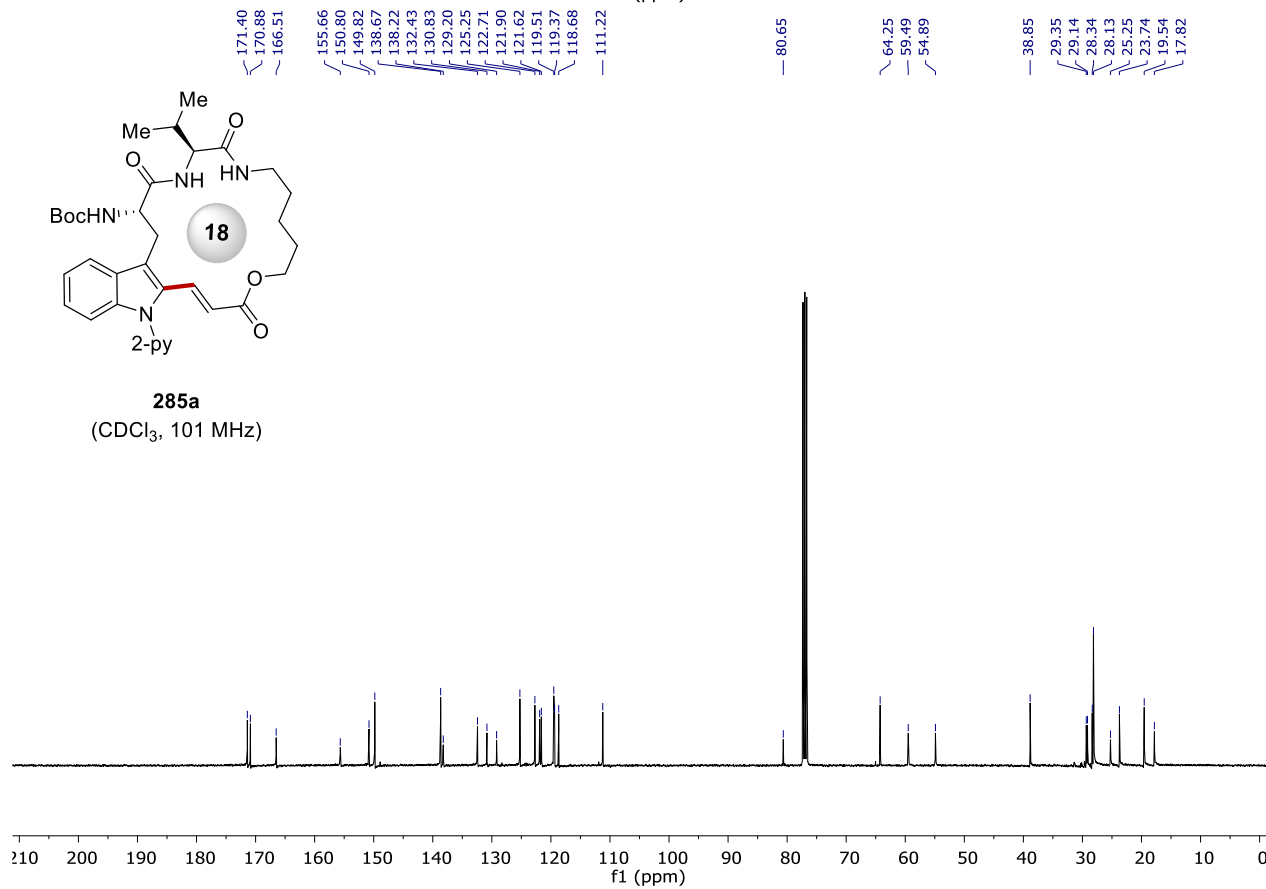
8. NMR Spectra

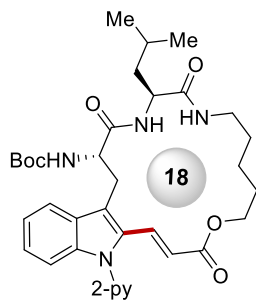


285a
(CDCl₃, 400 MHz)

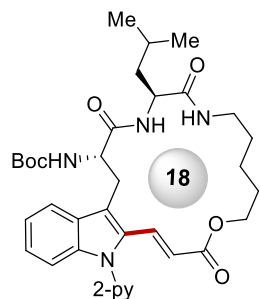
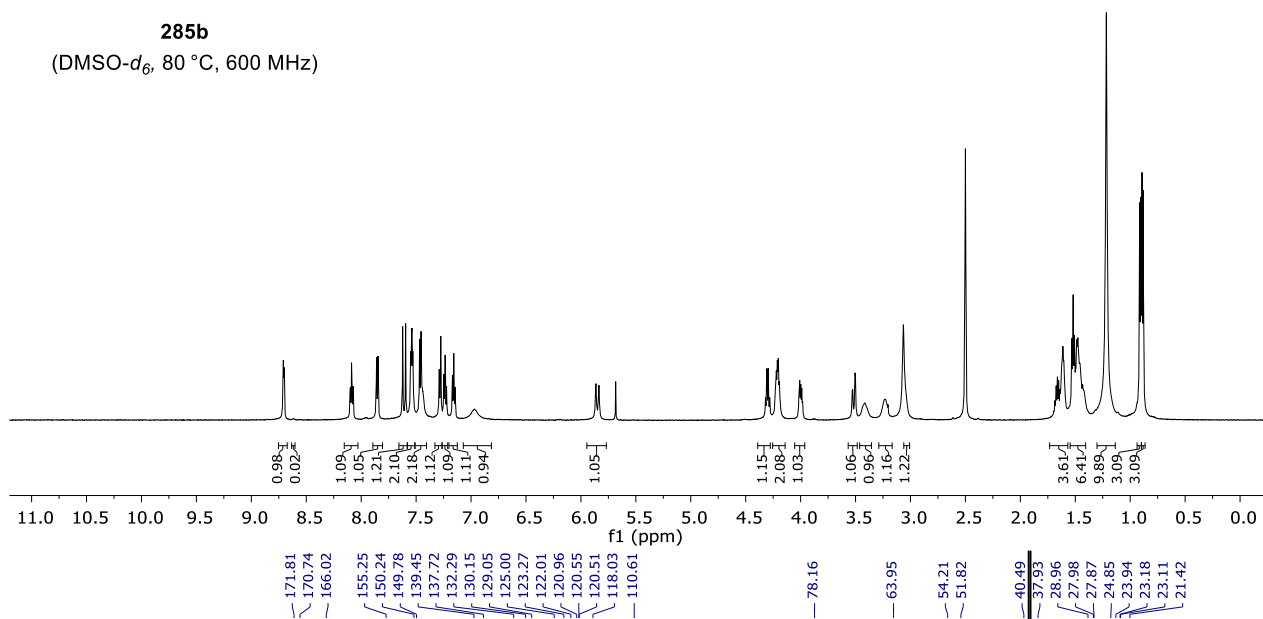


285a
(CDCl₃, 101 MHz)

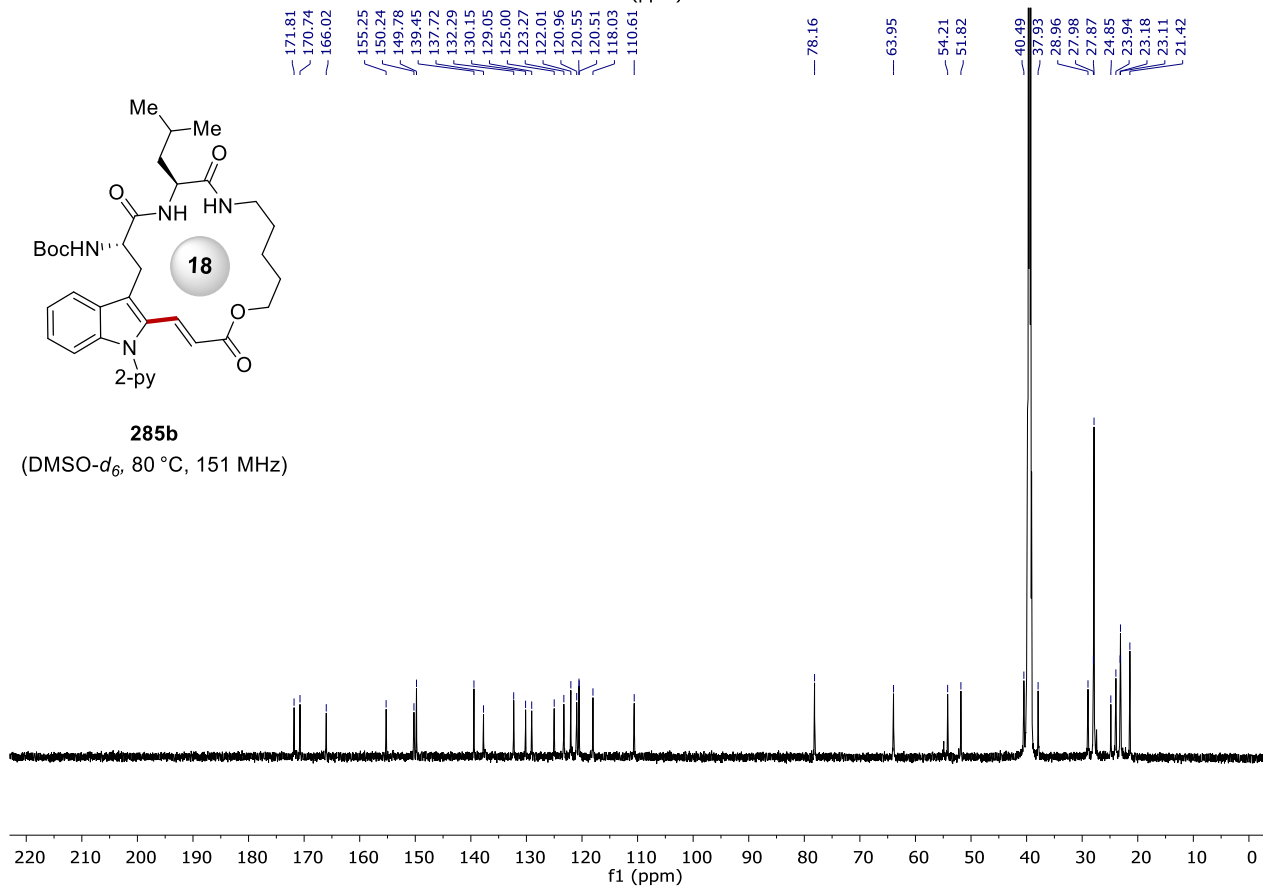




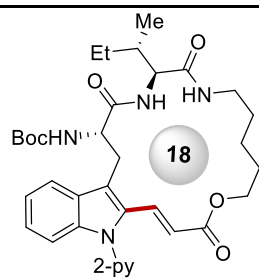
(DMSO- d_6 , 80 °C, 600 MHz)



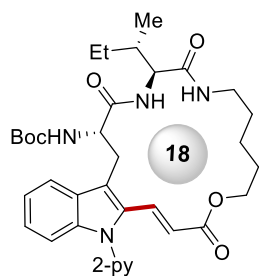
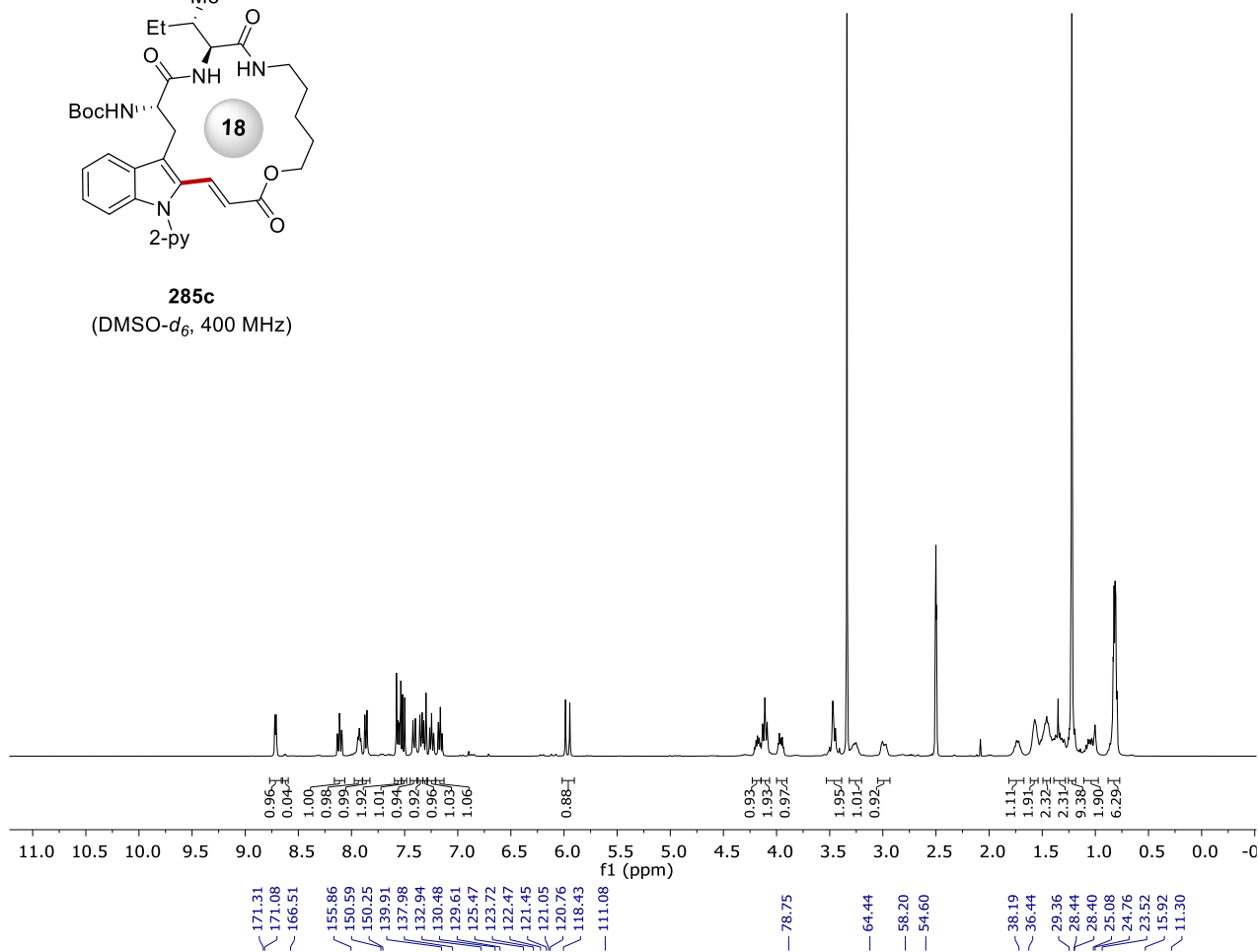
(DMSO- d_6 , 80 °C, 151 MHz)



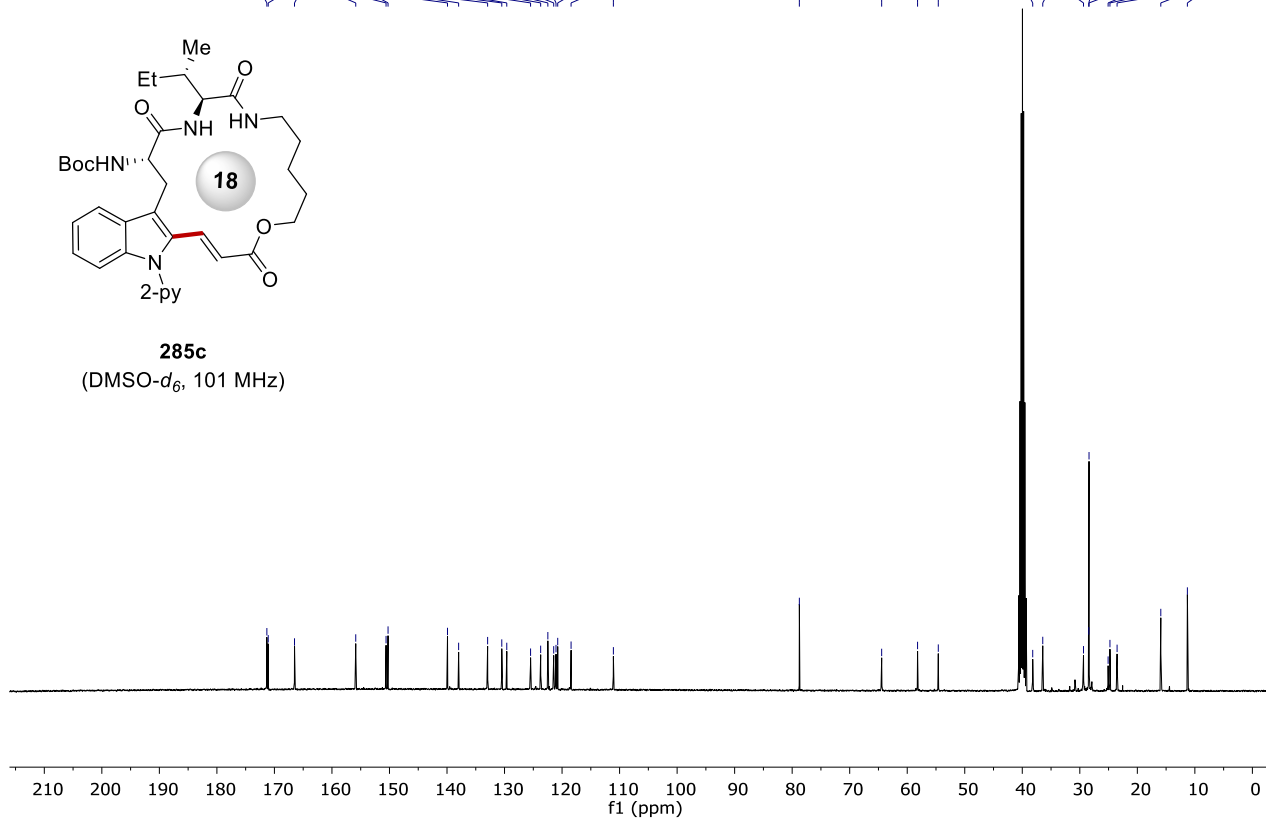
8. NMR Spectra

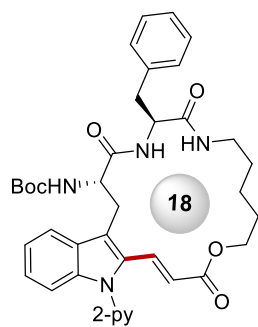


285c
(DMSO-*d*₆, 400 MHz)

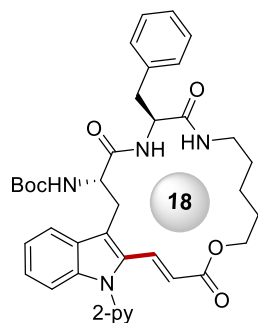
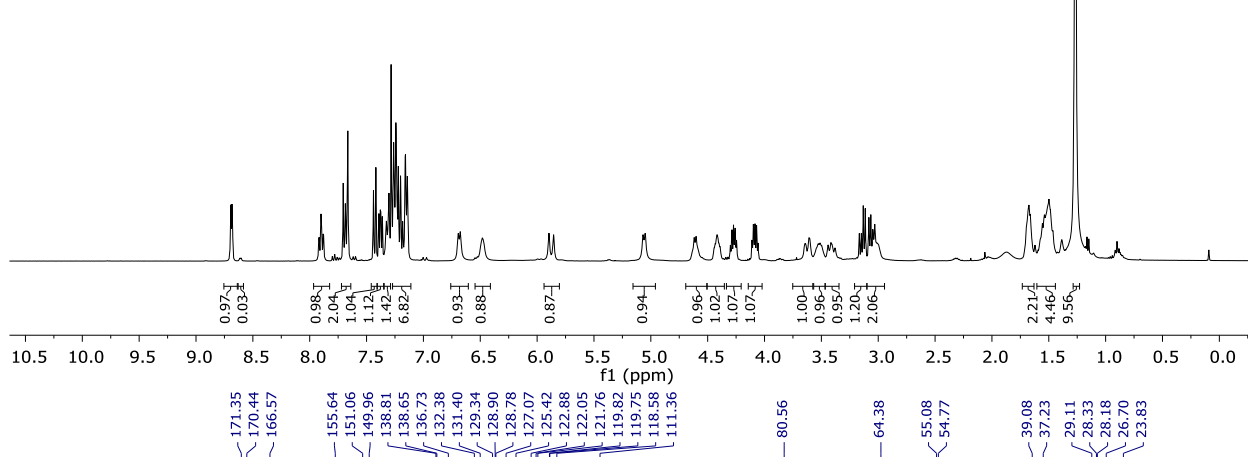


285c
(DMSO-*d*₆, 101 MHz)

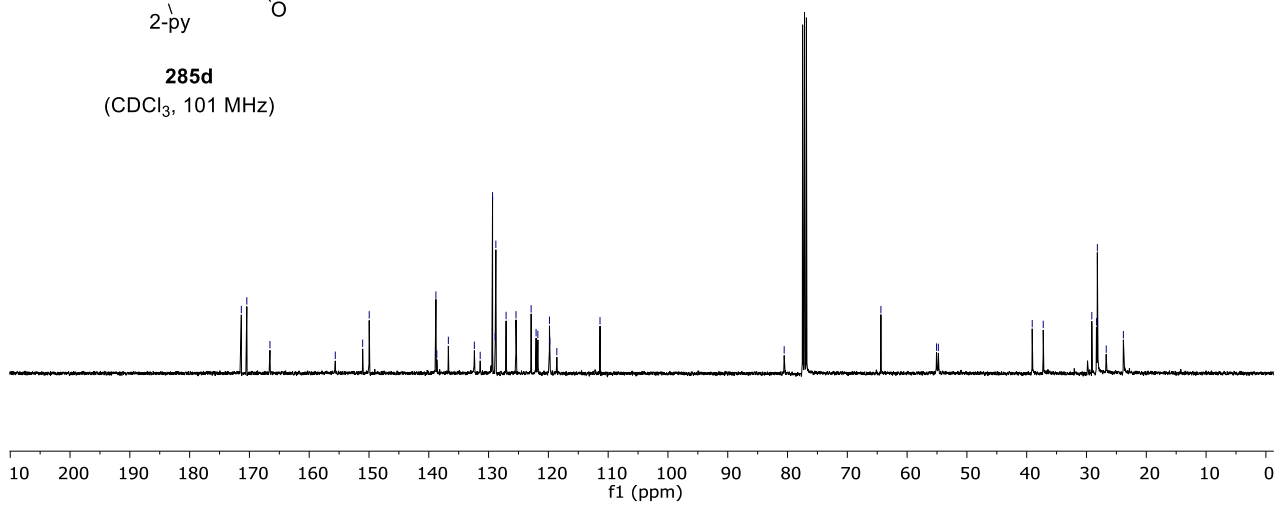




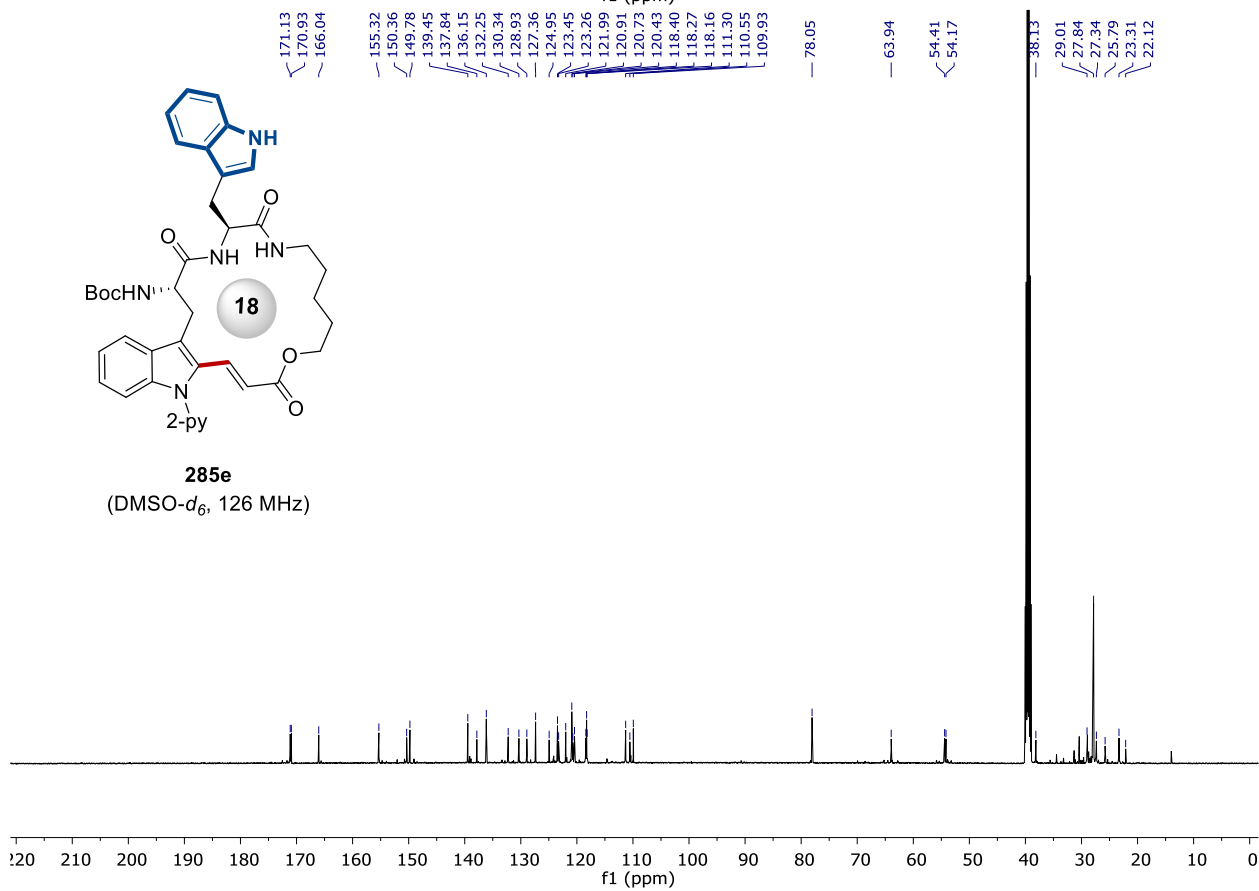
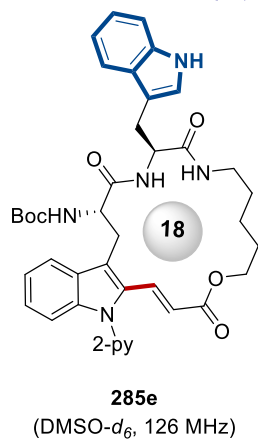
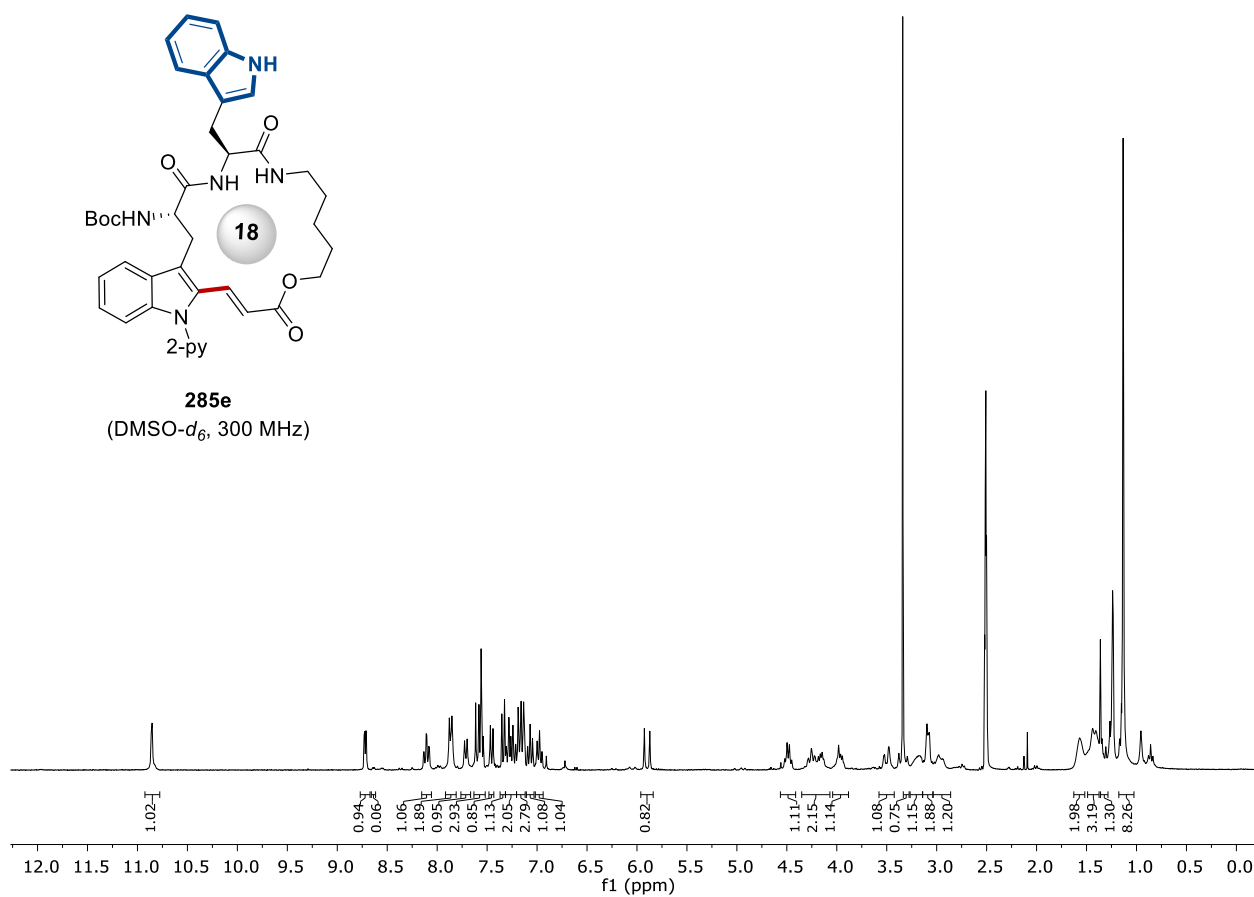
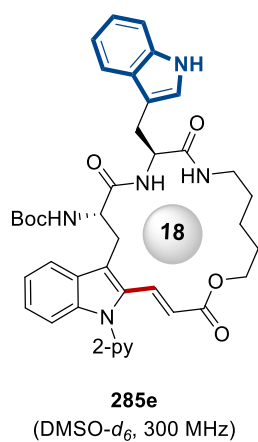
285d
(CDCl₃, 400 MHz)

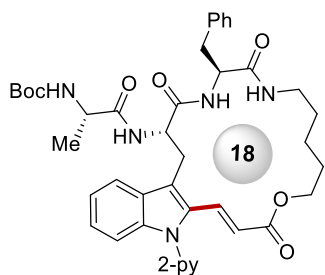


285d
(CDCl₃, 101 MHz)

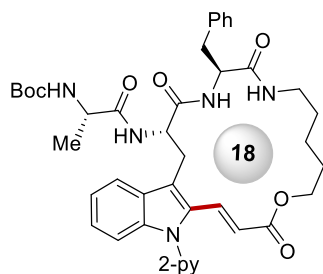
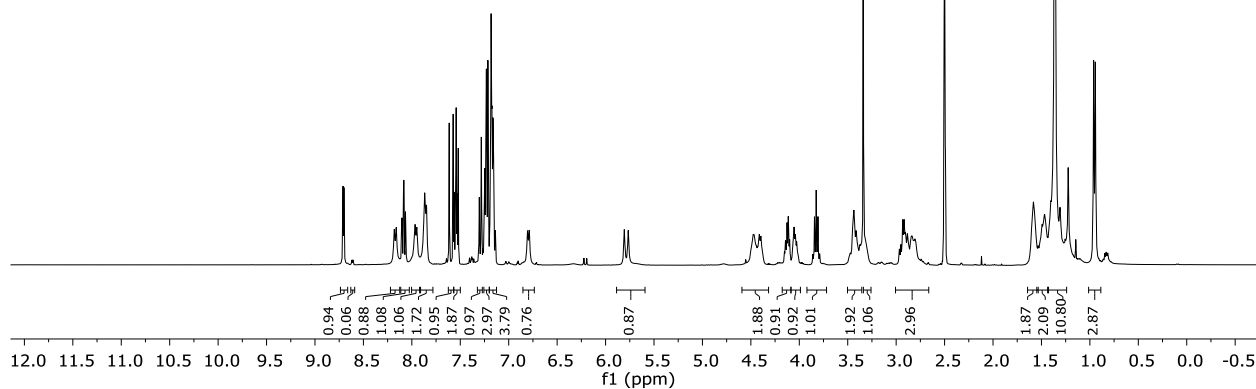


8. NMR Spectra

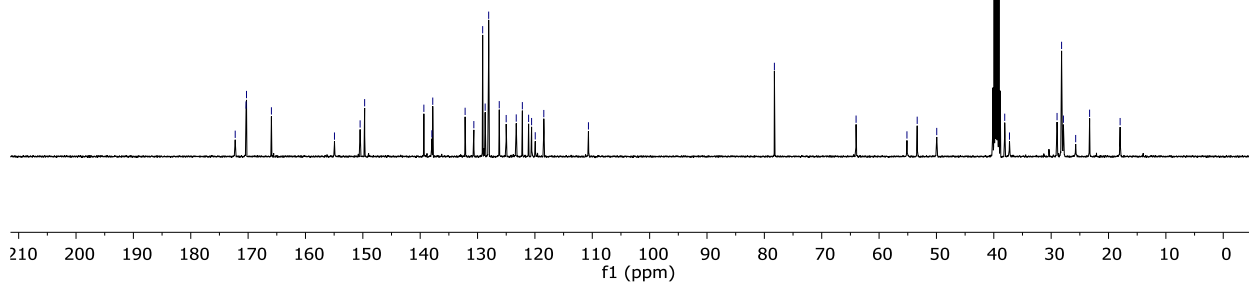




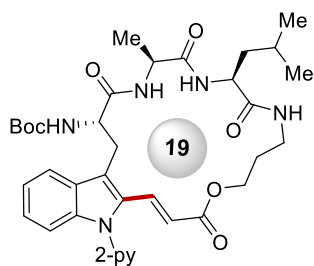
287a
(DMSO- d_6 , 400 MHz)



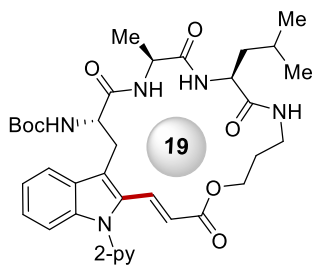
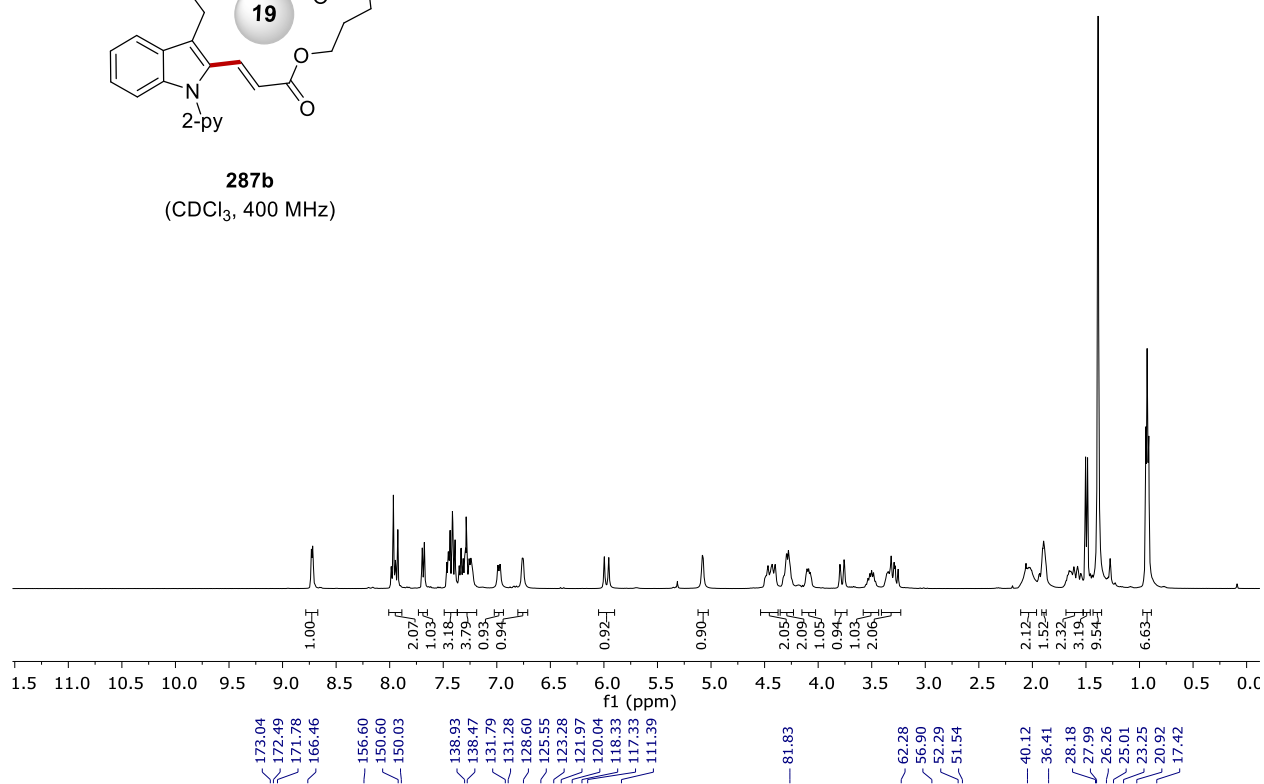
287a
(DMSO- d_6 , 101 MHz)



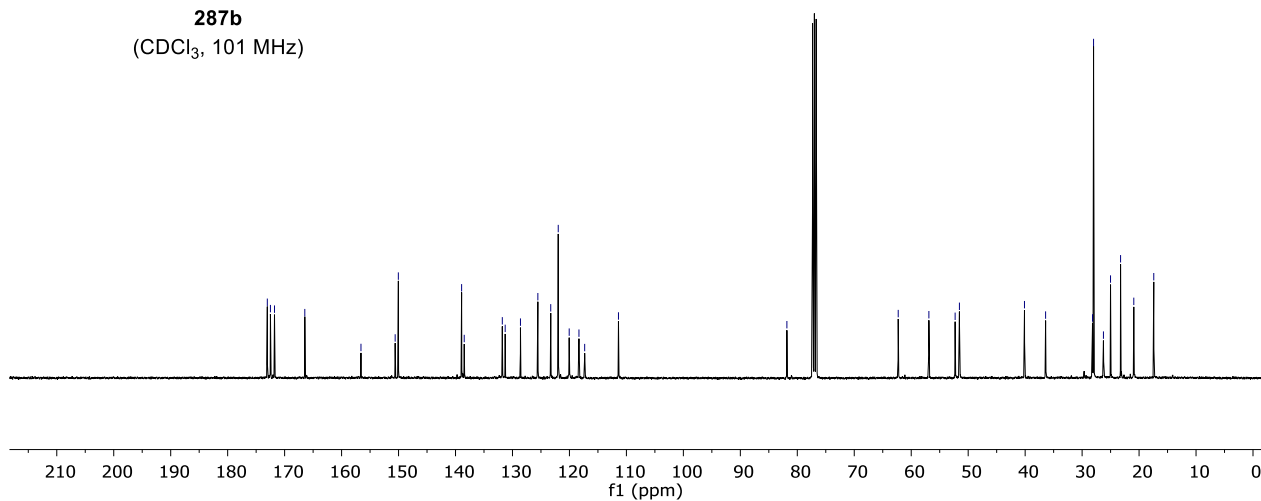
8. NMR Spectra

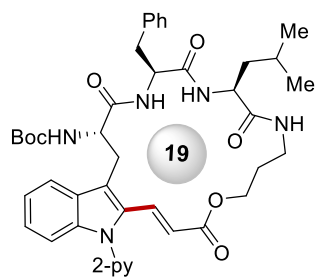


287b
(CDCl₃, 400 MHz)

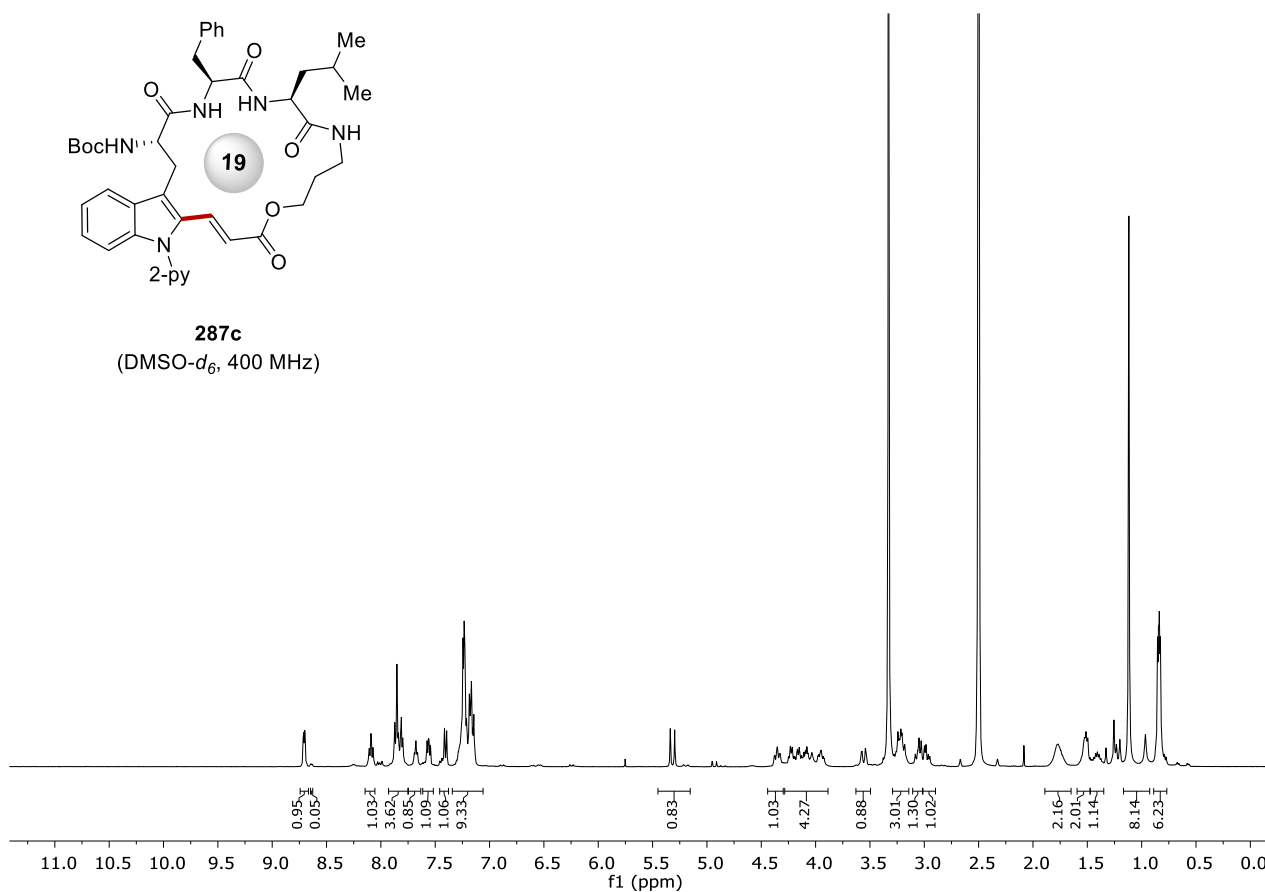


287b
(CDCl₃, 101 MHz)

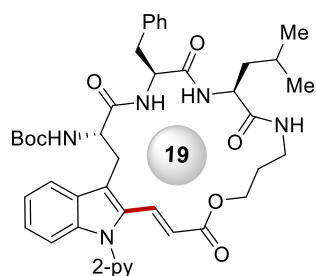




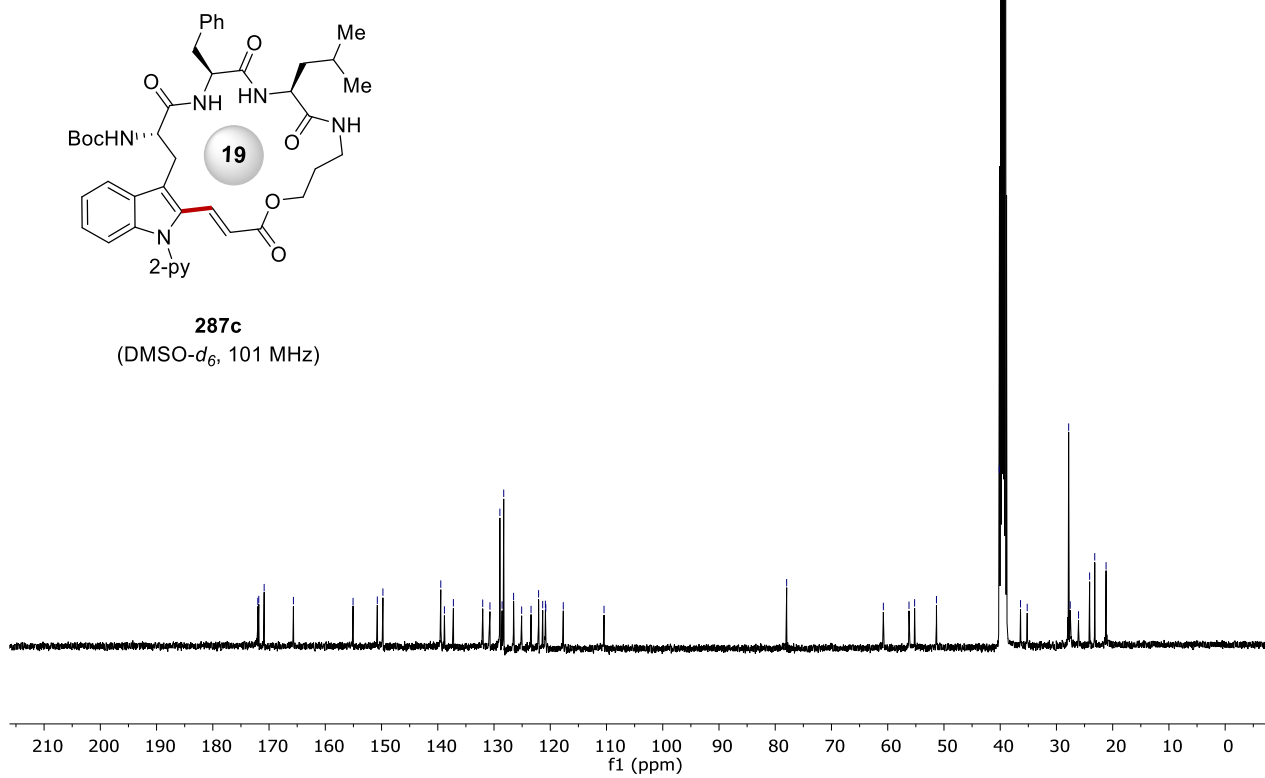
287c
(DMSO-*d*₆, 400 MHz)



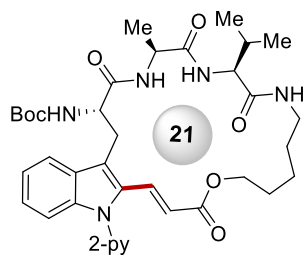
172.00
171.83
170.87
165.67
155.07
150.75
149.76
139.47
138.82
137.23
132.01
130.72
128.96
128.57
128.28
126.52
125.09
123.42
122.08
121.35
120.80
120.87
117.69
110.44
77.97
60.77
56.22
55.22
51.33
40.17
36.39
35.20
27.83
27.55
26.07
24.10
23.19
21.18



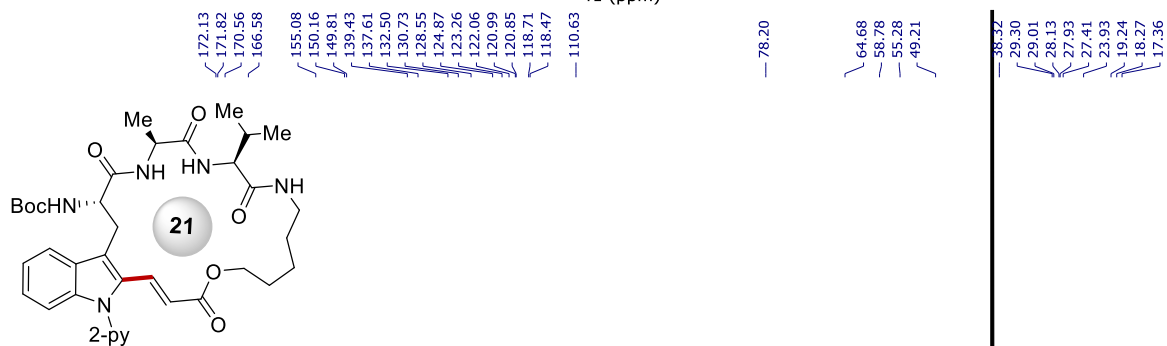
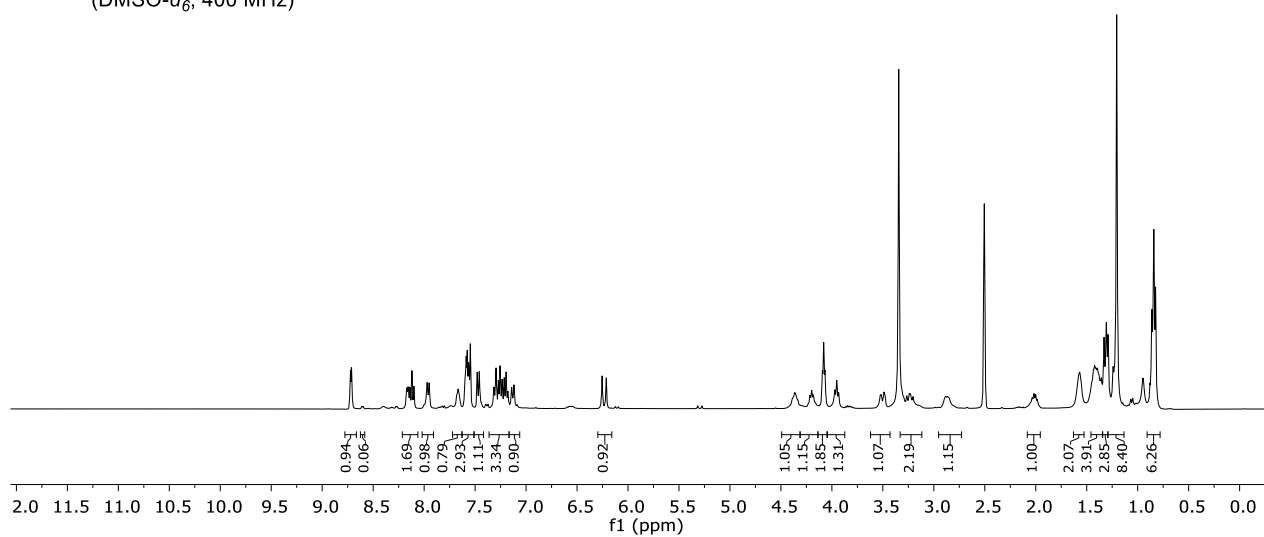
287c
(DMSO-*d*₆, 101 MHz)



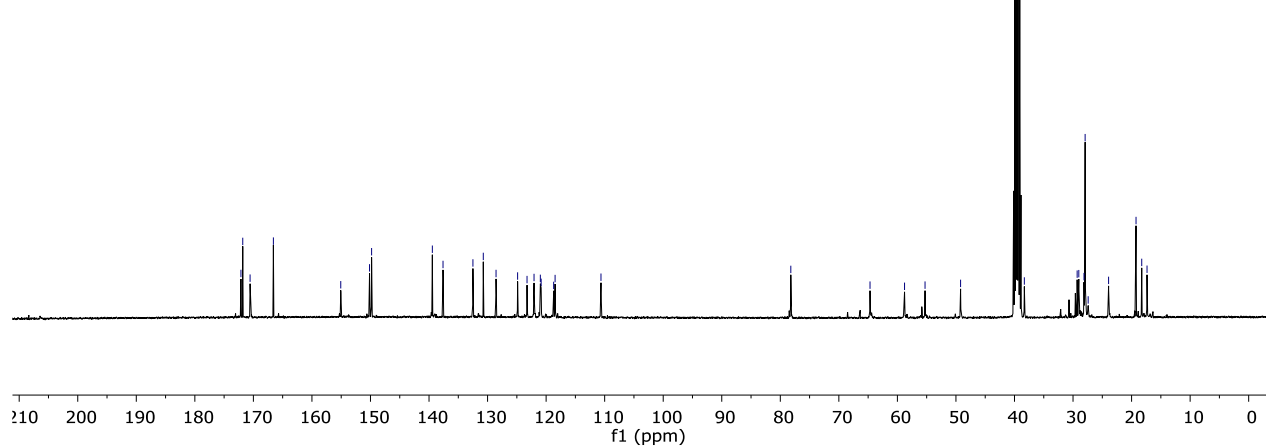
8. NMR Spectra

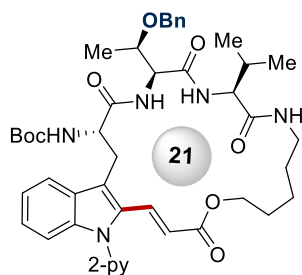


287d
(DMSO- d_6 , 400 MHz)

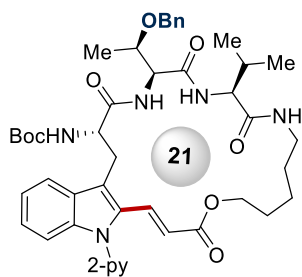
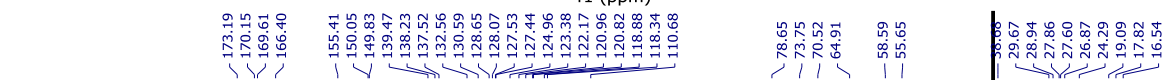
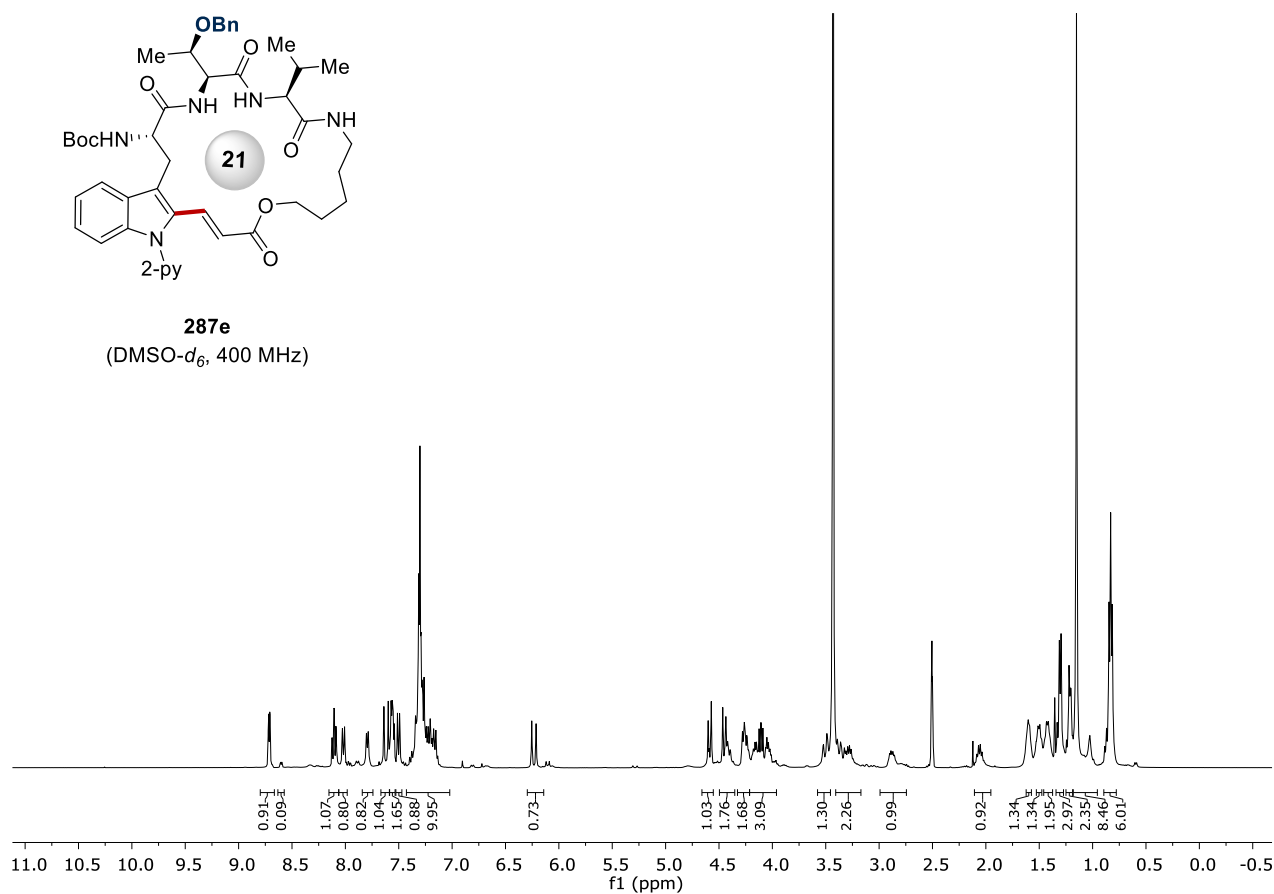


287d
(DMSO- d_6 , 101MHz)

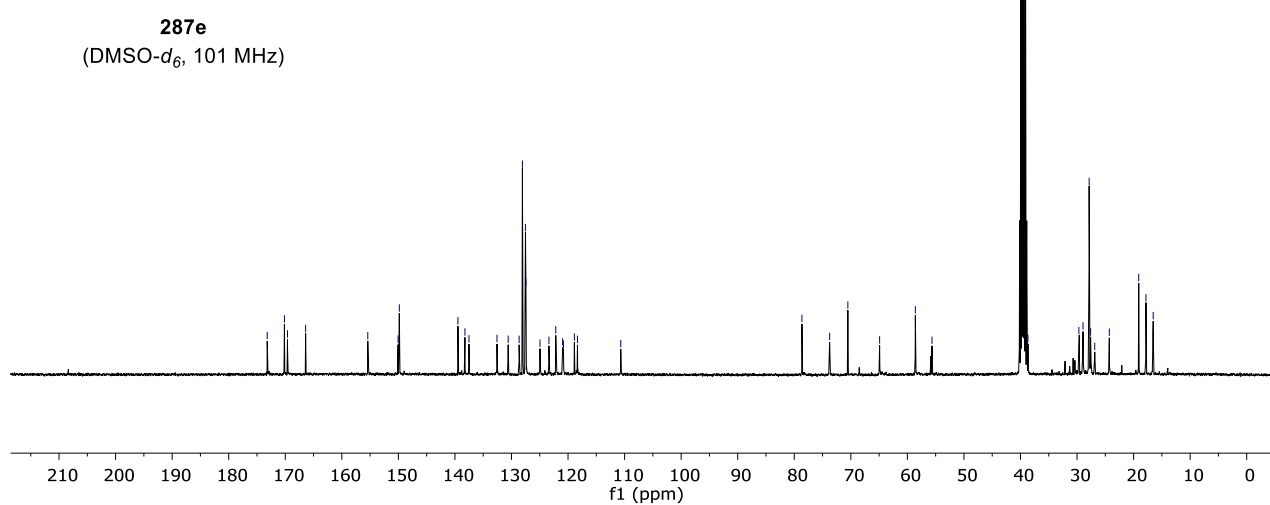




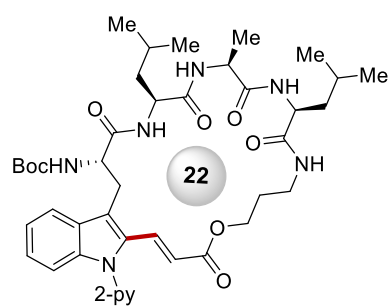
287e
(DMSO- d_6 , 400 MHz)



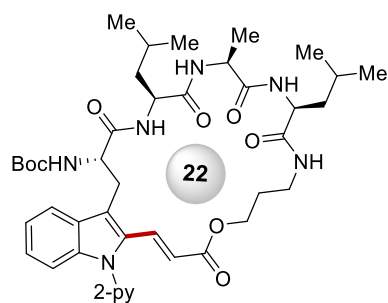
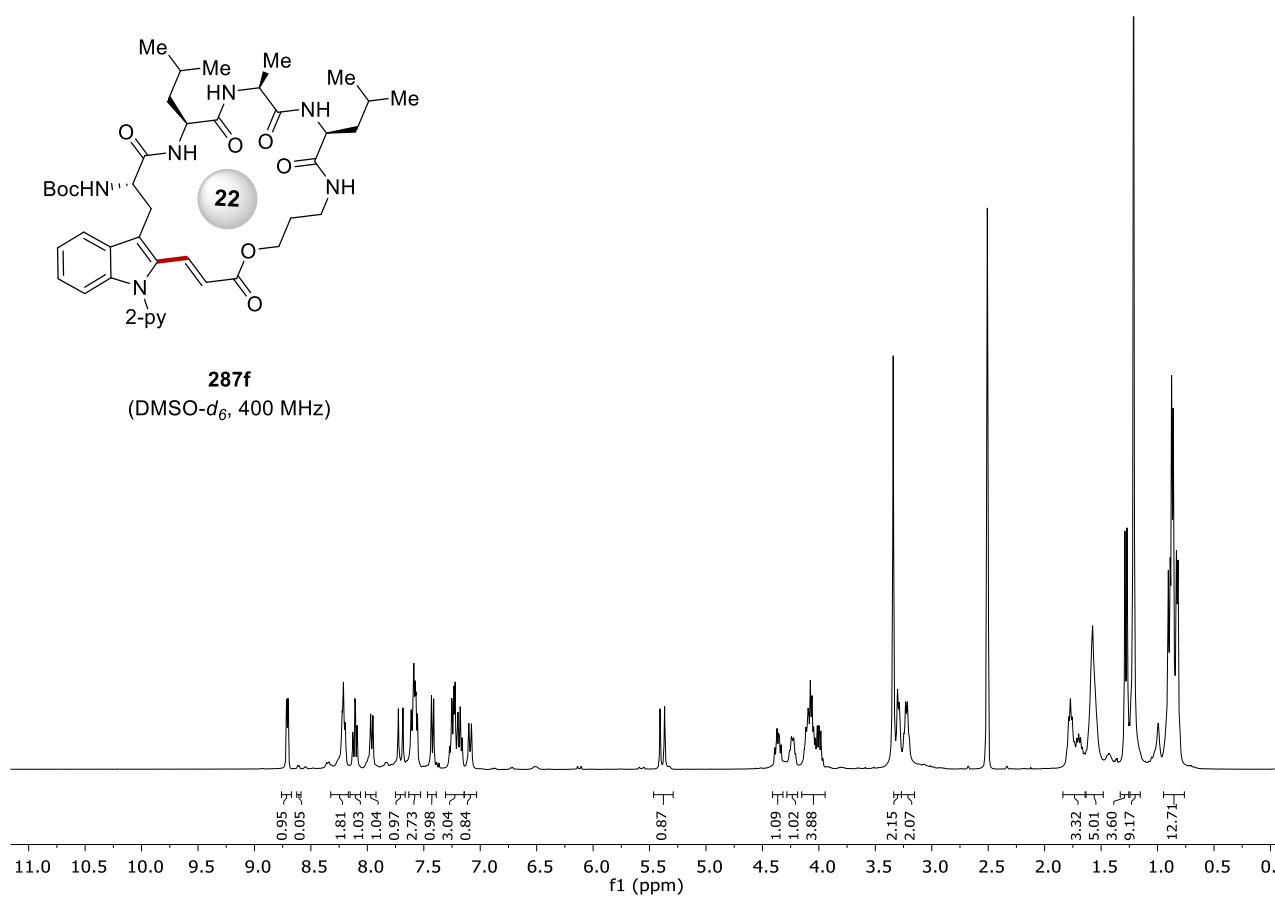
287e
(DMSO- d_6 , 101 MHz)



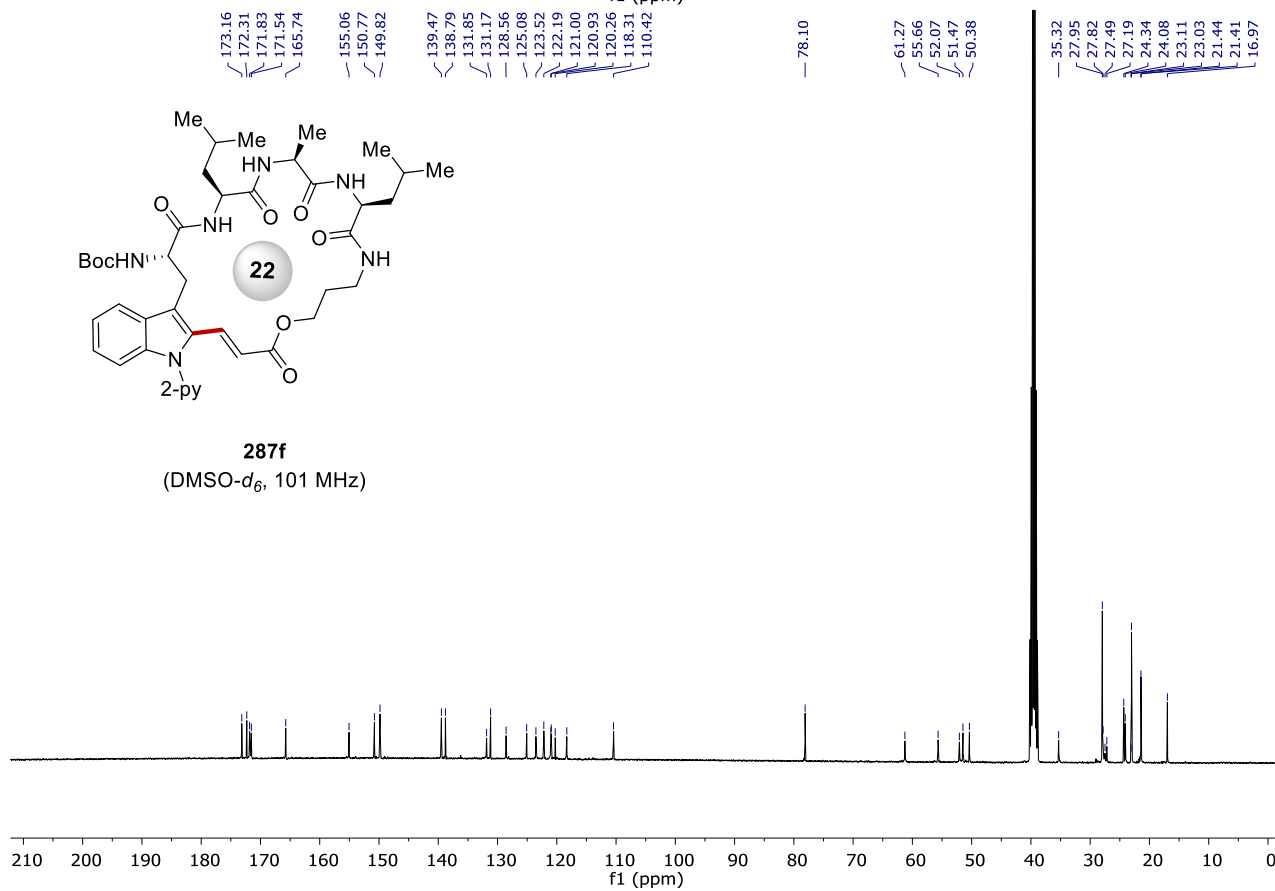
8. NMR Spectra

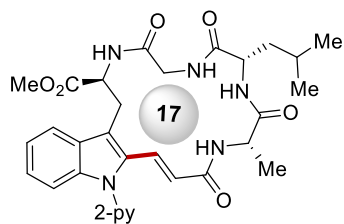


287f
(DMSO- d_6 , 400 MHz)

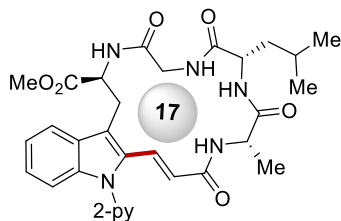
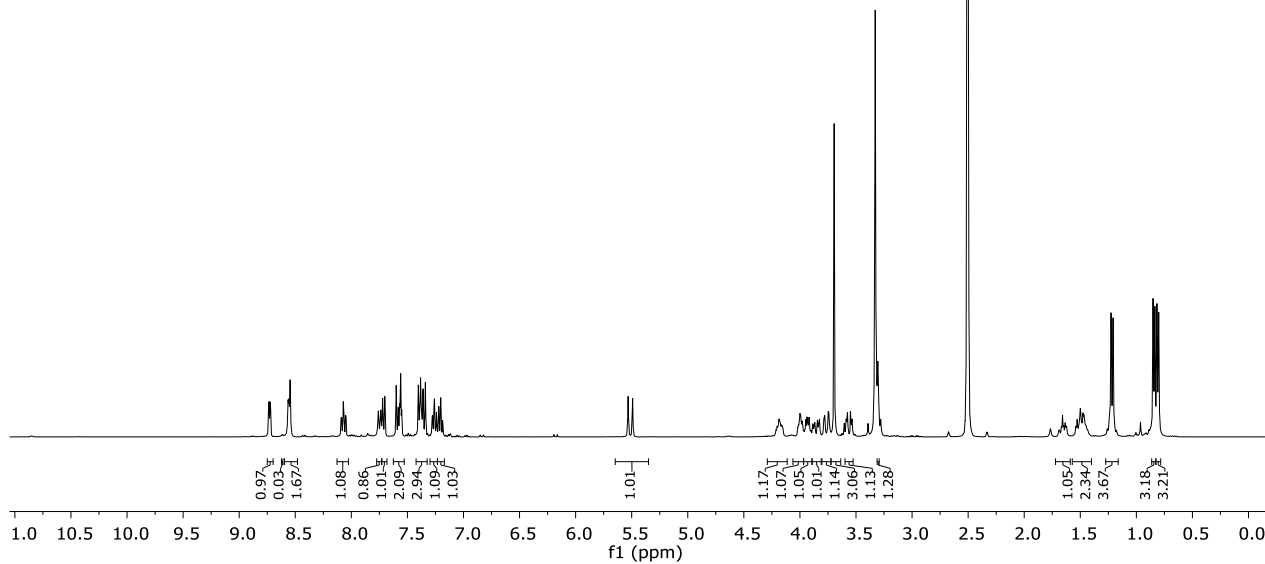


287f
(DMSO- d_6 , 101 MHz)

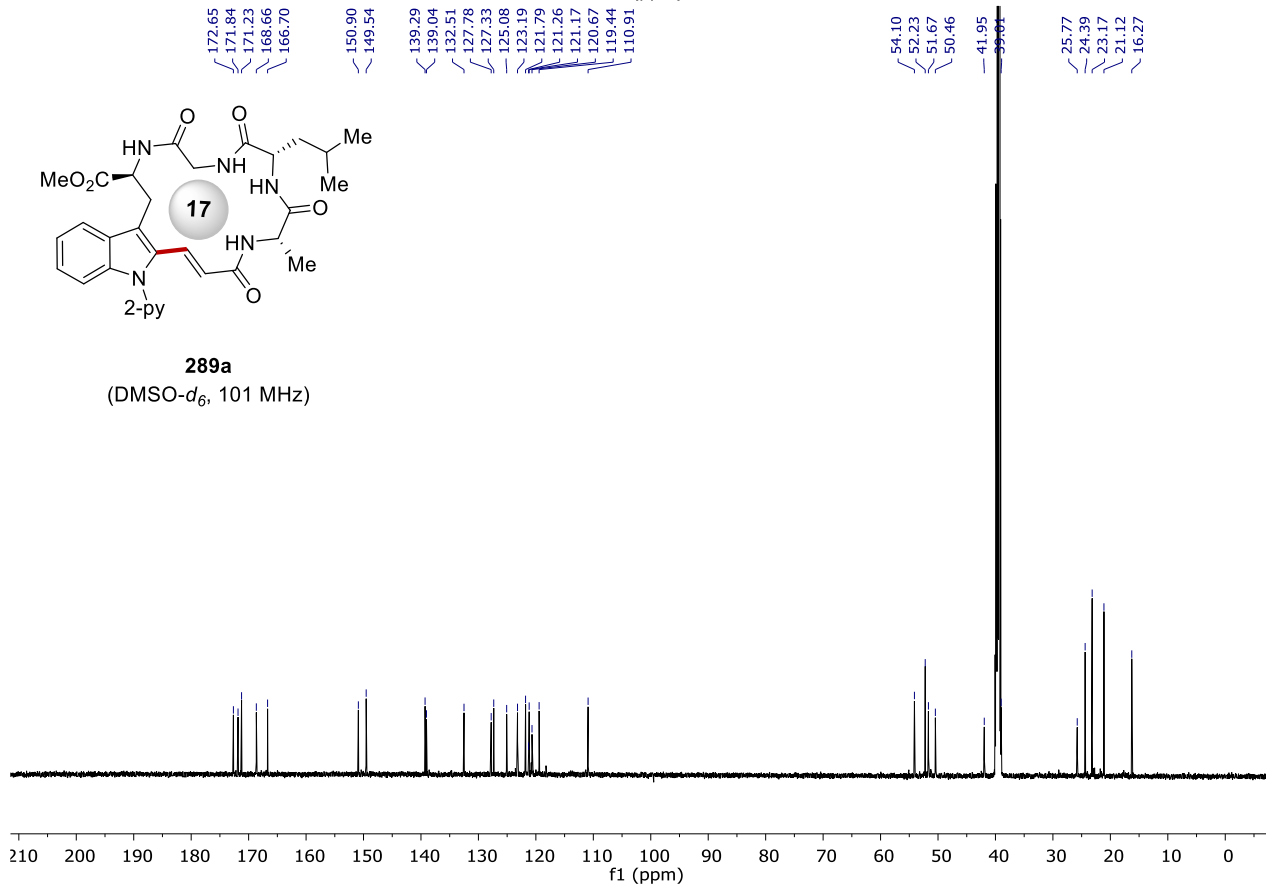




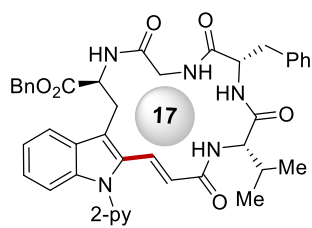
289a
(DMSO-*d*₆, 400 MHz)



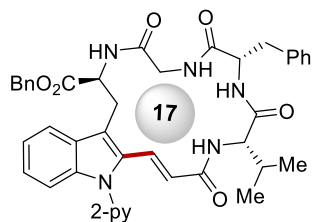
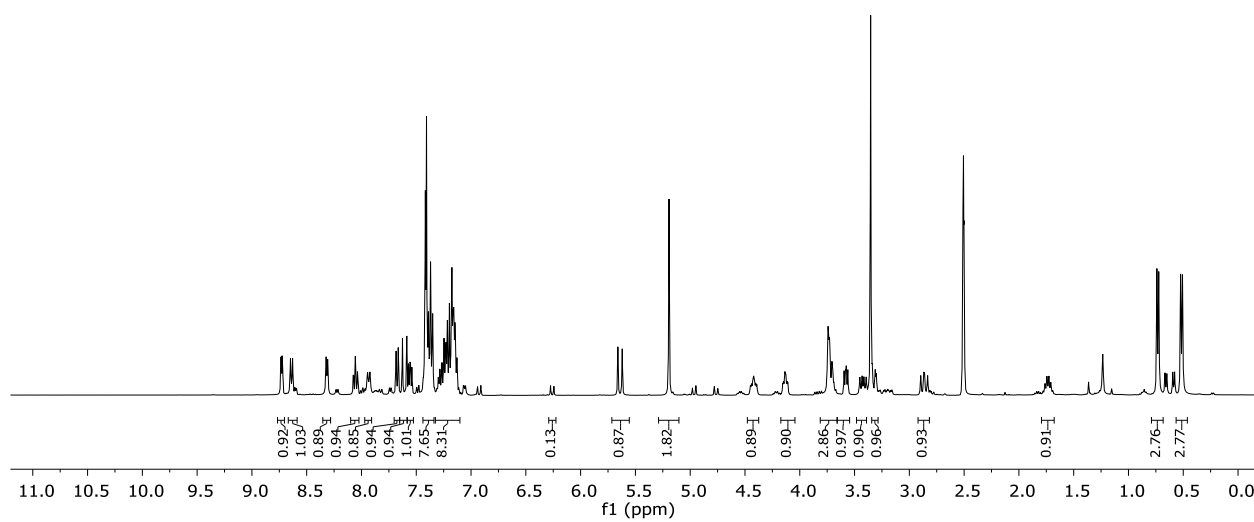
289a
(DMSO-*d*₆, 101 MHz)



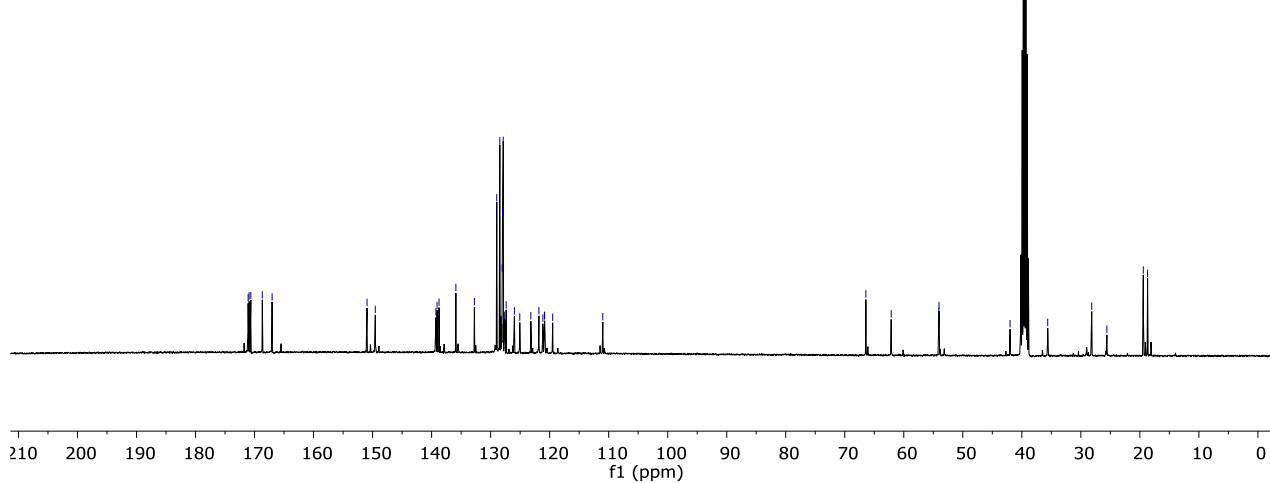
8. NMR Spectra

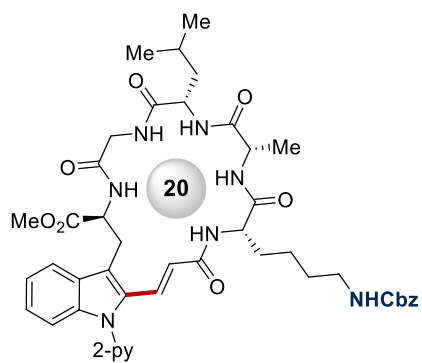


289b
(DMSO- d_6 , 400 MHz)

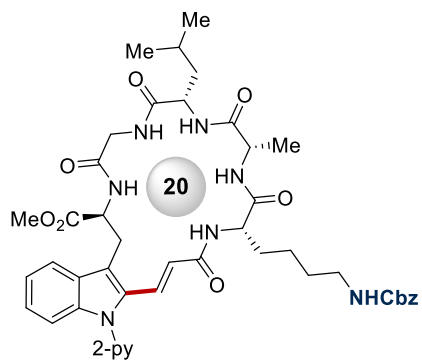
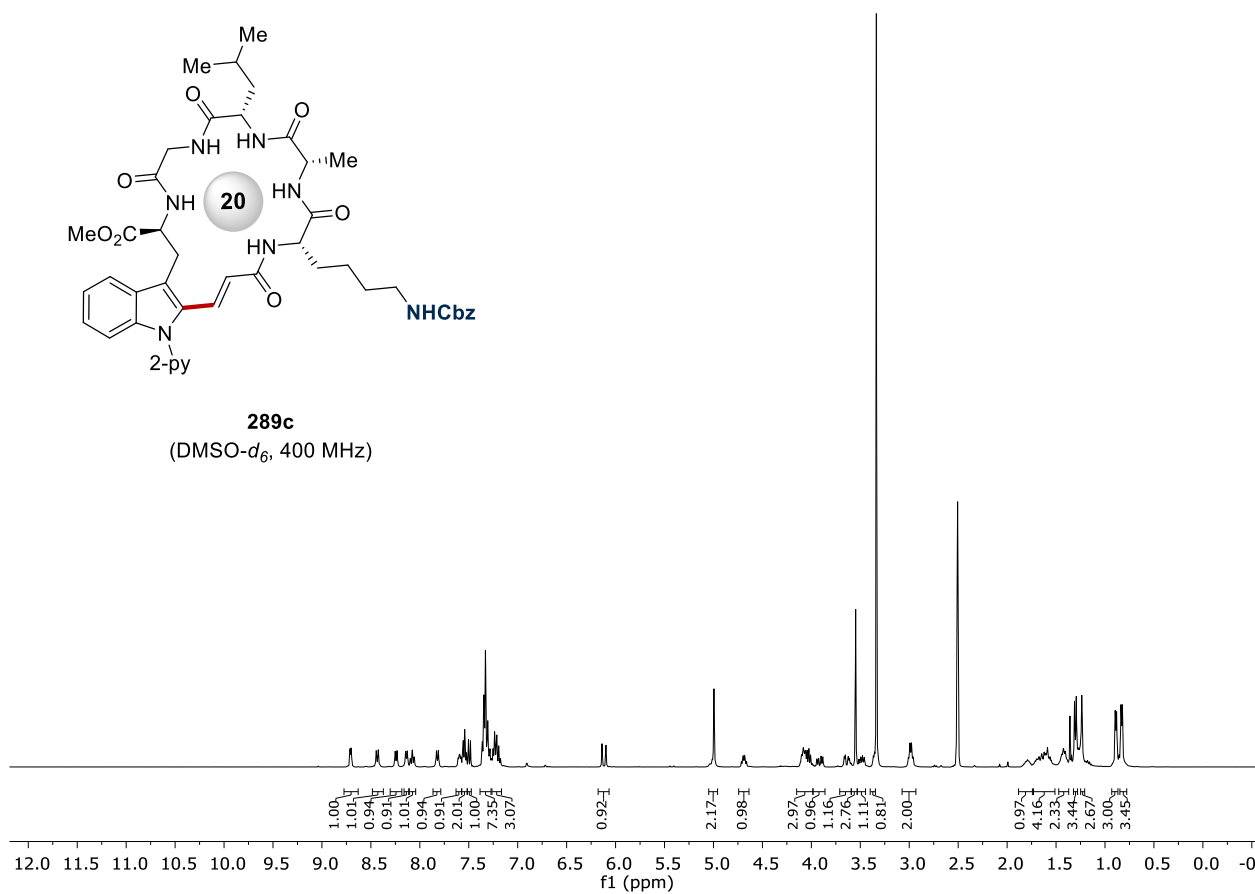


289b
(DMSO- d_6 , 101 MHz)

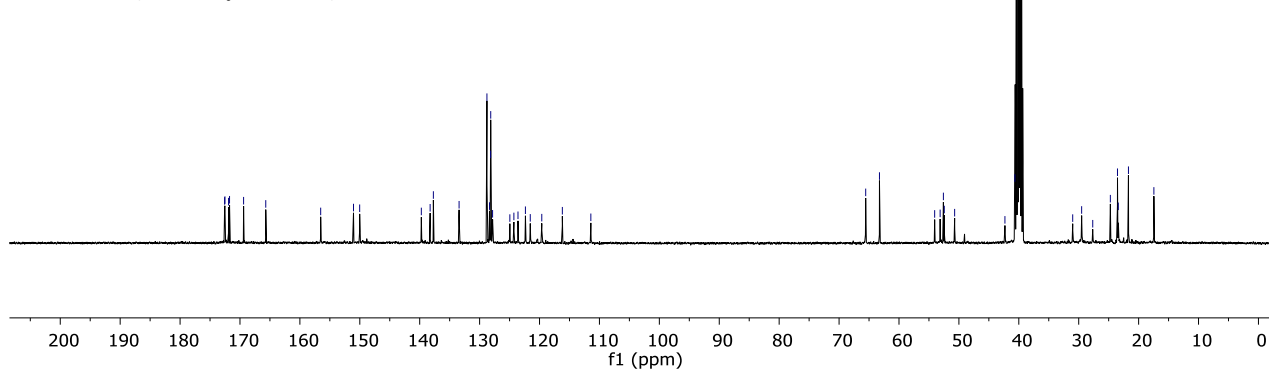




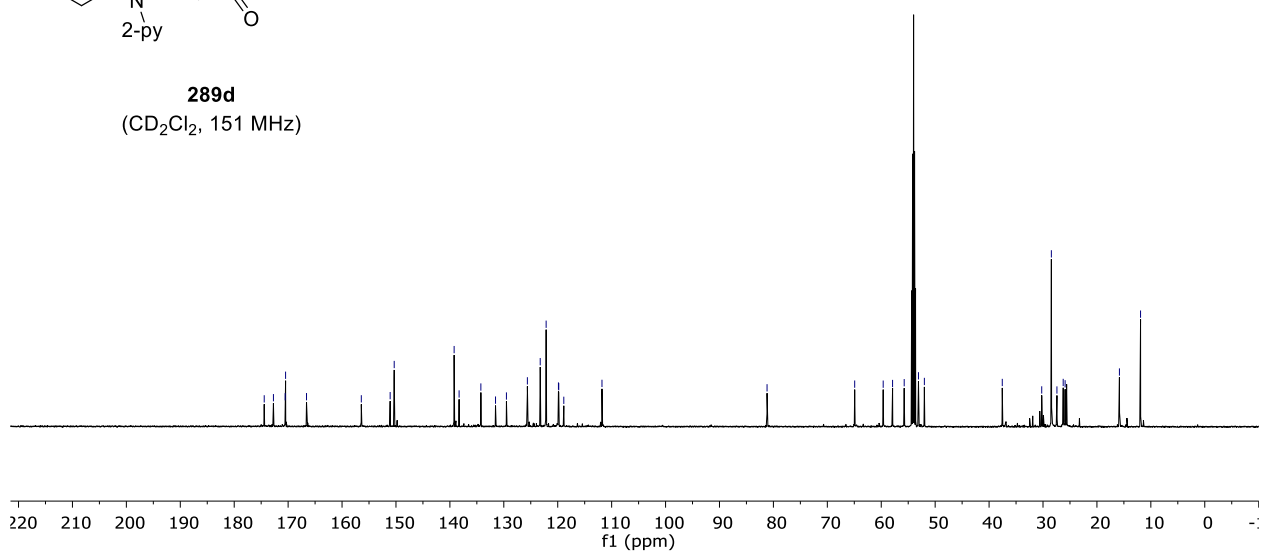
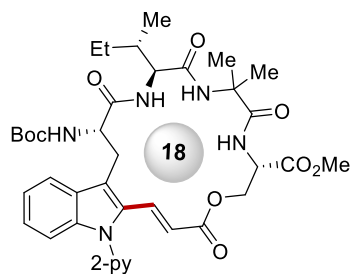
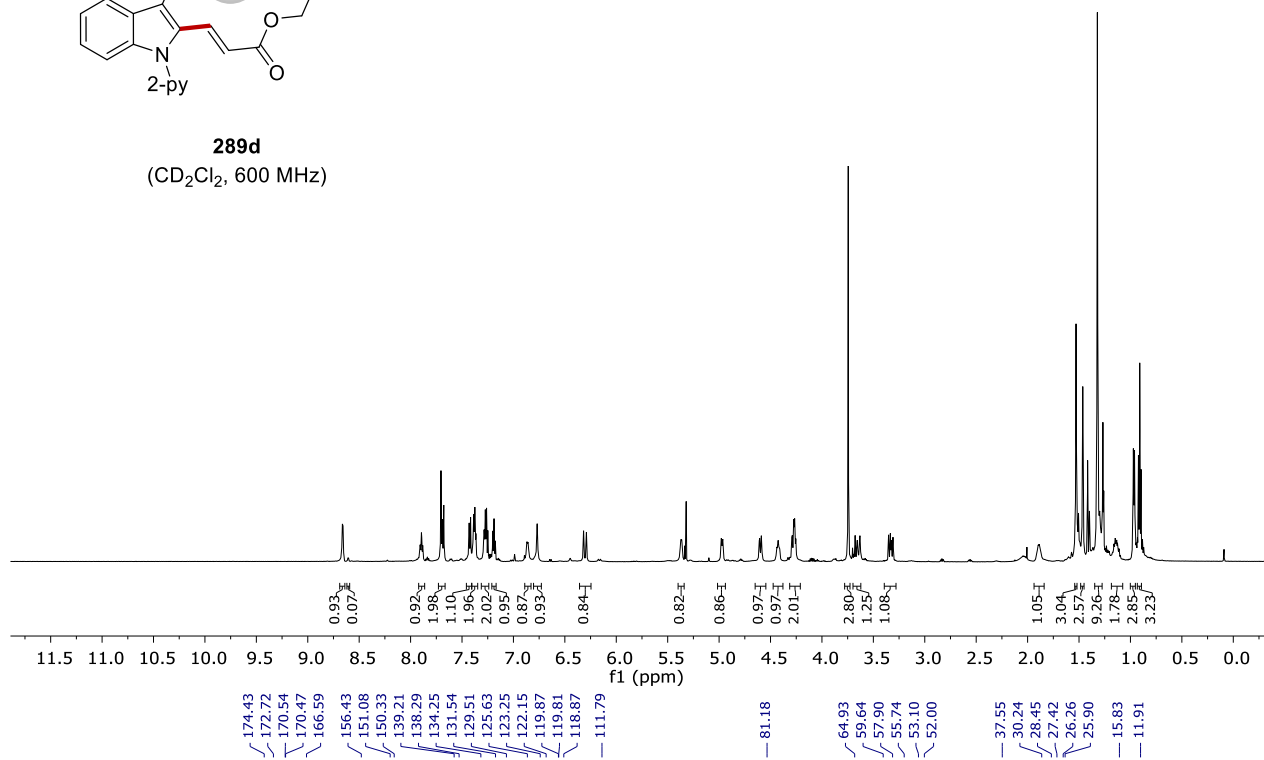
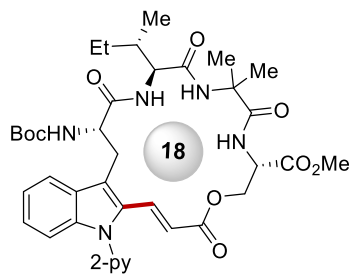
289c
(DMSO- d_6 , 400 MHz)

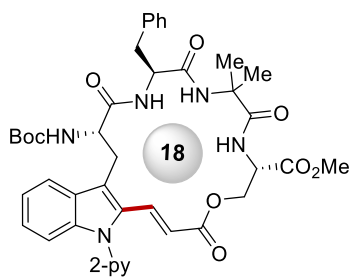


289c
(DMSO- d_6 , 101 MHz)

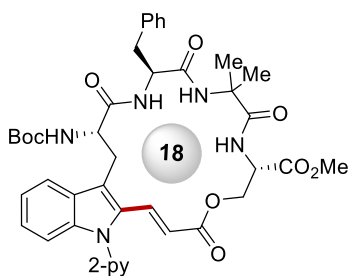
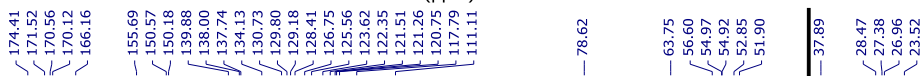
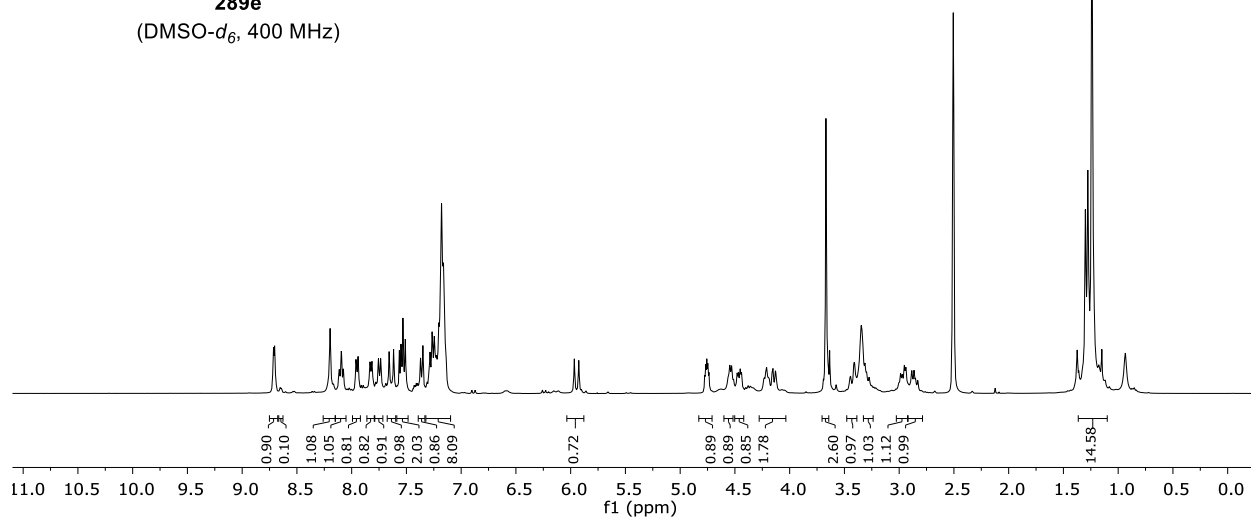


8. NMR Spectra

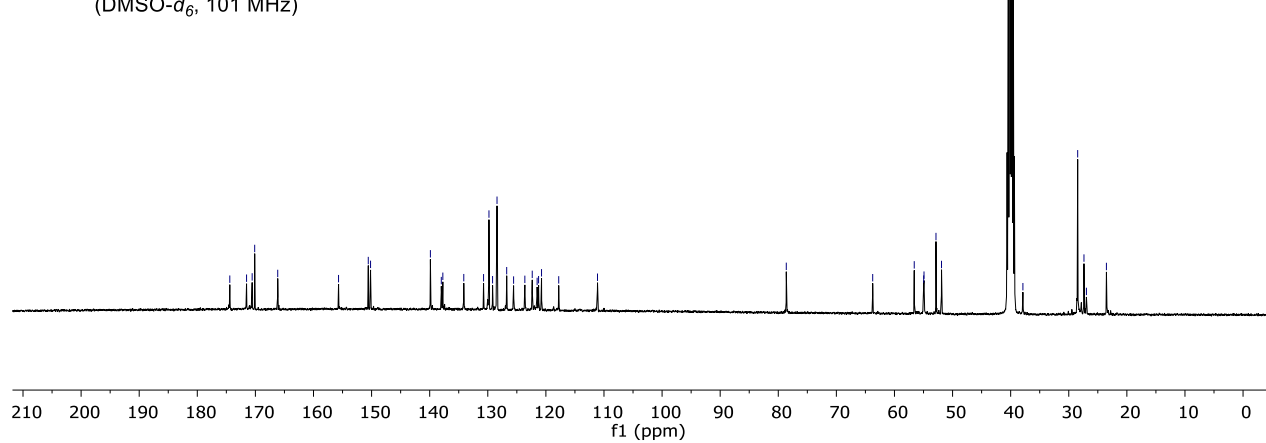




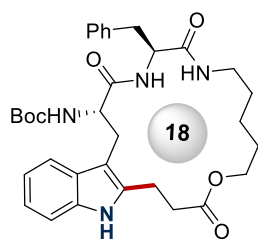
289e
(DMSO- d_6 , 400 MHz)



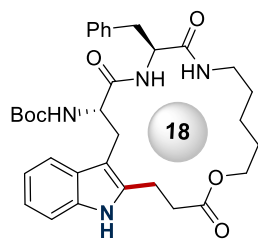
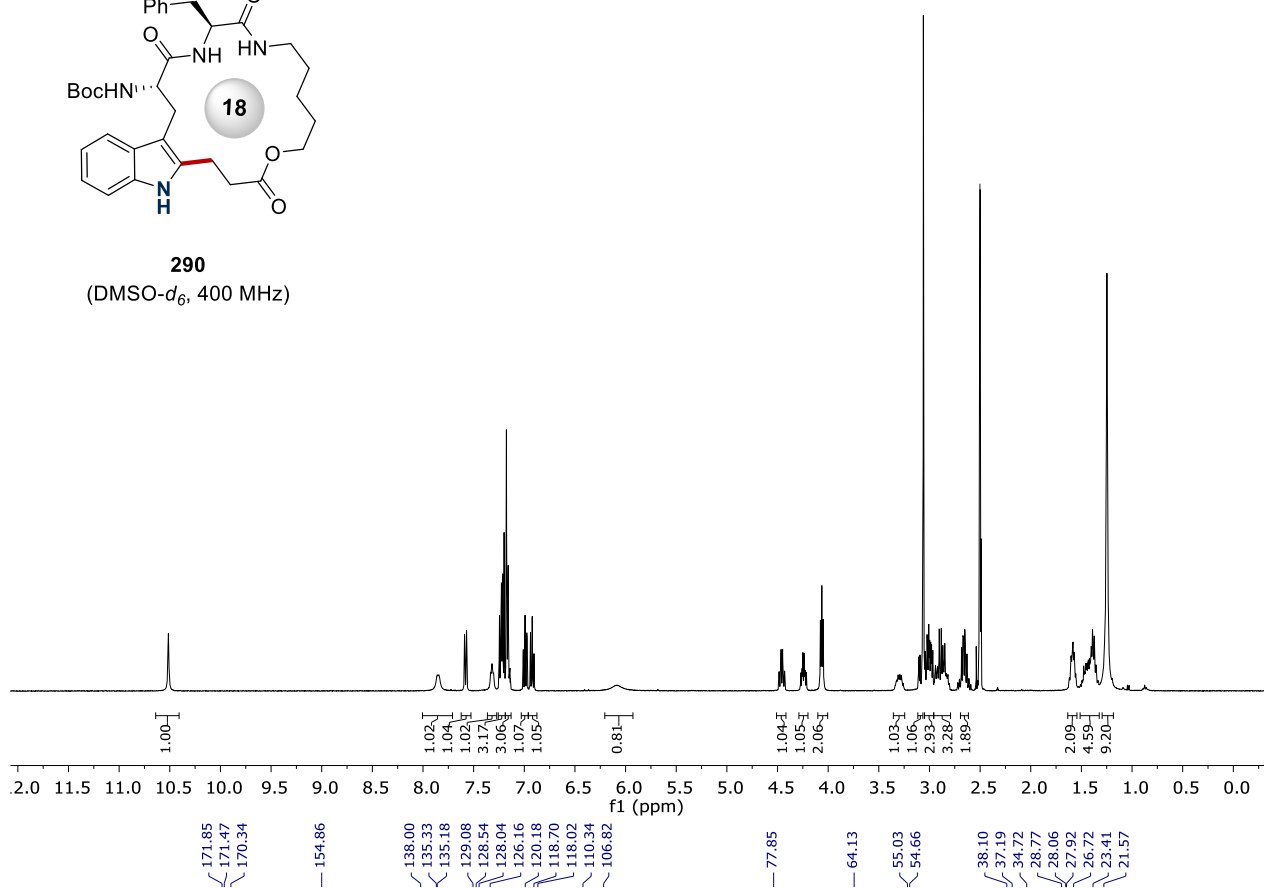
289e
(DMSO- d_6 , 101 MHz)



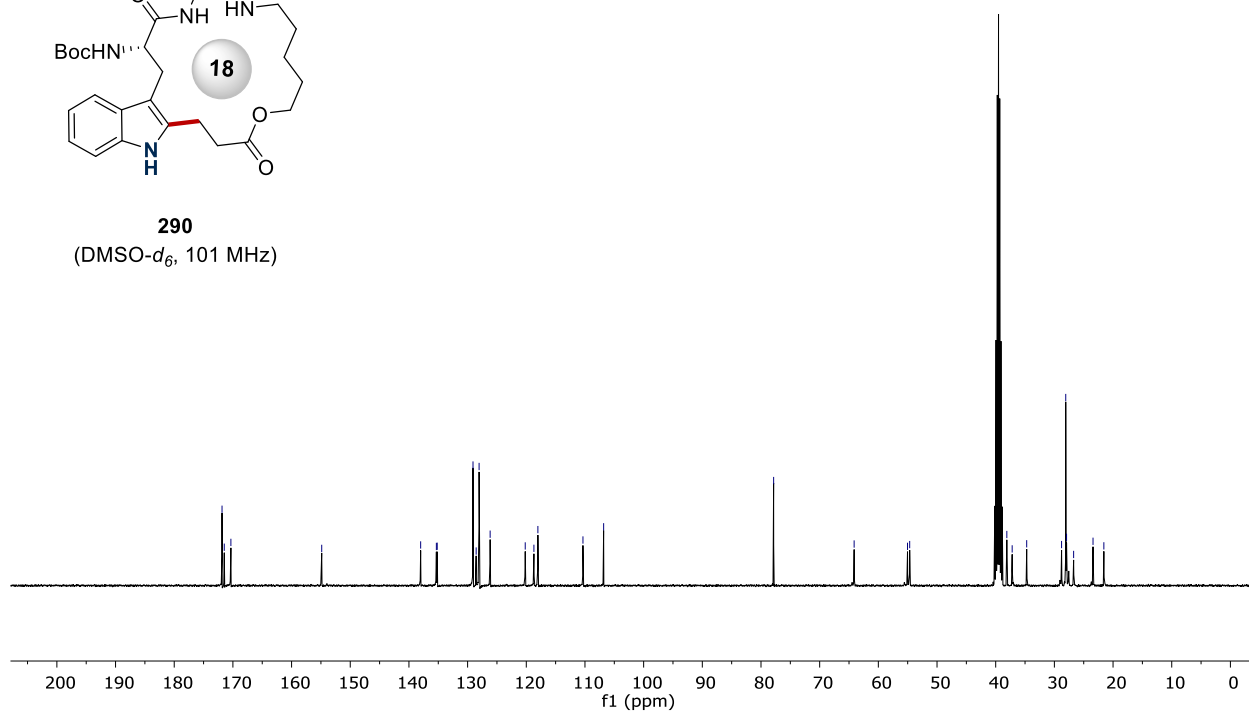
8. NMR Spectra

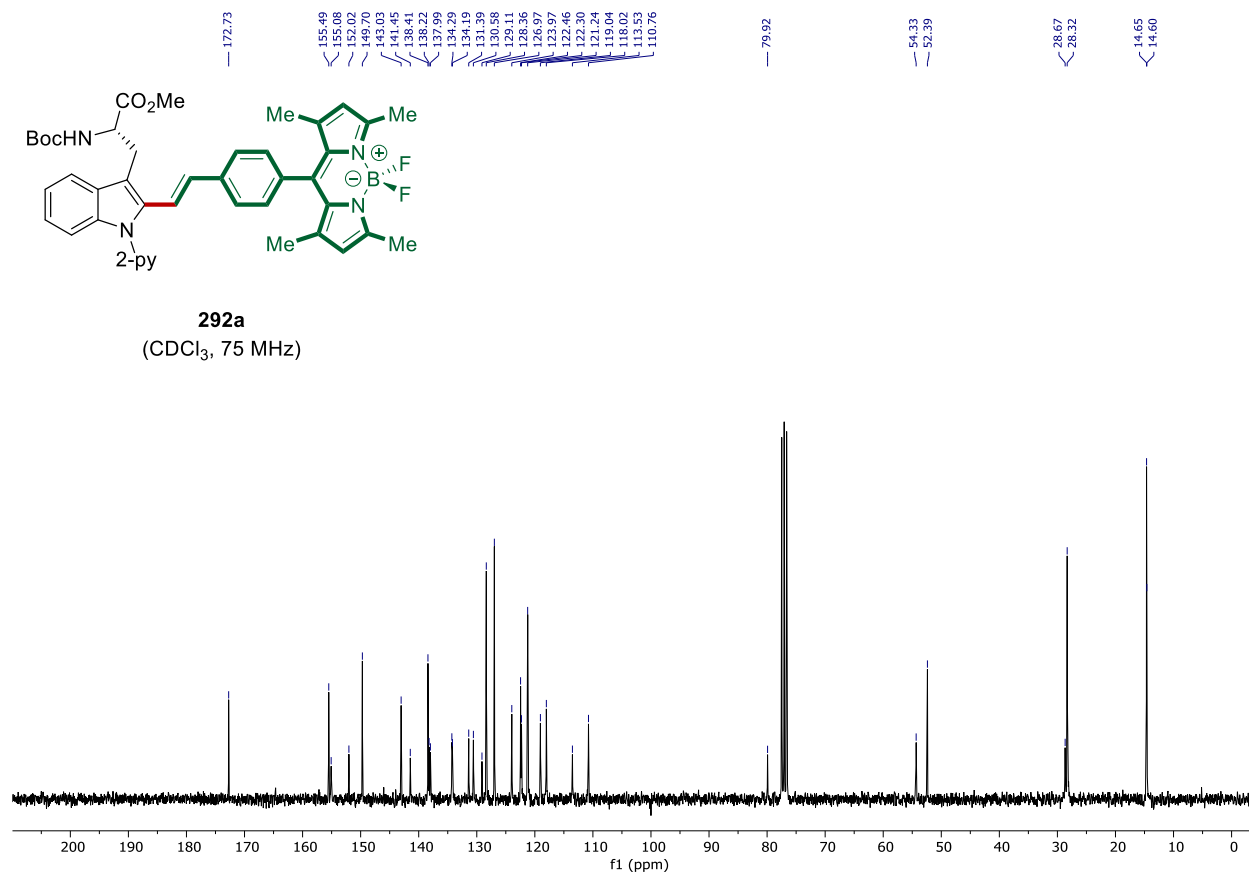
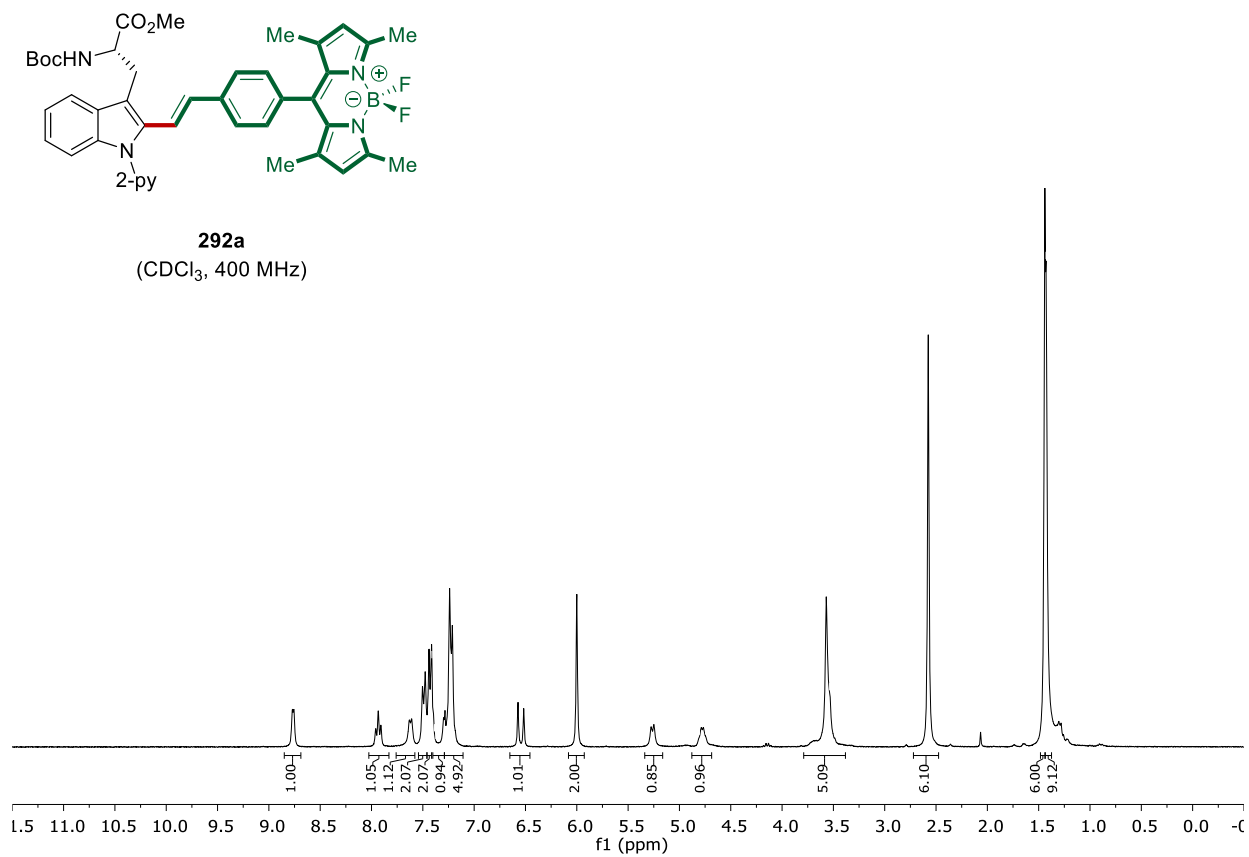


290
(DMSO- d_6 , 400 MHz)

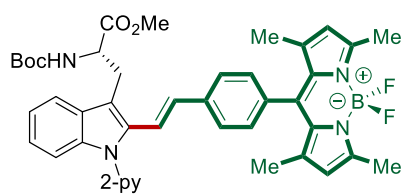


290
(DMSO- d_6 , 101 MHz)

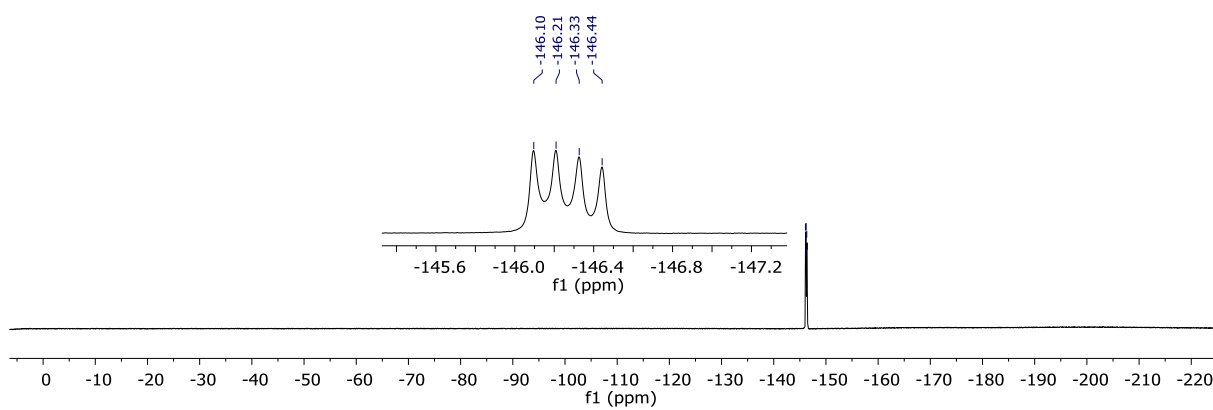


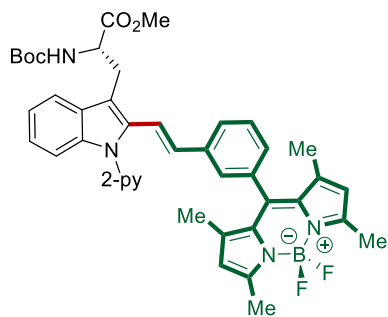


8. NMR Spectra

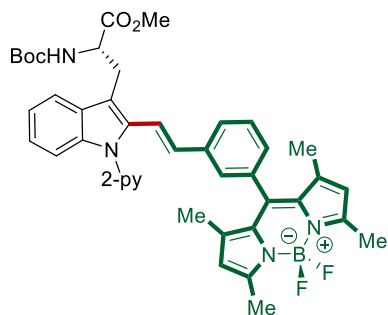
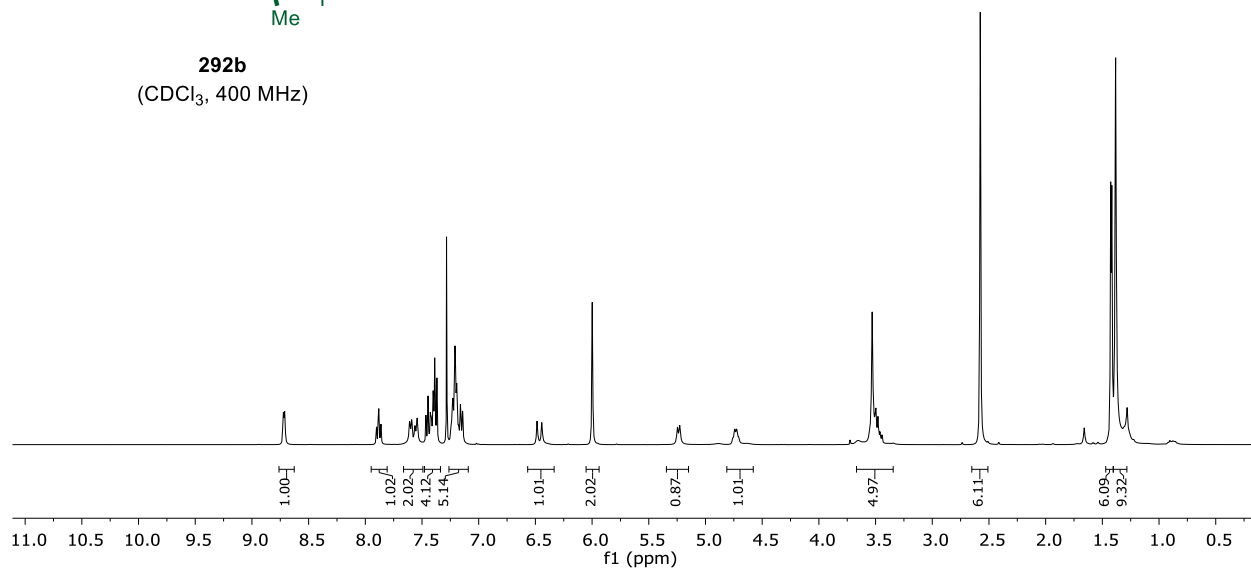


292a
(CDCl₃, 282 MHz)

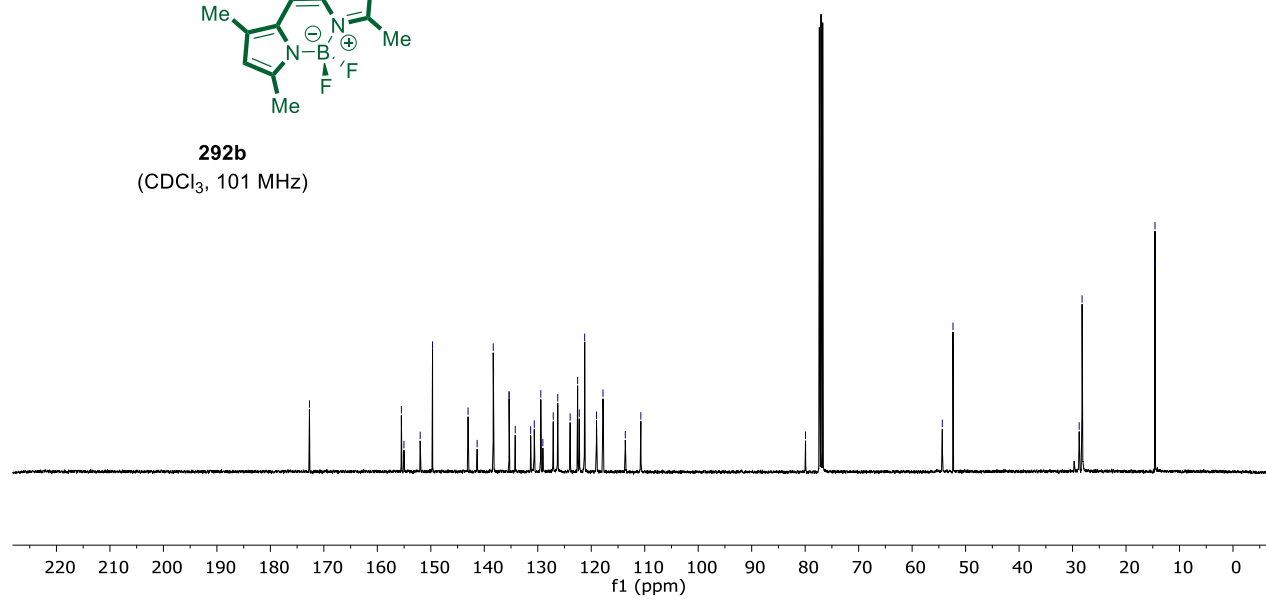




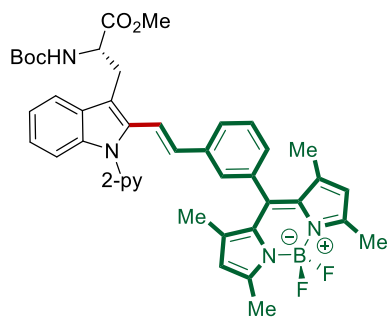
292b
(CDCl₃, 400 MHz)



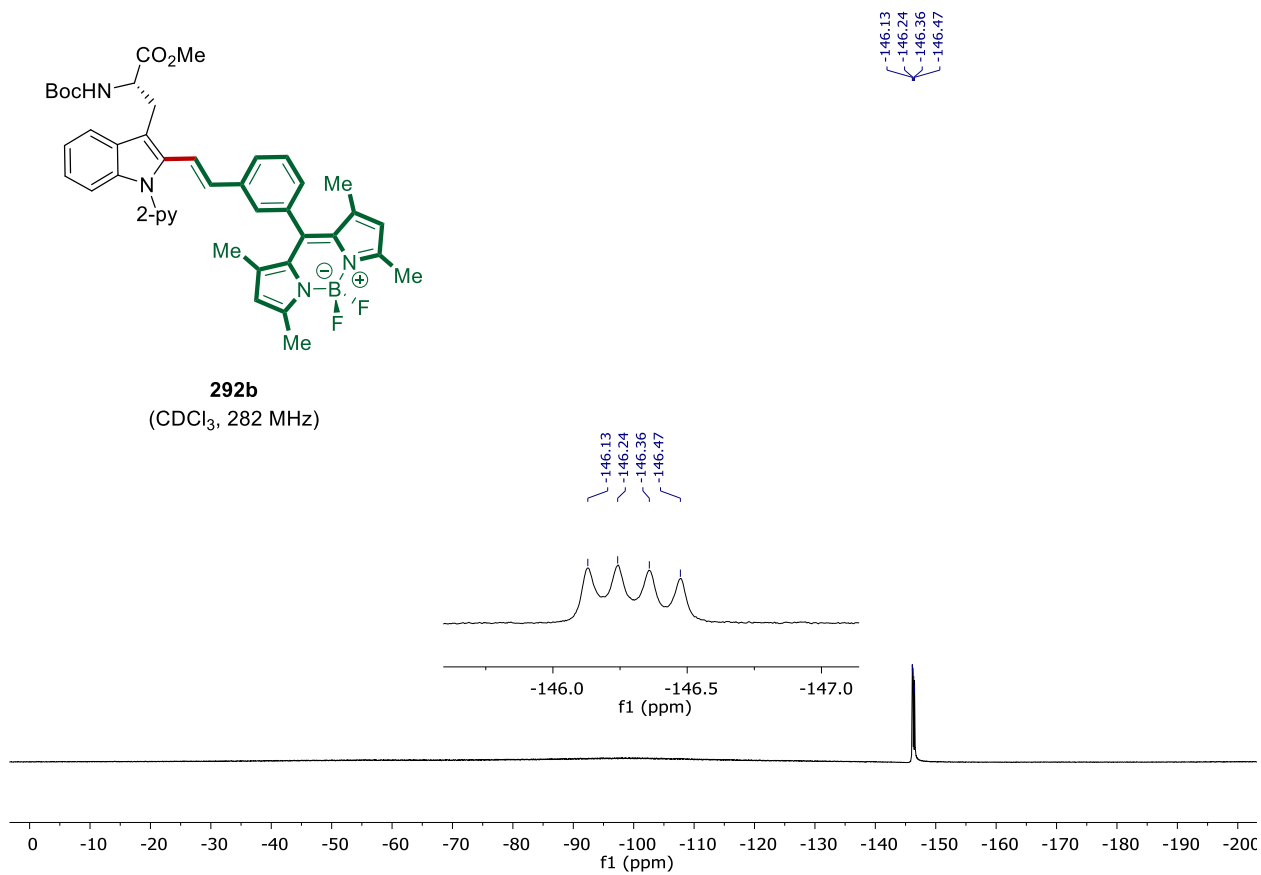
292b
(CDCl₃, 101 MHz)

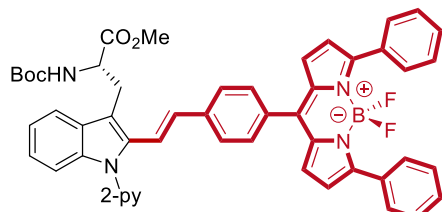


8. NMR Spectra

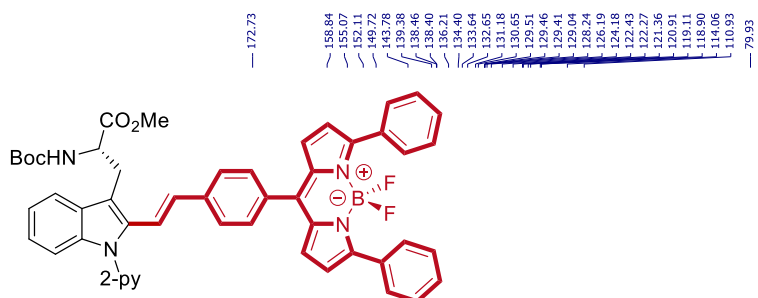
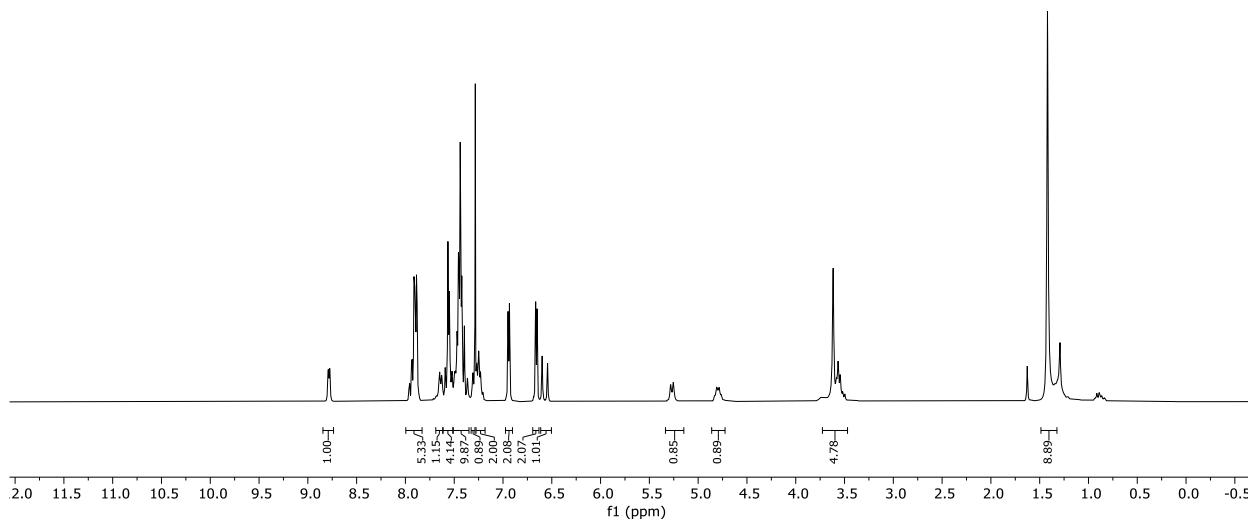


292b
(CDCl₃, 282 MHz)

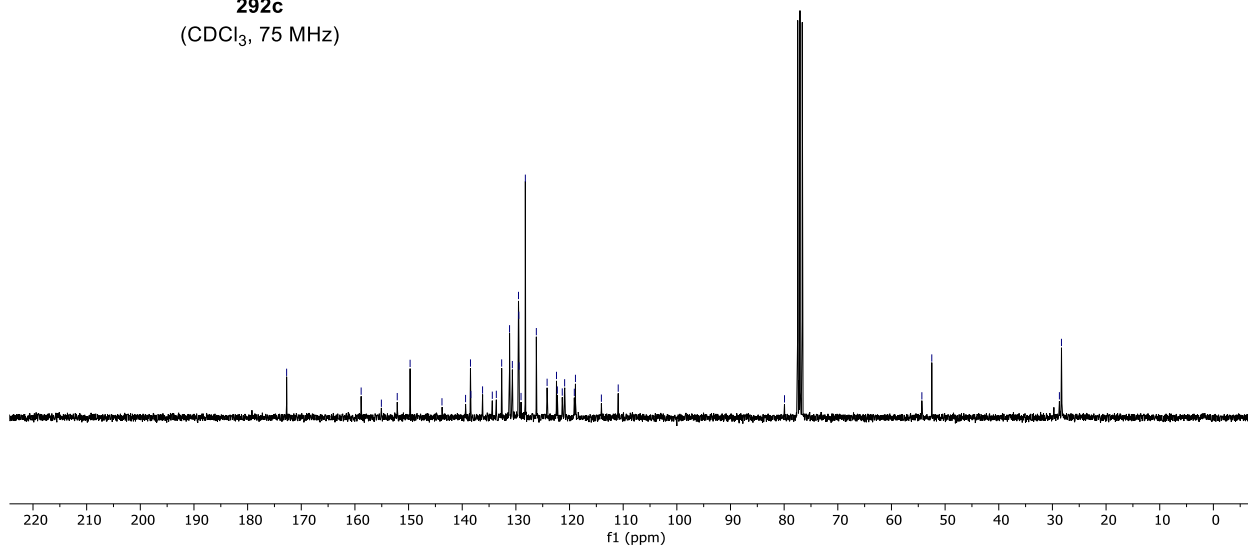




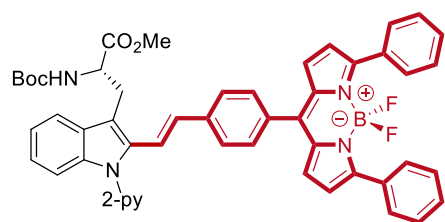
292c
(CDCl₃, 400 MHz)



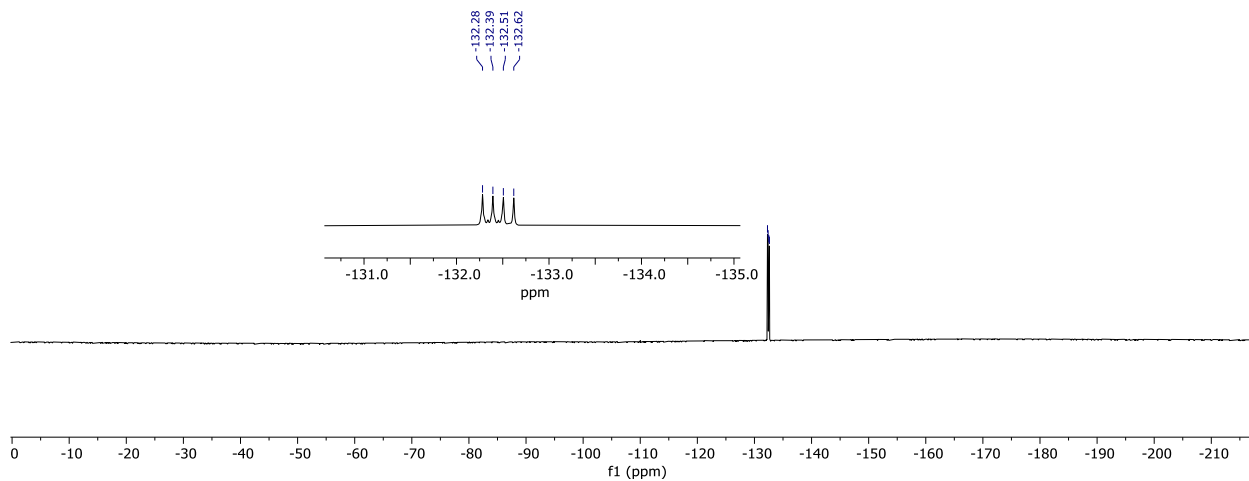
292c
(CDCl₃, 75 MHz)

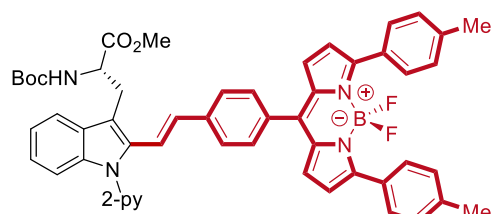


8. NMR Spectra

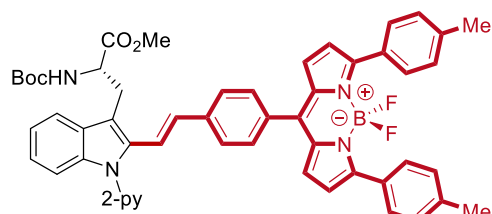
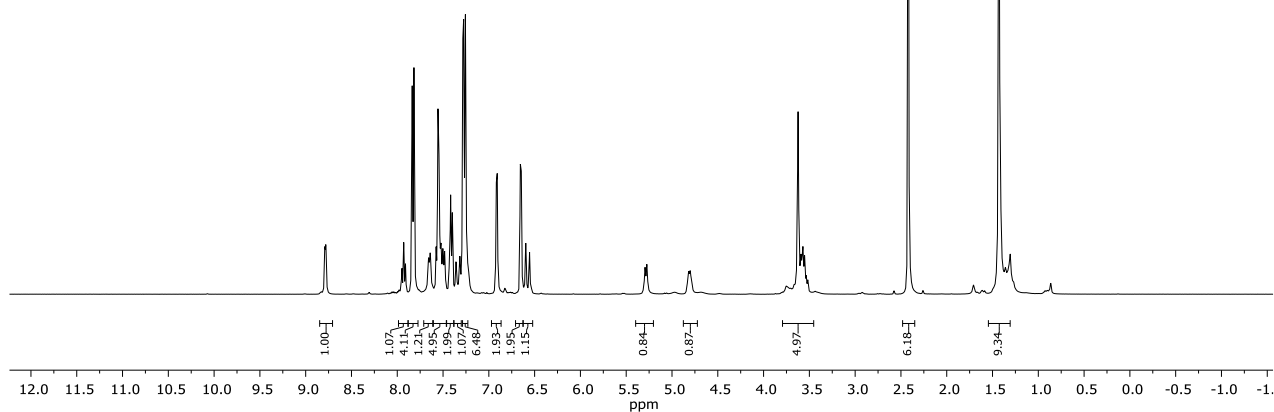


292c
(CDCl₃, 282 MHz)

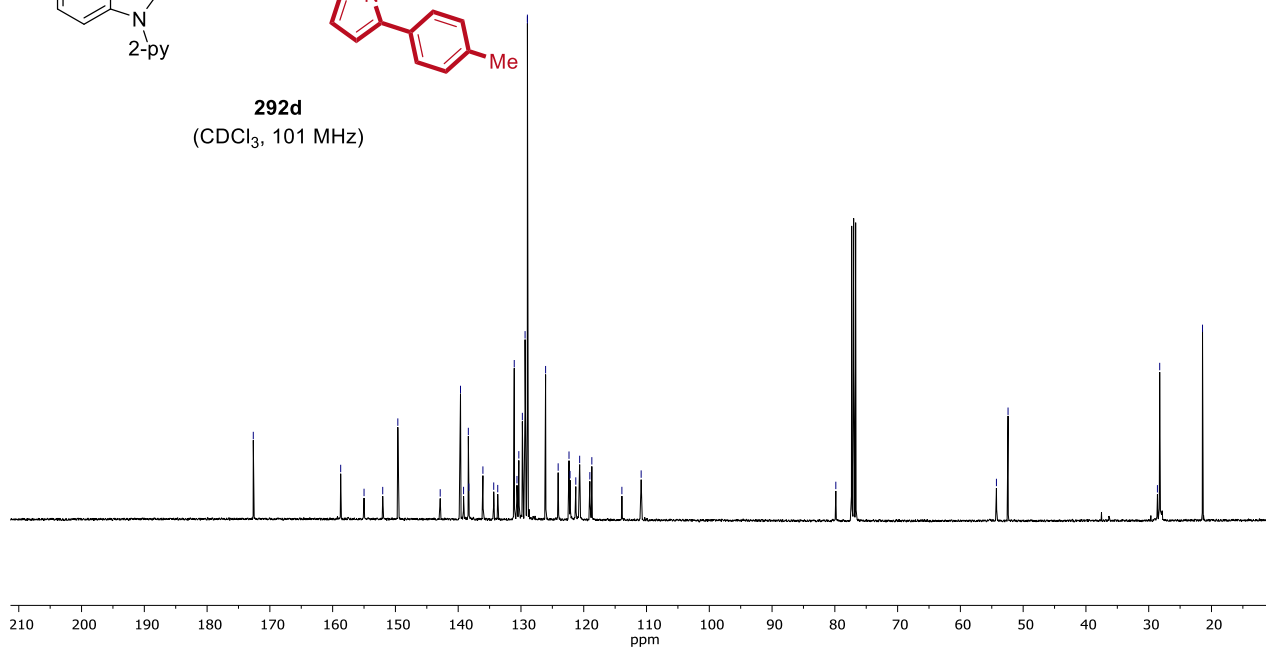




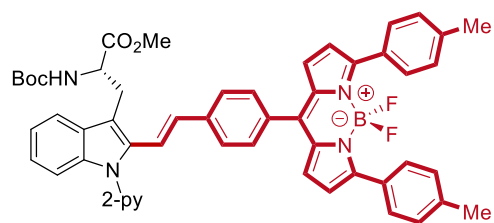
292d
(CDCl₃, 400 MHz)



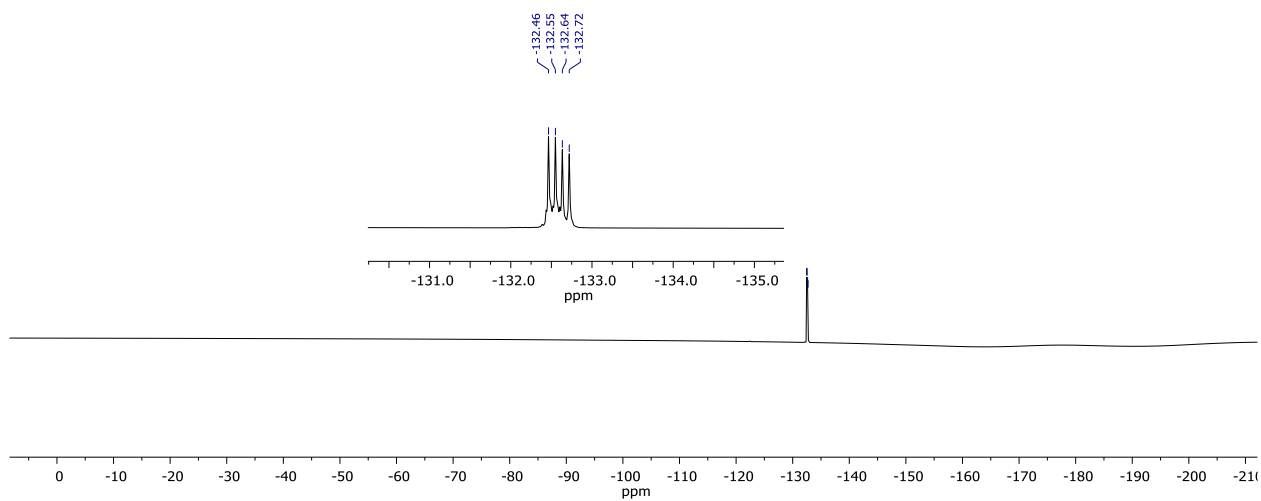
292d
(CDCl₃, 101 MHz)

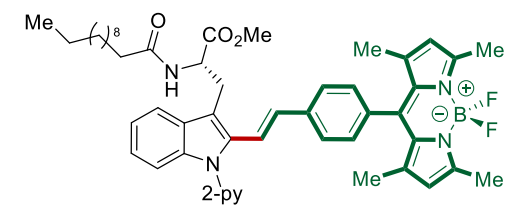


8. NMR Spectra

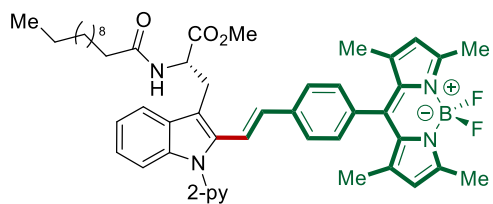
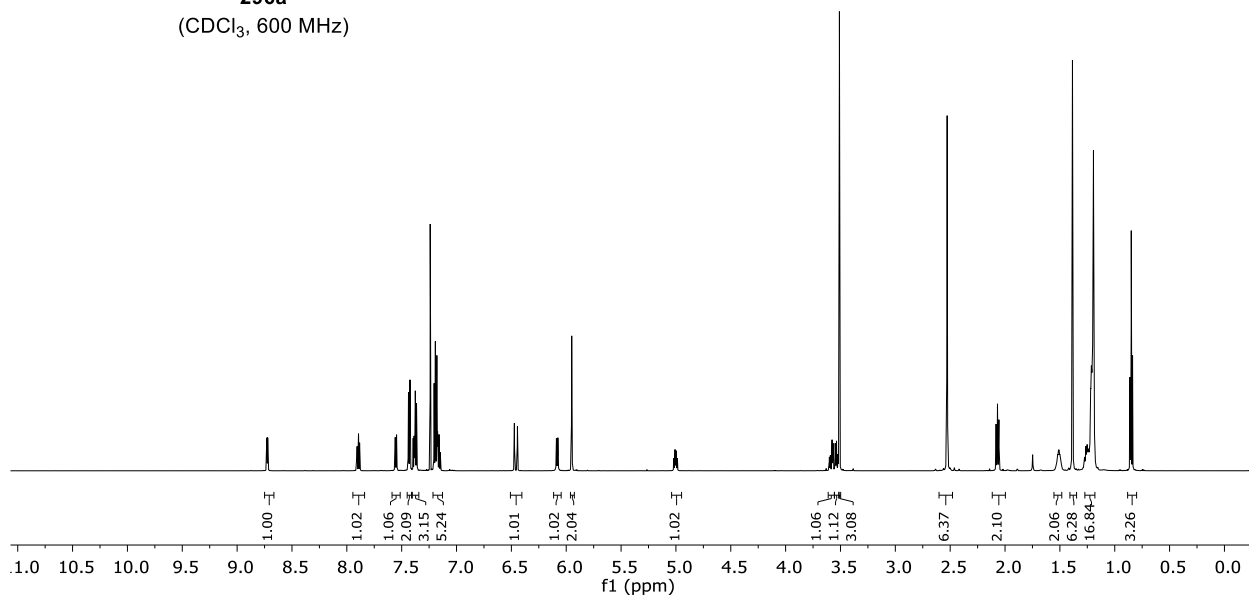


292d
(CDCl₃, 376 MHz)

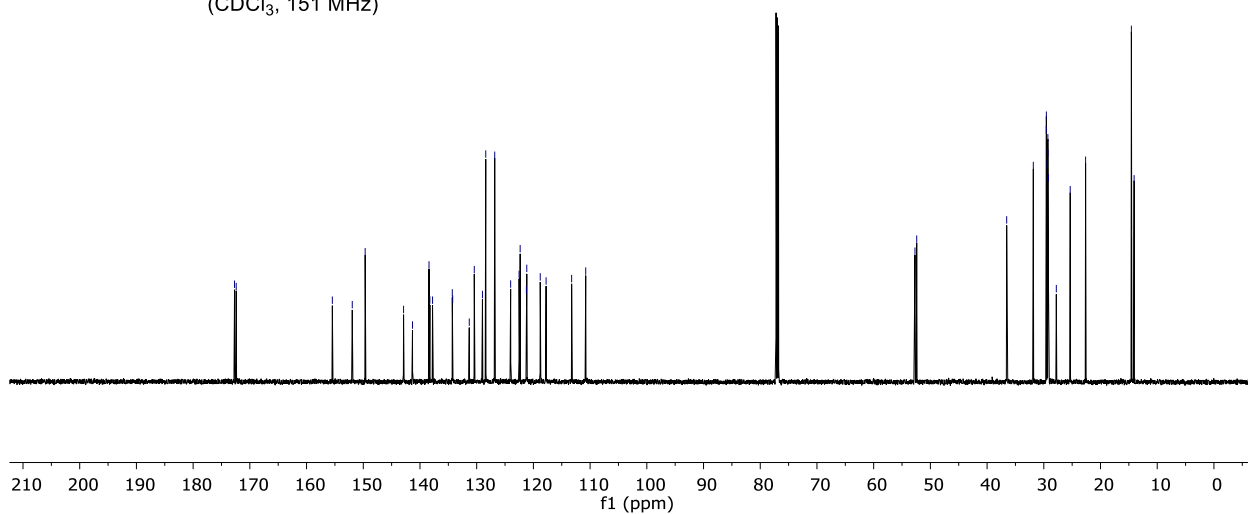




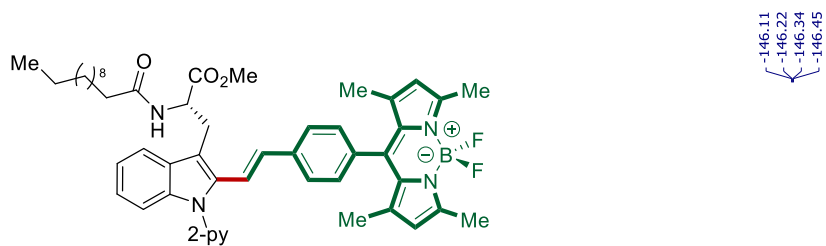
296a
(CDCl₃, 600 MHz)



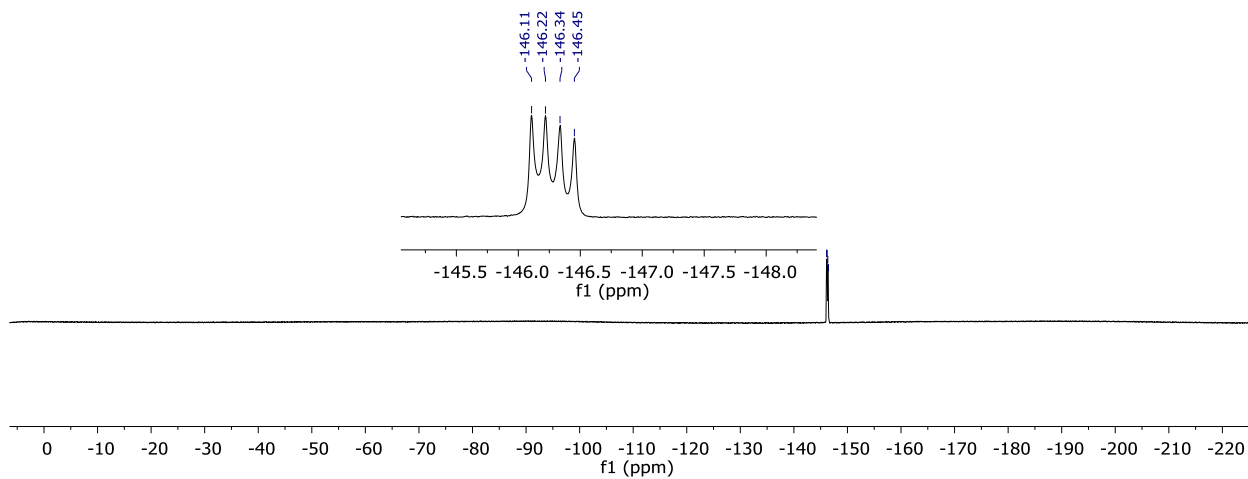
296a
(CDCl₃, 151 MHz)

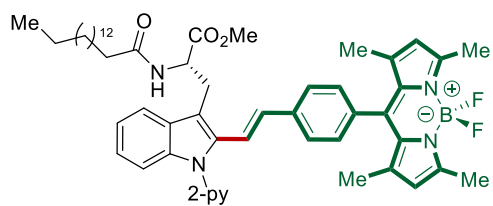


8. NMR Spectra

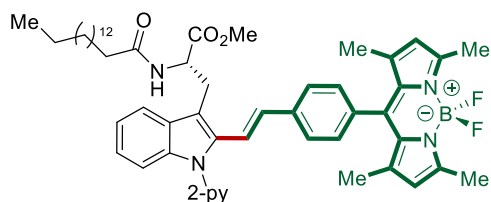
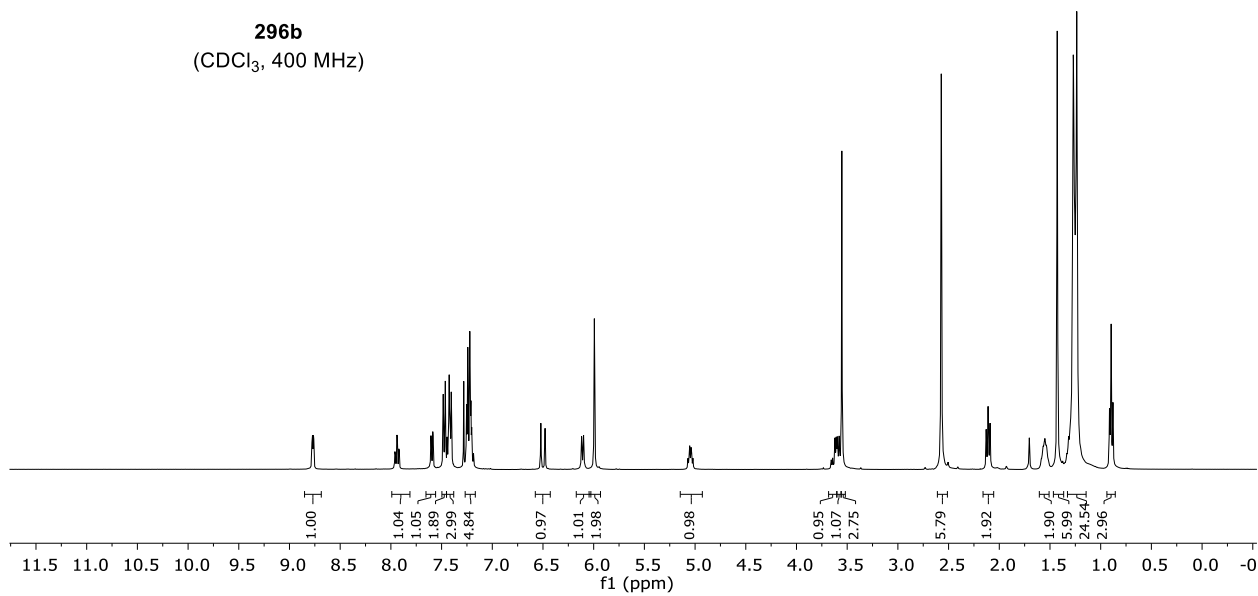


296a
(CDCl₃, 282 MHz)

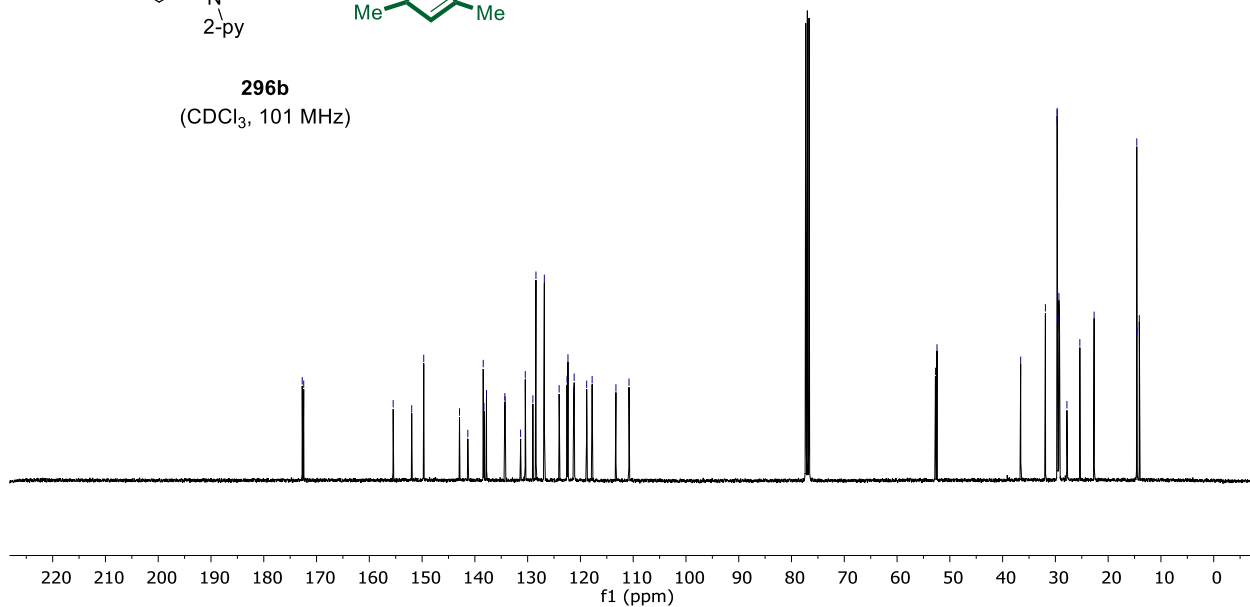




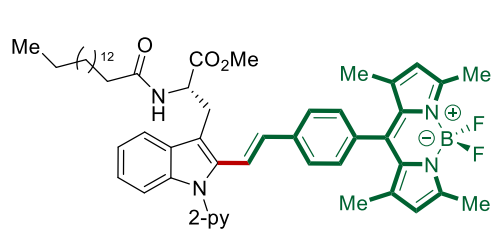
296b
(CDCl₃, 400 MHz)



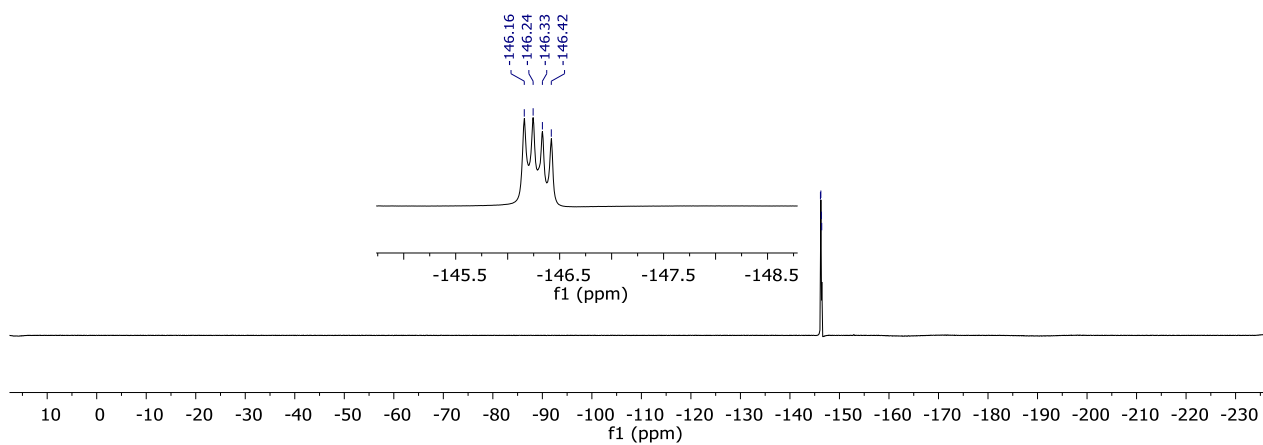
296b
(CDCl₃, 101 MHz)

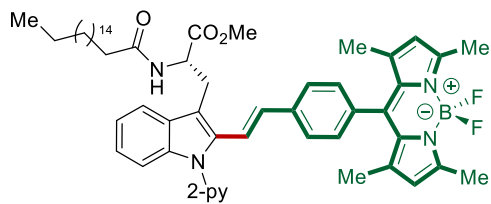


8. NMR Spectra

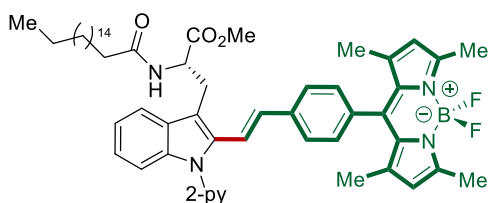
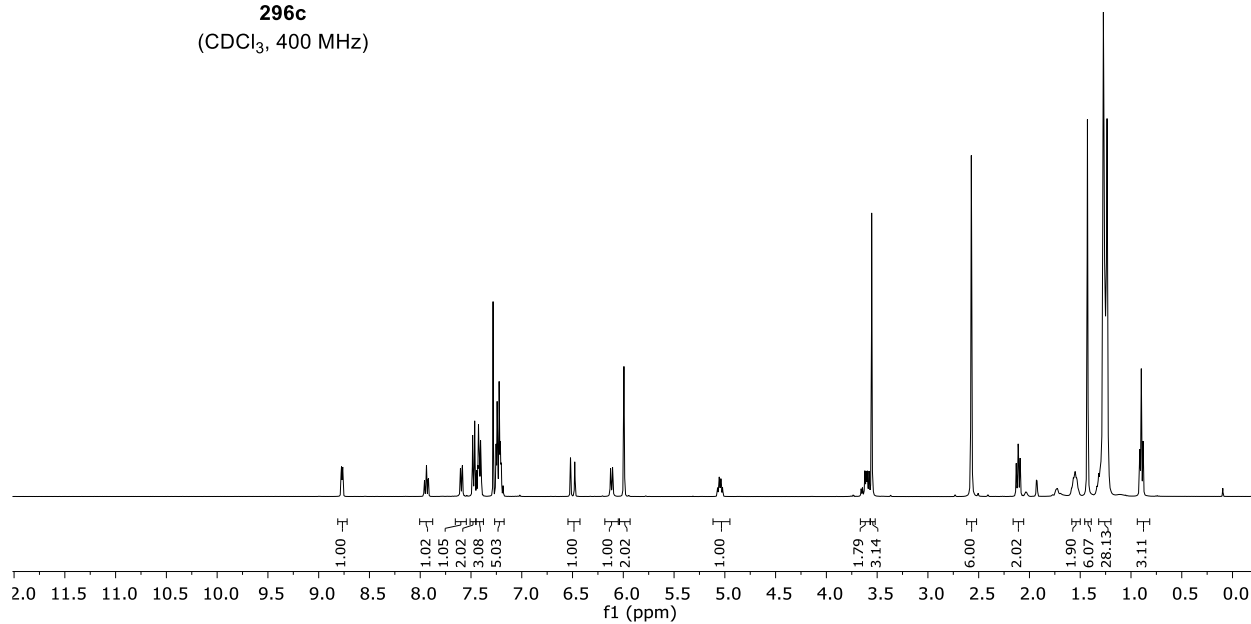


296b
(CDCl₃, 377 MHz)

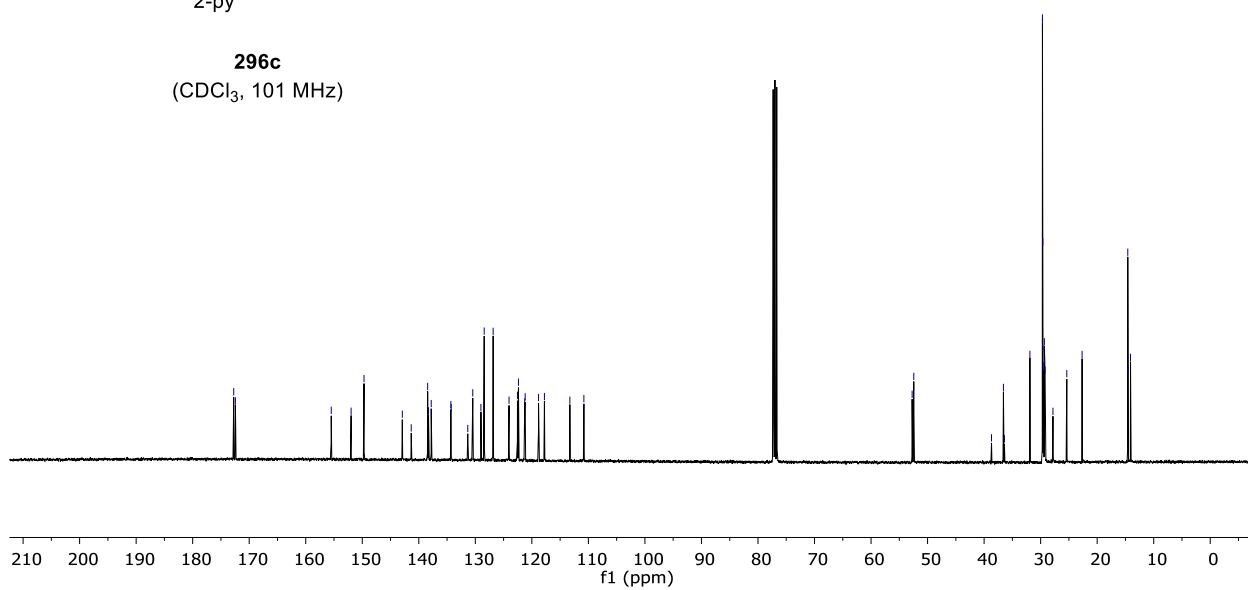




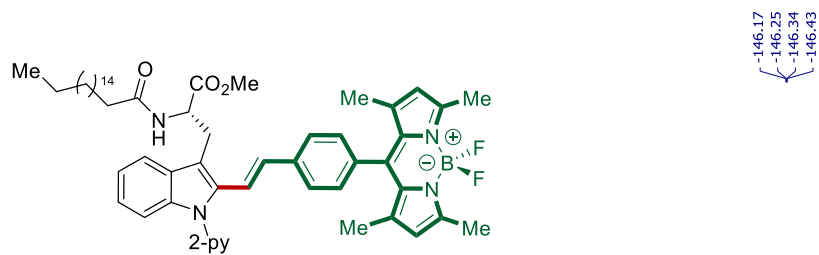
296c
(CDCl₃, 400 MHz)



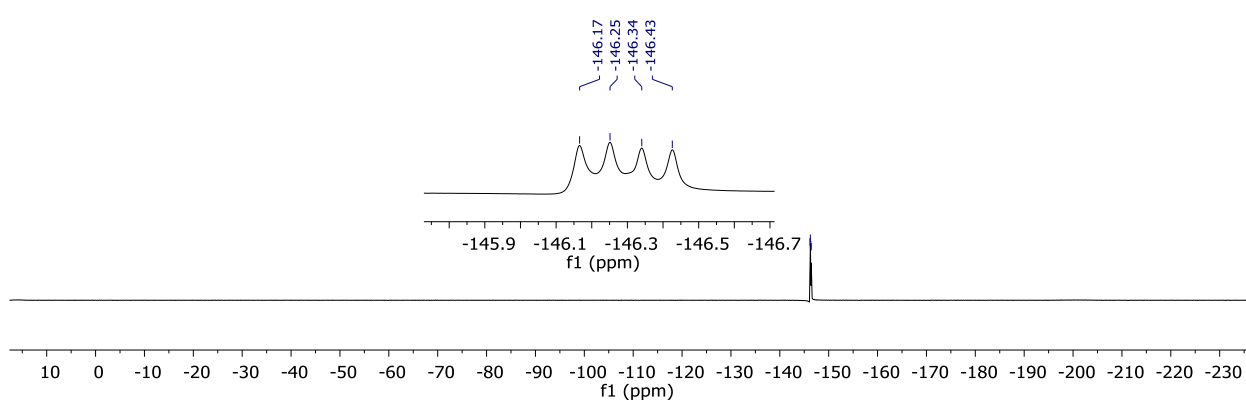
296c
(CDCl₃, 101 MHz)

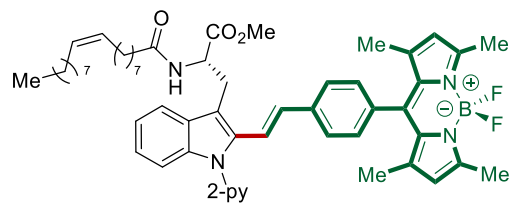


8. NMR Spectra

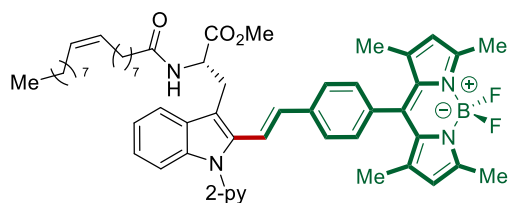
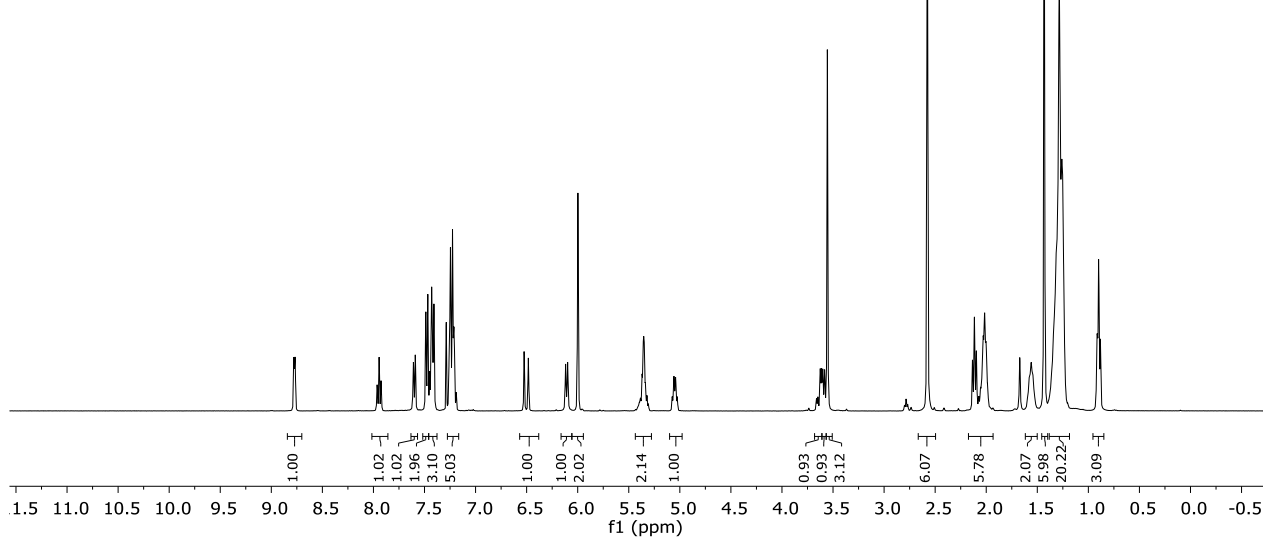


296c
(CDCl₃, 376 MHz)

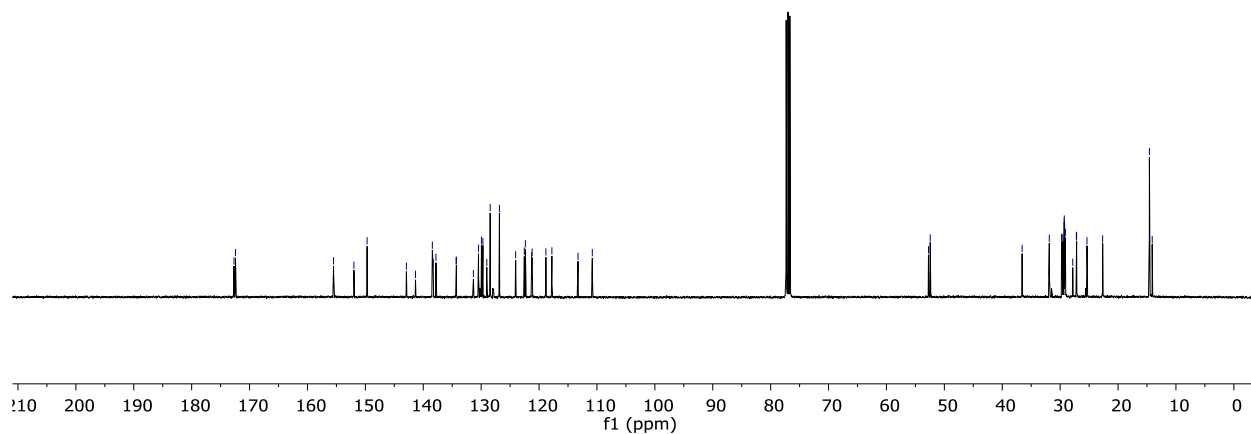




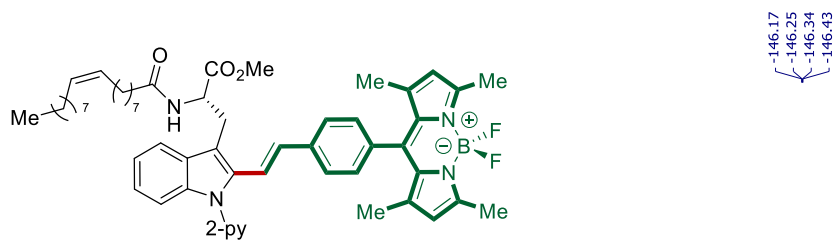
296d
(CDCl₃, 400 MHz)



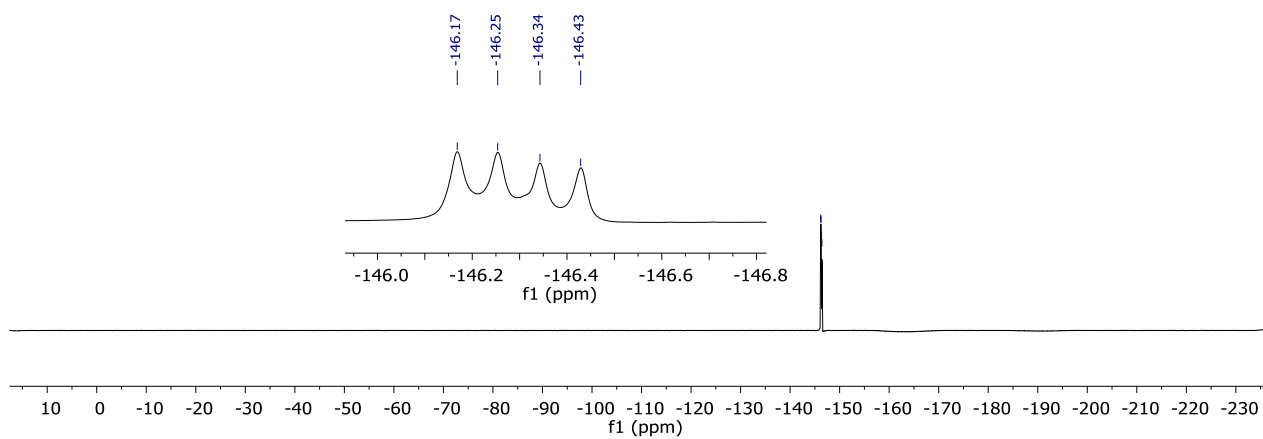
296d
(CDCl₃, 101 MHz)

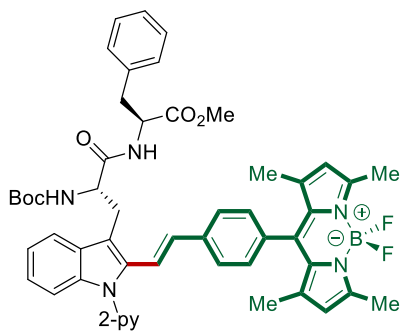


8. NMR Spectra

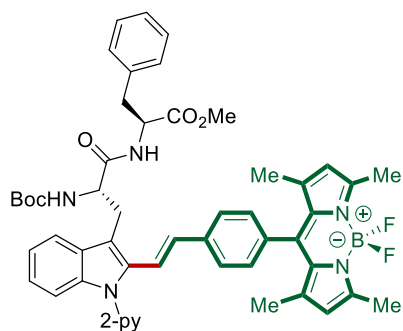
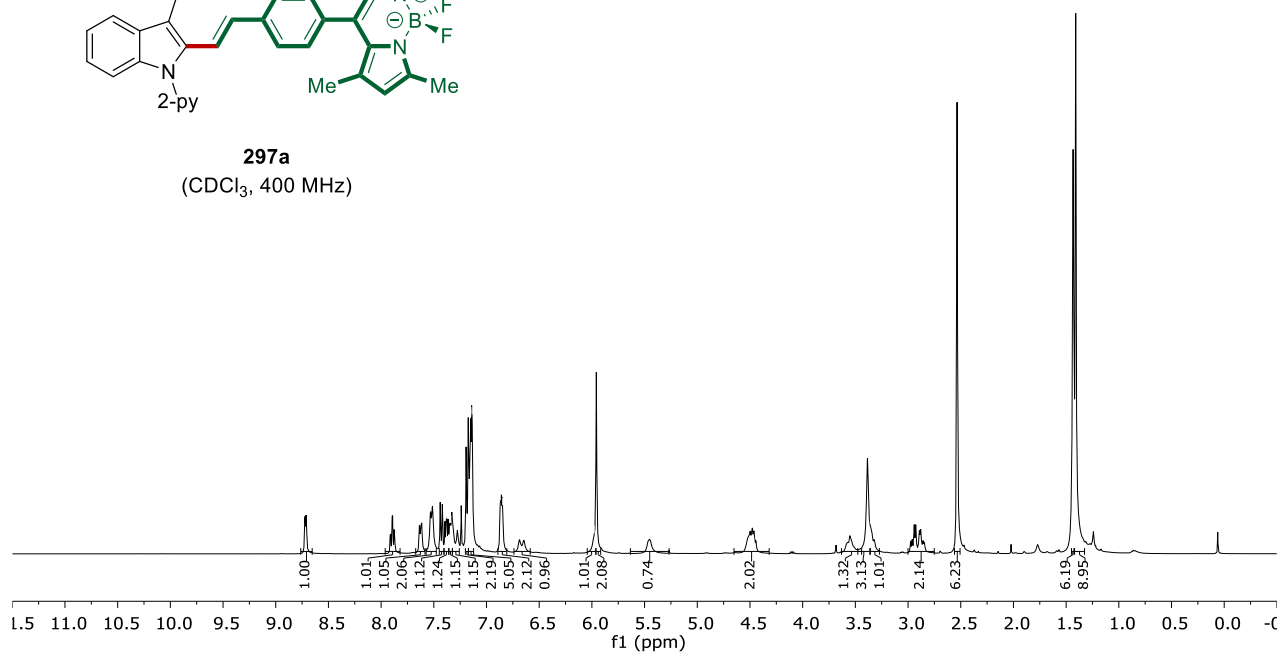


296d
(CDCl₃, 377 MHz)

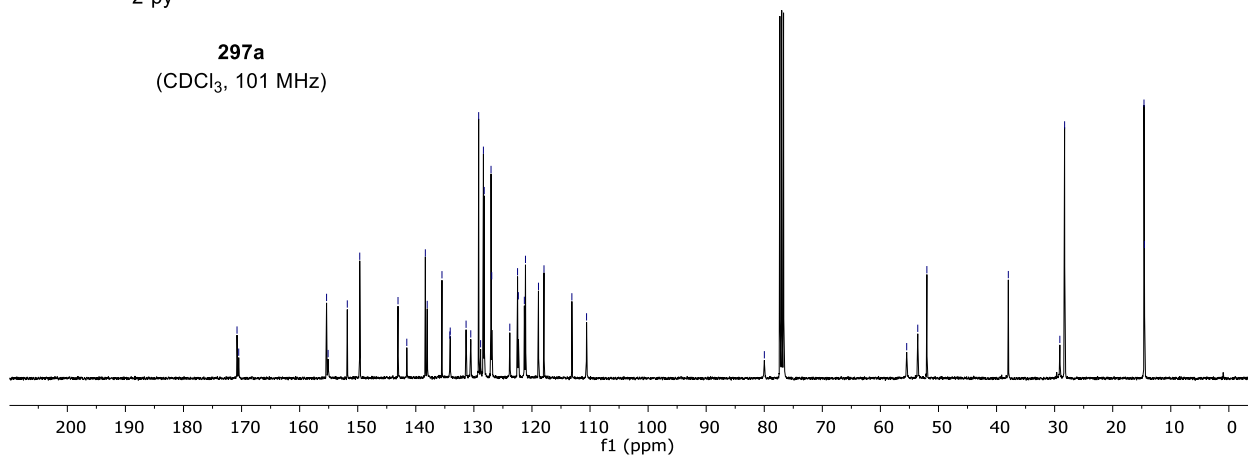




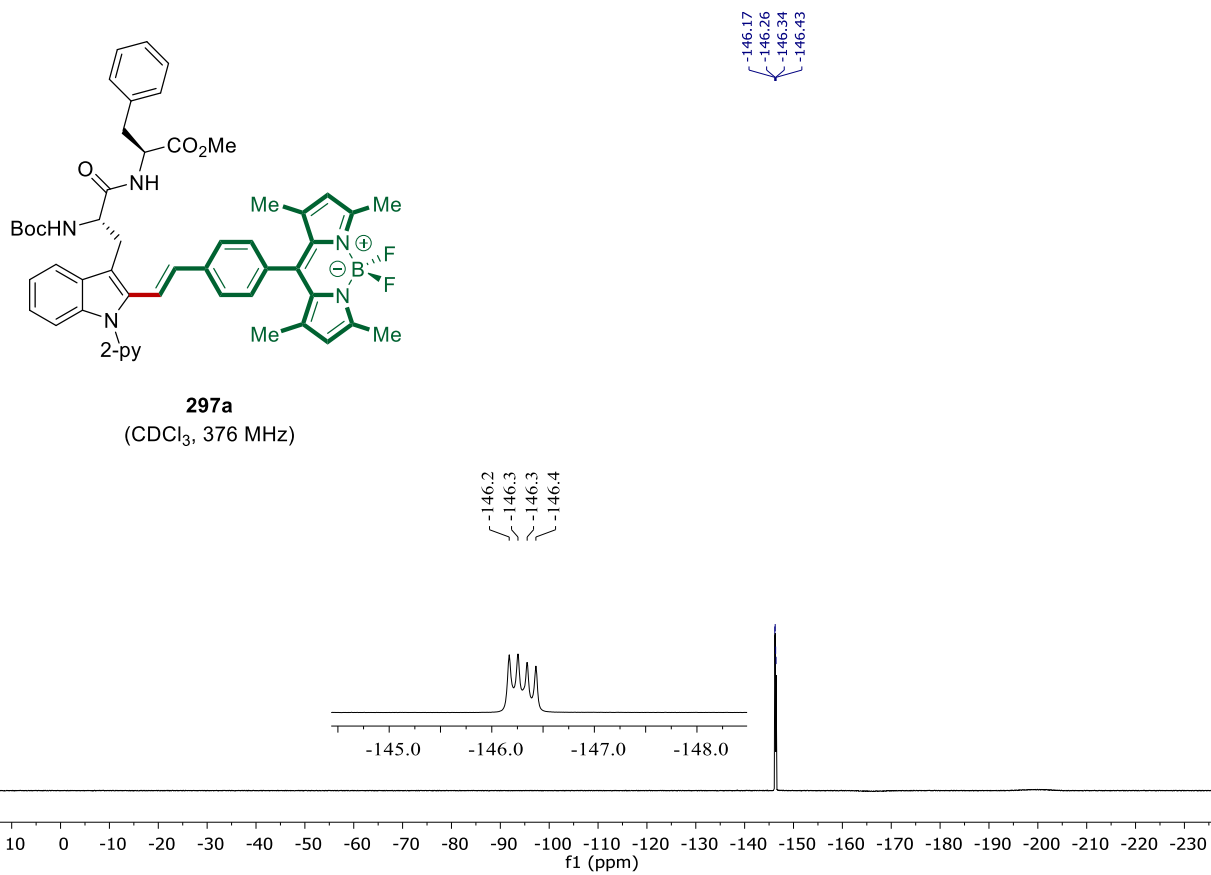
297a
(CDCl₃, 400 MHz)

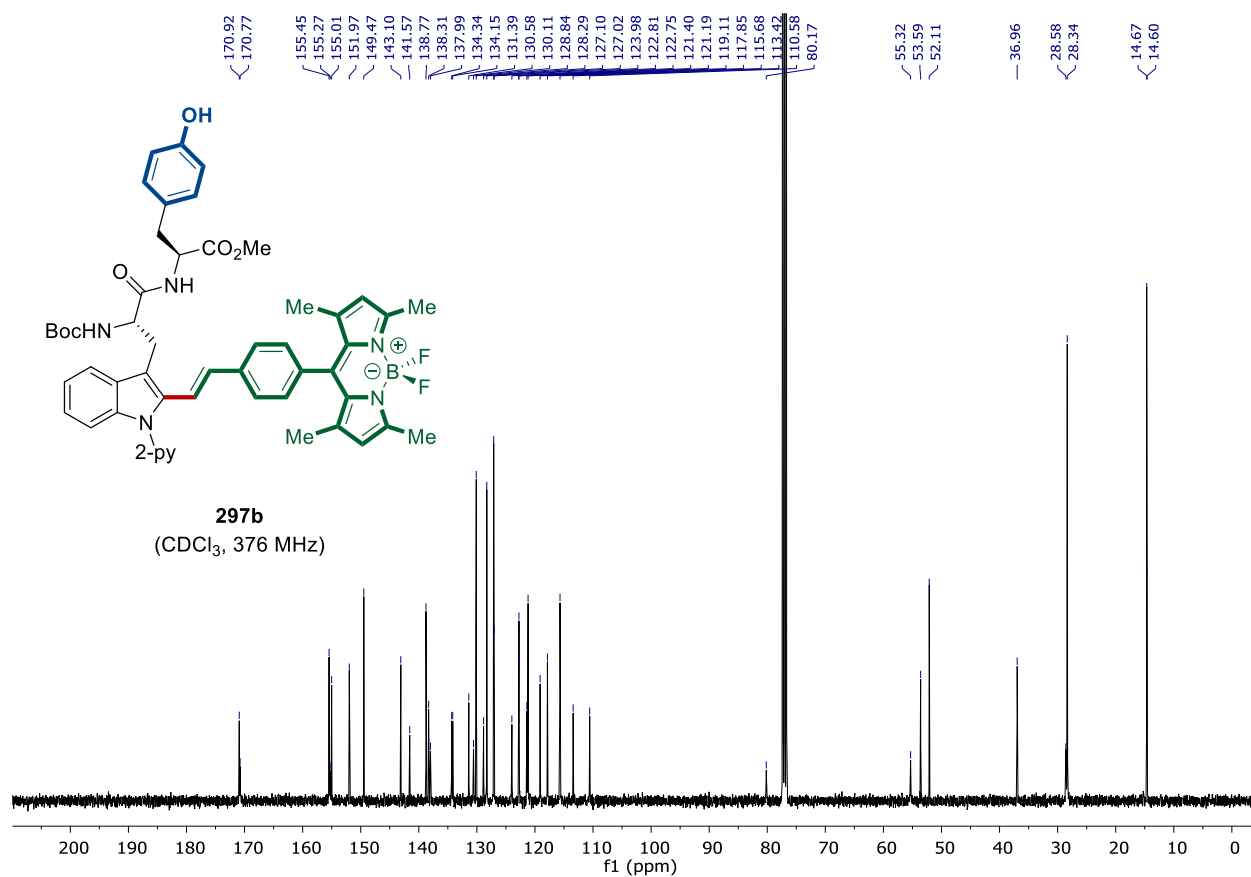
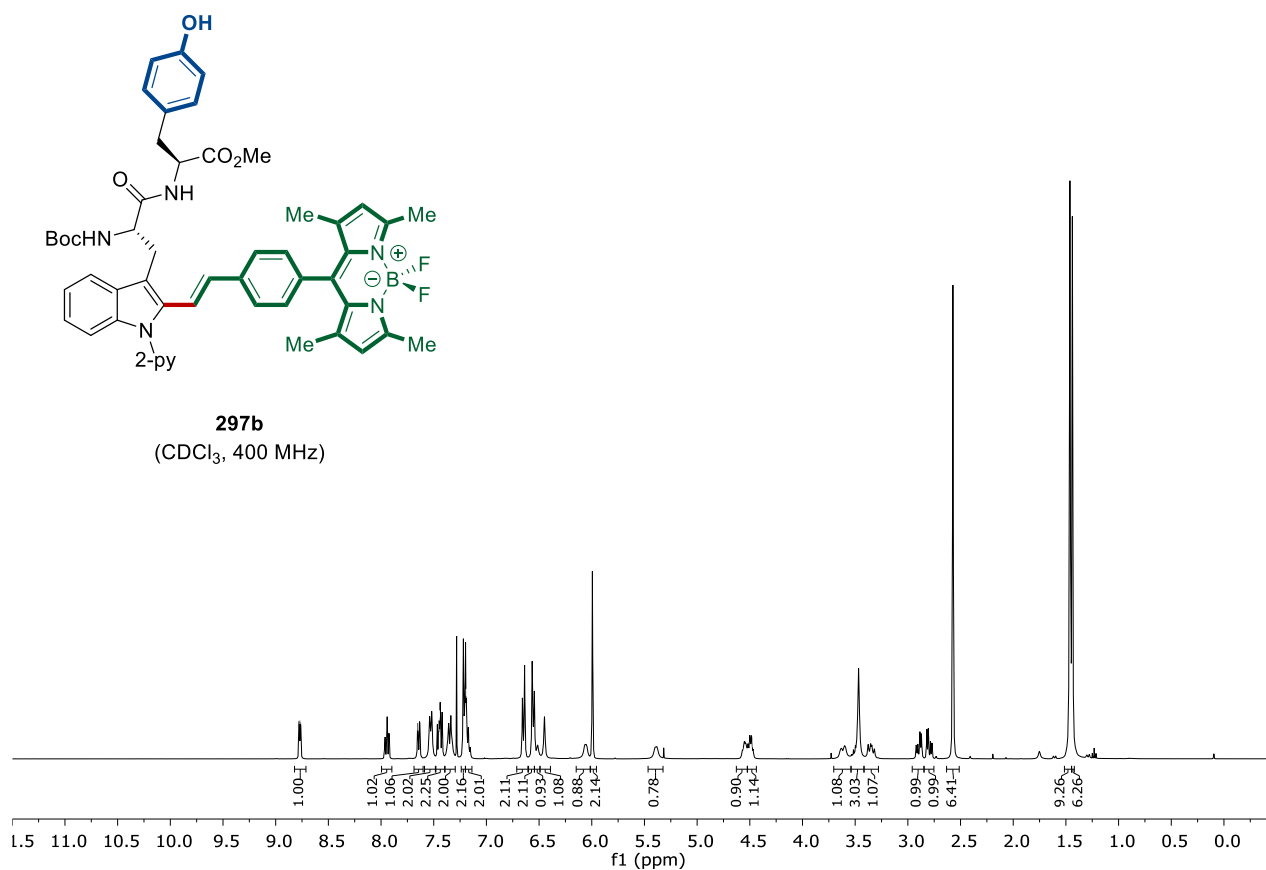


297a
(CDCl₃, 101 MHz)

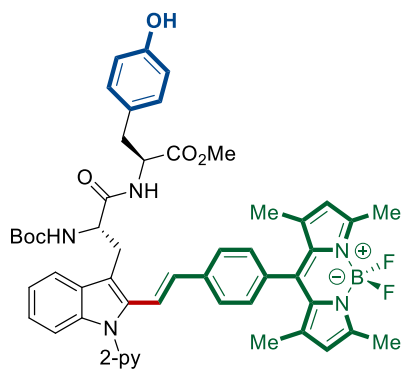


8. NMR Spectra

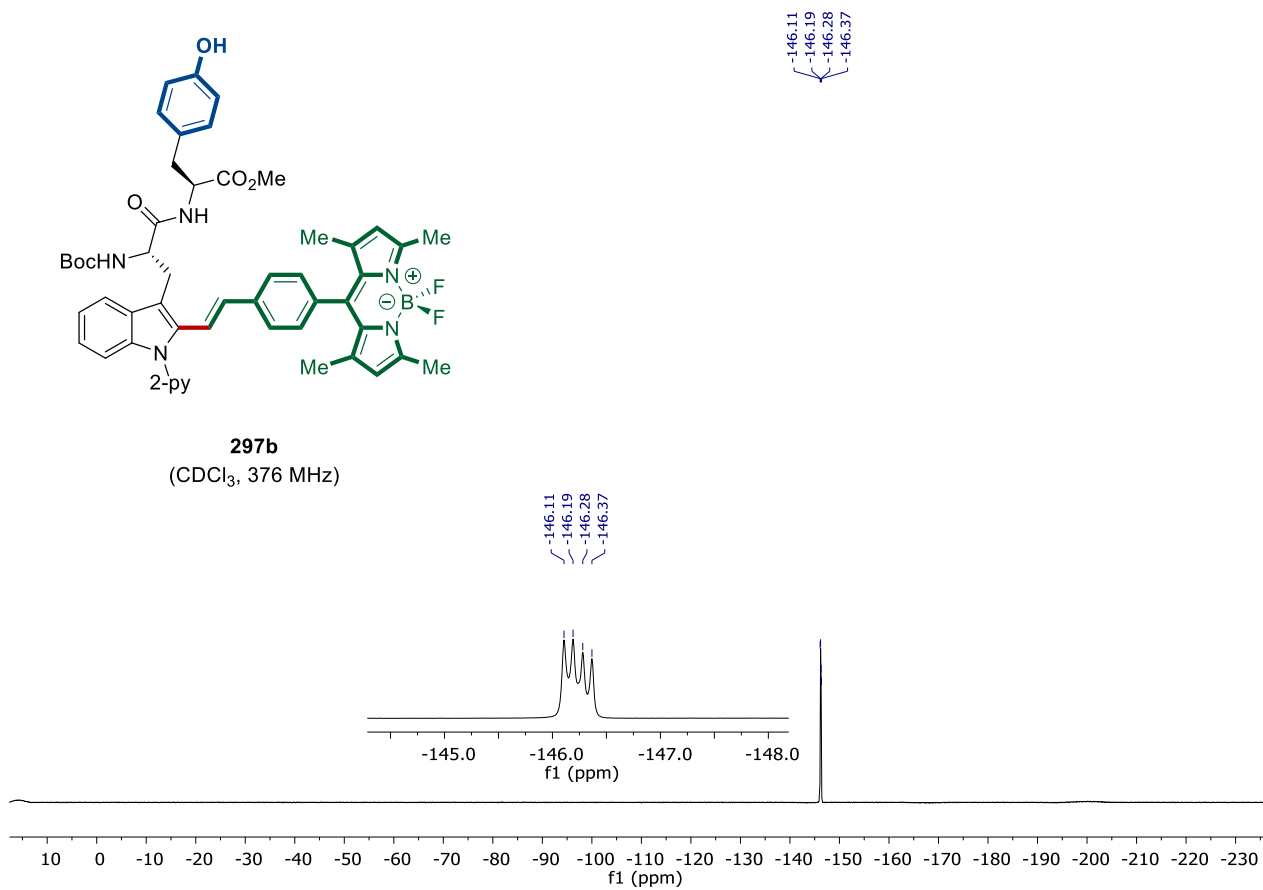




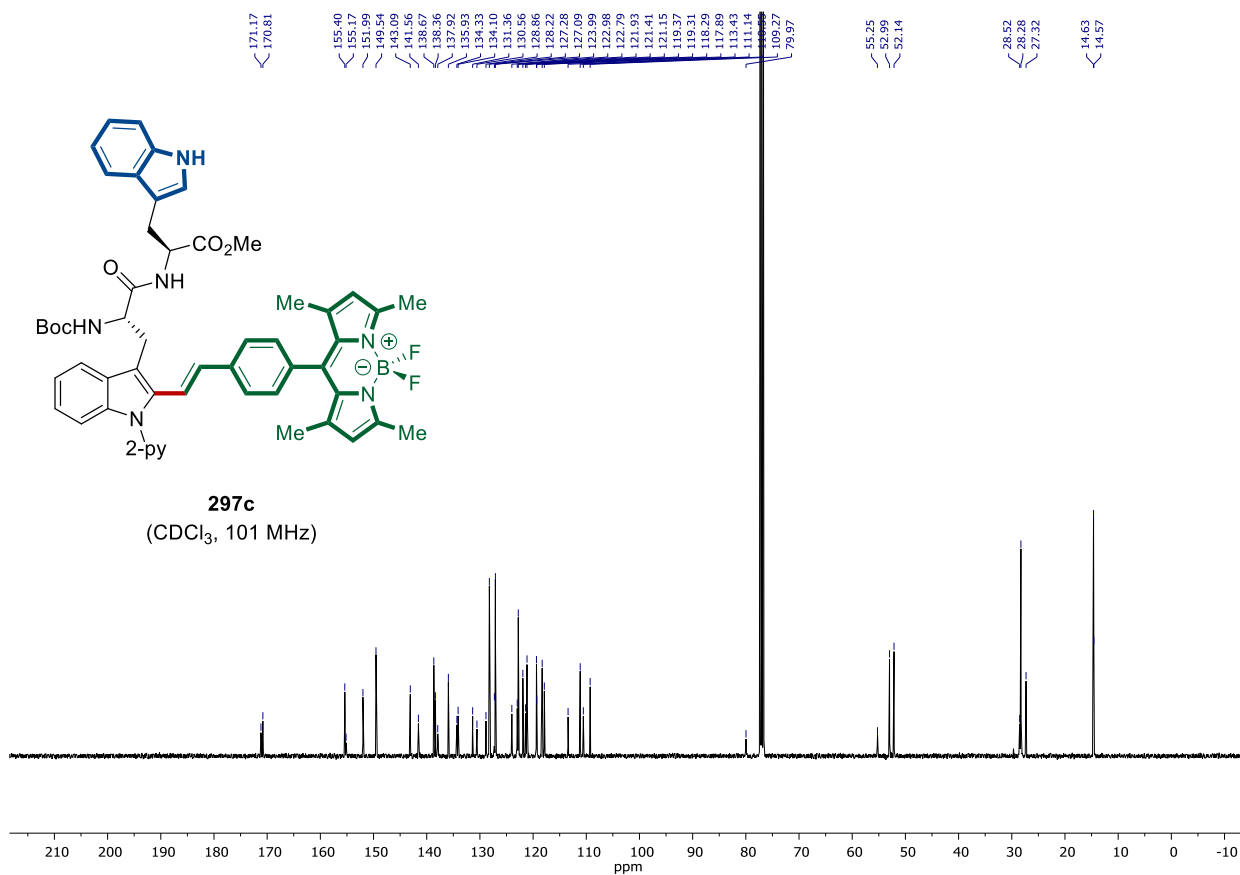
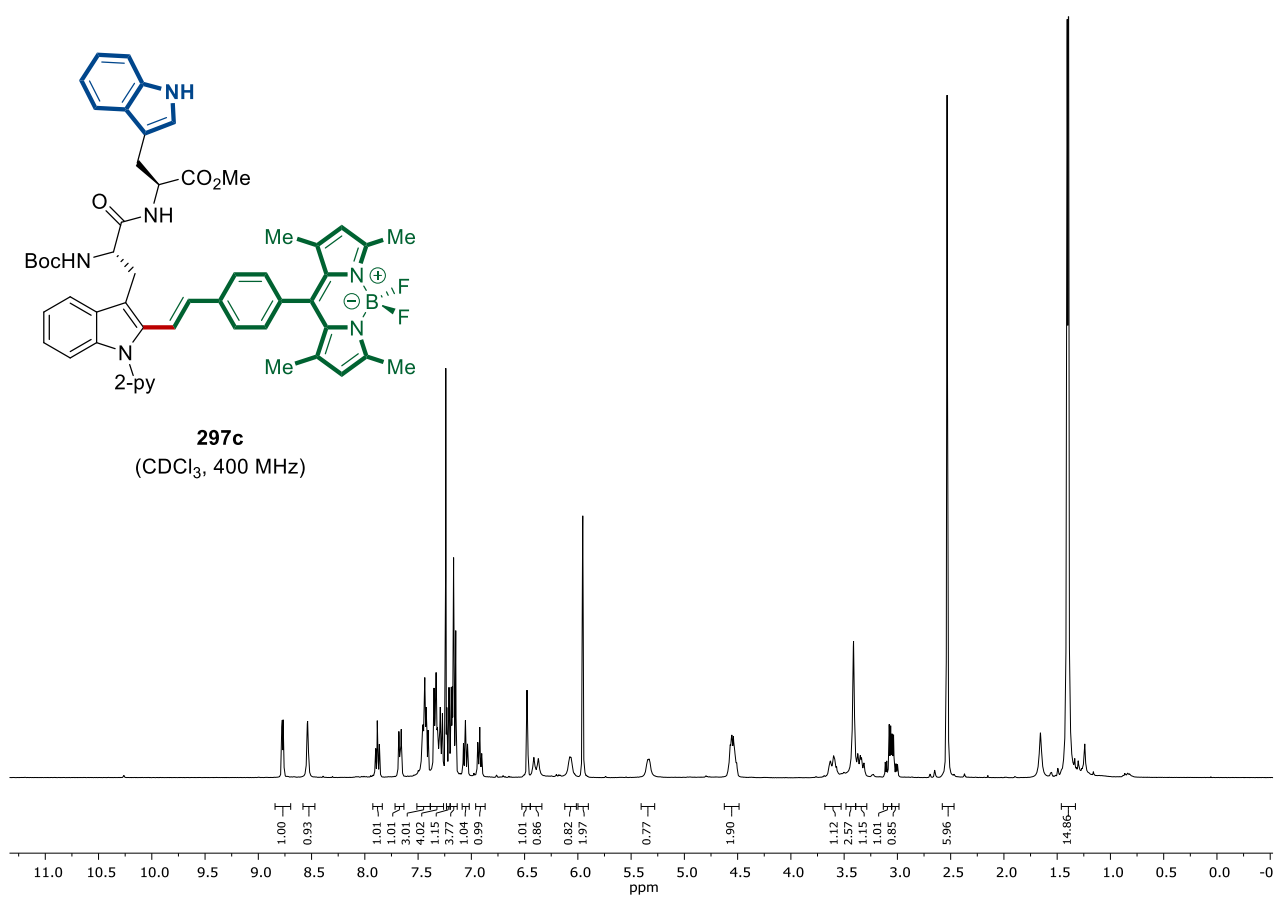
8. NMR Spectra



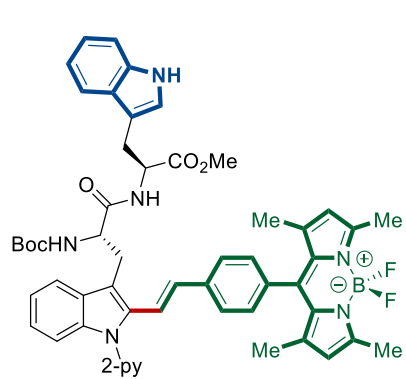
297b
(CDCl₃, 376 MHz)



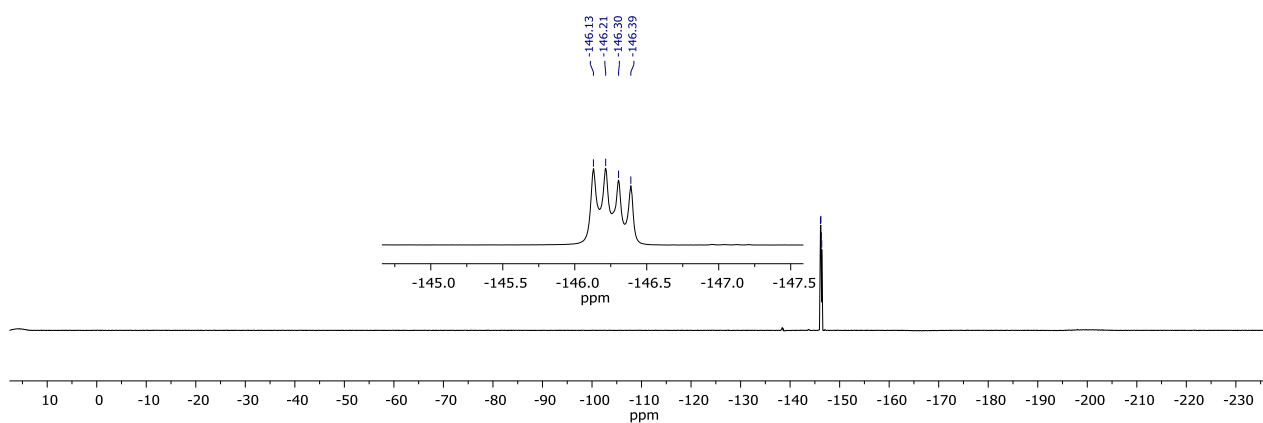
8. NMR Spectra

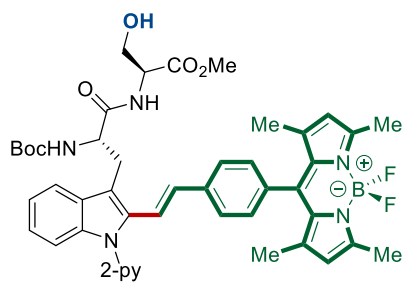


8. NMR Spectra

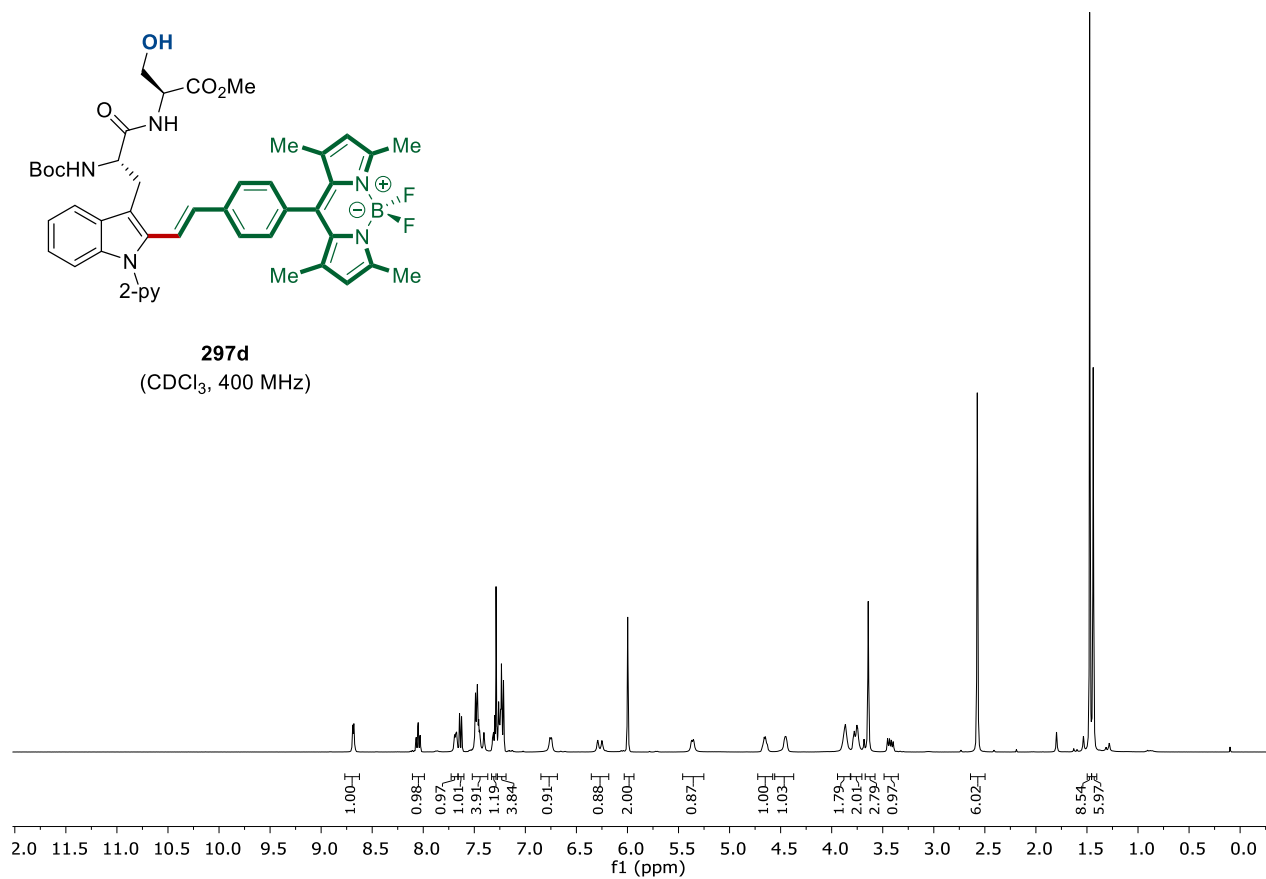


297c
(CDCl₃, 376 MHz)



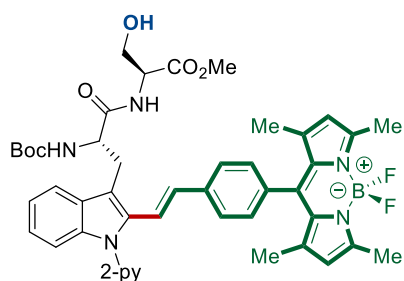


297d
(CDCl₃, 400 MHz)

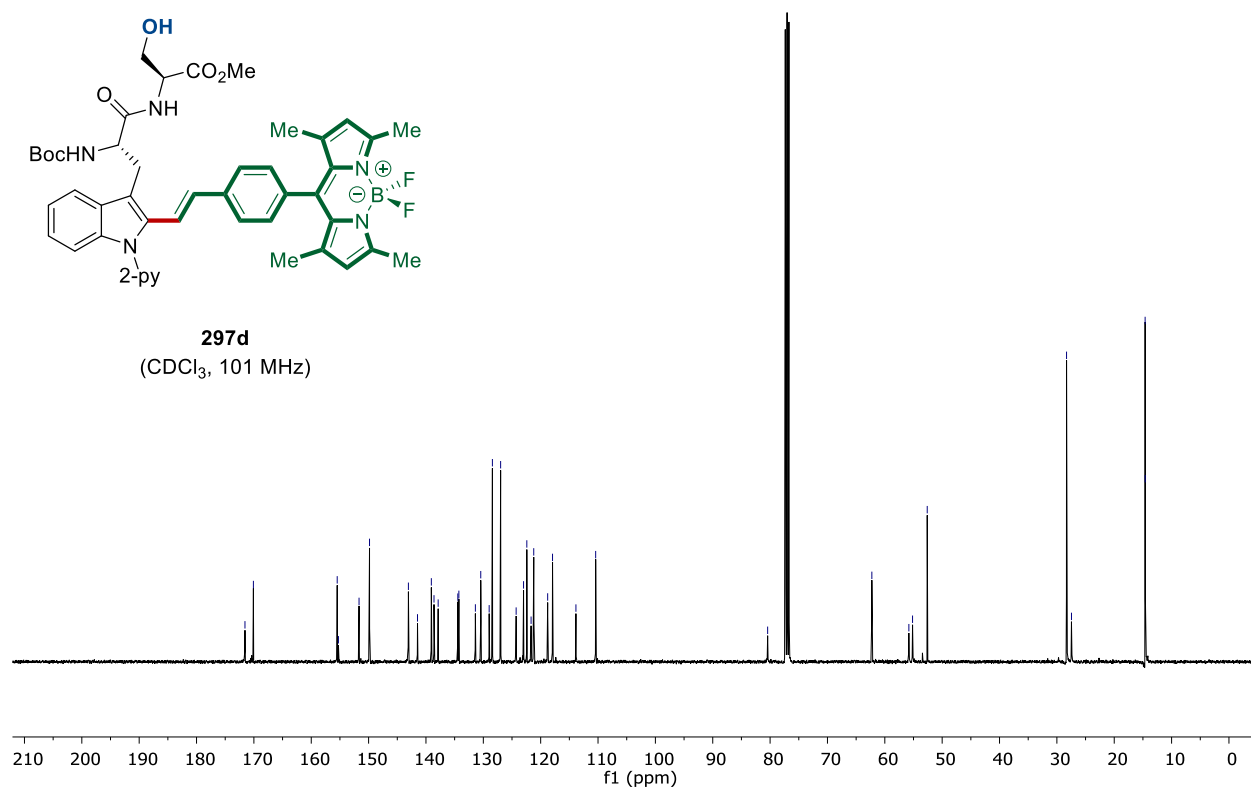


Chemical shift values (ppm) for ¹H NMR spectrum:

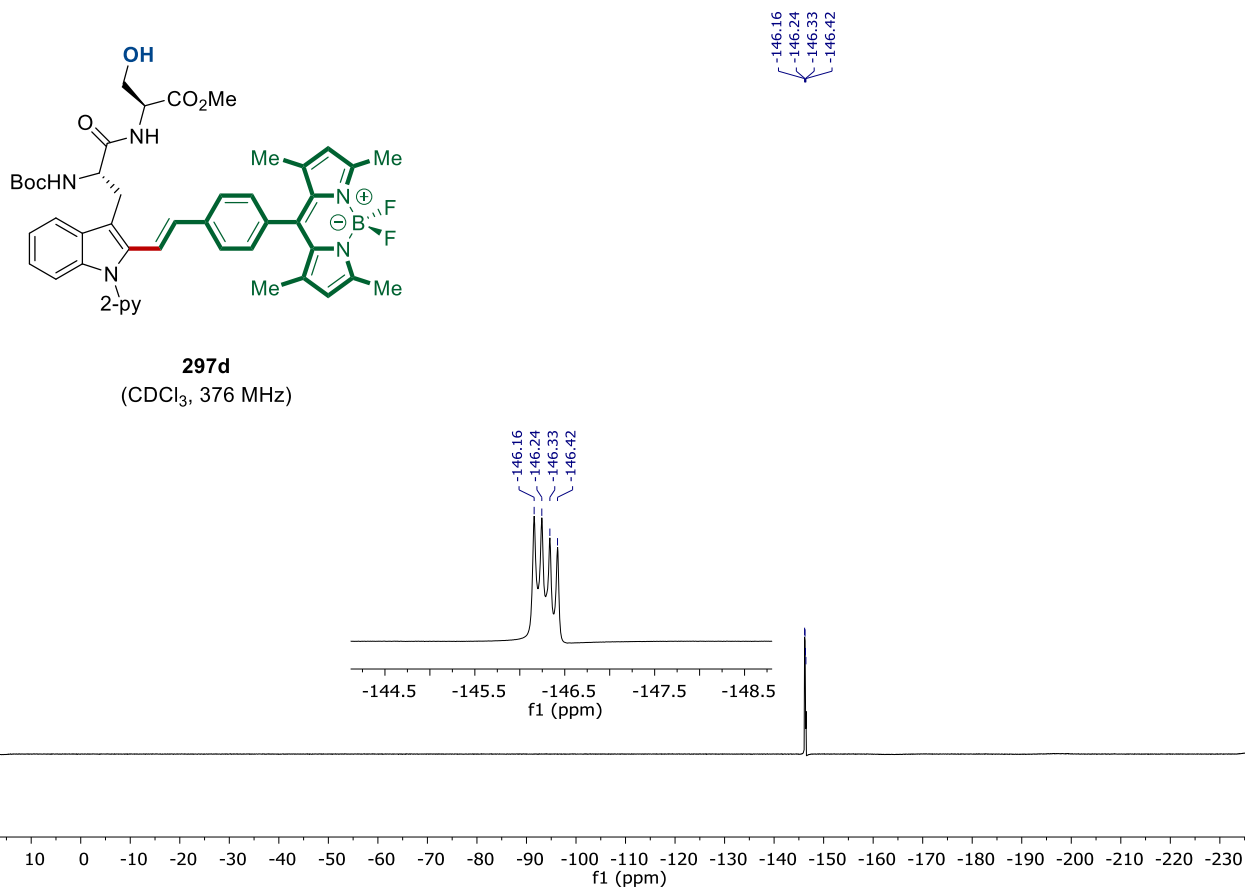
- 171.56
- 170.09
- 155.47
- 155.26
- 151.67
- 149.84
- 143.06
- 139.06
- 138.60
- 137.87
- 134.45
- 134.26
- 131.38
- 130.45
- 128.98
- 128.42
- 126.98
- 124.28
- 122.99
- 122.42
- 121.67
- 121.21
- 118.78
- 117.93
- 113.85
- 110.41
- 80.43
- 62.26
- 55.81
- 55.16
- 52.61
- 28.31
- 27.46
- 14.62
- 14.60

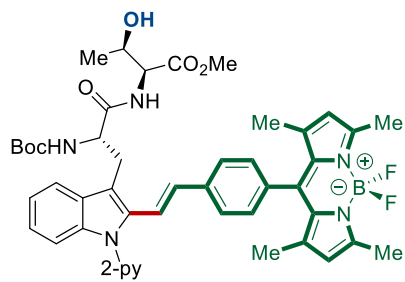


297d
(CDCl₃, 101 MHz)

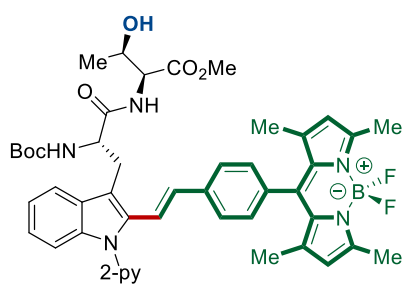
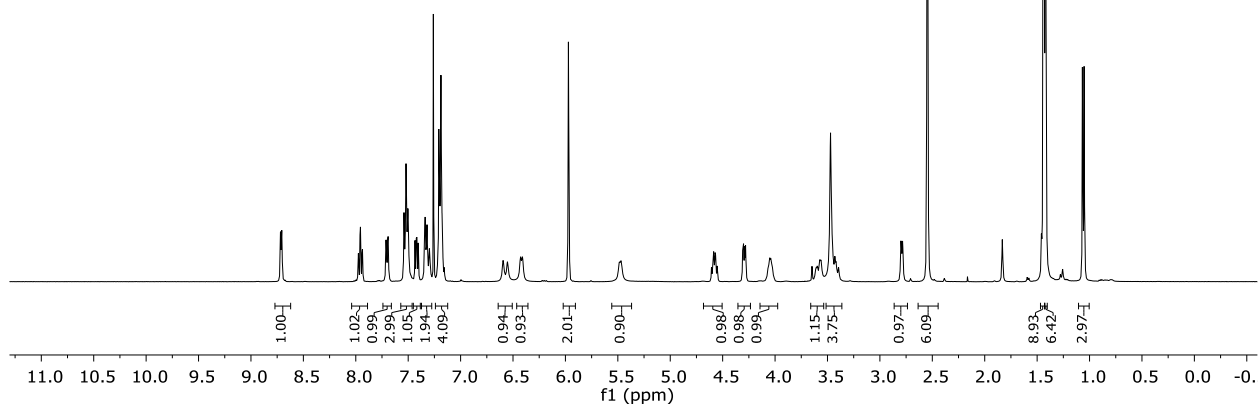


8. NMR Spectra

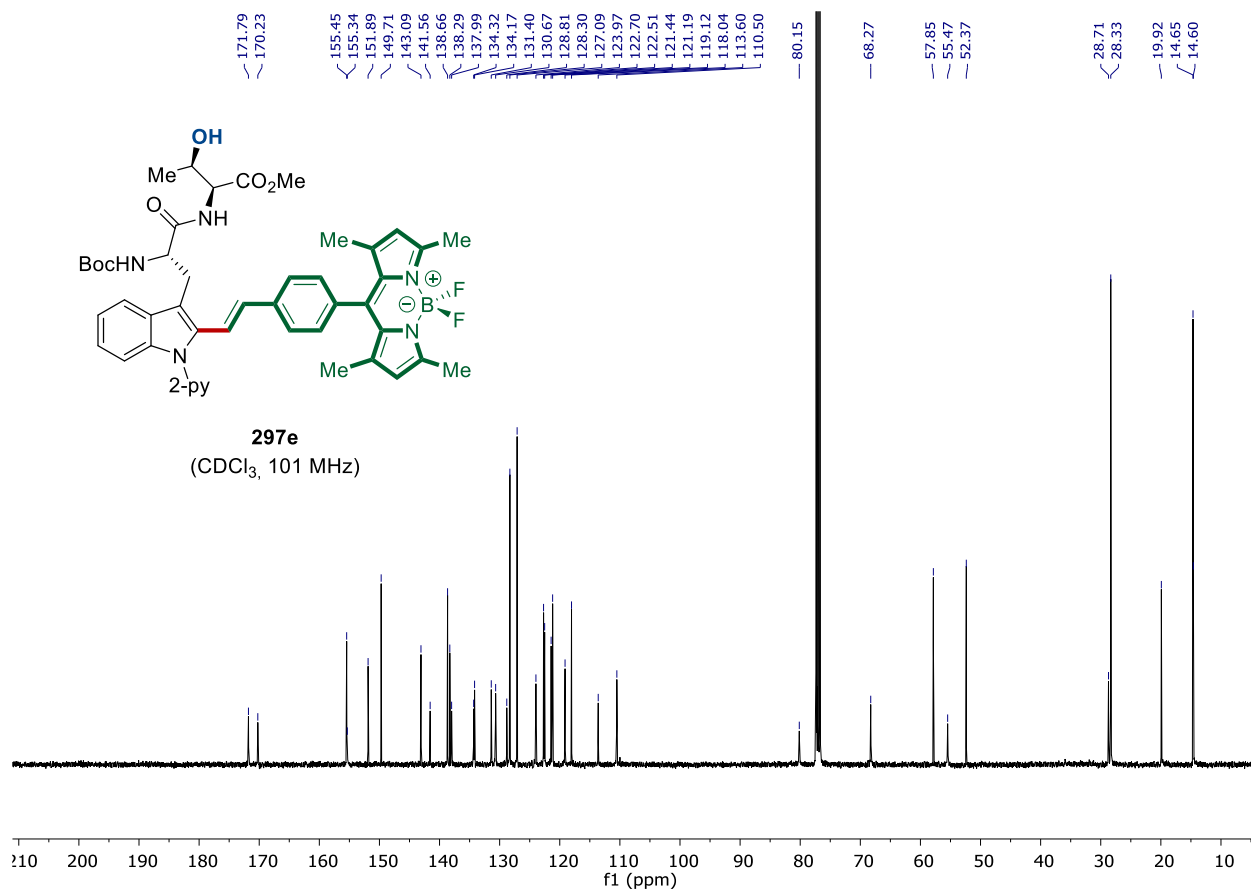




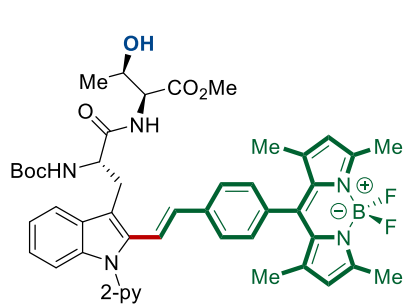
297e
(CDCl₃, 400 MHz)



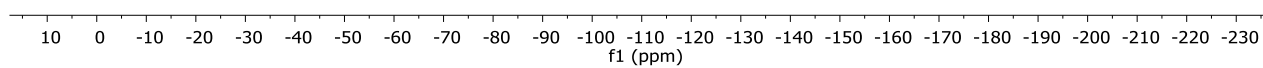
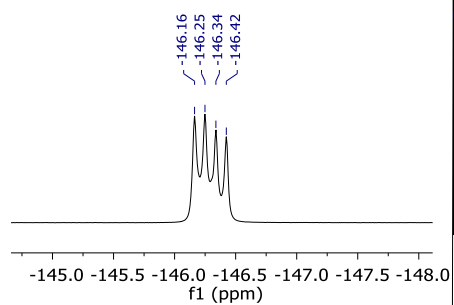
297e
(CDCl₃, 101 MHz)



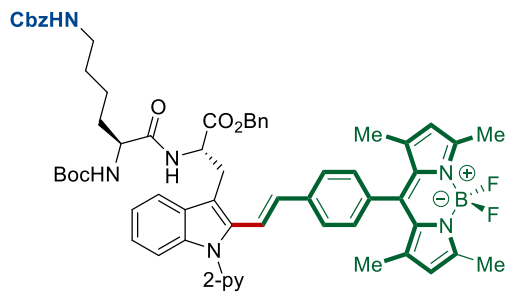
8. NMR Spectra



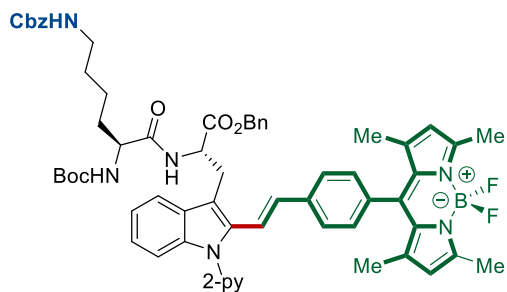
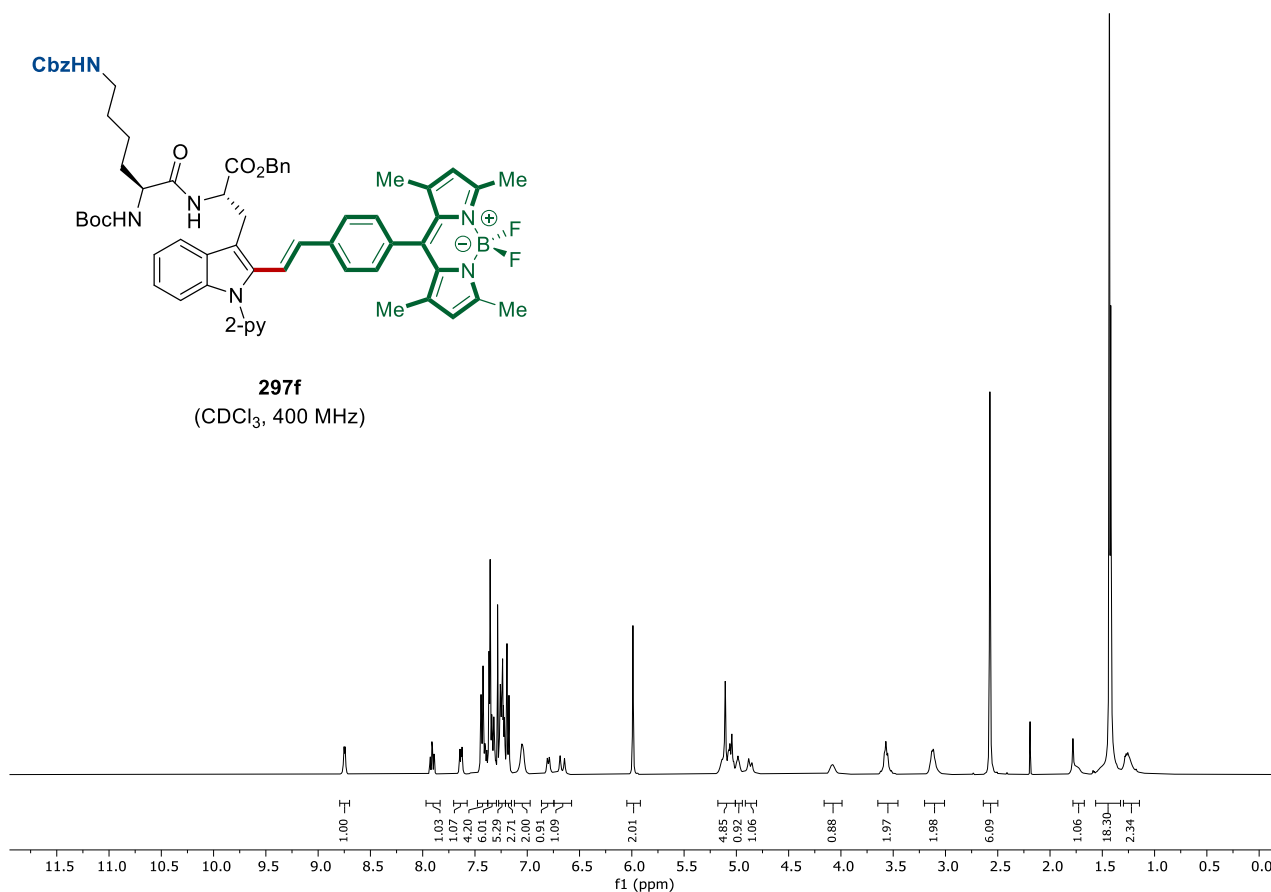
297e
(CDCl₃, 376 MHz)



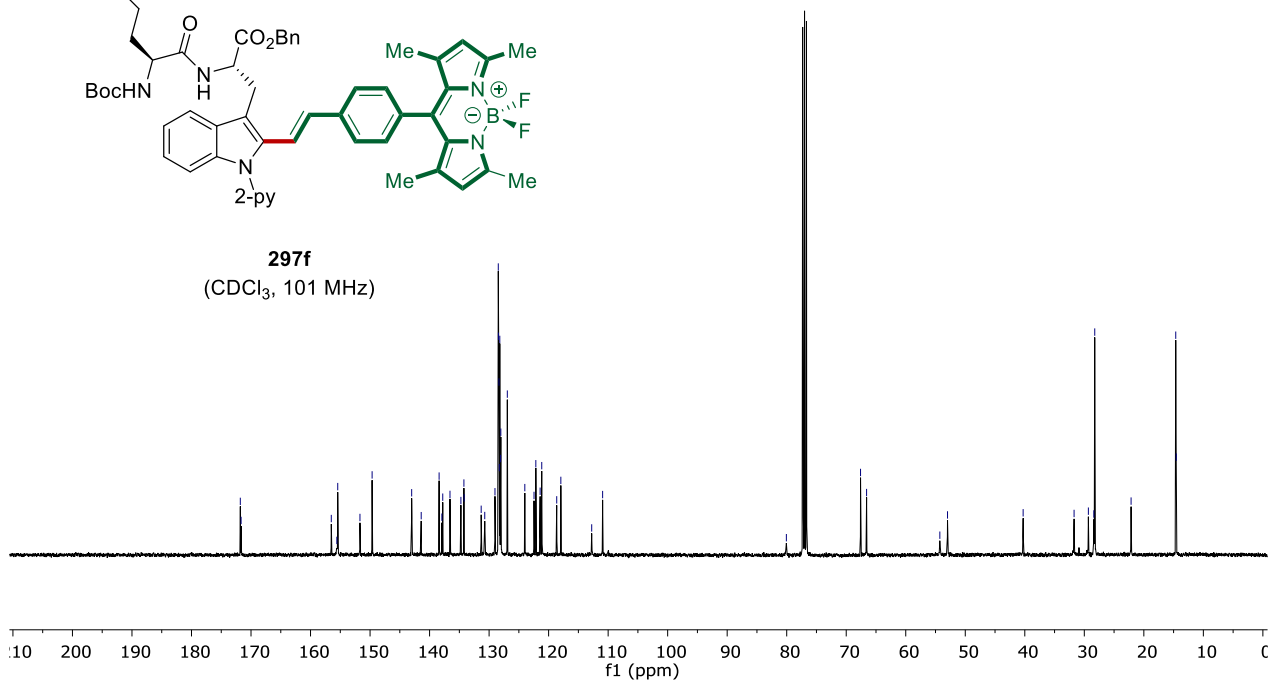
8. NMR Spectra



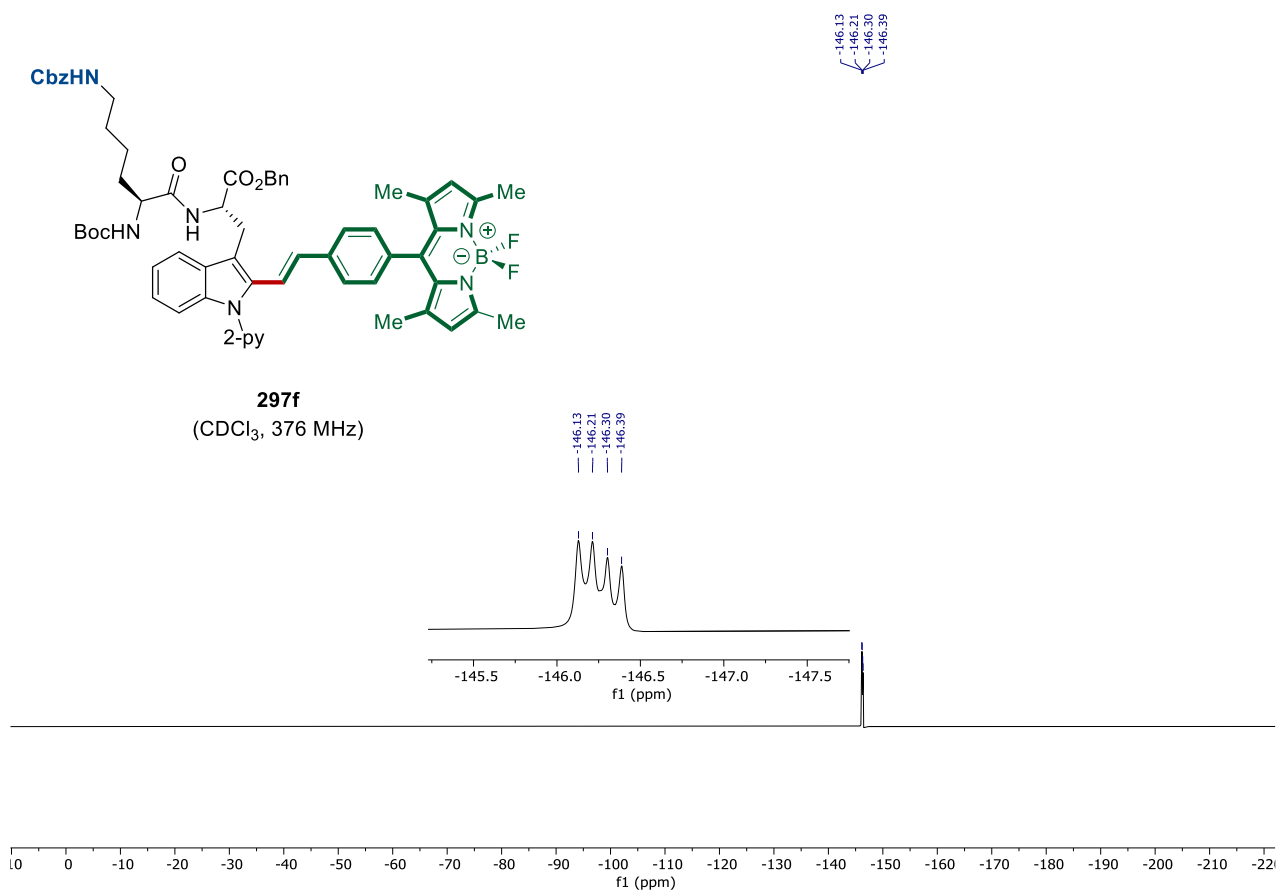
297f
(CDCl₃, 400 MHz)

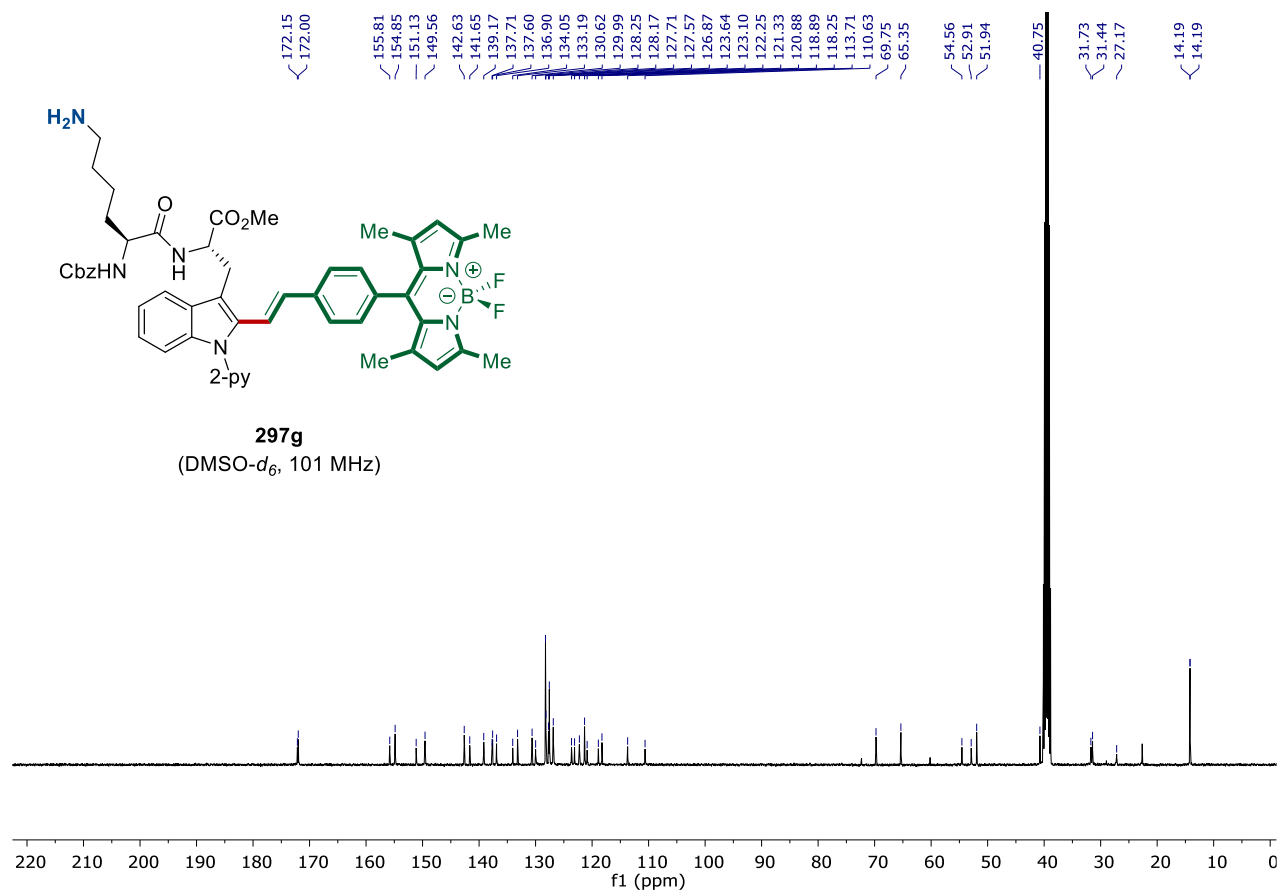
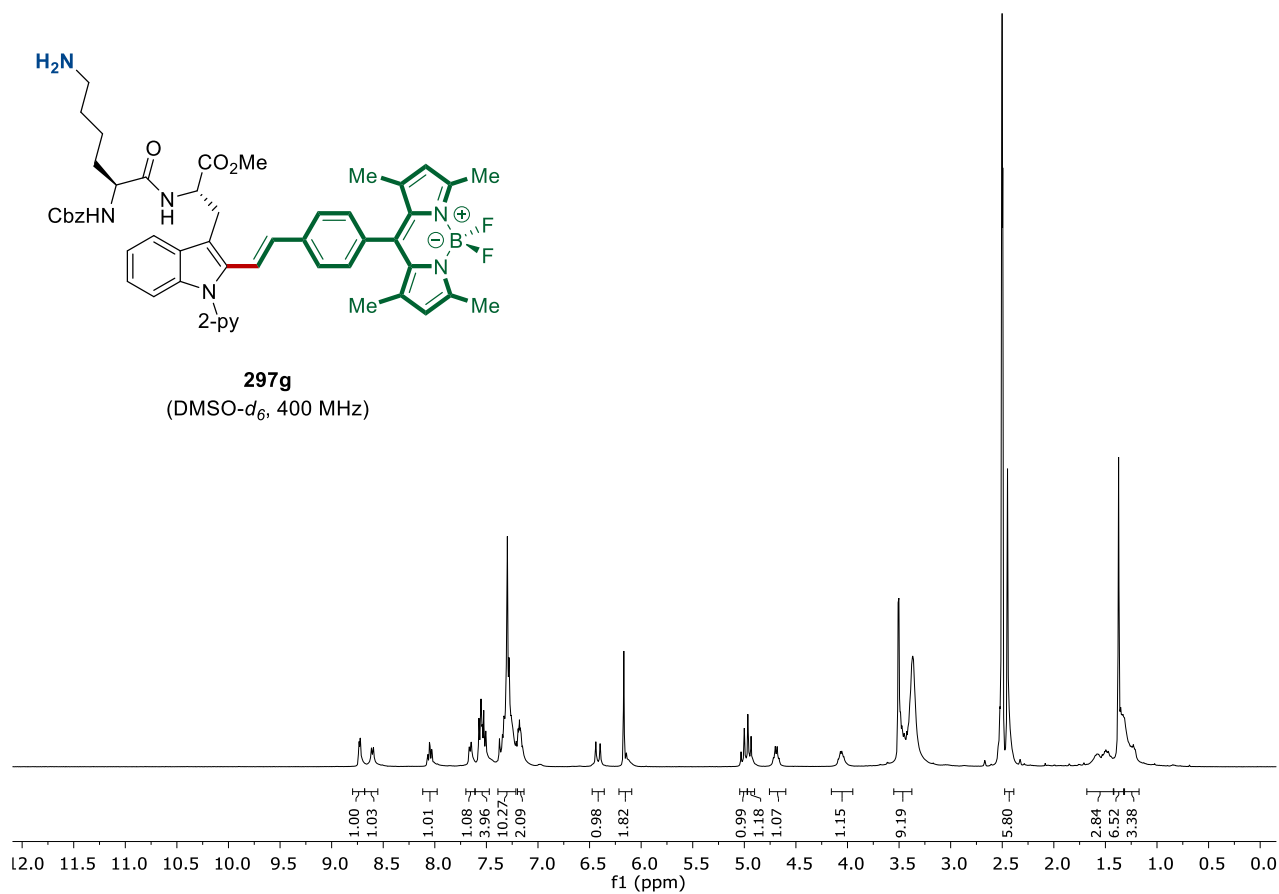


297f
(CDCl₃, 101 MHz)

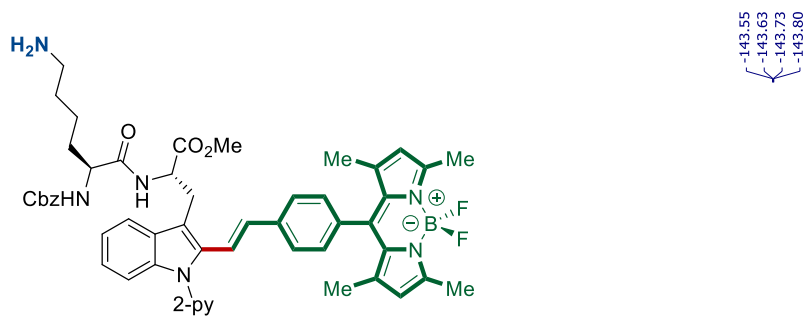


8. NMR Spectra

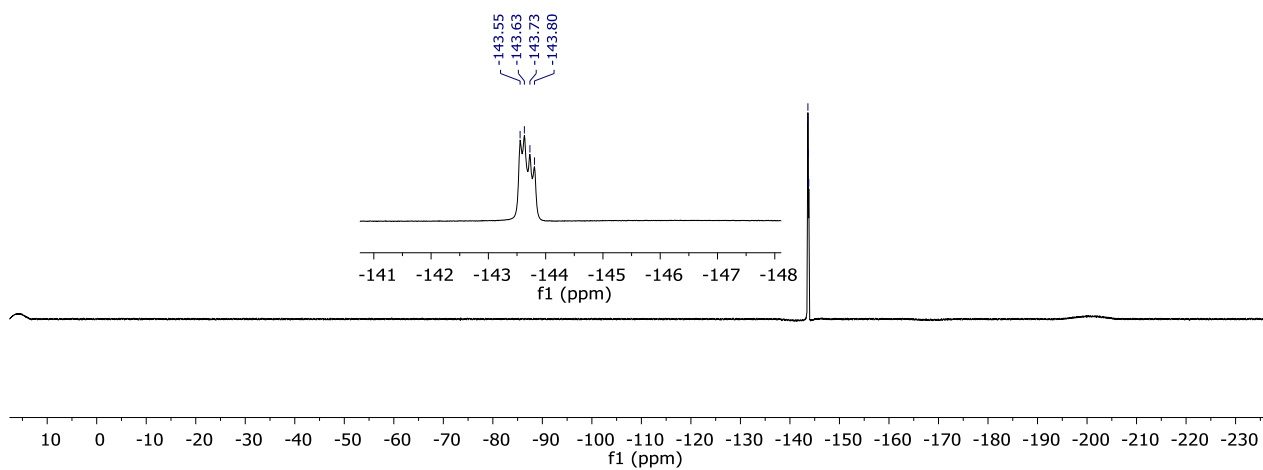


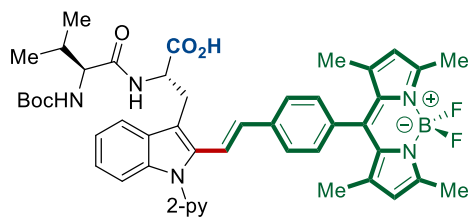


8. NMR Spectra

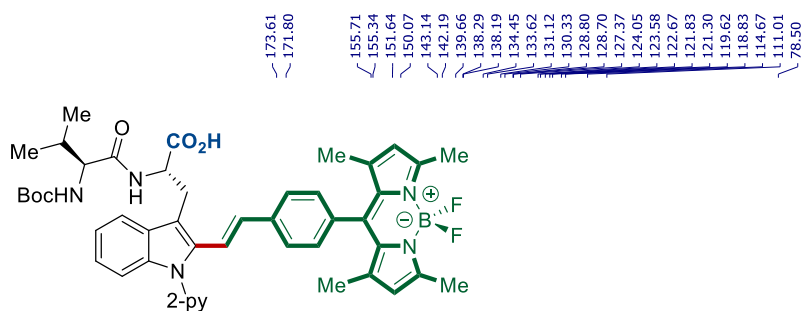
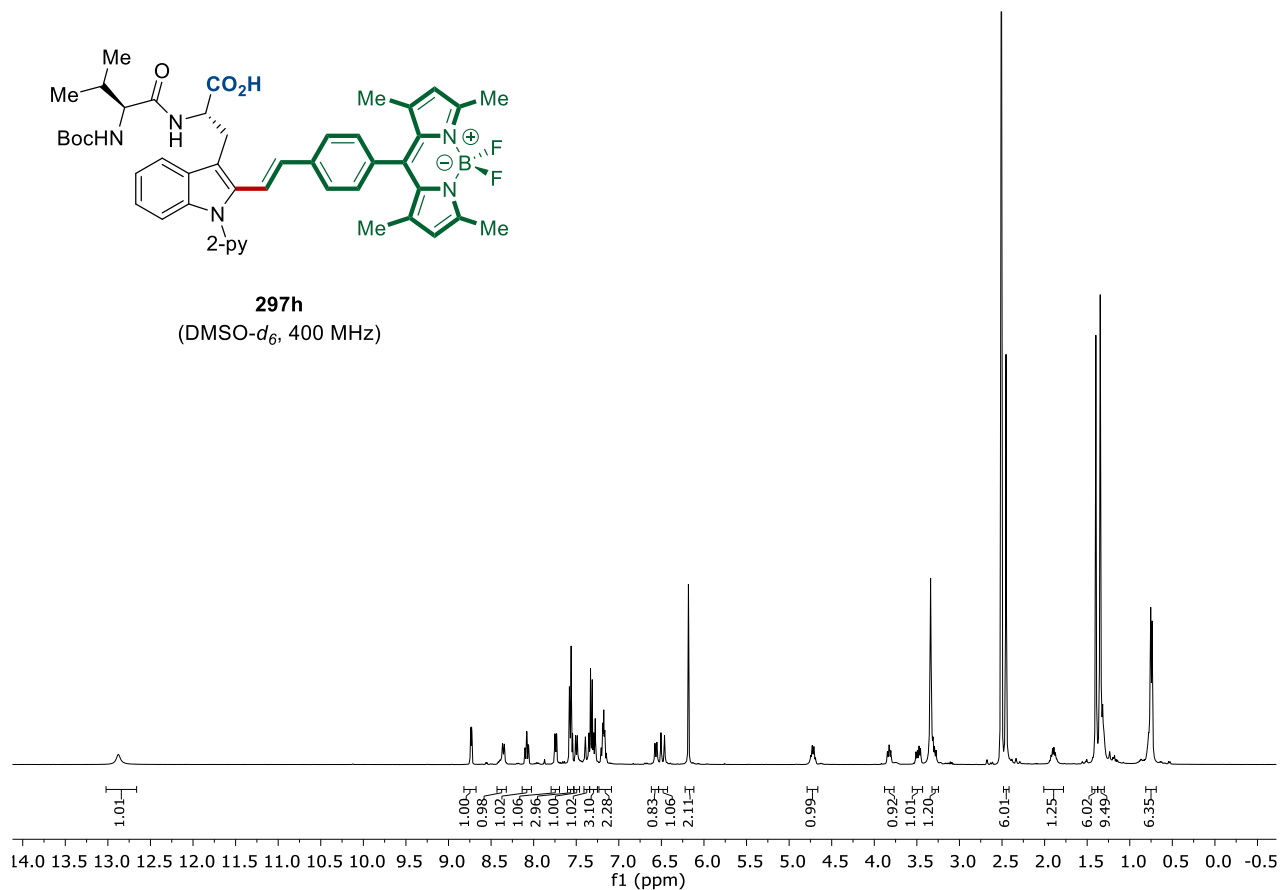


297g
(DMSO-*d*₆, 376 MHz)

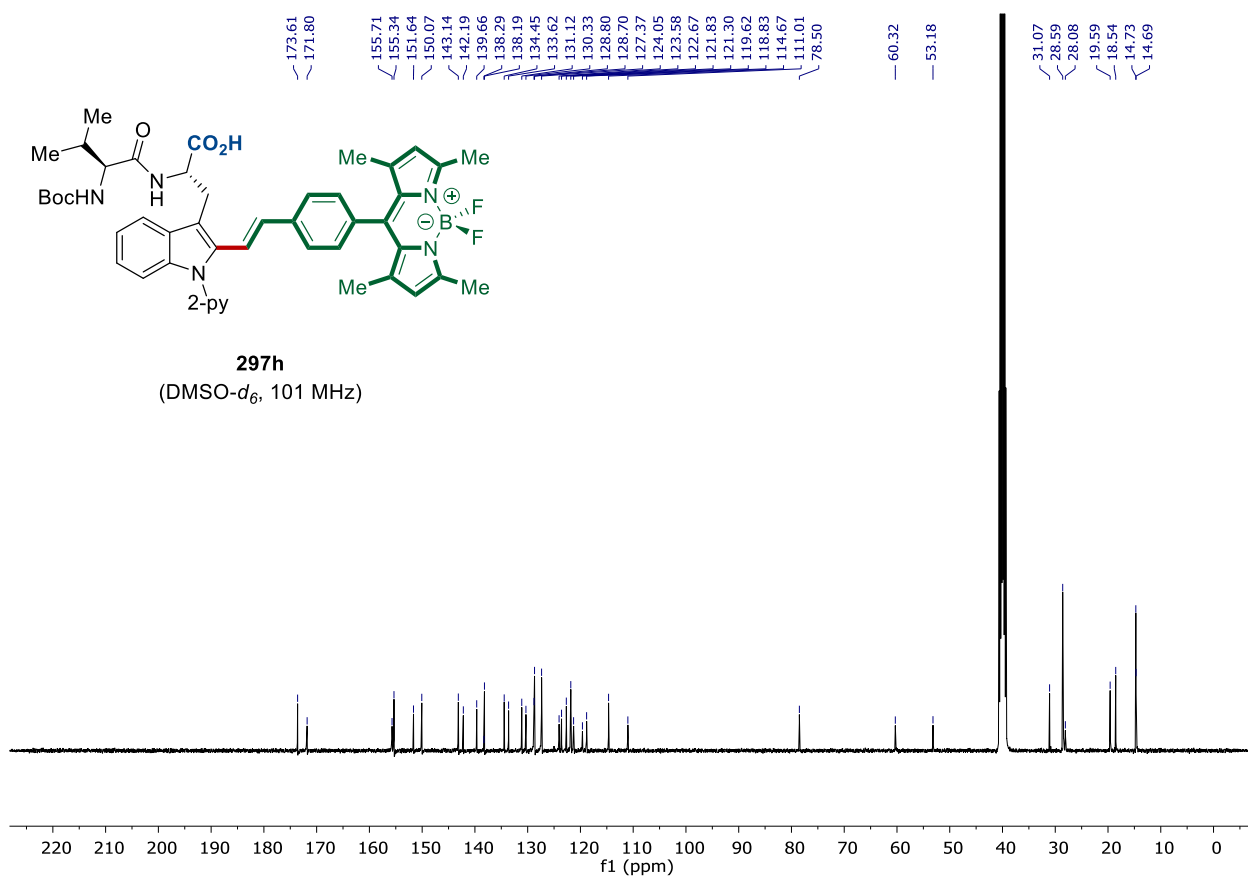




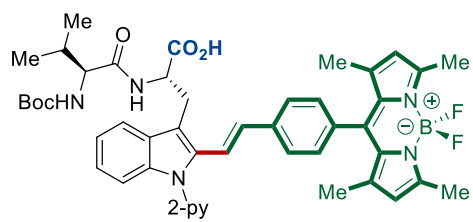
297h
(DMSO- d_6 , 400 MHz)



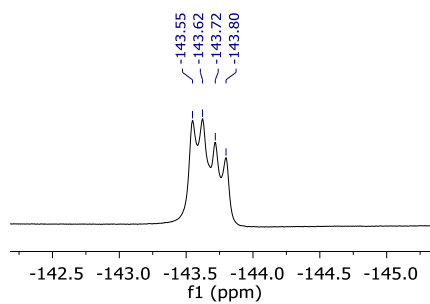
297h
(DMSO- d_6 , 101 MHz)



8. NMR Spectra



297h
(DMSO-*d*₆, 376 MHz)

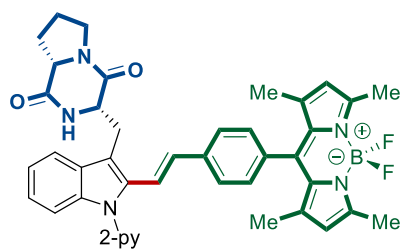


-143.55
-143.62
-143.72
-143.80

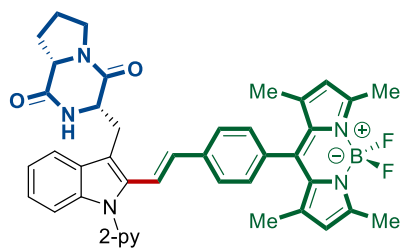
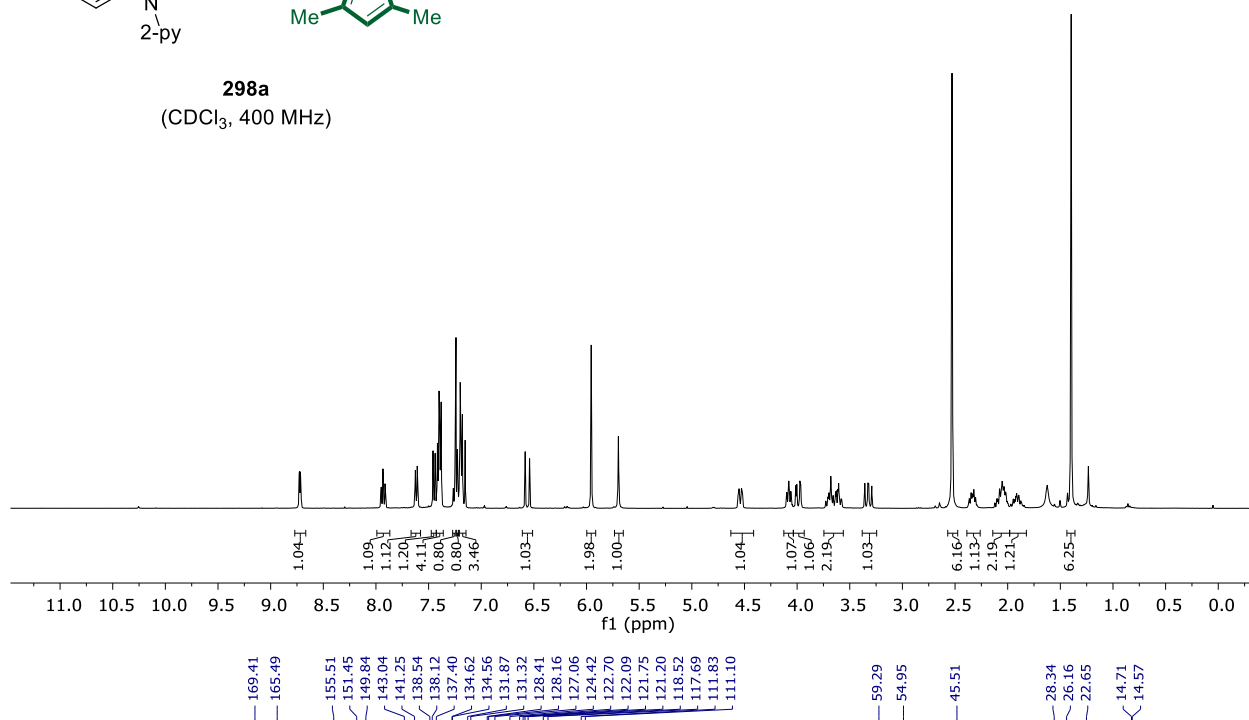
-143.55
-143.62
-143.72
-143.80

-142.5 -143.0 -143.5 -144.0 -144.5 -145.0
f1 (ppm)

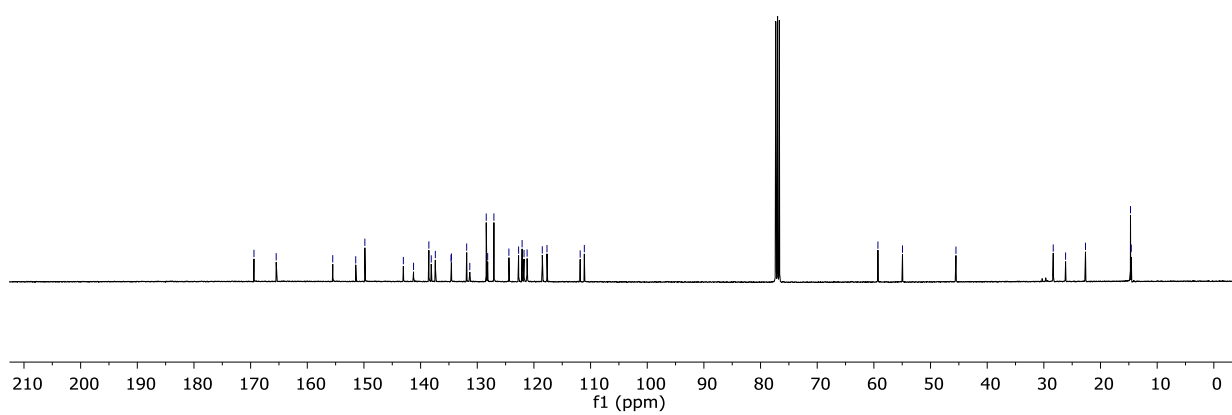
10 0 -10 -20 -30 -40 -50 -60 -70 -80 -90 -100 -110 -120 -130 -140 -150 -160 -170 -180 -190 -200 -210 -220 -230
f1 (ppm)



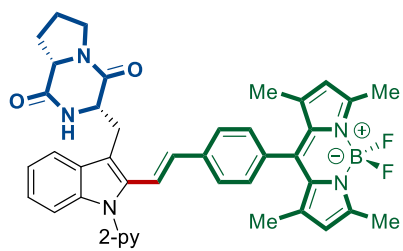
298a
(CDCl₃, 400 MHz)



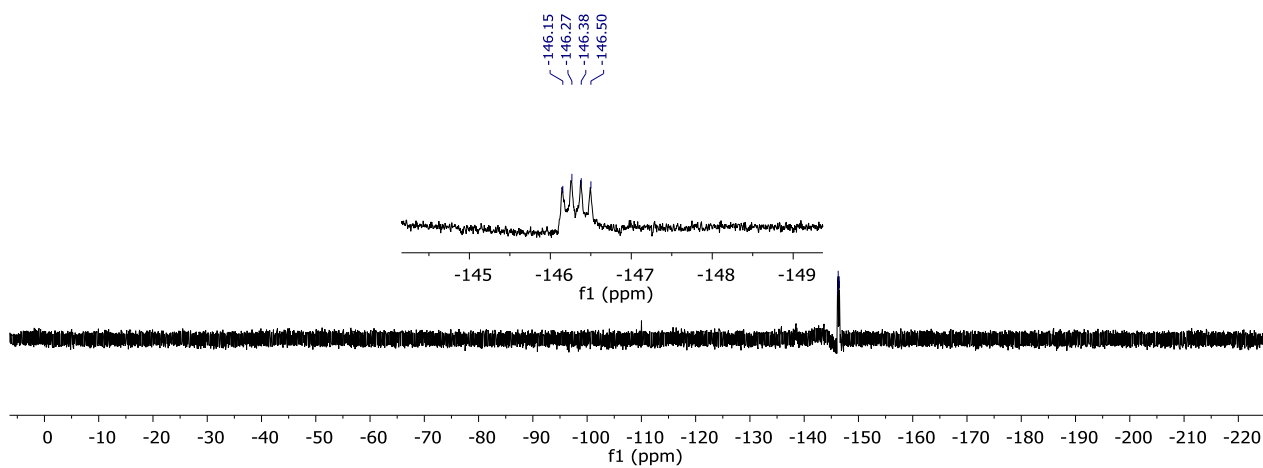
298a
(CDCl₃, 101 MHz)

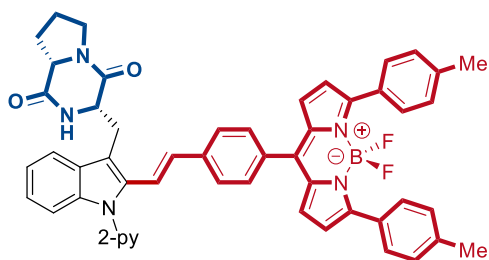


8. NMR Spectra

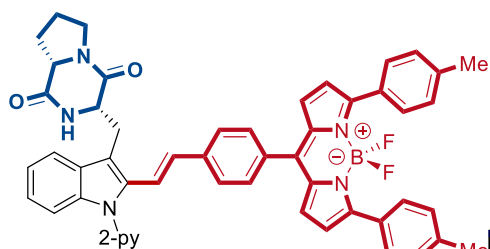
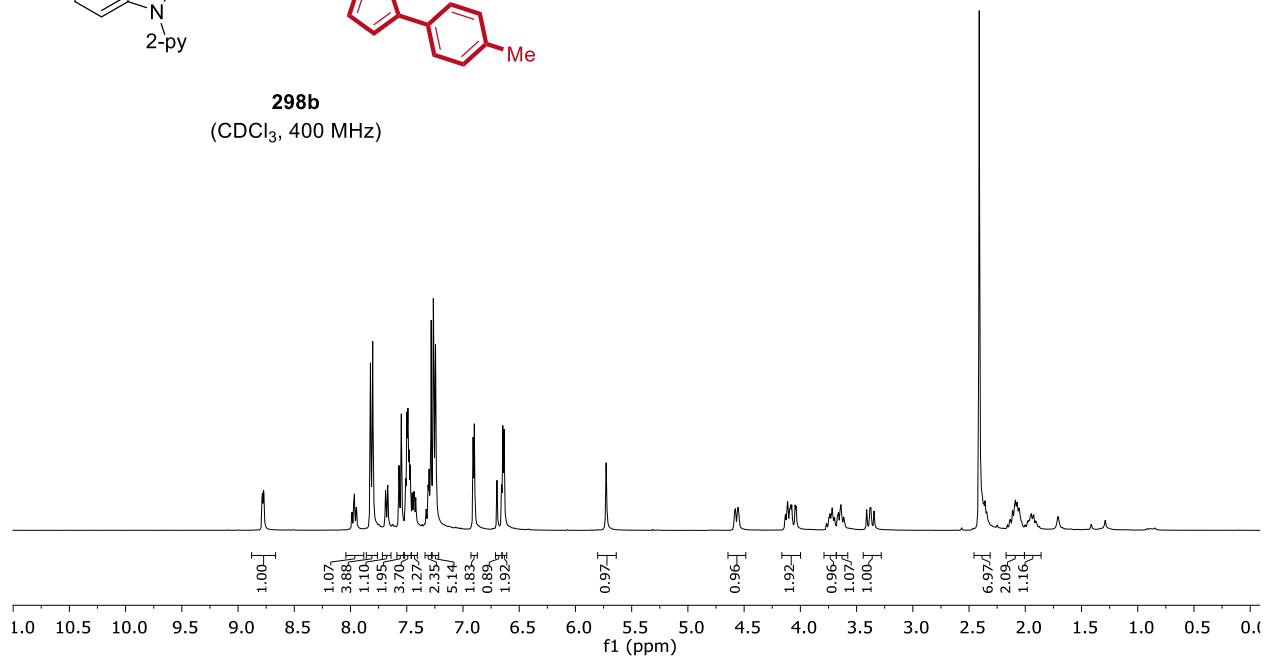


298a
(CDCl₃, 282 MHz)

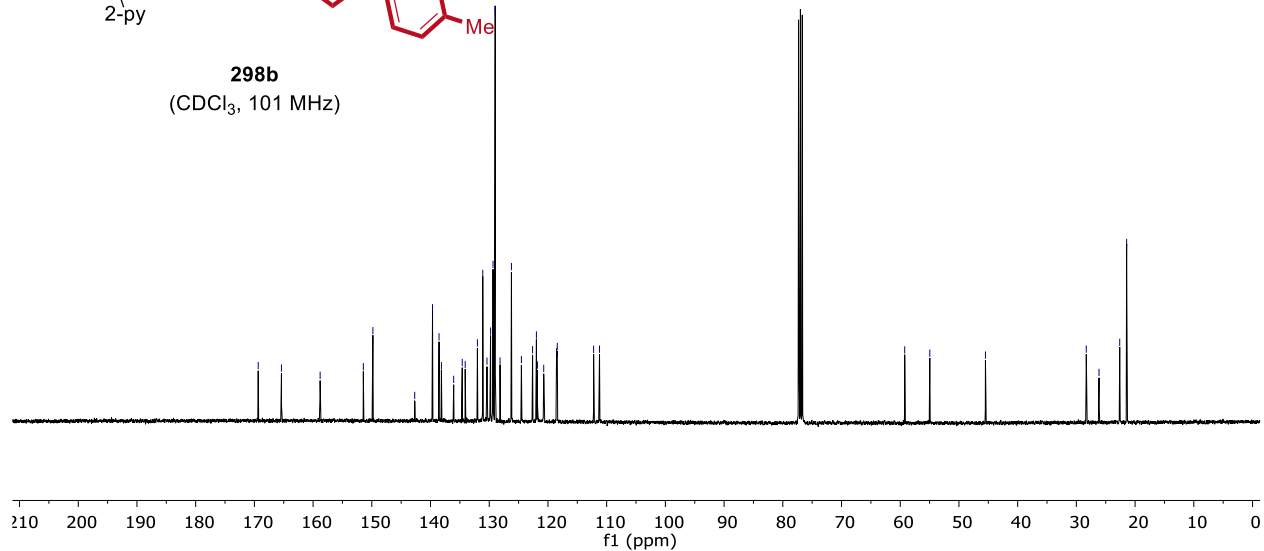




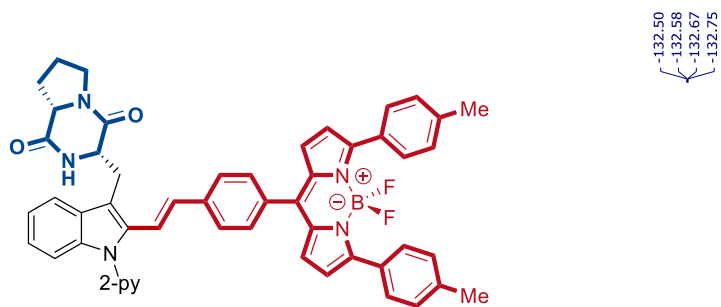
298b
(CDCl₃, 400 MHz)



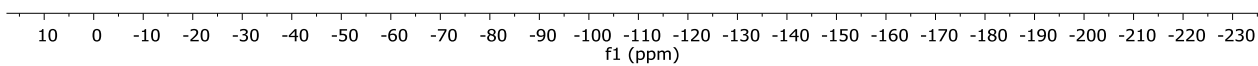
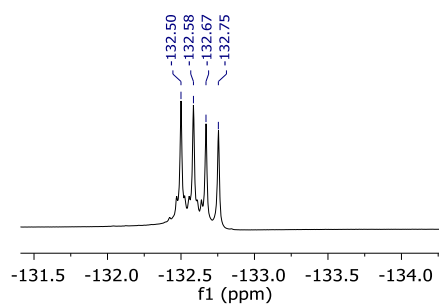
298b
(CDCl₃, 101 MHz)

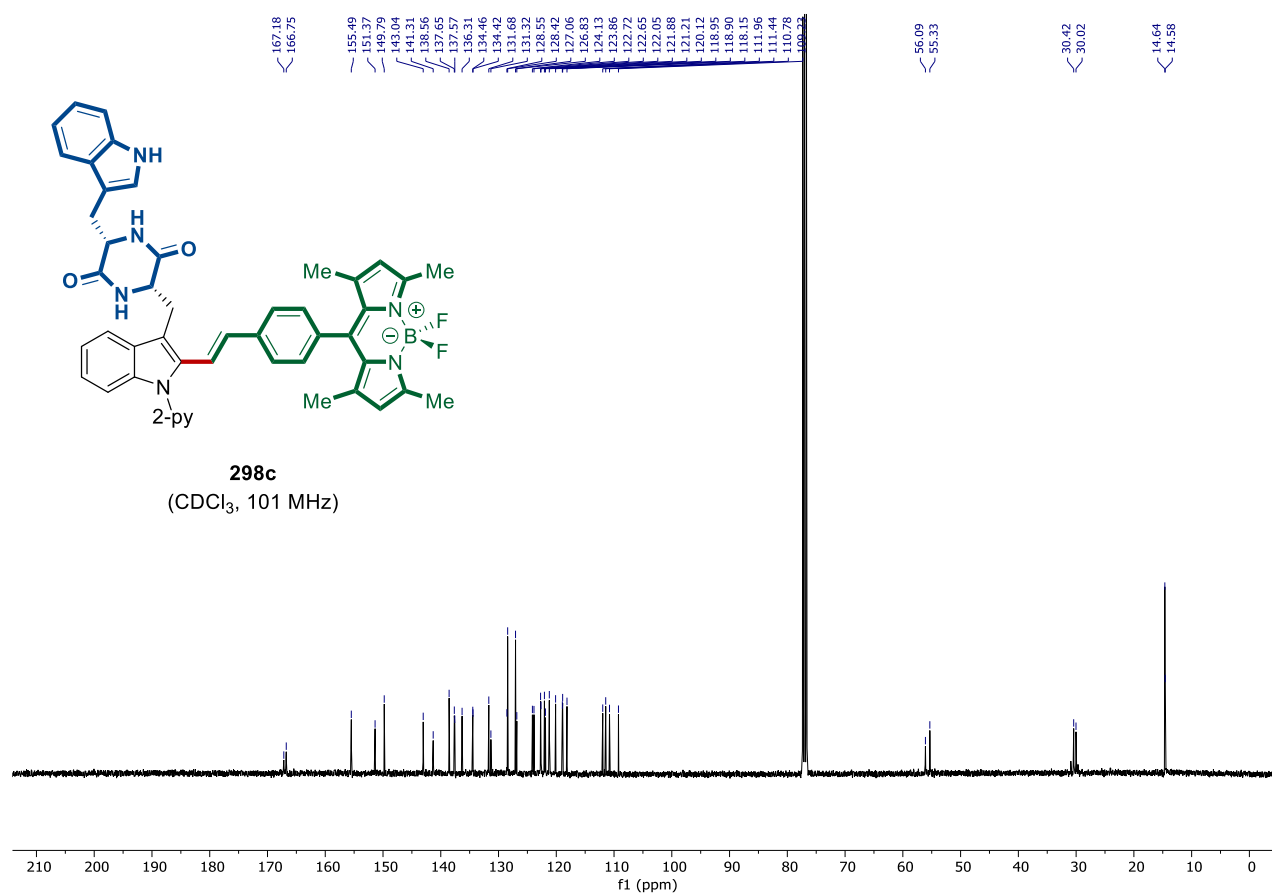
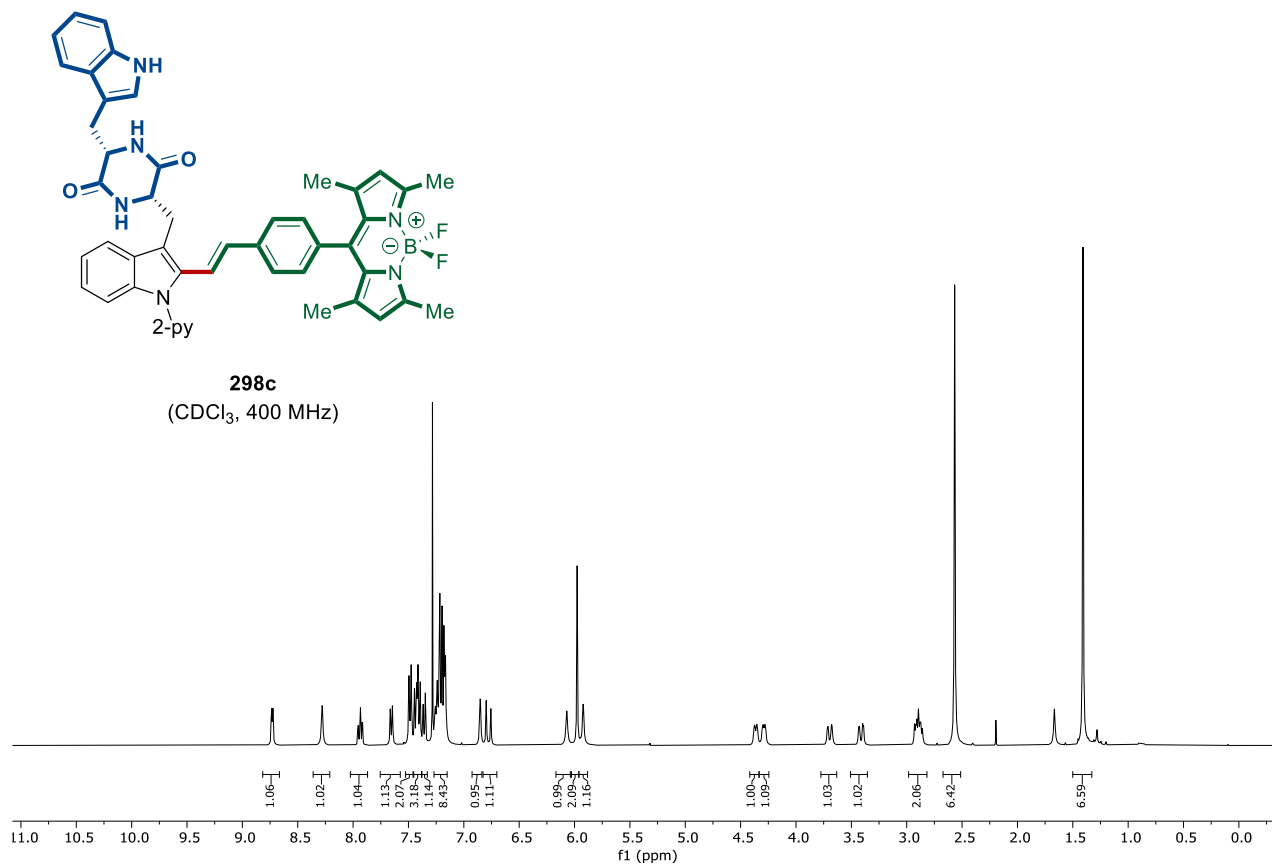


8. NMR Spectra

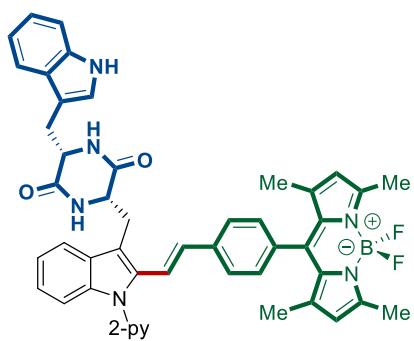


298b
(CDCl₃, 376 MHz)

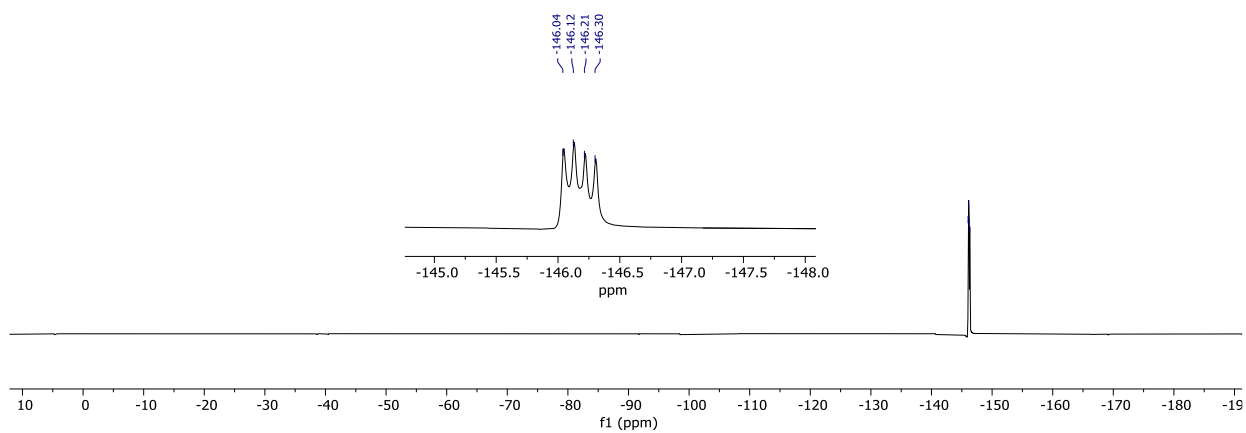


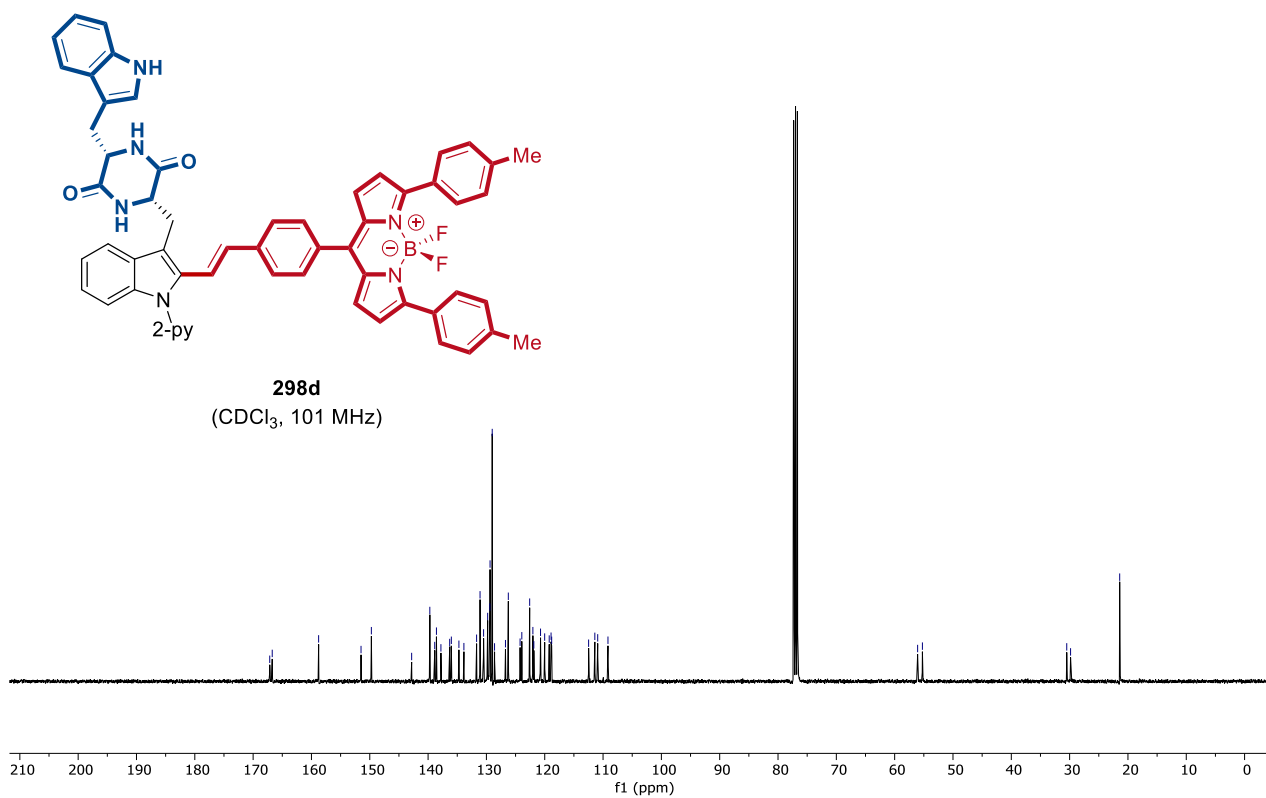
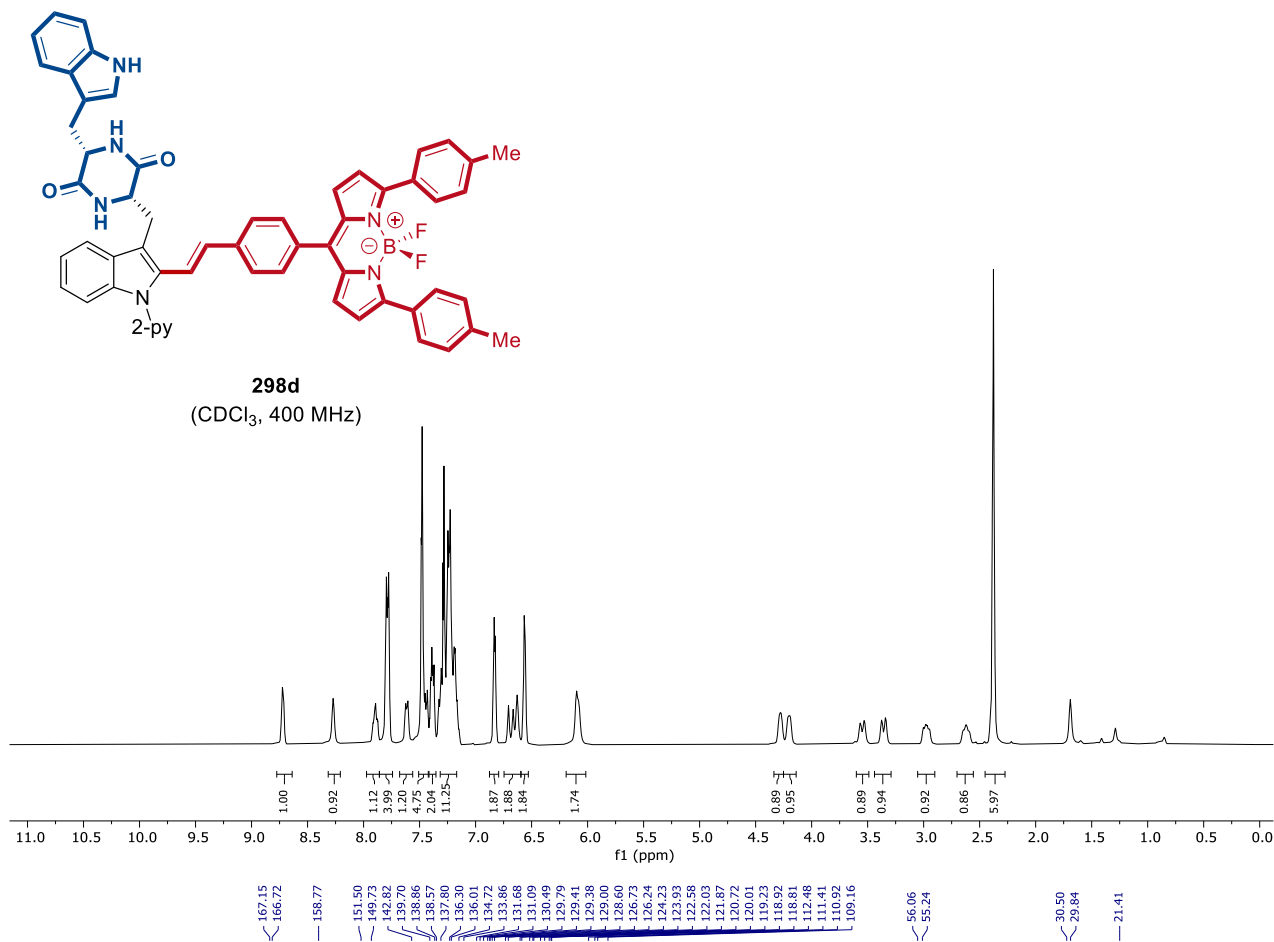


8. NMR Spectra

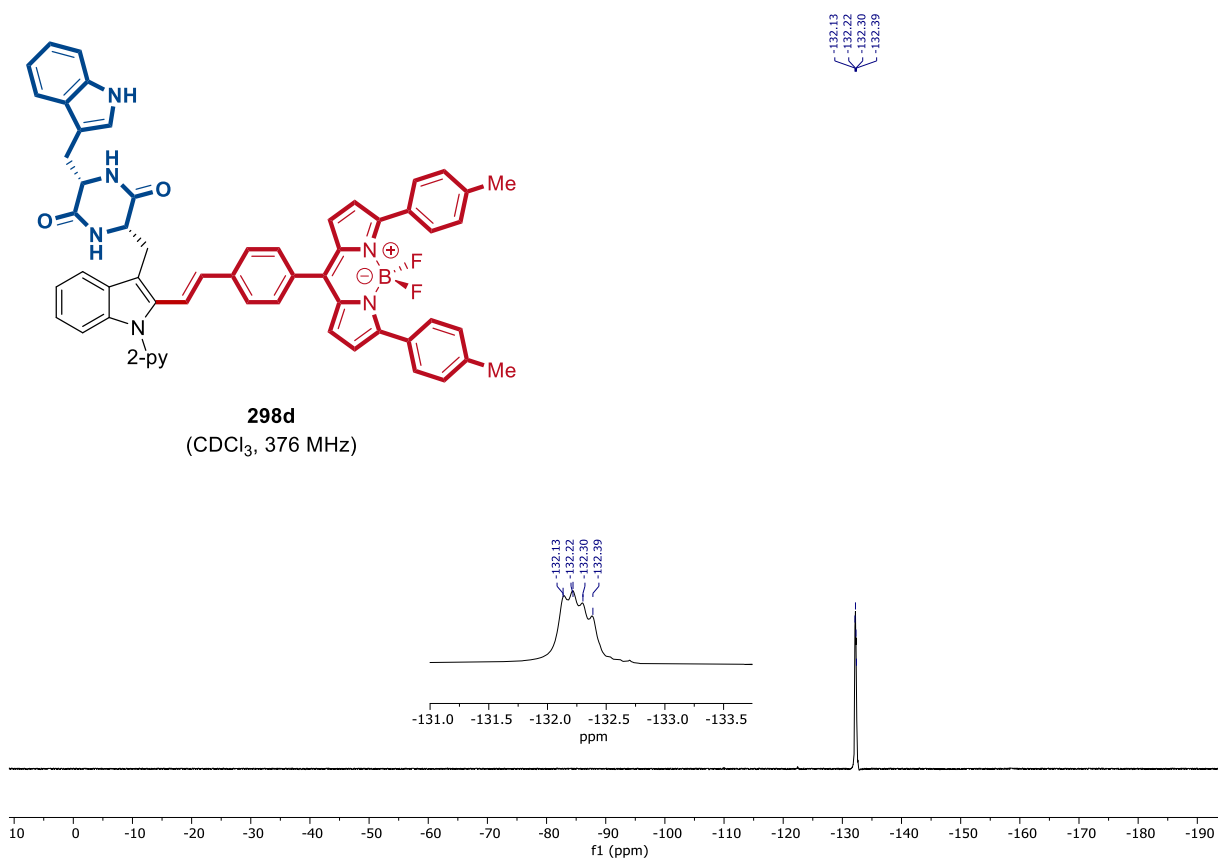


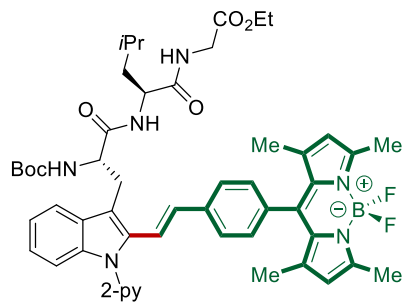
298c
(CDCl₃, 376 MHz)



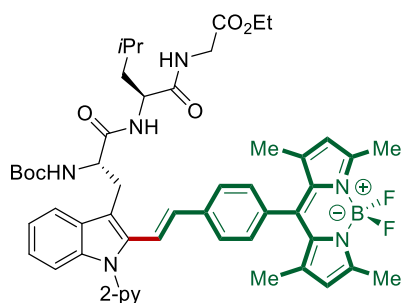
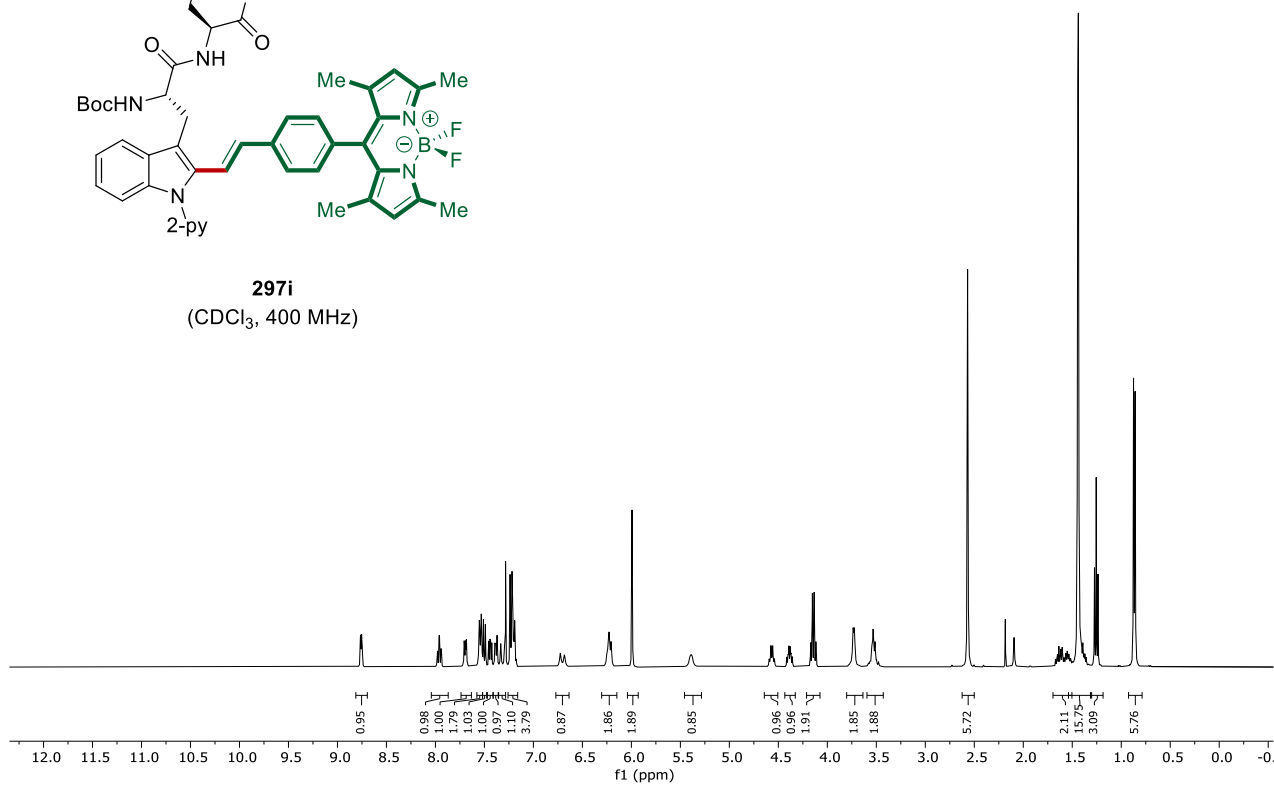


8. NMR Spectra

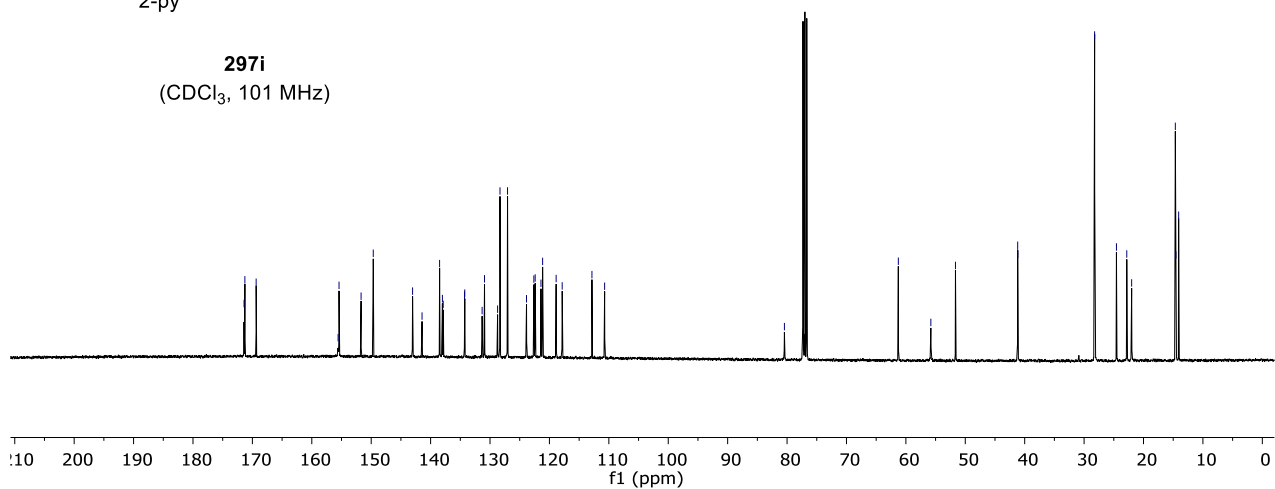




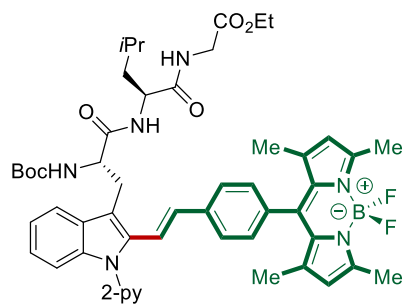
297i
(CDCl₃, 400 MHz)



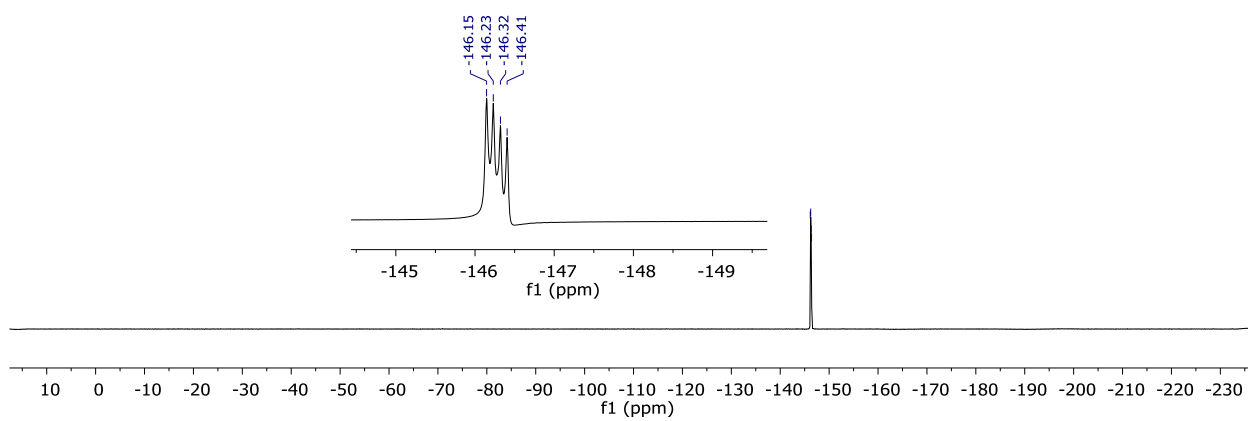
297i
(CDCl₃, 101 MHz)

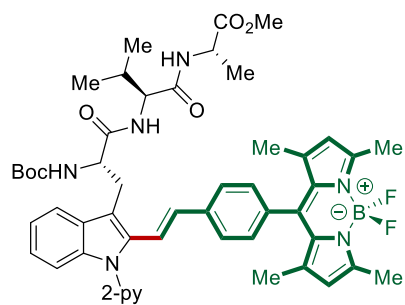


8. NMR Spectra

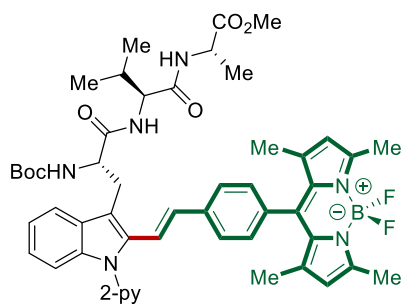
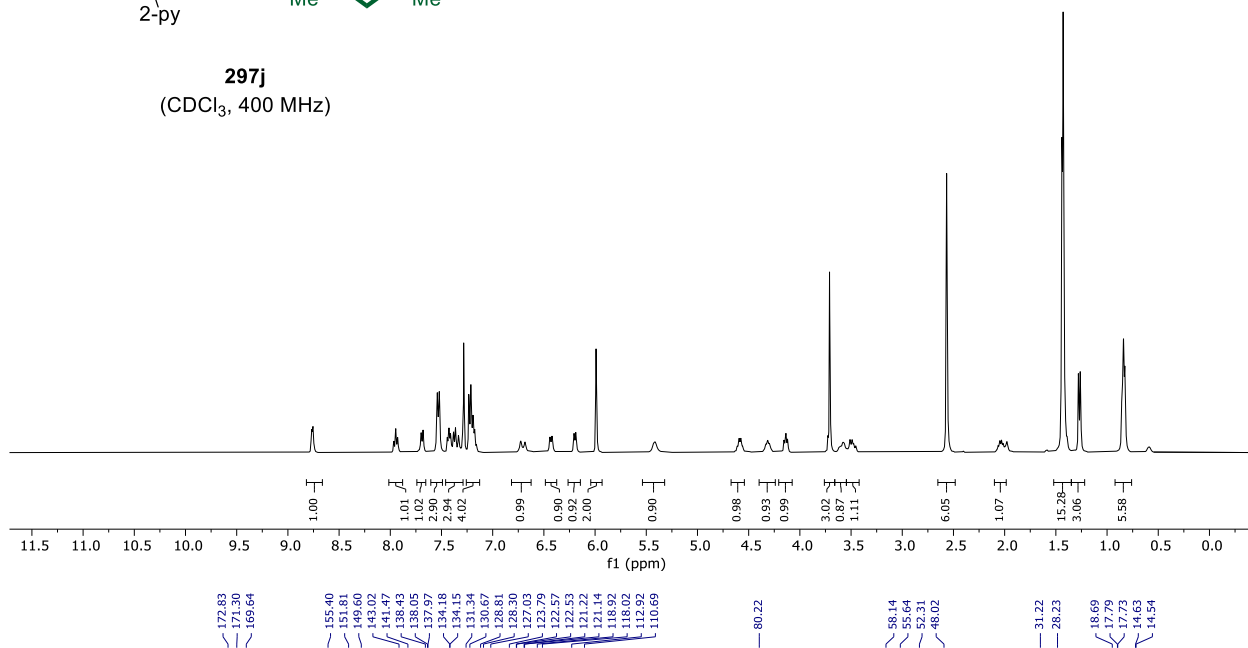


297i
(CDCl₃, 376 MHz)

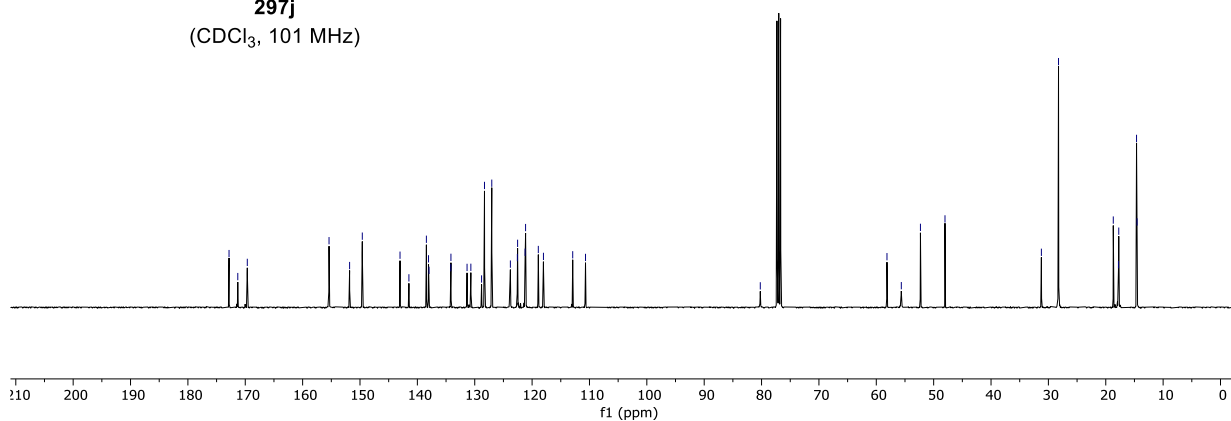




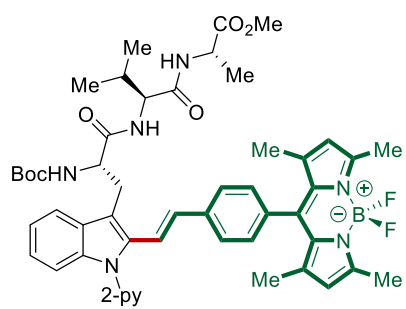
297j
(CDCl₃, 400 MHz)



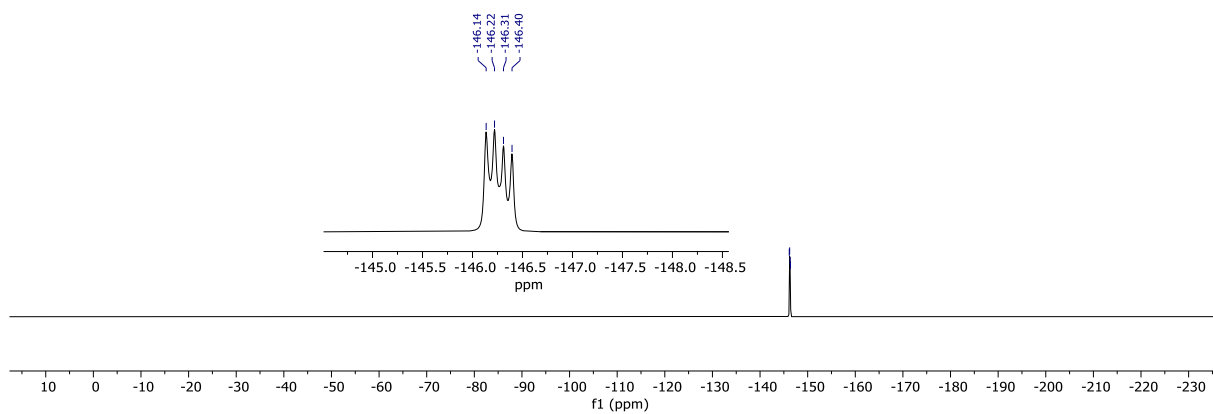
297j
(CDCl₃, 101 MHz)

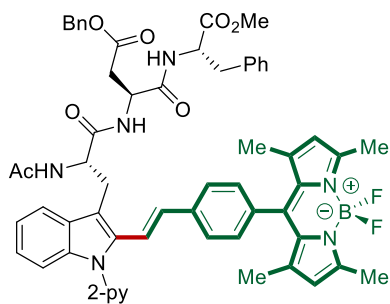


8. NMR Spectra

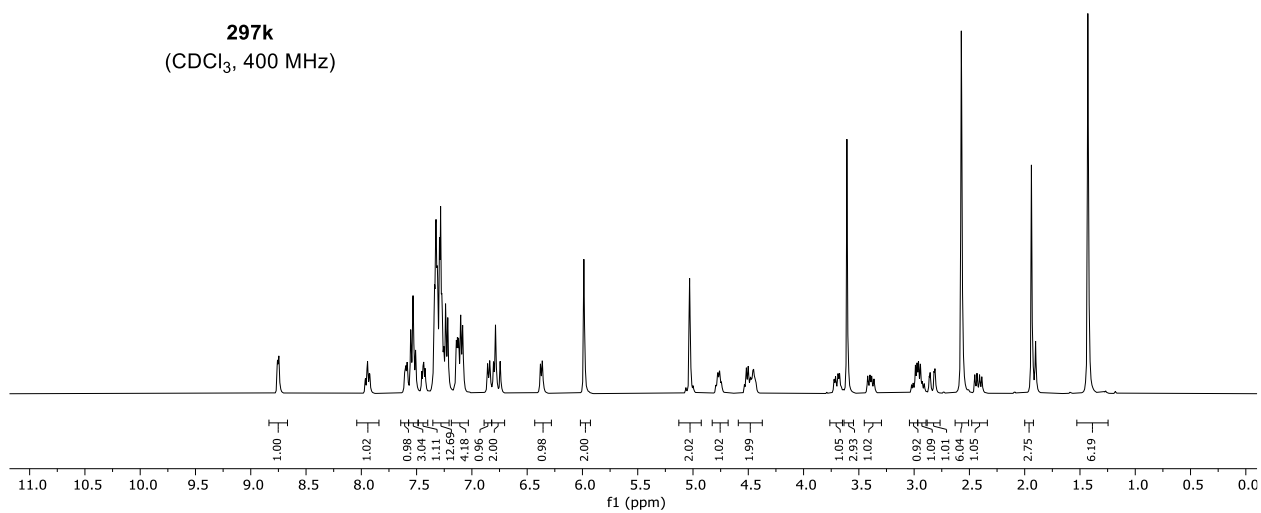


297j
(CDCl₃, 376 MHz)

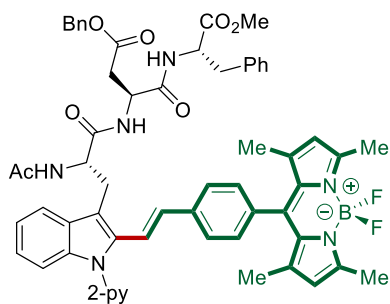




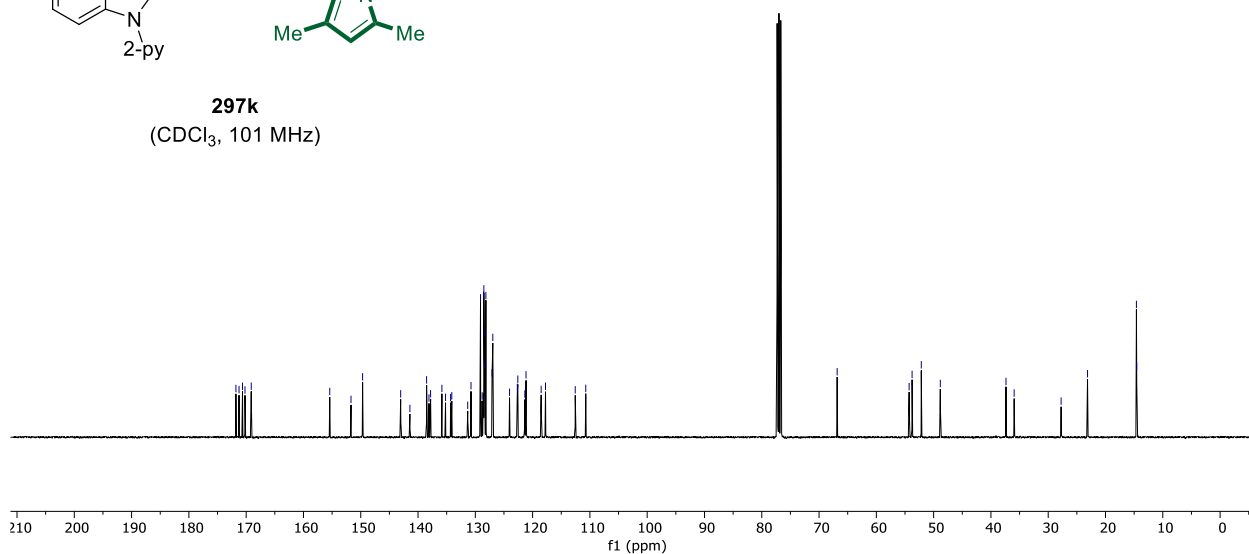
297k
(CDCl₃, 400 MHz)



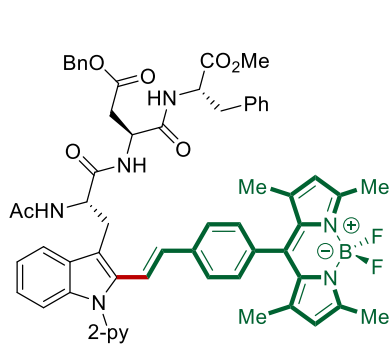
171.79, 171.25, 170.64, 169.71, 169.12, 155.41, 151.70, 149.68, 143.03, 141.42, 138.90, 138.09, 135.41, 135.83, 135.20, 134.32, 134.11, 131.33, 130.75, 129.09, 128.81, 128.96, 128.56, 128.41, 128.43, 128.33, 128.16, 127.09, 126.95, 124.03, 122.67, 122.58, 121.96, 119.75, 118.51, 117.75, 112.56, 110.72, 66.84, 54.28, 53.76, 52.16, 48.83, 37.37, 35.95, 27.75, 23.14, 14.60, 14.56



297k
(CDCl₃, 101 MHz)

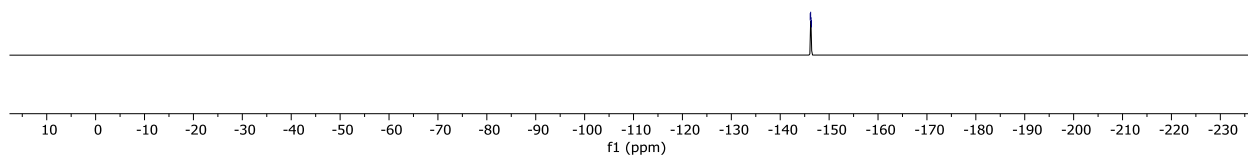
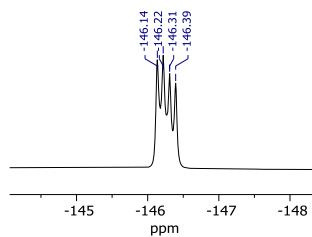


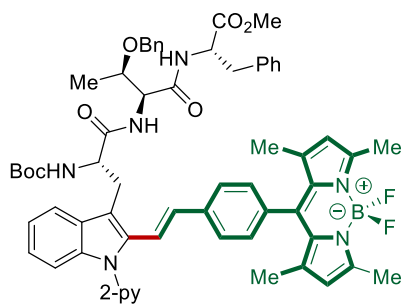
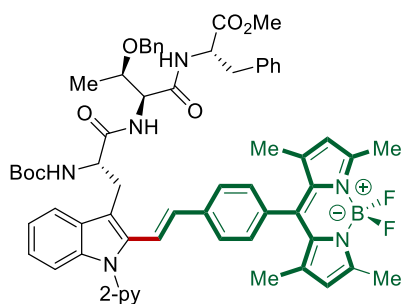
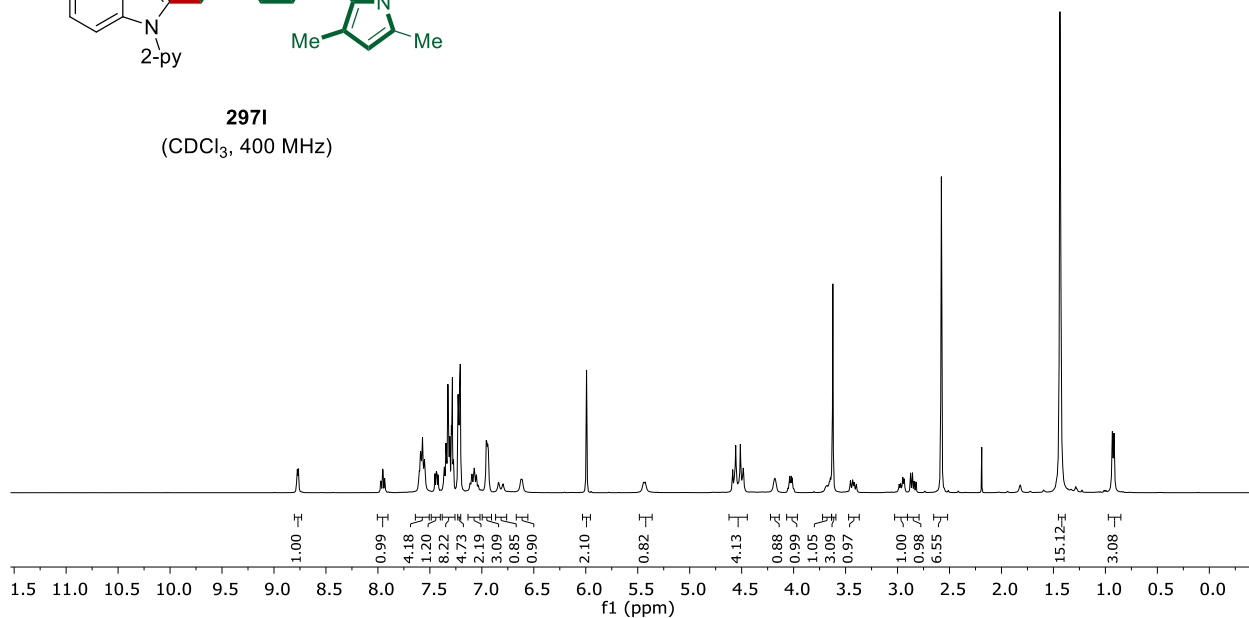
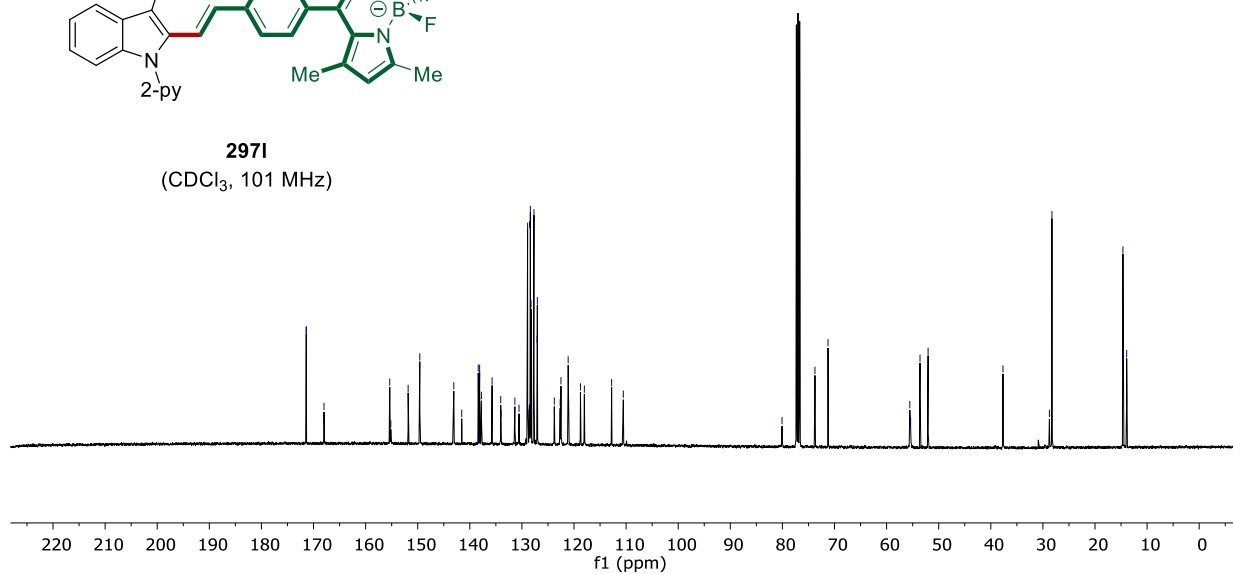
8. NMR Spectra



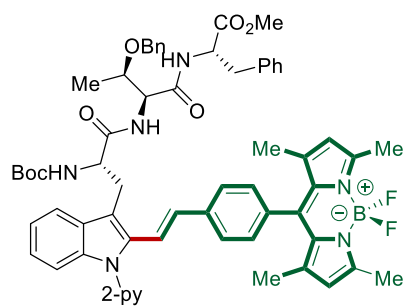
297k
(CDCl₃, 376 MHz)

-146.14
-146.22
-146.31
-146.39

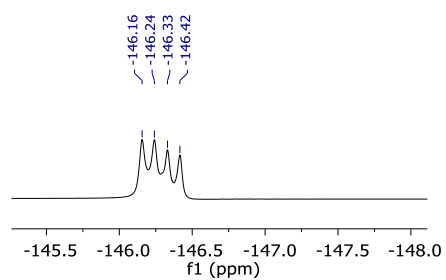


**2971**(CDCl₃, 400 MHz)**2971**(CDCl₃, 101 MHz)

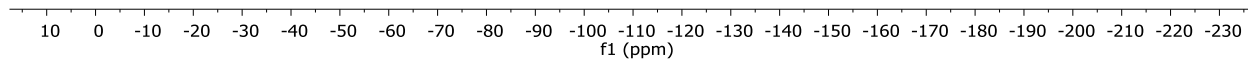
8. NMR Spectra

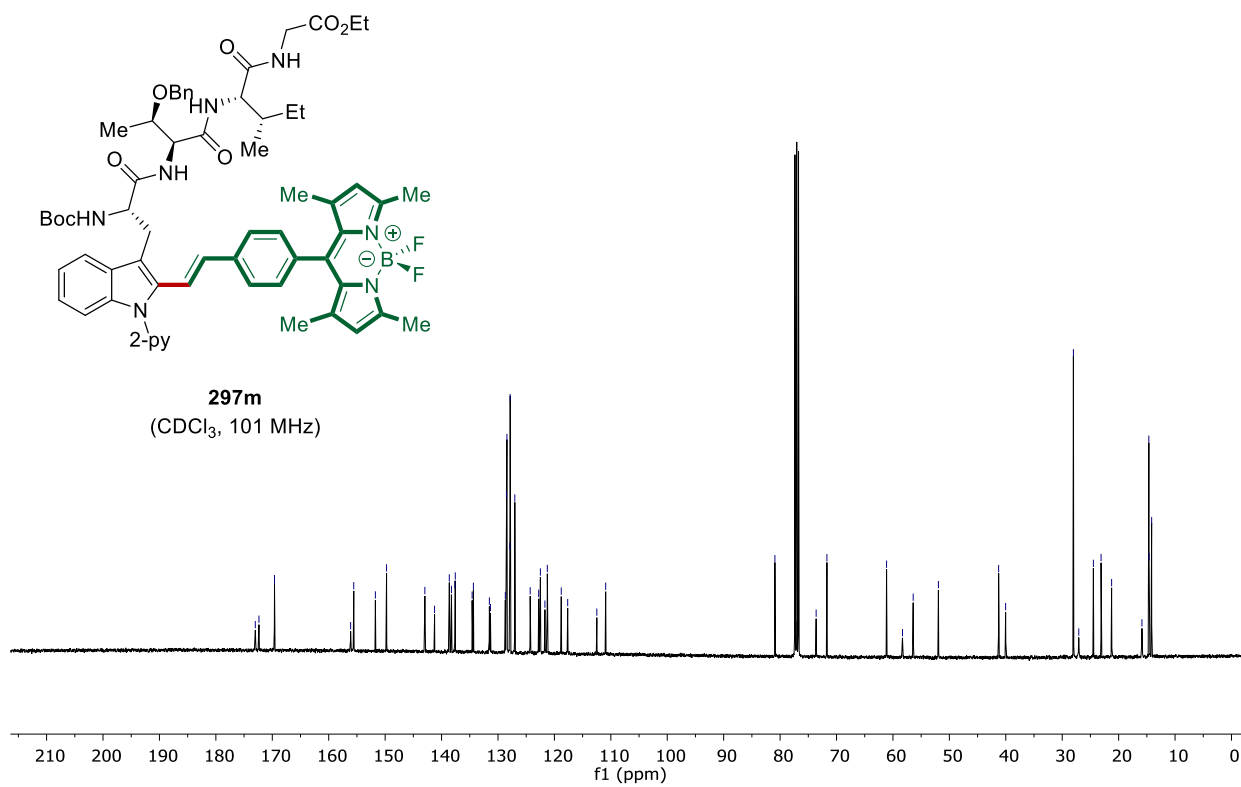
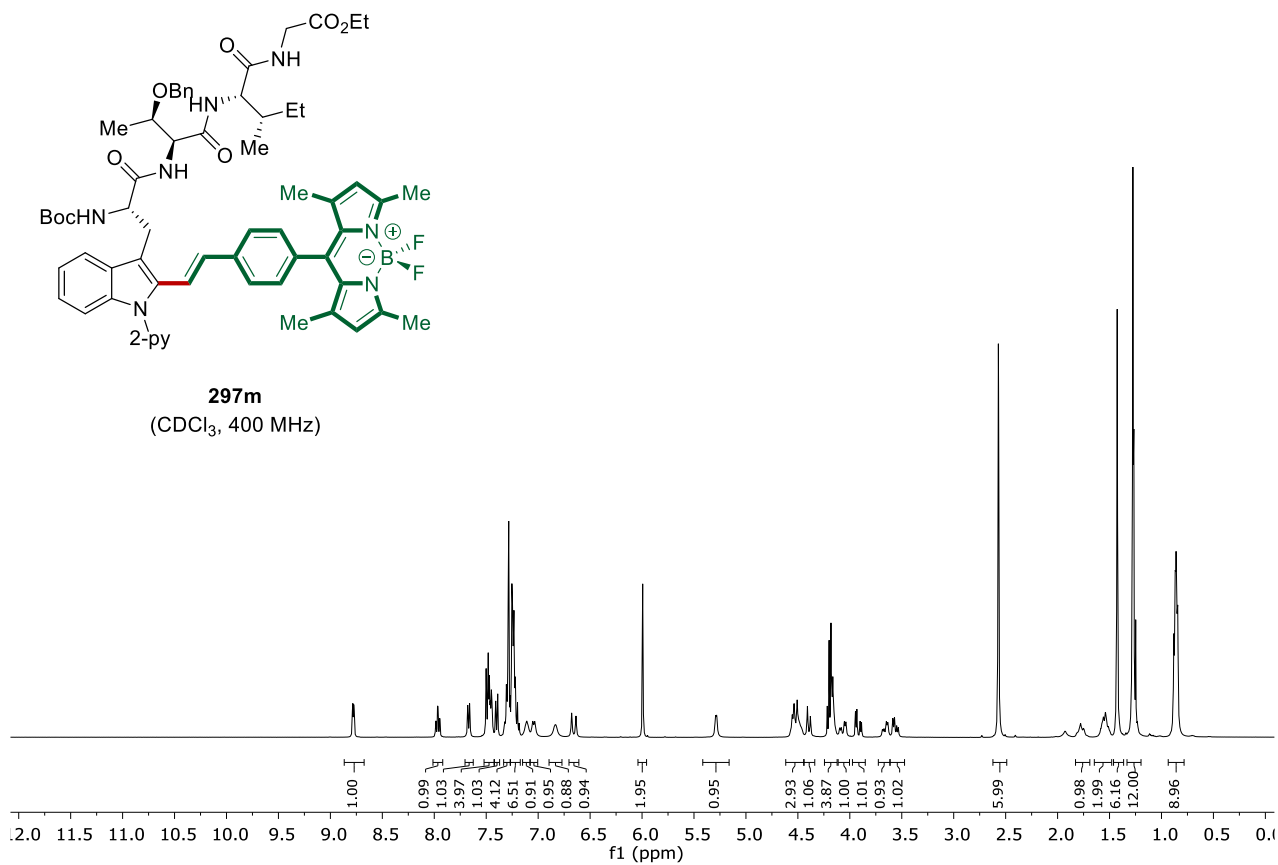


2971
(CDCl₃, 376 MHz)

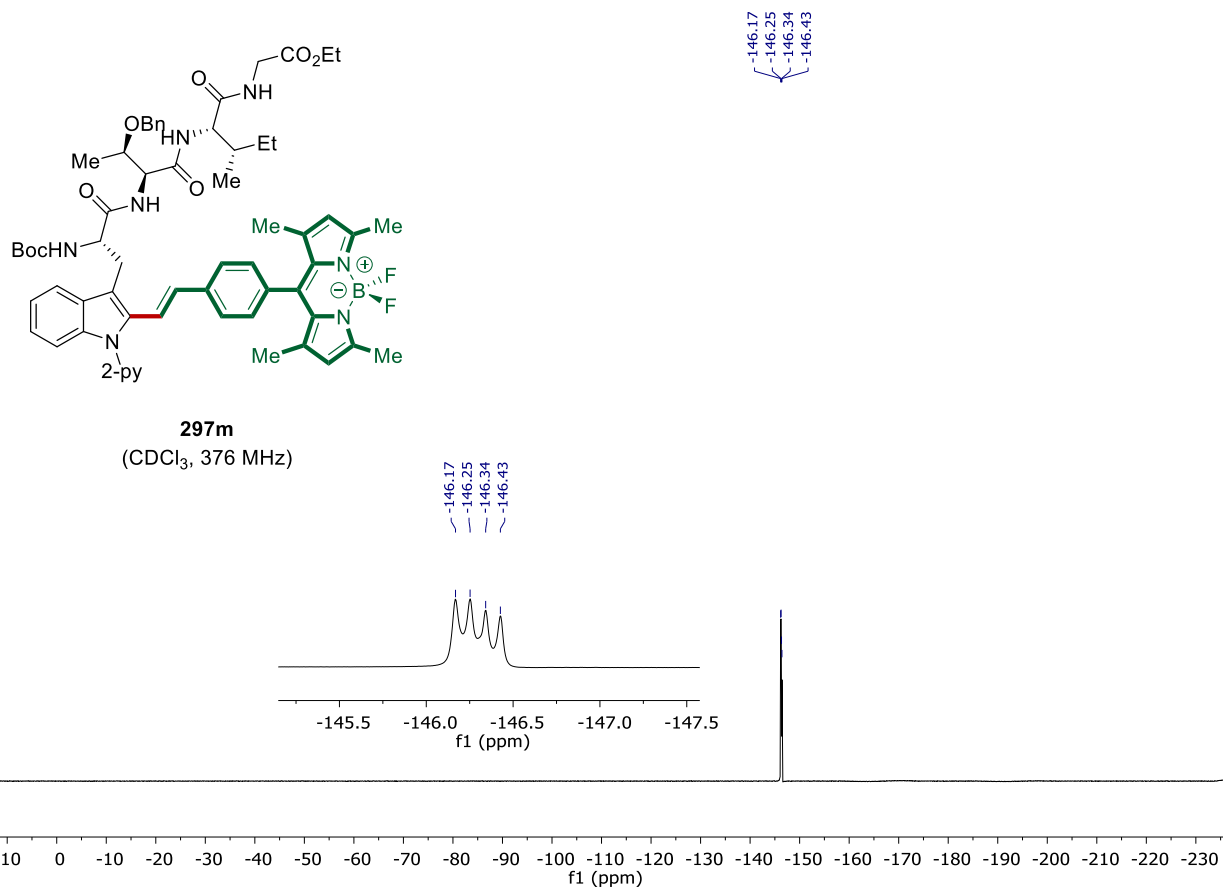


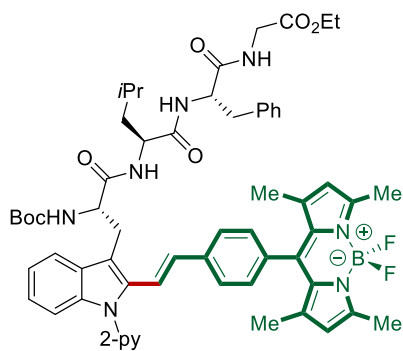
-146.16
-146.24
-146.33
-146.42



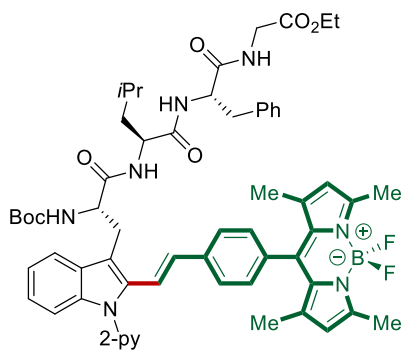
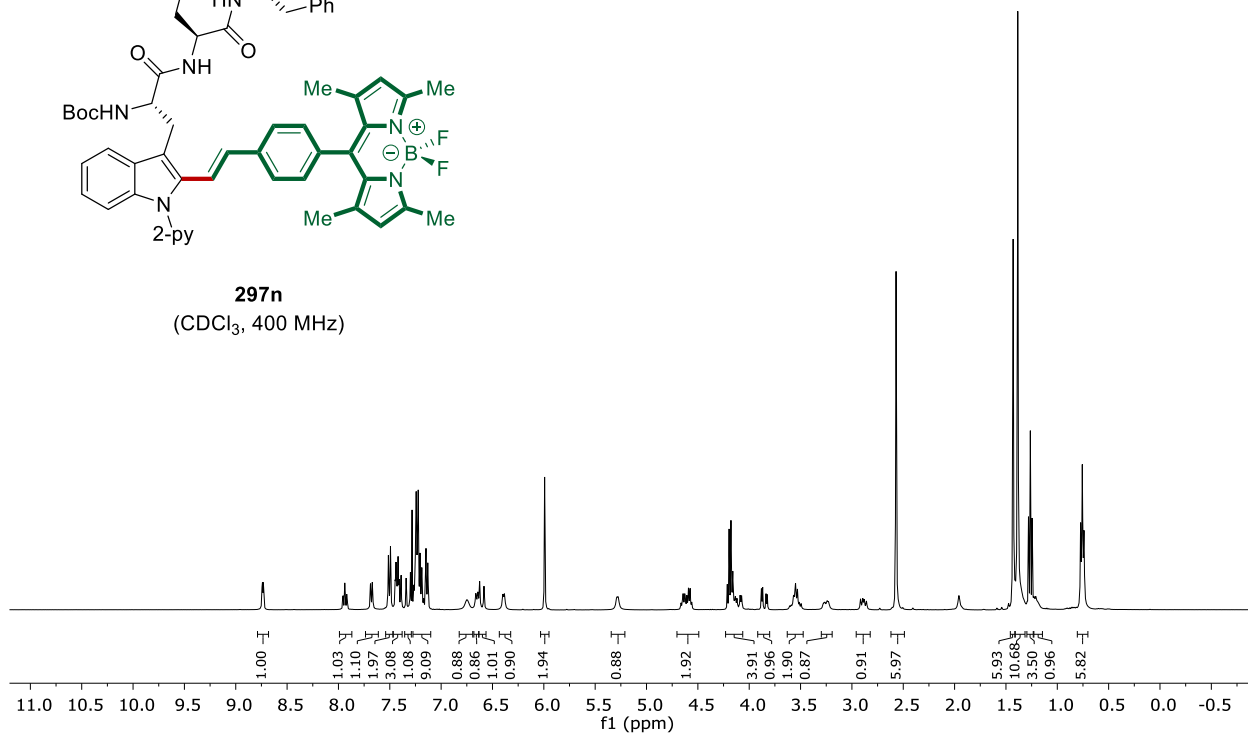


8. NMR Spectra

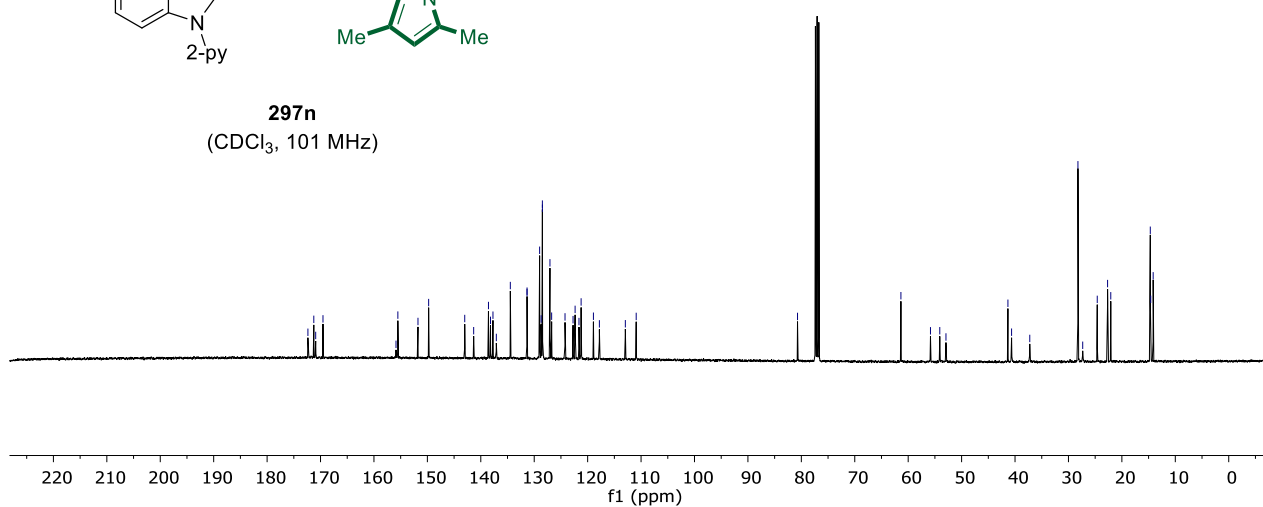




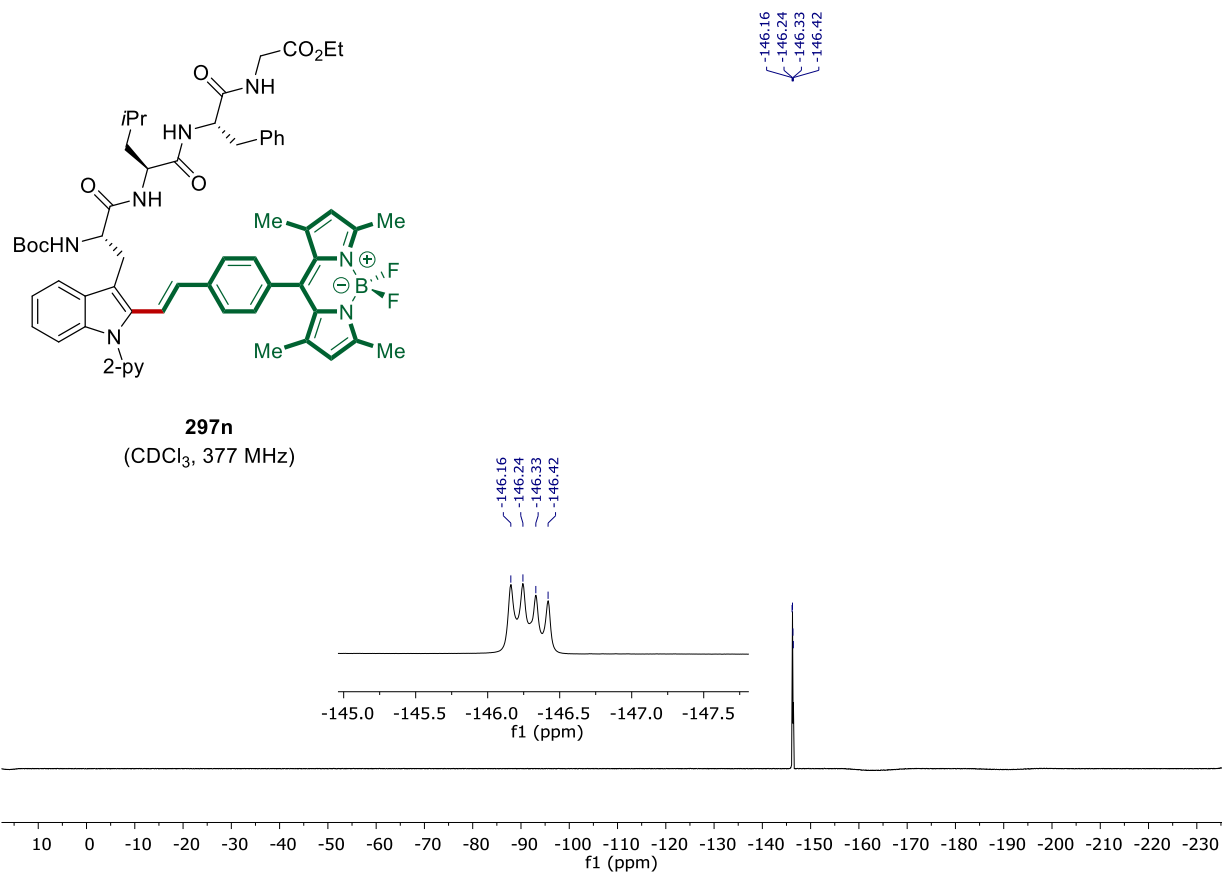
297n
(CDCl₃, 400 MHz)



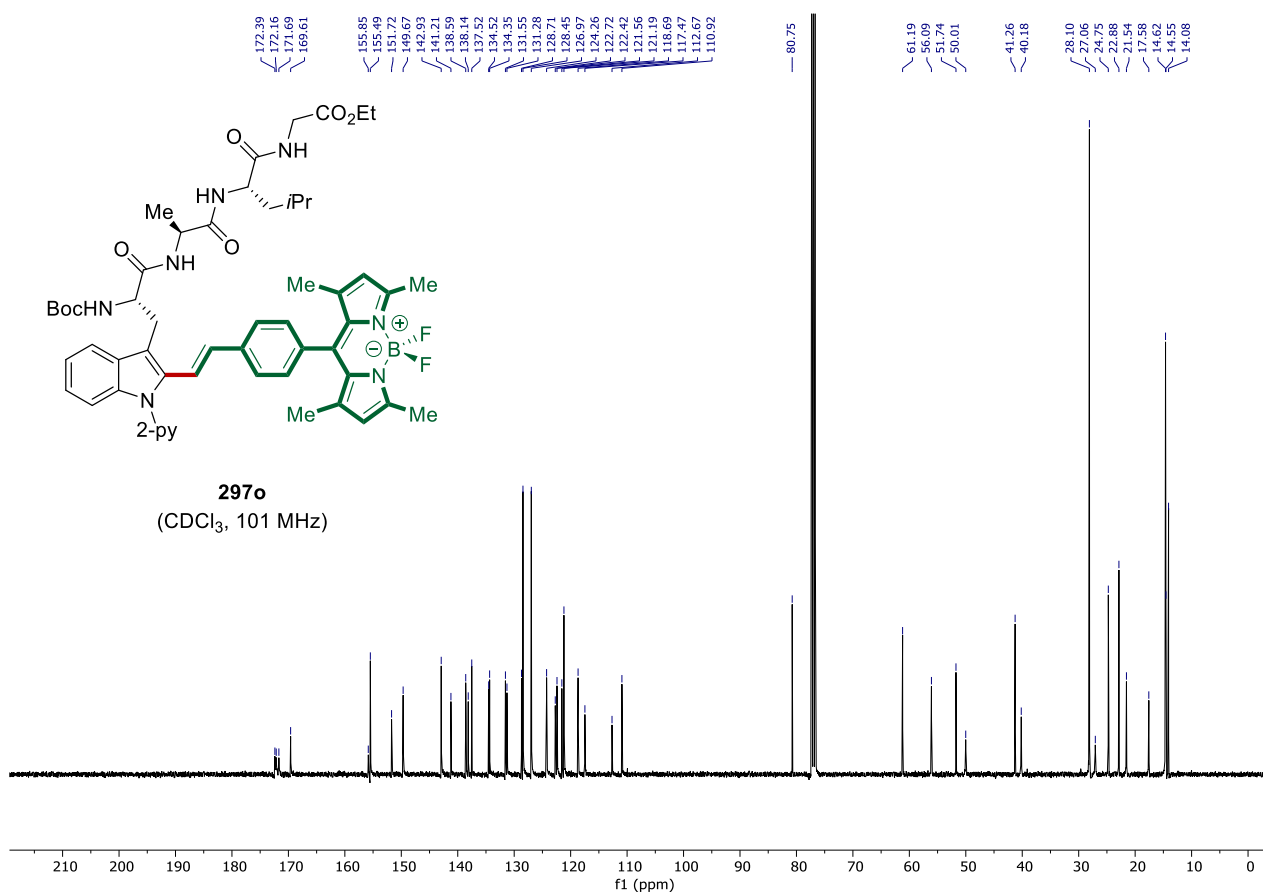
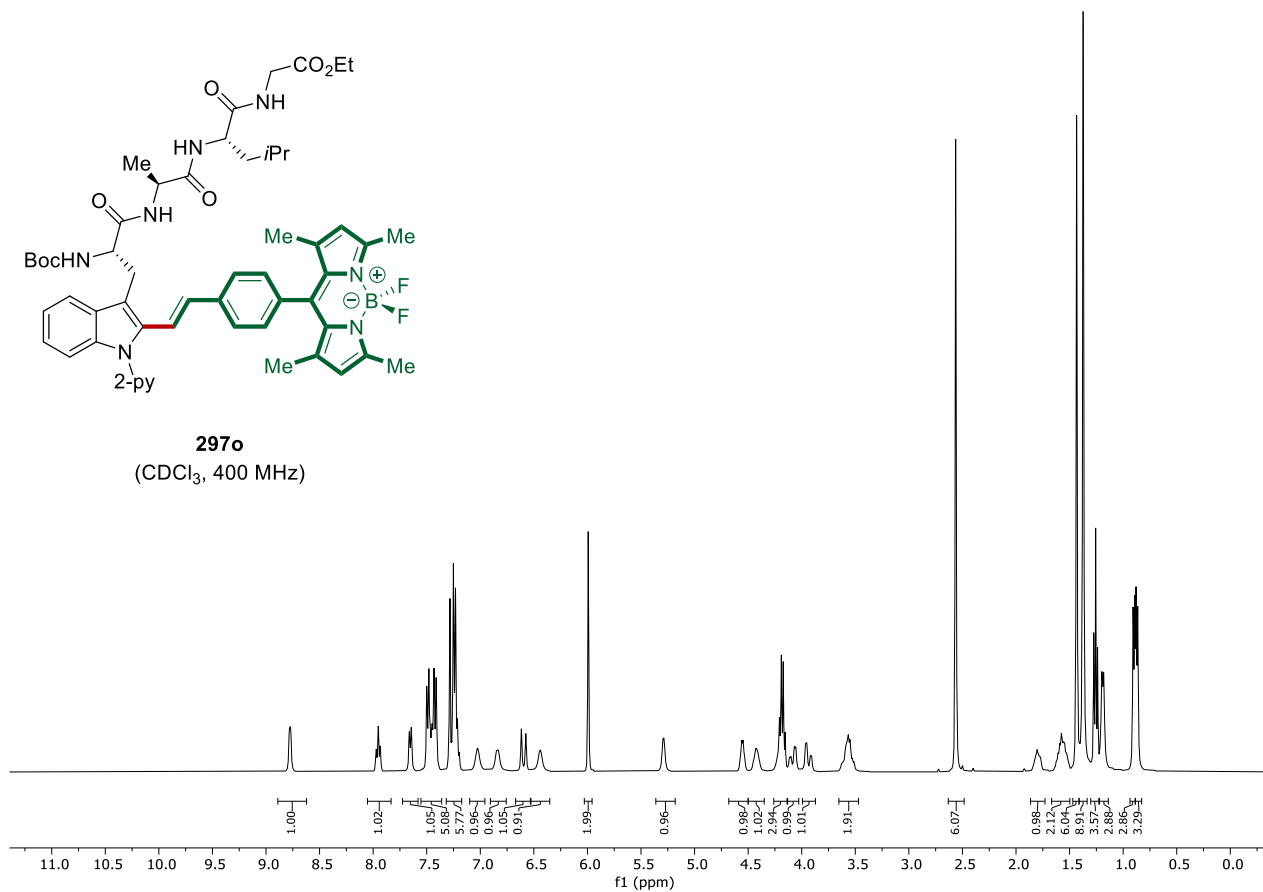
297n
(CDCl₃, 101 MHz)



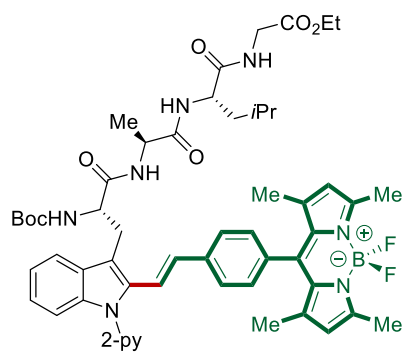
8. NMR Spectra



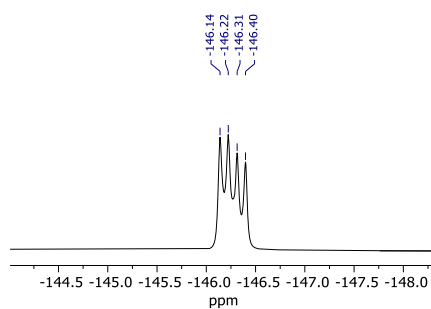
8. NMR Spectra



8. NMR Spectra

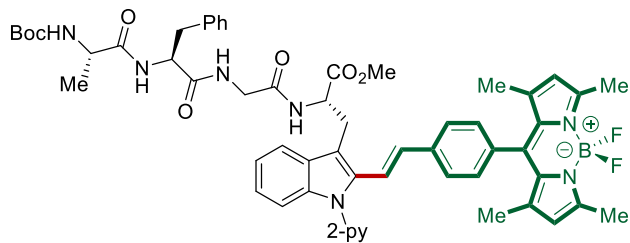


297o
(CDCl₃, 376 MHz)

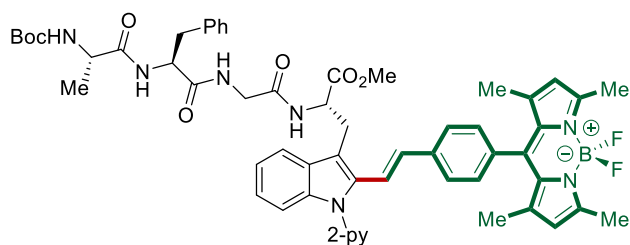
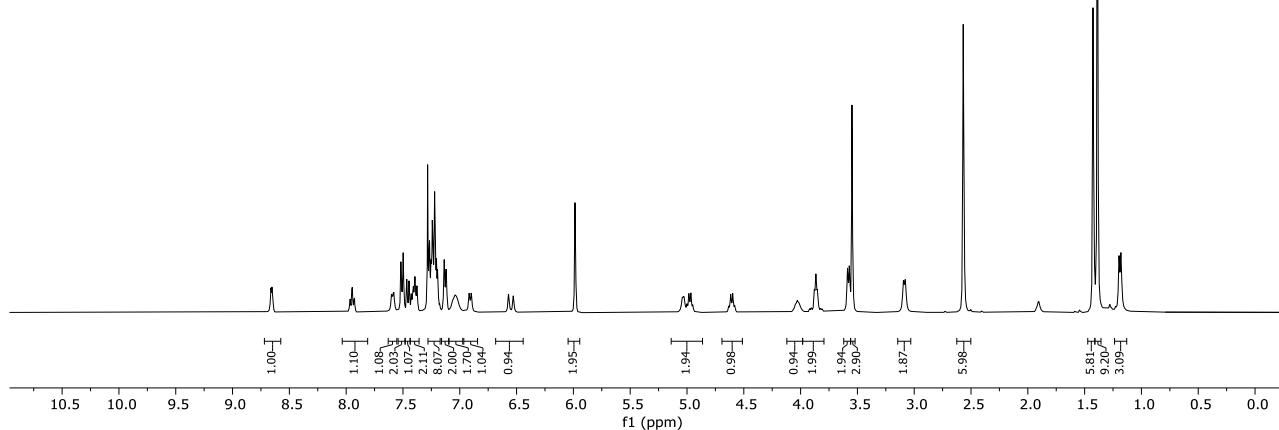


-146.14
-146.22
-146.31
-146.40

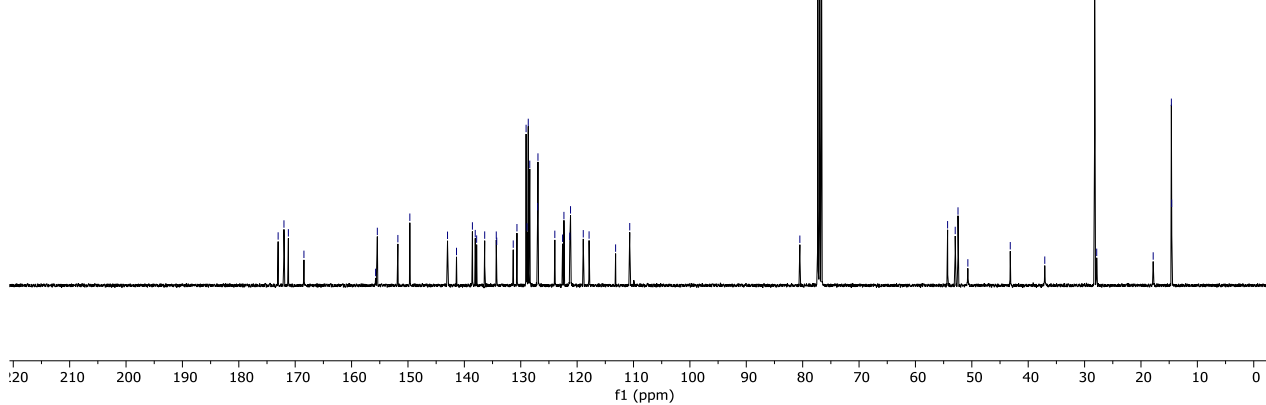
8. NMR Spectra



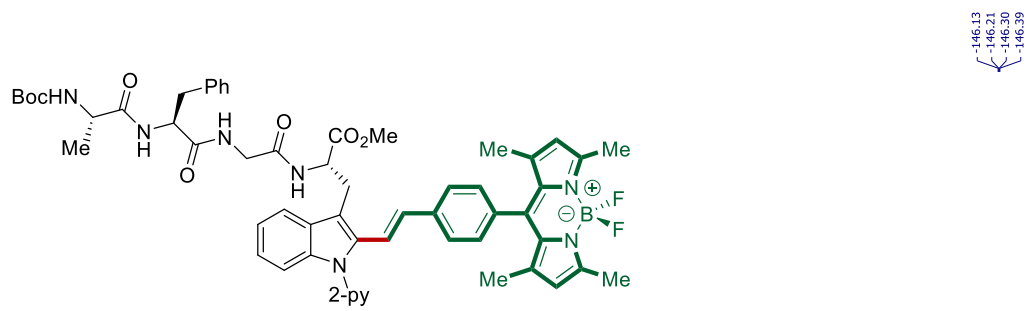
297p
(CDCl₃, 400 MHz)



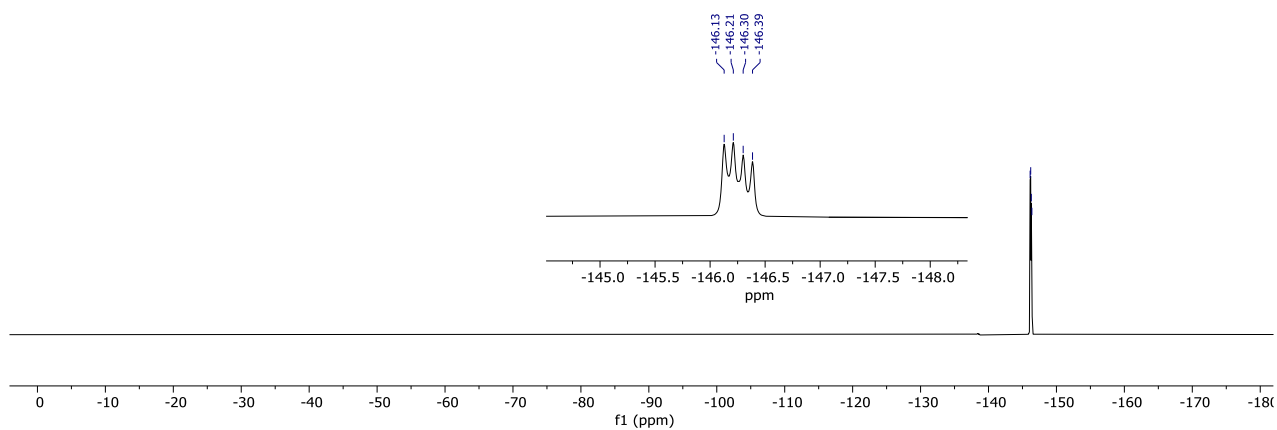
297p
(CDCl₃, 101 MHz)

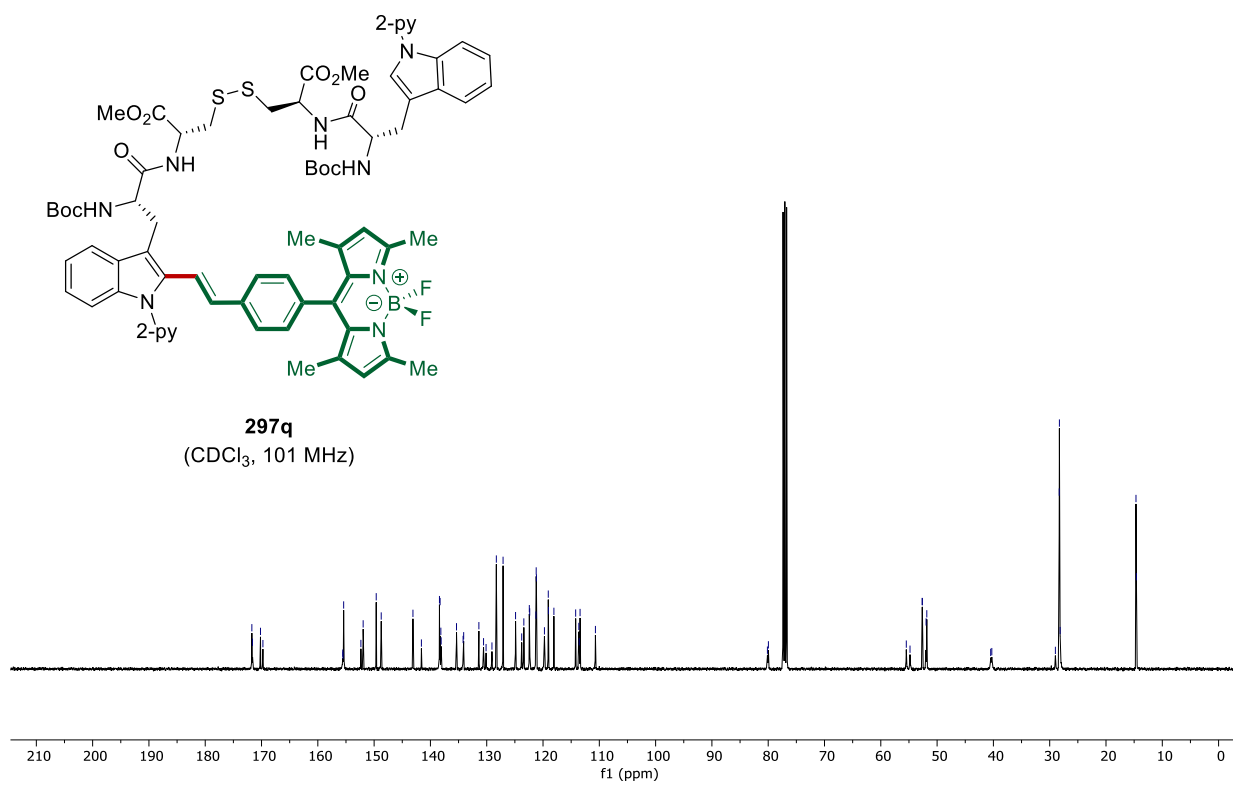
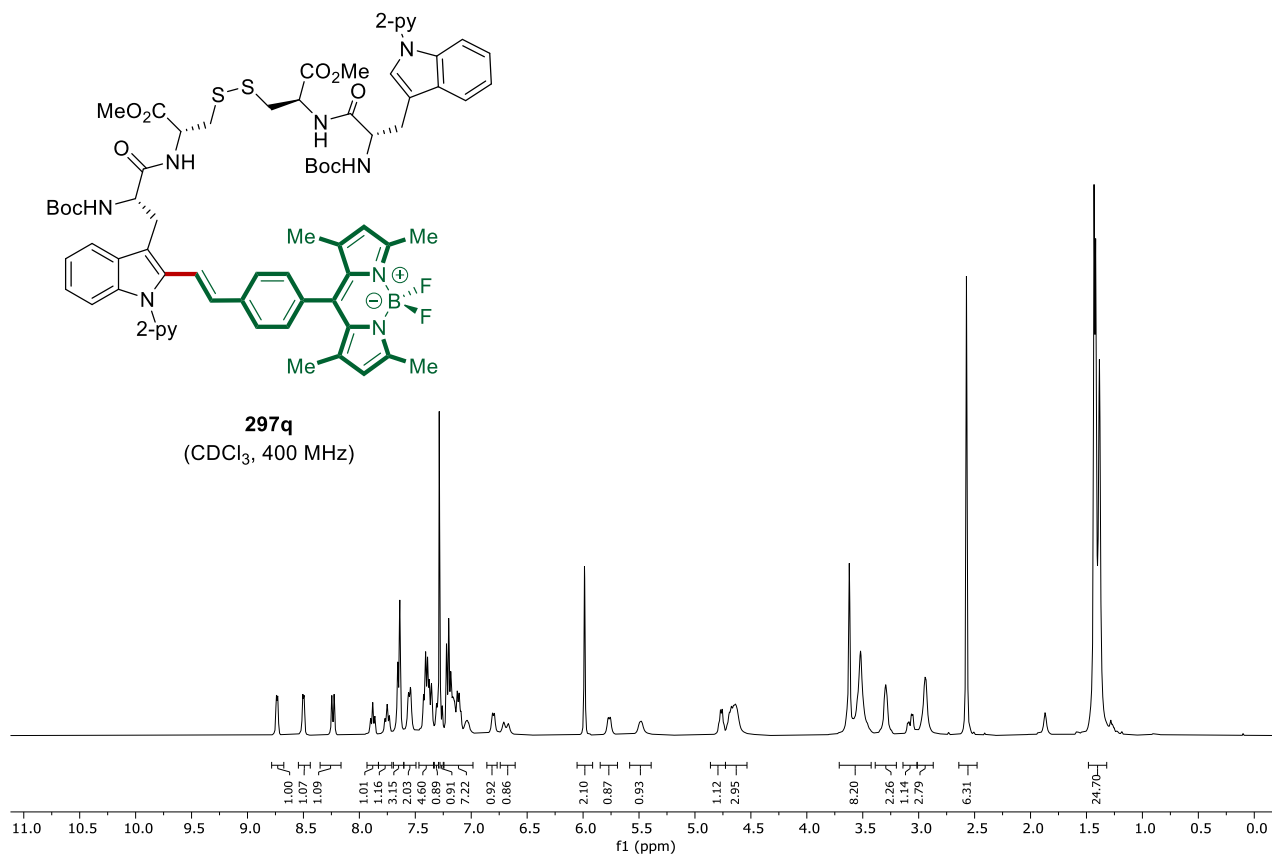


8. NMR Spectra

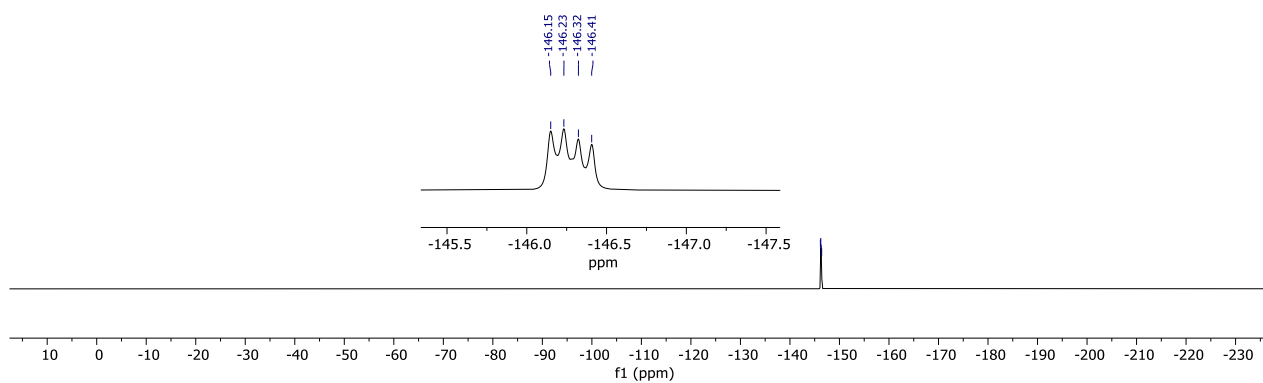
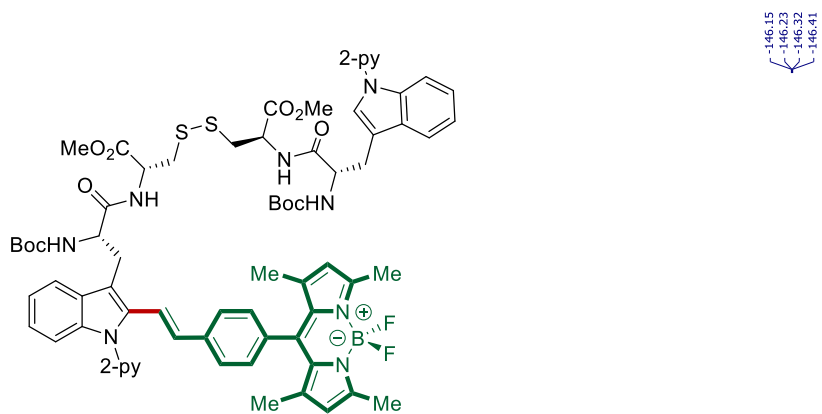


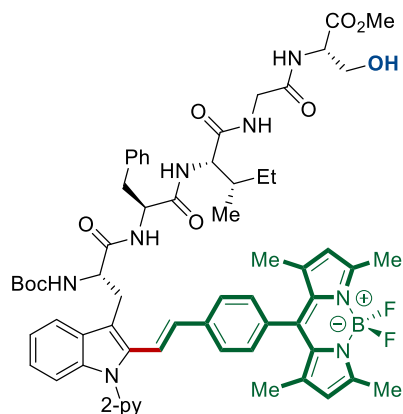
297p
(CDCl₃, 377 MHz)



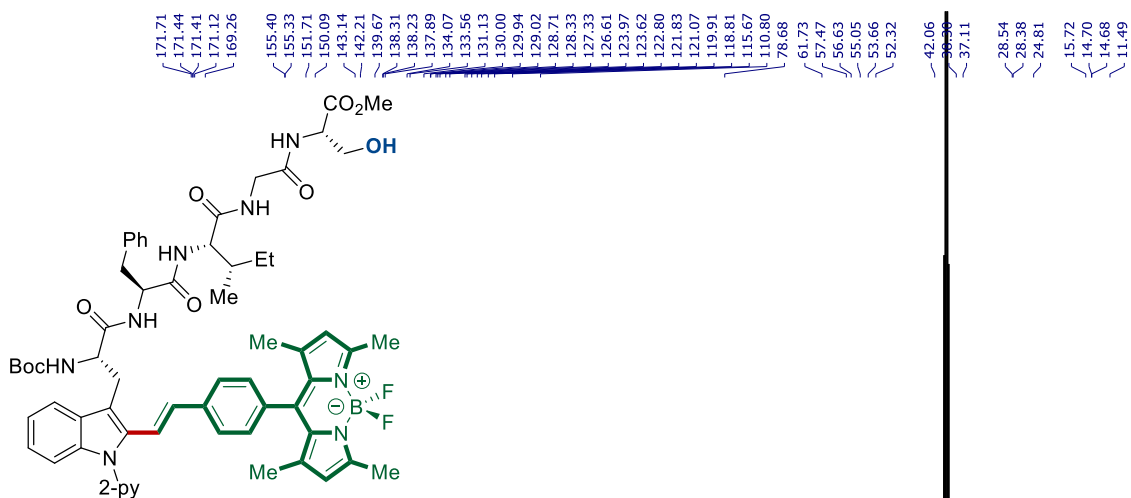
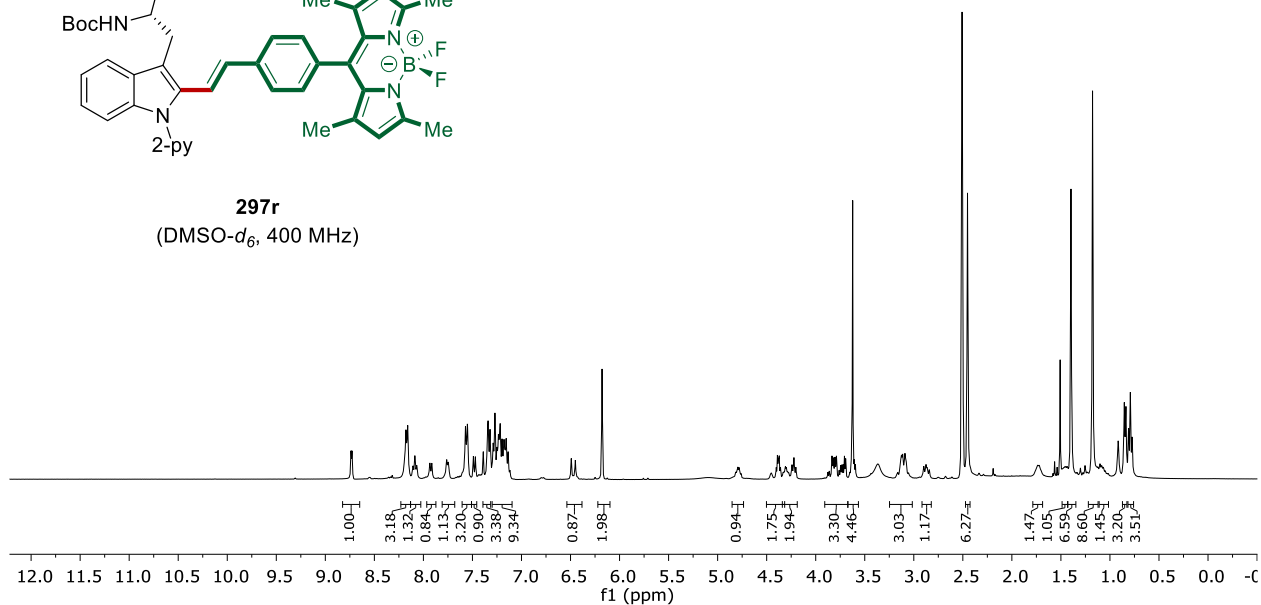


8. NMR Spectra

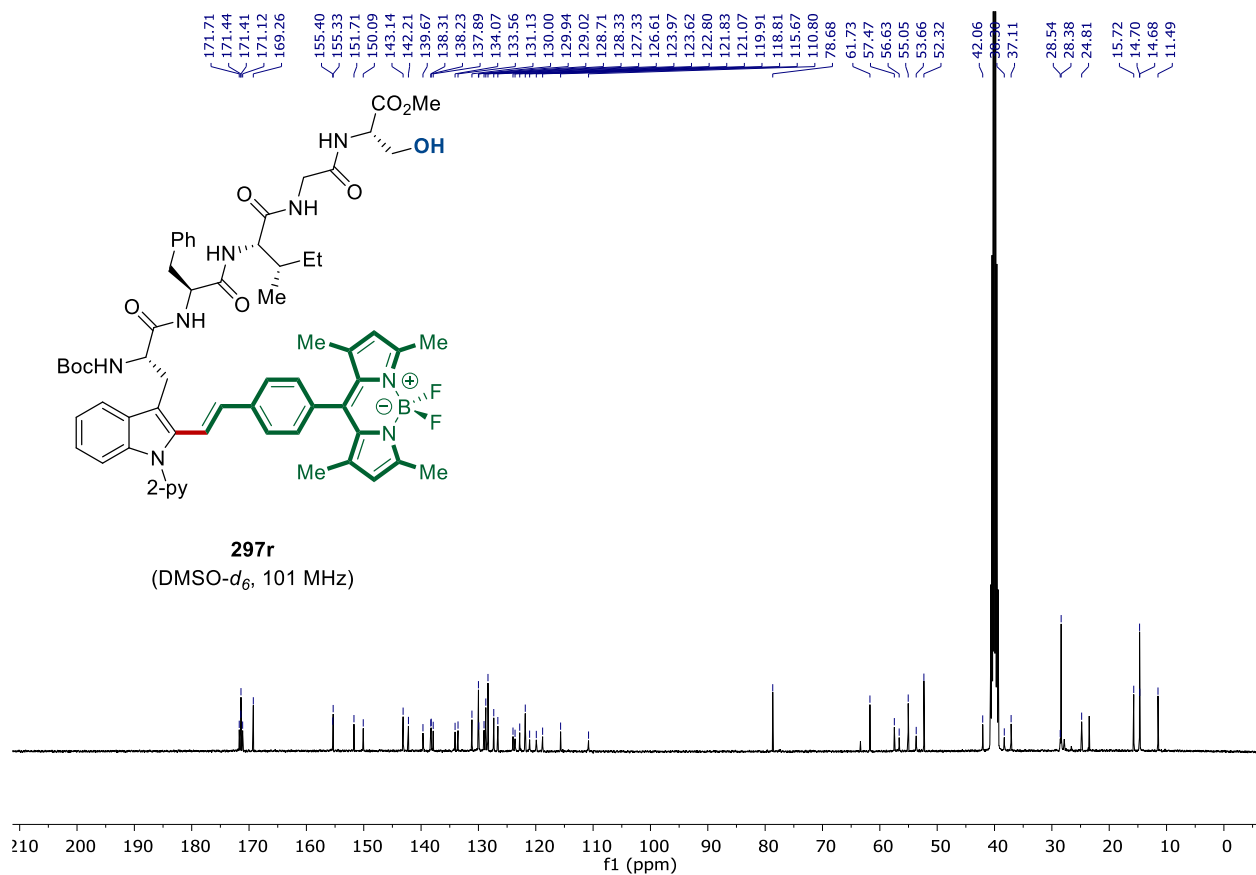




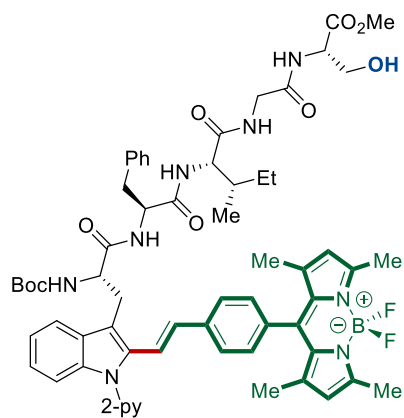
297r
(DMSO- d_6 , 400 MHz)



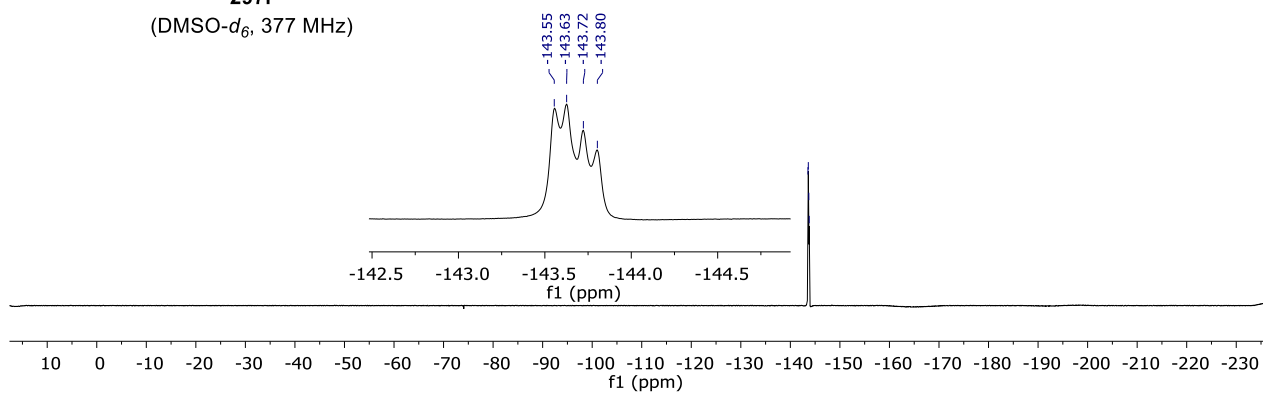
297r
(DMSO- d_6 , 101 MHz)



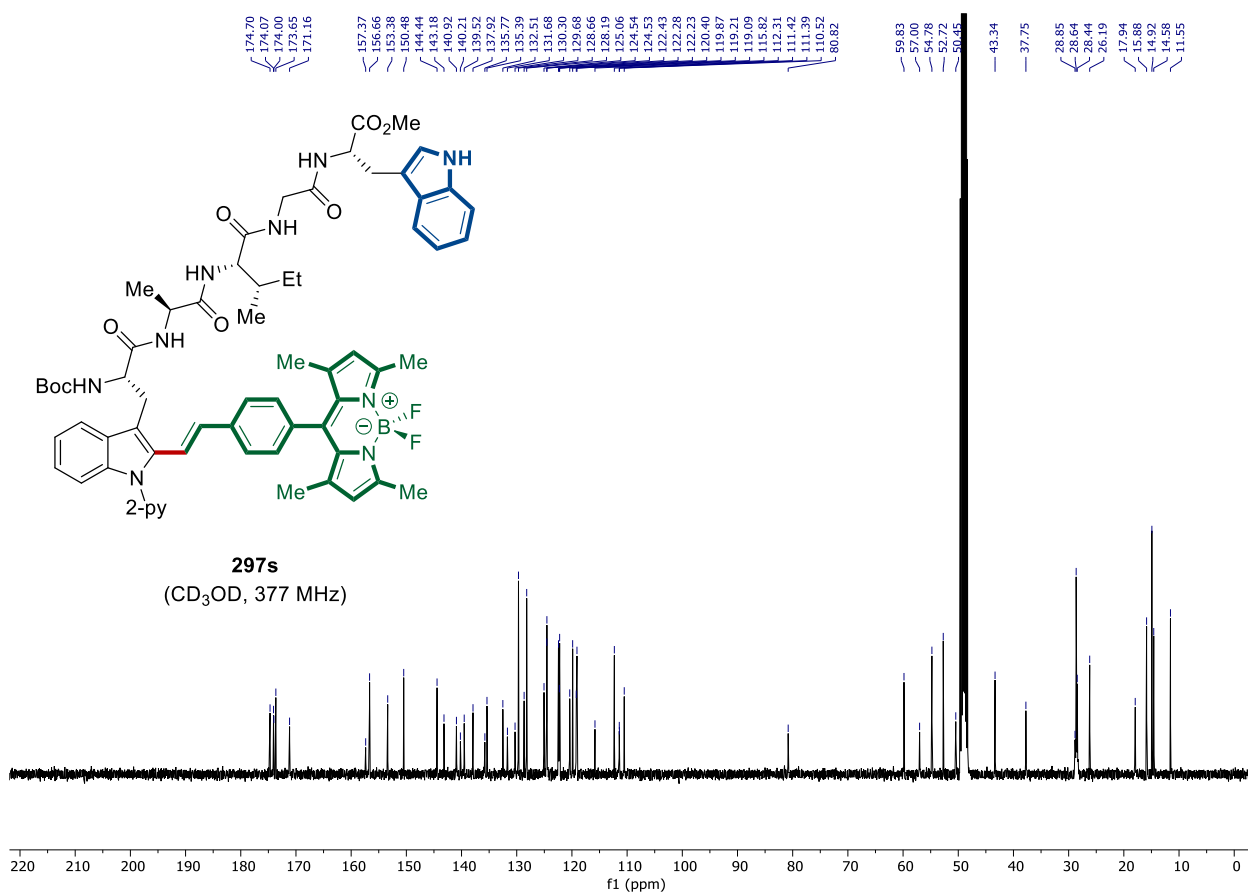
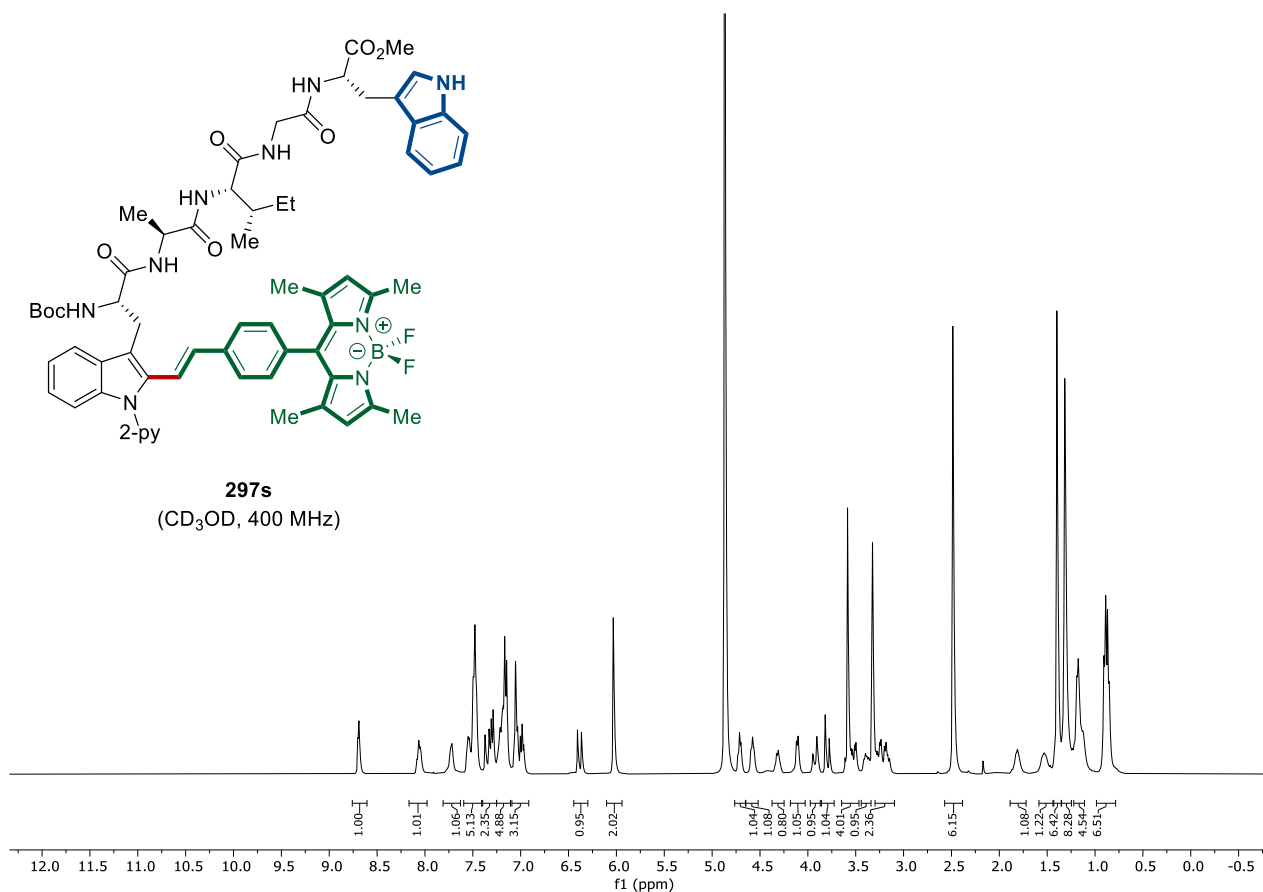
8. NMR Spectra



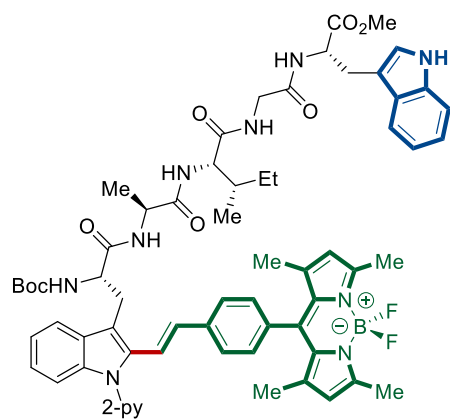
297r
(DMSO-*d*₆, 377 MHz)



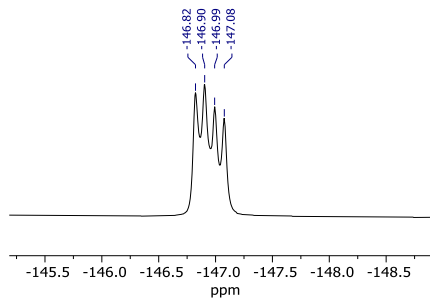
8. NMR Spectra



8. NMR Spectra

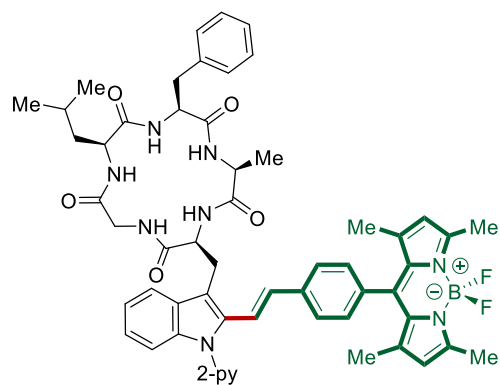


297s
(CD₃OD, 377 MHz)

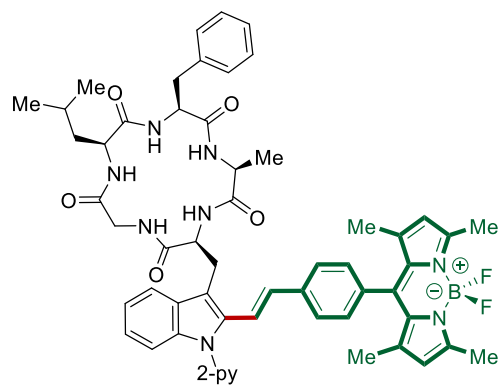
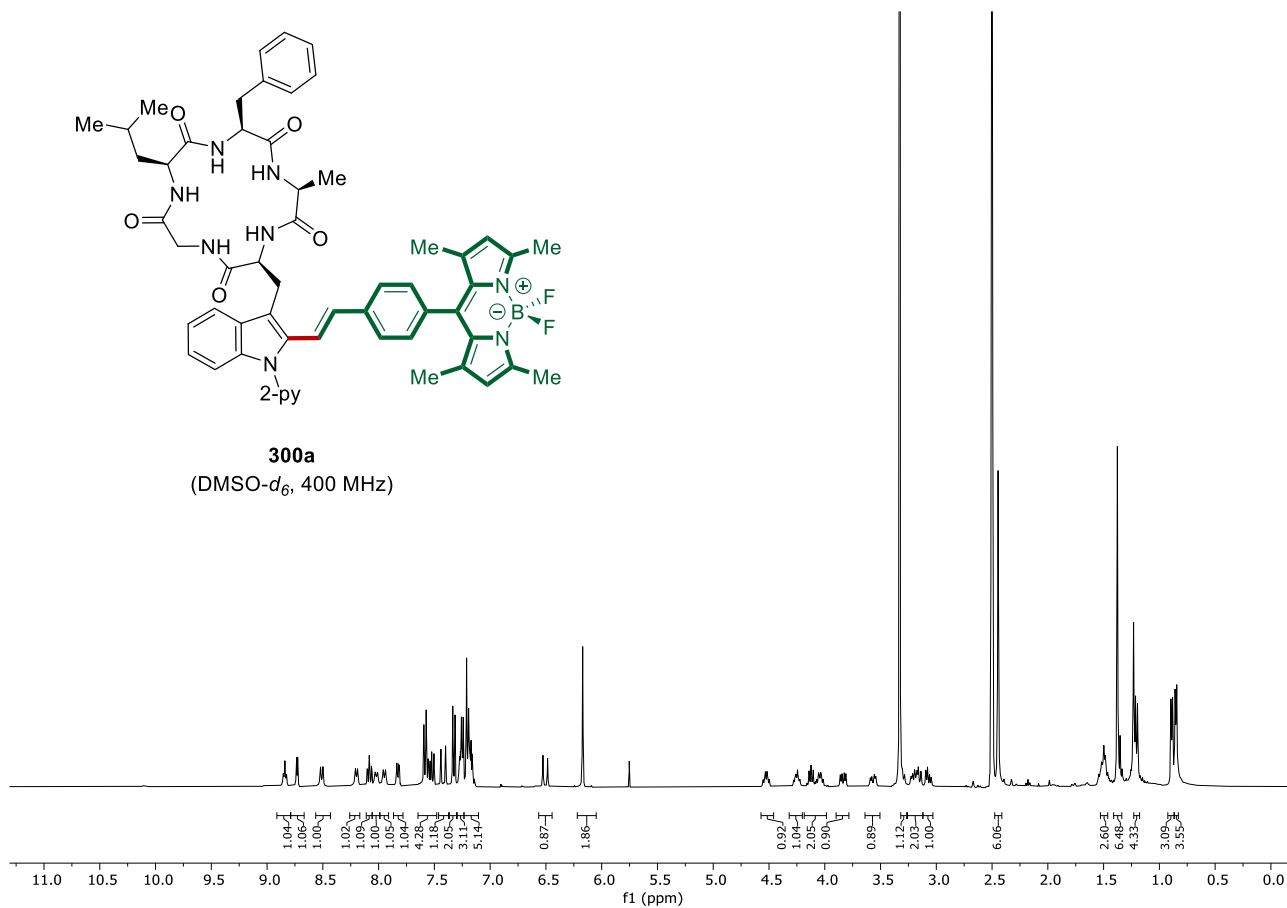


-146.82
-146.90
-146.99
-147.08

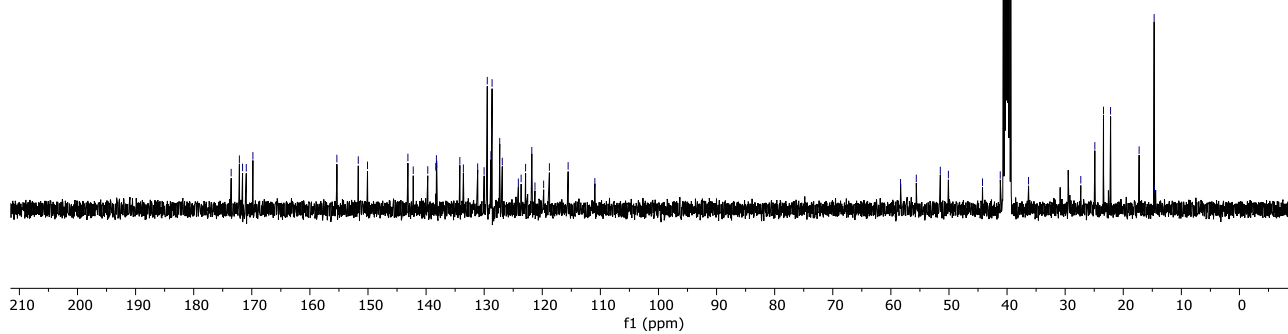
10 0 -10 -20 -30 -40 -50 -60 -70 -80 -90 -100 -110 -120 -130 -140 -150 -160 -170 -180
f1 (ppm)



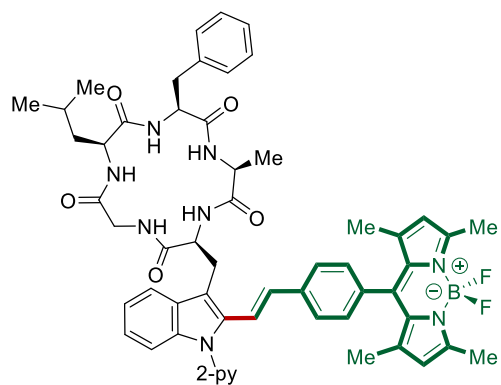
300a
(DMSO- d_6 , 400 MHz)



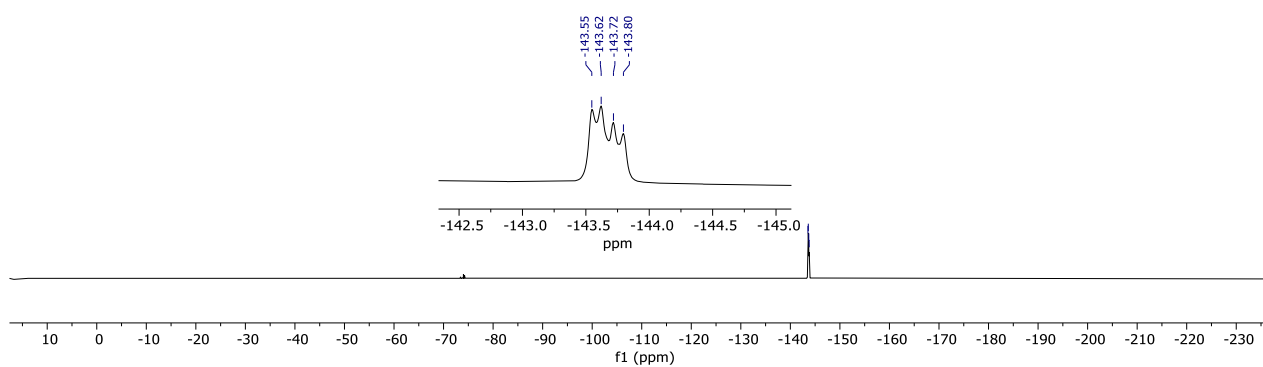
300a
(DMSO- d_6 , 101 MHz)

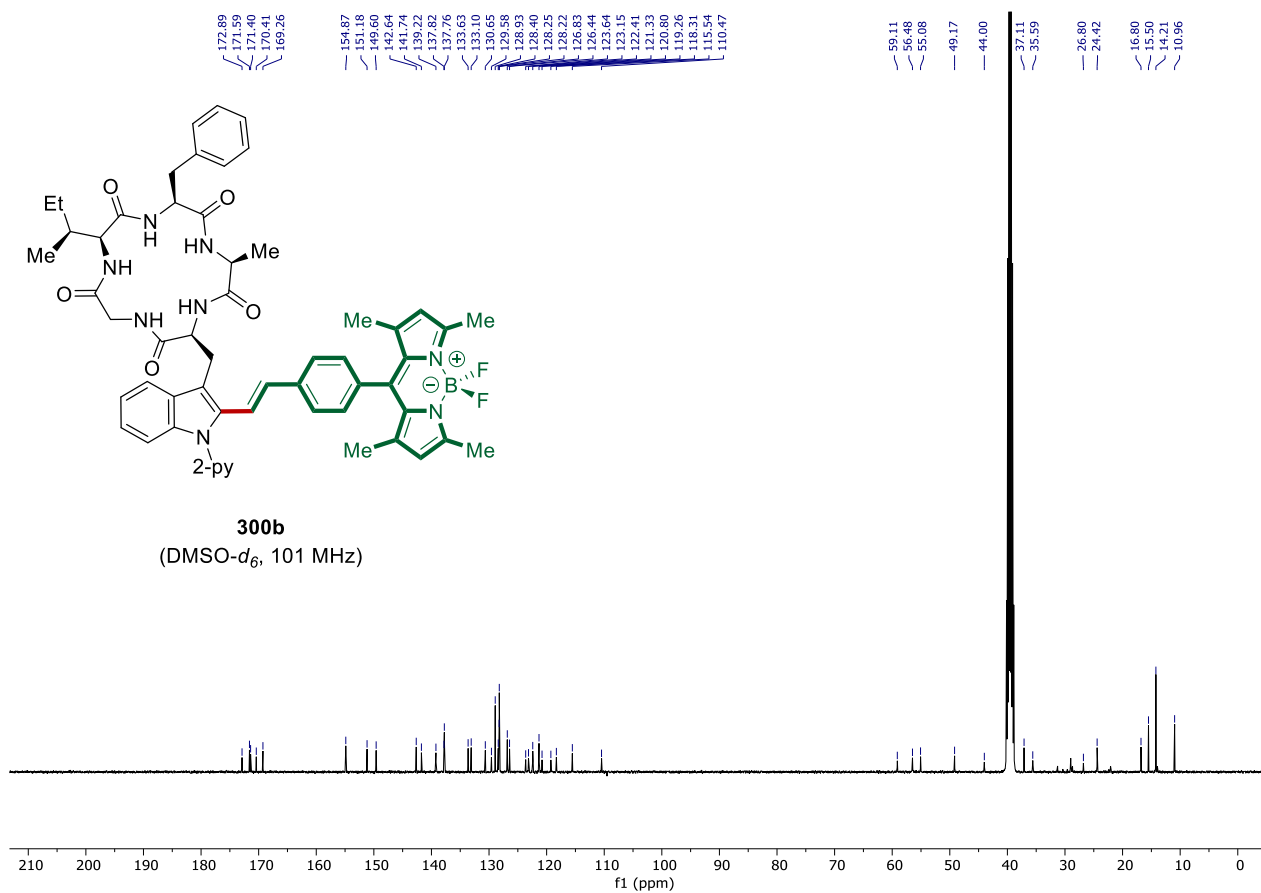
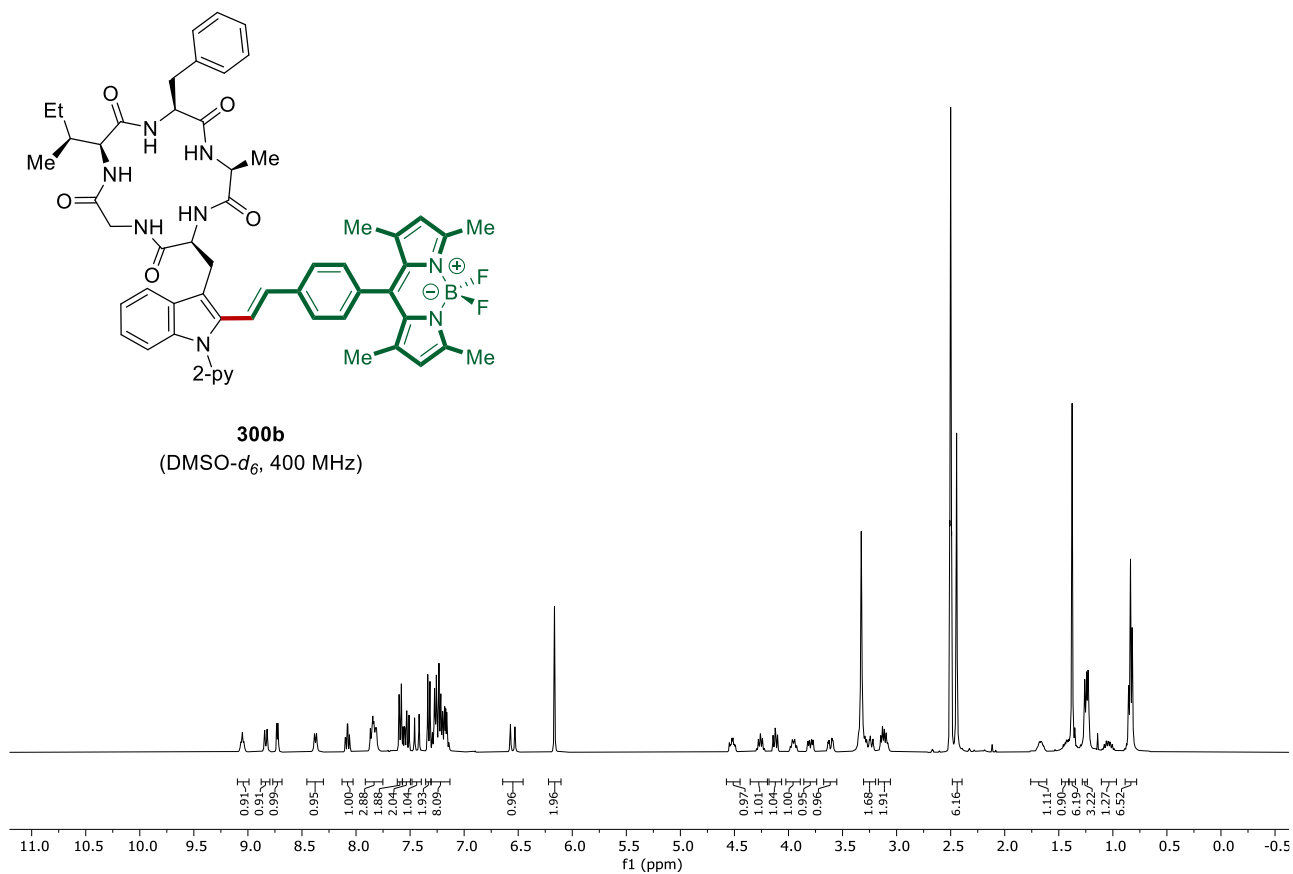


8. NMR Spectra

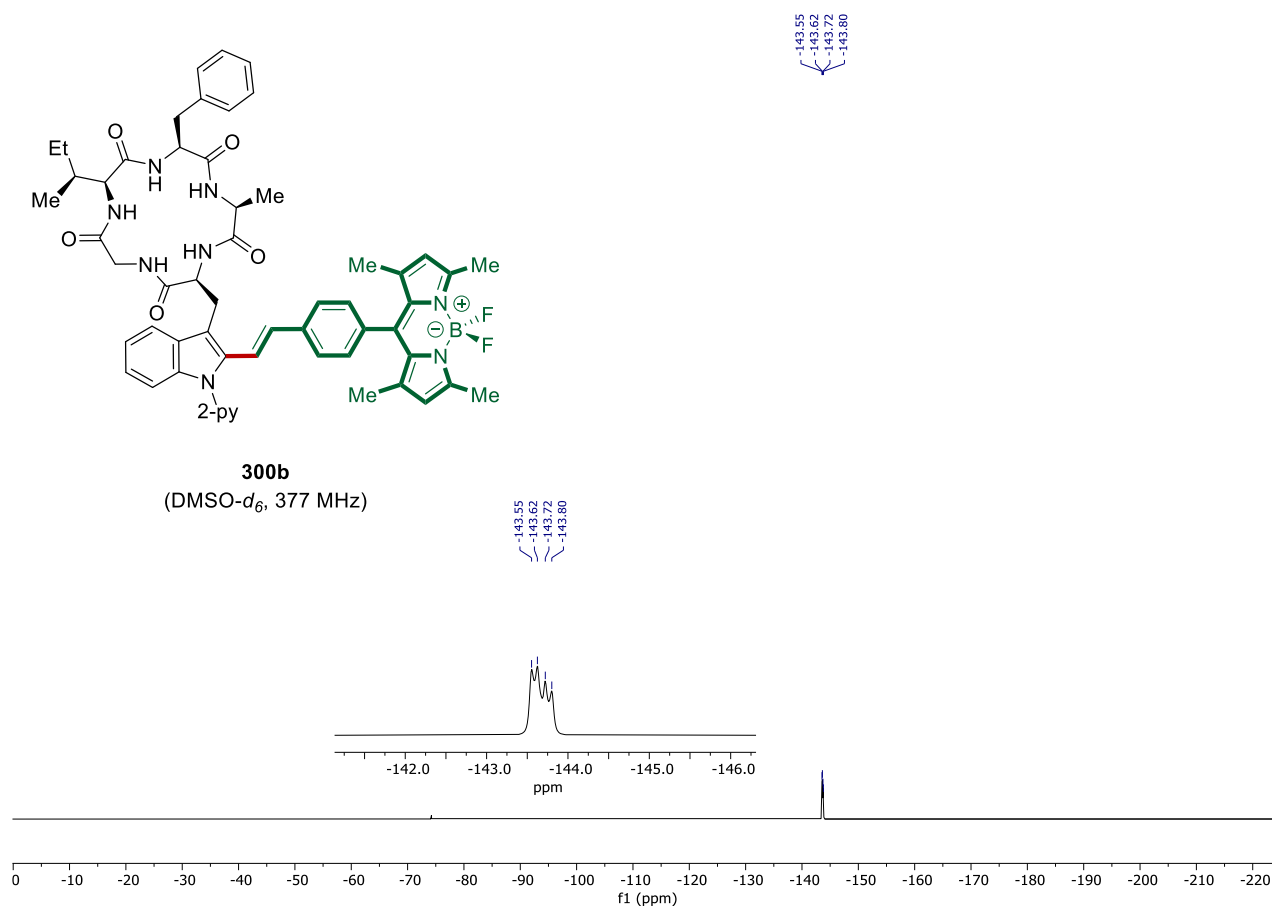


300a
(DMSO- d_6 , 376 MHz)

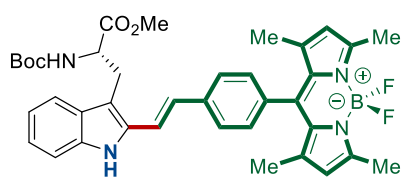




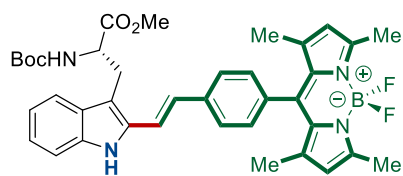
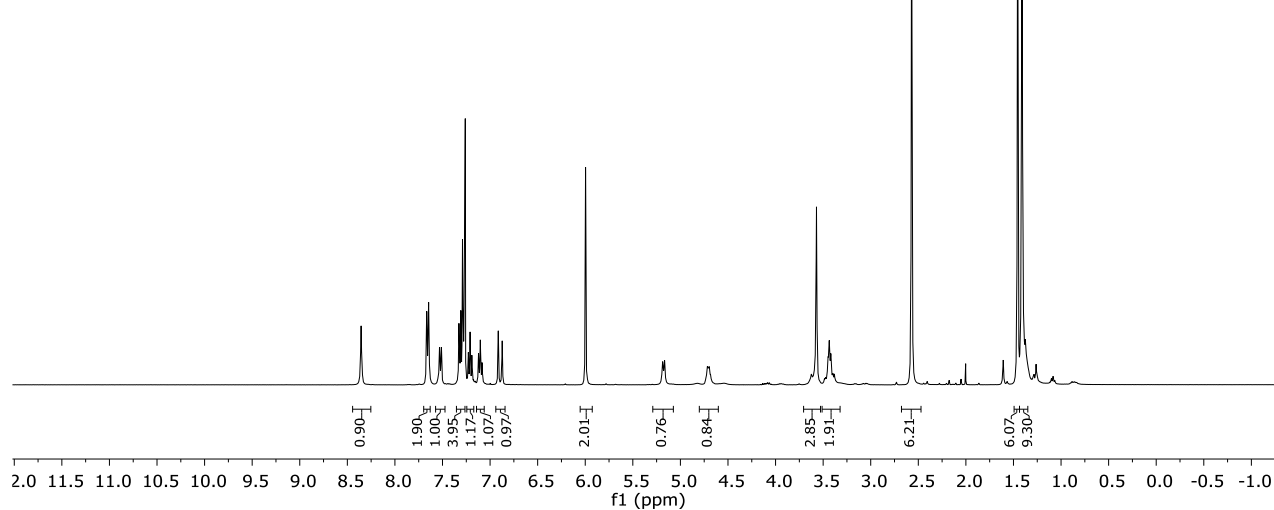
8. NMR Spectra



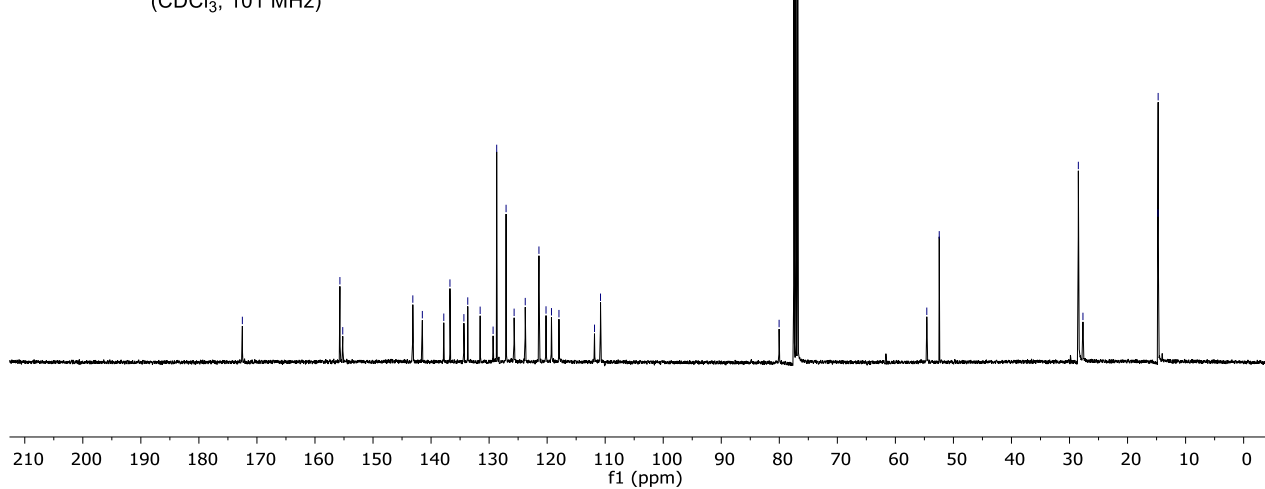
8. NMR Spectra



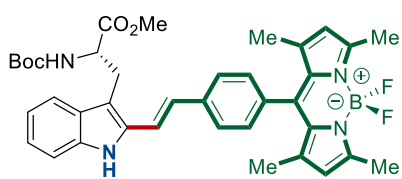
301
(CDCl₃, 400 MHz)



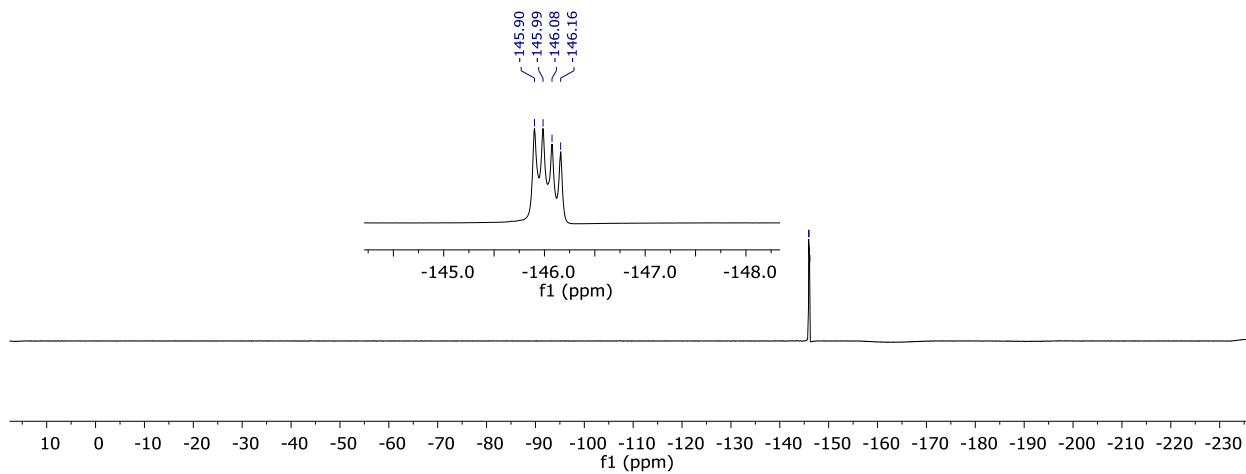
301
(CDCl₃, 101 MHz)



8. NMR Spectra



301
(CDCl₃, 377 MHz)



Erklärung

Ich versichere, dass ich die vorliegende Dissertation in dem Zeitraum von September 2016 bis Juni 2021 am Institut für Organische und Biomolekulare Chemie der Georg-August-Universität Göttingen

auf Anregung und unter Anleitung von

Herrn Prof. Dr. Lutz Ackermann

selbstständig durchgeführt und keine anderen als die angegebenen Hilfsmittel und Quellen verwendet habe.

Göttingen, den 30.06.2021